Spectrochemical Studies on the Anomalous Color Reactions of Some Iron(II) Chelate Compounds

By Kôzô SONE

(Received August 20, 1951)

Introduction

The colors of simple salts containing ferrous ion are generally light green and the absorption spectra of their aqueous solutions have a weak, split band in the infra-red region at *ca.* 1,000 mμ and also a weak, continuous absorption in the ultraviolet region.(1) It was found by Yamasaki and his collaborators,(2) however, that the ferrous complex salts containing 2, 2'-dipyridyl and 1, 10-phenanthroline ((I) and (II))

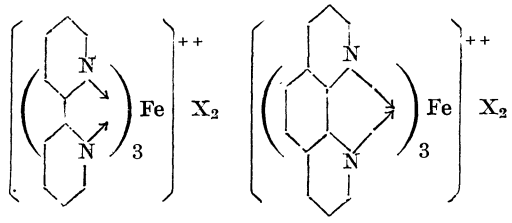

I II

show very strong absorption bands in the visible and near ultraviolet regions which differ substantially from the absorption bands due to the ferrous ion or to the organic ligand molecules of these complexes. The position of visible bands of dipyridyl- and phenanthroline ferrous complexes are 520, 510 mμ respectively (*cf.* Fig. 1). Complex salts of other metals, such as Cu, Zn, Co and Ni, containing these ligand molecules have no such bands; therefore, the appearance of these new, strong bands seems to be characteristic of the ferrous complexes themselves.(3)

The present study deals with the absorption spectra of the peculiar color reactions shown by ferrous ions with a number of organic substances. The following organic compounds are

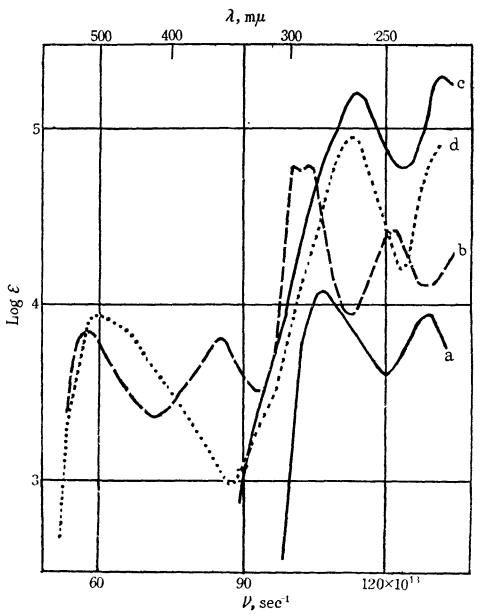

Fig. 1.—(a), 2, 2'-dipyridyl in H_2O; (b), $[Fe(dip)_3]Cl_2$ in H_2O; (c), 1, 10-phenanthroline in H_2O; (d), $[Fe(phen)_3]Cl_2$ in H_2O.

already known to show anomalous color reactions with a ferrous ion(4):

(A) 2, 2'-Dipyridyl, 1, 10-phenanthroline and their derivatives: red.

(B) Dimethylglyoxime and dioximes with similar structures: red.

(C) Compounds containing the group —C(:NOH)—CO—: blue or green.

(D) α-Carboxylic acids of pyridine, quinoline and their derivatives: brown, violet, etc.

(E) 8-Hydroxyquinoline: red.(5)

(F) Pyrocatechol and related polyphenols: violet.(6)

Of these six groups, (A) was already studied in our laboratory; also (D) was studied earlier by Ley and his collaborators(7) who showed

(1) Th. Dreisch, *Z. Phys.*, **40**, 714 (1927); Th. Dreisch and O. Kallscheuer, *Z. phys. Chem*, **B59**, 19 (1939); R. H. Potteril, O. J. Walker and J. Weiss, *Proc. Roy. Soc.*, **A156**, 561 (1936).

(2) K. Yamasaki, This Bulletin, **15**, 461 (1940); K. Yamasaki, H. Yokoi and K. Sone, *J. Chem. Soc. Japan*, **69**, 137 (1948); *Chem. Abst.*, **44**, 9295 (1950).

(3) It may be noted that the ferric complexes of these compounds also show similar bands(2), and that W. W. Brandt and G. F. Smith (*Anal. Chem.*, **21**, 1313 (1949)) reported that the dipyridyl complex of ruthenium also shows an analogous band.

(4) F. Feigl, "Chemistry of the Specific, Selective and Sensitive Reactions," 1949.

(5) R. Berg, "Die analytische Verwendung von *o*-Oxychinolin "Oxin" und seiner Derivate," 1938.

(6) Snell, "Colorimetric Methods of Analysis", Vol. II, 1937.

(7) H. Ley and C. Schwarte, O. Münnich, *Ber.*, **57B**, 349 (1924).

that the absorption spectra of such color reactions present great similarities with those of (A). Also in this case, a strong visible band appeared by chelate formation (III) (IV) which

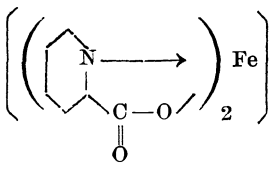

III

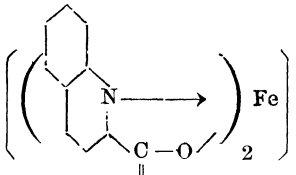

IV

is completely different from the ligand absorption. Therefore, compounds belonging to the remaining three (B), (C) and (E), such as dimethylglyoxime, 8-hydroxyquinoline, α-nitroso-β-naphthol and nitroso-R salt which are the most common analytical reagents, were studied spectrophotometrically in regard to their anomalous coloration with a ferrous ion.

Color Reaction with Dimethylglyoxime

Tschugaeff[4] discovered that a ferrous ion shows strong red coloration in the solutions containing dimethylglyoxime or dioximes having similar structures, and bases containing nitrogen such as NH_3, amines or pyridine. This coloration is, however, rather unstable, and readily fades away in contact with air, owing to the rapid oxidation of the ferrous to ferric state which is ineffective for color production; therefore small amounts of reducing agents must be added to the solution to obtain stable coloration. As the cause of the color, Tschugaeff assumed the formation of hexacoördinated complexes such as $[Fe(DH)_2A_2]$ (DH_2= dimethylglyoxime, A=NH_3 or amines) (V), although Cambi[8] prepared pyridine-containing complex salts of somewhat different composition, and Feigl[4] considered the possibility of ionic formula, such as $(AH)_2^+[FeD_2]^{-2}$ (VI).

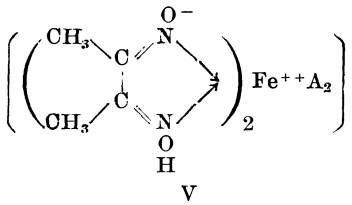

V

(8) Cambi, *Gazz. chim. ital.*, **63**, 767 (1393).

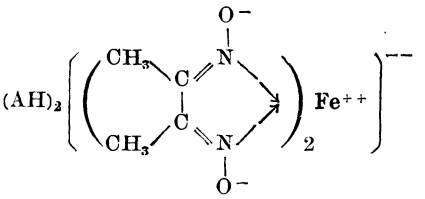

VI

By using hydrazine which is a reducing agent as the basic component, or by adding small amounts of sodium hydrosulfite crystals to the sample solutions, the present author has succeeded in preparing colored solutions containing a large exess of dimethylglyoxime and bases which were stable for about half an hour at least, and measured their absorption spectra in visible and near ultraviolet regions (Fig. 2). Dimethylglyoxime itself shows only

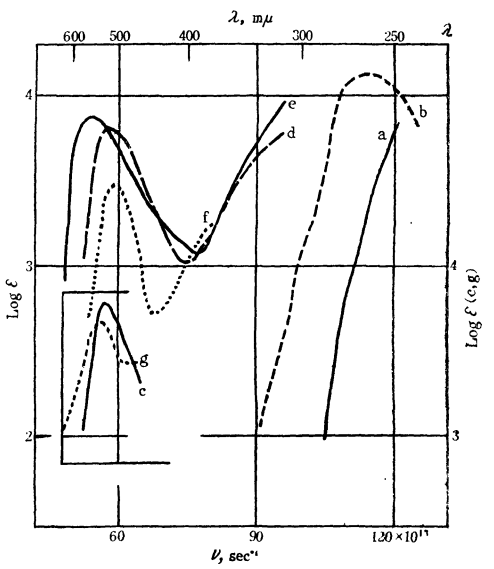

Fig. 2.—(a)~(b), dimethylglyoxime, (a) in alcohol and (b) in 0.05 N KOH; (c)~(f) Fe^{++} (0.00025 M) + DH_2 (0.0025 M), (c) +NH_3 (0.015 M), (d) +N_2H_4 (0.05 M), (e) +en (0.015 M) and (f) +pyridine (0.015 M); (g), Ni(DH)$_2$ colloidal solution (Juza).

a continuous absorption in the ultraviolet region which shifts in alkaline solutions to longer wave-lengths, a broad band appearing at *ca.* 260 mμ. However, the colored solution containing a ferrous ion and base shows a very strong, completely new absorption band in the visible region at *ca.* 510~550 mμ, which is quite similar to those bands of the dipyridyl, phenanthroline and α-pyridinecarboxylic acid complexes already mentioned above, and such close similarity makes it highly probable that

all of such bands are of similar origin in their electronic systems.

As is well known, the color of the nickel dimethylglyoxime complex is red unlike many nickel complex salts. Absorption spectra of this complex have never been reported, probably owing to its small solubility in ordinary solvents; however, the absorption curve of its colloidal solution reported by Juza[9] shows a band at *ca.* 530 mμ, which is analogous to that of ferrous complexes. This phenomenon may be connected with the fact that both the nickel atom in planar configuration and the ferrous iron atom in octahedral configuration postulated by Tschugaeff contain the same number of electrons, and they are both diamagnetic,[8] suggesting that their electronic states are much alike. Dimethylglyoxime complexes of other metals, such as Co^{III} and Cu, were known to show no similar bands.[10]

In addition to these spectral measurements, the author tried to test the validity of Tschugaeff's formula (V) or other possible structures for these complexes. The combining ratio Fe:DH determined by Job's method[11] was 1:2 (Fig. 3). However, additions of nitrogen-bearing bases are necessery for coloration, and

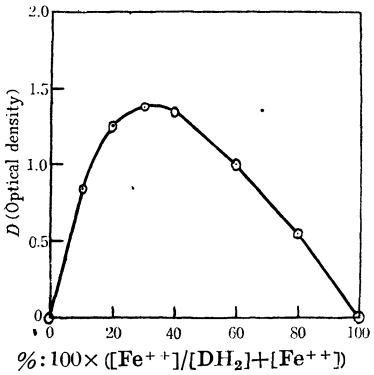

Fig. 3.—Composition curve for dimethylglyoxime-hydrazine complex; Pulfrich photometer, filter S47, $d=1$ cm., $[DH_2]+[Fe^{++}]=0.0025\,M$ in $0.05\,M$ N_2H_4.

the position of a visible band depends definitely on the nature of the base. These facts suggest the coördination of the base to the central iron atom; as the coördination number of ferrous iron is usually six, the number of base molecules coördinated to an iron atom can be supposed to be two. Therefore, Tschugaeff's formula (V) seems to be in accord with these spectrochemical observations; however, the recent observation of Mathews and Diehl[12] that the analogous complex with 1,2-cyclohexanedionedioxime has a negative charge in its solution is incompatible with this structure and it supports Feigl's formula. The author's opinion is that the complex has some intermediate structure, such as (VII),

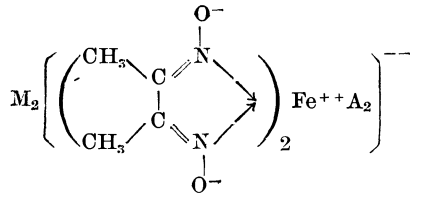

VII (M=H or cations)

which can explain all of these experimental evidences. The recent data of Mellon and Griffing[13] on the spectra of these complexes are in general agreement with ours.

Color Reaction with 8-Hydroxyquinoline

Most of the complex salts formed by 8-hydroxyquinoline with bivalent metals are yellow, orange or yellowish green in color, showing strong absorption bands in the region of 370~430 mμ with molecular extinction coefficients of several thousands; however, bands of comparable strengths are only rarely seen in the visible region.[14] From the fact that the ferrous complex is red in color,[5] it can be expected that some sort of special absorption band appears in the visible region also in this case. The author found that the ferrous complex precipitated from a weakly alkaline solution is reddish violet in color; however, this complex is very easily oxidized in air, like the dimethylglyoxime complexes, and changes into dirty black when brought in contact with air. It remains unchanged only in the mother solution containing strong reducing agents, *e. g.* hydrosulfite. Therefore the confirmation of its structure is extremely difficult, although it seems to be very probable that it has the structure (VIII) analogous

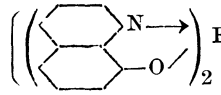

VIII

(9) Juza, R. Langheim, "Physikalische Methoden im Chemischen Laboratotium", 1937, p. 250; *Angew. Chem.* **50**, 255 (1937).

(10) H. S. French and H. E. Acly, *J. Amer. Chem. Soc.*, **48**, 847 (1927) (Cu complex); R. Tsuchida *et al.*, This Bulletin, **12**, 83, 350 (1937) (Co complexes).

(11) P. Job, *Ann. chim.*, (10) **9**, 113 (1928).

(12) J. Mathews and Jr., H. Diehl, *Iowa State Coll. J. Sci.*, **23**, 279 (1949).

(13) M. Griffing and M. G. Mellon. *Anal. Chem.*, **19**, 1017 (1947).

(14) K. Sone, unpublished results.

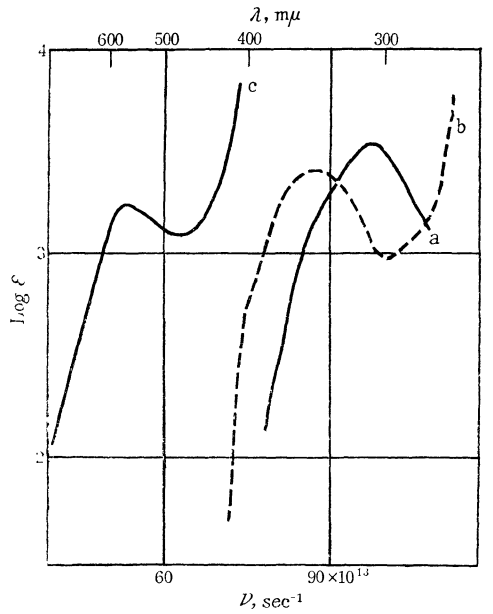

Fig. 4.—(a)～(b), 8-hydroxyquinoline, (a) in alcohol and (b) in 0.2 *N* KOH; (c), Fe^{++} (0.0003 *M*) +8-hydroxyquinoline (0.005 *M*) + KOH (0.2 *N*).

to the other metallic 8-hydroxyquinolinates precipitated under the same condition. The measurement of its absorption spectra is also difficult, and Fig. 4 (c) is that of a metastable solution of this complex produced by mixing dilute solutions of ferrous sulfate and 8-hydroxyquinoline with a large exess of the latter, which is stable for several hours in the presence of a small amount of hydrosulfite. Compared with the absorption curves of 8-hydroxyquinoline in neutral and alkaline solutions and the curves of metallic 8-hydroxyquinolinates mentioned above, it is clear that a new kind of absorption band appears at 560 mμ by the formation of this ferrous complex, the strong end absorption of its curve being due to the 8-hydroxyquinoline molecules present in excess.

Color Reaction with α-Nitroso-β-naphthol and Nitroso-R Salt

Organic compounds containing the group —C(NOH)—CO—, or the tautomeric group —C(NO):C(OH)— are known to produce blue coloration with the alkaline solutions containing ferrous ion, and complexes such as (IXa) or (IXb) are supposed to be responsible for these colors.

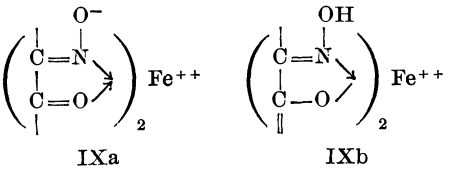

IXa IXb

Preliminary observations on isonitrosoacetone and isonitrosoacetacetic ester, the simplest compounds containing this group, revealed that the ferrous complexes of these substances possess a new strong absorption band at *ca.* 600 mμ, which is also quite different from the ligand absorption.

The same kind of reactions are observed also by aromatic compounds, and *o*-nitrosophenol and α-nitroso-β-naphthol are known to give green complexes. The latter substance and its sulfonate derivatives were studied earlier by Hoffman and Ilinsky and more recently by Sarver, Griffith and Ségal[15]. Although Hoffman considered the origin of color to be a ferric salt of the type (Xa), other authors preferred the formula (Xb) which, according to their experimental evidences, contains ferrous ion.

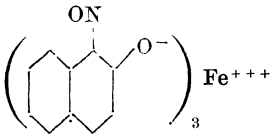

Xa

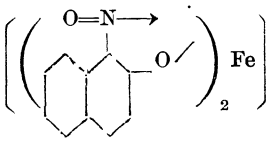

Xb

The present author studied the ferrous complex of α-nitroso-β-naphthol in ethyl acetate solution[16], and found that it has a strong visible band which is again quite different from the ligand absorption. The curve Fig. 5 (a) and (b) shows respectively the absorption spectra of α-nitroso-β-naphthol in alcoholic and alkaline solutions. In addition to the strong band at 370～385 mμ, a weak band appears in the latter curve at *ca.* 570 mμ. However, when the green precipitate formed

(15) O. Hoffmann, *Ber.*, **24**, 3741 (1891); M. Ilinsky and G. v. Knorre, *ibid.*, **18**, 2728 (1885); Sarvar, *Ind. Eng. Chem., Anal. Ed.*, **10**, 378 (1938); M. Griffing, M. G. Mellon, *Anal. Chem.* **19**, 1014 (1947); J. Ségal *Compt. rend.*, **227**, 1266 (1948).

(16) *Cf.* R. Vanossi *Anales soc. cient. argentina*, **131**, 226 (1941).

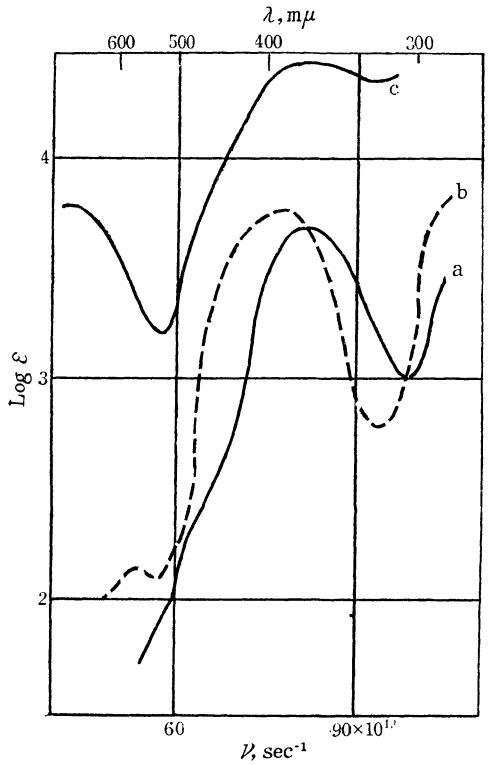

Fig. 5.—(a)～(b), α-nitroso-β-naphthol, (a) in alcohol and (b) in 0.2 *N* KOH; (c), ethyl acetate extract of ferrous complex, containing 0.000055 *M* of Fe^{++}, the initial mixing ratio of Fe^{++} to reagent being 1:6.

by the action of excess amounts of α-nitroso-β-naphthol with ferrous sulfate in weakly alkaline solution was extracted by ethyl acetate and the absorption spectra of the extracted solution was measured, a very strong band was found to appear in the neighborhood of 700 mμ, and although this complex is gradually oxidized in air changing into a black substance, It was found by rapid measurements that this new band attains its maximum absorption when about 3 moles of α-nitroso-β-naphthol are mixed with one mole of ferrous ion. Therefore the structure of this substance seems to be of hexacoördinated type, such as (Xc), instead of the conventinal formula (Xb) used by previous investigators.

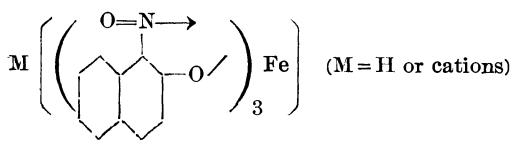

Xc

Nitroso-R salt, or the sodium salt of α-nitroso-β-naphthol-3, 6-disulfonic acid, produces green soluble complex which is very stable even after standing for many hours. The characteristics of the absorption spectra of this complex are quite similar to those of α-nitroso-β-naphthol, the absorption of the new band becoming still stronger. Owing to the higher stability of the colored solution, the

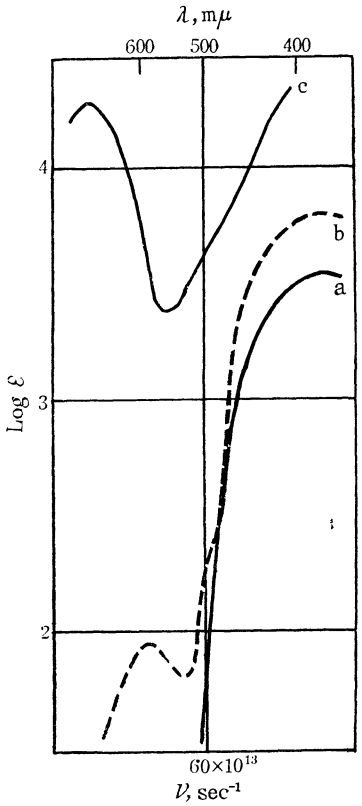

Fig. 6.—(a)～(b), nitroso-R salt, (a) in H_2O and (b) in 0.2 *N* KOH; (c), Fe^{++} (0.0001 *M*) +nitroso-R salt (0.0003 *M*) +NaOAc (0.05 *M*).

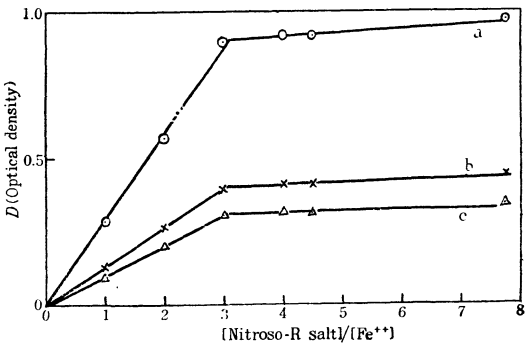

Fig. 7.—"Molar ratio" curve for nitroso-R salt complex; Pulfrich photometer, filter (a) S61, (b) S57, (c) S53, *d*=1 cm., Fe^{++} (0.00011 *M*) +nitroso-R salt (variable amt.) in 0.05 *M* NaOAc.

exact determination of the composition of the colored complex becomes possible in this case, with the result that the molar ratio of ligand to iron is 3:1, as in the case of α-nitroso-β-naphthol, showing the validity of analogous hexacoördinated formula (XI) in this complex (Figs. 6 and 7). Recent data of Griffith *et al.* agree fairly well with the author's.

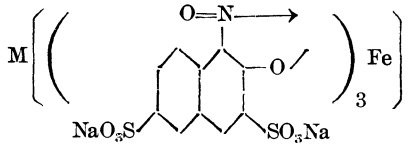

XI

Discussion

From the experimental results described above, it seems to be fairly clear that, although the structure of these complex salts are different, all of them show a strong absorption band in the visible region, with maximum wave-lengths ranging from 500 to 720 mμ and log ε of 3~4, which cannot be attributed to the ferrous ion or to the organic ligand molecules. They are only rarely observed in the complexes of other metals with these ligands and are therefore quite characteristic of these ferrous complexes studied (*cf.* Table 1).

Table 1

Reagent	Probable structure of the complex	Absorption, maximum mμ	log ε*
2, 2'-dipyridyl	(I)	520, 352	3.8
1, 10-phenanthroline	(II)	510	3.9
α-pyridine carboxylic acid and derivs.	(III), (IV)	500~560	2.5~3**
dimethylglyoxime			
+NH_3		525	3.8
+N_2H_4	(V), (VI) or	520	3.8
+en	(VII)	550	3.9
+pyridine		510	3.5
8-hydroxyquinoline	(VIII)	560	3.2
isonitrosoacetone and derivs.	(IX)	ca. 600	
α-niroso-β-naphthol	(Xc)	ca. 700	3.8
nitroso-R salt	(XI)	720	4.3

* Molecular extinction coefficients of the complexes were calculated for one mole of ferrous ion.

** Estimated values from the data of Ley *et al.*

From the examination of the probable structures of these complexes it becomes evident that some sort of unsaturated five-membered ring formation, such as (a) or (b), occurs in all of them in common.

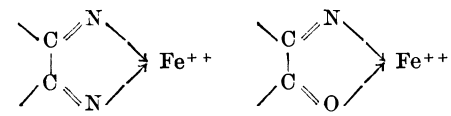

Of course, the positions of double bonds in these rings may be variable owing to the resonance effects. Therefore the existence of such an intramolecular ring can be assumed as a sort of chromophore which produces this kind of new absorption band. Thereby the unsaturated state of the whole ring, that is to say, the possibility of resonance of the π-electrons over all four non-metallic atoms composing the ring, seems to be essential for the color, because ethylenediamine does not form such a colored complex and 8-aminoquinoline, which has a similar structure with 8-hydroxyquinoline, only produces yellow ferrous complex[17] which may be due to the fact that their NH_2 groups become saturated with the coördination to the iron and therefore they are impossible to participate in the resonating system. It may be added that the violet compounds produced by *o*-diphenols and analogous polyphenols (*cf.* Introduction) with ferrous ion may contain an intramolecular ring of similar structure (c-1) or (c-2).

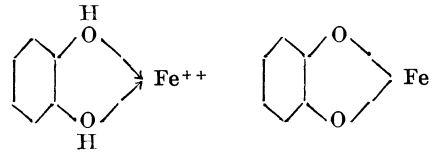

Similar chromophore action of an intramolecular organometallic ring was formerly observed by Willis and Mellor[18] in the case of diamagnetic nickel complexes, and the ferrous complexes reported in this study might be regarded as its second example. In the case of nickel complexes a close relation was found between the magnetic properties of the complexes and the appearance of a new absorption band; however, no definite relation can be found by ferrous complexes, as the band appears in both para- and diamagnetic complexes.[8]

(17) G. J. Burrows and E. Ritchie, *J. Proc. Roy. Soc. New South Wales* **72**, 113 (1939).

(18) Willis and Mellor, *J. Amer. Chem. Soc.*, **69**, 1237 (1947).

Experimental

Reagents.—Mohr's salt of extra pure grade was used as the source of ferrous ions. All the organic reagents are analysis grade samples and, when necessary, were purified by repeated recrystallization.

Preparation of Samples.—In the preparation of sample solutions with dimethylglyoxime and 8-hydroxyquinoline, a minute amount of hydrosulfite crystalls was added to the solutions, except in the case of the hydrazine complex to prevent air oxidations. Sample solutions of α-nitroso-β-naphthol were prepared by mixing the alcoholic solution of the organic reagent and aqueous solution of Mohr's salt in a 10% solution of sodium acetate, and by rapidly extracting the formed precipitate with ethyl acetate.

Spectral Measurements.—Measurements of absorption spectra were made by a Spekker spectrophotometer combined with a medium quartz spectrograph. A Pulfrich photometer was also used in the visible region. The measurements on nitroso-R salt were made with the Beckman DU spectrophotometer which was put at our disposal in the later stage of this study.

Summary

Absorption spectra of colored complex salts formed by ferrous ion with dimethylglyoxime, 8-hydroxyquinoline, α-nitroso-β-naphthol and nitroso-R salt were studied. The origin of a strong absorption band in the visible region in all of these complexes was attributed to the formation of unsaturated intramolecular five-membered rings. Determination of the composition of the complexes was made spectrophotometrically in the case of dimethylglyoxime, α-nitroso-β-naphthol and nitroso-R salt.

The author wishes to express his thanks to Prof. K. Yamasaki for his guidance. A part of the expense of this study was defrayed from a grant for Fundamental Scientific Research.

Chemical Institute, Faculty of Science
Nagoya University, Nagoya

The Structure of Surface-Denatured Protein. I. Molecular Weight and Surface Area of Horse Serum Albumin Molecule

By Kazutomo IMAHORI

(Received June 6, 1951)

As Bull and others have shown, it is possible to obtain a very thin protein film of the thickness of the order of 10 Å. by putting a small quantity of powdered protein or protein solution on the surface of concentrated salt solution[1] or water solution of propyl alcohol.[2] The protein molecule in such a film may lose its original globular shape; it is considered that the polypeptide linkage has the extended, to become the so called β-form, This can be shown by transferring the film to the surface of a solid and taking its photograph by x-ray diffraction.[3] The transformation from α-form to β-form is characteristic for the denaturation phenomenon. Therefore, the above-mentioned protein film is sometimes called surface-denatured protein. Neurath[4] has pointed out, that the surface denaturation is the most perfect denaturation. And it is quite interesting to investigate the structure of the surface-denatured protein as well as the mechanism of the surface denaturation.

This problem has been investigated by the present author from several points of view and in this paper the molecular weight and surface area of the surface-denatured horse serum albumin will be reported. The former was determined by H. B. Bull's method, but the latter by the measurement of the compressibility of the film.

Surface Balance

The author modified the so-called Wilhelmy[5]

(1) H. B. Bull, *J. Am. Chem. Soc.*, **67**, 4 (1946).
(2) H. Theorell, *Trans. Faraday soc.*, **35**, 1413 (1939).
(3) W. T. Astbury, F. O. Bell, E. Gorter and J. van Ormondt, *Nature*, **142**, 33 (1938).
(4) H. Neurath, J. P. Greenstein, F. W. Putnam and J. O. Erickson, *Chem. Rev.*, **34**, 157 (1945).
(5) Wilhelmy, *Ann. Physik.*, **119**, 177 (1863).

type surface balance and has used it instead of the Adam's type. One of the bowls of the chemical balance (made by E. Sartorius in Germany) is taken away, and a long metal wire is hung instead. A very thin glass plate is hung on the tip of the wire. The glass plate must by kept in the chromic acid mixture; it should be washed with distilled water and then dried before use, for even the slightest stain on the plate will make the measurement quite incorrect.

The length of the wire is controlled so that about one third part of the plate may be immersed under the water surface. An extremely thin glass needle is put on the tip of the needle of the balance. A scaled microscope of 40 magnification is fixed in front of the needle and is brought to its focus.

Then, putting some balance-weight on the bowl, the balance is brought in equilibrium and the position of the glass needle on the scale of the microscope is read. When some film is put on the water surface, its surface tension decreases, and the glass plate rises a little. The needle then moves to a new equilibrium position and the deflection of the needle ΔQ_1 can be expressed as

$$\Delta Q_1 = k\Delta\gamma. \qquad (1)$$

Here, $\Delta\gamma$ is the surface pressure, k is a constant indicating the sensivity of the balance, contact angle being assumed to be zero. Then the balance weight on the bowl is decreased so as to bring the needle to its original position. If the decrease in weight is expressed as ΔG, the following equation must hold.

$$g\Delta G = 2(t+b)\Delta\gamma \qquad (2)$$

Here, g is the gravity constant and t the thickness and b the width of the plate respectively. And thus the surface pressure can be calculated from (2) or the following relation, which can be derived from (2).

$$\Delta\gamma = \frac{g\cdot\Delta G}{2(t+b)} \qquad (3)$$

In the present experiment, $t = 2\times10^{-3}$ cm. and $b = 5.5$ cm.

But it is troublesome to bring the needle just to the original position by adjusting the weight on the bowl. In such a case, the surface pressure can be calculated as follows.

When the weight on the bowl is decreased by ΔG_1 and the needle is brought to the position which is deflected from the original position by ΔQ_2, the surface pressure can be expressed as

$$\Delta\gamma = \frac{g\cdot\Delta G_1}{2(t+b)}\left(1+\frac{\Delta Q_2}{\Delta Q_1-\Delta Q_2}\right) = \frac{g\cdot\Delta G}{2(t+b)}\times\frac{\Delta Q_1}{\Delta Q_1-\Delta Q_2} \qquad (4)$$

Thus $\Delta\gamma$ can be obtained from (4) by using the data of ΔQ_1 and ΔQ_2. In Fig. 1, the surface pressure—surface area curve of the horse serum albumin is shown, which is obtained by using this apparatus. Curve 1 is at pH=6, and curve 2 is at pH=10.

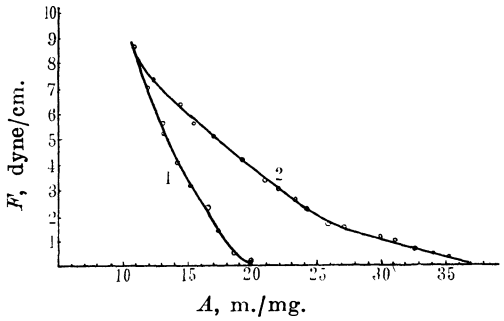

Fig. 1.—F-A curve of horse serum albumin.

Determination of Molecular Weight

The molecular weight of protein can be determined by H. B. Bull's method.[1] In Fig. 2, the film pressure F of the horse serum albumin monolayer multiplied by the film area A per milligram of protein is plotted against the surface pressure F. The experiment has been carried out under pH=6.

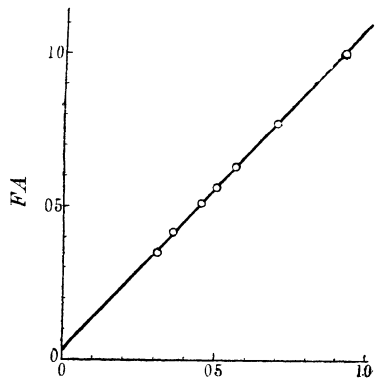

Fig. 2.—Relation between F and FA.

The protein used is the crystalline horse serum albumin which was purified by Dr. Sankichi Nakamura in Chemical Laboratory, Faculty of Science, University of Tokyo, by the sodium sulfate method. Water is distilled several times and is used as the substrate. The surface pressure is measured by the surface balance mentioned above.

Bull has pointed out that $FA-F$ curve should be given as a straight line, which is represented by the following equation:

$$FA = nRT + nS_pF. \qquad (5)$$

Here, n is the mol number of the protein on the water surface and S_p is the surface area covered by one mol protein. Accordingly the extrapolated value of FA at zero surface pressure should satisfy the equation,

$$FA = nRT = (m/M)(RT), \qquad (6)$$

where R is the gas constant, T the absolute temperature and m the weight of protein put on the water surface. Thus molecular weight M can be calculated from the above equation. nS_p is equal to the gradient of the curve and can be calculated from Fig. 2. From the points on Fig. 2, values of nRT and nS_p can be calculated by using the method of least squares as follows:

$$nRT = 0.034 \pm 0.006 \text{ and } nS_p = 1.05 \pm 0.11.$$

And therefore, equation (5) can be expressed as

$$FA = 0.034 + 1.05\,F. \qquad (7)$$

And as $T = 19°C.$, the molecular weight of the surface-denatured serum albumin proves to be about 70,000 ± 12,000, which agrees with the data from the measurement of osmotic pressure and others.[6] This tells us that serum albumin does not split into two or more pieces, although it may lose its original shape by surface denaturation.

The surface area covered by 1 mg. of serum albumin is equal to 1.05 m.^{2} This value can be checked by the following compressibility measurement.

The Measurement of the Compressibility of the Film

As expanded film is compressed, it gradually changes into condensed film, and it becomes less and less compressible. At last, at the point where the molecules on the surface are packed most closely, the compressibility comes to its minimum. If the film is further compressed, it will be broken and the compressibility will increase again. The compressibility δ may be defined by

$$\delta = \frac{1}{A}\frac{dA}{dF}. \qquad (8)$$

Where A is the surface area per milligram of protein and F is the surface pressure. Fig. 3 shows the compressibility of the horse serum albumin at various surface areas.

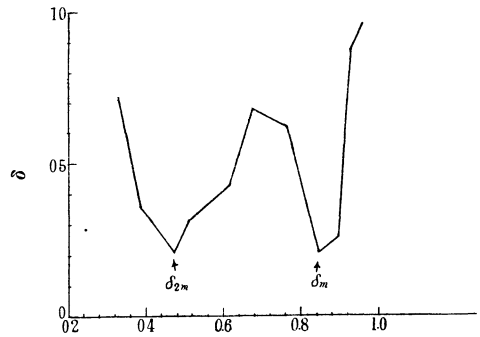

Fig. 3.—Compressibility of horse serum albumin.

As is seen from Fig. 3, the minimum compressibility δ_m has the value of 0.21. The surface pressure F_m and surface area A_m at this point have the value of 12 dyne/cm. and 0.845 m.^{2}/mg. respectively. From the value of A_m the surface area covered by one albumin molecule is calculated to be 9820 Å.^{2}

Fig. 3 shows also that the compressibility has the second minimum δ_{2m}. The surface area at this second minimum point has the value of 0.466 m.^{2}/mg. and this value is equal to about one half of that of A_m. This perhaps shows that at this point, protein has the doubled layer structure.

As is cited above, the surface area of the serum albumin molecule can be calculated from the $FA-F$ curve, and is obtained as 1.05 m.^{2}/mg. The disagreement of this value with that of A_m can be interpreted as follows.

Tonomura[7] has derived, from a statistical mechanical treatment, that if nS_p/A_m has the value of about two, the molecule on the surface is considered to have a round disk shape, while if the ratio has the value near one, it is considered to have an elongated disk shape.

From the present experiment, nS_p/A_m becomes to be equal to 1.24 and this indicates that the serum albumin molecule has an elongated disk shape.

Summary

1. The molecular weight of the surface denatured serum albumin molecule is measured from the $FA-F$ curve. The experiment has shown it to be about 70,000.

2. The surface area covered by one surface-denatured serum albumin molecule is determined to be 9820 Å.^{2} from the compressibility measurement.

(6) H. Neurath, G. R. Cooper, and J. O. Erickson, *J. Biol. Chem.*, **142**, 249 (1942); N. F. Burk, *J. Biol. Chem.* **98**, 353 (1982).

(7) Y. Tonomura, *Kagaku (Science)*, **19**, 565 (1949).

The author wishes to express his hearty thanks to Prof. Bun-ichi Tamamushi, Prof. San-ichiro Mizushima and Dr. Takehiko Shimanouchi for their very kind advice, discussions and encouragement. This work was aided by a grant from the Ministry of Education.

Chemical Laboratory, College of General Education, Tokyo University, Tokyo

The Structure of Surface-Denatured Protein. II. Relation between the Surface Diffusion Constant and the Shape of the Protein Molecule (Theoretical)

By Kazutomo IMAHORI

(Received July 2, 1951)

In the previous paper of this series[1], the molecular weight of the surface-denatured serum albumin has been obtained: 70,000 from the $FA-F$ curve. The surface area of the serum albumin is also obtained: 9820 Å.^{2} from the compressibility measurement. Now it is desired to clarify the shape of the surface-denatured protein.

The shape of the native protein molecule has already been investigated by the measurement of the viscosity of the solution, determination of its diffusion constant, measurement of the sedimentation equilibrium under the ultracentrifugal force, etc.

The shape of the surface-denatured protein is likely to be determined by the analogous experiment. Of those methods the measurement of the viscosity and the diffusion constant are applicable for the surface film.

In our laboratory the latter method has been carried on. In this paper the relation between the surface diffusion constant and the shape of the molecule will be derived theoretically.

Relation between the Diffusion Constant and the Friction Ratio

It is perhaps quite natural to postulate that the surface-denatured protein molecule has the form of an elliptic disk, which floats upon the water surface. Suppose at first the disk is circular.

If the relative speed of the disk and water be taken as U, then the frictional force K can be given as

$$K=6\pi\eta p'U \tag{1}$$

where, η is the viscosity coefficient of water. According to Lamb[2], p' is expressed as $8r/9\pi$, r being the radius of the disk. The driving force acting on the protein molecules which are contained in 1 cm.^{2} of area can be expressed as $-\mathrm{d}F/\mathrm{d}x$, where F is the surface pressure of protein film. One square centimeter of area containe $(\rho/M)\times N$ protein molecules, in which ρ is the mass of protein contained in 1 cm.^{2} of area, M is the molecular weight of protein, and N is the Avogadro's number. Thus, the driving force acting on one protein molecule can be shown as $-(M/\rho N)(\mathrm{d}F/\mathrm{d}x)$. This force must be equal to K in magnitude and must have the opposite sign to that of K. When surface film is gaseous we can put

$$F=\frac{R}{M}\rho T \tag{1'}$$

so that $\dfrac{\mathrm{d}F}{\mathrm{d}x}=\dfrac{R\cdot T}{M}\cdot\dfrac{\mathrm{d}\rho}{\mathrm{d}x}$ must hold, and finally we get

$$6\pi\eta p'U=\frac{RT}{\rho N}\frac{\mathrm{d}\rho}{\mathrm{d}x} \tag{2}$$

or

$$U=\frac{R\cdot T}{6\pi\eta\rho N p'}\frac{\mathrm{d}\rho}{\mathrm{d}x} \tag{2'}$$

The mass of protein which diffuses in one second across a line of 1 cm. long will be expressed as $U\rho$. On the other hand from Eq.

(1) K. Imahori, This Bulletin, **25**, 7 (1952).

(2) H. Lamb, "Hydrodynamics," 6th edition, Cambridge, 1932, p. 605.

(2) this can be expressed as follows:

$$U\rho = -\frac{RT}{6\pi\eta N p'}\frac{d\rho}{dx} \qquad (4)$$

As mentioned above, $p' = 8r/9\pi$, and the Eq. (4) may be expressed:

$$U\rho = -\frac{3RT}{16\eta N r}\frac{d\rho}{dx} \qquad (4')$$

The diffusion constant D_0 can be defined as

$$U\rho = -D_0\frac{d\rho}{dx} \qquad (5)$$

so that from Eqs. (4') and (5) the following relation will be obtained:

$$D_0 = \frac{3RT}{16\eta}\frac{1}{N\cdot r} \qquad (6)$$

The suffix 0 means that the molecule is circular.

As $16\eta r/3$ means the frictional force acting on the circular disk when it is floating at a unit speed, we can put

$$\frac{16\eta r}{3} = f_0$$

Then (6) reduces to:

$$D_0 = \frac{R\cdot T}{N}\cdot\frac{1}{f_0} \qquad (7)$$

When the disk is not circular, but elliptic, the frictional force may be expressed as f, and just like for the circular disk, the next relation can be obtained for the elliptic disk:

$$D = \frac{R\cdot T}{N}\frac{1}{f} \qquad (8)$$

From (7) and (8) is obtained:

$$\frac{D}{D_0} = \frac{f_0}{f} \qquad (9)$$

Now, the molecular weight M of a circular disk-shaped protein molecule can be expressed by r (the radius of disk), d (its thickness), V (the reciprocal of the density) and N (Avogadro's number), as follows

$$M = \pi r^2 d\frac{N}{V} \qquad (10)$$

Combining with (6) and (9), (10) can be expressed as

$$M = \frac{\pi d N}{V}\cdot\left(\frac{3}{16\eta}\right)^2\cdot\left(\frac{RT}{ND_0}\right)^2 = \frac{9\pi d R^2T^2}{256\,\eta^2 N D^2 V}\left(\frac{f_0}{f}\right)^2 \qquad (11)$$

This shows the relation between the diffusion constant D and the friction ratio f/f_0. In the equation, M can be determined by the method described in the previous paper[1]. The thickness d can be determined by the optical method which will be reported in the later paper[3]. And thus f/f_0 can be determined from equation (11), if the value of D is known. The method for determination of the value of D will be reported in part 3 of this series.

Relation between the Friction Ratio f/f_0, and the Ratio of Two Axes of Ellipse c/a

The friction ratio can be determined from the above equation (11). But in order to determine the actual shape of the ellipse, the relation between f/f_0 and c/a must be derived. In this section, this relation has been derived as follows.

The frictional force acting on the disk which floats on the water surface is supposed to be just a half of the force acting on the disk which moves through the water in its edgeways direction. And when the elliptic disk flows on the water surface, the frictional force acting upon the disk is expressed by

$$K = 6\pi\eta RU$$

where U is the relative velocity of the disk against water, η is the viscosity of water and R is the function of the magnitudes of two axes of the ellipse.

According to Lamb[2], for the movement in its a-axis direction, R can be expressed as R_a and is given by the relation:

$$R_a = \frac{4}{3}\frac{ac}{\chi_0 + \alpha_0 a^2} \qquad (13)$$

and

$$\chi_0 = ac\int_0^\infty \frac{d\lambda}{\sqrt{(a^2+\lambda)(c^2+\lambda)\lambda}} \qquad (14)$$

$$\alpha_0 = ac\int_0^\infty \frac{d\lambda}{\sqrt{(a^2+\lambda)^3(c^2+\lambda)\lambda}} \qquad (15)$$

The former integration can be carried out by setting $\lambda = t^2$

(3) K. Imahori and Y. Yoneyama, unpublished.

$$\int_0^\infty \frac{d\lambda}{\sqrt{(a^2+\lambda)(c^2+\lambda)\lambda}} = \int_0^\infty \frac{1}{t\sqrt{(a^2+t^2)(c^2+t^2)}} \cdot \frac{d\lambda}{dt} \cdot dt = \int_0^\infty \frac{2dt}{\sqrt{(a^2+t^2)(c^2+t^2)}} = \frac{2}{c} K(e) \tag{16}$$

$K(e)$ means the complete elliptic integral of the first order and e is the eccentricity of the ellipse as given by the following relation:

$$e^2 = \frac{c^2-a^2}{c^2}$$

The integration of α_0 can be carried out as follows. As in the case of χ_0, $\lambda=t^2$ is put in (14)

$$\alpha_0 = \int_0^\infty \frac{d\lambda}{\sqrt{(a^2+\lambda)^3(c^2+\lambda)\lambda}} = \int_0^\infty \frac{2dt}{\sqrt{(a^2+t^2)^3(c^2+t^2)}} = \frac{2}{c^2-a^2}\left[\int_0^\infty \sqrt{\frac{(c^2+t^2)}{(a^2+t^2)}}\, dt - \int_0^\infty \frac{dt}{\sqrt{(a^2+t^2)(c^2+t^2)}}\right]$$

The second term in the bracket is just equal to the integration of Eq. (15) and can be given as the complete elliptic integration of the first kind. The former term is the one of the modification of the complete elliptic integral of the second kind. And thus α_0 can be expressed as follows:

$$\alpha_0 = \frac{2}{c^2-a^2}\left[\frac{c}{a^2} \cdot E(e) - \frac{1}{c} \cdot K(e)\right] = \frac{2}{a^2c(c^2-a^2)}[c^2E(e)-a^2K(e)] \tag{17}$$

Putting (16) and (17) into (13), the following will be obtained

$$R_a = \frac{4}{3} \frac{1}{\frac{2}{c} \cdot K(e) + \frac{2}{c(c^2-a^2)}[c^2E(e)-a^2K(e)]} = \frac{2}{3} \frac{c}{K(e) + \frac{1}{c^2-a^2}[c^2E(e)-a^2K(e)]} \tag{18}$$

And the frictional force acting on the disk can be given from equation (12) as:

$$K_a = \frac{4\pi\eta Uc}{\frac{1}{c^2-a^2}[c^2E(e)-a^2K(e)]} \tag{19}$$

In the similar way for the movement in b-axis direction the frictional force K_b can be given as:

$$K_b = \frac{4\pi\eta Uc}{K(e) + \frac{1}{e^2}[K(e)-E(e)]} \tag{20}$$

The molecule on the surface moves quite at random, so frictional force must be averaged statistically for all directions. This can be done approximately by the following relation:

$$\frac{1}{K} = \frac{1}{2K_a} + \frac{1}{2K_b} \tag{21}$$

By putting (19) and (20) into (21), K can be expressed as

$$K = \frac{8\pi\eta Uc}{3K(e)} \tag{22}$$

while, as mentioned above, f_0 can be defined by

$$f_0 = \frac{16\eta r}{3} \tag{23}$$

Now, similarly f can be defined by

$$f = \frac{8\pi\eta c}{3K(e)} \tag{24}$$

This defininition is quite logical, because if the relation $c=a=r$ holds, f reduces to f_0, or when the disk is circular f becomes just equal to f_0.

From (23) and (24) and also by using the relation of

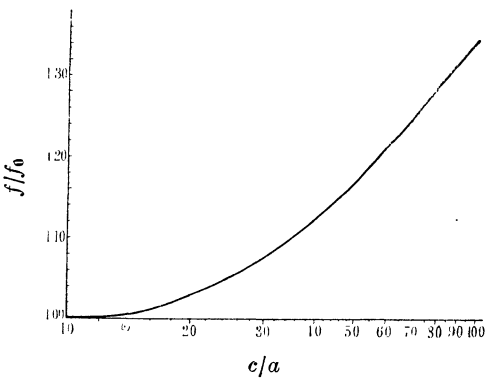

Fig. 1.—Relation between f/f_0 and c/a.

$$ac=r^2$$

the friction ratio is expressed as follows:

$$\frac{f}{f_0}=\frac{\pi}{2K(e)}\cdot\frac{c}{r}=\frac{\pi}{2K(e)}\sqrt{\frac{c}{a}}$$

$$=\frac{\pi}{2K\left(\sqrt{\frac{c^2-a^2}{c^2}}\right)}\cdot\sqrt{\frac{c}{a}} \qquad (25)$$

This shows the relation between f/f_0 and c/a. This relation can be expressed as Fig. 1, and the value of c/a can be derived when the value of f/f_0 is found by the method mentioned above.

Summary

1. The relation between the friction ratio and the surface-diffusion constant has been derived.

2. The relation between the friction ratio and the ratio of two axes of an ellipse has been derived.

3. The relation between f/f_0 and c/a has been shown in a curve which makes the estimation of c/a very simple.

The author wishes to express his best thanks to Prof. Bun-ichi Tamamushi, Prof. San-ichiro Mizushima and Dr. Takehiko Shimanouchi for their kind advice and encouragement. The author also owes much to Professor Isao Imai for helping the hydrodynamical calculation.

Chemical Laboratory, College of General Education, Tokyo University, Tokyo

The Structure of Surface-Denatured Protein. III. Determination of the Shape of Surface-Denatured Horse Serum Albumin

By Kazutomo IMAHORI

(Received July 24, 1951)

In the first paper[1] of this series, the molecular weight and the surface area covered by one protein molecule were reported. In the second paper,[2] theoretical treatment on the relation between the shape of the protein molecule and the surface diffusion constant has been given.

In the present paper, the method of calculating the surface-diffusion constant from the measurement of surface potential as well as its result will be reported.

Apparatus of Surface Potential Measurement

There are two methods of measurement of surface potential. One is the so-called vibrating plate method,[3] by Zisman, and the other is the ionization method adopted by Rideal and others.[4] Recently, several chemists in this country have constructed the apparatus which in all cases is of the former type. The present author has constructed one of the latter type, principally because the latter type is superior to the former in the experiment of surface diffusion, as the electrode of the latter type is so thin that the surface potential can be measured from point precisely. The apparatus is shown in Fig. 1.

In the figure, T is the trough, filled with water, upon which the protein film under investigation is spread. The trough is held on a bakelite stand, which is insulated from the earth electrically. The potential of T can be varied by potentiometer P, which is connected with T through caromel cell C and salt junction J. A is an air electrode —made of platinum wire of about 1 mm. diameter and coated with polonium. The polonium ionizes the air between A and T and conncets A electrically with the top of the surface film. A is supported by a pyrex glass bar which is fixed on a steel stand and can be freely moved vertically and horizontally. U is a vaccum tube, UX 54 made by the Tokyo Shibaura Electric Co. Ltd., which has a very large grid resistance ($10^{10}\Omega$). The filament current is 200 mA. R_1, R_2 and R_3 are all variable resistances of 25 Ω. R_0 and R_0' are also variable resistances of 500 kΩ and 100 Ω respectively. R_g is also a variable resistance, the value of which is just equal to the critical damping

(1) K. Imahori, This Bulletin, **25**, 7 (1952).
(2) K. Imahori, This Bulletin, **25**, 10 (1952).
(3) W. A. Zisman, *Rev. Sci. Instr.*, **3**, 367 (1932).
(4) J. E. Schulman and E. K. Rideal, *Proc. Roy. Soc.*, **130, A**, 259 (1931).

reistance of the galvanometer used, and equal to 1 kΩ in the present case.

R_a anc R_b are fixed resistances of 20 kΩ and 1 kΩ respectively. I_f is a milliammeter having a scale up to 500 mA. and G a galvanometer, sensitivity of which is about 2×10^{-8} A. The apparatus must be completely shielded electrically. The operation of this apparatus is as follows.

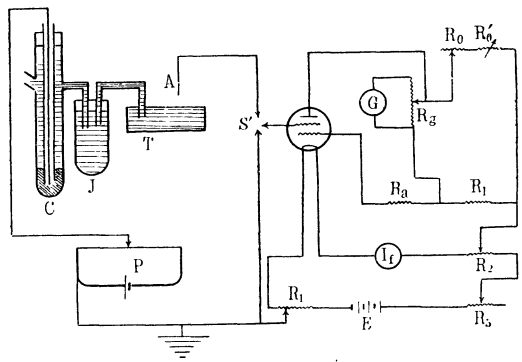

Fig. 1.—Apparatus for measuring the surface potential.

First the switch S in Fig. 1 is put downward and the grid is earthed. By adjusting R_0 and R_0', the needle of G is set to its zero point. Then A is brought about 1~2 mm. above the cleaned surface of the water contained in the trough T. S is switched upward and A is connected to the grid. The needle of the G moves then far from zero point and it is brought back again to near zero point by adjusting P. Now, S is put downward, then upward again and P is adjusted and this operation is repeated several times until the needle of G does not move by this operation. The value, which P indicates, is just equal to the contact potential between A and the water surface and can be expressed by V_1.

Then monomolecular film of protein is put on the water surface. The contact potential between A and water carrying the protein film can be measured by the similar way and is expressed as V_2. The surface potential ΔV of the protein film is equal to the difference of V_2 and V_1, or

$$\Delta V = V_2 - V_1.$$

The Relation between Concentration and Surface Potential

In the experiment of the surface diffusion constant, it is needful to measure the concentration of protein on the surface. There are probably only a few ways to measure this concentration. The present author has done this from the measurement of surface potential, because, in the region of low concentration, surface potential is thought to be proportional to surface concentration. This can be ascertained from the following experiments. The curve V_P in Fig, 2 shows the relation between the surface potential and the surface cencentration of serum albumin, while the curve F_P shows the relation between the surface pressure and the surface concentration. From these two curves it becomes evident that the surface potential is proportional to the surface concentration in the region of concentration below 0.1 mg./m.^{2} or in the region of surface pressure below 0.05 dyne/cm. Similarly, curves V_c and F_c show that the surface potential of castor oil monolayer is proportional to the surface concentration in the region of surface pressure below 0.5 dyne/cm.

When the mixed film of castor oil and protein monolayer is expanded on the surface, the surface potential varies according to the curve V_m in Fig. 2, where the amount of protein used is constant——2.085×10^{-7} g., while the amount of castor oil is varied.

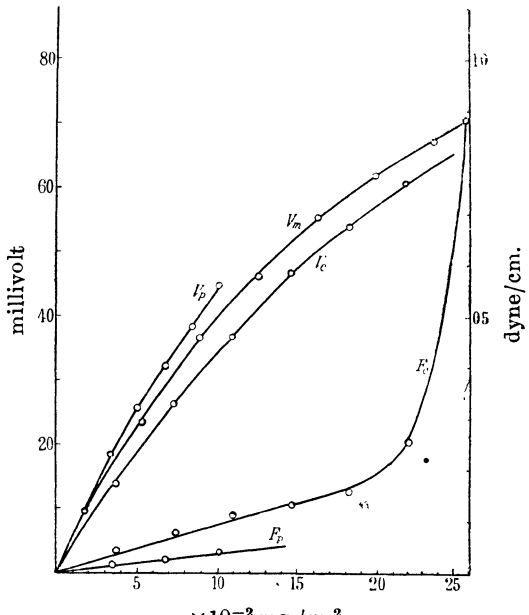

$\times10^{-2}$ mg./m.^{2}

Fig. 2.

From this curve it is also evident that the surface potential of the mixed film becomes just the sum of two partial surface potentials, namely, the surface potentials of two components expanded on the same surface area, each alone respectively. This shows that there is very little interaction between molecules of protein and castor oil on the surface, under very low surface pressure.

Mesurement of the Surface Diffusion Constant

As is shown in Fig. 1, a tray of 60 cm. long,

20cm. broad, and 4cm. deep, is filled with distilled water or other aqueous substrates. The surface of the water is cleaned with a moving barrier (M and M′ in Fig. 3) and then is divided into two

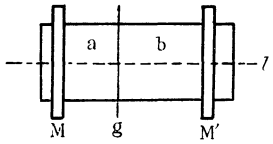

Fig. 3.

parts by a very thin glass rod (g), which is so thin and so light that it can be pushed away by even the slightest surface pressure. The contact potential V_1 of the water surface and the electrode is measured by the apparatus mentioned above. Serum albumin solution in water of 0.0209% concentration is put on one side (side a), of the water surfece, from a micrometer syringe, which makes the gaseous film of serum albumin, and the rod g is pushed to the other side (side b). The sample of serum albumin is just the same as that used in the first paper of this work.

Then a few drops of very dilute benzene (or ethylether) solution of castor oil are put on both sides of the rod until the surface pressures of the both sides balance with each other and the rod g comes to an equilibrium position. The balanced surface pressure must be less than 0.5 dyne/cm.

The air electrode A is carried along the line l of Fig. 3. The surface potential along l can be

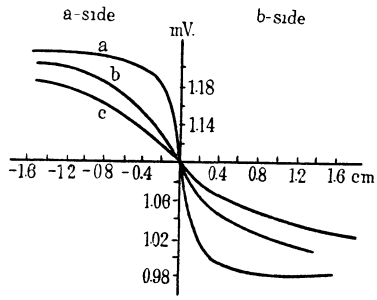

Fig. 4.—Surface potential curve.

shown schematically as the curve a in Fig. 4, in which the abscissa shows the the distance along l. The zero point corresponds with the point where the glass rod crosses the line l. The glass rod must be kept perpendicular to l.

Now, the glass rod is taken away from the water surface and the protein begins to diffuse into the b-side. If, however, castor oil had not been put on the b-side, the protein molecule would flow on the water surface just as a gas flows from a vessel of higher pressure into one of lower pressure, and soon all the surface will be covered by a homogeneous protein film. The velocity of such flow would not mean the true surface diffusion velocity. To avoid the error from this flow movement, some substance (such as castor oil) is put on the b-side so as to balance the surface pressures of both sides. And thus, the net diffusion constant on the surface can be determined.

As time elapses, the surface potential gradient at zero point becomes gradually less and less just as is shown schematically by the curves b and c in Fig. 4.

As is cited above, the experiment is carried out at low surface pressure, and under this condition the potential gradients at various points are proportional to the gradients of the concentration of protein molecules, just as is shown in the above section. The surface potential along l after 24 hours of diffusion is shown in Fig. 5 and the gradients at various points of this curve are shown in Fig. 6. The measurement can be carried out within the error of 0.5 mV.

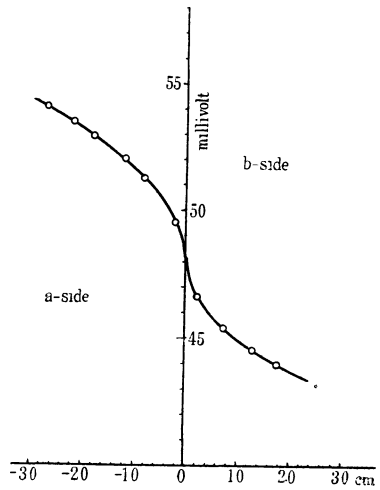

Fig. 5.

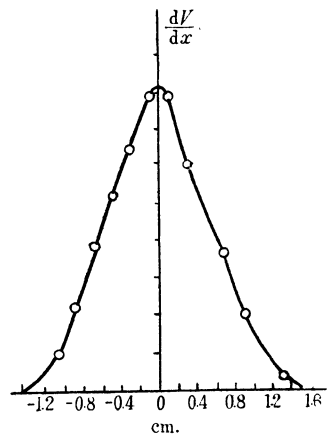

Fig. 6.—Surface potential gradient.

The curve in Fig. 6 also represents the gradients of the concentration of protein on

the surface at various points, so that, just as in the case of three-dimensional diffusion, the diffusion constant can be calculated by the inflection point method. If the distance from the zero point to the inflection point is expressed as μ and the time elapsed from the initiation of the diffusion to the measurement is expressed by t, the diffusion constant can be given as

$$D=\frac{\mu^2}{2t} \qquad (1)$$

From Fig. 6 and Eq. (1), and also by using the data of $\mu=0.14$ cm., D is calculated to be 1.1×10^{-6} cm.^{2}/sec. By putting this value into Eq. (11) given in the second report of this investigation,

$$M=\frac{9dR^2T^2}{256\eta^2ND^2}(f_0/f)^2$$

and also by using the data, V (reciprocal of the density of protein) $=0.748$,[5] d (thickness of the film) $=10$ Å.,[6] M (molecular weight of protein) $=70{,}400$,[1] f/f_0 (friction ratio) is given as 1.28. Using the relation shown in Fig. 1 of the same report mentioned above, the ratio of two axes turns out to be 8.0.

As was shown in the first report, the surface area covered by one serum albumin molecule is 9800 Å.^{2} and thus the length of the two axes are calculated as: $a=20$ Å. and $c=160$ Å. Therefore, the shape of the surface-denatured serum albumin molecule will be schematically expressed as in Fig. 7.

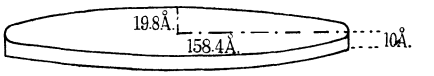

Fig. 7.—Shape of the surface-denatured serum albumin molecule.

(5) T. Svedberg, "Ultracentrifuge," 1940.
(6) K. Imahori and Y. Yoneyama, unpublished.

Summary

1. The apparatus for measuring surface potential by the so-called ionization method has been described.

2. The relation between the surface potential and concentration of serum albumin and castor oil monolayers have been obtained.

3. The method for determining the shape of surface-denatured protein molecules has been described. This can be carried out on the grounds of the determination of surface-diffusion constant by the surface potential measurement.

4. The shape of horse serum albumin has been decided to be an elliptic disk having the value of $a=20$ Å., $c=160$ Å. and thickness of 10 Å.

The author wishes to express his hearty thanks to Prof. Henry B. Bull, Prof. Bun-ichi Tamamushi, Prof. San-ichiro Mizushima and Dr. Takehiko Shimanouchi for their kind encouragement and advice. Thir experiment is aided by a Grant in sid for Fundamental Scientific Research defrayed from the Ministry of Education.

Chemical Laboratory, College of General Education, University of Tokyo, Tokyo

Synthesis of 2-Amino-4-methyl-5-cyanothiazole from Acetonitrile

By Kiku MURATA

(Received August 14, 1951)

For the purpose of obtaining 2-amino-4-methyl-5-aminometylthiazole (VII) which is presumed as the substance to be produced by reduction of 2-(*p*-acetylphenylazo)-4-methyl-5-(*p*-acetylphenylazomethyl)-thiazole (VI) believed[1),2),3)] to be an azo-color from thiamine as shown in Schema 2, a new thiazole, 2-amino-4-methyl-5-cyanothiazole (V) was synthesized from acetonitrile (I) according to the processes shown in Schema 1,

(1) K. Murata, *J. Chem. Soc. Japan*, **64**, 1379 (1943).
(2) K. Murata, *J. Chem. Soc. Japan*, **66**, 57 (1945).
(3) K. Murata, *J. Chem. Soc. Japan*, **66**, 59 (1945).

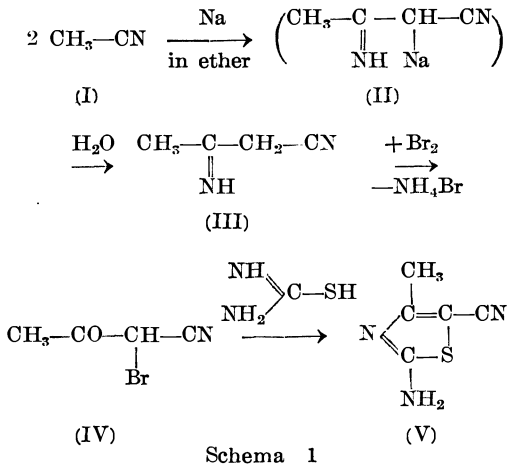

Schema 1

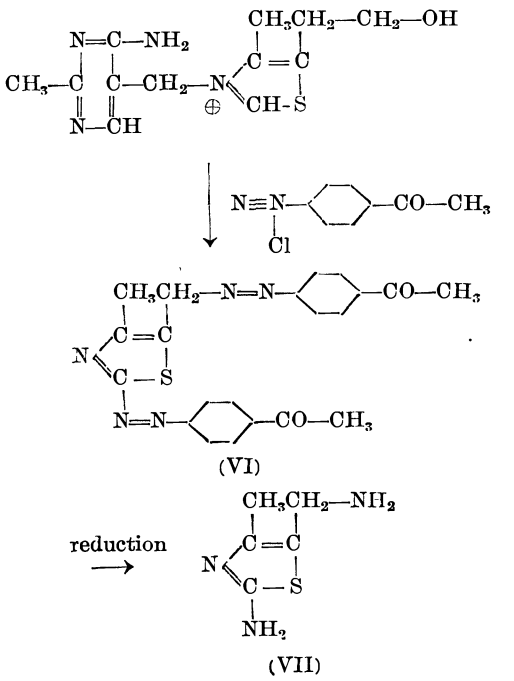

Schema 2

Catalytic reduction of 2-amino-4-methyl-5-cyanothiazole (V) is being carried on now under several conditions, but it is not yet completed, so the synthesis of this thiazole (V) is reported here.

Experimental

(1) β-Iminobutyronitrile (III).—The preparation of this substance was carried out according to Hortzwart[4]. A three-necked flask of 500 cc. content, equipped with a sealed stirrer, dropping funnel and reflux condenser under the protection of the moisture was used. Metallic sodium (8 g.) in small pieces were put in 300 cc. of absolute ether in the flask, and 25 g. of pure acetonitrile were gradually added with thorough stirring. After all of the metal had dissolved, the flask was warmed for 1 hour at 40° on a water-bath. The precipitates were separated from ether. The crude precipitates (30 g.) presumed as sodio-β-iminobutyronitrile (II) were dissolved in a little water (*ca.* 10 cc.), to which 50 cc. of ether were added and boiled on the water-bath or shaken with ether and water. Then the ether solution was evaporated to one third of its original volume. β-Iminobutyronitrile crystallized from ether after standing for 2 or 3 days in the ice chest. The crude crystals (m. p. 47—65°) (1 g.) were receystallized from benzene at room temperature. The stable form[4],[5]. (m. p. 47—48°) was obtained as crystals soluble in benzene and the labile form[6] (m. p. 74—78°) was obtained from the insoluble part, in yields of 0.3 g. and 0.1 g. respectively. When 4 g. of crystals, m. p. 47—80°, were boiled with benzene for 30 min. on the water-bath, the crystals, m. p. 46—60°, was obtained. When this crystal was boiled again in benzene, the crystals, m. p. 47—48°, separated out in a yield of 0.3 g.

Both specimens, m. p. 47—48° and 46—60°, gave the oxime, m. p. 98—100° (Found: C, 49.26; H, 6.45%) and the semicarbazone, m. p. 159—160° (Found: C, 42.97; H, 6.05%) of β-iminobutyronitrile as described in the literature[7].

(2) α-Bromo-β-ketobutyronitrile (IV).—Nineteen g. of bromine, *i. e.* theoretical amount, were dissolved in 200 cc. of ether and the solution was dropped into 400 cc. of ether solution containing 10 g. of β-iminobutyronitrile (m. p. 47—65° or 50—70°) cooled in an ice bath. The excess of bromine in the ether solution was removed by the treatment with aqueous solution of sodium bisulfite, and the solution was dried with sodium sulfate and evaporated. The resulting oil was separated from ammonium bromide and destilled in vacuum. α-Bromo-β-ketobutyronitrile, b. p. 70—73°/4 mm., was obtained in a yield of about 60% (Found; C, 29.94; H, 2.93%. Calcd. for $C_4H_4ON\,Br$: C, 29.64; H 2.47%.) The ammonium bromide recovered amounted to 70% of the theory.

(3) 2-Amino-4-methyl-5-cyanothiazole (V).—When the theoretical amount of powdered thiourea was mixed with α-bromo-β-ketobutyronitrile in water solution and warmed on the water-bath at 80°, the reaction went on gradually. The whole was allowed to stand overnight, and then dissolved in 10 cc. of water. After removing the unreacted substances by ether, the aqueous solution was fitlered and 2 *N* alkali solution (about 15 cc.) was added to the filtrate until *p*H 6.8. The precipitated substance was collected. The

(4) A. Holtzwart, *J. prakt. Chem.*, (2) **39**, 230 (1889).

(5) E. Meyer, *J. prakt. Chem.*, (2) **52**, 84 (1895).

(6) E. Meyer, *J. prakt. Chem.*, (2) **52**, 83 (1895).

(7) E. Meyer, *J. prakt. Chem.*, (2) **78**, 504 (1908).

crystallization from water gave 2-amino-4-methyl-5-cyanothiazole, colorless needles, m. p. 164—166°, easily soluble in benzene, alcohol and hot water, 50% yield. (Found: C, 43.40; H 3.95%. Calcd. for $C_5H_5N_3S$: C, 43.17; H 3.53%.)

Summary

A new thiazole, 2-amino-4-methyl-5-cyanothiazole (V) m. p. 164—166° was synthesized from thiourea and α-bromo-β-ketobutyronitrile (IV), b. p. 70—73°/4 mm., prepared by the action of bromine on β-iminobutyronitrile obtained from acetonitrile.

The author wishes to express her sincere thanks to Dr. Matsukawa of Takeda Institute who kindly helped her in this research. Thanks are also due to Mr. Ikehata who has assisted her during the experiments, and to Dr. Chachin of this Research Institute for his support in executing this work. The cost of this research has been partly defrayed from the Ministry of Education, to which the author's thanks are due.

Osaka Municipal Institute for Hygiene, Osaka

On the Properties of 1-Thiol-benzthiazole Derivatives as Photographic Addition Agents

By Yasushi OH-YAMA

(Received August 16, 1951)

Introduction

Previously the author reported several times about the derivatives of 2-mercapto-benzimidazole as addition agents for photographic emulsions and developers.[1],[2],[3],[4]

In this connection he has been examining from that time the probabilities or the properties as additions of 1-thiol-benzthiazole, usually called 2-mercapto-benzthiazole, intimately related compound of the above mentioned, and soon the practical importance of this compound in photography has been recognized.

It is interesting to know that the usefulness of this compound has been recently disclosed in other countries.[5],[6]

The author's intention, being interrupted with the short supply of materials during the war, to prepare and examine those derivatives of it, as were derived of 2-mercapto-benzimidazole, is now attained.

In this report, properties of two kinds of alkyl (and aralkyl) derivatives of this compound are described as additions in developer for pure silver chloride emulsion and as additions in emulsion for chloride and chloro-bromide emulsions and compared with similar derivatives of mercapto-benzimidazole already reported.

Relation between S-Alkyl- and N-Alkyl-derivatives

1-Thiol-benzthiazole is a single substance having two tautomeric configurations by proton transfer as shown below,

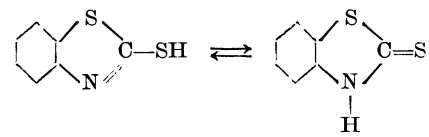

but those compounds, in which this replaceable hydrogen atom is substituted by alkyl (or aralkyl) radical, form two distinct compounds, S-alkyl-derivatives (I) and N-alkyl-derivatives (II), each must be called 1-alkylthio-benzthiazole (I) and 1-thio-2-alkyl-1:2-dihydro-benzthiazole (II), and it is not easy to convert one to the other.

Generally (II) is more stable than its corresponding compound of (I), and (I) can be converted to (II) through its quaternary ammonium salt

(1) Yasushi Oh-yama, *Bull. Inst. Phys. Chem. Research (in Japanese)*, **22**, 483 (1943).
(2) Yasushi Oh-yama, *ibid.*, **23**, Chem.-7 (1944).
(3) Yasushi Oh-yama, *J. Soc. Scientific Photography Japan (in Japanese)*, **9**, 1 (1943).
(4) Yasushi Oh-yama, *ibid.*, **9**, 57 (1943).
(5) A. Bycichin and L. Vlach, *Chem. Listy*, **41**, 136; *Sci. Ind. Phot.*, **18**, 33; *C. A.* **42**, 1518 (1948).
(6) W. H. Dimsdale and R. R. Robinson (Ilford Ltd.), U. S. P. 2, 432, 864; U. S. P. 2, 432, 865.

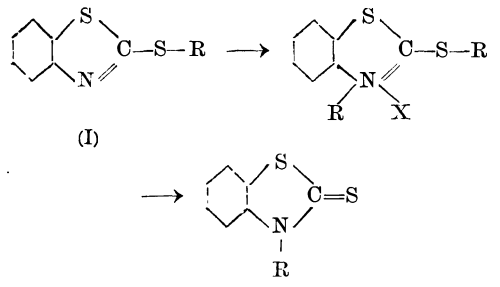

(I)

(II)

or by other means. And it is also possible to change its alkyl radical on this occasion.[7]~[10]

Experimental

In homologues of S-alkylthio-benzthiazole (I), methyl, ethyl, allyl, benzyl and carboxymethyl-derivatives, and in those of N-alkyl-compounds (II), methyl, ethyl, allyl[11] and benzyl derivatives were prepared and tested.

The similar S-alkyl-derivatives (III) of mercapto-benzimidazole

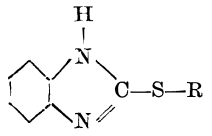

(III)

(*i. e.*, 2-thiol-benzimidazole), which were previously reported[1],[3], were tested in comparison with these compounds.

Strips of specially made gaslight paper which was coated with pure silver chloride-gelatin emulsion, were exposed at a fixed condition under optical wedge, developed 1 min. at 20°C., in an ordinary developer containing metol, hydroquinone, sodium sulphite, sodium carbonate but not potassium bromide and finally added varied amounts of above mentioned compounds dissolved in methanol (0.1~1%).

The relation between the time of appearance of images, the fog, the tone of images and the amount of substances added were examined.

The emulsion tests of these compounds were also carried out in some case of gaslight and chloro-bromide emulsions.

Results

Results of above experiments were illustrated in Fig. 1, Fig. 2 and Table 1:

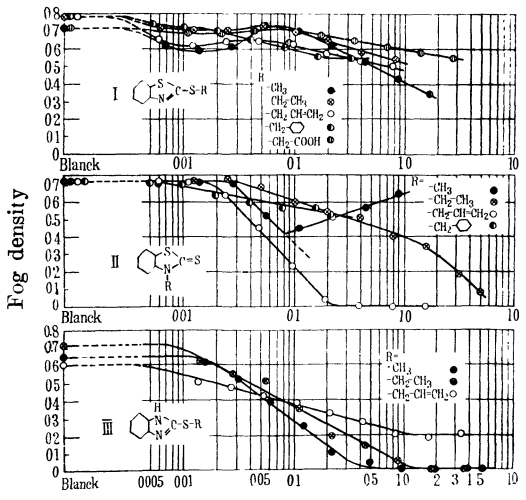

Fig. 1.—Relation between fog-density and concentration of addition in developer.

Table 1

Blue-black Developing Property of Derivatives of 1-Thiol-benzthiazole and 2-Thiol-benzimidazole

Substance added in developer	Minimum conc. to produce appreciable effect	Concentration to produce maximum effect	Bluishness of tone
1-Methylthio-denzthiazole	0.027< C <0.055	0.44 (approx.)	+
1-Ethylthio- 〃	0.025< C <0.051	0.20~0.40	+
1-Allylthio- 〃	0.024 (approx.)	0.39 (approx.)	++
1-Benzylthio- 〃	0.32 (approx.)	?	very weak
1-Thio-2-methyl-1:2-dehydro-benzthiazole	0.027< C <0.055	0.44 (approx.)	++++
1-Thio-2-ethyl-1:2- 〃	1.60< C <3.20	?	++
1-Thio-2-allyl-1:2- 〃	0.006< C <0.012	0.77 (approx.)	+++
1-Thio-2-benzyl-1:2- 〃	0.08 (approx.)	0.16 (〃)	very weak
2-Methylthio-benzimidazole	0.015< C <0.030	0.48 (approx.)	+
2-Ethylthio- 〃	C <0.014	0.45 (〃)	+
2-Allylthio- 〃	C <0.013	0.42 (〃)	+++

(7) C. Hasan and R. F. Hunter, *J. Chem. Soc.*, **1936**, 1672.
(8) J. D. Kendall (Ilford Ltd.), F. P. 821, 980; B. P. 475, 647.
(9) W. A. Sexton, *J. Chem. Soc.*, **1939**, 470.
(10) F. P. Reed, A. Robertson and W. A. Sexton, *J. Chem. Soc.*; **1939**, 473.
(11) Melting point of this compound (1-thio-2-allyl-1:2-dihydro-benzthiazole) is 66.5~67.0°C.

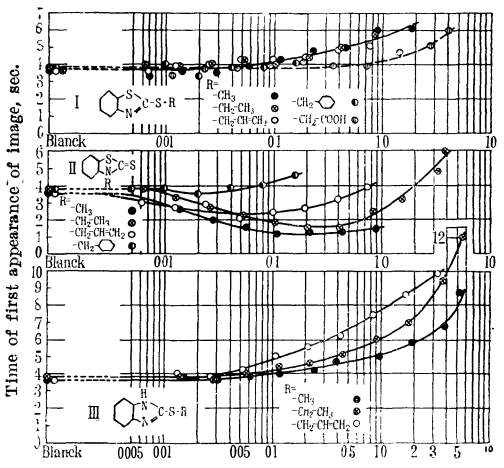

Fig. 2.—Relation between time of first appearance of image and concentration of addition.

Behaviors of these additions when added in emulsion, though these tests were not carried out systematically, keep parallel with those tendency they presented when added in developer. And it would be able to conclude as follows.

(A) Anti-fogging or Fogging Properties.—All of these compounds have fog-preventing or fog reducing property. Generally most of N-alkyl compounds (II) of 1-thiol-benzthiazole surpass even the marked fog-preventing property of any of the S-alkyl derivatives of 2-thiol-benzimidazole (III), on the contrary the S-alkylthio-benzthiazole (I) are inferior compared with the above mentioned and almost equal with its parent substance (1-thiol-benzthiazole).

The only exception is the methyl derivative of (II), which exhibits fog-preventing property at low concentration in developer and causes a considerable degree of fog at high concentration, and this tendency can also be seen when added in emulsion. The emulsion which contains such an amount of it that restrains fog when prepared, sometimes becomes heavily fogged during the storage or incubation test.

The ethyl or allyl derivative of (II) is not only good as a fog-reducer in developer, but can give the emulsions of very good durability. Similarly the benzyl derivative which cannot exhibit a noticeable effect in developer owing to its low solubility, can restrain fog and increase durability when added in emulsion.

(B) Blue-black-developing Property.—The tone or color of the developed silver image of chloride or chloro-bromide emulsion turns from neutral black or warm-black to blue-black, when most of these derivatives (I, II and III) are added in developer or in emulsion, and this property cannot be seen in their parent substances.

This tendency differs according to the substituents, in (I) and (III) it grows stronger when the alkyl radical is replaced by methyl, ethyl, allyl in turns, but benzyl derivatives of these are very weak probably because of their low solubility, and carboxymethyl ($-CH_2-COOH$) derivatives show no effect.

On the contrary N-methyl, ethyl and allyl derivatives (II) of this dihydro-benzthiazole show equally very strong blue-black developing effect, even the benzyl derivative of it, being very weak in developer, shows fairly good effect when added in emulsion.

(C) Development Accelerating or Retarding Property and Sensitizing or Desensitizing Effect.—Derivatives of (I) and (III) series retard development more or less, and derivatives of (II) series, to the contrary, accelerate it.

Plotting the time of first appearance of image against the concentration in developer of these additions (Fig. 2), it shows characteristic curves for each series (I, II and III) and in series (II) and (III) their effects differ regularly according to the number of carbon atoms in the substituted alkyl radical *e. g.*, methyl, ethyl, allyl, benzyl in turns, while in series (I) they bear no evidence of this difference except the carboxymethyl derivative.

The sensitizing and desensitizing properties of them in emulsions run parallel with their development accelerating and retarding properties, (II) has somewhat sensitizing property for silver chloride emulsion as one of the thions which Kendall[12] already pointed out, and derivatives of series (I) and (III) show rather desensitizing effect but not noticeable in ordinary case.

Discussion

The similarity of actions of (I) and (III) lies in parallel with the resemblance of their constitution, and it is supposed to be attributable to the imino group in the imidazole ring of (III) that it exceeds (I) in fog-preventing property and development retardation.

It is recognized from blue-black developing property of these three series, that the imino radical gives scarcely any effect upon this property and the relation between this property and development retardation is not basic.

The considerable difference between(I)and(II),

(12) J. D. Kendall, IXth. Cong. Phot. 1935, Paris, 235.

which is the influence of the same substituent in different positions of the molecule, is supposed mainly to be attributable to the change of the constitution of the sulfur atom of thio-ether type to more reactive thio-keto type.

It is easy to point out this thio-keto radical as the cause of sensitizing, development-accelerating or fog-preventing property of (II).

The sulfur atom of this radical forms complex with silver or silver salts and the stability, the solubility, the rate of decomposition or the delicate combination of those character of this complex compound will be the cause of complicated, sometimes contradictory behavior of these compounds as additions. The behavior of methyl derivative of the series (II) surely indicate the lack of this stability of the complex compound between the said derivative and silver chloride.

Summary

S-Alkyl-(I) and N-alkyl-derivatives (II) of 1-thiol-benzthiazole are prepared and tested as additions for silver chloride emulsions, and compared with previously reported S-alkyl-derivatives (III) of 2-thiol-benzimidazole. Properties of these substances as additions may differ according to alkyl radicals substituted, positions of substitution and their parent substances.

(1) Most of these compounds (I, II and III) show blue-black developing property which can not be seen in parent substances. This effect is the weakest in (I) and the strongest in (II), and as a whole, being the substituent methyl, ethyl or allyl, its activity rises in turn. Benzyl derivatives of them are almost inactive and carboxymethyl derivatives of (I) and (III) are inactive.

(2) As for the fog-preventing property, (II) and (III) have greater activity and increase activity as the number of carbon atoms in the substituent increases. (I) is not so active as (II) or (III) regardless of its substituents.

(3) It is remrakable that (II) has somewhat sensitizing property added in emulsion, and accelerate the development when both (I) and (III) retard it.

(4) The similarity of actions of (I) and (III) lies in parallel with the resemblance of their chemical constitution, but (I) is inferior to (III) in those properties which are supposed to be due to the imino group in the imidazole ring, as fog-preventing action.

(5) The considerable difference between (I) and (II) which is the influence of the same substituent in different position of the molecule, is supposed to be attributable to the change of the constitution of the sulfur atom of thio-ether type to more reactive thio-keto type. The sensitizing, fog-preventing or development-accelerating action of the latter is supposed to be intimately related to the complex forming character of this thio-keto group with silver or silver salts.

Research Section, Kyoto Factory,
Mitsubishi Paper Mills Co.,
Kyoto

On the Nature of Built-up Film. I. Adsorption of Ion on Built-up Film of Stearic Acid

By Mitsuo MURAMATSU and Tunetaka SASAKI

(Received September 3, 1951)

Introduction

It has been shown by several investigators that the heavy metallic ions exhibit remarkable effects on the surface properties of monolayer of fatty acid spread on water[1] or multilayer transferred onto a solid surface.[2],[3] That the built-up film of fatty acid on solid shows a high wettability when conditioned with the solution containing polyvalent ion, such as aluminum,[4] thorium,[5] or uranyl ion,[6] and that the protein molecules can be adsorbed on such a conditioned surface also suggest a special action of heavy metallic ion on fatty acid.

(1) I. Langmuir and V. J Schaefer, *J. Am. Chem. Soc.*, **58**, 284 (1936); **59**, 2400 (1937).
(2) K. B. Blodgett, *J. Phys. Chem.*, **41**, 975 (1937); K. B. Blodgett and I. Langmuir, *Phys. Rev.*, **51**, 964 (1937).
(3) I. Langmuir, "Recent Advances in Surface Chemistry and Chemical Physics", Science Press Printing Co., Lancaster, 1939, p. 1.
(4) I. Langmuir and V. J. Schaefer, *J. Am. Chem. Soc.*, **59**, 1406 (1937).
(5) I. Langmuir and V. J. Schaefer, *J. Am. Chem. Soc.*, **59**, 1762 (1937); **60**, 135 (1938).
(6) G. H. A. Clowes, "Recent Advances in Surface Chemistry and Chemical Physics," Science Press Printing Co., Lancaster, 1939, p. 61.

The experimental data, presented by Clowes[6], which showed that the built-up film adsorbed a maximum amount of protein when it was conditioned with the aqueous uranyl salt solution at *p*H 6.0~6.5, lead us further to the presumption that the metallic ion requires an optimum *p*H range for the adsorption. If we adopt the opinion of Kraus and Nelson, [7] insisting rather a complex nature of uranyl ion in aqueous solution, its adsorption may naturally be of a more complex nature than it appears. The present authors have also intended to study the action of polyvalent ion for the built-up film of stearic acid, concerning such a problem.

Experimental

a. Material.—Stearic acid used was Merck's pure chemical reagent. Barium, aluminum, and mercuric chlorides, copper sulfate, and thorium nitrate were recrystallized repeatedly. Substrate water was made pure enough so as no impurity could be detected from the detail of the pressure~area curve obtained for monolayers of fatty acid spread on it.

b. Method.—Most of the experiments were carried out in the temperature range of 23~28°C., in which, however, the monolayer of stearic acid on mere distilled water tends to expand when the pressure of the piston oil is too low, and collapses when it is high[6]. Since the collapsing effect readily appears (2 min. after the spreading), the echelon consisting of pure stearic acid could hardly be prepared while the monolayer on water is stable. For this reason, the following procedure was adopted. The highly polished stainless steel slide, on which a mixed multilayer of stearic acid and barium stearate was deposited, was immersed in *N*/100 hydrochloric acid in order to convert barium stearate to free fatty acid[9], and this converted layer was covered with a few layers of stearic acid by means of an ordinary technique. Thus, barium stearate could be converted to free acid in the depth of several layers at temperature above 25°C.

To minimize the accidental experimental error, a half part of the slide (called the treated side hereafter) was dipped in a solution containing metallic ion, and the other half (the control side) in a control solution. An apparent increase in thickness due to the adsorption was then determined by means of the optical interference method[10], assuming that the spacing and refractive index of barium stearate are 24.4 Å. per layer and 1.462 respectively[6]. The number of equivalent layers on which the ions were supposed to be compactly adsorbed was determined by the skeletonization with benzene.

The *p*H of the solution was adjusted simply by redistilled hydrochloric acid and aqueous ammonia solution when required.

Experimental Results and Discussion

a. Effect of Acid and Alkali.—When the echelon was treated with various kinds of acid or alkali solutions, an appreciable change in composition generally occurred, frequently the change reaching several layers in the depth. For instance, when the echelon was treated with solution of *p*H<2 for 30 sec., the thickness of echelon decreased, indicating presumably the conversion of barium stearate underneath into free acid. A more remarkable decrease appeared in a strong alkaline region. After treating the control side of the echelon with acid solution of *p*H=2 and the other half with that of varying *p*H, the difference in thickness between both echelons was measured as shown in Table 1. These changes may be ascribed to the dissolution of stearate ion into the bulk of solution.

Table 1

Change in Thickness of Echelon Treated by Acid or Alkali

*p*H	2.0	3.2	3.9	5.0	6.6
Change in thickness, Å.	control	0.0	−0.1	−0.8	−0.3
*p*H	7.3	8.3	8.8	9.0	9.4	9.8
Change in thickness, Å.	+0.4	+0.5	−5.2	−6.8	−34.3	−32.9

b. Adsorption of Various Ions. — The amounts of the adsorption of barium, mercuric, cupric, aluminum, and thorium ions from 10^{-4} mol/l. aqueous solutions of varying *p*H were determined and shown in Fig. 1, where the abscissa denoted *p*H and the ordinate, the amount of adsorption expressed by the difference in thickness (in Å.) between the treated and the control sides of a slide. The figure shows that there exists an optimum *p*H range of adsorption for each metallic ion. The adsorption is usually not remarkable in other region of *p*H, presumably due to the decrease in the concentration either of metallic ion in the solution or of stearate ion on the surface. It can therefore be expected that the optimum range of *p*H for the adsorption depends on the nature of metallic ion concerned.

The apparent increment in the ordinate in Fig. 1 at *p*H exceeding 9 may be accounted

(7) K. A. Kraus and F. Nelson, *J. Am. Chem. Soc.*, **71**, 2510, 2517 (1949).
(8) K. B. Blodgett, *J. Am. Chem. Soc.*, **57**, 1007 (1935).
(9) A. Rothen, *J. Am. Chem. Soc.*, **70**, 2732 (1948).
(10) T. Tachibana, *Seikagaku* (*Biochemistry*, in Japanese), **20**, 8 (1948).

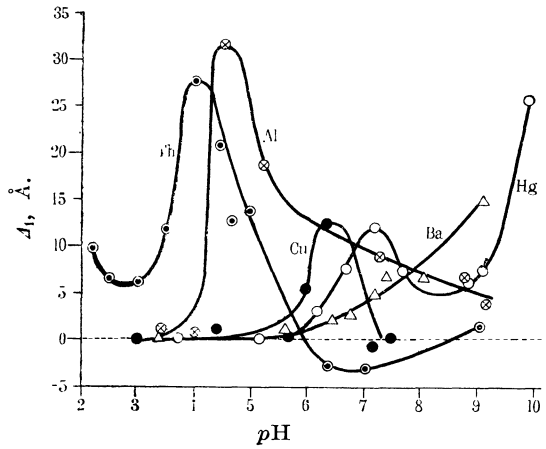

Fig. 1.—Apparent increase (Δ_1) in thickness due to adsorption.

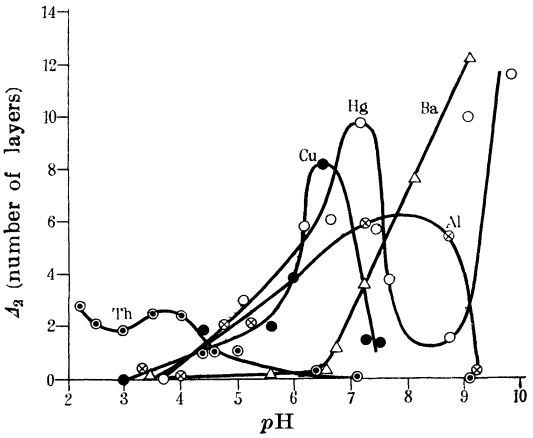

Fig. 2.—Apparent difference (Δ_2) in thickness between treated and control sides of echelon after skeletonization, taking the thickness of barium stearate monolayer as unit.

for by the dissolution of stearate molecules in the multilayers of the control side into the bulk of solution as shown in Table 1, and not by the increase in thickness on the treated side; practically a remarkable decrease was seen on the control side with increasing time of soaking, while only a little increment was observed on the treated side. Barium ion, and perhaps some other ions such as mercuric ion, when they were adsorbed on multilayers, showed a protecting effect against its dissolution into the alkaline medium, just as the effect of these ions on the monolayer spread on water[11].

c. Skeletonization of Adsorbed Layers. —The echelon treated as mentioned above was immersed into benzene for thirty seconds. This procedure brought a very striking difference in thickness between the control and the treated sides. It may be accounted for by the difference in resistance to the dissolution due to the presence of metallic soap on the treated side. Thus the amount of stearic acid which took part in the formation of metallic soap could be estimated by assuming that the metal stearate was practically insoluble in benzene, and that its structure in the multilayer could be preserved after skeletonization. Though it was doubtful whether the experimental conditions were good enough to allow these assumptions, the numbers of stearic acid layers taking part in the adsorption are roughly calculated as shown in Fig. 2. Judging from Figs. 1 and 2, it can be said that the increase in thickness due to the adsorption is rather pronounced in the case of a relatively few position of anchorage for the adsorbing ion. The ratio of the ordinate (Δ_1) of Fig. 1 to that (Δ_2) of Fig. 2 was calculated and illustrated in Fig. 3. This ratio is roughly

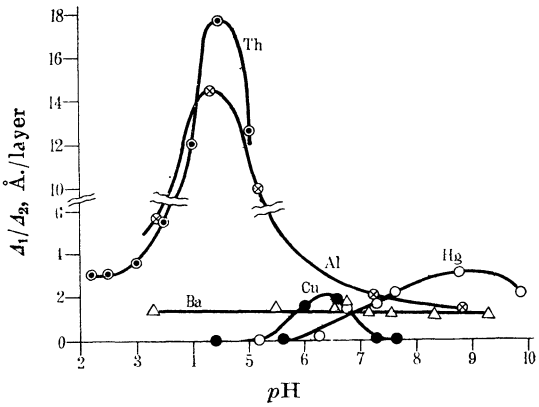

Fig. 3.—Adsorbed amount of ions per layer at various *p*H.

considered to be the increase in thickness when a stearic acid monolayer is completely changed to metallic soap, and a very specific nature of individual metallic ions can be seen in this figure. Thus, the adsorption of barium ion caused, irrespective of *p*H, the increment of 1.7 Å. in thickness, which was in a good agreement with that expected from the known spacing of stearic acid and barium stearate, whilst cupric and mercuric ions showed a maximum value of thickness in a specific *p*H range. It may be added further that one of the above mentioned assumptions could be valid for these three ions, namely, by contacting with vapor of *n*-octane, the

(11) T. Sasaki and R. Matuura, This Bulletin, **24**, 274 (1951).

skeletonized echelon almost restored the original thickness which it possessed before soaked into benzene.

On the other hand, the values of aluminum and thorium offered a question concerning the limit of the validity of skeletonization. The adsorbed amount per layer shown in Fig. 3 would be too large when compared with the adsorbed amounts of these ions on the multilayers of barium stearate[4),(5)] where it could be considered that the adsorption below a layer did not take place.[12] From the experience of the present authors, it seemed impossible to exceed 3 and 5 Å. in any case for alumiuum and thorium respectively. By contacting with *n*-octane vapor, it could be confirmed that the skeleton collapsed after the skeletonization. Furthermore, it has also been pointed out[2] that the meaning of skeletonization is obscure unless the content of metallic soap in the layer is more than 50 per cents. Therefore, we attempted further to determine the reliable value of the number of stearic acid layers taking part in the formation of metallic soap.

If the adsorption takes place in a few outermost layers of the built-up film, there exists a sandwich layer of pure stearic acid between the adsorbed layer and the base multilayer. As a result, when this echelon was skeletonized, the adsorbed layer would be partially detached from echeion into the solution, due to the dissolution of the underlying sandwich layer of stearic acid. Since this effect is considered to be remarkable when only a few surface layers take part in the adsorption, it is evident that the apparent amount of the adsorption per layer is also exaggerated in such a case. These circumstances are still more likely to occur in the case where a large or complex ion may suffer resistance to the penetration of the surface layers for the deeper adsorption.

These presumption could be confirmed from the following experiment. Instead of the multilayers of stearic acid converted from barium salt, definite multilayers of stearic acid were deposited from water the surface of water onto the barium stearate echelon at 8～12°C., at which the monolayers could be transferred repeatedly without collapse, and the experiments of the adsorption of ion and the successive skeletonization were carried out similarly. The experimental results showed that the amounts of the adsorption were nearly the same as in the former case in all *p*H region, while the detachment of stearate during skeletonization seemed to be fairly remarkable. This may be probable, since the stearic acid in this case can be completely removed by skeletonization, while, in the former case, the stearic acid layer contains some barium stearates which resist the detachment effect mentioned above. We could cite further evidence for this argument. From 2 to 10 layers of stearic acid were transferred onto the multilayers of barium stearate. Using these surfaces the similar experiments were repeated. The apparent amounts of the adsorption per layer as a function of the number of layers of stearic acid initially transferred were shown in Table 2. It was about 2 Å. for barium at *p*H 9.0 independent of the number of the layers. This value may be expected from the spacing of the built-up layers of barium stearate (24.4 Å.) and of stearic acid (23.1 Å.).

Table 2

Apparent Amount of Adsorption as a Function of the Number of Layers of Stearic Acid

No. of layers of stearic acid on echelon	Adsorbed amount per layer in Å.		
	Ba at *p*H 7.4	Ba at *p*H 9.0	Al at *p*H 4.3
2	2.6	1.6	5.0
4	3.2	2.1	3.9
6	27	2.5	20.0
8	35	2.1	52.1
10	50	1.9	68

On the other hand, there was a remarkable increase in thickness of the adsorbed film between 4 and 6 stearic acid layers of aluminum at *p*H 4.3 or for barium at *p*H 7.4. These results seem to show that these ions can penetrate only about 4 layers at the corresponding *p*H. This table does not only suggest the existence of the sandwich effect, but also enables us to calculate the adsorbed amount per layer for aluminum, being about 5 Å., which can be expected from the content (usually 60～80%) of barium stearate in the ordinary echelon and increment in thickness (～3 Å.), when it was conditioned with aluminum ion. That the aluminum ion could, even at the most favorable *p*H for the adsorption, penetrate only a few layers, suggests its complex nature as compared with barium ion, which has already been pointed out for instance by McGee[13]. Recently, Gerovich and Kaptsan[14] pointed out the anomalous surface potential of monolayers of stearic acid spread on water

(12) I. Langmuir, *Proc. Roy. Soc.*, **A 170**, 1 (1939).

(13) C. G. McGee, *J. Am. Chem. Soc.*, **71**, 278(1949); *etc.*

(14) M. Gerovich and O. Kaptsan, *Zhur. Fiz. Khim.*, **23**, 445 (1949); *C. A.* **43**, 6038 (1949).

containing thorium salt at *p*H 2.5. This also seems to have some relation to our experiment. Furthermore, it was reported by Sasaki and Matuura[11] of our laboratory that the monolayers of stearic acid spread on the aqueous solutions containing ions of copper, aluminum, thorium, etc., remarkably expanded at the *p*H ranges corresponding to those of Fig. 3. From the data shown in Figs. 1 to 3, it may also be reasonable to assume more or less large unit of the complicated structure at least in the specific *p*H range for cupric, mercuric, aluminum, and thorium ions in the solution, the degree of complexity being presumably as follows:

thorium ion>aluminum ion>cupric ion.

Summary

The adsorption of barium, mercuric, cupric, aluminum, and thorium ions on the built-up films of stearic acid both transferred from water the surface of water, and converted from barium stearate multilayers, was studied.

The adsorbed amount of barium ion increased with increasing *p*H, but the increase in thickness corresponding to the saturate adsorption for monolayer was constant for all *p*H. On the contrary, other ions studied showed the specific *p*H range for the optimum adsorption. A more or less complicated and large structure for these ions was concluded from the special nature of the adsorption hereby exhibited by these ions. Such a complex nature was most pronounced for aluminum and thorium ions.

The cost of this research has been defrayed from the grant of the Ministry of Education, to which the authors' thanks are due.

Department of Chemistry, Faculty of Science, Kyûshû University, Fukuoka

On the Nature of Built-up Film. II. Deposition of Monolayer of Stearic Acid from Surface of Water Containing Copper, Aluminum, and Thorium Ions

By Mitsuo MURAMATSU and Tunetaka SASAKI

(Received September 3, 1951)

Introduction

The built-up film of stearate can readily be prepared when the substrate water from which it is built up contains barium or calcium ion. If, however, it contains a trace of heavy metallic ion, the nature of this film is profoundly altered.[1] As pointed out by Blodgett,[2] this effect seems to be very remarkable in case of copper ion which hinders the deposition of monolayer on a metallic slide, even if the other conditions are favorable for the successive deposition. She also reported[3] that the monolayer spread on water containing aluminum chloride could not be deposited onto the slide. In the preceding report,[4] the authors were inclined to the opinion that some metallic ions, *e. g.*, cupric, mercuric, aluminum, and thorium ions, somewhat differ in the manner of adsorption from alkali earth ions. They seem to behave rather as a large unit of the complicated structure in a specific *p*H range, at which the adsorption is remarkable. This conclusion has also been supported by the experimental results on monolayer spread on water, carried out by Sasaki and Matuura of our laboratory.[5] In the present report, it was attempted to build up stearic acid monolayers by transferring from the surface of aqueous solutions containing cupric, aluminum, and thorium ions, and the properties of these films were studied.

Experimental

Materials used were purified similarly as describ-

(1) I. Langmuir, "Recent Advances in Surface Chemistry and Chemical Physics," p. 1, Science Press Printing Co., Lancaster (1939); I. Langmuir and V. J. Schaefer, *J. Am. Chem. Soc.*, **58**, 284 (1936); **59**, 2400 (1937).

(2) K. B. Blodgett, *J. Phys. Chem.*, **41**, 975 (1937),

(3) K. B. Blodgett, *J. Am. Chem. Soc.*, **57**, 1007 (1935).

(4) M. Muramatsu and T. Sasaki, This Bulletin, **25**, 21, (1952).

(5) T. Sasaki and R. Matuura, This Bulletin, **24**, 274 (1951).

ed in the preceding report.[4] Stearic acid was spread as benzene solution on the surface of aqueous solutions of copper sulfate (*p*H 6.5), aluminum chloride (*p*H 6.3), and thorium nitrate (*p*H 4.0), *p*H of which was properly adjusted using ammonia and hydrochloric acid. Concentration of salts was 10^{-4} mol/l. The method of deposition will be described in the following section. The spacing of film, transferred onto the echelon of barium stearate, was determined by means of the optical method as in the preceding report.[4] The contact angle was measured by an image method.[6] Thereby we ignored the disturbance due to the evaporation of water, but the results were quite satisfactory for the present purpose.

Results

a. Deposition of Monolayers onto the Slide.—It was confirmed by the preliminary experiments, that the difficulty of transference onto the slide of monolayers of stearic acid spread on aqueous solution containing copper, aluminum, and thorium ions, chiefly comes from their mechanical properties. High rigidity and brittleness spoil the fluidity and flexibility of monolayer which are necessary for building up monolayers. Actually, the piston oil could not exert a uniform pressure on a film. It must be noted further that, in this case, films are so sensitive even for a slight mechanical agitation accompanying dipping and withdrawing of the slide,[1] that the piston oil of high spreading pressure usually employed for this purpose can not be used. Moreover the heavy metal ions in a substrate water seem to influence the nature of an ordinary piston oil, such as castor oil, as it does for stearic acid. Taking into account of these circumstances, the following procedure was adopted to prepare a built-up film. Successive *Y*-multilayers of barium stearate, deposited onto the metal slide, were conditioned with aluminum chloride solution of *p*H 4.3 or with thorium nitrate of *p*H 4.0, and immersed in water containing ion under the investigation. Benzene solution of stearic acid was then applied to that surface of water by a micro-pipette, until only a small drop of benzene remained. The additional drops were put on several positions about 4 cm. apart from the place where the slide was withdrawn. As the slide was withdrawn and monolayer was transferred, drops of benzene spread with the irregular shape, as if they wedge into cracks formed in a rigid surface layer of stearic acid. Here drops behave as a piston oil of the spreading pressure of about 10 dynes per cm. presumably unaffected by a substrate ion. The spreading of drops was the indication of transference of monolayer. It must be noted that, although the first layer of copper, aluminum, and thorium stearates could be built up relatively easily, successive deposition of these films, especially of thorium stearate, occurred in an irregular manner, *i.e.*, we often encountered the folding or the defection of monolayers during its transference from the surface of water.

The first layers of built-up films thus obtained were wettable, to some extent, soon after withdrawal, but became very hydrophobic once they were dried. The contact angle in such a state towards water are shown in Table 1. Here, an *X*-film of barium stearate was built from substrate water of *p*H 9, and the contact angle value was the mean of four to eight experiments.

Table 1

Contact Angles of Built-up Films towards Water

Lower layer	45*Y* Ba-st.		47*Y* Ba-st.		
Upper layer	2*Y* Ba-st.	3*X* Ba-st.	1*B* Cu-st.	1*B* Al-st.	1*B* Th-st.
Contact angle, degree	99±12	102±10	104±11	106±10	110±6

Further the calculation was made for the apparent spacing of monolayers of these built-up films, using the value of 24.4 Å. for the spacing of barium stearate monolayer and refractive index of 1.462 which was assumed to be equal to that of base echelon. The result was shown in Table 2. The value of spacing was obtained from the results of five to seven experiments.

Table 2

Apparent Spacing of Copper, Aluminum, and Thorium Stearates

Film	Apparent spacing, Å.
Barium stearate	24.4
Copper stearate	23.0 ± 4.1
Aluminum stearate	17.8 ± 4.7
Thorium stearate	20.5 ± 3.6

b. Property of Conditioned Built-up Film.—As reported in the preceding paper, copper, aluminum, and thorium ions behave in the case of adsorption on stearic acid multilayers as a fairly large unit. They also render the treated surface highly wettable as

(6) E. Kneen and W. W. Benton, *J. Phys. Chem.*, **41**, 1195 (1937).

was already reported by Inaba of our laboratory,[7] but this effect was known to be more remarkable in the case of barium stearate multilayers than in the case of stearic acid.[8] We can also observe a characteristic behavior for wetting, when we examine the built-up layers of stearate of some other heavy metal, as are summarized in Table 3.

Table 3

Wettability of Variously Conditioned Built-up Film

Conditioning		Built-up Film			
Reagent	*p*H	Barium stearate (*Y*-layer)	Copper stearate (*B*-layer)	Aluminum stearate (*B*-layer)	Thorium stearate (*B*-layer)
Barium chloride	6.5	—	—	—	—
Copper sulfate	6.5	+++	++	—	—
Aluminum chloride	6.3	++++	+++	+	—
Thorium nitrate	4.0	++++	++++	++	—

—, Non-wettable after soaking for 1 hr.; ++++, perfectly wettable after soaking within 30 sec.; +, ++, and +++, more than a half of total area of a slide being wettable after soaking for 20 min., 5 min., and 30 sec., respectively, but water peeling back by the subsequent washing.

Discussion

In the data shown in Table 1, it will be noticed that the films of stearate of heavy metal are very hydrophobic, despite the difficulty of their deposition. Bikerman[9] reported that the monolayer is deposited as *Y*- or *X*-layer according to whether the contact angle being variable on both sides of 90° or variable only on the larger side of 90°. According to this view, *X*-layer should be transferred during down-trip which could be the case for copper stearate if it was built up with thorough precaution. However it was unsuccessful with aluminum and thorium stearates. This may perhaps come from their speciality in the mechanical behaviors. On the other hand, it will be noticed that the apparent spacings of all these films are smaller than that of barium stearate. Since the actual length of stearyl radical can not be considered to be affected by the presence of heavy metal, the results seem to indicate a smaller refractive index for stearate of copper, aluminum, and thorium than that of barium. The smaller refractive index in turn predicts that the stearyl radicals of these stearates exist uniformly separated in the built-up film, provided that the defection or the folding of monolayer mentioned above are absent in this case. This, together with the fact that the monolayer could hardly be transferred onto a slide on account of its mechanical resistance, leads us to the conclusion that these stearyl radicals are rigidly bound together by a somewhat long chain consisting of, say, aluminum and oxygen. Such a conclusion has been obtained also by Sasaki and Matuura[5] of our laboratory. In this connection we should refer to the macromolecular structure of aluminum soap which is recently proposed by many authors[10] to explain its peculiar and complex nature. Perhaps, we should not use the term aluminum stearate, as it was reported that we could merely find the adsorption complex consisting of hydrated alumina and stearic acid rather than the stearate.[11] But it is not a matter of fundamental importance for the present argument how they are combined together. Experimental result in Table 2 shows in agreement with these authors, that the substance thereby formed is of a complex nature.

Now, let us pay attension to the fact that the built-up films of barium, copper, aluminum, and thorium stearates exhibit nearly the same wettability towards water as shown in Table 1, which is due, of course, to the fact that a hydrocarbon part of the stearate constitutes an outermost layer in all cases. But precisely looking, we can arrange these ions in series of barium, copper, aluminum, and thorium according to the decreasing order of the wettability of their stearate, though it is not so distinct. This series is, of course, in contradiction to what would be expected from apparent spacing of stearate shown in Table 2, and can therefore be ignored as an experimental error, but we should like rather to take it for the slight indication of overturning effect allowed for molecules,[12] with the easiness decreasing in the order shown in the above series. Precisely speaking, it can reasonably be assumed that the stearate molecule is allowed to overturn itself in the surface layer, with the degree of difficulty proportional to the complexity of its structure.

A more clear evidence of this view can be

(7) A. Inaba, This Bulletin, **23**, 146 (1950).
(8) I. Langmuir and V. J. Schaefer, *J. Am. Chem. Soc.*, **59**, 1762 (1937).
(9) J. J. Bikerman, *Trans. Faraday Soc.*, **36**, 412(1940).
(10) V. R. Gray and A. E. Alexander, *J. Phys. Colloid Chem.*, **53**, 9, 23 (1949); C. G. McGee, *J. Am. Chem. Soc.*, **71**, 278 (1949); *etc.*
(11) L. J. Edwards, Thesis for Fellowship, Royal Institute of Chemistry (1946): Unfortunately the authors have not yet seen the original report.
(12) I. Langmuir, *Science*, **87**, 493 (1938).

found in Table 3. Here again it is confirmed that above ions hinder the overturning of stearic acid molecule and re-overturning of once overturned molecule, with the intensity increasing in the order mentioned above. The easiness of overturning was here corelated with the degree of wettability semiquantitatively expressed in this table. This order is also in agreement with that of the preceding report. [4] Thus we are inclined to the opinion that the metallic stearate increases the complexity of its structure in the order of barium, copper, aluminum, and thorium, among which aluminum and thorium stearates are complex enough to be called macromolecule or micelle, as was proposed by McGee *et al.*,[10] while barium stearate forms merely a simple stoichiometric compound as is usually considered. It is interesting in these relation to point out that although the film of free stearic acid or barium stearate can readily be conditioned (rendered wettable) by treating with aluminum or thorium salt solution, thorium stearate film itself is not wettable, and moreover can not be conditioned similarly, and further that stearic acid conditioned by aluminum salt proves to be fairly wettable, while aluminum stearate is well known as one of the efficient water-repellant. All these apparent contradictions can be explained reasonably. Special nature of water-repellent ferric stearate frequently employed for the coating of a trough for the surface film experiment[13] can also be understood from such a point of view.

Summary

Monolayer of stearic acid spread on water containing copper, aluminum, and thorium ions, has been transferred onto solid surface, and the apparent thickness of monolayer as well as its wettability towards water after the treatment with or without aqueous solution of salts were measured. Tentative explanations for these phenomena are given, taking into account of a macromolecular structure of aluminum soap.

The cost of this research has been defrayed from the grant of the Ministry of Education, to which the authors' thanks are due.

Department of Chemistry, Faculty of Science, Kyûshû University, Fukuoka,

(13) I. Langmuir, *Cold Spring Harbor Symposia Quant. Biol.* **6**, 171 (1938).

The Electrical Conductivity of the Condensed Polynuclear Aza-aromatic Compounds

By Hiroo INOKUCHI

(Received September 18, 1951)

Introduction

The molecules of the condensed polynuclear aza-aromatic compounds are composed of the net-work plane of the conjugated double bonds of carbon and nitrogen. These substances have some interesting properties as the dyestuff material, and also as the biochemical substance. These vat dyestuffs, for example, have no "light catalytic reaction character" and can be synthesized more easily than the corresponding condensed aromatic compounds.

Little has been known about the physical properties of these compounds. Fox example, when the resonance energy of simple aza-aromatic compounds are compared with the corresponding hydrocarbons, the difference is negligible as shown in Table 1.[1] And it is also known that the replacement of a conjugated carbon atom by a nitrogen atom does not greatly influence the ultraviolet absorption spectrum of the compound.

Table 1

The Resonance Energy of the Condensed Aza-aromatic and Aromatic Compounds

Substance	Benzene	Pyridine	Naphthalene	Quinoline
Resonance energy, kcal./mol	41	43	77	75

(1) G. W. Wheland, "The Theory of Resonance," p. 69-70 (1944).

In the previous report,[2] we have found that violanthrone, pyranthrone etc. have the character of an intrinsic semi-conductor concerning the electrical conductivity in powdered state of these crystals. From these results, the difference in the electrical conductivity is expected to be not so large between aza-aromatic compounds and condensed aromatic hydrocarbons or quinones.

Experimental Procedure

The electrical conductivity of cyananthrone (dark violet), indanthrone black (brownish black), flavanthrone (yellownish orange), indanthrone (violet), indanthrazine (brown), 5,6-(N)-pyridino-1,9-benzanthrone (yellow) and 1,9,4,10-anthradipyrimidine (brown) was measured. The molecular structures of these compounds are illustrated in Table 3.

Indanthrone black, flavanthrone and indanthrone were purified chemically from the commercial vat dyestuffs respectively,[3] and then they were sublimed repeatedly in a vacuum until the conductivity became constant. In the case of indanthrone black (Indanthrene Black B. I. G.), as it contained a large volume of by-products, repeated chemical purifications were needed.

Indanthrazine was made by the reduction of indanthrone with E. Clar method[4] by Mr. T. Handa. And recrystallization and sublimation were repeated alternately until indanthrone was perfectly removed. In the course of this experiment, it was found that the specimen of indanthrone, for the preparation of indanthrazine, could be reduced by zinc powder more easily when it was used as a precipitated form from the concentrated sulphuric acid solution, than the ordinary product or, for example, when it was purified by the sublimation. The cause of this difference can be understood by the following explanation.

Indanthrone (Indanthrene RSN) was purified chemically and was sublimated in vacuum 10^{-4} mm.Hg at 350°. This specimen has violet colour, and is here called specimen (A). Specimen (A) was dissolved in concentrated sulphuric acid, and then this solution was poured into a large amount of water under 10° with strong stirring. This precipitated specimen was then filtered, washed to be made free from acid and dried at 70°. It is believed that no sulphate salt of indanthrone is formed in this case. This specimen has blue colour, and is called specimen (B).

When we compare x-ray Debye-Scherrer patterns of thess (A) and (B), it was found that patterns of the specimen (B) were more diffuse than the specimen (A). And in the case of the specimen (B), some of the patterns which appeared on the photograph of specimen (A), disappeared. (see Table 2.) This fact indicates that the specimen (B) is more irregular in the arrangement of molecules in crystal than (A).[5] Therefore the reactive area of the specimen (B) will be larger than specimen (A). It coinsides with the fact that the specimen (B) is reduced by zinc powder more easily than (A).

Cyananthrone was synthesized from 5,6-(N)-pyridino-1,9-benzanthrone by Mr. Handa[6] and purified in the same manner as described above.

Table 2

X-ray Data for Iadanthrone. Values of Spacings (x-ray: Cu Kα Ni-filtered)

Specimen A sublimated in vacuum		Specimen B precipitated from conc. H_2SO_4	
d/n, Å.	intensity	d/n, Å.	intensity
7.80	f	8.10	f diffuse
5.96	mf		
4.60	mf		
3.39	ff	3.46	f diffuse
2.75	mf	2.75	pp very diffuse
2.66	mp		
2.51	mp		
2.36	mf		
2.24	mf	2.24	pp very diffuse
2.12	p		
2.08	mp		
1.99	pp		
1.92	mf		
1.85	mp		
1.79	mf		
1.68	p		
1.58	mp		
1.42	p		
1.32	p		
1.275	p		
1.230	p		
1.190	pp		
1.165	pp		
1.085	pp		

As in the cases of condensed polynuclear aromatic compounds, single crystals could not be obtained. Therefore seven samples were examined in the state of the compressed powdered form. The measuring method of the electrical conductivity has been already described. The specimen was compressed between the metal end and piston in a polished good quality ebonite cylinder, which had 0.8 cm. diameter. The height of the specimen was between 0.3 cm. and 0.5 cm. The electrical resistance was measured by the potential drop

(2) H. Akamatu and H. Inokuchi, *J. Chem. Phys.*, **18**, 810 (1950); H. Inokuchi, This Bulletin, **24**, 222 (1951).

(3) H. Akamatu and K. Nagamatsu, *J. Colloid Sci.*, **2**, 593 (1947).

(4) E. Clar, *Ber.*, **72**, 1645 (1939).

(5) It was found frequently that some dyestuffs were crystallized in various ways by which the particle shape and the colour were influenced greatly (*cf.* F. A. Hamm and E. V. Norman, *J. Appl. Phys.*, **19**, 1097 (1948).

(6) T. Maki, *J. Soc. Chem. Ind. Japan*, **37**, 505 (1934).

method with the aid of a direct current amplifier using UX-54 tube. This circuit is illustrated in Fig. 1. The supplied voltage was 400~500 V. per cm. The constancy of the electrical conductivity of these powdered specimens is obtained when the compressed pressure upon them is over 80 kg./cm.^{2} Therefore these specimens were compressed by a lever above 80 kg./cm.^{2}

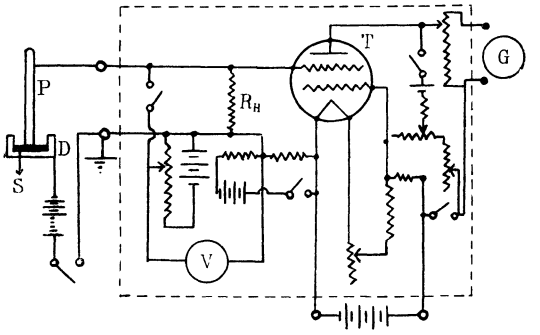

Fig. 1.—The circuit of direct current amplifier: T, electrometer tube UX-54 (This tube has the same character as FP-54); V, voltmeter. (Range is from 0.01 V. to 5 V.); R_H, high resistance ($10^9\Omega$ or $10^{10}\Omega$); G, galvanometer, (Sensitivity is 0.001 μA./mm.); P, piston (0.8 cm. diameter); D, Cyrindrical dish (made of brass coated by chromium); S, specimen. The height of this is between 0.1 cm. and 0.5 cm.

On the other hand, as 5, 6-(N)-pyridino-1, 9-benzanthrone (No. 6) and 1, 9, 4, 10-anthradipyrimidine (No. 7) have high electrical resistivity, these specimens(S)were compressed on a cylindrical dish (D), instead of the ebonite cylinder, by a piston (P) to 80 kg./cm.^{2} with a lever system as shown in Fig. 1 schematically. Because the ebonite cylinder was not used, the surface leakage of the cylinder could be avoided completely and the temperature could be increased to 300°. By this method we could measure the high electrical resistance of these substances.

Results and Discussions

The temperature coefficient of the electrical resistivity was negative in every specimen, and logarithm of electrical resistivity $\log \rho$ and the reciprocal of temperature $1/T$ have the linear relation for a large range of temperature,

$$\rho = \rho_0 \exp(\Delta\varepsilon/2kT) \qquad (1)$$

where $\Delta\varepsilon$ is the activation energy, corresponding to the interval of energy band on the model of semi-conductor.

About these behaviours, differences could not be found between this group and condensed polynuclear aromatic compounds.

Non-hysteresis of electrical resistivity and independency of the current upon the time prove the electronic conductance. Therefore the mechanism of semi-conductive character of those aza-aromatic compounds is assumed to be intrinsic, from their perfect molecular crystals as in the cases of the condensed polynuclear aromatic compounds.

The value of ρ_{15}, extrapolated to 15°, $\Delta\varepsilon$ and ρ_0 were tablulated in Table 3, and the relation of equation (1) were illustrated on Figs. 2 a, b and c.

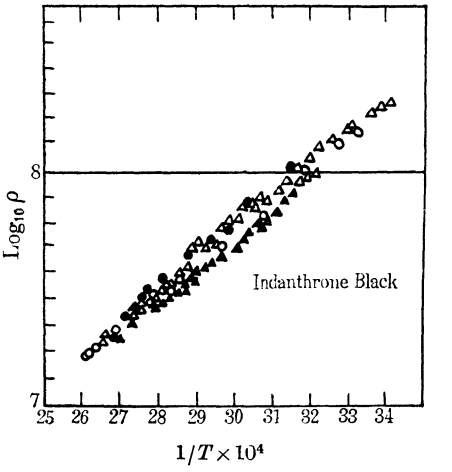

Fig. 2 a.—The relation between resistivity and temperature for indanthrone black: △82.1 kg./cm.^{2}, increasing temperature; ▲82.1 kg./cm.^{2}, decreasing temperature; ○119.5 kg./cm.^{2}, increasing temperature; ●119.5 kg./cm.^{2}, decreasing temperature.

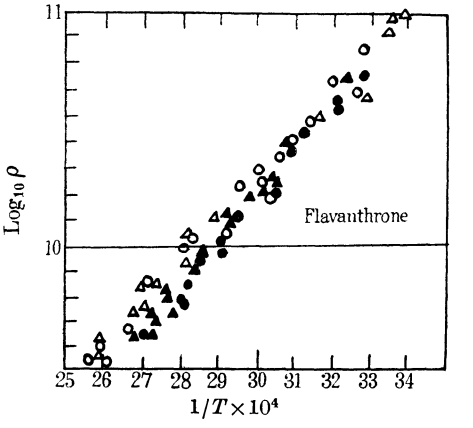

Fig. 2 b.—The relation between resistivity and temperature for flavanthrone. The same symbols as in Fig. 2 a.

Concerning the value of the electrical conductivity, cyananthrone and indanthrone black

Table 3

The Values of ρ_{15}, $\Delta\varepsilon$ and ρ_0 of the Condensed Polynuclear Aza-aromatic Compounds

No.	Substance	Structure	ρ_{15}, Ω cm.	$\Delta\varepsilon$, e. V.	ρ_0, Ω cm.
1	Cyananthrone	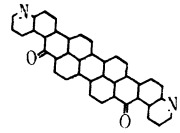	1.2×10^{7}	0.20	2.24×10^{5}
2	Indanthrone Black	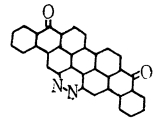	2.5×10^{5}	0.56	3.45×10^{3}
3	Flavanthrone	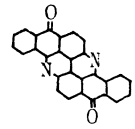	1.4×10^{11}	0.70	9.5×10^{4}
4	Indanthrone	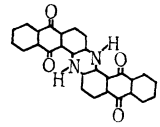	7.5×10^{14}	0.63	2.5×10^{9}
5	Indanthrazine	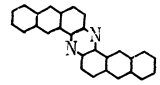	1.4×10^{15}	0.66	2.2×10^{9}
6	5, 6-(N)-Pyridino-1, 9-benzanthrone	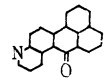	8.5×10^{22}	3.20	1.4×10^{-5}
7	1, 9, 4, 10-Anthradipyrimidine		8.8×10^{24}	3.21	1.3×10^{-3}

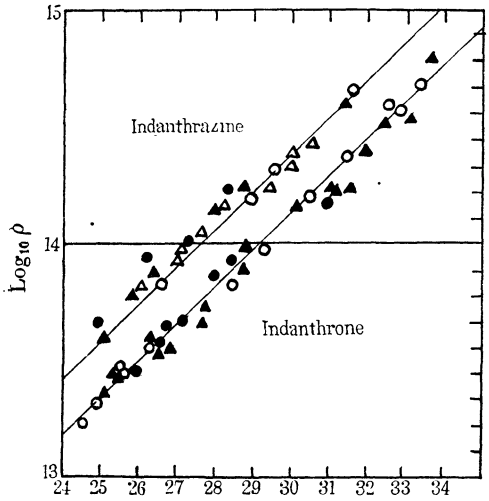

Fig. 2c.—The relation between resistivity and temperature for indanthrone and indanrthazine. The same symbols as in Fig. 2a.

have the typical values of semi-conductor, $10^{-7}\Omega^{-1}$cm.$^{-1}$~$10^{-8}\Omega$cm.$^{-1}$[7]

When the number of rings is increased, the illustration shows that the value of electrical conductivity and activation energy approach those of carbon. The electrical conductivity and the activation energy of commercial graphite is the order of $10^{2}\,\Omega^{-1}$ cm.$^{-1}$ and 10^{-2} e. V. respectively[8].

It is found that the values of the electrical resistivity of aza-aromatic compounds are much smaller than those of related aromatic compounds. A typical one is shown in Table 4. It is interesting to compare this result to the fact that intensities of flourescence spectra of aza-aromatic compounds (6-azachrysene and 1-azapyrene) are about ten times as great as those of the related hydrocarbons (chrysene and pyrene)[9].

(7) M. F. Manning and M. E. Bell, *Rev. Mod. Phys.*, **12**, 215 (1940).
(8) S. Mrozowski, *Phys. Rev.*, **77**, 838 (1950).
(9) R. Schoental and E. J. Y. Scott, *J. Chem. Soc.*, 1683 (1949).

Table 4

The Values of $\Delta\varepsilon$ and ρ_{15} of Pyranthrone and Flavanthrone

Substance	Pyranthrone 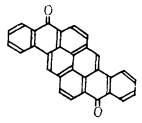	Fravanthrone 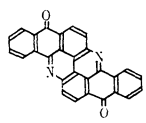
$\Delta\varepsilon$	1.06 e.V.	0.70 e.V.
ρ_{15}	$3.9\times10^{15}\Omega$ cm.	$1.4\times10^{11}\Omega$ cm.

The electrical conductivity of indanthrone is very poor as compared with the value of flavanthrone. We think that the cause of this irregularity is a spatial structure. The spatial structure of indanthrone has not yet been researched, but a magnetic susceptibility of this suggests non-coplaner structure.[10]

Summary

The electrical conductivity of the condensed polynuclear aza-aromatic compounds; (1) cyananthrone, (2) indanthrone black, (3) flavanthrone, (4) indanthrone, (5) indanthrazine, (6) 5, 6-(N)-pyridino-1, 9-benzanthrone and (7) 1, 9, 4, 10-anthradipyrimidine,—has the character of a semi-conductor. The electrical resistivity of these compounds can be expressed as $\rho=\rho_0\exp(\Delta\varepsilon/2kT)$ and the mechanism of the conduction is assumed to be that of the intrinsic semi-conductor as in the cases of the condensed polynuclear aromatic compounds. The value of $\Delta\varepsilon$ and ρ at 15° were found as; (1) 0.20 e.V., $1.2\times10^{7}\Omega$ cm., (2) 0.56 e.V., $2.5\times10^{8}\Omega$ cm., (3) 0.70 e.V., $1.4\times10^{11}\Omega$ cm., (4) 0.63 e.V., $7.5\times10^{14}\Omega$ cm., (5) 0.66 e.V., $1.4\times10^{15}\Omega$ cm., (6) 3.2 e.V., $8.5\times10^{22}\Omega$ cm. and (7) 3.21 e.V., $8.8\times10^{24}\Omega$ cm. The values of the electrical resistivity of this group are smaller than that of related condensed polynuclear aromatic compounds.

The author expresses his hearty thanks to Prof. H. Akamatu for his kind direction of this study and also to Mr. T. Handa who prepared the samples of this work. The Debye-Sherrer x-ray photograph was due to Mr. H. Takahashi's favour. The author wishes to thank him. The cost of this research has been defrayed from the Grant in Aid for Fundamental Scientific Research from the Ministry of Education, to which the author's thanks are due.

Department of Chemistry, Faculty of Science, Tokyo University, Tokyo

(10) H. Akamatu, suggestion.

On the Viscosity of Binary Mixture of Liquids[1]

By Mikio TAMURA and Michio KURATA

(Received September 20, 1951)

Introduction

If we attempt to derive an equation which should connect the viscosity coefficient of a mixture of liquids A and B with its composition and those of its constituents, it becomes necessary, in addition, to introduce a quantity in order to take the molecular interaction of A-B type into account inasmuch as the viscosity of a mixture depends upon the mutual action of the molecules constituting it. Dolezalek,[2] at first, and then Wijk[3] introduced the quantity relating the A-B type interaction in the form of a parameter called "mutual viscosity" η_{AB} and derived their own equations having simple form, but the agreement of their equations with the experimental values seems not to be enough as will be shown below, and their definitions of η_{AB} seem to be obscure. Recently, Powell, Roseveare and Eyring[4] and Kottler[5] proposed the semi-empirical equations respectively, which involve the quantities of different type from η_{AB}, but their equations are inconvenient for numerical

(1) The contents of this paper were read at the 1st and 2nd annual meetings of the Society in May, 1948 and in April, 1949 and were published partly in *Busseiron Kenkyu*, **11**, 20 (1948); **20**, 151 (1949) in Japanese.

(2) F. Dolezalek, *Z. phys. Chem.*, **83**, 73 (1913).

(3) A. J. A. van der Wijk, *Nature*, **138**, 845 (1936).

(4) R. E. Powell, E. Roseveare and H. Eyring, *Ind. Eng. Chem.*, **33**, 430 (1941).

(5) F. Kottler, *J. Phys. Chem.*, **47**, 277 (1943); **48**, 76 (1944).

calculation, and this is an important defect for practical use. In this paper, the authors will give the definition of η_{AB} explicitly and derive a new semi-empirical equation which has simple form and seems to be better than others.

Derivation of Equation

According to Frenkel and Eyring,[6] the viscosity coefficients, η_A and η_B, of liquids A and B are given by

$$\eta_A=(kT/v_A)\tau_A \quad \text{and} \quad \eta_B=(kT/v_B)\tau_B, \tag{1}$$

respectively, where k is the Boltzmann constant, T the absolute temperature and v's are the volumes occupied by one molecule; the subscripts indicate the molecular species. And τ's represent the relaxation times of flow and are given by

$$\left.\begin{aligned}&\tau_A=(h/kT)\exp(\chi_A/kT)\\ \text{and}\quad&\tau_B=(h/kT)\exp(\chi_B/kT),\end{aligned}\right\} \tag{2}$$

where h is the Planck constant and $\chi_A(\chi_B)$ is the activation free energy of flow relating only with A-A(B-B) contact of molecules. Quite similarly, the viscosity coefficient η of mixture of liquids A and B, should be given by

$$\eta=(kT/v)\tau \tag{3}$$

with

$$\tau=(h/kT)\exp(\chi/kT). \tag{4}$$

Here the letters with no subscript (τ, v and χ etc.) represent the quantities regarding the mixture.

Now, let us introduce the "mutual activation free energy of flow" χ_{AB} relating only with A-B contact of molecules in the same manner as χ_A (or χ_B) relates with A-A (or B-B) contact, and define τ_{AB} by

$$\tau_{AB}=(h/kT)\exp(\chi_{AB}/kT). \tag{5}$$

This is the relaxation time of flow of A molecule in liquid B or *vice versa*. And τ in Eq. (3) may be given as a kind of mean of τ_A, τ_B and τ_{AB}.

If we represent the molar fractions of each component by x_A and x_B, the probabilities of occurring of A-A, B-B and A-B contacts of molecules are given by x_A^2, x_B^2 and $2x_Ax_B$ respectively under the condition of random mixing. Then assuming that τ is given by the arithmetical mean of τ's, *i. e.*,

$$\tau=x_A^2\tau_A+x_B^2\tau_B+2x_Ax_B\tau_{AB}, \tag{6}$$

and defining the "mutual viscosity coefficient" η_{AB} by

$$\eta_{AB}=\{kT/(v_Av_B)^{1/2}\}\tau_{AB}, \tag{7}$$

we obtain

$$\eta=x_A^2\left(\frac{v_A}{v}\right)\eta_A+x_B^2\left(\frac{v_B}{v}\right)\eta_B+2x_Ax_B\left(\frac{v_Av_B}{v^2}\right)^{1/2}\eta_{AB}, \tag{8}$$

from Eqs. (1), (3), (6) and (7). If d be the density and w the weight fraction, we can obtain easily

$$x_Av_A/v=w_Ad/d_A \text{ and } x_Bv_B/v=w_Bd/d_B. \tag{9}$$

For the practical purposes, we can put

$$x_Av_A/v=\varphi_A \quad \text{and} \quad x_Bv_B/v=\varphi_B, \tag{10}$$

where φ's are the volume fractions, and obtain

$$\eta=x_A\varphi_A\eta_A+x_B\varphi_B\eta_B+2(x_Ax_B\varphi_A\varphi_B)^{1/2}\eta_{AB}, \tag{11}$$

since the volume change on mixing can be neglected in general. Although Eq. (11) appears to be rather similar to the Dolezalek equation,

$$\eta=x_A^2\eta_A+x_B^2\eta_B+2x_Ax_B\eta_{AB}, \tag{12}$$

it must be noticed that the agreement of the former with the experiments is considerably better than that of the latter as will be shown in the following section.

It is well-known that, if we use the harmonic oscillator model of liquids,[7] we can get the relations of the following type;

$$\left.\begin{aligned}&\tau=(1/\nu)\exp(\varepsilon/kT),\\ &\tau_A=(1/\nu_A)\exp(\varepsilon_A/kT)\\ \text{and}\quad&\tau_{AB}=(1/\nu_{AB}\nu_{BA})^{1/2}\exp(\varepsilon_{AB}/kT),\\ &\text{etc.},\end{aligned}\right\} \tag{13}$$

where ε's are the activation energies of flow and ν's are the frequencies of lattice vibration and ν_{AB} (or ν_{BA}) represents the frequency of A (or B) molecule surrounded by B (or A) molecules only. Then (1), (3) and (7) with (13) become

(6) J. Frenkel, "Kinetic Theory of Liquids," Oxford, 1947, Chap IV, § 2; S. Glasstone, K. J. Laidler and H. Eyring, "The Theory of Rate Processes," New York, 1941, Chap. IX.

(7) See, for example, R. H. Fowler and E. A. Guggenheim, "Statistical Thermodynamics," Cambridge, 1939, p. 319.

$$\left.\begin{aligned} &\eta=(kT/v\nu)\exp(\varepsilon/kT),\\ &\eta_A=(kT/v_A\nu_A)\exp(\varepsilon_A/kT)\\ \text{and}\quad &\eta_{AB}=\{kT/(v_Av_B\nu_{AB}\nu_{BA})^{1/2}\}\\ &\qquad\times\exp(\varepsilon_{AB}/kT). \end{aligned}\right\}\quad(14)$$

That is, the temperature dependency of η_{AB} may also satisfy the expression of Andrade's type.[8]

Comparison of η with the Experimental Values

The comparison of Eq. (11) with the experimental values of viscosity coefficient, η_{obs}, has been performed in regard to about 30 systems which are chosen from various types of mixtures as shown in Tables 1 and 2. In these tables are arranged the systems in three classes; mixtures of (A) non-polar and non-polar liquids, (B) non-polar and polar liquids and (C) polar and polar liquids, for convenience' sake. And $\bar{\Delta}$ denotes the arithmetical mean of the absolute values of $\Delta=(\eta_{calc}-\eta_{obs})\times100/\eta_{obs}$ at various compositions and max. or min. in the last column of these tables indicate that $\eta-x$ curve has a maximum or minimum. The unit of η_{AB} is "centi-poise" and the values of η of all systems except B-2, 4 and C-7 are adopted from "International Critical Tables," Vol. V. Some of the results of calculation are plotted in Figures 1~3, where the circles (○ or ①) and the full lines represent the observed

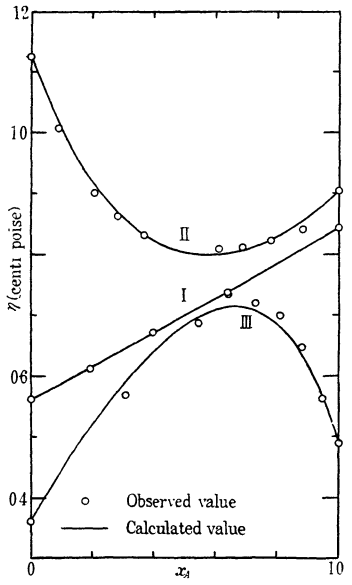

Fig. 1.—Observed and calculated values of η —1: Curve I, A=CCl_4, B=C_6H_6(30°C.); Curve II, A=CCl_4, B=CH_3COOH(25°C.); Curve III, A=H_2O, B=CH_3OH(60°C.).

(8) E. N. da C. Andrade, *Phil. Mag.*, **17**, 497, 698 (1934).

Table 1

List of the Systems Compared and the Results Obtained.—I

No.	System (Observer)	°C.	η_{AB}	$\bar{\Delta}$, %	
A-1	$CCl_4+C_2Cl_4$ (i)	25	0.752	0.5	min.
A-2	$CCl_4+C_2H_2Cl_4$ (i)	25	0.973	0.9	
A-3	$CCl_4+C_6H_6$ (ii)	0	1.134	0.0	
		10	0.941	0.0	
		20	0.797	0.2	
		30	0.688	0.2	
		40	0.596	0.1	
		50	0.522	0.0	
		60	0.463	0.2	
A-4	$CS_2+C_6H_6$ (iii)	25	0.474	0.6	
B-1	CCl_4+CHCl_3 (iii)	25	0.589	0.7	
B-2	CCl_4+CH_3COOH(xii)	25	0.657	0.9	min.
B-3	$CCl_4+CH_3COCH_3$(iv)	0	0.538	2.8	
B-4	$CCl_4+n\text{-}C_8H_{17}OH$ (xii)	25	1.112	3.7	
B-5	$CS_2+CH_3COCH_3$(v)	−13	0.450	0.2	min.
		−10	0.445	0.2	min.
		0	0.416	0.4	min.
		15	0.389	0.0	
		35	0.326	0.2	
B-6	$CS_2+C_2H_5OH$ (vi)	25	0.510	2.9	
B-7	$CS_2+C_6H_5CH_3$ (iii)	25	0.442	0.9	
B-8	$C_2H_2Cl_4+C_6H_5NO_2$ (vii)	5	3.41	1.4	max.
		76.5	0.958	0.7	max.
B-9	$C_6H_6+CHCl_3$ (iii)	25	0.572	0.2	
B-10	$C_6H_6+CH_3OH$ (viii)	25	0.636	0.2	
B-11	$C_6H_6+CH_3COOH$(vi)	25	0.464	2.9	min.
B-12	$C_6H_6+C_2H_5OH$ (vi)	25	0.524	1.8	min.
	〃 (ix)	15	0.668	1.9	
		20	0.614	2.5	
		25	0.567	2.0	min.
		30	0.522	1.4	
		35	0.481	0.9	
		40	0.445	0.9	
B-13	$C_6H_6+C_6H_5OH$ (x)	20	—	—	
B-14	$C_6H_6+C_6H_5CH_2CO_2C_6H_5$ (xi)	25	—	—	
		40	0.905	6.6	
		60	0.751	2.5	
		75	0.660	1.2	

Observer of η: (i) Herz and Rathmann, (ii) Thorpe and Rodger, (iii) Linebarger, (iv) Sakhanov and Ryakhovskii, (v) Faust, (vi) Dunstan, (vii) Drucker and Kassel, (viii) Bramley, (ix) Gertman, (x) Oholm, (xi) Bingham and Sarver, (xii) Jones, Bowden, Yarnold and Jones, *J. Phys. Coll. Chem.*, **52**, 753 (1948).

and the calculated values respectively. For purposes of comparison, we show also in Fig. 3 the values obtained from the Dolezalek equation, (12), and the Wijk equation,[3]

$$\log \eta = x_A^2 \log \eta_A + x_B^2 \log \eta_B + 2x_A x_B \log \eta_{AB}. \quad (15)$$

Table 2

List of the Systems Compared and the Results Obtained.—II

No.	System (Observer)	°C.	η_{AB}	$\overline{\Delta}$, %	
C-1	H_2O+CH_3OH (i)	0~30	—	—	
		40	1.510	5.1	max.
		50	1.232	4.2	
		60	0.997	2.1	
C-2	$H_2O+C_2H_5OH$(ii)	0~40	—	—	
		45	1.940	7.0	
		50	1.721	6.3	
		55	1.532	5.6	
		60	1.370	5.1	max.
		65	1.230	4.7	
		70	1.108	4.5	
		75	1.000	4.3	
C-3	$H_2O+C_3H_7OH$ (iii)	20	5.31	6.5	
		25	4.50	6.0	max.
		30	3.82	5.2	
C-4	$H_2O+C_3H_5(OH)_3$		—	—	
C-5	$CHCl_3+C_2H_5OC_2H_5$ (iv)	0	0.626	3.8	
		10	0.543	3.4	
		20	0.474	2.9	
		30	0.418	2.5	
C-6	$CHCl_2F+CH_3COCH_3$ (v)	0	0.562	1.2	max.
C-7	$CH_3OH+C_2H_5OH$(vi)	25	0.730	0.6	
		35	0.626	0.5	
		45	0.546	0.2	
		55	0.484	0.4	
C-8	$C_2H_5OC_2H_5+C_6H_5OC_6H_5$ (vii)		—	—	
C-9	i-$C_5H_{11}OH+HCONH_2$ (viii)	0	13.20	7.6	max.
		76.5	1.560	2.3	
C-10	i-$C_5H_{11}OH+C_6H_5NO_2$ (viii)	0	1.650	6.4	min.
		80	0.503	1.2	
C-11	i-$C_5H_{11}OH+C_6H_5N(C_2H_5)_2$ (viii)	0	2.77	6.1	min.
		76.5	0.559	1.2	
C-12	$C_6H_5CH_3+C_6H_5CO_2C_2H_5$ (ix)	25	0.782	1.2	

Observer of η: (i) Traube, (ii) Bingham and Jackson, (iii) Dunstan and Thole, (iv) Thorpe and Rodger, (v) Lacher, Walden and Park, *J. Am. Chem. Soc.*, **71**, 3026 (1949), (vi) Bingham, White, Thomas and Cadwell, (vii) Kendall and Wright, (viii) Drucker and Kassel, (ix) Kendall and Monroe.

It is nothing but the illustration of the satisfactory agreement of our equation (11) with the experimental values, that $\overline{\Delta}$ of almost all the systems is less than a small percentage. It must be noticed that $\overline{\Delta}$ of the mixture

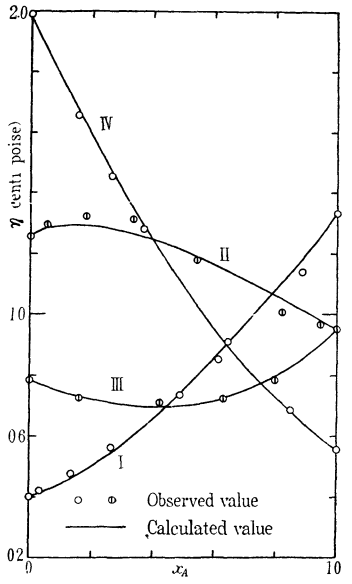

Fig. 2.—Observed and calculated values of η —2: Curve I, A=CCl_4, B=CH_3COCH_3 (0°C.); Curve II, A=*i*-$C_5H_{11}OH$, B=$HCONH_2$ (76.5°C.); Curve III, A=*i*-$C_5H_{11}OH$, B=$C_6H_5N(C_2H_5)_2$ (76.5°C.); Curve IV, A=$C_6H_5CH_3$, B=$C_6H_5CO_2C_2H_5$ (25°C.).

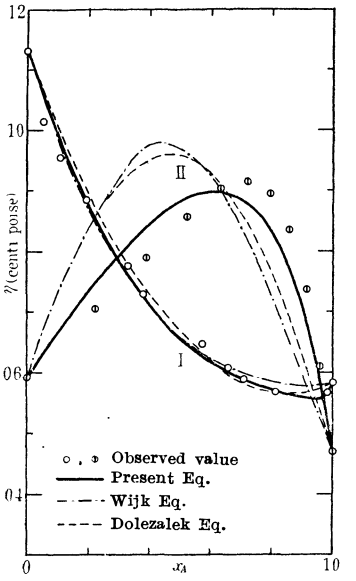

Fig. 3.—Observed and calculated values of η —3: Curve I, A=C_6H_6, B=C_2H_5OH(25°C.); Curve II, A=H_2O, B=C_2H_5OH(60°C.).

composed of liquids strongly associated becomes also less than a small percentage at a higher temperature (*cf.* Systs. C-1, 2 and 9~11). Consequently, the equation presented here seems to be better than the equation of either Dolezalek or of Wijk. However, our equation, as well as others, seems not to be applicable to the mixture in which the difference between η_A and η_B is very remarkable (for example, the mixture of water and glycerine).

Mutual Activation Energy of Flow

If we plot $\log \eta_{AB}$ against $1/T$, a straight line will be obtained according to the definition of η_{AB}, (7) or (14). The demand for this linearity is, indeed, satisfied by our results of calculation and, accordingly, we can estimate the value of ε_{AB} from the slope of this straight line. The values of ε_{AB} thus obtained are tabulated in Table 3. As is expected, ε_{AB} is approximately equal to $(\varepsilon_A+\varepsilon_B)/2$ in such systems as carbon tetrachloride+benzene or methyl alcohol+ethyl alcohol which are regarded as the so-called "ideal solutions." But in the mixture of water and alcohols, ε_{AB} is remarkably larger than ε_A or ε_B; ε of pure components of these systems being 3.30 kcal./mole for water, 2.51 for methyl alcohol and 3.52 for ethyl alcohol at about 60°C. This result may be related closely with the strong affinity of alcohols with water and with the remarkable volume contraction which results on mixing. In Table 3, the values of χ_{AB} calculated from (7) with (5) or

$$\chi_{AB}=kT\ln\{(v_Av_B)^{1/2}\eta_{AB}/h\} \qquad (16)$$

are also tabulated.

Table 3

Mutual Activation Energy of Flow.

Syst. No.*	ε_{AB}†	χ_{AB}(°C.)**	λ_{AB}	$\frac{\lambda_{AB}}{\varepsilon_{AB}}$	$\frac{\lambda_{AB}}{\chi_{AB}}$
A-3	2.69	3.13(60)	7.75	2.9	2.48
4	—	2.66(25)	6.50	—	2.44
B-5	1.19	2.47(35)	6.62	5.6	2.68
7	—	2.67(25)	6.70	—	2.51
8	3.46	—	—	—	—
9	—	2.86(25)	7.75	—	2.71
12	2.90	2.75(40)	8.73	3.0	3.12‡
14	1.98	—	—	—	—
C-1	4.52	2.82(60)	9.81	2.2	3.48‡
2	4.88	3.08(75)	10.22	2.1	3.32‡
3	5.18	—	—	—	—
5	2.20	2.76(30)	7.00	3.2	2.54
7	2.65	2.99(55)	9.50	3.6	3.51‡
9	5.31	—	—	—	—
10	2.86	—	—	—	—
11	3.98	—	—	—	—

* System No. is given in Tables 1 and 2.
** Temperatures at which χ_{AB} was calculated are put in parentheses.
† The unit of energies is kcal./mole.
‡ Compare with the values; $\lambda/\chi=4.98(H_2O)$, $3.78(CH_3OH)$ and $3.34(C_2H_5OH)$ at about 60°C.

In Table 3, the values of λ_{AB} calculated from (7) with (5) or

$$\lambda_{AB}=kT\ln\{(v_Av_B)^{1/2}\eta_{AB}/h\} \qquad (16)$$

are also tabulated.

Further, the empirical relations of ε and χ of pure liquid with its heat of vaporization, λ, proposed by Eyring seem to hold good for ε_{AB} and χ_{AB}, too, as shown in the table: that is,

$$\lambda_{AB}/\varepsilon_{AB}=3\sim4 \quad \text{and} \quad \lambda_{AB}/\chi_{AB}\fallingdotseq2.5, \qquad (17)$$

where λ_{AB} denote the "mutual heat of vaporization" and it can be obtained from the equations of vapor pressure P of binary liquid mixture,

$$P=x_A\varphi_AP_A+x_B\varphi_BP_B+2(x_Ax_B\varphi_A\varphi_B)^{1/2}P_{AB} \qquad (18)$$

with $P_{AB}=\text{constant}\times\exp(-\lambda_{AB}/kT)$.

In addition, the linearity of the $\log \eta_{AB}$ against $1/T$ is very useful for practical purposes, because we can calculate η_{AB} at any temperature so far as the values are known, at least, at two temperatures.

Activation Energy of Flow of Mixture

We can obtain the activation energy of flow of mixture ε from η_{obs} by

$$\varepsilon_{obs}=\left\{\frac{\partial\ln(\eta_{obs}v/T)}{\partial(1/kT)}\right\}_{x_A}. \qquad (19)$$

On the other hand, substituting (11) for (19) and performing the differentiation, we obtain the following expression for ε after some rewritings;

$$\varepsilon_{calc}=y_{AA}\varepsilon_A+y_{BB}\varepsilon_B+y_{AB}\varepsilon_{AB}, \qquad (20a)$$

with
$$y_{AA}=x_A\varphi_A\eta_A/\eta_{calc},$$
$$y_{BB}=x_B\varphi_B\eta_B/\eta_{calc} \qquad (20b)$$
and
$$y_{AB}=2(x_Ax_B\varphi_A\varphi_B)^{1/2}\eta_{AB}/\eta_{calc}.$$

Here y's are regarded as the occurring probabilities of molecular contacts of the indicated

(9) Eq. (18) will be published in future. As will be shown in our later paper, the value of λ_{AB} obtained from Eq. (18) agrees with the one estimated from the heat of mixing.

types. The comparison of ε_{calc} with ε_{obs} is given in Fig. 4. Here the mixture of carbon tetrachloride and benzene and that of water and ethyl alcohol are chosen as the examples of the ideal cases and non-ideal respectively. In this figure, the values calculated from the Wijk equation, (15) or

$$\varepsilon = x_A^2\varepsilon_A + x_B^2\varepsilon_B + 2x_Ax_B\varepsilon_{AB}, \qquad (21)$$

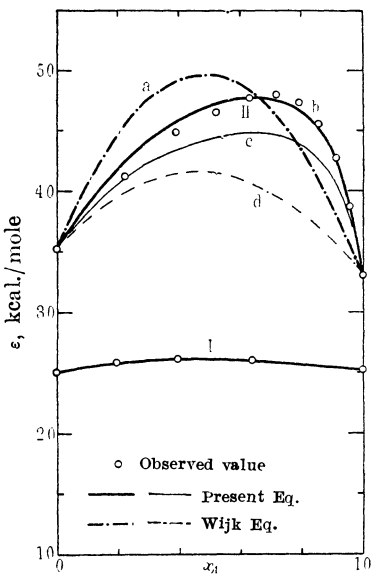

Fig. 4.—Observed and calculated values of ε: Curve I, A=CCl_4, B=C_6H_6, ε_{AB}=2.69 kcal./mole; Curve II, A=H_2O, B=C_2H_5OH (at about 60°C.), ε_{AB}=, (a), 6.50 (b), 5.30 (c and d) 4.88 kcal./mole.

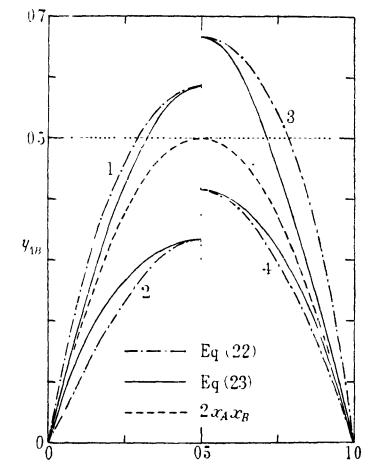

Fig. 5.—Occurring probabilities of A-B contact, y_{AB}: $\tau_A/\tau_{AB}=\tau_B/\tau_{AB}=1/\sqrt{2}$ (curve 1); 2 (curve 2); 1/2 (curve 3); $\sqrt{2}$ (curve 4). Eq. (23) nearly coincides with the Bethe-Fowler-Takagi approximation.

are also plotted for comparison's sake. Though in the former example, either (20) or (21) agree with ε_{obs} satisfactorily. In the latter, (21) used by Wijk does not agree with ε_{obs} even if the values of ε_{AB} were adjusted in any way. On the contrary, (20) agrees with ε_{obs} satisfactorily, if we adjust ε_{AB} so that ε_{calc} may agree with ε_{obs}. Though the values of ε_{AB} thus determined, 5.30 kcal./mole, is slightly different from that of ε_{AB} in Table 3, 4.88 kcal./mole, the inconsistency in this degree will be acceptable in such non-ideal systems as this example.

Now, let us examine the physical meaning of the assumption (6) used in order to derive Eq. (11). For that, it seems to be simplest to examine the meaning of y's which have been given by (20b). Substituting (1), (3), (6) and (7) into (20b), we obtain

$$\left.\begin{aligned} y_{AA} &= x_A^2\tau_A/(x_A^2\tau_A + x_B^2\tau_B \\ &\quad + 2x_Ax_B\tau_{AB}) = x_A^2\tau_A/\tau, \\ y_{BB} &= x_B^2\tau_B/\tau \end{aligned}\right\} \qquad (22)$$

and $y_{AB} = 2x_Ax_B\tau_{AB}/\tau$.

If the difference between τ_A and τ_B be not so remarkable, we can transform (22) to the following forms after some tolerable approximations:[10]

$$y_{AB} = 4x_Ax_B/(1+\beta) \quad \text{etc.}, \qquad (23a)$$

with $\beta \fallingdotseq [1+4x_Ax_B\{(\tau_A\tau_B/\tau_{AB}^2)-1\}]^{1/2}$. (23b)

These equations are to be compared with those of the Bethe-Fowler-Takagi (B-F-T) approximation for regular solutions.[11] That is, according to this approximation y's are, likewise, given by (23a) with

$$\beta = [1+4x_Ax_B\{\exp(\Delta\zeta/kT)-1\}]^{1/2}, \qquad (24)$$

where $\Delta\zeta$ denotes the increase of the free energy in the process,

$$\text{(A-A contact)} + \text{(B-B contact)} \rightarrow 2\times\text{(A-B contact)}.$$

Though (23b) and (24) seem to be slightly different, both expressions of β agree with

(10) Since the agreement of (22) with (23) is satisfactory as will be shown in Fig. 5, the rewriting from (22) to (23) seems to be reasonable.

(11) Ref. 7, p. 358; Y. Takagi, *Proc. Phys. Math. Soc. Japan*, **23**, 44 (1941).

(12) The free energies, ζ's of molecular contacts of the indicated types are given by

$\zeta_{AA} = (2\lambda_A/z) - (6kT/z)\ln\nu_A + (3kT/z)\ln(kT/2\pi m_A)$ etc., so far as the harmonic oscillator model of liquids is used (See, Ref. 7, p. 324). Since the last terms in the right hand side of these formulae are canceled in $\Delta\zeta = \zeta_{AA} + \zeta_{BB} - 2\zeta_{AB}$, we can obtain Eq. (25).

each other as shown in the followings. Using the harmonic oscillator model of liquids, we can put[2]

$$\exp\left(\frac{\Delta\zeta}{kT}\right)=\left(\frac{\nu_{AB}\nu_{BA}}{\nu_A\nu_B}\right)^{6/z} \exp\left\{\frac{\lambda_A+\lambda_B-2\lambda_{AB}}{kT}\left(\frac{2}{z}\right)\right\}, \quad (25)$$

where z is the number of the nearest neighbors. Then, using $z\fallingdotseq 8$, the result obtained by the x-ray diffraction, and the Eyring relation (17), we obtain

$$\exp\left(\frac{\Delta\zeta}{kT}\right)\fallingdotseq\left(\frac{\nu_{AB}\nu_{BA}}{\nu_A\nu_B}\right)^{3/4}\exp\left\{\frac{\varepsilon_A+\varepsilon_B-2\varepsilon_{AB}}{kT}\right\} \fallingdotseq\frac{\tau_A\tau_B}{\tau_{AB}^2}, \quad (26)$$

from (25) and (13), for $\nu_{AB}\nu_{BA}/\nu_A\nu_B\fallingdotseq 1$ in general. Accordingly, it can be concluded that (23), nearly, coincides with the B-F-T approximation. In Fig. 5, we show the values of y_{AB} calculated from (22) and (23) and the value of $2x_Ax_B$ for some values of τ's. In conclusion, our treatment involving (22) corresponds to the B-F-T approximation. From the fact mentioned here, the reason becomes obvious why Eq. (11) corresponding to (22) is better, as shown in before, than the Wijk equation corresponding to (21) or to the Bragg-Williams approximation. Furthermore, it will be one of the strong points of (22) in comparison with (21) that the effect of the difference between the sizes of constituent molecules is tacitly taken into consideration by the weight factor, τ's, having the values which are parallel with the molecular sizes in general.

Summary

A new semi-empirical equation for the viscosity coefficient of binary mixture of liquids, Eq. (11), has been derived and we have reached the conclusion that the assumption used in order to derive our equation corresponds to the Bethe-Fowler-Takagi approximation for regular assembly qualitatively. The equations for η and ε have been compared with the experimental values and satisfactory results have been obtained.

In conclusion, the authors would like to express their thanks to Prof. T. Watari and Mr. K. Maeda for some helpful discussions. This work was aided by a grant from the Ministry of Education.

Department of Industrial Chemistry, Faculty of Engineering, Kyoto University and Physicochemical Laboratory, Tokyo Institute of Technology

Note on the Ideal Mixture Law for Viscosity

By Tetsuya ISHIKAWA

(Received September 26, 1951)

Four interesting measurements on the viscosity of mixtures of the same crystal forms were seen in the recent literature, three[1] being those of ionic liquids with tests of Macleod's formula (1924), and one[2] that of the sodium and potassium system with test of Drucker-Kassel's formula (1911). According to their results these formulas hold good with at most 2 % and 1 % divergence respectively. Among the known formulas, however, there are two more worthy to be considered: the one is Kendall's formula (1913)[3]

$$\log \eta = (1-z_m)\log \eta_1 + z_m \log \eta_2$$

and the other is Ishikawa's formula (1929)[4]

$$\eta = \eta_1 + (\eta_2 - \eta_1)Kz_m/(1-z_m+Kz_m)$$

where η_1, η_2 and η denote the viscosities of component 1, 2 and mixture respectively, z_m molar fraction of component 2, K the characteristic constant which signifies, according to the latter's theory, the intensity of the molecular attraction field of component 2 relative to that of component 1.

Tests made with these four pairs are illustrated in tables, from Table 1 to Table 4, in which

(1) B. S. Harrap and E. Heymann, *Chem. Rev.*, **48**, 45 (1951).

(2) C. T. Ewing, J. A. Grand and R. R. Miller, *J. Am. Chem. Soc.*, **73**, 1168 (1951).

(3) J. Kendall, *Meddelanden f. K. Velensk, Novelinstituta*, **2**, No. 25, 1 (1913).

(4) T. Ishikawa, This Bulletin, **4**, 5 (1929).

only percentage deviations $100(\eta_{calc}-\eta_{obs})/\eta_{obs}$ are given for comparison of those obtained by the respective observers.

Table 1

AgBr (1) – AgCl (2), 500°C.[1]

z_m	Deviation, %		
	Macleod	Kendall	Ishikawa (K=1.21)
0.200	+0.5	+0.5	0
0.400	+0.5	0	0
0.599	+1	+0.5	0
0.732	−2	−0.5	−0.5

Table 2

$CdCl_2$ (1) – $CdBr_2$ (2), 600°C.[1]

z_m	Deviation, %		
	Macleod	Kendall	Ishikawa (K=0.82)
0.252	0	−0.5	−0.5
0.445	+1	+0.5	0
0.725	+0.5	+0.5	0

Table 3

$PbBr_2$ (1) – $PbCl_2$ (2), 510°C.[1]

z_m	Deviation, %		
	Macleod	Kendall	Ishikawa (K=0.33)
0.247	0	+3.5	−1
0.436	+1	+7.5	+0.5
0.769	−2	+9	+2

Table 4

Na (1) – K (2).[2]

z_m	°C.	Deviation, %		
		Drucker-Kassel	Kendall	Ishikawa (K=2.54)
0.214	103.7±0.2	−0.9	+6.6	−0.1
	121.5±0.2	−1.1	+6.1	−0.5
	147.0±0.2	−0.9	+6.0	−0.5
	167.4±0.2	−0.7	+5.9	−0.4
	192.8±0.2	−0.1	+6.4	+0.1
0.361	103.7±0.2	−0.5	+8.3	+0.3
	121.5±0.2	−0.4	+8.4	+0.2
	147.0±0.2	−0.6	+7.7	+0.2
	167.4±0.2	−0.2	+7.8	+0.0
	192.8±0.2	−0.2	+7.6	−0.1
0.683	103.7±0.2	+0.1	+6.5	+0.6
	121.5±0.2	−0.2	+6.3	+0.2
	147.0±0.2	−0.5	+5.6	−0.3
	167.4±0.2	−0.2	+5.8	−0.0
	192.8±0.2	−0.1	+5.7	0
Mean		−0.4	+6.7	±0.3

As seen from each table, the Kendall formula holds good for AgCl–AgBr and $CdCl_2$–$CdBr_2$ systems, but fails for $PbCl_2$–$PbBr_2$ and Na–K systems, whereas the Ishikawa formula holds good for all the pairs, although the constancy of K in $PbCl_2$–$PbBr_2$ system is somewhat doubtful, yet its superiority to other formulas may be accepted without hesitation.

For $PbCl_2$–$PbBr_2$ system, there exist two different opinions even in these years: Delgery[5] claimed the existence of a stable compound PbClBr and an unstable peritectic compound $PbBr^2$ $3PbCl_2$, but Calingaert, Lamb and Meyer[6] confirmed the former but denied the latter by thermal and x-ray diffraction analyses. The present viscosity analysis gives the result that K in $PbCl_2$(1)–$PbBr_2$(2) system takes a quite different value 3.0 (=1/0.33) as compared with K in AgCl(1)–AgBr(2) and $CdCl_2$(1)–$CdBr_2$(2) systems, taking 0.826 (=1/1.21) and 0.82 respectively.

For Na–K system, a peritectic melting compound Na_2K was confirmed recently by Mckisson and Bromley[7] from the measurement of heat formation. K of this system takes a unique value 2.54 throughout the observed temperature range.

Since K's in mixtures composed of like liquids differ not so much from unity,[8] K's in AgCl–AgBr and $CdCl_2$–$CdBr_2$ systems are regarded as being normal, but those in $PbCl_2$–$PbBr_2$ and Na–K systems as being abnormal. These anomalous values may clearly be explained by the supposition that the tendency of forming a peritectic compound $PbBr_2 3PbCl_2$ or Na_2K necessitates the activation of attraction field intensity of lead bromide or potassium to have nearly three times or two times that of its ordinary intensity respectively. These systems, therefore, belong to a quasi-ideal mixture. In fact, in Na–K system occurs slight volume contraction of the simplest form Δv (cc./g.)$=Cz(1-z)$ (z=weight fraction) on mixing, giving C 0.056, 0.051 and 0.048 at 103.7, 147.0 and 192.8 °C. respectively, which, though little in magnitude, suggests a compound of molecular ratio 2Na: K, if it forms.

Summary

Tests made with data in the recent literature show (1) that the Ishikawa formula is superior to the formulas of Macleod, Drucker-Kassel and Kendall which are often used as an ideal mixture law for viscosity, and (2) that the

(5) I. Delgery, *Compt. rend.*, **222**, 886 (1946); **223**, 401 (1946); **224**, 274, 915 (1947).

(6) G. Calingaert, F. W. Lamb and F. Meyer, *J. Am. Chem Soc.*, **71**, 3709 (1949).

(7) R. L. Mckisson and L. A. Bromley, *J. Am. Chem. Soc.*, **73**, 314 (1951).

(8) T. Ishikawa and T. Baba, This Bulletin, **11**, 64 (1936).

extraordinary values of K of his formula in $PbCl_2$–$PbBr_2$ and Na–K systems suggest the tendency of forming peritectic compounds of $PbBr_2 3PbCl_2$ and Na_2K respectively.

Sasebo Commercial Junior College
(Nagasaki Prefeotural), *Sasebo*

Surface Chemistry of Synthetic Protein Analogues. I. Surface Pressure-Area Relation of Synthetic Polypeptides as the Model of Proteins

By Toshizo ISEMURA and Kozo HAMAGUCHI

(Received October 8, 1951)

Introduction

Many investigations have been made of the monolayers of proteins at air-liquid or liquid-liquid interfaces to obtain some information about the nature of protein fiims.[1] The surface chemistry of proteins involves many problems to be solved, because of the fact that the proteins are of a rather complicated structure and consisted of various amino-acid residues which are not arranged in orderly manner with uniform distribution along the polypeptide chain. Recently, it became possible to synthesize simple protein analogues of the known structure and of the high molecular weight, by polymerization of N-carboxy-anhydride of α-amino acid.[2] It is well convinced that these synthetic protein analogues play a very important role as a model of natural protein, because of these simple constitutions having one or two known amino acids, though it is unfortunate that the molecular weight distribution is not so uniform as that of natural proteins. It is our aim to obtain some information of natural protein from the surface chemical study of these polymers and to approach to the structure of proteins.

Recently, some interesting studies by Ambrose,[3] Astbury[4] and their collabrators on the synthetic polypeptides by x-ray and infrared analysis have appeared. Whether the results obtained by the monolayer technique would coincide with these by x-ray and infrared data, or not, is also an interesting problem to be investigated.

The synthetic protein analogues examined in the present investigation were poly DL-α-aminocaproic, poly DL-α-aminocaprylic, poly DL-α-aminocapric, poly DL-α-aminolauric acid, and poly γ-methyl-L-glutamate. Poly ε-aminocaproic acid(amilan) was also examined in comparison with the polymers of α-amino acid.

At the first step, surface pressure-area (F-A) relations of the monolayers of these protein analogues on water were examined, and some results obtained were reported in the previous notes.[5],[6] It was found that the F-A curve of poly DL-α-aminocaproic acid which has shorter side chain and those given by natural proteins such as ovalbumin or pepsin resembled very closely in shape. The region which has a very high compressibility appeared in the F-A curves of the polypeptides of which side chains have more than six carbon atoms. It is believed that poly DL-α-aminocaproic, poly DL-α-aminocaprylic, poly DL-α-aminocapric, and poly DL-α-aminolauric acid have a structure of β-keratin type on the surface of water since the area which was found for every polymer to be in the closest packing of polypeptide backbone, was all 14.7 Å.^{2}/amino acid residue. This value is in good agreement with the area calculated by x-ray data for an

(1) J. S. Mitchell, *Trans. Faraday Soc.*, **33**, 1129 (1937); I. Langmuir and V. J. Schaefer, *Chem. Rev.*, **24**, 181 (1939).

(2) R. B. Woodward and C. H. Schramm, *J. Am. Chem. Soc.*, **69**, 1551 (1947); H. Tani, J. Noguchi, *et al.*, *Chem. High Polymers, Japan*, **8**, 51, 53, 57, 62, 65 (1951).

(3) E. J. Ambrose and W. E. Hanby, *Nature*, **163**, 483 (1949); C. H. Bamford, W. E. Hanby and F. Happey, *ibid.*, **164**, 138 (1949); C. H. Bamford, W. E. Hanby and F. Happey, *ibid.*, **164**, 752 (1949); A. Elliot and E. J. Ambrose, *ibid.*, **165**, 921 (1950); C. H. Bamford, W. E. Hanby and F. Happey, *ibid.*, **166**, 829 (1950).

(4) W. T. Astbury, C. E. Dagliesh, S. E. Darmon and G. B. B. M. Sutherland, *Nature*, **162**, 596 (1948); W. T. Astbury, *ibid.*, **163**, 722 (1949); W. T. Asthury, *ibid.*, **164**, 439 (1949).

(5) T. Isemura, K. Hamaguchi, H. Tani, J. Noguchi and H. Yuki, *Nature*, **168**, 165 (1951).

(6) T. Isemura and K. Hamaguchi, *Kagaku (Science)*, **22**, 87 (1952).

arrangement of β-configuration. Polyγ-methyl-L-glutamate occupied less area per residue than any other polypeptides. It may have a structure of α-keratin configuration. This supposition was comfirmed by the transformation of the film into a film constituted of the molecules of β-configuration by adding some acids to the substrate water.

Experimental

Experimental Method and Materials.—Surface pressure was registered by Sasaki's modification[7] of Harkins' method using the Wilhelmy balance.

The synthetic polypeptides used were prepared by Dr. H. Tani, Dr. J. Noguchi and their collabrators and the samples of amilan were presented by Toyo Rayon Co. The polypeptides were used without any further purification. Amilan was purified by the precipitation from the solution in formic acid by adding water.

Poly DL-α-aminocaproic, poly DL-α-aminocaprylic, poly DL-α-aminocapric, and poly DL-α-aminolauric acids were spread from benzene solution, poly γ-methyl-L-glutamate from pyrididine solution and amilan from a solution in a mixed solvent of cresol and benzene. The molecular weight of the poly DL α-aminolauric acid determined by the osmotic pressure measurement was 172,000. The molecular weight of poly α-aminocaproic acid by the surface technique was 1,060,000.

Results.—The F-A curves obtained with the five polypeptides described above on distilled water are shown in Figs. 1 and 2. The abscissa is the area (m.^{2}) per milligram of polypeptide in Fig. 1 and the area (Å.^{2}) per amino acid residue in Fig. 2. These curves were obtained for the films allowed to stand on water prior to the experiment for six minutes after spreading.

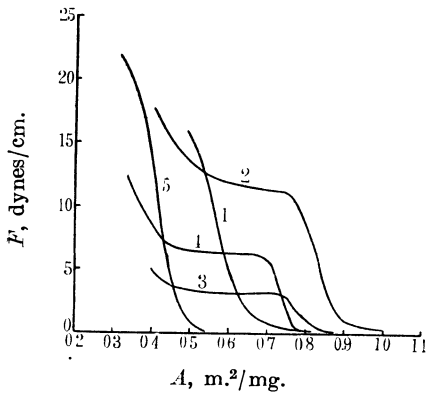

Fig. 1.—The surface pressure-area curves of polypeptide monolayers on distilled water (9°C.): Curve 1, poly DL-α-aminocaproic acid; curve 2, poly DL-α-aminocaprylic acid; curve 3, poly DL-α-aminocapric acid; curve 4, poly DL-α-aminolauric acid; curve 5, poly γ-methyl-L-glutamate.

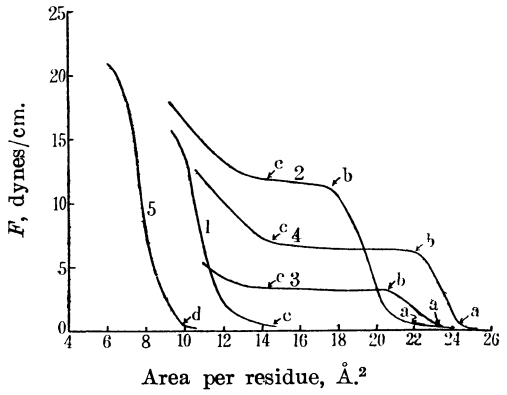

Fig. 2.—The surface pressure-area curves of polypeptide monolayers on distilled water (9°C.).

Poly DL-α-aminocaproic acid (curve 1) occupied the area of 0.68 m.^{2}/mg. (13 Å.^{2}/residue) at 1 dyne/cm., which is in good agreement with the area of 0.7 m.^{2}/mg. (about 14 Å.^{2}/residue) at 1 dyne for the egg albumin or pepsin.[8] The shape of the curve of this polymer was also very similar to that of these natural proteins.

The plateau which is a region of very high compressibility (from point b to c in Fig. 2), appeared in the F-A curves of poly DL-α-aminocaprylic (curve 2), poly DL-α-aminocapric (curve 3), and poly DL-α-aminolauric acid (curve 4). As far as our surface balance of hanging plate type was concerned, the plateau was not recognized for the curve of poly DL-α-aminocaproic acid, but was found to exist in very low pressure region (at about 0.05 dyne/cm.) by using the surface balance of Langmuir-Adam type which has the sensitivity of about 0.001 dyne/cm.

The areas at the points a, b, c, and d which are indicated by arrows for each curve in Fig. 2 are summarized in Table 1. The longer the side chain was, the larger the limiting area (at point a) became. The area at point c was almost the same irrespective of the monomer of α-amino acid. (about 14.7 Å.^{2}/residue). Poly γ-methyl-L-glutamate (curve 5) had a very small limiting area of 9.8 Å.^{2}/residue (at point d).

(7) T. Sasaki, *J. Chem. Soc. Japan*, **62**, 796 (1941).

(8) I. Langmuir and D. F. Waugh, *J. Am. Chem. Soc.*, **62**, 2771 (1940).

Table 1

Polypeptides	Side chain	Area, Å.²/residue Point a	b	c	d
α-Aminocaproic acid	$-(CH_2)_3CH_3$			14.6	
α-Aminocaprylic acid	$-(CH_2)_5CH_3$	22.0	18.0	14.7	
α-Aminocapric acid	$-(CH_2)_7CH_3$	23.0	21.0	14.8	
α-Aminolauric acid	$-(CH_2)_9CH_3$	24.2	22.2	14.7	
γ-methyl-L-glutamate	$-(CH_2)_2COOCH_3$				9.8

The *F-A* curves of poly DL-α-aminocaproic acid and poly γ-methyl-L-glutamate changed little with time after spreading, but the *F-A* curves of the other polypeptides which have longer side chains changed extremely with time. For instance, the effect of aging for poly DL-α-aminocaprylic and poly DL-α-aminolauric acid is shown in Figs. 3 and 4, respectively. The initial spreading concentrations of the former and the latter polymer were 0.51 and 0.48 mg./m.², respectively.

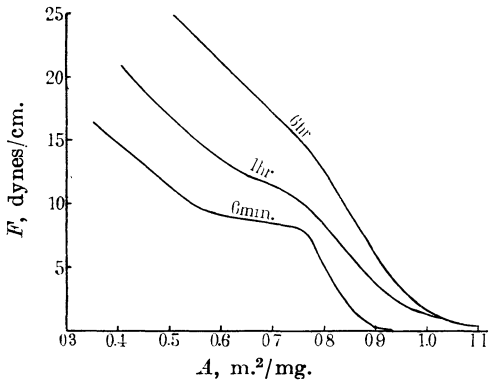

Fig. 3.—Poly DL-α-aminocaprylic acid aged on distilled water (16.5°C.).

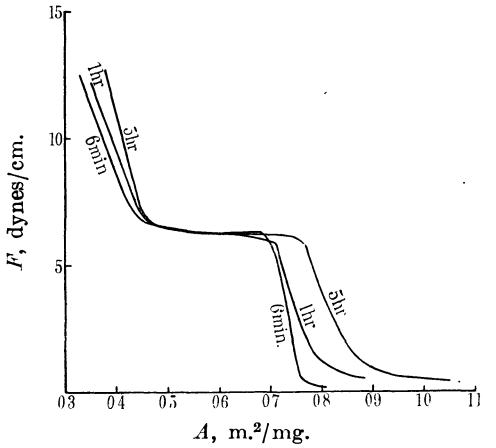

Fig. 4.—Poly DL-α-aminolauric acid aged on distilled water (9°C.).

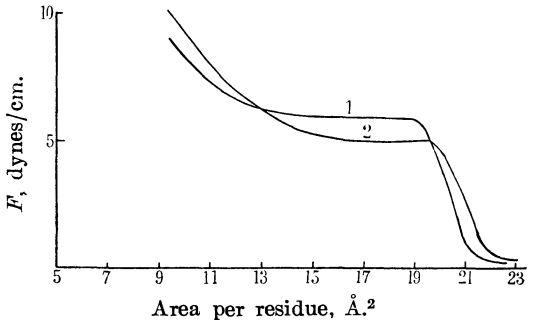

Fig. 5.—Effect of substrate on the acidity of monolayer of poly DL-α-aminocapric acid (21°C.): curve 1, on distilled water; curve 2, on 0.2 *M* formic acid.

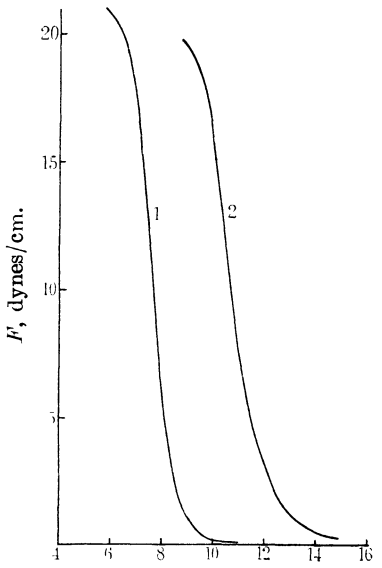

Fig. 6.—Effect of acidity of substrate on the monolayer of poly γ-methyl-L-glutamate (22°C.): curve 1, on distilled water; curve 2, on 0.02 *M* formic acid.

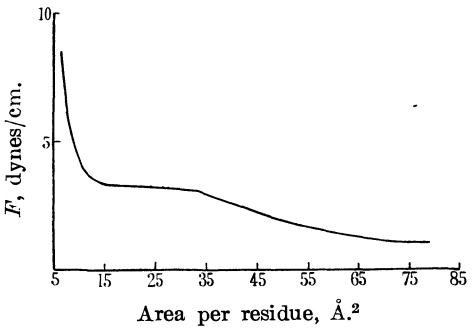

Fig. 7.—The surface pressure-area curve of poly ε-aminocaproic acid. (23°C.)

Acidic substrate exerted no detectable effect upon the monolayers of poly DL-α-aminocaprylic, poly DL-α-aminocapric and poly DL-α-aminolauric acid. For instance, the effect of 0.2 *M* formic acid on the monolayer of poly DL-α-aminocapric acid is shown in Fig. 5. The *F-A* curve of the monolayer on acidic substrate is shown by curve 2, together with the curve on distilled water (curve 1) in the figure.

On the other hand, when poly γ-methyl-L-glutamate was spread on acidic substrate, the limiting area was increased to larger area than on distilled water. Curve 2 in Fig. 6 shows *F-A* curve of the polymer on acidic substrate containing formic acid in concentration of 0.02 *M*. For comparison with the monolayer on acidic substrate, the curve of the monolayer on distilled water is shown by curve 1 in the figure. Using acetic or hydrochloric acid solution as substrate, the curves were practically the same as curve 2. The limiting area of the curve on these acid substrate was also 14.7 Å.^{2}/residue, corresponding to the area of the other polypeptides at point c in Table 1.

In Fig. 7, the *F-A* curve of amilan on distilled water is shown. The polymer of ε-amino acid gave the curve of an expanded type which was entirely different from those of the polymers of α-amino acid.

Discussion

As pointed out above, the *F-A* curve of poly DL-α-aminocaproic acid resembled those of natural proteins such as the egg albumin or pepsin, the reason of which may be that the carbon number of hydrocarbon side chain of the polymer (four) is very near to the average carbon number of side chain of natural proteins, that is, about three. The preliminary experiments on the surface viscosity of this polymer also bore a close resemblance to those of natural proteins.[9]

The plateau which is a region of very high compressibility was also found in the *F-A* curve of poly DL-α-aminocaproic acid at very low pressure. The results obtained by H. B. Bull from the experiments on the egg albumin[10] showed the existence of the plateau in very low pressure region. These facts also show the resemblance between the synthetic polypeptides having shorter side chains and natural proteins.

The curves for the other polypeptides having longer side chains had a plateau in higher pressure region, which is not found in the case of natural proteins. This fact may be attributed to the absence of longer side chains with more than six carbon atoms on the average.

At areas larger than that indicated by point a (Fig. 2), the polypeptide molecules are spread with chains flat on the surface. Between points a and b on the *F-A* curves, the surface pressure would be exerted mainly by the action of side chains. Surface viscosity measurement showed that the viscosity in this region was as large as that of the state of gel. From point b to c, the surface pressure was kept practically constant. It suggests that the molecules of polypeptide would be reorientated in this region by compression and the side chains would be compressed away from the surface, so that they might be forced upwards or downwards into the water. Thus, at point c, a film which is arranged in close packed polypeptide backbone of β-configuration would be formed, since the area at this point for every polymer was found to be 14.7 Å.^{2}/amino acid residue, and this value corresponds to the area calculated with the x-ray data for an arrangement of β-configuration. When the surface viscosity against area curve was registered for the monolayer of poly DL-α-aminocaproic acid, the sudden increase in slope of the curve occurred at 14.7 Å.^{2}/residue. The same value was found by Cumper and Alexander[11] from their investigation on the surface viscosity for polyalanine (at air-liquid and liquid-liquid interfaces) and polyphenylalanine (at air-liquid interface). From point c, the pressure was again increased by further compression. It might be considered that segments of the chain might be left the surface.

Polyorganosiloxanes,[12] Buna N,[13] and long chain urea derivatives[14] give the similar *F-A* curves as those of polypeptides with longer side chains, which have the plateau in the curve. The effect of temperature on these monolayers is also similar to that on the polypeptides. The higher the temperature of substrate is, the situation of the plateau passes to the lower pressure region. Fox, Taylor and Zisman[12] characterized the appearance of this plateau as the process of coiling of high linear

(9) M. Joly, *Research*, Supplement, "Surface Chemistry," Butterworth, 1949, p. 157.

(10) H. B. Bull, *J. Biol. Chem.*, **185**, 27 (1950).

(11) C. W. N. Cumper and A. E. Alexander, *Trans. Faraday Soc.*, **46**, 235 (1950).

(12) H. A. Fox, P. W. Taylor and W. A. Zisman, *Ind. Eng. Chem.*, **39**, 1401 (1947).

(13) K. Suzuki, *Koshitugaku-Ronso (Discussions Colloid Sci., Japan)*, **1**, 63 (1947).

(14) J. Glazer and A. E. Alexander, *Trans. Faraday Soc.*, **47**, 401 (1951).

polymer molecule by compression on the surface of water. Saraswat and Kalyanasundarm[15] presented the same idea. As far as the synthetic polypeptides are concerned, however, the process of coiling of the linear molecule would not be considered as the reason of the appearance of the plateau, because, contrary to polyorganosiloxanes, the longer the side chains of the polypeptides are, the more marked the existence of the plateau became and it would be impossible for polypeptide molecules of which side chains have six, eight, or ten carbon atoms to be coiled by compression. Merely, from the resemblance of the shape of *F-A* curves, it can hardly be concluded that the properties of the monolayers of polyorganosiloxanes and of polypeptides would be the same. From both points of view of chemical structure in which —CO—NH— group is contained and of the behaviors of monolayers, the most closely related films to that of polypeptide may be the films of hexadecyl and octadecyl urea which wer einvestigated by Glazer and Alexander[14]. The shape of *F-A* curves of these urea derivatives resembles closely those of polypeptides, and also it is the same for both substances that the physical state from point a to b is gel or solid. However, that the physical state of higher pressure region above point c is liquid in the case of urea derivatives, is different from those of polypeptides. They considered in the case of urea derivatives that the molecules are combined by hydrogen bonding with each other in the region from point a to b, and that in higher pressure region above point c, no inter-chain hydrogen bonding exists. Therefore, the appearance of the plateau was considered to be due to the breaking of hydrogen bonds. In the monolayer of synthetic polypeptides, however, there occurred reorientation of the molecules in the region from point b to c, being accompanied by the formation of inter-chain hydrogen bonds. The molecules are bound strongly by inter-chain hydrogen bond if the monolayer was sufficiently compressed, so that polypeptide could be drawn out as a string from the surface of water by a glass rod. This is in good agreement with the experimental results that the area at point c at which inter-chain hydrogen bonding may be completed are always 14.7 Å.^{2}/amino acid residue, regardless of the lengths of the side chains.

As pointed out above, the monolayer of poly γ-methyl-L-glutamate gave much smaller limiting area than the other polypeptides. It gave the limiting area of 9.8 Å.^{2}/residue on distilled water but this limiting area was increased to 14.7 Å.^{2} on acidic substrate. The difference of the limiting area dependent on the nature of the substrate may be due to the change of the configuration of the molecule. Some considerations were presented by us previously.[6]

It is known from the results of infra-red analyis by Ambrose *et al.* that poly γ-methyl-L-glutamate has a structure of α-configuration and is not transformed to β-configuration even if it is forcibly stretched.[16] Protein molecules having a folded structure would be generally unfolded on the surface of water probably transforming to β-type, since interface such as the surface of water exerts a strong force on the molecules. If the model of α-configuration for proteins, presented by Shimanouchi and Mizushima[17] and by Ambrose *et al.*[16] independently, is accepted, the area per amino acid residue when molecules are arranged in α-configuration must be two thirds of the area occupied by the molecule arranged in β-configuration. On the other hand, if the model of α-configuration presented by Astburty,[18] is accepted, the area occupied by the molecule of α-type must be half the area in the case of β-configuration. The experimental results obtained with this polymer are in good agreement with the former case (14.7 Å.^{2}×2/3=9.8 Å.^{2}). It is known that poly γ-methyl-L-glutamate having α-configuration is transformed to β-configuration by the treatment with formic or acetic acid.[19] When poly γ-methyl-L-glutamate was spread on the substrate containing hydrochloric, formic, or acetic acid, the surface pressure against the area curve shown by curve 2 in Fig. 6 was obtained, and the limiting area became to 14.7 Å.^{2}/residue, *i. e.*, the limiting area of the polypeptides having β-configuration. These results correspond to the α→β transformation due to the destruction of the intra-chain hydrogen bonding by the interaction of the polypeptide with the acids in substrate. The results obtained with the surface viscosity measurement, the details of which will be reported elsewhere, led to the same conclusion. On distilled water the surface viscosity of the monolayer formed by polypeptide of α-configuration is considerably greater than that of proteins even at lower pressure region and suddenly increased at the area of about 9.8

(15) H. C. Saraswat and A. Kalyanasundarm, *J. Polymer Sci.*, **6**, 82 (1951).

(16) E. J. Ambrose and W. E. Hanby, *Nature*, **163**, 483 (1949).

(17) T. Shimanouchi, and S. Mizushima, *Science (Japan)*, **17**, 24, 52 (1947); This Bulletin, **21**, 1 (1948).

(18) W. T. Astbury and F. O. Bell, *Nature*, **147**, 696 (1941).

(19) C. H. Bamford, W. E. Hanby and F. Happey, *Nature*, **166**, 829 (1950).

Å.^{2}/residue. On acidic substrate, however, the surface viscosity increased steeply at about 14.7 Å.^{2}/residue and at the area larger than this, the polymer exhibited the viscosity of the same order of magnitude as that of any other polypeptides. Moreover, acidic substrates exerted little effect on the monolayer of poly DL-α-aminocapric acid, which spread as a film of β-configuration as shown in Fig. 5. These facts must be the surface-chemical indications of the $\alpha \rightarrow \beta$ transformation of poly γ-methyl-L-glutamate.

The reason for the change of *F-A* curve of the monolayers of polypeptides having longer side chains as a function of time after spreading is not yet clear. This phenomena, however, may probably be caused by the decrease of the entanglement of the side chains of polypeptide molecules. The effect of aging on the monolayer of polyorganosiloxanes observed by Fox, Solomon and Zisman[20] are apparently analogous to those of the polypeptides. They considered that this effect may be due to the hydrolysis of polyorganosiloxanes by the interaction with substrate. The reason for the aging considered by them, however, may not be valid for the present case.

As previously mentioned, the behaviors of monolayers of the synthetic polypeptides are much influenced by inter and intra-chain hydrogen bonding. From this reason, the monolayer of poly ε-aminocaproic acid, was also examined, in which five methylene groups are placed between NH- and CO-groups. The *F-A* curve of this polymer is of very expanded type and is entirely different from that of the polymers of α-amino acid. It is concluded from this point of view that the poly ε-aminocaproic acid is inadequate as a model of natural proteins. Detailed consideration about this polymer will be reported elsewhere.

Summary

The surface pressure against area (*F-A*) curves of the monolayers of poly-DL-α-aminocaproic, poly DL-α-aminocaprylic, poly DL-α-aminocapric, poly DL-α-aminolauric acids, poly γ-methyl-L-glutamate and poly ε-aminocaproic acid (amilan) was measured. The results obtained were as follows:

(1) The *F-A* curve of poly DL-α-aminocaproic acid having four carbon atoms in the side chain resembled in shape very closely to those given by natural proteins such as the egg albumin or pepsin. This fact is due to the resemblance of the carbon number in the side chains of both of the polypeptide and proteins.

(2) The plateau which is a region of very high compressibility appeared in the *F-A* curves of the polypeptides having more than six carbon atoms in the side chains. The curves of these polypeptides were entirely different from those of natural proteins.

(3) The area per amino acid which was found for every polypeptide to be in the closest packing of polypeptide backbone was all 14.7 Å.^{2} This value is in good agreement with the area calculated from x-ray data for an arrangement of β-keratin configuration.

(4) Poly γ-methyl-L-glutamate occupied the limiting area of 9.8 Å.^{2}/amino acid residue on distilled water. This value can be sufficiently accounted for, if this polymer has a structure of α-configuration on water surface and the model of α-keratin configuration presented by Shimanouchi and Mizushima and by Ambrose *et al.* is accepted. On substrates containing hydrochloric, formic, or acetic acid, however, this polypeptide occupied the limiting area of 14.7 Å.^{2}/residue, this value corresponding to the area of the other polypeptides which are arranged in close packed β-configuration. The $\alpha \rightarrow \beta$ transformation of this polypeptide could be demonstrated by monolayer technique.

(5) The monolayer of the polymer of ε-aminocaproic acid is inadequate as a model of protein films.

The authors wish to express their sincere thanks to Dr. H. Tani in Faculty of Science, Osaka University and to Dr. J. Noguchi at Kanazawa University who gave them the valuable samples of synthetic polypeptides. A part of the expense for the experiment has been defrayed from a grant given by the Ministry of Education, to which the authors' thanks are due.

The Institute of Scientific and Industrial Research, Osaka University, Sakai, Osaka

(20) H. W. Fox, E. M. Solomon and W. A. Zisman, *J. Phys. Coll. Chem.*, **54**, 723 (1950).

The Relation between the Geometrical Configurations of Inorganic Complexes and their Absorption Bands. II.[1] The Configurations of Two Isomers of Sodium Disulfono-tetrammine-cobaltiate

By Yoichi SHIMURA

(Received October 9, 1951)

The two isomers of $Na[Co(NH_3)_4(SO_3)_2]$ were first prepared by Hofmann and Jenny,[2] who designated a brown, more insoluble dihydrate as *cis*-form and another golden yellow, more soluble tetrahydrate as *trans*-form. But this assignment was unreliable, since it was deduced from an uncertain analogy with two isomers of dinitro-tetrammine-cobalt(III) salt.

As will be shown in this report, however, the spectral data prove that the brown salt is *trans*-isomer and the golden yellow salt *cis*-isomer. There is, of course, a possibility of other isomerism, *i. e.*, sulfono-sulfito isomerism, which corresponds to nitro-nitrito isomerism of the complexes containing some NO_2^--radicals. In such case, the difference between both isomers consists in the difference of the atom which combines directly with the central cobalt (III) ion: in sulfono-isomer the S-atom of $SO_3^=$-radical is bound to the cobalt and in sulfito-isomer the O-atom is bound to it. But the spectral data exclude this possibility as will be seen later.

Results and Discussion

The absorption spectra of the two salts were measured at the spectral region from 55 to 125×10^{13}/sec. in 3% aqueous solutions of NH_3. The absorption curves are shown in Fig. 1.

The brown salt has three absorption maxima in this region and the yellow salt only two maxima. It has been well known[3] that the complex ions with a pair or pairs of negative ligands in *trans*-positions have the third absorption bands, which are situated almost always in the region $110\text{–}120\times10^{13}$/sec. for Co (III) or Cr (III) complex salts. Accordingly, the brown salt which has a third band at 113.6×10^{13}/sec. is *trans*-isomer concerning the positions of $SO_3^=$-radicals, and the yellow salt which has no absorption band in the region of $110\text{–}120\times10^{13}$/sec. is *cis*-isomer.

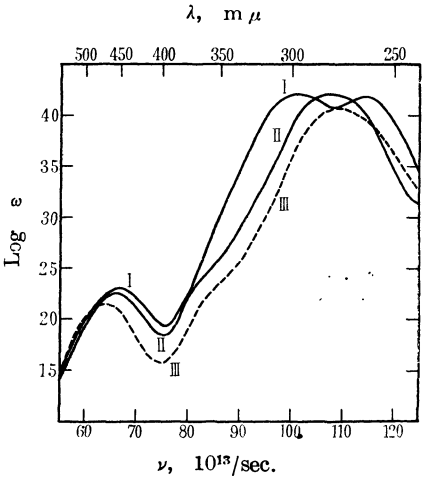

Fig. 1.—Absorption spectra of: I, brown salt, $Na[Co(NH_3)_4(SO_3)_2]\cdot2H_2O$ (*trans*) in 3% NH_3 aq.; II, golden yellow salt, $Na[Co(NH_3)_4(SO_3)_2]\cdot4H_2O$ (*cis*) in 3% NH_3 aq.; III, $[Co(NH_3)_5SO_3]Cl$ (Kiss and Czeglédy).

The larger absorption bands, which are distributed at 101.0×10^{13}/sec. for *trans*-compound and at 107.8×10^{13}/sec. for *cis*-compound, are the "$SO_3^=$-specific absorption bands" due to the coördinated $SO_3^=$-radicals. The absorption spectra of $[Co(NH_3)_5SO_3]Cl$ (Fig. 1, Curve III) and $Na_5[Co(CN)_4(SO_3)_2]$, which have been reported by Kiss and his co-workers,[4],[5] have also the similar $SO_3^=$-specific bands.

The $SO_3^=$-specific band of the *trans*-salt is more bathochromic than that of the *cis*-salt. In a previous paper,[1] the author has pointed out that the rhodanato- or nitro-specific bands

(1) Part I of this report: Y. Shimura, *J. Am. Chem. Soc.*, **73**, 5079 (1951).
(2) K. A. Hofmann and A. Jenny, *Ber.*, **34**, 3855 (1901).
(3) R. Tsuchida, This Bulletin, **13**, 388, 433 (1938).
(4) Á. v. Kiss and D. v. Czeglédy, *Z. anorg. Chem.*, **235**, 407 (1938).
(5) Á. v. Kiss, G. Auer and E. Major, *ibid.*, **246**, 28 (1941).

Table 1

First Band of $[Co(NH_3)_4A_2]$

Spectrochemical series of ligands	Complex ion	Position of first band, 10^{13}/sec.	Ref.
NO_2^-	*trans*-$[Co(NH_3)_4(NO_2)_2]^+$	68.2,[a] 68.9	(6), (7)
	cis-$[Co(NH_3)_4(NO_2)_2]^+$	67.0,[a] 69.0	(6), (7)
$SO_3^=$	*trans*-$[Co(NH_3)_4(SO_3)_2]^-$	66.6 [b]	
	cis-$[Co(NH_3)_4(SO_3)_2]^-$	65.9 [b]	
NH_3	$[Co(NH_3)_4(NH_3)_2]^{3+}$	63.4	(7)
H_2O	$[Co(NH_3)_4(H_2O)_2]^{3+}$	60.0	(8)
$C_2O_4^=$	$[Co(NH_3)_4C_2O_4]^+$	58.8	(7)
$CO_3^=$	$[Co(NH_3)_4CO_3]^+$	58.4	(7)
Cl^-	*trans*-$[Co(NH_3)_4Cl_2]^+$	<50	(8)

(a) in methanol-water solution. (b) in 3% NH_3 aq.

of *trans*-forms of Co(III) complexes have the longer wave-lengths than those of the *cis*-forms. Now it is recognized that such regularity is also true for the $SO_3^=$-specific absorption bands.

It has been shown by Tsuchida[3] that the near infra-red, the visible and the ultra-violet absorption bands of the complex salts are classified by their origins into the first, second, third and specific absorption bands. As is clear from Fig. 1, each of the isomers has the first band, but the second bands are inexplicit, since those are hidden under the larger $SO_3^=$-specific bands. The first band of the *trans*-salt is slightly shifted to the shorter wave-length than that of the *cis*-salt. In this connection, the relationship of the first band to the *cis-trans* isomerism will be discussed in the third report of this series. A small inflexion of the absorption curve of the *cis*-form at about 82×10^{13}/sec. is attributed to the second band. A similar hump is found in the absorption curve of the pentammine salt.

To determine the position of $SO_3^=$-radical on the spectrochemical series,[3] $[Co(NH_3)_4A_2]$ type complex ions (A = a molecule or a negative ion) were arranged in Table 1 in the order of frequencies of their first bands. From the table, $SO_3^=$-radical is located between NO_2^- and NH_3 on the series. This fact indicates that $SO_3^=$-radical coördinates around the central Co(III) ion by the lone pair of electrons of its S-atom, since it is expected that if $SO_3^=$-radical is bound to cobalt by O-atom, its position on the series should be behind NH_3. For instance, NO_2^--radical is ahead of NH_3 on the series when it coördinates by its lone pair electrons of N-atom, while it is behind NH_3 when it coördinates by O-atom forming the nitrito-complexes. The *cis*- and *trans*-salts studied in this paper, therefore, should be named sodium disulfono-tetrammine-cobaltiate, instead of disulfito-tetrammine-cobaltiate.

Moreover, the above discussion is confirmed from the following consideration. The absorption spectrum of a free $SO_3^=$-ion has a maximum at 100×10^{13}/sec.[4] All of the $SO_3^=$-specific bands of the complexes given in Fig. 1, are distributed in the more hypsochromic region than the absorption maximum of the free $SO_3^=$-ion. This shows that the coördinated $SO_3^=$-radical is more stable than a free $SO_3^=$-ion. $SO_3^=$-ion has a pyramidal structure, in which 3 $O^=$-ions and a lone pair of electrons are bound tetrahedrally around the central sulfur ion as $\left[\begin{array}{c} O \\ | \\ :S-O \\ | \\ O \end{array}\right]^=$, whilst this lone pair of S-atom is utilized in sulfono-Co (III) complexes, by which the structure should be compared to a sulfate type, *i. e.*, $\left[\begin{array}{c} O \\ | \\ Co-S-O \\ | \\ O \end{array}\right]$. In this manner, the sulfono-radical in coördination is more symmetrical and more stable than a free $SO_3^=$-radical. Thus the hypsochromic shift of the absorption band of $SO_3^=$ is observed. If the radical is coördinated by O-atom as $\begin{array}{c} Co-O \\ \diagdown \\ \quad S \quad : \\ \diagup \quad \diagdown \\ O \quad\quad O \end{array}$, this sulfito-radical in coördination becomes more unstable than a single $SO_3^=$-ion and in consequence the "sulfito-specific band" should appear in the long wave-length side as compared with the absorption maximum of a free $SO_3^=$-ion. Therefore, the specific bands given in Table

(6) F. Basolo, *J. Am. Chem. Soc.*, **72**, 4393 (1950).
(7) H. Kuroya, *J. Inst. Polytech., Osaka City Univ.*, **1**, No. 1, Ser. C, 29 (1950).
(8) R. Tsuchida, This Bulletin, **11**, 721 (1936).

2a, are undoubtedly the "sulfono-specific bands", and these salts are the disulfono-tetrammine- or sulfono-pentammine-cobaltiate. This is also clear from comparing the Table 2a with Table 2b.

Table 2

a: Position of Sulfono- or Sulfitoo-specific Absorption Band

	$\times 10^{13}$/sec.	Ref.
Sulfito-specific band	(smaller than 100)	
Absorption maximum of a free $SO_3^{=}$-ion	100(log ε=1.0)	(4)
Sulfon-specific band:		
trans-Na[Co(NH$_3$)$_4$(SO$_3$)$_2$]	101.0(log ε=4.22)	
cis-Na[Co(NH$_3$)$_4$(SO$_3$)$_2$]	107.8(log ε=4.21)	
[Co(NH$_3$)$_5$SO$_3$]Cl	109.5(log ε=4.08)	(4)

b: Position of Nitro- or Nitrito-specific Absorption Band

	$\times 10^{13}$/sec.	Ref.
Nitrito-specific band	83–84	(7)
Absorption maximum of a free NO_2^--ion	84.5(log ε=1.3)	(9)
Nitro-specific band:		
trans-[Co(NH$_3$)$_4$(NO$_2$)$_2$]Cl	86.8(log ε=3.90)	(7)
cis-[Co(NH$_3$)$_4$(NO$_2$)$_2$]NO$_3$	91.5(log ε=3.90)	(7)
[Co(NH$_3$)$_5$NO$_2$]SO$_4$	91.3(log ε=3.57)	(7)

Structure of $NH_4[Co(NH_3)_4(SO_3)_2]\cdot 3H_2O$— Two isomers of $NH_4[Co(NH_3)_4(SO_3)_2]$ have also been known, *i. e.*, a dark brown trihydrate and other reddish brown tetrahydrate. According to Hofmann and Jenny,[2] the dark brown isomer corresponds to the brown sodium salt and the reddish brown isomer to the golden yellow sodium salt. From the data of the photochemical decompositions of the salts, Schwarz and Tede[10] supported the theory that the dark brown salt is *cis*-isomer and the reddish brown salt is *trans*-isomer. Klement,[11] and Bailar and Peppard[12] also concluded, from the studies of reactions starting from the dark brown trihydrate, that the salt has two $SO_3^{=}$-groups in *cis*-positions. But the conclusions are not very reliable, since some rearrangements of ligands might have taken place in the course of such reactions.

The absorption spectrum of the dark brown isomer, however, is almost identical to that of the brown sodium salt (Table 3). This suggests that the salt is ammonium *trans*-disulfono-tetrammine-cobaltiate, although it is contrary to the several investigators' assignments of *cis*-configuration, and to solve this contradiction, it is hoped that the detailed reaction mechanism of the salt will be studied.

Experimental

Materials—*trans*-Na[Co(NH$_3$)$_4$(SO$_3$)$_2$]·2H$_2$O(brown salt) and *cis*-Na[Co(NH$_3$)$_4$(SO$_3$)$_2$]·4H$_2$O (golden yellow salt) were partly prepared by the method of Hofmann and Jenny,[2] and partly by a modification of that as follows: 21 grams of anhydrous cobaltous carbonate were dissolved in 250 ml. of *ca.* 30% acetic acid and mixed with 250 ml. of 28% NH_3 aq. A vigorous stream of air was drawn through the solution for 24 hours. Through the resultant solution gaseous sulfur dioxide was passed until a considerable amount of brownish orange precipitates appeared. After removal of the precipitates, a mixture of 38 grams sodium bisulfite dissolved in 100 ml. of water and 100 ml. of 28% NH_3 aq. was added to the filtrate. Leaving the mixture for 4 hours at room temperature, the precipitated dark yellow powder was removed by filtration. The filtrate, on cooling in water for 6 hours, precipitated the brown crystals of *trans*-Na[Co(NH$_3$)$_4$(SO$_3$)$_2$]·2H$_2$O. Then it precipitated, by cooling in ice for 10 hours, first a little amount of *cis-trans* mixtures and then the almost pure golden yellow crystals of *cis*-Na[Co(NH$_3$)$_4$(SO$_3$)$_2$]·4H$_2$O. The rough products of both the isomers were recrystallized from concentrated aqueous solutions by addition of 95% methanol. These were washed by methanol and dried in air. The absorption spectra of the two salts which were obtained by the above method com-

Table 3

Absorption Maxima of Three Disulfono-complexes

Complex salt	First band		Second band		Third band		Sulfono-specific band	
	ν_1, 10^{13}/sec.	log ε$_1$	ν_2, 10^{13}/sec.	log ε$_2$	ν_3, 10^{13}/sec.	log ε$_3$	ν_s, 10^{13}/sec.	log ε$_s$
trans-Na[Co(NH$_3$)$_4$(SO$_3$)$_2$]·2H$_2$O (brown salt)	66.6	2.32	?		113.6	4.19	101.0	4.22
cis-Na[Co(NH$_3$)$_4$(SO$_3$)$_2$]·4H$_2$O (golden yellow salt)	65.9	2.26	?		——	——	107.8	4.21
NH$_4$[Co(NH$_3$)$_4$(SO$_3$)$_2$]·3H$_2$O (dark brown form)	66.6	2.35	?		114.2	4.20	101.2	4.22

(9) H. Kuroya and R. Tsuchida, *J. Chem. Soc. Japan*, **59**, 1142 (1938).
(10) R. Schwarz and K. Tede, *Ber.*, **60**, 63 (1927).
(11) R. Klement, *Z. anorg. Chem.*, **150**, 117 (1926).
(12) J. C. Bailar, Jr. and D. F. Peppard, *J. Am. Chem. Soc.*, **62**, 105 (1940).

pletely accord with those of the salts obtained by the original direction of Hofmann and Jenny.

The dark brown form of ammonium disulfonotetrammine-cobaltiate, $NH_4[Co(NH_3)_4(SO_3)_2]\cdot 3H_2O$, was prepared by the method of 'Bailar and Peppard.[12]

Spectrographic Measurements—The formal extinction coefficient ε was calculated from the equation: $I=I_0\times 10^{-\varepsilon cd}$, where c is the concentration of the complex ion in gram-ion per liter and d the thickness of the layer in cm. The measurements were made in 3% aqueous solutions of NH_3, because aqueous solutions of the disulfono-complexes because turbid when allowed to stand for about 30 minutes in an open place, while in 3% NH_3 aq. the clearness could be kept almost perfectly for a long time. The comparison cell was also filled with 3% NH_3 aq. Measurements were done at room temperature, with concentrations of 2.5×10^{-3} and 1.0×10^{-4} gram-ion per liter and with varying thickness from 5 to 1 cm.

Summary

The visible and ultra-violet absorption spectra of $Na[Co(NH_3)_4(SO_3)_2]\cdot 2H_2O$ (brown salt) and $Na[Co(NH_3)_4(SO_3)_2]\cdot 4H_2O$ (yellow salt) have been measured. The results have proved that the $SO_3^=$-radical coördinates around the central cobalt (III) ion by the lone pair electrons of its sulfur atom, and that the brown salt has *trans*-configuration concerning the positions of the $SO_3^=$-radicals and the yellow salt *cis*-configuration.

The absorption spectrum of $NH_4[Co(NH_3)_4(SO_3)_2]\cdot 3H_2O$ (dark brown form) has also been studied and it has been assumed that the salt is *trans*-isomer contrary to several investigators' assignments of *cis*-structure.

The author expresses sincere thanks to Professor R. Tsuchida for his kind advice and encouragement.

Department of Chemistry, Faculty of Science, Osaka University, Osaka

The Relation between the Geometrical Configurations of Inorganic Complexes and their Absorption Bands. III.[1] A General Rule for the First and Second Bands of Co (III) Complexes

By Yoichi SHIMURA

(Received October 12, 1951)

Introduction

Many data have been reported in scientific literature about the absorption spectra of the geometrical isomers of Co(III) complex salts, but the relation between the *cis-trans* isomerism of the complexes and their absorption bands has not been completely clarified. It is well known that the visible and ultra-violet absorption bands of Co(III) complexes consist of the first, second, third and some other specific bands. The relations of these bands to the geometrical configurations, which have already been offered by some authors, are summarized as follows.

(1) **Third band.**—According to Shibata-Tsuchida's *trans*-anions hypothesis,[2] the Co(III) complexes which contain a pair or pairs of negative ligands in *trans*-positions are expected to have a third band at the region of 110-120 $\times 10^{13}$/sec. More recently, Basolo[3] reported the third bands of some *cis*-anions complexes in the shorter wave-lengths than the corresponding *trans*-isomers. These facts are applicable to the configurational determination of the complex salt.

(2) **Specific bands.**—The bands are due to the special ligands in the coördination sphere. In the previous reports,[4],[1] the author has shown that the nitro-, rhodanato- and sulfono-

(1) Part II of this report, Y. Shimura, This Bulletin, **25**, 46 (1952).

(2) R. Tsuchida, *ibid.*, **13**, 388, 436 (1938).
(3) F. Basolo, *J. Am. Chem. Soc.*, **72**, 4393 (1950).
(4) Y. Shimura, *ibid.*, **73**, 5079 (1951).

specific bands of the *trans*-isomers of Co(III) complexes have always the longer wave-lengths than those of the *cis*-forms. This relationship is also useful for the configurational determination of complex salt.

(3) **First band.**—The band is always in the visible region for Co(III) complexes and the color of the complex salt is due to the band. It has frequently been stated that the *cis*-isomers are more highly colored than the *trans*-isomers, but this rule is not reliable since many exceptions are known.

(4) **Second band.**—According to Tsuchida,[2] this band, which appears in the near ultra-violet region for Co(III) complexes, gives a measure of stability of the complex. Basolo[3] stated that the second band of *cis*-form is shifted towards the shorter wave-length as compared with that of *trans*-form, even though his "second band" is confused with the nitro- or rhodanato-specific band.

At the same time, Basolo assumed that whenever the stability differences of stereoisomers are sufficiently large to cause a shift in the absorption band positions, then the one that absorbs at the shorter wave-length is the *cis*-isomer. But it must be noticed here that in fact the first bands of *trans*-compounds containing some nitro- or sulfon-radicals are almost always shifted slightly more towards the shorter wave-lengths than the corresponding *cis*-compounds.

Thus, the relation of the third and some

Table 1

First Band of $[Co\ en_2\ A_2]$ or $[Co(NH_3)_4A_2]$ Type Complex Ion

No.	Spectrochemical series of ligand A	Complex ion	First band (10^{13}/sec.) of: *cis*-isomer, ν_c	First band (10^{13}/sec.) of: *trans*-isomer, ν_t
1	NO_2^-	$[Co(NH_3)_4(NO_2)_2]^+$	67.0	68.2
1a	NO_2^-	$[Co(NH_3)_4(NO_2)_2]^+$	65.5	67.9
1b	NO_2^-	$[Co(NH_3)_4(NO_2)_2]^+$	69.0	68.9
2	NO_2^-	$[Co\ en_2\ (NO_2)_2]^+$	69.0	69.9
2a	NO_2^-	$[Co\ en_2\ (NO_2)_2]^+$	68.5	69.3
3	$SO_3^=$	$[Co(NH_3)_4(SO_3)_2]^-$	65.9	66.6
4	NH_3	$[Co\ en_2\ (NH_3)_2]^{3+}$	63.8	63.8
5	H_2O	$[Co\ en_2\ (H_2O)_2]^{3+}$	60.6	60.4
6	NCS^-	$[Co\ en_2\ (NCS)_2]^+$	59.3	59.0
6a	NCS^-	$[Co\ en_2(NCS)_2]^+$	57.7	58.3
7	Cl^-	$[Co(NH_3)_4Cl_2]^+$	(57.3) (a)	<50.0
8	Cl^-	$[Co\ en_2\ Cl_2]^+$	56.6	48.0
8a	Cl^-	$[Co\ en_2\ Cl_2]^+$	55·8	48.4
9	Br^-	$[Co\ en_2\ Br_2]^+$	54.5	45.6

No.	$\nu_c - \nu_t$	Solvent	Ref.
1	−1.2	methanol-water	Basolo[3]
1a	−2.4	water	Kuroya and Tsuchida[5]
1b	+0.1	water	Kuroya[6]
2	−0.9	water	Kuroya and Tsuchida[5]
2a	−0.8	methanol-water	Basolo[3]
3	−0.7	3%-NH_3 aq.	Shimura[1]
4	0.0	water	Basolo[3]
5	+0.2	water *p*H 0.7	Basolo[3]
6	+0.3	water	Shimura[4]
6a	−0.6	methanol-water	Basolo[3]
7	>+7.3	water	Tsuchida[8]
8	+8.6	methanol-water	Basolo[3]
8a	+7.4	alcohol-water	Ernsberger and Brode[7]
9	+8.9	alcohol-water	Ernsberger and Brode[7]

(a) datum of the crystal.[9]

(5) H. Kuroya and R. Tsuchida, This Bulletin. **15**, 427 (1940).
(6) H. Kuroya, *J. Inst. Polytech., Osaka City Univ.*, **1**, No. 1, Ser. C, 29 (1950).
(7) M. L. Ernsberger and W. R. Brode, *J. Am. Chem. Soc.*, **56**, 1842 (1934).
(8) R. Tsuchida, This Bulletin, **11**, 721 (1936).
(9) R. Tsuchida and M. Kobayashi, *ibid.*, **13**, 619(1938).

Table 2

First Band of [Co en_2 A·B] or [$Co(NH_3)_4$ A·B] Type Complex Ion[a]

No.	Spectrochemical series of ligand B	Complex ion	First band (10^{13}/sec.) of: *cis*-isomer, ν_c	*trans*-isomer, ν_t	$\nu_c-\nu_t$	Solvent	Ref.
(a)	Monochloro-bisethylenediamine or -tetrammine series (A=Cl^-)						
1	NO_2^-	$[Co\ en_2\ Cl\cdot NO_2]^+$	64·5	64.4	+0.1	methanol-water	Basolo[3]
2	NCS^-	$[Co\ en_2\ Cl\cdot NCS]^+$	59.6	54.0	+5.6	water	Kuroya and Tsuchida[5]
2a	NCS^-	$[Co\ en_2\ Cl\cdot NCS]^+$	58.8	57.7	+1.1	methanol-water	Basolo[3]
3	H_2O	$[Co(NH_3)_4Cl\cdot H_2O]^{2+}$	58.5	50.0	+8.5	water	Tsuchida[6]
4	Cl^-	$[Co\ en_2\ Cl\cdot Cl]^+$	56.6	48.0	+8.6	methanol-water	Basolo[3], (b)
5	Br^-	$[Co\ en_2\ Cl\cdot Br]^+$	55.1	47.0	+8.1	alcohol-water	Ernsberger and Brode[7]
(b)	Mononitro-bisethylenediamine or -tetrammine series (A=NO_2^-)						
1	NO_2^-	$[Co(NH_3)_4NO_2\cdot NO_2]^+$	67.0	68.2	−1.2	methanol-water	Basolo[3], (b)
2	NO_2^-	$[Co\ en_2\ NO_2\cdot NO_2]^+$	69.0	69.9	−0.9	water	Kuroya and Tsuchida[5], (c)
3	NCS^-	$[Co(NH_3)_4NO_2\cdot NCS]^+$	62.6	64.0	−1.4	water	Shimura (present paper)
4	NCS^-	$[Co\ en_2\ NO_2\cdot NCS]^+$	64.8	65.3	−0.5	water	Kuroya and Tsuchida[5]
5	Cl^-	$[Co\ en_2\ NO_2\cdot Cl]^+$	64.5	64.4	+0.1	methanol-water	Basolo[3]
(c)	Monorhodanato-bisethylenediamine or -tetrammine series (A=NCS^-)						
1	NO_2^-	$[Co(NH_3)_4NCS\cdot NO_2]^+$	62.2	64.0	−1.4	water	Shimura (present paper)
2	NO_2^-	$[Co\ en_2\ NCS\cdot NO_2]^+$	64.8	65.3	−0.5	water	Kuroya and Tsuchida[5]
3	NH_3	$[Co\ en_2\ NCS\cdot NH_3]^{2+}$	60.0	58.8	+1.2	methanol-water	Basolo[3]
4	NCS^-	$[Co\ en_2\ NCS\cdot NCS]^+$	59.3	59.0	+0.3	water	Shimura[4], (b)
5	Cl^-	$[Co\ en_2\ NCS\cdot Cl]^+$	59.6	54.0	+5.6	water	Kuroya and Tsuhcida[5], (c)
(d)	Monoammine-bisethylenediamine series (A=NH_3)						
1	NH_3	$[Co\ en_2\ NH_3\cdot NH_3]^{3+}$	63.8	63.8	0.0	water	Basolo[3]
2	H_2O	$[Co\ en_2\ NH_3H_2O]^{3+}$	61.9	61.9	0.0	water pH 0.7	Basolo[3]
3	NCS^-	$[Co\ en_2\ NH_3\cdot NCS]^{2+}$	60.0	58.8	+1.2	methanol-water	Basolo[3]
4	OH^-	$[Co\ en_2\ NH_3\cdot OH]^{2+}$	60.6	60.6	0.0	water	Basolo[3]

(a) $[Co\ en_2NH_3\cdot Cl]^{2+}$ is excluded, because the absorption data[3] of its *trans*-isomer are very queer and not agree with its color.
(b) for the other investigator's data, see Table 1.
(c) for the other investigator's data, see Table 2 a.

specific bands to the *cis-trans* isomerism have thoroughly been clarified, but those of the first and second bands are yet in confusion. It is the purpose of the present paper to report on a new regularity about the first or second band and the geometrical isomerism.

Results and Discussion

First Band.—The first bands of the geometrical isomers of Co(III) complexes available in previous reports as well as in the author's measurements are presented in Tables 1 and 2.

In Table 1, the bands of [Co en_2A_2] and [Co$(NH_3)_4A_2$]type complex ions (A=a molecule or a negative ion) are arranged in the order of the spectrochemical series of the ligand A, *i.e.*,

CN^-, NO_2^-, $SO_3^=$, en, NH_3, ONO^-, H_2O, NCS^-, $SO_4^=$, NO_3^-, OH^-, $C_2O_4^=$, $CO_3^=$, $S_2O_3^=$, Cl^-, $CrO_4^=$, Br^-, I^-.

This represents a decreasing order of the frequencies at the maximum absorption of the first bands of the complexes having such ligands.[2),(1)] It is readily recognized from Table 1, that the frequency of the first band of [Co en_2A_2] or [Co$(NH_3)_4A_2$] type ion decreases in the order of the spectrochemical series of the ligand A. From the table, if the data 1b and 6a are omitted, the frequency difference of the first bands of *cis-* and *trans*-isomers, $\nu_c-\nu_t$, is minus for the ligand NO_2^- or $SO_3^=$, zero for NH_3, and plus for H_2O, NCS^- and Cl^-. Considering the very close distribution of NH_3 and en on the spectrochemical series, the fact is generalized as follows. The values $\nu_c-\nu_t$ of [Co X_4A_2] type ions are respectively minus or plus according as the position of the ligand A in the spectrochemical series is ahead of or behind the ligand X. This is interpreted as the result of a *trans*-influence of the ligands, that is, the substitution of two A, which is ahead of X on spectrochemical series, for the two X of [Co X_6], has a greater hypsochromic effect in the case of *trans*-[Co X_4A_2] as compared with the case of the *cis*-[Co X_4A_2], while when A is behind X, such substitution has a greater bathochromic effect in the case of *trans*-substitution than the case of *cis*. In summary, it seems that a *trans*-substitution causes a greater shift of the first band than corresponding *cis*-substitution and the direction of this shift is ruled by the relative positions of the ligands on the spectrochemical series. Thus the first bands of *trans*-isomers of dinitro-complexes are at the shorter wave-lengths than the *cis*-isomers, and the reverse relation is observed in the dichloro-complexes.

About[Co $X_4A{\cdot}B$] type complexes, the similar regularities are substantiated from the Table 2. As for monochloro-bisethylenediamine or -tetrammine series, $\nu_c-\nu_t$ is always plus, because Cl^- is far behind en or NH_3 on spectrochemical series. In the mononitro-bisethylenediamine or -tetrammine series, $\nu_c-\nu_t$ is for the most part minus according as the higher position of NO_2^- than that of NH_3 or en. In the mono-rhodanato-bisethylenediamine or -tetrammine series, the value starts from −1.4 for [Co$(NH_3)_4$ $NCS{\cdot}NO_2]^+$ and comes to +5.6 for [Co $en_2NCS{\cdot}$ $Cl]^+$. From the data of these three series, it is also shown that the farther separations occur between the ligand B and en or NH_3 on the spectrochemical series, the greater absolute value of $\nu_c-\nu_t$ is attained.

Finally in the monoammine-bisethylenediamine series (Table 2 d), $\nu_c-\nu_t$ is almost zero. This is distinctly due to the condition that the position of NH_3 on the spectrochemical series is very close to that of en and that these complexes are compared to a pentammine type, in which the *cis-trans* isomerism can not be taken place.

Second Band.—The data of the second are summarized in Table 3. Since the second bands of the complexes having NO_2^-, $SO_3^=$ and NCS^-, are generally covered by the large specific bands, the bands of such complexes could not be confirmed. From the table, it is clear that the tendency of $\nu_c-\nu_t$ is the same as that of the first band, though the example of minus

Table 3

Second Band of Geometrical Isomer of Co(III) Complex Ion

Complex ion	Second band (10^{14}/sec.)			
	cis-isomer, ν_c	*trans*-isomer, ν_t	$\nu_c-\nu_t$	Ref.
[Co en_2 $NH_3{\cdot}NH_3]^{3+}$	88.8	88.8	0.0	(3)
[Co en_2 $NH_3{\cdot}H_2O]^{3+}$	88.2	87.0	+1.2	(3)
[Co en_2 $H_2O{\cdot}H_2O]^{3+}$	84.5	*ca.* 84.5	*ca.* 0	(3)
[Co en_2 $NH_3{\cdot}OH]^{2+}$	83.3	82.2	+1.1	(3)
[Co$(NH_3)_4H_2O{\cdot}Cl]^{2+}$	82.5	74.5	+8.0	(8)
[Co en_2 $Cl{\cdot}Cl]^+$	*ca.* 76.9	66.7	*ca.* +10.2	(3)

value of $\nu_c - \nu_t$ is unknown.

Moreover, it must be noticed here that some difference values are observed in the case of $[Co\ en_2\ NH_3 \cdot H_2O]^{3+}$ and $[Co\ en_2\ NH_3 \cdot OH]^{2+}$, in which $\nu_c - \nu_t$ of the first band was zero. This indicates that the second band is more sensitive to the geometrical configurations as compared to the first band. Tsuchida[2] has offered a theory concerning the origins of the absorption bands, that the first band is due to the electron transitions in the unsaturated transition shell of the central ion and that the second band is attributed to the transitions of the coördination electrons. The above fact is smoothly explained by this theory of Tsuchida, since the coördination electrons are presumably more sensitive to the geometrical configurations than the electrons in the transition shell of the central ion.

Absorption Spectra and Configurations of Two Isomers of $[Co(NH_3)_4NO_2 \cdot NCS]^+$

The configurations of two stereoisomers of $[Co(NH_3)_4NO_2 \cdot NCS]^+$ have not been studied. The chloride of an isomer was prepared by Werner and Klien[10] from $[Co(NH_3)_4HO_2 \cdot Cl]Cl$, whose structure has been determined as *trans* from its method of preparation[11] and the spectral data.[12] The monohydrated bromide of another isomer was prepared by Werner[13] as the following process.

$$[Co[NH_3)_4(H_2O)_2]_2(SO_4)_3 \xrightarrow{NH_4NCS,\ KBr} [Co(NH_3)_4H_2O \cdot NCS]Br_2 \xrightarrow{NaNO_2} [Co(NH_3)_4H_2O \cdot NCS](NO_2)_2 \xrightarrow[KBr]{heat} [Co(NH_3)_4NO_2 \cdot NCS]Br \cdot N_2O$$

From their preparations, it can be expected that $[Co(NH_3)_4NO_2 \cdot NCS]Cl$ is *trans*-isomer and $[Co(NH_3)_4NO_2 \cdot NCS]Br \cdot H_2O$ is *cis*-isomer. For the purpose of confirming this point of view, the author has prepared the two salts and investigated their absorption spectra, comparing them with those of the corresponding bisethylenediamine salts, which have already been measured by Kuroya and Tsuchida.[5]

The spectrographic measurements were done at room temperature, in the aqueous solutions slightly acidified with acetic acid in order to avoid the decomposition of the salts. The results are shown in Fig. 1 with those of the corresponding bisethylenediamine salts.

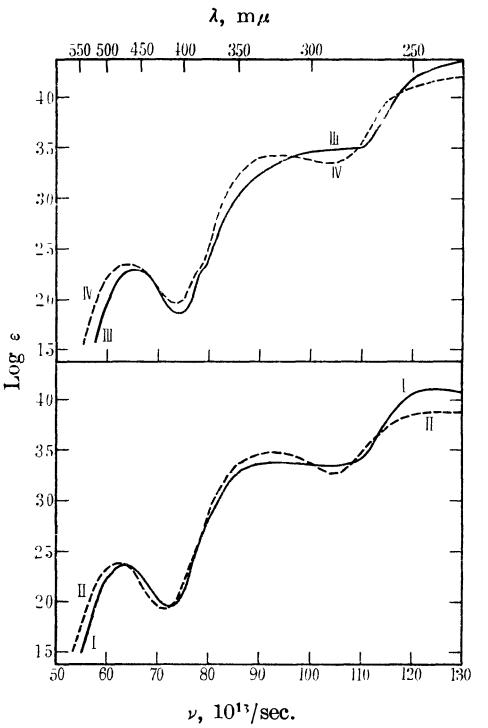

Fig. 1.—Absorption spectra of: I, *trans*-$[Co(NH_3)_4NO_2 \cdot NCS]Cl$; II, *cis*-$[Co(NH_3)_4NO_2 \cdot NCS]Br \cdot H_2O$; III, *trans*-$[Co\ en_2\ NO_2 \cdot NCS]NCS$ (Kuroya and Tsuchida); IV, *cis*-$[Co\ en_2\ NO_2 \cdot NCS]Cl$ (Kuroya and Tsuchida).

As is clear from the shapes of the curves and from the positions of the first bands, $[Co(NH_3)_4NO_2 \cdot NCS]\ Cl$ is analogous to *trans*-$[CO\ en_2\ NO_2 \cdot NCS]NCS$ and $[Co(NH_3)_4NO_2 \cdot NCS]Br \cdot H_2O$ to *cis*-$[Co\ en_2\ NO_2 \cdot NCS]Cl$. Thus the former is *trans*-salt and the latter *cis*-salt. This conclusion coincides with the above presumption from the method of preparations.

As for the first bands of both salts, the band positions and the logarithms of maximum formal extinction coefficients are as follows;

trans-$[Co(NH_3)_4NO_2 \cdot NCS]Cl$
64.0×10^{13}/sec. ($\log \varepsilon = 2.34$)

cis-$[Co(NH_3)_4NO_2 \cdot NCS]Br \cdot H_2O$
62.6×10^{13}/sec. ($\log \varepsilon = 2.36$).

With regard to the second or third band as well as the nitro- or rhodanato-specific band, it is impossible to explain the detail because of the intricated superposition of these bands.

Summary

A survey of the absorption data of the tetrammine- or bisethylenediamine-Co(III) complexes available in previous literature as well as in the author's measurements has shown that the frequency differences of the first bands

(10) A. Werner and R. Klien, *Z. anorg. Chem.*, **22**, 111 (1900).
(11) S. M. Jörgensen, *ibid.*, **7**, 290 (1894).
(12) R. Tsuchida and S. Kashimoto. This Bulletin, **11**, 785 (1936).
(13) A. Werner, *Ber.*, **40**, 776 (1907).

(or second bands) of the *cis*- and *trans*-isomers are closely related to the spectrochemical series of the ligands which coördinated in *cis*- or *trans*-positions. This correlation has been interpreted as the result of a *trans*-influence of the ligands, *i. e.*, a *trans*-substitution causes a greater shift of the first band (or second band) than corresponding *cis*- substitution. The visible and ultraviolet absorption spectra of two isomers of $[Co(NH_3)_4NO_2 \cdot NCS]^+$ have been measured and the steric configurations of both ions have been determined.

The author expresses sincere thanks to Professor R. Tsuchida for his continued interest and encouragement during the course of this work.

Department of Chemistry, Faculty of Science, Osaka University, Osaka

Antituberculous Compounds. I. Synthesis of *p*-Acetamidocinnamaldehyde Thiosemicarbazone

By Tamio NISHIMURA

(Received November 2, 1951)

Some thiosemicarbazones of *p*-substituted aromatic aldehydes have been shown to have the antituberculous activity by Domagk and Behnisch.[1] Among the few thiosemicarbazones active in vivo, *p*-acetamidobenzaldehyde thiosemicarbazone has recently gained much interest and many patients have been treated with this chemotherapeutic agent. The author became interested in preparing *p*-acetamidocinnamaldehyde thiosemicarbazone (VIII) in the expectation that this substance could have antituberculous activity.

This synthesis of (VIII) may be illustrated by the following series of reactions.

p-Nitrobenzaldiacetate (II) was prepared from *p*-nitrotoluene (I) by the method of Organic Syntheses[2] with certain modifications. The diacetate was easily converted to *p*-nitrobenzaldehyde (III) by hydrolysis. The aldehyde was condensed with acetaldehyde to form β-(*p*-nitrophenyl)-β-hydroxypropionaldehyde acetaldehyde addition compound (IV).[3] The dehydration of the addition compound to form *p*-nitrocinnamaldehyde (V) was accomplished by heating it with hydrochloric acid in acetic acid or methanol. The preparation of (V) by the method of Fecht[4] was also executed and found to give better yields compared with the

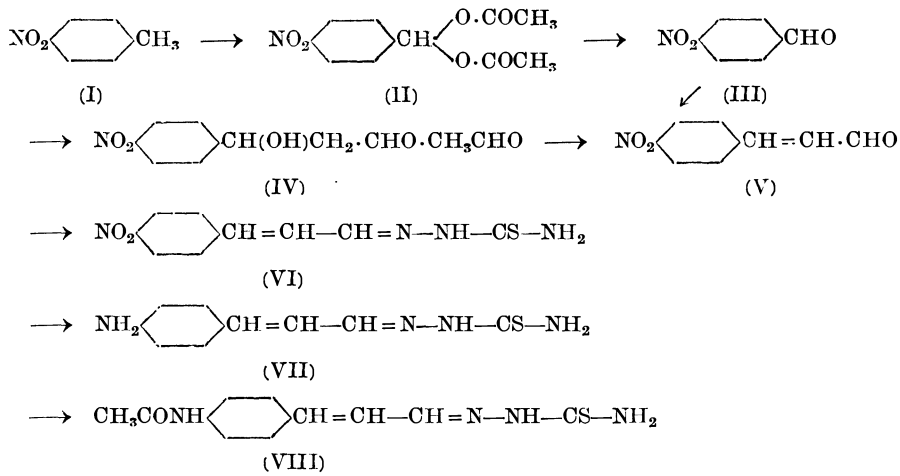

(1) G. Domagk, R. Behnisch, F. Mietzsch and H. Schmidt, *Naturwiss.*, **33**, 315 (1946).
(2) "Organic Syntheses," Vol. 18, 61.
(3) C. F. Göhring, *Ber.*, **18**, 372 (1885).
(4) H. Fecht, *Ber.*, **40**, 3898 (1907).

procedure mentioned above. The condensation of (V) with thiosemicarbazide to give *p*-nitrocinnamaldehyde thiosemicarbazone (VI) was performed by the usual procedure. The attempts to reduce (VI) with sodium sulfide or disulfide were unsuccessful; but when sodium hydrogen sulfide was employed, reasonable yields of *p*-aminocinnamaldehyde thiosemicarbazone (VII) were obtained. The reduction with ferrous sulfate also proceeded in ethanol but with lower yields. (VII) was readily acetylated by acetic anhydride in 50 % aqueous acetic acid or ethanol to yield *p*-acetamidocinnamaldehyde thiosemicarbazone (VIII). Another approach to (VIII) is illustrated in the following scheme.

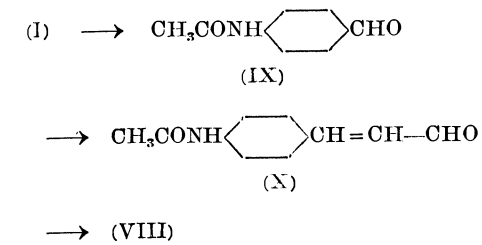

p-Acetamidobenzaldehyde (IX) was prepared from *p*-nitrotoluene (I) by refluxing with a solution of sulfur and sodium hydroxide in ethanol followed by acetylation of the ether extract, giving the product melting at 153—155° (yield: 24 % of the theoretical.[5],[6] For the preparation of *p*-acetamidocinnamaldehyde Beard's method was followed according to the description in Chemical Abstracts **44**, 8862 (1950) with the following modifications; (a) the product was recrystallized from water, omitting the ether extraction; (b) optimum reaction temperature was found to be −5—10°. From 3.3 g. of *p*-acetamidobenzaldehyde was obtained 0.46 g. (12 %) of the desired product melting at 174—175.5°.

Experimental[7]

p-Nitrobenzaldiacetate (II).—To a solution of 50 g. of *p*-nitrotoluene in 400 ml. of acetic anhydride is added 80 ml. of concentrated sulfuric acid.

When the mixture has been cooled to 0°, a solution of 100 g. (1.0 mole) of chromium trioxide in 400 ml. of acetic anhydride[8] is added slowly, with stirring, at such a rate that the temperature does not exceed 10°, and stirring is continued for two hours at 5°—10° in an ice-water bath after the addition is completed. Further treatment is similar to that described in Organic Syntheses. The product, after drying in a vacuum desiccator, weighs 63—69 g. (68—75% of the theoretical), m. p. 122°—124°.

p-Nitrocinnamaldehyde (V).—(a) A mixture of 2.3 grams of β-(*p*-nitrophenyl)-β-hydroxypropionaldehyde acetaldehyde addition compound,[3] 7 ml. of glacial acetic acid and 7 ml. of concentrated hydrochloric acid was heated on a steam-bath. When the aldehyde had dissolved (about one minute), 14 ml. of water were added to the mixture. After cooling, seperated crystals were filtered and washed with water; yield: 17 g. (94 %), m. p. 137—140°. (b) Fecht's method with the following modification.—In a 500 ml. three-necked flask fitted with a mechanical stirrer, a thermometer and a burette were placed 50 g. of *p*-nitrobenzaldhyde and 100 ml. of freshly distilled acetaldehyde. The mixture was stirred and cooled in an ice salt mixture. A solution (20 %) of potassium hydroxide in methanol was added dropwise to the mixture from the burette until the alkaline reaction was obtained and during the reaction period it was maintained to be alkaline by the additional dropping of the potassium hydroxide solution, amounting 4.8 ml.; the internal temperature was maintained at 0°—5° throughout the procedure, and for 40 minutes thereafter. At the end of this period, the mixture solidified. One hundred and sixty ml. of acetic anhydride were added and heated for 30 minutes on a steam-bath. The solution was poured into 1.2 l. of hot water and heated on a steam-bath for 20 minutes after the addition of 160 ml. of concentrated hydrochloric acid, where the yellow needles separated. The mixture was allowed to stand overnight and crystals were filtered by suction and washed with water. One crystallization from 1.6 l. of 30 % acetic acid gave 37.5 g. (64.4 %) of the desired product, melting at 140~142°.

p-Nitrocinnamaldehyde Thiosemicarbazone (VI).—To a solution of 18.2 g. of thiosemicarbazide in 700 ml. of hot ethanol was added 35.4 g. of *p*-nitrocinnamaldehyde and the mixture was heated on a steam-bath for 30 minutes. After cooling, yellow precipitates were filtered by suction, washed with ethanol and dried, giving 47 g. (94%) of the desired product, melting at 224° (decomp.). A small sample was recrystallized from ethanol to give the material with the same m. p. (Anal. Calcd. for $C_{10}H_{10}O_2SN_4$: N, 22.38 %. Found: N, 22.24 %).

(5) Friedl. **4**, 136.
(6) Gabriel and Herzog, *Ber.*, **16**, 2003 (1883).
(7) All temperatures are uncorrected.

(8) Recently, we encountered an explosion on dissolving chromium trioxide in acetic anhydride, the cause of which seems to be local heating of the mixture. Without any hazard, the cooling by tap water has been executed after the total acetic anhydride had been poured in one portion, into the flask containing chromium trioxide but the explosion which we experienced occurred before the cooling was started. Therefore, it is preferable to cool acetic anhydride before being mixed with chromium trioxide.

***p*-Aminocinnamaldehyde Thiosemicarbazone (VII).**—After saturation of a mixture of 200 ml. of ethanol and 64 ml. of 2 *N* aqueous sodium hydroxide solution with hydrogen sulfide, 20 g. of *p*-nitrocinnamaldehyde thiosemicarbazone was added to the mixture in one portion. The mixture was heated on a steam-bath without stirring. When the mixture began to boil, the bath was removed. After the boiling has subsided, the mixture was heated for 10 minutes with stirring and allowed to stand overnight at room temperature. Separated crystals were collected on a filter, washed with ethanol, water and finally ethanol giving 15.5 g. (70 %) of pure product, m. p. 207° (decomp.) (Anal. Calcd. for $C_{10}H_{12}SN_4$: C, 54.53; H, 5.50%. Found: C, 54.29; H, 5.27%).

***p*-Acetamidocinnamldehyde Thiosemicarbazone (VIII).**—(a) To 11 g. of *p*-aminocinnamaldehyde thiosemicarbazone suspended in 110 ml. of ethanol was added 11 ml. of acetic anhydride and the mixture was stirred for ten minutes. After standing overnight, precipitated solid was filtered and washed with water to give 10.4 g. (80 %) of the desired product, m. p. 223—225° (decomp.). Recrystalization from 500 ml. of ethanol yielded 8.4 g. (66 %) of *p*-acetamidocinnamaldehyde thiosemicarbazone, m. p. 224—225° (decomp.). Faint yellow plate was obtained by recrystallization of a small sample from ethanol, m. p. 225° (decomp.) (Anal. Calcd. for $C_{12}H_{14}OSN_4$: C, 54.95; H, 5.38 %. Found: C, 54.89; H, 5.48 %).

(b) Eight-tenths g. of *p*-acetamidocinnamaldehyde was dissolved in 30 ml. ethanol and to the solution 0.4 g. of thiosemicarbazide was added. The mixture was heated on a steam-bath and stirred for 30 minutes while yellow solid precipitated. After cooling, the solid was filtered and washed with ethanol. It weighed 1.1 g. (100 %), m. p. 224° (decomp.). After one recrystallization from ethanol, there was obtained pure material melting at 225° (decomp.).

The author wishes to acknowledge his indebtedness to Miss T. Harada (Agricultural Department, the University of Tokyo) for the microanalytical data.

Chemical Laboratory,
The Kitasato Institute

Studies on Nitrate Reductase. VI. Acceptor Specificity of the Enzyme

By Ryo SATO,* Mituo EBATA and Fujio EGAMI

(Received October 25, 1951)

Despite a considerable amount of knowledge obtained in our laboratory on nitrate reductase of *Escherichia coli*,[1]~[5] the acceptor specificity of this enzyme remains largely uninvestigated, except a few informations indicating that nitrate reductase of *E. coli* can reduce chlorate as well as nitrate,[1] and that molecular oxygen can not supplant the function of hydrogen acceptor for this enzyme.[6],[7]

Since there are a number of organic nitrogen compounds derived from or structurally related to nitrate, such as nitric acid esters, nitramines, and aliphatic and aromatic nitro compounds, it seems desirable to study whether these compounds can also serve as hydrogen acceptors for nitrate reductase. Among them, nitro compounds are of special interest in view of the long known facts that nitro groups of numerous aromatic compounds are reduced by many microorganisms and animal tissues. Furthermore, in recent years, a considerable attention has been paid to the biochemical significance of nitro groups, since two nitro compounds, chloramphenicol[8] and β-nitropropionic acid[9],[10] have been isolated from biological sources, contrary to the hitherto universally presumed idea that nitro compounds do not occur in nature. It appears, therefore, of interest to find a relation, if exists, between

* Present address : Faculty of Science, Kanazawa University.

(1) F. Egami and R. Sato, *J. Chem. Soc. Japan*, **68**, 39 (1947).

(2) F. Egami and R. Sato, *J. Chem. Soc. Japan*, **69**, 160 (1948).

(3) R. Sato and F. Egami, This Bulletin, **22**, 137 (1949).

(4) F. Egami and R. Sato, *J. Chem. Soc. Japan*, **70**, 397 (1949).

(5) R. Sato, *Scienca Revuo*, **2**, 122 (1950).

(6) M. Niwa, R. Sato and S. Taniguti, *Symposia on Enzyme Chem.*, **6**, 40 (1951).

(7) L. H. Stickland, *Biochem. J.*, **25**, 605 (1931).

(8) J. Ehrlich, Q. R. Bartz, R. M. Smith, D. A. Joslyn and P. R. Burkholder, *Science*, **106**, 417 (1947).

(9) C. L. Carter and W. J. McChesney, *Nature*, **164**, 575 (1949).

(10) M. T. Bush, O. Touster and J. E. Brockman, *J. Biol. Chem.*, **188**, 685 (1951).

the metabolism of these compounds and nitrate reductase.

The results described below, however, indicate that none of the nitrogen compounds tested can replace nitrate as hydrogen acceptor for nitrate reductase.

Materials and Methods

Dried cells of *E. coli*, which contain nitrate reductase and dehydrogenase systems with their carrier systems, were used as the enzyme preparation. The organism was grown on a peptone-bouillon-agar medium containing 0.1 per cent potassium nitrate for 24 hours at 37°. The cells were then harvested and washed thrice with physiological saline and once with distilled water. The washed cells were dried by lyophilization in the presence of phosphorous pentoxide and stored at 0° in a vacuum desiccator. Dried cell suspension was prepared just before the use by suspending 2—5 mg. of the dried cells in distilled water.

Most experiments were conducted at 37° under an anaerobic condition with the use of Thunberg tubes. Sodium formate was used as the hydrogen donator throughout the investigation. The reaction mixture usually consisted of 1 ml. of each dried cell suspension, *M*/10—*M*/25 sodium formate, substrate solution, *M*/5—*M*/15 phosphate buffer of *p*H 7.4 or 7.6, and distilled water (or inhibitor solution). At the end of incubation periods the reaction mixtures were deproteinized with 2 ml. of saturated uranyl acetate solution or 20 per cent trichloroacetic acid. The reduction of nitrate was followed by determining the formation of nitrite in the deproteinized filtrates. Determination of nitrite was performed by a colorimetric method using Griess-Ilosvay reagent,[11] and analysis for aromatic amines formed from the corresponding nitro compounds was made by the method of Smith and Worrel,[12] N-[1-naphthyl]-ethylene diamine being substituted by α-naphthylamine as coupling reagent.

Reoxidation of leuco form of methylene blue by nitrogen compounds was tested as follows. One ml. of each dried cell suspension (3 mg. of the cells), *M*/5 phosphate buffer of *p*H 7.4, *M*/25 sodium formate, and 10^{-4} *M* methylene blue was pipetted into the main room of a Thunberg tube, and 1 ml. of the solution of the compound to be tested into the side arm. The tube was then incubated at 37° until the dye was completely decolorized. Then the contents of the both parts were mixed. If the compound can reoxidize the leuco dye in the presence of the dried cells, recolorization of the dye takes place immediately after the mixing.

Results

Action of the Dried Cells upon Ethyl Nitrate.

—Ethyl nitrate was used as a representative of nitric acid esters. When the ester is acted by the dried cells of *E. coli*, one may anticipate the following four possibilities: (1) the ester is first hydrolyzed spontaneously or by an esterase to liberate inorganic nitrate, which is in turn reduced to nitrite by nitrate reductase; (2) the ester is enzymatically reduced to the nitrous acid ester; (3) the ester combines with nitrate reductase, but no further change takes place; and (4) no reactions occur at all.

The results of experiments (Curves I and II, in Fig. 1) showed that no nitrite is produced from ethyl nitrate by the action of the dried cells. The hydrolysis of the ester, therefore, seems to be improbable. To test the formation of the nitrous acid ester, the reaction mixture of Curve I was deproteinized after 3 hours incubation and acidified to *p*H 1.0 with hydrochloric acid and then boiled for 30 minutes to hydrolyze the ester. However, no nitrite liberation was detected by this procedure. This seems to exclude the second possibility. Heppel and Hilmoe[13] have reported an enzyme in hog liver which catalyzes the reduction of nitroglycerol and erythritol tetranitrate by glutathione or cysteine in the presence of cyanide. The addition of cysteine (10^{-2} *M*) and potassium cyanide (4×10^{-3} *M*), however, did not activate our preparation to reduce ethyl nitrate. It was further found, as is recorded in Fig. 1 (Curves III and IV), that nitrate reduction by the dried cells is entirely

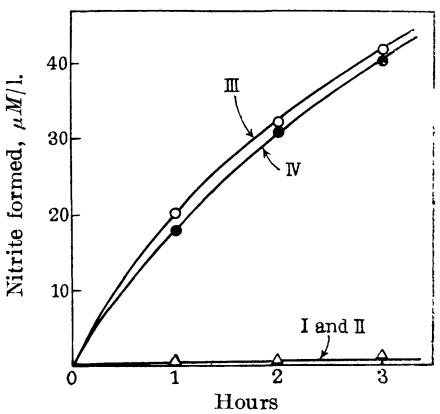

Fig. 1.—Action of the dried cells of *E. coli* on ethyl nitrate (4×10^{-3} *M*/l.) under aerobic (Curve I) and anaerobic (Curve II) conditions; and reduction of KNO_3 (2×10^{-4} *M*/l.) by the cells in the presence (Curve III) and absence (Curve IV) of ethyl nitrate (4×10^{-3} *M*/l.). *p*H = 7.6, and 3 mg. of the dried cells were contained in 5 ml. of medium.

(11) S. Yamagata, *Acta Phytochimica*, **10**, 283 (1938).
(12) G. N. Smith and C. S. Worrel, *Arch. Biochem.*, **24**, 216 (1949).
(13) L. A. Heppel and R. J. Hilmoe, *J. Biol. Chem.*, **183**, 129 (1950).

unaffected by the presence of ethyl nitrate at a concentration 20-fold as much as that of the inorganic nitrate supplied. This fact appears to show that the third possibility is also unlikely. After all, we are compelled to take the fourth possibility and assume that the ester is indifferent to nitrate reductase at all.

That ethyl nitrate has no affinity to nitrate reductase receives further support from the observation that the ester can not reoxidize leuco methylene blue in the presence of the cells, in contrast to the fact that inorganic nitrate can rapidly recolorize the leuco dye under the influence of nitrate reductase.[11]

Effect of Nitrourea on Nitrate Reduction.—Nitrourea, a nitramine, was found to be a strong inhibitory reagent for nitrate reductase. Nitrate reduction by the dried cells was almost completely inhibited by 4×10^{-3} *M* nitrourea. This compound failed to reoxidize leuco methylene blue.

Effect of Nitromethane on Nitrate Reduction.—As a means of elucidating an interaction between nitromethane and nitrate reductase, the effect of this aliphatic nitro compound on the activity of nitrate reductase was studied (Fig. 2). It was found that 4×10^{-3} *M* nitromethane exhibits no inhibition on nitrate reduction by the dried cells, concentrations of nitrate being varied from 2×10^{-5} *M* to 4×10^{-3} *M*. This fact may be thought to indicate that nitromethane has no affinity to nitrate reductase. Furthermore, leuco form of methylene blue was not recolorized by this compound in the presence of the cells.

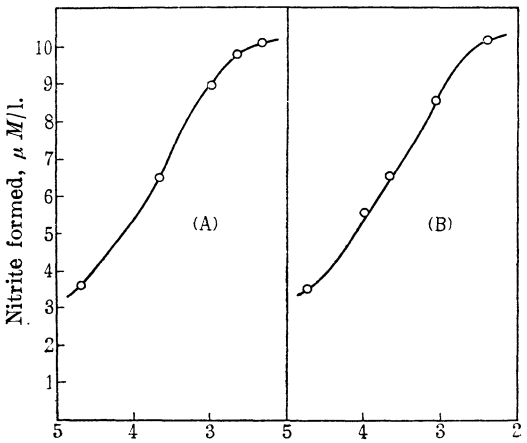

Fig. 2.—Activity-*p*S-curve of nitrate reduction by the dried cells of *E. coli* in the presence (A) and absence (B) of nitromethane (4×10^{-3} *M*/l.). *p*H = 7.6, and 3 mg. of the cells were contained in 5 ml. of medium. Incubation period = 120 minutes.

While rabbit liver homogenates have been reported to decompose nitromethane liberating nitrite ion both under aerobic and anaerobic conditions,[14] the dried cells of *E. coli* produced no nitrite from nitromethane under any conditions.

Reduction of *p*-Nitrobenzoic Acid to *p*-Aminobenzoic Acid.—The dried cells of *E. coli* were found to reduce *p*-nitrobenzoic acid (PNBA) to *p*-aminobenzoic acid (PABA) in the presence of formate. But the amount of PABA produced was very small (Table 1). This reduction was inhibited by 2×10^{-3} *M* cyanide about 80 per cent. Aerobic condition also retarded the reduction, and in the absence of formate the formation of PABA was decreased to 65 per cent of the complete system.

Table 1

The Reduction of PNBA to PABA by the Dried Cells of *E. coli*

Exp. No.	1	2	3	4	5	6
Dried cell suspension (3 mg. per ml.), ml.	1	1	1	1	1*	1
Phosphate buffer (*p*H 7.4, *M*/5), ml.	1	1	1	1	1	1
PNBA (2×10^{-3} *M*), ml.	1	1	1	1	1	—
Sodium formate(*M*/10), ml.	1	1	—	1	1	—
Distilled water, ml.	1	1	2	1	1	3
Condition	an.	an.	an.	ae.	an.	an.
Incubation period, min.	60	120	120	120	120	120
PABA formed (10^{-5} *M*)	0.2	0.3	0.2	0.2	0	0

* The suspension was heated at 100° for 5 minutes. an. = anaerobic; ae. = aerobic.

It was further found that PNBA reduction is also inhibited by nitrate to a small extent. At the first glance this fact was thought to be an evidence indicating that there may be a competitive interaction between PNBA and nitrate. Further study of the effect of PNBA on nitrate reduction, however, provided a strong evidence suggesting that PNBA is indifferent to nitrate reductase. As will be seen in Fig. 3, PNBA (1.4×10^{-3} *M*, a concentration 7-fold as much as the nitrate present) does not inhibit the reduction of nitrate (2×10^{-4} *M*), and, moreover, there is even a slight acceleration in nitrite production. These phenomena can be explained as follows. The

(14) F. Egami and R. Sato, *Nature*, **165**, 365 (1950), F. Egami and M. Itahashi, *J. Biochem.*, **38**, 329 (1951).

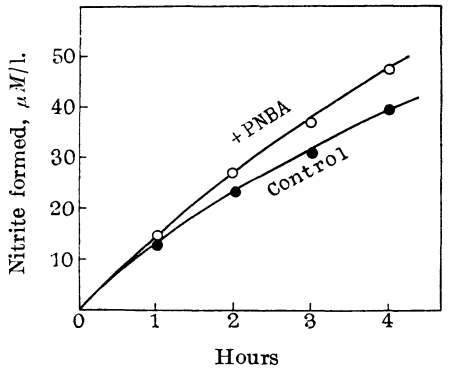

Fig. 3.—Effect of PNBA on nitrate reduction by the dried cells of *E. coli*. pH=7.4, PNBA=1.4×10^{-3} M/l., $KNO_3=2\times10^{-4}$ M/l., and 2 mg. of the dried cells were contained in 5 ml. of medium.

enzyme system responsible for PNBA reduction is not identical with that for nitrate reduction, but the observed reduction of PNBA is due to nitrite reductase system contained in the dried cells of *E. coli* at a minute concentration,* and consequently there exists a competitive relation between PNBA reduction and nitrite reduction (but not nitrate reduction). Thus the inhibitory action of nitrate to PNBA reduction mentioned above is not directly caused by nitrate itself, but by nitrite formed from nitrate as the product of its reduction. The slight acceleration of nitrite formation by PNBA is also explicable, since PNBA prevents in a competitive manner the further reduction of nitrite once formed. This competition between nitrite and aromatic nitro groups in their reduction by bacteria has been more clearly demonstrated with a cell-free extract from a bacterial strain, which lacks nitrate reductase, but possesses a much greater activity of nitrite reductase than *E. coli*. We have already published[15] such a competitive interaction between the reduction of the nitro group of chloramphenicol and that of nitrite.

The failure of PNBA to reoxidize leuco methylene blue in the presence of the dried cells of *E. coli* also supports the view that PNBA has no affinity to nitrate reductase.

Several aromatic nitro compounds tested other than PNBA (including chloramphenicol, nitrobenzene, and *p*-nitrosalicylic acid) were also found to behave similarly.

Discussion

From the evidence presented in this paper it seems very probable that all the nitrogen compounds tested are unable to accept hydrogen from formate by way of nitrate reductase system. Though the compounds tested in the present study are only a few representatives of many related compounds, it might be expected that all the other nitric acid esters, nitramines, and nitro compounds also behave similarly toward nitrate reductase. Thus, based on the results available up to the present, we might be able to state that only two compounds, nitrate and chlorate, can be reduced by this enzyme system. Chlorate has been known to be reduced to chlorite by *E. coli* and some other bacteria.[16] The ability of this compound to accept hydrogen from nitrate reductase was concluded by us[1] from the observations that chlorate, which may be regarded as a chlorine analog of nitrate, exihibts a marked competitive inhibition on nitrate reduction by a cell-free preparation of nitrate reductase from *E. coli*. We have further found, by analyzing the inhibition data, that the apparant Michaelis constant for chlorate reduction by this enzyme is $10^{-2.98}$ M/l., while that for nitrate reduction is $10^{-3.85}$ M/l. Chlorate reduction, however, could not be regarded as a normal function of this enzyme, since its reduction product, chlorite, has been shown to be a very powerful bacterial poison.[16] Quastel, Stephenson, and Whetham[16] claimed that for chlorate reduction is responsible an enzyme which is similar but distinct from nitrate reductase. It might be quite natural that Stephenson[17] was led by this opinion to a somewhat queer conclusion, which she wrote as follows: "Chlorate is a salt which so seldom forms a part of bacterial substrate that it can hardly worth while to possess an enzyme for using it.... the (chlorate reducing) enzyme can hardly be of service to the cell except for purposes of suicidal war". On the other hand, according to our demonstration of the identity of the chlorate reducing enzyme with nitrate reductase, such a queer consideration is not necessary; chlorate reduction is a mere result of a chemical resemblance of chlorate to nitrate, which permits the former to act as hydrogen acceptor for nitrate reductase.

* The content of nitrite reductase in *E. coli* varies from a strain to the other. One strain is completely devoid of it, while the other contains a relatively high activity. But our experiences indicate that the cell-free preparations of nitrate reductase extracted from many strains of *E. coli* by ultrasonic destruction of the cells are free from nitrite reductase activity.

(15) F. Egami, M. Ebata and R. Sato, *Nature*, **167**, 118 (1951).

(16) J. H. Quastel, M. Stephenson and M. D. Whetham, *Biochem. J.*, **19**, 304 (1925).

(17) M. Stephenson, in "Perspectives in Biochemistry", Cambridge, 1938, p. 92.

Summary

Evidence is presented to indicate that ethyl nitrate, nitromethane, and possibly also nitrourea are not able to accept hydrogen from nitrate reductase system of *E. coli*. *p*-Nitrobenzoic acid is reduced to *p*-aminobenzoic acid by the action of the dried cells of *E. coli* to a small extent. This reduction is, however, not achieved by nitrate reductase. Nitrite reductase contained in the organism is responsible for the reduction of aromatic nitro groups.

The cost of this research has been defrayed from the Grant in Aid for Fundamental Scientific Research from the Ministry of Education.

Chemical Institute, Faculty of Science,
Nagoya University

On the Hydrogen-Bond-Forming Powers of Atoms or Atomic Groups

By Masamichi TSUBOI

(Received November 10, 1951)

I. Introduction

It is well known that the energy of hydrogen bond, X—H···Y where X and Y denote two kinds of atoms, takes various values (from about 8 to 1 kcal./mol) depending upon the nature of the atomic groups which contain X and Y. However, as to how the energy relates with the nature of the atomic groups much is yet to be studied. Useful data concerning this question may be obtained from infrared absorption measurements of certain ternary solutions—the ternary solutions, each of which is composed of a large quantity of nonpolar solvent (such as CCl_4) and small quantities of two polar solutes (a proton-donator containing X—H and a proton-acceptor containing Y), and in which complex molecules with the hydrogen bond X—H···Y are present.* For, from these measurements the concentrations of hydrogen-bonded X—H and free X—H in the solutions at various temperatures are to be found, and on the basis of such data the bond energy of any X—H···Y can be determined. The difference in the values of energies thus obtained for different hydrogen bonds in the same medium must represent the difference in the nature of the atomic groups pertaining to the bonds, there being no difference in the environment in which the hydrogen bonds are formed.

This paper is concerned with preliminary investigations made with what have been stated above in mind. In the first place, some results of the infrared absorption measurements of certain ternary solutions are presented, with interpretations of them. Next, it is shown how the hydrogen bond energy can be determined from the results of these measurements, with a few examples of the values of the energy actually obtained. Lastly, the general relationship between the hydrogen-bond-forming powers of atoms and the nature of the atomic groups containing the atoms is discussed, on the basis of the data so far obtained.

II. Instrument and Samples

The instrument used is a reflection monochromator with a 60° prism of fluorite,(1) in conjunction with the thermocouple and galvanometer system.

The compositions of the ternary solutions examined are:(2)

phenol	+ ethyl ether	+ carbon tetrachloride
〃	+ hexamethylene tetramine	+ 〃
〃	+ benzaldehyde	+ 〃
〃	+ anisol	+ 〃
〃	+ nitrobenzene	+ 〃
〃	+ methyl benzoate	+ 〃
methanol	+ ethyl ether	+ 〃
〃	+ anisol	+ 〃
guaiacol	+ hexamethylene tetramine	+ 〃
o-nitrophenol	+ 〃	+ 〃
methyl salicylate	+ 〃	+ 〃
salicylic aldehyde	+ 〃	+ 〃
p-oxybenzoic methylester	+ 〃	+ 〃

* Of this idea the writer owes to Dr. T. Shimanouchi's suggestion.

(1) The fluorite prism used was kindly placed by O. Matsumura at the writer's disposal.

(2) Some of the materials used were kindly placed at the writer's disposal by Prof. S. Kambara, Mr. H. Tada, Mr. H. Baba, and Mr. T. Inukai.

For comparison, infrared absorption measurements were made also of the binary solutions with the following compositions:

phenol	+carbon	tetrachloride
methanol	+	〃
guaiacol	+	〃
o-nitrophenol	+	〃
methyl salicylate	+	〃
salicylic aldehyde	+	〃
ethyl ether	+	〃
hexamethylene tetramine	+	〃
benzaldehyde	+	〃
anisol	+	〃
nitrobenzene	+	〃
methyl benzoate	+	〃

III. Infrared Absorption Data and their Interpretations

Formation of Intermolecularly Hydrogen-bonded Complexes in Certain Ternary Solution.—Figs. 1—10 show the results of infrared absorption measurements of phenol and methanol in various solutions. In these figures the abscissas denote wave-lengths in the 3μ region and the ordinates the absorption coefficients of phenol or methanol. These absorption coefficients were obtained by subtraction: the absorption coefficients of the solutions containing phenol or methanol [*e. g.* solution composed of phenol (0.01 mol/l.)+ethyl ether (0.06 mol/l.)+carbon tetrachloride] minus the absorption coefficients of the solutions without phenol or methanol [*e. g.* solution composed of ethyl ether (0.06 mol/l.)+carbon tetrachloride].

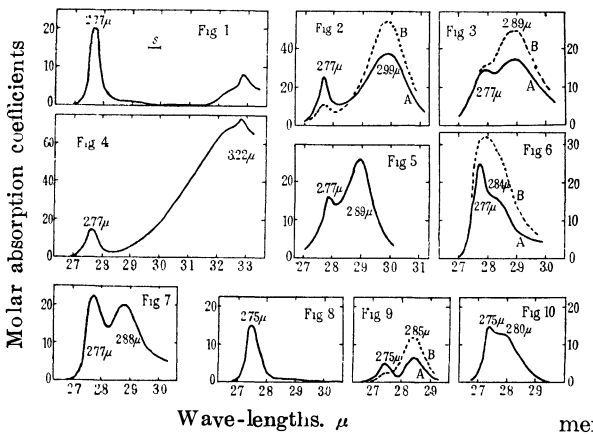

Fig. 1–10.—Infrared absorption curves of phenol and those of methanol in the solutions: Fig. 1, CCl_4+phenol 0.01 mol/l.; Fig. 2, (A) CCl_4+phenol 0.01 mol/l.+ethyl ether 0.06 mol/l., (B) CCl_4+phenol 0.01 mol/l.+ethyl ether 0.11 mol/l.; Fig. 3, (A) CCl_4+phenol 0.01 mol/l.+benzaldehyde 0.05 mol/l., (B) CCl_4+phenol 0.01 mol/l.+benzaldehyde 0.1 mol/l.; Fig. 4, CCl_4+phenol 0.01 mol/l.+hexamethylene tetramine 0.01 mol/l.; Fig. 5, CCl_4+phenol 0.01 mol/l.+anisol 0.5 mol/l.; Fig. 6, (A) CCl_4+phenol 0.01 mol/l.+nitrobenzene 0.08 mol/l., (B) CCl_4+phenol 0.01 mol/l.+nitrobenzene 0.18 mol/l.; Fig. 7, CCl_4+phenol 0.01 mol/l.+methyl benzoate 0.02 mol/l.; Fig. 8, CCl_4+methanol 0.02 mol/l.; Fig. 9, (A)CCl_4+methanol 0.01mol/l.+ethyl ether 0.1 mol/l., (B) CCl_4+methanol 0.01 mol/l.+ethyl ether 0.4 mol/l.; Fig. 10, CCl_4+methanol 0.02 mol/l.+anisol 0.5 mol/l. Temperature: 30°C. *s*: Effective slit-width.

The curve in Fig. 1 is for phenol in the solution of the composition: phenol (0.01mol/l.)+carbon tetrachloride. There is seen a single O—H band at 2.77μ. This indicates that the phenol molecules here are wholly in a free state without molecular association.

Figs. 2—7 show how the absorption is effected by adding proton-acceptors to the solution. For example, in Fig. 2, two curves A and B are for phenol in the ternary solutions, respectively with compositions: phenol (0.01 mol/l.)+ ethyl ether (0.06 mol/l.)+carbon tetrachloride and phenol (0.01 mol/l.)+ ethyl ether (0.11 mol/l.)+carbon tetrachloride. Here, two O—H bands are present, one at 2.77 μ and the other at 2.99 μ. A comparison of the three curves, that in Fig. 1 and A and B in Fig. 2, reveals that by adding ethyl ether to the solution, phenol (0.01 mol/l.)+carbon tetrachloride, the absorption intensity of the O—H band at 2.77 μ becomes weaker and there appears another O—H band at 2.99 μ. Further experiments have shown that, on increasing the concentration of ethyl ether in the solution, there occurs a decrease in the absorption intensity of 2.77 μ band and an increase in the intensity of 2.99 μ band, but no shifting occurs in the positions of these O—H bands. These facts, taken together, may be interpreted as indicating that in the above-mentioned solutions a molecular complex: $C_6H_5OH\cdots O(C_2H_5)_2$, to which the 2.99 μ band is attributable, is formed by the intermolecular hydrogen bond $O-H\cdots O$, and that this complex molecule coexists with free phenol and ether molecules in equilibrium: $C_6H_5OH+O(C_2H_5)_2 \rightleftarrows C_6H_5OH\cdots O(C_2H_5)_2$. The curves in Figs. 3—7 are for phenol in the ternary solutions, whose compositions are given in the notes under the figures. Each of these solutions contains, besides phenol, proton-acceptor. In these solutions phenol exhibits O—H bands at 2.89 μ, 3.22 μ, 2.89 μ, 2.84 μ, and 2.88 μ, besides that at 2.77 μ, indicating

that there are formed in the solutions complexes: $C_6H_5OH\cdots OCHC_6H_5$, $C_6H_5OH\cdots N_4(CH_2)_6$, $C_6H_5OH\cdots O(CH_3)C_6H_5$, $C_6H_5OH\cdots O_2NC_6H_5$, and $C_6H_5OH\cdots OC(OCH_3)C_6H_5$[3].

Figs. 8, 9, and 10 give data of the solutions in which methanol is present, instead of phenol, as a proton-donator. The curves here (for methanol) are much like those in Figs. 1, 2, and 5 (for phenol), and similar interpretations may be given of these data. Thus, Fig. 9 shows that in the ternary solution with the composition: methanol (0.01 mol/l.) + ethyl ether (0.1 or 0.4 mol/l.) + carbon tetrachloride, there is formed a molecular complex: $CH_3OH\cdots O(C_2H_5)_2$, to which the 2.85 μ band is attributable; and Fig. 10 shows that in solution with the composition: methanol (0.02 mol/l.) + anisol (0.5 mol/l.) + carbon tetrachloride, there is formed a molecular complex: $CH_3OH\cdots OCH_3C_6H_5$, to which the 2.80 μ band is attributable.

Summarizing, it may be said that in a carbon tetrachloride solution containing small quantities of a proton-donator (D) and a proton-acceptor (A), there is formed a molecular complex DA, where D and A are intermolecularly hydrogen-bonded, and that the complex DA, coexists with free D and free A in equilibrium: $D+A\rightleftarrows DA$.

Hindrance of the Presence of *Intra*-molecular Hydrogen Bond to the Formation of *Inter*-molecular Hydrogen Bond.— What has been said in the preceding section is of phenol or methanol without *intra*-molecular hydrogen bond; however another relation is revealed of *o*-substituted phenols with *intra*-molecular hydrogen bond. The data obtained from the infrared absorption measurements, as to the effects of adding proton-acceptor to dilute carbon tetrachloride solutions of some substituted phenols are given in Table 1. All the phenols here examined, excepting *p*-oxybenzoic methylester, have O—H's in intramolecularly hydrogen-bonded state; and the positions and the intensities of the O—H bands of these phenols in their dilute carbon tetrachloride solutions remain unchanged by adding hexamethylene tetramine (a powerful proton-acceptor) to the solutions. *p*-Oxybenzoic methylester, with no *intra*-molecular hydrogen bond, exhibits a different behavior. There, on adding hexamethylene tetramine to its dilute carbon tetrachloride solution, a new O—H band appears at 3.22 μ, besides the free O—H band (at 2.77 μ), just like nonsubstituted phenol. The facts as above may be interpreted as indicating that the presence of the *intra*-molecular hydrogen bond, even such a weak one as in guaiacol, hinders the OH group therein involved from forming an *inter*-molecular hydrogen bond.

Table 1

Composition of solution	Concentration, mol/l.	Wave-length (in μ) of O—H band; with molar absorption coefficient in parentheses	
Guaiacol Carbon tetrachloride	0.005	2.80 (80)	
Guaiacol Hexamethylene tetramine Carbon tetrachloride	0.005 0.03	2.80 (80)	
o-Nitrophenol Carbon tetrachloride	0.005	3.08 (80)	
o-Nitrophenol Hexamethylene tetramine Carbon tetrachloride	0.005 0.03	3.08 (80)	
Methyl salicylate Carbon tetrachloride	0.005	3.11 (120)	
Methyl salicylate Hexamethylene tetramine Carbon tetrachloride	0.005 0.03	3.11 (120)	
Salicylic aldehyde Carbon tetrachloride	0.005	3.1	
Salicylic aldehyde Hexamethylene tetramine Carbon tetrachloride	0.005 0.03	3.1	
p-Oxybenzoic methylester Hexamethylene tetramine Carbon tetrachloride	0.005 0.03	2.77 (20)	3.22 (120)

Effective slit width: 0.025 μ
Temperature: 10°C.

IV. On the Determination of the Intermolecular Hydrogen Bond Energy

The infrared absorption data of the solutions as those given above are useful for the determination of the energies of *inter*-molecular hydrogen bonds between proton-donating and proton-accepting molecules. From these data the values of energies are obtainable in the way as follows.

For the ternary solutions ($D+A+CCl_4$) with such low concentrations of D and A as those examined here, it is admissible to consider that there are present only the complex molecules DA and the free molecules, D and A, but none of other complex molecules such as D_2, D_2A, etc. Then the total concentrations

(3) As a result of the electron migration from the methoxyl O to the carbonyl group in the methyl benzoate molecule, the carbonyl O in this molecule is expected to have a stronger negative charge, and must therefore be a stronger proton-acceptor than the methoxyl O.

of D and of A in the solutions may be taken as equal respectively to the sum of the concentrations of DA and D, and to the sum of the concentrations of DA and A, *i. e.*,

$$\text{Total concentration of D} = (\text{DA}) + (\text{D})$$

$$\text{and Total concentration of A} = (\text{DA}) + (\text{A}),$$

where (DA), (D), and (A) denote the concentrations (mol/l.) of DA, D, and A, respectively.

Now, from the intensity of the absorption band due to DA or free D and the known total concentrations of D and A, is obtainable the value of the equilibrium constant:

$$K = \frac{(\text{DA})}{(\text{D}) \times (\text{A})} \qquad (1)$$

for $\text{D} + \text{A} \rightleftarrows \text{DA}$. In order to facilitate the finding of the values of K, Fig. 11 is constructed, where are given the relation between (DA)+(A) and

$$\alpha = \frac{(\text{DA})}{(\text{D}) + (\text{DA})} \qquad (2)$$

(which represents the degree of forming the complex DA for D), for various values of K and for the fixed concentration, 0.01 mol/l., of (D)+(DA).

The change of free energy (ΔF) accompanying the formation of DA is obtainable from K by the equation: $\Delta F = -RT \ln K$, and then the change of total energy (ΔE) and the change of entropy (ΔS) accompanying the formation of DA (in carbon tetrachloride medium) are obtainable from ΔF for different temperatures by the equation: $\Delta F = \Delta E - T\Delta S$.

Two examles of the actual determinations of the energies of *inter*-molecular hydrogen bonds between D and A in the carbon tetrachloride solutions are given below:

ΔE of the Hydrogen Bond between Phenol and Ethyl Ether.—A determination was made of the O—H···O bond energy from the intensity measurements of the 2.99 μ band which is due to the molecular complex: $C_6H_5OH\cdots O(C_2H_5)_2$ (*cf.* Fig. 2). By preliminary examinations, it has been ascertained that the relation between the observed transmittance and the absorption path-lengths of the solutions (phenol+ethyl ether+CCl_4) for the 2.99 μ ray accords with the Lambert's law, at any concentrations and temperatures (30—60°C.). Moreover, it has been ascertained that on the 2.99 μ band there is no superposition of other bands. These facts show that the observed molar absorption coefficient (κ) at 2.99 μ of phenol in these solutions may be taken as being proportional to α, thus

$$\kappa = \kappa_0 \alpha \qquad (3)$$

Here, the proportionality constant κ_0 corresponds to the maximum value of κ, *i. e.*, the molar absorption coefficient of the molecular complex: $C_6H_5OH\cdots O(C_2H_5)_2$, at 2.99 μ. The values of κ was observed of the solutions of various concentrations of ethyl ether and of constant concentration of phenol, 0.01 mol/l., and are given by ○ (at 30°C.), △ (at 45°C.), and □ (at 60°C.), in Fig. 12. The dotted lines in Fig. 12. represent the values of κ calculated from the equations (1), (2), and (3) by giving

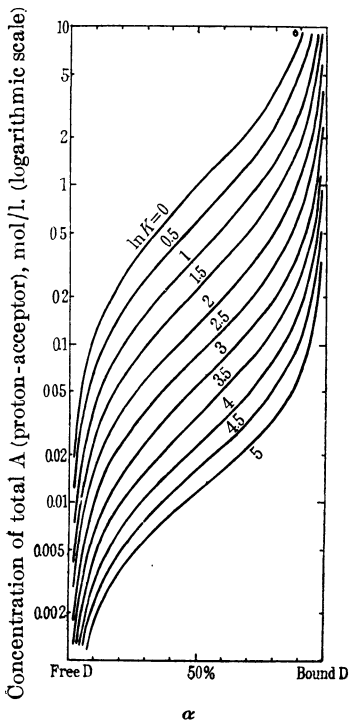

Fig. 11.

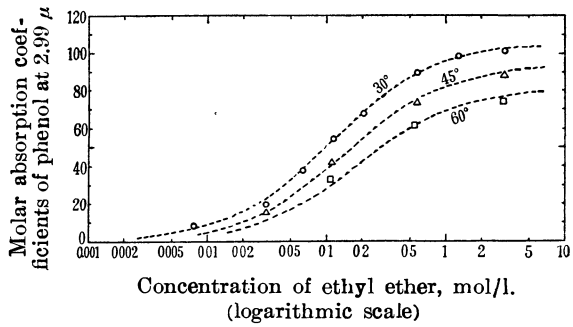

Fig. 12.

following values to κ_0 and K in them: $\kappa_0=105$, $K=10.0$ at 30°C.; $\kappa_0=94$, $K=7.4$ at 45°C.; $\kappa_0=82$, $K=5.75$ at 60°C.(4) (also *cf.* Fig. 11). As is seen in the figure, the observed and calculated values of κ are in close agreement with each other, and hence, from the values of K given here the values of ΔF, ΔS, and ΔE for the O—H···O bond formation can be calculated. These are tabulated below.

Table 2

Temperature, °C.	K	ΔF, kcal./mol	ΔS, E. U.	ΔE, kcal./mol
30	10.0	−1.38		
45	7.4	−1.26	−7.6	−3.7
60	5.75	−1.16		

ΔF (at 30°C.) of the Hydrogen Bond between Phenol and Hexamethylene Tetramine.—A determination was made of the ΔF (at 30°C.) of the O—H···N bond from the intensity measurement of the 2.77 μ band which is due to free phenol molecules (*cf.* Fig. 4). As a preliminary examination the transmittance of the 2.77 μ ray was measured in binary solutions composed of phenol+carbon tetrachloride, varying the concentration of phenol from 0 to 0.006 mol/l. but keeping the absorption path-length (6.11 cm.) and the temperature (30°C.) of the solution constant;(5) and then, similar measurements were made with the ternary solutions which contain hexamethylene tetramine of 0.03 mol/l. The results obtained are shown in Fig. 13. From this figure the concentrations of the phenol molecules in a free state and of those bound by the hexamethylene tetramine molecules were read. In Fig. 14, the ratio of the total concentration of hexamethylene tetramine to the concentration of bound phenol in each solution is plotted versus the reciprocal of the concentration of the free phenol. Here, all the plotted points fall approximately on a single straight line. From the inclination of this straight line, K and ΔF for the O—H···N bond formation at

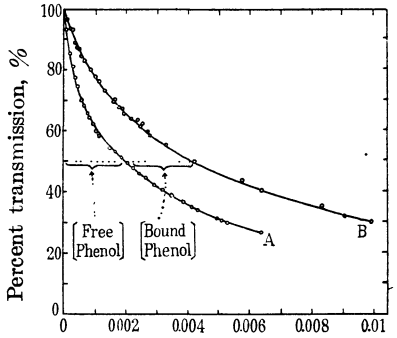

Fig. 13.—Percent transmittance of phenol in (A) binary solutions, CCl_4+phenol, and (B) ternary solutions, CCl_4 + phenol + hexamethylene tetramine (0.03 mol/l.). Wavelength: 2.77 μ. Cell thickness: 6.11 cm. Temperature: 30°C.

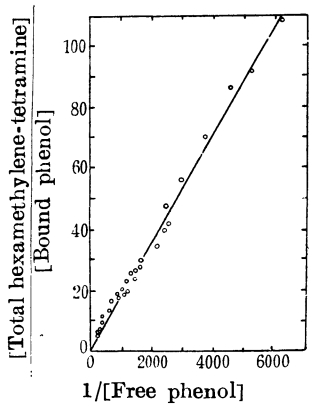

Fig. 14.

30°C. were obtained after I. M. Klotz's method,(6) with the results: $K=40$, $\Delta F=-2.4$ kcal./mol.

V. Hydrogen-Bond-Forming Powers of Atoms or Atomic Groups

The values of ΔF at 30°C. for the hydrogen bond between phenol and ethyl ether and for that between phenol and hexamethylene tetramine are, as have been given in the preceding section, −1.38 kcal./mol, and −2.4 kcal./mol, respectively;—*i. e.*, the latter bond is stronger than the former. While it is difficult to determine the exact values of ΔF and ΔE for

(4) On raising the temperature from 30 to 60°C., the position of the maximum absorption in the band due to the molecular complex shifts slightly (about 0.02 μ) to a shorter wave-length, and κ_0 decreases from 105 to 82. This fact shows that the structure of the molecular complex concerned is not strictly the same at different temperatures. In the present investigation, which aims at approximate estimation of ΔE, this difference in structure has been ignored.

(5) This preliminary examination was necessary because the observed absorption at 2.77 μ of phenol in carbon tetrachloride solution, even when its concentration is as low as 0—0.01 mol/l., does not obey Beer's law. This disobedience is but apparent, due to too low resolving power of the monochromator used (effective slit width: 0.05 μ) for the sharpness of the selective absorption of phenol at 2.77 μ.

(6) I. M. Klotz, F. M. Walker, and R. B. Pivan, *J. Am. Chem. Soc.*, **68**, 1486 (1946). Because of the low solubility of hexamethylene tetramine in CCl_4, it is impossible to use Klotz's method in determining the maximum number of phenol molecules that can be bound by one hexamethylene tetramine molecule. (Probably the maximum number is 4.)

the intermolecular hydrogen bonds in the other complexes examined, the order of the strengths of these hydrogen bonds in these complexes may be determined by observing the frequencies and the intensities of the O—H bands concerning the hydrogen bonds in question. Generally speaking, the frequency and the intensity of the hydrogen-bonded O—H band are taken as measures of the strength of the bond, if other conditions are equal. For, the lower frequency of the bonded O—H band indicates the greater loosening of the O—H accompanying the hydrogen bond formation, and the larger intensity indicates the higher concentration of the hydrogen-bonded O-H and accordingly indicates the larger value of K for the formation of the hydrogen-bonded complex. Inspections of Figs. 2, 5, 9, and 10, with what have been just stated in mind, reveal that the O—H···O bonds in the complexes: phenol-ethyl ether and phenol-anisol are stronger respectively than the O--H···O bonds in the complexes: methanol-ethyl ether and methanol-anisol, and that the OH of phenol is stronger than the OH of methanol in the tendency of donating its proton on its forming hydrogen bonds with other molecules. Similarly, from inspections of Fig. 2—7 and 9—10 it may be concluded that the proton-accepting powers of atoms in the molecules examined are in the following order, from stronger to weaker: N of hexamethylene tetramine, O of ethyl ether, O of benzaldehyde, O (carbonyl) of methyl benzoate, O of anisol, O of nitrobenzene.

From the order of the proton-donating and proton-accepting powers of the atoms and atomic groups as exemplified in the above, the following general rule may be advanced: The proton-donating power of X—H depends upon the tendency with which X attracts the electron of H to leave the proton bare; and the proton-accepting power of Y depends upon the tendency with which Y attracts electrons from the adjacent atoms or adjacent atomic groups to charge itself electrically negative. This rule agrees with and adds to what L. Pauling said concerning the strength of the hydrogen bond: "The strength of the hydrogen bond should increase with the increase in the electronegativity of the two bonded atoms (X and Y)."[7] The validity of the rule here advanced may be demonstrated also from the behavior of the O atom attached to the benzene ring. Thus, the electron migration in phenol molecule from O to benzene ring[8] results in an increase of the tendency of the H in OH to be left bare, and accordingly in increase of the proton-donating power of the OH group; this electron migration, on the other hand, results in a decrease of the negativity of the O atom attached to the benzene ring, and accordingly in the decrease of its proton-accepting power. (This last effect is apparent

Table 3

Inter-molecular hydrogen bonds	ν_{OH}, cm.$^{-1}$	$\Delta\nu_{OH}$, cm.$^{-1}$	*Intra*-molecular hydrogen bonds	ν_{OH}, cm.$^{-1}$	$\Delta\nu_{OH}$, cm.$^{-1}$
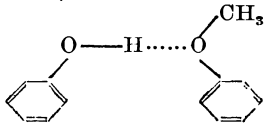	3460	150	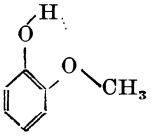	3560	50
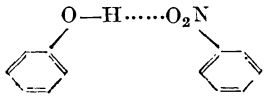	3520	90	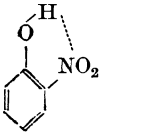	3250	360
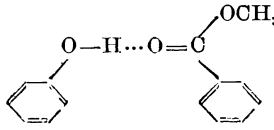	3470	140	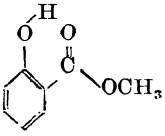	3220	390
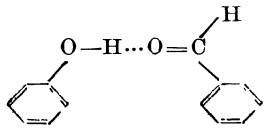	3460	150	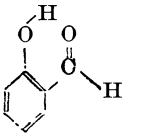	~3200	~400

(7) L. Pauling: The Nature of the Chemical Bond, 287 (1940). The words in the parentheses are the present writer's.

(8) K. F. Herzfeld: *Chem. Rev.*, **41**, 233 (1947); S. Nagakura and H. Baba: *J. Chem. Soc. Japan*, **71**, 527 (1950).

from the fact that the O atom in anisol has less proton-accepting power than that in ethyl ether.—*Cf.* the order in proton-accepting powers given above.)

Appendix.—In the course of the present investigation, an interesting fact has come to the writer's notice, *viz.*—The frequency of O—H, bonded with a certain atomic group, takes different values according as the bond is *intra*-molecular or *inter*-molecular. Table 3 gives the values of ν_{OH} (the frequency of O—H stretching vibration) and $\Delta\nu_{OH}$ (its difference from the frequency, 3610 cm^{-1}, of free O—H stretching vibration) given for some molecules and molecular complexes with *intra*-molecular and *inter*-molecular hydrogen bonds.

As is shown in the table, ν_{OH} in guaiacol is higher than that in the complex: $C_6H_5OH\cdots OCH_3C_6H_5$. This fact may be explained from the difference in the structural positions of oxygen atoms in these compounds; for, in guaiacol the oxygen atom of the methoxyl group which is the proton-acceptor, is situated at a position much displaced from the extention of the line representing the O—H bond vector. ν_{OH}'s for the other three O—H···O bonds listed in the table take lower values when the bonds are formed *intra*-molecularly than when they are formed *inter*-molecularly. This may be explained by assuming that there occurs a conjugation across the hydrogen bonds[9] when the bonds are formed *intra*-molecularly in *o*-nitrophenol, methyl salicylate, and salicylic aldehyde.

The writer wishes to express his sincere thanks to Professor San-ichiro Mizushima and Dr. Takehiko Shimanouchi for their kind guidance throughout this work. His thanks are also due to O. Matsumura for his lending the fluorite prism used, and to Professor S. Kambara, Mr. H. Tada, Mr. H. Baba, and Mr. T. Inukai for their placing some of the materials used at the writer's disposal. The cost of this research has been partly defrayed from Grant in Aid for Scientific Research from the Ministry of Education.

(9) R. S. Rasmussen, D. D. Tunnichiff, and R. Brattain, *J. Am. Chem. Soc.*, **71**, 1068 (1949); R. S. Rasmussen and R. Brattain, *ibid.*, 1073; I. M. Hunsberger, *J. Am. Chem. Soc.*, **72**, 5626 (1950).

1,2-Bis-(*p*-methoxyphenyl)-1-(methylthio)-butane, 1,2-Bis-(*p*-methoxyphenyl)-1-(methylthio)-2-methoxy-ethane, and 1,2-Bis-(*p*-methoxyphenyl)-1,2-bis-(methylthio)-ethylene. Estrogenic Sulfur Analogs of Hexestrol Dimethyl Ether and of Diethylstilbestrol Dimethyl Ether

By Yoshiyuki URUSHIBARA, Michinori ŌKI, and Reiji IKEDA

(Received November 12, 1951)

The syntheses of some estrogenic analogs of hexestrol have already been reported from this laboratory.[1][2] In the present paper the syntheses of further analogs of hexestrol dimethyl ether and of diethylstilbestrol dimethyl ether are described.

1,2-Bis-(*p*-methoxyphenyl)-1-(methylthio)-butane, $CH_3OC_6H_4CH(SCH_3)CH(C_2H_5)C_6H_4OCH_3$.—1,2-Bis-(*p*-methoxyphenyl)-butanol-(1), $CH_3OC_6H_4CHOHCH(C_2H_5)C_6H_4OCH_3$, m. p. 100-103°, was prepared by the reduction of the corresponding ketone, α-ethyldesoxyanisoin, with sodium amalgam in alcoholic solution.[3] The substituted butanol (1.0 g.) and methyl mercaptan (2 cc.) were dissolved in glacial acetic acid (30 cc.) and dry hydrogen chloride was passed into the solution for an hour, methyl mercaptan (1 cc.) being added every fifteen minutes. After the addition of a small amount of zinc chloride, the mixture was left to stand overnight under a stopper. The crystalline deposits were collected and recrystallized from ethyl acetate. 1,2-Bis-(*p*-methoxyphenyl)-1-(methylthio)-butane (0.55 g.) was obtained in colorless prisms melting at 152.5-154.5° and soluble with difficulty in alcohol.

(1) Y. Urushibara and M. Ōki, This Bulletin, **23**, 35 (1950).

(2) Y. Urushibara and T Takahashi, *ibid.*, **23**, 53 (1950).

(3) T. Takahashi, read before the annual meeting of the Chemical Society of Japan on April 2, 1950.

Yield: 49% of the theory. Found: S, 9.95%; molecular weight, 329. Calculated for $C_{19}H_{24}O_2S$: S, 10.13%; molecular weight, 316.

1, 2-Bis-(*p*-methoxyphenyl)-1-(methylthio)-2-methoxy-ethane, $CH_3OC_6H_4CH(SCH_3)CH(OCH_3)C_6H_4OCH_3$.—Anisoin methyl ether, $CH_3OC_6H_4CH(OCH_3)COC_6H_4OCH_3$, prepared by the action of methyl iodide and silver oxide on anisoin was reduced to hydranisoin methyl ether, $CH_3OC_6H_4CH(OCH_3)CHOHC_6H_4OCH_3$, with sodium amalgam.[4] The hydranisoin methyl ether (1.0 g.) was treated with methyl mercaptan and hydrogen chloride in the same way as described above. The product was recrystallized from ethyl acetate or alcohol. 1,2-Bis(*p*-methoxyphenyl)-1-(methylthio)-2-methoxy-ethane was obtained in colorless prisms melting at 190-191°, soluble in glacial acetic acid and in ethyl acetate, and soluble with difficulty in alcohol and in acetone. Yield: 55% of the theory (0.6 g.). Found: S, 10.25%; molecular weight, 305. Calculated for $C_{18}H_{22}O_3S$: S, 10.07%; molecular weight, 318.

Attempted preparation of anisoin methyl ether from α-bromodesoxyanisoin, $CH_3OC_6H_4CHBrCOC_6H_4OCH_3$, failed. The latter compound was prepared by the bromination of desoxyanisoin in direct sun light. α-Bromodesoxyanisoin melts at 101-103° with decomposition. Found: Br, 23.83%. Calculated for $C_{16}H_{15}O_3Br$: Br, 23.84%. It gave anisoin by the action of either sodium methoxide or sodium ethoxide.

1,2-Bis-(*p*-methoxyphenyl)-1,2-bis-(methylthio)-ethylene, $CH_3OC_6H_4C(SCH_3)=C(SCH_3)C_6H_4OCH_3$.—Anisoin (0.6 g.) was dissolved in glacial acetic acid (30 cc.). Methyl mercaptan (1 cc.) was added to the solution and dry hydrogen chloride was passed for an hour, while methyl mercaptan (0.5 cc.) was added every fifteen minutes. After the addition of a small amount of zinc chloride, the mixture was left to stand overnight. Deposited crystals were collected and recrystallized from ethyl acetate. 1,2-Bis-(*p*-methoxyphenyl)-1,2-bis-(methylthio)-ethylene was obtained in colorless prisms melting at 194-196° and soluble with difficulty in alcohol. Analysis gave the required result. Found: C, 65.65; H, 6.19; S, 19.12%; molecular weight, 337. Calculated for $C_{18}H_{20}O_2S_2$: C, 65.02; H, 6.06; S, 19.29%; molecular weight, 332. $C_{18}H_{22}O_2S_2$ would require H, 6.72%. The absorption spectrum of this substance gave a maximum at 235 mμ coinciding with the maximum given by diethylstilbestrol dimethyl ether, showing the presence of a similar dimethoxy-stilbene structure. Furthermore, it was different from the saturated 1,2-bis-(*p*-methoxyphenyl)-1,2-bis-(methylthio)-ethane, which was newly synthesized. The corresponding free phenol and its diacetate had already been synthesized.[1] The dimethyl ether was prepared from hydranisoin and from isohydranisoin as follows:

To obtain hydranisoin and isohydranison anisil was reduced with sodium amalgam in alcoholic solution. The two stereoisomeric products were separated by taking advantage of their different solubilities in ether and recrystallized from alcohol. Hydranisoin, $CH_3OC_6H_4CHOHCHOHC_6H_4OCH_3$, was treated with methyl mercaptan and hydrogen chloride in the same way as described above. Recrystallized from acetic acid, 1,2-bis-(*p*-methoxyphenyl)-1,2-bis-(methylthio)-ethane, $CH_3OC_6H_4CH(SCH_3)CH(SCH_3)C_6H_4OCH_3$, was obtained in colorless prisms melting at 188-190°. Found: S, 19.10%; molecular weight, 335. Calculated for $C_{18}H_{22}O_2S_2$: S, 19.17%; molecular weight, 334. Isohydranisoin, treated similarly, gave a viscous oil and a small amount of the same substance as obtained from hydranisoin. The oily product could not be purified.

Estrogenic Activities. — Since attempted demethylation to free phenols with thiophenol[5] was successful with neither of the hexestrol dimethyl ether analogs described above, the dimethyl ethers were tested on their physiological activities. The minimum doses to produce full estrus in ovariectomized mice by subcutaneous injection in two portions in oil solution were found as follows: 1,2-bis-(*p*-methoxyphenyl)-1-(methylthio)-butane 100 γ, 1,2-bis-(*p*-methoxyphenyl)-1-(methylthio)-2-methoxy ethane 100 γ, 1,2-bis-(*p*-methoxyphenyl)-1,2-bis-(methylthio)-ethylene 10 γ.

The authors thank the Ministry of Education for the Grant in Aid for Fundamental Scientific Research.

Department of Chemistry, Faculty of Science, Tokyo University.

(4) I. Moodie, *J. Chem. Soc.*, **1907**, 543.

(5) *Cf.* G. K. Hughes and E. O. P. Thompson, *Nature*, **164**, 365 (1949).

Studies on the Polarographic Analysis. XI. New Differential Polarography with One Dropping Electrode[1]

By Masayoshi ISHIBASHI and Taitiro FUJINAGA

(Received September 20, 1951)

Introduction

With the progress of polarography, interest in the differential technique has recently been aroused by Heyrovsky[2] and other workers.[3] Their methods depend on the use of two mercury electrodes dropping at the same rate, but this manipulation is very difficult. It was tried to make the drops fall at regular intervals by magnetic force or to make use of a streaming electrode and yet little has been gained in practice.

Delahay deviced to differentiate the electrometric titration curves with regard to time by inserting a condensor in series with a recording galvanometer and Lévèque and Roth have recently applied the method for differentiating the polarographic curves.[4] According to their method, therefore, the differential current can not be measured at any moment while the increase of the applied potential is stopped and also a good reproducibility is scarecely expected because of the use of an electrolytic condensor of a large capacity.

According to the authors' method, in which a rotating current-alternator similar to that of the Kalousek's method is used,[5] two applied potentials different by ΔE are applied by turns and the corresponding electrolytic currents flow through a galvanometer alternatively in reverse directions. Therefore, the differential current with one dropping electrode is easily measured at any applied potential and moreover, when the rotation of the current-alternator is stopped, it comes back to an ordinary polarograph without changing the circuit. These are the differences arising from the use of above mentioned methods.

In conclusion, however, the differential curves obtained by the authors' method show maetrially the differential curve of the ordinary polarogram only when the electrode reaction takes place so rapidly that the diffusion is a rate determinant and also when the reaction is irreversible. On the other hand they take on some different aspects in case of a reversible reaction or of a slow reaction rate.

Instrumentation

As seen from the circuit shown in Fig. 1, when potentiometer drum R and sliding contact C are used, potential difference between A and C, *i. e.*,

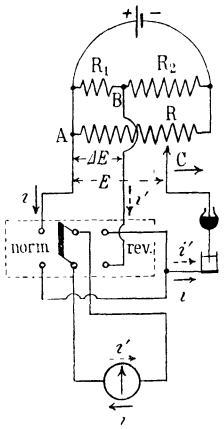

Fig. 1.—The principle of the differential polarograph.

E volt is applied to the cell and by inserting two resistances R_1 and R_2 in parallel with R and connecting B with anode, potential difference between B and C *i. e.*, $E-\Delta E$ volt is applied to the cell. Hence, if a four-poles-double-throw switch and a galvanometer are connected between A, B and the anode as indicated in the figure, a normal polarogram can be obtained when the switch is settled in side " norm.", while a polarogram in which the voltage is consecutively less by ΔE than in the former polarogram is obtained in the contrary direction when the switch is settled in one's turn in side " rev.", so the latter is $E-\Delta E$ *vs.* $-i'$ curve (Curve 2 in Fig. 3). Therefore the galvanometer will indicate $(i-i'/2)=\Delta i$ provided that the changing of the switch connection to side "norm." or "rev." is performed alternatively in regular intervals and moreover, so rapidly as the the galvanometer cannot correspond with the changing of currents because of its

(1) Presented at the annual meeting of the Chemical Society of Japan in 1951.

(2) J. Heyrovsky, *Chem. Listy*, **40**, 222 (1946).

(3) G. Semerano and L. Riccoboni, *Gazz. Chim. ital.*, **72**, 297 (1942).

(4) P. Lévèque and F. Roth, *J. Chim. Physique*, **46**, 480 (1949).

(5) M. Kalousek, Collection *Czech. Chem. Communs.*, **13**, 105 (1948).

inertia. In consequence of this, a differential polarogram, E *vs.* $\Delta i/\Delta E$ curve (Curve 3 in Fig. 3) should be obtained by sliding C continuously along R as in case of an ordinary polarography. To make in practice the connection change of the switch so rapid and at regular intervals, a cylindrical rotating switch shown in Fig. 2 is used and

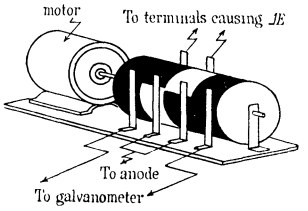

Fig. 2.—The rotating-current-alternator (the differentiator).

the rotation velocity is well adjusted at any interval from 500 to 1,500 r. p. m. Though this rotation velocity of the cylinder is influenced by characteristic properties of galvanometer, 700 to 1,000 r. p. m, is usually adopted (about four times faster than the Kalousek's experiment) and we can carry out the works with much reproducibilities even without using a synchronous motor.

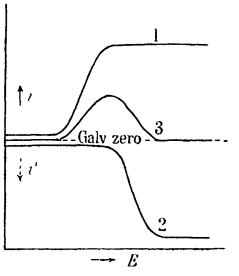

Fig. 3.—Schematic representation of the differential wave: curve 1, normal wave ($E\sim i$ curve); curve 2, reverse wave ($E-\Delta E\sim -i'$ curve); curve 3, composite differential wave ($E\sim\Delta i/\Delta E$ curve).

Results Obtained and Discussions

On the Reproducibility.—If ΔE is always fixed and there is not a large fluctuation in the rotation velocity, the results of a good reproducibility can be easily obtained. Fig. 4 indicates the reproducibility of the differential polarograms as for cadmium in chloride solution and as for zinc ammine solution.

On the Relation between the Peak Potential (E_h) of Differential Curve and the Half-Wave Potential ($E_{1/2}$) of Ordinary Curve.—The polarogram of simple metal ion is formulated as below by Heyrovsky and Ilkovic;

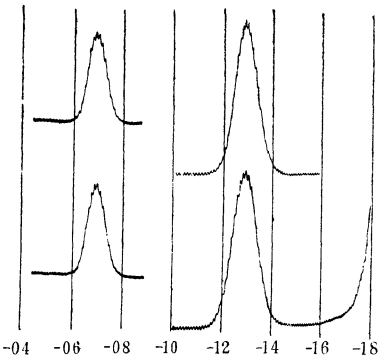

Fig. 4. — Reproducibility of the differential polarograms: left waves, Cd^{++} in KCl; right waves, Zn^{++} in NH_4Cl-NH_4OH.

$$E=E_{1/2}-RT/nF\cdot[\ln i/(i_d-i)] \qquad (1)$$

where E is potential of dropping electrode, $E_{1/2}$ half-wave potential, i electrolytic current corresponding to E, and i_d diffusion current. Here

$$i=i_d/e^{nF(E-E_{1/2})/RT}+1 \qquad (2)$$

Hence, differentiating current i with regard to applied potential E, we get

$$di/dE=-\frac{nF/RT\cdot i_d\cdot e^{nF(E-E_{1/2})/RT}}{\{e^{nF(E-E_{1/2})/RT}+1\}^2} \qquad (3)$$

Suppose d^2i/dE^2 to be zero, then $E=E_{1/2}$. Hence, from the formula (3) we get

$$(di/dE)_{E=E1/2}=-nF\cdot i_d/4RT \qquad (4)$$

So, let E be negative, the differential curve indicates its maximum value at $E_{1/2}$, which is denoted by $nF\cdot i_d/4RT$.

However, the formula (3) is only approximately effective even though ΔE is taken small enough and also the electrode reaction does not always take place fundamentally in accordance with the formala (1), it may be admitted that the peak potential of differential curve is not necessarily in accord with the half-wave potential, But taking $E-\Delta E/2$ instead of E for the potential axis, we can see usually a good accordance of them. (see Table 1). Accordingly, the precise half-wave potential is possible to be measured in qualitative analysis when ΔE is taken small enough.

On the Separability.—In the ordinary polarogram, the half-wave potential is generally on a gentle slope which is apt to give a cause for the overlap of two neighboring waves.

Table 1

Peak Potentials (E_h) and Half-Wave Potentials ($E_{1/2}$)

sample	ΔE, mV.	$Eh = E - \Delta E/2$ (*vs.* S.C.E.), V.		$E_{1/2}$ (*vs.* (S.C.E.),V.
Cd^{++} in KCl	20	-0.64_2,	-0.66_5*	-0.64_2
	40	-0.64_4		
	54	-0.64_4		
	54	-0.64_4		
	98	-0.64_6		
	206	-0.65_4		
Zn^{++} in NH_4OH	20	−1.36,	−1.38*	−1.36
	54		−1.38*	
	98		−1.39*	
	206		−1.36*	

* With damped galvanometer

While in the differential polarogram the half-wave potential is denoted by the potential which gives the maximum value of the curve, Moreover, according to this method, the increase in the current often occurs at maximum part owing to the dissolution of the deposited metals and the decrease of it after the maximum takes place by the stoppage of the dissolution phenomena and the minimum between two neighboring maximum is deeply notched. Hence in many cases it is possible to separate the waves whose difference is only 75 millivolts. This availability is more clearly observed particularly in separation at the last increasing domain (Fig. 5 and Fig. 6).

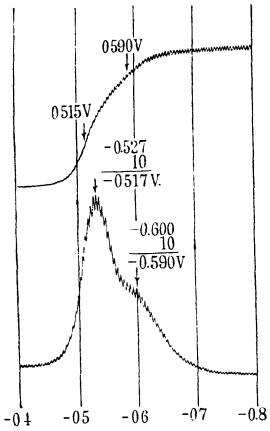

Applied potential, volt

Fig. 5.—Separability of the neighboring waves. Pb^{++} and Tl^{+} in 0.1 *N* KCl—0.1 *N* HNO_3: curve 1, ordinary curve; curve 2, differential curve (ΔE=20 mV.).

On the Elimination of the Components of the Diffusion Current and of the Residual Current. — The effect of the diffusion current is eliminated, so the imperfect detection and determination in the normal polarogram when much formerly discharging matters are present together are quite excluded or considerably lessened and that the sensitivity of the galvanometer is fairly magnified. The result of the experiment is shown in Fig. 7. In the

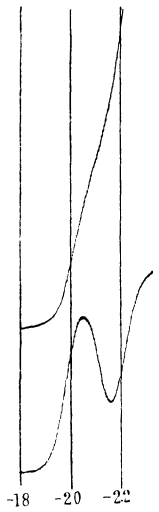

Applied potential, volt

Fig. 6.—Separability of the neighboring waves. Impurities in crude LiCl: curve 1, ordinary curve; curve 2, differential curve (ΔE=50 mV.).

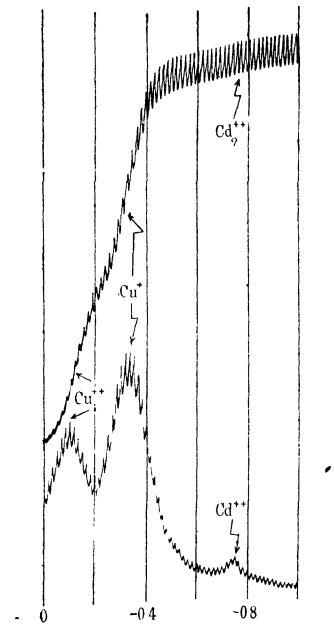

Applied potential, volt

Fig. 7.—Polarograms of brass dissolved in ammoniacal solution: curve 1, ordinary curve; curve 2, differential curve.

next place as for the residual current, it does not give much interference in the differential polarogram, since it always indicates the constant value. Therefore, the detection of the minute component is well carried out, which is inclined to be obstructed by the comparatively great residual current.

On the Elimination of the Current Vibration.—The current vibration caused by dropping of mercury drops is one of the factors which makes the measurements obscure in the normal polarogram. However, in the authors' differentical method this phenomena should be theoretically excluded; if the potential difference ΔE is enough infinitesimal. At any moment two reverse currents, which are yielded one after another, cancel themselves mutually in the domain of the diffusion current, namely in part excluding the peak in the differencial polarogram. (By the way this elimination does not take place in the Lévèque's method). In practice, however, the vibration is seen all the same in the part of the peak and larger the potential difference is, the larger the vibration becomes. (See also Fig. 7).

Summary

The authors studied on the new differential polarography; its instrumentation and result obtained were particularly reported in the present paper. Discussions for its quantitative analysis and for the electrode reactions and some utilities of current-alternator will be followed.

The authors express their sincere thanks to the Ministry of Education for its financial grant.

Laboratory of Analytical Chemistry,
Faculty of Science,
Kyoto University, Kyoto

Surface Films of Azo-proteins

By Taro TACHIBANA,[1] Kiyoshige FUKUDA, Kiyoshi INOKUCHI, Seisaburo YAMAOKA and Kan SUZUKI

(Received October 2, 1951)

Introduction

Numerous attempts[2] have been made to interprete the observed properties of the protein surface films in terms of the structure and the orientation of the film molecules. Though various hypotheses have been advanced, no definite conclusion has yet been reached. In order to throw some light on this problem, it seemed desirable to study the films of artificially modified proteins and to compare their behavior with that of the original native proteins. For this reason we made a study of the surface films of azo-protein, *i. e.* the protein to the side chains of which known chemical groups have been chemically conjugated through diazonium groups. As a sample of azo-protein, *p*-azo-phenylarsonic acid-conjugated ovalbumin (henceforth referred to as azo-ovalbumin) was chosen. With azo-ovalbumin, experiments were carried out to determine the force-area curves of the films spread on water.

Further, films were transferred, in various ways, onto metal slides and their antigenic activity to the antibody directed specifically against the diazonium groups was tested. In connection with the activity tests, the structure of protein monolayer was discussed. These are described in the present paper.[3]

Experimental

Material.[4]—The samples of azo-ovalbumin with various amounts of diazonium groups were prepared according to the method of Haurowitz[5] from purified hen ovalbumin by treating with different amounts of diazotized *p*-phenylarsonic

(1) Present address: Chemical Laboratory, Faculty of Science, Ochanomizu University, Bunkyo-ku, Tokyo.

(2) H. B. Bull, "Advances in Protein Chemistry," Vol. 3, 1947, p. 95—121.

(3) Following the present study, investigations were made on the relationship between the number of haptenic groups in azo-proteins and the number of adsorbed antibody molecules. These results will be reported elsewhere.

(4) Details on the material will be given by one of the present authors, S. Yamaoka, elsewhere.

(5) F. Haurowitz, *Hoppe-Seylers Z. physiol. Chem.*, **245**, 23 (1936~37).

acid. Each preparation was purified thoroughly until no further color was observed in the supernatant fluid after precipitation by adding hydrochloric acid followed by dialysis. The nitrogen analysis of the compounds was made by the Micro-Kjeldahl method modified by Elek and Sobotka[6] and the arsenic determination by the method of Sandell.[7] Each sample thus obtained was found to be electrophoretically uniform by the Tiselius method.

The number of diazonium groups per one molecule of azo-ovalbumin, x, was estimated by referring to Boyd and Hooker's[8] method of calculation. Then we may write the following equation

$$F_c = F(1-0.373\,R)+3.05\,R \qquad (1)$$

where F_c represents the ratio of the weight of azo-ovalbumin to total nitrogen in it, F, that of ovalbumin to nitrogen which was estimated as 6.62 according to Calvery,[9] and R, that of arsenic to total nitrogen in azo-ovalbumin.

When F_c is obtained from the value of F and R with an azo-ovalbumin, the percentage of arsenic content in azo-ovalbumin, As %, is calculated from the following equation,

$$\text{As}\,\% = 100\times\frac{R}{F_c} \qquad (2)$$

Thus, the value of x is obtained from the following equation

$$\text{As}\,\% = \frac{75\,x}{40000+228\,x}\times 100 \qquad (3)$$

where the molecular weight of ovalbumin is approximately taken as 40,000.

Procedure.—Preliminary experiments showed that although azo-ovalbumins had a tendency to spread on pure water, they appeared to dissolve partly into substrate. Therefore, solution of 0.01 N HCl or, more satisfactorily, a half saturated solution of ammonium sulfate was used as a substrate in a trough of chromium plated brass (60.0×14.6×2.0 cm.) In order to spread azo-ovalbumin monolayer, 0.05% aqueous solution of azo-ovalbumin was given on the surface of substrate solution from a capillary pipette. Force-area curves were obtained by using the Wilhelmy's method based on the principle of tensiometry.[10] The sensitivity of the instrument was of the order ±0.1 dyne per cm. For the measurement in low pressure regions, the sensitivity was raised to 0.01 dyne per cm., using thinner torsion wire (diameter 60 μ). All the experiments were made at a room temperature (about 20°C.). Next, the transfer of azo-ovalbumin monolayers onto metal slides was attempted. However, when acidic substrate water was used, it was frequently unsuccessful to obtain the built-up films of azo-ovalbumin using piston oil of castor oil (pressure, 15 dynes per cm.), because the detachment of the films occurred during the deposition. Thus, azo-ovalbumin was spread on distilled water at pH 5.5 and transferred onto chromium slides covered with the optical gauge of barium stearate multilayers, using castor oil as piston oil. One monolayer of azo-protein film can be transferred either by immersing the slide into the trough before the protein has been spread and withdrawing it through the protein monolayer (up-trip) or by immersing the slide through the protein monolayer previously spread (down-trip) and removing the monolayer from the surface before the slide is withdrawn.

According to Langmuir,[11] the monolayer deposited by down-trip is called an A-layer and that deposited by up-trip, a B-layer. In order to deposit a B-layer directly onto the optical gauge, it was necessary to condition the surface of barium stearate film by thorium nitrate solution (0.001 mol). One double-layer (AB-layer) of azo-ovalbumin can be transferred on stearate layers as easily as native proteins. It was found that a transfer of more than one double-layer on the barium stearate films was not successful, while successive transfer of B-layer was performed without difficulty. However, the increasing number of B-layer made further successive transfer gradually difficult. Possible mode of deposition will be described later.

To measure the deposition ratio, a floating barrier of a circular waxed paper disk was used. The displacement of the disk multiplied by the width of the trough gave the area of monolayer consumed.

The thickness of the built-up films of azo-ovalbumin was measured by using the Blodgett and Langmuir[12] method. The optical thickness (T) of the films was calculated from the following formula:

$$T = 24.4\left(N_1\frac{\cos r_1}{\cos r_2}-N_2\right), \qquad (4)$$

where T is the thickness in Å., N, the number of stearate layers which gives a minimum intensity in the reflected light for the angle of the refraction r_1 before the transfer of the film, N_2 the corresponding number of stearate layers after the film has been transferred, and r_2, the corresponding angle of refraction. The refractive index of protein film was assumed to be 1.495, being the same as that of barium stearate films. It was possible by using polarized sodium light to

(6) A. Elek and H. Sobotka, *J. Am. Chem. Soc.*, **48**, 501 (1926).

(7) E. B. Sandell, *Ind. Eng. Chem., Anal. Ed.*, **14**, 82 (1942).

(8) Boyd and Hooker, *J. Biol. Chem.*, **104**, 329 (1934). In Boyd and Hooker's paper the second term of the righthand side of formula (1) is represented as 3.20 R, but the coefficient should be corrected to 3.05.

(9) Calvery, *J. Biol. Chem.*, **94**, 613 (1931~32).

(10) A. Dognon and M. Abribat, *Compt. rend.*, **208**, 1881 (1939). T. Sasaki, *J. Chem. Soc. Japan.*, **62**, 796 (1941).

(11) I. Langmuir, *Cold Spring Harbor Symp.*, **56**, 171 (1938).

(12) K. B. Blodgett and I. Langmuir, *Phys. Rev.*, **51**, 964 (1937).

measure the thickness of built-up films within the error of approximately ±2Å. The increment of thickness by the adsorption of a antibodies onto azo-ovalbumin films was also measured by the above method.

Results and Discussion

Force-Area Relationships.—(i) High pressure region. Fig. 1 gives the force-area curves for the monolayer of native ovalbumin and azo-ovalbumin on a half-saturated solution of ammonium sulfate. These curves, A, B, C and D, show the relationships between pressure and specific area (m.²/mg.) for a series of azo-ovalbumins of increasing number of diazonium groups. As the number of diazonium groups in azo-ovalbumin molecule increases, the limiting specific area decreases. However, with the area per molecule, instead of specific area of azo-ovalbumin, practically identical force-area relationships were obtained for each sample of azo-ovalbumins irrespective of the number of diazonium groups. In other words, the limiting area (area extrapolated to zero pressure) per one azo-ovalbumin molecule is independent of the number of diazonium groups and is around 7000 Å.², although it tends to increase slightly with the coupling of diazonium groups. This means that diazonium groups introduced contribute not to the area but mainly to the thickness of azo-ovalbumin monolayer. The thickness of monolayer at 15 dynes per cm. can be evaluated from the correspondent specific area and the film density (assumed to be 1.3, the same as density in bulk). The results obtained with the samples of azo-ovalbumin are given in Column VIII of Table 1.

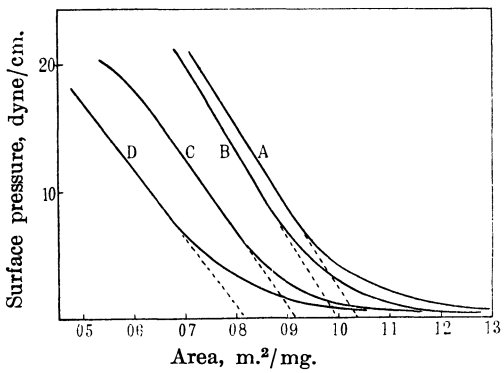

Fig. 1.—Force-area curves for azo-ovalbumin samples: curve A, Native ovalbumin; curves B, C and D, Azo-ovalbumin with 14, 30 and 58 diazonium groups per molecule.

On the other hand, the thickness is also found by the following consideration. Since the area per molecule of each sample is nearly the same at the pressure of 15 dynes per cm. *i. e.*, about 5500 Å.², the thickness (h_A) of their monolayers may be calculated from the following equation.

$$h_A = h_0 \frac{M_A}{M_0}, \qquad (5)$$

h_0 being the thickness of ovalbumin monolayer at the pressure of 15 dynes per cm., calculated from the specific area and density, M_A and M_0, molecular weight of azo-ovalbumin and ovalbumin, respectively, where the latter is taken as 40,000. The thickness values calculated are given in Column IX of Table 1, being in good agreement with that obtained from the specific area and density.

Thus, Eq. (5) is applicable for the estimation of molecular weight of azo-ovalbumins, on the basis of data available from force-area curves. The thickness of a single layer of azo-ovalbumin molecule, when measured directly using the built-up films, gave somewhat higher value than that obtained from force-area relationships (Column X, Table 1). As the deposition ratio of any of the samples of azo-ovalbumin was 0.83, the same as that of native ovalbumin, much higher thickness value should be expected with the film spread on distilled water. This may probably be due to incomplete spreading of azo-ovalbumin which was spread on distilled water so as to form the

Table 1

I	II	III	IV	V	VI	VII	VIII	IX	X
Sample	Number of azo-groups per molecule	Molecular weight	Limiting area per milligram, m.²	Area/mg. at 15 dynes/cm., m.²	Limiting area per molecule, Å.²×10⁸	Area per molecule at 15 dynes/cm., Å.²×10⁸	Thickness of monolayer calculated from specific area and density, Å.	Thickness of monolayer from Eq. (5), Å.	Thickness of monolayer observed at 15 dynes/cm., Å.
A	0	40000	1.04	0.81	6.9	5.3	9.5	9.5	9
B	14	43300	1.00	0.78	7.1	5.6	9.9	10.2	11
C	30	47100	0.92	0.69	7.4	5.4	11.1	11.1	12.5
D	58	53800	0.82	0.62	7.3	5.5	13.1	12.7	14

Temperature of measurements: 20~21°C.

built-up films.

It has now been established that the coupled diazonium groups do not contribute to the area of the compressed protein film molecule, but tend to increase the thickness. According to Pauly,[13] and Kapellar-Adler and Boxer[14] the diazonium groups are introduced into the side-chains of polypeptides, such as tyrosine and histidine residues. Accordingly, the present results seem to support the view[15] that under higher pressures the side-chains will be forced out of the surface until they are oriented perpendicular to the surface.

(ii) Low pressure region (below one dyne per cm.). The force-area curves of ovalbumin and azo-ovalbumin with 58 diazonium groups per molecule are shown in Fig. 2. It was found for both samples that a break occurs in force-area curves, denoting a higher order transformation point. A detailed description will be given in future.

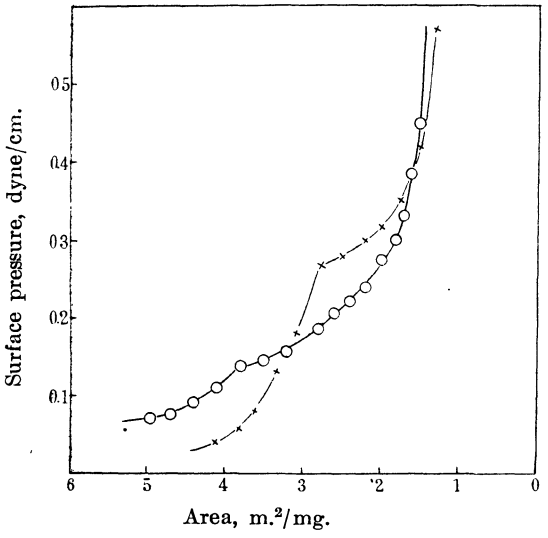

Fig. 2.—Force–area curves of azo-ovalbumin samples: Cross shows native ovalbumin and circle azo-ovalbumin with 41 diazonium groups per molecule. Underlying solution is 0.1 *N* HCl, and temperature, 23°C.

Various Types of Built-up Films of Azo-ovalbumin.—With ovalbumin various types of built-up films have been obtained by Langmuir[11] and coworkers. Langmuir indicated these films with the following symbols: PRA, PRAA, PRAB, PRBBB···, PRBAB, etc., where P stands for a metal plate, R for barium stearate multilayers, A for protein monolayers which is deposited by a down-trip and B for that deposited by an up-trip.

We examined the mode of deposition with azo-ovalbumins and found that it was possible to prepare the following types: PRA, PRABBB ···, PRTB, PRTBB, PRTBAB etc., where RT represents the barium stearate multilayers conditioned by thorium nitrate, the surface of which is hydorphilic. Contrary to ovalbumin, it was difficult to prepare the types of PRB and PRAA. According to our experience, it may be said that the more hydrophobic is the surface of underlying substrate, the easier is the deposition of A-layer, and the more hydrophilic the underlying surface, the easier the deposition of B-layer.

The order of wettability for various type of built-up films gave the following series:

$$\text{PRA} > \text{PRAB} > \text{PRTB}$$

i. e., PRA film is more hydrophilic than PRTB film. Langmuir[11] found, with ovalbumin, that PRA and PRB films differ very little in wettability. This fact has led him to the view that the hydrophobic and hydrophilic portions of protein molecule have no fixed orientations within the film, but can readily overturn by contact with water. In the present experiment, however, B-layer of azo-ovalbumin film was found to have adhered to the PRT film whose surface is highly polar. Then anchoring of hydrophilic groups to the surface of PRT film would occur, leaving the hydrophobic groups on the side exposed to air. This may be the reason why PRA film is more wettable toward water than PRTB film.

Antigenic Activity of Azo-ovalbumin Films.—The reactivity of protein films is evidently associated with the structure and orientation of film molecules. For instance, Langmuir and Schaefer[16] demonstrated that the activity of urease monolayers depends greatly on the type of films deposited. To obtain some insight into this problem, it was desirable to utilize azo–protein–antibody system. For this purpose, various types of the built-up film of azo–ovalbumin containing 29 diazonium groups in one molecule were treated with undiluted antiserum,[17] which contains an

(13) H. Pauly *Z. Physiol. Chem.*, **94**, 284 (1915).
(14) R. Kapellar-Adler and G. Boxer, *Biochem. Z.*, **285**, 55 (1936),
(15) *Cf.* H. Neurath and H. B. Bull, *Chem. Rev.*, **23**, 391 (1938).
(16) I. Langmuir and V. J. Schaefer, *J. Am. Chem. Soc.*, **60**, 1351 (1938).
(17) This serum was obtained from rabbits injected with *p*-phenylarsonic acid-conjugated horse serum and contained appreciable quantity of antibody specifically directed against the diazonium groups.

antibody specifically directed against the *p*-azo-phenylarsonic acid group, according to the following technique. The prepared plates were placed in antiserum during 15~20 hours. The plates were then removed and washed. After drying, the increment of thickness was measured. These results are summarized in Table 2.

Table 2

Type of film	Thickness increment after treatment with antiserum, Å.
PR	—
PRA	225
PRAB	400
$PR(AB)_E$	<20
$PR(AB)_EB$	250
$PR(AB)_EBB$	405
PRTB	90
PRTBA	180
PRTBB	180

The treatments with antiserum were performed at 0°C. The symbol $(AB)_E$ denotes one double-layer of ovalbumin which is ineffective to the adsorption of antibody used in these experiments. All the data were obtained with a pool of antisera in order to eliminate individual variation from serum to serum.

The treatment with antiserum produced a considerable adsorption on respective films, whereas the thickness increment on exposure to normal rabbit serum did not exceed a few Å. Obviously the prepared films demonstrated a clear-cut specificity.

Hereupon it would be of interest to compare the activity of A-layer with that of B-layer. For this purpose it seemed desirable to make a comparison between the activities of PRA and PRB films. However, it was impossible to make the film of type PRB with azo-ovalbumin. Therefore, for the sake of convenience the activity of B-layer on $PR(AB)_E$ film (barium stearate multilayer covered with one double-layer of ovalbumin) was compared with that of A-layer on PR film. The thickness increment with non-specific adsorption on one double-layer of ovalbumin alone ($PR(AB)_E$-film) did not exceed 20 Å. If this non-specific increment is taken from the data in Table 2, it would be found that the activity of a B-layer in $PR(AB)_EB$ is almost equal to that of an A-layer in PRA. Antigenic films of type $PR(AB)_EBB$ and PRAB, also, exhibited equal activity, and the activity of PRAB film was twice as much as that of PRA film. These results show that an A-layer and a B-layer of azo-ovalbumin film differ little in antigenic activity.

In the present experiments, however, the substrate films on which an A-layer or a B-layer was deposited were not the same. In this sense, the experiments using PRTBB and PRTBA as antigenic films would enable us to make the comparison between an A-layer and a B-layer, since then the underlying layer PRTB was common to both films. Thereupon, as shown in Table 2, the thickness increment on both films were almost equal and were twice as thick as that on PRTB film. From these data it may also be concluded that an A-layer and a B-layer have almost equal value in respect to antigenic activity. Similar results have been noticed in the behavior of a single layer of ovalbumin, bovine albumin or meta-kentrin by Rothen[18] and coworkers.

The results in Table 2 also show that the antigenic activity of azo-ovalbumin layer on PRT film is markedly less than those on PR or $PR(AB)_E$ film. This means that thorium nitrate conditioning of underlying substrate film has an effect of appreciably decreasing on the antigenic activity of azo-ovalbumin layer. This effect may be due to the anchoring of arsonic acid radicals in haptenic groups to highly polar surface of PRT film. The activity of PRTBB and PRTBA films are just twice as much as that of PRTB film which is less than that of PRA film. In other words, the effect of conditioning extends to the top layer of an antigen double-layer. Protein monolayer is of skeleton-like structure as considered by Blodgett[19] so that haptenic groups of top layer also could anchor to the polar surface of conditioned stearate multilayer.

The fact that the activity of two antigen layers is almost twice as much as that of one antigen layer, would require some explanation. Rothen[20] showed with bovine albumin that the amount of specifically adsorbed antibody is directly proportional to the number of underlying antigen layers up to a certain number. He explained this fact by "Long range forces" hypothesis. We also found a similar phenomenon by our experiments with azo-ovalbumin, some results of which were given in the previous paper.[21] In short, owing to the strong combining forces of antigen and antibody, antibody molecules could bind, penetrating into antigen films of skeleton-like structure, with the haptenic groups in the inside of films. Similarities of behavior in A-layer and

(18) A. Rothen: "Advances in Protein Chemistry," Vol. III, p. 123, (1947).
(19) K. B. Blodgett, *J. phys. Chem.*, **41**, 975 (1937).
(20) A. Rothen, *J. Biol. Chem.*, **168**, 75 (1947).
(21) T. Tachibana and K. Fukuda, This Bulletin, **24**, 4 (1951).

B-layer may also be explained along this line.

Summary

(1) Force-area curves were determined of monolayers of native ovalbumin and azo-ovalbumin with various number of diazonium groups. As a results it was found that the coupled diazonium groups do not contribute to the area of compressed protein film molecule, but tends to increase the thickness.

(2) The mode of deposition, when the monolayers of azo-ovalbumins are deposited on metal slides covered with multilayers of barium stearate, was examined. Various types of deposited azo-ovalbumin films thus obtained were tested as to their antigenic activity. The results were discussed in relation to the structure of protein films.

The authors wish to express their gratitude to Professor Jitsusaburo Sameshima (Department of Chemistry) and to Professor Tomio Ogata (Department of Serology) for their kind advice and encouragement throughout this work. The expense of this work has been defrayed from the Grant in Aid for Fundamental Scientific Research from the Ministry of Education, to which the authors' thanks are due.

Department of Chemistry, Faculty of Science and Department of Serology, School of Medicine, Tokyo University, Tokyo

Influence of Substituent Groups on Nuclear Reactivity in Formations of Substituted Biphenyls through Reactions of Aromatic Diazo and Cognate Compounds with Aromatic Liquids. II. The Bromine Atom

By Osamu SIMAMURA, Takashi INUKAI and Masaya KURATA

(Received November 24, 1951)

In a previous paper[1] the results of an investigation on the directive influence of the nitro group on the formation of isomeric nitrobiphenyls by the decomposition of N-nitrosoacetanilide or benzenediazo hydroxide in nitrobenzene have been reported. The nitro group has been found to activate all the nuclear positions of nitrobenzene towards substitution by the phenyl radical as compared with the reactivity of the nucleus of benzene itself. The present report is concerned with the results of a similar investigation on the influence of the bromine substituent on the formation of isomeric bromobiphenyls from bromobenzene by the decomposition of N-nitrosoacetanilide or of benzenediazo hydroxide produced by the reaction between benzenediazonium chloride and alkali:

$$C_6H_5Br + C_6H_5N(NO)COCH_3 \rightarrow C_6H_5C_6H_4Br + N_2 + CH_3COOH,$$

$$C_6H_5Br + C_6H_5N_2Cl + NaOH \rightarrow C_6H_5C_6H_4Br + N_2 + NaCl + H_2O.$$

At first we have tried to determine the ratio of *o*-, *m*- and *p*-bromobiphenyls in the product by oxidizing the isomeric mixture formed with chromic trioxide in acetic acid to a mixture of the corresponding bromobenzoic acids and then fractionating the latter. It was shown by preliminary experiments that this method could not give reliable results, because the isomeric bromobiphenyls undergo oxidation with different yields of the corresponding bromobenzoic acids, and, moreover, the yields were hardly reproducible enough to permit the accurate determination. However, it could be demonstrated in this way that all the possible isomerides of bromobiphenyls are produced in these reactions. Thus, the approximate percentages of the *o*-, *m*- and *p*-bromobiphenyls formed in the decomposition of benzenediazo hydroxide in bromobenzene were estimated to be 30.1, 25.5 and 44.4%, respectively, and the corresponding percentages in the decomposition of nitrosoacetanilide in bromobenzene were

(1) O. Simamura, T. Inukai and M. Kanazashi, This Bulletin, **23**, 205 (1950).

22.3, 26.5 and 51.1%, respectively. As the formation of only *o*- and *p*-bromobiphenyls in a similar reaction[2] is recorded in the literature, it is to be noted that the meta isomeride was formed in a considerable amount as in the reaction in nitrobenzene which gave as much as 23% of *m*-nitrobiphenyl along with *o*- and *p*-isomerides.[1] Competitive reactions carried out in a mixture of bromobenzene and benzene showed that bromobenzene reacted with phenyl radicals 1.4 to 2.6 times as fast as benzene.[3]

Snbsequently, infra-red spectrophotometric analysis of the reaction products carried out by Mr. K. Kuratani in the Institute of Science and Technology of this university revealed that the results shown above were too high in the percentage of the para isomeride. In this analysis, absorptions were measured at 9.70, 12.06 and 12.70 microns, each an absorption band characteristic of *o*-, *p*- and *m*-bromobiphenyls, respectively. Table 1 illustrates the accuracy of this analytical method. The results of reinvestigation performed by means of the spectrophotometric determination are summarized in Table 2.

Table 1

Percentages of isomerides in known mixtures

	Taken	Found	Taken	Found
Ortho	60	60	52	50
Meta	11	9	35	34
Para	29	29	13	16

Table 2

Expt. No.*	Reactants		Bromobiphenyls Yield, millimoles	Isomeric ratio *o*	*m*	*p*
1	$C_6H_5N_2OH$(from 6.5 g. aniline)	200 cc.	19.8	59	26	14
2	$C_6H_5N_2OH$(from 24 g. aniline)	335 cc.	52.4	53	26	21
3	$C_6H_5N_2OH$(from 6.5 g. aniline)	217 cc. +C_6H_6 373 cc.	9.18 +Biphenyl 5.96			
4	$C_6H_5N(NO)$-$COCH_3$ 5.0 g	287 cc.	28.8*	60	22	18
5	$C_6H_5N(NO)$-$COCH_3$ 39.5 g.	183 cc. +C_6H_6 155 cc.	22.5 +Biphenyl 8.77			

* See Experimental Part.

The percentage of the ortho isomeride formed was remarkably high, and this is in line with the preponderant formation of *o*-nitrobiphenyl in the reactions of N-nitrosoacetanilide, benzenediazo hydroxide and dibenzoyl peroxide with nitrobenzene, and of *o*-methoxybiphenyl in the decomposition of dibenzoyl peroxide in anisole as shown in Table 3.

Table 3

Reactants		Isomeric ratio of biphenyls formed *o*	*m*	*p*	Reference
$C_6H_5N_2OH$	$C_6H_5NO_2$	46	19	35	(1)
		55	4	41	(4)
$C_6H_5N(NO)Ac$	$C_6H_5NO_2$	58	23	19	(1)
		60	9	31	(4)
$(C_6H_5CO_2)_2$	$C_6H_5NO_2$	72	2	26	(4)
$(C_6H_5CO_2)_2$	$C_6H_5OCH_3$	67	18	15	(5)

In experiment 3, biphenyl and bromobiphenyls were formed in a molar ratio of 1:1.54, and as benzene was used in an amount about twice that of bromobenzene, the ratio of the reactivities of benzene and bromobenzene is 1:3.2. Since it may reasonably be assumed that the isomeric ratio found in experiment 1 obtains in the competitive reaction, the relative reactivities[6] of the *o*-, *m*- and *p*-nuclear positions of bromobenzene are calculated to be 5.7, 2.5 and 2.7, respectively, the reactivity of one position of the unsubstituted benzene nucleus being taken as unity. Similarly, from the data of experiments 4 and 5 the reactivities for the isomeric positions are found to be 4.6, 1.7 and 2.8, respectively.

The common tendency observed in the isomeric ratios of substituted biphenyls formed in the various reactions which include the decomposition of dibenzoyl peroxide and the activating influence of substituent groups, such as the bromine atom (Expts. 3 and 5) and the nitro group,[1] on the reactivity of the benzene nucleus to which these groups are attached towards attack by the phenyl group afford strong supports for a hypothesis that these reactions take place through a mechanism involving free phenyl radicals.[7]

Experimental

Materials.—N-Nitrosoacetanilide was prepared by the method of O. Fischer[8] as in the previous investigation. Benzene, bromobenzene and aniline were purified by repeated distillation.

(2) M. Gomberg and W. E. Bachmann, *J. Am. Chem. Soc.*, **46**, 2339 (1924).

(3) The above results were reported at the third annual meeting of the Chemical Society of Japan, Kyoto, April 1950.

(4) DeLos F. DeTar and H. J. Scheifele, *J. Am. Chem. Soc.*, **73**, 1442 (1951).

(5) T. Suehiro, *J. Chem. Soc. Japan, Pure Chem. Sect.*, **72**, 301 (1951).

(6) See reference 1.

(7) See, *e. g.*, W. A. Waters, "The Chemistry of Free Radicals," Oxford University Press, London, 1948.

(8) O. Fischer, *Ber.*, **9**, 463 (1876).

Reactions with Benzenediazo Hydroxide.—Experiment 1. Aniline (6.5 g.) dissovled in 6 cc. of water and 14 cc. of concentrated hydrochloric acid was diazotized by adding a solution of 5.1 g. of sodium nitrite in 10 cc. of water. The resulting solution was added to 200 cc. of bromobenzene, and to this mixture a solution of 6.7 g. of sodium hydroxide in 20 cc. of water was added dropwise with vigorous stirring at 5-8° in the course of thirty minutes. The stirring was continued for a further four hours. The reaction mixture was separated from the aqueous layer and distilled through a Vigreux column 30 cm. in length to remove bromobenzene. The residue was subjected to vacuum distillation and the distillate treated with a little zinc and hydrochloric acid. The colourless liquid thus obtained was distilled under diminished pressure to yield 4.61 g. of a mixture of bromobiphenyls boiling at 130 to 143° at 8.5 mm. Hg (Found: Br, 34.03%. Calcd. for $C_{12}H_9Br$: Br, 34.28%). Experiment 2 was carried out similarly.

Experiment 3. For a competitive reaction a mixture of 217 cc. (2.02 moles) of bromobenzene and 373 cc. (4.21 moles) of benzene was used instead of 200 cc. of bromobenzene, the amounts of the other reagents being equal to those in the run described above. After the usual treatment benzene and bromobenzene were removed through a fractionating column. The distillate was again fractionated and the residue in the distilling flask was combined with the residue from the initial distillation. The mixture was fractionated under diminished pressure, giving a very small amount of bromobenzene, and then a fraction, from which biphenyl deposited, and another containing bromobiphenyls. The crystallized biphenyl was separated and weighed. The mother liquor was combined with the crude bromobiphenyls, and the mixture was freed from traces of bromobenzene by fractional distillation under diminished pressure and analyzed for bromine in order to estimate the content of bromobiphenyls. Thus, it was found that 2.14 g. of bromobiphenyls and 0.9 g. of biphenyl were produced in this reaction, the yields being 13.2 and 8.5%, respectively, based on the aniline used.

Reactions with N-Nitrosoacetanilide.—Experiment 4. N-Nitrosoacetanilide (5 g.) was added to bromobenzene (286 cc.). The dissolution took place at 16.5 without evolution of heat and the decomposition proceeded gradually. Two such reaction mixtures were combined after three days and worked up as described above. The final product, b. p. 136-145° at 9.5 mm. Hg, weighed 6.72 g. (Found: Br, 34.49%. Calcd. for $C_{12}H_9Br$: Br, 34.28%).

Experiment 5. For a competitive run, 39.5 g. (0.24 mole) of N-nitrosoacetanilide was allowed to decompose in a mixture of 155 cc. of benzene and 183 cc. of bromobenzene (both 1.74 moles), and 5.25 g. of bromobiphenyls and 1.25 g. of biphenyl were obtained.

Summary

The reaction of N-nitrosoacetanilide or benzenediazo hydroxide with bromobenzene gives all three isomerides of bromobiphenyls, the yields decreasing in the order ortho > meta > para. All the nuclear positions of bromobenzene are more reactive than benzene towards attack by the phenyl radicals.

The authors thank Mr. K. Kuratani in the Institute of Science and Technology, Tokyo University for the spectrophotometric analyses and the Ministry of Eduction for a Grant-in-Aid for Scientific Research.

Department of Chemistry, Faculty of Science, Tokyo University, Tokyo

LETTER

A Note on the Identification of Ortho-, Meta- and Pyro-Phosphates by Means of Paper Chromatography[1]

By Toshio ANDO, Jiro ITO, Shin-ichi ISHI, and Tokuro SODA

(Received December 18, 1951)

It is often desired in the field of biochemical studies to identify easily ortho-, meta-, and pyro-phosphates in minute quantities. A characteristic yellow coloration produced with ammonium molybdate instantly from the ortho-phospahate and only after heating from meta- and pyro-phosphates, will be usefull for detecting them when combined with a development on filter paper. However, it is difficult to distinguish the spots clearly by this method unless the separation is quite complete, as they are all colored similarly. Only for the ortho-phosphate, several methods have been described for its identification, in which the phosphate was detected either on a paper without development by a blue stain formed by adding a drop of molybdate followed by that of benzidine[2] (a

(1) The present paper was read by one of the authors (J. I.) before the 8th Meeting of this institute held on Sept. 29, 1951.

(2) F. Feigl *Z. anal. Chem.*, **61**, 454 (1922); **74**, 386 (1928); **77**, 299 (1929).

spot test), or also on a paper with development by the yellow color of phosphomolybdate or by the blue color formed further from the latter by the action of hydrogen sulfide.[3] Nevertheless, none of these procedures has yet been applied for the identification of meta- and pyrophosphates.

The present authors have now developed a method of identifying the three types of phosphates accurately on paper chromatograms. About 0.005 cc. of 0.1 *M* aqueous solutions of sodium ortho-, meta- and pyro-phosphates, respectively alone or in their various mixtures, were developed on paper strips (1.8×20 cm. of the Toyo filter paper No. 2) at 25-30°C. with butanol-acetic acid-water (4:1:5 V/V) as a solvent, followed by spraying with a solution of ammonium molybdate in nitric acid[4] and by heating, and then by further spraying with a solution of benzidine in acetic acid.[4] On neutralizing in an atmosphere of ammonia, meta-, pyro- and ortho-phosphates were revealed successively as a blue spot with $R_F = 0$, a purplish red with $R_F = 0.15$, and a blue with $R_F = 0.21$. They were easily distinguished respectively, owing to the difference in color and also to the colorless boundary lines which always appeared among them.

Coexistence of arsenate or nitrate with phosphates was found not to disturb the present identification. Further experiments are now in progress, in which the development with a solvent mixture of modified ratio on the Toyo filter paper No, 50 and the influences of heavy metallic ions upon the chromatograms are respectively examined. Details will be published later elsewhere.

Institute of Science and Technology,
TokyoUniversity, Tokyo

(3) C. S. Hanes and F. I. Isherwood, *Nature*, **164**, 1107 (1949).

(4) *Cf.* F. Feigl, "Qualitative Analysis by spot Tests," 3rd English edition (translated by R. E. Oesper), New York, 1947, p. 251.

Molecular Structure of Monochloromethyl Chloroformate

By Minoru KASHIMA

(Received January 21, 1952)

The molecular structure of monochloromethyl chloroformate molecule in the gas phase was determined by electron diffraction studies. The sample was prepared by passing a mixture of methylformate vapour and chlorine through a silica tube exposed to the light from a mercury lamp, and redistilled at 52.5—53° under 100 mm.Hg. The photographs were taken in the usual way with an electron wave lengh of about 0.06 Å. and a camera distance of 8.5 cm.

The interatomic distances and valence angles determined are as follows:

$ClCOOCH_2Cl$.

Cl-C	1.74 ± 0.02 Å.
Cl—C (chloromethyl)	1.74 ± 0.02 Å.
C=O	1.20 ± 0.03 Å.
C—O (carboxyl)	1.40 ± 0.04 Å.
C—O (methoxyl)	1.40 ± 0.04 Å.
∠Cl—C—O	112 ± 4°
∠O=C—O	126 ± 4°
∠C—O—C	110 ± 4°
∠O—C—Cl (chloromethyl)	109.5 ± 3°

An angle between and 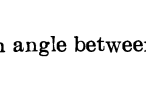 plane is 0°~90°, and the chlorine atom in the $-CH_2Cl$ group is *trans* to the carboxyl carbon atom.

The carboxyl C—O bond in this molecule is about 0.03 Å. shorter than the normal bond, corresponding about 5% of Pauling double bond character and thus in fair agreement with its non-planar constellation. J. M. O. Gorman *et al.* reported the structures of the methyl formate, methyl acetate and methyl chloroformate molecules by means of electron diffraction.[1] According to their investigation, all these molecules have approximately planar configurations with the ester methyl group *cis* to the carbonyl oxygen atom, and they have shorter carboxyl C—O distance (1.35-1.37 Å.), and longer methoxyl C—O distance (1.46-1.47 Å.), than the normal bond. The contrasting results for these esters are in agreement with the conclusions from dipole-moment studies for aliphatic carboxylic esters[2],[3],[4] but not for methyl carbonate and methyl and ethyl chloroformates, these molecules according to the dipole studies[5],[6] having rather large amplitudes of libration. However, the dipole moment data are not incompatible with a mainly planar structure, either *cis* or *trans*, with considerable libration and considerable resonance, the various, possibly large, resonance moment contributions having been neglected.[5],[6] Accordingly, the carboxylic C—O bond seems to have less double bond character and hindrance to

(1) J. M. O. Gorman, W. Shand, Jr. and V. Schomaker, *J. Am. Chem. Soc.*, **72**, 4222 (1950).
(2) A. Eucken and L. Meyer, *Physik. Z.*, **30**, 397 (1927).
(3) C. T. Zahn, *ibid.*, **33**, 730 (1933).
(4) R. J. B. Marsden and L. E. Sutton, *J. Chem. Soc.* **1936**, 1383.
(5) M. Kubo, Y. Morino and S. Mizushima, *Sci. Papers. Inst. Phys. Chem. Research (Tokyo)*, **32**, 129 (1937).
(6) S. Mizushima and M. Kubo, This Bulletin, **13**, 174 (1938).

libration in methyl chloroformate than in the simple esters, but more than in chloromethyl chloroformate; correspondingly, chlorine in either position probably diminishes the net contribution of the C—O (carboxyl) structures such as I, 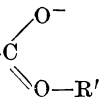 perhaps by giving rise predominantly to competing structures such as II, 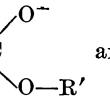 and III, 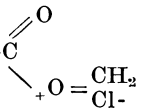

as well as by the destabilizing (inductive) effect of the chloromethyl dipole on structure I. Structure III would also account for the shortening of methoxyl C—O in monochloromethyl chloroformate.

The details of this research will be published elsewhere.

The author wishes to express his sincere appreciation to Dr. S. Yamaguchi, Prof. V. Schomaker and Prof. Y. Morino for their kind advice and discussion, and also to Prof. Y. Kuwata for his interest in carrying out of this research.

The Scientific Research Institute.
31, *Komagome-Kamifujimaecho,*
Bunkyo-ku, Tokyo

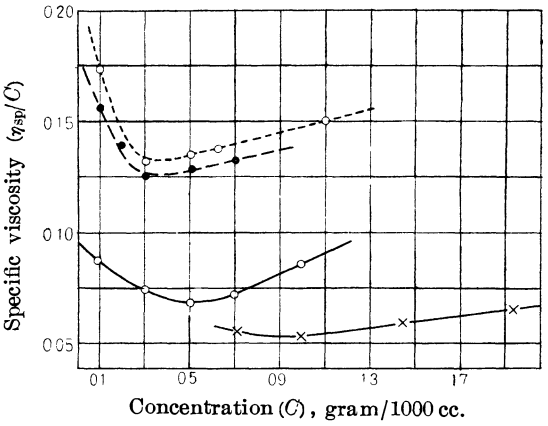

Fig. 1.—Viscosity of polyvinyl chloride in extremely dilute solution: × Sample 1 (average polymerization degree 600), ○ Sample 2 (*ditto* 1500), ● Sample 3 (*ditto* 2900), ——tricresyl phosphate, ... dioctyl phthalate, ---- cyclohexanone. Temperature: 80°C.

Abnormal Viscosity of Polyvinyl Chloride in Extremely Dilute Solutions

By Masatami TAKEDA and Eiiti TURUTA

(Received January 22, 1952)

With a view to determine the intrinsic viscosity of polyvinyl chloride[1] in solutions of some plasticizers, we have measured the viscosity in extremely dilute solutions of unfractionated polyvinyl chloride in dioctyl phthalate as well as in tricresyl phosphate by means of an Ostwald viscosimeter. The solutions were prepared by dispersing the sample in the plasticizer two days at room temperature and by heating four hours at 90°C. The results are shown in Fig. 1,[2] from which, however, the intrinsic viscosity cannot be calculated, since the relation between the specific viscosity divided by concentration (η_{sp}/C) and the concentration (C) dons not conform with the empirical equation of Huggins.[3] Besides, we have observed a similar abnormal behavior in cyclohexanone at extreme dilution, whereas, at higher concentrations no anomaly has ever been observed in this solvent, as reported in our previous paper.[4] In general, it has been found that the value of η_{sp}/C of polyvinyl chloride in extremely dilute solutions shows a minimum at a certain concentration, and then increases with further dilution. Such behavior has never been found with non-electrolytic high polymers, such as polyvinyl chloride, although similar abnormal phenomena have already been observed with high-molecular electrolyte.[5]

This somewhat unexpected phenomenon may be of particular interest in two respects. First, it is expected that the true intrinsic viscosity of chain polymer is estimated from these experimental results, the value of which is now frequently used for the estimation of the size and shape of chain polymers in solution by the aid of theories. Secondly the concentration of the minimum value of η_{sp}/C changes with the molecular weight of chain polymers and the nature of solvents, which is evident from Fig. 1. Thus, these phenomena together with theoretical considerations suggest that there may exist a certain special interaction between the polymer molecules in such dilute solutions.

Tokyo College of Science, Shinjuku, Tokyo

(1) Supplied by the Mitsui Chemical Industrial Company, and purified by precipitating once from a cyclohexanone solution with methanol.

(2) From the fluctuation of measured flow times of solution, the probable error of η_{sp}/C is estimated to be ±1% in the most dilute solution of cyclohexanone, ±3.5% in the most dilute solution of dioctyl phthalate and ±8% in the most dilute solution of tricreesyl phosphate.

(3) M. L. Huggins, *J. Am. Chem. Soc.*, **64**, 2716 (1942).

(4) Takeda and Turuta, *J. Phys. Soc. Japan*, **6**, 525 (1951).

(5) Fuoss, *J. Polymer Science*, **3**, 602 (1948).

Stereomerisierung der α-Bromallozimtsäure und eine vorläufige Bemerkung über das Additionsprodukt von Bromwasserstoff zu Phenylpropiolsäure

Von Hazime KASIWAGI

(Eingegangen am 6, August, 1951)

Bei zahlreichen Äthylenverbindungen ist es als Sauerstoffeffekt wohl bekannt, dass sie mit Bromwasserstoff in Gegenwart von Luft, Sauerstoff oder einem gewissen Peroxyde reagieren, und daraus das "abnormale," *d. h.* das zur Markownikowschen Regel in Widerspruch stehende Additionsprodukt bilden *bzw.* durch die sterische Umlagerung in ihre geometrischen Isomeren verwandeln *u. s. w.* Dieser Effekt beruht wesentlich auf einer Kettenreaktion, die durch das freie organische Radikal hervorgerufen wird. Dies letztere ist aus der Äthylenmolekel durch Addition des bei der Reaktion entstandenen Bromatoms als Reaktionsintermediat gebildet. Diese Auffassung ist heute festgestellt worden durch die Tatsache, dass derselbe Effekt durch Anwesenheit von einem "Antioxidant," *z. B.* Brenzkatechin, stark oder ganz verzögert wird.

Der Verfasser beabsichtigt den Vorgang zu untersuchen, wie der sauerstoffeffekt bei den Substanzen auftritt, die eine dreifache Bindung haben. Zu diesem Zwecke ist die Phenylpropiolsäure ausgewählt worden. Über die Addition von Bromwasserstoff zu dieser Substanz haben früher A. Michael und G. H. Shadinger bereits Bericht erstattet,[1] dass sie nämlich, der Verschiedenheit der gebrauchten Lösungsmitteln gemäss, bald α-Bromzimtsäure, bald β-Bromzimtsäure als Produkt erhalten haben. Bemerkenswert ist dabei, dass Phenyl und Carboxyl-gruppe immer eine *trans*-Stellung miteinander einnehmen. Hierauf fassen sie die Bildung solcher Säuren nur als den Effekt verschiedener Lösungsmittel auf, in den man den Bromwasserstoff auf Phenylpropiolsäure reagieren lässt, und infolgedessen lehnen den Kettenmechanismus durch Sauerstoffeffekt ab. Bei dem jetzigen Stand der Kenntnisse muss aber die Möglichkeit geprüft werden, dass die Reaktion durch Mechanismus des Sauerstoffeffekts herbeigeführt würde, was die Entstehung der verschiedenen Säuren zur Folge haben mag. Ferner wird man auch wohl mit Recht diejenigen Bromzimtsäuren, mindestens einen Teil derselben, sei es auch gering, als die sich wegen der sekundären Umlagerung der *cis*- oder Bromallozimtsäuren gebildeten *trans*-Säuren ansehen können.

Zur Erklärung dieser Fragen werden hier die Beobachtungen über die Stereomerisierung der α-Bromallozimtsäure und über die Addition des Bromwasserstoffs zu Phenylpropiolsäure mitgeteilt, die von mir in Gegenwart von Brenzkatechin durchgeführt worden ist.

Betreffs der terischen Umlagerung der α-Bromallozimtsäure ist die Tatsache schon längst bemerkt worden, dass sie durch Einwirkung einer kleinen Menge von Brom (noch besser, unter dem Sonnenlicht)[2] oder der Wärme[3] zustande kommt. Da wird übrigens die Umlagerung des einen geometrischen Isomeren in das andere durch Einwirkung von Bromwasserstoff nach der nachstehenden Formel des Dissoziationsgleichgewichts, durchgeführt, wenn die infolge des Sauerstoffeffekts entstandenen Radikale sich miteinander nicht vereinigen oder die Atome (H, Br *u. a.*) nicht einnehmen.[4]

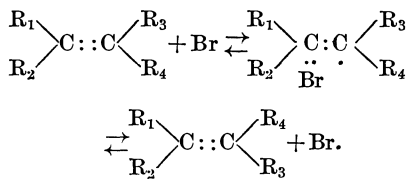

Die Isomerisierung Isostilbens in Stilben durch Bromwasserstoff, deren Verlauf im Gegenwart von Licht, Sauerstoff oder Peroxyde stark beschleunigt wird,[5] ist ein typisches Beispiel, das durch den oben erklärten Mechanismus vor sich geht.

Anderseits wird die Umwandlung des Maleinsäuremethylesters ins Fumaroid durch Ein-

(1) *J. Org. Chem.*, **4**, 128 (1939).

(2) R. Stoermer und P. Heymann, *Ber.*, **46**, 1258 (1913).

(3) J. J. Sudborough und K. J. Thompson, *J. Chem. Soc.*, **83**, 686 (1903).

(4) F. R. Mayo und C. Walling, *Chem. Rev.*, **27**, 404 (1940).

(5) Y. Urushibara und O. Simamura, Dieses Bulletin, **13**, 566 (1938); Y. Urushibara, *J. Chem. Soc. Japan*, **60**, 717 (1938).

wirkung von Bromwasserstoff,[6] abweichend von denen der dem Stilben ähnlich gebauten Verbindungen, weder durch Sauerstoff beschleunigt noch durch Brenzkatechin unterdrückt wird, aber durch Chlorwasserstoff durchgeführt, womit der Sauerstoffeffekt nicht in Frage kommen kann. Dies weist darauf hin, dass der Vorgang nicht etwa durch das durch Sauerstoffeffekt hervorgerufene Radikal gefördert wird, sondern wohl durch eine elektromerische Verschiebung der Doppelbindung wegen der Protonaufnahme des anliegenden Carbonylsauerstoffs.

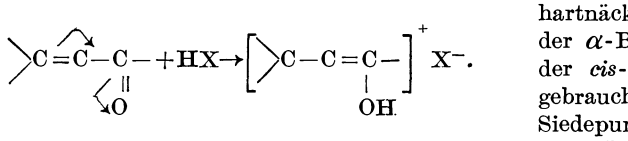

Wenn man α-Bromallozimtsäure in einem gewissen, den Bromwasserstoff enthaltenden Lösungsmittel auflöst und sie mehrere Stunden stehen lässt, so verwandelt sie grösstenteils in die *trans*- *d. h.* α-Bromzimtsäure, was man wohl durch den Mechanismus der Kettenreaktion erklären kann, die das durch Sauerstoffeffekt hervorgebrachte Bromatom enthält. Ferner kann man sich vorstellen, dass diese Auslegung sich dadurch bestätigt, dass die oben genannte Isomerisierung stark gehemmt wird von einer Substanz, *z. B.* Brenzkatechin, die den Sauerstoffeffekt zurückhalten kann.

Ferner hat man die Tetrachlorkohlenstofflösung der α-Bromallozimtsäure unter stetigem Chlorwasserstoffstrom auf längere Zeit erhitzt, was die Isomerisierung der zuständigen Säure in *trans*-Säure zur Folge gehabt hat, obzwar die Umwandlung dadurch nur partiell gewesen und viel langsamer als durch Bromwasserstoff oder Brom verlaufen sein mag.

Folglich hat man bewiesen, dass die α-Bromallozimtsäure durch den beiden Mechanismen isomerisieren kann, wie Allozimtsäureester,[7] der die struktuelle Eigentümlichkeiten der oben erwähnten beiden Reihen von Verbindungen hat, *d. h.* der Stilbenreihe, so wie der Maleinsäure.

Die Fähigkeit der Broms, die Isomerisierung der α-Bromallozimtsäure zu verursachen, führt zur Vermutung, daß diese auch durch Jod statt findet. Dies ist unter einer Bedingung der Fall. Nämlich wird die allo-Säure mit Jod in geschmolzenem Rohr vermengt und ein viertel Stunde auf 175°—180° erhitzt, dann wird die Wärmeisomerisierung der *cis*-Säure etwas beschleunigt und sie verläuft um 37.4 Prozente, während ihr Wert in der Abwesenheit des Jods höchstens halb des oben genannten Prozentsatzes (18%) beträgt. Diese Umlagerung würde wahrscheinlich dank des Jodatoms, wie die der *cis*-Zimtsäure verlaufen[8]. Unter den anderen Bedingungen, worin man eine Wirkung des Broms deutlich erkennen kann, entfernt sich jedoch das experimentelle Resultat weit von der Erwartung und man kann dabei keine Isomerisierung beobachten. Sie ist sogar gar nicht aufgetreten, wenn man auch α-Bromallozimtsäure in Gegenwart von Jod mit dem Lösungsmittel wie Tetrachlorkohlenstoff in seinem Siedepunkt lang erhitzt hat. Diese hartnäckige Abwehrung gegen Isomerisierung der α-Bromallozimtsäure ist etwas anders bei der *cis*-Zimtsäure, die im als Lösungsmittel gebrauchten Schwefelkohlenstoff bei seinem Siedepunkt leicht in *trans*-Säure übergehen kann.[9] Unter dieser Bedingung würde die Isomerisierung vielleicht durch Jod ein wenig gehemmt werden, da der Wert der Isomerisierung in seiner Gegenwart unmerkbar klein ist, der sonst einige Prozente beträgt. Dass diese Erscheinung darauf nicht beruht, dass die Umwandlung der α-Bromzimtsäure umgekehrt in ihren *cis*-Isomer, nämlich in α-Bromallozimtsäure, durch Jod erregt wird, wie durch die längere Bestrahlung mit ultraviolettem Lciht,[10] ist davon festgestellt worden, dass die α-Bromzimtsäure, nach dem gleichen Verfahren mit Jod behandelt, gar nicht isomerisiert ist.

Überdies zeigt das Jod eine sehr auffallende Erscheinung, dass es nämlich wie Brenzkatechin, aber auf eine etwas schwächere Weise, die durch Bromwasserstoff katalysierte Stereomerisierung hemmt. Da die Isomerisierung der α-Bromallozimtsäure durch Bromwasserstoff, wie oben erwähnt, grösstenteils durch Sauerstoffeffekt geleistet wird, ist es zweifellos anzunehmen, dass das Jod auf diesen Effekt schädlich wirkt.

Der grösste Teil der Produkte, die man aus Phenylpropiolsäure durch direkte Einwirkung von Bromwasserstoff auf ihre Benzollösung erhält, ist α-Bromzimtsäure, was Michael und Shadinger bestätigt haben. Warum wird die α-Bromallozimtsäure überhaupt nicht erhalten? Weist der Misserfolg, die α-Bromallozimtsäure vom Reaktionsgemisch aus zu isolieren, nicht darauf, dass der Sauerstoffeffekt sich an dieser Reaktion beteilige ?

Gesetzt, es sei richtig diese Vermutung, dann muss die Reaktion des Bromwasserstoffs auf

(6) O. Simamura, Dieses Bulletin, **14**, 22 (1939).
(7) O. Simamura, Dieses Bulletin, **14**, 29 (1939).
(8) R. G. Dickinson und H. Lotzkar, *J. Am. Chem. Soc.*, **59**, 472 (1937); A. Berthoud und Ch. Urech, *J. chim phys.*, **27**, 291 (1930).
(9) C. Liebermann, *Ber.*, **23**, 512 (1890).
(10) R. Stoermer und P. Heymann, *Ber.*, **46**, 1251 (1913).

Phenylpropiolsäure unter Benutzung von Antioxidant anders als die der gewöhnlichen Addition, *d. h.* nicht nach Vorschrift von Michael und Shadinger verlaufen. Dies ist tatsächlich der Fall, und die Wirkung des Brenzkatechins ist erheblich. Man konnte keine α-Bromzimtsäure in den Additionsprodukt finden.

Beschreibung der Versuche

α-Bromallozimtsäure wird dargestellt durch die Behandlung des Zimtsäuredibromids mit alkoholischer Kalilauge. Da die bezweckte Säure mit dem *trans*-Isomeren vermengt ist, werden die beiden Isomeren Vermöge des Unterschiedes der Löslichkeit ihrer Bariumsalze getrennt. Das Exemplar, das man sich aus dem leichten Petroleumäther-Chloroform dreimal umkristallisiert hat, ist bei 119—120° geschmolzen.

I. Isomerisierung durch Bromwasserstoff

(a) **Wirkung desselben allein.**—α-Bromallozimtsäure wird in schwefelfreiem Schwefelkohlenstoff aufgelöst, worin das Bromwasserstoffgas vorher durchgeleitet worden ist, und man lässt die Lösung auf die erforderliche Zeit stehen. Die Lösung wird zum Befreien von Bromwasserstoff mit Wasser durchschüttelt und abdestilliert. Löst man den erhaltenen gelblichen Rückstand in Ammoniakwasser auf und versetzt ihn mit einer ziemlich konzentrierten Bariumchloridlösung, so scheidet sich der Niederschlag so fort ab, was das Übergehen der gebrauchten Allosäure in die *trans*-Säure zeigt. Die unveränderte Allosäure aber bleibt in der Lösung als lösliches Bariumsalz zurück. Dann werden der Niederschlag und das Filtrat voneinander getrennt, jedes für sich, mit Salzsäure angesäuert und mit Äther mehrmals ausgeschüttelt. Nach dem Trocknen der beiden Ätherlösungen mit wasserfreiem Natriumsulfat, destilliert man den Äther ab und wiegt die erhaltenen Rückstände.

Zur Feststellung, dass diese beiden Substanzen reine Isomere sind, schmilzt man sie jede für sich mit den vorbreiteten Exemplaren zusammen, entweder ohne weitere Behandlung, oder nach Umkrystallisation aus dem leichten Petroleumäther-Chloroform, oder aus dem Tetrachlorkohlenstoff. Die zur Feststellung der isomerisierten Säure angewandte α-Bromzimtsäure ist nach dem Verfahren von Sudborough und Thompson[3] aus α-Bromallozimtsäure dargestellt worden. Die umkrystallisierte *trans*-Säure hat den Schmelzpunkt 130.5—131°. Über die Wirkung des Bromwasserstoffs gibt die Tabelle 1 eine folgerichtige Erklärung ab.

(b) **Einfluss des Lichts.**—Diese Reihe von Versuchen ist in der Dunkelkammer durchgeführt worden, die Luft aus dem Reaktionsraum aber nicht weggenommen, obgleich die Versuche unter strengem Luftausschluss ausgeführt werden sollen, um daraus eine sichere Schlussfolgerung über den Sauerstoffeffekt in dieser Stereomerisierung zu ziehen. Aber die Zahlen (Tab. 2) werden doch deutlich zeigen, dass die Abwesenheit des Lichts wahrscheinlich auf die Isomerisierung einen schädlichen Einfluss ausübt.

Die Werte auf der Tabelle 3 sind unter anderen Bedingungen erhalten worden. Das Lösungsmittel wird unter Lichtausschluss und im Stickstoffstrom in das Reaktionsgefäss eindestilliert, worin die Allosäure eingesetzt ist, um die Luft aus dem Reaktionsraum und aus der Lösung vollkommen auszuschliessen, und dann wird Bromwasserstoff, dessen Entwicklungsapparat auch mit Stickstoff voraus gesättigt ist, durchgeleitet. Man kann aber die Verminderung des Isomerisierungswerts aus

Tabelle 1

Anfangsmaterial, g.	CS_2, cc.	Reaktionsdauer, Stdn.	Totalsumme beider Isomeren, g.	Isomerisierter Teil, g.	Isomerisierter Teil, %
0.45	20	48	—	0.40	>88.9
0.125	13	24	0.116	0.108	93.1
0.191	20	24	0.184	0.170	92.4
0.689	40	24	0.663	0.652	98.3

Tabelle 2

Anfangsmaterial, g.	CS_2, cc.	Reaktionsdauer, Stdn.	Totalsumme beider Isomeren, g.	Isomerisierter Teil, g.	Isomerisierter Teil, %
0.138	13	24	0.127	0.099	78.0
0.182	18	48	0.169	0.124	73.4
0.199	20	48	0.181	0.135	74.6

Tabelle 3

Anfangsmaterial, g.	CS_2, cc.	Reaktionsdauer, Stdn.	Totalsumme beider Isomeren, g.	Isomerisierter Teil, g.	Isomerisierter Teil, %
0.944	45	48	0.913	0.648	71.0
0.567	30	48	0.547	0.382	69.8

diesen Zahlen nicht deutlich ersehen.

(c) **Wirkung des Brenzkatechins.**—Die zuständige Säure wird im mit Bromwasserstoff vorausgesättigten Schwefelkohlenstoff mit Brenzkatechin aufgelöst und stehen lassen. Die Menge des umgewandlten Säure nimmt beträchtlich ab, wie man aus der Tabelle 4 ersehen kann.

Man kann den Einfluss des Brenzkatechins auch deutlich erkennen, selbst wenn die durch Bromwasserstoff katalysierte Isomerisierung verhältnissmässig klein ist. Zu solchen Umstände kann man gelangen durch Abkürzen der Reaktionsdauer oder durch Anwedung von Lösungsmitteln, wie Tetrachlorkohlenstoff, worin das Anfangsmaterial schwer löslich ist und der grösste Teil desselben als Niederschlag unverändert bleibt. Die Tabelle 5 zeigt diese Verhältnisse.

Die zahlen auf der Tabelle 6 sind genügend, um damit zuzeigen, die hemmende Kraft des Brenzkatechins unter dem Gebrauch von einer äusserst geringen Menge desselben absinkt.

II. Wirken der Halogene

Das Wirken des Broms enthält kein Problem in sich, aber mit Jod steht es ganz anders. Wenn man auch die Tetrachlorkohlenstofflösung sieden lässt, tritt die erwartete Wirkung nicht auf, und es scheint, dass die Stereomerisierung dagegen gehemmt wird. Auf der Tabelle 7 sieht man einige Beispiele über die Wirkung der Halogene.

Ferner, wenn man die mit Jod beigemengte α-Bromallozimtsäure in den vorher mit Bromwasserstoff durchströmten Schwefelkohlenstoff auflöst, wird die sonst durch Bromwasserstoff zu katalysierende Isomerisierung stark verzögert (Tabelle 8). Auf der Tabelle sind die beiden Werte der Isomerisation, die durch Bromwasser-

Tabelle 4

Anfangsmaterial, g.	Brenzkatechin, g.	CS_2, cc.	Reaktionsdauer, Stdn.	Totalsumme beider Isomeren, g.	Isomerisierter Teil, g.	Isomerisierter Teil, %
0.530	0.0285	40	24	0.513	0.035	6.6
0.515	0.028	40	24	0.500	0.031	6.2

Tabelle 5

Anfangsmaterial, g.	Brenzkatechin, g.	Lösungsmittel, cc.	Reaktionsdauer	Totalsumme beider Isomeren, g.	Isomerisierter Teil, g.	Isomerisierter Teil, %
0.838	unbenutzt	40 CS_2	10 Min.	0.828	0.019	2,3
0.860	0.011	40 CS_2	10 Min.	0.849	0.004	0.5
0.854	0.057	40 CS_2	10 Min.	0.839	0.006	0.7
0.995	unbenutzt	40 CCl_4	36 Stdn.	0.972	0.060	6.2
0.556	0.0285	20 CCl_4	36 Stdn.	0.540	0.003	0.6

Tabelle 6

Anfangsmaterial, g.	Brenzkatechin, g.	CS_2, cc.	Reaktionsdauer, Stdn.	Totalsumme beider Isomeren, g.	Isomerisierter Teil, g.	Isomerisierter Teil, %
0.121	0.0015	12	22	0.108	0.075	69.4
0.196	0.0017	20	48	0.189	0.124	65.6

Tabelle 7

Anfangsmaterial, g.	Halogen, g.	Lösungsmittel, cc.	Reaktionsdauer, Stdn. auf Zimmer Temperatur	Reaktionsdauer, Stdn. auf Siedepunkt von CCl_4	Totalsumme beider Isomeren, g.	Isomerisierter Teil, g.	Isomerisierter Teil, %
0.090	0.0055 Br_2	7 CS_2	48	—	0.082	0.078	95.1
0.217	0.0042 Br_2	15 CS_2	96	—	0.203	0.190	93.6
0.098	0.0073 J_2	7 CS_2	48	—	0.095	0.001	1.2
0.215	0.0070 J_2	15 CS_2	96	—	0.200	0.002	1.0
0.547	0.0230 J_2	60 CCl_4	55	18	0.530	0.004	0.8
0.563	0.1003 J_2	35 CCl_4	55	18	0.546	0.002	0.4
0.498	unbenutzt	55 CCl_4	55	18	0.475	0.016	3.7
0.177	unbenutzt	20 CCl_4	85	12	0.162	0.008	5.1

Tabelle 8

Anfangsmaterial, g.	Antioxidant, g.	Lösungsmittel, cc.	Reaktionsdauer, Stdn.	Totalsumme beider Isomeren, g.	Isomerisierter Teil, g.	Isomerisierter Teil, %
0.689	unbenutzt	40 CS_2	24	0.663	0.652	98.3
0.530	0.0285 Brenzkatechin	40 CS_2	24	0.513	0.035	6.6
0.772	0.0565 J_2	40 CS_2	24	0.751	0.083	11.1
0.995	unbenutzt	40 CCl_4	36	0.972	0.060	6.2
0.556	0.0285 Brenzkatechin	20 CCl_4	36	0.540	0.003	0.6
0.996	0.061 J_2	40 CCl_4	36	0.977	0.014	1.4

Tabelle 9

Anfangs-material, g.	Lösungs-mittel, cc.	Reaktionsdauer, Stdn. auf Zimmer Temperatur	Reaktionsdauer, Stdn. auf Siedepunkt von CCl_4	Totalsumme beider Isomeren, g.	Isomerisierter Teil, g.	Isomerisierter Teil, %
0.391	20 CS_2	48	—	0.371	0.000	0.0
0.245	30 CCl_4	76	20	0.226	0.034	15.0
0.405	50 CCl_4	76	20	0.380	0.062	16.3

stoff sowohl in Gegewart von Brenzkatechin wie auch in dessen Abwesenheit ergeben werden, zum Vergleich wieder angegeben.

III. Einfluss des Chlorwasserstoffs

Wird die α-Bromallozimtsäure in Tetrachlorkohlenstoff aufgelöst, und unter Hindurchleiten des Chlorwasserstoffstroms gekocht, so erfährt sie eine Stereomerisierung, deren Menge deutlich grösser ist, als die der nur von Wärme hervorgebrachten Umwandlung (Tabelle 9). Bei gewöhnlicher Temperatur findet keine merkliche Veränderung statt.

IV. Direkte Einwirkung des Bromwasserstoffs auf Phenylpropiolsäure

(a) **In Benzol.**—Man löst 1 g. Phenylpropiolsäure in 15 cc. Benzol auf, leitet den getrockneten Bromwasserstoff eine Stunde lang durch, und lässt sie eine Nacht stehen; dann wäscht man die Lösung einmal mit Wasser, dampft das Lösungsmittel ab, und man erhält 1.47 g. (95% d. Theor.) sauren Rückstand als Additionsprodukt. Dieser Rückstand besteht aber aus mindestens zweierlei Säuren, da er beim Zusazt von konzentrierter Bariumchloridlösung zu seiner ammoniakalischen Lösung neben dem löslichen Bariumsalz eine kleine Menge von löslichem gibt. Die Menge der Säure, die aus dem ersteren durch Ansäuerung mit verdünnter Salzsäure erhalten wird, beträgt 1.29 g. Nach Umkrystallisation aus dem leichten Petroleumäther-Chloroform schmiltzt sie bei 128.0—129.5°, und stimmt mit α-Bromzimtsäure überein. Dagegen kann man aus dem löslichen Bariumsalz keine einheitliche Säure erhalten. Sie wird mit α-Bromallozimtsäure zusammengebracht, um dann bei einer weit tieferen Temperatur zu schmelzen.

(b) **In Gegenwart von Brenzkatechin im gleichen Lösungsmittel.**—In Gegenwart von genanntem Antioxidant lässt man den Bromwasserstoff auf die Benzollösung von 2 g. reiner Phenylpropiolsäure reagieren. Nach der Addition und dem Abdampfen des Benzols erhält man den Rückstand, der den sauren Teil enthält, der das lösliche Bariumsalz gibt. Diese Säure, aus Tetrachlorkohlenstoff umkrystallisiert, beträgt 1.25 g. Ihr Schmelzpunkt liegt bei 151—6°, während der des Gemisches mit α-Bromzimtsäure wohl unter 90° liegt, welche Tatsache zwanglos zur Feststellung führt, dass es keineswegs α-Bromzimtsäure ist, die in Abwesenheit von Antioxidant das Hauptprodukt gewesen ist. Unter den Reaktionsprodukten findet man ferner 1.22 g. sauren Stoff, der unlösliches Salz gibt und sich mit keiner einheitlichen Säure identifizieren lässt, von α-Bromallozimtsäure ganz zu schweigen. Abgesehen davon, dass die Trennungsmethode nicht scharf genug ist, um einzelne Stoffe völlig zu isolieren, kann man schliessen: es ergebe sich keine α-Bromzimtsäure bei dieser Reaktion.

Zusammenfassung

Die Einwirkung von Bromwasserstoff auf α-Bromallozimtsäure ruft keine Bildung des Zimtsäuredibromids hervor, sondern die Stereomerisierung, *d. h.* ihre Umwandlung in den *trans*-Isomere, α-Bromzimtsäure. Diese Umwandlung kann auch sowohl durch Brom als durch Chlorwasserstoff hervorgebracht werden, durch Jod aber geht dies keineswegs, wobei im Gegenteil der sonderbare Effekt desselben beobechtet wird, dass es auf die von Bromwasserstoff katalysierte Isomerisierung schädlich wirkt. Solche störende Wirkung auf die Isomerisierung tritt in Gegenwart von Brenzkatechin, einem bekannten Antioxidant, noch deutlicher auf im vorhergehenden fall. Diese Erscheinungen führen zwanglos zur Annahme, dass diese Reaktion hauptsächlich von den Mechanismus des Sauerstoffeffekts entstandenen Atomen oder freien Radikalen erregt werde. Doch darf man hier die Teilnahme des Ionenmechanismus, wenn diese auch gering sein mag, gar nicht wegleugnen.

Es sei noch hinzugefügt, dass die α-Bromzimtsäure, die aus Phenylpropiolsäure, gelöst in Benzol, durch unmittelbare Addition des Bromwasserstoffs erhalten wird, ihre Bildung dem Sauerstoffeffekt verdankt.

Zum Schluss muss der Verfasser den Herren Prof. Y. Urushibara und Prof. O. Simamura für ihre freundlichen Leitungen, sowie seinen Arbeitsgenossen für ihren Beistand durch lebhafte Diskussion über diesen Gegenstand den herzlichen Dank aussprechen.

Chemisches Institut,
Fakultät der Naturwissenschaften,
Tokyo Universität

The Salt Effect in the Aniline-Formaldehyde Condensation

By Yoshiro OGATA, Masaya OKANO and Tsutomu YAMAMOTO

(Received Octover 23, 1951)

In our previous paper the kinetic study of the aniline-formaldehyde condensation in aqueous hydrochloric acid media has been reported.[1] The rate has been found to be second-order with respect to the initial concentration of aniline and first-order with respect to the sum of the concentrations of formaldehyde and methylene-anilines present. The purpose of the present investigation is to find the effect of inorganic salts on the rate of this reaction in aqueous hydrochloric or sulfuric acid media. The results show that the catalytic action of the salts is explicable in terms of the primary and secondary salt effects.[2]

Experimental

Materials and General Procedures are substantially the same as those in the previous paper.[1]

Experimental Results are shown in Fig. 1 and Table 1. Fig. 1 shows the effect of pH on the

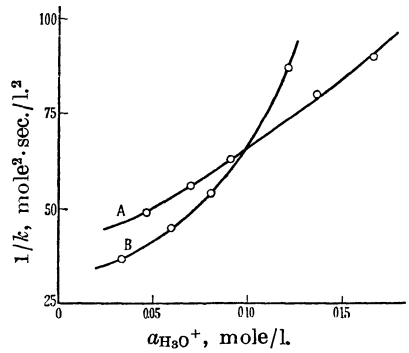

Fig. 1.—Relationship between $1/k$ and $a_{H_3O^+}$: A, 0.10 M $C_6H_5NH_2$+0.10 M CH_2O+0.15~0.30 M HCl; B, 0.10 M $C_6H_5NH_2$+0.10 M CH_2O+0.10~0.30 M H_2SO_4.

Table 1

The Effect of Various Salts on the Rate of the Aniline-Formaldehyde Condensation (25.0±0.1°C)

(A) Concentrations of reactants in original solutions: Aniline 0.1 M, HCl 0.2 M, Formaldehyde 0.1 M.

Added salt	M	pH	$a_{H_3O^+}M$	$k_f\times10^4$ (1/sec.)	$1/k_e$ (mole².sec./l.²)	$1/k_c$ (mole².sec./l.²)	μ_e	μ_c	β
None		1.05	0.090	1.57	64		0.20		
NaCl	0.50	0.99	0.105	1.88	53	67	0.70	0.22	0.6
〃	1.00	0.93	0.120	2.12	47	75	1.20	0.23	0.7
〃	2.00	0.79	0.160	2.66	38	89	2.20	0.30	0.9
KCl	1.00	0.96	0.110	2.32	43	71	1.20	0.22	0.8
$MgCl_2$	0.50	0.92	0.120	2.61	38	75	1.70	0.23	0.8
KBr	1.00	0.97	0.110	2.49	40	71	1.20	0.22	1.0
Na_2SO_4	0.10	1.40	0.040	2.78	36	46	0.50	0.15	0.9
K_2SO_4	0.10	1.42	0.038	2.82	35	45	0.50	0.15	0.9

(B) Concentrations of reactants in original solutions: Aniline 0.1 M, H_2SO_4 0.1 M, Formaldehyde 0.1 M.

None		1.48	0.033	2.67	37		0.30		
Na_2SO_4	0.10	1.64	0.023	3.87	26	34	0.60	0.26	1.1
〃	0.20	1.79	0.016	4.81	21	33	0.90	0.22	1.0
〃	0.30	1.84	0.014	5.63	18	32	1.20	0.22	0.9
K_2SO_4	0.10	1.65	0.023	3.84	26	34	0.60	0.26	1.1
$MgSO_4$	0.10	1.56	0.028	3.81	26	34	0.70	0.28	1.0
KBr	1.00	1.28	0.053	3.52	29	42	1.30	0.41	0.6
KCl	1.00	1.29	0.051	3.38	29	42	1.30	0.41	0.6

(1) Ogata, Okano and Sugawara, *J. Am. Chem. Soc.*, **73**, 1715 (1951).

(2) La Mer, *Chem. Rev.*, **10**, 179 (1932); Moelwyn-Hughes, "Kinetics of Reactions in Solution," Clarendon Press, Oxford, 1933, pp. 184.

rate with constant stoichiometric initial concentrations of aniline (0.1M) and formaldehyde (0.1M). In the figure, k is equal to k_f/a^2, where a is the initial concentration of aniline and k_f, the pseudo-first-order constant with respect to formaldehyde present. Table 1 tabulates the effect of the addition of several salts. Here, k_e corresponds to k described above and μ_e is the ionic strength of the solution; the definitions of k_c, μ_c and β will be given in the next paragraph. The salts employed are those alone which afford homogeneous solutions during rate measurements and do not interfere with titrimetric analyses.

Discussion of Results

Fig. 1 suggests that in sulfuric acid solution more attention should be paid to the concentration of free arylamino group together with undissociated arylammonium sulfate upon the rate than in hydrochloric acid solution. In order to derive the generalized rate equation in which undissociated aniline hydrochloride is taken into account as in dimethylaniline-formaldehyde condensation,[3] equilibria

$$ArNH_2+HCl \rightleftharpoons ArNH_3Cl \quad (a) \quad K_a$$
$$ArNH_3Cl \rightleftharpoons ArNH_3^+ + Cl^- \quad (b) \quad K_b$$

should be considered. Here, K_a is the average equilibrium constant of the formation of hydrochlorides of aniline and its condensate; K_b, that of their ionization. Consequently, the initial concentration of aniline is expressed as

$$a \doteqdot \sum[ArNH_2]+\sum[ArNH_3Cl]+\sum[ArNH_3^+]$$

or

$$\sum[ArNH_2]=a/\{(K_A/K_W)(1+[a_{Cl^-}/K_b])+1\}$$

in which K_A is the average ionization constant of aniline and its condensate, $ArNH_2$, and K_W is the ion product of water. Introduction of this value into the rate equation previously given,[1] *i.e.*,

$$dx/dt=K\,a_{H_3O^+}(\sum[ArNH_2])^2(f-x)$$
(K: a constant)

leads to

$$dx/dt=\frac{K\,a_{H_3O^+}a^2(f-x)}{\left\{1+\frac{K_A}{K_W}\left(1+\frac{a_{Cl^-}}{K_b}\right)a_{H_3O^+}\right\}^2}=k_f(f-x) \quad (1)$$

in which $a_{H_3O^+}$ etc. are the activities of the subscripted substances, H_3O^+ etc. Hence, the relation between a^2/k_f and $a_{H_3O^+}$ is given by

$$\frac{1}{k}=\frac{a^2}{k_f}=\frac{1}{K\,a_{H_3O^+}}+\frac{2K_A}{KK_W}\left(1+\frac{a_{Cl^-}}{K_b}\right)+\frac{K_A^2}{KK_W^2}\left(1+\frac{a_{Cl^-}}{K_b}\right)^2 a_{H_3O^+} \quad (2)$$

The plot of $1/k$ against $a_{H_3O^+}$ expressed in two curves in Fig. 1 should be consistent with this equation (2). If the equation is compared with equation (18) in the previous paper, it is apparent that the added terms $1/Ka_{H_3O^+}$ and a_{Cl^-}/K_b are related with free aniline and undissociated aniline hydrochloride, respectively. In hydrochloric acid media, a_{Cl^-}/K_b shows the ratio $[ArNH_3Cl]/[ArNH_3^+]$, and $1/K\,a_{H_3O^+}$ may be negligible in comparison with the other terms. In sulfuric acid media, however, the latter term should probably not be eliminated.

The dissociation of excess hydrochloric acid and that of hydrochlorides of aniline together with its condensate will be affected by adding salt. Although pH increases generally by adding inorganic salt into aqueous acid, the present results show that the pH decreases and therefore the concentration of hydrochloric acid ($HCl+H_2O \rightleftharpoons H_3O^+ + Cl^-$) as well as free aniline seems to increase as the amount of salt increases. Surely this change in pH will give rise to the change in the rate, *i.e.*, "secondary salt effect". The variation of k with pH was estimated from the curves in Fig. 1, while the effect of an increase in ionic strength on the rate will be considered later. These presumptive values of rate constant k_c and ionic strength μ_c in Table 1, where no inorganic salt is contained in the solution at the same pH's as shown in the third column of the same line, were measured by employing these curves. On the other hand, the change of the dissociation of arylammonium hydrochlorides seems to be difficult to evaluate, but probably it is reasonable to suppose that the value of $1/k$ decreases as the mean value of K_b increases by the addition of chloride in aniline sulfate solution. (See equation (2).)

The effect of salts on activity coefficients of reactants, so-called "primary salt effect," is expressed as equation (3) for the reaction between a neutral molecule and an ion at relatively high concentration.[4]

$$k=k_0(1+\mu\beta) \quad (3)$$

where k is a rate constant with ionic strength μ, k_0, that with the ionic strength zero, and β, a constant. In hydrochloric acid medeia, the above values of k_c together with those of

(3) Ogata and Okano, *J. Am. Chem. Soc.*, **72**, 1459 (1950).

(4) Glasstone, "Text-book of Physical Chemistry", D. Van Nostrand Company, New York, 1940, pp. 1115.

k_e, *i. e.*, the values of experimentally found, are expressed as

$$1/k_0=(1+\mu_c\beta)/k_c \quad (4)$$

$$1/k_0=(1+\mu_e\beta)/k_e \quad (5)$$

Therefore, β can be calculated by means of an equation

$$\beta=\{(1/k_c)-(1/k_e)\}/\{(\mu_e/k_e)-(\mu_c/k_c)\} \quad (6)$$

As shown in Table 1, β holds good constancy. In hydrochloric acid media, average value of β is equal to 0.8 and in sulfuric acid media, β, 1.0. Using these values of β and those of k at appropriate oxonium ion activity (*e. g.*, pH=1.5) in Fig. 1, k_0 may be calculated by means of equation (3). The values of k_0 calculated independently by using the data in hydrochloric and sulfuric acid solutions are in agreement; *i. e.*, $k_0=2.09\times10^{-2}$ and 2.11×10^{-2} (l^2./mole.^{2}·sec.), respectively. Abnormal values of β were obtained when either bromide or chloride was added into sulfuric acid media. These facts may be explained by assuming that the mean values of K_b are increased under these conditions. This catalytic effect of anions of salts may be ascribed to the acceleration of the rate-determining attack of carbonium ion $ArNHCH_2^+$ on the carbon atom of the benzene nucleus by attracting proton of the nucleus to the anion. A similar concerted mechanism has been suggested by Swain in other nucleophilic reactions.[5]

Summary

In the hydrochloric or sulfuric acid-catalyzed condensation of aniline with formaldehyde, it was found that the addition of inorganic salt, *e. g.*, sodium chloride or potassium sulfate, increases the rate and this fact is ascribed to the so-called primary and secondary salt effects.

The authors wish to express their thanks to Prof. T. Nishi for the assistance in pH measurement.

Department of Industrial Chemistry
Faculty of Engineering
Kyoto University, Kyoto

(5) Swain, *J. Am. Chem. Soc.*, **70**, 1119 (1948); **72**, 2794 (1950).

Spinnability of Liquid. A Visco-elastic State. I. Spinnability and Anomalous Viscosity

By Tsurutaro NAKAGAWA

(Received November 2, 1951)

Introduction

It is well-known that some substances which are usually considered as "liquids" have a marked thread-forming property as is shown by Fig. 1. The so-called mucilaginous fluids, such as egg-white, vitreous humour of the eye, saliva, secretion of the various mucous membranes, mucus from seaweeds, extraction of the root of *Abelmoschus Manihot* Medicus (*Hibiscus Manihot* L.), mucus of a taro, mucus of "nattô" (fermented beans), and other rotten or fermented things, all possess this peculiar property; furthermore in the laboratory, we see the phenomenon in a raw rubber-benzene solution, aq. solution of mercury sulphosalicylic acid, and in some coacervates. When we raise a stirring rod from these liquids, or when the liquids are poured out of a beaker, a very long and fine thread is spun which sometimes reaches a length of 30~40 cm. or more.

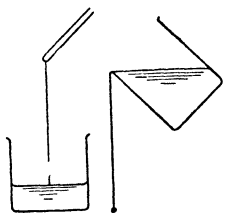

Fig. 1.

To what is this phenomenon attributed? One may ascribe it to the high viscosity which is characteristic of the solution of polymeric substances; but the impropriety of this assumption will be understood by the fact that the other high-viscous polymer solutions, for

example, starch solution, gelatin sol, or agar-agar sol, pectin sol, etc. show no spinnability. Recognizing that the spinnability of liquid is not solely related to the viscous flow, what is the other factor to be added?

Inspection of the examples cited above gives us two general ideas; first, from the chemical point of view, they are high-polymeric solutions, and second, from the physical point of view, they are in the colloidal state. Mechanical properties of these high-polymeric or colloidal states consist of many non-ideal peculiarities: their deformation is non-Hookean, and their flow is non-Newtonian. From the standpoint of relaxation phenomena, the time of mechanical relaxation λ of these high-polymeric, colloidal and the so-called "amorphous" substances is finite. Deviations from the ideal behavior of the mechanical properties of these high-polymeric materials depend chiefly upon this finite relaxation time. Because of the fact that λ is comparable with the time of our observation (t), the mechanical behavior of those amorphous substances usually appears as a relaxation phenomena. According to the relative magnitude of λ to (t), the apparent mechanical behavior of the subject shows much variety; in other words, the time-effect is remarkable in the mechanical properties of high-polymers.

One of the phenomenological treatments to describe systematically these non-ideal, time-sensitive mechanical properties is the theory of the "visco-elastic or elastic-viscous state". By this method, various actual anomalies of the mechanical behavior are described quantitatively as a function of the "magnitudes" of η (viscosity coefficient) and G (elasticity coefficient) and of the "type" of coupling of η and G. Now that our spinnable (thread-forming) liquids are generally high-polymeric or colloidal solutions, the above-stated concept of a visco-elastic state will be applicable to this peculiar mechanical property. Supporting this view, we actually observe some elastic property in these spinnable liquids; a liquid-thread springs back elastically when it breaks, or these liquids in a vessel turn back in the opposite direction when we rotate it in one direction and then hold it.

In this essay, the spinnability of liquids is treated from these points of view.

Tammann and Tampke[1] measured spinnability by the maximum length of a liquid thread formed when a rod is raised from a spinnable liquid as is shown by Fig. 2. This method seems to be the most convenient and popular.

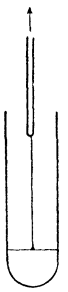

Fig. 2.

Jochims[2] found out that viscosity is not the single factor which causes spinnability and determines the degree of spinnability, and that an elastic scaffolding existing in such a liquid is another important factor.

H. Erbring[3] first treated it systematically and extensively as a colloid-chemical problem; his general conclusion drawn out of his experiments is outlined as follows. He used Tammann and Tampke's principle (Fig. 2) to express the degree of spinnability quantitatively. From his measurements on an extract of flax-seeds, mucilage of quince, solutions of gum Arabic, mercury sulphosalicylic acid, acetyl cellulose, cotton-yellow, aluminium soap, polystyrene, sodium stearate, sodium silicate, polyvinyl alcohol, and viscose etc., some coacervates, for example, a gelatin-phenol coacervate and a gelatin-starch coacervate etc., Erbring gained the following general aspects on the spinnability phenomenon; (a) spinnability does not simply depend upon viscosity of liquid, (b) surface tension also is not an important factor, its influence being negligible for markedly spinnable liquids, (c) a sort of "elasticity" plays a principal rôle in this phenomenon, (d) spinnability is a phenomenon relating to a particular colloid-chemical "state" of a substance, and not to a special chemical species, (e) spinnability seems to be owing to some "structure" in liquid, both a proper fluidity (viscosity) and a proper consistency (structure) being important for the appearance of spinnability, (f) the existence of rod-shape or long-chain molecules in liquid seems to be necessary, (g) structural viscosity (non-Newtonian flow) is closely related to spinnability.

Measurement of Spinnability

As the first step, the author constructed an apparatus for observing quantitatively the degree of spinnability after the Tammann-Erbring method,[3] in which the degree of spinnability is expressed by the maximum length of a liquid thread spun by a rod raised out of the liquid.

(A) **Apparatus**—Since the maximum length of a liquid thread depends appreciably upon the velocity of the ascending of a testing rod,

(1) G. Tammann and R. Tampke, *Z. anorg. allgem. Chem.*, **162**, 1 (1927).

(2) J. Jochims, *Koll. Z.*, **61**, 250 (1932).

(3) H. Erbring, *Koll. Beih.*, **44**, 171 (1936); *Koll. Z.*, **77**, 32, 213 (1936); *ibid.*, **80**, 20 (1937); *ibid.*, **98**, 164 (1942) or *Chem. Abs.*, **36**, 6393 (1942).

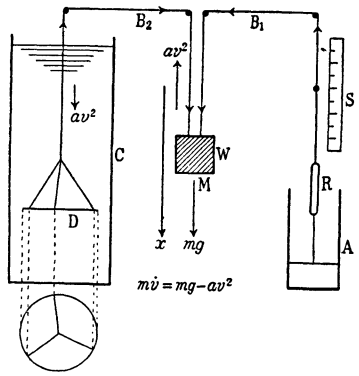

Fig. 3.

R, a velocity controlling device as is shown by Fig. 3 was constructed. The rod R is driven by a weight W and some pulleys, and acceleration of W is suppressed by a damper D moving in water, so that a constant terminal velocity is gained, which is voluntarily controlled if W is changed. The terminal velocity is attained soon after starting.

D is a disc of 16 cm. dia. Weight of W and D is 120 g. and 70 g. respectively, so that the effective driving weight of W is approximately 30 g., assuming empirically that the total frictional resistance at the mechanical contacts is equivalent to about 20 g. Then the velocity of R can be controlled in the neighbourhood of 5 cm./sec. Reproducibility is satisfactory. (Fluctuation of the measured maximum thread length is less than 5 mm.)

(B) Spinnability of simple high-viscous liquids: trivial case of spinnabiliy.— The most simple and trivial type of spinnability is one by very high viscosity of liquid, for then a liquid column is formed between the surface of the liquid and the tip of a rising rod because of the slowness of the liquid supply downward from a rod (Erbring's "Nachliefe-rungsvorgang"). From what value of viscosity does this simple spinnability due to the slow supply appear? The author experimented as follows.

As the comparatively high-viscous liquids whose flow are ideally Newtonian, exhibiting neither elastic property nor structural viscosity (anomalous viscosity), two solutions were taken, namely (a) conc. aq. solution of sucrose and (b) aq. solution of water glass (sodium silicate). Sucrose is suitable for preparing a high-viscous solution because of the difficulty of crystallizing out of a supersaturated solution.

Viscosities of these solutions at various concentrations and temperatures were measured by the falling-sphere method. The capillary method viscosimetry is not applicable on account of their high viscosity. In our case, η was calculated from the time t sec., necessary for a steel ball of radius 0.07875 cm. ($D=7.80$ g./cm.^{3}) to fall down 15 cm. along the central axis of a liquid column of radius 1.4 cm. and of height 30 cm. Thus, viscosities ranging in 2~600 poises were measured.

Taking these solutions, the author measured the degree of spinnability by the above-stated apparatus. The viscosity of a solution at the time when spinnability first appears is thus known.

In this way, the following conclusion was drawn out.

A solution of any concentration generally begins to exhibit spinnability at a temperature at which viscosity amounts to 40~50 poises; in other words, at least 40~50 poises of viscosity are necessary for a simple high-viscous liquid to produce spinnability. This critical viscosity is 4000~5000 times as large as the viscosity of water.

It should however be noticed that, as will be stated below, typically spinnable liquids exhibit marked spinnability at the viscosity far lower than this.

(C) Spinnability of raw rubber solutions.—Solutions of raw rubber in xylene, toluene, and benzene etc. are, as egg-white and saliva, typically spinnable. Using the above-mentioned apparatus, spinnability (expressed by the maximum thread-length, L cm. before breaking) of a raw rubber—xylene solution at various concentrations was measured, by changing a lifting velocity, v of the rod R (*cf.* Fig. 4). As is clear from Fig. 4, spinnability—concentration relation has a maximum, showing that the 3~4%

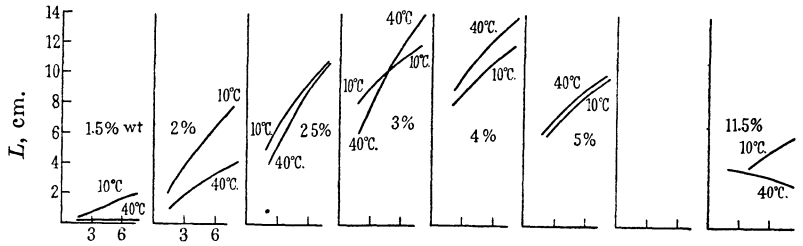

Fig. 4.

solutions exhibit the most remarkable spinnability. This result may be explained as follows by a concept of relaxation phenomenon. Spinnability increases with the increase of concentration or viscosity, but with too much increase of viscosity, a liquid becomes too rigid to follow the testing rod rising upwards with the velocity of several cm. per second, and the breaking occurs: in other words, spinnability is maximum when the time of relaxation of the solution is optimum in comparison with the time of observation or velocity of measurement. Optimum concentration, or the maximum in the concentration—spinnability curve thus takes place.

In marked contrast with sucrose solution in which at least 40~50 poises of viscosity are necessary for it to exhibit spinnability, raw rubber solution, as illustrated in Fig. 4, shows marked spinnability even at 2 poises corresponding to a concentration of 2%. Saliva is also said to have obvious spinnability in spite of viscosity less than 1 poise. The foresight of Jochims,[2] Erbring[3] etc. seems to be correct, for they sought to attribute the remarkable spinnability of such typical spinnable liquids of comparatively low viscosity to a sort of "elasticity" coexisting with viscosity. The concept that spinnability is a co-operation of "viscous flow" streaming down from the tip of a rod and "elastic deformation" analogous to the elongation of a rubber string, appears to be correct.

Anomalous Viscosity (Structural Viscosity)

(A) Anomalous Viscosity. — Non-Newtonian flow is characteristic of most colloidal solutions, especially lyophile ones. In these cases, viscosity η is not a constant independent of shearing stress of flow, but generally decreases with the increase of the velocity gradient. The so-called Hagen-Poiseuille s law in the capillary flow does not hold.

When the Newtonian liquids are made to flow through a capillary of radius r and length L by means of a pressure p, and a volume v of fluid passes through it in a time t_0 sec., then viscosity η of a liquid is according to Hagen-Poiseuille's law

$$\eta = \frac{\pi p r^4 t_0}{8vL} = \text{const.} \times pt_0 \qquad (1)$$

(provided v = const.)

In the ordinary Newtonian liquids, η or pt_0 is independent of p. In most of lyophile colloidal solutions, on the other hand, pt_0 is not independent of p, but generally decreases with the increase of p. Wo. Ostwald ascribed this effect to the destruction of an internal structure by the shearing stress of flow, and called it "structural viscosity"; but strictly, this effect might not always be attributed to this sole mechanism, and it will be rather safe simply to say anomalous viscosity or non-Newtonian flow (*cf.* Fig. 5).

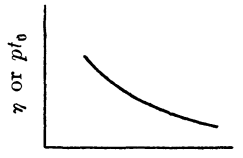

Fig. 5.

Philippoff[4] assumed a sort of elasticity in the non-Newtonian colloidal liquids, and presented the following formula,

$$\left.\begin{aligned} \eta^* &= \eta_\infty + \frac{\eta_0 - \eta_\infty}{1 + 2P_R^2/(3G^2)} \\ P_R &= rp/(2L) \end{aligned}\right\} \qquad (2)$$

where η^* is the apparent viscosity gained from Eq. (1) into which we insert the experimental data mechanically (though, strictly speaking, it is nonsense to use Eq. (1) for non-Newtonian liquids). P_R means the shearing stress at the wall of a capillary, whose radius and length are r cm. and L cm. respectively, when pressure p dyne/cm.^{2} is given on the end of a capillary; this is also a formal diversion of the relation which holds only in the Newtonian flow, in which shearing stress changes linearly from zero at the central axis of a capillary to a maximum value at the wall of it as is given by the under formula of Eq. (2). η_0 and η_∞ are constants and correspond to $[\eta^*]_{P_{R\to 0}}$ and $[\eta^*]_{P_{R\to\infty}}$ respectively. G is a coefficient of the so-called fluid-elasticity, and in the case of the capillary flow, means a torsional elastic constant or rigidity. Thus, if we adopt the standpoint of Philippoff, it is possible to estimate the magnitude of an elastic constant of a sol by means of an experimental η^*—P_R curve.

(B) Anomalous Viscosity of the Spinnable Solutions.—The author studied elasticity of the typically spinnable liquids following Philippoff.

Since η must be plotted as a function of pressure p, the common Ostwald's viscometer

(4) W. Philippoff, *Koll. Z.*, **71**, 1 (1935); *ibid.*, **75**, 142, 155 (1936); *ibid.*, **83**, 163 (1938).

is inapplicable. As the most suitable type for such experiments, the author used Tsuda's horizontal capillary viscometer.[5] A voluntarily changeable pressure p is applied from the two large glass vessels which are connected to each other and each is filled with a certain amount of water, and then p equals the difference of the water-head of the two vessels.

Strictly speaking, all capillary type viscometers are in principle improper for the study of anomalous viscosity, because, in the capillary flow, the shearing stress P varies with the radial distance from the center of a capillary, so that the shearing stress at the wall is maximum and is zero at the center of a tube. This fact is not consistent with our aim to know η in relation to the shearing stress P. Couette's rotational viscometer is the most rational, for in this case the shearing stress P is almost constant, independent of the radial distance as long as the gap between the two cylinders is small as compared with radii of the two cylinders. Nevertheless Tsuda's horizontal capillary viscometer is preferable to the rotation type from the practical point of view; the latter is accompanied with some faults, namely, the structural complexity and the difficulty in controlling temperature.

Experimental results on anomalous viscosity of xylene solution of raw rubber ("pale sheet") are illustrated in Fig. 6 and Fig. 7. For reference, the η^*—P_R curves for sucrose solution aq. and vanadium pentoxide sol are added in Fig. 6. Take three sets of (η^*, P_R) values, then from Eq. (2) three constants G, η_0 and η_∞ can be determined. Using, for example, from the lower curve about raw rubber—xylene system in Fig. 6, the following three points

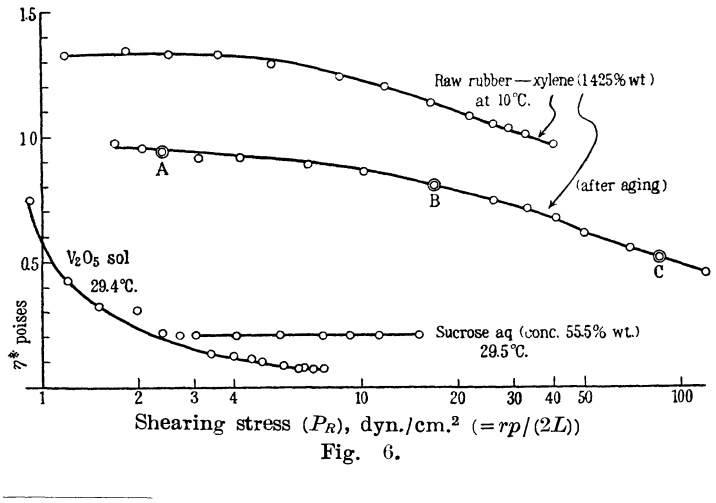

Shearing stress (P_R), dyn./cm.^{2} ($=rp/(2L)$)

Fig. 6.

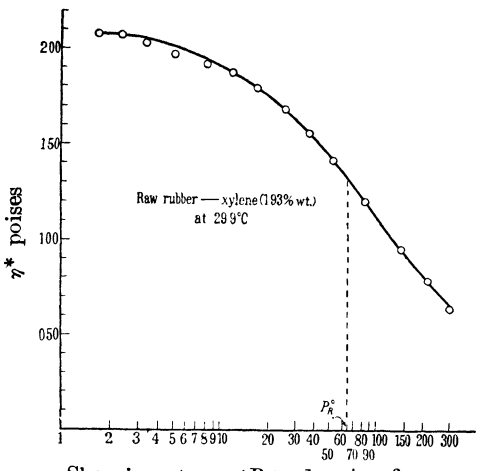

Shearing stress (P_R), dyn./cm.^{2}

Fig. 7.

$$\begin{cases} \text{A } (P_R = 2.43, & \eta^* = 0.933), \\ \text{B } (P_R = 17.2, & \eta^* = 0.791), \\ \text{C } (P_R = 85.6, & \eta^* = 0.497), \end{cases}$$

we obtain

$$G = 21.6 \text{ dyn./cm.}^2, \qquad \eta_0 = 0.935 \text{ poise}$$
$$\eta_\infty = 0.450 \text{ poise}$$

Or, since the inflection point of Eq. (2) can be determined from the condition

$$\frac{d^2\eta^*}{dP_R^2} = 0, \qquad (3)$$

it is obtained from Eq. (2) and Eq. (3), the next formula, provided P_R° means a value of P_R at the inflection point.[4]

$$G = \sqrt{\frac{2}{3}}\, P_R^\circ = 0.815\, P_R^\circ$$

Using, for example, $P_R^\circ = 60 \sim 70$ from Fig. 7,

$$G \fallingdotseq 50 \text{ dyn./cm.}^2$$

This is another procedure of determining G.

Maxwell's classical formula relating the time of mechanical relaxation λ

$$\lambda = \eta/G$$

becomes

$$\lambda = \eta_0/G$$

in the case of Philippoff's formulation of anomalous viscosity. From the above-gained

(5) S. Tsuda, *Koll.—Z.*, **45**, 325 (1928); Wo. Ostwald and H. Malss, *Koll.—Z.*, **63**, 61 (1933).

$\eta_0 = 0.935$, $G = 21.6$,

$$\lambda \fallingdotseq 0.04 \text{ sec.}$$

Since, on the other hand, our observation time, when we speak of the appearance of spinnability, is supposed to be 0.1～1 sec., the rubber solution of such a low concentration (1.5%) has a relaxation time much less than our observation time. Accordingly, the tendency to flow down is much stronger than the tendency to elongate to a liquid-thread, so that spinnability is not yet remarkable, as illustrated above (Fig. 4). However, as will be discussed later again in Part II, in a 3～4% rubber solution λ becomes the order of 0.5 sec., so that marked spinnability is observed on account of the fact that the relaxation time λ is comparable with our observation time. With the increase of the concentration moreover, λ of the fluid becomes presumably far larger than the observation time $\mathfrak{t}$. This situation, that the deformation of fluid can not follow the testing velocity, results in the snapping or breaking of a thread rather than extending or elongating it; spinnability decreases in this way (*cf.* Fig. 4).

Summary

Simple viscous liquids become thread-forming first at the viscosity of 40～50 poises or more.

Spinnability of typical thread-forming liquids is characterized by the co-operation of the far smaller viscosity and some "elasticity."

Department of Chemistry, Faculty of Science, Tokyo University, Tokyo

Spinnability of Liquid. A Visco-elastic State. II. Spinnability and Visco-elastic Property

By Tsurutaro NAKAGAWA

(Received November 2, 1951)

Spinnability as a Visco-elastic State

From the statements and examples in the previous paper, it seems to be almost admissible that a sort of "elasticity" accompanying the thread-forming liquids is an important factor of the spinnability phenomenon. As was stated above, by analysing the η^*—P_R curves of anomalous-viscous liquids exhibiting spinnability, we estimated the value of the elastic constant specifying that elasticity, and assumed it to be probable that spinnability is a co-operation of a viscous flow specified by a relatively small coefficient of viscosity ($\eta = 10^0 \sim 10^1$) on the one hand, and an elastic deformation corresponding to a coefficient of elasticity $G = 10^1 \sim 10^2$ on the other hand. But the determination of G by the analysis of anomalous viscosity is an indirect way, and it will not always be permissible to use Philippoff's equation without any reservation. As was mentioned already, the elasticity of spinnable liquids is not a theoretical parameter, but a physical reality which is actually observed. When a liquid thread snaps, it springs back elastically; or when these liquids are left free after a violent agitation, an elastic returning in the liquid actually occurs.

Is a direct measurement of such elasticity impossible? In our case, as is easily understood, the usual statical methods, namely, the methods of observing a static elastic equilibrium between stress and strain are inapplicable because of a marked relaxation or a flowing which accompanies an elastic deformation. The author designed thereupon the following dynamic method, in which is observed a mechanical resonance of a body which is oscillated by an oscillatory force transmitted through a torsion wire and is suffering, from a surrounding liquid, viscous resistance proportional to the deformation velocity and elastic resistance proportional to the deformation rate.

Principle of the Method for a Measurement of Visco-elastic Constants —Forced Oscillation Resonance Method

Consider a device as is illustrated in Fig. 1.[1] We shall discuss the motion of the inner cylinder when it is forced into oscillation through a torsion wire. The sinusoidal rotational displacement

$$\Theta(t)=\Theta_0 \sin \omega t$$

($\omega=2\pi\nu$; ν; frequency)

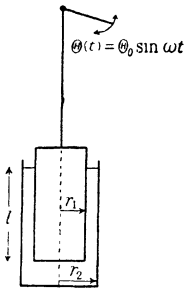

Fig. 1.

is given at the upper end of the torsion wire. The space between the inner and the outer cylinder is filled by a visco-elastic liquid.

Then

(inertial resistance of the cylinder)+(viscous resistance of the liquid)+(elastic resistance of the liquid)=(external elastic force from the torsion wire)

where

$$\text{(inertial resistance)}=I\ddot{\theta}$$

I: moment of inertia of the inner cylinder

$$\text{(viscous resistance)}=R_1\dot{\theta}$$

$$\text{(elastic resistance)}=E_1\theta$$

$$\text{(external force)}=k(\Theta-\theta)$$

k: torsion constant of the torsion wire

Therefore, the equation of motion of the inner cylinder is

$$I\ddot{\theta}+R_1\dot{\theta}+E_1\theta=k(\Theta-\theta) \qquad (1)$$

or

$$\ddot{\theta}+2\varepsilon\dot{\theta}+n_e^2\theta=L\sin\omega t \qquad (2)$$

where, $2\varepsilon\equiv R_1/I$

$n_e^2\equiv(k+E_1)/I$

$L\equiv k\Theta_0/I$

Since the transient term of the general solution of Eq. (2) damps soon, the singular solution is sufficient as long as we are concerned with a stationary state when the observation is made. The stationary state solution, therefore, is

$$\theta=\frac{L}{\sqrt{(n_e^2-\omega^2)^2+4\varepsilon^2\omega^2}}\sin(\omega t-\phi)$$

$$\equiv A\sin(\omega t-\phi) \qquad (3)$$

where, $\tan\phi=2\varepsilon\omega/(n_e^2-\omega^2)$

The amplitude of the forced oscillation of the inner cylinder is, therefore,

$$A=\frac{L}{\sqrt{(n_e^2-\omega^2)^2+4\varepsilon^2\omega^2}}\equiv L/\sqrt{f(\omega)} \qquad (4)$$

Condition of the amplitude resonance is

$$A=\text{max.} \quad \text{or} \quad f(\omega)=\text{min.}$$

namely $\dfrac{\partial A}{\partial\omega}=0$ or $\dfrac{\partial f}{\partial\omega}=0$

Calculation of this gives

$$\omega_{\text{res}}^2=n_e^2-2\varepsilon^2, \quad \text{or} \quad \nu_{\text{res}}=\frac{1}{2\pi}\sqrt{n_e^2-2\varepsilon^2} \qquad (5)$$

where ω_{res} and ν_{res} mean ω and ν at resonance respectively, and consequently

$$A_{\text{res}}=L/\sqrt{4\varepsilon^4+4\varepsilon^2\omega_{\text{res}}^2} \qquad (6)$$

where A_{res} means A when resonance.

If, therefore, A_{res} and ω_{res} are observed, ε and n_e are calculated from Eq. (6) and Eq. (5), so that R_1 and E_1 are known from Eq. (2).

We have, on the other hand, the next two relations[2],[3]

$$\begin{cases} \eta=\dfrac{R_1}{4\pi l}\left(\dfrac{1}{r_1^2}-\dfrac{1}{r_2^2}\right) & \text{poises} \\ G=\dfrac{E_1}{4\pi l}\left(\dfrac{1}{r_1^2}-\dfrac{1}{r_2^2}\right) & \text{dyn./cm.}^2 \end{cases}$$

where η and G are the viscosity coefficient and the elasticity coefficient (rigidity, here) respectively of the fluid between the two cylinders, and r_1 and r_2 are radii of the inner and the outer cylinder respectively, l being an immersion depth of the inner cylinder.

Description of the Apparatus

An apparatus as is illustrated in Fig. 2 was constructed. A rotating disc A and another disc B which oscillates rotationally are connected to each other by a connecting rod R. R is combined to A by a pin; A is provided with several holes

(1) *Cf.* T. Kuyama. "*Kagaku*" (*Science*), **16**, 149 (1946); J. R. Van Wazer and H. Goldberg, *J. Appl. Phys.*, **18**, 207 (1947); T. Nakagawa, "*Kagaku*" (*Science*), **20**, 327, 469 (1950); T. Nakagawa, *J. Chem. Soc. Japan*, **72**, 759 (1951); T. Nakagawa, This Bulletin, **24**, 191 (1951).

(2) E. Hatschek, "The Viscosity of Liquids," G. Bell and Sons, Ltd., London, 1928.

(3) Th. Schwedoff, *J. de Phys.*, [2] **8**, 341 (1889).

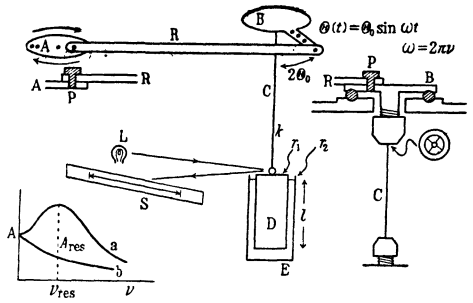

Fig. 2.

which are bored eccentrically at a distance of several millimeters to several centimeters from the center of the disc A, and is pinned by P to R by a certain suitable hole. The B—R coupling is made in a similar way by the holes bored eccentrically at the points several mm. to several cm. distant from the center of B, by using a pin P. A and B are both brass disc plates, 5~10cm. dia. and 5 mm.~1 cm. thick, R being also a brass square rod about 1 meter long. P are brass pins about 4 mm. dia. The under side of the disc B, as is shown in Fig. 2, is provided with a ball bearing to smooth its rotational oscillation. The upper and lower ends of the torsion wire C are each connected to the other body by a chuck whose head is divided in four (*cf.* Fig. 2). If the eccentricity at the A—R coupling is several millimeters, the one at the B—R coupling is several centimeters, and the length of R is about one meter, the rotational angular oscillation of B may be supposed to be almost perfectly sinusoidal. The torsion wire C is a properly selected piano wire, about 0.5 mm. dia. and about 30 cm. long. The inner cylinder D is a glass tube about 5 cm. dia. which is at the upper opening provided with a hard rubber plug to which is attached the above-stated chuck at the center, to be connected to the wire C, and this tube is filled with a proper amount of lead shot to prevent floating up on the one hand and to control the moment of inertia I on the other hand. Since ordinary piano wire has a habit of being bent, it is necessary to straighten it by giving an appreciable weight to D. The outer cylinder E is also a glass vessel about 6.5 cm. dia.

At the chuck which is the lowest end of the wire C, is attached a small galvanometer mirror which reflects a light from a lamp L onto the scale S, and we are able to observe the amplitude of rotational oscillation of D. It should be remembered here that the angle swept by light is double the actual angle of a deflection of the mirror or the body D. The disc A is driven by a phonograph motor, which is convenient to control the revolution speed.

Torsion constant k of the wire C is determined as follows from the observation of a natural frequency or a period T sec. of the free oscillation when a weight of a known moment of inertia I_{kn} is used in place of D.

$$k=4\pi^2\frac{I_{kn}}{T^2}$$

As a weight of a known moment of inertia, the author used a brass cylinder of several cm. dia. and height, whose moment of inertia is easily calculated by the formula

$$I=\frac{1}{2}Mr^2$$

(according to the rotation about the longitudinal axis)

where M and r are mass and radius of the cylinder respectively. It is recommended that several of these standard weights of various dimensions be prepared for the sake of calibrating a wide range of magnitude of torsion constant k. The standard weight, too, is provided with an above-stated fastening chuck to be easily connected to the wire. One of them, for example, which we used, has a value of $I=1.96\times10^3$ g. cm.^{2} ($M=791.2$ g., $r=2.23$ cm.).

With k thus determined, we are able to know the moment of inertia I of the inner cylinder D, by observing a period T sec. of its free oscillation, according to the formula

$$I=\frac{kT^2}{4\pi^2}$$

The procedure of the observation is as follows. A liquid to test is placed between D and E, and a dipping l is properly controlled. Oscillation is started. Inspecting the amplitude of a light spot on S, we vary a revolution speed of the motor or A, and consequeptly a frequency of oscillation of B. (In the case of a phonograph motor, we can easily perform this procedure by an accessory speed controlling arm.) As is shown in the curve (a) of Fig. 2, at a certain value of a frequency, the amplitude of the motion of D reaches a maximum which is of course greater than the amplitude of the driving disc B; in other words, a mechanical resonance of D occurs. Record the resonance frequency ν_{res} and the amplitude of a light spot on S at resonance. Then the above-mentioned analysis gives us the values of η and G of the sample; the amplitude of a light spot on S must be of course reduced to the value of the actual angular amplitude A_{res} of D. It must be remembered that when the dipping l, accordingly R_1, is too large, a maximum of the amplitude does not appear (*cf.* case (b) of Fig. 2).

Measurements were carried out under the following condition.

$k=1.89\times10^4$ dyn·cm.

I (of the inner cylinder) $=1.225\times10^3$ g. cm.^{2}

$\theta_0\fallingdotseq0.1$ radian

$r_1=2.4$ cm., $r_2=3.3$ cm.

$l=$ several cm.

The frequency of the free oscillation (for the determination of k or I), and the resonance frequency ν_{res} were all in the neighbourhood of

Table 1

Substance	Spinnability, cm.	η, poises	G, dyn./cm.^{2}	Conc., % wt.	Remarks
Rubber-xylene (I)	4.5	9.3	6.3		series coupling
Rubber-xylene (II)	11.0	51.	105.	3.6	series coupling
Extract of root of *Hibiscus Manihot* L.	1.0	11.3	27.6	2.9	series coupling
Hg sulphosalicylic acid aq. soln. (I)	5.5	4.2	27.8	4.2	series coupling
Hg sulphosalicylic acid aq. soln. (II)	4.5	4.2	35.0	3.1	series coupling
Starch paste	0	5.5	40.0		parallel coupling
Sucrose aq. soln.	0	11.9	0	68.	purely viscous
Water glass aq. soln.	0	16.6	0	61.	purely viscous

1 cycle per second. The resonance amplitude A_{res} was about 0.2 radian.

Experimental Results

In this way, Table 1 was acquired. As is seen in the table, the Newtonian liquids as a sucrose solution and a water glass solution do not exhibit spinnability even at the comparatively higher viscosities; that these purely viscous liquids require viscosity of 40~50 poises or more to become thread-forming, was already stated. Typically thread-forming liquids, on the other hand, as a rubber solution, an extract of a root of *Hibiscus Manihot* L., a solution of mercury sulphosalicylic acid etc. possess marked elasticity besides relatively low viscosity as is read in the table. Such co-operation of a simple viscous flow and an elastic deformation is responsible for the typical spinnability phenomenon. A thread-forming state is an elastic deformation like the elongation of a rubber string, superposed upon a viscous flow streaming down from above. This elastic deformation, however, is one which corresponds to a relatively small λ, time of relaxation. When this relaxation time is in the same order as our observation time ⓣ (0.1~1 sec.) at the spinnability test, displacement is nearly elastic (reversible). But for a test of a sufficiently long period the displacement becomes viscous (irreversible). So that even in the typically spinnable liquids spinnability does not appear when they are treated by means of a very slow observation speed; a liquid thread will not be formed when a rod is raised up too slowly from a liquid.

Starch paste exhibits no spinnability in spite of its typically visco-elastic nature; this fact will be discussed later.

Spinnability (cm.), as was already described in the paper I, means the maximum length of the liquid thread spun between the surface of the liquid and the tip of the ascending rod, which is an arbitrary measure of the thread-forming ability of a liquid.

Discussions

(A) Optimum Values of η and G for Spinnability.—We have thus an idea that spinnability or the thread-forming property of some liquids is a superposition of a simple viscous flow and an elastic deformation, and determined experimentally the value of a viscosity coefficient specifying the degree of flowing and an elasticity coefficient specifying the extent of an elastic deformation. Now the next problem is to know the optimum values of η and G for thread-forming liquids to exhibit the most remarkable spinnability. To estimate these values, the author experimented as follows.

As is shown in Fig. 4 of Part I, spinnability of a raw rubber—xylene solution has a maximum at a concentration of 3~4% by weight. Direct measurement of viscous elasticity of a 3.6% solution gives the following values (*cf.* Table 1)

$$\eta=51 \text{ poises}, \quad G=105 \text{ dyn./cm.}^2$$

These values will presumably indicate the order of the optimum values for spinnability. According to Maxwell's relation, the time of mechanical relaxation λ is

$$\lambda=\eta/G\fallingdotseq 0.5 \text{ sec.}$$

This value of λ is just the same order of the time-scale ⓣ of our experimental investigation or the experimenting speed when we test the existence of spinnability. That the mechanical relaxation velocity of a system just coincides with the testing velocity, is a necessary condition for the appearance of the most remarkable spinnability. The case stated here just satisfies this condition.

(B) The Problem of the Coupling Type of η and G.—As was referred to previously, starch paste, a typical visco-elastic substance, does not exhibit spinnability. How is it explained ?

The behavior of a material exhibiting a flow superimposed upon elasticity can be represented by means of mechanical models as follows (*cf.*

Fig. 3).[4),(5)] Here the elastic mode of response to stress is indicated by a "spring", and the flow mechanism by a "dashpot" in which a

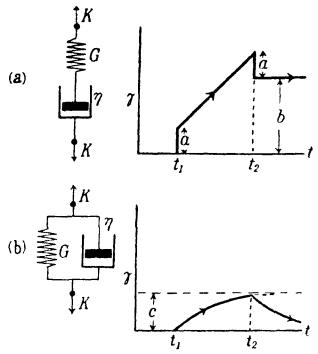

Fig. 3.

porous piston is assumed to move in viscous fluid. If stress is imposed, the ends can move either by a stretching of the spring, or by a flow in the dashpot. The response of the material to a stress can, in this way, be translated into the corresponding behavior of the mechanical model. As the simplest of such models of viscous elasticity, the next two types, as is illustrated by (a) and (b) of Fig. 3, are assumed. Take first the model (a). Impose a constant stress K at the ends, and plot the displacement γ against time t, then the behavior of the system will be as shown in the right-hand diagram of (a). When the stress K is applied at the time t_1, the spring instantaneously stretches to the amount a corresponding to (K/G), and at the time the dashpot begins to elongate steadily at the rate (K/η). When the stress K is removed at the time t_2, the spring instantaneously contracts by the amount a, but the dashpot remains in its elongated condition, and the amount of viscous flow b during the time (t_2-t_1) does not recover permanently.

Consider the second case (b). This device differs from that of the case (a) in that the spring and the dashpot are coupled in parallel, not in series. When the stress K is applied at t_1, the elastic stretching of the spring does not occur in phase with the stress, on account of the viscous damping resistance which is coupled in parallel with the spring. The equilibrium position of elastic deformation is reached asymptotically. And, moreover, unlike the case (a), total displacement does not exceed a value c corresponding to (K/G), even if the loading continues forever. When the load is removed at t_2, the ends return completely to the initial position of zero displacement through the same asymptotic path as above. Such a deformation type is called retarded elastic response, and such a time effect is called elastic after-effect.

Now the series mechanical model (a) is fit to symbolize the mechanical behavior of thread-forming fluids, for it is capable of elongating infinitely by a certain stress. The parallel model (b) is a case of a finite elongation for a certain stress, and the attempt to elongate it at a constant speed, seems to produce splitting or breaking into pieces, without forming a thread. When we call the former case (a) the series coupling and the latter (b) the parallel coupling of viscosity and elasticity, the mechanical behavior of starch paste may correspond to the latter *viz.* the parallel type of visco-elasticity.

Summary

According to the experiments and considerations presented above, a mechanical model as Fig. 4 is introduced for the thread-forming state of liquid. The thread-forming state is the "series" coupling of elasticity corresponding to $G=10^0\sim10^2$ dyn./cm.^{2} (some millionth of G for rubber) and viscosity which corresponds to $\eta=10^0\sim10^1$ poises (some thousands times η for water).

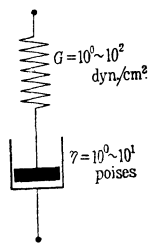

Fig. 4.

This is spinnability.

The author wishes to express his thanks to Prof. J. Sameshima and Prof. H. Akamatsu for their leadership. The expenses connected with this investigation have been defrayed by the grants from the Ministry of Education, to which his thanks are also due.

Department of Chemistry, Faculty of Science, Tokyo University, Tokyo

(4) T. Alfrey, "Mechanical Behavior of High Polymers," Interscience Publishers, New York, 1948.
(5) R. Houwink, "Elasticity, Plasticity and Structure of Matter," Cambridge Univ. Press, London, 1937, p. 64.

Pen Writing Polarograph with Direct Current Amplifier. — Study of *p*-Nitrosodiethylaniline —

By Sinichi KIKUCHI, Yoshikata SAKAGUCHI and Kenichi HONDA

(Received November 12, 1951)

Introduction

It is twenty-six years since polarography was born. There have been many studies of this subject especially in recent years as J. J. Lingane reported in Analytical Chemistry.[1],[2] Excited by the industrial use, the polarographic apparatus has gained remarkable progress and is ready for the new application. According to the progress of the apparatus, it is just now going to break new ground in polarography. The present authors feel keenly the importance of instrumentation for the above-mentioned considerations.

One of the eminent developments is the invention of a pen-writing device without photographic paper. It has been studied chiefly in U. S. A.,[1],[2] but to our disappointment, the structure of those devices has not been described in full.

Two of the present authors—S. Kikuchi and Y. Sakaguchi—employed the direct current amplifier and its recorder for silver potentiometric studies of photographic fog inhibitors,[3],[4],[5] while S. Kikuchi and K. Honda were studying the polarography for the research of the electrolytic preparation of diethylparamine from *p*-nitrosodiethylaniline.[6] The former is known as the developer of color photography.

Here we have combined both techniques, and have obtained excellent polarograms. We have compared the polarograms of *p*-nitrosodiethylaniline obtained with this recorder and those of ordinary photographic apparatus. We should like to report as follows, because we had satisfying results. We wish to write at this opportunity that the second and more improved apparatus is being made now.

Instrumentation

Direct Current Amplifier for Polarograph.—There are two systems which record the small potential difference, as a rule. The one is the recording potentiometer system, and the representative is Sargent visual recording polarograph[1] with Brown Electronik potentiometer recorder. The merits of this system are to keep good equilibrium notwithstanding the variation of voltage of alternating lines and to record with rectangular coordinates in a chart and so to have good reliance. On the other hand its defects are that half-period of the potentiometer is too long as it needs several seconds to cover all the range and the price is considerably expensive—this is an important problem in Japan.

The other is the direct current amplifier and recorder system and the representative is Polaro Analyzer[1] of Rutherford Instrument Co. The merit of this system is that half-period of recorder is within one second. This allows us to use it not only in the industial application, but also for theoretical studies. Among other instruments, this is very cheap, the predominant merit for us. The defects of this system are the use of the direct current amplifier for this purpose is very difficult, and especially difficult, in Japan, because of the bad quality of the electric line in Japan, and that it records with curved coordinates. Considering all these conditions, we adopted the latter.

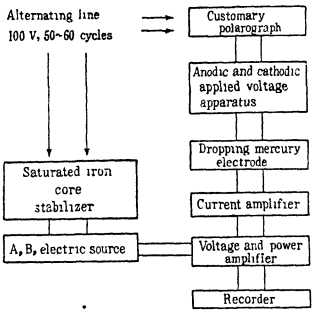

Fig. 1.—Block diagram of pen-writing polarograph with direct current amplifier.

(1) J. J. Lingane, *Anal. Chem.* **21**, 45 (1949).
(2) J. J. Lingane, *ibid*, **23**, 86 (1951).
(3) S. Kikuchi and Y. Sakaguchi, *J. Soc. Sci. Phot. Japan*, **12**, No. 4, 3 (1950).
(4) S, Kikuchi & Y. Sakaguchi, *ibid.*, **13**, No. 4, 6 (1951).
(5) S. Kikuchi & Y. Sakaguchi, "Seisan Kenkyu" published by Tokyo Univ. **3**, No. 4, 161, (1951).
(6) S. Kikuchi and K. Honda, *ibid.*, **2**, No. 6, 267 (1950).

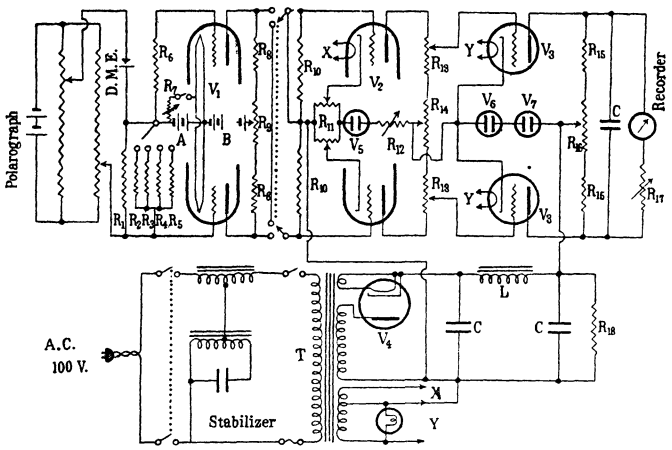

R_1	1	MΩ	R_{13}	50	KΩ V. R.	V_5	VRA 60/80	
R_2	1.5	KΩ	R_{14}	20	KΩ V. R.	V_6	VRB 135/60	
R_3	2	KΩ	R_{15}	10	KΩ	V_7	VRA 140/50	
R_4	3	KΩ	R_{16}	2	KΩ V. R.	A	two of 1.5 volts dry battery (special unit one)	
R_5	5	KΩ	R_{17}	5	KΩ V. R.			
R_6	3	KΩ	R_{18}	1	MΩ	B	67.5 v. piled dry battery	
R_7	10	Ω variable resistor	C	4	μF oil filled condenser	T	secondary 350 v. 70 mA. 6.3 v. × 2 5 v. for 40 watts	
R_8	30	KΩ	L	10	H 80 mA.			
R_9	5	KΩ V. R.	V_1	UZ30MC		D. M. E. dropping mercury electrode		
R_{10}	3	MΩ	V_2	US6SL7GT		Every resistors are for 1 watt.		
R_{11}	100	Ω V. R.	V_3	UY76				
R_{12}	600	Ω V. R.	V_4	KX80HK				

Fig. 2.—Circuit of the amplifier.

Then the amplifier is the main point of this report. The mechanism of this system is shown in Fig. 1 as the block diagram.

When the polarographic current I flows on the resistance R—1.5 KΩ~5 KΩ, the potential drop is IR which is amplified so as one can get the polarograms on the recording milli-ammeter. Suitable voltage amplification degree and power amplification degree to drive the recorder are possessive functions of course. The circuit of this amplifier is shown in Fig. 2.

Balanced type UZ 30 MC preamplifier with dry batteries was made to recover the shortage of amplification degree of main amplifier which had been made to potentiometric titrations. Its voltage gain was about 6 times. The main amplifier based on the balanced bridge of 6SL7GT and two of UY76 was a eliminator system and its voltage gain was about forty times, in other words it needed 400 mv. for a full swing of the recorder.

Stability of the amplifier was obtained by the next three methods. The first was the customary saturated iron core type stabilizer; the second was "μ balanced circuit"[7] which was composed of R_{11}, V_5, and R_{12} in 6SL7GT's circuit; the third was stabilo-volt tubes of V_6 and V_7 in UY 76's circuit. The "μ balanced circuit" is as follows,

$$\mu = (-dE_p/dE_g)I_p$$

where, μ is amplification factor, I_p is plate current E_p is plate voltage, and E_g is grid voltage. Controlling that $-dE_p/dE_g$ is equal to μ of the tube, one gets the constancy of plate current. It is that $1/\mu$ of dE_p is negatively fed back to the grid. The stabilo-volt tube is used for taking formulated ratio. If it is fed back to slightly excess, it is possible for one to avoid the variation of emission of

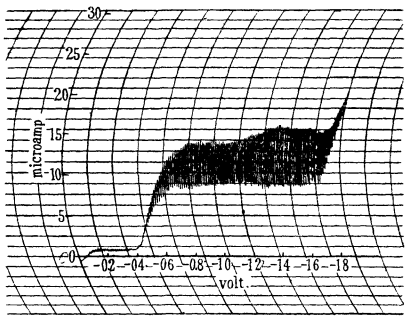

Fig. 3.—Micro-ampere and voltage graduation of the co-ordinates with the example of the polarogram by the amplifying method.

(7) G. P. Harnwell and S. N. Van Voorhis, *Rev. Sci. Instruments*, **5**, 244 (1934).

filament. Thus, the movement of zero-point of this direct current amplifier was within 1% between 90 and 110 volts of alternating lines.

Having combined pre-amplifier, main amplifier, and recorder, the micro-ampere and voltage graduation was shown in Fig. 3 where in-put resistance was 2KΩ.

Its stability was a function of A dry battery, which was able to be employed about five hours. The movement of zero-point was 3% of full range in fifteen minutes. B battery was not changed. The total error of this recording system was within 5%. The amplification degree was adjusted by R_2, R_3, R_4, R_5, and R_{17}: and zero-point was adjusted by R_9 and R_{14} roughly, and by R_{16} finely. The main amplifier was originally a voltage amplifier, then the potential difference of anode pool electrode *vs.* calomel electrode was recorded with this amplifier. The graduation in the chart on this case was as shown in Fig. 4.

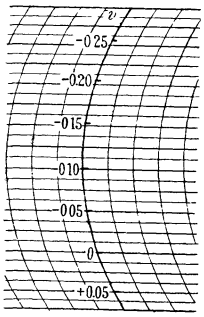

Fig. 4.—Voltage graduation of the anode potential *vs.* S. C. E.

There were four combinations of electric source, stabilizer, and main amplifier. Only one or two of them were suitable for good recording; then the combination was changed occasionally by inspection. The apparatus was not electrically grounded.

Recorder.—It was a direct current 2 milliamp. recorder and its inside resistance was 6000 Ω and its half-period was within one second. It had twelve chart speeds, but we used usually that of 20 mm./min. The effective width of the chart was twelve cm. and its length was 20 m., and it was moved with a clock. This recorder was made by Yokogawa Electric Works, Japan, in 1951.

Experimental

As described before, *p*-nitrosodiethylaniline was studied polarographically, using both our new pen-writing apparatus and ordinary photographic apparatus. The aim is to test the faculty of this new apparatus by comparing the data gained from both apparatuses and so to contribute to the study of electrolytic reduction of *p*-nitrosodiethylaniline.

(a) **Preparation.**—*p*-Nitrosodiethylaniline investigated here, was synthetized from diethylaniline and sodium nitrite,[8] and further recrystallized twice as dark green needles from methanol. Its m. p. was 84.5~85°C. This compound was dissolved in ethanol to the concentration of $5\cdot10^{-3}$ mol/l. as the stock solution. On the other hand, Sørensen's citrate-HCl, citrate-NaOH, borate-HCl, and borate-NaOH buffer solutions were prepared, which, were added to the stock solution with the ratio of 4:1~40:1 to make up the proper concentration of test solution. The electrolysis was carried out with the anode of mercury pool at the constant temperature of 20°C. in the liquid paraffin bath. The potential of the anode was measured with potentiometer or amplifying recorder referring to the saturated KCl calomel electrode after each electrolysis. The drop time of capillary was 5.7 sec. per drop and the value of $m^{2/3}t^{1/6}$ was found to be 1.8 $mg.^{2/3}$ $sec.^{-1/2}$ in water with no applied potential. To remove oxygen from the solution, nitrogen was bubbled. As for the photographic polarograms, they were recorded using Yanagimoto's pre-war type polarograph.

(b) **Results.**—*p*-Nitrosodiethylaniline gives only one typical reduction wave and its limiting current is very clear. The values of the half-wave potentials of this in buffered ethanol solution *vs.* various *p*H values, and also the values of the wave heights in the same solution at the concentration of 10^{-3} *M.*/l., are tabulated in Table 1. In this table, the half-wave potentials obtained by amplifying method which adopts the inserted resistance of 2 KΩ, and those of photographic are compared. The wave-heights in the table are measured from the polarograms by the former.

Table 1

Comparison of Half-wave Potential *vs.* *p*H by Both Methods. Concentration of the sample is 10^{-3} *M.*/l.

*p*H	$E_{1/2}$ v. (v. s. c.)		Wave height, microamp.
	pen-writing	photographic	pen-writing
1.93	+0.124		
3.36		+0.053	
4.16	−0.008	−0.031	6.9
5.98	−0.128	−0.229	6.6
7.93	−0.272	−0.287	6.0
9.91	−0.583	−0.598	6.1
11.7	−0.559		7.2

Inspecting this table, the differences between the $E_{1/2}$ of both methods are about 10 mv. with one exception. The present authors think that possible fluctuation of $E_{1/2}$ which often appears in the irreversible system of such organic compounds, can actually make this difference negligible, and consequently the potential drop by the

(8) Kopp, *Ber.*, **8**, 621 (1875).

inserted resistance which is $2 \cdot 10^3\,\Omega \times 6 \cdot 10^{-6}$ amp. $= 12$ mv. in this case, becomes not very important.

Now going back to the standpoint of polarographic study, it is concluded that the reduction mechanism would be the same in the whole pH range because of the similar wave form and the character of each polarogram. The half-wave potential of this compound is more positive than those of other nitro compounds and so it shows that this compound is very easily reducible. This corresponds to the results of the former investigation about electrolytic reduction.[6] Especially, in the solution of pH value 1, the reduction proceeds with no applied potential.

The relation between the $E_{1/2}$ and pH shows their complete linearity over the whole pH range with one exception which seems to be the experimental error. The increase of $E_{1/2}$ per unit pH value is about 75 mv.

The relation of concentration and wave height at the pH 9.91, in the case of using the amplifying method is shown in Table 2. It shows their linearity generally, between the range of 2.5×10^{-4} and 3×10^{-3} *M*./l.. From this result, it is proved that this pen-writing apparatus can be used especially for quick quantitative analysis.

Table 2

Relation between Concentration and Wave-height (pH = 9.91)

Concentration, *M*/l.	Wave-height, micro amp.
2.5×10^{-4}	1.88
5×10^{-4}	3.13
1×10^{-3}	6.72
2×10^{-3}	10.0
3×10^{-3}	15.6

Summary

A new type of polarographic apparatus which utilizes the amplifying method and recorder is described. And its faculty is studied by comparing it with usual photographic apparatus. At the same time, p-nitrosodiethylaniline is studied polarographically and the comparison of both apparatuses is achieved through that study.

Laboratory of Electrochemistry and Photochemistry, Institute of Indusrtial Science, Tokyo University, Chiba.

Studies on the Gas-Liquid Interface by Surface Potential Measurements III. The Surface Aging of the Solutions of the Long-chain Dibasic Acids

Hiroshi HOTTA and Toshizo ISEMURA

(Received September 13, 1951)

When a new surface is formed on the top of a solution by sweeping the surface with a glass barrier, the solute in the solution will begin immediately to be adsorbed on the freshly formed surface. The rate of adsorption depends mainly on the nature of the solute if the other conditions are the same, and is a problem of some interest in regard to the structure of the layer and the mechanism of adsorption. The adsorption equilibrium of polar organic compounds on the surface of its solution can be considered as a result of competition of the hydrophilic nature of polar groups and the hydrophobic nature of the nonpolar part of the amphipathic molecule. In a homologous series the solute of low molecular weight readily reaches a steady state. With the solute of moderate molecular weight, the formation of a completely adsorbed layer needs considerable time. On the other hand, the solute of high molecular weight requires so much longer time for equilibration, that the solution apparently reaches a steady state immediately. In a homologous series of the amphipathic compounds, it is generally expected that the lower the molecular weight of the solute is, the higher the solubility and the larger the mobility of the solute is.

The variation of a surface layer will be reflected on the surface tension and surface potential of the solution. Hence, the rate of adsorption can be readily followed by measuring the surface tension and the surface potential as a function of time. In the course of our previous investigation,[1] the change of surface

(1) T. Isemura and H. Hotta, *Bull. Chem. Soc. Japan*, **23**, 193 (1950).

potential with time was found with solutions of some ω, ω'-dicarboxylic acids.

In this respect, the measurements of surface tension and surface potential of the solution are the powerful means to study the change of the surface layer of the solution. In order to observe the change of the surface layer and to clarify its cause, we modified the apparatus used in the previous investigation to adapt it for this purpose. The change of the surface tension and the surface potential was determined with some dicarboxylic acids. From such experiments it was concluded that the adsorption may occur in two stages, initial rapid, and later slow adsorption. In our present experiments, the slow adsorption only was studied. The experimental results will be considered on the ground of the kinetic molecular theory.

Experimental

Experimental Methods.—The apparatus used in our present experiment was a combination of a surface balance of hanging plate type and a surface potentiometer of vibrating electrode type. A thick-walled shallow glass trough, $0.7\times7.0\times15.0$ cm. was used for the economy of the solution. The vibrating electrode of the diameter of 20 mm. was hung over the middle of the trough and the glass plate for the surface tension measurement was inserted into the solution by the side of the electrode. The other electrode made of platinum wire was immersed over-night in the same solution prior to the experiment by using such a syphon as shown in Fig. 1. In order to observe the surface aging of the solution, the surface of the solution was cleaned before starting by the paraffined glass barrier.

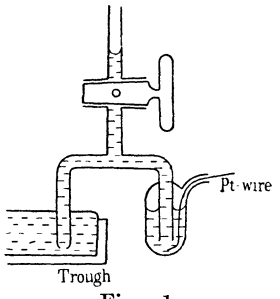

Fig. 1.

The amplifier of the surface potentiometer consists of two parts, *i. e.*, the pre- and main amplifier. The main amplifier is a three-stage tuned amplifier for *ca.* 500 c./s. using three CZ-501 D tubes.

The change of the surface tension was followed by the hanging plate method, and the displacement of the plate was measured by an optical lever.

The level of the surface of the solution was defined by using a telescope.

The materials used in the present experiment were adipic, suberic, azelaic, sebacic and γ,γ'-sulfonyl dibutyric acid. Most of the measurements were made with acidulated solution by hydrochloric acid (in a concentration of 0.015 *N* HCl) if without any special indications. With sebacic acid, a measurement was also made for comparison with aqueous solution. The monolayer of ω,ω'-hexadecadicarboxylic acid was also studied by the technique generally used for insoluble monolayer. All measurements were made at room temperature in a small closed chamber without any special temperature regulation. However, the variation of temperature in the course of measurement to obtain a single curve never exceeded more than 0.4°. At first, it was confirmed that the change of surface tension of pure water with time was not detectable during a course of experiment (within 1.5 hours). The effect of evaporation was also negligible in such a small closed chamber.

Results.—From such experiments as the above it was found that the rate of change of the surface tension was generally parallel to that of the surface potential. However, at the last stage of adsorption of the nearly saturated solution of sebacic acid after 60 minutes, both rates were not parallel to each other. (See curves *f* and *f'* in Fig. 3 and 4.) In this respect, some theoretical consideration will be given in the following section. No appreciable change of the tension and the potential could be observed with nearly saturated solutions of adipic acid (0.095 mol/l.) and of γ,γ'-sulfonyl dibutyric acid (0.017 mol/l.) at 22°.

A part of the experimental results is shown in the following figures (Fig. 2, 3 and 4). The snrface tension of suberic acid solution in the concentration of 4.5×10^{-3} mol/l. changed definitely by *ca.* 0.1 dyn./cm. during the first four minutes, although the change can hardly be recognized from the figure. Azelaic acid solution of 2.7×10^{-3} mol/l. showed the gradual change of the tension until after 93 minutes when the experiment was disrupted. On the other hand, azelaic acid solution of 1.35×10^{-3} mol/l. showed no change. Meanwhile, all the solutions of sebacic acid examined changed the tension even in a concentration as dilute as 1.87×10^{-4} mol/l.

From these results it can be concluded that the shorter the dicarboxylic acid is and the more dilute the solution is, the shorter is the time required for equilibration. In the case of sebacic acid, the surface tension and potential of the most dilute solution showed an appreciable change after a considerable time.

The absolute value of surface tension can hardly be determined by our present method without any uncertainty, even though the level of the surface of the solution was adjusted to

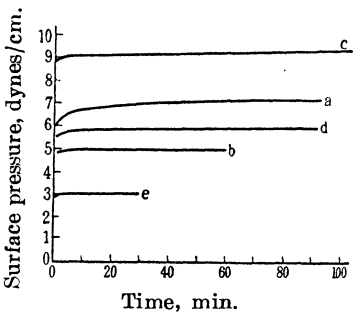

Fig. 2.—The change of surface pressure with time.
(I) Suberic acid solutions in 0.015 *N* HCl: curve a, 9.03×10^{-3} mol/l. (nearly saturated), 22°C.; curve b, 4.5×10^{-3} mol/l., 22°C.
(II) Azeraic acid solutions in 0.015 *N* HCl: curve c, 5.4×10^{-3} mol/l., 20.5°C.; curve d, 2.7×10^{-3} mol/l., 20.5°C.; curve e, 1.35×10^{-3} mol/l., 21.0°C.

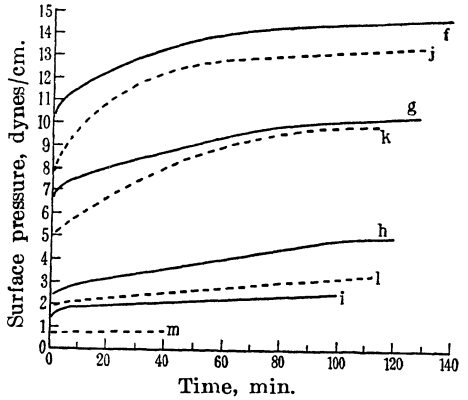

Fig. 3.—The change of surface pressure of sebacic acid solutions with time.—
(I) Solutions in 0.015*N* HCl (full line): curve f, 1.62×10^{-3} mol/l. (saturated), 22°C.; curve g, 8.1×10^{-4} mol/l., 22°C.; curve h, 4×10^{-4} mol/l., 22°C.; curve i, 2×10^{-4} mol/l., 23°C.
(II) Solutions in water (dotted line): curve j, 1.55×10^{-3} mol/l., 22°C.; curve k, 7.7×10^{-4} mol/l., 23°C.; curve l, 3.75×10^{-4} mol/l., 23 °C.; curve m, 1.87×10^{-4} mol/l., 22.5°C.

a fixed level by the aid of a telescope. Moreover, in the initial stage (5-10 seconds) the disturbance of the surface caused by dipping of the plate and the sweeping could not be avoided. However, the rate of surface tension lowering could be determined very accurately. On the other hand, the rate of change of surface potential was also determined quite correctly since we take care of equilibration, sufficiently for this purpose.

In comparison with our previous results,[1] the results on adipic and γ,γ-dibutyl sulphonic acid were in good agreement with previous

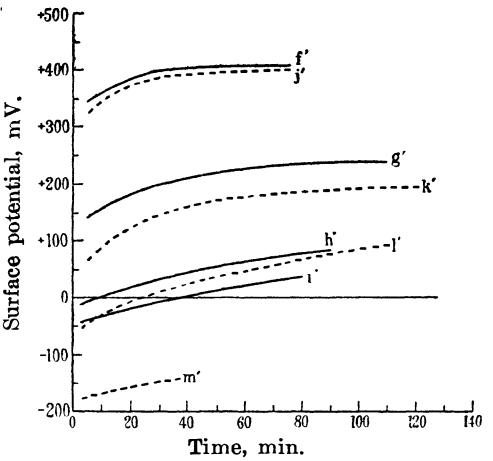

Fig. 4.—The change of surface potential of the sebacic acid solutions with time. Each curve corresponds to that with the same letter without prime in Fig. 3.

ones. The results on other acids showed slight discrepancies. These slight discrepancies may be caused by some fluctuation of the standard potential and by the adsorption of the solute on the electrode dipped in the solution. The electrode in the present experiment was used after equilibration between the solution and the electrode, while the electrode in the previous experiments was used without any such precaution.

ω,ω'-hexadecadicarboxylic acid was examined on 0.1 *N* HCl solution. It gave the film of gaseous type, however considerably deviated from the ideal law. The surface moment of hexadecadicarboxylic acid was determined from surface potential-area relation and was found 0.41 D at the molecular area of 100 Å.^{2}, 0.35D at 200 Å.^{2} and 0.32 D at 300 Å.^{2}. 0.35 D was used in the later calculation.

Discussion

The mechanism of the change of surface tension with time was recently studied by several investigators. Some of them[2,3,4] considered that the diffusion of the solute was one of the most important factors. In the case of the fast adsorption such as that studied by Addison,[5] the inference might be correct; however, in the case of slow adsorption such as in our present experiments, this is not

(2) A. F. H. Ward and L. Tordai, *J. Chem. Phys.* **14**, 453 (1946).
(3) S. Ross, *J. Am. Chem. Soc.*, **67**, 990 (1945).
(4) C. M. Blair, *J. Chem. Phys.*, **16**, 113 (1948).
(5) C. C. Addison, *J. Chem. Soc.*, **1943**, 535; **1944**, 252; **1945**, 98.

applicable.[6,7] In the latter case the rate of adsorption must be much slower than that of diffusion. The inference was examined quantitatively in the following manner. According to Ward and Tordai,[2] the rate of diffusion will be given by

$$\frac{\partial M}{\partial t} = D\frac{n_0}{\sqrt{\pi Dt}} \qquad (1)$$

where D is the diffusion constant, M the number of solute molecules per cm^2, n_0 the bulk concentration in molecules per cc., t the time in sec. If we assume values approximately as follows,

$$D=10^{-6}, \quad n_0=10^{17} \quad t=10^3$$

in relation to our present experiment, it will be obtained from (1)

$$\frac{\partial M}{\partial t} = 10^{13} \quad \text{(molecules per cm.}^2\text{ per sec).}$$

On the other hand we shall estimate the actual rate of adsorption to be 10^9 molecules per cm^2 per sec. from the present experimental results. The reasons for the estimation will be given in a later part of this report. Now we assume the final state of adsorption was reached by passing over an energy barrier which serves as the rate-determining factor. The adsorption was probably pursued through two stages. The first is the fast adsorption which is mainly concerned with diffusion, and the second is the slow adsorption with energy barriers, which are caused probably from dehydration, electrostatic repulsion, reorientation and so on. In our present experiment, only the second stage of adsorption was investigated, since our method did not fit the investigation of such a fast change occurring in the surface as that of the first stage,

In order to study this problem the cage model of a liquid by Fowler and Slater[8] was adopted as the ground. If we consider a sub-layer under the adsorbed monolayer in the surface, the concentration in the sub-layer may be equal to that of the bulk since the diffusion is enough to made up for the loss by adsorption quantitatively. Therefore, if the number of solute molecules in a unit area of a sublayer is n_{sub},

$$n_{sub} = \frac{2Nc\delta}{10^3}$$

where N is the Avogadro's number, c the bulk concentration in mol/l., 2δ the thickness of sub-layer in cm. The total number of collisions per unit time of a given molecule with the cage wall by the thermal agitation can be expressed by

$$\nu = \frac{3}{2\delta}\sqrt{\frac{2RT}{\pi M}}$$

according to them,[8] where M is the molecular weight. Now, if we assume that one-sixth of the total collision is effective to adsorption, the total number of the effective collisions, Z against unit area per unit time, is written by

$$Z = \frac{1}{6}n_{sub}\nu = \frac{Nc}{10^3}\sqrt{\frac{RT}{2\pi M}}. \qquad (2)$$

This result is formally analogous to the formula[9] previously proposed. Therefore, the number of the actually adsorbed molecules, n_{ads}, per unit area per unit time is given by

$$n_{ads} = \frac{Nc}{10^3}\sqrt{\frac{RT}{2\pi M}}e^{-\Delta F^*/RT} \qquad (3)$$

where ΔF^* is the free energy of activation for adsorption. According to the cage theory, of course, the size of the cage of the solute molecule is equal to that of the solvent molecule, and all molecules in a cage have a similar energy distribution with a perfect gas. We assume this first approximation is the case in our present experiment.

On the other hand we can estimate the actual rate of adsorption from the rate of the surface potential change as follows. It is generally accepted that the relation between the surface potential ΔV and the contribution of each adsorbed molecule to it, namely, the effective moment μ of each molecule is expressed by

$$\Delta V = 4\pi N_{ads}\mu \qquad (4)$$

where N_{ads} is the number of the adsorbed molecules in a unit area of the surface. Hence

$$\frac{d\Delta V}{dt} = 4\pi\left(\mu\frac{dN_{ads}}{dt} + N_{ads}\frac{d\mu}{dl}\right) \qquad (5)$$

If it is assumed as a first approximation that,

$$\frac{d\mu}{dt} = 0, \qquad (6)$$

that is the orientation of the molecule of ω, ω'-dicarboxylic acid is not changed by

(6) K. S. G. Doss, *Kolloid-Z.*, **86**, 205 (1939).
(7) A. E. Alexander, *Trans. Faraday Soc.*, **37**. 15 (1941).
(8) Fowler and Slater, *Trans. Faraday Soc.*, **34**, 81 (1938).
(9) Adam, "The Physics and Chemistry of Surfaces", Oxford, 1938, p. 6.

further adsorption, it is obtained from (5)

$$\Delta(\Delta V) = 4\pi\mu_s \Delta N_{ads} = 4\pi\mu_s n_{ads} \qquad (7)$$

where the symbol Δ means the change for a unit time. Therefore, if the magnitude of μ_s of the suitable standard substance is known, the rate of adsorption can be calculated from (7). There exists some doubt in respect to the validity of the equation (4). However, this may be cancelled by applying the same equation to a standard substance. In the present case, ω, ω'-hexadecadicarboxylic acid was used as the standard substance, which has *ca.* 0.35 Debye unit of μ_s in monolayer as mentioned above. Although this value may be somewhat smaller than that expected from the data of monocarboxylic acid[10] and μ_s should be dependent upon the state of the surface, the above value was adopted for the present calculation, and n_{ads} obtained was shown in the Table 1. With this value ΔF^*, the activation free energy of adsorption, can be estimated with (3), which is also listed in the Table 1.

This value of n_{ads} seems to be too large, because the surface energy per molecule is smaller than kT in the lower pressure region from our present result. This contradiction may, probably, be due to the unsuitable estimation of μ_s. On the other hand, we can at least point out the propriety of the assumptions that (I) all the adsorbed molecules are undissociated in the acidulated solution; and that (II) equation (6) is valid, that is, the contribution of the change of μ_s of the already adsorbed molecules to $\Delta(\Delta V)$ can be neglected. However these assumptions effect the estimation of ΔF^* by 0.5 Kcal./mol increase even at the highest, but considerable to that of surface energy per molecule. Neverthless n_{ads} should be smaller, consequently ΔF^* larger.

As already pointed out, in the case of the saturated sebacic acid solution (see curves f and f' in Fig. 3 and 4), the surface potential attained to the stationary state, while the surface pressure was still increasing. This means that in the fairly close-packed film a small increase of packing would produce a marked increase in surface pressure but scarcely any effect on surface potential as interpreted by Alexander.[7]

Also in Fig. 3 and 4 the effect of the hydrochloric acid was examined in comparison with the aqueous solution. It may be noticed that, in the concentrated solution, the equilibrium values of both acidulated and aqueous solution scarcely suffered any effect in spite of the considerable difference in the initial stage, while, in the dilute solution, the considerable difference on the equilibrium value was found. The surface potential of the aqueous solutions was far more negative than of the acidulated solution. This fact can be explained on the

Table 1

Rate and Activation Free Energy of Adsorption

Solute	Curve in figure	Total effective collison number per second	n_{ads} and ΔF^*	Time, min. 10 ~20	20 ~30	30 ~40	40 ~50	50 ~60	60 ~70	70 ~80	80 ~90	90 ~100	100 ~110	110 ~120
Suberic Acid	a	2.6×10^{22}	n_{ads} (10^9/cm^2/sec)	5.7	—	—	4.3		—	—	—	—	—	—
			ΔF^* (kcal./mol)	17.5	—	—	17.8		—	—	—	—	—	—
	b	1.3×10^{22}	n_{ads}	1.7	—	—	—	—	—	—	—	—	—	—
			ΔF^*	17.9	—	—	—	—	—	—	—	—	—	—
Azeraic Acid	c	1.5×10^{22}	n_{ads}			1.6				0.5			—	—
			ΔF^*			18.0				18.5			—	—
	d	7.5×10^{21}	n_{ads}					0.7					—	—
			ΔF^*					18.1					—	—
Sebacic Acid	f	3.9×10^{21}	n_{ads}	25	13	9.5	4.3	1.9	0	—	—	—	—	—
			ΔF^*	15.4	15.7	16.0	16.4	17.0	∞	—	—	—	—	—
	g	2.05×10^{21}	n_{ads}	30	—	15	—	11	—	—	—	2.5	—	2.2
			ΔF^*	15.0	—	15.4	—	15.6	—	—	—	16.5	—	16.6
	h	10^{21}	n_{ads}					11					—	—
			ΔF^*					14.1					—	—
	i	5×10^{20}	n_{ads}					11					—	—
			ΔF^*					13.8					—	—

(10) J. H. Schulman and E. K. Rideal, *Proc. Roy. Soc. (London)*, **A 130**, 270 (1930).

ground that, the dissociation degree at the surface is somewhat larger on the aqueous solution than on the acidulated solution, if the surface concentration is low, while, the difference of dissociation between both solutions disappears, if the surface concentration is high. The effect of acidulation is not so considerable as in the case of soap.[11] This difference is because of the small dissociation constant of the free acid compared with that of soap. This will be further investigated in future for more evidences.

Summary

The surface aging of the solutions of some ω,ω'-dicarboxylic acids was investigated by measuring the surface tension and surface potential, in a function of time. Only the slow adsorption process was studied in the present experiment.

Adipic, suberic, and azelaic acid reached readily an equilibrium. Sebacic acid showed considerable surface aging. The mechanism of adsorption was assumed in the light of kinetic molecular theory, and the free energy of activation for adsorption was calculated. We obtained the free activation energy, 17.5-17.9 Kcal. for suberic acid, 18.0-18.5 Kcal. for azelaic acid and 13.8 Kcal. or more than this for sebacic acid. Free energy of activation for adsorption was increased to some extent with the surface concentration of already adsorbed solute molecules and consequently, for a certain solution, with the surface age.

Thanks are due to Mr. N. Numasaki for his aid in the construction of the amplifier. The authors' sincere thanks are also due to the Ministry of Education for the financial grant.

The Institute of Scientific and Industrial Research, Osaka University, Osaka

(11) G. C. Nutting and F. A. Long, *J. Am. Chem. Soc.*, **63**, 84 (1941).

Identification of Halogens in Organic Compounds by Means of Paper Chromatography[1]

By Toshio ANDO and Shin-ichi ISHII

(Received November 17, 1951)

In order to identify halogens contained in organic compounds, a usual method of qualitative inorganic analysis has been applied to the solutions obtained by decomposition of the compounds. However, such an analysis is somewhat troublesome and needs a considerable amounts of samples. Lederer[2] has recently described a chromatographic method for the separation of inorganic halides on paper with butanol-ammonia as solvent, but the resolution of chloride and bromide especially was not complete, and the instability of composition of the solvent resulting from vaporization of ammonia was also found undesirable.

Now the present authors have developed a method of identifying halogens of organic substances accurately on paper chromatograms, in which a few drops of Lassaigne's solution obtained by decomposing the compounds in the usual way with sodium were developed favorably with a solvent consisting of butanol-picoline. The spots of chloride, bromide, and iodide were then revealed separately as brown coloration of silver sulfide. A spot of iodide could also be located by a characteristic violet coloration of iodine-starch compound.

Experimental Method

Sample.—0.1 *M* solutions of sodium chloride. bromide, and iodide in water and in aqueous sodium hydroxide of 0.5, 1.0, 1.5, and 3.0 *N* in concentration were used at first for the sake of control. Those of sodium cyanide, sodium sulfide, and potassium rhodanate were also used. The organic substances containing halogen which were used were as follows: benzene hexachloride, chloronitrophenol and aniline hydrochloride (both containing Cl and N), dibromocholestanedione,

(1) The present paper was read by one of the authors (S. I.) before the 7th Meeting of this Institute (Nov. 9, 1950) and also before the 4th Annual Meeting of the Chemical Society of Japan in Tokyo University held on April 7, 1951.

(2) M. Lederer, *Science*, **110**, 115 (1949).

bromophenol blue and bromothymol blue (Br and S), ammonium bromocamphorsulfonate (Br, N and S), and diiodotyrosine (I and N), and also some combinations of them.

Decomposition of the organic compounds.—A small quantity of organic halogenocompound was fused with 3~5 parts of metallic sodium, and the mixture was poured into water of 30~40 times the weight of sodium used. 0.01~0.005 cc. of the Lassaigne's solution thus prepared was applied to a strip of paper.

Filter paper.—A strip (1.8×22 cm.) of the Toyo filter paper No. 131 was used. The Toyo filter paper No. 2 was found unsuitable for the present purpose, as it always contained a slight quantity of chloride and the chromatogram obtained on it was not so fine as to distinguish the spots clearly.

Development and revelation.—One-dimensional ascending type of development was adopted in a test-tube (2.5×25 cm.) containing solvent in the bottom.

Solvents used were as follows: (a) butanol-picoline-water (1:1:0.8 V/V), (b) butanol-propanol-water (1:1.1:1 V/V), and (c) butanol-1.5*N* aqueous ammonia (5:1 V/V). Temperatures were given respectively in the foot-notes of the table.

After development and drying, the paper was sprayed with 0.2 *N* aqueous solution of silver nitrate, followed by washing away the excess of silver nitrate twice with 0.1 *N* nitric acid. Then the paper was either sprayed with 0.2 *N* solution of sodium sulfide or exposed to the atmosphere of hydrogen sulfide. The spot of halide was revealed as brown coloration of the resulting silver sulfide.

In a case of iodide, the following method was also used and proved more sensitive than the former: after development the paper was sprayed with 3% aqueous hydrogen peroxide and then with 0.2% aqueous solution of starch. A fine bluish violet spot of iodine-starch appeared instantly.

Results and Discussions

R_F values of various solutions of inorganic halides, sulfide, and rhodanate when developed with butanol-picoline, butanol-propanol, and butanol-ammonia, and also those of halides obtained from organic compounds containing halogens were summarized in the accompanying table.

Chromatograms of aqueous solutions of inorganic halides.—In aqueous solution of sodium chloride, bromide, or iodide, the butanol-picoline system was found most suit-

Table

R_F Values of Several Halides and Salts Dissolved in Water or Alkaline Solutions of Various Concentrations and Developed with Several Solvents[a]

Developing Solvent	Solution of Sample (0.1 *M*) in	Halide			Other Relating Salt	
		NaCl	NaBr	NaI	Na_2S	KCNS
Butanol-Picoline[b]	Water	0.22§	0.31	0.59	0.03	0.64
	0.5*N*-NaOH	0.19	—	—		
	1*N*-NaOH	0.18	0.28	0.56		
	1.5*N*-NaOH	0.15	—	—		
	3*N*-NaOH	0.10	—	—		
	Decomposition Solutions of Organic Halogenocompounds*	0.19 ±0.02	0.27 ±0.02	0.56 ±0.03		
Butanol-Propanol[c]	Water	0.28	0.32	0.40	0.14	0.48
	0.5*N*-NaOH	0.27	—	—		
	1*N*-NaOH	0.23	0.26	0.34		
	1.5*N*-NaOH	0.21	—	—		
	3*N*-NaOH	0.18	—	—		
Butanol-Ammonia[d]	Water	0.05	0.08	0.14	0.00_6	0.20
	0.5*N*-NaOH	—	—	—		
	1*N*-NaOH	0.05	0.07	0.13_5		
	1.5*N*-NaOH	—	—	—		
	3*N*-NaOH	—	—	—		

(a) By an ascending method. (b) Butanol-picoline-water (1:1:0.8 V/V); picoline was collected between b. p. 120~155° of pyridine base. Developing temperature was 5~10°. (c) Butanol-propanol-water (1:1.1:1 V/V). Temperature was about 25°. (d) Butanol-1.5*N* aqueous ammonia (5:1 V/V). Temperature was about 28°.

* Summarized results were given.

§ KCl and $CaCl_2$ in aqueous solutions gave R_F values of 0.22 and 0.23 respectively, while $CuCl_2$ and HCl those of about 0.38 and 0.40 respectively, forming presumably salts with picoline.

able to resolve the halides.[3] It was also found that, with the same solvent, an elevation of temperature caused a tendency of decreasing in R_F values, while a dilution of the solution caused a tendency of increasing in R_F.

Application of 0.005 cc. of 0.1 *M* solution proved most adequate, yet the spot could be detected even with 0.01 *M* solution.

An aqueous solution of the chloride of potassium or calcium was also developed with the same solvent and was found to show the same R_F value for the chloride. That of cupric chloride or hydrogen chloride, in contrast, gave somewhat greater value in R_F, where the halides seemed to move forming salts with picoline (see the foot-note marked with § in the table).

The butanol-propanol system proved also useful as a solvent, although differences among R_F values of the chloride, bromide, and iodide became somewhat smaller, whereas butanol-ammonia gave too small R_F values for all halides and only too small differences among them to distinguish spots clearly. Only in the case of iodide, which often appears as a partly diffused spot on a butanol-picoline chromatogram, development with either one of the other two solvents, if necessary, will be useful.

Influence of alkali on the chromatogram.—As the decomposition solution of organic halogenocompound is alkaline, the influence of alkali on the chromatogram was examined using 0.1 *M* solutions of halides in 0.5~3.0 *N* sodium hydroxide. As shown in the table, an aqueous caustic soda was found to decrease slightly the R_F values of halides with an increase in its concentration. It may, however, be considered that no such remarkable effect as to disturb identification of halides was seen in practice on the R_F values or on the shapes of the spots, so far the concentration of alkali lower than *ca.* 1.5 *N* was used.

Chromatograms of the decomposition solutions of organic substances containing halogens.—According to the directions given before for the decomposition of organic substances, just an alkaline solution of 1~1.5 *N* concentration should be prepared, in which practically no influence on the spots of halides could be observed as described above.

R_F values with butanol-picoline of halides of such solutions obtained from various organic halogenocompounds used alone or in some admixtures, either containing nitrogen and sulfur in addition to halogen or not, were always in good agreement respectively with those obtained in control experiments (see the table), shapes of the spots being also unaffeted. Halogen of organic compound containing one atom at least per molecular weight 1,000 is to be successfully identified by this procedure, taking into account the limit of detection observed before with control test.

When the solution to be tested, if necessary, is applied by the side of or mixed with an authentic specimen of sodium halide in question and developed, the resulting figure will add a more reliable fact. Separation and identification of halogens in organic compounds were thus found satisfactory.

The present method of analysis seems to be applied also to the solution obtained microtechnically by decomposing organic halogenocompound on heating with the mixture of magnesium and anhydrous potassium carbonate (Foulke-Schneider method[4]). But no solvent could yet be found applicable for the solution obtained by the Carius method of decomposition with fuming nitric acid.

Chromatograms of sulfide and rhodanate.—In the case of an organic substance containing nitrogen or sulfur, or both together, there may be produced cyanide or sulfide, or both and sometimes rhodanate in the decomposition solution with sodium. Accordingly, specimens of such salts were also developed.

When revealed in the usual way except washing with water instead of with dilute nitric acid, sodium cyanide showed only a very faint spot near the original point with every solvent used in the experiment. Sodium sulfide gave a spot of low R_F value as shown in the table merely by spraying with aqueous silver nitrate. By the usual method of revelation, on the contrary, potassium rhodanate alone or even in admixture with halides showed a spot located always above that of iodide in case of every solvent, as shown in the last column of the table. In fact, on dealing with the solution from an organic compound containing (besides halogens) both nitrogen and sulfur, such a spot often appeared just at the point accounted above.

It was thus confirmed that these salts gave influence neither upon R_F values nor on shapes of halides existed together.

Summary

Paper chromatograms of sodium halides such

(3) It appears that each halide moves mainly in a form of the salt as it was. When developed with butanol-picoline, especially when halides dissolved in water were used, a faint ghost was always found just above each spot of halides, and seemed likely to consist of a salt of picoline with halide ion partly separated.

(4) G. Foulke and F. Schneider, *Ind. Eng. Chem., Anal. Ed.*, **10**, 102 (1938).

as chloride, bromide, and iodide, dissolved in water or in aqueous caustic soda of various concentrations, were studied with butanol-picoline, butanol-propanol, or butanol-ammonia as a developing solvent, in order to identify such halides accurately by their RF values on chromatograms, and further to apply the result for the identification of halogens contained in organic substances.

The spots of halides after development were revealed by their brown coloration of silver sulfide formed through silver halides. Iodide was better identified by means of a characteristic starch method.

It was found that butanol-picoline was a suitable solvent to separate spots of the three halides completely, and that these suffered little influence on RF value or on shape by caustic soda contained in solutions so far as its concentration was within *ca.* 1.5 *N*. Sodium cyanide and sulfide, and potassium rhodanate were also chromatographed and it was found that they were located quite separately from halides and did not disturb the identification of the latter.

On chromatographing a few drops of the decomposition solution with sodium (the alkaline concentration being within the limit quoted above) of various organic substances, which, in addition to halogen, may sometimes contain either nitrogen or sulfur, or both together, halogens contained in them were identified quite satisfactorily based on the results obtained above.

The authors wish to express their hearty thanks to the Ministry of Education for the Scientific Research Grant given for this work.

Institute of Science and Technology,
Tokyo University, Komaba-machi,
Meguro-ku, Tokyo

Estrogenic Action and Molecular Structure

By Michinori ŌKI and Yoshiyuki URUSHIBARA

(Received November 20, 1951)

This paper presents a hypothesis regarding an optimum molecular thickness as a structural requirement for the development of a strong estrogenic activity.

The preparation of various estrogenic oxygen and sulfur analogs of hexestrol or its dimethyl ether, reported from this laboratory,[1],[2],[3] has demonstrated that the similarity in the structural features, consisting of the shapes of molecular skeletons and the nature and the positions of functional groups, may cause similar physiological properties. It was shown by X-ray crystallography[4] that the stereochemical arrangement of the atoms in hexestrol is very closely related to the stereochemical form of the natural estrogens. On the other hand, diethylstilbestrol would possess a planar structure, significantly thinner than those of hexestrol and natural estrogens, if its two ethyl groups did not exert a steric interference upon the benzene nuclei and thus the whole system were completely conjugated.

F. W. Schueler[5] suggested that a given substance may be estrogenic if it consists of a rather large, rigid, and inert molecular structure with two active hydrogen bond-forming groups located at an optimum distance of 8.55 A. from one another. E. R. Clark[6] modified Schueler's hypothesis by introducing the conception of "anchoring" in order to explain the estrogenic activity of non-rigid molecules. There are, however, many substances which have little activity even though they apparently satisfy Schueler's requirements, as exemplified by 4, 4'-dihydroxystilbene and 4, 4'-dihydroxy-2, 2'-diethylstilbene. Schueler seems to find an example to meet his hypothesis in *trans-p, p'*-dihydroxyazobenzene which is said to show definite estrogenic activity in dosages of from 10 to 15 mg. when injected subcutaneously in.

(1) Yoshiyuki Urushibara and Michinori Ōki, this Bulletin, **23**, 35 (1950).
(2) Y. Urushibara and Takeyoshi Takahashi, *ibid.*, **23**, 53 (1950).
(3) Y. Urushibara, M. Ōki, and Reiji Ikeda, *ibid.*, **25**, 66 (1952).
(4) C. H. Carlisle and D. Crowfoot, *J. Chem. Soc.*, **1941**, 6.
(5) F. W. Schueler, *Science*, **103**, 221 (1946).
(6) E. R. Clark, *J. Chem. Soc.*, **1950**, 3397.

rats. But it should be considered that this substance is rather weak in spite of its fulfilment of the requirements, because Schueler gives examples of substances more active but not meeting his requirements.

The present authors measured the absorption spectra and the extinction coefficients of 4,4′-dimethoxystilbene, $CH_3OC_6H_4CH=CHC_6H_4OCH_3$, and its α,α'-dialkyl homologs. They are shown in the accompanying figure with the absorption curve of *p*-cresol methyl ether. The unsubstituted dimethoxystilbene shows a maximum at the longest wave length with the greatest molecular extinction coefficient. The dimethyl homolog gives a maximum at a shorter wave length and a smaller molecular extinction coefficient, and, as a larger alkyl group is substituted, the absorption curve is displaced further toward a shorter wave length and a smaller molecular extinction coefficient, until, presumably, that of *p*-cresol methyl ether is reached at the extremity.

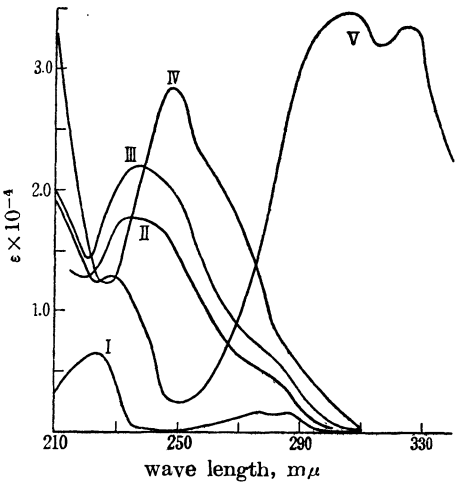

Fig. 1.—Ultraviolet absorption spectra of *p*-cresol methyl ether (I), 4,4′-dimethoxy-α,α'-dipropylstilbene (II), 4,4′-dimethoxy-$\alpha.\alpha'$-diethylstilbene (diethylstilbestrol dimethyl ether)(III), 4,4′-dimethoxy-α,α'-dimethylstilbene (IV), and 4,4′-dimethoxystilbene (V) in 95% ethanol.

The displacement of the absorption curves from that of unsubstituted dimethoxystilbene can be interpreted as showing the extent of decrease in the degree of conjugation, which in turn can be attributed to a deviation of the benzene nuclei from the coplanar structure due to a rotation about the 1,4- and 1′,4′-axes enforced by the steric interference of the alkyl groups at the α,α'-positions. Then, it will be proved that diethylstilbestrol does not possess a planar structure, and it is natural to suppose that it will possess an optimum molecular thickness (the dimension perpendicular to the plane of the ordinary projection formula) as the most potent member of its series. Since steric interference is mutual, the two ethyl groups may not be able to rotate freely or independently of the benzene nuclei. Thus, the ethyl groups will be arranged in a manner coördinated with the rotated benzene nuclei, and it can be said that the ethyl groups impart the most appropriate structural features to the molecule of diethylstilbestrol by their own bulks on one hand, and, on the other, by exerting a steric interference on the benzene nuclei to cause their deviation from a coplanar conjugation.

It must be noticed that the molecular thickness is of course correlated with the width for a given structural formula and the width may possibly have no less importance on the physiological properties, but the thickness is mentioned here to express explicitly the significance of the definite deviation from a planar structure and to put a primary stress on the nature of the flatness of the molecule, because the natural estrogens and consequently hexestrol are known to possess rather flat structures.

Examination of scale models also reveals that diethylstilbestrol is sterically hindered while the 2,2′-diethyl isomeride is not hindered. There exists no steric interference in 4,4′-dihydroxystilbene as is shown by the absorption spectrum of its dimethyl ether and also in *trans*-*p*,*p*′-dihydroxyazobenzene as is understood from its constitution. The small activity of these substances capable of taking the most conjugated planar structures can be explained by considering that their structures are too thin to develop a strong activity although they are favored with the location of the two hydrogen bond-forming groups at the optimum distance.

In a previous paper[3] the authors and R. Ikeda described the synthesis of 1,2-bis-(*p*-methoxyphenyl)-1,2-bis-(methylthio)-ethylene, $CH_3OC_6H_4C(SCH_3)=C(SCH_3)C_6H_4OCH_3$, which was active in the dosage of 10γ in mice. It gave an absorption spectrum indicating that the steric interference of the methylthio groups corresponds nearly to that of the propyl groups in 4,4′-dimethoxy-α,α'-dipropylstilbene.

In this connection, it may be pointed out that it is dangerous to attempt a determination of *cis*- and *trans*-forms of stilbene derivatives from absorption spectra.[7]

(7) D. H. Hey and O. C. Musgrave, *J. Chem. Soc.*, **1949**, 3156.

Experimental Part

The absorption spectra were recorded with a Beckman Model DU photoelectric quarz spectrophotometer. The length of solutions was 5 mm. The concentrations of the solutions are shown below: *p*-Cresol methyl ether (b. p. 176°) 17.75×10^{-5} mol./l.
4,4'-Dimethoxystilbene (m. p. 212—213°) 5.25 〃
4,4'-Dimethoxy-α,α'-dimethylstilbene (m. p. 140.5—142°) 5.26 〃
4,4'-Dimethoxy-α,α'-diethylstilbene (Diethylstilbestrol dimethyl ether) (m. p. 121.5—123°) 2.80 〃
4,4'-Dimethoxy-$\alpha.\alpha'$-dipropylstilbene (m. p. 111—113°) 6.45 〃

4,4'-Dimethoxystilbene, $CH_3OC_6H_4CH=CH-C_6H_4OCH_3$. Prepared by the methylation of 4,4'-dihydroxystilbene.

4,4'-Dimethoxy-α,α'-diethylstilbene (Diethylstilbestrol dimethyl ether), $CH_3OC_6H_4C(C_2H_5)=C(C_2H_5)C_6H_4OCH_3$. Synthesized by the method of Vargha and Kovács.[8]

***p*-Methoxyacetophenone-hydrazone,** $CH_3OC_6H_4-C(CH_3)=NNH_2$. *p*-Methoxyacetophenone (5.0 g.), prepared from anisole and acetic anhydride,[9] and 72% hydrazine hydrate (3.3 g.) were dissolved in warm alcohol (5 cc.) and the solution was heated on a water bath for 5 hours. After cooling, the formed crystalline product was collected and recrystallized from alcohol. Colorless needles (Yield 5.0 g.), m. p. 118.5—120°. Found: N, 17.03%. Calculated for $C_9H_{12}ON_2$: N, 17.06%.

4,4'-Dimethoxy-α,α'-dimethylstilbene, $CH_3-OC_6H_4C(CH_3)=C(CH_3)C_6H_4OCH_3$. The above hydrazone (4.0 g.) and yellow mercuric oxide (8.0 g.) suspended in petroleum ether (b. p. 40—60°) (100 cc.) were shaken at 23—24° for 16 hours. The resulting red solution was filtered and sulfur dioxide was passed vigorously into the solution under cooling, until the color disappeared and instantly bubbles were generated. Petroleum ether was evaporated and the residue was heated to 150° to complete decomposition. The substance, dissolved in benzene, was adsorbed chromatographically on alumina and recrystallized from alcohol. Colorless plates (Yield 0.6 g.), m. p. 140.5—142°. Found: C, 80.45; H, 7.59%. Calculated for $C_{16}H_{20}O_2$: C, 80.56; H, 7.51%. Dodds *et al.*[10] give m. p. 127—128°.

4,4'-Dimethoxy-α,α'-dipropylstilbene, $CH_3O-C_6H_4C(C_3H_7)=C(C_3H_7)C_6H_4OCH_3$. *p*-Methoxybutyrophenone, prepared from anisole and butyryl chloride,[11] gave a difficultly crystallizable hydrazone. The crude hydrazone (5 g.) and yellow mercuric oxide (10 g.) were treated in the same way as described above. Recrystallized from alcohol, the product was obtained in colorless rhombic prisms (Yield 0.3 g.), m. p. 111—113°. Found: C, 81.77; H, 8.90%. Calculated for $C_{22}H_{28}O_2$: C, 81.44; H, 8.70%. The minimum active dose in mice was found 100 γ. Dodds *et al.*[10] give a boiling point 178—181°/0.8 mm. but no melting point. They record a minimum active dose of 100 γ in rats for the corresponding free phenol.

The authors thank the Ministry of Education for the Grant in Aid for Fundamental Scientific Research.

Department of Chemistry, Faculty of Science, Tokyo University, Tokyo

(8) F. L. Vargha and E. Kovács, *Ber.*, **75**, 794 (1942).
(9) J. B. Conant and C. R. Kinnet, "Org. Syntheses" Coll. Vol., I, p. 105.
(10) E. C. Dodds, L. Golberg, W. Lawson, and R. Robinson, *Proc. Roy. Soc.*, B, **127**, 140 (1939).
(11) P. M. Baranger, *Bull. soc. chim. France*, [4], **49**, 1214 (1931).

Estrogenic Thio-Analogs of the Dimethyl Ethers of Diethylstilbestrol, its Homologs, and Hexestrol

By Michinori ŌKI

(Received December 10, 1951)

The author and Y. Urushibara[1] have presented a hypothesis postulating that it is essential for a highly estrogenic substance to possess not only two groups carrying active hydrogen atoms, located at the optimum distance from one another,[2] but also a moderate thickness of the molecule. Estradiol is endowed *a priori* with such favorable structural features and hexestrol shares the fame of strong estrogens with the natural hormone due to its privilege of being a meso form, while diethylstilbestrol, which otherwise would have a planar structure, acquires its molecular thickness qualifying it for an estrogen of the same rank through the steric interference between the benzene rings and the ethyl groups, the former enforced to rotate to a moderate extent and the latter arranged in a coördinated manner. The steric interference and the rotation of the benzene rings caused by it have been deduced from a comparison of the absorption spectra of the dimethyl ethers of diethylstilbestrol and its lower and higher homologs with that of the unsubstituted 4, 4′-dimethoxystilbene on the assumption that the deterioration in the light absorption is associated with the loss in conjugation.

The substitution of the methoxy group or the methylthio group for the ethyl groups in hexestrol and diethylstilbestrol may cause no radical change in the shapes of the molecules. Thus, various oxygen and sulfur analogs in this line have been synthesized and proved to be estrogenic as reported from this laboratory.[3],[4],[5]

The present paper contains the following thio-analogs, derived from dimethyl ethers of diethylstilbestrol, its homologs, and hexestrol, by replacing the phenolic oxygen atoms with sulfur atoms. The methods of preparation of these substances are described in the Experimental Part.

4, 4′-Bis-(methylthio)-α, α'-dimethylstilbene, $CH_3SC_6H_4C(CH_3)=C(CH_3)C_6H_4SCH_3$ (I)

4, 4′-Bis-(methylthio)-α, α'-diethylstilbene, $CH_3SC_6H_4C(C_2H_5)=C(C_2H_5)C_6H_4SCH_3$ (II)

4, 4′-Bis-(methylthio)-α, α'-dipropylstilbene, $CH_3SC_6H_4C(C_3H_7)=C(C_3H_7)C_6H_4SCH_3$ (III)

4-Methoxy-4′-(methylthio)-α, α'-diethylstilbene, $CH_3OC_6H_4C(C_2H_5)=C(C_2H_5)C_6H_4SCH_3$ (IV)

3, 4-Bis-[*p*-(methylthio)-phenyl]-hexane, $CH_3SC_6H_4CH(C_2H_5)CH(C_2H_5)C_6H_4SCH_3$ (V)

The steric arrangements of the groups constituting the molecular skeletons of these compounds are expected to be similar to those of the corresponding dimethoxy compounds, because the skeletons of the members of the present series are constructed in the same manner as those of the corresponding members of the dimethoxy series. The absorption data of the unsaturated members presented in Table 1 show that the steric interference and consequently the rotation of the benzene rings caused by it grow greater as the alkyl groups at the α, α'-positions become larger (I, II and III), although the maxima are displaced in the whole to longer wave lengths than in the dimethoxy series probably due to the influence of the methylthio groups. It is noticed that the absorption spectrum of substance IV, a combination of one half each of the corresponding dimethoxy and dimethylthio compounds, shows two maxima, one being located very close to the maximum (236 mμ) of the dimethoxy compound, namely, diethylstilbestrol dimethyl ether, and the other to that of the

Table 1

Substance	$\lambda_{max.}$ (mμ)	$\varepsilon_{max.} \times 10^{-4}$
I	271	3.1
II	266.5	2.7
III	265	2.5
IV	233	1.2
	263.5	2.0

(1) M. Ōki and Y. Urushibara, this Bulletin, **25**, 109 (1952).
(2) F. W. Schueler, *Science*, **103**, 221 (1946).
(3) Y. Urushibara and M. Ōki, this Bulletin, **23**, 35 (1950).
(4) Y. Urushibara and T. Takahashi, *ibid.*, **23**, 53 (1950).
(5) Y. Urushibara, M. Ōki, and R. Ikeda, *ibid.*, **25**, 66 (1952).

dimethylthio compound (II).

It is expected that the methylthio group, as well as the methoxy group, is demethylated *in vivo*, and thus two hydrogen bond-forming groups required for the development of estrogenic activity become available in these substances, although the distance between them may be a little greater than in the corresponding dihydroxy compounds, and the thiol group to be formed by demethylation may be subject to ready oxidation to a disulfide group *in vivo*. Estrogenic activities were evaluated by the vagina smear test with ovariectomized mice by subcutaneous injection of oil solutions in two portions. Substance I produced estrus in 50% of animals in the dosage of 300 γ. Substance II was fully active in 40 γ. Substance III showed activity, partially incomplete, in all the animals used in the dosage of 200 γ. Here, too, in the dimethylthio series, the medium member with a moderate molecular thickness shows the greatest activity. Substance IV was found very potent, being fully active in all the animals used in the dosage of 5 γ, while diethylstilbestrol dimethyl ether showed a minimum active dose of 2.5 γ by the same test method. Substance V showed an unexpectedly small potency, its minimum active dose being 200 γ. It may possibly be a racemic form instead of a meso form, which is also made probable by its low melting point and high solubility in organic solvents.

Experimental Part

The preparation of 4,4'-Bis-(methylthio)-α,α'-dialkylstilbenes

***p*-(Methylthio)-acetophenone**, $CH_3SC_6H_4COCH_3$. To a mixture of 12.4 g. of thioanisole, prepared from thiophenol and dimethyl sulfate[6] and dissolved in 30 cc. of carbon disulfide, and 20.0 g. of aluminum chloride, 7.9 g. of acetyl chloride was gradually added with thorough cooling and stirring. The mixture was left to stand for 2 hours and then gently boiled for 30 minutes. After being treated with ice and hydrochloric acid (30 cc.), the mixture was extracted with benzene. The benzene solution was washed with 10% aqueous sodium hydroxide and with water, dried over calcium chloride, and distilled. *p*-(Methylthio)-acetophenone distilled over at 154-156°/12 mm. and was recrystallized from petroleum ether. Colorless prisms, m. p. 84°. Yield 10.5 g. (63% of the theory). Found: S, 19.36%. Calculated for $C_9H_{10}OS$: S, 19.29%.

The structure of the ketone was proved by its oxidation to *p*-methanesulfonylbenzoic acid, $CH_3SO_2C_6H_4CO_2H$. Namely, oxidation with potassium bichromate and 50% sulfuric acid gave a substance melting at 268-268.5° and containing S, 16.05%. *p*-Methanesulfonylbenzoic acid melts at 267-268°[7] and requires S, 16.02%.

***p*-(Methylthio)-acetophenone-hydrazone.** A Mixture of 3.5 g. of *p*-(methylthio)-acetophenone dissolved in 5 cc. of hot alcohol and 2.7 g. of 72% hydrazine hydrate was refluxed for 5 hours. The crystalline product was recrystallized from benzene-petroleum ether. *p*-(Methylthio)-acetophenone-hydrazone was obtained in colorless leaflets melting at 96-96.5°. Yield 3.7 g. (97% of the theory). Found: N, 15.53; S, 17.55%. Calculated for $C_9H_{12}N_2S$: N, 15.54; S, 17.79%.

4,4'-Bis-(methylthio)-α,α'-dimethylstilbene (I). A suspension of 4.0 g. of *p*-(methylthio)-acetophenone-hydrazone and 9.0 g. of yellow mercuric oxide in 100 cc. of petrolem ether was shaken for 8 hours at 22-23°. The resulting red solution was filtered from solids and sulfur dioxide was rapidly introduced, when yellowish crystals separated out. The solvent was distilled off, the remainder was dissolved in benzene, and the benzene solution was passed through an aluminum oxide column. From the colorless part of the column, 4,4'-(methylthio)-α,α'-dimethylstilbene was obtained in colorless needles melting at 132.5-133.5° after recrystallization from alcohol. Yield 0.3 g. Found: S, 21.39%. Calculated for $C_{18}H_{20}S_2$: S, 21.35%.

***p*-(Methylthio)-propiophenone**, $CH_3SC_6H_4CO-C_2H_5$. Prepared in the same way as *p*-(methylthio)-acetophenone, using 9.3 g. of propionyl chloride instead of 7.9 g. of acetyl chloride. *p*-(Methylthio)-propiophenone distilled at 167-169°/14 mm. Recrystallized from petroleum ether, it was obtained in colorless prisms melting at 59-60°. Yield 12.2 g. (68% of the theory). Found: S, 17.95%. Calculated for $C_{10}H_{12}OS$: S, 17.79%. The structure was proved by its transformation into *p*-methanesulfonylbenzoic acid.

***p*-(Methylthio)-propiophenone-hydrazone.** Prepared from 3.0 g. of *p*-(methylthio)-propiophenone and 1.0 g. of hydrazine hydrate, and recrystallized from benzene-alcohol. Colorless prisms, m. p. 75.5-76.5°. Yield 3.0 g. (94% of the theory). Found: N, 14.52; S, 16.73%. Calculated for $C_{10}H_{14}N_2S$: N, 14.42; S, 16.50%.

4,4'-Bis-(methylthio)-α,α'-diethylstilbene (II). A suspension of 4.0 g. of *p*-(methylthio)-propiophenone-hydrazone and 8.0 g. of yellow mercuric oxide in 50 cc. of petroleum ether was shaken for 6 hours at 16-18°, and the reaction mixture was treated in a manner similar to the case of 4,4'-bis-(methylthio)-α,α'-dimethylstilbene. A chromatographical separation followed by recrystallization from alcohol gave 4,4'-bis-(methylthio)-α,α'-diethylstilbene in colorless rhombic prisms melting at 132-132.5°. Yield 0.5 g. Found: S, 19.83%. Calculated for $C_{20}H_{24}S_2$: S, 19.52%. The same substance was obtained by catalytic hydrogenation of the reaction products with colloidal

(6) H. Gilman and N. J. Beaber, *J. Am. Chem. Soc.*, **47**, 1449 (1925).

(7) J. Walker, *J. Chem. Soc.*, **1945**, 630.

palladium in acetic acid followed by recrystallization from ethyl acetate.

A direct recrystallization of the products from alcohol gave *p*-(methylthio)-propiophenone-azine, m. p. 139-140°, identified with the specimen described below, and a small yield (0.01 g.) of a compound in prisms melting at 70-73° from the mother liquor. The latter is presumably *cis*-4, 4'-bis-(methylthio)-α, α'-diethylstilbene. Found: S, 19.30%. Calculated for $C_{20}H_{24}S_2$: S, 19.52%.

p-(Methylthio)-butyrophenone, $CH_3SC_6H_4CO\text{-}C_3H_7$. Prepared in the same way as *p*-(methylthio)-acetophenone, 10.7 g. of butyryl chloride being used. *p*-(Methylthio)-butyrophenone distilled at 168.5-171.5°/13 mm. Recrystallization from petroleum ether gave colorless needles melting at 69.5-70.5°. Yield 11.7 g. (61% of the theory). Found: S, 16.80%. Calculated for $C_{11}H_{14}OS$: S, 16.50%. The structure was proved by the formation of *p*-methanesulfonylbenzoic acid on oxidation.

p-(Methylthio)-butyrophenone-hydrazone. Prepared analogously from 9.5 g. of the above ketone and 4.5 g. of 72% hydrazine hydrate in 10 cc. of alcohol. Colorless needles, m. p. 71-72°. Yield 9.0 g. (90% of the theory). Found; N, 13.31; S, 15.35%. Calculated for $C_{11}H_{16}N_2S$: N, 13.45; S, 15.39%.

4, 4'-Bis-(methylthio)-α, α'-dipropylstilbene (III). Synthesized analogously to its lower homologs. Chromatographical separation with alumina and recrystallization from alcohol gave colorless prisms melting at 99-99.5°. Yield 0.2 g. from 4.0 g. of the hydrazone. Found: S, 18.22%. Calculated for $C_{22}H_{28}S_2$: S, 17.99%.

From the mother liquor of recrystallization a small amount of a viscous oil, presumably the *cis*-isomeride, was obtained, but not characterized.

The Preparation of 4-Methoxy-4'-(methylthio)-α, α'-diethylstilbene (IV)

The steps of synthesis are shown below schematically:

$$p\text{-}NO_2C_6H_4CH_2COCl + C_6H_5SCH_3 \rightarrow p\text{-}NO_2C_6H_4CH_2COC_6H_4SCH_3\text{-}p$$

$$\rightarrow p\text{-}NO_2C_6H_4CH(C_2H_5)COC_6H_4SCH_3\text{-}p$$

$$\rightarrow p\text{-}H_2NC_6H_4CH(C_2H_5)COC_6H_4SCH_3\text{-}p$$

$$\rightarrow p\text{-}HOC_6H_4CH(C_2H_5)COC_6H_4SCH_3\text{-}p \text{ (not isolated)}$$

$$\rightarrow p\text{-}CH_3OC_6H_4CH(C_2H_5)COC_6H_4SCH_3\text{-}p$$

$$\rightarrow p\text{-}CH_3OC_6H_4CH(C_2H_5)\text{-}C(C_2H_5)(OH)C_6H_4SCH_3\text{-}p$$

$$\rightarrow p\text{-}CH_3OC_6H_4C(C_2H_5)=C(C_2H_5)C_6H_4SCH_3\text{-}p$$

p-Nitrobenzyl-p-(methylthio)-phenyl-ketone, $NO_2C_6H_4CH_2COC_6H_4SCH_3$. To a solution of 6.2 g. of thioanisole in 50 cc. of carbon disulfide 15.0 g. of aluminum chloride was added. *p*-Nitrophenylacetyl chloride, prepared from 10.0 g. of *p*-nitrophenylacetic acid and 11.6 g. of phosphorus pentachloride,[6] was dropped into the mixture while the solvent was gently boiled. The mixture was boiled further 30 minutes to complete the reaction. The upper carbon disulfide layer was decanted off and the greenish-black viscous addition compound was decomposed with ice and hydrochloric acid (30 cc.). The yellowish fine granular product was collected, and washed well with water. (Sodium hydroxide cannot be used to remove aluminum compounds because the ketone is soluble in caustic alkali in purple color.) Recrystallization from acetone gave pale yellow crystals melting at 183-185°. Yield 12.2 g. (85% of the theory). Found: N, 4.73; S, 11.40%. Calculated for $C_{15}H_{13}O_3NS$: N, 4.88; S, 11.16%.

1-(p-Nitrophenyl)-propyl-p-(methylthio)-phenyl-ketone, $NO_2C_6H_4CH(C_2H_5)COC_6H_4SCH_3$. The above ketone (25 g.) was added in small portions to a hot solution of 1.2 g. of metallic sodium in 50 cc. of absolute alcohol, when an intensive violet color resulted. The mixture was heated on a water bath for 15 minutes, cooled slightly, mixed with 8.0 g. of ethyl iodide, and heated again for 2 hours. When the violet color almost disappeared, an alcoholic solution containing 0.6 g. of sodium ethoxide and then 2.0 g. of ethyl iodide were added. The mixture was further refluxed until the violet color completely disappeared (about 2 hours). The resulting light-brownish solution with crystals of sodium iodide in it was poured into 100 cc. of water. Alcohol was evaporated off under a reduced pressure and the remainder was extracted with ether. The ethereal solution was washed with aqueous sodium thiosulfate and then with water, and evaporated. The residue was distilled under a reduced pressure. A viscous orange oil distilled at 202-205°/0.02mm. Yield 11.0 g. (70% of the theory). On standing for a long time it solidified and was recrystallized from alcohol. Pale yellow needles, m. p. 64-65°. Found: N, 4.63; S, 10.06%. Calculated for $C_{17}H_{17}O_3NS$: N, 4.44; S, 10.17%.

1-(p-Aminophenyl)-propyl-p-(methylthio)-phenyl-ketone, $H_2NC_6H_4CH(C_2H_5)COC_6H_4SCH_3$. To a solution of 15.8 g. of the above ketone in 100 cc. of hot alcohol, 22.5 g. of granulated tin was added and 65 cc. of concentrated hydrochloric acid was gradually added in small portions. The mixture was refluxed until no violet coloration occurred on addition of a small portion to alcoholic sodium hydroxide (about 1.5 hours). On pouring the reaction mixture into 100 cc. of water a complex product separated out in a viscous brown oil soluble with difficulty even in hot water. After evaporation of alcohol *in vacuo*, the oily addition product and the upper hydrochloric acid layer were poured together into an excess of hot aqueous 10% sodium hydroxide, and the whole was boiled for a while to complete the decomposition of the addition product. A yellow viscous oil separated out and solidified on cooling. Recrystallized from benzene-petroleum ether,

(8) E. Wedekind, *Ann.*, **378**, 289 (1911).

the amino compound was obtained in colorless prisms melting at 100.5-102.5°. Yield 12.5 g. (81% of the theory). Found: N, 4.86; S, 11.56%. Calculated for $C_{17}H_{19}ONS$: N, 4.91; S, 11.23%.

1-(*p*-Methoxyphenyl)-propyl-*p*-(methylthio)-phenyl-ketone, $CH_3OC_6H_4CH(C_2H_5)COC_6H_4SCH_3$. The above amino compound (7.1 g.) and 20 cc. of 30% sulfuric acid were refluxed to a clear solution (about 15 minutes), which was poured on 100 g. of ice with vigorous stirring. To the resulting pasty mass 1.8 g. of sodium nitrite dissolved in 5 cc. of water was gradually added. After standing for 30 minutes the excessive nitrous acid was decomposed with urea. The diazonium sulfate solution was poured into 100 cc. of boiling 30% sulfuric acid in small portions while the mixture was kept boiling, and the whole was further boiled for a few minutes. A black viscous oil separated out, turning to a resinous mass on cooling. The aqueous layer was decanted off and the remainder was well washed with cold water. The phenol thus obtained could not be purified. The crude substance was dissolved in 25 cc. of 10% aqueous sodium hydroxide. (When 15% sodium hydroxide was used the sodium salt of the phenol could be dissolved in it with difficulty.) To the solution 4.0 g. of dimethyl sulfate was added with occasional shaking. The mixture was heated for 30 minutes on a water bath, then cooled, and extracted with benzene. The benzene extracts were dried over calcium chloride and evaporated. The methoxy compound distilled at 200-205°/0.15 mm. and solidified on cooling. Recrystallization from alcohol gave colorless needles melting at 76.5-78°. Yield 3.3 g. (44% of the theory). Found: S, 10.31%. Calculated for $C_{18}H_{20}O_2S$: S, 10.67%.

1-(*p*-Methoxyphenyl)-propyl-*p*-(methylthio)-phenyl-ethyl-carbinol, $CH_3OC_6H_4CH(C_2H_5)$-$C(C_2H_5)(OH)C_6H_4SCH_3$. A mixture of 3.0 g. of the above ketone dissolved in 10 cc. of warm benzene and a Grignard reagent prepared from 7.8 g. of ethyl iodide, 1.2 g. of magnesium, and 20 cc. of ether, was refluxed for 2 hours. Then the reaction mixture was treated with 50 cc. of 20% aqueous ammonium chloride and 50 g. of ice. The aqueous layer was extracted with benzene, and the combined benzene solution was dried over anhydrous sodium sulfate and evaporated. The residue gave a pale yellow oil distilling at 172-175°/0.14 mm. and boiling at 160-162°/0.10 mm. on redistillation. On standing, the distillate partially solidified and it was pressed on a porous plate. Recrystallization from alcohol gave colorless prisms melting at 75.5-77.5°. Yield 1.5 g. (45% of the theory). Found: S, 9.82%. Calculated for $C_{20}H_{26}O_2S$: S, 9.70%. The oily fraction contained perhaps a stereoisomeride with a lower melting point.

4-Methoxy-4'-(methylthio)-α, α'-diethylstilbene (IV). The above carbinol did not react with acetyl chloride and acetic anhydride.

The carbinol (0.5 g.) was fused with potassium bisulfate at 230-240° for 30 minutes. After cooling, the salt was washed out. On standing, the oily product partially solidified and was pressed on a porous plate. Recrystallization from alcohol gave colorless prisms melting at 107-108°. Yield 0.02 g. (4% of the theory). Found: S, 10.17%. Calculated for $C_{20}H_{24}OS$: S, 10.26%.

The Preparation of 3, 4-Bis-[*p*-(methylthio)-phenyl]-hexane (V)

***p*-(Methylthio)-propiophenone-azine,** $CH_3SC_6H_4$-$C(C_2H_5)=NN=C(C_2H_5)C_6H_4SCH_3$. A mixture of 30 g. of *p*-(methylthio)-propiophenone dissolved in 30 cc. of hot alcohol, 4.5 g. of hydrazine hydrate, and 7 cc. of acetic acid, was heated on a water bath, when suddenly a vigorous reaction took place and orange-colored crystals separated out. After completion of the reaction by heating further for 10 minutes, the reaction mixture was cooled and the crystalline product was collected. On recrystallization from benzene-alcohol the azine was obtained in yellow needles melting at 139.5-140°. Yield almost quantitative. Found: N, 8.16; S, 17.94%. Calculated for $C_{20}H_{24}N_2S_2$: N, 7.86; S, 17.99%.

3, 4-Bis-[*p*-(methylthio)-phenyl]-hexane (V). The above azine (1.0 g.) was suspended in a mixture of 20 cc. of methanol and 3 cc. of acetic acid, 0.1 g. of palladium chloride was added, and the mixture was shaken with hydrogen. Every time when the absorption of hydrogen slowed down, the evolved nitrogen was swept out from the hydrogenating apparatus, until no more hydrogen was absorbed. The solution filtered from the catalyst was diluted with water, when a pale yellow oil separated out and solidified on standing. Recrystallization from alcohol gave colorless plates melting at 62-63°. Yield 0.8 g. Found: S, 19.54%. Calculated for $C_{20}H_{26}S_2$: S, 19.40%.

The hydrogenation of the azine gave directly the ultimate product, and neither tetrahydro- nor dihydro-azine was isolated. It seems that the dihydro-azine is unstable and decomposed immediately to yield the dibenzyl compound and nitrogen.[9]

Ultra-Violet Absorption Spectra

The absorption spectra were recorded with a Beckman Model DU photoelectric quartz spectrophotometer in 95% ethanol solutions. The length of the solutions was 5 mm. Concentrations are given below:

Substance	Concentration
I	2.40×10^{-5} mol/l.
II	2.47
III	2.02
IV	2.76

The author thanks Professor Y. Urushibara for his kind guidance and encouragement.

(9) Cf. H. Bretschneider, A. de Jonge-Bretschneider, and N. Ajtai, *Ber.*, **74**, 571 (1941); *Z.* Földi and G. von Fodor, *ibid.*, **74**, 589 (1941); B. R. Baker, *J. Am. Chem. Soc.*, **65**, 1674 (1943).

Thanks are due also to Mr. F. Ueno of the Teikoku Hormone Manufacturing Co., Ltd., Kawasaki, for the bio-assays and to the Ministry of Education for the Grant in Aid for Fundamental Scientific Research.

Department of Chemistry, Faculty of Science, Tokyo University, Tokyo

The Photopolymerization of Acetylene. On the Formation of Cycloöctatetraene

By Zenichiro KURI and Shoji SHIDA

(Received October 1, 1951)

Introduction

Ultraviolet light of wave lengths shorter than 2537 Å. induces polymerization of gaseous acetylene. A considerable number of investigations have been made on this reaction, concerning the reaction rate[3),(7),(8)] and the reaction mechanism[4),(5),(9),(10)] as well as the reaction products.[1),(2),(4),(6),(10)]

The photopolymerization of acetylene is generally assumed to be propagated by a chain mechanism. Polymer is formed by the successive addition of acetylene molecules to the activated ones. The dimer of the chain polymerization is considered to be vinylacetylene by W. Kemula and S. Mrazek,[4)] while recently B. L. Dunicz[10),(11)] assumes that the dimer consists of cyclobutadiene, which so far has not been found to exist. Dunicz makes this assumption from the following facts; the reaction of mixtures of acetylene and vinylacetylene proceeds in a different way from that of acetylene only, and the cyclobutadiene structure has the considerable stability in its triplet state according to the theory of Wheland.[12)]

From the cyclobutadiene theory of Dunicz, assuming the following reaction,

$$2C_4H_4(\text{Cyclobutadiene}) \rightarrow C_8H_8(\text{Cycloöctatetraene})$$

we expected cycloöctatetraene to form in the process of the photochemical change of acetylene. We investigated it in detail.

Experiments and Results

(1) Photochemical Properties and Analysis of Cycloöctatetraene (abbr. C. O. T.)

Photochemical Change of C. O. T.—It is not known whether C. O. T. changes photochemically or not, under the ultraviolet light. We tested it and found that C. O. T. in the gaseous state made the photochemical change in the irradiation of ultraviolet light. Spectra of irradiated C. O. T. show two new absorption bands, one of which is characteristic for benzene and the other one is of unknown substances. But the irradiation of one minute or

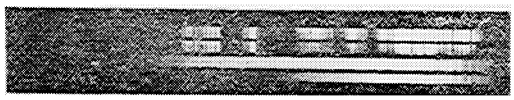

Fig. 1.—Photolysis of C. O. T.: (1) spectrum at the pressure of 0.1 mm. Hg; (2) the same at the lower pressure. (Spectrum of benzene is seen.); (3) and (4) iron spectrum.

(1) D. Berthelot and H. Gaudechon, *Compt. rend.*, **150**, 1169 (1910).
(2) S. Kato, *Bull. Inst. Phys. Chem. Research (Tokyo)* **10**, 343 (1931).
(3) S. C. Lind and R. Livingston, *J. Am. Chem. Soc.*, **54**, 94 (1932).
(4) W. Kemula and S. Mrazek, *Z. Physik. Chem.*, **B23**, 358 (1933).
(5) S. C. Lind and R. Livingston, *J. Am. Chem. Soc.*, **56**, 1550 (1934).
(6) R. Livingston and C. H. Schiflett, *J. Phys. Chem.*, **38**, 377 (1934).
(7) J. C. Jungers and H. S. Taylor, *J. Chem. Phys.*, **3**, 338 (1935).
(8) H. W. Mellville, *Trans. Faraday Soc.*, **32**, 258 (1936).
(9) W. Kemula and B. L. Dunicz, *Z. Phys. Chem.*, **181**, 389 (1938).
(10) B. L. Dunicz, *J. Am. Chem. Soc.*, **63**, 2461 (1941).
(11) B. L. Dunicz, *J. Chem. Phys.*, **12**, 37 (1944).
(12) G. W. Wheland, *Proc. Roy. Soc. (London)*, **A164**, 397 (1938).

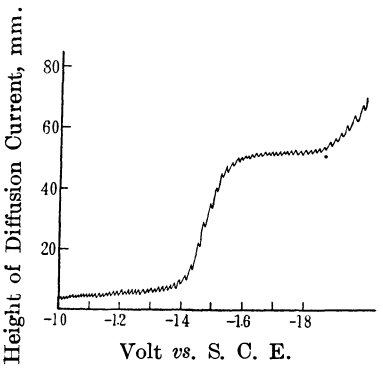

Fig. 2.—Polarogram of 4.6×10^{-4} M solution of C. O. T.: the diffusion current is 4.8 μA and the half wave potential is -1.49 volts *vs.* S. C. E. The sensitivity is 1.2×10^{-7} ampere per mm.

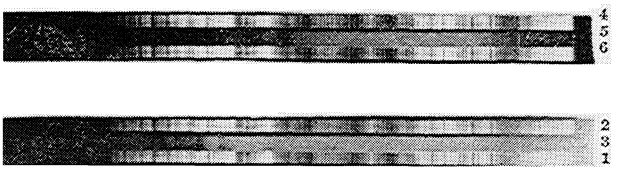

Fig. 3.—Spectra of the products: (5) photopolymerization products at 1.5 mm. Hg; (2) the same products at 0.5 mm. Hg; (1) (3) (4) and (6) iron spectra.

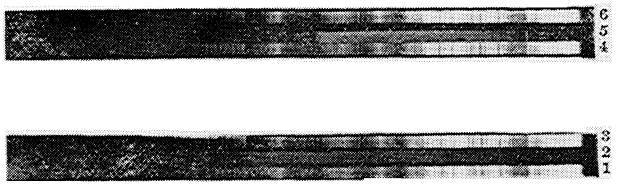

Fig. 4.—Spectra of benzene and styrene: (5) styrene at 0.2 mm. Hg; (2) benzene at 0.1 mm. Hg. (1) (3) (4) and (6) iron spectra.

two does not change the character of absorption spectra of C. O. T. So, in order to get C. O. T., acetylene should be passed in a few seconds under the ultraviolet light, avoiding the photolysis of C. O. T. It is to be found in Fig. 1.

Polarography of C. O. T.—The best way for the quantitative analysis of C. O. T. is the polarographic method.[13] We adopted Elofson's receipt as follows: Ethanol solution of C. O. T. 1 cc., 0.1 M solution of tetramethylammonium bromide 1 cc., sodium sulfite solution 0.1 cc.

The half wave potential was -1.49 volt *vs.* S. C. E. at pH=7. The diffusion current was linear against the concentration of C. O. T. from 1×10^{-5} to 2×10^{-3} M solution. At the sensitivity of 2.4×10^{-3} μA/mm. of the galvanometer, one mm. displacement of the diffusion current corresponds to 2.79×10^{15} molecules of C. O. T. in the cell solution mentioned above. Fig. 2 shows one of the polarograms of C. O. T.

(2) Irradiation of Acetylene in a Continuous Flow

(a) Products of the Reaction.—In order to obtain a larger fraction of the lower polymers, especially smaller than C_8H_8, formed during the reaction, products of irradiation were quickly removed out of the reaction tube to be frozen into the trap cooled by the dry ice at the end of the tube. After passing the dry ice trap, unchanged acetylene was frozen out into another trap cooled by the liquid air.

After the experiment, the thin yellow film was visible at the wall right in front of the light source mercury lamp and a light yellow volatile liquid stayed in the dry ice trap.

Fig. 3 gives the absorption spectra of the products at the pressures of 0.5 and 1.5 mm. Hg respectively. Spectra of pure benzene and pure styrene are given in Fig. 4. Besides benzene, we see a small amount of styrene in the spectral lines characterized by 2877, 2800, and 2780 Å. 2808, 2720, and 2687 Å. lines belong to the unknown substance which is called "c" group and is expected to correspond to acetylene-1-cyclobutene-1 by Dunicz.

C. O. T. was analysed by polarographic method dissolving the products in the cell solution of Elofson's receipt. We found a small but definite quantity of C. O. T., as was expected.

(b) The Rate of Formation of C. O. T. under the Varied Light Intensity.—Acetylene was made to flow continuously through the reaction tube irradiated with the mercury lamp at the space velocity of 2 cm./sec. and at the pressure of 175 mm. Hg for 180 minutes in each experiment. The total gas volume which flowed was 1.45×10^5 cc. and the passing time under mercury light was 5 sec. Light intensity of mercury lamp was varied by the electric current intensity from 3 to 10.4 amp. and was proportional to the current intensity. The weaker light intensity was obtained by the net screening.

The result is shown in Fig. 5. The amount of C. O. T. in 180 minutes, H, expressed in mm. of diffusion current of the polarograph at the sensitivity mentioned, is plotted against the abscissa i, the current intensity of mercury lamp. The maximum point was obtained at $i=3.5$ amp. Under the higher intensity of light, the amount of C. O. T. had decreased unexpectedly.

(13) R. M. Elofson, *Anal. Chem.*, **21**, 917 (1949).

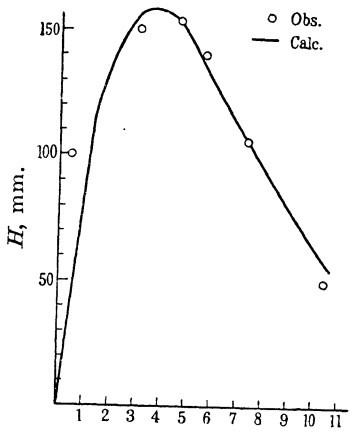

Fig. 5.—Rate of formation of C. O. T. *vs.* intensity of light.

A small percent of air added, quite obstructed the formation of C. O. T. perhaps by the oxydation. The use of a glass filter which is transparent 50% at 2600 Å., decreased the amount of C. O. T. but this was natural.

(c) The Rate of Formation of C. O. T. under the Varied Pressure of Acetylene. —Acetylene gas was made to flow in just the same way as in (2)-b, but the pressure was varied while the light intensity was maintained constant at 4.6 amp. Fig. 6 shows the results.

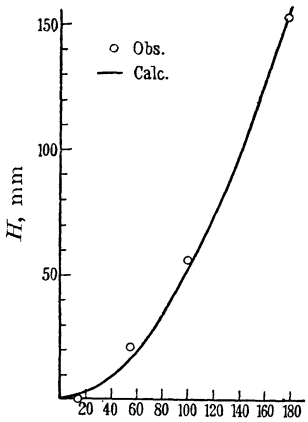

Fig. 6.—Rate of formation of C. O. T. *vs.* acetylene pressure.

The higher the pressure, the greater the rate of formation of C. O. T. However it is not linear to the pressure of acetylene but rather of somewhat higher exponents.

Experimental Details

Acetylene gas was purified by the normal method. The whole arrangement for the experiment is shown in Fig. 7. Purified acetylene is led through A into the liquid air freezing trap B, where the solidified acetylene is rid of the non-condensable gas through L and is fractionated into the reservoir C. From the reservoir, pure acetylene goes through a quartz reaction tube irradiated with mercury lamp E, passing the dry ice cooled trap F into the liquid air trap B. Pressure of acetylene in the tube is read by Bourdon gauge J or mercury manometer K. Reaction products caught in the trap F are evaporated into the reaction tube D, after evacuating the unchanged acetylene. The spectrographic system consists of a hydrogen lamp G, the reaction tube equipped with quartz windows on both ends, and a spectrograph H. An iron spark was used for the standard spectrum.

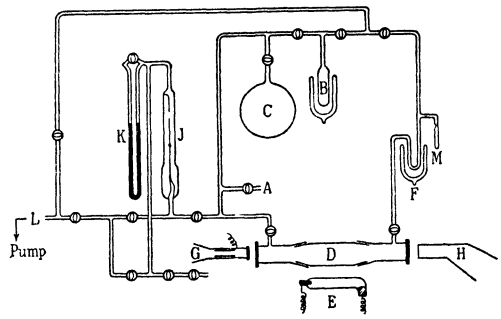

Fig. 7.

For the analysis of C. O. T., products in the trap F were directly distilled into a tiny ampoule M using the dry ice bath, and then the ampoule was cut at the top. Its contents were dissolved in ethanol-tetramethylammonium bromide solution which was submitted to polarographic analysis.

After each experiment, the reaction tube was heated in the air until the sediment on the wall had been removed.

Discussions of the Experimental Results

Now we have been able to find C. O. T. as one of the reaction products. Although straight chain dimers such as vinylacetylene can be an intermediate product, we can well expect on the basis of molecular structure that the steric factors for the formation of C. O. T. from such dimers are much smaller than that for the recombination of two cyclobutadiene molecules.

Assuming cyclobutadiene as dimeric intermediate, we propose the following reaction steps for the photopolymerization of acetylene, at least under the conditions employed.

$$\begin{matrix} CH \\ \| \\ CH \end{matrix} \quad + \quad h\nu \quad \overset{k_1}{\rightarrow} \quad \begin{matrix} CH^* \\ \| \\ CH \end{matrix} \qquad (1)$$

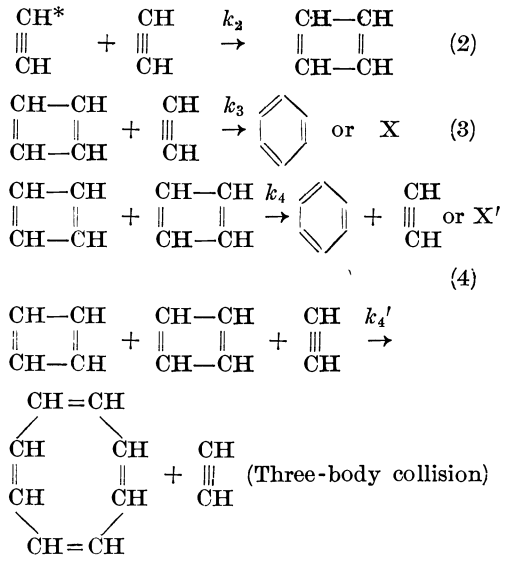

(2)

(3)

(4)

(Three-body collision)

(4)'

For simplicity we will use the abbreviation: acetylene A; cyclobutadiene D; benzene B; C. O. T. C; trimers and tetramers of unknown structures X and X' respectively. Under the condition of rapid flowing, we can ignore steps forming higher polymers than C_8H_8. Then in the stationary state

$$dA^*/dt = k_1 I_{abs} - k_2 A^* A = 0 \quad (5)$$

$$dD/dt = k_2 A^* A - k_3 DA - k_4 D^2 = 0 \quad (6)$$

$$dB/dt = k_3 DA \quad (7)$$

$$2dC/dt = k_4' D^2 A. \quad (8)$$

In Eq. (6) we ignored the consumption of D by (4') compared with that by (3) and (4).

As cyclobutadiene formed is assumed to be in a higher energy (biradical or triplet) state, three-body collision would be necessary to couple one cyclobutadiene molecule with another to form C. O. T., which is a more stable form of C_8H_8. Bimolecular collision, on the contrary, will lead to the formation of either benzene and acetylene or some other substances. Benzene will be mainly formed by (3).

On the Light Intensity Absorbed.— Although we did not measure the absolute value of light intensity, the following considerations may be made on this respect. In Fig. 8, the light of intensity I_0 from the mercury lamp passes through the precipitated film on the wall of the reaction tube, where it diminishes to the intensity I. Then the light, being partially absorbed by acetylene, leaves the vessel with intensity I_t. Thus the light intensity absorbed by acetylene I'_{abs} is $I'_{abs} = I - I_t$. Here we assume that the time-averaged light-absorbing power of the film produced in a definite time of irradiation is proportional to the light intensity I_0, *i. e.*, $I = I_0 e^{-I_0\beta}$, where β is a constant. On the other hand, the light intensity which passes through is represented by $I_t = Ie^{-\varepsilon Ad}$, where ε denotes the absorption coefficient of acetylene, A the concentration of acetylene, d the thickness of acetylene layer. So, $I'_{abs} = I - Ie^{-\varepsilon Ad} \fallingdotseq dI\varepsilon A$. Then the mean value of light absorbed per cm.^{3} across the layer is given by $I_{abs} = I'_{abs}/d = I\varepsilon A = I_0 \varepsilon A e^{-I_0\beta}$. The light intensity of the mercury lamp was found to be proportional to the current intensity i at constant voltage, *i. e.*, $I_0 = iq$, where q is a constant. Therefore

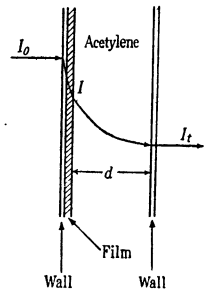

Fig. 8.—Mechanism of light absorption.

$$I_{abs} = \varepsilon A q i e^{-iq\beta} = QAie^{-i\alpha}, \quad (9)$$

where α and Q are constants.

Rate Equation of C. O. T. Formation.— From eqs. (5) and (6) we obtain as the stationary dimer concentration

$$D = [-k_3 A \pm (k_3^2 A^2 + 4k_1 k_4 I_{abs})^{1/2}]/2k_4. \quad (10)$$

Here the negative sign must be omitted. The rate constant k_4' is that for the three-body collision reaction and its collision factor is assumed to be 1/1000 of that for the binary collision of k_4 at the acetylene pressure A of 1 atm. Then

$$dC/dt = 1/2\, k'_4 D^2 A = 1/2000\, k_4 D^2 A, \quad (11)$$

where A is to be expressed in atm. unit and the same, zero or very small, activation energy is assumed for k'_4 and k_4. Inserting eq. (10) into eq. (11), we obtain

$$dC/dt = k_3^2/4k_4 \times 10^3 \cdot A^3[1 - \{1 + (2k_1 A/k^2{}_3 A^2/4k_4) I_{abs}\}^{1/2}] + k_1 A/2 \times 10^3 \cdot I_{abs}. \quad (12)$$

If the amount of C. O. T. produced is represented by H in terms of the height of

polarographic diffusion current, then

$$dC/dt = Hn/Vt \text{ molecules, cc.}^{-1} \text{ sec.,}^{-1}$$

where V is the total gas volume passed at the pressure under the experimental conditions, 1.45×10^5 cc., t the pass-time under irradiation, n sensitivity of polarograph for C. O. T. 2.79×10^{15} molecules mm.$^{-1}$ Using the values of constants given here, it follows

$$dC/dt = 3.84\times10^9 H = n_0 H. \qquad (13)$$

From Eqs. (9), (12) and (13) we obtain finally

$$H = k_3^2A^3/4k_4n_0\times10^3[1-\{1+(2k_1Q/2n_0 \times10^3A^2/k^2{}_3A^3/4k_4n_0\times10^3)ie^{-i\alpha}\}^{1/2}] + k_1QA^2/2n_0\times10^3\cdot ie^{-i\alpha}. \qquad (14)$$

Effect of Light Intensity.—The $H-i$ curve shown in Fig. 5 indicates the apparent effect of the light intensity on the rate of formation of C. O. T. Its true effect may be elucidated by using Eq. (14) as follows. At constant acetylene pressure A_0, putting

$$k^2{}_3A^3{}_0/4k_4n_0\times10^3 = a \qquad (15)$$

and

$$k_1QA^2{}_0/2n_0\times10^3 = K, \qquad (16)$$

we get

$$H = a[1-(1+2K/a\cdot ie^{-i\alpha})^{1/2}] + Kie^{-i\alpha}. \qquad (17)$$

From $dH/di=0$, $i=1/\alpha$ or ∞ follows. Comparing this result with the experimental curve in Fig. 6, we obtain $\alpha=1/3.5$. When this value of α is inserted into Eqs. (15) and (16), the constants a and K can be determined from two equations with different values of i; that is, $a=4$ and $K=151$. As seen in the figure, the theoretical curve obtained from Eq. (17) using these values of a and K is in good agreement with the observed values.

If the steric factors, the collision numbers and the activation energy for the reactions (3) and (4) are denoted by P, Z and E respectively, Eq. (15) can be rewritten in the form

$$a = k^2{}_3A^3{}_0/4k_4n_0\times10^3 = P^2{}_3Z^2{}_3e^{-2E_3/RT}/ 4P_4Z_4e^{-E_4/RT}n_0\times10^3\cdot A^3{}_0. \qquad (18)$$

Assuming[14] that $P_3=P_4=10^{-2}$ and that E_4 for the activation energy of the reaction between the two biradical (triplet) molecules is equal to zero, and using the values $n_0=3.84\times10^9$ molecules cc.$^{-1}$ sec^{-1}. mm.$^{-1}$, $A_0=175/760$ atm., $Z_3=Z_4=8.6\times10^{28}$ and $T=303$°K., we obtain $E=7.8$ Kcal./mol, which is not unreasonable for the activation energy of a propagation process in polymerization reaction.

Combination of Eq. (10) with Eqs. (15) and (16) leads to the expression

$$D = -k_3A/2k_4 + k_3A/2k_4\cdot(1+2K/a\cdot ie^{-i\alpha})^{1/2}. \qquad (19)$$

When $i=4.6$ amp., using the numerical values obtained above, we obtain

$$D = 1.85\times10^{-3} \text{ mm. Hg.}$$

Effect of Acetylene Pressure.—When the acetylene pressure was varied, even if the light intensity of mercury lamp remaining constant, the light intensity absorbed by acetylene was also varied. The light absorbing power of the colored film on the wall might therefore, possibly be changed with the pressure. However, this effect seemed to be relatively small and neglected, because the coloring of the film was observed to depend on the irradiating, not absorbed, intensity of light. Then, if we gather the constants in Eq. (14) as follows,

$$k^2{}_3/4k_4n_0\times10^3 = m \text{ and } k_1Q/2n_0\times10^3 = n,$$

Eq. (9) becomes

$$H = mA^3[1-(1+2n/mA\cdot ie^{-i\alpha})^{1/2}] + nA^2ie^{-i\alpha}. \qquad (20)$$

The numerical values of m and n in the present experimental conditions are

$$m = a/A^3{}_0 = 3.28\times10^2 \text{ and } n = K/A^2{}_0 = 2.85\times10^3.$$

Eq. (20) gives the relation between the amount of C. O. T. produced and the pressure of acetylene A. The calculated values from this equation of H at $i=4.6$ amp. are plotted against A in Fig. 7 and compared with the observed values. The agreement is satisfactory.

Acknowledgements are made to Mr. H. Shimojima of the Laboratory of Chemical Analysis of this Institute for his kind cooperation in carrying polarographic measurements, and to Dr. N. Hagiwara of the Osaka University who gave us a pure sample of C. O. T. We are indebted to the budget of the Ministry of Education for our experiments.

Laboratory of Physical Chemistry,
Tokyo Institute of Technology, Ōokayama, Tokyo

(14) *cf.* M. G. Evance and M. Szwarc, *Trans. Faraday Soc.*, **45**, 940 (1949).

The Structure of Surface-Denatured Protein. IV. The Molecular Weight, Surface Area and Shape of the Surface-Denatured Hemoglobin Molecule

By Kazutomo IMAHORI

(Received November 7, 1951)

In the previous three papers of this series the author has illustrated the apparatuses for measuring surface pressure and surface potential and by using these apparatuses, the molecular weight, surface area and shape of the surface denatured horse serum albumin have been measured.[1] And in the second paper a theory for the determination of the shape of the protein molecule has been developed.[2]

In this paper the structure of hemoglobin molecule is dealt with. As in the case of horse serum albumin, the molecular weight is first determined by H. B. Bull's method. Then the surface area is determined from the compressibility measurement. And finally the shape of the molecule is determined by the surface diffusion experiment.

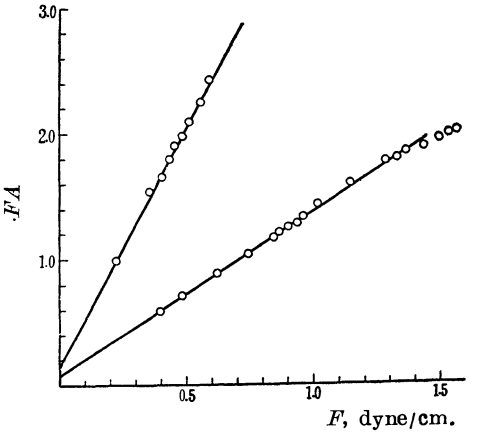

Fig. 1.—FA-F curves at pH=6 and pH=1.8.

Molecular Weight Determination

The method for the determination of molecular weight of surface denatured hemoglobin is just the same as that described in Part I.

Hemoglobin has been purified and crystallized from horse blood by Dr. T. Hosoya of the Institute of Science and Technology, Tokyo University, according to the ethanol method. About 0.2 M KCl solution was used as the substrate, because of the electric measurement purpose. Using the apparatus described in Part I and a thin glass plate, the result was obtained as shown in Fig. 1. The curve of Fig. 1 can be represented by the following equation being obtained by the least squares method:

$$FA=(0.064\pm0.017)+1.32F \qquad (1)$$

Here, F means the surface pressure expressed in dyne/cm. and A means the surface area expressed in m.^{2}/mg. From the equation (10) in Part I, the molecular weight of the surface-denatured hemoglobin is obtained as 35,000$\pm$9,300, which is about a half of that of the native hemoglobin molecule, obtained by sedimentation, diffusion or osmotic pressure measurement.[3],[4] The result is reasonably accounted for by assuming that the hemoglobin molecule splits into two pieces by surface denaturation. This result agrees fairly well with that obtained recently by Michel and Benhamou.[5] Tonomura[6] has calculated the molecular weight of surface denatured hemoglobin to be about 4,000 from the data of Jonix[7] and has concluded that the hemoglobin molecule splits into about sisteen pieces when it is denatured on the surface. However, the measurement of Jonix was carried out under the surface pressure above 1 dyne/cm., and the result obtained by the extrapolation to zero pressure could hardly be expected to be correct. As shown in Fig. 1, the curve deviates from the straight line in the range above 1.5 dyn./cm. Now, if the curve above 1 dyne/cm. is extrapolated to zero pressure the FA value becomes far larger than that of the present experiment.

(1) K. Imahori, This Bulletin, **25**, 7 (1952) hereafter called Part I.
(2) K. Imahori, This Bulletin, **25**, 10 (1952) hereafter called Part II.
(3) N. Gralen, *Biochem J.*, **33**, 1907 (1939).
(4) Svedberg and Pedersen, "Die Ultrazentrifuge," p. 308 (1939).
(5) J. Michael and N. Benhamou, *Compt. rend.*, **228**, 1577 (1949).
(6) Y. Tonomura, *Kagaku*, **19**, 565 (1949).
(7) Jonix, *Biochem. Journ.*, **33**, 1745 (1939).

Guastalla[8] has measured the molecular weight of hemoglobin molecule expanded on the 0.01 *N* HCl solution and obtained the value of 12,000. The present author has measured the molecular weight of hemoglobin expanded on the ammonium sulphate solution of *p*H 1.8. The result is shown in Fig. 1 (curve b). The molecular weight is calculated to be 13,000±2,800. These data may indicate that the molecule splits into four pieces.

Compressibility Measurment

The method for measuring the compressibility of hemoglobin is just the same as that of serum albumin which has been described in Part I.

The modified Wilhelmy Balance is used. Hemoglobin used is from the same sample as is used in the previous experiment. Distilled water containing KCl is used as the substrate. As is shown in Fig. 2, the obtained curve has

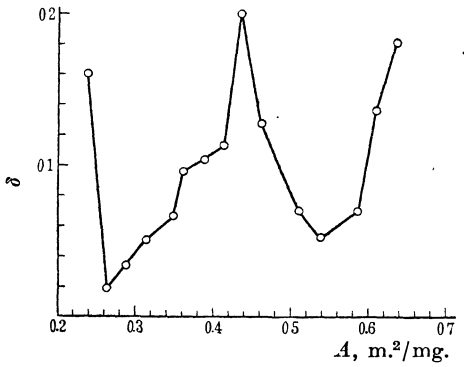

Fig. 2.—Compressibility of hemoglobin Film.

two minima. The one, A_m, is at the surface area of 0.535 m.²/mg. and the other, A_{2m}, is at the surface area of 0.262 m.²/mg. At the first minimum, compressibility, δ_m, is 0.054, and the surface pressure, F_m, is 17.1 dyn./cm., while at the second minimum δ_{2m} is 0.0197, and F_{2m} is 36.6 dyn./cm.

Taking into account that the molecular weight of the surface-dentatured horse hemoglobin is about 35,000 as obtained in the previous experiment, the area per one molecule is estimated te be 3065 Å.² at the first minimum. Davidson and others[9] have reported that horse methemoglobin is like a right-circular cylinder with the diameter of 57 Å. and the height of 34 Å.

The thickness of the hemoglobin film transferred on the metal surface under the surface pressure of about 16 dyn./cm. is measured by the optical method,[10] and found to be about 19 Å. This value is about one half of the height of the methemoglobin molecule described above. The molecular weight of the surface-denatured hemoglobin is about a half of that of the native one. Therefore, it is probable that the horse hemoglobin molecule splits into two pieces and takes the shape just as shown in Fig. 3.

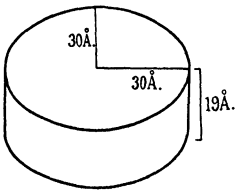

Fig. 3.—The shape of the surface-denatured hemoglobin molecule.

The area of the base of the cylinder-shaped methemoglobin molecule is calculated to be 2560 Å.² from the data by Davidson. On the other hand, even when this cylinder-shaped molecule is packed in one layer compactly on the water surface there is some space around each molecule and the area per one molecule should be about 10% larger than the area of the base of the cylinder, namely, 2816 Å.² per one molecule.

The area at the first minimum is obtained to be 3065 Å.² and this fact shows that the surface-denatured hemoglobin molecule at this point is in the state of closest packing.

If the film were compressed still more it would collapse, or two denatured homoglobin molecules would begin to join into the one original cylinder-shaped molecule. Taking into account that the A_{2m} is about one half of A_m, the film is considered to be doubled at the second minimum. Because, at A_{2m} one molecule covers about 1490 Å.² or two molecules cover about 2980 Å.², which is nearly equal to the above calculated value 2816 Å².

Moreover, δ_{2m} is somewhat smaller than one half of δ_m—the film at δ_{2m} is more than twice as incompressible as that at δ_m.

The Shape of the Surface-Denatured Horse Hemoglobin Molecule

From the result of the previous experiment it is supposed that the surface denatured hemoglobin molecule would have the shape as shown in Fig. 3.

The shape can be determined from the

(8) Guastalla, *Compt.* rend., **208**, 1078 (1939).
(9) J. Bones-Watson, E. Davidson and M. F. Perutz, *Proc. Roy. Soc.*, **191A**, 83 (1947).
(10) K. Imahori and Y. Yoneyama, unpublished.

measurement of the diffusion constant on the surface. The theoretical treatment, on which the present experiment has its foundation, has been dealt with in Part II of this series.

The method for measuring the surface diffusion constant is just the same as that used in the case of serum albumin. Distilled water containing KCl is used as the substrate and castor oil is used as the balancing substances in the present case. The surface pressure is about 0.8 dyne/cm.

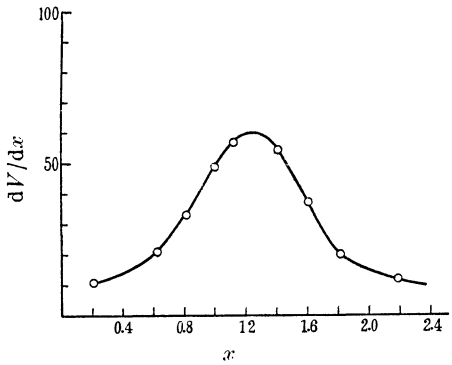

Fig. 4.—Concentration gradients after 7.2 hours of diffusion.

The result is shown in Fig. 4, which shows the gradients of surface potential at various points after 7.2 hours diffusion. In the figure, V means the surface potential expressed in Volt, and x means the distance expressed in cm. From this curve the diffusion constant is calculated, by the inflection point method, to be 2.78×10^{-6} cm.^{2}/sec. Using this value, and also other data such as $V=0.749$[4], $d=$ 19 Å. and $M=35.000$, f/f_0 is calculated from the equation (11) of part II to be 1.003. And thus c/a can be obtained from the Fig. 1 of Part II to be 1.12.

From this result it would seem that the surface-denatured hemoglobin molecule is an almost perfectly circular disk. In conclusion, the hemoglobin molecule is considered to split into two equal disks, the radius and the height of which are calculated to be about 30 Å. and about 19 Å., respectively, when it is denatured on the surface of the distilled water.

Summary

1. The molecular weight of the surface-denatured hemoglobin is calculated from the FA-F curve, to be about 35,000, which shows that the hemoglobin molecule splits into two pieces by surface denaturation at pH $=6$.

2. From the compressibility data, and surface denatured hemglobin molecule is considered to cover about 3065 Å.^{2} of area.

3. The ratio of two axes is obtained by the surface diffusion experiment to be 1.12.

4. The thickness of the molecule is determined to be 19 Å. by the optical method, and the surface-denatured hemoglobin molecule is considered to be a perfectly circular disk, the radius of which is about 30 Å. and the thickness about 19 Å.

The author wishes to express his hearty thanks to Prof. Henry B. Bull, Prof. Bun-ichi Tamamushi, Prof. San-ichiro Mizushima and Dr. Takehiko Shimanouchi for their kind discussions, advice and encouragement. This experiment is aided by the Scientific Research Grant of the Ministry of Education.

Chemical Institute, College of General Education, Tokyo University, Tokyo

On the Viscosity of Solutions of Non-electrolytes[a)]

By Mikio TAMURA, Michio KURATA and Susumu SATA

(Received December 6, 1951)

1. Introduction

The viscosity of solutions composed of liquids (solvent) and solids (solute) can be treated from different standpoints: the first,[2] in which the solvents are regarded as the continuous medium and, then, the equations of Einstein's type based on the hydrodynamics are used; and the second, in which the solutions are regarded as the special case of the liquid mixture. Since the molecular sizes of solvent and of solute are comparable, inasmuch as the ordinary solutions, except polymer solutions, are concerned, it is obvious that the second viewpoint is more excellent than the first. The theory of Kendall and Monroe proposed in 1917 is probably the only treatment based on the second standpoint.[3] They extended their equation,

$$\eta^{1/3}=x_A\eta_A^{1/3}+x_B\eta_B^{1/3}, \qquad (1)$$

(which had been proposed for the viscosity η of the binary liquid mixture) to solutions of non-electrolytes such as benzene solution of naphthalene and calculated the "viscosity coefficient of solute" η_B as a parameter. According to them, η_B is a constant, independent of the concentration. But η_B of the same solute given by them shows different values from solvent to solvent as will be shown in Table 1. This is nothing but the illustration of the defect of Eq. (1), for η_B must be characteristic of the solute and independent of the nature of the solvents according to its definition.

Two of the present authors[4] proposed the following equation to represent the viscosity coefficient of a mixture of two liquids and showed that the equation agrees with the experimental data satisfactorily:

$$\eta=x_Aw_A\frac{d}{d_A}\eta_A+x_Bw_B\frac{d}{d_B}\eta_B+2\left(x_Ax_Bw_Aw_B\frac{d^2}{d_Ad_B}\right)^{1/2}\eta_{AB}, \qquad (2)$$

where x's denote the molar fractions, w's denote the weight fractions, d, d_A and d_B are the densities of the solution, the solvent and the solute respectively. η_{AB} is a parameter called "mutual viscosity coefficient", which has its origin in the mutual interaction between solvent and solute molecules, and is independent of the composition of the solution. In this paper, we applied the equation (2) to the benzene or toluene solutions of naphthalene or diphenyl and obtained reasonable results.

2. Independency of η_B in relation to the Nature of Solvent

We applied at first the equation (2) to the experimental data obtained by Kendall and Monroe.[3] In the case of a mixture of liquids, η_{AB} is the only unknown quantity that must be evaluated. In the present case, not only η_{AB} but also η_B is unknown. and we have two unknown parameters. To evaluate these, we rewrite Eq. (2) as follows:

$$\frac{\eta-(x_Aw_Ad/d_A)\eta_A}{x_Bw_Bd/d_B}=\eta_B+2\left(\frac{x_Aw_Ad/d_A}{x_Bw_Bd/d_B}\right)^{1/2}\eta_{AB}. \qquad (3)$$

If there occurs neither contraction nor expansion on mixing, then w_Ad/d_A etc. can be replaced by the volume fractions, φ_A etc., and we get

$$\frac{\eta-x_A\varphi_A\eta_A}{x_B\varphi_B}=\eta_B+2\left(\frac{x_A\varphi_A}{x_B\varphi_B}\right)^{1/2}\eta_{AB}. \qquad (4)$$

If we plot the value on the left hand side of the equation (4) against $(x_A\varphi_A/x_B\varphi_B)^{1/2}$, a straight line will be obtained so far as our equation is applicable. The results of our calculation give, indeed, straight lines as shown in Fig. 1; thus we can evaluate easily the values of η_B and η_{AB} in the usual way. As shown in Fig. 1, η_B, which is given by the ordinate of the point of intersection of the straight line and the ordinate, is constant, and is independent in relation to the nature of the

(1) Read at the 3rd annul meeting of the Society in April, 1950.
(2) For example, H. L. Bredeé and J. de Booys. *Kolloid Z.*, **91**, 39 (1940).
(3) J. Kendall and K. P. Monroe, *J. Am. Chem. Soc.*, **39**, 1802 (1917).
(4) M. Tamura and M. Kurata, This Bulletin, **25**, 32 (1952).

solvent at a constant temperature. η_B is a kind of viscosity coefficient characteristic of the solute and should be independent of the solvent, as it is in our case, while η_B given by Kendall and Monroe depends upon the nature of the solvent, which is obviously inconsistent with the definition of η_B. The values of η_B and η_{AB} are given in Table 1.

Table 1

η_B and η_{AB} at 25°C. (Comparison of Eq. (2) with the Kendall and Monroe equation)

Solute / Solvent		Naphthalene: Benzene	Naphthalene: Toluene	Diphenyl: Benzene	Diphenyl: Toluene
K.-M. Eq.	η_B	2.25	1.825	3.44	2.82
Eq. (2)	η_B	1.98	1.92	2.87	2.85
	η_{AB}	1.030	0.912	1.197	1.004

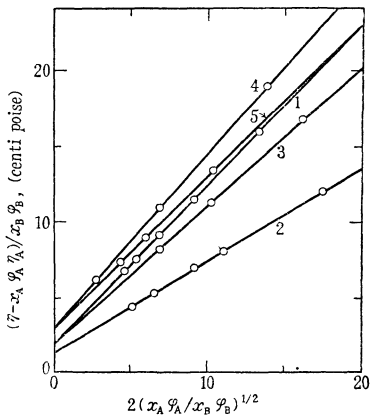

Fig. 1.—Comparison of Eq. (4) with experiments: lines 1, 2, benzene+naphthalene (25° and 60°C.); line 3, toluene+naphthalene (25°C.); line 4, benzene+Diphenyl (25°C.); line 5, toluene+diphenyl (25°C.).

3. Experimental

There are few data concerning the viscosity coefficient of such solutions as are under discussion, especially of solutions of high concentrations and those at various temperatures. So we conducted experiments on the viscosity of benzene solution of naphthalene. Benzene was purified in accordance with the instruction given by Richards and Schipley ("Organic Solvent" (1935)), and had melting point of 5.7°. Naphthalene was purified by sublimating twice in a vacuum and had a melting point of 80.0°.

In order to avoid the change in concentration due to the evaporation of benzene, we used the Ostwald type viscometer modified by Ostwald and Luther.[5] The temperature of the thermostat was regulated to ±0.005°. The measurements of the density and the viscosity were carried out at 25°, 30°, 40°, 50° and 60°. The results are shown in Table 2.

4. Temperature Dependency of η_B

In our calculation we used the equation (3). As for d_B at $t°$, the values calculated by the following equation were used,[6]

Table 2

Experimental Data of d, η and Calculated Values of η

A = Benzene and B = Naphthalene

100 x_B, %		0	2.82	6.90	8.98	13.41	15.87	20.89	25.33
100 w_B, %		0	4.55	10.85	13.93	20.27	23.63	30.23	35.76
25°C.	d	0.8733	0.8787	0.8883	0.8922	0.9009	0.9058	0.9169	0.9239
	η_{obs}	0.6020	0.6309	0.6732	0.6932	0.7423	0.7733	0.8330	0.8891
	η_{calc}		0.6298	0.6734	0.6957	0.7445	0.7730	0.8330	0.8871
	Δ		−0.2	0	+0.4	+0.3	0	0	−0.2
30°C.	d	0.8680	0.8736	0.8827	0.8872	0.8959	0.9007	0.9127	0.9170
	η_{obs}	0.5632	0.5882	0.6269	0.6448	0.6897	0.7181	0.7723	0.8222
	η_{calc}		0.5879	0.6268	0.6470	0.6912	0.7164	0.7723	0.8185
	Δ		−0.1	0	+0.3	+0.2	−0.2	0	−0.5
40°C.	d	0.8563	0.8634	0.8725	0.8771	0.8862	0.8908	0.9017	0.9097
	η_{obs}	0.4932	0.5160	0.5478	0.5665	0.6017	0.6263	0.6698	0.7200
	η_{calc}		0.5155	0.5487	0.5660	0.6041	0.6259	0.6749	0.7154
	Δ		−0.1	+0.2	−0.1	+0.4	−0.1	+0.7	−0.6
50°C.	d	0.8415	0.8529	0.8624	0.8666	0.8755	0.8807	0.8915	0.8992
	η_{obs}	0.4344	0.4564	0.4838	0.4993	0.5290	0.5509	0.5871	0.6319
	η_{calc}		0.4544	0.4824	0.4967	0.5296	0.5489	0.5909	0.6294
	Δ		−0.4	−0.3	−0.5	+0.1	−0.4	+0.6	−0.4
60°C.	d	0.8226	0.8425	0.8516	0.8551	0.8631	0.8705	0.8817	0.8894
	η_{obs}	0.3852	0.4059	0.4294	0.4418	0.4695	0.4925	0.5209	0.5572
	η_{calc}		0.4070	0.4308	0.4425	0.4695	0.4869	0.5211	0.5523
	Δ		+0.2	+0.3	+0.2	0	−1.2	0	−0.9

(5) See, for example, E. Hatschek, "The Viscosity of Liquids (London, 1928)," p. 47.

(6) International Critical Tables, Vol. III, (1928).

Table 3

Values of d_B, η_B and η_{AB} at Various Temperatures

Temp.	d_B	η_B	η_{AB}
25°C.	1.018	1.975	1.026
30	1.014	1.830	0.941
40	1.007	1.587	0.819
50	1.000	1.384	0.715
60	0.993	1.215	0.619

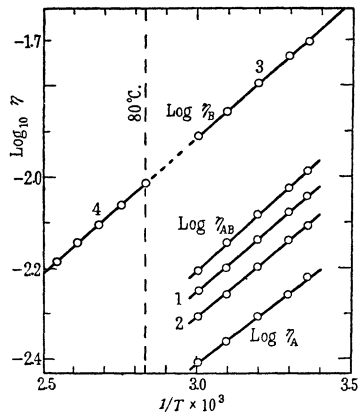

Fig. 2.—Temperature dependence of η of the system, benzene+naphthalene: line 1, $\log\eta$ ($x_B=0.2533$); line 2, $\log\eta$ ($x_B=0.1587$); line 3, $\log\eta_B$ (obtained by Eq. (3)); line 4, $\log\eta_B$ (liquid naphthalene)

$$d_B=0.9779+0.7670\times10^{-3}\times(80-t)-0.755\times10^{-6}\times(80-t)^2. \quad (5)$$

This equation holds for temperature higher than 80° (melting pt.). We extrapolated to lower temperatures to get d_B, for we thought it might be reasonable to use the densities of supercooled liquid naphthalene in our case. The values of d_B are shown in Table 3, with the values of η_B and η_{AB} at various temperatures which are obtained by the method mentioned in **2**. Using these values, we calculated the viscosity coefficient of the solutions. The results are given in Table 2 compared with the observed values. Δ in the table represents $100\times(\eta_{calc}-\eta_{obs})/\eta_{obs}$. The coincidence between the calculated and the observed values is very satisfactory.

Now let us investigate into the relation between η_B and the absolute temperature T. If η_B represents the "viscosity coefficient of naphthalene", it may satisfy the following equation, as is often the case with the viscosity coefficient of pure liquid in general.

$$\log\eta_B=a+(b/T), \quad (6)$$

where a and b are constants. In fact, the equation (6) is satisfied as shown in Fig. 2. (See the straight line No. 3 which lies to the right hand side of the dotted line indicating the melting point of naphthalene.) The straight line No. 4 in Fig. 2 is the plot of $\log\eta_B$ of the liquid naphthalene at temperatures higher than the melting point against $1/T$. Two plots, No 3 and No. 4, lie on a straight line, and this fact suggests an interesting conclusion that η_B, which we evaluated in **2** and in this section, may be none other than the viscosity coefficient of supercooled liquid naphthalene. And this shows that the coincidence between the observed values of η and the calculated values by eq. (2) is not a fictitious result coming from the regulation of the values of two parameters, η_B and η_{AB}.

In the lower part of the right hand side of Fig. 2, we plotted $\log\eta$ at various concentrations, $\log\eta_A$ and $\log\eta_{AB}$ against $1/T$, respectively. These give straight lines, whose slopes give the following activation energies of flow:

$\varepsilon_A=2.50$, $\varepsilon_B=2.74$ and $\varepsilon_{AB}=2.75$ kcal./mole.

Even in such a case as under discussion, where two components are rather similar to each other in construction, ε_{AB} is not always equal to $(\varepsilon_A+\varepsilon_B)/2$, and this fact indicates that the introduction of the term containing η_{AB} is necessary even in the case of apparently ideal solutions.

In conclusion, we wish to expess our thanks to Dr. S. Shida of Tokyo Institute of Technology for his kind and effective help concerning the experimental part, and also to acknowledge our indebtedness to the Ministry of Education for a grant-in-aid.

Department of Industrial Chemistry, Faculty of Engineering, Kyoto University and Physico-chemical Laboratory, Tokyo Institute of Technology

(7) The experimental values of η_B of liquid naphthalene are as follows: 0.97(80°), 0.86(90°), 0.78(100°), 0.71(110°), 0.65(120°), 0.59(130°), 0.54(140°) and 0.49 centipoise (at 150°).

These values have been tabulated in K. Shiba, Tables of Physical Constants (in Japanese, Iwanami, Tokyo, 1947), p. 78.

Spectrochemical Study of Microscopic Crystals. II. Dichroism of Cobalt (III)-Praseo Salts

By Shoichiro YAMADA and Ryutaro TSUCHIDA

(Received December 7, 1951)

The crystal of the hydrochloride of the so-called "praseo-salts", 1, 6-dichloro-bis-(ethylenediamine)-Co(III) hydrochloride dihydrate, shows a striking dichroism. while that of the nitrate exhibits only a little dichroism compared with the former. This seems to be very interesting, being related to the fact that the hydrochloride easily effloresces in the air to lose its hydrogen chloride of crystallization and that the nitrate, stable in the air, is much less soluble than the hydrochloride. No research on these compounds, however, has been made in the crystalline state, nor has the analysis of the crystal structure or absorption spectrum of the crystal ever been reported. Previously, one of the present authors and M. Kobayashi, in the researches on pleochroism of the crystals of the metallic complex salts,(1) and the present authors, in the researches on dichroism of metallic planar complexes,(2),(3) showed that the measurement of pleochroism of the crystals was of great use to studies on the crystal structure and on the state of the complex ions in the crystals.

In this report, we can give the results of the measurement of dichroism with praseo-Co(III)-hydrochloride and nitrate, and discuss the orientations which the complex ions take in these crystals.

Experimental

Materials.—1, 6-$[Co(en)_2Cl_2]Cl \cdot HCl \cdot 2H_2O$(4) was prepared by the method of Werner.(5) The crystals obtained were green tablets on {001} bounded laterally by {110} (Fig. 1). These belong to the monoclinic system and exhibit extinction in the direction of the b- and the a-axis. The crystal shows marked dichroism in the above two directions, *i. e.*, blue by polarized light with electric vector parallel to the a-axis and yellow with a slight tint of green by that parallel to the b-axis. Analysis of the crystal structure has not been performed as yet. In this work dichroism measurement was made with microcrystals by light polarized in the above two directions.

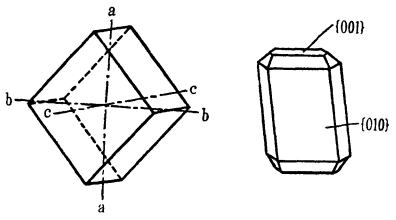

(a) (b)

Fig. 1.—A modification of the crystal usually obtained: (a) praseo-hydrochloride dihydrate, (b) praseo-nitrate.

1, 6-$[Co(en)_2Cl_2]NO_3$ was prepared as green monoclinic crystals by adding concentrated nitric acid to the concentrated aqueous solution of the hydrochloride, acidified with hydrochloric acid. The crystals usually obtained are elongated in the c-direction, bounded by prism faces of {010} and {110} type. Very slight dichroism, as compared with the hydrochloride, can be observed in most faces, and the most distinct dichroism is found in {010}, *i. e.*, green by polarized light with electric vector parallel to the plane formed by the a- and the b-axis and greenish blue by that perpendicular to it. Dichroism measurement was made in that face by polarized light with electric vector in the above two directions. A little less distinct dichroism of a similar nature can be seen in {110}. Dichroism is discerned only slightly in {001} and{100}. The crystal structure has not been determined as yet.

Quantitative Dichroism Measurement. — The microscopic method(1),(6) was applied. The measurements were made with microcrystals of the respective salts by polarized light in the region covering about 7500 Å. to nearly 2000 Å. The crystals used in the measurements were several hundredths of mm. thick. The b- or a-absorption in Fig. 2 for the hydrochloride represents, respectively, absorption by polarized light with electric vector parallel to the b- or a--axis. $/\!/$- or $\perp$-absorption in Fig. 3 for the nitrate represents absorption by polarized light with electric vector parallel or perpendicular to the plane formed by the a-

(1) R. Tsuchida and M. Kobayashi, "The Colours and the Structures of Metallic Compounds," Zoshindo, Osaka Japan (1944), (in Japanese).

(2) R. Tsuchida, S. Yamada and H. Yoneda, *J. Chem. Soc. Japan*, **69**, 145 (1948), (in Japanese).

(3) (a) S. Yamada, *J. Am. Chem. Soc.*, **73**, 1579 (1951); (b) This Bulletin, **24**, 125 (1951).

(4) en represents ethylenediamine molecule.

(5) A. Werner, *Ber.*, **34**, 1733 (1901).

(6) S. Yamada, *J. Am. Chem. Soc.*, **73**, 1182 (1951).

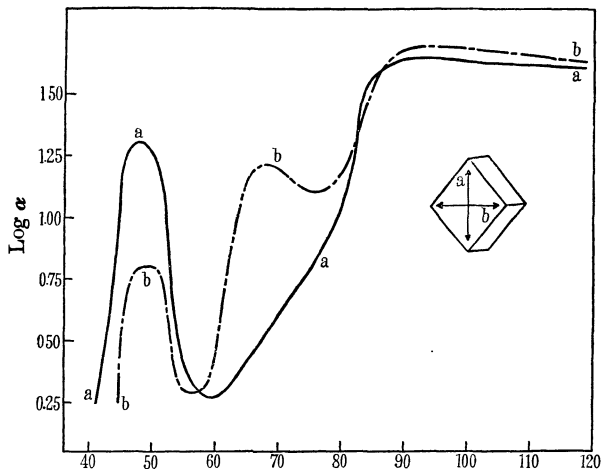

Fig. 2.—Dichroism of 1,6-[$Co(en)_2Cl_2$]Cl·HCl·$2H_2O$.

and the *b*-axis. α denotes absorption coefficient per mm. of the crystal. Results of the measurements are shown in the figures 2 and 3, and summarized in Table 1.

Discussion

The Orientation of the Complex Ions in the Crystal of the Hydrochloride.—As is seen in Fig. 2, *b*- and *a*-absorption of the hydrochloride are quite different from each other. The difference between them is so large, as compared with that for planar complexes with four ligands, which was formerly determined,[6] that it may be inferred that all the complex ions take the same, at least almost the same, disposition in the crystal of this compound, since otherwise the crystal would not exhibit such a large difference between each of the absorptions. In the following, we shall discuss the orientations which the complex ions take in the crystal of the hydrochloride.

As to the first absorption band, a great difference in the extinction coefficient at the absorption maximum is observed between *a*- and *b*-abrorption, which we shall consider below. The transition probability in a certain direction for the first absorption band of a complex ion, which is considered as due to an electronic transition in an unsaturated transition shell,[7] can be, in general, supposed to be influenced most strongly by the ligands in that direction. On the basis of the above assumption the present authors found that there exists what we call "the hyperchromic series of ligands" which represents the decreasing order as to their effects on magnitude of molar extinction coefficient of a complex ion at an absorption maximum of its first absorption band.[8] In case of such a complex ion as 1,6-$[Co(en)_2Cl_2]^+$, it is reasonable to suppose that the effect of ligands on transition probability for the first band in the direction connecting the central Co atom with two Cl atoms is quite different from that in the direction perpendicular to the above, *i.e.*, in the plane containing one Co and four N atoms of two ethylenediamine molecules around the central Co atom. Since ethylenediamine stands much higher in the hyperchromic series than Cl^-, it is supposed that the extinction coefficient of the first band is much larger for the absorption by polarized light with electlic vector in the en-Co-en plane than for that by polarized light with electric vector in the direction of the straight line, Cl-Co-Cl.

Thus, it is presumed that *a*-absorption in Fig. 2 corresponds to the absorption by polarized light with electric vector parallel to the en-Co-en plane, that the *b*-absorption corresponds to that by polarized light with electric vector in the Cl-Co-Cl direction, and, therefore, that in the crystal of the hydrochloride the line connecting Co at the center of a complex ion with two Cl atoms is parallel to the *b*-axis and that the plane containing Co and four N atoms of ethylenediamine molecules around Co is perpendicular to the *b*-axis of the crystal.

As to the second absorption band, a great difference in intensity as well as in the wave length at absorption maximum can be found between *a*- and *b*-absorption. In the same way as for the first band, the effect of ligands on the second absorption band is expected to be different in the en-Co-en plane from that in the direction of the straight line binding one Co and two Cl atoms. As for the order in hypsochromic effects of ligands on the second absorption band of metallic complexes, there have been known "the spectrochemical series,"[7] in which Cl stands much lower than ethylenediamine, meaning that Cl, as a ligand, has much more bathochromic effect on the second band of a complex than en. Therefore, it is suggested that the second absorption band by polarized light with electric vector in the direction of the line, Cl-Co-Cl, lies in the region of a considerably longer wave length than that

(7) R. Tsuchida, This Bulletin, **13**, 388, 436 (1938).

(8) The report dealing with the subject will be submitted later.

perpendicular to the above, and, in consequence that the former corresponds to *b*-absorption and that the latter corresponds to *a*-absorption in Fig. 2.

From the foregoing discussion on the first and the second absorption band, it is inferred that all the complex ions take the same or at least almost the same disposition to the crystal axes in the crystal of the hydrochloride, that the straight line connecting Co and two Cl atoms is parallel to the *b*-axis, and that the plane containing Co and four N atoms of the two ethylenediamine molecules coincides with the plane formed by the *a*- and the *c*-axis.

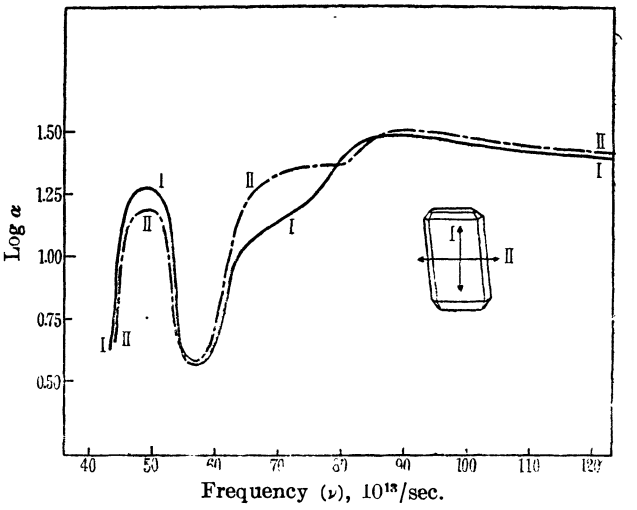

Fig. 3.—Dichroism of 1,6-$[Co(en)_2Cl_2]NO_3$.

Thus it is found that the dichroism of the praseo-hydrochloride in Fig. 2 represents that for the single ion, 1,6-$[Co(en)_2Cl_2]^+$ (Table 1). The dichroism of the single ion, as determined above, is in good accordance with the regularity as to the dichroism for the first and the second band of *trans*-disubstituted complex ions.[9] The fact that the nature of the dichroism for the first absorption band differs considerably from that for the second band suggests that the origins for those bands are different from each other. It was formerly stated[10] that extinction coefficients at absorption maxima of the first and the second band for complexes of some metals had almost equal magnitude, and it has been insisted that this is one of the principal grounds for the hypothesis that the first and the second band originate from similar transitions of electrons of the same kind. It is quite clear, however, that extinction coefficients at the absorption maxima of the first and the second band for the praseo-ion have remarkably different magnitudes in both the absorptions (Table 1) and that the two bands should be attributed to the electronic transitions of different kinds which are not related directly to each other.

Arrangement of the Complex Ions in the Crystal of the Praseo-nitrate and its Comparison with that of the Hydrochloride. —Since the dichroism for the crystal of the nitrate is found to be very slight as compared with that of the single praseo-complex ion, which has been determined from the dichroism measurement with the crystal of the hydrochloride, it must be presumed either that the complex ions in the crystal of the nitrate take considerably different orientations to one another, marked dichroism of single ions compensating for one another to such an extent that only a little dichroism is left in the crystal of the nitrate, or that the complex ions, all of which have the same orientations with refer-

Table 1

Absorption Maxima of Co(III)-Praseo-Ion

	1st Band		2nd Band		3rd Band	
Crystal	ν_{max}	log α_{max}	ν_{max}	log α_{max}	ν_{max}	log α_{max}
Cl-Co-Cl	48.7	0.80	68.0	1.21	flat	1.70
en-Co-en	48.0	1.30	(75)	—	flat	1.65
Solution[a]	ν_{max}	log ε_{max}	ν_{max}	log ε_{max}	ν_{max}	log ε_{max}
	48.0	1.54	66.7	1.41	119.0	4.31
			78.9	1.64		

(a) F. Basolo, *J. Am. Chem. Soc.*, **72**, 4393 (1950). This measurement was made with Methanol-H_2O solution of praseo-chloride.

(9) Detailed report on the subject will be submitted later.

(10) K. Sone, *J. Chem. Soc. Japan*, **71**, 316 (1950), (in Japanese).

ence to the crystal axes, make considerably large angles to all of the three crystal axes so that absorption spectra in respective directions are not so distinctive as in the case of hydrochloride. In the same way as in the case of hydrochloride and on the basis of the results obtained in that case, the orientation of the complex ions in the nitrate can be inferred from observations as to the dichroism in some faces. Thus, by comparing the dichroism in {010} of the crystal of the nitrate with that of the single praseo-ion (Fig. 3), it is presumed that the en-Co-en plane of the praseo-complex ion in the crystal is, on the average, inclined at an angle considerably larger than 45° to the plane formed by the *a*- and the *b*-axis. Similarly, since the crystal does not exhibit distinct dichroism in {001}, showing only a little more greenish tone by polarized light with electric vector parallel to the *b*-axis than by polarized light perpendicular to it, it is supposed that the straight line, Cl-Co-Cl, in the complex ions makes to the *b*-axis an angle a little smaller than 45°, when viewed perpendicularly to the *ba*-plane. It is also suggested by comparing the nature of dichroism in {100} with that of the single complex ion that the straight line, Cl-Co-Cl, is, on the average, inclined to the *b*-axis at an angle only a little less than 45° when viewed perpendicularly to the *bc*-plane.

It seems that the complex ions are not usually arranged more disorderly in the crystal of the nitrate which contains planar nitrate ions than in the crystal of the hydrochloride with spherical chlorine ions instead of planar nitrate ions. Taking into consideration the fact that the crystal of the praseo-hydrochloride undergoes decomposition in the air at room temperature to give away one molecule of hydrogen chloride, it is suggested that the molecule of crystallization, HCl, plays an important part in holding the complex ions together so that all the complex ions take the same or at least almost the same orientation with their en-Co-en planes parallel to the *ac*-plane. This seems to be closely related to the fact that the violeo-salt in solution acidified with hydrochloric acid is readily changed into the praseo-salt and that the hydrochloride has not been found for the violeo-series whereas it is found for the praseo-series.

Summary

The dichroisms of 1,6-$[Co(en)_2Cl_2]Cl \cdot HCl \cdot 2H_2O$ and of 1,6-$[Co(en)_2Cl_2]NO_3$ have been measured by the microscopic method. From consideration of the results, it has been presumed that, in the crystal of the hydrochloride, the line connecting Co with two Cl atoms is almost parallel to the *b*-axis, that the plane containing one Co and four N atoms of two ethylenediamine molecules around Co is almost parallel to the plane formed by the *a*- and the *c*-axis. The nature of absorption bands of metallic complexes has been discussed on the basis of dichroism for the single praseo-ion, which has been determined from the above assumption. Arrangement of the complex ions in the nitrate has been inferred from observations as to the nature of dichroism in several faces. From comparison of the crystal structures of the two compounds and consideration of other properties, it has been suggested that the HCl molecule of crystallization in the crystal of the hydrochloride plays an important part in holding the complex ions together so that all the complex ions take the same orientation.

This investigation was supported in part by a grant from the Ministry of Education.

Department of Chemistry, Faculty of Science, Osaka University, Nakanoshima, Osaka

LETTER

Eine neue Bestimmungsmethode von Ligninsulfosäure in Sulfitzellstoffablauge

von Ryoichi SENJU

(Eingegangen am 11, Januar, 1952)

Um die Bestimmungsmethode von Ligninsulfosäure festzustellen, haben viele Forscher sich bisher vergebens angestrengt, von organischen Aminen ein gutes Fällungsmittel für Ligninsulfosäure zu entdecken. Ich wählte als Fällungsmittel ein neues hochmolekulares Amin (Polyglykolglucosamin), und es ist mir gelungen, die gesamte Ligninsulfosäure in Sulfitablauge damit quantitativ fällen zu lassen. Das Prinzip der Bestimmungsmethode besteht darin, dass man eine bekannte Menge von Polyglykolglucosamin (abgekürtzt P. G. G. A.) gegen das negative Polyvinylalkohol-Schwefelsäureester (abgekürtzt P. V. A. S.) zurückzutitriert.

Zu 5 cc. der zwanzigfach verdünnten Ablauge wird unter Umschütteln 5 cc. von $N/100$ P. G. G. A. (berechnet auf NH_2-Gruppe) zugesetzt. Ein Teil des Niederschlags der Ligninsulfosäure wird durch das überschüssige P. G. G. A. kolloid verteilt. Diese trübe Kolloidlösung wird gegen $N/400$ P. V. A. S. titriert. Sobald die äquivalente Menge von P. V. A. S zugesetzt ist, wird die trübe Lösung augenblicklich klar, und dann der Niederschlag sammelt sich flockig. Der Endpunkt dieser Kolloidtitration kann sehr genau bestimmt werden.

Bei der Titration der stark verdünnten Ablauge ist es vorteilhaft, Toluidinblau, das die stärke "Metachromasie" gibt, als Indikator zu benutzen. Wenn man das Gewicht des Niederschlags bei der Kolloidtitration wägen will, ist es zweckmässig, soviel Menge von Ablauge zu nehmen, wie man damit Niederschlags von 0.1-0.2 g. erhält.

Die Verbindung der negativen Ligninsulfosäure mit dem positiven P. G. G. A. weist ein sauberes stöchiometrisches Verhältnis auf. Daher ergibt sich aus dem Gewicht des ausgefällten Niederschlags die Menge der aus einem Mol NH_2-Gruppe entstehenden Verbindung.

Zieht man von diesem Gewicht das bekannte Äquivalentgewicht des verwendeten P. G. G. A. (C_8 H_{16} O_5 N=206) ab, so erhält man das Äquivalentgewicht der Ligninsulfosäure gegen NH_2-Gruppe (Tabelle 1, Spalte 5). Um die Ligninsulfosäure in Sulfitablauge zu bestimmen, braucht man aber nicht den Niederschlag bei der Kolloidtitration im einzelnen zu wägen, weil das Äquivalentgewicht von Ligninsulfosäure in Ablauge im allgemeinen Konstant(etwa 380) ist. Durch Verbrauch von P. G. G. A. kann man gleich die Menge der Ligninsulfosäure berechnen.

Diese Methode ist besonders darin überlegen, dass man die Bestimmung auf volumetrische Weise sehr genau und schnell ausführen kann. Deshalb ist diese Methode als eine Kontrollmethode für den Sulfitkochprozessverwendbar. Infolge des Mangels an schnellen Bestimmungs methoden von Ligninsulfosäure in Kochsäure sind die chemischen Techniker von Sulfitzellstoff-Fabriken dazu gezwungen, durch die mittelbaren Methoden wie die Bestimmung der Schwefligen Säure, des Farbtones und des spezifischen

Table 1

Die Bestimmung der Ligninsulfosäure in Kochsäure der Kunstseide Sulfit Zellstoff-Fabrik

1	2	3	4	5
Kochzeit in Min.	Verbrauch $N/100$ P. G. G. A. cc./cc. Ablauge	Niederschlag aus 1 cc. Lauge, g.	Ligninsulfosäure-Gehalt, g./cc.	Äquivalentgewicht von Ligninsulfosäure
420	19.13	0.1118	0.0724	378
450	21.40	0.1256	0.0815	381
480	24.27	0.1410	0.0910	375
510	24.66	0.1440	0.0932	379
570	25.00	0.1490	0.0975	394
600	26.38	0.1477	0.0954	376
690	26.05	0.1522	0.0985	378

Gewichtes von Kochsäure den Kochprozess zu kontrollieren. Daher glaube ich, dass diese Methode sowohl von den rein-wissenschaftlichen als auch von den technisch-wissenschaftlichen Forschern freudig angenommen wird.

Institut für Wissenschaft und Industrie
der Universität Kyushu

Atomic Polarization of Aliphatic Alcohols in the Liquid state

By Masasi YASUMI, Michio SHIRAI and San-ichiro MIZUSHIMA

(Received March 15, 1952)

The refractive index n and absorption coefficient k of methyl, ethyl, i-propyl, n-butyl,

Table 1.

	methyl alcohol	ethyl alcohol	*i*-propyl alcohol	*n*-butyl alcohol	*i*-butyl alcohol	*tert*-butyl alcohol
ε_0	31.5	24.3	18.0	16.0	16.0	9.90
ε' (3.24 cm.)	5.55	4.08	3.06	3.08	2.94	2.80
ε''(3.24 cm.)	5.12	2.58	1.18	1.08	1.01	0.85
n_D^2	1.76	1.85	1.89	1.95	1.94	1.92

Table 2.

	methyl alcohol	ethyl alcohol	*i*-propyl alcohol	*n*-butyl alcohol	*i*-butyl alcohol	*tert*-butyl alcohol
ε_∞	4.54	3.76	2.96	2.99	2.86	2.70
P_E	8.2	13.0	17.6	22.1	22.2	22.2
M/d	40.7	58.6	79.6	91.9	92.9	94.8
$\frac{\varepsilon_\infty-1}{\varepsilon_\infty+2}\frac{M}{d}$	22.1	28.7	30.4	36.6	35.5	34.3
P_A	13.9	15.7	12.8	14.5	13.3	12.1

i-butyl, and *tert*-buthyl alcohols have been measured at the wave length of 3.24 cm. and at the temperature of 25°C. by the improved free wave method reported previously.[1] From the values of n and k the dielectric constant ε' and the loss factor ε'' have been calculated through the following equation.

$$\varepsilon'-i\varepsilon''=(n-ik)^2 \qquad (1)$$

The calculated values are shown in Table 1 with the static dielectric constant ε_0 and the square of refractive index n_D^2 for D-line.

If we assume a single relaxation time, we have the following relations irrespective of the dielectric model

$$\varepsilon'=\varepsilon_\infty+\frac{\varepsilon_0-\varepsilon_\infty}{1+\omega^2\tau^2}=\varepsilon_\infty+\frac{\varepsilon_0-\varepsilon_\infty}{1+(\lambda_s/\lambda)^2} \qquad (2)$$

$$\varepsilon''=\frac{\varepsilon_0-\varepsilon_\infty}{1+\omega^2\tau^2}\omega\tau=\frac{\varepsilon_0-\varepsilon_\infty}{1+(\lambda_s/\lambda)^2}(\lambda_s/\lambda) \qquad (3)$$

$$\lambda_s=2\pi c\tau \qquad (4)$$

where τ is the relaxation time corresponding to a critical wave length λ_s (Sprungswellenlänge) and λ, ω, and c have their usual significance. ε_∞ is the value of ε' at high frequencies at which the orientation effect of dipole disappears completely. The values of ε_∞ shown in Table 2 (and those of λ_s) have been chosen as to give the best fit with the experimental data through Fqs. (2), (3) and (4). From ε_∞ we can calculate the values of atomic polarization P_A by the following equation:

$$P_A=\frac{\varepsilon_\infty-1}{\varepsilon_\infty+2}\frac{M}{d}-P_E$$

where M is the molecular weight, d the density, $P_E=\frac{n_D^2-1}{n_D^2+2}\frac{M}{d}$ the electronic polarization for D-line. The vaules of $\frac{\varepsilon_\infty-1}{\varepsilon_\infty+2}\frac{M}{d}$, P_E and P_A are shown in Table 2.

We see that the atomic polarization of each alcohol in the liquid state has almost the same value which is about 14 cc. and is much larger than that in the gaseous state which is estimated as less than 10% of the electronic polarization: *i.e.* less than 2 cc.

The large values of atomic polaization of these alcohols in the liquid state are, therefore, attributable to the structure of the liquid and the approximate constancy of these values may be explained by considering that the hydrogen bond plays the most important part in this problem.

Detailed discussion will be published elsewhere.

Institute of Science and Technology
and Faculty of Science of Tokyo University

(1) M. Yasumi, This Bulletin, **24**, 53 (1951); M. Yasumi, K. Nukazawa and S. Mizushima, This Bulletin, **24**, 60 (1951).

Concentration Polarization and the Polarographic Current-Time Curve. I. Rate of the Consecutive Reaction Consisting of the Linear Diffusion Process and the Electrode Reaction

By Tomihito KAMBARA and Isamu TACHI

(Received October 2, 1951)

Introductory Remarks on the Consecutive Reaction

As the simplest consecutive reaction, let us suppose the reaction:

$$A \xrightarrow{k_1} B \xrightarrow{k_2} C, \qquad \text{(i)}$$

where k_1 and k_2 are the rate constants. Let C_A, C_B and C_C represent the respective concentrations, and if the initial condition is given by

$$C_A = a, \quad C_B = C_C = 0 \text{ when } t = 0, \qquad \text{(ii)}$$

it can be demonstrated that,[1],[2]

$$C_C = a\left\{1 - \frac{k_2}{k_2 - k_1}\exp(-k_1 t) + \frac{k_1}{k_2 - k_1}\exp(-k_2 t)\right\}, \qquad \text{(iii)}$$

where it is assumed that $k_1 \neq k_2$. It is clear that the condition

$$k_1 \gg k_2 \qquad \text{(a)}$$

reduces the Eq. (iii) to the form:

$$C_C = a\{1 - \exp(-k_2 t)\}. \qquad \text{(iii-a)}$$

And it is seen that this is equivalent to the supposition that the overall reaction is controlled by the process

$$A \xrightarrow{k_2} C. \qquad \text{(i-a)}$$

Similarly the condition

$$k_2 \gg k_1 \qquad \text{(b)}$$

reduces Eq. (iii) to the form:

$$C_C = a\{1 - \exp(-k_1 t)\}. \qquad \text{(iii-b)}$$

This result can be readily obtained, if we assume that the whole reaction is equivalent to the process

$$A \xrightarrow{k_1} C. \qquad \text{(i-b)}$$

From the above-stated deductions, it can be readily seen that the velocity of the overall reaction is approximately equal to the velocity of the slowest process, *i.e.* of the rate-determining step; but comparison of Eq. (iii) with Eqs. (iii-a) and (iii-b) clearly shows that this simplification is not always legitimate.

We have been hitherto accustomed to the conception that the velocity of the heterogeneous reaction in liquid phase, *e.g.* the electrode reaction, is governed by the rate of the slower one of the two processes, *i.e.* the rate of diffusion of the depolarizer transported from the bulk of the solution to the electrode surface and the rate of the electrode reaction of depolarizer at the surface. In this article, the author will discuss a rigorous mathematical treatment for the rate of heterogeneous reaction, in which neither of the rates of these two elementary processes can be neglected.

Basic Theory for the Overall Velocity of the Electrode Reaction Including the Diffusion Process

Electrolysis by means of the polarographic method gives one of the most convenient methods for the theoretical consideration; *viz.* the applied E. M. F. shows the potential of the dropping electrode relative to the constant potential of the impolarizable bottom electrode, and the depolarizer is obliged to reach to the dropping electrode surface only by diffusion. In this way the depolarizer diffuses towards the electrode surface and then the electrode reaction takes place; the reaction product thus produced also moves by thermal agitation. (When the product is soluble in the electrolytic solution, it diffuses away into the solution,

(1) S. Glasstone, "Textbook of Phys. Chemistry" (1940) p. 1055.
(2) E.A. Moelwyn-Hughes, "Phys. Chemistry" (1940) p. 526, 639.

and when the product forms an amalgam with the electrode mercury, it diffuses into the electrode.) In general we must consider the movements of two matters, *i. e.*, the depolarizer (denoted by the suffix 1) and the product (denoted by the suffix 2); and neglecting the curvature of the electrode surface, the following two equations hold:

$$\frac{\partial C_1}{\partial t}=D_1\frac{\partial^2 C_1}{\partial x^2} \quad \text{and} \quad \frac{\partial C_2}{\partial t}=D_2\frac{\partial^2 C_2}{\partial x^2}\ . \tag{1}$$

In these equations D_1 and D_2 are the diffusion coefficients and x_1 is the distance from the interface to the solution, and x_2 is also the distance from the interface, the sign of which depends on the nature of the reaction product. In our case we will suppose that

$$x=x_1=-x_2. \tag{2}$$

This simplification does not lose the generality of the mathematical procedure given below (This corresponds to the case that the cadmium ion in solution deposits on the mercury cathode).

The initial condition is given by

$$C_1={}^*C_1,\ C_2={}^*C_2 \text{ when } t=0,\ x>0, \tag{3}$$

where ${}^*C_1$ and ${}^*C_2$ are the concentrations in the body of solution. The boundary condition is controlled by the electrode reaction and is manifested by

$$D_1\frac{\partial C_1}{\partial x}=k_1{}^\circ C_1-k_2{}^\circ C_2=-D_2\frac{\partial C_2}{\partial x} \quad \text{when} \quad x=0,\ t>0, \tag{4}$$

where k_1 and k_2 are the specific rates of the forward and reverse reactions, respectively, and ${}^\circ C_1$ and ${}^\circ C_2$ represent the concentrations of the depolarizer and the reaction product at the electrode surface ($x=0$), and are the functions of time t. In some cases, k_1 or k_2 includes the product of the concentrations of the chemical species which take part in the reaction. This boundary condition results from the conception that the rate of depolarization process is given by

$$v_1=k_1\cdot{}^\circ C_1$$

and that the rate of reverse process is given by

$$v_2=k_2\cdot{}^\circ C_2.$$

In general this condition depends on the mechanism of the electrode reaction and is written in the form:

$$D_1\frac{\partial C_1}{\partial x}=k_1'\cdot{}^\circ C_1{}^{n_1}-k_2'\cdot{}^\circ C_2{}^{n_2}=-D_2\frac{\partial C_2}{\partial x} \quad \text{when} \quad x=0,\ t>0. \tag{4 a}$$

The physical meaning of Eqs. (1) and (4) can be readily seen, *i. e.*, the depolarizer and the reaction product move according to the law of diffusion, but their amount which penetrate the plane $x=0$, *i. e.* the velocity of the electrode reaction is governed by the law of chemical kinetics, and the flow of materials must be continuous even at the plane $x=0$.

In order to integrate the system of differential equations (1), we will employ the Laplace transformation[3] defined by

$$\mathfrak{L}C_i(x,\ t)=p\int_0^\infty e^{-pt}\cdot C_i(x,\ t)\cdot dt=u_i(x,\ p). \quad (\text{for } i=1,\ 2.)$$

Then it is found that

$$\mathfrak{L}\frac{\partial C_i}{\partial t}=[p\cdot C_i\cdot e^{-pt}]_0^\infty+p^2\int_0^\infty e^{-pt}\cdot C_i\cdot dt =-p^*C_i+pu_i. \quad (\text{for } i=1,\ 2.)$$

Hence we obtain the following system of ordinary differential equations

$$\left.\begin{aligned}\frac{p}{D_1}(u_1-{}^*C_1)&=\frac{\partial^2 u_1}{\partial x^2};\\ \frac{p}{D_2}(u_2-{}^*C_2)&=\frac{\partial^2 u_2}{\partial x^2}.\end{aligned}\right\} \tag{5}$$

The general integral of these two equations are:

$$\left.\begin{aligned}u_1&={}^*C_1+A_1\cdot\exp\left(\sqrt{\frac{p}{D_1}}x\right)+B_1\cdot\exp\left(-\sqrt{\frac{p}{D_1}}x\right);\\ u_2&={}^*C_2+A_2\cdot\exp\left(\sqrt{\frac{p}{D_2}}x\right)+B_2\cdot\exp\left(-\sqrt{\frac{p}{D_2}}x\right).\end{aligned}\right\} \tag{6}$$

Since u_1 and u_2 must be finite even at $x\to\infty$, two constants A_1 and A_2 must be zero; *i. e.*,

$$A_1=A_2=0 \tag{7}$$

and

$$\left.\begin{aligned}u_1&={}^*C_1+B_1\cdot\exp\left(-\sqrt{\frac{p}{D_1}}x\right);\\ u_2&={}^*C_2+B_2\cdot\exp\left(-\sqrt{\frac{p}{D_2}}x\right)\end{aligned}\right\} \tag{8}$$

(3) K. W. Wagner, "Operatorenrechnung nebst Anwendungen in Physik und Technik." (1940); Japanese Translation by H. Tahara (1943) Kagaku-Shinko-Sha.

Differentiation of these equations gives

$$\left.\begin{aligned}\frac{\partial u_1}{\partial x}&=-B_1\sqrt{\frac{p}{D_1}}\exp\left(-\sqrt{\frac{p}{D_1}}x\right);\\ \frac{\partial u_2}{\partial x}&=-B_2\sqrt{\frac{p}{D_2}}\exp\left(-\sqrt{\frac{p}{D_2}}x\right).\end{aligned}\right\}\quad(9)$$

Hence from the Eqs. (4) and (9), it is found that

$$\begin{aligned}-B_1\sqrt{pD_1}&=k_1({}^*C_1+B_1)\\ -k_2({}^*C_2+B_2)&=B_2\sqrt{pD_2}.\end{aligned}\quad(10)$$

Thus the two integral constants B_1 and B_2 are found to be

$$\left.\begin{aligned}B_1&=-\frac{k_1{}^*C_1-k_2{}^*C_2}{\sqrt{pD_1}+k_1+k_2\sqrt{\frac{D_1}{D_2}}};\\ B_2&=-\frac{k_1{}^*C_1-k_2{}^*C_2}{\sqrt{pD_2}+k_2+k_1\sqrt{\frac{D_2}{D_1}}}.\end{aligned}\right\}\quad(11)$$

Accordingly it is shown that

$$\left.\begin{aligned}u_1&={}^*C_1-\frac{\alpha\sqrt{D_2}}{\lambda}\cdot\frac{\lambda}{\lambda+\sqrt{lp}}\\ &\quad\cdot\exp(-a_1\sqrt{lp});\\ u_2&={}^*C_2+\frac{\alpha\sqrt{D_1}}{\lambda}\cdot\frac{\lambda}{\lambda+\sqrt{lp}}\\ &\quad\cdot\exp(-a_2\sqrt{lp});\end{aligned}\right\}\quad(12)$$

where

$$\left.\begin{aligned}l&=D_1D_2;\quad\alpha=k_1{}^*C_1-k_2{}^*C_2;\\ \lambda&=k_1\sqrt{D_2}+k_2\sqrt{D_1};\\ a_1&=\frac{x}{D_1\sqrt{D_2}};\quad a_2=\frac{x}{D_2\sqrt{D_1}}.\end{aligned}\right\}\quad(13)$$

Now let us perform the inverse transformation of Eq. (12) in order to evaluate the quantity C_1 and C_2; for this purpose, the following theorem is valid[3]:

If $$\mathfrak{L}^{-1}f(p)=A(t),$$

it is found that

$$\mathfrak{L}^{-1}f(lp)=A(t/l),\quad(14)$$

where l is a coefficient. Further it is known that

$$\left.\begin{aligned}&\mathfrak{L}^{-1}\frac{\lambda}{\lambda+\sqrt{p}}\cdot\exp(-a\sqrt{p})\\ &\quad=1-\operatorname{erf}\frac{a}{2\sqrt{t}}-\Psi(t);\end{aligned}\right\}\quad(15)$$

$$\Psi(t)\equiv\exp(a\lambda+\lambda_2 t)\times\left\{1-\operatorname{erf}\left(\frac{a}{2\sqrt{t}}+\lambda\sqrt{t}\right)\right\},$$

where $\operatorname{erf}\xi$ is the Gauss' error function defined by

$$\operatorname{erf}\xi\equiv\frac{2}{\sqrt{\pi}}\int_0^{\xi}\exp(-z^2)\cdot dz.$$

Accordingly it is found finally that

$$\left.\begin{aligned}\mathfrak{L}^{-1}u_1&=C_1={}^*C_1-\frac{k_1{}^*C_1-k_2{}^*C_2}{s\sqrt{D_1}}\\ &\quad\times\left[1-\operatorname{erf}\frac{x}{2\sqrt{D_1t}}-\exp\left(\frac{sx}{\sqrt{D_1}}+s^2t\right)\right.\\ &\quad\left.\times\left\{1-\operatorname{erf}\left(\frac{x}{2\sqrt{D_1t}}+s\sqrt{t}\right)\right\}\right];\\ \mathfrak{L}^{-1}u_2&=C_2={}^*C_2+\frac{k_1{}^*C_1-k_2{}^*C_2}{s\sqrt{D_2}}\\ &\quad\times\left[1-\operatorname{erf}\frac{x}{2\sqrt{D_2t}}-\exp\left(\frac{sx}{\sqrt{D_2}}+s^2t\right)\right.\\ &\quad\left.\times\left\{1-\operatorname{erf}\left(\frac{x}{2\sqrt{D_2t}}+s\sqrt{t}\right)\right\}\right];\end{aligned}\right\}\quad(16)$$

where s is given by

$$s=\frac{k_1}{\sqrt{D_1}}+\frac{k_2}{\sqrt{D_2}}.\quad(17)$$

Hence it is obvious that the concentrations at the interface ($x=0$) are shown by

$$\left.\begin{aligned}{}^\circ C_1&={}^*C_1-\frac{k_1{}^*C_1-k_2{}^*C_2}{s\sqrt{D_1}}\\ &\quad\times\{1-\exp s^2t\cdot(1-\operatorname{erf}s\sqrt{t})\};\\ {}^\circ C_2&={}^*C_2+\frac{k_1{}^*C_1-k_2{}^*C_2}{s\sqrt{D_2}}\\ &\quad\times\{1-\exp s^2t\cdot(1-\operatorname{erf}s\sqrt{t})\}.\end{aligned}\right\}\quad(18)$$

Applications of the Theory

(1) In the case that the Reverse Reaction dose not Take Place.—In this case k_2 equals zero, and from Eqs. (16) and (18) it is seen that

$$\begin{aligned}\lim_{k_2\to0}C_1&={}^*C_1\left[\operatorname{erf}\left(\frac{x}{2\sqrt{D_1t}}\right)\right.\\ &\quad+\exp\left(\frac{k_1^2}{D_1}t+\frac{k_1}{D_1}x\right)\\ &\quad\left.\times\left\{1-\operatorname{erf}\frac{x}{2\sqrt{D_1t}}+\frac{k_1\sqrt{t}}{\sqrt{D_1}}\right)\right\}\Bigg];\end{aligned}\quad(19)$$

$$\lim_{k_2\to 0} {}^{\circ}C_1 = {}^{*}C_1 \cdot \exp\left(\frac{k_1^2}{D_1}t\right) \times\left\{1-\mathrm{erf}\left(\frac{k_1}{\sqrt{D_1}}\sqrt{t}\right)\right\} . \quad (20)$$

This result can be obtained when we solve the equation

$$\partial C_1/\partial t = D_1 \cdot \partial^2 C_1/\partial x^2 \quad (1)$$

with the conditions

$$C_1 = {}^{*}C_1 \quad \text{when} \quad t=0, \quad x>0;$$

$$D_1\frac{\partial C_1}{\partial x} = k_1 \cdot C_1 \quad \text{when} \quad t>0, \quad x=0.$$

I. e., it can be readily found that the solution given by Fürth[4] is quite in harmony with Eq. (19).

(2) The final Concentrations at the Electrode Surface.—For large value of ξ, it can be shown that

$$\sqrt{\pi}\,(1-\mathrm{erf}\,\xi) = 2\left(\int_0^{\infty} - \int_0^{\xi}\right) \sim \exp(-\xi^2) \times\left(\frac{1}{\xi} - \frac{1}{2\xi^3} + \frac{3}{4\xi^5} - \cdots\right), \quad (21)$$

i. e.,

$$\exp\xi^2 \cdot (1-\mathrm{erf}\,\xi) \sim \frac{1}{\sqrt{\pi}} \times\left(\frac{1}{\xi} - \frac{1}{2\xi^3} + \frac{3}{4\xi^5} - \cdots\right). \quad (22)$$

Hence it follows that

$$\lim_{t\to\infty} {}^{\circ}C_1 = \frac{k_2({}^{*}C_1\sqrt{D_1} + {}^{*}C_2\sqrt{D_2})}{k_1\sqrt{D_2} + k_2\sqrt{D_1}} = {}^{\circ}C_1(\text{fin.}), \quad (23)$$

$$\lim_{t\to\infty} {}^{\circ}C_2 = \frac{k_1({}^{*}C_1\sqrt{D_1} + {}^{*}C_2\sqrt{D_2})}{k_1\sqrt{D_2} + k_2\sqrt{D_1}} = {}^{\circ}C_2(\text{fin.}), \quad (24)$$

and accordingly it is found that

$$\lim_{t\to\infty} \frac{{}^{\circ}C_1}{{}^{\circ}C_2} = \frac{{}^{\circ}C_1(\text{fin.})}{{}^{\circ}C_2(\text{fin.})} = \frac{k_2}{k_1} = K, \quad (25)$$

where k_1, k_2, and the equilibrium constant K depend on the electrode potential. Thus it is found that the depolarizer and the reaction product finally reach to their equilibrium concentrations.

(4) R. Fürth, "Wärmeleitung und Diffusion" in "Die Differential und Integralgleichungen der Mechanik und Physik." Bd. II. Herausgegeben von Ph. Frank und R. v. Mises. (1927) S, 234.

(3) Electro-deposition of Solid Metal or Alloy on a Solid Cathode.—In this case the concentration of the deposited material is considered to show a constant value ${}^{\circ}C_s$. Hence we must solve the equation

$$\partial C_1/\partial t = D_1 \cdot \partial^2 C_1/\partial x^2 \quad (1)$$

with the initial condition given by Eq. (3) and with the boundary condition given by

$$D_1\frac{\partial C_1}{\partial x} = k_1 \cdot C_1 - k_2 \cdot {}^{\circ}C_s \quad \text{when} \quad t>0, \quad x=0. \quad (4b)$$

And it is found finally that

$$C_1 = {}^{*}C_1 - \frac{k_1{}^{*}C_1 - k_2{}^{\circ}C_s}{k_1}\left[1-\mathrm{erf}\frac{x}{2\sqrt{D_1 t}} - \exp\left(\frac{k_1 x}{D_1} + \frac{k_1^2 t}{D_1}\right) \times\left\{1-\mathrm{erf}\left(\frac{x}{2\sqrt{D_1 t}} + \frac{k_1}{\sqrt{D_1}}\sqrt{t}\right)\right\}\right]. \quad (26)$$

Hence it follows that

$$\lim_{t\to\infty} {}^{\circ}C_1 = \frac{k_2}{k_1}\,{}^{\circ}C_s, \quad (27)$$

i. e., when the considerable time has elapsed after the beginning of electrolysis, the equilibrium concentration is established at the interface.

(4) Current-Time Curves.—

(a) Stationary Electrode.—Ilkovic etc[5~11] have solved the differential equation

$$\partial C_1/\partial t = D_1 \cdot \partial^2 C_1/\partial x^2 \quad (1)$$

with the condition

$$\left.\begin{aligned} C_1 &= {}^{*}C_1 && \text{when} \quad t=0, \quad x>0; \\ C_1 &= {}^{\circ}C_1\ (\text{fin.}) && \text{when} \quad t>0, \quad x=0, \end{aligned}\right\} \quad (28)$$

and the result is

$$C_1 = {}^{\circ}C_1\,(\text{fin.}) + \{{}^{*}C_1 - {}^{\circ}C_1\,(\text{fin.})\} \cdot \mathrm{erf}\frac{x}{2\sqrt{D_1 t}}, \quad (29)$$

(5) D. Ilkovic. *Collection Czech. Chem. Communs.*, **6**, 498 (1934).
(6) D. Ilkovic, *Jour. chim. physique*, **35**, 129 (1938).
(7) D. MacGillavry and E. K. Rideal, *Rec. trav. chim. Pays-Bas*, **56**, 1013 (1937).
(8) M. v. Stackelberg, *Z. Elektrochem.*, **45**, 466 (1939).
(9) H. Strehlow und M. v. Stackelberg, *Ibid.*, **54**, 51 (1950).
(10) T. Kambara, M. Suzuki and I. Tachi, *This Bulletin*, **23**, 219 (1950).
(11) T. Kambara and I. Tachi, *This Bulletin*, **23**, 225 (1950).

where it is supposed that the concentration of the depolarizer at the electrode surface shows a constant value ${}^{\circ}C_1$ (fin.) according to the electrode potential immediately after the commencement of the electrolysis. From Eq. (29), it follows that

$$\left(\frac{\partial C_1}{\partial x}\right)_{x=0} = \frac{{}^{*}C_1 - {}^{\circ}C_1\,(\text{fin.})}{\sqrt{\pi D_1 t}}, \qquad (30)$$

and therefore if q is the surface area of the electrode, and nF (F: Faraday) is the electricity required for the electrolysis of one mol of the depolarizer, it can be seen that the instantaneous current intensity i is given by

$$i = nFqD_1\left(\frac{\partial C_1}{\partial x}\right)_{x=0} = nFqD_1\frac{{}^{*}C_1 - {}^{\circ}C_1(\text{fin.})}{\sqrt{\pi D_1 t}}, \qquad (31)$$

i.e., it is shown that

$$i \propto t^{-1/2} \qquad (32)$$

Hence just at the beginning of the electrolysis the current intensity is given by

$$i_{t=0} = \infty, \qquad (33)$$

which is clearly an inadequate result.

According to the above-developed theory it is seen that

$$i/nFq = k_1{}^{\circ}C_1 - k_2{}^{\circ}C_2 = (k_1{}^{*}C_1 - k_2{}^{*}C_2) \times \exp s^2 t \cdot (1 - \operatorname{erf} s\sqrt{t}), \qquad (34)$$

and therefore it follows that

$$i_{t=0} \simeq nFq(k_1{}^{*}C_1 - k_2{}^{*}C_2), \qquad (35)$$

which is a quite rational conclusion. On the other hand, when the long time has elapsed after the commencement of electrolysis, it is shown from Eq. (22) that

$$i \simeq nFq\left({}^{*}C_1 - \frac{k_2}{k_1}{}^{*}C_2\right)\cdot\frac{D_1}{\sqrt{\pi D_1 t}} \times \frac{1}{1+\dfrac{k_2}{k_1}\sqrt{\dfrac{D_1}{D_2}}}.$$

Further, it is seen from Eq. (23) that

$${}^{*}C_1 - {}^{\circ}C_1\,(\text{fin.}) = \frac{k_1{}^{*}C_1\sqrt{D_2} - k_2{}^{*}C_2\sqrt{D_2}}{k_1\sqrt{D_2} + k_2\sqrt{D_1}} = \left({}^{*}C_1 - \frac{k_2}{k_1}{}^{*}C_2\right)\Big/\left(1+\frac{k_2}{k_1}\sqrt{\frac{D_1}{D_2}}\right),$$

and hence it can be found that

$$i \simeq nFqD_1\{{}^{*}C_1 - {}^{\circ}C_1\,(\text{fin.})\}/\sqrt{\pi D_1 t}, \qquad (36)$$

which perfectly coincides with Eq. (31). Analogously it can be readily found that

$$i \simeq nFqD_2\{{}^{\circ}C_2\,(\text{fin.}) - {}^{*}C_2\}/\sqrt{\pi D_2 t}. \qquad (36a)$$

It may be concluded that the boundary condition given by Eq. (28), and also the expessions shown by Eqs. (30) and (31) are merely approximate formulae representing the limiting case of our general theory.

On the contrary, when the electrode process is the rate-determining step, it is seen that k_1 and k_2 are much smaller than $\sqrt{D_1}$ and $\sqrt{D_2}$ and so the quantity s given by Eq. (17) is vanishingly small, *i. e.*

$$s \fallingdotseq 0. \qquad (37)$$

Then it can be seen from Eq. (34) that

$$i \simeq nFq(k_1{}^{*}C_1 - k_2{}^{*}C_2). \qquad (38)$$

This equation indicates that the overall reaction rate is nearly equal to the rate of electrode reaction.

In Fig. 1 (a) is shown the change of concentrations of the depolarizer and the product with time according to the conditions given by

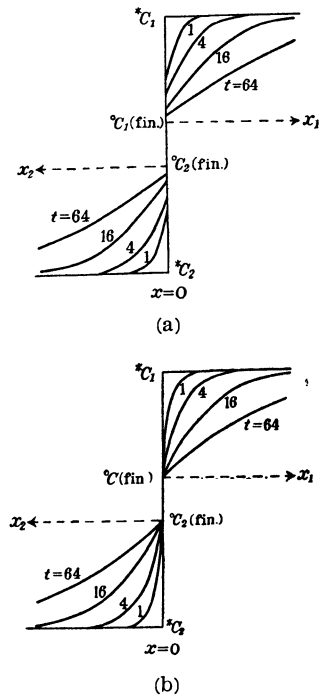

Fig. 1.—Schematic representation of the structure of diffusion layer. Variation of C-x curves with time.
Curve (a): The present theory. Curve (b): Ilkovic theory.

Eqs. (3) and (4), and in Fig. 1 (b) is illustrated the change which is controlled by the conditions given by Eq. (28). The change of the diffusion current with time is illustrated in Fig. 2; curve (a) represents the current intensity given by Eq. (34) and the curve (b) shows that given by Eq. (36). In the Table are given the numerical values employed therefor.

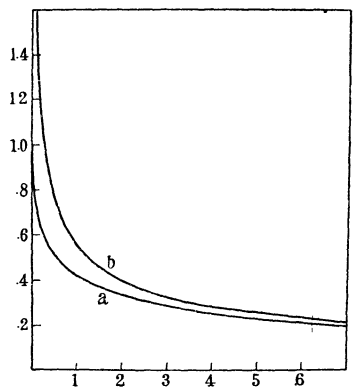

Fig. 2.—Current-time curve at the stationary electrode.

There is no doubt that the general formula for the linear diffusion current, *i.e.* Eq. (34), is reduced to the hitherto employed old formulae shown by Eq. (36) or Eq. (38) according to the simplification that the overall reaction rate is equal to either the rate of diffusion or the rate of electrode process; this is reasonably comparable to the relation between Eq. (iii) and the Eqs. (iii-a) and (iii-b).

(b) Dropping Mercury electrode.—Investigations by MacNevin with Balis[12] and by Smith[13] show that at the instant when the growth of the new drop has just begun, the new drop exposes a residual surface. Ilkovic[14] describes in his paper on the theory of polarographic maxima that at the beginning of the growth of the new drop, its radius would be equal to the internal radius of the capillary. Taking these opinions into account, it may be supposed that the volume of the mercury drop V is given by

$$V = V_0 + vt, \qquad (39)$$

where V_0 is the residual volume at $t=0$ and v is the rate of flow of mercury out of the capillary in ccm/sec. Accordingly the radius

Table

Numerical Values of Functions Appearing in Eqs. (34), (36), (42) and (47)

s^2t	$s\sqrt{t}$	$f_1(t)$*	$f_2(t)$*	$f_3(t)$*	$f_4(t)$*
0	0	1.000,0	∞	1.000,0	0
0.000,001	0.001	0.998,9	564.19	0.999,6	5.642
0.000,004	0.002	0.997,7	282.10	1.000,4	7.106
0.000,009	0.003	0.996,6	188.06	1.002,6	8.135
0.000,016	0.004	0.995,5	141.05	1.006,1	8.955
0.000,1	0.01	0.988,8	56.419	1.053,7	12.15
0.000,4	0.02	0.977,8	28.210	1.223,7	15.31
0.000,9	0.03	0.967,0	18.806	1.483,4	17.53
0.001,6	0.04	0.956,4	14.105	1.808,4	19.30
0.002,5	0.05	0.946,0	11.284	2.180,5	20.79
0.003,6	0.06	0.935,8	9.403	2.588,3	22.11
0.004,9	0.07	0.925,7	8.060	3.022,3	23.25
0.006,4	0.08	0.915,8	7.052	3.477,1	24.32
0.008,1	0.09	0.906,0	6.268	3.950,3	25.28
0.01	0.1	0.896,5	5.641,9	4.434	26.18
0.04	0.2	0.809,0	2.821,0	9.617	32.99
0.09	0.3	0.734,6	1.880,6	14.861	37.77
0.16	0.4	0.670,8	1.410,5	19.846	41.57
0.25	0.5	0.615,7	1.128,4	24.499	44.78
0.36	0.6	0.567,8	0.940,3	28.763	47.63
0.49	0.7	0.525,9	0.806,0	32.729	50.09
0.64	0.8	0.489,1	0.705,2	36.365	52.39
0.81	0.9	0.456,5	0.626,8	39.708	54.46
1.00	1.0	0.427,6	0.564,2	42.759	56.42
1.21	1.1	0.401,7	0.512,9	45.573	58.19
1.44	1.2	0.378,9	0.470,2	48.284	59.92
1.69	1.3	0.357,6	0.434,0	50.762	61.60
1.96	1.4	0.338,7	0.403,0	53.039	63.11
2.25	1.5	0.321,5	0.376,1	55.202	64.57
2.56	1.6	0.305,9	0.352,6	57.241	65.97
2.89	1.7	0.291,7	0.331,9	59.171	67.33
3.24	1.8	0.278,6	0.313,4	60.998	68.63
3.61	1.9	0.266,5	0.296,9	62.667	69.82
4.00	2.0	0.255,5	0.282,1	64.386	71.08
4.84	2.2	0.235,2	0.256,5	67.282	73.35
5.76	2.4	0.219,0	0.235,1	70.377	75.55
6.76	2.6	0.207,0	0.217,0	74.018	77.58

* $f_1(t) = \exp s^2t \cdot (1-\mathrm{erf}\, s\sqrt{t})$;

$f_2(t) = \dfrac{1}{\sqrt{\pi s^2 t}}$;

$f_3(t) = \left(1+\dfrac{v}{V_0}t\right)^{2/3} \cdot \exp s^2t \cdot (1-\mathrm{erf}\, s\sqrt{t})$;

$f_4(t) = \left(\dfrac{v}{V_0}t\right)^{2/3} \cdot \dfrac{1}{\sqrt{\pi s^2 t}}$;

$v/V_0 = 10^{\gamma}$.

of drop at any instant t is shown by

$$r = \{3(V_0+vt)/4\pi\}^{1/3},$$

and therefore the surface area q of drop is seen to be

(12) W. M. MacNevin and E. W. Balis, *J. Am. Chem. Soc.*, **65**. 660 (1943).
(13) G. S. Smith, *Trans. Faraday Soc.*, **47**, 63 (1951).
(14) D. Ilkovic, *Collection Czech. Chem. Communs.*, **8**, 13 (1936).

$$q=4\pi\cdot(3/4\pi)^{2/3}\cdot(V_0+vt)^{2/3}, \qquad (40)$$

and the residual surface area q_0 is demonstrated by

$$q_0=4\pi(3V_0/4\pi)^{2/3}. \qquad (41)$$

Hence the instantaneous current intensity at the dropping electrode is manifested by

$$i=nF\cdot q_0\cdot\left(1+\frac{v}{V_0}t\right)^{2/3}\cdot(k_1{}^*C_1-k_2{}^*C_2)$$
$$\times\exp s^2t\cdot(1-\mathrm{erf}\, s\sqrt{t}). \qquad (42)$$

From this equation, the current which flows at the instant when the preceding drop has just fallen off is given by

$$i_{t=0}\simeq nFq_0(k_1{}^*C_1-k_2{}^*C_2). \qquad (43)$$

According to the Ilkovic theory, it is known that

$$i\propto t^{1/6},$$

and hence it follows that

$$i_{t=0}=0. \qquad (44)$$

Many oscillographic observations,[10] however, indicate that the current intensity at $t=0$ does not diminish away to zero, but shows a finite, although small, value. Differentiating Eq. (42) with respect to the time and putting $t=0$ gives

$$(\mathrm{d}i/\mathrm{d}t)_{t=0}=-\infty. \qquad (45)$$

It is required by the Ilkovic theory that

$$(\mathrm{d}i/\mathrm{d}t)_{t=0}=+\infty, \qquad (46)$$

which does not agree with the oscillogaphic findings. For the large value of t, since vt is much greater than V_0, it follows from Eqs. (22) and (42) that

$$i\simeq nF\cdot 4\pi(3/4\pi)^{2/3}\cdot(vt)^{2/3}\cdot D_1$$
$$\{{}^*C_1-{}^\circ C_1\,(\mathrm{fin.})\}/\sqrt{\pi D_1t}, \qquad (47)$$

which is completely in accordance with the old theory of Ilkovic,[5] neglecting the effect of compressions of the diffusion layer by the expansion of mercury drop.

It may be concluded that the instantaneous current at the dropping electrode starts from a certain small value given by Eq. (43) and at first decreases rapidly but soon it begins to increase as indicated by Eq. (42) and finally becomes asymptotically identical with that predicted by the Ilkovic theory. Such a course of current change as is reported by McKenzie[15] and by us[10] is first comprehensible from our theory which takes the diffusion process and the electrode reaction into consideration at the same time.

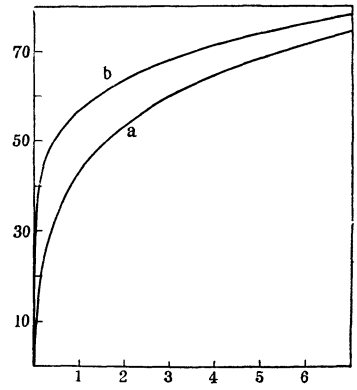

Fig. 3.—Current-time curve at the dropping electrode.

In the Table are given the numerical values of the functions appearing in Eqs. (42) and (47). For the sake of simplicity, it is assumed that $s=1$ and $v/V_0=10^3$. Randles[16] gives the value 6×10^{-3} for the electrode reaction constant of zinc ion in potassium chloride solution. The internal radius of capillary electrode is said to be about 20~30 μ, and v under the ordinary condition is about 10^{-4} cc./sec. Curve (a) in Fig. 3 shows the theoretical current-time curve plotted according to Eq. (42) and curve (b) is drawn by Eq. (47). In the above considerations the effects produced by the convection of solution due to the expansion[5~8] of drop and by the curvature[9~11] of mercury drop are ignored; it may be said, however, that the reason why the current intensity increases very slowly in the infancy of drop-life is cleared up.

Randles[16] states that the rate constant k decreases remarkably with the addition of gelatine. On the other hand, it is well known that the mobility of an ion, and hence the diffusion coefficient, are hardly effected thereby.[17] It is noteworthy that the polarographic current-time curve is much effected by the addition of gelatine, as observed by us[10]; this will be elucidated by the above theory which regards the electrode reaction as an ensemble of the diffusion and electrode process.

(15) H. A. McKenzie, *J. Am. Chem. Soc.*, **70**, 3147 (1948).
(16) J. E. B. Randles, *Discuss. Faraday Soc.*, No. 1., 11 (1947).
(17) H. Ulich, "Elektrische Leitfähigkeit. Flüssigkeiten und Lösungen" in "Hand- und Jahrbuch der chemischen Physik" herausgegeben von A. Eucken und K. L. Wolf. Bd. 6/Abschnitt II. (1933) S. 150.

Note:—(1) The investigation by Koutecky and Brdicka[18] on the reaction current is the direct motive for the present paper. In their communication the numerical value of the integral defined by

$$f(y_1)=\int_0^{y_1} y^{2/3}\cdot\exp y\cdot(1-\mathrm{erf}\sqrt{y})\cdot dy$$

is tabulated, and this tabulation may be convenient for the study of the polarographic mean diffusion current; but it is pointed out that this table contains some miscalculations.[19]

(2) In the monograph by Frank and v. Mises,[20] the special case that is shown by

$$k_1=k_2=D^*;\ D_1=D_2=D;\ {}^*C_2=0:$$

is discussed. This condition corresponds to the problem of diffusion through a diaphragm, and its conclusion is immediately obtainable from Eq. (18).

(18) J. Koutecky and R. Brdicka, *Collection Czech, Chem. Communs.*, **12**, 337 (1947).

(19) J. Koryta, *Proceedings of the I. Intern. Polarographic Congress in Prague*, Part 1., p. 794, 798. (1951)

(20) Reference 4, p. 237.

Summary

The differential equation of linear diffusion was solved with the boundary condition controlled by the chemical kinetics. The result obtained gives the rate of the consecutive reaction consisting of the diffusion process and the electrode process. This theory can explain the course of the polarographic current-time curve very well.

Agricultural Chemical Laboratory
Faculty of Agriculture, Kyoto
University, Kyoto

Amperometric Titrations. IV. The Use of Metal Electrode of High Negative Potential and its Application to the Determination of Sulfur in Pyrite

By Masayoshi ISHIBASHI and Taitiro FUJINAGA

(Received November 28, 1951)

In the previous paper,[1] the authors reported on the use of reference electrodes having high negative potential, *e. g.* the mercuric sulfide electrode ($E = -0.8$ volt *v. s.* S. C. E.) in the short-circuited amperometric titration of some organic reagents with copper sulfate.

In the present paper, some fundamental experiments on the short-circuited amperometric titration by the use of metal electrode of high negative potential, especially of metallic zinc-potassium chloride electrode, are presented and their application to the determination of sulfur in pyrite after its oxidation to sulfate is reported.

Experimental.

In amperometric titrations, different from the polarographic method where the electrolytic current is a function of the electrode potential, the current is a function of the concentration of the reducible ion in question, and the potential of the indicator electrode is invariant, so in spite of the change in the composition of the titrating solution, the potential of the opposite electrode (anode) must be kept constant while the titration is carried out. In the polarographic method, the mercury pool is generally used as anode of the constant electrode potential, and the potential of dropping electrode is proportional to the applied voltage. In amperometric method, however, if the naked mercury pool is used as the opposite electrode, a very indefinite result is apt to occur. The example is shown in the argentometric titration of cyanide (see Fig. 1). From curve 1 in Fig. 1, where the mercury pool is used as the opposite electrode, the end point is difficult to be determined. The reason is clearly shown by tracing the change of the electrode potential of mercury pool electrode, which is shown by curve 2 in the Fig. 1. As is shown in the curve, the mercury pool electrode has a highly negative potential in the original cyanide solution, but it comes to have a highly positive potential in excess of silver ion against the saturated calomel

(1) M. Ishibashi, T. Fujinaga, this bulletin, **23**, 229 (1950).

electrode and so the amperometric titration curve comes to show irregularity. These effects are thought to occur more or less in all titration reactions. In this case, however, when the separated metallic silver-potassium chloride electrode is used, the titration curve becomes a straight line as is shown in curve 3 in the Fig. 1 and the end point is clearly shown by the cross point of two straight lines (see also Fig. 2)

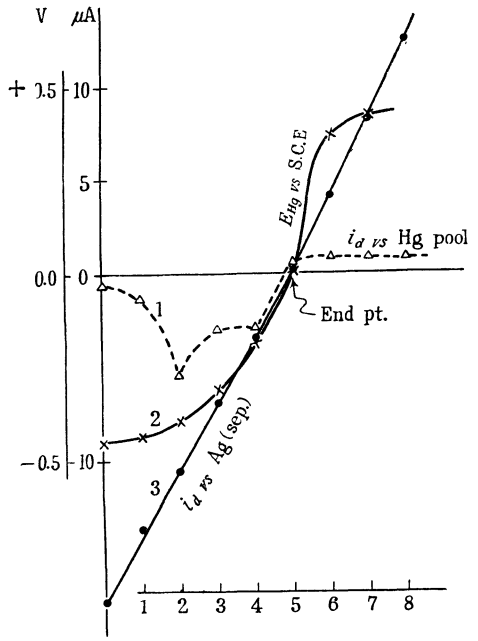

Fig. 1.—Argentometric titration curves of cyanide: curve 1, amperometry using mercury pool as opposite electrode; curve 2, potential change of mercury pool electrode; curve 3, amperometry using separated silver electrode.

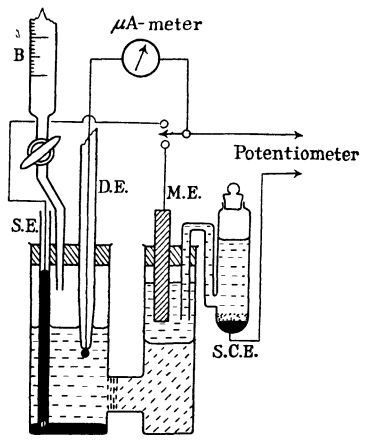

Fig. 2.—Titration cell for the measurement of diffusion current and electrode potential: B, burette; D. E., dropping electrode; M. E., separated metal electrode, S. C. E., saturated calomel electrode; S. E., stationary mercury pool electrode.

These metal electrodes are supposed to be unstable, but from the authors' experiments, an even baser metal like zinc can be used as a stable reference electrode for the amperometric purpose. Table 1 shows the change in the electrode potential of metallic zinc (surface amalgamated) inserted in the anodic solution of potassium chloride,

Table 1

Potential of Zinc Electrode

Discharge time, min.	Electrode potential, volts *vs.* S. C. E.	Discharge current, μA
0 (not connected)	−1.120	0
5	−1.122	21.1
60	−1.118	21.1
150	−1.122	20.0

while the cathodic solution containing 10^{-2} M. lead ion is discharged on the dropping mercury electrode for 2.5 hours by short-circuiting both electrodes. In these experiments, 21.1 microamperes flowed continuously, but the electrode potential was kept constant at $E_c = -1.1$ volts *v.s.* S. C. E. So it appears that such natural electrodes are stable and usable for the amperometric titration at E_c of up to −1.1 volts *v. s.* S. C. E. instead of those produced by the battery-potentiometer method. The examples of other metal electrodes and thereby reducible ions are shown in Table 2.

Table 2

Electrode Potential of Some Metal Electrodes

Electrode	Electrode potential, volts *vs.* S. C. E.	Reducible ion
Ag/sat. KCl	−0.08	Ag^+, Hg^+, Fe^{+++}, CrO_4^{--} etc.
Cu/sat. KCl	−0.325	Bi^{+++}
Sb/buffer soln.	−0.1∼−0.6	
Cd/sat. KCl	−0.820	Cu^{++},$Cu(NH_3)_4^{++}$
Zn/sat. KCl	−1.120	Cd^{++}, Pb^{++}

Determination of Sulfur in Pyrite.

Sulfate can be determined by the amperometric titration with lead nitrate standard solution.[2] In this titration, the potential of −1.2 volts *v. s.* S. C. E. was applied to the dropping mercury electrode; therefore this outside e. m. f. can be replaced by the zinc-potassium chloride electrode. The apparatus is the same as that shown in Fig. 2 (the calomel electrode and the mercury pool electrode are unnecessary).

(2) I. M. Kolthoff, Y. D. Pan, *J. Am. Chem. Soc.*, **62**, 3332 (1940).

Reagents Used: Pure sodium sulfate was accurately weighed out and 0.1N-sodium sulfate solution was prepared as the standard of sulfate. The titre was again determined as barium sulfate by the gravimetric method. 0.1N-lead nitrate solution (1 ml. of 0.1N-nitric acid is added per litre of the solution to prevent the hydrolysis of lead nitrate) was prepared and also the concentration was determined as lead sulfate. Other reagents such as nitric acid, sodium hydroxide and alcohol were all c. p. grade.

Procedure: The fundamental experiment was carried out using the standard sodium sulfate and lead nitrate solution. To 10 ml. of 0.1N-sodium sulfate solution is added 10 ml. ethyl alcohol and 10 ml. of water and one drop of 0.1% methyl red, and titration is worked out with 0.1N-lead nitrate standard solution using the same electrode and the titration cell as mentioned above. The procedure is the same as reported in the previous paper.[1]

By the experiments, it is observed that the presence of less than 1N-sodium nitrate does not interfere in this titration. However, the acidity of the titrating solution gives much influence on the results of titration because of the amphotericity of lead ion. So in strong alkaline or acidic medium, the current increases from the beginning of the addition of lead ion, and lead sulfate does not precipitate. Near the *p*H of 9, owing to the coprecipitation of lead oxide with lead sulfate, a larger result is obtained. So, before the titration is carried out, it is preferred to regulate the *p*H of the solution to be about 3 to 5 using nitric acid or sodium hydroxide, and to titrate in 30% alcoholic medium. The recommended procedure for the determination of sulfur in pyrite is, therefore, as follows.

Sample (*ca.* 1g.) is dissolved in 20 ml. of aqua regia and heated to boiling point and then evaporated to a syrupy state. Nitric acid is then added to the solution and is again concentrated to the same state. After the oxidation of sulfur to sulfate is completed, 20 ml. of water are added to it to dissolve the residue and 10 ml. of sodium hydroxide are added, heated to boiling point, filtered and washed with hot water. The precipitate is dissolved with hot 3N-nitric acid and reprecipitated with sodium hydroxide at boiling state and filtered and washed again. Both filtrates are transferred to a 100 ml. measuring flask and diluted with water to the mark. The aliquot portion is transferred to the cell and neutralized with 3N-nitric acid using phenolephtalein as an indicator. The same volume of alcohol is added to it and the solution is titrated with 0.1N-lead nitrate. The results are shown in Table 3.

Table 3

Determination of Sulfate

No.	0.1N-Na_2SO_4, ml.	Kind of indifferent Salt	0.1N-$PbSO_4$ used (f:1.058), ml.	Error or Result
1	10	None	9.45, 9.45, 9.45	0
2	10	*p*H=3	9.25, 9.30	−2.2%, −1.5%
3	10	1N-$NaNO_3$	9.45	0
4	10	*p*H=9	10.20	+8.0%
5	10	*p*H $\begin{matrix}>12\\<1\end{matrix}$	not found	.....
6	Pyrite(0.05 g.) (S=25.71%)		7.48 7.54 7.50	S=25.71% 25.58% 25.44%
7	Pyrite(0.10 g) (S=3.56%)		2.14 2.14 2.16	S= 3.63% 3.63% 3.66%

Conclusion

The amperometric titration of sulfate with lead nitrate standard solution by the use of metallic zinc-potassium chloride electrode as an anode was examined and this method was applied to the determination of sulfur in pyrite. A satisfactory result was obtained. These natural electrodes are sufficiently stable and reproducible for the use in short-circuited amperometric titrations.

Laboratory of Analytical Chemistry
Faculty of Science, Kyoto University, Kyoto.

The Spatial Configurations and the Ultraviolet Absorption Spectra of the Stilbene Derivatives[1]

Hiroshi SUZUKI

(Received December 1, 1951)

The ultraviolet absorption spectrum of *trans*-stilbene has a maximum at λ 2940 A., which is shifted progressively toward shorter wave lengths as one, and then two methyl groups are introduced into the α- and α'-positions of the molecule.[2] These hypsochromic shifts have been explained as being due to the steric interferences of the substituents which prevent the molecule from assuming a planar configuration.

On the other hand, *cis*-stilbene has an absorption maximum at shorter wave lengths than the trans isomer. This has been also explained by the inference that in this compound the two phenyl groups can not be simultaneously coplanar with the central ethylenic linkage owing to the steric necessities. For the same reason, it is inferred that the resonance energy is less in the cis isomer than in the trans isomer. This provides a reasonable explanation for the fact the cis isomer is more labile and is easily converted to the trans isomer by the action of heat or of various reagents.[3]

Similar hypsochromic effects have been observed also in other cases; for examples, *ortho*-substituted biphenyls,[4] *N*, *N*-dimethylanilines,[5] and acetophenones,[4,a] and have been explained in a similar manner by the steric interferences by the substituents.

These prevailing explanations are based on the rather vague assumption that the spectrum is related to resonance and hence to the planar configuration of the molecule, and that the destruction of the planar configuration may cause a change in the spectrum. But how the spectrum changes when the planar configuration is prevented to any extent is not satisfactorily accounted for by these explanations.

Jones[6] has divided several stilbene derivatives into three groups: compounds which have spectra similar to that of styrene, compounds which have spectra similar to that of *trans*-stilbene, and compounds which have spectra intermediate between these two extremes. In triphenylethylene and tetraphenylethylene, all the phenyl groups cannot be accommodated in a strainless planar structure, so that one, or two, phenyl groups are turned out from the plane, leaving the two remaining *trans*-related phenyl groups in the plane of the central ethylenic linkage, hence these compounds have the spectra similar to that of *trans*-stilbene; that is, these compounds have the structures containing a "stilbene chromophore". Also, a close similarity of the spectra between 1,1-diphenylethylene and styrene has been explained by assuming a rotation of one of the phenyl groups of the former compound out of the plane of the ethylenic linkage, giving rise to a molecule containing a "styrene chromophore". In a similar manner, the fact that *trans*-α, α'-dimethylstilbene has a spectrum similar to that of styrene has been explained by the assumption that only one phenyl group is turned out, leaving a structure containing a "styrene chromophore".

But such considerations can not explain the "intermediate" spectra of *cis*-stilbene and α-methylstilbene. Further, the two phenyl groups in α, α'-dimethylstilbene are in equivalent positions with regard to the molecular structure, so that; even when one of these is turned out from the plane, the steric strain cannot be relieved. Rather, both should be considered as turned out to the same extent from the plane of the central ethylenic linkage. According to this assumption, the so-called "stilbene chromophore" or "styrene chromophore" must be absent in α, α'-dimethylstilbene. But it may be rather reasonable to think that the deviation of both phenyl groups to some extent from the plane of the ethylenic linkage does result not in the notable deformation or the simple destruction of the

(1) Presented at the Symposium on the π-electron held under the auspices of the Chemical Society of Japan in Tokyo, June 24th, 1951.

(2) (a) H. Ley and F, Rinke, *Ber.*, **56**, 771 (1923).
(b) B. Arends, *Ber.*, **64**, 1936 (1931).

(3) G. Egloff, G. Hulla, and V. I. Komarewsky, "Isomerization of Pure Hydrocarbons" Reinhold, 1942, p. 164-167.

(4) (a) W. H. Rodebush, *et al.*, *J. Am. Chem. Soc.*, **62**, 2906 (1940); **63**, 3018 (1941); **68**, 896 (1946).
(b) D. W. Sherwood and M Calvin, *J. Am. Chem. Soc.*, **64**, 1360 (1942).

(5) Remington, *J. Am. Chem. Soc.* **67**, 1838 (1945).

(6) R. N. Jones, *J. Am. Chem. Soc.*, **65**, 1818 (1943).

spectrum characteristic of stilbene, but only in the shift of the absorption maximum toward shorter wave lengths, with the result that the spectrum of α, α'-dimethylstilbene happens to resemble that of styrene. This assumption implies that the perfect coplanarity is not prerequisite to the appearance of a spectrum characteristic of such a conjugated system as stilbene or biphenyl but that the necessity of coplanarity is a question of degree.

From such a view point, and generally, in order to obtain a clearer understanding of the relationship between the resonance and the absorption spectrum which is frequently apt to be misunderstood, the present author has carried out new measurements of the absorption spectra of several stilbene derivatives and has performed calculations to assess the quantitative relations between the degree of the deviation from the coplanarity and the absorption spectrum as well as the resonance energy for the stilbene derivatives.

Calculations

The calculations have been performed according to the usual molecular orbital method[7] and therefore require no detailed description. Since, for this treatment, the stilbene molecule can be considered as belonging to the symmetry group D_2, the secular equation for the determination of the fourteen approximate molecular orbitals as linear combinations of $2p\pi$ atomic orbitals is factorized into the following four equations:

$$A_1,\ x^5+\gamma x^4-(5+\alpha^2)x^3-5\gamma x^2+(4+3\alpha^2)x+4\gamma=0,$$

$$B_2,\ x^5-\gamma x^4-(5+\alpha^2)x^3+5\gamma x^2+(4+3\alpha^2)x-4\gamma=0,$$

$$B_1,\ x^2-1=0,$$

$$B_3,\ x^2-1=0,$$

where $x=W/\beta=(Q-E)/\beta$, Q, E, and β having their usual meanings. By parameters α and γ allowances are made for the situation that the 1−2, 1′−2′ and 1−1′ bonds have lengths different from those in the phenyl group, $\alpha\beta$ and $\gamma\beta$ denoting the exchange integral for the 1−2 or 1′−2′ and the 1−1′ bond respectively. (See Fig. 1.)

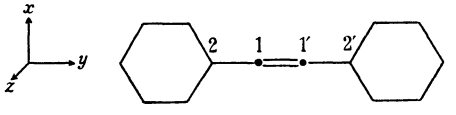

Fig. 1.—Stilbene molecule skeleton.

Now, since the exchange integral can be taken to be approximately proportional to the overlap integral S,[8] the overlap integal for some $\pi-\pi$ bond divided by that for the $\pi-\pi$ bond in benzene whose length is 1.39 A., namely S/S (1.39 A.), represents the coefficient of β in the exchange integral for this $\pi-\pi$ bond. The relation between the $\pi-\pi$ bond length and the corresponding overlap integral can be obtained from Mullikens' Tables.[9] Thus, using the value of 1.34 A. for the length of the 1−1′ bond which is assumed to be not varied to any important extent by resonance,[10] γ is estimated to be 1.08.

According to the results of X-ray diffraction measurement reported by Robertson and Woodward,[10] stilbene has a planar configuration and the length of the bonds joining the phenyl groups to ethylenic carbon atoms, namely the 1−2 and 1′−2′ bonds, is 1.45 A.. With this value, α is estimated to be 0.900 for stilbene. This value of α must become smaller as the phenyl groups are turned out from the plane of the central ethylenic linkage. Thus we can see how the energy levels change as the phenyl groups are twisted gradually from the plane, by taking decreasing values such as 0.9, 0.8, 0.7,....., 0.1, 0, in turn for α in the above equations and solving them.

The results of such calculations are shown in Fig. 2, where the values of W are plotted against α. The solid lines represent the energy levels belonging to A_1 and the broken lines the energy levels belonging to B_2. In addition to these levels, there are two two-fold degenerate levels at $-\beta g$ and $+\beta$ belonging to B_1 and B_3, whose energies do not vary with the value of α. In the lower part of Fig. 2, the calculated extra-resonance energy, R. E., is plotted against α.

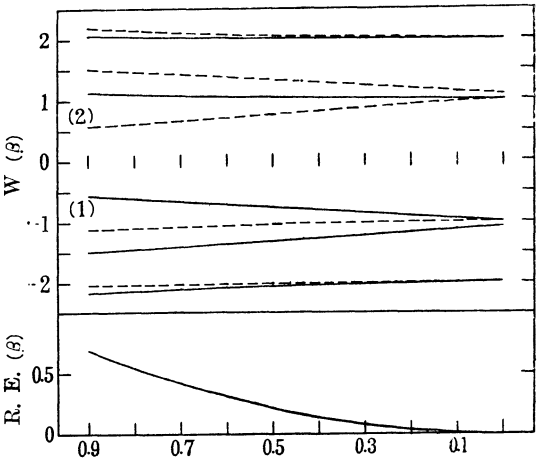

Fig. 2.—The energy levels and the resonance energy as functions of α for stilbenes.

(7) H. Eyring, J. Walter, and G. E. Kimball, "Quantum Chemistry", John Wiley & Sons, Inc., 1944, p. 255.

(8) (a) R. S. Mulliken, C. A. Rieke, and W. G. Brown, *J. Am. Chem. Soc.*, **63**, 41 (1941).
(b) J. Van Dranen and J. A. A. Ketelaar, *J. Chem. Phys.*, **17**, 1338 (1949).

(9) R. S. Mulliken, C. A. Rieke, D. Orloff, and H. Orloff, *J. Chem. Phys.*, **17**, 1248 (1949).

(10) J. M. Robertson and I. Woodward, *Proc. Roy. Soc.* (London), **A 162**, 568 (1937).

In the ground state, the levels lower than zero are all occupied by pairs of electrons, and the levels higher than zero are all vacant. According to the group theory, the transition from A_1 to B_2 is allowed by the absorption of the light polarized in the y-direction. Therefore, since the present calculations apply to vertical excitation, that is, to electron jumps without change in nuclear configuration, the absorption band characteristic of stilbene derivatives is assumed to correspond to the energy difference between the (1)- and (2)-levels in Fig. 2, which is denoted by ΔE. From Fig. 2, it can be seen that the value of ΔE, which is $1.150\,\beta$ when $\alpha=0.900$, that is, for stilbene itself, increases with the decrease of the value of α, and simultaneously, the resonance energy decreases. Thus, the present calculations indicate clearly that the absorption maximum is shifted progressively toward shorter wave lengths, and simultaneously, the resonance energy decreases, as the departure from the planar configuration becomes gradually larger. When $\alpha=0$, the energy levels reduce to those of benzene and ethylene, and the value of ΔE becomes 2β. In Table 1, the values of ΔE and R. E. for various values of α are recorded.

Table 1

α	0.9	0.8	0.7	0.6	0.5
$\Delta E(\beta)$	1.150	1.236	1.326	1.422	1.522
R. E. (β)	0.690	0.548	0.418	0.312	0.216
α	0.4	0.3	0.2	0.1	0
$\Delta E(\beta)$	1.624	1.730	1.838	1.940	2
R. E. (β)	0.134	0.076	0.032	0.009	0

According to Platt,[11] in the absorption spectrum of benzene, the "center-of-gravity of singlets", 48,000 cm.$^{-1}$ in wave number, *i.e.* the average of the energies of the three singlet levels measured in solution, corresponds to the energy difference of 2β calculated by the molecular orbital method of the same order of approximation as the present treatment. On the other hand, the wave number 34,014 cm.$^{-1}$ of the observed absorption maximum of stilbene corresponds to the calculated energy difference ΔE of $1.150\,\beta$. Therefore, in order to correlate the position of the absorption maximum with the calculated energy difference ΔE, it is assumed that the former expressed in wave number changes linearly with respect to the change in the latter from 34,014 cm.$^{-1}$ corresponding to $\Delta E=1.150\,\beta$ to 48,000 cm.$^{-1}$ corresponding to $\Delta E=2\beta$.

The next problem to be settled is in what manner the value of α varies as the phenyl groups are gradually turned out. Denoting by θ the angle through which the axis of the $2p\pi$-orbital on C atom 2 or 2′ is twisted about the 1—2 or 1′—2′ bond axis against the axis of the $2p\pi$-orbital on C atom 1 or 1′ which lies perpendicular to the plane of ethylenic linkage, it is easily verified that the overlap integral $S(\theta)$ in the case where the angle of twist is θ is equal to the overlap integral $S(0)$ when θ is zero, multiplied by $\cos\theta$. If it is assumed that the exchange integral is approximately proportional to the overlap integral in such a case also, and further that the bond length R is maintained constant even when the phenyl groups are turned out to any extent, α would be $S(R)\cos\theta/S(1.39\,\text{A.})$. But any deviation from the planar configuration must inevitably inhibit the $\pi-\pi$ interaction to the corresponding extent, and consequently must be accompanied by change in the bond length. Therefore, we need to take into consideration the variation of α due to the change in the bond length resulting from the twist. This problem may be very complicated, but we can proceed approximately as follows.

The length R of the 1—2 bond was tentatively assumed to vary with θ according to the relation

$$\{S(R)-S(1.54\,\text{A.})\}/\{S(1.45\,\text{A.})-S(1.54\,\text{A.})\} = S(\theta)/S(0)=\cos\theta,$$

since R will vary from 1.45 A. for stilbene to 1.54 A., the length of the normal $C-C$ single bond, as θ varies from 0° to 90°. When the angle of twist θ is given, the corresponding value of $S(R)$ is easily obtained, and then the value of α is given by $S(R)\cos\theta/S(1.39\,\text{A.})$. Thus the position of absorption maximum for a stilbene derivative in which the phenyl groups are twisted from the coplanar position to any extent is inferred by estimating the ΔE by means of Fig. 2 for an appropriate value of α and then the corresponding wave number by means of the linear relationship assumed above between the absorption maximum and ΔE.

Conversely, when the position of the absorption maximum is known experimentally for some stilbene derivative, the values of ΔE, α, θ, R, and R. E. can be successively estimated by reversing the above procedure.

A few examples of the results of such estimations are shown in Table 2. In the calculations of the extra-resonance energies, the value of 21.74 kcal. was used for β, which was deduced from the calculated value $0.690\,\beta$ and the observed value 15 Kcal.[12] for the extra-resonance energy for stilbene itself. In α-methylstilbene, the positions of the two phenyl groups are not equivalent, and therefore, their angles of twist may not be equal. But they were assumed to be so in deducing the above values.

The difference in resonance energy between the trans and the cis isomers of stilbene as calculated above is 3.9 kcal./mol in satisfactory agreement with the experimental value of 3 kcal./mol estimated from the results of the thermal isomerization by Kistiakowsky and Smith[13] and by Taylor

(11) J. R. Platt, *J. Chem. Phys.*, **18**, 1168 (1950).

(12) L. Pauling and J. Sherman, *J. Chem. Phys.*, **1**, 606 (1933).

(13) G. B. Kistiakowsky and W. R. Smith, *J. Am. Chem. Soc.*, **56**, 638 (1934).

Table 2

	λ(A.)obs.	$\Delta E(\beta)$	α	R. E.		θ	R(A.)
cis-Stilbene	2780	1.268	0.765	0.51 β	11.1 kcal.	29°	1.462
trans-α-Methylstibene	2720	1.318	0.709	0.43	9.3	36°	1.467
trans-α, α'-Dimethylstilbene	2435	1.578	0.445	0.17	3.7	58°	1.492
trans-α, α'-Diethylstilbene	2400	1.616	0.408	0.14	3.0	60°	1.496

Table 3

The Absorption Maxima of the Stilbene Derivatives

	Trans	λ(A)	$\varepsilon\times10^{-4}$	*Cis*	λ(A.)	$\varepsilon\times10^{-4}$
Stilbene	(1) m. p. 123–4°	2940	2.76	(1′) b. p. 136–7°/10 mm.	2780	0.98
α-Methylstilbene	(2) m. p. 83.0-83.5°	2720	2.10	(2′) b. p. 151–5°/14 mm.	2670	0.934
α, α'-Dimethylstilbene	(3) m. p. 107°	2435	1.226	(3′) m. p. 67°	2520	0.878
α-Methyl-α'-ethylstilbene	(4) m. p. 47–8°	2400	1.195			
α, α'-Diethylstilbene	(5) m. p. 77–8°	2375	1.102	(5′) b. p. 177–8°/22 mm.	2440	0.774
Methyltriphenylethylene	m. p. 88–9°	2750 2260	0.986 1.372			

and Murray.[14]

Regarding the angle of twist, there is no available experimental evidence such as X-ray diffraction measurement. But these values may be guessed from purely geometrical considerations. Thus, according as we assume a twisted structure for *trans*-α, α'-dimethylstilbene in which the ortho hydrogen atom of a phenyl group just touches the methyl group attached to the same ethylenic carbon atom as the phenyl group or a structure in which that hydrogen atom just touches the other methyl group, the angle of twist is calculated to be 60° or 56°, the following values for distances and angles being used: C=C, 1.34A.; C–CH_3, 1.54 A.; C_6H_5–C, 1.49 A.; C–C in C_6H_5, 1.39 A.; C_6H_5–H, 1.08 A.; angles C=C–CH_3 and C=C–C_6H_5, 124°20′[15]; CH_3-radius, 2.0 A.; H-radius, 0.9 A. (the "Wirkungsradius" of Stuart[6]) (Fig. 3.).

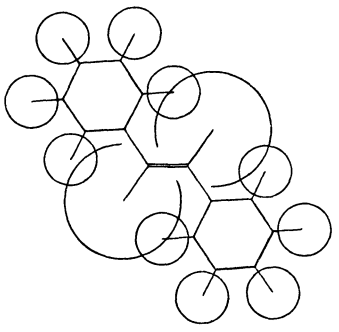

Fig. 3.—Scale drawing of *trans*-α, α'-dimethylstilbene.

For *cis*-stilbene, using the same values except for C_6H_5-C, for which the length is assumed to be 1.46 A., the angle of twist of both phenyl groups out of the plane of the ethylenic linkage is calculated to be about 25°. These values for the angles of twist are in fair agreement with the values calculated above from the absorption spectra. Although to these agreements too much significance should, perhaps, not be attached mainly because of uncertainties in the values for bond lengths, bond angles, and interference radii, it may be supposed that the quantitative relation between the angle of twist and the absorption spectrum has been satisfactorily assessed here.

Results of Measurements of Spectra

The results of the measurements of the absorption spectra are shown in Fig. 4 and in Table 3.

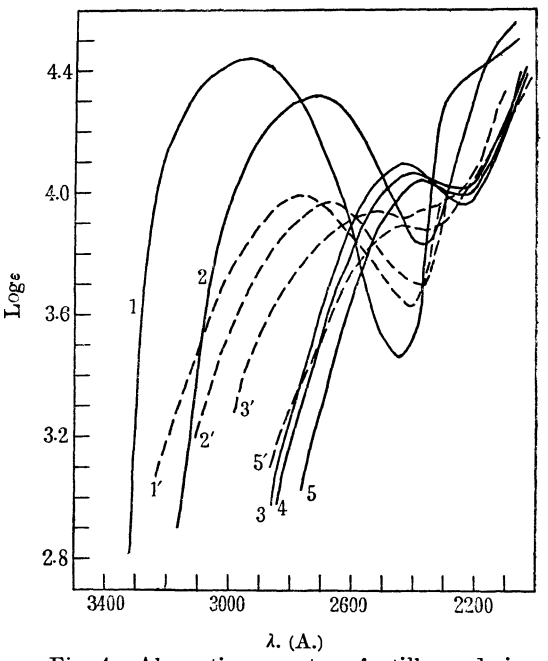

Fig. 4.—Absorption spectra of stilbene derivatives. The solid lines are those for *trans* compounds and the broken-lines those for *cis* compounds listed in Table 3.

(14) T. W. J. Taylor and A. R. Murray, *J. Chem. Soc.*, 2078 (1938).

(15) L. Zechmeister and A. L. LeRosen, *J. Am. Chem. Soc.* **64**, 2755 (1942).

It can be seen that the absorption maximum is shifted progressively toward shorter wave lengths and decreases in intensity gradually, as a larger substituent is introduced into the α- and α'-positions of *trans*- or *cis*-stilbene. In addition it may be noticed that the absorption spectra for the trans and those for the cis isomers form two groups quite distinct from each other in that the former shows a larger molecular extinction coefficient than the latter. This fact may be explained on the basis of the theory advanced by Mulliken[16] and applied to the interpretation of the spectra of carotenoids[17] that the longer the conjugated system in the direction of the electric vector of the light wave responsible for an absorption band, the greater is the intensity of the absorption maximum. On account of this fact, it is believed that the present measurements make it possible to make assignment of trans or cis configuration to these compounds, even when the difference in the position of the absorption maximum between the trans and the cis isomers is very small as compared with that between the two isomers of stilbene, or even when the maximum of a trans isomer is at shorter wave lengths than that of the corresponding cis isomer as in the case of dimethylstilbene. Thus, the geometrical configuration has now been determined as shown in Table 3 for diethylstilbene, methylstilbene and methylethylstilbene for which either only one of the possible geometrical isomers is known or, when both isomers are known, the geometrical configuration has not been unambiguously established.

The cis isomer of α,α'-dimethylstilbene has the absorption maximum at longer wave lengths than the trans isomer. Therefore, it would be anticipated from the above arguments that the former is more stable than the latter. Actually, it was reported by Lamart-Lucas and coworker[18] that the isomerization of the trans isomer to the cis isomer took place by heat whereas the reverse isomerization did not. But the results of the experiments by the present author were contrary to this theory. The isomerization by heat at 210°C. in the presence of traces of sulfuric acid gave an equilibrium mixture, in which the ratio of the amounts of the cis and the trans isomers was about 45:55, whether the starting material was the trans or the cis isomer. From this result, the difference in the stability between the two isomers of dimetylstilbene is concluded to be very small, the trans isomer to be slightly more stable. This conclusion is contrary to the anticipation from the absorption spectra alone. But a more careful examination of the stereochemistry of dimethylstilbenes shows that such may actually be the case, because, while in the trans isomer the steric repulsion between the large substituents may be almost completely relieved by the rotation of the two phenyl groups out of the plane of the molecule, in the cis isomer on the other hand, the steric repulsion between the two methyl groups can not be reduced by the rotation of the phenyl groups, the steric strain still remaining causing the cis isomer to be the less stable one.

Methyltriphenylethylene has the two absorption maxima at 2750 A. and 2260 A., and the absorption curve near the maximum at longer wave lengths coincides almost perfectly with that of *cis*-stilbene. On the other hand, the absorption spectrum of tetraphenylethylene resembles that of *trans*-stilbene. These facts may be thought to indicate that the two *trans*-related phenyl groups in tetraphenylethylene, if rotated out of the plane, permit the other *trans*-related phenyl groups to assume the configuration coplanar with the othylenic linkage, and that, if one of the rotated phenyl groups is replaced by a methyl groud, even the *trans*-related phenyl groups cannot assume the coplanar configuration.

A similar relation may be found on comparison of the spectrum of *trans*-α-methylstilbene with that of triphenylethylene.

Experimental

The measurements of the spectra.—The absorption spectra were determined with a Beckman Quartz Spectrophotometer Model DU. 95% Ethanol was used as the solvent. The concentrations of the solutions were approximately 10^{-4} mole per liter in all the cases.

Materials. — α, α'-Dimethylstilbene was prepared by dehydration of 2,2-diphenylbutanol-(3), which was obtained by the action of methylmagnesium iodide on methyldiphenylcarbinal.[19] The trans and the cis isomers were separated by fractionational crystallization from petroleum ether.

Other compounds were prepared by analogous methods.

Isomerization of α,α'-dimethylstilbene.—About 0.8 g. of *cis*-or *trans*-α,α'-dimethylstibene and pumice impregnated with concentrated sulfuric acid were placed in a sealed tube, and heated in boiling nitrobenzene for about 20 hours. The composition of the products were determined by comparing the melting-points with those of the standard mixtures prepared from known amounts of the two isomers.

Summary

(1) With certain simple assumptions, calculations based on the molecular orbital method have been performed to assess the quantitative relations between the degree of the deviation from the coplanarity of the molecular configuration and the ultraviolet absorption spectrum as well as the resonance energy for the stilbene derivatives.

(16) R. S. Mulliken, *J. Chem. Phys.*, **7**, 364 (1939).
(17) L. Zechmeister, *Chem. Rev.*, **34**, 207 (1944).
(18) Ramart-Lucas and M. E. Salmon-Legagneur, *Bull. soc. chim. France*, [4] **45**, 718 (1929).
(19) E. Ott, *Ber.*, **61**, 2135 (1928).

(2) New measurements of the spectra of the several stilbene derivatives have been carried out.

(3) By these calculations and the measurements of the spectra, it has been clarified that the absorption maximum is shifted progressively toward shorter wave lengths with the increasing angle of twist of the phenyl groups out of the plane of the ethylenic linkage.

(4) Further, from the results of these calculations and the observed position of the absorption maximum, it is possible to deduce the adequate values of the angle of twist and the resonance energy for any stilbene derivative.

(5) It has been shown that the absorption spectra for the trans isomers and those for the cis isomers of the stilbene derivatives form two groups quite distinct from each other in hat the former shows a larger molecular t extinction coefficient than the latter. On the basis of this fact, the assignments of the geometrical configurations have been determined for some stilbene derivatives.

(6) The experiments on the geometrical isomerization of α, α'-dimethylstilbene by heat have been carried out and the results have been interpreted, based on a consideration of the spatial configurations of the two isomers.

The author expresses his sincere thanks to Prof. Osamu Simamura, Drs. Saburo Nagakura and Makoto Takahashi for their kind guidance and encouragement throughout this study. Thanks are also due to the Ministry of Education for a Grant-in-Aid for Scientific Research.

The College of General Education (Kyoyo-Gakubu), Tokyo, University Tokyo

The Near Ultraviolet Absorption Spectra of Acetophenone and Benzophenone Vapors and the Long Wave-lengths Absorption System of Benzaldehyde Vapor

By Sunao IMANISHI, Kimio SEMBA, Mitsuo ITO and Toshinobu ANNO

(Received January 9, 1952)

Introduction

Recently, one of the authors[1] analyzed the near ultraviolet absorption band system lying in the 2480-2970 A. region and arising from the electronic transition of the type $^1A_1-{}^1B_1$, which is allowed in C_{2v} symmetry, of the benzaldehyde molecule. The present paper is concerned with similar attempts for the acetophenone and benzophenone spectra, together with some accounts on another, wave absorption region in the benzaldehyde spectrum which has longer wave-lengths than that mentioned above.

Absorption measurements for acetophenone and benzophenone in alcohol or hexane solutions have been reported, but their vapor spectra have not been studied in detail.[2] There are two absorption regions in each of these spectra, just as in the case of benzaldehyde. The long wave-lengths absorption region fo acetophenone, and both the short and long wave-lengths regions of benzophenone are continuous. Only the short wave-lengths absorption region of acetophenone has a discrete band structure, which, however, is much more diffuse than that of the benzaldehyde referred to above. The general diffuseness of these spectra are attributable to the introduction of heavier and more complicated substituents into the molecule.

(1) S. Imanishi, *J. Chem. Phys.*, **19**, 389 (1951).
(2) Y. Hukumoto, *Sci. Rep. Tohoku Univ.*, **25**, 1162 (1936). S. Kato and F. Someno, *Sci. Pap. Inst. Phys. Chem. Res.*, **12**, 329 (1944)

Experimental

The spectra of acetophenone and benzophenone were photographed with a Hilger $E-2$ medium quartz spectrograph having a linear dispersion of about 10 A. per mm. at 2700 A. The absorption cell was a quartz tube 40 cm. in length and 3 cm. in diameter, to which a side recess was attached for placing the substance to be investigated in liquid form and sealed in a small thin-walled glass ampoule. The cell was evacuated and the liquid was vaporized by raising the temperature of the cell in an electrically heated mantle, after

breaking the ampoule containing the liquid. The continuous background was supplied by a water-cooled hydrogen discharge lamp consuming about 2.5 kW. at 5,000 volts terminal voltage. To cover the great change in absorbance of the vapors with wave-length it was necessary to make many exposures, each of 40 min. duration on Fuji panchromatic plates, at different temperatures of the vapor and liquid, ranging from 20 to 100°C for acetophenone, and from 70 to 170°C for benzophenone. Iron arc was used to supply the comparison spectrum for the calibration of wave-lengths. Wave-lengths were determined from dispersion curves for each set of measurements of a spectrogram negative.

Acetophenone used was supplied by Takeda-Seiyaku Co. Ltd., and was redistilled before use, and benzophenone was synthesized from benzene and benzoyl chloride which had been prepared by the chlorination of benzoic acid in the presence of phosphorus pentachloride in carbon disulfide solution. The sample thus obtained was purified and distilled several times in vacuum.

Table 1

Wave-lengths Regions of Absorption (A.)

Substance	Long wave-lengths region		Short wave-lengths region	
	Vapor	Liquid	Vapor	Liquid
Acetophenone	3060 ~3500	3204 (alc. sol.)[3]	2480 ~2610	2785 (alc. sol.)[3]
Benzophenone	3270 ~3510	3389 (hexane sol.)[4]	2500 ~2910	2550 (hexane sol.)[4]

Analysis and Interpretation of Spectra

Short Wave-lengths Absorption Regions of Acetophenone and Benzophenone

The symmetry of the carbon-oxygen skeleton of the acetophenone molecule belongs to the point group C_s, in which the electronic transition derivable from the forbidden transition ${}^1A_{1g}-{}^1B_{2u}$ of the benzene molecule (D_{6h} symmetry) is of the type $A'-A'$, and is allowed in this symmetry having the transition moment in the plane of symmetry, *i. e.* the molecular plane. The electronic terms of representations A_{1g} and B_{2u} in D_{6h} symmetry go over into the A_1 and B_1 terms in molecules of C_{2v} symmetry, and the transition between these two terms is allowed having the transition moment in the molecular plane and perpendicular to the C_2 axis. The vibrational structures in the strong absorption systems lying in the 2500~2800 A. region of mono-substituted benzenes, *e. g.* mono-chlorobenzene[5] and benzaldehyde,[1] have been analyzed from this viewpoint. In these substituted benzene spectra the "forbidden" character of the benzene 2650 A. system still remains in that non-totally symmetric vibrations of proper symmetries, excited to an odd quantum state, can interact with the electronic transition to make bands bearing their frequencies to be observed.

Now, the B_1 term in C_{2v} is symmetric with respect to the molecular plane and anti-symmetric with respect to the plane perpendicular to it, so that by dropping the latter symmetry element both A_1 and B_1 terms go over into A' type terms in C_s.[6]

Wave-numbers of the observed band heads in the acetophenone short wave absorption are given in Table 2.

The strong and sharp head at 35375 cm^{-1} is taken to be the 0,0 vibrational transition.

Table 2

The Short Wave-lengths Absorption Bands of Acetophenone Vapor

Wave-length A.	Wave-number $cm.^{-1}$	Intensity	Distance from the 0,0 band $cm.^{-1}$	Combination
2826	35375	s.	0	0,0
2797	35742	v. w.	367	0,367
2783	35922	v. w.	547	0,547
2752	36326	s.	951	0,954
2724	36700	w.	1325	0,367+954
2711	36876	w.	1501	0,547+954
2681	37288	m. w.	1913	0,2×954
2645	37796	v. w.	2421	0,547+2×954
2615	38230	v. w.	2855	0,3×954

In the intensity column: s. strong; w. weak; m. medium.

Table 3

Fundamental Vibration Frequencies of the Acetophenone Molecule found in U. V. Absorption

Raman effect (ground state)[7]			U. V. Absorption (excited state)	Symmetry	
$\Delta\nu$ $cm.^{-1}$	Intensity	Depolarization Factor ρ		C_{2v}	C_s
368	3b	p?	367	α_1	α'
406	1/2	—			
617	6s	0.78	547	β_1	α'
999	15s	0.10	954	α_1	α'

(3) J. Bielecki and V. Henri, *Ber.*, **47**, 1690 (1914).
(4) International Critical Tables, Vol. V.
(5) H. Sponer and S. H. Wollman, *J. Chem. Phys.*, **9**, 816 (1941).
(6) H. Sponer and E. Teller, *Rev. Mod. Phys.*, **13**, 75 (1941).

This band and the three bands at 36326, 37288, and 38230 cm.$^{-1}$ form the main progression, giving a frequency interval of 954 cm.$^{-1}$, which is the mean value obtained from these four bands and other bands containing multiples of this frequency in combination with other fundamentals. This 954 cm.$^{-1}$ must be the excited state value of the 999 cm.$^{-1}$ frequency found in the Raman effect for this substance. The intensity decreases regularly along this progression in accordance with the Boltzmann law. Two weak bands with wave-numbers 35742 and 35922 cm.$^{-1}$ are separated from the 0,0 band by 367 and 547 cm.$^{-1}$, respectively, on its violet side. These distances probably represent the upper state values of the 368 and 617cm.$^{-1}$ ground state frequencies observed in Raman effect, and are analogues of the 404 and 549 cm.$^{-1}$ excited state frequencies of the benzaldehyde molecule observed in ultraviolet absorption,[1] whose ground state values are 439 and 623 cm.$^{-1}$, respectively. We may apply to these bands the same interpretation as done for benzaldehyde, and say that they arise from the splitting of the degenerate 606 cm.$^{-1}$ (ground state value) ε_g^+ vibration of the benzene molecule into one of the β_1 type non-totally symmetric vibration of a frequency nearly of the unchanged magnitude, and another of the α_1 type totally symmetric vibration of a much lower frequency in going over into mono-substituted benzenes having C_{2v} symmetry. In such cases usually the α_1 type vibration appears with a much higher intensity than the β_1 type. In acetophenone, however, these bands are observed with almost the same intensity. This may be understood if we assume that the symmetry of the molecule is still lowered to C_s, and, by the same reason as stated above for the electronic states (which applies as well to the symmetry properties of molecular vibrations), the two types of vibration have become indistinguishable. On the other hand, polarization measurements of Raman lines clearly indicate the C_{2v} characters of these vibrations as seen in Table 3, so that we may consider there still remains a pronounced two-fold axis in the acetophenone molecule.

Other bands on the shorter wave-length side are all very diffuse, but several peaks can be measured and assigned to combinations of the fundamental frequencies found above as given in Table 2.

The short wave-lengths absorption of benzophenone vapor (2910-2500 A.) is continuous as stated earlier. This is to be expected because chances of the occurrence of predissociation increase as the molecule becomes more complex, and although this absorption region arises from electronic transition of the same type as the acetophenone short wave region, it has lost the discrete vibrational structure possessed by the latter.

Long Wave-lengths Absorption Regions of Acetophenone, Benzophenone and Benzaldehyde

The absorption region between 3060 and 3500 A. of acetophenone and that between 3270 and 3510 A. of benzophenone are both very weak and continuous. In connection with these weak absorptions, we may consider the corresponding long wave absorption bands of benzaldehyde vapor previously reported by Almasy.[8] This system (Almasy's première région) extends from 3160 to 3747 A., and contains a large number (159 measured by Almasy) of narrow weak bands, showing a pronounced group appearance. We have re-examined this region using the 1st. order of a 3 meter focus concave grating spectrograph,

Table 4

Long-wave Absorption System in Benzaldehyde Vapor

Wave-number cm.$^{-1}$	Relative intensity	Wave-number distance from band 26915 cm.$^{-1}$	Vibrational assignment
26892	s.	−23	
26915	v. s.	0	0
26943	v. s.		
26973	s.		
27636	s.	721	721
28005	s.	1090	1090
28098	s.		
28156	s.		
28229	v. s.	1314	1310
28253	s.		
28280	s.		
28357	m.	1442	2×721
28386	s.		
28949	m.	2031	721+1310
29319	s.	2404	1090+1310
29340	s.		
29404	s.		
29440	s.		
29528	v. s.	2613	2×1310
29559	v. s.		
30259	s.	3344	721+2×1310
30627	s.	3713	1090+2×1310
30842	m.	3927	3×1310

(7) K. W. F. Kohlrausch, "Ramanspektren", Akademische Verlagsges. Leipzig, 1943.

(8) F. Almasy, *J. Chim. Phys.*, **30**, 528, 634, 713 (1933).

and an absorption path of 1 meter at saturation pressures of benzaldehyde corresponding to 180°C at the highest (over 1 atmosphere). The total absorption intensity of this system appears to be of the order of 10^{-3} or smaller compared with that of the short wave system. Stronger bands in this system, according to our measurements, are listed in Table 4, together with probable vibrational assignments.

The three excited state frequencies 721, 1090 and 1310 cm.$^{-1}$ found in the above analysis may be identified in mode with the ground state frequencies of the benzaldehyde molecule 799, 1208 and 1434 cm.$^{-1}$, respectively, found in the analysis of the short wave absorption system.[1] All of these are of the α_1 type, and the ratio of the excited state value to the ground state value is 0.90 in all cases. The completely different appearances of the vibrational structures of the short and the long wave systems are due to the fact that no common vibrational modes are excited in the respective upper electronic states. This may be understood by considering the difference in nature of the two upper electronic states as stated below, but the fact that the carrier molecule is the same for the two systems is established unambiguously by the relations found above.

McMurry[9] has discussed, using mainly liquid phase data, the elctronic transition of the long wave-lengths absorption near 3500 A. invariably appearing in spectra of aliphatic and aromatic aldehydes and ketones, and has concluded that the upper state of this transition is the one which arises from the excitation of one of the non-bonding electrons localyzed on the oxygen atom of the C=O group, while the short wave system corresponds to the excitation of the ring π electron. The weakness of the long wave absorption is attributed to the fact that its upper state is one of the ^{1}E states theoretically predicted by Mulliken, to which the electronic transition from the ground state ^{1}N is forbidden.

Assuming this interpretation to be true, and if the forbiddenness is due to the symmetries of the electronic eigenfunctions, the band 26915 cm.$^{-1}$, the strongest first member of the progression with the 1310 cm.$^{-1}$ interval which is arbitrarily chosen as the origin in the above analysis (Table 4), may not be the 0,0 band of the system, and the 0,0 frequency may lie, just as in th case of the benzene 2650 A. forbidden transition, at a still longer wave-length shifted by the frequency of a certain non-totally symmetrical vibration which makes this system to be observed on the spectrum.

The authors express their thanks to the financial aids given them by the Scientific Research Funds of the Board of Education.

Chmical Laboratory, Faculty of Science, Kyushu University, Fukuoka.

(9) H. L. McMurry, *J. Chem. Phys.*, **9**, 231, 241 (1941).

The Near Ultraviolet Absorption Spectrum of *p*-Cresol Vapor

By Sunao IMANISHI and Mitsuo ITO

(Received January 23, 1952)

Introduction

The near ultraviolet absorption by *p*-cresol in the vapor phase, extending in the spectral region between 2480 and 2950 A., and having the strongest band corresponding to the 0,0 vibrational transition at 2829 A., was studied by Purvis and McCleland,[1] and by Savard.[2] Savard's photograph of this absorption system is reproduced in Sponer and Teller's surveying article on "The Electronic Spectra of Polyatomic Molecules".[3] Robertson and his coworkers[4] utilized the spectra of *p*-, *o*-, and *m*-cresol vapors for their quantitative chemical analysis of synthetic cresol mixtures, and also reproduced their spectrograms in their paper.

As to the more modern interpretation of the origin of the *p*-cresol spectrum, Sponer,[5] and Cave and Thompson,[6] both on re-examining

(1) J. Purvis and N. McCleland, *J. Chem. Soc.*, **103**, 1088 (1913).

(2) J. Savard, *Ann. de chim.*, **11**, 287 (1929); *Compt. rend.* **188**, 762 (1929).

(3) H. Sponer and E. Teller, *Rev. Mod. Phys.*, **13**, 75 (1941), on page 120.

(4) W. W. Robertson, N. Ginsburg, and F. A. Matsen, *Ind. Eng. Chem.*, **18**, 746 (1946).

(5) H. Sponer, *J. Chem. Phys.*, **10**, 672 (1942).

(6) W. T. Cave and H. W. Thompson, Farad. Soc. Discussions, 1950, p. 35.

Savard's published data, found out several conclusive features completely in line with results obtained recently for many of closely related molecules, *i. e.* mono- and di-substituted benzenes.

Savard's work, while appearing to contain the most reliable experimental informations on this spectrum so far published, gives us only three or four fundamental vibrational frequencies of the molecule, all of them belonging to the excited electronic state involved in the absorption transition. In order to complete the observational data for this band system, and also for the corresponding systems of *o*- and *m*-cresols appearing in the same wave-lengths region, at least to the extent achieved for their parent substance toluene,[7] we have photographed them anew, varying the concentration of the absorbing molecules in much wider range than by the previous workers. In this paper results of analysis for the *p*-cresol spectrum will be reported.

Experimental

For photographing the cresol vapor spectra a laboratory-built quartz spectrograph having a 120 cm. focus (for visible light) camera lens and a mean linear dispersion of 6 A. per mm. in this region was employed. The light source, absorption cell, and procedures of photography etc. are the same as described in our previous paper published in this journal on the near ultraviolet absorption spectra of acetophenone and other vapors.[8]

Commercial *p*-cresol sample supplied by Kanto-Kagaku Chemcals Mfg. Co. was used after several careful distillations in air. Unfortunately a very small trace of *o*-cresol could not be completely removed by such ordinary distillations, and a few of the strongest bands due to the latter isomer were recorded on some of our spectrograms. These could easily be identified and eliminated by comparing with our measurements of *o*-cresol bands, except perhaps in several cases where the close superposition might have affected the measured *p*-cresol wave-lengths slightly.

Exposures were made at the following temperatures of the liquid reservoir (Table 1), but the vapor filling the absorption cell (length 40 cm.) was always kept at a temperature 5 to 10 degrees higher than that of the liquid reservoir to prevent condensation on the windows and wall of the cell.

The finer details of the structure on the shorter wave-length side of the 0,0 band are best observed on exposures made at temperatures below 60°C. At higher temperatures the absorption in this region becomes so intense that a complete continuum results, and as we elevate the temperature and pressure, bands corresponding to excitations of higher frequency vibrations in the ground electronic state of the molecule gradually appear on the red end of the continuum. All bands of this system are degraded towards the longer wave-length side. Wave-lengths of band heads measured on different spectrograms are averaged and the correspondingv acuum wave-numbers are listed in Table 2. Head wave-lengths observed at very different vapor densities and temperatures may differ slightly from each other, depending mainly on different photographic densities, and, to some extent, on different developments of the rotational structure. But in the majority of cases they agree within 0.1 A. which is about the limit of accuracy of our measurements for sharp heads. A few bands, especially those "satellites" accompanying closely on the longer wave side of very strong bands, show no heads, and for them positions of maximum intensity are measured and given in Table 2 with the letter m affixed in the intensity column. In the notation adopted in the last column of the table, numbers standing on the left of the comma refer to excitations of ground state vibrations, and those on the right, to electronically excited state vibrations.

Interpretation of Spectrum and Discussion

The electronic transition responsible for this absorption system is an "allowed" one as in all substituted benzenes, and the 0,0 band must be the strongest, as the one at 35338 cm.$^{-1}$ actually is. Fundamental vibrational frequencies of the molecule participating in this transition are listed in Table 3 against the published Raman and infra-red data observed in the liquid

The difference frequency -23 cm.$^{-1}$ used in the above analysis occurs always with satellite bands mentioned in the preceding section, for which heads could not be measured. If examined under much higher resolution, these bands would be more satisfactorily explained as arising from the 1-1 transition of a certain low frequency fundamental, or superposition of 1-1 transitions of several different fundamentals, accompanying each strong main transition.

The *p*-cresol molecule has, strictly speaking, no

Table 1

Temperature of liquid (°C.)	20	30	40	50	60	70	80	90	100	110	120	130	140
Saturated Vapor pressure (mm.Hg)	.08	.18	.40	.83	1.7	3.3	6.1	11	18	30	47	71	108

(7) N. Ginsburg and W. W. Robertson, *J. Chem. Phys.*, **14**, 511 (1946).

(8) S. Imanishi, K. Semba, M. Ito and T. Anno, *This Bulletin*, **25**, 150 (1952).

Table 2

Near Ultraviolet Absorption Bands of *p*-Cresol Vapor.

m: Intensity-maxima data.

*: Measurement probably affected by superposition of a strong *o*-cresol band.

Wave-Number ($cm.^{-1}$)	Intensity, °C												Interpretation
	140	130	120	110	100	90	80	70	60	50	40	30	
(33964)	00	00											1374, 0; 3×458, 0
34004	00	00											839+499, 0
042	0	0											1296, 0; 2×648, 0
079	0	0	00										1259, 0
107	00	00											1231, 0
147	0	0											458+734, 0
186	3	2	00	00									1152, 0
226	5	4	0	00									2×230+648, 0; 648+458, 0
264	8	8	1	0	00								230+839, 0
339			8	0	00								2×499, 0
385				3	0								458+499, 0
423				10	3								2×458, 0
460				10	4								230+648, 0; 734+839. 694
499				10	7	0	00	00					839, 0
562				10	2								2×734, 694
604					5								734, 0
654					10	00							230+458, 0
690						00							648, 0
718						00	00						2×310, 0; 839, 217
764						0							230+310+458, 422
804						4	0	00					310+648, 422
839						8	2	1					499, 0
880						10	5	2	0				458, 0; 1152, 694; 2×230, 0
940							0	00					2×230, 217
993							1	0					1152, 808
35028							5	4	00				734, 422, ; 310, 0
069								3	0				230+734, 694
108							10	7	3	1	00		230, 0; 648, 422
179									2	0	00		159, 0: 230+734, 808
229									4	2	00		1259, 1153
261								10	10	7	3	1	499, 422
283												3	230+734, 217+694
298										10	7	5	734, 694
308										7m	4m	5m	839, 808
317											5m	4m	0, −*23*
338									10	10	10	8	0, 0
397							10	7	2	1	0	00	159, 217
469							5	3	00				458, 585
515								4	0				734, 217+694
536								3	0				499, 694
555							8	5	2	0	00		0, 217
650									2	00	00		839, 1153; 499, 808
686									3	0	00		458, 808
719									3	1	0		734, 422+694
725									1m	00m			839, 1226; 1152, 1536; 310, 694; 1231, 2×808
738									2m	0m			0, 422-*23*
760								10	5	2	1	1	0, 422; 734, 1153
(807)								3	0				1152, 2×808
879									0				
901									0	00			

Wave-Number (cm^{-1})	Intensity, °C												Interpretation
	140	130	120	110	100	90	80	70	60	50	40	30	
35923									2	0	00		0, 585
981									1	0	00		0, 217+422
36032										2	0	00	0, 694; 458, 1153
068									10	8	3	2	499, 422+808
103											8	2	734, 694+808; 458, 1226
109											3m	2m	458, 422+808
120											3m	2m	0, 808-*23*; 839, 2×808
146									10	10	10	8	0, 808
205*									4	3	1	0	159, 217+808
294									2	2	1	0	458, 217+1196
354*										7*	5*	4*	0, 217+808
454									4	1	0		499, 2×808
491									5	3	2		0, 1153; 458, 2×808
534									8	6	4	3	0, 1196; 939, 808+1226; 1231, 3×808
564									6	4	2	1	0, 1226; 310, 1536; 0, 422+808
610									5	4	2	2	0, 1272; 1152, 3×808
730									0	00	00		0, 585+808; 0, 2×694; 230, 2×808
830*									4	3	2	0	0, 217+1272
874									5	3	1	00	0, 1536; 499, 1226+808
918									7	5	3		458, 422+2×808; 734, 694 +2×208; 839, 3×808
955*									8	7	5	3	0, 2×808
37011*									1	0	0		159, 217+2×808
176*									0	00	00		0, 217+2×808
258*									0	00	00		499, 3×808;
305*									1	0			458, 3×808; 0, 1153+808; 0, 694+1272
318									3	1			0, 1196+808-*23*
341											1		0, 1196+808; 839, 1126 +2×808; 1231, 4×808
375									2	1			0, 422+2×808; 0, 1226+808
420								10	3	2	2	0	0, 3×694; 0, 1272+808; 1152, 4×808
476								3	1	00	00		499, 217+3×808
629								5	3	2	1	0	0, 217+1272+808
679*									2	0			0, 1536+808
723									2	1			734, 694+3×808; 839, 4×808
763								10	3	3	1	0	0, 3×808; 0, 1153+1272
807									4	2	0	00	0, 1196+1272
921*								3	1	0	00	00	648, 4×808
975								0	00	00			0, 217+3×808
38072*								8	3	1	1	0	499, 4×808; 0, 1196+1536
111								4	2	0	00		458, 4×808; 0, 4×694
148								5	2	0	00		0, 1196+2×808
197								2m	0m				1152+839, 6×808
227							5	5	2	0	0	00	0, 1272+2×808; 1152, 5×808
272							6	4	0				648, 1153+3×808
350							4	0					230, 4×808
410*							6	4	00				0, 2×1536
450							3	00					
469							3						
527							5	2	00				734, 694+4×808
567							6	5	1				0, 4×808
610							3	2	00				734+458, 422+5×808
(645)								0					734, 5×808

Wave-Number (cm^{-1})	Intensity, °C												Interpretation
	140	130	120	110	100	90	80	70	60	50	40	30	
38702							2	1					159+734, 217+5×808
786							1	00					0, 217+4×808
857							3	2					458+1296, 422+6×808
891							1	1					1296, 6×808
952							2	1					1231, 6×808; 0, 1196+3×808
39004							2	1					0, 2×1196+1272
042							00	00					0, 1272+3×808; 1152, 6×808
284							00	00					
346						7	1	1					839, 6×808
380						2	0	00					0, 5×808
362						3	0	0					458+734, 422+6×808
447						1	00	00					734, 6×808
494						2	00	00					
545						1							
(583)						1							(0, 217+5×808)
(647)						1							
(699)						1							(499, 6×808)
(795)							0						(0, 422+5×808)
(829)						0							(0, 1272+4×808; 1152, 7×808)
(887)						0							(310, 6×808)
(982)						00							(230, 6×808)
(40233)						00							(0, 6×808)

Table 3

Fundamental Vibrational Frequencies of *p*-Cresol Molecule.

Raman Effect (Liquid)				Ultraviolet Absorption (Vapor)					Infra-Red Abs. (Liquid) [11]
				Ground State	Excited State				Ground State
				Present Work				ref. 5,6	
$\Delta\nu$ (Intensity) [9]		Depolarization Factor[9], ρ	Assignment[10] (C_{2v})						
				159					
				230	β_1	or	α_2	217	
338	(4)	1.00	ω_{10}, β_1	310	β_1				
465	(5)	0.52	ω_{11}, α_1	458	α_1		422	419	
507	(0)			499					
649	(5)	0.92	ω_2, β_1	648	β_1		585		
703	(0)	0.87							680~690 (w)
736	(1)			734	α_1		694		720~730 (w)
822	(3)	0.15							818 (st)
842	(10)	0.07	ω_1, α_1	839	α_1		808	808	860~870 (w)
1016	(00)								910~920 (m) 1000~1010 (w) 1080 (m)
1171	(2)	0.34	δ_3, α_1	1152					1170~1180 (st)
1214	(5)	0.09	ω_4, α_1	1231			1153		
1256	(3)	0.07	ω_3, α_1	1259			1196	1187	
1297	(0)	0.55		1296			1226		
1381	(3)	0.49		1374			1272	1268	
1450	(00)	0.92							
1615	(4)	0.74					1536		
2864	(1/2)	p							
2922	(2)	p							
3015	(1/2)	p							
3046	(3)	0.47							

(9) K. W. F. Kohlrausch u. A. Pongraz, *Monatsh. f. Chem.*, **63**, 427 (1933).

(10) O. Paulsen, *Monatsh. f. Chem.*, **72**, 244 (1939).

(11) J. Lecomte, *J. Phys. radium*, **9**, 13 (1938).

symmetry element, but as far as the ultraviolet absorption is concerned, skeleton vibrations involving only heavy-atom-containing bonds chiefly come into question. In this sense the molecule has approximately the C_s or even C_{2v} symmetry if we take the oxygen atom of the OH group as lying in the ring plane. Then its mass distribution is nearly the same as in the *p*-fluorotoluene molecule, the ultraviolet absorption of which was investigated by Cave and Thompson in the vapor phase.[6] They found the following fundamental frequencies in this molecule.

p-Fluorotoluene. 0,0 band at 36876 $cm.^{-1}$

Excited State	185,	—,	—,	398,	584,	794,
Ground State	217,	311,	377,	453,	641,	825,

Excited State	843,	1014,	1194,	1229 cm^{-1}.
Ground State	844,	1156,		cm^{-1}.

From the close parallelism between these and the *p*-cresol fundamentals given in Table 3, we may identify 230 (217) $cm.^{-1}$ in *p*-cresol wlth 217 (185) $cm.^{-1}$ in *p*-fluorotoluene in mode of vibration, even though no corresponding Raman shifts are reported. At the same time we notice the characteristic structure-sensitiveness of this low-frequency fundamental in that its values are approximately in the inverse ratio of the masses of the OH group and the F atom in both the electronic states. There is another set of frequencies 734 (694) $cm.^{-1}$ in *p*-cresol and 825 (794) $cm.^{-1}$ in *p*-fluorotoluene, which, apparently, is also structure-sensitive, but in comparing the respective Raman values the physical correspondence of these fundamentals in the two molecules seems doubtful. Now the structure-sensitive 230(217)$cm.^{-1}$ frequency of *p*-cresol must be of the mode in which the C-OH bond chiefly changes, and we suggest that it is the bending of this bond in the ring plane (β_1 type) or perpendicular to it (α_2 type), the single quantum excitation of either of which can produce a transition moment with the elec tronic transition under consideration (A_1-B_1). This is supported by the fact that the manner in which the 217 $cm.^{-1}$ excited state frequency combines with other α_1 type fundamentals clearly indicates its non-totally symmetric nature (see Table 2).

In mono-substituted benzenes we find the analogous behavior of a low frequency fundamental around 200 $cm.^{-1}$, so far judged from vapor ultraviolet absorption data. Thus in phenol,[12] monofluorobenzene,[13] aniline,[14] benzaldehyde,[15] benzonitrile,[16] and benzotrifluoride[17] fundamental frequencies 245, 240 (assigned to α_2), 231, 223 (α_2 or β_1), 170 and 141 (assigned to β_1) $cm.^{-1}$, respectively, are reported. These are again in the inverse order of the masses of theOH, F, NH_2, CHO, CN and CF_3 groups or atom, and their corresponding Raman lines are all depolarized, suggesting their belonging to the similar bendings of the substitution bonds in these mono-substituted benzene molecules.

Returning to *p*-cresol, we have taken another low frequency fundamental 159 $cm.^{-1}$ in the ground state from the appearance and intensity of the 35179 $cm.^{-1}$ band on the longer wave-length side of the 0,0 band, although an alternative interpretation can be given to this band as shown in Table 2. The weakly excited β_1 type 310 $cm.^{-1}$ ground state frequency has its analogue 311 $cm.^{-1}$ in *p*-fluorotoluene, while their closely coinciding Raman counterparts are not found. Another β_1 type frequency 648 (585) $cm.^{-1}$, which originated from the ε_g^+ type 606 $cm.^{-1}$ degenerated vibration in benzene is also weakly excited in both states. Correspondence between other structure-insensitive fundamentals and the Raman values is generally good as we see in Table 3.

The authors express their gratitude to the financial aids from the Scientific Grant of the Ministry of Education.

Chemical Laboratory, Faculty of Science, Kyushu University, Fukuoka

(12) F. A. Matsen, N. Ginsburg, and W. W. Robertson, *J. Chem. Phys.*, **13**, 309 (1945).
(13) S. H. Wollman, *J. Chem. Phys.*, **14**, 123 (1946).
(14) N. Ginsburg and F. A. matsen, *J. Chem. Phys.*, **13**, 167 (1945).
(15) S. Imanishi, *J. Chem. Phys.*, **19**, 389, (1951)
(16) H. C Hirt and J. P. Howe, *J. Chem. Phys.*, **16**, 480 (1948).
(17) H. Sponer, *J. Opt. Soc. Am.*, **39**, 840 (1949); also reference (6).

Dipole Moments of Some Hydroxyl Compounds

By Keniti HIGASI

(Received December 12, 1951)

In this note the present author wishes to report some unpublished values of dipole moments of phenol derivatives and also discuss the influence of solvent upon the moments of hydroxyl compounds in general.

In Table 1 the electric moments of three isomers of cresol, chlorophenol and nitrophenol are recorded with those of phenol and chlorobenzene. The values of the table were obtained by the dilute solution method, toluene being chosen as solvent; and the following equation was used in the calculation of moments: $\mu=0.127\sqrt{P_{2\infty}-MR_D}$, the symbols having the usual significance.

Table 1

Dipole Moments in Debye Unit

Cresols			
temp. (°C.)	ortho	meta	para
0	1.35	1.66	1.62
25	1.35	1.61	1.58
50	1.35	1.58	1.57
75	1.38	1.58	1.54
Chlorophenols			
0	1.23	2.06	2.26
25	1.24	2.08	2.24
50	1.24	2.10	2.25
75	1.24	2.12	2.23
Nitrophenols			
0	3.06	3.66	—
25	3.12	3.76	4.72
50	3.16	3.86	4.63
75	3.16	3.86	4.60

Phenol and Chlorobenzene		
temp. (°C.)	Phenol	Chlorobenzene
0	1.52	1.54
25	1.49	1.56
50	1.44	1.57
75	1.43	1.57

As toluene is seldom used as the solvent for dipole moment work, a comparison is made with the values in benzene[1] for the substances measured (see Table 2). In spite of the difference in polarity between the two solvents, no appreciable deviation* is found between the values of the second and third columns of the table.

Table 2

Dipole Moments and Solvents

Solute	Solvent	
	Benzene	Toluene
o-Cresol	1.41	1.35
m- 〃	1.54	1.61
p- 〃	1.57	1.58
o-Chlorophenol	1.33	1.24
m- 〃	2.10	2.08
p- 〃	2.22	2.24
o-Nitrophenol	3.11	3.12
m- 〃	3.90	3.76
p- 〃	5.02	4.72
Phenol	1.56	1.49
Chlorobenzene	1.57	1.56

On inspection, it is seen in Table 1 that the moments of most of the ortho and meta disubstituted compounds increase with the increase in temperature. One might interpret this increase as the change of the equilibrium-ratio of the *cis-trans* isomers with temperature, or one might instead favor the hypothesis of inner-molecular rotation. Indeed, one could succeed in calculating the moments on any of these assumptions. However, such calculations are equally unreliable, since the moment of phenol itself is not independent of temperature. It is also to be noted that para derivatives of phenol show the same decrease with temperature in moment, which is certainly either due to association or to solute-solvent interaction.

Recently Nagakura and Baba[2] pointed out that the electron migration plays an important role in moments of aromatic molecules. It is not unlikely that such an effect is also included in the moments recorded here, but admittedly the observed temperature-variation should not be regarded as arising solely from this cause.

(1) "Table of Electric Dipole Moments" Massachusetts Institute of Technology, 1949.

* Exceptions to this rule occur in the cases of *m*- and *p*-nitrophenols.

(2) Nagakura, and Baba Shortly to be printed in J. Am. Chem. Soc., **74** (1952)

It is a well-known fact that hydroxyl compounds are apt to associate together into groups by the formation of hydrogen bonds. Further, it has often been pointed out that these molecules easily interact with hydrogen bonding solvents such as dioxane and ethers.[2][3] The present author once examined the use of ethyl ether as a solvent for dipole moment studies and found that it reduces the degree of association of alcohol to a remarkable extent, that there should be no peak in P_2—x curve in ether solution[4] (Fig. 1). This remarkable phenomenon can be explained by the hypothesis that on account of the strong interaction between the solute and the solvent there are scarcely any associated solute molecules in the diluted part of the ether solution. This explanation is in good accord with the higher moment of alcohols in ether, *viz.*, 1.8-1.9D., while further support may be found in the recent work of Nagakura and Baba.[2] Moreover, the high dielectric constant of ether is certainly able to reduce the degree of association, but it cannot possibly be the dominant cause of this phenomenon.

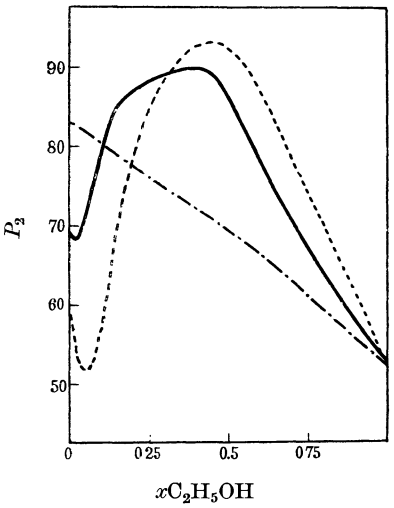

Fig. 1.—The molecular polarization of ethyl alcohol in various solvents. P_2 are plotted against the concentrations of alcohol: ——benzene; ····hexane; -·-· ethyl ether.

The formation of hydrogen bonds with benzene is not certain. But a very weak tendency to form such a solute-solvent interaction may be suspected, since benzene also gives a less pronounced maximum of polarization and a slightly higher moment for alcohols than any other normal solvents. Consequently, the result in toluene, which resembles benzene in many respects, may not be free from the possible errors arising from this sort of solute-solvent interaction.

Summary

Dipole moments of cresols, chlorophenols and nitrophenols were measured in toluene at 0°, 25°, 50° and 75°C. They are found to be in general agreement with the corresponding values measured in benzene. Further, factors which may affect the moment are considered in detail. As a connected topic it is shown that some anomalies of hydroxyl compound in ether are explainable by the hypothesis of hydrogen bond formation with the solvent.

Research Institute of Applied Electricity
Hokkaido University, Sapporo

(3) Curran and Estok, *J. Am. Chem. Soc.*, **72**, 4575(1950).
(4) Higasi, *Sc. Pap. I. P. C. R.* (Tokyo) **24**, 57 (1934).

On the Molecular State of Water Bound to the Peptide Linkage

By Masamichi TSUBOI

(Received February 8, 1952)

According to A. M. Buswell *et al*[1] and K. Kuratani[2] the water molecules bound to gelatin and other proteins cause infrared absorption bands which range from 2.85 μ to 3.03 μ. As Sponsler, Bath, and Ellis[3] have pointed out, these water molecules must be of

(1) A. M. Buswell, K. Krebs and W. H. Rodebush, *J.Am. Chem. Soc.*, **59**, 2603 (1937); *J. Phys. Chem.*, **44**, 1126 (1940).

(2) K. Kuratani, *Raports of the Radiation Chemistry Research Institute (Tokyo Univ.)*, Vol. III, 14 (1949).

(3) O. L. Sponsler, J. D. Bath and J. W. Ellis, *J. Phys. Chem.*, **44**, 996 (1940).

two kinds—(1) those bound to the peptide linkages in the backbone of protein and (2) those bound to the polar groups in the side chains. In order to obtain information about the molecular state of water bound exclusively to the peptide linkage, the present writer made 3μ region infrared absorption measurements of a film of "amilan" (Poly ε-capramide),[4]

$$\ldots\ldots-(CH_2)_5-CONH-(CH_2)_5-CONH-\ldots,$$

in dry as well as in wet state, and found that there exists a band at about 2.86 μ which is attributable to the water bound to the peptide linkage in this compound. The result obtained and its interpretation are given in this paper.

The dried specimen of amilan used here was prepared by keeping an amilan film for two weeks in a sealed tube specially made of silica glass with plane-parallel windows as shown in Fig. 1, which contained concentrated H_2SO_4

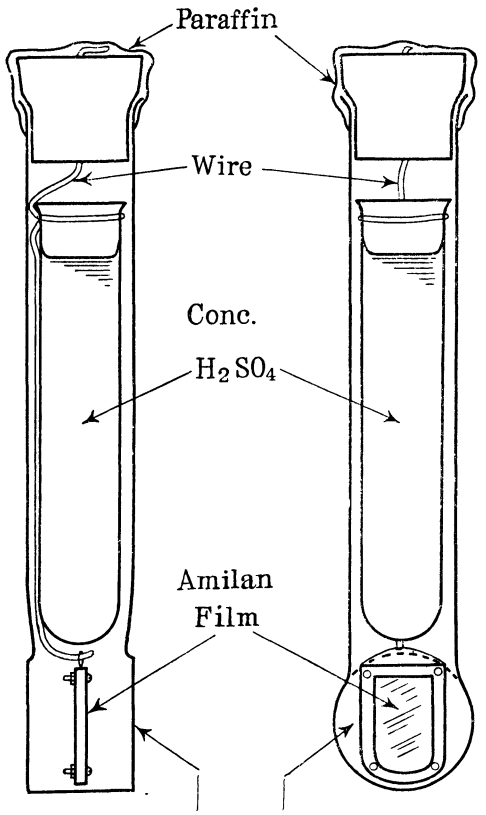

Windows of plane parallel silica glass plates

Fig. 1.

as is illustrated.[5] The dried film within the tube was subjected to the spectroscopic measurement without being taken out, by passing the infrared radiations through the film between the plane parallel windows. The result of this measurement is shown graphically by curve A in Fig. 2, where the infrared absorptions due to the silica glass plates of the windows have been eliminated. Curve B in Fig. 2 is obtained on the same amilan film, measured after it was taken out from the tube

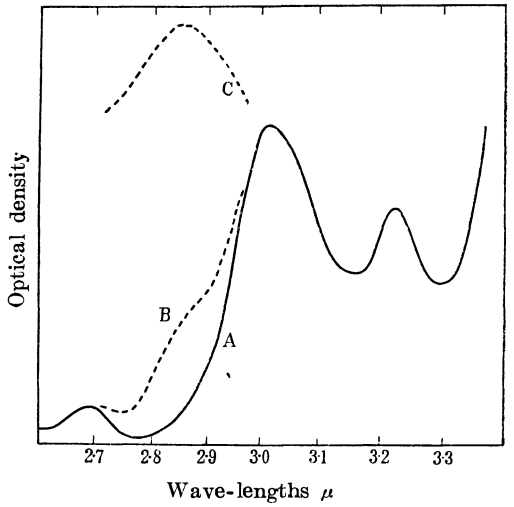

Fig. 2.—Infrared absorption curves for (A) conc. H_2SO_4-dried amilan film, (B) amilan film under water vapor of 0.01 atm., and (C) water bound to amilan.

and exposed to the air of 76% relative humidity at 11°C. (*i. e.* 0.01 atmospheric pressure of water vapor). According to the private communication of Mr. H. Yumoto, amilan contains in the air of this humidity about 0.3 mole of H_2O per $-(CH_2)_5-CONH-$ unit (=113 g.) in equilibrium. As is seen in the figure, deviation of the absorption spectrum of wet amilan from that of dry amilan is conspicuous in 2.8-2.9μ region. Curve C in Fig. 2 represents the absorption spectrum due to the water bound to amilan as obtained by subtraction of the data of curves A from B (B —A). It shows an absorption peak at about 2.86μ, which may be associated to the O—H stretching vibrations in the bound-water molecules. It is noteworthy that, while bound-water of gelatin and other proteins always shows absorptions not only in 2.85-2.90μ region but also in 2.90-3.03μ region, the amilan-bound-water shows an absorption only at 2.86μ and not in the 2.90-3.03μ region. This fact may be taken as indicating that the water molecules which cause the absorption in the 2.90-3.03μ region are those bound to side chains of the proteins, and those bound to the peptide linkages cause the absorption at about 2.86μ.

(4) Material of synthetic fibers made by the Toyo Rayon Co.

(5) The writer owes to Mr. H. Yumoto's suggestion in devising this drying apparatus.

Table 1

Molecules and their states	Number of perturbing hydrogen bonds versus maximum possible number of perturbing hydrogen bonds	Positions of O—H bands	Observers
		μ	
H_2O in CCl_4	0/4	2.70	Fox and Martin[7]
in amilan	2?/4	2.86	Tsuboi
pure water	4/4	2.95	Fox and Martin[7]
ice	4/4	3.08	Fox and Martin[7]
gelatin		2.85—3.03	Buswell, Krebs, and Rodebush[1]; Kuratani[2]
ROH in CCl_4 (dil.)	0/2	2.74	Fox and Martin[8] Smith and Creitz[9]
in 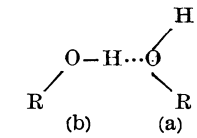 (b) (a)	1/2	(a) 2.76	Fox and Martin[8] Smith and Creitz[9]
		(b) 2.86	Smith and Creitz[9]
$ROH\cdots O(CH_3)C_6H_5$	1/2	2.80	Tsuboi[10]
$ROH\cdots O(C_2H_5)_2$	1/2	2.85	Tsuboi[10]
pure liquid	2/2	2.95	Smith and Creitz[9], and others
pyridine	1/2	3.00	Errera and Sack[11]

It is also noticed that the O—H band of amilan-bound-water or peptide-bound-water is situated at a wave-length much shorter than the O—H band of pure water (at 2.95μ). This indicates that the water molecule in peptide linkage is in a less distorted state than the water molecule in pure water.

Further details of the molecular state of the peptide-bound-water may be conjectured from the position of its O—H band in the following way.

The positions of the O—H bands of H_2O as well as of other hydroxy molecules (ROH) depend upon how far O—H vibrations in these molecules are perturbed through hydrogen bondings by other molecules. Each of these molecules has two possible types of perturbing hydrogen bonds—*i. e.* (I) hydrogen bonds through the hydrogens of the molecule under consideration and (II) hydrogen bonds through

(type I) O—H....X
X—H....O—H (type II)

the hydrogens of molecules other than the one under consideration.[6] In Table 1 are listed the positions of some of the O—H bands known for water and alcohol molecules perturbed in various ways. As may be seen from the table, the number of the perturbing hydrogen bonds of each type is a factor determining the degree of perturbation; and the strength of the proton-accepting or proton-donating powers of molecules with which the molecule under consideration is hydrogen-bonded is another factor. Thus, an alcohol molecule perturbed through the single hydrogen bond of type II by another alcohol molecule gives an O—H band at 2.76μ, and that perturbed through the single hydrogen bond of type I by another alcohol molecule (or ether molecule) gives an O—H band at about 2.86μ. While, an alcohol molecule perturbed through hydrogen bonds of both types (I and II) by other alcohol molecules gives an O—H band at 2.95μ. The carbonyl O in the peptide linkage is considered to be a stronger proton-acceptor than the ether or hydroxy O, because there is the electron migration from NH group towards the carbonyl group in the peptide linkage. It is expected, therefore, that the hydrogen bond O—H....O between the peptide C=O and the alcohol molecule, if it exists, should give O—H band at a longer wave-length than 2.86μ (Let its position be $2.86+\alpha\mu$).

Since the perturbation through the hydrogen bond of type II is weak as shown above, it is unlikely that the N—H....O bonding between the peptide N—H group and the bound-water molecule, which is one of the possible perturbing hydrogen bonds, is responsible by

(6) P. C. Cross, J. Burnham and P. A. Leighton, *J. Am. Chem. Soc.*, **59**, 1134 (1937).
(7) J. J. Fox and A. F. Martin, *Proc. Roy. Soc.(London)*, **A 174**, 234 (1940).
(8) J. J. Fox and A. F. Martin, *Trans. Faraday Soc.*, **36**, 897 (1940).
(9) F. A. Smith and E. C. Creitz, *J. Resear. Nat. Bur. Stand.*, **46**, 145 (1950).
(10) M. Tsuboi, This Bulletin **25**, 60 (1952).
(11) J. Errera and H. Sack, *Trans. Faraday Soc.*, **34**, 728 (1938).

itself for shifting the water band from 2.70μ (due to free H_2O) to 2.86μ. On the other hand, simultaneous perturbations of two types (I and II) as those in pure water may be ruled out for the bound-water molecule, because the O—H band under consideration is situated at a much shorter wave-length than that of pure water. The simple perturbation through hydrogen bonds of type I is the probable one for the present case. Calculations of the vibration frequencies of H_2O molecule[12] show that, if one of the two O—H's of a water molecule is perturbed through the hydrogen bond of type I by a peptide oxygen atom and the other O—H is left free, the molecule will give two O—H bands at about 2.7μ and at $2.86+\alpha\mu$, while, if both of its two O—H's are perturbed by peptide oxygen atoms, it will give two O—H bands, at a little longer wave-length than $2.86+\alpha\mu$ (corresponding to the symmetric stretching vibration) and at a little shorter wave-length than $2.86+\alpha\mu$ (corresponding to the antisymmetric stretching vibration). In the case now at issue no band attributable to the peptide-bound-water has been observed in the vicinity of 2.7μ,[13] showing that the bound-water molecule has no free O—H. Then, a view may be set forth here tentatively that the peptide-bound-water molecule has both of the two O—H's perturbed through O—H....O bondings by two peptide oxygen atoms (located near to each other),[14] and that the 2.86μ band corresponds to the antisymmetric vibration of that water molecule. The band due to the symmetric vibration, which, according to the above view, should appear at a little longer wave-length than $2.86+\alpha\mu$ has not been observed. This, however, may not necessarily be taken as vitiating the above view, for it is conceivable that this band is too weak to be observed, the dipole-moment-oscillation due to the symmetric vibration being smaller in amplitude than that due to the antisymmetric vibration.[15]

The bound-water band in the 2.90-3.03μ region observed on proteins may be attributed either to water molecules bound by much stronger proton-acceptor groups in the side chains such as ionized carbonyl groups, or to water molecules forming an aggregate around the polar groups just as those in liquid water.

A few words may be added here concerning the bound-water band at 2.86μ. In the writer's previous measurements of the 3μ region infrared absorption on egg albumin and horse serum albumin,[16] remarkable peaks at about 2.86μ were observed. This fact suggests that the water molecule bound to the carbonyl O in the backbone in the manner shown above are abundant in these proteins. On the other hand, the present writer's recent study on a film of poly-D, L-norleucine[17] (an isomer of amilan),

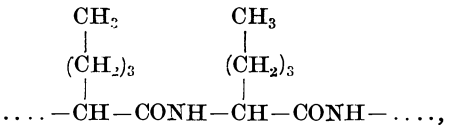

indicated that the film shows no absorption band at 2.86μ in the air of equal humidity as the air in which the measurement corresponding to the curve B for amilan (Fig. 2) was made. The crowded hydrophobic side chains ($-CH_2-CH_2-CH_2-CH_3$) seem to prevent the water molecule from reaching the backbone.

(12) In order to get knowledge about the coupling between the vibrations of two O-H's in a water molecule, the normal vibration frequencies of the water molecule were calculated, assuming the potential energy (V) of the molecule as,

$$V=\frac{1}{2}f_1(\Delta r_1)^2+\frac{1}{2}f_2(\Delta r_2)^2+\frac{1}{2}f_3(r_0\Delta\alpha)^2,$$

where r_1 and r_2 are the bond lengths of the two O-H's, r_0 the equilibrium O-H distance, α the angle HOH, and f_1 etc. the force constants. If we put $f_1=f_2=7.54655\times10^5$ dyne/cm, $f_3=0.70195\times10^5$ dyne/cm; we obtain three normal vibration frequencies: 3702, 3648, and 1600 cm^{-1}, which are close to the frequencies observed for water vapor (3750, 3650, and 1595 cm^{-1}). Fig. 3 and 4 show the two O-H stretching frequencies of H_2O molecule, as calculated by assuming that $f_1=f$(variable), $f_2=7.54655\times10^5$ dyne/cm., $f_3=0.70195\times10^5$ dyne/cm. (Fig. 3); and that $f_1=f_2=f$ (variable), $f_3=0.70195\times10^5$ dyne/cm. (Fig. 4). The dotted lines in the figures indicate the frequencies calculated for the case when the two O-H's vibrate independently of each other.

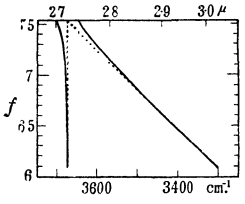

Fig. 3.

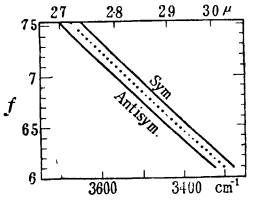

Fig. 4.

(13) Amilan shows a weak band at 2.7μ, but its intensity remains unchanged even when amilan is dried.

(14) The heat of adsorption of water into amilan from liquid water is, according to K. Hoshino and H. Yumoto (*J. Chem. Soc. Japan*, **70**, 104 (1949)), about -1 kcal/mol. From this the heat of adsorption from water vapor is calculated to be about -11 kcal/mol. This value is just as may be expected from the molecular state of the bound water here assumed.

(15) For instance, the symmetric O-H stretching vibration of H_2O gives much weaker infrared absorption band than the antisymmetric one in the CCl_4 solution (see reference (7)).

(16) M. Tsuboi, This Bulletin **22**, 255 (1949).

(17) This material was kindly placed by Dr. H. Tani (Osaka Univ.) at the writer's disposal.

In conclusion the writer wishes to express his sincere thanks to Professor San-ichiro Mizushima and Dr. Takehiko Shimanouchi for their kind guidance in this work, and to Mr. Hirosuke Yumoto for his valuable suggestions and for his placing the amilan film at the writer's disposal. The cost of this research has been partly defrayed from a Grant in Aid for Scientific Research from the Ministry of Education.

Department of Chemistry, Faculty of Science, Tokyo University, Tokyo

On the Electronic Structure of the Carbonyl and the Amide Groups

By Saburo NAGAKURA

(Received December 27, 1951)

Introduction

To the state of the molecule with the carbonyl or the amide group, the partially ionic structure, $\begin{matrix} R \\ R' \end{matrix}\!\!>\!C^+\!-\!O^-$ or $\begin{matrix} O^- \\ R \end{matrix}\!\!>\!C\!=\!N^+\!<\!\begin{matrix} R' \\ R'' \end{matrix}$ is expected to make large contributions.[1] By the use of these resonance structures, very satisfactory results have been obtained in the qualitative interpretation of many interesting physico-chemical properties of these groups, such as the large dipole moment[2] and the relatively low basicity of amide.[3]

In the present paper, the contributions of the partially ionic structures are theoretically treated by the molecular orbital method. The values of energy levels, resonance energies and π-electron densities are calculated for these two groups. Then these theoretical predictions are checked by the experimental values of resonance energies, dipole moments and near ultraviolet absorption spectra. Especially, as to absorption spectra, measurements were made in this laboratory with acetone, acetylchloride, acetic acid, ethyl acetate and N-methylacetamide. From these theoretical and experimental investigations, it is suggested that the weak near ultraviolet absorption spectrum characteristic of the unconjugated carbonyl group is due to the $n\rightarrow\pi^*$ transition, as was shown by Mulliken,[4] McMurry,[5] Baba[6] and Kasha.[7]

Theoretical

As is usual, only the π-electrons, of which there are two in the carbonyl group and four in the amide group, are considered. The molecular π-orbitals ψ_j $(j=1, 2, 3)$ in amide may be taken as linear combinations of the $2p$ atomic orbitals of oxygen, carbon and nitrogen atoms which are denoted by φ_O, φ_C and φ_N respectively. Using this approximation (LCAO), the following equation is obtained

$$\psi_j=a_{Oj}\varphi_O+a_{Cj}\varphi_C+a_{Nj}\varphi_N \qquad (1)$$

Neglecting the overlap integral S_{AB} between two atomic orbitals φ_A and φ_B, ies energthe E of these molecular orbitals are given approximately as the solutions of the following secular equation,

$$\begin{vmatrix} \alpha_O-E & \beta_{CO} & 0 \\ \beta_{CO} & \alpha_C-E & \beta_{CN} \\ 0 & \beta_{CN} & \alpha_N-E \end{vmatrix}=0 \qquad (2)$$

where α_A is the coulomb integral of A-atom and β_{AB} is the exchange integral between adjacent atomic orbitals φ_A and φ_B.

To evaluate the values of E, the following assumptions were made

$$\alpha_A=\chi_A\alpha/\chi_C,^{(8)}\ \beta_{AB}=S_{AB}\beta/S,^{(9)}\ \alpha=k\beta^{(8)} \qquad (3)$$

where χ_A represents the electronegativity of A-atom, S is the overlap integral between atomic orbitals belonging to adjacent carbon atoms

(1) L. Pauling, The Nature of the Chemical Bond, Cornell University Press 1940, p. 75, 133.
(2) W. D. Kumler and C. W. Porter, *J. Am. Chem. Soc.*, **56**, 2549 (1934).
(3) M. J. S. Dewar, The Electronic Theory of Organic Chemistry, Oxford University Press (1949), p. 94.
(4) R. S. Mulliken, *J. Chem. Phys.*, **3**, 564 (1935).
(5) H. L. McMurry, *J. Chem. Phys.*, **9**, 231 (1941).
(6) H. Baba, *J. Chem. Soc. Japan*, **72**, 214 (1951).
(7) M. Kasha, Discuss. Farad. Soc., Spectroscopy and Molecular Structure, 14. (1950),
(8) C. Sandorfy, *Bull. soc. chim. France*, (1949), 615.
(9) G. W. Wheland, *J. Am. Chem. Soc.*, **64**, 900 (1942).

Table 1

The Final Results of the Molecular Orbital Calculation with Amide

	I*	II*	III*	IV*	V*	VI*
α_C	4.297β	4.078β	4.378β	4.301β	4.085β	4.383β
α_O	5.355β	5.098β	5.546β	5.362β	5.106β	5.551β
α_N	5.109β	4.864β	5.331β	5.096β	4.849β	5.323β
β_{CO}	0.889β	0.891β	0.884β	0.919β	0.919β	0.919β
β_{CN}	0.822β	0.822β	0.818β	0.761β	0.761β	0.761β
E_1	6.081β	5.841β	6.240β	6.075β	5.833β	6.240β
E_2	5.213β	4.963β	5.422β	5.196β	4.945β	5.408β
E_3	3.466β	3.236β	3.593β	3.489β	3.262β	3.610β
Q_C	+0.360	+0.346	+0.404	+0.366	+0.356	+0.408
Q_O	−0.700	−0.680	−0.712	−0.700	−0.676	−0.702
Q_N	+0.338	+0.336	+0.308	+0.338	+0.324	+0.294

* Values of various parameters used in each calculation are as follows: $\chi_C=2.5$ in all calculations; $\chi_O=3.5$ and $\chi_N=3.0$ in I, II, IV and V; $\chi_O=3.6$ and $\chi_N=3.15$ in III and VI; $k=4.1$ in I, III, IV and VI; $k=3.9$ in II and V; $r_{CO}=1.23$ A. and $r_{CN}=1.32$ A. in I, II and III; $r_{CO}=1.21$ A. and $r_{CN}=1.37$ A. in IV, V and VI.

in benzene, α and β are the coulomb and the exchange integrals in the same molecule respectively, and k is the constant representing the ratio between α and β. Sandorfy has assigned 4.1 for the value of k. In the present calculation, two values of k, 4.1 and 3.9 were adopted. The latter value was determined as the ratio of the ionization potential of the carbon atom to the value of β estimated by Platt.[10] The overlap integrals necessary for the determination of the exchange integrals were obtained from the Table of Mulliken *et al.*[11] using the following two sets of bond distances:

C=O, 1.23 A., C−N, 1.32 A.;[12]

C=O, 1.21 A., C−N, 1.37 A..[13]

Under these conditions, three values of E can be evaluated in units of β. Then the values of a_{ai} in Eq. (1) can be calculated for each value of E. And it is possible to determine the π-electron density q_a of a-atom by the following equation,[14]

$$q_a=2\sum_j a^2_{aj} \qquad (4)$$

where the summation extends over the molecular orbitals which are occupied in the ground state.

From the value of q_a obtained by Eq. (4), the formal charge Q_a (in electron units) of a-atom can be known. Each atom having the positive or negative formal charge, correction terms for the electronegativity χ_a and the overlap integral S_{ab} should be considered. Corrections for these two quantities were made by the method of Pauling[15] and by the use of the table of Mulliken *et al.*[11] respectively. Thus it is possible to calculate new values of α_a and β_{ab} by Eq. (3). Using these new values, E, q_a and Q_a are calculated again by Eqs. (2) and (4). These procedures are repeated seven or eight times until the final results of these quantities are self-consistent.[16] They are given in Table 1, together with values of several parameters used in the last calculation.

Next, the similar calculation was made with

Table 2

The Final Results of the Molecular Orbital Calculation with the Carbonyl Group

	I′	II′	III′
χ_C	2.5	2.5	2.5
χ_O	3.5	3.5	3.6
k	4.1	3.9	4.1
α'_C	4.35β	4.16β	4.40β
α'_O	5.44β	5.20β	5.62β
β'_{CO}	0.838β	0.838β	0.838β
E'_1	5.895β	5.666β	6.045β
E'_2	3.895β	3.694β	3.975β
Q'_O	−0.544	−0.528	−0.590
Q'_C	+0.544	+0.528	+0.590

(10) The value of β estimated by Platt is −23,000cm.$^{-1}$ = −2.84 ev. J. R. Platt, *J. Chem. Phys.*, **18**, 1168 (1950).

(11) R. S. Mulliken, C. A. Rieke, D. Orloff and H. Orloff, *J. Chem. Phys.*, **17**, 1248 (1949).

(12) R. B. Corey and J. Donohue, *J. Am. Chem. Soc.*, **72**, 2899 (1950).

(13) The private communication from Mr. M. Kimura in Department of Chemistry, University of Nagoya.

(14) G. W. Wheland and L. Pauling, *J. Am. Chem. Soc.*, **57**, 2086 (1935).

(15) L. Pauling, The Nature of the Chemical Bond, Cornell University Press, 1940, p. 65.

(16) G. W. Wheland and D. E. Mann, *J. Chem. Phys.*, **17**, 264 (1949); Y. Kurita and M. Kubo, This Bulletin **24**, 13 (1951).

the carbonyl group because it was necessary for the evaluations of the resonance energy of the amide group and of the shift in the wave length due to the substitution of the methyl group of acetone by the amino group. In this case, the distance between carbon and oxygen atoms was set equal to 1.24 A.[17]

Experimental

N-methylacetamide is the same sample as used in the previous investigation.[18] Acetylchloride was prepared from glacial acetic acid and phosphorous trichloride. It was purified by the distillation in the atmosphere excluding moisture (b. p. 51.3°C.). Acetic acid, ethyl acetate and acetone were purified by the method of "Organic Solvent." Petroleum benzine used as the solvent was shaken with concentrated sulphuric acid for several days. Then it was treated with potassium permanganate and distilled after drying with sodium metal.

The absorption spectrum was measured with a Beckman spectrophotometer model DE. The results of the measurements are shown in Figs. 1 and 2. In these figures, molar extinction coefficients ε_M are plotted against wave lengths in mμ.

It was observed that the absorption intensities of ethyl acetate and acetylchloride decrease during the absorption measurements. This fact seems to mean that the decomposition of these molecules is induced by the near ultraviolet light. So the measured values of absorption intensities of these two molecules may not be said to be very accurate. But the wave length of the absorption maximum can be determined reliably as 220 mμ and 207 mμ for acetylchloride and ethyl acetate respectively in their solutions of petroleum benzine. The absorp tion maximum of acetic acid cannot be observed in this experiment, but it may be inferred from its absorption curve that its maximum probably appears near 200 mμ.[19] The absorption maximum of N-methylacetamide seems to appear in the side of shorter wave lengths rather than those of the above three substances as shown in Fig. 2.[20] This maximum cannot be measured with a Beckman spectrophotometer model DU.

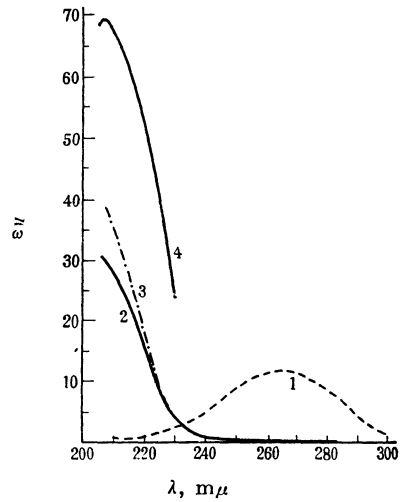

Fig. 1.—Absorption spectra of acetone, acetic acid and ethyl acetate: 1, acetone in water; 2, acetic acid in petroleum benzine; 3, ethyl acetate in water; 4, ethyl acetate in petroleum benzine.

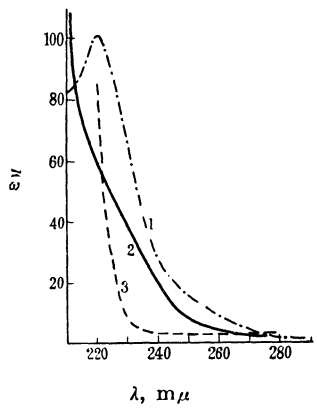

Fig. 2.—Absorption spectra of acetylchloride and N-methylacetamide: 1, acetylchloride in petroleum benzine; 2, N-methylacetamide in petroleum benzine; 3, N-methylacetamide in water.

At all events, it is evident from the above-mentioned experiments that the weak absorption band of acetone is intensified and shifted to the side of shorter wave lengths when one of the methyl groups is substituted by Cl atom, OR or NR_2 group.

Discussion

Calculated values of the resonance energies, π-electron distributions, and ground or exited energy levels of carbonyl and amide groups will be discussed comparing them with the observed or the estimated values of these quantities.

(17) M. Kimura and Y. Kurita, *J. Chem. Soc. Japan*, **72**, 396 (1951).

(18) S. Mizushima, T. Shimanouchi, S. Nagakura, K. Kuratani, M. Tsuboi, H. Baba and O. Fujioka, *J. Am. Chem. Soc.*, **72**, 3490 (1950).

(19) Ley and Arends observed the absorption maximum of acetylchloride, methyl acetate and acetic acid in pure liquids at 234.5 mμ, 208.5 mμ and 204 mμ respectively. The value of acetylchloride, which differs from that of the present experiment, seems to be incorrect because their measurements are not made in the wave lengths near the maximum. H. Ley and B. Arends, *Z. physik. Chem.*, (B) **17**, 177 (1932).

(20) Anslow pointed out with amide that very weak absorption maximum appeared about 280 mμ. In the present experiment, the similar phenomenon is observed in the concentrated aqueous solution of N-methylacetamide. Anslow regarded this absorption as due to associated amide molecules, but it seems more probable to consider that it is due to 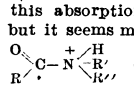 or some impurities.

G. A. Anslow, Discuss. Farad. Soc., Spectroscopy and Molecular Structure, 299 (1950).

Table 3

Calculated Values of ΔE_{res}, μ_π, and $\Delta\nu$ of Amide

	I	II	III	IV	V	VI
ΔE_{res}[a] (kcal./mole.)	19.2	18.3	18.0	18.2	17.3	17.5
μ_π (D)	5.54	5.38	5.42	5.51	5.32	5.32
$\Delta\nu$ ($cm.^{-1}$)[b]	7910	8200	7090	7550	7780	6810

a) The value of β is assigned -20 kcal./mole.
b) The value of β is assigned -23000 cm^{-1}.

(A) Resonance Energy of the Amide Group.—According to Pauling,[21] the resonance energy of amide is 21 kcal./mole. From the standpoint of the molecular orbital theory, this quantity can be represented approximately by the following equation, $\Delta E_{res}=2(E'_1+\alpha'_N)-2(E_1+E_2)$, where α'_N is the value of the coulomb integral for the neutral nitrogen atom. Calculated values of ΔE_{res} are given in Table 3. It is to be noticed that the values of ΔE_{res} evaluated by different methods I-VI may be regarded as almost the same,--that is to say, they are little affected by the values of various parameters used in each method. And it may be seen that the agreement between the calculated and the observed values are fairly good.

(B) π-Electron Densities and Dipole Moments of Carbonyl and Amide Groups.—The values of π-electron density, q_a calculated by the Eq. (4) indicate that in the carbonyl group about half of a π-electron moves from carbon to oxygen (see Table 2). This fact is in good accord with the conclusion derived by Pauling[1] from the study on the contribution of the polar resonance structure to the dipole moment of acetone or similar substances.

As to the amide group, it is shown that the non-bonding electrons in nitrogen partially migrate into the C=O bond. As the result of this electron migration, the nitrogen atom comes to have a partially positive charge. Thus it will be seen that the dipole moment of amide group becomes large, and the basic property of it decreases. From the values of Q_a, the dipole moment due to π-electron distributions, μ_π, can be calculated as shown in Table 3. The observed value of the dipole moment is 3.79D for dimethylacetamide in dioxan. So the calculated values are somewhat larger than the observed one.[22]

(C) Excited Electronic Levels and Near Ultraviolet Absorption Spectra of Carbonyl and Amide Groups.—Low intensity absorption band characteristic of unconjugated carbonyl bond appears at 279 mμ and 265 mμ in petroleum benzine and in water respectively. This absorption has been studied in detail by McMurry[5]; and from the theoretical investigation of the absorption intensity, it considered that this absorption might be due to the transition of non-bonding oxygen electron to the excited π-electron level of carbonyl group. This transition is shown schematically in Fig. 3. And it has been called the $n\rightarrow\pi^*$ or the $1\rightarrow\pi$ transition by Kasha[7] or Baba[6] respectively.

The results of our molecular orbital calculation on the electronic levels of carbonyl group are consistent with this view. The energy difference $\Delta E'$ between energy levels of the upper π-molecular orbital and of non-bonding oxygen electrons may be approximately represented by the following equation, $\Delta E'=E'_2-\alpha'_0$. The values of this quantity calculated by the methods I', II' and III' become -1.54, -1.51 and -1.64β respectively. The observed value can be determined as -1.56β, if the said absorption spectrum of acetone is due to the $n\rightarrow\pi^*$ transition. Therefore both values are in good agreement. But if it is assumed that this absorption band is due to the $\pi\rightarrow\pi^*$ transition, energy differences between upper and lower π-electron levels become -2.00, -1.97 and -2.07β. These values are larger than the observed value. Furthermore, the solvent effect of this absorption spectrum can be also explained from the same point of view. As shown in Table 4 the value of $\Delta E'$ calculated by the above equation becomes larger with the increase of $|\alpha'_0|$. This means that the above-mentioned absorption band shifts to the side of shorter wave lengths the contribution of the partially ionic resonance structure increases. The experimental result, namely that its wave length becomes smaller with he increment of the polarity of solvents,[23] conforms to the above theoretical expectation.

Table 4

The Relation between $\Delta E'$ and α'_0

α'_0	4.92β	5.41β	5.74β	6.07β	6.56β
Q'_0	-0.570	-0.640	-0.678	-0.710	-0.748
$\Delta E'$	-1.34β	-1.72β	-1.99β	-2.28β	-2.72β

Values of k, α'_c and β'_{co} used in these calculations are 4.1, 4.1β and 0.838β respectively.

Next the effect of substitution on the absorption spectrum of acetone will be discussed. When the methyl group of acetone is replaced by the group with non-bonding π-electrons such as amino or hydroxyl group, the absorption band shifts to the side of shorter wave lengths as shown in Figs. 1 and 2. On the other hand, in benzene the absorption spectrum due to the $A_{1g}\rightarrow B_{2u}$ transition shifts to the side of the longer wave lengths by

(21) L. Pauling, The Nature of the Chemical Bond, Cornell University Press (1940), p. 138.

(22) The dipole moment due to σ-electron distribution is expected to be very small for dimethylacetamide as well as C=O bond(1) So their dipole moments will be principally determined by π-electron distribution alone.

(23) According to Burawoy, this experimental result was regarded as one of the facts which could not be explained from the stand-point of $n\rightarrow\pi^*$ transition. But this difficulty for the $n\rightarrow\pi^*$ transition is surely removed by the present theoretical consideration. A. Burawoy, Discuss. Farad. Soc., Spectroscopy and Molecular Structure, 70 (1950).

the same substitutions.[24][25] It is interesting that the effect of the substitution on the absorption spectrum is quite different in acetone and benzene. This difference was discussed by Baba.[6] He applied the theory of the electron migration developed by Sklar[25] and Herzfeld[25] to explain qualitatively this fact. The same phenomenon can be treated by the LCAO molecular orbital method as follows. As shown in Fig. 3 and Tables 1 and 2, the calculated value of the empty π-electron level of amide group is higher than

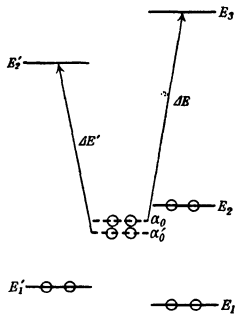

Fig. 3.—Energy levels of acetone and amide

that of acetone. So it may be regarded as reasonable that the absorption maximum of acetone appears in a longer wave length than that of amide. This fact can be readily understood by a glance at Fig. 3. And it is possible to calculate the wave number difference $\Delta\nu$ between these two absorption spectra by the equation, $\Delta\nu = (\Delta E - \Delta E')/ch = (E_3 - \alpha_0 - E'_2 + \alpha'_0)/ch$. The calculated values of $\Delta\nu$ are given in Table 3. The absorption maximum of N-methylacetamide appears probably below 205 mμ in petroleum benzine solution. So the observed value of $\Delta\nu$ may be estimated to be larger than 12900 cm.$^{-1}$ The calculated value for this quantity is smaller than the observed one. But it will be difficult to obtain more accurate values by the simple approximation of LCAO.

The shift of absorption spectra of acetylchloride, acetic acid and ethyl acetate can also be understood on the basis of the $n\rightarrow\pi^*$ transition. In these molecules as well as amide, the substituents have the non-bonding π-electrons which are able to migrate into carbonyl group, and the rate of electron migration probably increases in the order of Cl atom, OR and NR_2 groups as observed in the case of monosubstituted benzene.[25][27] It can be shown on the hand, that the value of E_3 becomes larger with the increment of the electron migration.[26] So it is expected from the standpoint of the $n\rightarrow\pi^*$ transition that these absorption spectra shift to the side of the shorter wave lengths in the order of acetylchloride, acetic acid or ethyl acetate, and N-metylacetamide. This expectation is qualitatively fulfilled by the present experiment.

Summary

1) Electronic structures of carbonyl and amide groups were investigated by the use of the molecular orbital method; calculated values of resonance energy and π-electron densities may be regarded as reasonable compared with these which were observed.

2) Near ultraviolet absorption spectra were measured with acetone, acetylchloride, acetic acid, ethyl acetate and N-methylacetamide. As the result of these measurements, it becomes evident that the low intensity absorption band of acetone shifts to the side of shorter wave lengths when the methyl group of acetone is replaced Cl atom or OR and NR_2 groups. These results can be explained by the present theoretical consideration if this absorption band is due to the $n\rightarrow\pi^*$ transition.

I wish to express cordial thanks to Prof. S. Mizushima and Prof. K. Higasi for stimulating and directing this research and to Mr. H. Baba for his helpful discussion. My thanks are also due to Mr. A. Kuboyama and Miss C. Tsurumi for their kind co-operation in performing this research. I am indebted to the budget of the Ministry of Education for this investigation.

Institute of Science and Technology, University of Tokyo, Tokyo

(24) S. Nagakura and H. Baba, *J. Chem. Soc. Japan*, **71**, 527 (1950).
(25) K. F. Herzfeld, *Chem. Rev.*, **41**. 233 (1947).
(26) A. L. Sklar, *J. Chem, Phys.*, **7**, 984 (1939).
(27) F. A. Matsen, *J. Am. Chem. Soc.*, **72**, 5243 (1950).
(28) This is apparent from the fact that $\partial E_3/\partial\alpha_N$ is positive.

Heats of Wetting of Polysaccharides. I. Heats of Wetting of Various Polysaccharides

By Toshio NAKAGAWA

(Received February 4, 1952)

Introduction

The interaction between polysaccharides and water has been investigated chiefly by graphing adsorption isotherms or X-ray patterns, and their heats of wetting have been relatively overlooked.

About fifty years ago, Rodewald and Kattein[1] measured heats of wetting of various starches, then in 1917 Katz[2] reported his data concerning adsorptions and heats of wetting of many substances including cellulose and inulin. More recently Schrenk *et al*[3]., Dumanskii and his collaborators[4], and Wahba[5] published their results in starch and cellulose.

The present writer also measured heats of wetting of various polysaccharides, such as potato starch, potato amylose, potato amylopectin, inulin, glycogen and konjac mannan, but found no regularity between heat of wetting and molecular constitution.

Apparatus and Procedure

The apparatus used resembles the one constructed by Harkins and his collaborator,[6] and is illustrated in Fig. 1a.

When the rod A is pushed down, the ampoule S breaks and the content is immersed into water, the temperature in D_1 rises owing to the heat of wetting of the sample and electrical potential difference appears at the ends of the thermocouple. This potential is measured with a potentiometer. Then a known amount of electric current is passed through H, the potential difference produced is measured again. We can estimate the heat of wetting by comparing these two potential differences.

The actual procedure of measurement is as follows. The apparatus is arranged as illustrated in Fig. 1a. When the thermal equilibrium is roughly attained, L is started. Potential difference at the ends of the thermocouple is recorded once every minute. The temperature in D_1 rises slowly because of the mechanical work of the stirrer (AB in Fig. 2). When the temperature-time curve results in a straight line, S is broken. The temperature is elevated rapidly owing to the heat of wetting (BC in Fig. 2), but in a short time returns again to a straight line (CD). When an amount of electric current is passed for a certain time through H, the temperature-time curve behaves as before (DEF).

Extrapolating these two straight lines (CD, EF), we can get temperature elevation S_1 by the heat of wetting and S_2 by the electrical work, and calculate the heat of wetting by comparing S_1 and S_2.

When the heat generation is relatively slow, necessary correction is given to S_1 and S_2. However in this experiment these corrections were usually small, and in most cases unnecessary.

If the value of an evacuated sample is to be obtained we put the sample in a thin walled ampoule S', evacuate under 1/1000 mm. Hg, and fuse off the neck, which remains an L-shaped

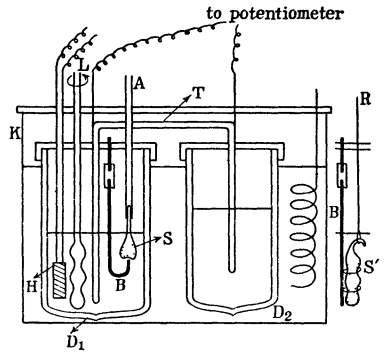

Fig. 1a. 1b.

K thermostat (constant within 1/100°C.)
D_1, D_2 Dewar's vessels
T Cu-constantan thermocouple with 36 pairs of junctions
S ampoule containing sample (usually ahout 0.8 g.)
A rod grasping ampoule
B brass rod with keen needle
H electric heater with resistance about 4.7 Ω
L glass stirrer
R string

(1) H. Rodewald and A. Kattein, *Z. phys. Chem.*, **33**, 579 (1900).
(2) J. R. Katz, *Kolloid. Beih.*, **9**, 1 (1917).
(3) W. G. Schrenk, A. C. Andrews and H. H. King, *Ind. Eng. Chem.*, **39**, 113, (1947).
(4) A. V. Dumanskii, Ya. F. Mezhennyi and E. F. Nekryach, *Kolloid. Zhur.*, **9**, 335 (1947); *Chem. Abst.*, **43**, 6042 (1949).
(5) M. Wahba, *J. Phys. Colloid. Chem.*, **52**, 1197 (1948).
(6) W. Harkins and Roy Dahlstrom, *Ind. Eng. Chem.*, **22**, 897 (1930).

hook. The rod A is removed and S' is fixed tightly to B, as shown in Fig. 1b. By pulling up the string R fastened to the hook, we can break the neck and bring out the sample into the water. In this case, heat development is somewhat slower, but the measurement can be performed without difficulty.

The accuracy of the apparatus was estimated in taking account of the sensibility of the potentiometer, and the exactness in determining electrical work. This is calculated to be about one per cent.

Furthermore, it is also deduced that the measured heat amount in the calorimeter has always uncertainty amounting to 0.05 cal., and this means, when we measure the heat smaller than 5 cal., the accuracy becomes less than one per cent.

The experimental values endorse the above presumption.

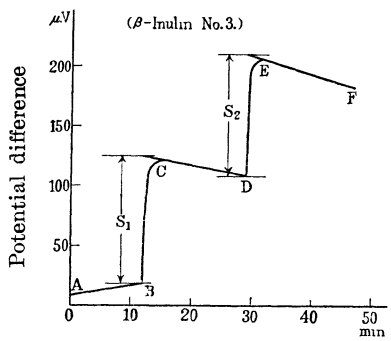

Fig. 2.

(1) Native potato starch: Native potato starch was dried in Abderhalden's desiccator under reduced pressure (2/100 mm. Hg.) so long as to reach constant weight.

(2) Potato starch in the form of paste: 6.5 g of native potato starch was mixed with 3 cc. of water, heated to 100°C. and dried at 100°C. Starch so treated was called by Katz "Verkleisterte" starch. It swelled to give paste when immersed into water.

(3) Retrograded potato starch: Potato starch paste was laid under saturated water vapor for a long time (from 22 to 162 days). Retrograded starch did not make paste.

(4) Potato amylose: Potato amylose was isolated by Schoch's method.(7) Potato starch was autoclaved with water for 3 hours at 110°C. To the 3 percent solution thus treated, excess amount of *n*-butanol was added and filtered. The filtrate which contained amylopectin, served as the source of the sample (6). Filtered precipitate was dissolved in hot water; then the solution was poured into a large amount of methanol, precipitating amylose. The resulting precipitate was filtered, washed with methanol and dried. This substance swelled well in cold water, dissolved partly in cold and perfectly in hot water, giving blue color with iodine.

(5) Retrograded amylose: The above-mentioned amylose was exposed to saturated water vapor for 25 days. The sample swelled in cold water but less than sample (4), and dissolved in hot water with difficulty.

(6) Potato amylopectin: The solution containing amylopectin (cf. sample (4)) was mixed with a large amount of methanol, the resulting precipitate was centrifuged, washed and dried. This sample swelled and partly dissolved in cold water. Iodine color was reddish violet.

(7) Retrograded amylopectin: Exposure of sample (6) to saturated water vapor for 29 days, gave retrograded amylopectin which swelled a little in cold water, but was entirely insoluble. This was confirmed by addition of iodine to the supernatant, which gave no color reaction.

(8) β-Inulin: "Takeda's" inulin was dissolved in hot water with active charcoal and filtered. The filtrate was cooled and frozen with freezing mixture; then melted. It remained a deposit. The precipitate was recrystallized three more times. β-Inulin is insoluble in cold water.

(9) α-Inulin: β-Inulin was dissolved in hot water, the solution was poured into a large amount of alcohol, the precipitate was centrifuged, washed and dried. α-Inulin dissolves in cold water.

(10) Retrograded inulin: α-Inulin was exposed to saturated water vapor for 10 days. This was insoluble in cold water.

(11) Konjac powder: Native konjac powder sold as "special grade", was dried under reduced pressure. This powder swells and dissolves in cold water. However, as the dissolution needed a very long time, it dissolved imperfectly in the course of the heat measurement.

(12) α-Konjac mannan: Native konjac powder was dissolved in cold water by shaking, and the solution filtered with cloth was mixed with alcohol. The resulting precipitate, after being washed and dried surves as the sample. α-Konjac mannan swelled and dissolved in cold water, but the perfect dissolution was not attained in the course of measurement because of slowness of the reaction.

(13) β-Konjac mannan: One per cent solution of α-konjac mannan was heated with $Ba(OH)_2$, and filtered. The deposit was treated with one per cent acetic acid solution for several days to remove Ba, then washed with water. The sample swelled a little in water, but did not dissolve even when boiled.

(14) Glycogen: "Takeda's" glycogen was dissolved in water, precipitated with alcohol, dissolved in water again, electrodialized, then precipitated with alcohol containing a trace of potassium acetate and washed thoroughly with alcohol. Glycogen dissolved well in cold water and gave a slightly turbid solution.

(7) T. J. Schoch, "Advances in Carbohydrate Chemistry." Vol. I. The fractionation of starch.

Results and Discussion

The results obtained are shown in Table 1. Each value is the mean of two or three experiments.

Table 1

		Heat of wetting cal./g.	
		in the presence of air	evacuated
1	Native potato starch	28.2	27.2
2	Potato starch paste	24.6	
3	Retrograded potato starch	25.6 (22 days) 25.5 (162 days)	
4	Potato amylose	22.8	
5	Retrograded amylose	23.5	
6	Potato amylopectin	21.2	
7	Retrograded amylopectin	21.8	
8	β-Inulin	23.1	23.2
9	α-Inulin	17.9	
10	Retrograded inulin	21.2	
11	Konjac powder	21.3	
12	α-Konjac mannan	23.7	
13	β-Konjac mannan	16.2	16.7
14	Glycogen	23.5	

We see that the heats of wetting of polysaccharides lie in the range from 10 to 30 calories per gram of dried substance. The value of native potato starch (28.2 cal./g.) is in good accordance with that of Schrenk *et al*[3]. (29.1) and Dumanskii *et al*[4]. (28.06). The elevation of drying temperature from 34° to 64° or 100°C caused no decrease of weight and no change of heat-of-wetting exceeding experimental error (0.2 cal.). It is somewhat interesting that potato starch gives a higher value than either of its fractions (potato amylose, potato amylopectin.)

Inulin gives 23.1 cal./g. in agreement with Katz's[2] result. Heats of wetting of evacuated samples were also measured in three cases, namely potato starch, inulin aud konjac mannan, but no or little effects were observed.

It seems to the present writer that there exists no correlation explicitly between the heat of wetting and the molecular constitution of polysaccharides.

Summary

Heats of wetting of various polysaccharides, such as potato starch, potato amylose, potato amylopectin, inulin, glycogen, and konjac mannan were measured, but no correlation between heat of wetting and molecular constitution was found.

The author wishes to express his hearty gratitude to Prof. Sameshima for his kind guidance and advice.

Department of Chemistry, Faculty of Science, Tokyo University, Tokyo

Heats of Wetting of Polysaccharides. II. A Rule Which Exists Between Adsorption Isotherms and Heats of Wetting of Polysaccharides

By Toshio NAKAGAWA

(Received February 4, 1952)

Net Heat of Adsorption

Net heat of adsorption defined by heat of adsorption minus heat of condensation, can be experimentally acquired by means of measuring heats of wetting of dried and partially saturated substance.

Denote the heat of wetting, obtained by throwing one gram of a dry substance into water, by H, and that obtained by a partially saturated substance, which consists of one gram of dry substance and m grams of water, by $H(m)$, then $H-H(m)$ gives the net heat of adsorption $N(m)$, generated when one gram of dry substance adsorbs m grams of water.[1]

$$N(m)=H-H(m) \qquad (1)$$

However, it should be remembered, that the processes are tacitly assumed to be reversible ones.

(1) A. B. Lamb and A. S. Coolidge, *J. Am. Chem. Soc.*, **42**, 1146 (1920).

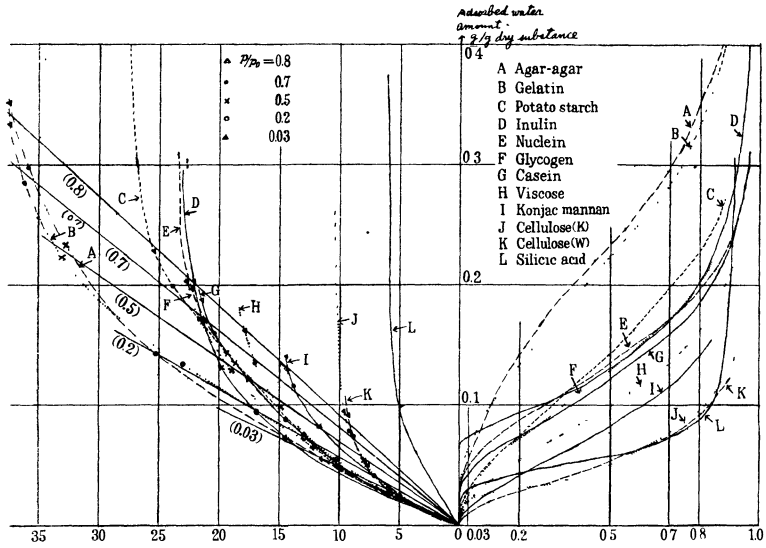

←Net heat of adsorption. cal./g. dry substance Relative humidity p/p_0→

Fig. 1.

The Rule Found by the Author

The present writer arranged the data concerning heats of wetting, which were reported by J. R. Katz,[2] E. Rosenbohm,[3] A. V. Dumanskii *et al*,[4] and M. Wahba,[5][6] together with the author's own data, and plotted net heats of adsorption against water amounts adsorbed.

By comparing the curves thus obtained with the adsorption isotherms obtained by Katz,[2] H. Sato,[7] Wahba[6] and the author, it was found that there exists a simple rule, between the net heats of adsorption and water amounts adsorbed among the following substances: starch, inulin, cellulose, viscose, glycogen, konjac mannan, casein, nuclein, gelatin, and agar-agar.

The rule states: "When we bring one gram of each of the above-mentioned substances under the same relative humidity $x(p/p_0)$, generated net heats of adsorption $N(m)$ (heat of adsorption minus heat of condensation) are proportional to the amounts m of water adsorbed, independently of the varieties of substances, in the range of x smaller than 0.8".

The author wishes to expound the rule in further detail. In the right half of Fig. 1. are represented adsorption isotherms taking relative humidity x in abscissa and adsorbed quantity m (g. water/1 g. of dry substance) in coordinate.

The data were gathered from the works of the following investigators, Katz[2] (inulin, cellulose (K), casein, nuclein, gelatin, agar-agar at room temperature), H. Sato[7] (potato starch 20°C), Wahba[6] (cellulose (W), viscose 30°C), and the author (konjac mannan, glycogen 20°).

It should be mentioned here that in this paper Katz's values slightly differ from his original report. Katz obtained the relation between relative humidity and adsorbed water amount, by exposing the samples over sulfuric acid solution with various concentrations. To estimate the water vapor pressure over sulfuric acid solution, he used Regnault's[8] data, but it seems inadequate particularly at a concentration higher than 50 per cent. Relative humidities were therefore amended by Greenewalt's[9] report.

In the left half, net heats of adsorption $N(m)$, obtained using the method discussed above are plotted against adsorbed quantities m, taking the former in abscissa, and the latter in coordinate.

The data were collected from the experiments of the following investigators, Rosenbohm[3] (gelatine), Katz[2] (inulin, cellulose (K), casein, nuclein, agar-agar at room temperature), Dumanskii *et al*[4]. (potato starch, 30°C), Wahba[5][6] (cellulose (W), viscose 30°), and the author (konjac mannan, glycogen 30°C).

(2) J. R. Katz, *Kolloid Beih*, **9**, 1 (1917).
(3) E. Rosenbohm, *Kolloid Beih*, **6**, 177 (1914).
(4) A. V. Dumanskii, Ya. F. Mezhennyi and E. F. Nekryach, *Coiloid Zhur.*, **9**, 355 (1917); *Chem. Abs.*, **43**, 6042 (1949).
(5) M. Wahba, *J. Phys. Colloid Chem.*, **52**, 1197 (1948).
(6) M. Wahba, *J. Phys. Colloid Chem.*, **54**, 1148 (1950).
(7) H. Sato, *J. Chem. Soc. Japan, Pure Chem. Sect.*, **72**, 790 (1951).
(8) Regnault, Landolt Tab. 3. Aufl. 166 (1905).
(9) G. H. Greenewalt, *Ind. Eng. Chem.*, **17**, 522 (1925).

The samples used in the two sets of experiments are the same excepting gelatin and starch. In the case of starch, it is ascertained by the author that Sato's sample has almost the same value of heat of wetting as the one used by Dumanskii (Sato's sample 28.2 cal./g., Dumanskii's 28.06 cal./g.).

When we draw a parpendicular line at a certain value of x in the right half of Fig. 1, its intersecting points with adsorption isotherms give the water amounts adsorbed by respective substances. Next we draw horizontal lines from these intersecting points toward the left half of Fig. 1. Intersecting points of these lines with net-heat-of-adsorption curves gives the values of net heats of adsorption, which will be developed when these substances are brought under the same relative humidity x. It will be recognized from Fig. 1. that these intersecting points lie on a straight line passing origin.

This rule holds well in the region from very small value of x (0.03) to relatively large value ($x=0.8$). This fact seems to the author too consistent to be considered as merely an accident. The rule cannot hold at any larger value of x, exceeding 0.8. The above-mentioned rule can be expressed mathematically as follows:

$$N(m)=a(x)m(x) \qquad (2)$$

where $N(m)$: a function of m, and depends also on the kind of substance.

$m(x)$: a function of x, and depends on the kind of substance.

$a(x)$: a function of x independently of the variety of substance.

Equation (2) indicates that net heat of adsorption is proportional to m at same x, independently of the variety of substance. Heat of adsorption $A(m)$ is also proportional to the adsorbed water amount m, because net heat of adsorption is defined by heat of adsorption minus heat of condensation.

$$\text{Thus} \quad A(m)=N(m)+Lm=(a+L)m \qquad (3)$$

L: heat of condensation of 1 g. water.

From Fig. 1, values of $a(x)$ are obtained as follows relating to several values of x.

x	0.03	0.2	0.5	0.7	0.8
$a(x)$	205	178	145	123	109 cal./g. water

For the purpose of comparison, adsorption isotherm and net-heat-of-adsorption curve of silicic acid[2] are also represented in Fig. 1. Clearly it does not obey the rule.

It is difficult to explain why the rule holds in the above-mentioned substances, but it is also noticeable that these substances are polysaccharides, proteins, or their relatives.

The approximate value of net heat of adsorption can be obtained by drawing only one adsorption isotherm, in the case of the substance which obeys the rule, so it is interesting to explore what kinds of substances are governed by the rule.

The above-mentioned relation does not hold when x exceeds 0.8. Possibly this fact is due to the rapid increase of different kinds of adsorption in such a high humidity.

To the author, it seems an interesting fact that a regularity is found in the integral rather than in the differential heat of adsorption.

An example of polysaccharide which does not obey the rule, is reported. Namely, comparing the adsorption isotherm of "Künstliche Stärkekörper" obtained by Katz,[2] with the net heat of adsorption of the same substance reported by H. Rodewald and his collaborator,[10] we find the rule does not hold well. The net heat of adsorption expected from the adsorption isotherm using the above-mentioned rule, is lower than the experimental value.

But there is some reason to think the value given by Rodewald *et al.* is somewhat too high, possibly for the sake of lower experimenting temperature. For example, among the heats of wetting of potato starch reported by them and other more recent investigators, their value alone is somewhat higher than the others.

H. Rodewald *et al*[10].	(1900)	32.68 cal./gr. (at 0°C)	
A. V. Dumanskii *et al*[4].	(1947)	28.06	(20°)
W. G. Schrenk *et al*[11].	(1947)	29.2	(30°)
T. Nakagawa[12]	(1949)	28.2	(30°)

Experiments

The samples of glycogen and konjac mannan, of which data are employed in the above discussion are the same ones as glycogen and β-konjac mannan in the preceding report of this series.[12]

A sample of each spread in a wide bottle, was put into a desiccator containing sulfuric acid solution with varying concentrations, and exposed for several months until constant weight was reached.

Adsorbed amount was measured as the increase of weight, relating to relative humidity.

Heats of wetting of partially saturated substances were measured using the same apparatus described in the preceding report. In this case, the sample enclosed in an ampoule, was put into the same desiccator that was mentioned above,

(10) H. Rodewald and A. Kattein, *Z. Phys. Chem.*, **33**, 579 (1900).

(11) W. G. Schrenk, A. C. Andrews and H. H. King, *Ind. Eng. Chem.*, **39**, 113 (1947).

(12) T. Nakagawa, Preceeding report in this journal.

and the ampoule was sealed off after the adsorption equilibrium had been roughly attained. Net heats of adsorption were then readily calculated.

In Fig. 1, curves thus obtained are represented with those derived from other investigators' data.

Summary

A simple rule which correlates adsorption isotherms and heats of wetting of polysaccharides was described.

The rule states: "When we bring one gram each of polysaccharides (and several other substances belonging to organic high polymer) under the same relative humidity, generated net heats of adsorption are proportional to the amounts of adsorbed water, independently of the varieties of substances."

The author wishes to express his sincere thanks to Prof. Sameshima for his kind guidance and encouragement.

Department of Chemistry, Faculty of Science, Tokyo University, Tokyo

Wettability of Solid Surface. V. The Effect of Metallic Cations on Wettability of Stearic Acid[1]

By Ayako INABA

(Received December 25, 1951)

Introduction

In one of the preceding reports,[2] it was pointed out that the wettability of stearic acid surface was increased by treating with aluminum or thorium salt solution, while it was not increased by treating with potassium or calcium salt solution. Langmuir also showed that the wettability of barium stearate built-up film was increased by treating with aluminum or thorium salt solution,[3][4] and further that some properties of stearic acid monolayer were changed by adsorption of these metallic ions.[5] However, the present author has found no explanation for the mechanism of wetting due to ions like aluminum and thorium. The present paper describes the effect of various metallic ions on the wettability of stearic acid as well as the explanation of its mechanism.

Experimental

Material.—Stearic acid of Kahlbaum was used after recrystallization from alcohol. Salts used were LiCl, NaCl, RbCl, $MgSO_4 \cdot 7H_2O$, $Ca(NO_3)_2 \cdot 4H_2O$, $Sr(NO_3)_2$, $BaCl_2 \cdot 2H_2O$, $Al_2(SO_4)_3 \cdot 18H_2O$, $CuSO_4 \cdot 5H_2O$, $AgNO_3$, $ZnSO_4 \cdot 7H_2O$, $3CdSO_4 \cdot 8H_2O$, $HgCl_2$, $Pb(NO_3)_2$, $Th(NO_3)_4$, $MnSO_4 \cdot 6H_2O$, $FeK(SO_4)_2 \cdot 12H_2O$, $Co(NO_3)_2$, and $NiSO_4 \cdot 7H_2O$. These salts were recrystallized from redistilled water before use. Special purification was made prior to the recrystallization if necessary. Water used for the wettability experiment was also redistilled using the apparatus of Vidrex glass of Kokura Glass Co. and was made free from carbon dioxide.

Measurement.—A clean glass rod of about 5 mm. diameter and 50 mm. length was dipped into molten stearic acid, withdrawn, and thus coated with a layer of stearic acid which was solidified in air. The surface of stearic acid thus obtained was treated with various salt solutions for about seventeen hours, after which the wettability of the surface was measured in relation to the same solution. The concentration of the solution used was kept to 10^{-4} mol unless mentioned otherwise. pH of the solution was controlled simply using hydrochloric acid or sodium hydroxide solution.

For wettability measurement, the sessile drop method was used. Namely, a drop of 0.5 mm. diameter was placed on the surface for measurement with the aid of a glass capillary having a paraffined tip. The image of the drop was magnified by a microscopic objective, projected on a screen, and sketched upon a piece of paper. A tangent was drawn for the silhouette thus obtained, and the contact angle θ was measured using a protracter. pH of the solution was determined by the color indicator method before and after each treatment of the surface. As the solution had no buffer action, the experiment was

(1) Reported before the annual meeting of the colloid chemistry held by the Chemical Society of Japan on Nov. 19th (1950).
(2) A. Inaba, This Bulletin, **23**, 146 (1950).
(3) I. Langmuir and V. J. Schaefer, *J. Am. Chem. Soc.*, **59**, 1406 (1937).
(4) I. Langmuir and V. J. Schaefer, *J. Am. Chem. Soc.*, **59**, 1762 (1937).
(5) I. Langmuir and V. J. Schaefer, *J. Am. Chem. Soc.*, **59**, 2400 (1937).

mainly conducted in the air free from carbon dioxide in the case of pH > 6. The use of a buffer solution was avoided owing to the probable effect of polyvalent anions and concentrated alkali ions which might obscure the effect of cation under investigation.

Results

The wettability of stearic acid surface treated by water, pH of which was controlled simply by hydrochloric acid or sodium hydroxide, is shown as a control curve in Fig. 1. In this case, wettability was constant in the range of pH < 8, being equal to that of untreated stearic acid towards distilled water ($\theta = 110°$), while the increase of wettability was remarkable at pH > 10, θ being reduced to almost 0°.

Addition of various metallic ions to the dipping solution affected the wettability of the stearic acid surface. These effects were divided into three types as follows:

(1) The Effect Produced by the Addition of Sodium, Potassium and Rubidium Salts.—The addition of these salts in concentration of 10^{-4} mol showed no effect on the wettability of stearic acid compared with the control as shown in Fig. 1. However, the increase of the concentration of the salts lowered pH at which wettability began to increase. For example, the addition of 0.05 mol Na_2HPO_4 or 0.2 mol KCl caused the wettability of stearic acid already at pH 7 (Fig. 1) to increase.

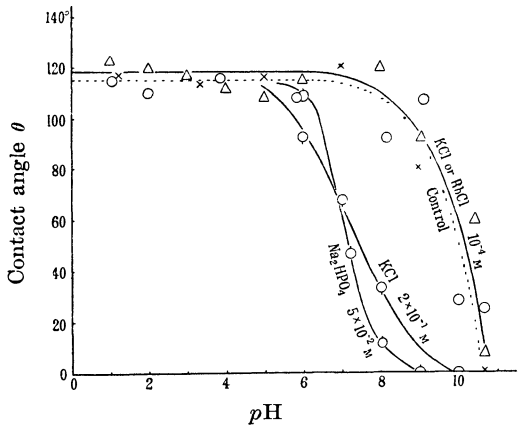

Fig. 1.—The effects of Na, K, and Rb ions (the 1st group) upon the wettability of stearic acid surface.

(2) The Effect Produced by the Addition of Thorium, Aluminum, Ferric, Chromic, Cobaltous and Cupric Salts.—These salts enhanced the wettability of the stearic acid surface in the pH region characteristic for each salt (Fig. 2a), although stearic acid showed only a small wettability in the absence of these salts (control curve). Cadmium, zinc, silver, and magnesium salts showed no effect at concentration of 10^{-4} mol but showed a perceptible wetting power at concentration of 10^{-3} mol (Fig. 2b). These salts may also be considered to belong to the preceding class, but for the reason mentioned later we should like to classify them as belonging to this class.

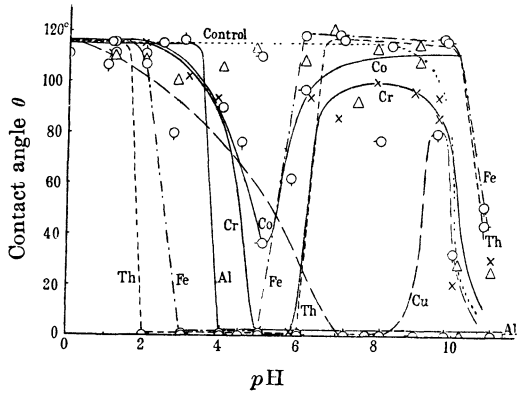

Fig. 2a.—The effects of Th, Fe, Al, Cr, Co, and Cu ions (the 2nd group) in concentration of 10^{-4} mol upon the wettability of stearic acid surface.

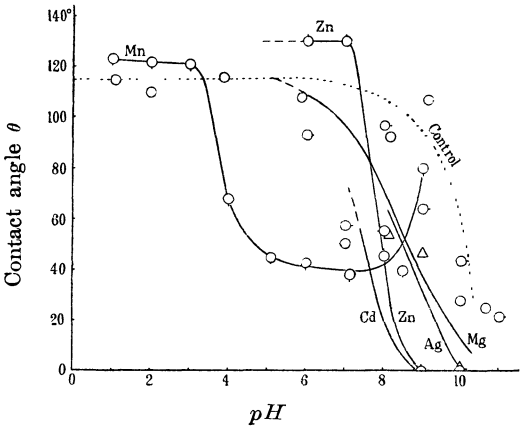

Fig. 2b.—The effects of Mn, Cd, Zn, Ag, and Mg ions (the 2nd group) in concentration of 10^{-3} mol upon the wettability of stearic acid surface.

(3) The Effect Produced by the Addition of Barium, Strontium, Calcium and Lithium Salts.—These salts reduced the wettability of stearic acid at pH > 10 (Fig. 3), in the region of which, however, stearic acid was wettable in the absence of these metallic ions except sodium ion which came from alkali for pH control. In this case increase in concentration of the ions of this group promoted the non-wetting properties of stearic acid as shown in Fig. 3. Mercuric, nickel, and lead salts showed apparently the similar effect (Fig. 4).

Discussion

Wettability of the stearic acid surface towards distilled water was small, the contact angle being

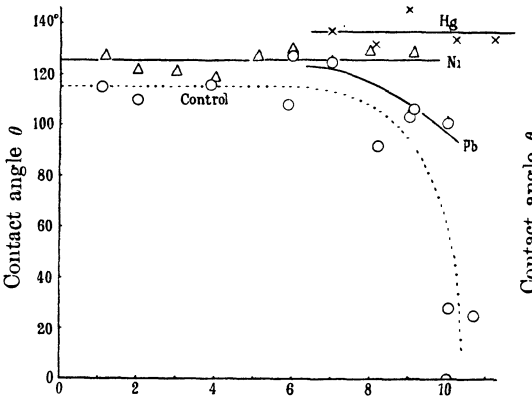

Fig. 3.—The effects of Ba, Sr, Ca, and Li ions (the 3rd group) upon the wettability of stearic acid surface.

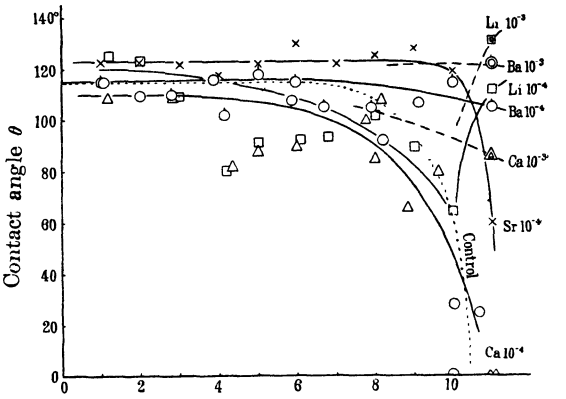

Fig. 4.—The effects of Hg, Ni, and Pb ions in concentration of 10^{-3} mol upon the wettability of stearic acid surface.

about 110°, and it did not change by being treated with hydrochloric acid. However, the surface showed increase in wettability towards sodium hydroxide solution. This increase can be explained by the polarity of the surface caused by the surface dissociation of stearic acid as follows:

$$StH+Na^+ + OH^- = St^-Na^+ + H_2O.$$

This will explain the control curve of Fig. 1. A more detailed calculation can even predict the wettability $\sim p$H curve similar to that found experimentally as shown in Fig. 1. It may be presumed that the addition of neutral salt like KCl or Na_2HPO_4 promotes the dissociation and that as a result wettability is increased. In fact, the wettability began to increase already at pH 7 as shown in Fig. 1.

Now we come to place where we can explain the effect of various metallic ions on the wettability of stearic acid. There have been some informations available for this purpose. For instance, we can cite Langmuir's study[5] on the stearic acid monolayer on the substrate containing metallic ions. There he confirmed the adsorption of metallic ions to the monolayer. Especially, in the case of barium salt, stearic acid monolayer was considered to be composed of neutral barium soap at pH 11,[6] and its built-up film was not wetted with water.[3] The author's experiment showed that the surface of stearic acid treated with 10^{-4} mol cupric salt so ution at pH $6\sim8$ was bright blue and the color was not removed after rinsing with water. From these and also other similar phenomena encountered we can safely conclude the adsorption or chemical reaction taking place between stearic acid and the metallic ions in solution, which profoundly affect the wetting condition of stearic acid surface. We can also confirm this point more precisely. Langmuir and others[5] introduced the following equation for this adsorption.

$$\log\{\gamma_1/(1-\gamma_1)\} = C_1 + m_1 \log[M_1^{Z+}] + Zm_1\,(p\mathrm{H})$$

Here γ_1 is the fraction of the number of surface cells occupied by the adsorbed substance, C_1 and m_1 are constants proper to M_1^{Z+} ion. According to this equation, it can be expected that apart from the characteristic properties of ions, higher valency ions can be adsorbed at still lower pH than that at which the lower valency ions are adsorbed. Langmuir's results showed that ferric ions were strongly adsorbed by stearic acid monolayer at pH 2, and aluminum ions at pH 3 to 5, barium at pH 6, and sodium at pH 8. On the other hand, in the author's experiment the various effects of the ions upon wettability appeared in the pH regions shown in Table 1, which were based upon the data of Figs. 2a, 2b, 3 and 4. It can be noted that these pH regions for various cations as a whole are in close relationship with those given for cations by Langmuir in the case of adsorption. The fact again confirms the above view, that the adsorption of ions is an important factor affecting the wettability of stearic acid. Disappearence of the remarkable wetting

Table 1

pH Regions at which Metallic Ions Affect the Wettability of Stearic Acid Surface.

Ion	pH	Ion	pH	Ion	pH	Ion	pH
Th^{++++}	2~6	Fe^{+++}	3~5	Co^{++}	5	Li^+	>10
		Al^{+++}	>4	Cu^{++}	7~8		
		Cr^{+++}	5~6	Mn^{++}	5~8 (10^{-3} mol)		
				Zn^{++}	>9 (10^{-3} mol)		
				Cd^{++}	>9 (10^{-3} mol)		
				Ba^{++}*	>10		

* Ba^{++} is considered to be partially adsorbed already at pH 6 or 7, but we cannot distinguish this surface from that of stearic acid at this pH, for both surfaces are non-dissociating and behave similarly at this pH.

(6) I. Langmuir and V. J. Schaefer, *J. Am. Chem. Soc.*, **58**, 284 (1936).

Table 2

Relation between Wetting Power and Co-ordination Tendency of Metallic Ions

Ion	Type of wetting	Degree of wetting*	Ionic potential	Ionization potential (1st), e. v.	Normal electrode potential, volt	Heat of hydration, kcal./mole	Free energy decrease of complex formation with stearate radical
Na^+	1st class	0	1.02	5.12	−2.71	114	—
K^+	〃	0	0.75	4.32	−2.92	94	—
Rb^+	〃	0	0.67	—	−2.92	—	—
Li^+	3rd class	−	1.28	5.37	−2.96	136	1.3
Ca^{++}	〃	−	1.89	6.09	−2.81	410	1.2
Sr^{++}	〃	−−	1.57	5.67	—	376	—
Ba^{++}	〃	−−	1.40	5.19	—	346	(1.1)
Ni^{++}	(3rd class)	−	2.56	7.61	−0.234	516	2.5
Hg^{++}	(〃)	−	1.79	10.38	+0.85	480	6.1
Pb^{++}	(〃)	−	1.52	7.38	−0.13	—	(3.4)
Mg^{++}	2nd class	+	2.56	7.61	−1.87	490	1.4
Cd^{++}	〃	+	1.94	8.96	−0.40	462	2.7
Zn^{++}	〃	+	2.41	9.36	−0.76	528	2.9
Mn^{++}	〃	+	2.20	7.41	−1.03	479	—
Ag^+	〃	+	0.88	7.54	+0.80	162	3.5
Co^{++}	〃	++	2.44	8.5	−0.26	504	2.2
Cu^{++}	〃	++	1.98	7.68	+0.35	536	3.4
Cr^{+++}	〃	++	4.69	6.74	−0.51	—	(4.3)
Fe^{+++}	〃	++	4.48	7.83	−0.04	185	(3.6)
Al^{+++}	〃	+++	5.26	5.96	−1.69	1149	(9.7)
Th^{++++}	〃	+++	3.64	—	—	—	—

* 0: Degree of wetting power exhibited under control condition.
−, −−: Relative degree of non-wetting power perceptible at 10^{-3} mol and 10^{-4} mol respectively.
+, ++: Relative degree of wetting power perceptible at 10^{-3} mol and 10^{-4} mol respectively.
+++: Remarkable wetting power exhibited at 10^{-4} mol.

power of ferric, thorium, chromic, cobaltous, and cupric, ions in high pH region can be attributed to the decrease of concentration of these ions in solution due to the precipitation as hydroxide.

Now, we feel much interest in the question, "What is the chief factor determining the wetting or non-wetting power of an ion?" To answer this question, we must know the nature of these adsorption products of metallic ions on stearic acid, which may presumably be attributed to the structural characteristics of the metallic ions themselves. In this connection, it is best to pay attention to the co-ordination tendency of the individual metallic ion concerned.

First of all, let us consider the aluminum ion which showed remarkable wetting power. It was known to have a marked co-ordination tendency and to form an aquo ion, $Al(H_2O)_6^{+++}$, in water, which was considered further to form so-called ol-compound and oxo-compound through hydrolysis and association of more than two aquo ions.[7] On the other hand, many fatty acid-aluminum compounds were considered by many investigators[8] to be hydrated macro-molecules. Sasaki and Matuura of our laboratory also confirmed the fact that stearic acid monolayer on the aqueous substrate containing aluminum ions showed a remarkable expansion and rigidity, while the monolayer on a substrate containing barium or calcium ions had no such properties.[9] Muramatsu and Sasaki observed that the thickness of the built-up film of stearic acid conditioned with aluminum salt solution, was remarkably increased compared with that without conditioning.[10] All these results lead us to the conclusion that the adsorption product or chemical compound between aluminum and stearic acid is composed of relatively large molecules of a complicated structure, which are also suitable for the explanation of the wetting power of aluminum ion. The complexity of the adsorption product may of course come from the marked co-ordination tendency exhibited by aluminum ion. From this point of view we may postulate further, that a marked co-ordination tendency of any metallic ion towards both water molecule and stearate

(7) N. Bjerrum, *Z. physik. Chem.*, **A 59**, 336, 581 (1907), **73**, 724 (1910), **110**, 656 (1924).

(8) V. R. Gray and A. E. Alexander, *J. Phys. & Colloid Chem.*, **53**, 26 (1949); E. Eigenberger and A. Eigenberger-Bittner, *Kolloid-Z.*, **91**, 287 (1940); Hi. Ikeda, K. Shiroyanagi and Ha. Ikeda, *Reports of The Scientific Research Institute*, **25**, 353 (1949); I. S. McRoberts and J. H. Schulman; *Proc. Roy. Soc.* (London), **A 200**, 136 (1950).

(9) T. Sasaki and R. Matuura, This Bulletin, **24**, 274 (1951). R. Matuura, This Bulletin **24**, 278 (1951)

(10) M. Muramatsu and T. Sasaki, This Bulletin, **25**, 21,25 (1952).

radical favors the wettability of the treated surface. To ascertain this presumption, we examined the parallelism required to exist between the co-ordination tendency of metallic ion and wettability of stearic acid treated with the solution containing the same ions.

As the measure of co-ordination tendency or something closely related to this, the following factors are selected as shown in Table 2, namely free energy decrease of complex formation in aqueous solution, ionic potential,[11] ionization potential (1st ionization),[12] normal electrode potential,[13] and heat of hydration.[14] The value of free energy decrease of complex formation, $N/Z \cdot \log k + \log 55$ (Z, the co-ordination number of metallic ion, N, the number of ligands co-ordinated to central metallic ion,

$$\log k = \frac{1}{N} \log \frac{[MA_N]}{[M_{aq}]\,[A]^N}, \quad [MA_N], [M_{aq}] \text{ and } [A]$$

being the concentration of the complex, hydrated cation, and ligand respectively), which is proposed by Bjerrum,[15] is calculated for the case of stearate radical as ligand using the data for other ligand. As a whole, these five series are parallel to the series of the wetting power of metallic ions mentioned above (Table 2), though there are minor irregularities not completely explained yet. Among these the series of Bjerrum's free energy shows a good parallelism. In this case, it must be kept in mind that Bjerrum calculated the value for the complete exchange of aquo-molecule for other ligands, whereas in our case, we rather require the value for the exchange of the certain fraction of exchangeable aquo-molecule for stearate radical. The latter quantity may, however, be considered to be roughly parallel to the former.

Now, we should like to consider that cadmium, silver, and zinc ions belong to the second class because they have a rather large co-ordination tendency as can be expected from Table 2. The results of Muramatsu, Matuura and Sasaki[9][10] also confirm this view. It can be noted however that nickel, mercuric and lead ions, in spite of their marked co-ordination tendency for stearate and of rather large heat of hydration, not only showed no effect of promoting the wettability of stearic acid but also exhibited a further reduction, when compared with the case of untreated stearic acid. These facts together with those obtained by Sasaki and Matuura lead us to postulate that these three ions might form another group. The author will refer to this point in a paper which will follow. Apart from these exceptions, the effect of the second group ions is considered to come from the macro-molecular structure of their adsorption product formed on stearic acid surface as mentioned already.

Sonders and others[16] insisted that the polarizability of metallic ions played an important role in the wettability when they were adsorbed on the surface of glass or clay. But their idea does not explain the wetting phenomena observed in the author's experiment.

It is required further to explain the effect of reducing the wettability due to the third group ions such as barium or calcium. Here, contrary to the macro-molecular structure of aluminum soap, barium soap is known to be a simple compound composed of the linkage of principal valency only, similarly as in the case of stearic acid. Therefore, the surface of barium soap is probably non-wettable as in the case of stearic acid in the region of low pH. The non-wetting power of barium stearate at pH>10, being different from the wettable property of stearic acid, is explained by the consideration that barium-soap is more stable against surface dissociation than free stearic acid in alkaline region. The stability is probably caused by a stronger binding force of stearate radical to barium than to hydrogen.

Thus, the wetting or non-wetting effect of the ions towards the stearic acid surface is briefly explained by either macro or simple molecular structure of the adsorption product. For the support of this view, it is worth while to point out further the following facts. It is generally recognized that the wettability is profoundly affected by the orientation or overturning of the surface molecules.[3] According to this view, together with our opinion concerning wettability, it may be expected that aluminum salt treatment renders the surface layer of stearic acid more difficult to overturn than in the case of barium salt treatment. Certainly, an easiness of overturning contributes to some extent to the non-wetting properties of a surface treated by barium salt. Thus the overturn theory not only does not contradict the experimental results and the opinion mentioned above, but also supports the result of measurements on wettability of stearic acid built-up film, which was already reported briefly by Muramatsu and Sasaki,[10] and will be described by the present author in detail in a paper which will follow.

Summary

The effect of the solution of various metallic ions at varying pH upon the wettability of stearic acid surface has been studied. These ions are adsorbed by stearic acid surface in characteristic pH region and are classified into the following three groups, according to their effects on wettability.

(11) The values were calculated from those of ionic radii from W. L. Bragg, "Atomic Structure of Minerals", Cornel University Press, New York (1937).

(12) R. F. Bacher and S. Gaoudsmit, "Atomic Energy States" McGraw-Hill Book Co., Inc., New York and London (1932).

(13) M. de K. Thompson, "Theoretical and Applied Electrochemistry" The Macmillan Co., New York (1939).

(14) J. D. Bernal and R. H. Fowler, *J. Phys. Chem.*, **1**, 515 (1933).

(15) J. Bjerrum, *Chem. Rev.*, **46**, 381 (1950)

(16) L. R. Sonders, D. P. Enright and W. A. Weyl, *J. Applied Phys.*, **21**, 338 (1950).

(1)	Wetting ions 1	Formation of ionic adsoption compound (surface dissociation).	Na, K, and Rb.
(2)	Wetting ions 2	Formation of hydrated, macromolecular adsorption compound.	Al,Th,Fe, Cr,Co,Cu, Zn,Cd,Mn and Ag.
(3)	Non-wetting ions	Formation of simple molecular non-dissociating compound of mere principal valency.	Ba, Sr, Ca, and Li.

The classification has been based upon the structural characteristics of the ions, especially the co-ordination tendency of the ions. The theory of overturning of molecules in surface layer is also one of the probable supports of these opinions.

The author wishes to express her gratitude to Prof. T. Sasaki for his kind advice and encouragement, and also to Miss. S. Miyazaki for her kind assistance throughout this study. The cost of this research has been defrayed by the Grant of the Ministry of Education given to Prof. Sasaki.

Department of Chemistry, Faculty of Science, Kyûshû University

Studies on the Conjugated Double Bond Systems. VIII. On the Electronic Structures of Furan, Pyrrole and Thiophen

By Saburo NAGAKURA and Toichiro HOSOYA

(Received January 21, 1952)

Introduction

Recently, remarkable advances have been made in the theoretical study on the electronic structures of unsaturated hydrocarbons containing conjugated double bonds. In particular, the electronic structures of benzene and other relatively simple molecules have been investigated in detail. Under these circumstances, therefore, the study on the electronic structure of hetero-cyclic compounds may be regarded not only as desirable from the stand-point of the theory of resonance, but also as necessary for the progress of the electronic theory of organic chemistry.

The first quantum mechanical treatment on hetero-cyclic compounds was made, probably, by Wheland and Pauling,[1] who used the molecular orbital method. It was, however, no more than merely making a guess at the π-electron distributions in the molecule which, apparently agreed with experimental facts on the condition that their assumed constant of electron affinity for the hetero-atom and of induced affinity for the adjacent atoms was suitable. Longuett-Higgins and Coulson[2] applied the same method to many hetero-cyclic compounds containing nitrogen, under some originai assumptions about coulomb integrals. The method of Orgel *et al.*[3] which was applied to many hetero-cyclic molecules was essentially identical with that of Longuett-Higgins and Coulson. They calculated the values for dipole moment and compared them with the experimental results.

In the present paper, the molecular orbital method has been employed in the investigation of electronic structures of furan, pyrrole and thiophene under suitable assumptions about coulomb- and exchange-integrals. The results have been used for discussiug resonance energies, dipole moments and near ultraviolet absorption spectra of these substances.

Outline of Method

In our treatment of furan, pyrrole and thiophene, we assume that they are all planar, and consider five $p\pi$ orbitals and six electrons, including an unshared pair on the hetero-atom. With the approximation of LCAO, the wave functions of molecular orbitals are as follows:

$$\Psi_j = C_{1j}\varphi_1 + C_{2j}\varphi_2 + C_{3j}\varphi_3 + C_{4j}\varphi_4 + C_{5j}\varphi_5 \quad (j=1,2,\ldots 5) \qquad (1)$$

(1) G. W. Wheland and L. Pauling, *J. Am. Chem. Soc.*, **57**, 2086 (1935).

(2) H. C. Longuett-Higgins and C. A. Coulson, *Trans. Faraday Soc.*, **43**, 87 (1947).

(3) L. E. Orgel, T. L. Cottrell, W. Dick and L. E. Sutton, *ibid.* **47**, 113 (1951).

where φ_1 is the $2p\pi$ or $3p\pi$ wave function of the hetero-atom, O, N or S, respectively, and $\varphi_2 \sim \varphi_5$ are the $2p\pi$ wave functions of the carbon atoms numbered as in Fig. 1. Assuming that φ_ts are all

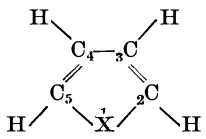

X=O, NH, S

Fig. 1.

normalized and mutually orthogonal, we reach to the following equation by the usual variation method:

$$\begin{vmatrix} H_{11}-E & H_{12} & H_{13} & H_{14} & H_{15} \\ H_{21} & H_{22}-E & H_{23} & H_{24} & H_{25} \\ H_{31} & H_{32} & H_{33}-E & H_{34} & H_{35} \\ H_{41} & H_{42} & H_{43} & H_{44}-E & H_{45} \\ H_{51} & H_{52} & H_{53} & H_{54} & H_{55}-E \end{vmatrix} = 0 \qquad (2)$$

where E is the energy of the molecular orbital Ψ_j, and $H_{rs} = \int \varphi_r H \varphi_s d\tau$.

Since these molecules belong to the symmetry group C_{2v}, the equation (2) is reduced to the following form

$$\begin{vmatrix} \alpha_1-E & \sqrt{2}\beta_1 & \sqrt{2}\beta_1' & 0 & 0 \\ \sqrt{2}\beta_1 & \alpha_2+\beta'_3-E & \beta_2+\beta_2' & 0 & 0 \\ \sqrt{2}\beta_1' & \beta_2+\beta_2' & \alpha_3+\beta'_3-E & 0 & 0 \\ 0 & 0 & 0 & \alpha_2-\beta_3'-E & \beta_2-\beta_2' \\ 0 & 0 & 0 & \beta_2-\beta_2' & \alpha_3-\beta_3-E \end{vmatrix} = 0 \qquad (3)$$

where following notations have been used, considering the symmetry of these molecules,

$$H_{11}=\alpha_1, \quad H_{22}=H_{55}=\alpha_2, \quad H_{33}=H_{44}=\alpha_3$$
$$H_{12}=H_{15}=\beta_1, \quad H_{23}=H_{45}=\beta_2, \quad H_{34}=\beta_3$$
$$H_{13}=H_{14}=\beta'_1, \quad H_{24}=H_{35}=\beta'_2, \quad H_{25}=\beta'_3.$$

That is, β_t $(t=1, 2, 3)$ is the exchange integral between adjacent atoms, and β_t' $(t=1, 2, 3)$ is the exchange integral between non-adjacent atoms. β_t' used to be neglected so far, but we will not neglect it, because in the penta-cyclic compounds, $|\beta_t'|$ is relatively large, owing to the smaller atomic distances compared with that of benzene. To make this point clear we have made calculations with and without neglecting β_t' in the case of furane and the results of two calculations have been compared with each other. (The method neglecting β_t' is named the first method, and the one including it, the second.)

These integrals are all represented with β[4], using the following approximations:

(a) the coulomb integral of the carbon atom in benzene is 4.1 β.[5]

(b) the coulomb integral of each atom is proportional to the electronegativity,[5] for which Pauling's values[6] have been adopted.

(c) the exchange integral is proportional to the overlap integral between two atoms.[7]

We have calculated the overlap integral with the aid of the table of Mulliken *et al.*[8] and the values of the atomic distances determined by Schomaker and Pauling.[9]

Under these assumptions, eigen values E_j $(j=1, 2, \ldots, 5$, numbered from the lowest level to the upper level) are evaluated and then C_{rj}s are determined for each value of E. With these values of C_{rj}s we can readily calculate the π-electron density q_r of r-atom by the following equation[1]

$$q_r = 2\sum_{j=1}^{3} C_{rj}^2$$

Now, it is possible to evaluate the formal charge of r-atom which is caused by π-electron migration from hetero- to carbon-atom. Owing to this formal charge, the correction term for the electronegativity and the overlap integral should be taken into consideration. We have obtained the correction for electronegativity according to Pauling,[10] and by the use of this corrected value the coulomb integral can be recalculated by the application of the above approximation (b). New values of overlap integrals are obtained from the tables of Mulliken *et al.*[5] and β_t's and β_t''s can be recalculated by the approximation (c). Using these values of the integrals, the equation (3) is resolved and q_rs are found.

These calculations are repeated several times until the final results are self-consistent.

Results and Discussion

In Table 1 are given our final values of energy integrals, energy levels and π-electron densities in the normal state.

Resonance Energy:—From the preceding results, we have calculated the resonance energy by the use of the following formula:

$$2(E_1+E_2+E_3)-2(\alpha_1+\alpha_2+\alpha_3+2\beta_2)$$

where α_1, α_2, α_3, and β_2 are the initial values of coulomb- and exchange integrals, *i. e.* the values

(4) β is the exchange integral between adjacent atoms of benzene.

(5) C. Sandorfy, *Bull. soc. chem. France*, (1949), 615.

(6) L. Pauling, "The Nature of the Chemical Bond," Cornell University Press, (1940) p. 64.

(7) G. W. Wheland, *J. Am. Chem. Soc.*, **64**, 900 (1942).

(8) R. S. Mulliken, C. A. Rieke, D. Orloff and H. Orloff, *J. Chem. Phys.*, **17**, 1248 (1949).

(9) V. Schomaker and L. Pauling, *J. Am. Chem. Soc.*, **61**, 1769 (1939).

(10) L. Pauling, "The Nature of the Chemical Bond" Cornell University Press, (1940) p. 65.

Table 1[a]

Values of Various Energy Integrals, Energy Levels and π-electron Densities.

	Furan (The First Method)	Furan (The Second Method)	Pyrrole (The Second Method)	Thiophene (The Second Method)
α_1	5.811	5.796	5.062	4.327
α_2	4.092	4.080	4.069	4.046
α_3	4.074	4.092	4.061	4.040
β_1	0.575	0.576	0.718	0.674
β_2	1.077	1.076	1.085	1.096
β_3	0.900	0.892	0.936	0.945
β_1'	—	0.086	0.116	0.147
β_2'	—	0.197	0.201	0.177
β_3'	—	0.193	0.204	0.130
E_1	6.304 (A_1)	6.515 (A_1)	6.429 (A_1)	6.221 (A_1)
E_2	5.383 (A_1)	5.364 (A_1)	4.876 (A_1)	4.512 (B_1)
E_3	4.804 (B_1)	4.488 (B_1)	4.453 (B_1)	4.360 (A_1)
E_4	3.190 (A_1)	3.174 (A_1)	3.026 (A_1)	2.908 (A_1)
E_5	2.462 (B_1)	2.599 (B_1)	2.536 (B_1)	2.499 (B_1)
q_1	1.869	1.896	1.745	1.578
q_2, q_5	1.011	1.036	1.060	1.100
q_3, q_4	1.055	1.016	1.068	1.111

a) In this Table, the energy values are represented in units of β.

obtained without the consideration of the resonance of π-electrons. The results are given in Table 2 together with the observed values[9] [11] which are obtained from the heat of combustion or hydrogenation. By a glance at the table, it is seen that the observed values themselves are different from each other. However, the following values may be regarded as the most probable: the resonance energy of thiophene, *i. e. ca.* 30 kcal./mol, and the difference between the resonance energy of furan and of pyrrole, *i. e. ca.*, 8 kcal./mol, which was deduced by Schomaker and Pauling[9] considering the resonance energies of many derivatives of furan and pyrrole. If these values are reliable, it is evident that the calculated values of these two quantities agree with the observed ones. In general, however, the calculated values are smaller than the observed, except in the case of the first method on furan. In addition, there is a serious difficulty in thiophene which requires a further discussion. It will be mentioned in the following section.

Dipole Moment:—The so called resonance moment which is caused by the migration of π-electron from the hetero-atom to the carbon atoms, *i. e.* μ_{mig}, can be calculated from the formal charges of the atoms and the atomic distances. The results are given in Table 3 together with the values which were determined by Schomaker and Pauling[9] using the observed values of dipole moments of these molecules and their tetrahydro-derivatives. As for pyrrole, however, they stated that it seemed to be impossible to make a reliable estimate for resonance moments on account of uncertainty regarding the orientation of the N-H bond in pyrrole and pyrrolidine, and further that various methods of making the calculation gave values lying between 1.0 and 2.5 D, 1.5 D being the most probable value.

Table 2

Resonance Energy (kcal./mol)

		Furan	Pyrrole	Thiophene
Calculated Values[a]	1st Method	17.6	—	—
	2nd Method	11.6	20.0	26.2
Observed Values	Schomaker and Pauling[9]	23	31	(31)
	Wheland (from heat of combustion)[11]	24	24	29
	Wheland (from heat of hydrogenation)[11]	17.2	—	—

(a) It is assumed that β is equal to -20 kcal./mol

Table 3

μ_{mig} (D)

		Furan	Pyrrole	Thiophene
Calculated Values	1st Method	1.21	—	—
	2nd Method	0.62	1.33	2.50
Estimated Values by Schomaker and Pauling[9]		0.95	*ca.* 1.5	1.25

If, μ_{mig} of pyrrole is calculated by the rule of vector addition using the bond moments 1.3 and 0.4 D for N-H and N-C bond,[9] respectively and assuming that pyrrole is planar, it will be found that μ_{mig} is about 1.0 D. Anyhow, in the case of pyrrole, the calculated value may be considered to be reasonable. Though the calculated value for furan by the first method is larger and by the second is smaller than the value estimated by Schomaker and Pauling, the discrepancies are not serious. On the contrary, in the case of thiophene, the calculated value is very large compared with that estimated by them. This disagreement seems to be due to the fact that the non-bonding electrons of sulphur have been represented only by the $p\pi$ wave function in our calculation. Longuett-Higgins[12] treated this molecule theoretically using the hybridisation functions of $3p\pi$ and $3d$ wave functions as those of the non-bonding electrons of sulphur atom.

Bond Order:—The bond order between neighbouring atoms r and s is defined[13] as

$$p_{rs} = 2 \sum_j C_{rj} C_{sj}$$

(11) G. W. Wheland, "The Theory of Resonance" John Wiley and Sons, New York (1947), Chapter III.

(12) H. C. Longuett-Higgins and C. A. Coulson, *Trans. Farad. Soc.*, **43**, 83 (1947).

(13) C. A. Coulson, *Proc. Roy. Soc.* (London), **A 169**, 413 (1939).

where the summation is extended over all occupied molecular orbitals. Calculated bond orders of present molecules are given in Table 4.

Table 4

Calculated Values of Bond Orders

	Furan	Furan	Pyrrole	Thiophene
	(The First Method)	(The Second Method)		
p_{12}	0.30	0.26	0.41	0.50
p_{23}	0.87	0.91	0.85	0.79
p_{34}	0.45	0.38	0.45	0.52

The difference between p_{12}, p_{23} and p_4 in the same molecule tends to decrease in the order of furan, pyrrole and thiophene. The result seems to be in agreement with the order of aromaticity of these molecules.(14)

Transition Energy and Near Ultraviolet Absorption Spectrum: — When the transition energies are calculated assuming that the electronic transition from E_3 to E_4 corresponds to the absorption spectra of the longest wave length and $\beta = 2.84$ e.V.,(15) it is found that they are 3.7, 4.0 and 4.1 e.V. in furan, pyrrole and thiophene, respectively. It is difficult to compare them with observed values, because we can not find reliable experimental data, but it seems that these values correspond to the absorption spectra,(16) 2650-2480 A. (4.6-4.9 e.V.), 2880-2540 A. (4.3-4.8 e.V.) and 2522-2246 A. (4.9-5.5 e.V.), respectively.

(14) The above mentioned view, however, is somewhat obscure owing to the following two reasons. Though it is reasonable to consider that p_{23} and p_{34} correspond to the strength of each bond, p_{12} does not do so, because as to the oxygen, nitrogen and sulphur atoms, which all have non-bonding electrons, the increase of the value of C means the decrease of bond formation character of these atoms. And as for thiophene, there is one more difficulty discussed in the preceding section.

Summary

Electronic structures of furan, pyrrole and thiophene were investigated by the use of the molecular orbital method. And values of energy levels, resonance energies, π-electron densities and bond orders were calculated. As the result of these calculations, it was found that non-bonding electrons of hetero-atoms migrate into carbon atoms and the degree of these electron migrations increases in the order of furan, pyrrole and thiophene.

The authors wish to express their sincere thanks to Prof. S. Mizushima and Prof. K. Higasi for their advice and encouragement throughout this research.

Institute of Science and Technology, and College of General Education, University of Tokyo, Meguro-ku Tokyo

(15) J. R. Platt, *J. Chem. Phys.*, **18**, 1168 (1950).
(16) H. Sponer and E. Teller, *Rev. Mod. Phys.*, **13**, 75 (1941).

Monolayers of Branched-Chain Fatty Acids I*

By Masami IZAWA

(Received February 18, 1952)

Branched-chain fatty acids have received much attention from biological points of view. Some of them are found in the normal cell of several kinds of bacteria, while some of them are strongly bactericidal. The bactericidal activity of a number of branched-chain fatty acids has been studied extensively by Adams and his coworkers,[1] and it has been stated that there is parallelism between the bactericidal activity and the surface activity of these acids. However, the exact mechanism of the bactericidal activity is still obscure.

A number of new branched-chain fatty acids have been synthesized at the Chemical Department, Institute for Infectious Diseases, Tokyo University, and their biological and chemical properties have been thoroughly investigated.[2]

* Part of this work was presented at the Meeting of the Chemical Society of Japan, held at Tokyo, Sept, 13 1947.

(1) W. M. Stanley and R. Adams, *J. Am. Chem. Soc.*, **54**, 1548 (1932).

(2) M. Asano, U. Kameta, T. Komai and I. Ishino, *Igakusōran (Japan)*, **1**, 41 (1945); M. Asano, U. Kameta and T. Wada, *J. Pharmaceut. Soc. Japan.*, **64**, 25 (1944); M. Asano and T. Yamakawa, *J. Pharmaceut. Soc. Japan*, **70**, 474 (1950); M. Asano, J. Ota and U. Ariyoshi, *Igakusōran (Japan)*, **1**, 42 (1945).

A detailed study of the monolayer behavior of these compounds may throw light on the mechanism of their action. In fact, it has been reported that there is a relation between the biological activity of alkyl substituted succinic acid half esters and the orientation of the molecules at air-water interface.[3] Unfortunately, at the present stage of our knowledge, it is not possible to correlate directly the surface properties of these acids with the biological activity. But, if we consider the surface behavior together with other properties of these acids, clearer understanding may be expected.

In this report, the measurements of force-area relations were made and the results were correlated with the structure and configuration of the molecules in the monolayer.

Techniques

The apparatus for measuring force-area curves was Langmuir-Adam type surface balance. It consisted of a nickel-plated brass trough and copper float with platinum ribbons. To avoid contamination, the whole surface of the trough, float system and glass barriers were heavily coated with solid paraffin in the usual manner, and they were rinsed with tap water about one hour before use.

The sample was dissolved with redistilled benzene and was spread on water by means of a micropipette. The volume of the micropipette was calibrated against the cross-sectional area of palmitic acid monolayer on distilled or acidic water substrates. The sensitivity of the torsion balance was 0.200 dyne per cm. per degree, and the surface pressure could be measured with the accuracy of ± 0.05 dyne/cm.

Since these compounds formed more stable films on acid substrates than on neutral or alkaline solutions, and since it was necessary to minimize the influence of heavy metal ions, experiments were made on 0.01 N hydrochloric acid solution.

Measurement was started at about one minute after spreading the material at zero pressure, and the time interval between adjacent points on the force-area curves was about thirty seconds. If the pressure changed rapidly with time owing to the hysteresis, it was read when no appreciable change was observed on the value within one minute. Generally, the coincidence between curves obtained by compression and expansion was relatively poor. Whether this is due to the instability of the monolayer or to the true hysteresis is uncertain. Each point on the curve was the mean of at least three independent measurements and was accurate within 3 per cent.

Materials

The branched-chain fatty acids used in this experiment were obtained from the Chemical Department, Institute for Infectious Diseases, Tokyo University, by courtesy of the late Prof. Asano. Palmitic acid was purchased from Dr. Theodor Schuchardt G. M. B. H. Chemische Fabrik, and was recrystallized from methanol. Its melting point was 62°C.

Results and Discussions

1. Trialkylacetic Acids.—Fig. 1 shows the force-area curves for two trialkylacetic acids with two long hydrocarbon chains at 20°C. These films are liquid-expanded, the limiting area of which is 75~80 A.^{2} per molecule, and are compressible to 60~65 A.^{2} The film of methylundecyldodecylacetic acid (I) collapses at about 7 dynes per cm., whereas monolayer of ethyldecyldodecylacetic acid (II) withstands higher pressures of 12~13 dynes. The reason for this difference may be due to the fact that while I is solid, II is liquid in

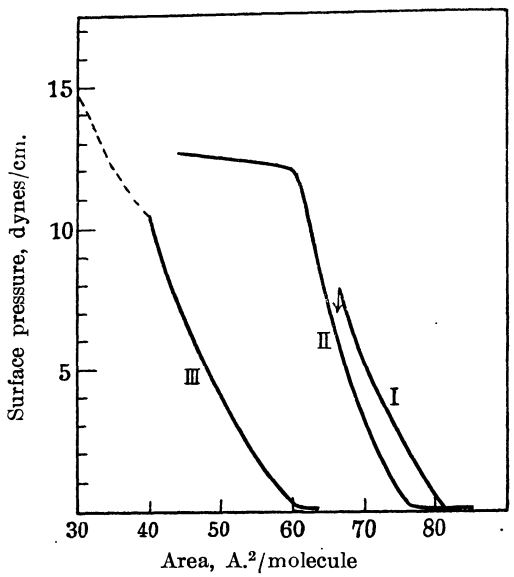

Fig. 1.—Force-area curves for methylundecyldodecylacetic acid(I)and ethyldecyldodecylacetic acid (II). Curve for phthioic acid (III) after Stenhagen is also shown in the figure. Substrate: 0.01 N HCl, 20°C.

(3) J. H. Schulman and W. McD. Armstrong, "Surface Chemistry", Interscience Publishers Inc., (1949), p. 263.

bulk state at room temperature. Below 60 A.^{2}, the curve of II shows a flat portion which indicates the existence of equilibrium between the monolayer and three-dimensional liquid drops on the substrate.

In Fig. 1, the curve for phthioic acid at 20°C (III), reported by Stenhagen,[4] is also shown. Phthioic acid is one of the normal constituents of tubercle bacillus with the formula $C_{26}H_{52}O_2$, isolated by Anderson,[5] and its molecular structure has been assumed to be a trialkylacetic acid, especially ethyldecyldodecylacetic acid (II), by Stenhagen[4] and Robinson.[6] Later, Polgar and Robinson[7] investigated the structure of the acid extensively and concluded that it was 3, 13, 19-trimethyltricosanoic acid. But the exact constitution still remains to be solved. It may be concluded at least from our results that phthioic acid is not identical with I or II.

2. β-Methylpalmitic Acid. — β-Methylpalmitic acid (IV) forms liquid-expanded film, whose limiting area is 63 A.^{2}, and compressible to about 30 A.^{2} as shown in Fig. 2.

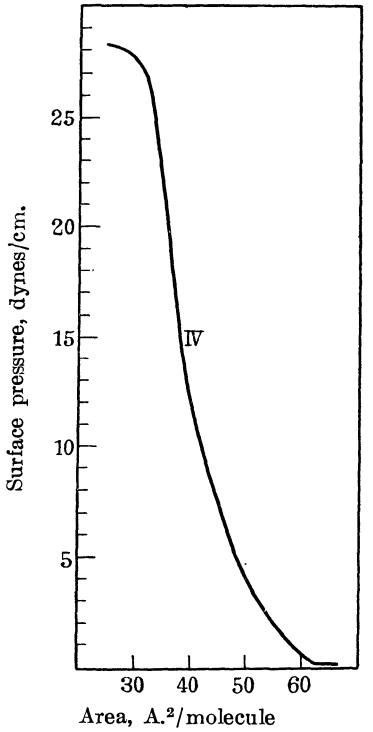

Fig. 2.—Force-area curve for β-methylpalmitic acid. Substrate: 0.01 N HCl, 25°C.

(4) E. Stenhagen and S. Ställberg, *J. Biol. Chem.*, **139**, 345 (1941).
(5) R. J. Anderson, *J. Biol. Chem.*, **97**, 639 (1932).
(6) R. Robinson, *J. Chem. Soc. (London)*, 505 (1940).
(7) N. Polgar and R. Robinson, *J. Chem. Soc., (London)*, 389 (1945).

3. β, β′, β″ - Trialkylpropionic Acids Having Only One Long Chain.—Fig. 3 shows the curves for β-methyl-β′-ethyltridecanoic acid (V) and β-methyl-β′-ethylpentadecanoic acid (VI). Both films are liquid-expanded and compressible to about 35 A.^{2}

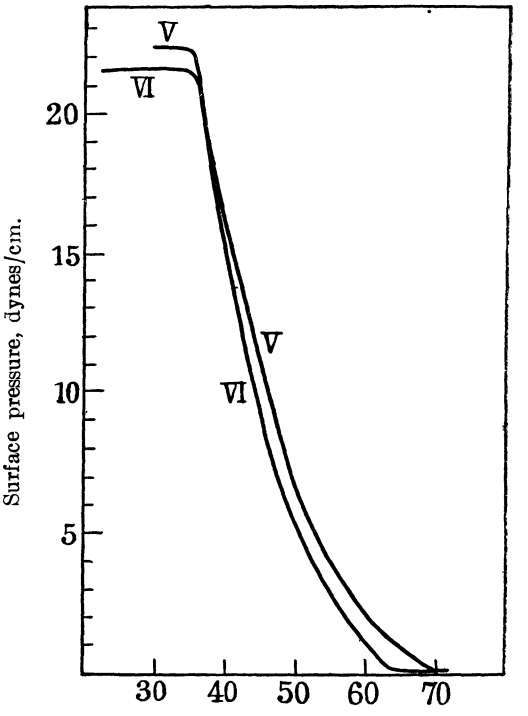

Fig. 3.—Force-area curves for β-methyl-β′-ethyltridecanoic acid (V) and β-methyl-β′-ethylpentadecanoic acid (VI). Substrate: 0.01 N HCl, 20°C.

4. Diheptylacetic Acid, β, β′-Diheptylpropionic Acid and γ, γ′-Diheptylbutyric Acid.—The effect of the position of diheptylmethyl group $[(C_7H_{15})_2—CH—]$ with respect to the carboxyl group of the acids was examined (VII, VIII and IX). As shown in Fig. 4, the limiting areas become smaller and the force-area curves steeper as the position of the substitution is separated from the carboxyl group. These monolayers collapse at about 50 A.^{2}

5. α-Ethyl Fatty Acids.—α-Ethylnonylic, α-ethylpalmitic (X), α-ethylstearic (XI) and α-ethylarachidic acids(XII) were examined (Fig. 5). α-Ethylnonylic acid does not form a stable monolayer, probably because of the high solubility of the compound. The monolayer of X is liquid-expanded, whereas monolayers of

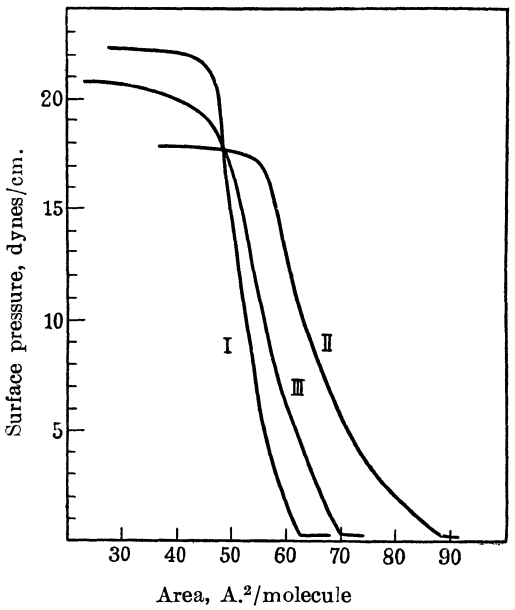

Fig. 4.—Force-area curves for diheptylacetic acid (VII), β,β'-diheptylpropionic acid (VIII) and γ,γ'-diheptylbutyric acid (IX). Substrate: 0.01 N HCl, 12°C.

XI and XII show a transition from liquid-expanded to condensed states. The latter two substances show a marked temperature effect as shown in Fig. 6.

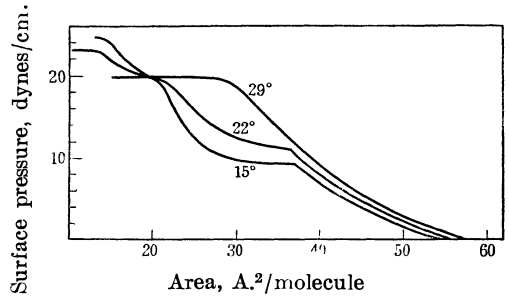

Fig. 6.—Temperature effect on the force-area curve for α-ethylstearic acid. Substrate: 0.01 N HCl.

6. α-Methyl-and α-Propylmyristic Acids. —The effect of α-substituted groups of myristic acid on the force-area curve is shown in Fig. 7 (XIII and XV). As the side chain becomes longer, the limiting area is larger and the equilibrium pressure is lower. The curve for

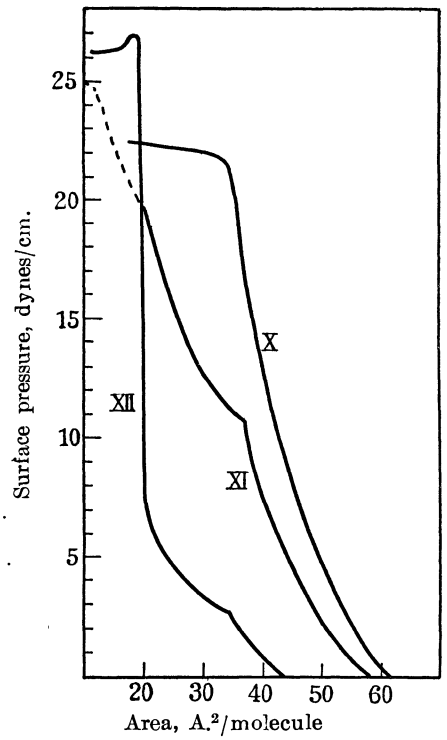

Fig. 5.—Force-area curves for α-ethylpalmitic acid (X), α-ethylstearic acid (XI) and α-ethylarachidic acid (XII). Substrate: 0.01 N HCl. 20°C.

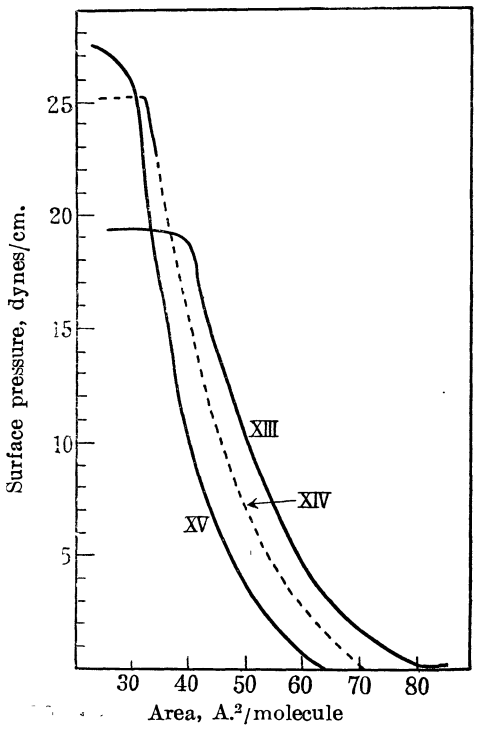

Fig. 7.—Force-area curves for α-propyl- (XIII) and α-methyl- (XV) myristic acids. XIV indicates the curve for α-methylpentadecylic acid after Stenhagen. Substrate: 0.01 N HCl, 20°C (XIV and XV) and 18°C (XIV).

α-ethylpalmitic acid (XIV) reported by Stenhagen[8] falls between these curves as indicated by a dotted line in the figure.

The monolayers reported above are all of liquid-expanded type. In 1933, Langmuir proposed a theory for the liquid-expanded state.[9] According to his theory, liquid-expanded films are composed essentially of two layers, the upper being an insoluble oil layer consisting of the hydrocarbon portion of the molecules, and the lower a layer of hydrophilic groups of the molecules which exists at the interface of oil and water phases and which acts as a gaseous film. The force-area relation for this state can be represented by the following equation:

$$(F-F_0)(a-a_0)=kT,$$

where F: surface pressure,
a: area per molecule,
k: Boltzmann constant,
T: absolute temperature,
F_0: a constant relating to the spreading coefficient of an assumed oil layer consisting of the hydrocarbon portion of the molecules in the film.
a_0: a constant relating to the actual cross-sectional area of one molecule on the surface.

The force-area relations for the branched-chain fatty acids examined fit this equation well. This theory has been opposed by several authors,[10] but essentially it will be right, as was pointed out by Adam,[11] irrespective of minute difficulties.

Since two constants, F_0 and a_0, in the equation may be considered as relating to the structure of molecules in the monolayer, it may be reasonable for these constants as well as the limiting area or the area at collapse to be characteristic to the molecular structure. The values of F_0 and a_0 calculated from the experimental curves are listed in Table 1. From the table, it can be seen clearly that there are close relations between the structure of the molecules and the values of F_0 and a_0. These relations are summarized as follows:

i) When two long hydrocarbon chains exist in the molecule, constant a_0 becomes about 40 A.^{2} This is shown in series 1 (except phthioic acid) and 4. Especially in series 4, the a_0 value of the three acids is determined by the diheptylmethyl radical $[(C_7H_{15})_2-CH-]$ and is about 40 A.^{2}, which is twice the value of the cross-sectional area of one hydrocarbon chain, in spite of the quite different shapes of the force-area curves. Shereshefsky and Wall[12] reported that dilauryl maleate forms a liquid-expanded film, the a_0 of which is 39.0 A.^{2} Hence, two long hydrocarbon chains of these compounds consist of a hydrophobic portion of the molecules, and stand side by side in the monolayer. It may be mentioned here that a_0 is practically equal to the "area at collapse", because the force-area curves are nearly vertical at the collapse point.

ii) The a_0 of the films which possess only one long chain in the molecule is about 20 A.^{2} Series 2, 3, 5 and 6 correspond to this structure. But as shown in series 6, the longer the side chain is, the larger is a_0, and, presumably, the smaller is $-F_0$. The value of the a_0 of tuberculostearic acid $[C_8H_{17}-CH(CH_3)-(CH_2)_8-COOH]$ is also about 20 A.^{2} if calculated from the published data.[4]

iii) An increase in the length of the long chain results in the increase in $-F_0$ value, but a_0 seems to be independent of it. Calculations were made on two other acids of similar structure (α-ethyltridecanoic and α-ethylpentadecanoic acids) based on the curves reported by Stenhagen,[4] and they are included in Table 1. From these figures, the influence of the chain length on the F_0 value will be evident. It has been reported by Langmuir[9] that, in normal chain fatty acids, there is a linear relation between the number of carbon atoms of the acids and F_0 as follows:

$$F_0=4.8-1.3n,$$

where n is the number of carbon atoms of the alkyl portion of the acid ($C_nH_{(2n+1)}COOH$). It can be concluded that there is a similar relation in the branched-chain fatty acids examined here at least qualitatively.

iv) As the branching shifts from the position of α, through β, to γ, with respect to the carboxyl group, $-F_0$ increases in this order. This is shown in series 4.

v) As the side chain in the α position becomes longer, a_0 increases and, apparently, $-F_0$ diminishes. Series 6 shows this regularity.

These relations are of a qualitative nature, and hold as long as films are of the liquid-expanded type. Using these relations, it should be expected that branched-chain fatty acids or other compounds newly synthesized or extracted from natural products can be identified, and in favorable cases, information about the

(8) E. Stenhagen, *Trans. Faraday Soc.*, **36**, 597 (1940).
(9) I. Langmuir, *J. Chem. Phys.*, **1**, 756 (1933).
(10) For example, W. D. Harkins and E. Boyd, *J. Phys. Chem.*, **45**, 20 (1941).
(11) N. f. Adam, "The Physics and Chemistry of Surfaces", Oxford University Press, (1938), p. 67.
(12) J. L. Shereshefsky and A. A. Wall, *J. Am. Chem. Soc.*, **66**, 1072 (1944)

Table 1

The Values of F_0 and a_0 in the Langmuir Equation for Liquid-Expanded Films of Branched-Chain Fatty Acids

Series No.	Sample No.	Formula	Temperature	a_0	$-F_0$
1	I	$\begin{matrix}CH_3\\C_{11}H_{23}\\C_{12}H_{25}\end{matrix}\!\!>\!CHCOOH$	20°	45.0	11.8
	II	$\begin{matrix}C_2H_5\\C_{10}H_{21}\\C_{12}H_{25}\end{matrix}\!\!>\!CHCOOH$	20°	45.5	12.9
	III†	Phthioic acid	20°	20.	9.8
2	IV	$\begin{matrix}CH_3\\C_{13}H_{27}\end{matrix}\!\!>\!CHCH_2COOH$	25°	22.0	10.4
3	V	$\begin{matrix}CH_3\\C_2H_5\\C_{10}H_{21}\end{matrix}\!\!>\!C\ CH_2\ COOH$	20°	24.9	9.1
	VI	$\begin{matrix}CH_3\\C_2H_5\\C_{12}H_{25}\end{matrix}\!\!>\!C\ CH_2\ COOH$	20°	24.3	10.4
4	VII	$\begin{matrix}C_7H_{15}\\C_7H_{15}\end{matrix}\!\!>\!CHCOOH$	12°	42.0	8.6
	VIII	$\begin{matrix}C_7H_{15}\\C_7H_{15}\end{matrix}\!\!>\!CH\ CH_2\ COOH$	12°	38.5	12.5
	IX	$\begin{matrix}C_7H_{15}\\C_7H_{15}\end{matrix}\!\!>\!CH\ CH_2CH_2COOH$	12°	37.2	15.8
5	†	$\begin{matrix}C_2H_5\\C_{11}H_{23}\end{matrix}\!\!>\!CHCOOH$	18°	22	6.9
	X	$\begin{matrix}C_2H_5\\C_{14}H_{29}\end{matrix}\!\!>\!CHCOOH$	20°	22.2	9.9
	XI	$\begin{matrix}C_2H_5\\C_{16}H_{33}\end{matrix}\!\!>\!CHCOOH$	20°	20.2	10.1
	XII††	$\begin{matrix}C_2H_5\\C_{18}H_{37}\end{matrix}\!\!>\!CHCOOH$	20°	(13)	(11.9)
6	XIII	$\begin{matrix}C_3H_7\\C_{12}H_{25}\end{matrix}\!\!>\!CHCOOH$	20°	26.3	7.5
	XIV†	$\begin{matrix}C_2H_5\\C_{13}H_{27}\end{matrix}\!\!>\!CHCOOH$	18°	22	7.6
	XV	$\begin{matrix}CH_3\\C_{12}H_{25}\end{matrix}\!\!>\!CH\ COOH$	20°	19.1	9.8

† F_0 and a_0 were calculated from the $F-a$ curves reported by Stenhagen *et al.*[4]

†† The values of F_0 and a_0 are uncertain because the film shows a transition from liquid-expanded to condensed states.

structure of them may be obtained.

Summary

(1) Force-area relations for the monolayers of a number of branched-chain fatty acids have been investigated.

(2) These monolayers are of the liquid-expanded type, on acidic substrates, and force-area curves fit the Langmuir equation well.

(3) Constants F_0 and a_0 in the Langmuir equation have been calculated from the curves. It has been shown that there is a definite regularity between these constants and the structure of the molecules in the films.

(4) It was revealed that the structure of phthioic acid is not of the trialkylacetic acid type as postulated by Stenhagen and Robinson.

This work was started at the Department of Chemistry, Faculty of Science, Tokyo University under the direction of Prof. Sameshima. The author wishes to express his sincere appreciation to Prof. Sameshima for his kind direction, and also to Dr. Akamatsu and Dr. Tachibana of Tokyo University, and Dr. Umezawa of the National Institute of Health for their advice in the present study. He is also greatly indebted to the late Prof. Asano for a number of samples of branched-chain fatty acids.

National Institute of Health, Tokyo

The Crystal Structure of Trinitrotriammine-cobalt (III), $[Co(NH_3)_3(NO_2)_3]$

By Yoshimichi TANITO, Yoshihiko SAITO and Hisao KUROYA

(Received December 19, 1951)

Introduction

According to Y. Shibata and R. Tsuchida,[1] the third absorption bands of co-ordinated compounds in aqueous solutions may be attributable to a pair or pairs of negative radicals co-ordinated in *trans*-positions and, from this point of view and because of the existence of the third absorption band at 120.4×10^{13} sec^{-1} ($\lambda=2492$ A.) with $\log\varepsilon=3.81$, it has been postulated that, to the trinitrotriammine-cobalt (III), $[Co(NH_3)_3(NO_2)_3]$, a *cis-trans*-configuration, instead of a *cis-cis* form, should be assigned (Fig. 1).

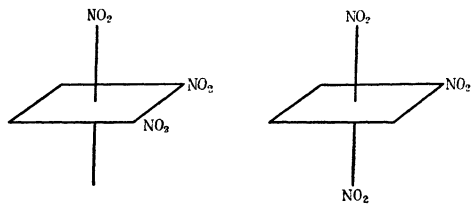

Cis-cis form *Cis-trans* form

Fig. 1.—Two possible forms of trinitrotriammine-cobalt (III).

In order to verify the above-mentioned conclusion by determining directly the configuration of the complex molecule, we have attempted to investigate the crystal structure of this compound.

Material

Trinitrotriammine-cobalt (III) was prepared by the method of Jörgensen.[2] Recrystallization from water containing a small amount of acetic acid yielded thin tabular crystals. The crystals belonging to the orthorhombic bisphenoidal class, are usually platy in habit with (010) extended.

According to Jaeger[3] the axial ratios are:

$$a:b:c=0.8682:1:0.6020\ ;$$

and the density is 1.992 g./cc. at 25°C.

Experimental

The X-ray work was carried out with Fe K_α radiation ($\lambda=1.937$ A.)

The crystals selected for the present study were $1\times1\times0.1$ mm. in effective dimensions. Only very thin platy crystals were available. Oscillation photographs about [100] and [001] gave the dimensions:

$$a=10.20\text{ A.},\ b=11.77\text{ A. and }c=6.99\text{ A.},$$

with the axial ratios

$$a:b:c=0.867:1:0.594$$

in agreement with the values obtained morphologically.

The space group is $D_2^4-P2_12_12_1$. There are four molecules in the unit cell, the calculated density being 1.972 g./cc. All the atoms are in the general positions: xyz; $1/2+x, 1/2-y, -z$; $1/2-x, 1/2+y, 1/2-z$; $-x, -y, 1/2+z$.

The reflections were estimated visually by comparison with a time calibrated scale of exposures, and they were converted into structure amplitudes by applying the appropriate correction factors, as shown in Fig. 2.

Analysis

At the outset of the analysis the following characteristics of intensity distribution were found:

(hkl); $h+l=2n$: strong
$(hk0)$; $h=2n$: strong
$(0kl)$; $k=2n$, $l=2n$: strong
and $(h0l)$; $h+l=2n$: strong.

This may indicate that the cobalt atoms are at $(x, 1/4, 1/4)$ etc., the arrangement of cobalt atoms alone thus having the symmetry D_{2h}^7-Bbmm. This was confirmed by synthesizing Patterson projections $I(xy)$ and $P(yz)$. These lead us to fix the positions of the cobalt atoms at 0.0686, 0.2500, 0.2500, etc.

Preliminary Fourier projections of electron density upon (001) and (100) were synthesized using $F(hk0)$'s with h even and $F'(0kl)$'s with k, l

(1) Y. Shibata, *J. Chem. Soc. Japan*, **36**, 1243 (1915); R. Tsuchida, *J. Chem. Soc. Japan*, **59**, 586 (1938).
(2) S. M. Jörgensen, *Z. anorg. Ch.*, **17**, 463 (1898).
(3) F. M. Jaeger, *Z. Krist.*, **39**, 568 (1904).

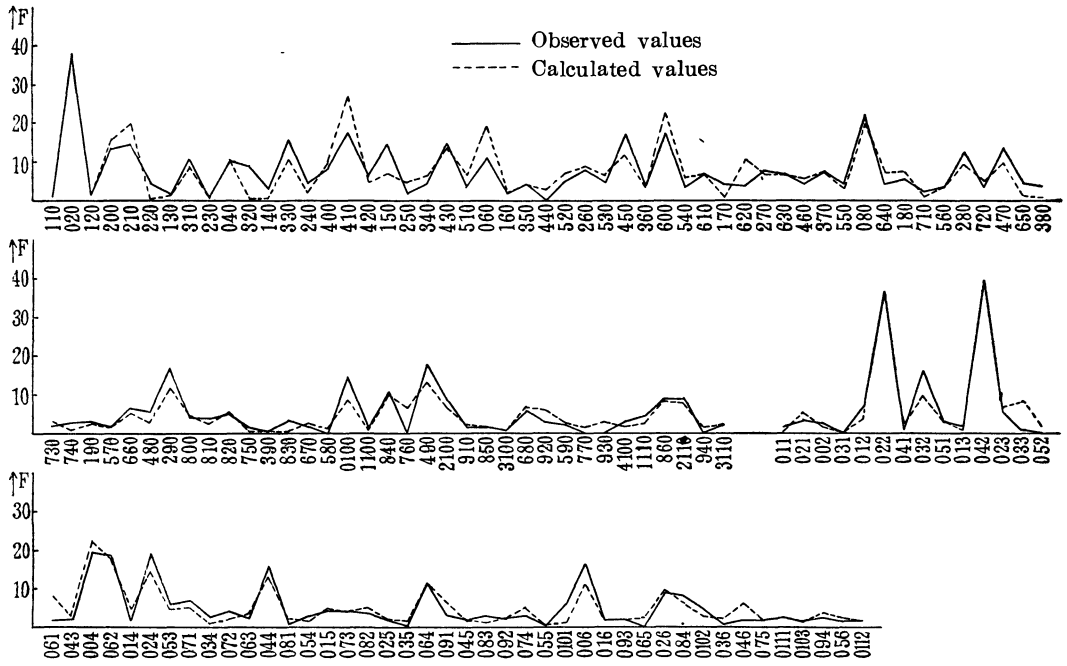

Fig. 2.—Observed and calculated F-values for trinitrotriammine-cobalt (III).

all even respectively, the signs of which were calculated from the parameter values of cobalt. From these projections we could assign approximate parameters for nitrogen atoms which form a distorted octahedron around each cobalt atom. These were in good accord with the conclusion drawn from Patterson projections $P(xy)$ and $P(yz)$. However, from the Fourier maps so obtained we could not locate the oxygen atoms unequivocally and we tried to determine the positions of these by trial and error. Bond angles and distances usual in nitro-compounds were used to locate oxygen atoms. Since the structure amplitudes $F(hk0)$ and $(F(0kl)$ could be accounted for only by one of the models having the *cis-trans* configuration, we regarded it as an approximate structure of trinitrotriammine cobalt (III) and started to determine the atomic parameters by successive approximations. The final parameters are listed in Table 1.

Table 1

Parameters of atoms in trinitrotriammine-cobalt (III)

	x/a	y/b	z/c
Co	0.0686	0.2500	0.2500
N(1)	−0.116	0.210	0.227
N(2)	0.020	0.360	0.450
N(3)	0.118	0.140	0.050
NH_3(1)	0.255	0.288	0.273
NH_3(2)	0.049	0.366	0.046
NH_3(3)	0.088	0.134	0.455
O(1)	−0.139	0.119	0.143
O(2)	−0.199	0.275	0.300
O(3)	0.135	0.393	0.472
O(4)	−0.068	0.401	0.558
O(5)	0.240	0.153	0.072
O(6)	0.076	0.054	−0.036

The values of $F(hk0)$ and $F(0kl)$ calculated from the parameter values in Table 1 are generally in good agreement with the observed values as shown in Fig. 2. In the calculation of the structure factors the atomic scattering curves in Internationale Tabellen (1935) were employed and corrected for temperature according to the Debye-Waller formula, the constant B being given the value 2.50×10^{-16} cm^2. For nitrogen belonging to the NH_3 group an appropriate correction,[4] due to the embedded hydrogen atoms, was made. A correction[5] for the anomalous dispersion for the Co atom ($\Delta f=2.2$) was also taken into account.

Description of the structure

The structure projected on the plane (001) is shown in Fig. 3 and the Fourier diagram in Fig. 4.

The cobalt atom occupies a general position. The arrangement of the cobalt atoms themselves has the symmetry D_{2h}^7—*Bbmm*. The proper symmetry of a cobalt atom is C_1-1 and this is surrounded by three nitrogen atoms of nitro-groups and three ammonia molecules, which form

(4) T. Watanabé, M. Atoji and C. Okazaki, *Acta Cryst.*, **3**, 405 (1950).

(5) H. Hönl, *Ann. Phys. Lpz.*, **18**, 625 (1935); R. W. James, "The Optical Principles of the Diffraction of X-rays" p. 609, G. Bell and Son, London, (1950).

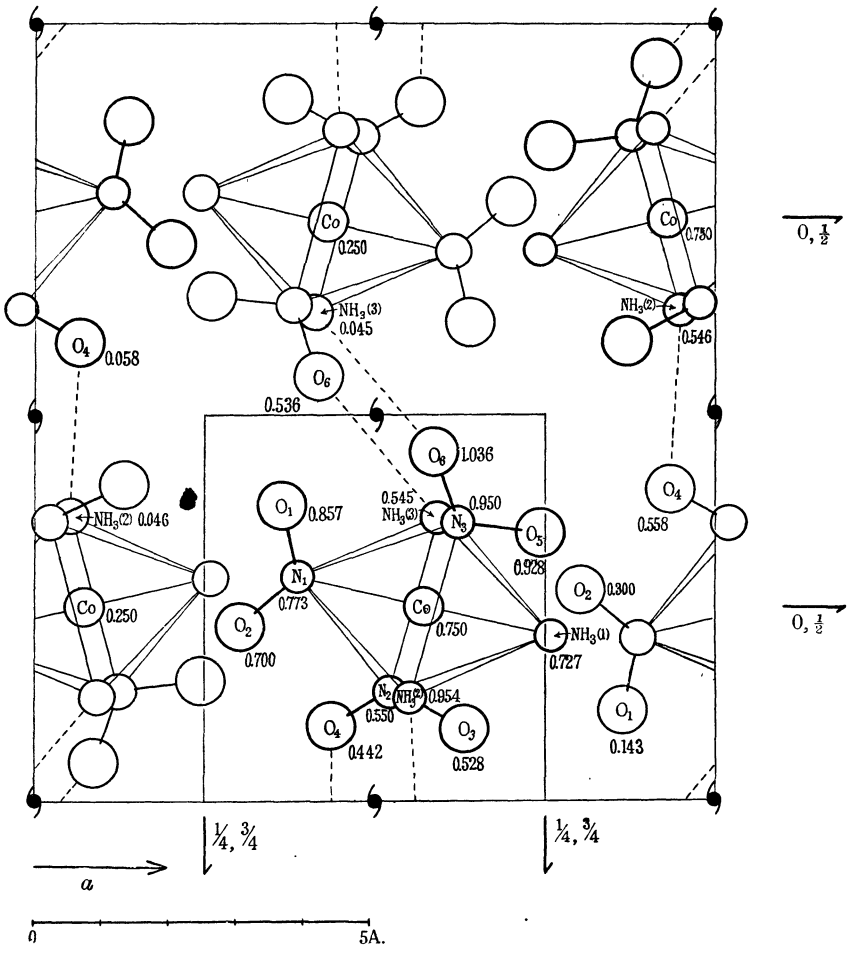

Fig. 3.—Projection of the structure upon (001) for trinitrotriammine-cobalt (III). Numbers give the height of atoms from (001) as fractions of the translation. N—H...O bonds are shown by dotted lines. The part of the cell corresponding to Fig. 4 is indicated.

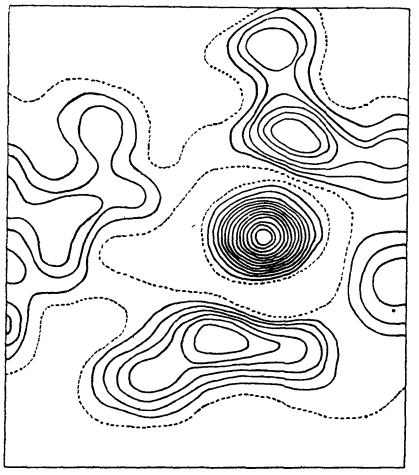

Fig. 4.—A Fourier projection of electron density of trinitrotriammine-cobalt(III). Contours at intervals of 2 e. A^{-2}., the first being broken.

a slightly distorted octahedron around the cobalt atom. Two of the nitro-groups are co-ordinated to a cobalt atom in *trans*-positions with respect to each other.

The interatomic distances as well as interbond angles are listed in Table 2.

Owing to the complexity of this crystal structure, involving the determination of 39 parameters and the overlapping of atomic peaks in both of the Fourier projections of electron density $\rho(xy)$ and $\rho(yz)$ it was not possible to determine the interatomic distances and interbond angles very accurately. The shape and size of the nitro-groups (N-O=1.25 A., $\angle$ONO=120°) may be compared with the values (N-O=1.25 A.. $\angle$ONO=112°) for the Erdmann's salt,(6) or with the values recently obtained for aromatic nitro-compounds.(7)

(6) A. F. Wells, *Z. Krist.*, **94**, 74 (1935).
(7) For example, F. J. Llewellyn, *J. Chem. Soc.*, **1947**, 884.

Table 2

Interatomic distances and angles in trinitro-triammine-cobalt (III).

Within a complex radical			Between neighboring molecules		
		A.			A.
Co	N(1)	1.96	$NH_3(2)$	0(4)	2.74
	N(2)	1.97	$NH_3(3)$	0(6)	2.78
	N(3)	1.97	$NH_3(1)$	0(1)	3.29
Co	$NH_3(1)$	1.97	$NH_3(1)$	0(2)	3.10
	$NH_3(2)$	1.98	0(1)	0(6)	3.10
	$NH_3(3)$	1.99	0(2)	0(5)	2.76
N(1)	0(1)	1.24			
	0(2)	1.25			
	∠ONO	127°			
N(2)	0(3)	1.25			
	0(4)	1.27			
	∠ONO	119°			
N(3)	0(5)	1.27			
	0(6)	1.25			
	∠ONO	121°			
0(1)	0(6)	2.65			
0(2)	0(4)	2.69			
$NH_3(1)$	0(3)	2.23			
	0(5)	2.13			

The closest approach of the molecules is between O atom of NO_2 group of one molecule and NH_3 of another. It seems likely that the binding forces between the molecules are mainly due to the N-H...O bonds between ammonia and nitro-groups. This N-H...O bonds are evidenced by characteristic short NH_3-O distances (2.75 A., 2.80 A.). They are shown in Fig. 3 by dotted lines. Somewhat analogous hydrogen bridges have been recently reported in the case of ammonium tetrametaphosphate.[8] Such bridges of length 2.8 A. have also been reported in several other cases.

By these NH...O bonds the complex molecules form a spacial network parallel to the plane (010). The NH_3...O distances between the molecules in the adjacent (010) layers (3.10 A., 3.29 A.) are longer by far than those between the molecules in the (010) layers. This fact may suggest that the interactions which are responsible for uniting molecules in the (010) planes would be greater than those which exert between the molecules of adjacent (010) layers. It is to be noted here that the shorter N-H...O bonds are formed between the nitro-groups in *trans*-positions and the ammonia groups also in *trans*-coordination.

Unlike other complex salts consisting of neutral molecules, trinitrotriammine-cobalt (III) is fairly soluble in water (0.177 g. in 100 parts of water at 16.5°C.[9]) This fact may be related to the presence of hydrogen bonds between molecules in crystals and also between these molecules and water in solution.

Summary

The crystal structure of trinitrotriammine-cobalt (III) prepared accoding to the method of Jörgensen has been studied by X-rays, using rotation methods (Fe K_α, $\lambda=1.937$ A.). This structure belongs to the orthorhombic system and the dimensions of the unit cell which contains four molecules of $[Co(NH_3)_3(NO_2)_3]$ are $a=10.20$ A., $b=11.77$ A., and $c=6.99$ A. The space group is $D_2^4-P2_12_12_1$. The cobalt atom is surrounded by six nitrogen atoms approximately in octahedral coordination. The shape and size of the nitro-groups are like those in $Ag[Co(NH_3)_2(NO_2)_4]$. Two of the nitro-groups are found to be (coordinated to) the cobalt atom in the *trans*-positions with respect to each other in conformity with the conclusion drawn from spectroscopic investigations.

The authors express their hearty thanks to Profs. I. Nitta and R. Tsuchida of the Osaka University for their kind advice and encouragement in the course of this study. Part of the cost of this study has been defrayed by a Grant of the Ministry of Education, to which the authors' thanks are due.

Institute of Polytechnics, Osaka City University, Osaka

(8) C. Romers, J. A. A. Ketelaar and C. H. MacGillavry, *Acta Cryst.*, **4**, 114 (1951).

(9) A. Werner, P. Larish and F. Ephraim., *Ber.*, **56**, 1532, (1923).

The Crystal Structure of Alpha-amino Isobutyric Acid*

By Sakutaro HIROKAWA, Shunsuke KURIBAYASHI and Isamu NITTA

(Received January 9, 1952)

Introduction

Since the war, crystal structures of some amino acids have been determined by several authors[1],[2],[3],[4] using the three-dimensional Fourier method. These works have revised several points of older knowledge; for example, the value of C—N distance has now turned out to be nearly equal to the sum of covalent radii of carbon and nitrogen atoms. Still it is desirable to collect more X-ray data extended to other amino acids in order to study the nature of chemical bonds as well as protein structure. Thus the present authors have carried out the investigation on the crystal structure of α-amino isobutyric acid, of which an account will be given below.

Crystallographic and Other Data

Alpha-amino isobutyric acid $(CH_3)_2C(NH_2)COOH$ was for the first time found by T. Yabuta[5] in 1938 in the decomposition products of a protein. The melting point of this new substance is 319~320°C. and it sublimes already fairly below the melting point like many other amino acids. The reaction of this substance with thymol-hypobromite is shown to be positive.

Single crystals used in this investigation were prepared from aqueous solution by slow evaporation. These show monoclinic symmetry, and cleavage parallel to (110) is very perfect and that cleavage parallel to (001) is fairly perfect. Specimens were cut into cylindrical shape being not more than 0.05 mm. in diameter. From the oscillation photographs of a-, b- and c-axes respectively, the unit cell of this crystal was determined to be of the following dimensions; $a=10.59\pm0.04$ kx, $b=8.97\pm0.01$ kx, $c=11.34\pm0.03$ kx and $\beta=94\pm0.5°$, the number of molecules in this unit being calculated to be eight from the density $\rho=1.27_5$ measured by the flotation method. The determined space group is C^6_{2h}—C2/c.

Determination of the Structure

The eight molecules in the unit cell should be arranged so that every set of eight atoms all occupy the eight-fold general positions of C2/c. The Patterson and Harker series were synthesized along a-, b- and c-axes, of which $P(x, y)$, $P(y, z)$ and $H(x, 1/2, z)$ were especially useful to find the atomic parameters. These are shown in Figs. 1, 2 and 3.

Using the results of the trial and error

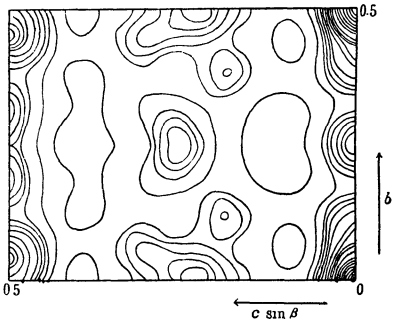

Fig. 1.– P(y, z). The contour lines are drawn at equal intervals of an arbitrary scale.

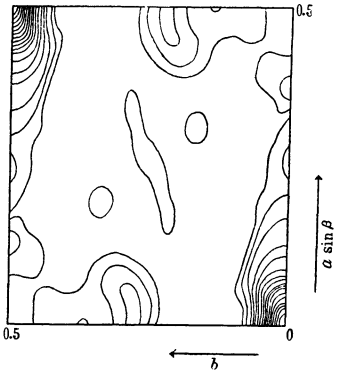

Fig. 2.—P(x, y). The contour lines are drawn at equal intervals of an arbitrary scale.

* A preliminary study of this problem was reported at the anual Meeting of the Chemical Society of Japan in April, 1950.

(1) E. W. Hughes and W. T. Moor, *J. Am. Chem. Soc.*, **71**, 2618 (1949).

(2) J. Donohue, *J. Am. Chem. Soc.*, **72** 949 (1950)

(3) G. B. Carpenter and J. Donohue, *J. Am. Chem. Soc.*, **72**, 2315 (1950).

(4) D. Shoemaker, J. Donohue, V. Schomaker and R. B. Corey, *J. Am. Chem. Soc.*, **72**, 2328 (1950).

(5) T. Yabuta, *Gakuj yutsu Kyokai (Japanese Scientific Association) Ho*, **13**, 80 (1938).

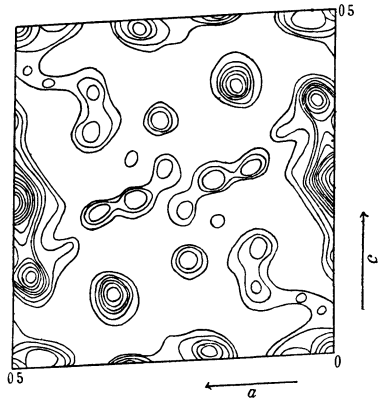

Fig. 3.—H $(x, 1/2, z)$. The contonr lines are drawn at equal intervals of an arbitrary scale.

method, the two-dimensional Fourier series were synthesized along the three principal axes. As the resolution of the obtained projections for the whole unit cell was rather poor, the part-cell projections were prepared. However, in these projections the atoms were not yet sufficiently resolved. Thus we proceeded to the three-dimensional Fourier analysis, which was done by the method of the Beevers-Lipson strips. The result is shown in Fig. 4.

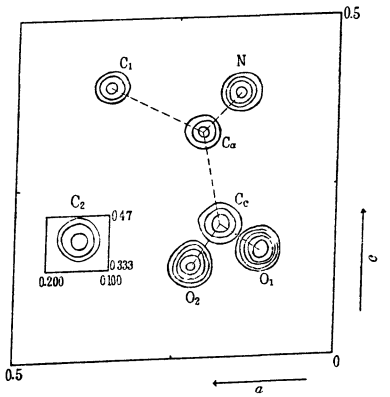

Fig. 4.—Composite drawing of electron density which were made from a section of $\rho\,(x, y, z)$ at several values of y. The contour lines are drawn at equal intervals of an arbitrary scale.

The refined locations of peaks were calculated by the method proposed by G. B. Carpenter and J. Donohue[3] in the paper on *N*-acetylglycine. Final parameter values obtained are listed in Table 1. Another table of comparison between observed and calculated *F*-values is omitted because of scarcity of space. Copies of this table will be available if required. In calculting structure factors a temperature factor with B=2.25 A.^{2} was used. For the accuracy of determination expressed in the usual way as

$$\Sigma(|F_{obs.}| - |F_{calc.}|)/\Sigma|F_{obs.}|$$

a figure of 0.199 was obtained for 1110 (*hkl*) reflections. It is to be added that this determination neglects the contributions of the hydrogen atoms.

Table 1

Parameter Values of Atoms

	N	C_c	C_α	C_1	C_2	O_1	O_2
x	0.154	0.178	0.212	0.355	0.148	0.112	0.224
y	0.100	−0.025	−0.031	−0.027	−0.167	0.083	−0.121
z	0.388	0.199	0.331	0.365	0.382	0.159	0.138

Discussion of the Structure

The determined atomic configuration and dimensions of the α-amino isobutyric acid molecule in the crystal are shown in Fig. 5. as well as in Table 2.

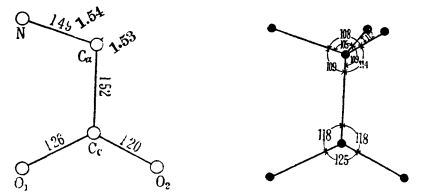

Fig. 5.—The molecule of the α-amino isobutyric acid, showing interatomic distances and bond angles. The hydrogen atoms are not drawn.

Table 2

Interatomic Distances and Bond Angles

Distances kx	Angles
$O_1-C_c=1.26$	$O_1-C_c-O_2=125.3°$
$O_2-C_c=1.20$	$O_1-C_c-C_\alpha=117.9°$
$C_c-C_\alpha=1.52$	$O_2-C_c-C_\alpha=117.7°$
$C_\alpha-N=1.49$	$C_c-C_\alpha-N=108.8°$
$C_\alpha-C_1=1.53$	$C_c-C_\alpha-C_1=114.0°$
$C_\alpha-C_2=1.54$	$C_c-C_\alpha-C_2=108.7°$
	$N-C_\alpha-C_1=107.5°$
	$N-C_\alpha-C_2=104.9°$
	$C_1-C_\alpha-C_2=112.2°$

The two C_α—C (methyl) distances and the C_α—N distance were found to be 1.53, 1.54 and 1.49 kx, respectively, in agreement with the sum of the covalent radii of Pauling. Among the bond angles of carbon atoms which are mostly nearly equal to the standard tetrahedral angle, there are observed some appreciable

deviations, for example, $C_c-C_\alpha-C_1=114.0°$ and $N-C_\alpha-C_2=104.9°$. As for the structure of the carboxylic group it was found that the bond distances $C-O_1$ and $C-O_2$ are somewhat

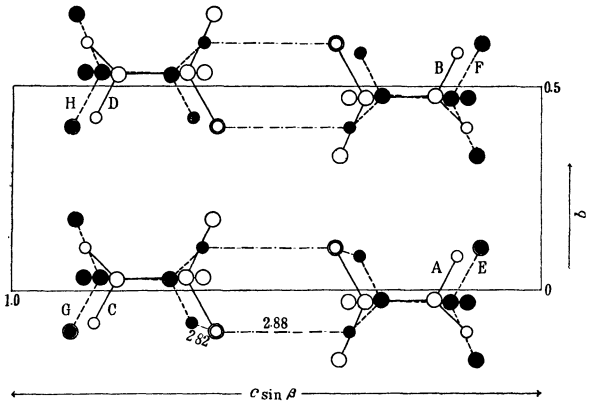

Fig. 6a.—Projection of molecules upon the (100) plane of the crystal, showing some significant interatomic distances. To distinguish molecules which superpose one another, atoms of one kind are drawn in white circles and those of the other kind are drawn in black circles.

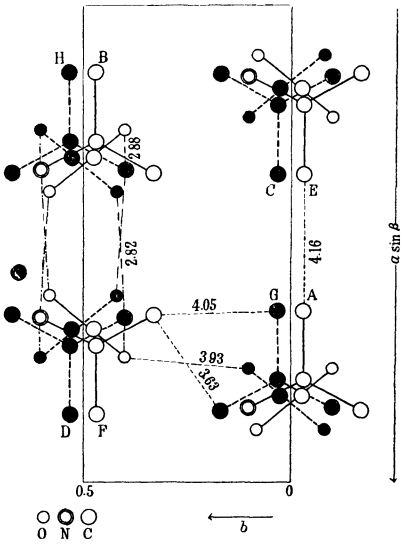

Fig. 6b.—Projection of molecules upon the (001) plane of the crystal, showing some significant interatomic distances. To distinguish molecules which superpose one another, atoms of one kind are drawn in white circles and those of the other kind are drawn in black circles.

different, 1.26 and 1.20 kx. respectively. It is to be noted that in the case of DL-alanine $C-O_1=1.21$ Å. is shorter than $C-O_2=1.27$ Å. Like all the amino acids hitherto analysed, the *N* atom lies approximately in the same plane as the carboxylic group. The value of the interatomic distance between N and O_1 in the molecule was calculated to be 2.61 kx.

The projections of the molecules along *a* and *b* axes respectively are given in Figs. 6a and 6b. The principal intermolecular interatomic distances between molecules are listed in Table 3. In these, the letters A to H refer to equivalent points in the space group as follows:

A: x, y, z; B: $1/2+x, 1/2+y, z$; C: $-x, -y, -z$; D: $1/2-x, 1/2-y, -z$; E: $-x, y, 1/2-z$; F: $1/2-x, 1/2+y, 1/2-z$; G: $x, -y, 1/2+z$; H: $1/2+x, 1/2-y, 1/2+z$.

It is seen that there are two types of hydrogen bonds in intermolecular contacts, one of which is formed between N and O_1, *e. g.* N in (B) and O_1 in (F) and its dimension is 2.82kx, and the other is between N and O_2, *e. g.* N in (B) and O_2 in (H) and its dimension 2.88 kx. It can be said that the molecules are tied to one another with hydrogen bonds in two dimensions between amino groups and carboxylic groups. There is seen considerably short intermolecular contact with respect to methyl groups, *e. g.* C_2 in (F) and C_2 in (G). The dimension of this contact is 3.63 kx. still shorter than that 3.79 A. in L-threonine crystal.

Considering the intermolecular contacts observed, the cleavages parallel to (110) and to (001) are interpreted quite naturally. For reference molecular dimensions found in some crystals of amino acids are listed in Table 4, where those of α-amino isobutyric acid are given in the last column.

Table 3

Principal Intermolecular Atomic Distances (kx)

N (B) – O (F) = 2.82	N (A) – O (B) = 5.56
N (B) – O (H) = 2.88	N (A) – O (G) = 4.20
O (A) – O (B) = 3.20	C (F) – C (G) = 3.63
N (A) – N (C) = 4.61	C (F) – C (G) = 4.05
N (A) – N (D) = 4.14	C (A) – C (E) = 4.16
N (A) – N (E) = 4.23	O (F) – O (G) = 3.93
N (A) – O (E) = 4.50	C (F) – O (G) = 5.86
N (A) – O (F) = 4.75	

Summary

X-ray examination of crystals of α-amino isobutyric acid shows them to be built upon a composite monoclinic unit having $a=10.59$ kx, $b=8.97$ kx, $c=11.34$ kx, and $\beta=94°$, containing eight molecules. The space group is $C2/c$ with all atoms being in the general positions with the following parameters which were determined by the three-dimensional

Table 4

A Comparison of Dimensions found in Some Crystals of Amino Acid.

	N-acetyl-glycine.	*β*-glycyl-glycine.	DL-alanine.	L-threonine.	*α*-amino isobutyric acid.
C_c-O	1.19	1.21	1.21	1.24	1.26
	1.31	1.27	1.27	1.25	1.20
C_c-C_α	1.51	1.53	1.54	1.52	1.52
$C_\alpha-N$	1.45	1.48	1.50	1.49	1.49
$C_\alpha-C$	—	—	1.51	1.54	1.53
	—	—	—	—	1.54
$C_\beta-C$	—	—	—	1.50	—
$O_1...N$	—	—	2.69	2.67	2.61
Hydrogen Bond;					
O...N	3.03	2.80	2.88	2.90	2.88
	—	2.81	2.84	2.80	2.82
Bond Angles;					
$O-C_c-O$	124	125	125	127	125
$O-C_c-C_\alpha$	124	123	121	117	118
	112	112	113	116	118
$C_c-C_\alpha-N$	110	111	108	110	109
$C_c-C_\alpha-C$	—	—	111	113	114
	—	—	—	—	109
$N-C_\alpha-C$	—	—	110	108	108
	—	—	—	—	105
$C-C_\alpha-C$	—	—	—	—	112
$C_\alpha-C_\beta-O_H$	—	—	—	104	—
$O-C_\beta-O_H$	—	—	—	111	—

Fourier analysis; nitrogen: $x=0.154$, $y=0.100$, $z=0.388$; carboxylic carbon: $x=0.178$, $y=-0.025$, $z=0.199$; α-carbon: $x=0.212$, $y=-0.031$, $z=0.331$; methyl carbon 1: $x=0.355$, $=-0.027$, $z=0.365$; methyl carbon 2: $x=0.148$, $y=-0.167$, $z=0.382$; oxygen 1: $x=0.112$, $y=0.083$, $z=0.159$; oxygen 2: $x=0.224$, $y=-0.121$, $z=0.138$. Bond distances are 1.26 and 1.20 kx. for carbon-oxygen, 1.52, 1.53 and 1.54 kx. for carbon-carbon and 1.49 kx. for carbon-nitrogen. There are observed a considerably close intramolecular approach between nitrogen and oxygen atoms and also close contact between two methyl groups.

The authors are indebted to Dr. J. Noguchi who kindly supplied the material for the present experiment. The cost of this investigation was partly defrayed by a grantfic of the Ministry of Education, to which the authors wish to express their thanks.

Faculty of Science, Osaka University, Osaka

X-Ray Study of Carbon Brushes

By Tokiti NODA and Shinya SATO

(Received February 7, 1952)

Carbon brushes for electrical machines must have specific qualities requisite for their uses. There are quite a good many kinds of carbon brushes on the market made from various kinds of raw materials by different procedures, details of which, however, are generally kept secret. The properties of carbon brushes depend on their structures, such as the mode of aggregation and distribution of carbon particles, and the form, size and degree of distortion or

Table 1

Unit Cell Dimensions of Graphite Crystal

Name of brush	c Dimension from (004)	(006)	a Dimension from (110)	(112)	mean	$C=c/a$ from (004)	(006)
	A.		A.				
HM-5	6.66_0	6.702	2.446	2.447	2.447	2.72_7	2.739
HM-6	6.71_2	6.708	2.461	2.462	2.462	2.72_6	2.725
PD-2	6.69_0	6.690	2.455	2.457	2.456	2.72_4	2.724
GE-D	6.72_4	6.699	2.460	2.461	2.460	2.73_2	2.723
8601-N	6.76_4	6.738	2.454	2.457	2.455	2.75_5	2.745
NCC-258	6.74_6	—	2.457	—	2.457	2.74_5	—
NCC-259	6.76_6	—	2.453	—	2.453	2.75_9	—
NCC-255	6.79_9	—	2.458	—	2.458	2.76_6	—
SA-45	6.79_6	—	2.455	—	2.455	2.76_6	—
E	6.71_2	6.720	2.458	—	2.458	2.73_2	2.736
Graphite							
Bacon[2]	6.708±0.001		2.4614			2.725_7	
Hofmann[3]	6.69 ±0.01		2.455 ±0.002			2.725	

imperfection of graphite crystallites in carbon particles. The structure may be divided into macroscopic, microscopic and submicroscopic ones. Although there are many studies concerning the macroscopic and microscopic structures, the apparent and true densities, the porosity, and other physical properties, no one has yet succeeded in making clear the relationship between the dynamic characteristics and the structure of brushes by having recourse to the macroscopic and microscopic observations alone. The authors now intend to make clear the submicroscopic structure of carbon brushes by X-ray and electronmicroscopic methods.

K. Hayashi and Y. Uto[1] measured the unit cell dimensions of graphite crystallites of several carbon brushes and divided them into three groups, *i. e.* (a) the natural graphite type, (b) the 2600 type or the pitch coke type, and (c) the SA-type or the soot type. The a dimension of graphite crystallite was constant for all kinds of brushes, but the c dimension was not uniform, being 6.72 A. for the natural graphite type, 6.78 A. for the 2600 type, and 6.85 A. for the SA-type. In the present paper, the results of the measurements of the unit cell dimensions and crystal sizes of graphite crystallites of several natural graphite and electrographite type of carbon brushes are reported.

Experimental

Specimens of carbon brush powder pulverized to pass 300 mesh per inch sieve and packed in a cellophane tube of about 0.3 mm inner diameter were employed, using FeK radiation in a 6.1 cm. camera. The diameter of the camera was calibrated by NaCl reflexions. Samples investigated were,

HM-5 (Morganite), natural graphite type,
HM-6 (Morganite), natural graphite type,
PD-2 (Hitachi), electrographitized pitch coke type (electrode for a vaccum tube),
GE-D (General Electric), electrograph itized pitch coke type,
8601-N (Ringsdorff), electrograph itized pitch coke type,
NCC-258 (National Carbon), electrographitized pitch coke type,
NCC-259 (National Carbon), electrographitized soot type,
NCC-255 (National Carbon), electrographitized soot type,
SA-45 (National Carbon), electrographitized soot type,
E (Nippon Carbon), electrographitized pitch coke type (Laboratory product).

Unit Cell Dimensions and Calculate Density.— The results of the meaurements of unit cell dimensions are shown in Table 1. The spacing values of HM-6, GE-D, 8601-N, NCC-255, and SA-45 were taken as the mean of those found from two films, but the others from one film.

The c dimensions were calculated from the (004) and (006) reflexions. For the a dimensions, the measurements were of the (110) and (112) reflexions. The c dimension from the (006) reflexion was used to calculate the a dimension from the (112) reflexion. The coincidence of the a dimensions from the (110) and (112) reflexions on the same film is satisfactory. The (006) and (112) reflexions could not be detected on films of some of the specimens, especially those of the soot type brushes. On the films of the soot type brushes, the (100) and (101) reflexions could not be resolved.

(1) K. Hayashi and Y. Uto, *Journ. Inst. Elec. Engrs., Japan*, **63**, 452, 592 (1943).
(2) G. E Bacon, *Acta Cryst.*, **3**, 137 (1950).
(3) U. Hofmann und D. Wilm, *Z. Elektrochem.*, **42**, 504 (1936).

The accurate measurement of the graphite unit cell dimensions of Bacon[2] (1950) showed that the value of the c dimension increased inversely proportionally with the thickness of graphite crystal, and that the value of the a dimension showed no change for graphite samples investigated, whose thicknesses of graphite crystals were larger than *ca.* 100 A. According to Taylor's paper[4] (1942), there was no genuine change of the a dimension for carbon layers having widths greater than a few tens of Ångstron unit. As shown later, graphite crystallites of our samples have width larger than 100 A. and overall height H larger than a few tens of Ångstron unit, it may reasonably be assumed that the a dimension of all the samples has the same value as that of the natural graphite. As all the spacings of HM-5 have smaller values than the other samples, there must be a systematic error due to the film treatment. Mean value of the a dimension of the eight samples except HM-5 is 2.457± 0.001 A. This value is almost equal to Hofmann's value 2.455 A., but smaller than the more accurate value of Bacon by 0.004 A. The main source of the error came from the camera diameter determination, as the camera diameter was calculated from NaCl reflexions on a separate film. We can eliminate the film error and compare the degree of graphitization of each sample by taking the axial ratio $C=c/a$. The (004) and (006) reflexions occur at 35° and 60° respectively. As the mean error of the a dimensions calculated from the (110) ($\theta=52°$) and (112) reflexions ($\theta=57°$) is ±0.0001 A., the mean error of the c dimension from the (006) reflexions may be the same as or less than that of the a dimensions. Therefore the mean error of the C (006), the axial ratio calculated from the (006) reflexions and the a dimension, was assumed to be ±0.001. The accuracy of the C (004) may be less than the C (006). From the standard deviation of the C (004) to the C (006) and the mean error of the C (006), the mean error of the C (004) was calculated to be ±0.008.

Among five specimens of which the values of C were obtained from the (006) reflexions, the values of C (006) of HM-6, PD-2, and GE-D should be looked upon as equal to the value of the natural graphite of Hofmann and Bacon. These brushes could be regarded as being composed of well crystallized graphite crystallites. The C (006) value of HM-5 is greater than the above three values, but smaller than that of 8601-N. The C (006) value of E is smaller than that of 8601-N, but larger than that of GE-D. The larger value of C indicates the smallness of graphite crystallite. From the C (004) values, it is difficult to tell the difference between HM-6, PD-2, GE-D, E and HM-5. The C (004) value of NCC-258 can be distinguished from that of PD-2, but not from that of GE-D. The C (004) value of 8601-N can be distinguished from that of GE-D, but not from that of NCC-258. The value of NCC-259 can barely be distinguished from that of NCC-258, but it cannot be distinguished at all from that of 8601-N. The value of NCC-255 is equal to those of SA-45 and NCC-259, but can clearly be distinguished from that of NCC-258. Summarizing the above observation, the order of the value of C of the brushes can be shown by the following inequality.

$$\text{HM-6}=\text{PD-2}=\text{GE-D}<\text{E}\leq\text{HM-5}<\text{8601-N},$$
$$\text{GE-D}\leq\text{NCC-258}\leq\text{8601-N}\leq\text{NCC-259}\leq$$
$$\text{NCC-255}=\text{SA-45}.$$

Densities d (X) of the graphite crystallites were calculated from the C (004) or C (006) values taking the a dimension as 2.461_4 A. from Bacon's paper. This value is also very near to the value 2.461_2 A., previously obtained by Nelson and Riley[5]. Both values are shown in Table 2 with densities d(p) measured by the picnometer method. Calculated *Kryptoporen*[6] are also shown in the table.

Table 2

Density and *Kryptoporen* of Carbon Brushes

Name of brush	d (X) from (006)	d (X) from (004)	d (P)	*Kryptoporen* from (006)	*Kryptoporen* from (004)
HM-5	2.240	2.24_9	2.101	6.20	6.6
HM-6	2.251	2.25_0	2.229	0.98	0.9
PD-2	2.252	2.25_2	2.254	0.00	0.0
GE-D	2.253	2.24_4	2.210	5.90	5.5
8601-N	2.235	2.22_6	1.999	10.5	$10._6$
NCC-258	—	2.23_5	2.120	—	5.1
NCC-259	—	2.22_3	2.068	—	7.0
NCC-255	—	2.21_6	2.000	—	9.8
SA-45	—	2.21_8	1.990	—	$10._3$
Graphite					
Bacon	2.250_6				
Hofmann	2.251				

Crystallite Size and Intensity Ratio of Reflexions.—Relative intensities of the (100), (101), (110) and (112) reflexions and widths at half intensity of the (004), (110) and (112) reflexions were measured from the microphotometric curves of the X-ray photographs. Sizes of graphite crystallites were calculated from the widths at half intensity by Laue's equation. Sizes of crystallites larger than 200 A. could not be determined and it was possible to compare sizes smaller than 100 A. The true thickness of the graphite crystal t ($=m_3c$) was calculated from the (112) reflexion, the width of the crystal w ($=m_1a$) from the (110) reflexion, and the overall height of the crystal H from the (004) reflexion. The results are shown in Table 3 with the values of $I(101)/I(100)$ and $I(112)/I(110)$. The t value and the intensity ratio of reflexions of the soot type brushes could not be obtained, as their (112) reflexions were not observed, and their (100) and

(4) A. Taylor, *Nature*, **152**, 462 (1942).

(5) J. B. Nelson and D. P. Riley, *Proc. Phys. Soc., London*, **57**, 477 (1945).

(6) *Kryptoporen*$=[d(\text{X})-d(\text{p})]\times 100/d(\text{X})$.

Table 3

Crystal Size and Intensity Ratio

Name of brush	Crystal Size×10 A. H	t $(=m_3c)$	w $(=m_1a)$	Intensity Ratio I (101)/I(100	I (112)/I(110)
HM-5	>20	15	>20	1.8	0.9
HM-6	>20	12	>20	4.3	1.8
PD-2	>20	10	>20	3.2	1.6
GE-D	>20	7	>20	2.5	1.2
8601-N	7	2	15	1.6	0.6
NCC-258	10	7	>20	1.6	0.9
NCC-259	10	—	15~20	—	—
NCC-255	10	—	15~20	—	—
SA-45	10	—	10	—	—
Natural graphite (Hofmann)				4.9	1.6

(101) reflexions could not be resolved.

Discussion

HM-6 and HN-5 are the natural graphite-carbon type brushes. From the C value or the calculated density and the value of the *Kryptoporen* of HM-5, it was shown that HM-5 must contain α considerable amount fo amorphous (or ungraphitized) carbon. By the influence of the presence of amorphous carbon, calculated thicknesses of crystallites of HM-5 and HM-6 appeared to be too small. Intensity ratios of the reflexions of HM-6 are approximately the same as those of the natural graphite, but those of HM-5 are far smaller. The content of amorphous carbon of HM-5 must be large enough to influence the intensities of reflexions. The fact that the C value or the calculated density of PD-2 is equal to the values of the natural graphite and that the value of *Kryptoporen* is zero shows the completeness of the graphitization of PD-2, the electrographitized pitch coke. The C value of GE-D is equal to that of the natural graphite, but the value of *Kryptoporen*, 6 %, shows that the degree of graphitization is not yet sufficient. But among the electrographitized pitch coke type brushes, GE-D is the most highly graphitized one. Judging from the C values, the crystallite sizes, and the intensity ratios of the reflexions, NCC-258 is next to GE-D in the graphitization. 8601-N is the least graphitized one among these three piteh coke type brushes. Among the electrographitized soot type brushes, the degree of graphitization of NCC-259 is larger than the degrees of NCC-255 and SA-45. The thickness of crystallites of the soot type brushes must be very small, though the (*hkl*) reflexions of these brushes could not be observed on the films. SA-45 appeared to be composed of graphite crystallites of the smallest size among the above three soot type brushes.

The X-ray study of carbon brushes may be said to be useful, and a finer conclusion may be obtained by improving the experimental method.

This research was supported by the Grant in Aid for Developmental Scientific Research of the ministry of Education and was made as a part of the work of the committee No. 117 (Carbon Materials for Electrical Machines) of the Japan Society for the Promotion of Scientific Research.

Department of Applied Chemistry, Faculty of Engineering, Nagoya University, Nagoya.

On the Acidity of Boric Acid. I. Neutral-Salt Effect Observed by Alkali-titration

by Shunsuke SHISHIDO

(Received January 21, 1952)

Introduction

It is a well known fact that the solution of boric acid is too weak to be determined by alkali-titration. But the solution is so strongly acidified by the addition of polyalcohol, glycerine, mannit, etc., that it can be titrated by adopting phenolphthalein as indicator. This is one of the methods of quantitative analysis of boric acid.[1] A. Deutsch and S. Osoling[2] studied the complex formation between boric acid and mannit by the conductometric and potentiometric methods and concluded that the equilibrium is as follows:

$$H_3BO_3 = H^+ + H_2BO_3^-$$
$$H_2BO_3^- + \text{Mannit} = [H_2BO_3\ \text{Mannit}]^-$$
$$H_2BO_3^- + 2\ \text{Mannit} = [H_2BO_3\ 2\ \text{Mannit}]^-.$$

Recently, D. Setten[3] has shown that the boric acid solution becomes more acidic than expected from the law of mass action in the case of concentrated solution (above 0.1 M), and that the polymerization of H_3BO_3 molecule occurs.

It is clear that the increase of acidity could be caused by the stabilization of the dissociated ion $H_2BO_3^-$ or H^+ owing to the complex formation or polymerization, but the reason why the stabilization and the ionization could be correlated directly with each other has not been explained sufficiently.

The new fact of neutral-salts effect has been discovered in this laboratory, which gives the hint for the explanation of this phenomena as shown in the following section.

Experimental Procedure and Result

(A) Titration by the addition of mannit, glycerine, ethylene glycol and methyl alcohol.—20 cc. of the solution of boric acid (0.1 M/1) added with 10 cc. of distilled water the mixture is titrated with 0.2 N. sodium hydroxide solution in the presence of phenolphthalein. The alkali solution is added until the colour of the solution turns to light pink (*p*H-8.5) and the added volume of alkali solution is read. This is the initial titration volume (itv). Then, the moderate volume of alcohol (volume added) is added. When the solution discolours, it is again titrated with the alkali solution in order to read the second titration volume. The titration is repeated and the titration curves can be obtained. When the quantity of alcohol is enough, the colouring points (each end point) become clearer, because the dissociation constant is increased. Some results are shown in Fig. 1. We can easily understand from these

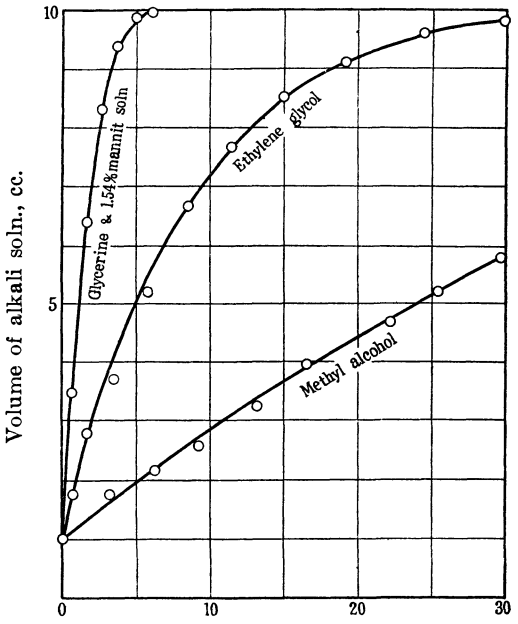

Fig 1.

curves that the strength of acidifying effect is demonstrated by the initial inclination of the titration curve. These values are listed in Table 1. Similar effects are observed in the system of two components of CH_3OH-$C_2H_4(OH)_2$ and CH_3OH-$C_3H_5(OH)_3$, and the results are shown in Table 2 and Fig. 2.

Supplementally, the effect of aceton and dioxan has been investigated without virtue, and the results are rather negative.

(B) Titration by the addition of neutral-salts.—20 cc. of the solution of boric acid (0.1 M) is added

(1) F. P. Treadwell, "Analytische Chemie".
(2) A. Deutsch and S. Osoling, *J. Am. Chem. Soc.*, **71**, 1637 (1949).
(3) D. Setten, *Anal. Chem.*, **23**, 1777 (1951).

Table 1

Subst.	Initial inclination cc./cc.	cc./mol	Relative value
Methyl alcohol	1/6	6.7	1
Ethylene glycol	4/6	36	5.4
Glycerin	4/1	280	42
1.54% Mannit Soln.	4/1	4000	100

Table 2

Methyl alcohol~Ethylene glycol Mol ratio (M:E)	Init. incli., cc./cc.	Methyl alcohol~Glycerin Mol ratio (M:G)	Init. incli., cc./cc.
4 : 0	0.17	4 : 0	0.17
3 : 1	0.35	3 : 1	2.2
2 : 2	0.60	2 : 2	3.2
1 : 3	0.65	1 : 3	4.0
0 : 4	0.67	0 : 4	4.0

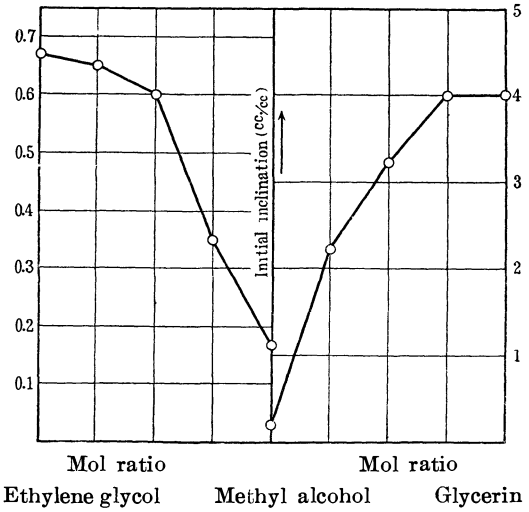

Fig. 2.

by the neutral-salt at first and 10 cc. of distilled water, and then the mixture is titrated by the similar way described in (A). The titration curves are obtained mainly with ethylene glycol. The results in the presence of NaI and K_2SO_4 are shown in Fig. 3. The curves are displaced from the original (ethylene glycol only) mainly in the next two points:

(1) initial titration volume (itv).

(2) sufficient quantity of ethylene glycol which needs to reach the final end point decreases when the initial titration volume increases as compared with the case of ethylene glycol only.

From these observations, the effects examined are divided into three classes, which are,

(a) strongly effecting salts: LiCl, $CaCl_2$, $BaCl_2$, NaBr, NaI, $Ca(NO_3)_2$, $Ba(NO_3)_2$,

(b) moderately effecting salts: NaCl, $NaNO_3$, KBr, KI,

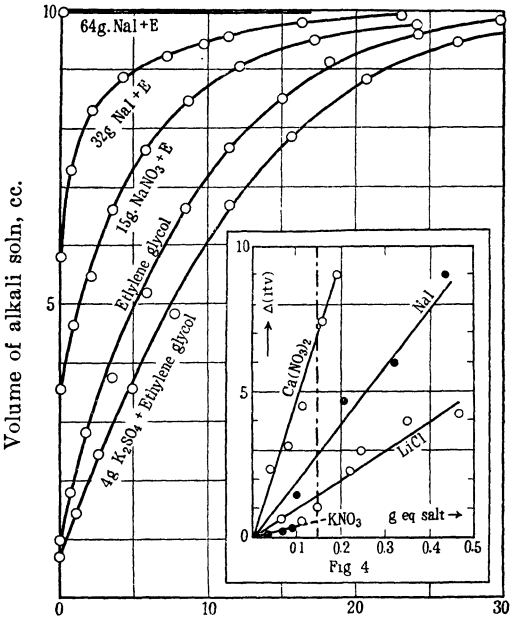

Flg. 3.

(c) little or negatively effecting salts: KNO_3, Na_2SO_4, K_2SO_4.

In order to discuss the effect quantitatively, the author examined the relation between initial titration volume and salt concentration. Generally, the change of initial titration volume $\triangle$(itv) is linear with the salt concentration. Some results are shown in Fig. 4. From this linearity, we can determine the strength of acidifying effect as the change of initial titration volume $\triangle$(itv)* at the salt concentration of one gram equivalent to the solution of 20 cc. of 0.1 M boric acid and 10 cc. of distilled water. These values are listed in the last column in Table 3.

Result and Discussion

The effects of polyalcohols and their mixtures, as well as acetone and dioxan, showed the results expected from the previous works. But the neutral-salt effect was remarkable. Therefore, it is important to discover the correlation between the acidifying effect and the other properties of salts.

After various speculation, the author has concluded that there is a distinct relation between the strength of the acidifying effect ($\triangle$(itv)*) and the energy of hydration of ions. When we compare the $\triangle$(itv)* with the difference of the hydration energy between positive and negative ions ($\triangle U$(Cal./g. eq. ion) $= U_+ - U_-$) in Table 3,[4] we can easily perceive the simple relation as

(4) J. D. Bernal and R. H. Fowlers, *J. Chem. Phys.*, **1**, 538 (1933). The values for NO_3^- and 1/2 SO_4^{--} are assigned as 58 kcal./g.eq. ion and 85 kcal. respectively from the expectation that the effect of KNO_3 and Li_2SO_4 lies on the curve on Fig. 5.

Table 3

Salts	Hydration energy, kcal./g. eq. ion				△(itv)*, cc.
	U_+	U_-	ΣU	$\triangle U$	
LiCl	136	65	200	75	+1.7
$LiNO_3$	136	(56)	(192)	(80)	+1.8
NaCl	114	65	179	49	+1.6
NaI	114	47	161	67	+3.0
$NaNO_3$	114	(56)	(170)	(58)	+1.2
$\frac{1}{2}Na_2SO_4$	114	(85)	(199)	(29)	±0
KCl	94	65	159	29	±0
KBr	94	57	151	37	+0.5
KI	94	47	141	47	+1.4
KNO_3	94	(56)	(150)	(38)	+0.6
$\frac{1}{2}K_2SO_4$	94	(85)	(179)	(9)	−1.0
$\frac{1}{2}CaCl_2$	207	65	272	142	+4.5
$\frac{1}{2}Ca(NO_3)_2$	207	(56)	263	(151)	+6.7
$\frac{1}{2}BaCl_2$	174	65	239	109	+4.7
$\frac{1}{2}Ba(NO_3)_2$	174	(56)	230	(118)	+3.0

shown in Fig. 5, that is, △(itv)* is larger as $\triangle U$ increases.

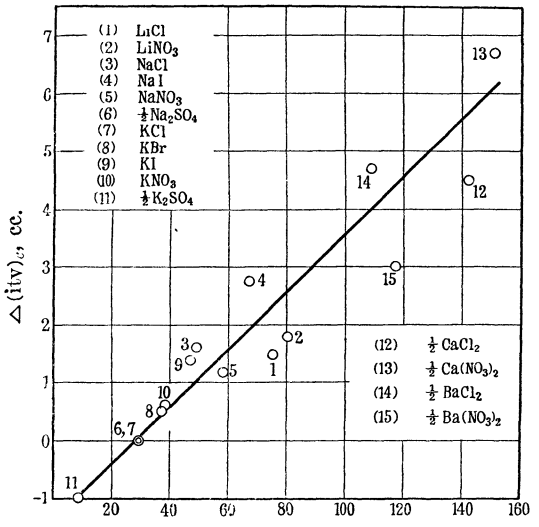

Fig. 5.

Concerning the acidity of boric acid solution, the following three principal features have been discovered;

(1) complex formation with polyalcohol[1][2]

(2) polymerization of itself in concentrated solution[3]

(3) present neutral-salt effect.

In virtue of the effort to obtain the consistent explanation of these three features, the author has reached the following conclusion:

(A) Since the electron configuration in boron atom is $(1s)^2\,(2s)^2\,(2p)^1$, it could be bound in either of two ways; that is, tricovalent bond as trimethyl boron B $(CH_3)_3$ molecule (pyramidal) or of tetracovalent bond as fluoroboronate ion $(BF_4)^-$ (tetrahedral). Actually, the various structures, which are derived from the above principal bond, are reasonating.[5]

(B) The structure of crystalline boric acid is considered, from the various facts,[5] to be a resonance form mainly among the tetravalent plane structures (Fig. 6) accompanied with the separation of formal charge, rather than tricovalent.

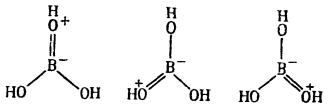

Fig. 6.

Therefore, when there are favourable circumstances for the separation of the formal charge of bond as in H_3BO_3 and $(BF_4)^-$, boron prefers to be bound in tetracovalent. In the case of aqueous solution of boric acid, the separation of charge becomes more easy in the process of electrolytic dissociation (complete separation of charge):

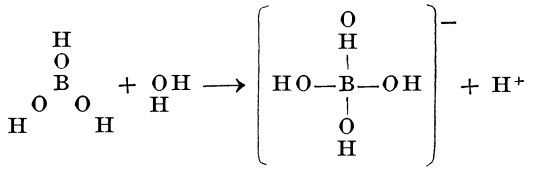

This is the mechanism of electrolytic dissociation of H_3BO_3, although it is very weak. The unstabilization accompanied slightly with the complete separation of charge can be cancelled by the increase of bond energy of regular tetrahedral bond which may be larger than that of the deformed tetravalent plane structure of H_3BO_3 molecule.

(C) When methyl alcohol coexists in an aqueous solution of boric acid the combination can form the methyl ester of boric acid more or less by the dehydrating action owing to the strong affinity of methyl alcohol to water. The separation of formal charge in the molecule of this ester becomes more difficult. Consequently, the bond nature should be inclined to tricovalent and becomes more unstable (for an example $B\cdot(OCH_3)_3$ molecule). But, if the ionization of methyl ester is easy, it can be stabilized by the possibility of complete separation of charge (*i.e.*, ionization) and of formation of regular tetracovalent bond.

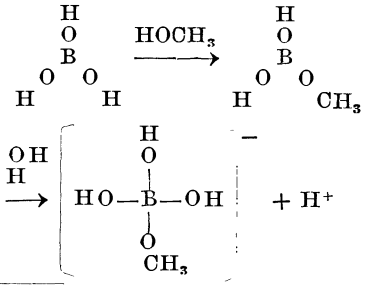

(5) L. Pauling, "The Nature of the Chemical Bond".

The ester formation and the ionization are parallel in this example, because any system should be existing in the most stable state. This is the acidifying mechanism of these compounds and their mixtures, and it depends mainly on the possibility of ester formation. Aceton and dioxan may have the sufficient affinity of water, but not the possibility of ester formation, therefore, they can not show the acidifying effect, but are rather negative.

(D) The fact that the acidity of the more concentrated aqueous solution of boric acid is larger than the value predicted from the law of mass action in the dilute solution is considered to be caused from polymerization.[3] According to the author's theory, this is the expectable result of the cooperative separation of charge to form a regular tetracovalent bond, for an example:

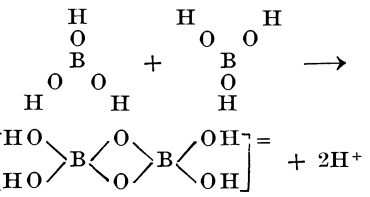

(E) Since the water molecule in the salt solution is hydrated strongly by the ion as in Fig. 7,

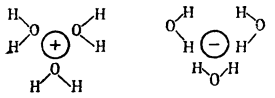

Fig. 7.

the water molecule behaves like the OH radical in polyalcohol or the O atom in the aceton and dioxan molecule in the neighborhood of the cation or anion, respectively. In a more concentrated neutral-salt solution, these two tendencies are counter-balancing, according, to the relative strength of hydration of cation and anion.

When the hydration of cation is greater than that of anion, the water molecule of the solution may behave like polyalcohol, and for the above reasons (A, B, C and D) the acidity of boric acid is increased. On the contrary, when the anion hydrates the water molecule more strongly than cation, the water molecule behaves like aceton or dioxan and rather decreases the acidity of boric acid solution.

This is the mechanism of the acidifying effect of neutral-salt solution. The author will give the quantitative explanation in detail later on.

Summary

The acidifying effect of various solutions (CH_3OH, $C_2H_4(OH)_2$, $C_3H_5(OH)_3$, $C_6H_8(OH)_6$, their mixture, CH_3COCH_3, $O(CH_2CH_2)_2O$, and neutral-salts) is measured by the alkali-titration method, and the simple relation between the hydration energy of neutral-salts and their acidifying effect is found. The consistent explanation for these phenomena is proposed on the view of the nature of the tricovalent and tetracovalent bond of boron atom.

Chemical Department, Faculty of Science, Niigata University, Niigata

Studies on Nitrate Reductase. VII. Reinvestigation on the Identity of the Enzyme with Cytochrome *b*[1]

By Ryo SATO[2] and Makoto NIWA

(Received November 22, 1951)

Previous studies in this laboratory,[3~6] together with informations from other laboratories,[7~10] have clarified that nitrate reductase is the enzyme functioning as the terminal component of the catalytic system, by which hydrogen atoms (or electrons) are transported from metabolites such as succinate, formate and alanine to the final acceptor

(1) The results and discussions described in this paper were, for the most part, already presented at the 3rd Symposium on Enzyme Chemistry, October 1950, TOKYO. Its abstract has been published in Japanese (*Symp. Enzyme Chem.*, **6**, 40 (1951))

(2) Present address: Faculty of Science, Kanazawa University.

(3) F. Egami and R. Sato, *J. Chem. Soc. Japan*, **68**, 39 (1947).

(4) F. Egami and R. Sato, *J. Chem. Soc. Japan*, **69**, 160 (1948).

(5) R. Sato and F. Egami, This Bulletin, **22**, 137 (1949).

(6) R. Sato, *Scienca Revuo*, **2**, 122 (1950).

(7) S. Yamagata, *Acta Phytochimica*, **10**, 283 (1938).

(8) S. Yamagata, *Acta Phytochimica*, **11**, 145 (1939).

(9) E. Aubel and F Egami, *Compt. rend. acad. sci.*, **202**, 675 (1936).

(10) E. Aubel and F. Egami, *Bull. soc. chim. biol.*, **18**, 301 (1936).

nitrate. The role of this enzyme in nitrate reduction is therefore quite analogous to that of the terminal heme enzyme in respiratory mechanisms. Corresponding to this functional similarity, one of the present authors (Sato) and Egami[5] suggested in an earlier report of this series that nitrate reductase of *Escherichia coli* may be an iron enzyme and is probably identical with cytochrome *b* of *E. coli* type.[11] This view appeared to be able to account for almost all the results obtained up to that time. As to this identity, however, some doubts were presented even at that time, since there was no evidence to indicate that the cytochrome in question does combine with cyanide, a well known inhibitor of nitrate reductase. On the contrary, Pappenheimer and Hendee[12] have reported that cytochrome *b* of *Corynebacterium diphtheriae*, apparently identical with that of *E. coli*, is insensitive to cyanide in its aerobic function. Sato (one of the present authors) and Egami[5] themselves also failed to observe any change in the absorption bands of the cytochrome *b* contained in a cell-free preparation of nitrate reductase from *E. coli* when cyanide was added to this preparation. In order to correlate this observation with the above view, they had to assume a rather incredible fact: cyanide does combine with the cytochrome *b* and so inhibit the activity of nitrate reductase, but this combination causes no alteration of the absorption spectra of the cytochrome (at least α- and β-bands of the reduced cytochrome). It has been since considered desirable to study the problem more extensively and to settle the contradictory points.

In our attempts to solve the problem, it was discovered that thiourea inhibits nitrate reductase considerably. This reagent differed from the other known inhibitors of nitrate reductase such as cyanide, azide and carbon monoxide in exerting only a slight inhibition upon the oxygen uptake by *E. coli*. The fact that such an inhibitor as thiourea does exist seemed to provide another support for the invalidity of the suggested identity, because it was clear that the very cytochrome *b* is required in this thiourea-insensitive respiration.

Further investigations were then carried out using thiourea as a tool in order to obtain more advanced informations on the nature of nitrate reductase. The results of these investigations as well as consideration of the other data have shown that the previously proposed hypothesis is incorrect. Instead, it has been now clarified that cytochrome *b* of *E. coli* type is not identical with nitrate reductase itself, though it is closely related to the nitrate-reducing activity of this organism. The "nitrate reductase" which we previously so called is in fact a complex system consisting of the cytochrome *b* and a cyanide- and thiourea-sensitive factor, nitrate reductase itself.

Despite the revision of the view, it seems still tenable that nitrate reductase is an iron enzyme, because the carbon monoxide inhibited-activity of the enzyme can be restored by light.

Experimental

Materials and Methods

The resting cell suspension of *E. coli* grown on a nitrate-containing peptone-bouillon-agar medium was prepared as described in the preceeding paper.[13] The cell-free preparation of nitrate reductase employed in this investigation was obtained from *E. coli* by ultrasonic destruction of the cells and ammonium sulfate precipitation as previously described.[5] In the present study, however, the preparation was brought to dryness by lyophilization after 10 hours dialysis against a stream of water and stored at 0° in a vacuum desiccator. The presence of cytochrome *b* of *E. coil* type in this preparation was readily demonstrable by a hand spectroscope. It also contained a powerful activity of formic dehydrogenase as measured by the methylene blue technique.

Nitrate reduction was carried out anaerobically using Thunberg tubes. The rate of the reduction was measured by determining the amount of nitrite formed in the reaction mixtures by a colorimetric method as used in the previous studies.[13] The activity of dehydrogenases was followed by the ordinary Thunberg method. Manometric experiments were conducted with the use of a Warburg manometer. Spectroscopic observations with the resting suspension were made as follows. A Thunberg tube containing the samples was illuminated by a projector from a distance of about 5 cm. and the spectrum was observed by a hand spectroscope. A Beckman spectrophotometer was employed in spectroscopic investigations with the cell-free preparation.

Further details of the experimental conditions and methods are given in the tables and figures.

Results

Effect of Thiourea on Nitrate Reductase, Dehydrogenase and Oxygen Uptake of E. coli.— Fig. 1 shows the effect of thiourea on nitrate reduction by the cell-free preparation of nitrate

(11) This type of cytochrom *b* is also called cytochrome b_1, according to D. Keilin and C. H. Harpley (*Biochem. J.*, **35**, 688 (1941)).

(12) A. M. Pappenheimer Jr. and E. D. Hendee, *J. Biol. Chem.*, **177**, 701 (1947).

(13) R. Sato, M. Ebata and F. Egami, *This Bulletin*, **25**, 56 (1952).

reductase using sodium formate and methylene blue as hydrogen donator and intermediary carrier respectively.[3] It can be seen that the reduction was completely inhibited by about 0.1 M. of thiourea; half maximum inhibition was attained by $10^{-2.9}$ M. of the inhibitor. Under these conditions, however, the reduction occurs by a co-operative action of formic dehydrogenase and nitrate reductase; the former reducing methylene blue and the latter transfering electrons from the reduced dye to nitrate.[3,7] It was therefore necessary to decide which of the two enzymes concerned was actually inhibited by thiourea. This problem was pursued by studying the effect of the inhibitor on formic dehydrogenase using Thunberg technique. The results of these experiments, together with those on succinic dehydrogenase, are recorded in Table 1. As is shown in the table, the activity of formic dehydrogenase as well as that of the succinic enzyme was not inhibited by thiourea even at a concentration of 0.2 M. It is accordingly evident that nitrate reductase was the actual site of the thiourea inhibition.

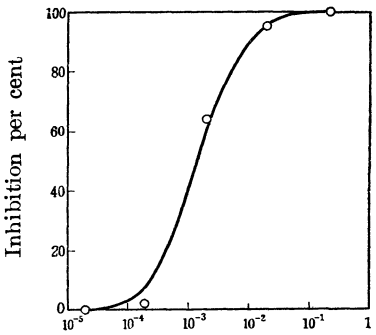

Fig. 1.—Inhibition of nitrate reduction by varying concentrations of thiourea. Each Thunberg tube contained 1 mg. of the cell-free enzyme preparation, 0.004 M. KNO_3, 0.02 M. sodium formate, 10^{-5} M. methylene blue, 0.1 M. phosphate buffer (*p*H 7.4), and varying concentrations of thiourea in a final volume of 5 ml. Temperature: 35°. Reaction time: 50 minutes. Control experiment without thiourea produced 165 μ M./l. nitrite under these conditions.

The effect of thiourea on the oxygen uptake by *E. coli* using formate (Fig. 2) and succinate (Fig. 3) as substrate was then studied. As shown in

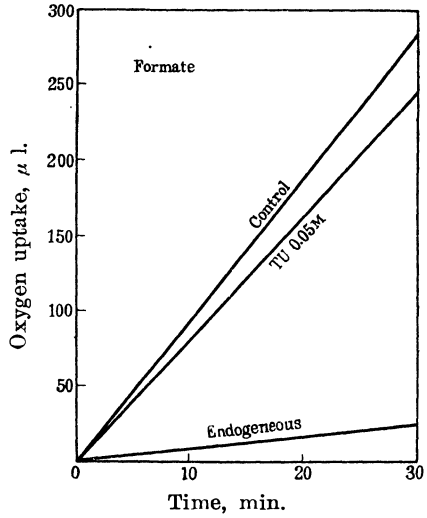

Fig. 2.—Effect of thiourea on respiration of *E. coli* (formate as substrate). Each vessel contained 2.5 mg. of the resting cells, 0.017 M phosphate buffer (*p*H 7.4), 0.017 M. sodium formate with or without thiourea (0.05 M.) in a final volume of 3 ml. Endogeneous respiration was measured without the addition of formate. Temperature: 36°. TU = thiourea.

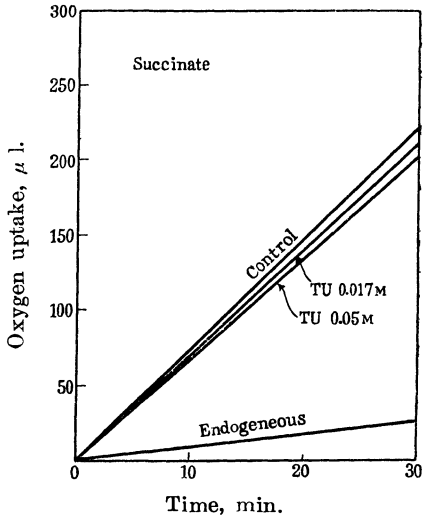

Fig. 3.—Effect of thiourea on respiration of *E. coli* (succinate as substrate). The same conditions as Fig. 2 except sodium succinate was used as substrate instead of formate.

Table 1

Effect of Thiourea on Formic and Succinic Dehydrogenases of *E. coli*.

Each Thunberg tube contained 12 mg. of the resting cells, 0.1 M. phosphate buffer (*p*H 7.6), 0.002 M. substrate, and 1 : 25000 methylene blue in a final volume of 5 ml. Temperature: 36°. Figures indicate the decolorization time of the dye (in minutes).

Substrate	Without thiourea	With thiourea		
		0.2 M	0.1 M	0.01 M
Formate	15	—	16	16
〃	14	10	—	—
Succinate	8	—	—	5
〃	5	9	5	—

Table 2

Qualitative Spectroscopic Observations using Resting Cell Suspension of *E. coli*

In the main compartment of a Thunberg tube the reactants in Column A were placed, and in the hollowed stopper those in Column D. After evacuation, the tube was incubated at 37° for about 20 minutes. The absorption bands of the ferrocytochrome *b* (at 560 mμ and 530 mμ) and the color of methylene blue (Mb) were observed and recorded in Column B. Then air was introduced into the mixture by removing the stopper and shaking vigorously. Changes observed after this procedure were recorded in Column C. The stopper was again plugged and the tube was incubated as before. Then the contents of the two parts of the tube were mixed and changes which occurrod as a result of this mixing were observed and recorded in Column E. All observations were conducted at room temperature. The *E. coli* suspension contained 7.5 mg. of the cells per ml. (in 0.2 M phosphate buffer of *p*H 7.6). ⧺, +, and ± indicate the intensity of the bands or the color. − shows the absence of the bands or the color.

	A (Main compartment)						B		C		D (Hollowed stopper)		E	
	E. coli suspension	Na succinate (0.1 M.)	Na formate (0.1 M)	KCN (0.1M)	Thiourea (1 M.)	Mb (0.02 %)	Bands of cytochrome	Color of Mb	Bands of cytochrome	Color of Mb	KNO_3 (0.5M)	Mb (0.02 %)	Bands of cytochrome	Color of Mb
1	2.0ml	0.5					⧺		−		0.5		±	
2	2.0		0.5				⧺		−		0.5		±	
3	2.0	0.5		0.5			⧺		⧺		0.5		⧺	
4	2.0		0.5	0.5			⧺		⧺		0.5		⧺	
5	2.0	0.5			0.5		⧺		−		0.5		+	
6	2.0		0.5		0.5		⧺		−		0.5		+	
7	2.0	0.5				0.5	⧺	−	−	⧺	0.5		±	⧺
8	2.0	0.5		0.5		0.5	⧺	−	⧺	+	0.5		⧺	−
9	2.0	0.5			0.5	0.5	⧺	−	−	⧺	0.5		⧺	±
10	2.0	0.5					⧺		−			0.5	−	⧺
11	2.0	0.5		0.5			⧺		⧺			0.5	−	⧺
12	2.0	0.5			0.5		⧺		−			0.5	−	⧺

Fig. 2 and Fig. 3, thiourea caused only a slight inhibition on the respiration of formate and that of succinate; only 12 per cent inhibition was seen in the respiration of formate by 0.05 M. of thiorea, a concentration sufficient to inhibit nitrate reductase almost completely. De Ritis and Scalfi[14] have also reported that thiourea does not appreciably influence the respiration of bacteria.

Spectroscopic Observations using Resting Suspension of E. coli.—One of the facts on which Sato and Egami[5] depended in suggesting the identity of nitrate reductase with cytochrome *b* of *E. coli* type was their spectroscopic observation that the reduced cytochrome *b* was rapidly oxidzed by the addition of nitrate. It seemed, therefore, of interest to use thiourea as an inhibitor in such spectroscopic experiments. Thus, we set ourself first to a qualitative investigation with the use of the resting cell suspension of *E. coli*. A hand spectroscope was employed for this purpose.

The results of this investigation are summarized in Table 2. On anaerobic incubation of the suspension with formate or succinate, the cytochrome *b* was converted to the reduced (or ferro-) form as indicated by the appearance of the absorption bands of the ferrocytochrome *b* (α-band at 560 mμ and β-band at 530 mμ). Thiourea and cyanide did not prevent this reduction. When air was introduced into the mixture, the bands disappeared at a rapid rate and the spectrum became that of the oxidized (or ferri-) cytochrome *b*. This aerobic oxidation of the ferrocytochrome *b* was completely inhibited by cyanide, but thiourea failed to inhibit it. In confirmation of the previous data,[5] the bands of the reduced cytochrome also greatly decreased their intensity by the addition of potassium nitrate. This oxidation by nitrate was also found to be sensitive to cyanide just like the aerobic process. A remarkable difference was, however, recognized between the two oxidation processes; in the former case, nitrate as oxidant, the disappearance of the reduced cytochrome bands was greatly inhibited by the presence of thiourea, in contrast to what was seen in the aerobic oxidation.

Incubation of the suspension with succinate or formate in the presence of methylene blue under anaerobic conditions resulted in, as is well known, the decolorization of the dye; the addition of nitrate into the decolorized mixture caused the immediate recolorization of the leuco methylene blue as previously reported.[3,7] This oxidation of the leuco dye by means of nitrate was found to be also inhibited by thiourea as well as by cyanide. Spectroscopically, it was confirmed that this recolorization of methylene blue was always accompanied by the disappearance of the bands of the reduced cytochrome *b*.

(14) F. De Ritis and L. Scalfi, *Boll. soc. ital biol sper.*, **22**, 703 (1946); *Chem. Abst.*, **41**, 3167 (1947).

Moreover it was found that the reduced cytochrome bands also disappeared when methylene blue was added to the mixture. But this disappearance was not inhibited by either cyanide or thiourea.

Finally, the effect of thiourea on the absorption spectra of the cytochrome *b* was examined. No change, however, could be detected in the spectra of either the oxidized or the reduced cytochrome even when 0.2 M. of thiourea was added.

Spectroscopic Experiments using the Cell-free Preparation.—A quantitative investigation by the use of a Beckman spectrophotometer was then undertaken with the object of ascertaining the findings of the above qualitative observations using a hand spectroscope. The cell-free preparation of nitrate reductase was adopted for this purpose.

Due to the turbidity and the relatively minute concentration of the cytochrome *b* contained in the preparation, the spectra obtained were rather indistinct. Nevertheless, it was not so difficult to identify the absorption maxima due to the reduced cytochrome *b*. Fig. 4 illustrates the spectra of the preparation at both the oxidized and reduced states measured at the wave length region ranging from 525 mμ to 575 mμ. The reduced state was realized by two methods; by the addition of sodium hydrosulfite and by incubation of the preparation with formate under an anaerobic condition (using liquid paraffin as a seal). In the latter procedure the incubation was carried out without any added intermediary hydrogen carrier such as methylene blue, but the cytochrome *b* was reduced to about 80 per cent of completion after 30 minutes (the reduction by hydrosulfite being assumed complete). This enzymatic method was used in the later experiments in preference to the hydrosulfite method; the reason of which was described in the previous paper.[5] It is clearly shown in Fig. 4 that the reduced spectra have two peaks at 560 mμ and 530 mμ corresponding to the α- and β-bands of the ferrocytochrome *b* respectively. On the other hand, no absoption maxima could be detected in the oxidized spectrum at least in this wave length region. The increasing optical density toward the shorter wave length region is not largely due to true absorption; the most part of this apparent absorption is a mere result of the scattering of light caused by the turbidity. (It is known that light scattering intensifies itself as the wave length becomes shorter). Net absorption at 560 mμ caused by the ferrocytochrome *b*, therefore, may

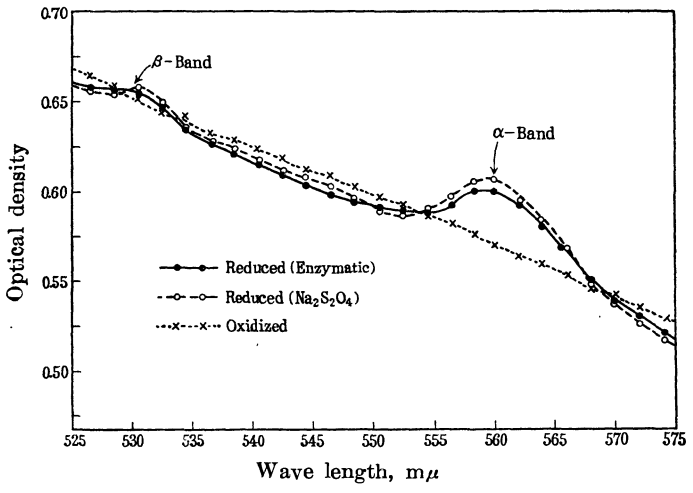

Fig. 4.—Absorption spectra of cell-free preparation of nitrate reductase. Each cuvette of the Beckman spectrophotometer (light path 1 cm.) contained 200 mg. of the cell-free preparation in a final volume of 4 ml. (phosphate buffer, 0.05 M, *p*H 7.4). Enzymatic reduction was carried out by incubating with 0.05 M sodium formate for 30 minutes at 37°. Liquid paraffin (1.5 cm. thick) was placed on the mixture to keep the anaerobic condition. Nonenzymatic reduction was carried out by adding a small amount of solid $Na_2S_2O_4$ and then placing liquid paraffin.

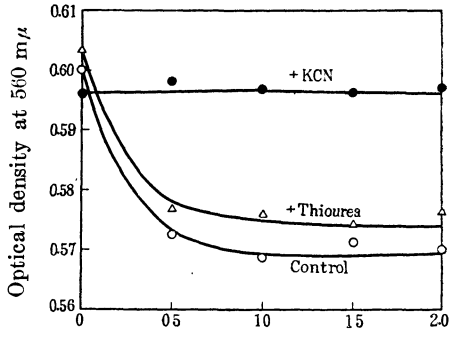

Fig. 5. Effect of KCN and thiourea on aerobic oxidation of ferrocytochrome *b*. The cell-free preparation of nitrate reductase was dissolved in 0.05 M. (*p*H 7.4) phosphate buffer containing 0.05 M. sodium formate (200 mg. of the preparation per 3 ml.). 3 ml. of this solution was pippetted into a cuvette of the Beckman spectrophotometer and liquid paraffin (1.5 cm. thick) was placed on it. The cuvette was then incubated for 30 minutes at 37°. Then each 1 ml. of either distilled water (control), or 0.04 M. KCN (+KCN), or 0.2 M. thiourea (+Thiourea) was added and the optical density at 560 mμ was measured. Then the liquid paraffin was removed by pipetting out as quickly as possible and air was bubbled into the mixture by a small syringe. The changes of the optical density was followed at each 30 seconds interval. Measurements were conducted at room temperature.

be estimated as about 0.03—0.04 in optical density unit.

By following the decrease of optical density at 560 mμ, the oxidation of the ferrocytochrome *b* by atmospheric oxygen (Fig. 5) and by potassium nitrate (Fig. 6) together with the effect of cyanide and thiourea on these processes were then studied. As shown in Fig. 5 and Fig. 6, it was confirmed that the reduced cytochrome *b* undergoes rapid oxidation by either introduction of air or by addition of nitrate. In both the cases the oxidation proceeded to completion within 30 seconds. In confirmation of the qualitative observations, it was further found that cyanide prevented both

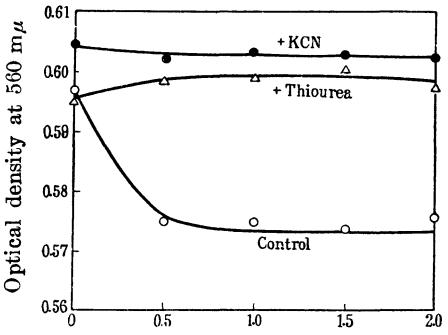

Fig. 6.—Effect of KCN and thiourea on oxidation of ferrocytochrome *b* by nitrate. Conditions and methods were the same as Fig. 5, except the following. Instead of removing the liquid paraffin and bubbling air, small amounts of solid potassium nitrate was added at zero time.

of the processes completely, but thiourea was inhibitory only for the oxidation by nitrate. No appreciable retardation of the aerobic oxidation was observed by the presence of thiourea (0.05 M.).

Attempts were also made to test the possibility that methylene blue may oxidize the ferrocytochrome suggested by the qualitative observation. But high concentration of methylene blue (0.001 per cent) used in these experiments made it impossible to conduct desirable measurements due to the intense general absorption of the dye. Even at lower concentrations of the dye no definite results were obtained.

Discussion

Nitrate reductase can be defined as the terminal enzyme of hydrogen (or electron) transporting pathways from suitable hydrogen (or electron) donators to nitrate; *viz.*, it is the enzyme which reacts directly with nitrate. If this enzyme is actually identical with cytochrome *b* of *E. coli* type as previously suggested,[5] the only possible scheme accounting for both the nitrate reduction and the aerobic respiration by *E. coli* should be as follows:

H-donators—dehydrogenases—····

····—cytochrome *b* (nitrate reductase) —oxidase?—O_2

—NO_3^-

↑

KCN, CO, Thiourea

Here, the arrow indicates the site of action of the inhibitors. The intermediary components between dehydrogenases and the cytochrome *b* are not shown in this scheme for several reasons; (1) no definite information is as yet available, (2) this part of the scheme may be different according to the hydrogen donators, and (3) they are not important for the later discussions. The oxidase inserted between the cytochrome *b* and molecular oxygen will be discussed later.

The results reported in the present study, however, suggest that the above scheme as such is unlikely. First of all, this scheme can not provide any satisfactory explanations for the finding that thiourea does not appreciably influence the aerobic respiration of *E. coli*, in contrast to its fairly marked inhibitory action upon the nitrate reduction. Spectroscopic evidence also indicates that thiourea is not capable of preventing the oxidation of the ferrocytochrome *b* by atmospheric oxygen, while the disappearance of the reduced cytochrome bands by nitrate is completely inhibited by the same reagent. Furthermore, as already mentioned the above scheme is not consistent with the observations that no changes occur in the cytochrome bands by the addition of cyanide. The view claimed by Pappenheimer and Hendee[12] that diphtherial cytochrome *b* is not inhibited by cyanide further makes a protest against the scheme.

A satisfactory settlement of the matter, however, suggests itself on the basis of the very results obtained in the present study. The marked inhibition exerted by thiourea upon the nitrate reduction and the failure of the same reagent to inhibit the respiration necessarily lead to the assumption that a certain thiourea-sensitive factor may be involved in the nitrate-reducing mechanism; whereas no such factor may be required in the respiratory system. The role of this factor is suggested by the spectroscopic results to consist in the catalysis of the oxidation of the ferrocytochrome *b* by nitrate (but not by molecular oxygen). We should therefore regard this factor, according to the definition, as nothing but nitrate reductase itself. The contradiction concerning the cyanide inhibition of the nitrate reduction

mentioned above would also be able to be settled by taking this factor into consideration, because it seems more reasonable to attribute the cyanide inhibition to this new factor (nitrate reductase) rather than to the cytochrome *b*.

On the basis of the above considerations, a more acceptable scheme can be drawn for the processes in question instead of the former one.

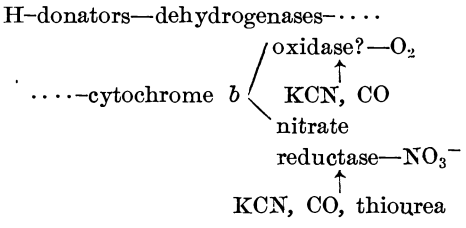

This revised scheme is in agreement with all the results reported in this paper as well as with those in the foregoing studies. The reason why thiourea exerts marked inhibition upon the nitrate reduction without seriously affecting the aerobic respiration will be readily explained by this scheme. (The slight inhibition of the respiration by thiourea may be due to an entirely different mechanism from that for the nitrate reduction.) This scheme can also interpret the spectroscopic findings with ease. Furthermore, the cytochrome *b* is shown in this scheme not to be inhibited by either cyanide or carbon monoxide in accordance with the generally held concept that the cytochrome does not combine with these reagents. Thiourea should also be regarded as being inert to the cytochrome because of the inability of this substance to inhibit the respiration which requires the cytochrome as an essential catalyst.

A brief account of the aerobic pathway presented in the scheme seems desirable. Although there remains little doubt about the participation of the cytochrome *b* in the respiration of *E. coli*, further details of the process are as yet obscure. Pappenheimer and Hendee[12] have obtained evidence indicating that diphtherial cytochrome *b* is autoxidizable and the greater part of the oxygen uptake by a cell-free diphtherial extract can be accounted for in terms of this autoxidation. It is not clear, however, whether the same respiratory mechanism is functioning also in *E. coli*. From our spectroscopic observations it appears preferable to consider that the autoxidation of the cytochrome, if any, does not greatly contribute to the respiration of *E. coli*, because the aerbic oxidation of the reduced cytochrome *b* was strongly inhibited by cyanide. This fact in turn suggests that a cyanide-sensitive oxidase is necessary as a link between the cytochrome and oxygen. Keilin and Harpley[11] have already suggested that an iron enzyme, designated cytochrome a_2, functions as an oxidase of the cytochrome *b* in *E. coli*. Moreover, it has been found spectroscopically that this cytochrome combines with cyanide and carbon monoxide. The presence of a similar oxidase in Type I Pneumococcus and some other bacteria which lack cytochrome *c* and cytochrome oxidase has been reported by Sevag and Shelburne,[15] who found that the respiration of these bacteria is sensitive to both cyanide and carbon monoxide and attributed the inhibitions to this oxidase. It seems therefore by no means unreasonable to assume such an oxidase as the terminal enzyme in the aerobic mechanism of a group of bacteria characterized by the lack of cytochrome *c*-cytochrome oxidase system. The absence of this system in *E. coli* has been confirmed by the negative indophenol oxidase reaction of the organism.[16]

The role of methylene blue as an intermediary hydrogen carrier between dehydrogenase systems and nitrate reductase in the reconstructed system[3] may require an explanation. Previously, assuming the identity of the cytochrome *b* with nitrate reductase, the dye was simply considered as an artificial link between dehydrogenase systems and the cytochrome. Our spectroscopic observations, however, have provided indications, though qualitative and inconclusive, that the dye can serve also as an oxidant of the ferrocytochrome *b*. In addition, it has been confirmed that the reoxidation of the leuco dye by nitrate is sensitive to both cyanide and thiourea. These facts lead to the view that methylene blue might mediate between the cytochrome and nitrate reductase in this simple reconstructed system.

Throughout the above arguments the selective inhibition by thiourea on the nitrate reduction has been taken as the most conclusive evidence in favour of the nonidentity of nitrate reductase with the cytochrome *b*. A selective toxicity[17] of this compound on nitrate metabolism has been also reported by Fleury,[18] who found that thiourea exerts a strong fungistatic action on *Aspergillus niger* in media with nitrate as the sole source of nitrogen, while the toxicity is much less (or absent) when ammonium salts or organic nitrogen

(15) M. G. Sevag and M. Shelburne, *J. Gen. Physiol.*, **26**, 1 (1942).

(16) R. Sato, Unpublished data.

(17) W. W. Wainio *et al.* have reported (*J. Biol. Chem.*, **192**, 349 (1951)) that thiourea, even at a concentration of 10^{-2} M., does not exert any inhibition on cytochrome oxidase activity of a heart muscle preparation.

(18) C. Fleury, *Bull. soc. suisse botan.*, **58**, 462 (1948); *Chem. Abst.*, **43**, 3880 (1949).

sources are available. From these findings Fleury has concluded that thiourea inhibits the nitrate-reducing enzyme system of the mold. The precise mechanisms involved in these specific inhibitions, however, are left to be clarified. Presumably, the capacity of thiourea to form complexes with various metal ions might play a part in these phenomena in some manners. At any rate, further research about this point appears to be of promise for the elucidation of the nature of nitrate reductase.

As a result of the denial of the identity previously suggested between nitrate reductase and cytochrome *b* of *E. coli* type, the necessity has come to the fore again to consider the chemical nature of this enzyme. Neverthless, it seems still valid that the activity of nitrate reductase of *E. coli* is inseparably associated with the presence of iron in the molecule. The most clear-cut support for this view comes from the results of the previous study[5] showing the carbon monoxide inhibition of this enzyme and its reversal by light. Recently it has been further confirmed in this laboratory[19] that a small but definite inhibition by carbon monoxide is also seen in the nitrate reduction by *Bacillus subtilis* and *Acetobacter xylinum*; light reversed the inhibition also in these cases, This suggests that a similar iron enzyme may be responsible for the reduction also in these organisms. Its detailed features, however, are not yet clear.

The iron-protein nature of nitrate reductase receives further indirect support from an investigation dealing with the effect of iron-deficiency on the nitrate-reducing activity of *E. coli*.[20] It has been shown that the organism grown on iron-deficient media has a considerably low activity of nitrate reductase as compared to the cells supplied with a sufficient amount of iron. The activity of succinic dehydrogenase was not influenced by the iron content of the media. Similar results has also been obtained with *C. diphtheriae*.[21] In this connection, observations by Granick and Gilder[22] are worthy of special attention. Studying the growth-promoting activity of various porphyrin derivatives on strains of *Hemophilus influenzae*, they found that several iron porphyrin compounds such as iron meso- and iron hematoporphyrin can substitute iron protoporphyrin as an essential growth factor for this organism. But the organism grown on these unnatural growth factors was found to be completely devoid of the nitrate-reducing activity. On the basis of these observations they have concluded that iron protoporphyrin is required either for the formation of the function of the nitrate-reducing mechanism, the vinyl side chains of protoporphyrin being assumed to be essential.

There are, however, no definite indications in support of the possibility that nitrate reductase is actually a heme protein enzyme, and the clarification of the chemical nature of this enzyme is largely left for the future.

Summary

1. It has been found that thiourea has a marked inhibitory effect on the nitrate reduction by *E. coli*, but dehydrogenase activity and the aerobic respiration of the same organism are not considerably influenced by this compound.

2. Spectroscopically it has been further clarified that thiourea completely prevents the anaerobic oxidation of the ferrocytochrome *b* by means of nitrate, whereas the same reagent can not inhibit the aerobic oxidation of the cytochrome. Cyanide prevents both of the oxidation processes.

3. On the basis of these findings the previously suggested identity of nitrate reductase with cytochrome *b* of *E. coli* type has been criticized and it has been concluded that the cytochrome *b* is not identical with nitrate reductase itself, though it is closely associated with the nitrate-reducing mechanism of *E. coli*.

4. A scheme has been proposed which can account for both the nitrate-reducing and the respiratory mechanisms of *E. coli*.

5. The chemical nature of nitrate reductase has been discussed and the iron-protein nature of this enzyme has been again emphasized.

Addendum I: In a review quoting a previous paper[5] of this series, Wurmser[23] wrote that in the nitrate reduction nitrogen replaces oxygen for the Slater's respiratory scheme. In spite of the validity of this statement, it should be considered that nitrate, but not nitrogen, replaces it.

Addendum II: After this paper had been submitted to the editors, we were informed of the criticism by G. N. Cohen[24] against our earlier hypothesis on the identity of nitrate reductase with the cytochrome *b*. The nitrate-reducing mechanism of strict anaerobes and its differences from that of *E. coli* have been

(19) I. Yamashina, Unpublished data.
(20) M. Niwa, Unpublished data.
(21) R. Sato and M. Yoneda, Unpublished data.
(22) S. Granick and H. Gilder, *J. Gen. Physiol.*, **30**, 1 (1946).
(23) R. Wurmser, *Ann. Rev. Biochem.*, **20**, 8 (1951).
(24) G. N. Cohen, *Ann. Rev. Microbiol.*, **5**, (1951).

investigated by Mr. Tadao Katsura at the Institute of Infectious Diseases of Tokyo University in connection with us. This material will be published shortly.

The present authors are deeply indebted to Prof. F. Egami for his continuous encouragement and valuable advice for this study. The spectroscopic experiments by the use of a Beckman spectrophotometer were carried out at the National Institute of Health (Japan). The kindness of Dr. H. Fukumi and Mr. H. Uchida who permitted us to use the instrument is gratefully acknowledged. Thanks are also due to Prof. S. Hosoya of the Institute for Infectious Diseases for his kindness in giving us many conveniences in preparing the cell-free enzyme preparation. A part of the cost of this investigation was defrayed from the Scientific Research Encouragement Grant from the Ministry of Education.

Chemical Institute, Faculty of Science,
Nagoya University

Études sur les Lactones dérivés des Acides Chrysanthémiques

par Masanao MATSUI, Takashi OHNO, Seiichi KITAMURA et Misao TOYAO

(Reçu Octobre 1, 1951)

Si l'on chauffe l'acide chrysanthémique jusqu'à 400° dans un tube à vide, la majeure partie des substances se transforme en lactones. Ainsi, on obtient le pyrocin qui fond à 83.5-84.5° de l'acide chrysanthémique naturel[1][2] et de la même façon on obtient le (±)-pyrocin qui fond à 61-62° des acides chrysanthémiques synthétiques.[2] Mais, la majeure partie des lactones reste à l'état d'huile. Si l'ouverture de l'anneau se produisait à quelques degrés par le chauffage, des lactones se produiraient comme exprimé par les formules suivantes.

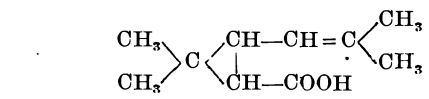

I.

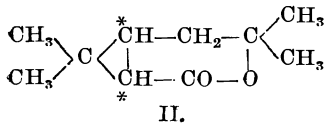

II.

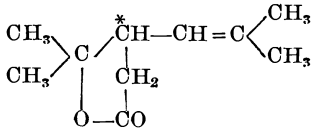

III.

* carbone asymétrique.

L'un de nous a suggéré que la formule constitutionelle du pyrocin pourrait être II d'après les produits d'oxydation et les réactions par son radical alcoolique du pyrocin.[2]

Il y a huit ans, le Dr. Makoto Nagase et l'un de nous[1] ont oxydé le pyrocin avec le permanganate de potassium et nous avons obtenu l'acétone et un corps qui fut considéré comme de l'acide *trans*-caronique par son point de fusion (212.5°) et par le résultat de la microanalyse.

Après cela, la constitution du pyrocin fut discutée sur la base de cette expérience. Cette même année, pourtant, nous avons su que le Dr. S. H. Harper[3][4] avait obtenu avec de l'acide (±)-*cis*-chrysanthémique en le traitant par l'acide sulfurique dilué un lactone qui fond à 52° et il proposait que ce corps est le lactone de l'acide 2-(2-hydroxyisobutyl)-3,3-diméthylcyclopropane - 1 - carboxylique (II). Pourtant, l'un de nous a aussi obtenu des acides (±)-*cis*·*trans*·chrysanthémiques synthétiques en chauffant dans un tube à vide, un lactone qui fond à 62° et il a conclu aussi à la même constitution que le Dr. Harper. L'abaissement du point de fusion du mélange de ces deux corps indique qu'ils sont des corps tout à fait différents.

Nous avons, alors, réexaminé des réactions

(1) Makoto Nagase et Masanao Matsui, *J. Agr. Chem. Soc. Japan*, **20**, 250 (1944).

(2) Masanao Matui, *Botyu-Kagaku* (Japan) **15**, 1(1950).

(3) S. H. Harper, Pyrethrum Post, Janvier et Avril (1949), **1**, No. 3, 9-15, No. 5, 10-16.

(4) Nous tenons à remercier ici Monsieur le Docteur S. H. Harper des précieux specimens qu'il nous a prodigués.

de pyrocins et essayé, de nouveau, l'oxydation du pyrocin et du (±)-pyrocin purifiés avec soin. Les deux corps décolorisèrent la solution alcoolique ou acétonique de permanganate de potassium. Alors, nous avons ozonisé les deux lactones et nous avons obtenu de l'ozonide du pyrocin l'acide (+)-térébinique qui fond à 200° et qui fond à 202° mélangé avec l'acide (+)-térébinique fondant à 201-204° [207.5-210.5° (corrigé)] qui est obtenu par nous de l'acide (±)-térébinique par son sel de cinchonine. Mme. Arne Fredga[5] a obtenu de l'acide térébinique actif qui fond à 201-205°, $[\alpha]_D^{25°}$, ±13.2° par oxydation de l'acide isopropylsuccinique. Or le corps fondant à 212.5° (corrigé) qui est obtenu par le Dr. Nagase et l'un de nous par l'oxydation du pyrocin avec le permanganate de potassium et regardé comme de l'acide *trans*-caronique[1] était réellement l'acide (+)-térébinique.

Nous avons obtenu aussi de l'ozonide du (±)-pyrocin l'acide (±)-térébinique qui fond à 173 et à 174°, étant mélangé avec l'acide (±)-térébinique fondant à 175°.

Alors la formule consitutionelle du pyrocin doit être le lactone lévogyre de l'acide 3-isocrotyl-4-méthyl-4-hydroxyvalerianique.

Le (±)-pyrocin se transforme en un corps $C_{10}H_{18}O_3$ qui fond à 159° ajoutant une molécule d'eau par le traitement de l'acide sulfurique dilué. Il donne l'éther-sel de *p*-bromophénacyl. Pourtant, à cause du point de fusion bas on ne peut pas le purifier suffisamment. Ce corps probablement est VI, parce que γ-lactone ne donne pas ordinairement l'ether-sel de *p*-bromophénacyl; On ne peut pas obtenir l'éther-sel de *p*-bromophénacyl du pyrocin.

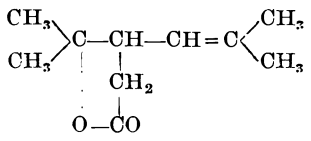

III.

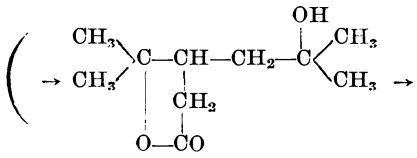

IV.

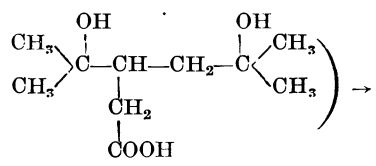

V.

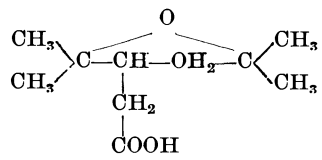

VI.

En outre, nous avons ozonisé aussi les liqueurs-mères du (±)-pyrocin. Pourtant nous n'avons pas obtenu des ozonides des corps cristallins sauf une petite quantité d'acide (±)-térébinique qui fond à 174°.

Alors, nous avons essayé de synthétiser du pyrocin et du (±)-pyrocin d'après la formule constitutionelle présomptive, en partant de l'acide (+)-térébinique et de l'acide (±)-térébinique respectivement, suivant les schèmes ci-dessous.

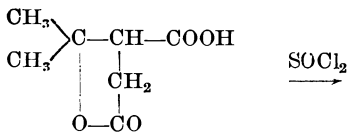

VII.

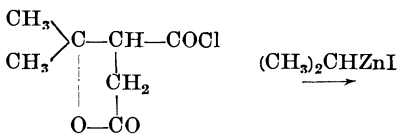

VIII.

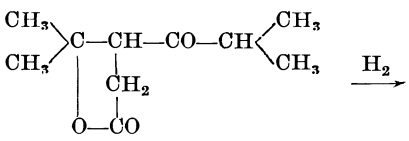

IX.

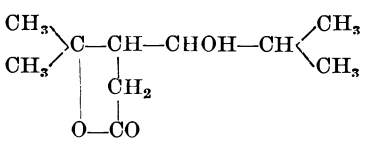

X.

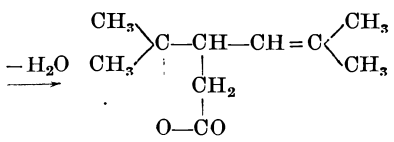

III.

La réaction de VIII à IX n'a pas été normale. Nous avons obtenu directement III par la réaction entre le chlorure de l'acide térébinique et l'iodure de zinc-isopropyl. Il

(5) Arne Fredga, Svensk Papperdtidn, **50**, No. 11, B 91-3 (1947), (*Chem. Abs.*, **42**, 123 (1948).

s'est manifesté par l'action réductrice de l'iodure de zinc-isopropyl suivi par la déhydration.

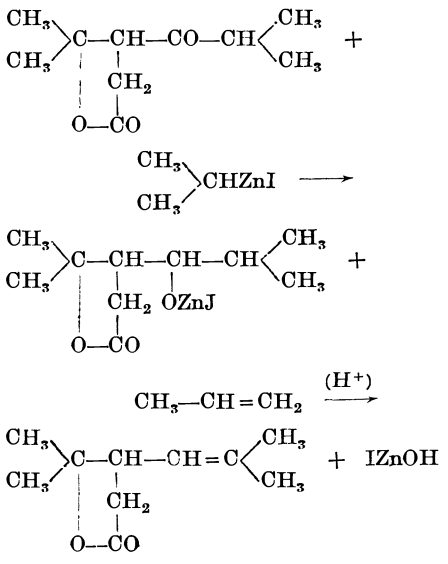

Les points de fusion des corps synthétiques sont 83-84° et 61-62° en partant de l'acide (+)-térébinique et l'acide (±)-térébinique respectivement et le point de fusion mélangé de ce corps-là avec le pyrocin fondant à 83.5-84.5° a été 83-84° et celui de ce corps-ci avec le (±)-pyrocin fondant à 61-62° a été 61-62°.

Le (±)-pyrocin totalement synthétique via l'acide (±)-térébinique aussi se transforme en corps qui fond à 159° ajoutant une molécule d'eau en chauffant dans l'acide sulfurique à 5% que le corps transformé de l'acide (±)-*cis-trans*-chrysanthémique par le chauffage.

Or, nous avons confirmé enfin que le pyrocin et le (±)-pyrocin sont respectivement la forme lévogyre et la forme racémique du lactone de l'acide 3-isocrotyl-4-méthyl-4-hydroxyvalérianique.

Pourtant par les études ci-dessus il est mis en évidence comme par miracle que le point de fusion de l'acide térébinique actif est présque celui de l'acide *trans*-caronique et le point de fusion de l'acide térébinique racémique est celui de l'acide *cis*-caronique. Alors dans des études de terpènes, il y a probablement des travaux qu'il faudra examiner de nouveau.

Partie Expérimentale

(Les points de fusion ne sont pas corrigés.)

1) Le pyrocin[1][2] et le (±)-pyrocin,[2] (III).—On a obtenu ces corps de la façon décrite dans le rapport précédent.[1][2] C'est-à-dire, on chauffe l'acide (+)-chrysanthémique naturel ou l'acide (±)-*cis-trans*-chrysanthémique dans un tube vide jusqu'à 400° pendant 30 minutes. Le contenant est pris dans l'éther et lavé plusieurs fois à la solution de carbonate de sodium à 10% et après avoir distillé le solvent dans le bain-marie, le sirop résiduel est saponifié par la potasse alcoolique. De l'eau est ajoutée et l'alcool est débarrassé de la solution. La solution restante est extraite à l'éther et on abandonne les corps neutres. On acidule la solution alcaline en ajoutant l'acide sulfurique dilué et on l'extrait à l'éther. On lave la solution d'éther à l'eau deux ou trois fois et on chasse l'éther de la solution. Le pyrocin ou le (±)-pyrocin se cristallisent dans la glacière. On les recristallise dans de l'éther de pétrole. F. du pyrocin: 83.5-84.5°, et F. du (±)-pyrocin: 61-62°. Rendement ca. 10% de la théorie.

$[\alpha]_D^{25°}$ du pyrocin = −57.7° (C: 0.6163 dans l'alcool).

2) Ozonisation du pyrocin actif.—Un courant d'air ozonisé passe pendant 50 minutes au travers de la solution de 120 mg. du pyrocin dans 50 cc. de chloroforme que l'on maintient à 0°. On chasse le chloroforme dans le vide et le résidu est bouilli avec de l'eau pendant une heure. On débarrasse une petite quantité de résine par passage sur une couche de norite. Après évaporation à sec dans le bain-marie, le résidu se cristallise. On recristallise les cristaux dans l'eau. Le point de fusion de ces cristaux (30 mg) est 200°.

$C_7H_{10}O_4$	calculé	C%	53.16	H%	6.33
	trouvé		52.93		6.77

Le point de fusion en mélange avec l'acide (+)-térébinique (F; 201-204°) est 200-201°, et le point de fusion en mélange avec l'acide (−)-térébinique (point de fusion 200°) est 175°. Il est sans aucun doute l'acide (+)-térébinique.

3) Résolution de l'acide térébinique.

a) L'acide (±)-térébinique, (VII).

Ce corps est obtenu par la méthode de Bruno Frost[6], mais la préparation est un peu modifiée: on ajoute 108 g. de méthylate de sodium dans 400 cc. d'éther anhydre et en réfroidissant à la glace on ajoute goutte à goutte un mélange de 120 g. d'acétone et 145 g. de succinate de méthyl. Après avoir laissé reposer deux jours, on y ajoute un mélange de 350 cc. d'acide hydrochlorique concentré et 350 cc. d'eau. Après évaporation de l'éther sur le bain-marie, on chauffe à reflux la solution pendant 12 heures. On ajoute 500 cc. d'eau chaude et on débarrasse la résine par passage sur une couche de norite et on laisse reposer une nuit. On sépare les cristaux et on lave deux fois à l'eau refroidie. Après recristallisation dans 200 cc. d'eau, on obtient 60 g. d'acide (±)-térébinique qui fond à 175°. On peut obtenir encore une petite quantitié de ce produit par évaporation des liqueurs-mères.

$C_7H_{10}O_4$	calculé	C%	53.16	H%	6.33
	trouvé		53.13		6.57

(6) Bruno Frost, *Ann.*, **226**, 363 (1884).

b) Sel de cinchonine de l'acide (+)-térébinique.

Six grammes et demi d'acide (±)-térébinique (F. 175°) dans 50 cc. d'alcool sont mêlés avec 12.5 g. de cinchonine dans 50 cc. d'alcool. On laisse reposer la solution résultante une nuit. Les cristaux séparés sont recristallisés dans 80 cc. d'alcool bouillant. Le produit (5 g.) fond à 222°. $C_{26}H_{32}O_5N_2$ calculé C% 68.35 H% 6.64 N% 6.68

trouvé 68.96 6.74 6.45

$[\alpha]_D^{25°} = +151°$ (c: 1.0 dans l'alcool à 12%).

c) L'acide (+)-térébinique.

Neuf grammes de cristaux de sel en haut sont dissous dans 160 cc. d'eau, on ajoute 10 cc. d'ammoniaque à 25%. Après refroidissement, la cinchonine qui est précipitée, est séparée et lavée à 100 cc. d'eau. La solution est évaporée à 25 cc. et acidulée en ajoutant 15 cc. d'acide hydrochlorique à 35%. Les cristaux se précipitent sous la forme de fragments carrés très jolis. Après recristallisation dans 30 cc. d'eau, l'acide (2 g.) fond à 201-204°.

$C_7H_{10}O_4$ calculé C% 53.16 H% 6.33

trouvé 52.84 6.00

$[\alpha]_D^{25°} = +9.0°$ (c: 4.0 dans l'alcool).

d) L'acide (−)-térébinique.

On laisse reposer 3 jours les liqueurs-mères du sel de cinchonine de l'acide (+)-térébinique et on débarrasse tous les cristaux séparés. Après l'évaporation d'alcool à sec, le résidu est repris dans 120 cc. d'eau et on ajoute 40 cc. d'ammoniaque à 25%. La cinchonine précipitée est débarrassée par filtration et la solution filtrée est évaporée à 40 cc. sur le bain-marie et on y ajoute 30 cc. d'acide chlorhydrique concentré. L'acide (−)-térébinique se sépare premièrement sous la forme de fragments carrés très jolis qui fondent à 198°. Après recristallisation dans 50 cc. d'eau, on obtient 1.5 g. du produit fondant à 200°.

$C_7H_{10}O_4$ calculé C% 53.16 H% 6.33

trouvé 52.60 6.54

$[\alpha_D]^{26.5°} = -7.95°$ (C; 3,333 dans l'alcool).

4) Ozonisation du (±)-pyrocin.—Un courant d'air ozonisé passe pendant deux heures à travers de la solution de 750 mg. du (±)-pyrocin dans 50 cc. de chloroforme que l'on maintient à 0°. Après évaporation à sec du chloroforme dans le vide à la température ordinaire, on décompose l'ozonide résiduel en chauffant avec de l'eau. Après avoir débarrassé une petite quantité de resine par passage sur une couche de norite, on évapore à sec la solution aqueuse. Il se sépare lentement des cristaux. Ils sont recristallisés dans de l'acide chlorhydrique dilué. On obtient ca. 300 mg. de produit fondant à 173° (pas encore tout-à-fait pur). En mélange avec l'acide (±)-térébinique fondant à 175° on trouve F. 174°.

$C_7H_{10}O_4$ calculé C% 53.16 H% 6.33

trouvé 52.93 6.47

5) Traitement du (±)-pyrocin par l'acide sulfurique dilué.—On chauffe à 100° dans un tube fermé 750 mg. du (±)-pyrocin et 50 cc. d'acide sulfurique à 5% pendant 12 heures et puis on laisse reposer une nuit dans une glacière. Les cristaux se séparent. Par recristallisation dans de l'eau on obtient 0.4 g. de cristaux fondant à 159°.

$C_{10}H_{16}O_3$ calculé C% 64.52 H% 9.69

trouvé 64.44 9.46

6) Le (±)-pyrocin, (III).—D'abord, on chauffe à reflux 45 g. d'acide (±)-térébinique, 200 cc. de benzène anhydre et 75 cc. de chlorure de thionyl pendant 20 heures sur le bain-marie. Après la distillation de benzène et excès de chlorure de thionyl on distille dans le vide. On obtient ainsi 45 g. de chlorure d'acide qui distille à 123° sous 10 mm.

On chauffe dans un ballon 55 g. d'iodure d'isopropyl, 30 cc. d'éther de pétrole et 65 g. de l'alliage éffacé de zinc et cuivre (10 : 1). Après que la réaction se produit on chauffe à reflux le mélange pendant deux heures. On ajoute 100 cc. de benzène anhydre. Les boues sont décantées et la solution versée dans un autre ballon muni d'une ampoule à brome contenant le chlorure d'acide (45 g.) susdit en solution dans 100 cc. de benzène anhydre. Le ballon est refroidi à 0° au moyen d'un mélange réfrigérant glace-sel et l'on introduit goutte à goutte le chlorure d'acide en agitant constamment. On laisse reposer une nuit, puis le produit de condensation est versé sur de la glace, extrait à l'ether, lavè à fond à l'acide sulfurique à 10%, au carbonate et enfin à l'eau.

On sépare ainsi 10 g. de parties neutres. Elles sont distillées dans le vide, on obtient 7 g. de produit distillant à 138-139° sous 35 mm. Il se cristallise dans une glacière. On sépare les cristaux et on recristallise dans de l'éther de pétrole. Ainsi on obtient 2 g. de cristaux qui fond à 61-62°. En mélange avec le (±)-pyrocin de 1) on observe F, 61-62°.

$C_{10}H_{16}O_2$ calculé C% 71.43 H% 9.52

trouvé 71.55 9.55

Il se cristallise lentement des liqueure-mères encore plus de cristaux.

7) Traitement du (±)-pyrocin de[6] par l'acide sulfurique dilué.—On chauffe dans un tube fermé 300 mg. du lactone derivé de l'acide (±)-térébinique et 23 cc. de l'acide sulfurique à 5% pendant 12 heures à 100°, et puis on laisse reposer dans une glacière une nuit. On sépare les cristaux et on recristallise dans de l'eau, F. 159°. En mélange avec le corps[5] dérivé de l'acide chrysanthémique, on observe F. 159°.

$C_{10}H_{15}O_3$ calculé C% 64.52 H% 9.68

trouvé 64.80 9.64

8) Le pyrocin, (III).—Comme pour la préparation du (±)-pyrocin, d'abord on prépare le chlorure de l'acide (+)-térébinique (6 g.) partant 6 g. d'acide, 40 cc. de benzène anhydre et 15 cc. de chlorure de thionyl par chauffage à reflux pendant

5 heures. Eb. 10 mm. 123°. Et puis on prépare la solution d'iodure de zinc isopropyl de la même façon que pour le cas[5] partant de 16 g. d'iodure d'isopropyl, 7 g. d'alliage éffacé de zinc et cuivre et 10 cc. d'éther de pétrole. Et traitant de la même façon qu'au cas du (±)-pyrocin,[6] on obtient 0.8 g. du produit qui fond à 83-84° après recristallisation dans de l'éther de pétrole. Le point de fusion en mélange avec le lactone derivé de l'acide (+)-chrysanthémique naturel qui fond à 83.5-84.5° est 83-84°.

$C_{10}H_{16}O_2$	calulé	C% 71.43	H% 9.52	
	trouvé	71.20	9.74	
$(\alpha)_D^{25°}$	$= -56.5°$	(C : 0.7512 dans l'alcool)		
	$-54.8°$	(C : 0.2993 dans l'alcool).		

Résumé

A la pyrolyse des acides chrysanthémiques quelques lactones se produisent. Le pyrocin et le (±)-pyrocin sont les deux qu'on obtient sous la forme cristalline. Nous avons fait de nouvelles recherches et par des synthèses totales nous avons confirmé ces formules constitutionelles. Le pyrocin est le lactone lévogyre de l'acide 3-isocrotyl-4-méthyl-4-hydroxy-valérianique et le (±)-pyrocin est le corps racémique.

Nous tenons à remercier ici M. le Docteur Ryo Yamamoto et M. le Professeur Ryuzaburo Nodzu de précieux conseils qu'ils nous ont prodigués.

Laboratoire de la Compagnie Chimique de Nissin

On the Hydrazinolysis of Proteins and Peptides: A Method for the Characterization of Carboxyl-terminal Amino Acids in Proteins

By Shiro AKABORI, Ko OHNO and Kozo NARITA

(Received January 21, 1952)

The problem of determining the amino acid sequence in proteins has attracted the interest of many investigators because of its bearing on protein structures. Although several chemical methods[1-5] have been published heretofore for the characterization of carboxyl-terminal amino acids in peptides, most of them are not entirely suitable to be applied for proteins practically. C. Fromageot *et al.*[6] have reported the most eminent method, in which insulin was treated with lithium aluminium hydride and only carboxyl-terminal amino acids were reduced to amino alcohols. However, it seems to be worth-while to study some other methods, because the applicability of the methods cited is for practical reasons restricted.

The present authors have investigated the hydrazinolysis of peptides for the purpose of finding a simple method of the characterization of carboxyl-terminal amino acids in proteins. It is well known that acylamino compounds are easily decomposed by hydrazine to acylhydrazines and amines. But, so far as the present authors are aware of hydrazinolysis of protein has never been studied, except that A. Stoll *et al.*[7] have studied the degradation of ergot alkaloids which contain peptide linkages.

When proteins are treated with anhydrous hydrazine under certain conditions, only carboxyl-terminal amino acids are liberated as free amino acids and other amino acid residues are converted to amino acid hydrazides. On treating with benzaldehyde the latter residues condense with it to form water-insoluble dibenzal compounds while the former remain in solution and can be identified by paper chromatography as amino acids. The reactions are shown in the following scheme:

(1) P. Schlack and W. Kumpf, *Z. physiol. Chem.*, **154**, 125 (1926).
(2) F. Bettzieche, *Z. physiol. Chem.*, **161**, 178 (1926).
(3) E. Abderhalden and H. Brockmann, *Biochem. Z.*, **225**, 386 (1930).
(4) M. Bergmann and L. Zervas., *J. Biol. Chem.*, **113**, 351 (1936).
(5) N. Lichtenstein, *J. Am. Chem. Soc.*, **60**, 560 (1938).
(6) C. Fromageot, N. Jutisz D. Meyer and L. Penasse, *Biochim. Biophys. Acta*, **6**, 238 (1950); *Compt. rend.*, **230**, 1905 (1950).
(7) A. Stoll, T. petrzilka and B. Becker, *Helv. Chim. Acta.*, **33**, 57 (1950).

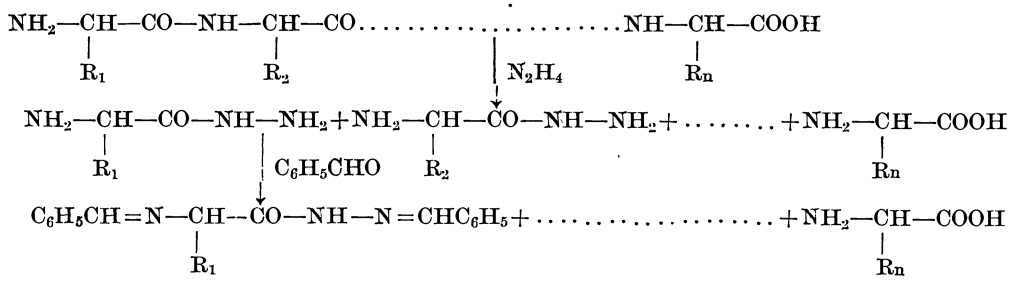

Amino acid hydrazides can also be detected on a paper chromatogram by their reducing power against ammoniacal silver nitrate solution as described in the experimental part.

Experimental

(I) Syntheses of Amino Acid Hydrazides and Their Dibenzal Compounds.—Amino acid hydrazides have not yet been synthesized except glycine-,[b] aspartic acid-[9] and tyrosine-hydrazides.[10] The authors synthesized, therefore, several new hydrazides as described below:

DL-Valine Hydrazide.—To DL-valine ethyl ester, which had been prepared as usual, a small excess of anhydrous hydrazine was added and heated in a water-bath for 10 minutes. On storing the reaction mixture *in vacuo* over sulfuric acid overnight, fine white needle valine hydrazide crystallized out. This was dissolved in hot chloroform and precipitated by addition of 3–4 volumes of ether. Thus, white crystalline DL-valine hydrazide, m. p. 96–7°C. (uncorrected), was obtained. This is very soluble in cold water (somewhat hygroscopic), ethanol and hot chloroform but insoluble in ether.

Analysis (Micro Dumas): N found, 31.06 %;* calcd. for $C_5H_{13}ON_3$, 32.05 %.

DL-Phenylalanine Hydrazide.—This was synthesized in the same manner as DL-valine hydrazide from DL-phenylalanine ethyl ester. After recrystallization from ethanol it melted at 123–4°C. (uncorrected).

Analysis: N found, 22.53%;* calcd. for $C_9H_{13}ON_3$, 23.45 %.

L-Leucine Hydrazide Dihydrochloride.—L-Leucine ethyl ester was treated with anhydrous hydrazine as usual and white plate crystals were obtained. But free hydrazide was so hygroscopic that conc. hydrochloric acid was added to it and heated for a few minutes. Leucine hydrazide dihydrochloride thus crystallized out, which, after evaporation of excess hydrochloric acid *in vacuo* over potassium hydroxide, was recrystallized from absolute ethanol, m.p. 275°C. (uncorrected), fine needles.

$[\alpha]_D^{15} = +30.6°$. (5% in distil. water).

Analysis: N found, 19.16%; calcd. for $C_6H_{17}ON_3Cl_2$ (as 2 HCl), 19.26%.

Other amino acid hydrazides synthesized in the same manner are cited in Table 1. Glycine-, alanine- and tryptophan-hydrazides were obtained not in crystalline but in syrupy forms, although these were sufficiently pure for paper chromatography. L-Tyrosine hydrazide[10] and L-glutamic acid-γ-hydrazide[11] were obtained in crystalline forms.

Amino acid hydrazides react with ninhydrin to give reddish purple color, with ammoniacal silver nitrate solution to give dark brown color, and reduce iodine and permaganate solutions. For the color reagent for paper chromatography, n-butanol solution saturated with ammoniacal silver nitrate aqueous solution is preferable. The chromatograms

Table 1

R_F Values of Several Amino Acid Hydrazides and Corresponding Amino Acids. Solvent for Paper Chromatography is Pyridine Base-aniline-water (9 : 1 : 4)

Amino acid hydrazides	R_F	Amino acids	R_F
Glycine hydrazide	0.26	Glycine	0.17
L-Alanine hydrazide	0.36	L-Alanine	0.24
DL-Valine hydrazide	0.56	DL-Valine	0.40
L-Leucine hydrazide	0.65	L-Leucine	0.51
DL-Phenylalanine hydrazide	0.71	DL-Phenylalnine	0.52
L-Tyrosine hydrazide	0.71	L-Tyrosine	0.55
L-Tryptophan hydrazide	0.70	L-Tryptophan	0.50
L-Glutamic acid-γ-hydrazide	0.15	L-Glutamic acid	0.11

(8) T. Curtius, *J. prakt. Chem.*, (2) **76**, 102 (1904).
(9) T. Curtius, *ibid.*, (2) **95**, 354 (1917).
(10) T. Curtius, *ibid.*, (2) **95**, 330 (1917).
* As there is a long time lag between the syntheses and analyses of these hydrazides, low values of found nitrogen must be due to their decomposition during their storage.
(11) S. Akabori and K. Narita, to be published shortly.

thus obtained can be stored after dipping them into thiosulfate solution, washing with water and drying. As the developing solvent for paper chromatography, pyridine base-aniline-water (9 : 1 : 4 : by volume) is found to be best. The "pyridine base" used is a high boiling fraction (b.p. 130–150°C.) of pyridines, *i. e.* a mixture of picolines and lutidines.

Amino acid hydrazides can be quantitatively estimated by oxidative titration using bromate or iodine standard solution. For example, we carried out the titration of leucine hydrazide dihydrochloride according to I. M. Kolthoff's analytical method for hydrazine.[12]

(1) **Potassium bromate method.**—Leucine hydrazide dihydrochloride (49 mg.) was dissolved in 2 ml. distilled water, added 2 ml. conc. hydrochloric acid and titrated with 0.100 N $KBrO_3$ using indigo as indicator. The sample required 2.22 ml. of the bromate. The calculated value for the next equation is 2.20 ml.: $RCH(NH_2)CONHNH_2 + 2/3KBrO_3 \rightarrow RCH(NH_2)COOH + N_2 + H_2O + 2/3KBr$

(2) **Iodine method.**—Leucine hydrazide dihydrochloride (18.8 mg.) was dissolved in 10 ml. distilled water containing 0.4 g. sodium bicarbonate and titrated with 0.1057 N iodine solution. The sample required 3.20 ml. of the iodine solution. The calculated value for the next equation is 3.25 ml.: $RCH(NH_2)CONHNH_2 + 2I_2 + H_2O \rightarrow RCH(NH_2)COOH + N_2 + 4HI$

In both cases the solution after titration was found to contain only free leucine by paper chromatography.

Dibenzal Compounds of Amino Acid Hydrazides.—Amino acid hydrazides condense with benzaldehyde in neutral aqueous solution to form white cold-water-insoluble dibenzal compounds, which develop no color by either ninhydrin or silver nitrate reagents. These benzal compounds, however, decompose to hydrazides and benzaldehyde in strong acidic solution. We synthesized dibenzal compounds of L-leucine- and L-alanine-hydrazides.

Dibenzal L-Leucine Hydrazide.—Crystalline L-leucine hydrazide dihydrochloride was dissolved in a small amount of water and an excess of benzaldehyde was added under cooling and stirring. As no precipitation occurred, the solution was neutralized with dil. NaOH until the precipitate separated out (*p*H 7.5). After standing over night in an ice box, the precipitate was collected on a filter and recrystallized from absolute ethanol. Thus white needle crystals, m.p. 149–50°C. (uncorrected), were obtained.

Analysis (Micro Dumas): N found, 13.20%; calcd. for $C_{20}H_{23}ON_3$, 13.10%.

Dibenzal Alanine Hydrazide.—Syrupy alanine hydrazide was dissolved in a small portion of water and an excess of benzaldehyde was added under cooling and stirring. On standing over night in an ice box, the white precipitate formed was collected on a filter and recrystallized from a large amount of water, whereby dibenzal L-alanine hydrazide was deposited in needles, m.p. 110–1°C. (uncorrected)

Analysis (Micro Dumas): N found, 15.06%; calcd. for $C_{17}H_{17}ON_3$, 15.05%.

Curtius[8] reported that he had obtained monobenzal compound of glycine hydrazide from acidic aqueous solution of the hydrazide, and that it was soluble in water, but for the present purpose it is preferable to precipitate hydrazides as dibenzal compounds. To accomplish this precipitation care must be taken not to shift the *p*H of the solution to acidic.

(II) Hydrazinolyses of Peptides.—As preliminary experiments we carried out the hydrazinolysis of several synthetic di- and tri-peptides. Peptides examined were as follows:

Dipeptides: glycyl-L-leucine, glycyl-L-tyrosine, glycyl-L-aspartic acid and L-leucyl-glycine.

Tripeptides: glycyl-glycyl-L-leucine and glutathione (SH form). All of these experiments gave successful results with ease. For example, two of them are described below.

Hydrazinolysis of Glycyl-L-Leucine.—Glycyl-L-leucine (73 mg.) was dissolved in 1 g. anhydrous hydrazine and heated under reflux at 125°C. (oil bath) for 1 hour. All glass apparatus was preferred in this treatment. After cooling the hydrazinolysate was poured into a watch glass and excess hydrazine was evaporated as perfectly as possible *in vacuo* over conc. sulfuric acid. The residue was dissolved in water and examined by paper chromatography. Using ammoniacal silver nitrate solution as color reagent, only glycine hydrazide developed the black spot, whereas on spraying ninhydrin solution two spots corresponding to glycine hydrazide and free leucine appeared. Therefore the carboxyl-terminal amino acid in this peptide was confirmed to be leucine.

Hydrazinolysis of Glutathione.—Glutathione (reduced form) (26 mg.) was dissolved in 1 g. anhydrous hydrazine and treated in the same manner. The paper chromatogram of the hydrazinolysate showed four spots indicating hydrazine, glutamic acid-γ-hydrazide, cysteine hydrazide and free glycine. The terminal amino acid, glycine, was confirmed further by treating as follows: The hydrazinolysate was dissolved in 1 cc. water and an excess of benzaldehyde was dropped into it under cooling and stirring, whereupon hydrazides condensed with benzaldehyde to form pale yellow amorphous precipitate (the yellow color is due to the formation of benzalazine from remaining hydrazine), and free glycine remained in the solution. After filtering the precipitate off, the colorless filtrate was examined by paper chromatography. Only one spot corresponding to glycine was found on the chromatogram, and no spot which reduced the silver nitrate solution was found. Fig. 1 shows the chromatograms of the hydrazinolysate and benzaldehyde-treated hydrazinolysate.

(III) Hydrazinolyses of Proteins.—In the case

(12) I. M. Kolthoff, *J. Am. Chem. Soc*, **46**, 2009 (1924).

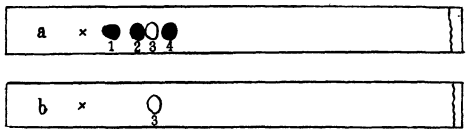

Fig. 1—a-Hydrazinolysate and b-benzaldehyde -treated hydrazinolysate of glutathione. Black spots, silver nitrate positive; white spots, ninhydrin positive. 1, cysteine hydrazide, 2, glutamic acid-γ-hydrazide; 3, glycine, and 4, hydrazine.

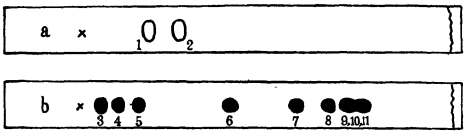

Fig. 2—a-Terminal amino acids of insulin: 1, glycine; 2, alanine. b-Hydrazinolysate of tyrocidin. Spots are hydrazides of ornithine (3), aspartic acid (4), glutamic acid (5), prolin (6), valine (7), leucine (8), tryptophan (9), tyrosine (10) and phenylalanine (11).

of lower peptides, the hydrazinolysis was completed in 1 hour, but in the case of proteins it was suspected that the time was not enough to hydrazinolyse proteins completely, and it was proved to be the case in a preliminary experiment. Hereby we hydrazinolysed glycyl-L-leucine for 10 hours and confirmed the fact that the other by-reaction such as hydrazidation of free amino acids did not occur in such a time. Therefore we decided to treat proteins with anhydrous hydrazine for 10 hours. This time of hydrazinolysis was enough to degrade proteins into amino acid hydrazides and free amino acids.

Hydrazinolysis of Insulin.—C. Fromageot *et al.*[6] reported by lithium aluminium hydride method that the carboxyl-terminal amino acids in beef insulin are glycine and alanine. On the other hand A. C. Chibnall and M. W. Rees[13] showed recently by means of the lithium boron hydride method that they are two alanines, one glycine and one as yet undetermined amino acid. We applied the hydrazinolysis to beef insulin, kindly supplied by Dr. J. Lens, N. V. Organon, Oss (the Netherlands), to compare its result with those of investigators mentioned above.

Crystalline insulin (55 mg.) was dissolved in 1 g. anhydrous hydrazine, heated to 125°C. for 10 hours, and after cooling, the excess hydrazine was evaporated *in vacuo* over sulfuric acid. The residue was taken up in water, an excess of benzaldehyde was added in small portions, and precipitates thus formed were filtered off. If hydrazides could not be completely precipitated, the *p*H of the solution was to be adjusted and made neutral by addition of dilute alkali. The mother liquor was concentrated *in vacuo* and free amino acids in it were identified by paper chromatography. Only glycine and alanine were detected on chromatogram (Fig. 2 a) showing good agreement with the result of Fromageot *et al.* Although we did not determine the result quantitatively, the intensity of the color and the area of the spots indicated that both amino acids existed in the protein in equal portions. From this result we reconfirmed the validity of this hydrazine treatment.

Hydrazinolysis of Tyrocidin.—Tyrocidin hydrochloride (200 mg.), which was kindly provided by Prof. Ohtani, Osaka Municipal University, was treated with 2 g. hydrazine for 9 hours. The hydrazinolysate gave, after evaporation of excess hydrazine, silver nitrate- and ninhydrin-positive 8 spots on paper chromatogram (Fig. 2 b), which corresponded to the hydrazides of amino acids composing tyrocidin. The chromatogram of the benzaldehyde-treated mother liquor gave no spots by spraying either ninhydrin or silver nitrate solutions. Therefore, tyrocidin was proved to be a cyclic peptide as reported heretofore.

Discussion

The present method has two excellent points: one of which is that anhydrous hydrazine is a good solvent for proteins. All proteins and peptides can be dissolved even at room temperature. The other point is that, being identified as amino acids themselves in respect to the terminal amino acids, there is no need to synthesize authentic amino acid derivatives and, if necessary, the quantitative estimations can be made by some suitable methods for microdetermination of amino acids published heretofore. Further, this method is very simple and can be carried out easily.

Besides the above mentioned experiments, the completion of the hydrazinolysis of proteins in 10 hours, on which we shall report elsewhere with details, was confirmed, in the following way: the benzaldehyde treated with mother liquor of protein hydrazinolysate was found to undergo no change in its amino acid either by further treatment with anhydrous hydrazine for 10 hours or by hydrolysis with 6 N HCl.

The applications of the hydrazinolysis to several crystalline proteins shall be reported in near future.

Summary

(1) A brief method for the characterization of carboxyl-terminal amino acids in peptides and proteins was investigated.

(2) Several new amino acid hydrazides were synthesized.

(3) Soveral di- and tri-peptides were hydrazinolyzed and identified their carboxyl-

(13) A. C. Chibnall and M. W. Rees, *Biochem. J.*, **48**, xlvii (1951).

terminal amino acid.

(4) The method was applied to beef insulin and tyrocidin for the demonstration of its applicability.

The authors wish to express their thanks to Dr. J. Lens, Organon, Oss (the Netherlands) for the supply of pure beef insulin, to Prof. Ohtani, Osaka Municipal University, for tyrocidin, and to Messrs. Fujii and Toki for the technical assistance offered in the syntheses of amino acid hydrazides. Hydrazine hydrate and sulfate were obtained through the courtesy of Mr. S. Yasuda of Mitsui Co. Ltd. and Messrs. Kumamoto and Harada of Ajinomoto Co. Inc.

Department of Chemistry, Faculty of Science, Osaka University

Fungus and Enzyme Preparation of Aspergillus Oryzae Amylase and its Use

By Taichi HARADA

(Received September 26, 1951)

Introduction

In 1934, the author[1] discussed the relation between various chemicals and fungi, and pointed out that thiourea exhibits a definite toxic value for fungi combined with neutral and harmless properties for human tissue. Application of this finding on the preparation or food and its value to fruits has aroused great interest which has appeared in recent literatures.[2],[3],[4]

The present paper of this series of investigations deals chiefly with a practical application of fungal amylase to the textile industry.

The fungal amylase taka-diastase[5] is a group of a great many enzymes among which protease, invertase and a few others are important ones. The mixture of such enzyme gives an undesirable result in one case but in an other case it gives a much better result than when used as a relatively pure amylase. The former case is seen in bread making[6] and the latter in desizing textiles in which the starch for sizing is not always pure.

Therefore, it is desirable to know how much of these enzymes are present in the amylase preparation before they are used in practice.

1) **Hydrolysis of starch.**—Saccharogenic hydrolysis of Lintner's starch by taka-diastase is found roughly to be a zero order of reaction since the value of n in the equation $\frac{dx}{dt}=K(a-x)^n$ is found to be -0.34.[7]

2) **Estimation of Invertase.**—To estimate this enzyme the author described the method[8] in which the amount of glucose is present and convenient for its calculation in accordance with the number of titer cc. which is not exactly reciprocally proportional to the true amount of produced sugar. This amount can now be calculated by the following equation with a fairly experimental agreement.

$$X=\left(0.5000\div\frac{Y}{5}\right)+\frac{0.5000(Y-5)}{1000}$$

X=glucose % in the case of 0.1-0.5% titer solution, Y=titer cc.

3) **Use in Banana Powder Making.**—In bread making, from two to three percent of sucrose is usually added to the flour for baking bread leavened with yeast which contains a considerable amount of invertase compared with that in the amylase preparation. Therefore, when a relatively small amount of the preparation is added to the dough, the invertase itself might not affect the

(1) T. Harada, This Builetin, **9**, 186 (1934).
(2) Denny, *Contrib. Boyce Thompson Inst.*, **7**, 55 (1935); *C. A.*, **29**, 6966 (1935).
(3) Childs and Siegler, *Science*, **102**, 68 (1945); *Ind. Eng. Chem.*, **38**, 82 (1946).
(4) Hartzell, *Contrib. Boyce Thompson Inst.*, **12**, 472 (1942); also refer Reineke and Turner, *Poultry Sc.*, **24**, 340 (1945); *C. A.*, **39**, 4968 (1945).
(5) The amylase preparation from pure culture on bran does not show the presence of alcohol oxidizing enzyme.
(6) T. Harada, This Bulletin, **24**, 105 (1951); *J. S. R. I.*, **44**, 189 (1950).
(7) This value was formally represented by the author as 2.34 and it was, therefore, thought that the reaction is to be a bimolecular one *Ind. Eng. Chem.*, **22**, 1424(1931).
(8) T. Harada, *Ind. Eng. Chem., Anal. Ed.*, **3**, 1 (1931).

Table 1

Titer cc. and Glucose %

No.	Titer, cc.	Glucose % obtained	Glucose % calculated	Error
1	5.00	0.5000	0.5000	0
2	6.25	0.4000	0.4000	0
3	7.50	0.3380	0.3346	0.1
4	8.50	0.3000	0.2959	0.1
5	10.00	0.2550	0.2525	1.4
6	13.00	0.2000	0.1986	1.0
7	17.50	0.1500	0.1492	0.5
8	21.75	0.1250	0.1234	1.5
9	29.00	0.1000	0.0982	1.8

bread compared with the control. However, in the banana powder making industry, the preparation helps a great deal to give a more digestive and nutritious product since a considerable amount of sucrose and the amylase preparation are both used. The analytical result was made by the author for one of the samples prepared by North-John's company, U. S. A. It is given in Table 2.

Table 2

Analysis of the banana powder obtained by treating with amylase and the control

	Untreated, %	Treated, %
Reducing sugar as glucose	28.14	43.84
Sucrose	52.00	41.23
Starch	7.68	3.53
Total carbohydrate	90.96	90.96

4) Effect of Electrolyte upon the Liquefaction of Starch Paste by Amylase.—The action of fungal amylase upon a swollen starch or starch paste is presumed to take three steps; that is to say, the starch is first transferred into soluble starch, then to dextrine and finally to sugar. The ratio of liquefying power to saccharogenic power differs depending on the origin of amylase and the process of the preparation and the condition.

The viscosity of starch paste in enzyme treatment is greatly influenced by the addition of an electrolyte. Among the electrolytes, ammonium, sodium and potassium chlorides, ammonium sulphate, potassium bromide and iodide, have the greatest effect, and these are followed in order by ammonium sulphate, potassium chloride, potassium bromide and iodide respectively when they are used by percent in weight; that is $NaCl \fallingdotseq NH_4Cl > (NH_4)_2SO_4 > KCl > KBr > KI$.

The activating power of the enzyme as measured by the liquefaction of starch is quickly established with a trace of the electrolyte NaCl in the case of pancreatic amylase, the maximum being obtained with a concentration of approximately 0.0025-0.0100 percent in the buffered starch solution (200 cc. with 50 cc. of 0.2 M H_2KPO_4 and 17.80 cc. of 0.2 M NaOH) to *p*H 6.6, and then is slowly decreased as the concentration increases. This buffer istelf decreases the viscosity of starch paste solution about 8.56 percent. The experimental results are shown in Tables 4, 5, 6, 7 and 8.

It appears that a trace of NaCl is essential for the liquefaction of starch by pancreatic amylase; in other words, the enzyme can not be liquefied without NaCl. The small decreases (0.010) in the viscosity is due probable to an experimental error in this type of experiment. In this, it differs from malt and fungal amylases. The last named two enzymes are not essential for liquefying action but are greatly activated by the salt.

The decrease of viscosity of starch paste by electrolyte alone is cosiderable. The action of electrolyte on starch is not clearly known. There is a lack of information regarding the effect of electrolyte on the viscosity of solution or paste of starch. In this connection, Boutaric and Chapeaux's report[9] appeared recently in the chemical abstract; however, unfortunately neither the details nor the original paper of the above authors are available to the author at present in Japan.

As the result of experiment, it was found that the viscosity is not alone due to the degree of acidity of the solution, since the chloride of the alkaline earth metal $CaCl_2$ liquefies much more than that of $AlCl_3$. Among phosphates, the acid one gives a greater effect than that of the alkaline one. Moreover (addition of 5 cc. of 0.2 M) sodium hydroxide in many experiments gives only a little change on the liquefaction of starch paste on standing at room temperatures.

5) Viscosity of Native Starch Solution and Time of Heating at 50°C.—The viscosity of the solution of starch paste, relative to that of water is calculated by means of the formula:

$$\eta\ (\text{starch solution}) = \frac{(\text{time} \times \text{density})_{\text{starch}}}{(\text{time} \times \text{density})_{\text{water}}}$$

The viscosity of 0.5 percent native potato starch solution was little influenced (not more than 5 percent) by heating at 50°C. for more than one hour.

As experiment, five grams of native potato starch were introduced into a large beaker with a small amount of water (about 30 cc.) to which about

Table 3

Relation between the Viscosity of 0.5 percent Native Starch Solution and Time of Incubation at 50°C. (viscosity relative to that of water at 25°C.)

No.	1	2	3	4
Time in min.	0	5	10	15
η change	2.4375	2.5000	2.4375	2.5000

No.	5	6	7
Time in min.	20	25	30
η change	2.4375	2.4375	2.4375

(9) Boutaric and Chapeaux, *Compt. rend.* **214**, 949 (1942); *C. A.*, **39**, 236 (1945).

Table 4

Influence of NaCl on Starch Liquefying Action of Fungal Amylase (Viscosity relative to that of water at 25°C.) with 0.0050% Solution

No.	A		B	C	D	E	F
	NaCl %	pH	η controls water +NaCl +NaOH +enzy.	η controls starch soln. +NaCl +NaOH +enzy.	η starch soln. +NaCl +enzy. then add. NaOH	η reduced, due to NaCl (C_1-C_n)	η actively reduced by enzy. (C_1-D_n)
1	—	6.2	1.0002	2.3134	2.0004	—	0.3130
2	0.0050	6.2	1.0002	2.2509	1.6257	0.0625	0.6877
3	0.0100	6.2	1.0315	2.1884	1.4378	0.1250	0.8756
4	0.0200	6.2	1.0327	1.9383	1.3755	0.3751	0.9379
5	0.2000	6.2	1.0628	1.6884	1.1882	0.6250	1.1252
6	0.5000	6.2	1.0632	1.5012	1.1259	0.8122	1.1875

No.	G	H	I	J	K	L
	η reduced, due to enzy. (C-D)	η starch soln. (C-B)	η reduced, due to NaCl and enzy. combined (D_1-D_n)	η starch soln. alone by enzy. (D-B)	η reduced, due to enzy. activation by NaCl (H_1-H_n)	η corresp. soluble starch soln. (0.5%)
1	0.3130	1.3132	—	1.0002	—	1.0627
2	0.6252	1.2507	0.3747	0.6255	0.0625	1.0627
3	0.7506	1.1569	0.5626	0.4063	0.1563	1.0627
4	0.5628	0.9056	0.8754	0.3428	0.4076	1.0638
5	0.5002	0.6252	1.0627	0.1254	0.6880	1.0630
6	0.3753	0.4380	1.1250	0.0627	0.8752	1.0634

Table 5

Influence of NaCl on Starch Liquefying Action of four different Amylase Preparations (viscosity relative to that of water at 25°C.) with 0.0050% Solution

P. D. = pancreatic diastase, T. D. = taka-diastase, M. D. = malt diastase, B. D. = bacterial diastase (Minagawa's commercial, is mixed with salt ?).

No.		P. D.	T. D. No. 1	T. D. No. 2	M. D.	B. D.*
	NaCl %	η decreased, due to enzy.	η decreased, due to enzy. (L. V. 3000)	η decreased, due to enzy. (L. V. 2030)	η decreased, due to enzy. (L. V. 780)	η decreased, due to enzy. (L. V. 570)
1	—	0.010	0.313	0.188	0.063	0.813
2	0.0025	1.576	—	—	—	—
3	0.0050	1.675	0.625	0.625	0.438	0.813
4	0.0100	1.513	0.751	0.751	0.469	0.743
5	0.0200	—	0.563	0.563	0.375	0.532
6	0.1000	1.274	—	—	—	—
7	0.2000	—	0.500	0.500	0.250	0.313
8	0.2500	1.183	—	—	—	—
9	0.5000	0.978	0.375	0.375	0.156	0.219

* The author thanks Dr. T. Minagawa for his bacterial amylase which was kindly given for this experiment.

300 cc. of boiling distilled water was added with a moderate constant stirring by means of a glass rod. The solution was boiled by heating for about ten minutes or over, cooled, then transferred to a 500 cc. volumetric flask and then diluted to the mark with freshly boiled and cooled distilled water.

A series of glass-stoppered Erlenmeyer's flasks containing 50 cc. of the solution of starch were incubated in a 50°C. thermostat for about 30 minutes until the internal temperature reached the temperature of the thermostat.

Each of the seven solutions was treated further for zero, 5, 10, 15, 20, 25 and 30 minutes respectively, and exactly at the end of the time of incubation, the solutions were treated with 5 cc. of 0.2 M NaOH and of water and mixed.

The rate of flow and the density of the respective solutions were determined by means of an Ostwald's viscosimeter and a picnometer at 25°C. respectively.

6) Method of Measuring the Liquefaction of

Starch Paste by Amylase.—150 cc. of the 0.5 percent starch solution prepared as above in (5) was transferred by means of a pipette very carefully free from saliva into several 250 cc. glass-stoppered Erlenmeyer's flasks containing respectively 0.0038, 0.0075, 0.0150, 0.1500, 0.3750 and 0.7500 g. of sodium chloride so as to give the solutions of 0.0025, 0.0050, 0.0100, 0.2500 and 0.5000 percent as the examples.

Two series of 100 cc. capacity of Erlenmeyer's flasks with glass stoppers, each containing 50 cc. of starch solution as above described, were prepared by means of a thoroughly cleaned 50 cc. pipette. The series of flasks were placed in a 50°C. thermostat for about 30 minutes and then they were treated as follows: Five cc. of a clear enzyme solution (0.005 percent) was added by means of a 5 cc. pipette to each solution and allowed to stand for exactly 5 or 7 minutes according to the strength of the enzyme preparation. At the end of this time 5 cc. of 0.2 M NaOH solution was added to destroy the activity of the enzyme. However, for the controls the NaOH solution was first added and then the enzyme solution followed. The viscosity of the each solution was determined as described above.

In the experiment, the substrate starch solution for liquefying power test of amylase was not buffered except in the case of pancreatic enzyme, since it has little meaning in the textile desizing factory, or is rather a contamination. The results are given in the following tables which are the average values of at least three experiments.

7) **Desizing of Cotton.**—The wetting agent Nekal BX, as the example, gives great help for desizing of cotton cloth when it is added to the enzyme solution. However, when the cotton material is, previously, treated with boiling water, the agent gives little help for the purpose of desizing. In practiec in the factory, it is suggested that the sized material be first passed through a boiling NaCl or other salt solution and then through the enzyme solution containing NaCl or other salt at the temperature of 45-50°C. This is the conclusion of many desizing experiments.

The order of salts with respect to decreasing the viscosity of starch solution was $CaCl_2 > NaCl > AlCl_3 \fallingdotseq KH_2PO_4 \fallingdotseq KCl > Na_2HPO_4$.

8) **Making of "Ame".**—Fungal amylase preparation gave a slightly colored product, to "ame", a favorite kind of Japanese candy, when potato starch paste was treated with the amylase in the usual process; while malt amylase preparation gave a much better white product.

Summary

The liquefaction of starch by means of electrolytes and of amylase preparations of various origins has been studied by the viscosity method. It appears that the presence of NaCl is necessary for the liquefaction of starch paste by pancreatic one. Nevertheless, for other enzymes, NaCl is not essential for the liquefaction but the presence of NaCl accelerates greatly the enzymatic action.

The maximum activation appears at about 0.01 percent cocentration. The relation between various salts and viscosity of starch solution has been also studied.

The Scientific Research Institute, Komagome, Bunkyo, Tokyo

Table 6

Influence of NaCl on Starch Liquefying Action of Two different Amylase Preparations (viscosity relative to that of water at 25°C.) with 0.0100% Solution.

No.	NaCl %	T.D. No. 1 η decreased, due to enzy. G (C–D)		η decreased, due to enzy. M. D. G (C–D)	
1	—	0.3755	opaque	0.2505	opaque
2	0.0050	0.8131		0.5631	
3	0.0100	1.0632	transparent	0.6250	
4	0.0200	0.8755		0.5004	
5	0.2000	0.6254		0.3127	
6	0.5000	0.4378		0.2502	

Table 7

Influence of various Salts on Starch Liquefying Action of Taka-diastase Preparation (viscosity relative to that of water at 25°C.)

No.	Salt 0.0100%	η obs.	η reduced by enzy.	order of salts
1	NaCl	1.4065	0.9069	$NaCl \fallingdotseq NH_4Cl$
2	NH_4Cl	1.4065	0.9069	$(NH_4)_2SO_4 > KCl >$
3	$(NH_4)_2SO_4$	1.4375	0.8759	$KBr > KI$
4	KCl	1.4692	0.8442	
5	KBr	1.5945	0.7189	
6	KI	1.7201	0.5933	

Table 8

Relation between Salt and Viscosity of Starch Solution at 25°C.

No.	Salt 0.2000%	*p*H	η obs.	η reduced by salt
1	NaCl	6.2	1.5764	0.7882
2	$CaCl_2$	6.4	1.5461	0.8185
3	$AlCl_3$	4.8	1.6067	0.7579
4	KH_2PO_4	5.0	1.6067	0.7579
5	KCl	6.2	1.6067	0.7579
6	Na_2HPO_4	7.8	1.6370	0.7276

The Bitter Substance, Produced in Black-rotten Sweet Potato. II. On the Constitution of Ipomoeamarone. Part 1

By Takashi OHNO

(Received December 21, 1951)

In a previous report,[1] some properties of ipomoeamarone, the main constituent of the bitter subtance obtained from black-rotten sweet potato, have been reported. Now I report more findings about its functional groups and degradation products.

Crude ipomoeamarone was isolated as the fraction, b.p. 140–155°/7 mm., from neutral part of the ethereal extract of sweet potato which was inoculated with *Ceratostomella fimbriata*. The semicarbazone, $C_{16}H_{25}O_3N_3$, m.p. 131–2°, and oxim, $C_{15}H_{23}O_3N$, b.p. 153–6°/6mm., were obtained from this fraction. Pure ipomoeamarone was regenerated from the semicarbazone by hydrolysis with oxalic acid, and it accorded with formula $C_{15}H_{22}O_3$; b.p. 146–9°/5 mm., d_4^{20} 1.0290, n_D^{20} 1.4808, $[\alpha]_D^{20}+10.0°$.

It is obvious by its attitude to potassium permanganate and bromine that ipomoeamarone is an unsaturated compound. By catalytic reductions, free ipomoeamarone absorbed 2 or 3 mols of hydrogen according to conditions, but the products could not lead to the crystalline derivatives. If the semicarbazone was hydrogenated, it gave tetrahydroipomoeamarone semicarbazone, $C_{16}H_{29}O_3N_3$, m.p. 95°, taking 2 mols of hydrogen. The hydrogenated compounds did not absorb bromine, but decolorised potassium permanganate after some minutes. Under some condition, the semicarbazone absorbed 3 mols of hydrogen, but the products did not crystallise, and hydrolysed ketone was tetrahydroipomoeamarone, $C_{15}H_{26}O_3$, b.p. 180° (bath)/5 mm. The ketone did not absorb bromine, but decolorised potassium permanganate after some minutes. The fact that dihydrocompound could not be obtained by stopping reduction when it absorbed one mol of hydrogen, shows two ethylenic linkages having same resistance to hydrogen.

With sodium and alcohol, ipomoeamarone formed an alcohol, ipomoeamarol, b.p. 162°/9 mm., which gave no ketonic reactions, and was derived to 3, 5-dinitrobenzoyl ester which, although liquid, gave the crystalline additional product with α-naphthylamine, m.p. 107–9°. By catalytic reduction, ipomoeamarol absorbed 3 mols of hydrogen, but the product could not be made into crystalline derivatives. This fact leads to the conclusion that two ethylenic linkages cannot be in the $\alpha\beta$-position to the carbonyl group, nor conjugated with each other.

Of three oxygen atoms, one was confirmed to be ketone. The other two were probably oxide types, since all the reactions about hydroxyl groups, including Zerewitinoff-Fraschenträger method, were negative. In spite of the presence of three oxygen atoms, ipomoeamarone is liquid and it is difficult to obtain crystalline compounds from its derivatives; these facts, also, prove the absence of hydroxyl group in the molecule.

Although I cannot yet give evidences of whether two oxydic oxygens are aliphatic ether, cyclic ether, peroxide, or methylene-dioxide, it is rational to suppose that ipomoeamarone is a derivative of sesquiterpene and is an open-chain diolefinic ketone containg two oxide rings.

By oxidation of ipomoeamarone with potassium permanganate at room temperature, oxalic acid and a liquid keto-acid (supposed to be $C_{12}H_{20}O_4$) were obtained. For the latter, we propose the name ceratonic acid after the genus name of the fungus, *Ceratostomella fimbriata*.

This acid will be discussed in my next report.

By oxidation of ipomoeamarone semicarbazone at 100°, acetone, acetic acid, oxalic acid and a liquid acid were obtained. Production of acetone shows the presence of an isopropyl group in the molecule, and this suggests that it is a terpenic substance.

When a drop of ipomoeamarone or ipomoeamarol was added to a solution of vanillin in concentrated hydrochloric acid, pink color was produced and it turned gradually to dark red, then violet. Ipomoeamarone gave, also, color reactions by acetic anhydride and sulfuric acid (turning from blue-violet to brown), and glacial acetic acid and sulfuric acid (turning from dark red to brown). It is interesting that all of these color reactions are common through many terpenic compounds which contain oxide groups.

(1) T. Ohno and T. Takeuchi, *Botyu-Kagaku (Scientific Insect Control)* **12**, 26-9 (1949).

F. H. McDowall has been isolated ngaione[2] (pronounced "ny-one") which resembles to ipomoeamarone, from the essential oil of the leaves and terminal branchlets of *Myoporum laetum* of New Zealand. He has reported; ngaione, $C_{15}H_{22}O_3$, the main fraction of the essential oil, was a lemon-yellow oil with faint odour, b.p. 182–3°/27 mm., d_{20}^{20} 1.0276, $[\alpha]_D$ -26.20°, n_D^{20} 1.4804, the semicarbazone, m.p. 120–2° (decomp.), *p*-nitrophenylhydrazone, m.p. 103°, and was an open-chain compound with two non-conjugated double bonds, one ketonic group, and two separated oxide rings. Although his work has been interrupted and the results of his research have taken no definite form, many resemblances of the properties of both subtances and their derivatives suggest that these are mutually optical isomers, or, at least, analogous substances.

Recently, H. Watanabe and H. Iwata[3] reported nearly the same recognitions about ipomoeamarone.

Experimental

Ipomoeamarone.—Sweet potato (518 kg.) was treated as reported in a previous paper, and 125 kg. of dry black-rotten sweet potato was extracted with ether by a large scale Soxhlet extraction apparatus in batches of about 20 kg. About 6 kg. of extract was obtained. Its neutral part, obtained by treatment with aqueous alkali, was a reddish-brown, extremely bitter oil. The oil was fractionated.

B.p.	up to 141°/7 mm.	799 g.
	141–147°/7 mm.	686 g.
	147–160°/7 mm.	237 g.
	over 160°/7 mm.	93 g.
Total		1,815 g.

Residue *ca.* 1 kg.

Repeated distillation of these fractions gave the following fractions:

Lower fraction	b.p.	up to 140°/7 mm.	
Fraction 1.	b.p.	140–145°/7 mm.	467 g.
Fraction 2.	b.p.	145–150°/7 mm.	517 g.
Fraction 3.	b.p.	150–155°/7 mm.	262 g.
Higher fraction	b.p.	over 155°/7 mm.	

The physical constants and the analytical values of these main fractions were as follows:

Fraction 1,	d_4^{15} 1.0353,	n_D^{15} 1.4869,	$[\alpha]_D^{15}$ 13.3° (*c*, 17.5 in benzene)
Fraction 2,	1.0351,	1.4859,	15.2° (*c*, 18.4 in benzene)
Fraction 3,	1.0346,	1.4880,	13.5° (*c*. 19.2 in benzene)

Anal-Found: Fraction 1, C, 71.24; H, 7.17%. Fraction 2, C, 73.23; H, 8.30%. Fraction 3, C, 71.09; H, 9.04%. Calcurated for $C_{15}H_{22}O_3$: C, 72.00; H, 8.80%.

Ipomoeamarone Semicarbazone.—A mixture of 100 g. of crude bitter oil (above-mentioned fractions), 46 g. of semicarbazide hydrochloride, 40 cc. of pyridin, 200 cc. of alcohol and 100 cc. of water was allowed to stand at room temperature. After a few days the crystals of the semicarbazone were deposited. It was filtered, once dissolved in alcohol for the isolation of disemicarbazide, concentrated and recrystallised with dilute ethyl alcohol repeatedly. M.p. 131–2°, $[\alpha]_D^{29}$+85.0° (*c*, 2.0 in benene). The pyridine method gave better yield in shorter time than sodium acetate method.

Hydrolysis of the Semicarbazone.—A mixture of 6 g. of the semicarbazone and 6 g. of oxalic acid in 100 cc. of water was distilled with steam. From the distillate, pure ipomoeamarone was isolated with ether. B.p. 145–9°/5 mm., $[\alpha]_D^{27}$+10.0° (*c*. 2.5 in benzene), d_4^{20} 1.0290, n_D^{20} 1.4808, $[R]_D$ 69.0 (calc. for $C_{15}H_{22}O_3$, F_2; 69.43). (*Anal.* Found: C, 71.89; H, 9.02%. Calc. for $C_{15}H_{22}O_3$: C, 72.00; H, 8.80%.)

It gave the same semicarbazone again, but the yield was low; probably it was accompanied by a certain amount of racemisation.

Ipomoeamarone Oxim.—A mixture of 50 g. of the crude bitter oil (fraction 1), 14 g. of hydroxylamine hydrochloride, 11.5 g. of sodium carbonate, 40 cc. of water and 100 cc. of alcohol was refluxed on the water bath. After fifteen hours, alcohol was distilled off, ether was added, and this was followed by washing with dilute acid and alkali, and an ethereal layer was dried and concentrated. The residue was fractionated.

b.p.	118–133°/6 mm.	30 g.
b.p.	153–156°/6 mm.	11 g.

The first fraction, non-oximable oil was a pale yellow, mobile liquid, giving negative color reaction with sodium nitroprusside; d_4^{15} 1.0087, $[\alpha]_D^{15}$ +12.8° (*c*, 12.5 in benzene), n_D^{15} 1.4850. (Found: C, 75.44; H, 9.21)

The second fraction, ipomoeamarone oxim, was a pale yellow, very viscous liquid; d_4^{15} 1.0633, $[\alpha]_D^{15}$ +23.3° (*c*, 6.0 in benzene), n_D^{15} 1.5032. $[R]_D$ 73.7 (calc. for $C_{15}H_{23}O_3N$, F_2: 73.91). (*Anal.* Found: C, 67, 39; H, 8.38; N, 5.24%. Calc. for $C_{15}H_{23}O_3N$: C, 67.90; H, 8.68; N, 5.28%.)

Hydrogenation of the Crude Bitter Oil.—One gram of crude bitter oil in presence of 0.5 g. of Pd-$BaSO_4$ and 10 cc. of alcohol absorbed 225 cc. (2.5 mols) of hydrogen during nine hours. The resulting oil was a pale yellow oil of sweet odour

(2) F. H. McDowall, *J. Chem. Soc.*, **1925**, 220; **1927**, 731; **1928**, 1324.

(3) H. Watanabe and H. Iwata, Lecture at the meeting of Agricultural Chemical Society of Japan, 3rd Nov. 1951.

and decolorised $KMnO_4$ only after a few minutes. But it did not give any crystalline derivatives.

Hydrogenation of Ipomoeamarone Semicarbazone.—1) The semicarbazone (3.07 g.) in 55 cc. of ethyl acetate was treated with a stream of hydrogen and 2.00 g. of Pd-$BaSO_4$. During nine hours, 492 cc. (2.2 mols) of hydrogen were absorbed. The reduced product crystallised by treatment with dilute alcohol.

Tetrahydroipomoeamarone semicarbazone, m.p. 95-6°, was soluble in common organic solvents except petroleum ether, did not absorb bromine and decolorised $KMnO_4$ only slowly. (*Anal.* Found: C, 61.70; H, 9.25; N, 13.58%. Calc. for $C_{16}H_{29}O_3N_3$: C, 61.73; H, 9.33; N, 13.51%.)

The oil, obtained by treatment of the hydrogenated semicarbazone with dilute mineral acid or aqueous oxalic acid, gave color reaction with sodium nitroprusside.

Other experiments of hydrogenation derived to the same tetrahydroipomoeamarone semicarbazone as follows;

a) Semicarbazone 0.45 g., acetone 16 cc., Pd-$BaSO_4$ 0.45 g. Absorbed H_2 60 cc. (1.8 mols), during 2 hrs.
b) Semicarbazone 0.92 g., alcohol 15 cc., Pd-$BaSO_4$ 1.0 g. Absorbed H_2 186 cc. (2.8 mols), during 12 hrs.
c) Semicarbazone 0.92 g., alcohol 20 cc., PtO_2 0.05 g. Absorbed H_2 183 cc. (2.7 mols), during 6.5 hrs.

2) One gram of the semicarbazone in presence of 0.50 g. of Pd-$BaSO_4$ and 25 cc. of ethyl alcohol absorbed 232 cc. (3.12 mols) of hydrogen during thirteen hours. The product was a very viscous oil which did not crystallised for a long period. This was treated with aqueous oxalic acid. The resulting pale yellow oil (720 mg.), which gave color reaction with sodium nitroprusside, was distilled twice under 5 mm. (bath temp. 180°), yielding 410 mg. It did not absorb bromine, decolorised $KMnO_4$ after a few minutes, kept colorless for long time, and was shown to be tetrahydroipomoeamarone by analysis. (*Anal.* Found: C, 71.13, 70.82; H, 10.13, 10.39%. Calc. for $C_{15}H_{24}O_3$: C, 71.43; H, 9.52%. Calc. for $C_{15}H_{24}O_3$: C, 70.87; H, 10.24%. Calc. for $C_{15}H_{26}O_3$: C, 70.31; H, 10.94%)

Half-Hydrogenation of Ipomoeamarone Semicarbazone.—Five grams of the semicarbazone in 50 cc. of ether was shaken with 2.5 g. of Pd-$BaSO_4$ in the stream of hydrogen. Reaction was interrupted at the absorption of one molecule of hydrogen. Repeated crystallisation of the resulting product yielded ipomoeamarone semicarbazone (m.p. 128°, and there was no depression of melting point with the specimens which melt at 131°). After the decolorisation of total half-hydrogenated products with active carbon, reduction was continued and tetrahydroipomoeamarone semicarbazone was obtained after the absorption of another molecule of hydrogen.

Reduction of Ipomoeamarone with Sodium and Alcohol; Ipomoeamarol.—Five grams of crude ipomoeamarone was reduced with 5 g. of sodium and 100 cc. of alcohol. The product, which boiled at 162°/9 mm. (3.33 g.), was a pale yellow oil, having a bitter taste, hardly ever colorised with sodium nitroprusside, and decolorised $KMnO_4$ at once.

A 0.3 g. portion of the substance in 10 cc of benzene was refluxed with 0.5 g. of 3, 5-dinitrobenzoyl chloride and a few drops of pyridine on the water bath for half an hour. 3, 5-Dinitrobenzoyl ester (0.44 g.), thus obtained, was a very viscous oil and did not crystallise.

To 0.4 g. of the liquid ester, a solution of 0.2 g. of α-naphthylamine in 80% alcohol was added. Addition products of α-naphthylamine were separated, m.p. 107-9°, dark-red crystals, but could not be purified because of their unstability.

Ipomoeamarol (0.85 g.) in alcohol was hydrogenated with 0.50 g. of Pd-$BaSO_4$. About 3 mols (228 cc.) of hydrogen was absorbed during ten hours. The pale yellow oil obtained, did not produce any crystalline derivatives.

Analysis of the Active Hydrogen by Zerewitinoff-Fraschenträger Method.—By the analysis, ipomoeamarone, regenerated from the semicarbazone, showed absence of active hydrogen.

111.6 mg. of substance; 0.02 cc. of CH_4 (15°, 759 mm.). Calcurated for one active hydrogen; 10.00 cc.

Oxidation of Ipomoeamarone with Potassium Permanganate at Room Temperature.—A 1.8 g. portion of ipomoeamarone, which was regenerated from the semicarbazone, was suspended in 50 cc. of water. Small portions of powdered $KMnO_4$ were added to the mixture successively under shaking and occassional cooling with water. Four and a quarter grams (8.55 atoms of oxygen) of $KMnO_4$ were required. Manganese dioxide was removed by filtration and washed with hot water. There were no neutral substances in the oxidised solution. Then, after this solution was concentrated, it was acidified with dilute sulfuric acid, and was distilled with steam. The distillate required only a small amount of aqueous alkali by titration. The non-volatile part was, then, extracted with ether. The extract (1.06 g.) was a brown viscous oil, and gave ketonic reaction with sodium nitroprusside. By distillation under 4.5 mm. (bath temp. 145-190°), 0.45 g. of the oil was obtained, which gave neither semicarbazone, nor 2, 4-dinitrophenylhydrazone, showed negative iodoform reaction, and was with difficulty soluble in cold water. Three months later, the crystals grew in the oil. After five months, large crystals were picked up and washed with ether. This was proved to be oxalic acid (m.p. 98°) by mixed melting point determination and analysis. (*Anal.* Found: C, 20.17; 19.95; H, 5.21, 5.12%. Calc. for $C_2H_2O_4 \cdot 2H_2O$: C, 19.05; H, 4.76%.)

The liquid acid, separated from oxalic acid, was redistilled under 5 mm. (167-180° bath temp.). It gave ketonic reaction with sodium nitroprusside. For this liquid keto-acid, I suggest the name ceratonic acid. This will be discussed in my next report.

Oxidation of Ipomoeamarone Semicarbazone with Potassium Permanganate at 100°.—Five grams of the semicarbazone was suspended in 100 cc. of boiling water. Small portions of powdered $KMnO_4$ were added successively. During the operation, vapor from the top of the reflux condenser was lead to the solution of 2, 4-dinitrophenylhydrazine (mixture of 0.5 g. of 2, 4-dinitrophenylhydrazine, 2.0 cc. of H_2SO_4, and 20 cc. of alcohol). About 43 g. (25 atoms of oxygen) of $KMnO_4$ were required. From the solution of 2, 4-dinitrophenylhydrazine orange-yellow crystals were isolated. This, after several recrystallisations from alcohol, was proved to be acetone 2, 4-dinitrophenylhydrazone (m.p. 127°) through mixed melting point determination and analysis. (*Anal.* Found: C, 45.76, 45.70; H, 4.08, 4.39; N, 23.57, 23.75%. Calc. for $C_9H_{10}O_4N_4$: C, 45.38; H, 4.20; N, 23.53%.)

From the oxidised solution, no other neutral product was isolated except a small amount of the recovered semicarbazone (m.p. 129°). As to volatile acid, acetic acid was caught as the *p*-bromophenacyl ester (m.p. 82°) and proved by mixed melting point determination and analysis. (*Anal.* Found: C, 46.73, 46.41; H, 3.68, 3.41%. Calc. for $C_{10}H_9O_3Br$: C, 46.69; H, 3.50%.) As to non-volatile acid, crystalline and liquid acids were obtained by ether extraction. The former was proved to be oxalic acid through mixed melting point determination and analysis. (*Anal.* Found: C, 19.59, 19.47; H, 4.87, 5.39%. Calc. for $C_2H_2O_4 \cdot 2H_2O$: C, 19.05; H, 4.76%.) The latter was distilled under 6 mm. (bath temp. 170–200°). The pale yellow oil gave negative reaction with sodium nitroprusside.

Summary

Ipomoeamarone is an open-chain ketone with two oxide rings and two ethylenic linkages. It gives a liquid keto-acid and oxalic acid by oxidation with potassium permanganate at room temperature, and acetone, acetic acid, oxalic acid and a liquid acid by oxidation with the same reagent at 100°.

I wish to express my sincere gratitude to Dr. M. Ohno for his guidance and to Dr. M. Matsui for his helpful advice given to me during the research. I also express my hearty thanks to Mr. T. Takeuchi, Miss M. Toyao and other members of Osaka Factory of Nisshin Chemical Co. for their helpfulness and friendship which facilitated my work.

Takei Laboratory, Insitute for Chemical Research, Kyoto University, and Osaka Factory of Nisshin Chemical Co.

LETTER

X-Ray Investigation of Trimethylacetic Acid Crystal

By Yoshiyuki NAMBA and Tsutom ODA

(Received April 30, 1952)

Timmermans[1] elucidated that trimethylacetic acid (pivalic acid) crystal possesses a very small entropy of fusion, 2.6 e.u./mole, and is an example of the organic plastic crystals so called by him. Hence, we have now carried out an X-ray investigation of this crystal in order to amplify our knowledge on the structures of such plastic crystals as cubic pentaerythritol,[2] tetranitromethane,[3] cyclohexane,[4] cyclohexanol[5] and hexachloroethane.[6]

The present material was prepared by the method of Puntambeker and Zoellner[7] and the product was subjected to fractional recrystallization and distillation, m. p. 33—34°. Samples of this compound were sealed in thin-walled glass capillary tubes and the single crystals were grown from the liquid by slow cooling of the tubes previously warmed to 40°. Rotation and oscillation photographs were obtained with these crystals using Cu

(1) J. Timmermans, *J. chim. phys*, **35**, 331 (1938).
(2) I. Nitta and T. Watanabé, This Bulletin, **13**, 28 (1938).
(3) T. Oda, T. Iida and I. Nitta, *J. Chem. Soc. Japan*, **64**, 616 (1943); T. Oda and T. Watanabé, *ibid.*, **65**, 154 (1944); T. Oda and I. Nitta, *ibid.*, **65**, 621 (1944); T. Oda and T. Matsubara, *X-Rays*, **6**, 27 (1950).
(4) T Oda, *ibid.*, **5**, 26 (1948).
(5) T. Oda, *ibid.*, **4**, No. 4, 2 (1945); *ibid.*, **5**, 95 (1949).
(6) M. Atoji, T. Oda and T. Watanabe, The 2nd Congress of the International Union of Crystallography (1951).
(7) S. V. Puntambeker and E. A. Zoellner, "Organic Syntheses", Coll. Vol. I, A. H. Blatt, Ed., John Wiley and Sons, Inc., New York, N. Y., 1947, p. 524.

radiations. From the results it was found that the crystal conforms to a face-centered cubic lattice, containing four molecules of $(CH_3)_3CCO_2H$ in the unit cell with the edge $a=8.82$ A. The calculated density is 0.98, which is reasonable in comparison with values extraporated from the known[8] densities of the liquid. The space group is T^2–$F2_13$, T^3_h–$Fm3$, T^2_d–$F\bar{4}3m$, O^3–$F43$ or most probably O^5_h–$Fm3m$. From the symmetry consideration it is shown that the molecules arranged at 0, 0, 0; 0, 1/2, 1/2; 1/2, 0, 1/2; 1/2, 1/2, 0 take either orientational or rotational disorder.

Such structure is seen to be in harmony with the extraordinarily rapid decrease of the intensities for increasing angle of scattering. On the other side, on several Laue photographs there appeared intense diffuse spots such as accompanied by {111} and {200}. These results are quite in resemblance to certain cases[2],[4],[5] of the above examples and those of *t*-butyl chloride, *t*-butyl bromide and neohexane recently published by Schwartz, Post and Fankuchen.[9]

It may be added that we have confirmed optically that the isotropic[8] crystals transform at about −2° to small birefringent needles. The transition may be due to cessation of the molecular rotation.

This investigation is aided by the Scientific Research Encouragement Grant from the Ministry of Education to which the authors' thanks are due. We are also indebted to the interest and helpful suggestions of Professors Isamu Nitta and Tokunosuké Watanabé of Osaka University.

Chemical Laboratory Osaka Liberal Arts University, Osaka

(8) A. Butlerow, *Ann.*, **173**, 355 (1874).

(9) R. S. Schwartz, B. Post and I. Fankuchen, *J. Am. Chem. Soc.*, **73**, 4490 (1951); *ibid.*, **73**, 5113 (1951). See also *ibid.*, **69**., 2502 (1947).

New Colorimetric Determination of Chloride using Mercuric Thiocyanate and Ferric Ion[1]

By Iwaji IWASAKI, Satori UTSUMI and Takejiro OZAWA

(Received April 22, 1952)

A new colorimetric method for the determination of low concentrations of chloride using slightly dissociating mercuric thiocyanate and ferric ion is mainly based on the following reactions:

$$2Cl^- + Hg(CNS)_2 \rightleftharpoons HgCl_2 + 2CNS^-$$
$$4Cl^- + Hg(CNS)_2 \rightleftharpoons HgCl_4^{--} + 2CNS^-$$
$$CNS^- + Fe^{+++} \rightleftharpoons Fe(CNS)^{++}$$

The orange color of ferric thiocyanate formed in the solution is determined colorimetrically.

Reagents:

A series of standard potassium chloride solutions containing 0.2, 0.5 ppm., 1 to 10 ppm. with differences of 1 ppm. and 10 to 20 ppm. with differences of 2 ppm., of chloride is prepared.

Mercuric thiocyanate solution is prepared by dissolving 0.3 g. of mercuric thiocyanate in 100 cc. of 95% ethyl alcohol.

Ferric alum solution is prepared by dissolving 6 g. of ferric ammonium sulfate in 100 cc. of 6 N nitric acid.

Procedure:

Ten cc. of the sample solution and 10 cc. of standard chloride solution are poured into the matched test tubes with stopper. Then 1.0 cc. of mercuric thiocyanate solution and 2.0 cc. of ferric alum solution are added to each solution. Comparisons are carried out after ten minutes from mixing. It is better to observe the colors from above against a white background.

Interfering substances are: bromide, iodide, cyanide, thiosulfate, and nitrite.

Results:

The lowest concentration of the standard solution whose color can be easily distinguished from that of the blank test, is 0.05 ppm. Cl^-. Therefore this is the minimum determinable concentration. However this colorimetric method is applied with best results in the concentration range of 0.1-20 ppm. of chloride. The colored solution has an absorption maximum at 460 mμ and its orange color is stable for several hours. The colored substance is not extracted with organic solvents such as ether or amyl alcohol.[2]

Table 1

Present. Cl^-	0.3	0.5	1.0	5.0	10.0	15.0 ppm.
Found. Cl^-	0.3	0.5	1.1	5.0	10.0	15.5 ppm.

There are excellent agreements.

This rapid and simple colorimetric method for the determination of low concentrations of chloride can be widely applied to the detrmination of chloride in water, rocks etc.

Laboratory of Analytical Chemistry and Geochemistry, Tokyo Institute of Technology, Tokyo

(1) This report was presented at the 5th annual Meeting of the Chem. Soc. Japan, April, 1952.

(2) Reported by I. Iwasaki and H. Shimojima at the 5th annual Meeting of the Chem. Soc. Japan, April, 1952.

Equilibrium of the CO_2-NH_3-Urea-H_2O System under High Temperature and Pressure. II. Liquid-Vapor Equilibrium in the Loading Mole Ratio of $2NH_3$ to CO_2[1]

By Schōhachi KAWASUMI

(Received December 17, 1951)

It is an established experimental fact that the yield of urea in urea-synthesis from ammonia and carbon dioxide depends upon the loading density or ratio of the weights of the materials to the total volume of the reaction vessel at a given temperature. The writer showed in the previous paper[2] that the equilibrium pressure as well as the urea-yield is a fnnction of the loading density at a given temperature, and explained that the diversity of the equilibrium pressure is based upon that of the equilibrium composition of the liquid and vapor phase.

The object of the present paper is to show the relations within the equilibrium composition of the liquid and vapor phase, the loading density and the temperature, by analysing the composition of the two phases under high temperature and pressure. For this purpose the vapor composition, or mole ratios of ammonia, carbon dioxide and water in the vapor-phase, the liquid composition, or mole ratio of unconverted ammonia to carbon dioxide in the liquid-phase, the converted amount to urea, and liquid-vapor volume ratio have been determined respectively by the following analytical methods in the loading mole ratio of 2 ammonia to 1 carbon dioxide.

The liquid- and vapor-phase compositions in the equilibrium state of the system have been calculated from these data. From these results the effects of the loading density and the temperature respectively on the calculated equilibrium compositions and the equilibrium constant of the following reaction have been discussed.

$$CO_2+2NH_3 \rightleftarrows CO(NH_2)_2+H_2O \qquad (1)$$

Experimental Procedure

Method of Determining the Vapor Compositions.—It is concluded that the reaction in urea-synthesis from ammonia and carbon dioxide takes place in the liquid phase, with which the vapor phase composed of CO_2, NH_3 and H_2O is in a state of equilibrium in the reaction vessel. The writer investigated the mole ratio of CO_2, NH_3 and H_2O is in a state of equilibrium in the reaction vessel. The writer investigated the mole ratio of CO_2, NH_3 and H_2O in the vapor phase by the following method.

(1). **Experimental Apparatus.**— The experimental apparatus consists of the reaction vessel (A), vapor holder (B), and gas-analyzing apparatus (C) as shown in Fig. 1. A is just the same as the apparatus used for pressure measurement reported in the previous paper[2]. The vapor and liquid were kept in a state of equilibrium in the reaction vessel (A-3). The readings of equilibrium pressure by the pressure gauge (A-2) became constant after 5 to 6 hours at such a high temperature as 160°C. The gas sample was withdrawn from the vapor phase after 20 hours of being in a state of equilibrium. The vapor-holder (B) is a bottle of 3 liter capacity (B-1), which is dipped in the thermo-regulated water bath at 90°C. and provided with a mercury-dropping apparatus. A part of the vapor in A-3 which is under high temperature and pressure is discharged into B-1 at the state of 90°C. and 1 atm. The gas-analyzing apparatus (C) consists of a washing bottle of 1 normal sulphuric acid aqueous solution (C-1), which is kept in the thermostat at 70°C., U-tubes with calcium chloride (C-2 and C-4) and kali-bulb (C-3). The mole ratio of CO_2, NH_3 and H_2O in the vapor was analyzed, sending the vapor in B-1 through this apparatus (C) gradually.

(2). **Procedure of Vapor Sampling.**—After heating the reaction vessel at a given temperature for 20 hours, the vapor in a state of equilibrium with the liquid was gently withdrawn through a 4 mm. high pressure valve (A-1) into a previously evacuated vapor-holder (B-1), which had been kept at the constant temperature of 90°C. to avoid the condensation of ammonium carbamate. To keep the condition of equilibrium between the vapor and the liquid in A-3, the valve (A-1) was adjusted by the reading of mercury head in a closed mercury manometer (B-6).

The sampling procedure through the valve (A-1) as described above—a method to get a gas sample at 90°C. and at the ordinary pressure—is the most

(1) A part of this paper was presented at the annual meeting of the Chemical Society of Japan held at Tokyo, on 6 April 1951.

(2) S. Kawasumi, This Bulletin, **24**, 148 (1951).

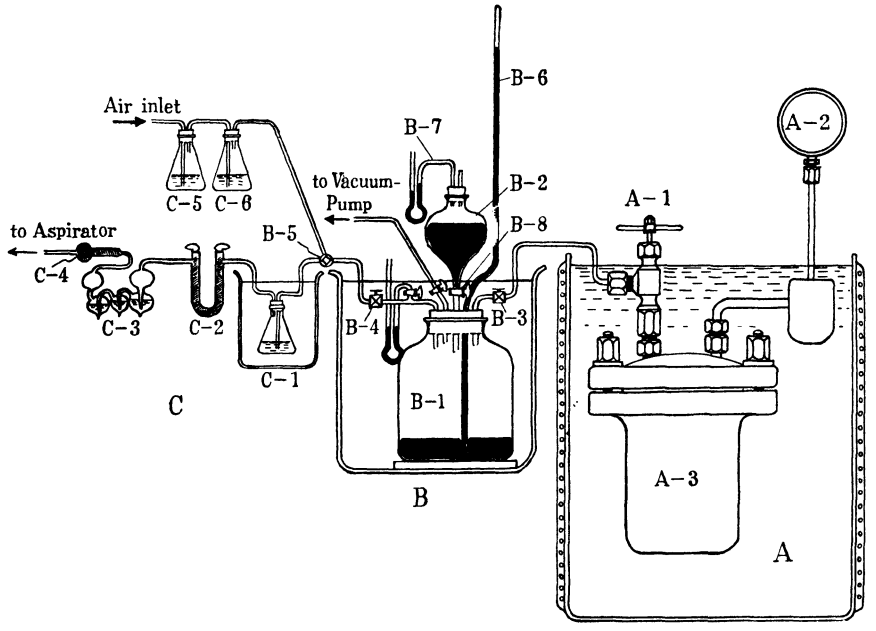

Fig. 1. –Apparatus for measuring the vapor compositions.

important. When the pressure of B-1 reached about 760 mmHg, the valve (A-1) and a screw-cock (B-3) were closed. At the temperature of 160°C. and the equilibrium pressure 70 to 150 kg./cm.^{2}, the readings of pressure drop were constantly between 5 and 7 kg./cm^2. The pipe between A-1 and B-3 which is exposed in the air, was heated to more than 70°C. by gas heating in order to avoid the condensation of the ammonium carbamate while withdrawing the vapor.

(3). **Determination of Mole Ratios of CO_2, NH_3 and H_2O.**—After the vapor was withdrawn, the vapor in B-1 was sent into an analyzing apparatus (C) at the constant velocity by dropping mercury in B-2 into B-1. The dropping velocity of mercury was regulated by a cock (B-8) according to pressure difference of a manometer (B-7). The dropping rate of mercury at each time was regulated on the average to about 40 cc. per minute. Ammonia was absorbed in C-1, water vapor in C-2 and C-4, and carbon dioxide in C-3. After the mercury-dropping procedure was finished, ammonia, carbon dioxide and water vapor in the dead space of C were completely driven into the absorbers by sending air which was introduced after being washed by concentrated KOH solution (C-5) and H_2SO_4 solution (C-6), by manipulating a three-way cock (B-5).

After the gas-absorbing procedure was finished, the four apparatuses C-1, C-2, C-3 and C-4 were weighed to obtain their increments. The increments of the kali-bulb (C-3) is the amount of carbon dioxide absorbed. And the amount of ammonia absorbed was found by titrating the solution in C-1 with 1-N NaOH solution. The amount of water vapor absorbed in C is the difference between the sum of the increments of both C-1 and C-2 and the absorbed amount of ammonia. In one gas-sampling procedure, the average value of the gas-analysis of two or three times was taken by dividing the sample in B-1 into two or three parts.

C-1 was kept at the constant temperature of 70°C. to minimize the absorption or solution of carbon dioxide into the dilute H_2SO_4 solution (C-1). The writer examined the analytical error which happened by the absorption or solution of carbon dioxide in the preliminary experiment, in which C-1 was kept over the temperature range 10 to 80°C. The amount of carbon dioxide absorbed in the kali-bulb (C-3) was measured by sending the decomposition gas which had been generated by heating 0.50 g. (0.00641 Mole) of ammonium carbamate, into the apparatus (C). The amount of N/2 H_2SO_4 solution in C-1 was 130 cc. The experimental results showed that the temperature of C-1 has to be kept at 70 to 80°C. by all means.

(4) **Accuracy of analysis.**—The above-mentioned analysis requires skill in the procedure, especially in the quantitative analysis of water vapor, or else the error becomes larger. It was confirmed by analyzing samples of known composition that the experimental error of this analytical procedure was less than 1 % in ammonia, but about 3 to 5 % in carbon dioxide and water vapor respectively. Obviously in most cases, carbon dioxide shows a tendency to negative error and water vapor to positive error.

Method of Determining Liquid Compositions.—A liquid sample which had been withdrawn from the equilibrium vessel under high temperature and pressure was analyzed by the following

procedure to study the mole ratio of the unconverted ammonia to carbon dioxide in it.

(1). **Experimental Apparatus.**—The experimental apparatus consists of the equilibrium vessel of the urea-synthesis reaction (A) and of the apparatus of withdrawing the liquid sample (B) as given in Fig. 2. A is just the same as the

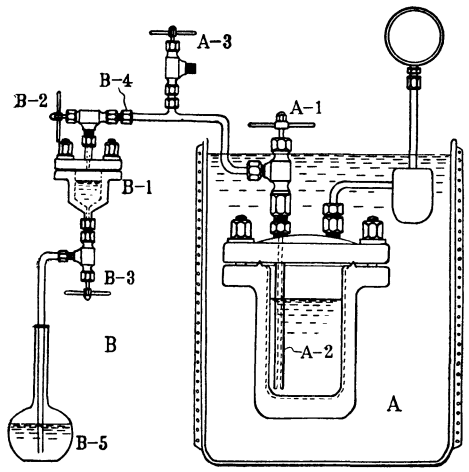

Fig. 2.—Apparatus for measuring the liquid compositions.

apparatus used for the pressure measurement described in the previous paper[2], with the exception that the cover of the equilibrium vessel is fitted with a lead pipe (A-2) of inner diameter 3 mm., outer diameter 10 mm. and length 12 cm. to discharge the liquid through the high pressure valve (A-1). B-1 is a high pressure vessel of capacity 56 cc. made of stainless steel and provided with two high pressure valves (B-2 and B-3), employed for introducing and withdrawing the liquid sample respectively, since the liquid discharged into B-1 exerts more than atmospheric pressure even at the ordinary temperature.

(2) **Procedure of Sampling.**—The procedure of withdrawing the liquid sample is more difficult than that of the sampling of vapor. The least analysable quantity of the liquid sample must be withdrawn without disturbing the liquid-vapor equilibrium by the opening of the valve (A-1), and it must be accomplished as quickly as possible, since a slow manipulation will bring about the vaporisation of the liquid through the valve (A-1). Moreover, the liquid in B-1 at the ordinary temperature is solidified too readily to be discharged from B-1. But these difficulties were nearly overcome by the following method. After the contents of the reaction vessel (A) had arrived at a condition of equilibrium at a given temperature, a very small liquid sample was expelled through the two valves (A-1 and A-3), and then the liquid was driven into B-1 through the two valves (A-1 and B-2) and the steel pipe between A-1 and B-2. This steel pipe had previously been heated at 80 to 100°C. by gas heating. A suitable amount of water had previously been charged in B-1 in order to prevent the solidification of the liquid sample. The amount of the liquid sample could be regulated by the amount of water in B-1. Under a condition of the equilibrium vessel at 160°C. and 90 kg./cm^2., for example, the pressure falls to 85 kg./cm^2. by the withdrawal of the liquid sample, but recovers and rises again after a while. After B had been separated from A by disconnecting the nut (B-4), B-1 was intensely shaken to make the contents in it homogeneous, and then by opening the valve (B-3) gently, the aqueous solution in B-1 was discharged into a measuring flask (B-5) of capacity 500 cc., in which some water had previously been charged to catch even a small amount of the vapor from the solution. By pouring the washing water into B-1 through the valve (B-2), the sample in B-1 was completely washed out to make the total amount of the sample 500 cc.

(3). **Determination of the Mole Ratio of Ammonia to Carbon Dioxide.**—The mole ratio of ammonia to carbon dioxide in the aqueous solution withdrawn by such a method as stated above was determined by the following method. An aliquot portion (50 cc.) of the sample 500 cc. was taken for determination of the unconverted ammonia by titration with 1-N sulphuric acid. Unconverted carbon dioxide in the sample was analyzed in an apparatus as shown in Fig. 3.

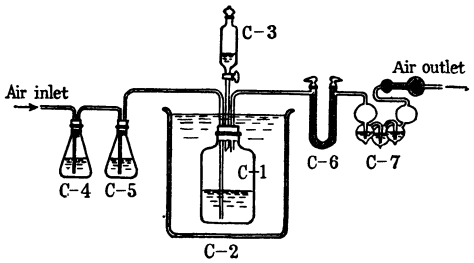

Fig. 3.—Apparatus for determination of carbon dioxide.

The other aliquot portion (50 cc.) was taken into a bottle (C-1), together with a few drops of methyl-orange as the indicator. Carbon dioxide generated by dropping concentrated sulphuric acid from a funnel (C-3) after the bottle (C-1) was immersed into a thermostat (C-2) at 70°C., was absorbed in potassium hydroxide solution (C-7) through a U-tube with calcium chloride (C-6). The dropping of sulphuric acid was continued until the color of the indicator in C-1 changed. After the generation of carbon dioxide had ended, carbon dioxide in the dead space was completely made to absorb in C-7 by sending air refined through concentrated potassium hydroxide solution (C-4) and sulphuric acid (C-5) by means of an aspirator. The increment of kali-bulb (C-7) is equal to the amount of carbon dioxide absorbed. Each sample was analyzed three times and the mean value was taken.

(4). **Accuracy of Analysis.**—At the above

method of analysis, though the excess addition of sulphuric acid for the generation of carbon dioxide after the neutralisation was reached, should result in a hydrolysis of urea and a consequent increase in the analytical value of carbon dioxide, an experiment showed that even when 50 cc. more sulpburic acid than necessary for the neutralisation was used, the value of carbon dioxide was only 0.15 % higher than theoretical. Therefore, it has become evident that the above method is not made invalid by the reaction of urea-decomposition.

Experimental Results

Relation between Vapor Composition and Loading Density.—As mentioned in detail in the previous paper[2], the equilibrium pressure of the urea-synthesis reaction greatly depends upon the loading density, that is to say, the former increases with the latter at a given temperature under a condition in which the loading mole ratio of carbon dioxide to ammonia is one by two. It is an important problem to clear up how the vapor composition depends upon the loading density in this case. The writer studied the relation between the vapor composition and the loading density at 160°C.

The experimental results showed that the mole ratio of ammonia to carbon dioxide in the vapor is less than two at each loading density, and the more loading density increases, the richer the carbon dioxide in the vapor composition becomes,

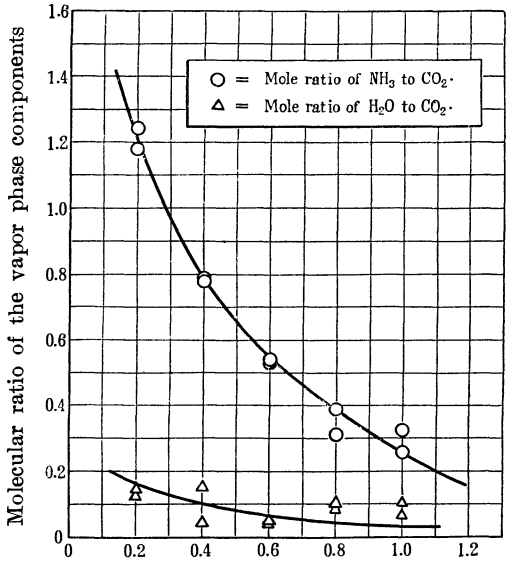

Fig. 4.—Relation between the vapor composition and the loading density at 160°C.

as shown in Fig. 4. Therefore, it is clear that the equilibrium pressure increases with the loading density, as the increase of the loading density accompanies at the same time the increase of carbon dioxide content in the vapor phase. These experimental results are based on the fact that the solubility of ammonia into the liquid phase is more than that of carbon dioxide. Moreover, the experimental results showed that the measured mole ratio of water to carbon dioxide in the vapor,—though there exists a very small quantity of water vapor—, is nearly within the range of 0.03 to 0.16.

Relation between Vapor Composition and Temperature.—The equilibrium pressure rises with temperature at a constant loading density as explained in the previous paper.[2] At the same time, it is expected in this case that the vapor composition undergoes a change with the change in temperature. The result of the experiments in which the vapor composition was measured at the loading density 0.60 g./cc. and over the temperature range of 140 to 180°C., is shown in Fig. 5. The observed mole ratio of ammonia to carbon

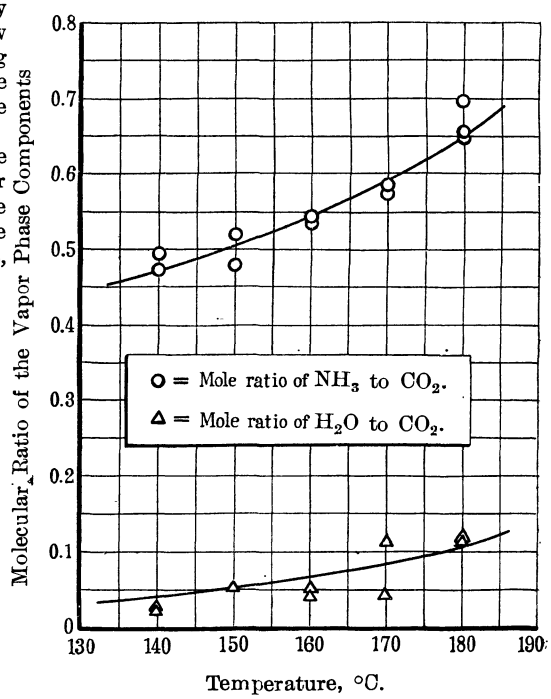

Fig. 5.—Relation between the vapor composition and the temperature at a loading density of 0.60 g./cc.

dioxide ranges from 0.47 to 0.65 under this condition and the vapor composition becomes richer in ammonia with the rise of temperature. The relation between the mole ratio of carbon dioxide to ammonia and temperature is nearly linear within the range of the experiments. Mole ratio of water to carbon dioxide ranges from 0.02 to 0.12.

Relation between Liquid Composition and Loading Density.—The effect of the variation of

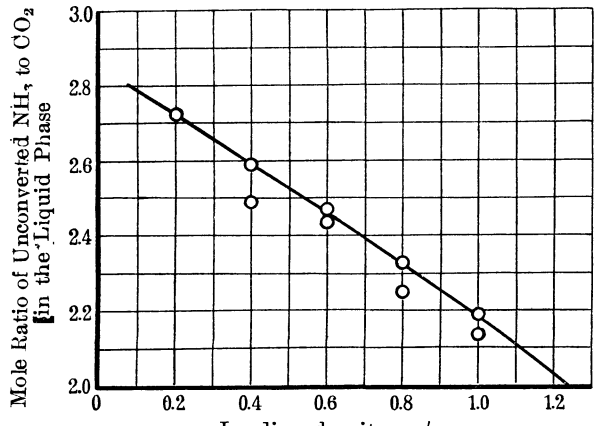

Fig. 6.—Relation between the liquid composition and the loading density at 160°C.

the loading density on the mole ratio of ammonia to carbon dioxide in the liquid phase which is in equilibrium with the vapor was studied at 160°C. and the loading densities of 0.20 to 1.00 g./cc. The experimental results are shown in Fig. 6. The mole ratio of ammonia to carbon dioxide increases from 2.18 to 2.72 within the range of the experiments; thus the liquid composition becomes richer in ammonia, with decrease of the loading density. This is closely connected with the facts that the vapor composition becomes richer in ammonia as described above and the yield of urea decreases, with decrease of the loading density. The point where the curve intersects the abscissa in Fig. 6 is nothing but the loading density where the mole ratio of ammonia to carbon dioxide in the liquid phase becomes equal to the loading mole ratio, or where the equilibrium vessel is filled up with only the liquid phase. This loading density is 1.24 g. per cc., being consistent with the maximum loading density which will be derived from the relation between the ratio of liquid volume to vessel volume and the loading density in the following section of this paper.

Relation between Liquid Composition and Temperature.—The effect of the change in temperature on the mole ratio of ammonia to carbon dioxide in the liquid phase was studied at the loading density 0.60 g./cc. and over the temperature range of 140 to 180°C. The experimental results are shown in Fig. 7. The mole ratio of unconverted ammonia to carbon dioxide increases from 2.26 to 2.67 within the range of the experiments; thus the liquid composition becomes richer in ammonia, with the rise of temperature. The mole ratio in the liquid composition is approximately a linear function of the temperature as shown in Fig. 7. This line intersects the abscissa at about 115°C. and this point is nothing but the temperature where the mole ratio of ammonia to carbon dioxide in the liquid phase becomes equal to the loading mole ratio, or the transition temperature, where the content in the equilibrium vessel undergoes a change from the solid- to the liquid-phase reaction. This transition temperature has been fully investigated by Kitawaki, Hori and Shimoda.[3] According to their investigations, a junction of the decomposition pressure-temperature curve of solid ammonium carbamate and the equilibrium pressure-temperature curve of the mixed solution of the CO_2-NH_3-Urea-H_2O system was 114.6°C., being consistent with the transition temperature from the solid- to the liquid-phase reaction, where a discontinuous point appears, in a plot of the yield of urea against the temperature, as shown in Fig. 8.

Relation among Urea-Yield, Loading Density and Temperature.—Fichter and Becker[4] discovered in 1911 that the

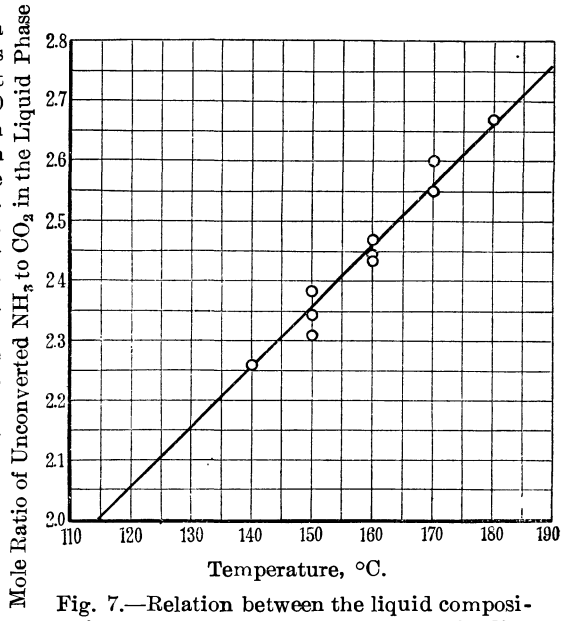

Fig. 7.—Relation between the liquid composition and the temperature at a loading density of 0.60 g./cc.

equilibrium yield of urea increaes with the loading density at a given temperature. Thereafter, the effect of the loading density on the equilibrium yield of urea was studied by Clark, Gaddy and Rist,[5] and M. Tokuoka,[6] the former specially studied the effect at such a higher loading density as 1.0 g./cc. over the temperature range of 135 to 200°C. The writer also studied the relation between the equilibrium yield of urea

(3) Kitawaki, Hori and Shimoda, *Bull. Gov. Chem. Ind. Res. Inst. Tokyo*, **32**, No. 6 and 10 (1937).
(4) Fichter and Becker, *Ber.*, **44**, 3473 (1911).
(5) Clark, Gaddy and Rist, *Ind. Eng. Chem.*, **25**, 1092 (1933).
(6) M. Tokuoka, *J. Agr. Chem. Soc. Japan*, **10**, 1333 (1934); *ibid.*, **11**, 107 (1935); *ibid.*, **11**, 174 (1935).

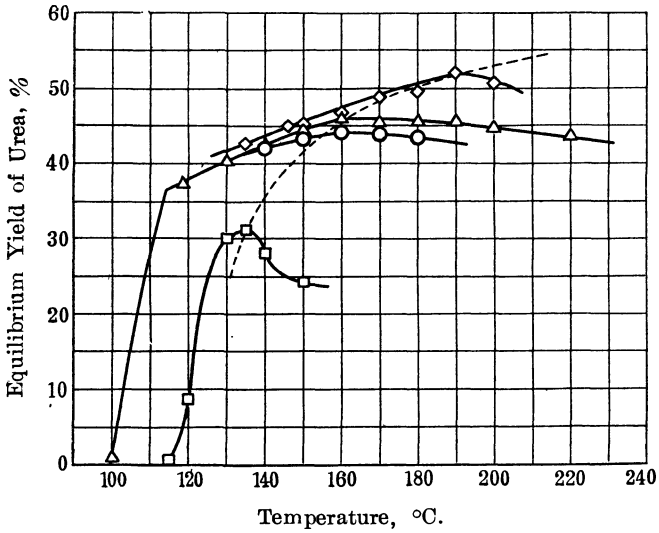

Fig. 8.—Relation between the yield of urea and the temperature.

Symbol	Loading density, g./cc.	Investigator
◇	1.00	Clark, Gaddy and Rist[5]
△	0.65	Kitawaki, Hori and Shimoda[3]
○	0.60	Present Measurement
□	0.11	Fichter and Becker[4]

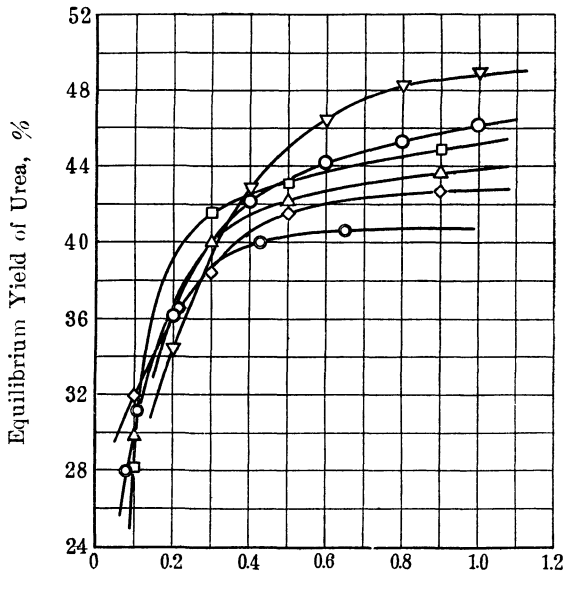

Fig. 9.—Relation between the yield of urea and the loading density.

Symbol	Temp. °C.	Investigator
▽	170	Clark, Gaddy and Rist[5]
○	160	Present Measurement
□	150	M. Tokuoka[6]
△	145	
◇	140	
◎	135	Fichter and Becker[4]

and the loading density at 160°C., in order to calculate the liquid- and the vapor-phase compositions in a state of equilibrium. Experimental results showed that the average yields of urea are 36.2, 42.2, 44.2, 45.3, and 46.2 % at the loading densities 0.20, 0.40, 0.60, 0.80, and 1.0 g./cc., respectively. The data cited above are shown graphically in Fig. 9.

In general it had been thought that the yield of urea increases with the rise of temperature at a given loading density, but Fichter, and Becker[4] showed that the yield of urea at a loading density of 0.11 g./cc. attains to the maximum at 135°C. Thereafter, the maximum yields of urea were experimentally shown at about 160°C. and 0.65 g./cc. by Kitawaki, Hori and Shimoda,[3] and at about 190°C. and 1.0 g./cc. by Clark, Gaddy and Rist,[5] respectively, as given in Fig. 8. The writer also studied the effect of the temperature on the equilibrium yield of urea at a loading density of 0.60 g./cc. Experimental results showed that the average yields of urea are 42.1, 43.3, 44.2, 44.0, and 43.5 % at 140°, 150°, 160°, 170°, and 180°C., respectively. Clark and others[5] explained that the lower yield of urea obtained above 190°C. may be attributed to the complications introduced by the more active corrosion of the reactor and to the increased tendency for the thermal dissociation of urea and the catalytic cracking of ammonia. However, the reason why these experiments showed increasing conversion of ammonium carbamate into urea with temperature up to the maximum at a given loading density, must essentially be attributed to the inevitable relations among the urea-yield, the loading density and the temperature, which result from the liquid- and the vapor-phase equilibrium of the CO_2-NH_3-Urea-H_2O system. Evidently, according to the data cited above, the temperatures where the equilibrium yield of urea attains to the maximum, rise with the increase of the loading density, drawing such a locus as a dotted line shown in Fig. 8.

In Fig. 10 which is a schematic expression of Fig. 9, it can readily be understood that the urea-yield Y_1 at the temperature T_1 is less than Y_2 at the lower temperature

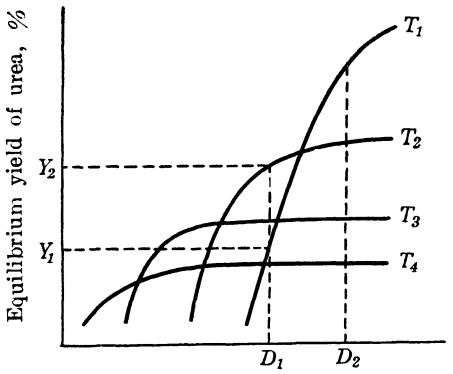

Fig. 10.—Schematic diagram of relation among the yield of urea, the loading density and the temperature.

Photo. 1

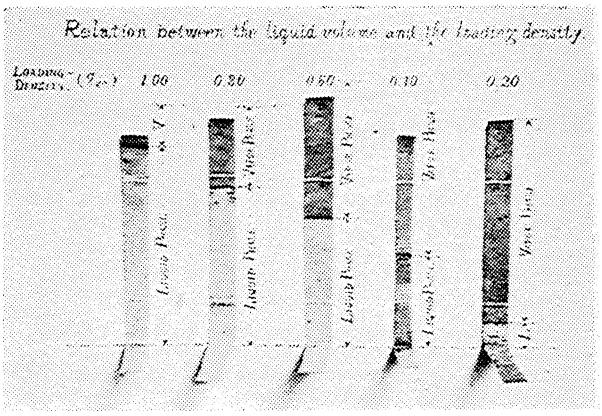

T_2, and Y_2 is the maximum urea-yield at a given loading density of D_1. Therefore we must raise the temperature and increase the loading density at the same time in order to increase the yield of urea. It is because of the decrease of vapor-phase volume, or of the incrase of ratio of the liquid-phase weight to the initial loading weight, that the yields of urea increase, with the increase of the loading density at a given temperature, as pointed out by Matignon and Fréjacques.[7] Krase and Gaddy[8] have also explained that since the equilibrium is established in the liquid phase and presumably only a negligible amount, if any, of urea is in the gaseous phase, the extent of conversion of carbamate to urea is dependent on the ratio of the volumes of liquid and gas phases. Similarly the existence of the maximum yield of urea in a plot of the yield against the temperature at a given loading density is attributable to the circumstances; while the conversion of ammonium carbamate to urea in the liquid phase increases, the quantity of liquid phase itself decreases with the rise of temperature. Ultimately the reason why such relations as shown in Fig. 10 arise among the urea-yield, the loading density and the temperature, must be accounted for by the fact that the equilibrium yields of urea depend not only upon the equilibrium of the reaction of urea-synthesis in the liquid-phase, but also upon the liquid- and vapor-phase equilibrium.

Volume-Ratio of Vapor- to Liquid-Phase.—As the equilibrium state between the vapor and liquid in an autoclave under high temperature and pressure is difficult to survey with the naked eyes, the writer tried to measure the volume-ratio of the vapor to the liquid by the following method in order to calculate the vapor- and liquid-density.

In the urea-synthesis reaction from ammonia and carbon dioxide, the corrosive action of the reacting system for the materials of the reaction vessel is so violent, that there appears a distinct corrosive line on the material which corresponds to the boundary of the two phases. Aluminium or 18Cr-8Ni stainless steel of about 20 cm. long, 15 mm. wide and 1 to 2 mm. thick, was bent at right angles as shown in Photo. 1 and inserted into the reaction vessel so that the plate might not move in it. After heating the reaction vessel at a given temperature for about 20 hours, the plate was taken out from the vessel. As shown in Photo. 1, a part of the plate which was dipped in the molten reaction mixture suffered more corrosive action and grew thinner than the other part exposed in the vapor; especially at the boundary of the two phases it suffered a violent corrosion. We can readily determine the volume-ratio of the two phases with about ±1 % error

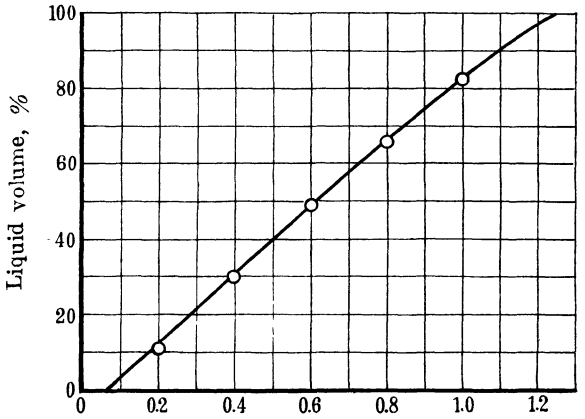

Fig. 11.—Relation between liquid volume and loading density at 160°C.

(7) Matignon and Fréjacques, *Bull. soc. chim.*, **31**, 394 (1922).
(8) Krase and Gaddy, *Ind. Eng. Chem.*, **14**, 611 (1922).

from the plate. The volume of the autoclave is about 750 cc. The data from these experiments concerning the percentage of liquid volume to vessel volume at 160°C. and over the loading density range of 0.2 to 1.0 g./cc., is given in Fig. 11 and Photo. 1. The loading density, in which the liquid volume to the total volume of the autoclave is 100 %, is nothing but the liquid density in the case of the autoclave filled up with the liquid. It will be sought by the extrapolation from Fig. 11 that the maximum loading density is about 1.24 g./cc. at 160°C. which is in good agreement with that which was derived from the relation between the mole ratio of unconverted ammonia to carbon dioxide in the liquid phase and the loading density.

The experimental results on the percentage of liquid volume to vessel volume at the loading density 0.60 g./cc. and over the temperature range of 140 to 180°C. is given in Table 1. The experiments showed that the percentage of liquid volume is nearly constant and independent of the temperature at a given loading density within the experimental error.

Table 1

Relation between Liquid Volume and Temperature at a Loading Density of 0.60 g./cc.

Temp., °C.	Equilibrium pressure, atm.	Leiquid volume to the vessel volume, %
140	52	48.2
150	67	47.1
160	88	48.8
170	115	48.5
180	149	47.5

Discussion of Results

Relation between Equilibrium Composition and Loading Density.—For the purpose of calculating the equilibrium compositions, it is assumed that the system consists of three components, ammonia, carbon dioxide and water, in the vapor phase and of four components, urea, water, unconverted ammonia and carbon dioxide, in the liquid phase, or that there exists neither gaseous- nor melted-ammonium carbamate in the two phases under high temperature and pressure, since it is impossible to measure the amount of ammonium carbamate distinguished from unconverted ammonia or carbon dioxide, although much amount of ammonium carbamate must exist in the liquid phase. In such a case that "c" gram moles of ammonium carbamate (equivalent of "$2c$" moles of ammonia and "c" moles of carbon dioxide) were initially loaded into a reaction vessel of 1 litre volume, we obtain from the material balance respectively;

$$n_{\text{urea}}+n_{CO_2}+n'_{CO_2}=c \tag{2}$$

$$2n_{\text{urea}}+n_{NH_3}+n'_{NH_3}=2c. \tag{3}$$

Let us put,

$$n'_{NH_3}/n'_{CO_2}=R' \tag{4}$$

$$n'_{H_2O}/n'_{CO_2}=S' \tag{5}$$

$$n_{NH_3}/n_{CO_2}=R \tag{6}$$

$$n_{\text{urea}}=cY \tag{7}$$

and

$$n_{H_2O}=n_{\text{urea}}-n'_{H_2O}. \tag{8}$$

From these seven equations (2) to (8), we can derive the following relations (9) to (14) which allow the equilibrium concentration of each component to be calculated.

$$n'_{CO_2}=\frac{c(1-Y)(R-2)}{R-R'} \tag{9}$$

$$n'_{NH_3}=\frac{cR'(1-Y)(R-2)}{R-R'} \tag{10}$$

$$n'_{H_2O}=\frac{cS'(1-Y)(R-2)}{R-R'} \tag{11}$$

$$n_{CO_2}=\frac{c(1-Y)(2-R')}{R-R'} \tag{12}$$

$$n_{NH_3}=\frac{cR(1-Y)(2-R')}{R-R'} \tag{13}$$

$$n_{\text{urea}}=cY \tag{7'}$$

$$n_{H_2O}=c\left\{Y-\frac{S'(1-Y)(R-2)}{R-R'}\right\}. \tag{14}$$

The compositions of the liquid- and vapor phase in the equilibrium state at a temperature of 160°C. and over the loading density range of 0.20 to 1.0 g./cc. are shown in Table 2. The equilibrium constants (K_{N_1}) of the reaction (1) represented by mole fraction (N_i) of each component in the liquid phase $K_{N_1}=\frac{N_{\text{urea}}N_{H_2O}}{N_{CO_2}N^2_{NH_3}}$ are also given in the last line of Table 2. These values of the equilibrium constant at 160°C. are approximately constant, independent of the loading density. A plot of mole fraction x_i of each component in two phases against the loading density is drawn in Fig 12. It is conjectured from Fig. 12 that the equilibrium yields of urea increase at a given temperature because the vapor-phase decreases or the boundary surface between the two phases rises up in the reaction vessel, with increasing loading density.

Effect of Loading Density on Liquid- and Vapor-Density.—The liquid- and vapor-density of the system under high temperature and pressure are given by dividing the weight

Table 2

Effect of Loading Density on Liquid- and Vapor-Phase Compositions in Equilibrium State at 160°C.

D, g./cc.		0.20	0.40	0.60	0.80	1.00
c, mole/l.		2.562	5.123	7.685	10.247	12.808
P, atm.		69	76.5	89	107.5	136.5
R'		1.347	0.816	0.547	0.405	0.325
S'		0.164	0.103	0.066	0.045	0.033
R		2.725	2.590	2.460	2.326	2.180
Y		0.362	0.422	0.442	0.453	0.462
Equilibrium Concentration, mole/l.	n'_{CO_2}	0.859	0.984	1.031	0.951	0.669
	n'_{NH_3}	1.158	0.803	0.564	0.385	0.217
	n'_{H_2O}	0.141	0.102	0.068	0.043	0.022
	n_{CO_2}	0.774	1.975	3.257	4.654	6.222
	n_{NH_3}	2.109	5.115	8.012	10.823	13.563
	n_{urea}	0.928	2.164	3.397	4.642	5.918
	n_{H_2O}	0.787	2.063	3.329	4.599	5.895
Equilibrium mole fraction	N'_{CO_2}	0.398	0.521	0.620	0.690	0.737
	N'_{NH_3}	0.537	0.425	0.339	0.279	0.239
	N'_{H_2O}	0.065	0.054	0.041	0.031	0.024
	N_{CO_2}	0.168	0.175	0.181	0.188	0.197
	N_{NH_3}	0.459	0.452	0.445	0.438	0.429
	N_{urea}	0.202	0.191	0.189	0.188	0.187
	N_{H_2O}	0.171	0.182	0.185	0.186	0.187
K_{N_1}		0.976	0.977	0.974	0.968	0.963

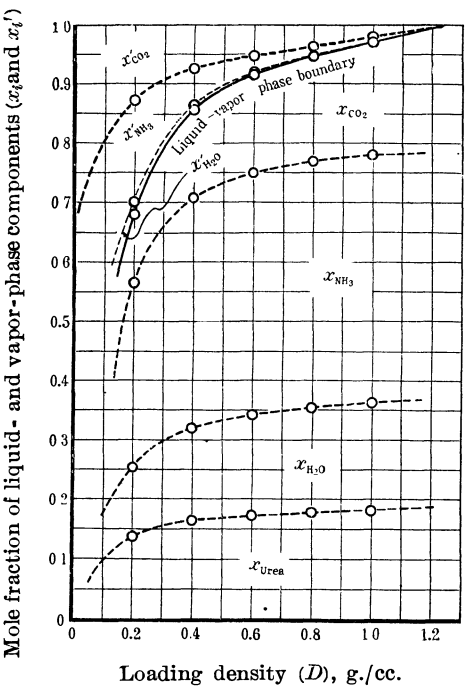

Fig. 12.—Liquid-vapor equilibria diagram of the CO_2-NH_3-Urea-H_2O system at a temperature of 160°C.

of each phase obtained from Table 2 by the liquid- and vapor-volume respectively. The densities (d and d') of the two phases at 160°C. and over the loading density range 0.20 to 1.00 g./cc. increase with the loading density as shown in Fig. 13. The extrapolation of the liquid-density curve in Fig. 13 shows that the liquid density at the maximum loading density of 1.24 g./cc. is identical with the latter. The vapor density (d') is approximately a linear function of the equilibrium pressure as shown in Fig. 14.

Relation between Equilibrium Composition and Temperature.—The results of calculation of the liquid- and vapor-phase compositions in the equilibrium state at a loading density of 0.60 g./cc. and over the temperature range of 140 to 180°C. are shown in Table 3. A plot of mole fraction x_i against the temperature is shown in Fig. 15. It is conjectured from Fig. 15 that the maximum yield of urea in a plot of the yield against the temperature

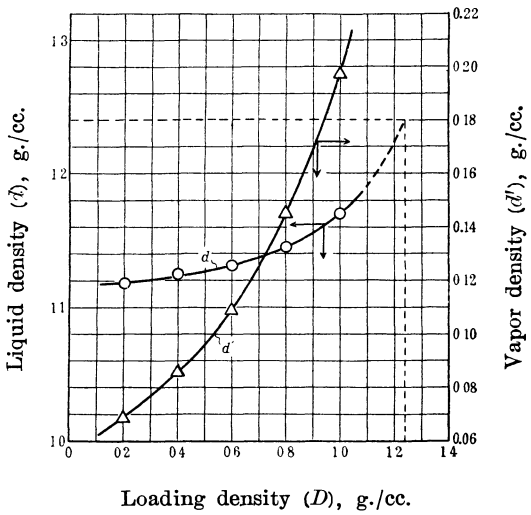

Fig. 13.—Effect of loading density on liquid- and vapor-density at 160°C.

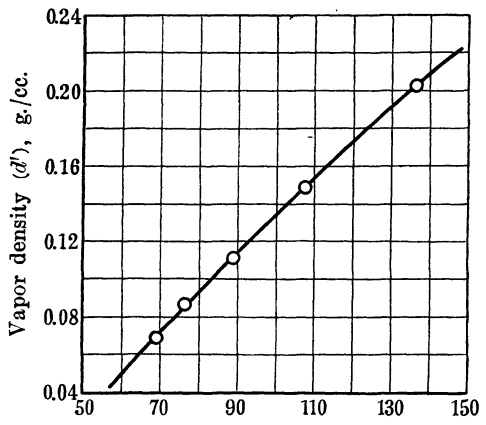

Fig. 14.—Relation between vapor density and equilibrium pressure at 160°C.

Table 3

Effect of Temperature on Liquid- and Vapor-Phase Compositions in Equilibrium State at a Loading Density of 0.60 g./cc.

Temp., °C.	140	150	160	170	180
c, mole/l.	7.685	7.685	7.685	7.685	7.685
P, atm.	50.5	68	89	117	151
R'	0.470	0.505	0.545	0.592	0.650
S'	0.040	0.052	0.066	0.082	0.105
R	2.260	2.360	2.460	2.562	2.665
Y	0.421	0.433	0.442	0.440	0.435
Equilibrium Concentration, mole/l. n'_{CO_2}	0.646	0.845	1.031	1.227	1.432
n'_{NH_3}	0.303	0.427	0.564	0.726	0.931
n'_{H_2O}	0.026	0.044	0.068	0.100	0.150
n_{CO_2}	3.803	3.512	3.257	3.076	2.910
n_{NH_3}	8.590	8.290	8.012	7.880	7.760
n_{urea}	3.235	3.327	3.397	3.381	3.343
n_{H_2O}	3.209	3.283	3.329	3.281	3.193
Equilibrium mole fraction N'_{CO_2}	0.662	0.642	0.620	0.597	0.570
N'_{NH_3}	0.311	0.324	0.339	0.354	0.370
N'_{H_2O}	0.027	0.034	0.041	0.049	0.060
N_{CO_2}	0.202	0.190	0.181	0.174	0.169
N_{NH_3}	0.456	0.451	0.445	0.448	0.452
N_{urea}	0.172	0.181	0.189	0.192	0.194
N_{H_2O}	0.170	0.178	0.185	0.186	0.185
K_{N_1}	0.697	0.833	0.974	1.021	1.046

at a given loading density is based on the fact that the vapor-phase increases with the rise of temperature. The equilibrium constants K_{N_1} of the reaction (1) represented by mole fraction N_i are shown in the last line of Table 3. There appears a discontinuous point at 160°C. in a plot of the equilibrium constant against the temperature. Hori and Ogami [9]

(9) Hori and Ogami, *J. Soc. High Pressure Gas Ind. Japan*, **6**, 256 (1942).

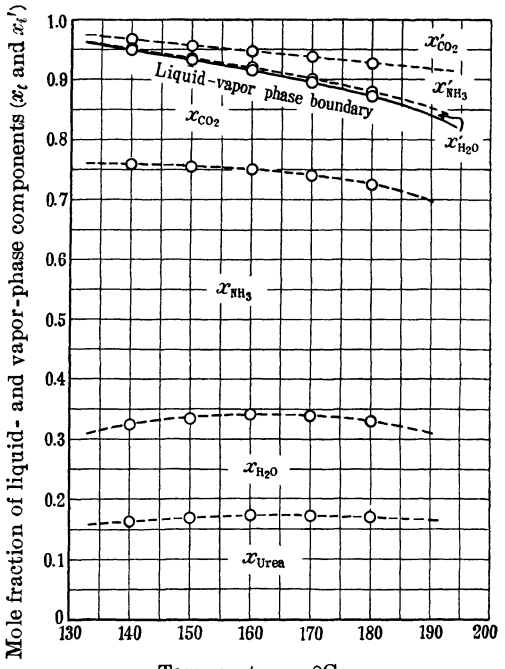

Fig. 15.—Liquid-vapor equilibria diagram of the CO_2-NH_3-Urea-H_2O system at a loading density of 0.60 g./cc.

have already found that a plot of the logarithm of the equilibrium constant[10] against the reciprocal of the temperature results in two straight lines intersecting at 154°C. This conclusion was reached in their experiment which was effected at a loading density of 0.65 g./cc. in a reaction vessel of sealed glass tube, and explained that the existence of the discontinuous point may possibly be based on the difference between the phases in the equilibrium state of the system at each temperature, that is to say, between the solid- and vapor-phase equilibrium at lower temperature than 154°C. and the liquid- and vapor-phase equilibrium at higher temperature than 154°C., because this point perfectly coincides with the melting point 153.5 to 155.8°C. of ammonium carbamate observed by Kitawaki, Hori and Shimoda[3]. The other values of the melting point of ammonium carbamate which were reported by Terres and Behrens[11], E. Jänecke[12], and Krase, Gaddy and Clark[13] are 147 to 150°C.,

(10) The equilibrium constant employed by Hori and Ogami was represented by mole fraction derived from the initial loading composition and the yield of urea without distinction between the liquid- and the vapor-compositions.

(11) Terres and Behrens, *Z. physik. Chem.*, **139 A**, 695 (1928).

(12) E. Jänecke, *Z. Elektrochem.*, **35**, 716 (1929).

(13) Krase, Gaddy and Clark, *Ind. Eng. Chem.*, **22**, 289 (1930).

153 and 145°C. respectively.

The fusion of ammonium carbamate, however, is a complicated phenomenon connected inevitably with the formation of equi-molar urea and water, as pointed out by Kitawaki and others,[3] because its melting point depends on the rate of heating carbamate and in cooling the molten ammonium carbamate, in which even a small quantity of urea was always detected, it is not solidified at the temperature where pure solid carbamate itself began to melt in heating it. In other words, the respective temperature observed in such a way is only an apparent melting point of carbamate, which may possibly depend upon the initial loading density of carbamate in a vessel. Since the equilibrium system, which is the subject under consideration, is a homogeneous liquid phase at a higher temperature than the transition point 115°C., the explanation that the discontinuous point corresponds to the melting point of ammonium carbamate is unreasonable. Preferably it ought to be considered that the discontinuous point corresponds to the maximum yield of urea in Fig. 8 and consequently varies depending on the initial loading density of carbamate.

This unaccountable relation between the equilibrium constant and the temperature might result from the inadequate initial assumption that the system consists of four components of urea, water, ammonia and carbon dioxide in the liquid phase. In other words, it seems to be impossible to represent the reaction of the urea formation by such a simple reaction as the equation (1). Therefore, for the complete explanation of the relation, further consideration should be tried from other stand-points and on other assumptions.

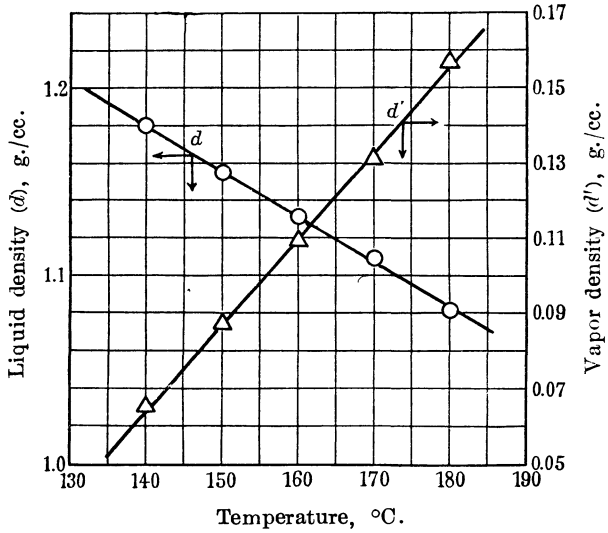

Fig. 16.—Effect of temperature on liquid- and vapor-density at a loading density of 0.60 g /cc.

Effect of Temperature on Liquid- and Vapor-Density.—From the weight of each phase obtained from Table 3 and the volume of each phase, the liquid- and vapor-density at a loading density of 0.60 g./cc. and over the temperature range of 140 to 180°C. has been calculated as shown in Fig. 16. The liquid-density decreases and the vapor-density increases linearly with the rise of temperature, respectively.

Summary

(1) For studying the liquid-and vapor-phase equilibrium of the CO_2-NH_3-Urea-H_2O system under high temperature and pressure, details of methods to determine mole ratios of ammonia, carbon dioixde and water in the vapor phase, mole ratio of ammonia to carbon dioxide in the liquid phase, and volume-ratio of the vapor-to liquid-phase in an autoclave have been described.

(2) Experimental results at temperatures between 140 and 180°C. and over the loading density range of 0.20 to 1.00 g./cc. have been shown in the case of the loading mole ratio of $2NH_3$ to 1 CO_2.

(3) The relations among the equilibrium yield of urea, the loading density and the temperature were discussed from the stand-point of the liquid- and vapor-phase equilibrium.

(4) The liquid- and vapor-phase compositions in the equilibrium state of the system have been calculated on an assumption that the system consists of three components, ammonia, carbon dioxide and water, in the vapor phase and of four components, urea, water, ammonia and carbon dioxide, in the liquid phase.

(5) The equilibrium constant of the following reaction represented by mole fraction of each component in the liquid phase is approximately constant independent of the loading density at a given temperature.

$$CO_2 + 2NH_3 \rightleftarrows CO(NH_2)_2 + H_2O$$

(6) A discontinuous point appearing in a plot of the equilibrium constant against the temperature at a given loading density has been discussed.

(7) The liquid- and vapor-densities of the system under high temperature and pressure have been calculated from

the equilibrium compositions.

Nomenclature

Symbols-

c—Number of moles of ammonium carbamate loaded initially into the reaction vessel, gram mole per litre

d—Density of liquid, g. per cc.

D—Loading density, or ratio of the weights of materials to the total volume of the reaction vessel, gram per cc.

K_{N_1}—Equilibrium constant of the reaction(1) represented by mole fraction N_i, no units

n_i—Number of moles of a component "i" in the liquid phase per litre of the reaction vessel, gram mole per litre

N_i—Mole fraction of a component "i" in the liquid phase, or ratio of gram moles to the total gram moles in the liquid phase, no units

P—Equilibrium pressure, atm.

R—Mole ratio of unconverted ammonia to carbon dioxide in the liquid phase, no units

S—Mole ratio of water to carbon dioxide in the liquid phase, no units

x_i—Mole fraction of a component "i" in the liquid phase, or ratio of gram moles to the total gram moles in the two phases, no units

Y—Equilibrium yield of urea, or ratio of gram moles of urea to initial loading moles of ammonium carbamate ($= n_{urea}/c$), no units

Superscript

$'$ (dash)—sign to denote the vapor phase

The writer wishes to express appreciation for the kind guidance and the advice received throughout this work from Dr. Shinjiro Kodama, Prof. of Kyoto University, and for the encouragement received from Dr. Kenji Fujimura, the chief of the Research Department.

Research Department, Niihama Works,
Nissin Chemical Co., Ltd., Niihama

Studies on the Polarographic Analysis. XII. New Differential Polarography with One Dropping Electrode (2)

By Masayoshi ISHIBASHI and Taitiro FUJINAGA

(Received February 27, 1952)

Introduction

In the previous paper,[1] the authors reported on the construction of the new differential polarograph and its application was discussed from the standpoint of qualitative analysis. Here, they discuss the differential technique from the standpoint of quantitative analysis and of electrode reactions there-of.

Results and Discussion

On the Relation between the Peak Current (i_h) of the Differential Method and the Diffusion Current (i_d) of the Ordinary Method.—As easily concluded from Eq. (4) shown in the previous paper,[1] the peak current should be proportional to the diffusion current, taking ΔE small enough to get the ideal differential curve. And also it would be less than one half of the diffusion current even though ΔE is taken as large enough to cover the whole increasing part of the ordinary wave.

However, in many cases it is observed that the peak current is several times the height of the ordinary diffusion current, proving the increase of the sensitivity. But in some cases, contrary to this, the diminishing of the sensitivity is observed. So the differential curve obtained by the authors' method is not always the resultant one of $E\sim i$ curve and $E-\Delta E\sim -i'$ curve.

The authors studied to clear these phenomena from the standpoint of electrode reaction, using the analysing circuit shown in Fig. 1. In the circuit of 1-a, when the switch is rotated, the electrolytic current i corresponding to the

(1) M. Ishibashi and T. Fujinaga, This Bulletin, **25**, 68 (1952).

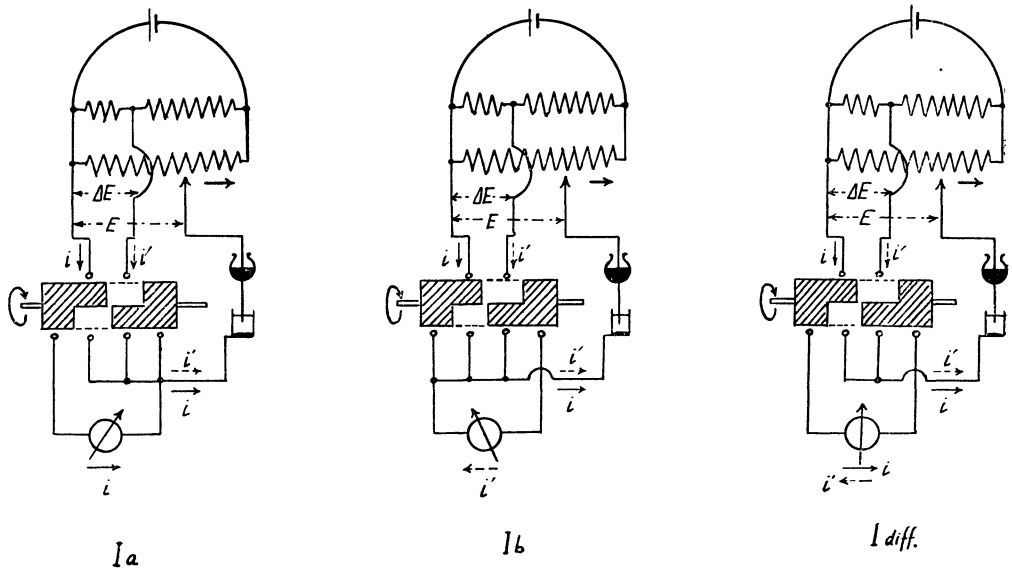

Fig. 1.—Scheme of the differential polarograph (1-diff.) and its analysing circuits (1-a and 1-b).

potential E flows through the galvanometer in the normal direction, while the current i' corresponding to the potential $E-\Delta E$ does not flow through it, but is short-circuited to the cell. We call the polarogram thus obtained by the rotation of the alternator in the circuit 1-a as $E\sim i$ rot. curve and to the contrary, in the circuit 1-b, the current i corresponding to E is short-circuited and i' corresponding to $E-\Delta E$ flows in the reverse direction through the galvanometer and we call this as $E-\Delta E\sim -i'$ rot. curve.

It is readily admitted that the differential polarogram obtained by the authors' method is the resultant curve of the $E\sim i$ rot. curve and $E-\Delta E\sim -i'$ rot. curve and that the experimental findings explain this point fairly well and are in good agreement with the considerations (see Fig. 2 and others). In addition, the scheme 1-a corresponds to the scheme 1-b in the experiment of Kalousek[2] and the scheme 1-b is a reversed circuit of the scheme 1-a in his experiment. Therefore, the authors' differential polarogram is explained to be the deduced curve of the two curves obtained by Kalousek's experiment.

(a) **A case when the electrode reaction is reversible and the dissociation rate of the reducible substances is fast.**—Cadmium and its ion can be oxidized or reduced reversibly at the dropping mercury electrode. The behavior of electrolytic dissolution and deposition of cadmium in potassium chloride solution is shown in Fig. 2. The curve 1 shows the ordinary polarogram i. e. the $E\sim i$ curve (taken with the switch stopped in 1-a or 1-

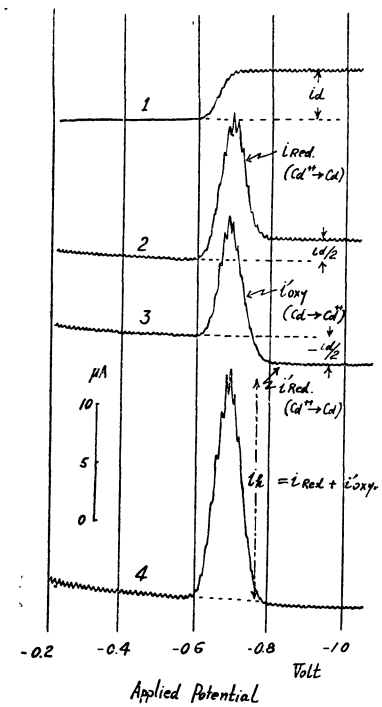

Fig. 2.—Polarograms of cadmium ion in potassium chloride:
ΔE= 50 millivolts, sensit. = 1:200.

(2) M. Kalousek, *Collection Czech. Chem. Communs.*, **13**, 105 (1948).

diff.), the curve 2 the $E\sim i$ rot. curve (the switch rotated in 1-a), the curve 3 the $E-\Delta E\sim -i'$ rot. curve (the switch rotated in 1-b) and the curve 4 the resultant differential curve *i.e.* $E\sim \Delta i/\Delta E$ curve (the switch rotated in 1-diff.). In these polarogram ΔE is 50 millivolts. Comparing the curve 1 with the curve 4, the diffusion current i_d is 4.1 microamperes in the ordinary polarogram while the peak current i_h is 18.3 microamperes in the differential one; in short, the sensitivity is increased by *ca.* 4.5 times. In the curve 2, the maximum is seen at the half-wave potential of the ordinary curve and the magnitude is about 2.7 $\times i_d$ and in the part of the diffusion current, the current falls down to about $i_d/2$. And in the curve 3 analogous maximum is seen and the current falls down to *ca.* $-i_d/2$ in the same part. Considering the isochronism of the rotating switch, it is well recognized that the current of *ca.* $i_d/2$ flows in normal and reverse directions in the part of diffusion current. As for the maximum at the halfwave potential, it could be explained, as Kalousek did, to depend on the reversibility of the electrode reactions. However, as for the curve 3, the current flows in the reverse direction contrary to Kalousek's scheme 1-a by the change of the switch connection. More precisely, the current caused by the reduction of cadmium ions flows in normal direction at the potential E, but in the next instant when E-ΔE is applied the reduction of them takes place no longer, but the dissolution of cadmium begins from the cadmium amalgam yielded by the reduction at the potential E thus effecting the oxidation current, which flows through the galvanometer still in normal direction. At the next instant when the potential E is again applied, the cadmium ions dissolved out of the electrode are again reduced at the same time together with other diffused ions. As a result of these, the concentration of cadmium ion at the electrode surface becomes much larger than it is in the ordinary polarography and the concentration instead of the diffusion layer is brought at the mercury-solution interface. Therefore the concentration of cadmium amalgam at the electrode surface also becomes larger in the same manner. Thus in the circuit 1-a the large reduction current and in the circuit 1-b the large oxidation current are yielded respectively, but by the action of the switch both these currents flow always in normal direction through the galvanometer in spite of the opposite electrode reaction. As the result, as shown in curve 4 of Fig. 2, the prominent maximum is seen in the differential method. Now, when the applied potential is so increased as both the potential E and $E-\Delta E$ come into the part of diffusion current, the above mentioned reverse reaction no longer takes place and consequently the currents have each definite value, $i_d/2$ or $-i_d/2$. The differential curve 4 which is a resultant curve of these curves 2 and 3, therefore, indicates zero current in the stationary parts before and after the wave. Thus the peak current (i_h) is larger by several times than the diffusion current (i_d) of the ordinary polarogram.

From the view-point of quantitative analysis this magnification ratio i_h/i_d would be constant, since then, the peak current is proportional to the concentration. In practice, however, taking ΔE small enough the magnification ratio is particularly large in dilute solution and it diminishes as the concentration increases. Nevertheless, when ΔE is taken as large enough to cover the potential width of the ordinary wave, the ratio becomes constant independently of the concentration and so the peak current is directly proportional to the concentration (see Fig.3). This increase in

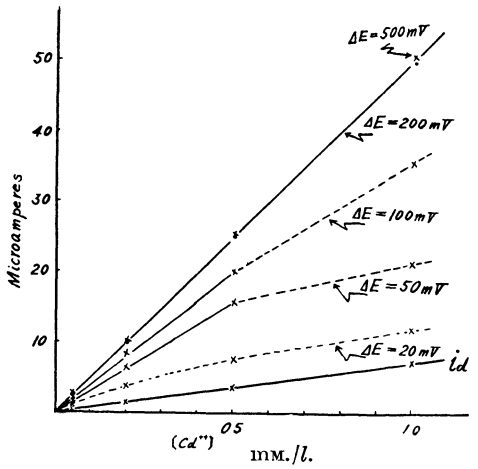

Fig. 3.—Relation between the peak current (i_h) and the diffusion current (i_d) of the cadmium ion in potassium chloride.

sensitivity based upon the reversibility is observed as well with the following ions and substances; free ions of copper, zinc, lead etc. and alkali-metal ions and ammonium ion also and oxygen.

(b) **A case when the electrode reaction is irreversible and the dissociation rate of the reducible substance is fast.**—Zinc ion indicates an irreversible electrode reaction in ammoniacal solution. Fig. 4 as well as Fig. 2 shows the normal order, curve 1; $E\sim i$ curve, curve 2; $E\sim i$ rot. curve, curve 3; $E-\Delta E\sim -i'$

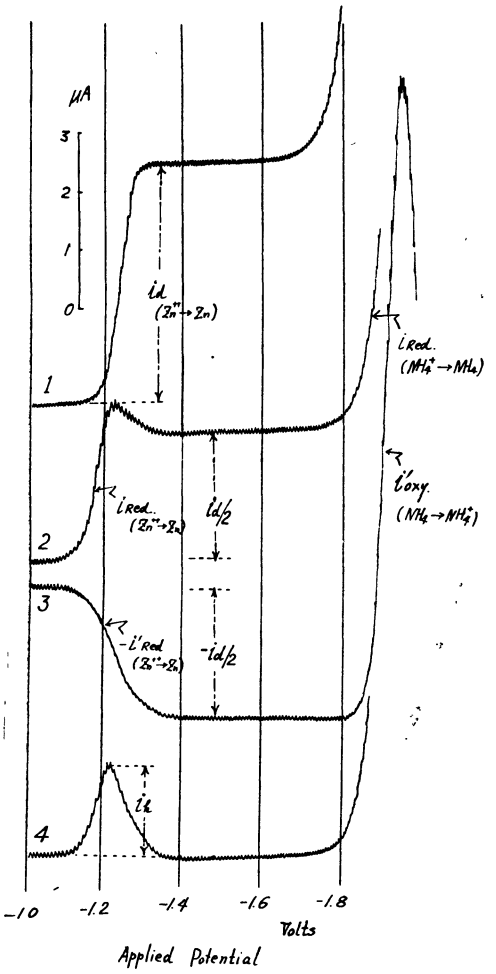

Fig. 4.—Polarograms of zinc ion in ammoniacal solution: ΔE=40 millivolts, sensit.=1:50.

rot. curve and curve 4; $E \sim \Delta i/\Delta E$ curve, which are all in regard to the same zinc ammine solution. The explanation about the case of such irreversible reaction is very easy and the differential curve in this case is in almost a perfect agreement with that in an ideal state. The electrode reaction is scarcely different from cases of ordinary polarography. It would be needless to discuss the curves 1 and 3. Though the curve 2 has likewise its maximum, this maximum is never beyond the height of diffusion current so long as ΔE is less than 300 millivolts. This maximum is explained as follows; the reduction takes place when the potential E is applied and the vacuum layer is formed on the electrode surface. In the next instant when the potential falls to $E-\Delta E$ its reduction still does not take place and also the oxidation does not happen due to the irreversible process. Therefore the vacuum layer is soon almost filled with zinc ions by the diffusion from the bulk of the solution at the potential $E-\Delta E$. In the next instant, when E is again applied, those zinc ions are together reduced at this time. Therefore the height of the peak in curve 2 is greater than

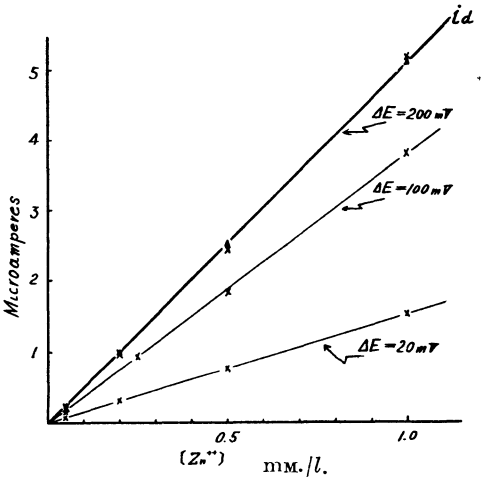

Fig. 5.—Relation between the peak current (i_p) and the diffusion current (i_d) of the zinc ion in ammoniacal solution.

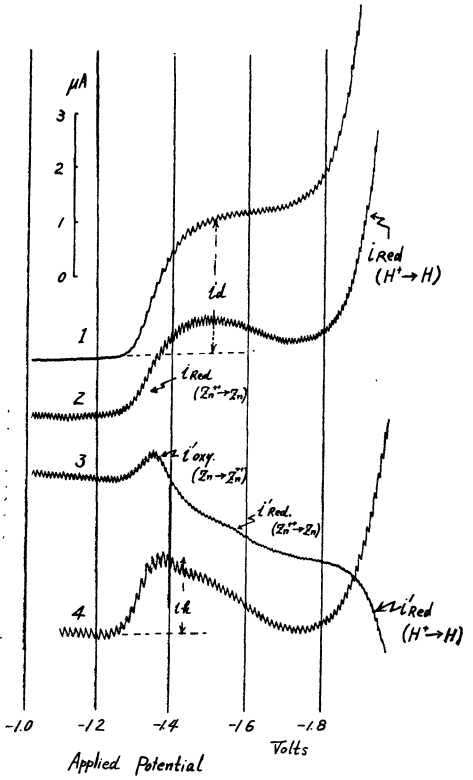

Fig. 6.—Polarograms of zinc ion in acidic tartrate solution: ΔE=100 millivolts, sensit.=1:50.

$i_d/2$ and less than i_d. Increasing the applied potential as high as the potential $E-\Delta E$ is sufficient to reduce zinc ion, the current drops to $i_d/2$ owing to the stop of supplying the ions at $E-\Delta E$. Thus the little peak appears in the curve 2 and also in the differential curve (curve 4), but differing from the case of reversible reaction, the peak current is always less than i_d. Viewed from the standpoint of quantitative analysis, such a case is the most ideal one in which the peak current is proportional to the concentration even though ΔE is small. The results obtained are shown in Fig. 5. Such irreversibility like that of zinc ammine should also be observed as to bismuth ion in tartrate solution, hydrion, many organic substances and hydrogen peroxide.[2]

(c) **A case when the dissociation rate is slow.**—In the ordinary polarogram, zinc in tartrate solution shows a wave of more gentle slope than the theoretically expected one. The differential polarogram shows only a little peak even when ΔE is taken so large. Judging from this fact, it is concluded that the rate of the dissociation of zinc ion from its tartrate complex is very slow compared with the electrodeposition of zinc from its simple ion. Fig. 6 shows from above to below, curve 1; $E\sim i$, curve 2; $E\sim i$ rot., curve 3; $E-\Delta E\sim -i'$ rot., and curve 4; $E\sim \Delta i/\Delta E$ curves. In the electrode reaction the over-voltage is required for the dissociation, and with the increase of the applied potential the dissociation is reasonably accelerated and the reduction current increases gradually to the extent of diffusion control. However, until the appearance of its influence, the potential interval is so wide that the peak becomes very low compared with the expected one. Concerning the little peak of the curve 3, it may be concluded that the electrode reaction has yet reversibility to some extent. The similar phenomena are expected in the following cases; the complex ions of nickel or cobalt and some organic substances which generate, for instance, the kinetic current. These cases are now under investigation.

Laboratory of Analytical Chemistry, Faculty of Science, Kyoto University, Kyoto

Analytical Chemistry by Means of Oxalic Acid. I. On the Quantitative Analysis of Strontium[1]

By Tamotsu MATSUMOTO

(Received July 9, 1951)

The method of determining a metal as its oxalate had been employed only in the case of calcium. The present writer applied this method to strontium, which is similar to calcium.[2]

Precipitating strontium as its oxalate was studied by Souchay, Lenssen, Herz, Muss and others[3],[4] who got various hydrates of strontium oxalate which were fairly soluble in water. The present writer tried the following experiments in order to apply the precipitate of strontium oxalate to gravimetric as well as volumetric analysis. In the gravimetric method strontium oxalate was weighed as its monohydrate, while in the volumetric determination the oxalic acid in strontium oxalate was titrated with potassium permanganate.

Experimental

Preparation of 0.1 M strontium nitrate was as follows:—Ishizu Chemicals' strontium nitrate was recrystallized. On analysing 50 ml. of the solution containing 10 g. of this salt, there were found no heavy metals, no alkali earths but strontium, and no alkalis in the sample. One litre of 0.1 M

Table 1

No.	$SrSO_4$ g.	Sr		
		Found g.	Calc. g.	Error mg.
1	0.4583	0.2186	0.2189	−0.3
2	0.4582	0.2186	0.2189	−0.3
3	0.4585	0.2187	0.2189	−0.2
mean	0.4583	0.2186	0.2189	−0.3

(1) Presented at the 6th Regular Meeting of the Chugoku-Shikoku Branch of the Chemical Society of Japan in January, 1952.
(2) Souchay and Lenssen, *Ann.*, **100**, 313 (1856).
(3) Souchay and Lenssen, *Ann.*, **102**, 35 (1857).
(4) Souchay. Lenssen, Herz and Muss, *Ber.*, **36**, 3717 (1903).

solution was prepared by dissolving 21.150 g. of this salt in distilled water, and 25 ml. of this solution was employed for each determination. In the first place the strontium in 25 ml. of this solution was determined by the ordinary sulfate method. The results are shown in Table 1.

1. Gravimetric Method.—In order to precipitate strontium as its oxalate, 5% ammonium oxalate solution was employed.

Procedure for precipitating strontium oxalate:—To 25 ml. of hot 0.1 M strontium nitrate solution which is acidified with dilute hydrochloric acid so that a small quantity of strontium oxalate precipitate once formed is redissolved, a definite quantity of hot 5% amm. oxalate solution is added and the whole is well stirred. When dilute ammonia is added drop by drop to the solution agitating strongly all the while, until the latter becomes just pink with phenolphthalein, a crystalline precipitate is produced. Now the whole is warmed in the water-bath for about 2 hrs., left to stand over night and filtered with 1.G.4. glass filter. The precipitate is washed with 1% amm. oxalate, distilled water or 50% alcohol, dried at 100—105°C. for 2 hrs. in the air-bath, and weighed.

A) Influence of washing solution.—In this case, 10 ml. of hot 5% amm. oxalate solution was employed for each determination. The precipitate was washed by decantation with one of the following washing liquids.

(1) 100 ml. of distilled water.

(2) 30 ml. of 1% amm. oxalate first, and 70 ml. of distilled water.

(3) 100 ml. of 50% alcohol.

The results are shown in Table 2.

Table 2 (Sr used is 0.2189 g.)

Washing liquid	$SrC_2O_4 \cdot H_2O$ g.	Sr	
		Found g.	Error mg.
water 100 ml.	0.4791	0.2168	−2.1
	0.4790	0.2167	−2.2
	0.4790	0.2167	−2.2
1% amm. oxalate 30 ml. and water 70 ml.	0.4810	0.2177	−1.2
	0.4812	0.2177	−1.2
	0.4813	0.2178	−1.1
50% alcohol 100 ml.	0.4837	0.2189	±0
	0.4835	0.2183	−0.1
	0.4835	0.2188	−0.1

The washing with distilled water (1) produces a remarkable negative error, the solubility of strontium oxalate being fairly large, while 50% alcohol (3) is found to be most effective, better results being given than by the ordinary sulfate method (Table 1). The error found in the case of washing with 1% amm. oxalate and water (2) is about the mean value of (1) and (3).

For the above reason, in the case where 50% alcohol is employed as the washing liquid, the determination of strontium can be carried out quantitatively.

Solubility of strontium oxalate.—The precipitate of strontium oxalate prepared by the above process and completely washed in hot water is put in a 300 ml. Erlenmeyer flask together with 200 ml. of solvent. The whole is set in a thermostat and shaken till the solution is saturated. After a definite time the solution is filtered, 50 ml. of the filtrate is put in the beaker and evaporated to dryness in the water-bath. The residue is dried at 100—105°C for 1 hr. and weighed. Table 3 shows the solubilities of strontium oxalate in distilled water, and 50% alcohol at 25—26°C.

Table 3

Solvent	Time in contact with solvent and precipitated, hr.	$SrC_2O_4 \cdot H_2O$ dissolved in 50 ml. mg.	Solubility (25-26°C) mg./l.	mol/l.
water	8	2.0		
	24	2.4	43.5	2.5×10^{-4}
	35	2.3		
50% alcohol	8	0.2		
	24	0.3	3.6	—
	35	0.2		

B) Influence of amount of amm. oxalate.—To find out the most suitable amount of amm. oxalate for precipitation of strontium oxalate and also to study the influence of dilution of the sample solution, a series of experiments were carried out, the results of which are shown in Table 4. In these experiments 100 ml. of 50% alcohol was employed as the washing solution.

Table 4 (Sr used is 0.2189 g.)

Water added ml.	5% Amm. Oxalate		$SrC_2O_4 \cdot H_2O$ g.	Sr found g.	Error mg.
	ml.	molar ratio to Sr			
—	10	1.4	0.4835	0.2188	−0.1
—	20	2.8	0.4836	0.2188	−0.1
—	40	5.6	0.4835	0.2188	−0.1
—	80	11.2	0.4838	0.2189	±0
50	10	1.4	0.4835	0.2188	−0.1
100	10	1.4	0.4834	0.2187	−0.2

The amounts of amm. oxalate and the partial dilution of the sample solution do not affect the exactness of the analysis.

C) Influence of *p*H.—To 25 ml. of 0.1 M strontium nitrate, a suitable indicator is added, and *p*H of the solution is adjusted to a certain value with dilute ammonia or hydrochloric acid. Then, with 10 ml. of hot 5% amm. oxalate solution the precipitate of strontium oxalate is formed.

From the results shown in Table 5, it is evident that the precipitation is completely carried out if the *p*H value of the sample solution is larger than 3.

Table 5 (Sr used is 0.2189 g.)

*p*H (Indicator)	$SrC_2O_4 \cdot H_2O$ g.	Sr g.	Error mg.
11.0 (Nitramine)	0.4835	0.2188	−0.1
8.2 (Phenolphthalein)	0.4835	0.2188	−0.1
6.3 (Methyl red)	0.4837	0.2189	±0
3.1 (Methyl orange)	0.4835	0.2188	−0.1
1.2 (Thymol blue)	0.4778	0.2162	−2.7
0.1 (Methyl violet)	none	—	—

D) Influence of various salts present.—The influence of various salts such as sodium chloride, potassium chloride, potassium nitrate, ammonium chloride or ammonium nitrate was examined. In each experiment, 25 ml. of 0.1 M strontium nitrate solution was mixed with a definite quantity of the salt, and this solution was treated in the manner described before. The results are shown in Table 6.

Table 6 (Sr used is 0.2189 g.)

salt	Mixed g.	$SrC_2O_4 \cdot H_2O$ g.	Sr g.	Error mg.
NaCl	2	0.5998	0.2714	+52.5
KCl	1	0.5324	0.2409	+22.0
KNO_3	2	0.5381	0.2435	+24.6
NH_4Cl	2	0.4833	0.2187	− 0.2
NH_4NO_3	2	0.4836	0.2188	− 0.1

Sod. chloride, pot. chloride, and pot. nitrate seem to be adsorbed in the precipitate of strontium oxalate so that the value of strontium is made very high. Amm. chloride and nitrate have no influence.

2) Volumetric Method.—When the strontium oxalate prepared by the above method is decomposed by sulfuric acid, oxalic acid is formed in the solution. By titrating this oxalic acid with potassium permanganate, the amount of strontium in the sample solution can be determined. The present writer applied this method to the volumetric analysis of strontium, and compared the results with those obtained by the gravimetric method.

Procedure:—From 25 ml. of 0.1 M strontium nitrate solution the precipitate of strontium oxalate is prepared under the best condition required in the former method. When 6 N sulfuric acid is added to the precipitate in a glass filter, strontium sulfate is formed and it is filtered out with suction, being stirred continuously with a glass rod. As the strontium sulfate probably adsorbs the oxalic acid, it should be washed well with distilled water. All the filtrate is kept in a measuring flask and diluted accurately to 250 ml. The 25 ml. of the filtrate, acidified with sulfuric acid, is titrated with 0.1 N potassium permanganate and from its volume the amount of strontium may be calculated.

Table 7 (Sr used is 0.2189 g.)

Gravimetrically		Volumetrically		
$SrC_2O_4 \cdot H_2O$ g.	Sr g.	0.1N-$KMnO_4$ (factor=1.0046) ml.	Sr found g.	diff. to grav. mg.
0.4837	0.2189	49.70	0.2188	−0.1
0.4835	0.2188	49.66	0.2186	−0.2
0.4835	0.2188	49.71	0.2188	±0

The results are shown in Table 7. Judging from the fact that the amount of strontium determined by the volumetric method is nearly equal to that given by the gravimetric, it may be said that the volumetric analysis by means of oxalic acid brings on satisfactory results.

Summary

1. Quantitative precipitation of strontium as its oxalate monohydrate is made possible by employing 50% alcohol as the washing solution and by drying the precipitate at 100-105°C for 2 hrs., and as a consequence a new method for determining strontium gravimetrically was established.

2. It was found that strontium can be determined volumetrically by titrating with potassium permangante the oxalic acid which is formed when the strontium oxalate prepared by the above method is decomposed with sulfuric acid.

The writer wishes here to express his hearty thanks to Prof. Masayoshi Ishibashi at Kyoto Univ. and Prof. Koichi Emi at Okayama Univ. for their kind guidance and encouragement. The expenses of this research were defrayed by the Grant in Aid for Fundamental Scientific Research from the Department of Education, to which the writer's thanks are due.

Chemical Institute, Faculty of Science, Okayama Univ.

A Study on the Mechanism of the Catalytic Action of Manganese Dioxide on the Decomposition of Potassium Chlorate by Use of Heavy Oxygen as an Isotopic Tracer

By Shouzow FUKUSHIMA, Yoshio HORIBE and Toshizo TITANI

(Received March 15, 1952)

Introduction

It is a well-known fact that various metallic oxides, especially manganese dioxide, show a remarkable catalytic action for the thermal decomposition of potassium chlorate.(1) Thus, the potassium chlorate, which melts at 370°C. without chemical change in the absence of catalyst, decomposes at such low temperature as 235~290°C.(2), when it is mixed with manganese dioxide which alone does not evolve oxygen gas below 520°C.

Ever since the reaction was studied by Döbereiner(3) in 1832, various hypotheses have been proposed for the mechanism of the catalytic action of manganese dioxide. But among these hypotheses the one which postulates the formation of an intermediate compound is presumably most probable.(4) According to this hypothesis, primarily an unstable intermediate compound is formed between potassium chlorate and manganese dioxide, and the subsequent decomposition of this intermediate compound is accompanied by the evolution of oxygen gas and the production of potassium chloride, manganese dioxide being regenerated. Although this hypothesis seems very probable from the recent point of view about the general mechanism of catalytic reactions, only few direct verifications for this mechanism have been found in the literatures so far as we know.

If, however, oxygen is evolved through the intermediate formation of an unstable compound between potassium chlorate and manganese dioxide, the evolved oxygen must contain oxygen atoms which are originated not only from potassium chlorate but also from manganese dioxide used as catalyst. And this may easily be shown by an isotopic analysis of the evolved gas, if either the oxygen atoms of potassium chlorate or those of manganese dioxide are labeled with heavy oxygen as an isotopic tracer. From this point of view, we studied the isotopic composition of oxygen gas evolved when potassium chlorate labeled with heavy oxygen was decomposed in the presence of an ordinary manganese dioxide.

Experimental

The potassium chlorate labeled with heavy oxygen was prepared by the anodic oxidation of potassium chloride in the solution of heavy water, of which content of heavy oxygen had been whose increased above its natural abundance by fractional distillation.

The product was purified by repeated recrystallizations in aqueous solution of ordinary water for the exchange reaction of oxygen atoms between water and chlorate ion can be ignored.(5)

The heavy potassium chlorate prepared in such a way was decomposed by heating in the presence of an ordinary manganese dioxide under various conditions as described below and the evolved oxygen was converted into the form of water by recombining with an ordinary tank hydrogen by the aid of a copper catalyst. At the same time a part of the same heavy potassium chlorate was non-catalytically decomposed in the absence of manganese dioxide catalyst by heating at 650°C. and the evolved oxygen gas was converted into the form of water in the same way as above, using the same tank hydrogen.

Another sort of water was also prepared by reducing, with the same tank hydrogen, a part of the same manganese dioxide which was used for the decomposition of heavy potassium chlorate as the catalyst. Although in this case manganese dioxide was to be reduced only to manganese monoxide, the isotopic separation between oxygen atoms contained in the produced water and those which remained in manganese monoxide was ignored.

The densities of these three sorts of water were then compared by the ordinary sinker

(1) Gmelin, "Handbuch der anorganischen Chemie", Kalium **22**, 473: Chlor, **6**, 342.

(2) Brown, Burrow and McLaughlin, *J. Am, Chem. Soc.*, **45**, 1343 (1923): Neville, ibid., **45**, 2331 (1923): Burrow and Brown, ibid., **48**, 1790 (1926): Balarew, *Kolloid-Z.*, **66**, 317 (1934).

(3) Döbereiner, *Ann.*, **1**, 236 (1832).

(4) McLeod, *J. Chem. Soc.*, **55**. 184 (1889); Sodeau, *J. Chem. Soc.*, **81**, 1066 (1902): *Proc. Chem. Soc.*, **18**, 136(1903); Dhar, *J. Phys. Chem.*, **28**, 953 (1924): Deniges, *Bull. trav. Soc. pharma. Bordeaux*, **74**, 93 (1936); Bhatnagar, et al, *J. Indian Chem. Soc.*, **17**, 124 (1940).

(5) T. Titani and K. Goto, This Bulletin, **13**, 667(1938).

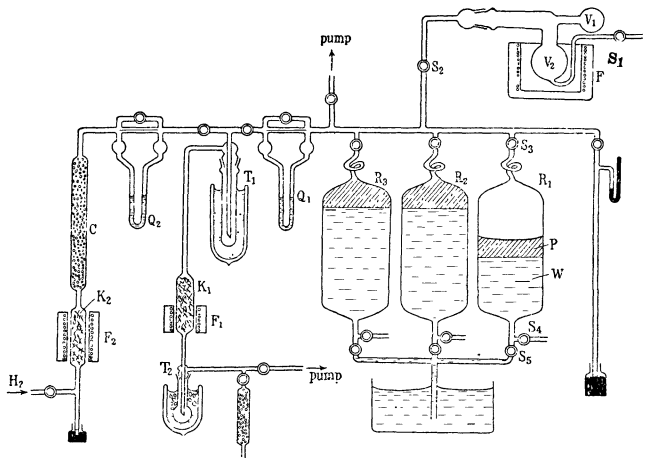

Fig. 1.

method, after a careful purification by heating with a small quantity of caustic soda and potassium permanganate and vacuum distillations. For each measurement, 0.5~0.8 ml. of water was needed.

The apparatus used for the thermal decomposition of heavy potassium chlorate in the presence and the absence of manganese dioxide is shown in Fig. 1 and the details of each run of the experiments are given below, where $KClO_3$* denotes the potassium chlorate whose oxygen is labeled with heavy oxygen, and $MnO_2 \cdot H_2O$ the manganese dioxide used as catalyst, because the manganese content of the catalyst determined by pyrophosphate method corresponds to that of this formula.

Exp. I.—Carefully powdered samples of 0.051 mole of $KClO_3$* and 0.045 mole of $MnO_2 \cdot H_2O$, were placed separately in V_1 and V_2. $KClO_3$* was dried in a vacuum for three hours at 20°C. and $MnO_2 \cdot H_2O$ was dried first in dry air current passed through S_1 and S_2 for two hours at 320°C. then in a vacuum for three hours at 20°C. Then, two reagents were mixed thoroughly in V_2 in a vacuum and the mixture was heated carefully by means of an electric furnace F at the desired temperature, which was measured by a thermocouple placed closely to the wall of the reaction vessel V_2. Oxygen gas was found to evolve at moderate rate at 320°C. and it took about fifty minutes until the reaction was completed, during this period the temperature inside the furnace being kept constant within a range of ±3°C. All of the evolved oxygen was collected in receiver R_1 by opening stopcocks S_2, S_3 and S_5. A thick layer of liquid paraffin P was placed to cover the surface of water W in the receiver in order to isolate the sampled oxygen from the air dissolved in the water. Then the oxygen gas was pushed out of R_1 to the catalyst tube K_1 through the flowmeter Q_1 and the dry ice trap T_1 by applying a hydropressure through S_4. The catalyst tube K_1 was filled with copper catalyst and heated at 400°C. in an electric furnace F_1. On the other hand, an excess quantity of tank hydrogen, which was freed from oxygen and water vapor by passing through the heated copper catalyst tube K_2 and the calcium chloride tube C and the dry ice trap T_1, was introduced into the catalyst tube K_1, the flow rate being checked by flowmeter Q_2. And thus the water, which was formed in the catalyst tube K_1 by the combination of the sample oxygen and the tank hydrogen, was collected in the ice water trap T_2.

Exp. II.—The experimental procedures and conditions were the same as Exp. I, except that 0.053 mole of $KClO_3$* was taken.

Exp. III.—The experimental procedures of this Exp. III, where 0.093 mole of $KClO_3$* and 0.095 mole of $MnO_2 \cdot H_2O$ were taken, were different from preceding Exps. I and II in two respects. In the first place $MnO_2 \cdot H_2O$ used in this experiment was pretreated under more severe conditions than in the preceding experiments. It was at first desiccated in the current of dry air for two hours at 480°C. and then treated for three hours in a vacuum at 320°C. By this severe treatment the catalytic activity of $MnO_2 \cdot H_2O$ seemed to be somewhat injured, for with this $MnO_2 \cdot H_2O$ the moderate rate of oxygen evolution was not observed until the temperature was raised up to 345°C. which is much higher than 320°C. the temperature used in the preceding experiments. The second characteristic of the procedure of this run was that the fractions of oxygen gas which were evolved at three different stages of the reaction were collected separately in three receivers, namely, the first fraction (1.05 l.) in R_1, the middle fraction (1.05 l.) in R_2 and the last fraction (0.35 l.) in R_3, and these three fractions of sampled oxygen were separately converted to water by use of the same tank hydrogen.

Exp. IV.—The purpose of this experiment was quite different from the purposes of the preceding Exps. I, II, and III and it is to investigate the possibility of a supposed secondary exchange reaction of oxygen atoms between manganese dioxide and gaseous oxygen which is evolved by the decomposition of potassium chlorate.

A gaseous oxygen which has the same isotopic composition as that of $KClO_3$* was prepared by the non-catalytic thermal decomposition of $KClO_3$*. The prepared heavy oxygen gas was then passed slowly through a reaction vessel which contains $MnO_2 \cdot H_2O$ pad at 350°C. and at the rate of 1.85 l. per hour. The $MnO_2 \cdot H_2O$ used in this experiment was preliminarily dried in the same way as in Exps. I and II, and the temperature of the reaction vessel (350°C.) was chosen much higher than the temperature (320°C.) at which the reaction mixture was heated in Exps. I and II. The heavy oxygen gas after being passed through the reaction vessel was converted to water in the same way as in the preceding experiments.

Results and Discussions

Results of the experiments are shown in Table 1; the third column gives the excess

Table 1

Results of the Experiments

Number of the sample	Sample	Excess density due to heavy oxygen in the sample[6] (in p. p. m.)	Density difference (in p.p.m.)
1	$KClO_3$*	48.3±0.8	Standard
2	$Mn_2O \cdot H_2O$	0.8±0.5	−47.5
3	Oxygen gas evolved in Exp. I	32.6±1.0	−15.7
4	Oxygen gas evolved in Exp. II	34.6±1.0	−13.7
5	Oxygen gas evolved in the first stage of Exp. III	37.8±0.2	−10.5
6	Oxygen gas evolved in the middle stage of Exp. III	48.5±0.3	+ 0.2
7	Oxygen gas evolved in the last stage of Exp. III	46.5±2.6	− 1.8
8	Oxygen gas after exchange reaction in Exp. IV	48.0±0.2	− 0.3

densities of recombined water due to the enrichment of heavy oxygen above the tap water in Osaka city,[6] and the last column the same, but with sample 1 taken as the standard. It will be seen from this table, by comparing the excess densities of samples No. 1 and 2, that the oxygen in $KClO_3$* is 47.5 p. p. m. heavier than that in $MnO_2 \cdot H_2O$. Accordingly the oxygen gas, which is evolved by the thermal decomposition of the mixture of $KClO_3$* and $MnO_2 \cdot H_2O$, must show the same excess density as that of $KClO_3$*, if the gas is exclusively originated from $KClO_3$*. But in fact the evolved gas has a much lower excess density than that of $KClO_3$*, as is seen from samples No. 3 to 5. On the other hand, the possibility of the secondary exchange reaction between evolved oxygen gas and $MnO_2 \cdot H_2O$ can be excluded by the result of Exp. IV, where the heavy oxygen, which was prepared by the noncatalytic decomposition of $KClO_3$* and passed over the same $MnO_2 \cdot H_2O$ as used in Exp. I and II, at higher temperature than that in these experiments, showed the same excess density as that of $KClO_3$* (see sample No. 8 in Table 1). From these experimental results, it can be concluded that a part of the oxygen gas, which is evolved by the catalytic decomposition of potassium chlorate in the presence of manganese dioxide, originates from the latter, presumably through an unstable compound, formed intermediately between the two substances. The result obtained in Exp. III is highly interesting, because it has been found there that the first fraction of the oxygen, which is evolved at the beginning of the reaction, shows the lower excess density than that of $KClO_3$*, as is seen in the preceding Exps. I and II, whereas the densities of the middle and last fractions agree with that of $KClO_3$* within the limit of the experimental error (see samples No. 5, 6 and 7 in Table 1). This result can, however, be explained under the following assumptions.

Although the oxygen is liberated through the decomposition of the intermediate compound, which is formed between potassium chlorate and manganese dioxide, only a small part of the manganese dioxide has the activity to form such an intermediate compound, with potassium chlorate. It follows therefore that an isotopic exchange equilibrium is quickly established between the oxygen atoms contained in this active part of manganese dioxide and those of potassium chlorate through the repeated formation and decomposition of the intermediate compound between the two substances, when a limited quantity of manganese dioxide is heated with potassium chlorate. And when this equilibrium is once attained, the oxygen liberated from the mixture of both substances must have the same isotopic composition as that of potassium chlorate, whereas a part of the gas originates from manganese dioxide. This may be the reason why in Exp. III the oxygen, evolved after a certain period of the reaction, has the same excess density as that of potassium chlorate.

If it is so, the ratio of the number N of oxygen atoms contained in the active part to the total number N_0 of oxygen atoms contained in the whole manganese dioxide can be calculated from the quantity of potassium chlorate and manganese dioxide used in the experiment and the isotopic composition of the liberated oxygen and that contained in the potassium chlorate. The results of the calculation are shown in Table 2.

Although nothing can be said on the exact nature of this active part of manganese dioxide without further study, it may be a reasonable assumption that it would be a thin layer on the surface of each manganese dioxide particle. It has been found further by a microscopic observation that the manganese dioxide particles used in the present experiment may be

(6) Corrected for the difference in the isotopic composition of hydrogen between the tank hydrogen and tap water.

Table 2

Ratio of the Active Part and Thickness of Active Layer of Manganese Dioxide

Sample	N/N_0	Thickness of active layer ($m\mu$)
$MnO_2 \cdot H_2O$ used in Exp. I	0.37	2.2
$MnO_2 \cdot H_2O$ used in Exp. II	0.32	1.8
$MnO_2 \cdot H_2O$ used in Exp. III	0.072	0.4

regarded as a sphere having a mean diameter of 30 μ. The thickness of the active layer given in the last column of Table 2 has been calculated by using the ratio N/N_0 given in the second column of the table, under the assumption that the active part forms a complete shell layer on the surface of a spherical particle of manganese dioxide having a diameter given above. From the figures given in Table 2, it will be seen that the active part of $MnO_2 \cdot H_2O$ used in the last Exp. III is much smaller than those used in Exps. I and II. This result is, however, in good accordance with the experimental fact that $MnO_2 \cdot H_2O$ used in Exp. III has a much weaker activity than those used in the other experiments as has already been stated. And if it is taken into consideration that $MnO_2 \cdot H_2O$ used in Exp. III has been pretreated under more severe conditions than in other experiments, namely, heated in a vacuum at much higher temperatures than others, it may be concluded that a large portion of the active part of manganese dioxide catalyst has been lost or destroyed by this severe treatment.

Summary

By use of heavy oxygen as an isotopic tracer, the following facts have been found;

1. At the catalytic decomposition of potassium chlorate in the presence of manganese dioxide, an unstable compound is formed between potassium chlorate and manganese dioxide, and oxygen gas is liberated by the decomposition of this intermediate compound.
2. The active part of manganese dioxide capable of composing such an intermediate compound with potassium chlorate is only a limited small portion of the particle.
3. Such an active part is readily destroyed by such a severe treatment as the heating of the catalyst in a vacuum at high temperature.

A part of the expense for the present research has been defrayed by the Scientific Research Encouragement Grant from the Ministry of Education, to which the authors' thanks are due.

Department of Chemistry, Faculty of Science, Osaka University, Osaka

Über die Reinigung des Rubidiums. — Umkrystallisation des Rubidiumtetraoxalates —

Von Airi SUETUNA

(Eingegangen am 25 Dezember, 1951)

Einleitung

Die Reinigung des Rubidiums wurde durch Umkrystallisation des Rubidiumtetraoxalates[1], [2] an Stelle des Rubidiumbitartrates versucht, welches als das entsprechende Cäsiumsalz weit schwerer löslich in Wasser ist und darum bisher für die Entfernung des Cäsiums von Rubidiumsalz oft benutzt wurde. Die Löslichkeit der Tetraoxalate wurde nun von neuem bestimmt, und somit wurde die Tatsache gefunden, daß trotz der Literaturenangabe der Löslichkeitsunterschied zwischen Tetraoxalaten des Cäsiums

(1) Neulich erschien eine Abhandlung von J. D'ans (*Angew. Chem.*, **62**, 118 (1950)), der für die Abscheidung des Rubidiums aus dem reinen Rubidiumcarnallit die Oxalsäure an Stelle von Weinsäure benutzte. Man saugt das abgeschiedene Rubidiumtetraoxalat ab und krystallisiert es aus Wasser um. Nach einer kurzen Fraktionierreihe geht das Cäsium als die leichter lösliche Komponente in die Mutterlauge.

(2) J. Formánek (*Österr. Chem. Ztg.*, **2**, 309 (1899)) benutzte die Normaloxalate zur Trennung von Kalium, Rubidium und Cäsium. Dabei ist wohl das Kaliumoxalat das wenigst lösliche

und des Rubidiums leider nicht so groß sei. Um diesen Nachteil zu überwinden, wurde die Umkrystallisation des Rnbidiumtetraoxalates so oftmals wiederholt, daß ganz unerwartet nicht nur das Cäsium sondern auch das Kalium dabei zugleich entfernt und das reine Rubidiumpräparat erhalten wurde. Dies stellt wirklich einen neuen Typus der Reinigung des Rubidiums dar.

(A) Löslichkeit der Tetraoxalate in Wasser

Ältere Angaben stehen in Tabelle 1.

Tabelle 1

Löslichkeit der Tetraoxalate.
g. Salz/100 g. H_2O (Ältere Angaben)

Salz	21°	25°	30°
$KH_3(C_2O_4)_2 \cdot 2H_2O$	4.96[3] (20.6°)	3.16[4] 5.2[5]	5.05[6]
$RbH_3(C_2O_4)_2 \cdot 2H_2O$	2.1[7]		
$CsH_3(C_2O_4)_2 \cdot 2H_2O$		25[8]	

Unter den Hydrooxalaten des Kaliums, des Rubidiums und des Cäsiums lassen sich nur die Tetraoxalate $MH_3(C_2O_4)_2 \cdot 2H_2O$ unverändert aus Wasser umkrystallisieren. Die Löslichkeit der Tetraoxalate wurde hier folgenderweise bestimmt: das reine Präparat der Tetraoxalate wurde in mäßiger Menge Wasser heiß aufgelöst, die Lösung in einem Thermostaten unter Schütteln abgekühlt, und einige Zeit stehen gelassen, dann ein Teil Mutterlauge gewogen und das darin vorhandene Oxalat-ion mit Kaliumpermanganatlösung titriert. In Tabelle 2 stehen die so erhaltenen Resultate. Die Werte sind die Mittel von je 2 bis 4 Messungen. Der Fehler beträgt bei jedem Falle höchstens 1%.

Tabelle 2

Löslichkeit der Tetraoxalate. g. Salz/100 g. H_2O
(von neuem bestimmt)

Salz	21°	25°
$KH_3(C_2O_4)_2 \cdot 2H_2O$	2.46	
$RbH_3(C_2O_4)_2 \cdot 2H_2O$	2.03	
$CsH_3(C_2O_4)_2 \cdot 2H_2O$	4.34	5.93

(3) J. J. Pohl. *Ber. Wien. Akad.*, **6**, 597 (1851).
(4) H. Hartley, J. Drugman, usw. *J. Chem. Soc.*, **103**, 1747 (1913).
(5) berechnet aus dem Diagramm des Systems $K_2C_2O_4$-$H_2C_2O_4$-H_2O bei 25° von H. W. Foote, I. A. Andrew. *Am. Chem. J.*, **34**, 162 (1905).
(6) I. Koppel, M. Cahn. *Z. anorg. Chem.*, **60**, 106 (1908).
(7) F. Stolba. Sitzungsber. Böhm. Ges. Wissensch,, 278 (1877).
(8) berechnet aus dem Diagramm des Systems $Cs_2C_2O_4$-$H_2C_2O_4$-H_2O bei 25° von H. W. Foote, I.A. Andrew. *Am. Chem. J.*, **34**, 162 (1905).

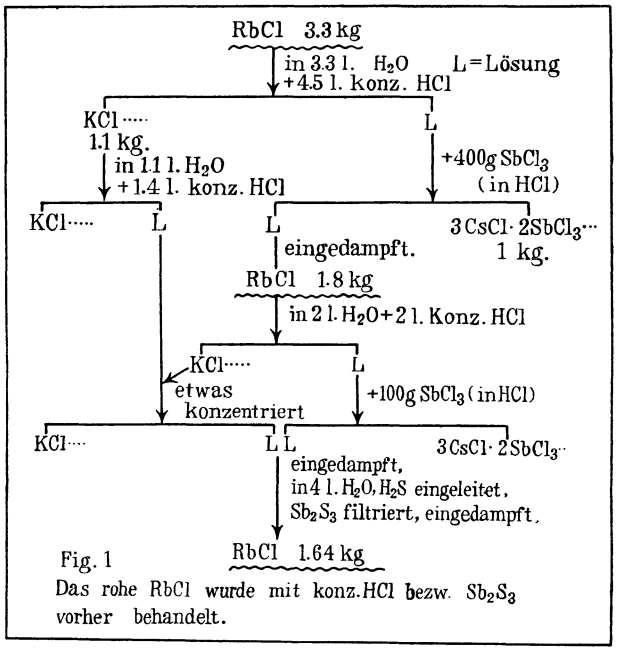

Fig. 1
Das rohe RbCl wurde mit konz.HCl bezw. Sb_2S_3 vorher behandelt.

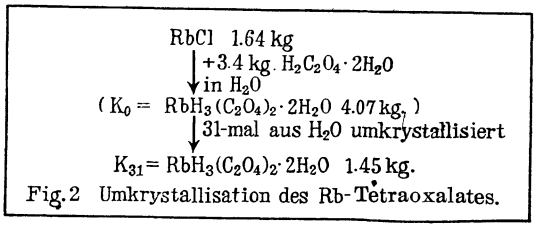

Fig. 2 Umkrystallisation des Rb-Tetraoxalates.

(B) Umkrystallisation des Rubidiumtetraoxalates

Das rohe Rubidiumchlorid, anscheinend K 15~20%, Rb 60~70%, Cs 15~20%, wurde wie üblich zur Beseitigung der Hauptteile des Kaliums und des Cäsiums mit konzentrierter Salzsäure bezw. Antimontrichlorid vorher behandelt. Fig. 1 veranschaulicht dieses Verfahren.

Das solcherweise vorbereitete Rubidiumchlorid wurde mit der berechneten Menge Oxalsäure in Wasser aufgelöst. Beim Abkühlen scheidet sich das Tetraoxalat fast ohne Verlust aus. Dies wurde durch Dekantieren von der Mutterlauge getrennt und weiter 31-mal wiederholt aus Wasser umkrystallisiert. Fig. 2 zeigt dieses Verfahren.

Das Rubidiumtetraoxalat ist äußerst günstig zur Umkrystallisation : das in kaltem Wasser wening lösliche Salz löst sich in heißem leicht und glatt, nach 31-maliger Umkrystallisation wurde 35.6% der anfänglichen Salzmenge gewonnen, und daher darf man annehmen, daß die Ausbeute 1- und 10-maliger Umkrystallisation 96.7% bezw. 71.7% betragen solle.

Weil das Salz beim Glühen leicht zerfällt und ins Carbonat übergeht, dient es sehr zweckmäßig als das Ausgangsmaterial beim Herstellen anderer Rubidiumsalze.

(C) Chemische Spektralanalyse der Produkte

Ungefähr um jede fünfte Umkrystallisation wurde ein Teil Salz zur Probe genommen, die auf einer Platinschale mäßig erhitzt, bis das Aufblasen der Schmelze sich aufhörte, und somit zur Analyse vorbereitet wurde. Die chemische, semi-quantitative Spektralanalyse wurde mit Littrowschem Spektrogramm nach Glimmschicht-spaltabbildungsmethode ausgearbeitet. Die so erhaltenen Resultate stehen in Tabelle 3.

Tabelle 3

Die Resultate der semi-quantitativen Analyse der Produkte

Produkt	Li(%)	Na(%)	K(%)	Cs(%)
K_5	0.001>	0.01	0.5~1	0.5~1
K_{10}	〃	〃	~0.5	0.1~0.5
K_{15}	〃	〃	0.1~0.5	0.05~0.1
K_{21}	〃	〃	~0.1	~0.001
K_{25}	〃	〃	0.05~0.1	~0.001
K_{31}	〃	〃	0.05~0.1	~0.001

K_n: Krystall nach n-maliger Umkrystallistation.

Wie aus dem Löslichkeitsunterschied hervorgeht, wurde das Cäsium rascher als das Kalium entfernt und gegen Ende der Umkrystallisierreihe wurde reines Rubidiumpräparat erhalten. Die letzten Mengen des Kaliums (0.05~0.1%) haften hartnäckig dem Rubidiumpräparat an und werden auch durch andere, geeignete Methoden schwer beseitigt. Wohl mag dies nicht nur auf Verbrauch der Glasgeräte zurückzuführen sein.

Zusammenfassung

(1) Die Löslichkeit der Tetraoxalate des Kaliums, des Rubidiums und des Cäsiums wurde von neuem bestimmt. Die des Cäsiumtetraoxalates wurde viel geringer als die ältere Angabe gefunden.

(2) Das rohe Rubidiumtetraoxalate wurde 31-mal aus Wasser umkrystallisiert.

(3) Die chemische Spektralalyse zeigt, daß bei der Umkrystallisation des Salzes das Cäsium sowie das Kalium in die Mutterlauge geht und allein das Rubidium im Krystall sich anreichert.

(4) Die Endprodukte stellten reines Rubidiumpräparat dar.

(5) Die Nach-und Vorteile dieser Methode werden hier nicht wiederholt erwähnt.

Herrn Prof. K. Kimura möchte ich für seine wertvollen Ratschläge bei dieser Untersuchung meinen besonderen Dank aussprechen.

Die chemische Spektralanalyse wurde von Herren H. Kakihana und M. Fujimoto durchgeführt. Dafür bin ich ihnen auch herzlich dankbar.

Chemisches Institut der Wissenschaftlichen Fakultät, Universität zu Tokyo.

Infrared Absorption Studies of Tropolone and Allied Compounds

by Kenji KURATANI, Masamichi TSUBOI and Takehiko SHIMANOUCHI

(Received March 5, 1952)

Introduction

The chemistry of the seven-membered unsaturated ring has rapidly developed in recent years. A number of new compounds with this ring have been synthesized and their structural formulas determined.[1a][1b] Of their spectroscopy, however, much work is yet to be done.[2] The present paper describes the infrared absorption spectra of tropolone and the related compounds prepared by Dr. T. Nozoe and his coworkers (Tohoku University, Sendai) who have carried out an extensive work in tropolone chemistry.[1a]

Experimental

Infrared absorption measurements were made by means of the Baird Infrared Spectrophotometer with a NaCl prism. Of the absorptions in the region above 2800 cm.$^{-1}$, measurements were also made by using a quartz spectrometer with higher resolving power, which was described in a previous paper.[3] The absorption curves obtained are shown in Figs. 1—6. Names, and

(1a) Nozoe, *Sci. Pap. Tohoku Univ. Ser.* 1, **34**, 199 (1950). *Proc Japan Acad.*, **26**, 30 (1950). Nature, **167**, 1055 (1951). *Chem. and Ind.* (Chem. Soc. Japan), **4**, 348 (1951).

(1b) Cook and London, *Quart. Rev.*, **5**, 99 (1951). Johnson, *Sci Progr.*, **39**, 405 (1951).

(2) Scott and Tarbell. *J. Am. Chem. Soc.*, **72**, 240 (1950). Doering and Knox, *J. Am. Chem. Soc.*, **73**, 828 (1951).

(3) Tsuboi, this Bulletin, **22**, 215 (1949).

melting points of the compounds examined are listed in Table 1. On dissolving the dried sample

Table 1

Substances	Melting points °C.	Absorption curves	References
tropolone	50—51	a	(i)
o-isopropyltropolone	33.2—34	b	(ii)
m-isopropyltropolone	51—52	c	(iii)
p-isopropyltropolone	77—78.5	d	(iv)
o-methyltropolone	49.5—50.5	e	(v)
m-methyltropolone	75—76	f	(v)
p-methyltropolone	108—110	g	(v)
o-bromotropolone	107—108	h	(i)
p-bromotropolone	190—191	i	(i)
o, *o'*-dibromotropolone	159—160	j	(vi)
o, *o'*, *p*-tribromotropolone	125—126	k	(i)
tropolone methyl ether	b.p. 125/5 mm.	l	(vii)
tropolone methyl ether+$^1/_2H_2O$	40.5	—	(vii)
tropolone acetate	69.5—70.5	m	(viii)
2-phenyltropone	85.8—86.5	n	(ix)
2-aminotropone	106—107	o	(x)

(i) Nozoe, Seto, Kitahara, Kunori and Nakayama, *Proc. Japan Acad.*, **26** (1950), 38.
(ii) Nozoe, Yasue and Yamane, *Proc. Japan Acad.*, **27** (1951), 15.
(iii) Nozoe and Katsura, *J. Pharm. Soc. Japan*, **69** (1944), 181.
(iv) Nozoe. Seto, Kikuchi and Takeda, *Proc. Japan Acad.*, **27** (1951), 146.
(v) Nozoe, Mukai and Matsumoto, *Proc. Japan Acad.*, **27** (1951), 110; Nozoe, Mukai and Matsui, *Proc. Japan Acad.*, in press.
(vi) Nozoe, Kitahara, Yamane and Yoshikoshi, *Proc. Japan Acad.*, **27** (1951), 18.
(vii) Nozoe, Seto, Ikemi and Arai, *Proc. Japan Acad.*, **27** (1951), 102.
(viii) Nozoe, Seto and Sato, to be published.
(ix) Nozoe, Mukai and Mineguchi, *Proc. Japan Acad.*, **27** (1951), 419.
(x) Nozoe, Seto, Takeda, Morosawa and Matsumoto, *Proc. Japan Acad.*, **27** (1951), 556.

of tropolone methyl ether in carbon tetrachloride or carbon disulphide, special care was taken to prevent it from being moistened because of its highly hygroscopic property.

Hydrogen Bond and Conjugated Double Bonds in the Tropolone Ring.—That tropolone has an intramolecular hydrogen bond of the form:

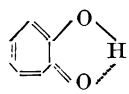

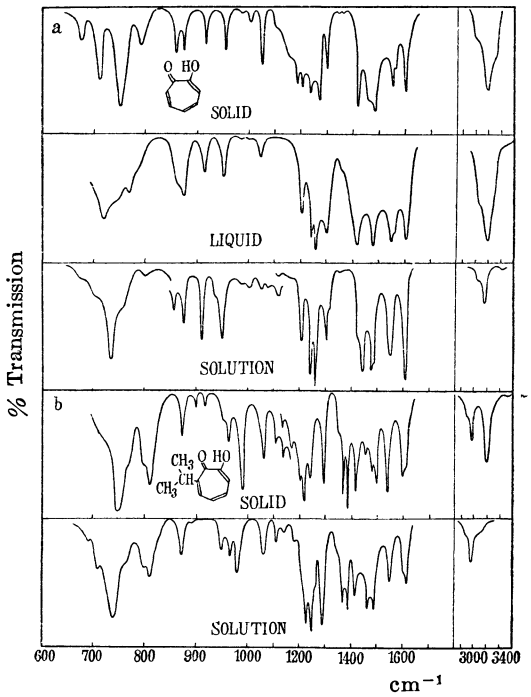

Fig. 1 A.—Infrared spectra of tropolone and *o*-isopropyltropolone.
Spectra in solids: samples molten and solidified between the two sylvine plates.
Spectra in solutions: 1300—630 cm.$^{-1}$, about 5% CS_2 solutions 4000—900 cm.$^{-1}$, about 5% CCl_4 solutions, cell thickness 0.1 mm.

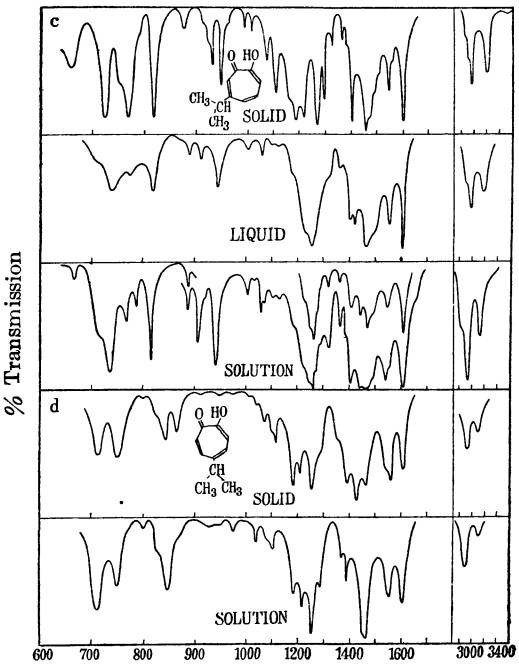

Fig. 1 B.—Infrared spectra of *m*- and *p*-isopropyltropolone.

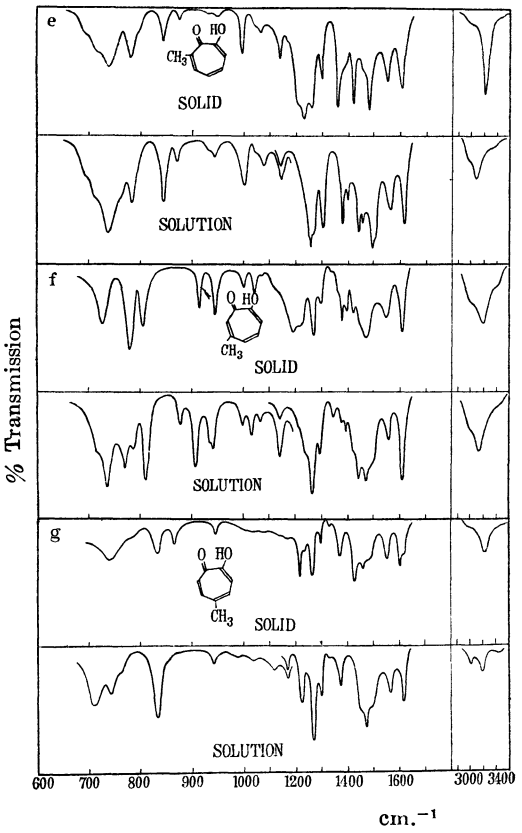

Fig. 1 C.—Infrared spectra of *o*-, *m*- and *p*-methyltropolone.

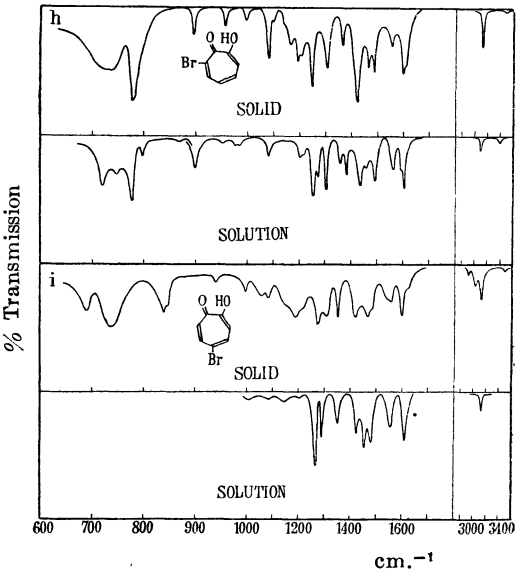

Fig. 1 D.—Infrared spectra of *o*- and *p*-bromotropolone.

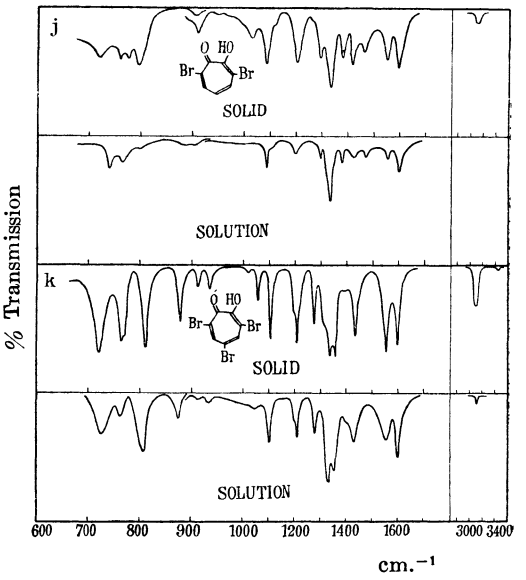

Fig. 1 E.—Infrared spectra of di- and tribromotropolone.

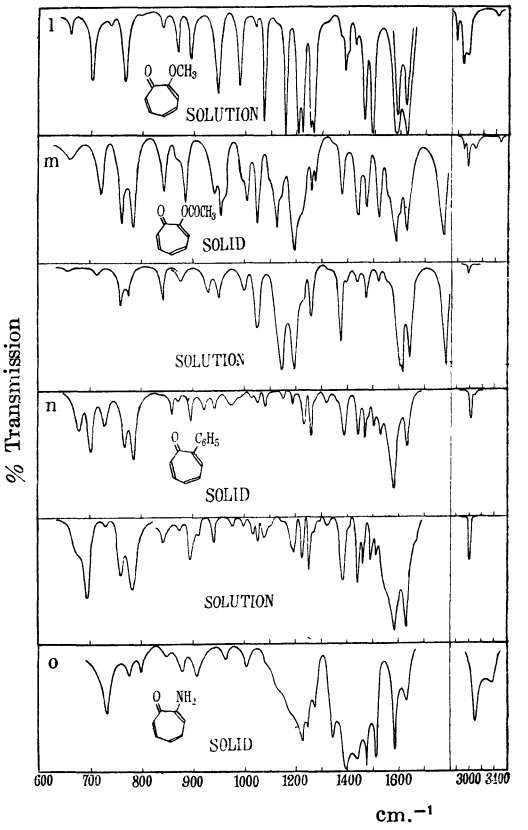

Fig. 1 F.—Infrared spectra of tropolone methyl ether, tropolone acetate, phenyltropone, and aminotropone.

has already been shown from the result of its dipole moment measurement[4] and from its infrared spectra.[5] The present studies have afforded further evidence for this conclusion. Thus, the O—H stretching band of tropolone observed in 0.01 mol./l. carbon tetrachloride solution is located at 3.2 μ (Fig. 2A), a position much displaced from that of the free O—H band, 2.8 μ,

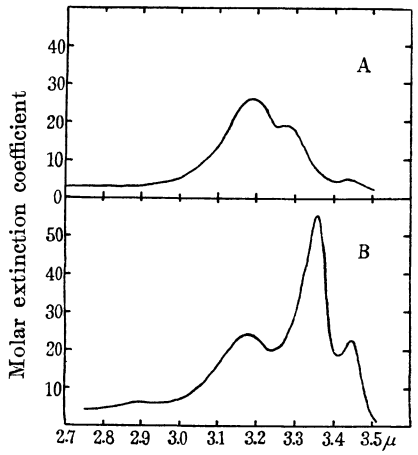

Fig. 2.—Near infrared absorption curves for (A) tropolone and (B) hinokitiol in 0.01 mol./l. CCl_4 solutions.

showing that the OH is hydrogen-bonded. Further, no change has been observed in the feature of the spectrum at all, even the concentration of the solution was changed from 0.004 to 0.1 mol./l., indicating that the hydrogen bonding is intramolecular. The unusually great shift of the O—H band of tropolone from that of free O—H band shows that the hydrogen bonding is correlated with the conjugation of the double bonds in tropolone—in other words, there is a kind of so-called "conjugated chelation"[6] in tropolone molecule. It may also be seen that the chelation in tropolone is stronger than those of *o*-substituted phenols (with O—H band at about 3.1 μ) and is weaker than those of the enol-forms of acetyl acetone and acetoacetic ethyl ester (with O—H band at about 3.7 μ[6]).

The C—H stretching absorption of tropolone is found at 3.3 μ but not in the 3.4—3.5 μ region Fig. 2A). This is consistent with the wellknown fact that all the carbon atoms in the tropolone molecule are unsaturated.

The near infrared spectra of *m*-isopropyltropolone (hinokitiol) and *o*- and *p*-isopropyltropolone (α- and γ-thujaplicin) (Fig. 1, b and d) are similar to that of tropolone in most respects, except the presence of the 3.4—3.5 μ bands in the former, which are due to the isopropyl group. Bromotropolones (Fig. 1, h, i, j, and k) exhibit their hydrogen-bonded O—H band 3.2 μ and unsaturated C—H band at 3.3 μ, just as tropolone does. On the other hand, tropolone methyl ether, 2-phenyltropone, and tropolone acetate exhibit no band at 3.2 μ, corresponding to the fact that they have no O—H group. Moreover tropolone methyl ether containing 1/2 H_2O shows its O—H band at 2.86 μ (Fig. 3).

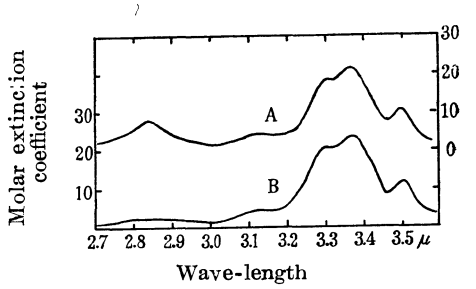

Fig. 3.—Near infrared absorption curves for (A) tropolone methyl ether with 1/2 H_2O and (B) dried tropolone methyl ether in 0.02 mol./l. CCl_4 solutions.

Special attention is called to the double bond region (1700—1500 cm.$^{-1}$) of the absorption spectra of troponoid[7] compounds. In tropolone methyl ether as well as tropolone acetate and 2-phenyltropone, the stretching vibrations of the C=O and C=C bonds are found, respectively, at 1630 and 1580 cm.$^{-1}$ (Fig. 1, l, m, and n), instead of at their normal positions which are respectively at 1720 and 1660 cm.$^{-1}$. This may be ascribed to the conjugation between the C=C and C=O bonds. Further, in tropolone as well as methyl-, isopropyl- and bromo-tropolones with the intramolecular hydrogen bonds the C=C and C=O frequencies appear in still lower frequency regions ——*i.e.* respectively at 1610 and 1560 cm.$^{-1}$ (Fig. 1, a-k). This fact may be taken as indicating that the intramolecular hydrogen bonding affects the electronic state of the tropolone ring, and, accordingly, affects the force constants of the C=C and C=O bonds in the ring.

The effect of intramolecular hydrogen bonding upon the electronic state of tropolone ring is also shown from the observation of its ultraviolet spectrum. Tropolone methyl ether and tropolone acetate exhibit one strong absorption band at about 320 mμ in the near ultraviolet region, while tropolone anion:

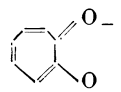

exhibits two bands at 330 and 393 mμ. The ultraviolet absorption spectra of tropolone and

(4) Kurita, Nozoe and Kubo, this Bulletin, **24**, 10 (1951).
(5) Koch, *J. Chem. Soc.*, 512 (1951).
(6) Rasmussen, Tunnicliff and Brattain, *J. Am. Chem. Soc.*, **71**, 1068 (1949).
(7) Dr. Nozoe gives a name "troponoids" to the allied compounds of tropone.

hinokitiol with intramolecular hydrogen bond possess features intermediate between those of tropolone methyl ether (or tropolone acetate) and tropolone anion, indicating that they are intermediate in electronic state.[8]

The Proton-Accepting Powers of Tropolone Methyl Ether and Hinokitiol Methyl Ether.—As has been mentioned above, tropolone has the stronger intramolecular hydrogen bond than *o*-substituted phenols. In order to obtain further information about the hydrogen-bond-forming powers of the compounds with the seven-membered unsaturated ring, the methyl ethers of tropolone and hinokitiol were compared with benzaldehyde as to their proton-accepting powers, by the method described in a previous paper.[9] The hydrogen-bonded complexes:

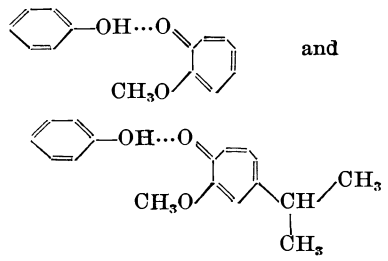

exhibit O—H bands at 3.00 and at 3.02 μ in dilute carbon tetrachloride solutions respectively (Fig. 4), while the complex:

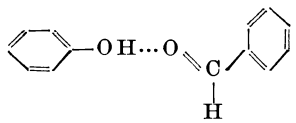

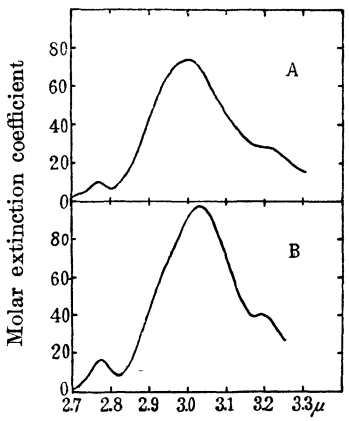

Fig. 4.—Near infrared absorption curves of phenol in (A) phenol (0.01 mol./l.)+tropolone methyl ether (0.02 mol./l.)+CCl_4 and in (B) phenol (0.01 mol./l.)+hinokitiol methyl ether (0.02 mol./l.)+CCl_4

exhibits O—H band at 2.89 μ. From the amount of these complexes in the solutions (estimated from the intensity measurement of these O—H bands) and from the amount of shifting of these O—H bands from free-phenol O—H band (2.77 μ), it is concluded that the proton-accepting powers of the methyl ethers of tropolone and hinokitiol are stronger than that of benzaldehyde.

The Vibrational Spectra and the Structure of Troponoid Compounds.—Corresponding to the arrangement of the substituent groups of benzene, characteristic absorption bands due to the out-of-plane C—H deformation vibrations are found in the region of 900—750 cm.$^{-1}$.[10] In the case of sevenn-membered unsaturated ring compounds, similar strong characteristic bands are found as shown in Table 2. The data given in the table will be useful for the determination of the structural formulas of the tropolone derivatives.

Table 2

Types of substitutions	Examples	Frequencies
1, 2-substituted	tropolone	735 cm.$^{-1}$
	tropolone methyl ether	770
	tropolone acetate	750 or 770
1, 2, 3-substituted	*o*-isopropyltropolone	800
	o-methyltropolone	782
	o-bromotropolone	770
1, 2, 4-substituted	*m*-isopropyltropolone	820
	m-methyltropolone	812
1, 2, 5-substituted	*p*-isopropyltropolone	850
	p-methyltropolone	830
	p-bromotropolone	850

Spectra of Troponoids in the Solid State.—Infrared spectra of tropolone and isopropyltropolones in the solid state are considerably different from those in solutions (Fig. 1, a—d). When they are brought from the solutions into the solid state, some of their absorption bands increase in relative intensity (for example, 1190—1210 cm.$^{-1}$ bands probably due to O—H deformation vibrations contained in them) and some become doublets (Fig. 1, b and c). The hydrogen-bonded O—H bands become, on solidification, stronger (in comparison with the C—H bands) and sharper, and at the same time shift towards shorter wave lengths (Fig. 1, b, e, f, g; Fig. 2 and 5). This indicates that the correlation between conjugation and hydrogen bonding in tropolonoid molecules is less remarkable in solid states than in solutions. According to the private communication of Prof. I. Nitta and Dr. K. Osaki, the presence of ring dimer with intermolecular double hydrogen bonds:

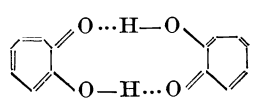

(8) Ultraviolet absorption studies of troponoids will be published elsewhere.

(9) Tsuboi, this Bulletin, **25**, 60 (1252).

(10) For example, Colthup, *J. Opt. Soc. Am.*, **40**, 397 (1950).

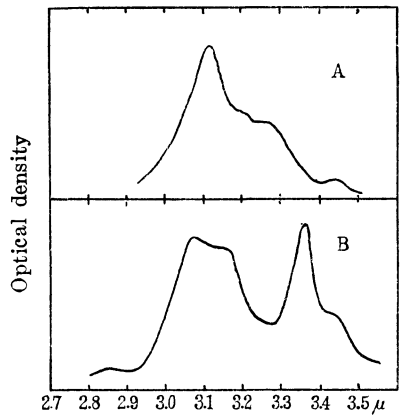

Fig. 5.—Near infrared absorption curves for (A) tropolone and (B) hinokitiol in solid states.

in tropolone crystal is recently proved from its x-ray analysis. Since tropolone in solutions has an intramolecular hydrogen bond and is in monomeric state, there must be a change in the behavior of hydrogen-bonding on its solidification. The observed changes in the spectra of tropolone and the allied compounds may be attributed to such changes in the behavior of hydrogen-bonding. A fact, perhaps worthy of note in this connection, is that the spectra of tropolone and hinokitiol in liquid states are closer to those in solutions than to those in the solid state, as may be seen from the comparison of the absorption curves shown in Fig. 1, a and c. The infrared spectra of some of the bromo-substituted tropolones are almost independent of their phase changes (Fig. 1, h—k).

Spectrum of Aminotropone.— Aminotropone exhibits two N—H stretching absorption bands at 2.83 μ (3530 cm.$^{-1}$) and 2.97 μ (3360 cm.$^{-1}$) (Fig. 6). This fact may be explained from the structure of this compound:

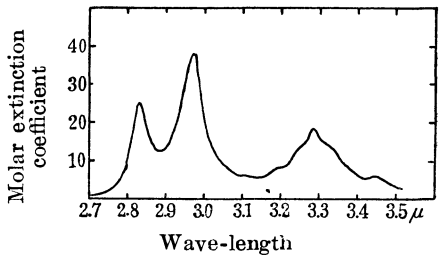

Fig. 6.—Near infrared absorption curve for aminotropone in 0.02 mol./l. CCl_4 solution.

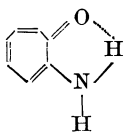

the former band being assigned to the free N—H vibration and the latter to the hydrogen-bonded N—H vibration. On the other hand, double-bond absorption bands observed for this compound are situated at 1624 and 1590 cm.$^{-1}$ (Fig. 1, o)——positions not much displaced from those observed for tropolone methyl ether. This shows that the internal hydrogen bond of aminotropone is weak.

In conclusion the writers wish to express their sincere thanks to Professor San-ichiro Mizushima for his kind guidance in this work, and to Professor Tetsuo Nozoe, Shuichi Seto, Yoshio Kitahara, Toshio Mukai, and other members of the Laboratory of Organic Chemistry, Faculty of Science, Tohoku University for their placing the samples at the writers' disposal and for their valuable suggestions. The cost of this work has been partly defrayed by a grant from the Ministry of Education.

Department of Chemistry,
Faculty of Science, University of Tokyo.

Dichroisms of Benzene Rings. III. The Dichroism of *m*-Nitronitrosobenzene Monomer

By Kazuo NAKAMOTO

(Received March 6, 1952)

Introduction

In the previous works, the dichroisms of aromatic compounds[1],[2] and molecular compounds[3] have been measured, and the general rules about the π-band have been found in respective cases. Throughout these works, however, the band at the longest wave length side

(1) K. Nakamoto, *J. Am. Chem. Soc.*, **74**, 390 (1952).
(2) K. Nakamoto, ibid., **74**, 392 (1952).
(3) K. Nakamoto, ibid., **74**, 1739 (1952).

was always superposition of the strong π-band and the weak band due to the substituents of the benzene ring. Accordingly, it was impossible to observe the dichroism characteristic of the substituents.

To measure the dichroism of the substituent band independently of the intense π-band, it is necessary to select a substance whose spectrum in crystalline state shows the band of the former, far apart from the latter in the ultraviolet region. As was shown in the spectrum of anthraquinone crystal,[2] the carbonyl band is superposed on the intense π-band, although they show definite peaks in solution. So the substance, which has both the bands far apart in the spectrum of the solution, is suitable for our purpose.

Nitrosobenzene derivatives have, generally, their characteristic bands due to the nitroso group at 700~800 mμ, and the π-bands due to the benzene ring at 300~400 mμ. They are therefore expected to appear separately even in the crystalline state.

In the present study, the spectra of *m*-nitronitrosobenzene monomer in crystalline state as well as in solution have been measured, and the results have been discussed in comparison with that of *m*-dinitrobenzene which had been reported before.[2]

Experimental

Material.—*m*-Nitronitrosobenzene was prepared by reduction of *m*-dinitroboenzene according to the method of Alway and Gortner.[4] Colourless powder (dimer). It melts at 91° to become a green liquid (monomer). For the purpose of getting fine crystals suitable for the measurement of dichroism, the ordinary method of recrystallization from the solution is not available, because the substance is unstable and apt to polymerize. By mixing the alcoholic solutions of *m*-nitronitrosobenzene and *m*-dinitrobenzene in the molar ratio of 1:1, light green acicular crystals were obtained. They are isomorphous to pure *m*-dinitrobenzene crystal, and have similar properties to it. Spectroscopic measurement, described later, revealed that they are composed of 25 per cent nitroso compound and 75 per cent dinitro compound. They show straight extinction, and dichroic property; light green by linearly polarized light with the electric vector vibrating parallel to the c-axis (needle axis), and light yellow, by the light with those vibrating perpendicular to it (b-axis).

Measurements.—Absorption spectra in solution were measured by the rotating sector method. Dichroism of the crystal was measured by the microscopic method mentioned in the former work.[1] Throughout these experiments, infrared sensitive photo-plates were used to measure the green region.

Results and Discussion

(1) The Spectrum of the Solution

Absorption spectra of *m*-dinitrobenzene and pure *m*-nitronitrosobenzene in alcoholic solutions are shown in Fig. 1. Numerical data characterizing these spectra are given in the following table.

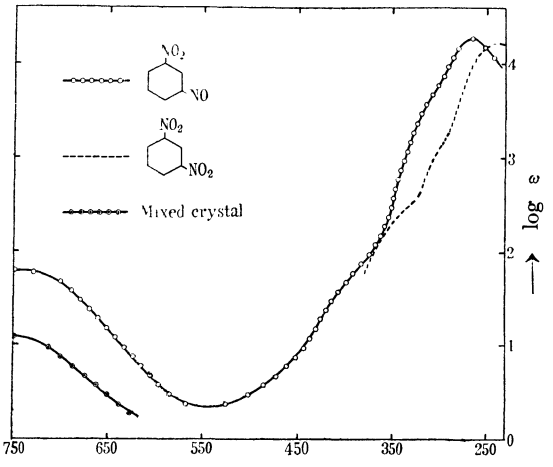

Fig. 1.—Absorption spectra of *m*-nitronitrosobenzene, *m*-dinitrobenzene and their mixed crystal in alcoholic solutions.

	Nitroso band	Nitro band	π-band	σ-band
m-Dinitrobenzene		330(2.5)	300(3.1)	250(4.2)
m-Nitronitrosobenzene	750(1.8)	390(1.8)	320(3.4)	265 (4.25)

Here the $\lambda_{max.}$ is expressed in mμ, and the log $\varepsilon_{max.}$ is given in brackets, respectively.

As is shown above, the substitution of one of the nitro groups by the nitroso group causes the occurrence of the nitroso band at about 750 mμ, and gives bathochromic and hypochromic effects to the nitro band. But the same substitution gives only small bathochromic and hyperchromic effects to the π- and σ-bands in the ultraviolet region. These changes in the spectrum can be easily explained by the facts that the nitroso group is more unstable than the nitro group, and a substitution of an unstable group for a stable group gives, generally, bathochromic and hyperchromic effects to all the bands in a molecule.

The absorption spectrum of an alcoholic solution of the mixed crystal is also shown in Fig. 1. From the comparison of log ε at 750 mμ in these two curves, the crystal was estimated to contain as much *m*-nitronitrosobenzene as 25 per cents.

(2) The Dichroism of the Crystal

The crystal used for the measurement contains

(4) F. J. Alway and R. A. Gortner, *Ber.*, **38**, 1900 (1905).

25 per cent nitroso compound, as spectroscopically shown before. Practically, two components can mix at any ratio in crystal, and, moreover, no colour change can be seen at the mixing of their solutions. These chemical facts suggest that in the crystal used, the two components exist merely in a mixed state and not as a molecular compound.

So far, its crystal structure is unknown, although that of pure *m*-dinitrobenzene has been thoroughly studied.[2] So the Debye-Scherrer photographs of both the crystals have been taken, as shown in Fig. 2. The resemblance of the two photographs means that the two crystals have similar structure and so, its crystal structure can be presumed as follows: the planar molecules* of *m*-nitronitrosobenzene in *m*-dinitrobenzene crystals are piled up along the needle axis (c-axis), making their molecular planes almost parallel to the a-axis and inclined by about 20° to the b-axis, as graphically shown in Fig. 3.

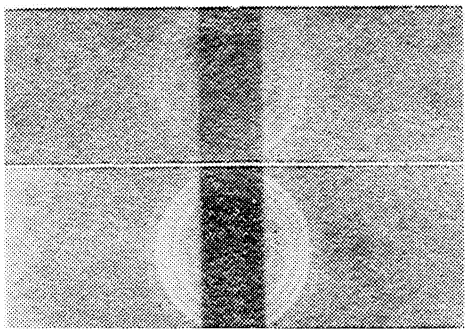

Fig. 2.—Debye-Scherrer photographs of pure *m*-dinitrobenzene (A) and the mixed crystal (B)

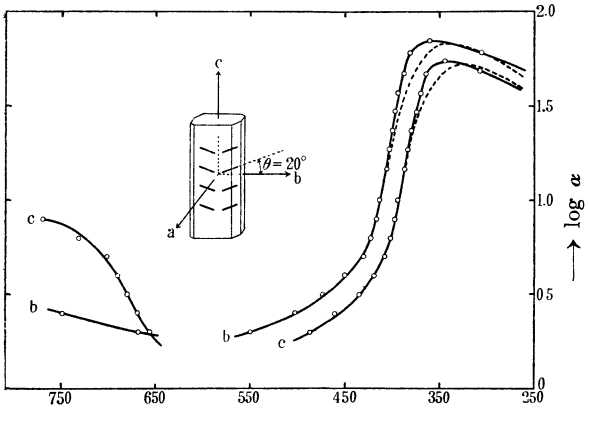

← Wave length, mμ.

Fig. 3.—Absorption spectra of the mixed crystal (solid lines) and *m*-dinitrobenzene (broken lines) in crystalline states.

* The steric configuration of nitrosobenzene derivatives is a subject of much discussion. None of these crystals, however, have ever been studied by X-ray analysis. So, in the present paper, the C-N-O bond is assumed to be nearly linear and coplanar with the benzene plane.

Absorption curves by linearly polarized lights with the electric vectors vibrating parallel to the b- and c-axes are shown in Fig. 3. As the angle θ between the molecular plane and the b-axis is only 20° and smaller than 45°, the light with the electric vector parallel to the b- (or c-) axis is abundant with the parallel (or perpendicular) component to the molecular plane. Conforming to these discussions with the experimental result, we can reach the conclusion that the ∥-absorption in the ultraviolet region is bathochromic and hypsochromic to the ⊥-absorption, whereas the former in the visible region is remarkably hypsochromic to the latter.

(3) The Dichroisms of pure *m*-Nitronitrosobenzene Monomer

If the absorption due to pure *m*-dinitrobenzene is reduced from the above results, the dichroism of pure *m*-nitronitrosobenzene is obtained.

(i) Visible Region

As is clearly shown in the former work, *m*-dinitrobenzene has no absorptions in the visible region. So the above result in this region is exclusively due to pure nitroso compound. Thus, it is concluded that the ⊥-absorption is hypsochromic to the ∥-absorption. The origin of this band is the nitroso group in the molecule, as is definitely shown in the spectrum of the solution. As a result, the absorption responsible for the green colour of *m*-nitronitrosobenzene is concluded to be due to the electronic transition polarized perpendicularly to the C—N—O bond. Recently Fenimore[5] obtained the same result as above. He, however, used the assemblage of many microcrystals which orientated practically parallel to each other, and measured the dichroism in the narrow range between 700~800 mμ. Whereas, we used only one single crystal, and measured in a wider range between 750~250 mμ.

(ii) Ultraviolet Region

Broad bands seen in the ultraviolet region consist mainly of the π-absorption, as already discussed in the former paper.[2] In Fig. 3 is shown the present result (solid lines) along with the dichroism of *m*-dinitrobenzene (broken lines). Both spectra are very similar to each other, except that the former is slightly bathochromic in comparison with the latter. This result suggests that both substances have similar dichroic property, and the dichroism of the π-band does not suffer any considerable change, even if *m*-dinitrobenzene in the crystal is replaced by *m*-nitronitrosobenzene.

Thus, we conclude that the ∥-absorption in pure *m*-nitronitrosobenzene is bathochromic and hypsochromic to the ⊥-absorption. If both molecules formed a molecular compound, the feature of the spectrum would be quite different.[3] This result, along with the above mentioned chemical facts, confirms the theory that the crystal observed here is only a mixed crystal, and not a molecular compound.

(5) C. P. Fenimore, *J. Am. Chem. Soc.*, **70**, 3114 (1948).

Summary

Absorption spectra of *m*-nitronitrosobenzene monomer in crystalline state as well as in solution have been measured quantitatively in the visible and the ultraviolet regions. In its π-band of the ultraviolet region, the general rule about the π-band of the benzene ring was found to hold also for the present case. In regard to the nitroso band of the visible region, the absorption by linearly polarized light with the electric vector vibrating perpendicular to the C—N—O bond was hyperchromic to the absorption by the light with those vibrating parallel to it. This result suggests that the green colour of *m*-nitronitrosobenzene is due to the electronic transition polarized perpendicularly to the C—N—O bond.

The author wishes to express sincere thanks to Prof. R. Tsuchida for his kind guidance and Mr. H. Matsuda for his help in X-ray work.

Department of Chemistry, Faculty of Science, Osaka University, Osaka

The Infrared Dichroism of Amides

By Kenji KURATANI

(Received February 26, 1952)

The measurement of the infrared dichroism is a useful method of determining the position of hydrogen atoms in molecules. With regard to the structure of amide groups this technique was first applied to urea by Keller[1] and then to acetanilide by Brown and Corbridge.[2] The author suggested in a previous paper[3] that Keller's conclusion was inaccurate and that the correct determination of planarity of urea should be made, using the dichroism of NH stretching vibrations. Recently using the grating spectrometer, Waldron and Badger[4] measured the dichroism of NH stretching vibrations and the planarity of urea molecule was accurately proved. In this paper, the infrared absorption spectra of trichloroacetamide and deuterated monochloroacetamide were measured and the observed vibrational frequencies of amide groups were assigned. With this result together with the measurement of infrared dichroism of benzamide and monochloroacetamide, the position of hydrogen atoms in these molecules is discussed.

Experimental

Infrared spectra of trichloroacetamide and deuterated monochloroacetamide were measured with a Baird spectrophotometer. Infrared dichroism of benzamide and monochloroacetamide were measured with the apparatus described in our previous papers,[5] though we also used a selenium reflexion polarizer (the incident angle about 70°) to provide plane polarized infrared radiation. The direction of the electric vector of the incident radiation was parallel to the entrance slit.

A small amount of the solid was molten between a pair of sylvine plates. The specimens were cooled in such a way as to induce as far as possible the crystallization in oriented linear fashion. Absorption intensities of these specimens were measured with the direction of the orientation of crystals either parallel or perpendicular to the electric vector of the incident plane-polarized radiation.

Materials.—The samples of amide were obtained as follows: benzamide was recrystallized from water (m.p. 127—8°), and monochloroacetamide was prepared from ethyl monochloroacetate and ammonia and then recrystallized from water by Mr. I. Nakagawa (m.p. 120°). Deuterated monochloroacetamide was obtained by repeating the exchange reaction with heavy water, and trichloroacetamide was prepared from ethyl trichloroacetate and ammonia by Mr. T. Sugita (m.p. 140°).

Results

Infrared absorption spectra of deuterated

(1) Keller, *J. Chem. Phys.*, **16**, 1003, (1948).
(2) Brown and Corbridge, *Nature*, **162**, 72 (1948).
(3) Kuratani, *J. Chem. Soc. Japan*, **71**, 22 (1950).
(4) Waldron and Badger, *J. Chem. Phys.*, **18**, 566 (1950).
(5) Shimanouchi, Tsuruta and Mizushima, *Sci. Pap. I. P. C. R.*, **42**, 165 (1945).

monochloroacetamide and trichloroacetamide are given in Fig. 1. and 2.

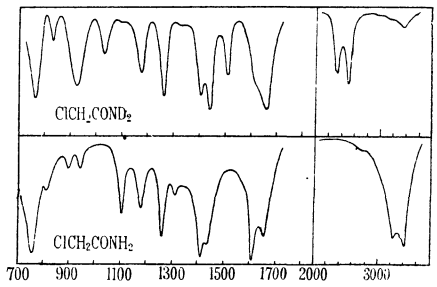

Fig. 1.—Infrared spectra of monochloroacetamide and partially deuterated monochloroacetamide.

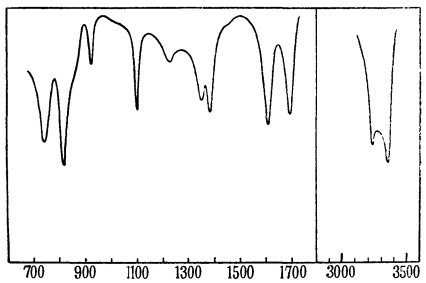

Fig. 2.—Infrared spectrum of trichloroacetamide.

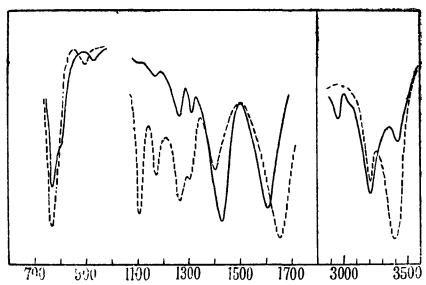

Fig. 3.—Polarized spectra for oriented crystals of monochloroacetamide. Electric vector of the beam is parallel (dotted curve) and perpendicular (full curve) to the direction of the crystal growth.

The absorption spectra of monochloroacetamide with the orientation of crystals parallel or perpendicular to the incident radiation are given in Fig. 3. The experimental results of the absorption spectra of benzamide were in agreement with those of Mann and Thompson.[6] The absorption peaks are summarized in Table 1, in which we have used the term

(6) Mann and Thompson, *Proc. Roy. Soc.* (*London*), **A, 192**, 489 (1948).

Table 1

Monochloroacetamide		Benzamide	
Bands	Dichroism	Bands	Dichroism
766 s	∥	768 s	⊥
804 w	⊥ ?	790 s	⊥ ?
890 w	∥ ?	805 s	⊥ ?
924 w	⊥ ?	920 m	?
1100 m	∥	1020 m	?
1180 s	∥	1120 m	∥ ?
1265 s	∥	1140 m	∥
1310 m	∥	1300 m	∥
1410 s	∥	1405 s	⊥
1430 s	⊥	1450 m	?
1610 s	⊥	1575 s	∥
1660 m	∥	1620 s	⊥
2960 m	⊥	1660 s	∥
3200 s	⊥	3200 s	⊥
3400 s	∥	3400 s	∥

"parallel dichroism" to describe larger absorption when the electric vector vibrates parallel to the axis of orientation than when it vibrates in a perpendicular direction, and the term "perpendicular dichroism" which is the reverse. Benzamide has other weaker bands, i. e., 843, 995, 1070, 1175, 1250 and 1495 cm.$^{-1}$, but the dichroism of these bands have not been determined.

Discussion

a) Vibrational Modes of Amide Group. —In the 9 vibrational modes of -$CONH_2$- group, OCN skeletal deformation vibration is not dealt with since this vibration lies beyond the observed frequency region. The remaining 8 modes are indicated in the first column of Table 2.

Table 2

Vibrational Modes	Notations	Assignment
NH_2 symmetric stretching	$\nu(NH_2)_s$	−3400 cm.$^{-1}$
NH_2 antisymmetric stretching	$\nu(NH_2)_a$	−3200
C=O stretching	$\nu(C=O)$	−1660
C−N stretching	$\nu(C-N)$	−1400
NH_2 symmetric deformation	$\delta(NH_2)$	−1600
NH_2 rocking, NH_2 wagging, NH_2 twisting; NH_2 rocking*	$\gamma(NH_2)$	−1150, —, —

(* The distinction of these 3 bands is not necessary for the following discussion.)

The characteristic vibrational frequencies of amide groups, i. e., the vibrational frequencies which are commonly found in amide groups are 3400, 3200, 1660, 1600, 1400, and 1150 cm.$^{-1}$.

These absorption frequencies are also observed in the case of trichloroacetamide which has no C—H bond (see Fig. 2). There is no doubt about the assignment of the first 3 bands and, therefore, only the assignment of the last 3 bands is discussed.

Based on the numerous experimental results, Randall[7] assigns the 1400 cm.$^{-1}$ band to ν(C—N) vibration. This conclusion is also supported by the presence of 1385 cm.$^{-1}$ band in trichloroacetamide (see Fig. 2), since in this case there is no possibility of the presence of $\delta(CH_3)$ vibration. (In general $\delta(CH_3)$ and $\delta(CH_2)$ vibrations are found in 1380—1480cm.$^{-1}$ region.)

The weakness of absorption bands at 1600 and 1100 cm.$^{-1}$ and the appearance of the bands at 830, 925 and 1030 cm.$^{-1}$ in the spectrum of deuterated monochloroacetamide, support the assignments of 1600 and 1100 cm.$^{-1}$ to NH_2 bending vibrations. These assignments are also confirmed by the frequency shift of 1600 and 1150 cm.$^{-1}$ bands in $CO(NH_2)_2$ to 1250 and 990 cm.$^{-1}$ in $CO(ND_2)_2$,[8],[9] and the shift of 1150 cm.$^{-1}$ band in CH_3CONH_2 to lower frequency region in CH_3COND_2.[10] The fact that primary amines have 1600 and 1150 cm.$^{-1}$ bands and secondary amines have only 1150 cm.$^{-1}$ band proves the assignments of 1600 cm.$^{-1}$ band to symmetric deformation vibration, and 1150 cm.$^{-1}$ band to NH_2 or NH rocking vibration. This conclusion is consistent with the assignment of Axford, Janz and Russel[11] on methylhydrazine, and that of Kahovec and Kohlrausch[12] on the Raman lines of various amides. Cleaves and Plyler[13] made the same assignment for 1625 and 1150 cm.$^{-1}$ bands of methylamine measuring the band contours of these bands. These considerations confirm the assignment of vibrational bands of amide groups as indicated in the right column of Table 2.

b) Relation between the Molecular Structure and Infrared Dichroism.—In the first place let us discuss the cofiguration of CNH_2 groups of amide molecules. For CNH_2 group, we may consider 2 configurations, in one of which C—N bond is almost perpendicular to the plane of NH_2 group as in the case of methylamine molecule, and in the other the C—N bond is in the NH_2 plane as in the case of urea molecule.

When the C-N bond is nearly perpendicular to the plane of NH_2 group, the vibrational modes of 1600 and 1150 cm.$^{-1}$ bands become as shown in Fig. 4.[14] In this case the direction of the dipole moment change of ν(C—N)

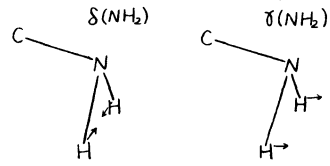

Fig. 4.—Vibrational modes for the nonplanar form.

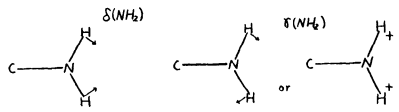

Fig. 5.—Vibrational modes for the planar form.

mode coincides with that of $\gamma(NH_2)$ mode and, therefore, ν(C—N) shows the same dichroism as $\gamma(NH_2)$. However, the direction of the dipole moment change of $\delta(NH_2)$ is perpendicular to that of ν(C—N) and the dichroism of $\delta(NH_2)$ is opposite to that of ν(C—N).

On the other hand, when the 2 hydrogen atoms lie on the same plane with carbon and nitrogen atoms as in the case of urea molecule, the vibrational modes of 1600 and 1150 cm.$^{-1}$ bands become as shown in Fig. 5.[14] In this case ν(C—N) band shows the same dichroism as $\delta(NH_2)$ and the opposite dichroism as $\gamma(NH_2)$. Accordingly the planarity of C—NH_2 group, i. e., whether C—NH_2 group is more similar to methylamine or to urea, is determined from the dichroism of 1600, 1400, and 1150 cm.$^{-1}$ bands. Of course, the accurate angle between C—N bond and NH_2 plane will be determined from the measurement of the pleochroism of these bands, but in the present experiment only the dichroism was measured and only the more favorable form was determined.

Monochloroacetamide.—Since chloroacetyl chloride, bromoacetyl chloride and bromoacetyl bromide[15] have their CH_2 deformation frequencies in the range of 1390—1400 cm.$^{-1}$, the

(7) Randall, Fowler, Fuson and Dangl, "Infrared Determination of Organic Structures" New York (1949).
(8) Kellner, *Proc. Roy. Soc. (London)*, **A. 177**, 456 (1941).
(9) Otvos and Edsall, *J. Chem. Phys.*, **7**, 632 (1939).
(10) Lenormant, *Compt. rend.*, **228**, 1861 (1949).
(11) Axford, Janz and Russel, *J. Chem. Phys.*, **19**, 709 (1951).
(12) Kahovec and Kohlrausch, *Z. phys. Chem.*, B. **51**, 49 (1942).
(13) Cleaves and Plyler, *J. Chem. Phys.*, **7**, 563 (1939).

(14) Since 1150 cm.$^{-1}$ Raman line of formamide is a polarized one, vibrational modes of this frequency are confined to these figures.
(15) Mizushima and Nakagawa, to be published shortly.

1410 and 1430 cm.$^{-1}$ bands of monochloroacetamide are most reasonably interpreted as being a CH_2 deformation and a C—N stretching vibration, respectively. The propriety of the planar structure as shown in Fig. 5 is deduced from the fact that 1430 and 1610 cm.$^{-1}$ bands have the same dichroism and 1100 cm.$^{-1}$ band has the dichroism opposite to them.

This conclusion is verified by the experiment in the 3 micron region. The same dichroism of ν(C—N) and $\nu(NH_2)_s$, i. e., 1430 and 3200 cm.$^{-1}$ bands, is the excellent evidence of the planarity of C—NH_2 group.

Benzamide.—The opposite dichroism of 1400 and 1140 cm.$^{-1}$ bands assigned, respectively to ν(C—N) and $\gamma(NH_2)$ vibrations of benzamide, prefers the planar structure without the discussion of the dichroism of $\delta(NH_2)$ vibration. The same dichroism of ν(C—N) and $\nu(NH_2)_s$ vibrations confirms this conclusion.

On account of the planarity of carbon, nitrogen and hydrogen atoms, remaining possibilities of amide structure are confined to 2 forms. In one of these, NH_2 group lies on the same plane with C—O—N skeleton (form I), and in the other, CNH_2 plane intersects the plane of C—O—N skeleton at right angles (form II). (Only the more symmetrical forms are considered.)

The depolarization degree of Raman lines assigned to NH_2 stretching vibrations will be useful to distinguish the 2 forms, because in structure I both Raman lines due to NH_2 symmetric and antisymmetric stretching vibrations are polarized, while in structute II, the depolarized Raman line due to NH_2 antisymmetric stretching vibration should be observed. However, the depolarization degree of Raman lines of amides has not yet been measured.

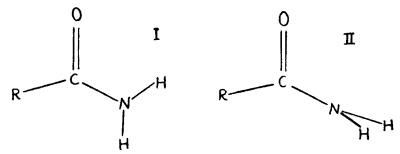

Fig. 6.

The direction of the dipole moment change of $\nu(NH_2)_a$ vibration is parallel to that of ν(C=O) vibration in structure I, and perpendicular in structure II. Therefore from the relation between the dichroism of $\nu(NH_2)_a$ and ν(C=O) (3400 and 1660 cm.$^{-1}$ bands), we can determine whether the structure of amides is consistent with I or II. The experimental result supports structure I for monochloroacetamide and benzamide molecules.

The writer wishes to express his sincere thanks to Professor San-ichiro Mizushima, and Assistant Professor Takehiko Shimanouchi for their kind guidance. The writer also thanks to Messrs. Tatsuo Miyazawa, Tadao Sugita, and Ichiro Nakagawa for their kind assistance throughout this work. The cost of this work has been partly defrayed by a grant from the Ministry of Education.

Institute of Science and Technology,
Tokyo University, Tokyo

The Change of Molecular Weight of Egg Albumin in Aqueous Solutions

By Kazuo SHIBATA and Koichi MURAI

(Received September 13, 1951)

Heller and Klevens[1] have recently measured the molecular weight of egg albumin in aqueous solutions by the light transmission method, and obtained a value of 47,000 immediately after the preparation of the sample at 4°C. With the lapse of time after the preparation, however, the value obtained gradually increased, namely 64,000 after 24 hours and 81,000 after 72 hours. This phenomenon was considered to be due to the occurence of aggregation, but the details of the process were not relevantly worked out by these authors. The purpose of this study is to elucidate the nature of the process, with special reference to the effect of temperature upon the phenomenon in question.

(1) W. Heller and H. B. Klevens, *Phys. Rev.*, **67**, 61 (1945). W. Heller, ibid., **68**, 5 (1945).

The solution used was a 0.3% aquous solution of egg albumin, which was prepared by dissolving egg albumin (preparation of Takeda Pure Chemicals LTD.) in distilled water. The relative value of the molecular weight of egg albumin in aqueous solution was measured by determining the turbidities of solutions, using a Pulfrich photometer provided with a special device for measuring the scattered light. The change of the molecular weight was observed at several intervals of time in the aqueous solution of egg albumin, which was immersed in the water baths regulated at 30°C., 40°C. and 50°C., respectively.

The results obtained are shown in Fig. 1, where the abscissa is the time in hours and the ordinate is relative value W of the weight average molecular weight, assuming the value immediately after the preparation of the solution as unity. As will be seen from this figure, the value of W increased rapidly within a few hours and reached the maximum value in four hours. In one experiment observation was continued over night, but from the fifth hour on, the value W was found to remain practically unchanged. To one of the samples (200 cc.), in which W had already reached its maximum value at 30°C., 5 cc. of 10 N urea solution were added, whereby no change of W could be observed. The rise of temperature caused both the increase of the initial velocity and the increase of the maximum value of W.

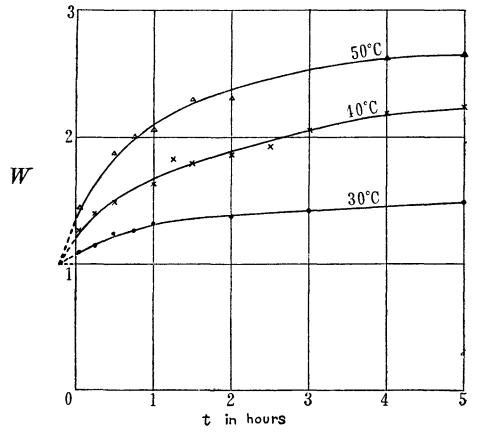

Fig. 1.

As was suggested by Heller and Klevens, the observed increase of molecular weight may be due to the process of aggregation. Let us assume that the aggregation takes place in the manner of the following polymerization reaction.

$$M_1+M_1 \xrightarrow{k} M,\quad M_1+M_2 \xrightarrow{k} M_3,\quad M_1+M_3 \xrightarrow{k} M_4,\ldots\ldots$$
$$M_2+M_2 \xrightarrow{k} M_4,\quad M_2+M_3 \xrightarrow{k} M_5,\ldots\ldots\ldots\ldots$$
$$\ldots\ldots\ldots\ldots\ldots\ldots\ldots\ldots\ldots\ldots$$
$$M_i+M_i \xrightarrow{k} M_{2i},\ldots\ldots M_i+M_j \xrightarrow{k} M_{i+j},\ \ldots\ldots$$
$$\ldots\ldots\ldots\ldots$$

where M_1, M_2..... indicate monomer, dimer and so on, i and j being assumed to be any integer. The velocity constant for each step of aggregating reactions is assumed to be the same. For such a type of multistep reactions, a theory had already been develoded by Flory,[2] according to whom, the number of moles of i-mers, N_i, which has been formed at the time t, is given by the following equation;

$$N_i = N_0 p^{i-1}(1-p)^2 \qquad (1)$$

in which

$$p = \frac{kt}{2+kt}.$$

N_0: Total number of moles of the monomer at the beginning. It has already been shown by Doty, Zimm and Mark[3] that whereas osmotic pressure measurements yield a number average molecular weight, turbidity measurements give a weight average. Therefore, the value W which we have observed is the relative value of weight average molecular weight M to the molecular weight of the monomer M_0. Hence,

$$W = M/M_0 = \frac{1}{M_0}\cdot\frac{\sum_i (iM_0)^2 N_i}{\sum_i iM_0 N_i} = \frac{\sum i^2 N_i}{\sum iN_i} = \frac{\sum i^2 p^{i-1}}{\sum ip^{i-1}} \qquad (3)$$

Using the relations

$$\sum_i ix^{i-1} = (1-x)^{-2} \qquad (4)$$

$$\sum_i i^2 x^{i-1} = (1-x)^{-3}(1+x), \qquad (5)$$

equation (3) becomes

$$W = \frac{1+p}{1-p}$$

(2) P. J. Flory, *J. Am. Chem. Soc.*, **58**, 1877 (1936); **59**, 241 (1937); **61**, 1518, 3334 (1939); **62**, 1057, 1561, 2255, 2261 (1940); **63**, 3083, 3091, 3096 (1941).

(3) P. M. Doty, B. H. Zimm and H. Mark, *J. Chem. Phys.*, **13**, 159 (1945).

$$=1+kt. \qquad (6)$$

This equation indicates that the initial velocity of the increase of W is k. The value k for each temperature can be evaluated from the data of our experiments. Based on the temperature dependency of k, the activation energy of the reaction was calculated to be 7 kcal./mole.

If we further assume that each reaction step has the same equilibrium constant (K), then the following relation must hold for the number fractions $m_i=N_i/N_0$;

$$K=\frac{m_{i+j}}{m_i \cdot m_j}.$$

This equation must hold for any choice of i and j, but the equations thus obtained are not necessarily independent of each other. Actually, the relation $(i=2, j=2)$ can be derived from the equations for $(i=1, j=1)$, $(i=1, j=2)$ and $(i=1, j=3)$. As will be seen from this example, the independent relationship will be the following;

$$m_i K=x^i, \qquad (7)$$

in which

$$x = Km_1.$$

Using equations (4), (5) and (7), the relative value of weight average molecular weight at equilibrium may be expressed by

$$W=\frac{1}{M_0}\cdot\frac{\sum_i (iM_0)^2 Ni}{\sum_i iM_0 Ni}$$

$$=\frac{\sum i^2 mi}{\sum imi}$$

$$=\frac{\sum i^2 x^i}{\sum ix^i}$$

$$=\frac{1+x}{1-x}. \qquad (8)$$

For obtaining the relation between K and W, we shall use the following relation;

$$\sum_i im_i=1, \qquad (9)$$

which must be true according to the definition of m. Substituting equation (7) in (9), we have

$$K=\frac{x}{(1-x)^2}. \qquad (10)$$

Since we have equation (8) relating x to W, we can express K in terms of W at equilibrium; that is

$$K=\frac{1}{4}(W^2-1). \qquad (11)$$

Using this equation, we evaluated K at each temperature, and calculated the change of heat content from the temperature dependency of K, which amounted to 7 kcal./mole. If we extrapolate our result of analysis to the case of lower temperatures, the value of W at equilibrium is calculated to be 1.04 at 0°C., which shows that almost no egg albumin molecules will aggregate at 0°C. Whether or not this conclusion is valid, it remains to be checked by further investigations.

The author is much indebted to Dr. Hiroshi Tamiya for his constant help and advice.

Tokugawa Institute for Biological Research

Synthetic Studies on the Δ^2-Derivatives of Selenazolines

By Yutaka MIZUHARA

(Received March 18, 1952)

The possible heterocyclic syntheses according to the schema which follow

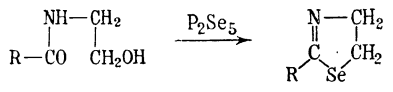

were pursued in our laboratory, with the desire to obtain selenium-containing ring compounds.

From N-acylethanolamine, H. Wenker[1] synthesized Δ^2-oxazolines and Δ^2-thiazolines.

(1) H. Wenker, *J. Am. Chem. Soc.*, **57**, 1080 (1935).

The procedure was not applied for the preparation of Δ^2-selenazolines.

Recently A. Van Dormael[2] made report on the formation of 2-methylselenazoline by a similar method to Wenker's procedure for the preparation of 2-methylthiazoline.

Hitherto 2-methylselenazoline has been prepared from diacetyldiaminoethyl-β-diselenide hydrochloride and phosphorus pentachloride.[3] It has also been synthesized from bromoethylamine hydrobromide and selenoacetamide.[4]

Unintentionally I have investigated also the reaction between N-acyletanolamine and phosphorus pentaselenide, which was found later to be similar to A. Van Dormael's procedure. This report* describes five homologues of Δ^2-selenazolines, three of which are 2-alkyl derivatives—2-methylselenazoline, 2-ethylselenazoline, and 2-*n*-propylselenazoline; and two of which are 2-aryl derivatives—2-phenylselenazoline, 2-benzylselenazoline. I found that the 2-aryl derivatives were solid and did not give picrates. Contrarily, the 2-alkyl derivatives were liquid and gave picrates easily. In the three 2-alkyl derivatives, the boiling point rises according to the increase of alkyl group weight. However the relation between the melting point of their picrates and the boiling point of free bases is reverse. The higher homologues are more stable and the yields are better.

This procedure is much simpler than the methods which so far have been devised and is convenient to obtain Δ^2-derivatives of selenazolines.

Experimental

Phosphorus pentaselenide.—Phosphorus pentaselenide was prepared by the methods described by W. Bogen[5] and by W. Muthmann & A. Clever.[6]

N-Acylethanolamines. — N-Acylethanolamines were synthesized by the double decomposition of ethanolamines and acid esters. The boiling points of the acylethanolamines used here were as follows:

Acetylethanolamine, b.p. 161°/4.5 mm. Hg,
Propionylethanolamine, b.p. 155—156°/7 mm. Hg,
Butyrylethanolamine, b.p. 159.5°/5 mm. Hg,
Benzoylethanolamine, b.p. 202—203°/4 mm. Hg,
Phenylacetylethanolamine, b.p. 207~209°/6.5 mm. Hg.

Δ^2-Selenazolines

(i) **2-Propylselenazoline.**—The procedure described here for 2-propylselenazoline was also used for the preparation of the other two 2-alkylselenazolines. In a 500 cc. Claisen distilling flask N-butyrylethanolamine (20 g.) and phosphorus pentaselenide (20.9 g., 5:1.5 mol.) were placed. The flask was connected with a condenser set for downward distillation. A Y-type adaptor was attached tightly at the place between the lower end of the condenser and a receiver. A tube then ran from the side arm of the adaptor to some bottles of granular sodium hydroxide and strong caustic soda to dissolve and decompose any hydrogen selenide which might be formed. The mixture was heated gently in an oil bath to 70—90°, when the reaction commenced violently with a rapid evolution of hydrogen selenide. The heat source was withdrawn until the reaction moderated. After the vigorous reaction had subsided, the flask was arranged for distillation under diminished pressure. The yellow-green liquid was collected at 110—135°/120—150 mm. Hg. During the distillation the bath temperature was maintained at about 200—230°. The liquid collected weighed 16.9 g. (yield 63%). By repeated redistillation 2-*n*-propylselenazoline, a light green liquid (8.7 g., yield 32.4%) which boiled at 116°/70.5 mm. Hg was obtained. The picrate was obtained by adding the base to a saturated alcoholic solution of picric acid. When this material was recrystallized from hot alcohol, it was often decomposed. The crude picrate was recrystallized from chloroform-ligroin, yellow crystals, m.p. 100.5—101°. (Found: C, 35.62; H, 3.33; N, 13.60. Calculated for $C_{12}H_{14}O_7N_4Se$: C, 35.56; H, 3.48; N, 13.82%).

(ii) **2-Ethylselenazoline.**—The procedure for 2-ethylselenazoline was similar to the procedure described above in the preparation of 2-*n*-propylselenazoline. The yellow orange liquid (2.4 g., yield 34.8%) distilled at 70—90°/60—70 mm. Hg (bath temperature of 180—190°) was made from propionylethanolamine (5 g.) and phosphorus pentaselenide (5.85 g., 5:1.5 mol).

The redistillation of the crude material gave light green liquid which boiled at 110—111°/135 mm.Hg (1.3 g., yield 19.4%). The picrate was labile in alcoholic solution. The recrystallization of the crude picrate from chloroform-ligroin yielded yellow prisms, m.p. 127—127.5° (Found: C, 34.07; H, 3.03; N, 14.25. Calculated for $C_{11}H_{12}O_7N_4Se$: C, 33.77; H, 3.09; N, 14.32%).

(iii) **2-Methylselenazoline.**—By the same procedure as mentioned above, the orange-yellow liquid (6.8 g., yield 18.2%) distilled at 80—92°/50—60 mm.Hg (bath temperature of 160—175°) was made from N-acetylethanolamine (26 g.) and phosphorus pentaselenide (34.4 g., 5:1.5 mol.). Repeated redistillation gave a light yellow liquid

(2) A. Van Dormael, *Chem. Abstr.* **44**, 144 (1950).
(3) W. Michels, *Ber.*, **25**, 3048 (1892).
(4) F. L. White, *Chem. Abstr.* **27**, 5550 (1933); *Brit. Pat.* 392,410.
* The present paper was read at the 4th Annual Meeting of the Chemical Society of Japan in Tokyo held in April 6, 1951.
(5) W. Bogen, *Ann.*, **124**, 57 (1862).
(6) W. Muthmann and A. Clever, *Zeit. anorg. Chem.*, **13**, 191 (1897).

(5.2 g., yield 13.9%) which boiled at 102°/145 mm. Hg. This boiling point coincided with b.p. 160—162°/752 mm. Hg,[3] 71—72°/35 mm. Hg[4] shown in the literatures. The crude picrate recrystallized from chloroform, yellow crystals, m.p. 159—159.5°, which also coincided with the melting point in the literature.[3]

(iv) **2-Phenylselenazoline.**—N-Benzylethanolamine (5 g.) and phosphorus pentaselenide (2.75 g., 5:1 mol.). were placed in a flask. The thermometer was inserted nearly to the bottom of the flask. The reaction started at about 80°, proceeded rapidly at about 120° with the evolution of white smoke, and the temperature rose spontaneously to about 140—160°. Soon the reaction ended. The yellow transparent resinous product was dissolved in chloroform, first washed with about 60 cc. of 5% sodium hydroxide solution and then washed with distilled water. White needles crystallized in the chloroform solution. The chloroform was distilled off under reduced pressure, leaving white yellow solid (3 g.). The recrystallization from benzene (70 cc.) gave white needles, m.p. 116—118°, softening at 105° (2.3g., yield 36.2%). (Found: C, 51.69; H, 4.39; N, 6.72. Calculated for C_9H_9NSe; C, 51.45; H, 4.32; N, 6.67%). The crystals obtained here did not give picrate, differing from the 2-alkylselenazolines.

(v) **2-Benzylselenazoline.**—By the same procedure as mentioned in 2-phenylselenazoline, a yellow-brown transparent resin was obtained from N-phenylacetylethanolamine (5 g.) and phosphorus pentaselenide (2.55 g., 5:1 mol.). The resinous mass was dissolved in chloroform (10 cc.), washed with 5% sodium hydroxide solution (50 cc.) and with distilled water. The chloroform was distilled under reduced pressure, leaving a yellow solid (3.45 g.). The recrystallization from benzene (100 cc.) gave yellow crystals, m.p. 122—124°, softening at 117°. Recrystallization thrice from benzene raised the melting point to 123—126°, softening at 122° but without being decolourized. The elementary analysis showed a fair coincidence with the theoretical value. (Found: C, 53.55; H, 5.30; N, 6.19. Calculated for $C_{10}H_{11}NSe$: C, 53.58; H, 4.95; N, 6.25%). The crystals also did not give picrate.

Summary

(i) Several derivatives of Δ^2-selenazolines were synthesized from N-acylethanolamine and phosphorus pentaselenide.

The larger the alkyl group was, the better the yield became.

(ii) 2-Arylselenazolines were solid and did not give picrates, differing from 2-alkylselenazolines.

The above results are largely due to the kind guidance of Professor Sumio Umezawa and the assistances of Kazuo Suzuki, and Yoshiro Itō who have helped me. Many thanks for their continual kindness.

Department of Applied Chemistry, Engineering Faculty of Keiō University, Tokyo.

Walden Inversion of Amino Acids. VI. The Synthesis of D-Surinamine (N-Methyl-D-tyrosine)

By Nobuo IZUMIYA and Atsuo NAGAMATSU

(Received March 27, 1952)

The synthesis of L-surinamine was carried out by Fischer and Lipschitz[1] from L-tyrosine through *p*-toluenesulfonyl derivatives. Recently, Corti[2] treated L-tyrosine with dimethyl sulfate and obtained L-surinamine. But no synthesis of D-surinamine has yet been attempted. The present study was undertaken to accomplish the synthesis of D-surinamine, and the reactions utilized were as follows:

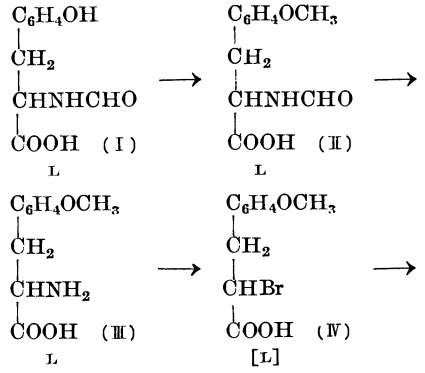

(1) E. Fischer and W. Lipschitz, *Ber.*, **48**, 360 (1915).
(2) U. A. Corti, *Helv.*, **32**, 681 (1949).

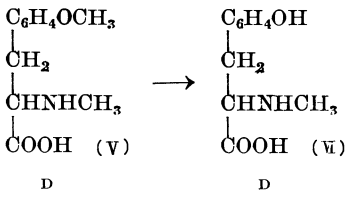

One of us (N. I.) has reported the results of his studies on Walden inversion of some amino acids,[3] such as δ-benzoyl-L-ornithine, ε-benzoyl-L-lysine, L-methionine, S-methyl-L-cysteine, S-butyl-L-cysteine, S-benzyl-L-cysteine, O-methyl-L-threonine, β-methoxy-DL-norvaline and 1 (or 3)-benzyl-L-histidine, and recognized a certain regularity in the case of amination and methylamination at 0 and 100° of the [L]-α-bromo acid prepared by the action of nitrosyl bromide on L-amino acid.

O-Methyltyrosine produced by the action of ammonia on the bromo acid (IV) at 100° was racemic, but O-methyltyrosine obtained at 0° was of D-form and showed the occurrence of Walden inversion. In the case of methylamination either at 100 or 0°, the obtained O, N-dimethyltyrosine was of D-form. But it must be noted that Rivers and Lerman[4] synthesized O-methyl-D-tyrosine before we did by the reaction of ammonia on bromo acid (IV) at 0°.

Though N-formyl-L-tyrosine was synthesized by Fischer[5] in 1907, we obtained a good yield of the substance by the method of Fruton and Clarke.[6] O-Methyl-L-tyrosine had already been prepared by Behr and Clarke[7] by methylation and subsequent hydrolysis of N-acetyl-L-tyrosine, and by Rivers et al.[4] by catalytic reduction of O-methyl-N-carbobenzoxy-L-tyrosine. But, the method adopted by the present authors seems preferable to the existing methods described above in the yield and the procedure. The compound (III) had $[\alpha]_D^{17} = -5.7°$ (the authors), $[\alpha]_D^{29} = -5.9°$[7] and $[\alpha]_D^{17} = -10.0°$.[4] Therefore, it was expected that we might obtain a partly racemized product after formylation. But actually, L-tyrosine obtained by the hydrolysis of our -O methyl-L-tyrosine and D-surinamine by the methylamination of bromo acid (IV) and subsequent hydrolysis were optically pure substances.

Experimental

N-Formyl-L-tyrosine (I).—L-Tyrosine (18.1 g.), having m.p. 314~316° (decomp.) and $[\alpha]_D^{10} = -12.1°$ (c=2.81, 3N HCl), was treated with 85% formic acid (220 cc.) and acetic anhydride (65 cc.) by Fruton and Clarke's method of formylation. At the end of the reaction, the solution was evaporated under reduced pressure. An ice cold N-hydrochloric acid was added to the remaining product to dissolve tyrosine not reacted on, and the compound (I) was collected by filtration, and washed with a small amount of cold water. It was recrystallized from water, and obtained 16.3 g. (yield 78%). It had no crystal water and remained as a non-hydrated compound even when exposed to the air for a long time. It has m. p. 170~171° and $[\alpha]_D^{10} = +89.4°$ (c=1.74, ethyl alcohol). Found: N, 6.64%; neut. equiv., 213. Calculated for $C_{10}H_{11}O_4N$: N, 6.70%; neut. equiv., 209.1.

Fischer[5] has described this substance as having one mole of crystal water, m. p. 171° and $[\alpha]_D^{25°} = +84.8°$ (dried substance, c=2.20, alcohol).

O-Methyl-N-formyl-L-tyrosine (II).—The compound (I) (20.9 g.) was dissolved in 4N-sodium hydroxide (50 cc.). The solution was then treated alternately with 4N-sodium hydroxide (10 cc.) and dimethyl sulfate (4.76 cc.) with mechanical stirring, the temperature being held at 30~35° by cooling; the addition was repeated four times in all. Stirring was continued for two hours at room temperature after all of the dimethyl sulfate had been added. The solution was acidified with 8N-nitric acid, and the crystal was collected and recrystallized from water. 20.3 g. was obtained (yield 91%). It had m. p. 152~154° and $[\alpha]_D^{10} = +94.7°$ (c=2.11, alcohol). Found: N, 6.31%; neut. equiv., 226. Calculated for $C_{11}H_{13}O_4N$: N, 6.28%, neut. equiv., 223.1.

The compound (I) was methylated with methyl iodide and sodium hydroxide in the usual way,[1] and the product obtained had m. p. 151~154°, showing correct elementary analysis. But, in this case, the fact that the product contained a small amount of the compound (I) was recognized in the paper chromatogram of the hydrolysate of this product.

O-Methyl-L-tyrosine (III).—The compound (II) (11.2 g.) was hydrolysed with 3N-hydrochloric acid (100 cc.) for 2 hours. The solution was evaporated under reduced pressure, and the concentration was repeated with the addition of water. The residue was dissolved in a small amount of water and neutralized with ammonia. After cooling, the resulting crystal was collected. This was recrystallized from hydrochloric acid and ammonia, and 8.6 g. was obtained (yield 88%). It had m. p. 263~265° (decomp.) and $[\alpha]_D^{10} = -5.7°$ (c=2.02, 3N HCl). Its phenylhydantoic acid had m. p. 176° and $[\alpha]_D^{15} = +127.5$ (c=3.89, alcohol).

Its *p*-toluenesulfonyl derivative had m. p. 66~

(3) N. Izumiya, *J. Chem. Soc. Japan, Pure Chem. Sect.*, **71**, 500 (1950), **72**, 26, 149, 445, 550, 702, 1050 (1951); The result of concerning, 1 (or 3)-benzyl-L-histidine is unpublished.

(4) R. P. Rivers and J. Lerman, *J. Endocrinol.*, **5**, 223 (1948).

(5) E. Fischer, *Ber.*, **40**, 3716 (1907).

(6) J. S. Fruton and H. T. Clarke, *J. Biol. Chem.*, **106**, 667 (1934).

(7) L. D. Behr and H. T. Clarke, *J. Am. Chem. Soc.*, **54**, 1630 (1932).

67° and $[\alpha]_D^{15}=+32.8°$ (c=3.34, alcohol). Found: N, 3.88%. Calculated for $C_{17}H_{19}O_5NS$: N, 4.01%.

The compound (III) was converted into L-tyrosine by the action of hydroiodic acid. The resulting L-tyrosine was confirmed as optically pure, and had $[\alpha]_D^{10}=-11.9$ (c=2.57, 3N HCl).

Behr et al.[7] have reported the compound (III) as having m. p. 264~265° (decomp.) and $[\alpha]_D^{29}=-5.9°$ (2% in N HCl), and its phenylhydantoic acid as having $[\alpha]_D^{21}=+123.6°$ (4% in alcohol). Rivers et al.[4] have reported the compound (III) as having m. p. 259~260° (decomp.) and $[\alpha]_D^{17}=-10.0°$ (2% in N HCl).

[L]-α-Bromo-β-(p-methoxy phenyl) propionic acid (IV).—The compound (III) (0.1 mol.) and potassium bromide (0.35 mol.) were dissolved in 2.5N-sulfuric acid (0.52 mol.). To the mixture was added sodium nitrite (0.16 mol.) in the usual way.[3] The resulting pale yellow crystal was collected, washed with water. Ths yield was 84 %. It had m. p. 85~89° and $[\alpha]_D^{10}=+13.8°$ (c=1.74, alcohol). It became oily when it was recrystallized from alcohol and water. Found: Br, 29.4%. Calculated for $C_{10}H_{11}O_3Br$: Br, 30.8%.

Rivers et al.[4] have reported it as having m. p. 98~99°.

O-Methyl-DL-tyrosine.—The brome acid (IV) (5.18 g.) was dissolved in 60 cc. of ammonia (saturated at 0°) and heated in a sealed tube at 100° for 1 hour. The solution was evaporated to dryness under reduced pressure, and the residue was collected by the aid of a small amount of cold water. It was recrystallized from hydrochloric acid and ammonia, and 3.20 g. was obtained (yield 82%). This had m. p. 285~287° (decomp.) and no rotation. Found: N, 7.24%. Calculated for $C_{10}H_{13}O_3N$: N, 7.18%. Its phenylhydantoic acid had m. p. 192~193° and showed no appreciable rotation. Found: N, 9.07%. Calculated for $C_{17}H_{16}O_4N_2$: N, 8.92%.

Dakin[8] has reported O-methyl-DL-tyrosine as having m. p. 295° (decomp.).

O-Methyl-D-tyrosine.—The bromo acid was dissolved in ammonia in the manner described above and kept at 0° for 7 days. The yield was 79%. It had m.p. 262~263° (decomp.) and $[\alpha]_D^{10}=+5.4°$ (c=2.11, 3N HCl). Its phenylhydantoic acid had m. p. 176° and $[\alpha]_D^{10}=-124.6°$ (c=2.84, alcohol).

O, N-Dimethyl-D-tyrosine (V).—(A) The bromo acid (5.18 g.) was dissolved in 36 cc. of aqueous methylamine (33%) and heated in a sealed tube at 100° for 30 minutes. The solution was concentrated under reduced pressure, and the residue was collected. It was recrystallized from hydrochloric acid and ammonia, and 2.38 g. was obtained (yield 57%). It had m. p. 247~248° (decomp.) and $[\alpha]_D^{10}=-3.9°$ (c=2.02, 3N HCl). Found: N, 6.74%. Calculated for $C_{11}H_{15}O_3N$: N, 6.70%. (B) The bromo acid was treated in the manner described above and kept at 0° for 5 days. The yield was 64%. It had m. p. 247~249° (decomp.) and $[\alpha]_D^{10}=-3.8°$ (c=2.54, 3N HCl). Found: N, 6.77%. Calcd.: N, 6.70%.

D-Surinamine (VI).—(A) The compound (V) (2.09 g.), $[\alpha]_D^{10}=-3.9°$, was dissolved in 20 cc. of hydroiodic acid (saturated at 0°) and warmed in a sealed tube at 70° for 30 minutes. The solution was concentrated under reduced pressure repeatedly by adding some water each time. The residue was dissolved in a small amount of water and neutralized with ammonia. The resulting product was recrystallized from hydrochloric acid and ammonia, and 1.74 g. was obtained (yield 89 %). It had m. p. 273~274° and $[\alpha]_D^{15}=-18.9°$ (c=1.74, 3N HCl). Found: N, 7.07%. Calculated for $C_{10}H_{13}O_3N$: N, 7.18. (B) In the manner described above, D-surinamine was obtained from the compound (V) ($[\alpha]_D^{10}=-3.8°$). It had m. p. 273~275° (decomp.) and $[\alpha]_D^{15}=-19.1$ (c=2.02, 3N HCl).

Fischer et al.[1] have reported L-surinamine as having $[\alpha]_D^{21}=+19.8°$ and Corti[2] as having m. p. 273° (decomp.) and $[\alpha]_D^{19}=+19.1$~19.3.

Rf values of paper chromatography.—The composition of each solvent was as follows:—phenol: water=100:15, collidine:lutidine=2:5 (saturated with water); acetic acid-n-butanol:water=1:4:1. The figures denote the volumes. The amino acids were dissolved in N-hydrochloric acid and tested.

Amino acid	Solvent		
	Phenol	Collidine + Lutidine	Acetic acid + Butanol
L-Tyrosine	0.57	0.61	0.60
D-Surinamine	0·83	0.66	0.66
O-Methyl-L-tyrosine	0.77	0.59	0.70
O, N-Dimethyl-D-tyrosine	0.86	0.64	0.78

This work was carried out partly by the aid of the Scientific Research Funds of the Ministry of Education. The authors wish to thank Prof. Dr. R. Hirohata for his guidance in carrying out this work, and also Mr. S. Saeki for his microanalysis of the substances.

Department of Medical Chemistry, Faculty of Medicine, Kyushu University, Fukuoka

(8) H. D. Dakin, *J. Biol. Chem.*, **8**, 20 (1911).

Dichroic Study on Polyvinylalcohol Fiber. II. Effect of the Crystallinity and Moisture Content of the Fibers on Their Deformation

By Saburo OKAJIMA and Yasuji KOBAYASHI

(Received February 11, 1952)

Introduction

The authors studied previously the deformation of the regenerated cellulose fiber,[1] so now the Polyvinylalcohol (PVA) fibers are being studied. The chain molecule of PVA is considered to be very flexible as compared to that of the cellulose and this difference may be expected to appear also in the deformation course. Moreover, the mechanical properties of PVA gel changes remarkably with the crystallinity and the moisture content, and the crystallinity itself can be controlled easily by the heat treatment.[2] The study of these effects of inner structure upon the deformation is considered to be very important and very interesting not only from the theoretical standpoint but also as the basic phenomena in the synthetic fiber industry, especially of Japanese vinylon.

As to the method of study of the orientation degree changed by the deformation, the X-Ray method is not necessarily effective as the crystallinity of the non-heat-treated PVA is very poor and only the dichroic method is useful for the quantitative study, because it gives the orientation of the PVA molecules by using that of a direct dye as a parameter. The dichroic data of Congo Red has already been studied by the authors[3] in the case of the cellulose fibers. PVA fibers can be dyed with direct dyes.

The double refraction and the refractive indices methods are not useful at present as their basic data of PVA fiber of ideal orientation has not been found. These data will possibly be found in the future when the orientation of PVA fiber will be determined dichroitically.

Experiment

(1) Preparation of the isotropic PVA filament.—The isotropic model filament of PVA is prepared by melt-spinning as described in the first report;[4] A sample of PVA powder containing 50% moisture was melted at 140—150°C under 4 atm. and extruded through a glass nozzle in the air of room temperature. The obtained filament has a circular cross section and a smooth surface. The diameter is about 0.17 mm and nearly equal to that of the glass nozzle.

As to the isotropy of the filament it is not perfect, but it has a slight anisotropy and the outer layer of the filament has a positive double refraction and the core a negative one as P. H. Hermans described in the case of the cellulose fiber.[5] But this anisotropy is so slight that it can be used in the following study.

(2) Crystallization of the filament.—In the two series B and C the samples were partially crystallized by heating at 140°C for one hour in the aqueous solutions of 40 and 50% ammonium sulfate respectively. The autoclave required 30 min. to be heated to 140°C from the room temperature and also to be cooled from the same temperature. The treated filaments were washed thoroughly with water and air-dried.

(3) Stretching of the isotropic filaments.—The isotropic filaments, both the non-heat-treated seires A and the heat heat-treated B and C, were dyed with Congo Red and then conditioned and stretched. The dyeing conditions are described in the next section.

The conditioning was carried out in three desiccators at 20°C for 48 hours. The desiccators contained water and the saturated solutions of Na_2SO_4 10 H_2O and $(NH_4)_2SO_4$ and the relative humidities in each desiccator are 100, 93 and 81% respectively at 20°C. It has been confirmed by a preliminary test that the 48 hours' conditioning was sufficient to get the equilibrium states.

The conditioned samples were then stretched from l_0 to l (ca. 26 cm) and then air-dried after being placed in each desiccator for 48 hours more. The degree of stretching is given by $v=l/l_0$. In this case the change of the filament volume caused by stretching was so small that the correction in the value of v was not necessary.

The middle part of the stretched filament was

(1) S. Okajima and others, *J. Soc. Chem. Ind. Japan*, **48**, 85, 86 (1945); **49**, 52, 168 (1946); S. Okajima and Y. Kobayashi, This Bulletin **24**, 85 (1951); S. Okajima and S. Hayama, ibid., **24**, 90 (1951).

(2) I. Sakurada and K. Futino, *Bull. Inst. Phys. and Chem. Research, Japan*, **21**, 1077 (1942).

(3) S. Okajima, *Japan Science Review*, **1**, No. 2, 71(1950).

(4) S. Okajima and Y. Kobayashi, *J. Soc. Chem. Ind. Japan*, **52**, 794 (1951).

(5) P. H. Hermans, Physics and Chemistry of Cellulose Fiber, Elsevier, 1949, p. 387.

placed on the deck glasses, A and B in Fig. 1, and fixed on them at the points F with celluloid solution. Cutting off the filaments at C, A and B were used as the preparates for the measurement of D.

PVA filament can be stretched at its maximum to some 6-fold under the appropriate conditions as shown below and in this case the diameter of the sample decreased and became so thin that a special device was necessary to prevent the slippage at the clamps.

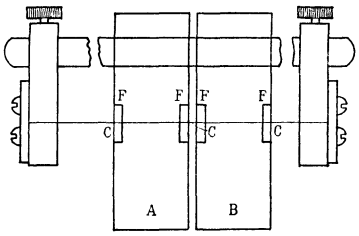

Fig. 1.

Dyeing condition of PVA filament for the dichroic study

As already shown,[3] it is necessary to dye the fiber suitably to obtain the reasonable value of D as the over-dyeing lowers the value enormously. This condition has already been determined in the case of the cellulose fibers, but the properties of PVA are so remarkably different from that of the cellulose that the composition of the dyeing bath was newly determined as below after many trials:

Congo Red: 0.025%,

Solvent: 50% Ethanol aqueous solution.

The filament was dyed in this bath for 48 hours at room temperature. The 48 hours' dyeing was confirmed to be necessary for the complete penetration of the dye in our filament. The ethanol solution was used to prevent the swelling of the non-heat-treated PVA filament.

The sample was taken out of the dye bath and air-dried by hanging in the room air after rinsing with water.

The fixed filament on a deck glass as above was mounted in Tricresylphosphate and the two principal coefficients of absorption, $K_{\parallel}$ and $K_{\perp}$, were determined as previously described.[3] $K_{\parallel}$ and $K_{\perp}$ are the coefficients of absorption of the dyed filament for D-line, oscillating parallel and perpendicular to the fiber axis, and $D=K_{\parallel}/K_{\perp}$ is a measure of the orientation degree of the filament.

Now dyeing to various deepnesses by controlling the dye concentration in the bath and plotting the values of $K_{\parallel}$ and $K_{\perp}$ of these filaments which have been stretched by 6-fold (the maximum stretching), the points appear as shown in Fig. 2. In the figure the points are likely to belong to a linear relation (1) till $K=0.5$, but for the larger values of $K_{\parallel}$ they deviate remarkably (over-dyeing).

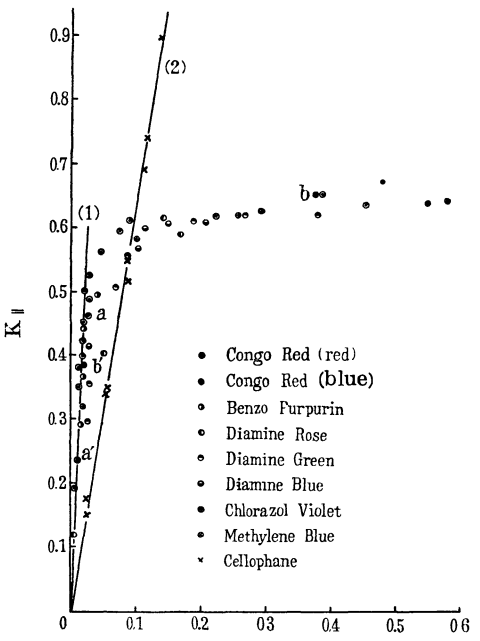

Fig. 2.

This phenomenon is the same as already shown in the case of the cellulose fibers.[3] In order to determine the value of D exactly the value of $K_{\perp}$ must be measured accurately and for this purpose it is desirable that the range of linear relationship extends sufficiently. So the similar experiments were repeated by using the following direct dyes: Diamine Rose, Diamine Green, Diamine Blue, Chlorazol violet, Benzopurpurine, and Methylen Blue. But the results are negative and the observed points begin to deviate from the same value of $K_{\parallel}$ as in the case of Congo Red. The filaments dyed with Congo Red are usually red but change to blue when they come in contact with HCl vapor and, at the same time, their coefficients of absorption increase, even when the $K_{\parallel}-K_{\perp}$ relation is kept unchanged.

A point (a) of a red filament, which has a larger $K_{\parallel}$ but is still on the line, moves to the point (b) when the filament changes to blue, but the point (a') of smaller $K_{\parallel}$ goes to (b') on the line unless $K_{\parallel}$ of (b') is smaller than 0.5. This change is reversible and the points come back to the initial points when the filaments are exposed to NH_3-gas.

The reason of this phenomenon is that the critical values of $K_{\parallel}$ and $K_{\perp}$ are the functions of the specific coefficients of absorption of the filament and not of the total absorption. The linear relationship seems to extend more in the case of the thicker filament of smaller specific absorption coefficient than the thinner filament of larger specific coefficient of absorption even though their total absorption are equall to each other.

This is proved experimentally as shown by a

line (2) in Fig. 2. In this case the values of $K_{\parallel}$ and $K_{\perp}$ were controlled by piling the strips of cellophane, which had been dyed with Congo Red and stretched. The specific coefficient of absorption of this cellophane ($K_{\parallel}$) is 0.16 and smaller than that of the above filament so the linear relationship holds good for $K_{\parallel}$ larger than 0.5. Of course the relation can be expected from the previous calculation.[3]

From these results the dyeing was carried out in this experiment so that $K_{\parallel}$ of the filament stretched to maximum did not exceed 0.5.

Results and discussion

Six series of stretching were carried out as shown in the next table:

Treatment	Relative humidity at the stretching at 20°C		
	100%	93%	81%
A. non-treated	A−1	A−2	A−3
B. heated in 40% $(NH_4)_2SO_4$ soln.	B−1		
C. heated in 50% $(NH_4)_2SO_4$ soln.	C−1	C−2	

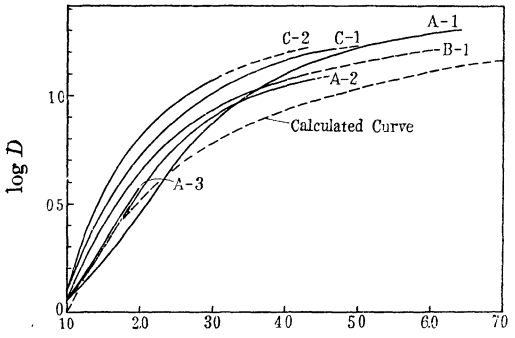

Fig. 3.

Fig. 3 shows $\log D$ as the measure of the orientation degree caused by the stretching given on the abscissa. The broken curve is the calculated one with the assumption of the first theory of O. Kratky.[6] The starting point of each curve does not coincide with the origin because of the slight anisotropy of the original filament. The curves are the mean of the several experiments.

From the figure some interesting facts can be observed as follows.

A-series. In this case the curves are slightly sigmoid but the tendency becomes slighter as the moisture content of the sample decreases, and, at the same time, the maximum degrees of stretching also decrease in the order from A−1 to A−3. The maximum stretching of A−1 is 6.4 and those of A−2 and −3 are 4.5 and 2.0 respectively, and the corresponding values of $\log D$ are 1.31, 1.09 and 0.57 respectively. The orientation degree of $\log D = 1.3$ is almost comparable to that of the ramie as reported previously[3] and, therefore, the orientation of A−1 can be said to be almost complete, while the filament of lower moisture content breaks at the lower degree of orientation.

It is well known that the moistened gel of PVA has a rubber-like elasticity but it loses the high elasticity and becomes rigid as it dries. This behaviour can be considered to be due to the decreasing microbrownian motion with the lowering of the moisture content. The above phenomena in the stretching may be due to the same cause, and therefore, generally speaking, the polymer having a more flexible chain molecule can be oriented more completely by stretching.

The authors repeatedly[7] maintained that in the case of the regenerated cellulose fiber the orientation degree at break is far from the complete orientation. This is because the chain molecule of the cellulose is too rigid to be arranged parallel in the ordinary processing. But this flexibility of the chain molecule is affected by many factors and even in the case of PVA it becomes rigid as said above because of the decaying microbrownian motion and the growing coherent force between the segments. And indeed, the deformation process of A−3 is very similar to that of the cellulose fiber. So, on the contrary, the isotropic cellulose fiber may possibly be stretched to a more highly oriented state in the properly selected conditions.

B−1. The curve is the saturation type in this case. The change is steep at first but later becomes inferior to that of A−1. The maximum value of v and $\log D$ are 6.1 and 1.21 respectively.

C-series. The curves are also the saturation type and very similar to that of B−1, and the changes of these are steeper than of the latter. But in this case the anisotropy of the original sample increased slightly by the heat-treatment, so correcting this factor, the difference between B−1 and C−1 becomes very slight although the above tendency also remains unchanged. The effect of the moisture content is also seen in this series.

Now an interesting observation will be added. It has been observed that when an isotropic fiber of regenerated cellulose is stretched higher under some conditions it appears milky due to the occurrence of a number of small lateral crackings. According to one of the authors' experiment on the cellulose fiber, this milkiness occurred in the dry stretching only and it was seen that the higher the stretching, the more anisotropic the original fiber was.

The same phenomena also appeared in the present study. The table below shows the degrees of stretching when the filaments began to appear

(6) O. Kratky, Kolloid, Z. 64, 213 (1933).

(7) S. Okajima, *J. Soc. Chem. Ind. Japan*, **49**, 168 (1946); *Bulletin of the Yamagata University, Natural Science*, No. 1, 21 (1951).

milky under their conditions, from which it is clear that even in dry stretching the phenomenon

A-1	A-2	A-3	B-1	C-1	C-2
—	4.4	—	4.3	4.7	3.1

is difficult in the moist state (A-1, not occurred) but becomes easy as the filament is demoistened (C-1, C-2) and crystallizes (C-1). The broken curves of A-2, B-1, C-1 and C-2 in Fig. 3 indicate the occurrence of this milkiness.

Conclusion

From the above results it is concluded that the relation of $\log D$ versus v of PVA filament is nearly saturation type as the first theory of Kratky requires. The demoistening and the partial crystallization of the filament does not change the tendency, but the former affects remarkably the degree of maximum stretching and the corresponding orientation, while the latter lowers the maximum stretching degree but not the degree of orientation.

Of course dichroism can indicate the orientation of the amorphous region and not the state in the crystallite. The crystallinity of the series A is very poor, so the orientation of this series may be given reasonably by $\log D$. But in the case of the filaments of higher crystallinity, the problem is not so simple because it is not yet proved whether the orientation of the amorphous part is not different from that in the crystalline region in the case of PVA. The study must await the future work. So the above results must be considered from the present stage of our knowledge.

The authors are indebted to Dr. S. Yazawa for the sample of PVA used. The cost of this research has been defrayed by the Grant in Aid for Fundamental Scientific Research from the Ministry of Education, to which the author's thanks are due.

Faculty of Engineering, Yamagata University, Yonezawa

Heterogeneous Structure of Rayon. I. Some Observations of the Heterogeneous Acetylation of Rayon

By Saburo OKAJIMA, Shigeru HAYAMA and Koichiro KOBAYASHI

(Received February 11, 1952)

It has long been known that the viscose rayons have the skins whose microstructures differ from those of the cores, but until recently there was no attempt to clear up these differences by studying the microstructures of the skin and core separately, excepting a short report by Nakayama,[1] who studied separately their orientation degrees by preparing a longitudinal section of rayon.

But this method requires extreme skill, so the authors studied the same problem since 1950 with a completely different method and have gained some interesting results. Recently the authors learned that some papers referring to the same problem have already appeared since 1946 by Elöd,[2] Preston,[3] and Hermans,[4] among which we could read the original papers by Preston and Hermans, according to which the similar experiments seem to be carried out by Elöd to get some similar results. But some discrepancies are thought to exist between the results of these authors, including the authors of this present paper, so our data are also reported here.

Consideration about the heterogeneous acetylation suitable for peeling-off the rayons

A method can easily be considered to trace radially the heterogeneous structure by peeling-off the rayon from the surface toward the center. And the authors also tried this chemically by acetylating the outer layers of the filament to the various depths by acid-catalyzed heterogeneous

(1) T. Nakayama, *Textile Review, Japan*, **40**, 60 (1949).
(2) E. Elöd & H. G. Fröhlich, *Melliand Textilb.*, **27**, 103 (1946); *Textile Research J.*, **18**, 487 (1948).
(3) J. M. Preston, *J. Textile Inst.*, **39**, T 211 (1948); **40**, T 327 (1949).
(4) P. H. Hermans, *Textile Research J.*, **20**, 553 (1950).

reaction by keeping the fibrous state and subsequent dissolution of the acetylated shell. The topochemical acetylation of the cellulose fiber was precisely studied by I. Sakurada,[5] who concluded that the acetylation is also a micelle-heterogeneous reaction and the fiber must be swollen for the sake of the rapid and smooth acetylation.

But for our present purpose, it is desirable that the penetration velocities of the acetylation reagents through the inter-micellar region be as equal as possible to that through the micell itself, although then the acetylation velocity may necessarily be very much smaller. So the heterogeneous acetylation of rayons was tried under the deswollen states in the following experiments.

Nitration, which is more speedy than acetylation, may also be used instead of acetylation for the above purpose, on which the study is now in progress.

Experiment

(1) **Sample.**—Five rayons were used as samples:

V-1: a viscose rayon on the market, 120/25 denier.

V-2: a viscose rayon, manufactured some 15 years ago, 120/25 denier.

V-3: an old viscose rayon, manufactured on trial some 40 years ago by Prof. Hata, who was one of the famous pioneers of the Japanese rayon industry.

T: a viscose tire cord.

C-1: a cuprammonium rayon on the market.

These samples were extracted with ether for 10 hours, washed with hot distilled water (60°C) repeatedly. The purified samples were vacuum-dried and acetylated; in some experiments the air-dried samples were also used. The effect of the moisture content of the sample will be discussed in the following paper.

(2) **Acetylation.**—1 gm. of a sample was poured into an acetylating bath, contained in an ordinary test tube stoppered lightly by a cork stopper and acetylated at the constant temperature. Four bath compositions shown in Table 1 were tried, among which the bath A is the most suitable and was used successfully for the most experiments at 40 ~60°C. At 100°C the integration of the fiber was too remarkable for bath A to be used.

Table 1

Bath composition	A	B	C	D
Benzol	30 g.	30 g.	30 g.	
Acetic anhydride	10 g.	10 g.	10 g.	40 g.
Sulfuric acid (1.84)	0.05cc.	0.025cc.	0.10 cc.	
Potassium acetate				12 g.
Glacial acetic acid				10 g.

The bath C contains too much sulfuric acid and disintegrated the fiber considerably, although the reaction proceeds rapidly in this case; when B is used, on the contrary, the reaction is too slow due to the too small content of the catalyst. These two baths are, therefore, not suitable. In the bath D, the fiber form was retained completely even when it was used at 100°C, but the acetylated product did not dissolve in any usual solvents and this was abandoned.

When the samples had been acetylated for the desired time (0.5~1160 hours), they were taken out, washed with benzol, and with hot distilled water (60°C) repeatedly and air-dried at room temperature.

(3) **Measurement of the acetic acid content.**—0.5 g. of the acetylated product was poured into a 20 cc. of N/2 NaOH aq. solution in a tightly closed flask and saponified for 48 hours at the room temperature, after which the consumed alkali was titrated and acetic acid content was calculated as usual. The saponification was ascertained to be enough and it needed to be continued for 48 hours under the present conditions.

The observation of the acetylation process

(1) **Partial dissolution of the fiber during the acetylation.**—If W g. of a sample is acetylated under an ideal condition and if we obtain W_A g. of the partially acetylated product, whose degree of acetylation is x mole. per glucose residue and the acetic acid content is 100 A%, then

$$A = 60x/(162+42x) \tag{1}$$

and therefore,

$$x = 162A/(60-42A), \tag{2}$$

and

$$W_A = \frac{W}{162}(162+42x) = \frac{W}{1-0.7A}. \tag{3}$$

But the observed value of W_A was always smaller than that calculated from the relation (3), and this decrease in weight became larger and larger as the acetylation time elongated and A also grew larger. This is thought to be due to the partial dissolution of the acetylated part of the rayon.

Now this partially dissolved cellulose, actually dissolving as triacetylcellulose, is assumed to be L_1 g, them

$$W_A = (W-L_1)/(1-0.7A). \tag{4}$$

So L_1 can be calculated from W_A, W and A.

Fig. 1 shows the relations of L_1 and A of the samples V-1 and V-3, acetylated under various conditions (see the next report), according to which L_1 grows linearly but slowly with A, (α-range), and beyond a certain point K the curve is very steep (β-range). Similar phenomena are also seen in the cases of the other samples as shown in

(5) I. Sakurada, *J. Soc. Chem. Ind. Japan*, **35**, 123 B, 283 B, (1932); **36**, 280 B, 299 B, (1933); **37**, 53 B, 599 B, (1934).

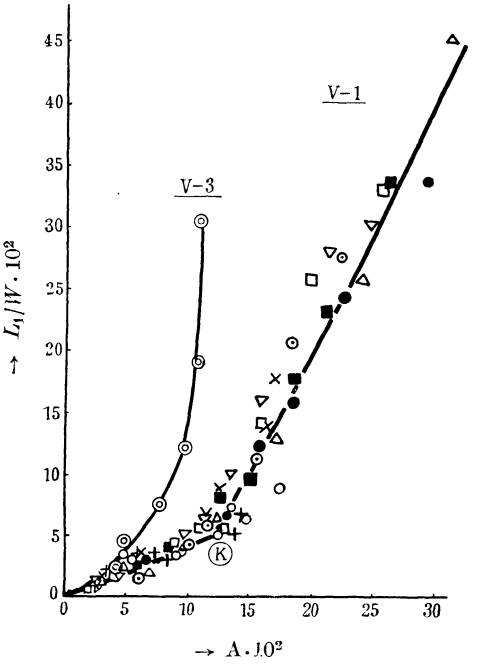

Fig. 1.

Fig. 2. In the α-range the fluctuation of the points is comparatively small, and its slope is independent upon the type of the rayon, while they are dispersed in the β-range and the slopes also vary from sample to sample. The position of K and the slopes of the curves in the β-range are characteristic to each sample, but not remarkably affected by the acetylating conditions. The characteristic of the curve will be described in the following paper. Because of these facts, acetyl content A did not obey the diffusion formula as suggested by I. Sakurada,[5] but after a certain time of reaction, the acetylation velocity increased again.

(2) Microscopic observation of the acetylated fibers.—As well known, many stripes running parallel to the fiber axis can be seen under a microscope on the surface of our viscose samples (Fig. 3 A), but as the acetylation proceeds the surface of the fiber becomes very rugged and many small cracks which cover the stripes appear on them (Fig. 4). But when the yarn is poured

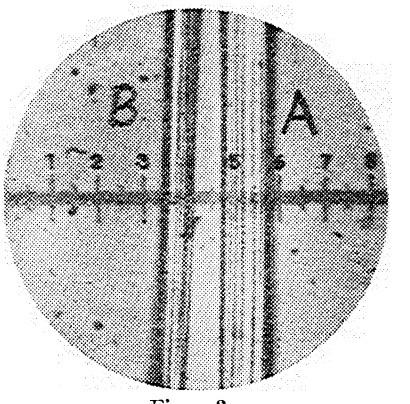

Fig. 3.

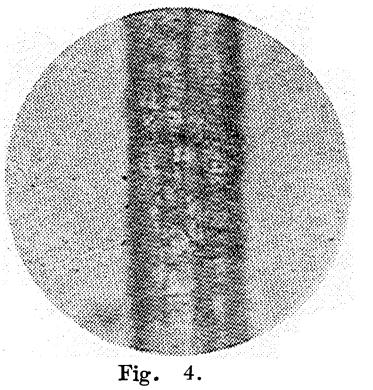

Fig. 4.

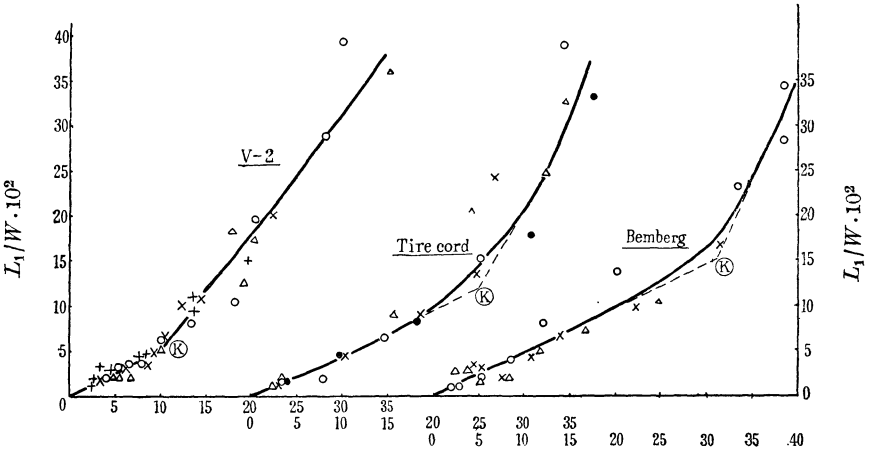

Fig. 2.

into chloroform and warmed at 60°C for 3—4 hours, the stripes reappear again and at the same time the fiber becomes transparent and the external appearance recovers, excepting that its diameter becomes slender (Fig. 3 B). This observation can be clearly explained by considering that the outer layer of a certain thickness, corresponding to the acetylation time, changed to triacetyl cellulose. These acetylated layer depolymerized considerably during the acetylation, so it is partly soluble in the acetylation bath and also its mechanical strength is also very poor and it cracks as the result of the mechanical shocks. This layer can be removed by treating with chloroform. If the acetylation proceeds fiber-heterogeneously the dissolution by chloroform occurs concentrically and, again, the stripes can be seen on the new surface of the rayon, and of course, then, the fiber becomes slender.

The fiber shown in Fig. 5 is an example of the partially acetylated yarn stretched a little, where a part of the peeled layer is seen, and in Fig. 6 the outer shell is more clearly shown.

The degrees of polymerisation of the acetylated shell and the non-acetylated core are separately measured in Table 2, in which DP of the acetylated part was measured viscometrically by dissolving in chloroform and that of the core in cuprammonium solution. The extremely low degree of polymerisation of the acetylated layer allows us to consider its poor mechanical property. As shown in Figs. 1—2 the larger dispersion of the points in the β-range may partly be due to the mechanical removing during the treatment as well as the extraction with the solvent. On the contrary the core is thought not to be degraded to some extent. This is very important when we discuss the mechanical properties of the skin and core separately by such a peeling-off method. But this problem requires further precise study.

Table 2

Sample	Degree of Peeling-off, %	Degree of Polymerization: Original rayon	Acetylated shell	Core
V-1	18.8	250	—	270
	19.3	240	60	230
	11.8	240	55	220
V-2	10.0	270	75	250

(3) Solubility of the acetylated product.—If the acetylation proceeds from the outer layer concentrically as considered above, the amount of cellulose, L_2, which changed to triacetylcellulose and remained undissolved during the reaction and the corresponding weight of triacetylcellulose, L_A, can be calculated from the value of A as follows:

$$L_A = \frac{291}{162} L_2 = 1.778\, L_2 \qquad (5)$$

And the value of L_1+L_2 can be also obtained directly by measuring the difference between W and the residue after extracting the acetylated shell with chloroform followed by saponification

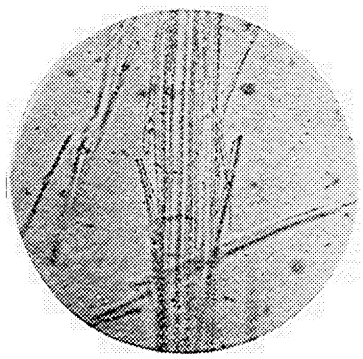

Fig. 5.

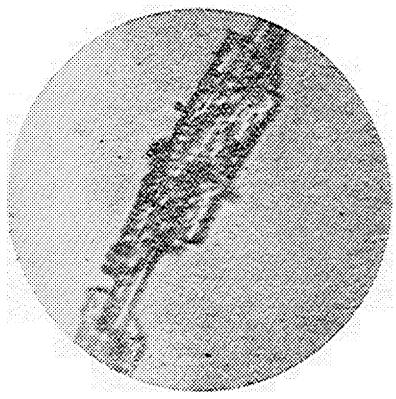

Fig. 6.

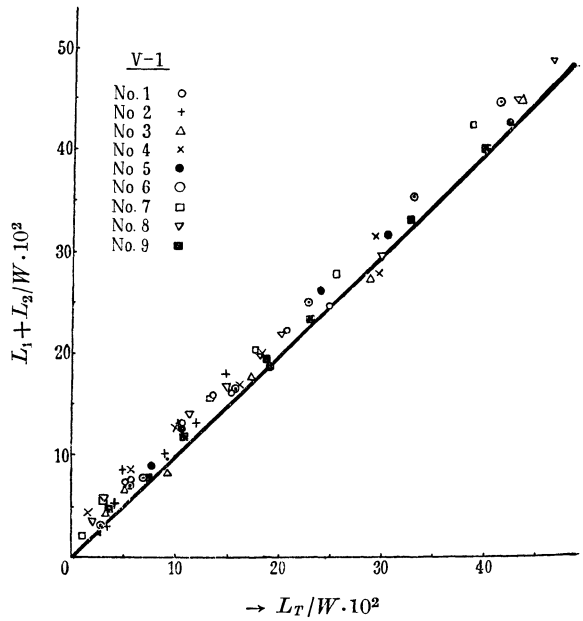

Fig. 7.

with N/5 NaOH aq. solution. If this is denoted by L_T, it must be equal to L_1+L_2, provided that the fiber is acetylated completely heterogeneously. And indeed this is nearly true as shown in Fig. 7. In the figure $(L_1+L_2)/W$ is plotted against L_T/W, where a nearly theoretical relation can be seen (a line in the figure is bisecting between the coordinates), although there is a tendency that the former values are slightly (1—2%) larger than the latter ones, which may probably be due to the incomplete extraction. There is necessarily a continuous distribution of the acetyl groups between the outer layer of triacetylcellulose and the completely unchanged core, and therefore, the smaller part of the acetyl groups remain unextracted.

The Fig. 7 shows the case of V-1 as an example; in the other cases the same relation holds good, excepting values larger than 50%, where the relation is inverse and L_T/W is larger than $(L_1+L_2)/W$, which may perhaps be due to the disintegration of the sample and the loss during the treatments, as the fiber becomes too slender.

Observing th fibers, which were extracted with only chloroform and not treated with dilute alkali, the refractive indices, $n_{\parallel}$ and $n_{\perp}$, are equal to these of the extracted one followed by saponification, in spite of the fact that the remarkable difference of the refractivity has been known between the cellulose and triacetylcellulose. So the surface layer of the core containing acetyl group is considered to be very thin in other words, the acetylated layer can be removed almost quantitatively. In order to ascertain this point the next experiment was carried out.

Two samples of V-1 were acetylated at 60°C for 6 (P) and 15 (Q) hours. Their respective acetyl contents are 3.06 and 6.14% and the thickness of the acetylated layers are estimated to be nearly 0.8 and 2.9% of their radius respectively (see the next paper). The denier of the single filament in this case is 5.04 and its mean diameter is nearly 10 micron. Therefore the thickness of the acetylated layers are 900 and 3000 A. respectively.

Observing the sample Q under a microscope existence of a thin layer of different refractivity can be clearly recognized on the surface of the fiber by the appearance of the two Becke's lines. But in the case of P, a single Becke's line appears ordinarily and the outer layer can not be recognized. Therefore, it is thought that the unextracted acetyl content of some 1—2% does not cover the refractivity of cellulose itself. This observation can support the above consideration. The critical thickness of this diffuse layer may be the order of the wave length.

Conclusion

The acetylation type of the not-swollen rayon is fiber-heterogeneous and it proceeds concentrically from the outer surface and the acetylated layer can be removed nearly quantitatively by chloroform. This reaction may be suitable for the peeling-off the rayons.

The cost of this research has been defrayed by the Grant in Aid for Fundamental Scientific Research from the Ministry of Education, to which the authors' thanks are due.

Faculty of Engineering,
Yamagata University, Yonezawa

Heterogeneous Structure of Rayon. II. Orientation Degree of the Skin and Core of Rayons

By Saburo OKAJIMA, Shigeru HAYAMA and Koichiro KOBAYASHI

(Received February 11, 1952)

In the previous report a possibility of peeling-off the rayon fiber by a heterogeneous acetylation was recognized. So now the orientation degrees of the skin and core are measured optically, applying this method, and the effect of the conditions of acetylation upon them is discussed.

Experiment

Five samples of rayon were acetylated by using the bath A as already described in the preceding report. In some cases the other bath compositions were used, where only the diluent benzol was substituted by carbon tetrachloride or toluol. The moisture content of the sample was also controlled.

The acetylated fiber was extracted with chloroform, treated with N/5 NaOH aq. solution, washed with distilled water and air-dried. The refractive indices, $n_{\parallel}$ and $n_{\perp}$, of the peeled-off fiber were measured with the Becke's method and the observed values were corrected on the

standard value of $n_{iso}=1.5356$ with the authors' method.[1] $n_{\parallel}$ and $n_{\perp}$ are the refractive indices for the plane-polarized D-line, oscillating parallel and perpendicular to the fiber axis; then the intrinsic double refraction Γ is given by $n_{\parallel}-n_{\perp}$.

The amount of the peeled-off cellulose is expressed by P_r %, which indicates the thickness of the peeled-off shell. If the sectional area and the length of the single fiber are denoted by S_0 and l, then its weight is

$$W=S_0ld,$$

and

$$L_T=(S_0-S)ld,$$

where d is the density of the original fiber and S_0 and S are the cross sectional areas before acetylation and after acetylation and extraction, followed by saponification respectively, providing, of course, that the length is very long compared to S_0, the form of the cross section remains similar during the peeling-off process, and the density is equal through the cross section. Then

$$1-L_T/W=S/S_0.$$

Therefore,

$$(S/S_0)^{1/2}=(1-L_T/W)^{1/2}=r/r_o,$$

and

$$P_r=1-r/r_0=1-(1-L_T/W)^{1/2},$$

where r_0 and r are the radii before and after the peeling-off.

The above assumptions are not thought to hold exactly good in the actual case, and P_r is, therefore, only an apparent representation, although it is right in the dimension.

Conditions of treatment

The results obtained are given in Figs. 1—4, from which some interesting phenomena can be seen.

(1) **Effect of moisture of the sample.**—The moisture content of the sample poured into the acetylation bath does not affect the orientation of peeled-off fiber according to P. H. Hermans,[2] but in our data the effect is clearly seen. Some of the examples are given in Fig. 1, where the samples V—1 and —2 were acetylated under the following conditions; the vacuum-drying was carried out at 60°C in each case.

Table 1

Conditions of Acetylation

Sample		Conditioning	Acetylation temp., °C	Diluent
V—1	(1)	Air-dried	45	Benzol
	(3)	Air-dired, acetylated after immersion into benzol overnight	60	Benzol
	(4)	Vacuum-dried	60	Benzol
	(5)	Vacuum-dried	60	Toluol
	(8)	Vacuum-dried, conditioned to the moisture content of 4.23%	60	Benzol
	(9)	Vacunm-dried, conditioned to the moisture content of 14.1%	60	Benzol
V—2	(1)	Air-dried	45	Benzol
	(2)	Air-dried	60	Benzol
	(3)	Vacuum-dried	45	Benzol

The vacuum-dried samples (4) and (5) of V—1 show the existence of the outermost layers and the cores of the completely and almost constant birefringence and the transition layers between them, while in the cases of the air-dried ones Γ decreases continuously from the surface toward the core and this tendensy is more remarkable

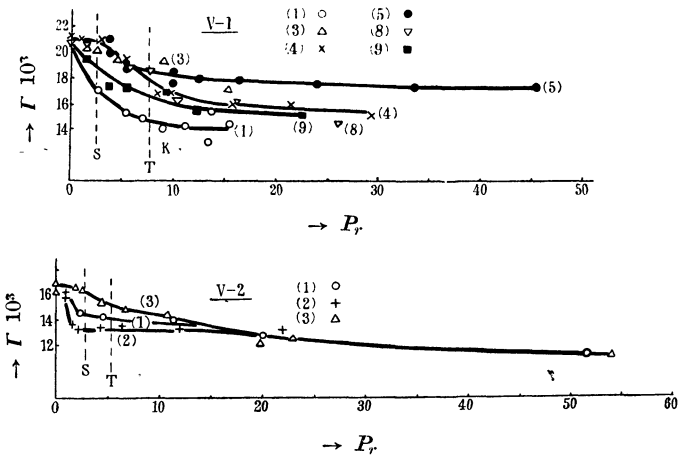

Fig. 1.

(1) S. Okajima and Y. Kobayashi, *J. Soc. Chem. Ind. Japan*, **46**, 941(1943). S. Okajima, Bull. Yamagata University, *Natural Science*, No. 1, 21(1950).

(2) P. H. Hermans, *Textile Research J.*, **20**, 553 (1950).

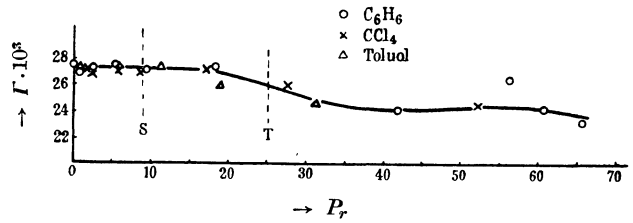

Fig. 2.—Bemberg.

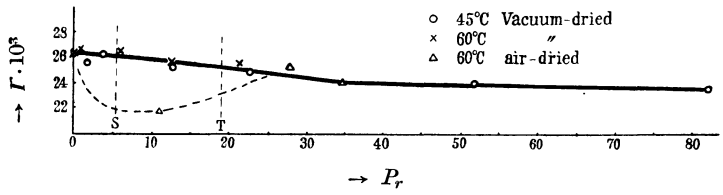

Fig. 3.—Tirecord.

the larger the moisture content of them is (rf. the samples V—1, 1, 3, 8, 9).

The cause of this phenomenon is not clear but the authors believe that the factor causing this difference is the moisture of the sample and not the vacuum-drying because the immersion of the air-dried one into benzol overnight gives the vacuum-dried type (rf. V—1, 3) and also the conditioning after the vacuum-drying gives the air-dried type again (rf. V—1, 8 and 9).

The same phenomenon can also be seen in the case of V—2, where the effect disappears as the reaction proceeds; this is because the loosely absorbed moisture is substituted by the molecules of benzol.

As the results, the moisture effect appears especially in the early stage of reaction so the vacuum-drying is thought to be necessary to recognize the existence of the outermost skin, if any, so all of the samples were vacuum-dried in the following experiments, excepting ones which were especially described.

(2) **Effect of diluent.**—Two samples of V—1 were peeled-off by acetylating in the bath C, but with using toluol and benzol as the diluent (rf, 4 and 5). Fig. 1 indicates that the curves are similar in shape but Γ of the core are more or less different.

A cuprammonium rayon was also examined by using benzol, toluol and carbon tetrachloride as the diluents. In this case the three curves coincide completely with each other as shown in Fig. 2, therefore, the effect of diluent seems to be negligible.

(3) **Effect of the acetylation temperature.**—A sample of tire cord was examined by acetylating at 45 and 60°C. Their results coincide completely as shown in Fig. 3 and, therefore, the temperature effect can be disregarded.

In the series (3) the acetylation was carried out without vacuum-drying, so the first point (P_r=10.8%) is remarkably low but the other two points are normal. The reason was already described in the section of the moisture effect.

Distribution of the orientation degree and the type of rayon

Now it is clear that the careful treatment can give the reasonable results, and observing the curves $\Gamma - P_r$ of the vacuum-dried samples, they indicate some interesting facts.

(1) **The distribution of the orientation degree and the skin structure.**—Observing the radial distribution of Γ of V—1, —2 and also —3 (Fig. 4), whose skin structures are clearly shown by the microscopical observation of the stained cross sections, the outermost skin, the core and the transition layer are recognized in each case. The orientation of the outermost skin, whose thickness is 2—4% of the total radius is constant, while that of the core decreases very faintly toward the center.

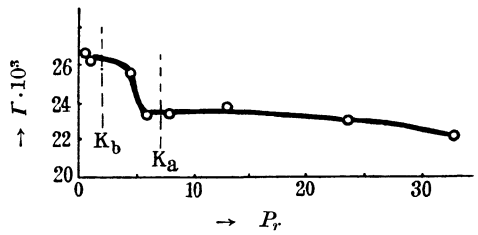

Fig. 4.—V-3.

Moreover in the case of the tire cord or the cuprammonium rayon, one of which is said to have a thickened skin and the other no skin, the similar distribution of the orientation can be seen, although the tendency is slight, as the results of the thickening of the outermost and the transition layers and also the smaller difference of orientation between the skin and core.

This difference of orientation between the skin

and core is much smaller than that which was expected from the impression hitherto given by the optical observation of its cross section.

(2) **Structure of the skin.**—Some of the microstructures of the skin were tested by many authors. The density of the skin has been thought to be larger according to the methacromasic[3] observation, but the result of Hermans[2] was opposite. As to this problem a phenomenon of some importance is seen in the above data.

As shown in Figs. 1 and 2 of Report I, there is a knick point K on each curve of L_1/W versus A. The curve indicate the ratio of the rate of acetylation of the fiber and the rate of dispersion of the acetylated layer in the bath, so the appearance of a knick point means the occurence of the abrupt change of this ratio, which may probably be caused by the dissolving away of the skin, providing, of course, that the resistance of the skin toward the penetration of the acetylating agents and dispersing away in the bath is larger than that of the core. The behaviour is the same in the case of the air-dried sample and this seems to indicate a priori existence of the outermost skin in the original fiber.

This presumption is supported by the following consideration. If the amount of cellulose which was lost in the acetylating bath (actually as triacetylcellulose) up to the knick point K is L'_K per 100 part of the original sample and the acetic acid content at K is 10^2.A %, then the weight of the partially acetylated sample, W_K, is given by the formula (1) of Report I as follows,

$$W_K=(100-L'_K)/(1-0.7\,\mathrm{A}) \qquad (1)$$

If the corresponding value of L_2 at K is denoted by L''_K, then

$$100-L'_K-L''_K+1.778\,L''_K=W_K \qquad (2)$$

$$L''_K=\frac{0.7\mathrm{A}(100-L'_K)}{(1-0.7\mathrm{A})\times 0.778} \qquad (3)$$

The value of L_T/W is smaller than $(L'_K+L''_K)/W$ by some 1.5 according to Fig. 7 in the preceding report, therefore in this case

$$L_T=L'_K+L''_K-1.5 \qquad (4)$$

This gives the corresponding value of P_r.

The table below contains these values at the knick point, where the values of L'_K and A of each sample are obtained on each curve in Figs. 1 and 2 of the preceding paper. In the case of $V-3$, the curve is too steep to obtain the correct value of K, so K_a and K_b are used as the limiting values as shown in Fig. 5; the acutal value must be between them.

Table 2

Sample	$V-1$	$V-2$	$V-3$ (a)	$V-3$ (b)	T	C
A (%)	12	11	8.5	4	25	31
L'_K/W	5.3	6	8	1.8	12	15
L_T/W	15.0	10.5	14.1	3.9	34.5	43.8
P_r (%)	7.8	5.4	7.3	2.0	19.1	25.0

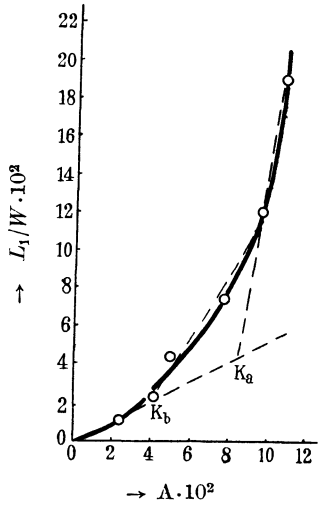

Fig. 5.—V-3.

The calculated value of P_r is indicated by a broken line (T) on each curve of $\Gamma-P_r$; then all of them seem to be in the transition layer of each sample. And in the case of $V-3$ also the transition layer is held between the above two limiting lines.

The same behaviour is also seen in the tire cord or the cuprammonium rayon. This fact is thought to support the existence of the skin structure as described above even in a case, where the existence of the skin has been denied. Of course the skin structure of these rayons are not so remarkable and correspondingly the knick points are less distinct.

These results allow us to venture to calculate the thickness of the outermost skin. If we suppose that the knick point K appears when the outermost skin of the least porosity has dispersed away in the bath liquor and the resistance for the acetylation and the dispersion have decreased abruptly, then L_1 indicates the amount of the outermost skin, which is easily calculated from the $L_1/W-A$ curve.

As shown in Figs. 1—3, in which the calculated value is indicated by a broken line (S), the above supposition is proved to be nearly true in the cases of $V-1$ and -2 and the tire cord. But the value of the cuprammonium rayon which is obtained is too thin. This is probably because the microstructure of the cuprammonium rayon is more or less different from that of the viscose rayon due to the different nature of the spinning reaction.

(3) K. Ohara, *Scientific Paper. I. P. C. R.*, **25**, 154 (1934).

As to $V-3$ it is very difficult to obtain exactly as already described, so it was omitted from the present discussion.

Furthermore, it is worthy to note that the slope of curve $L_1/W-A$ between the origin and K is constant but thereafter it varies according to the type of rayon, which may indicate that the microstructures of the skin of the various rayons are nearly equal to each other but not of the core.

Conclusion

A peeling-off method by the heterogeneous acetylation can give reasonably the radial distribution of the degree of orientation when it is carried out under the appropriate conditions. The skin structure is shown by this method in the cases of the tire cord and even the cuprammonium rayon. And the resistance of the skin against penetration and dispersion seems larger than that of the core.

The cost of this research has been defrayed by the Grant in Aid for Fundamental Scientific Research from the Ministry of Education, to which the authors' thanks are due.

Faculty of Engineering,
Yamagata University, Yonezawa.

LETTER

Electron Microscopic Observation of Aluminum Chloride

By Sho SUZUKI

(Received April 3, 1952)

A smoke of aluminum chloride, one of the halide catalysts of the Friedel-Crafts' type, was observed by means of electron microscopy. With regard to the same material, the electron microscopic observation has not yet been reported in the literatures I could see. This paper presents interesting micrographs obtained on the same material.

Aluminum chloride used here was prepared

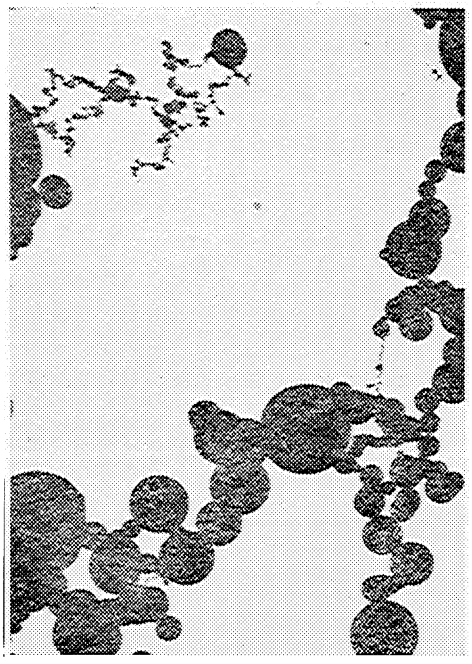

Electron micrographs of aluminum chloride.
Fig. 1.—Magnification: 20,000. Fig. 2.—Magnification: 18,000.

as follows: A stream of chlorine was flowed over pure aluminum foils (99,9%) heated at about 250°C in order to obtain the aluminum chloride smoke.

Figs. 1 and 2 show the micrographs obtained from the aluminum chloride smoke. In these micrographs there are found the two types of particles. One of them has the forms (size: 200 A.—0,2 μ) as recognizable in the case of the usual smoke of metal oxides. Another of them has spherical forms (size: 500 A.—1 μ). The spherical particles seemed to be the hydrate of chloride, because the number of these spherical particles increased always on exposure of the specimen to the air.

Since the wet aluminum chloride can not play a role of a catalyst, the spherical particles remarked in Figs. 1 and 2 will not behave as an active catalyst, but the smoke-like particles in Fig. 1 will be active in catalytic reaction.

The sample prepared by subliming the commercial aluminum chloride gave the same micrographs as are shown in Figs. 1 and 2.

Governmental Chemical Industrial Research Institute, Tokyo

A New Method of Catalytic Hydrogenation[1]

By Yoshiyuki URUSHIBARA

(Received July 4, 1952)

The author with co-workers has found that precipitated nickel and copper are active catalysts for hydrogenation in the presence of caustic alkali or when treated with aqueous caustic alkali before use in hydrogenation. In the hydrogenation in aqueous caustic alkali, metallic aluminum or zinc can be used as well as hydrogen gas. In this preliminary note some examples are presented with no detailed accounts.

Metallic nickel is precipitated by adding zinc dust to an aqueous solution of nickel chloride heated on a water bath until the supernatant liquid becomes colorless. It is washed with water by decantation, digested with 10 percent aqueous sodium hydroxide or potassium hydroxide on a water bath for one hour or two, and again well washed with water. The nickel catalyst thus prepared is shaken with hydrogen for two hours in the hydrogenating medium, aqueous caustic alkali, alcohol, or alcoholic caustic alkali, and then is ready for use as the catalyst in the hydrogenation of organic compounds by shaking with hydrogen at the ordinary temperature and pressure. Thus, estrone is reduced to estradiol either in aqueous caustic potash or in neutral alcoholic solution. Cholestenone is reduced to cholestanol in alcoholic solution, neutral or alkaline. Cinnamic acid is reduced to hydrocinnamic acid in alkaline aqueous solution. Nitrobenzene is reduced to aniline in alkaline alcoholic solution.

The time needed for hydrogenation naturally depends on the amount of nickel, and the use of a large amount seems desirable especially in the hydrogenation in the neutral medium. The metallic nickel precipitated from the chloride solution contains adsorbed chloride ions and the preparatory treatment with caustic alkali seems advantageous even in the hydrogenation in the alkaline medium, because the digestion with caustic alkali desorbs much of the adsorbed chloride. The nickel treated with caustic alkali retains a considerable quantity of adsorbed alkali even though washed several times with hot water, the washings keeping persistently alkaline to phenolphthalein, while it loses the retained alkali promptly if digested with a sodium chloride solution. The adsorbed alkali probably plays an important rôle in the hydrogenation, because the nickel not treated with caustic alkali, and the nickel treated with caustic alkali and then washed with acetic acid, are totally inactive. In conclusion, it may be added that the author has come to understand why Raney nickel is an active catalyst.

Department of Chemistry, Faculty of Science, Tokyo University, Tokyo.

(1) Patent applications were received by the Japanese Patent Bureau: Nov. 7, 1951; Dec. 7, 1951; and Apr. 24, 1952. Read before the 5th Annual Meeting of the Pharmaceutical Society of Japan on April 30, 1952, and before the ordinary meeting of the Chemical Society of Japan on June 21, 1952.

Concentration Polarization and the Polarographic Current-Time Curve. II. The Spherical Diffusion Current

By Tomihito KAMBARA

(Received February 22, 1952)

Mathematical Part

It is reported in our preceding paper[1] that the problem of linear diffusion current can be treated reasonably when the boundary condition demonstrates the equality of the three quantities, i.e., the rate of diffusion of the depolarizer, the rate of the electrode reaction, and the rate of diffusion of the reaction product. In this article, the mathematical treatment for the spherical electrode will be given. Suppose that a spherical electrode is immersed in an infinite solution of depolarizer and the suitable supporting electrolyte and that the electrode reaction product is water soluble. Two movements of the depolarizer and the reaction product are shown by the following system of equations:

$$\left.\begin{aligned}\frac{1}{D_1}\frac{\partial C_1}{\partial t}&=\frac{\partial^2 C_1}{\partial r^2}+\frac{2}{r}\frac{\partial C_1}{\partial r}\ ;\\ \frac{1}{D_2}\frac{\partial C_2}{\partial t}&=\frac{\partial^2 C_2}{\partial r^2}+\frac{2}{r}\frac{\partial C_2}{\partial r}\end{aligned}\right\} \qquad (1)$$

where r is the distance from the center of the spherical electrode, t is the time, and C and D are the concentrations and the diffusion coefficients, respectively. The suffices 1 and 2 indicate the quantities concerning the depolarizer and the product, respectively. The initial condition is shown by

$$t=0,\quad r\geq r_e,\quad C_1={}^*C_1,\quad C_2={}^*C_2, \qquad (2)$$

where $^*C$'s represent the initial uniform concentrations and r_e is the radius of the electrode.

Employing the Laplace transformation defined by

$$\mathfrak{L}C_i=p\int_0^\infty e^{-pt}\cdot C_i(x,\ t)dt=u_i(x,\ p)\ \text{ for } i=1,\ 2, \qquad (3)$$

it is found that Eqs. (1) are converted into the system of the ordinary differential equations. Further, the proper boundary condition is given by

$$t>0,\ r=r_e,\ D_1\frac{\partial C_1}{\partial r}=k_1C_1-k_2C_2=-D_2\frac{\partial C_2}{\partial r}, \qquad (4)$$

where k_1 and k_2 are the rate constants of the forward and reverse reactions. Thus we obtain finally the expressions:

$$\left.\begin{aligned}u_1&={}^*C_1-K_r\cdot\sqrt{D_2}\left(\frac{\xi_1}{\sqrt{p}+m}+\frac{\eta_1}{\sqrt{p}+n}\right)\\&\quad\cdot\exp\left(-z_1\sqrt{p}\right);\\ u_2&={}^*C_2+K_r\cdot\sqrt{D_1}\left(\frac{\xi_2}{\sqrt{p}+m}+\frac{\eta_2}{\sqrt{p}+n}\right)\\&\quad\cdot\exp\left(-z_2\sqrt{p}\right).\end{aligned}\right\} \qquad (5)$$

In these equations:

$$\left.\begin{aligned}&z_1=\frac{r-r_e}{\sqrt{D_1}}\ ;\quad z_2=\frac{r-r_e}{\sqrt{D_2}}\ ;\\ &K_r=\frac{r_e(k_1{}^*C_1-k_2{}^*C_2)}{r\sqrt{D_1D_2}}\ ;\quad \xi_1=\frac{m-d_1}{m-n}\ ;\\ &\xi_2=\frac{m-d_2}{m-n}\ ;\quad \eta_1=\frac{d_1-n}{m-n}\ ;\quad \eta_2=\frac{d_2-n}{m-n}\ ;\\ &m=\frac{b+\sqrt{b^2-4ac}}{2a}\ ;\quad n=\frac{b-\sqrt{b^2-4ac}}{2a}\ ;\\ &a=\sqrt{D_1D_2}\ ;\quad b=k_1\sqrt{D_2}+k_2\sqrt{D_1}\\ &\qquad+\frac{\sqrt{D_1D_2}}{r_e}(\sqrt{D_1}+\sqrt{D_2});\\ &c=\frac{1}{r_e}\left(k_1D_2+k_2D_1+\frac{D_1D_2}{r_e}\right);\\ &d_1=\frac{\sqrt{D_2}}{r_e}\ ;\quad d_2=\frac{\sqrt{D_1}}{r_e}\ .\end{aligned}\right\} \qquad (6)$$

And it it is seen that between these quantities the following relationships hold:

$$\left.\begin{aligned}&m+n=\frac{b}{a}\ ;\quad m-n=\frac{\sqrt{b^2-4ac}}{a}\ ;\quad mn=\frac{c}{a}\ ;\\ &\xi_1+\eta_1=1;\quad \xi_2+\eta_2=1.\end{aligned}\right\} \qquad (7)$$

(1) T. Kambara and I. Tachi, This Bulletin, **25**, 135 (1952).

Now let us perform the inverse transformation. For this purpose, the following rule is favorable.

$$\left.\begin{aligned}&\mathfrak{L}^{-1}\frac{\lambda}{\lambda+\sqrt{p}}\cdot\exp(-z\sqrt{p})=G(z,\ \lambda,\ t)\\&=1-\mathrm{erf}\frac{z}{2\sqrt{t}}-\Psi(z,\ \lambda,\ t);\\&\Psi(z,\ \lambda,\ t)=\exp(z\lambda+\lambda^2 t)\\&\times\left\{1-\mathrm{erf}\left(\frac{z}{2\sqrt{t}}+\lambda\sqrt{t}\right)\right\}.\end{aligned}\right\}\quad(8)$$

Hence it is found that the appropriate integrals are shown by

$$\left.\begin{aligned}C_1&={}^*C_1-K_r\sqrt{D_2}\left\{\frac{\xi_1}{m}G(z_1,\ m,\ t)+\frac{\eta_1}{n}G(z_1,\ n,\ t)\right\};\\C_2&={}^*C_2+K_r\sqrt{D_1}\left\{\frac{\xi_2}{m}G(z_2,\ m,\ t)+\frac{\eta_2}{n}G(z_2,\ n,\ t)\right\}.\end{aligned}\right\}\quad(9)$$

Verification of the Above Developed Theory

(1) Linear Diffusion Current at the Plane Electrode.—The above stated theory must become identical with that reported in the Part 1 of this study, when the conditions given by

$$r_e\to\infty;\quad r-r_e\equiv x;\quad r/r_e=1\qquad(10)$$

are fulfilled. Then it is found that

$$c=n=d_1=d_2=\eta_1=\eta_2=0;\ \xi_1=\xi_2=1;\quad z_1=x/\sqrt{D_1};\ z_2=x/\sqrt{D_2},\qquad(11)$$

where x is the distance from the electrode surface. It is also found that the quantities η_1/n and η_2/n are finite and that

$$\left.\begin{aligned}&\lim_{r_e\to\infty}m=\frac{b}{a}=\frac{k_1}{\sqrt{D_1}}+\frac{k_2}{\sqrt{D_2}}=s;\\&\lim_{n\to0}G(z,\ n,\ t)=0;\end{aligned}\right\}\quad(12)$$

$$\left.\begin{aligned}&\lim_{r_e\to\infty}C_1={}^*C_1-\frac{k_1{}^*C_1-k_2{}^*C_2}{s\sqrt{D_1}}\cdot G\left(\frac{x}{\sqrt{D_1}},\ s,\ t\right);\\&\lim_{r_e\to\infty}C_2={}^*C_2+\frac{k_1{}^*C_1-k_2{}^*C_2}{s\sqrt{D_2}}\cdot G\left(\frac{x}{\sqrt{D_2}},\ s,\ t\right);\end{aligned}\right\}\quad(13)$$

Thus the conclusions obtained with the plane electrode can be derived as the limiting case of the present treatment.

(2) Final Concentrations at the Electrode Surface.—Concentrations at the electrode surface can be obtained by putting $r=r_e$ Writing

$$\left.\begin{aligned}&K=\frac{k_1{}^*C_1-k_2{}^*C_2}{\sqrt{D_1D_2}};\\&F(y)=\exp y\cdot(1-\mathrm{erf}\sqrt{y});\end{aligned}\right\}\quad(14)$$

it is found that the interfacial concentrations ${}^\circ C_1$ and ${}^\circ C_2$ are shown by

$$\left.\begin{aligned}{}^\circ C_1&={}^*C_1-K\sqrt{D_2}\left[\frac{\xi_1}{m}\{1-F(m^2t)\}+\frac{\eta_1}{n}\{1-F(n^2t)\}\right];\\{}^\circ C_2&={}^*C_2+K\sqrt{D_1}\left[\frac{\xi_2}{m}\{1-F(m^2t)\}+\frac{\eta_2}{n}\{1-F(n^2t)\}\right].\end{aligned}\right\}\quad(15)$$

Putting $t\to\infty$ gives the final concentrations at the interface, *i. e.*

$$\left.\begin{aligned}{}^\circ C_1(\mathrm{fin.})&=\frac{k_2'({}^*C_1D_1+{}^*C_2D_2)+({}^*C_1D_1D_2/r_e)}{k_1D_2+k_2D_1+(D_1D_2/r_e)};\\{}^\circ C_2(\mathrm{fin.})&=\frac{k_1({}^*C_1D_1+{}^*C_2D_2)+({}^*C_2D_1D_2/r_e)}{k_1D_2+k_2D_1+(D_1D_2/r_e)}.\end{aligned}\right\}\quad(16)$$

(3) Diffusion-Controlled Current Intensity.—If the electrode reaction of one mol of the depolarizer requires the electricity of n Faraday, it is seen that the current intensity i is shown by

$$\left.\begin{aligned}&i/nFq=i'=k_1{}^\circ C_1-k_2{}^\circ C_2=i_1'+i_2';\\&i_1'=(k_1{}^*C_1-k_2{}^*C_2)-K\times\left\{k_1\sqrt{D_2}\left(\frac{\xi_1}{m}+\frac{\eta_1}{n}\right)+k_2\sqrt{D_1}\left(\frac{\xi_2}{m}+\frac{\eta_2}{n}\right)\right\};\\&i_2'=K\left\{\left(k_1\sqrt{D_2}\frac{\xi_1}{m}+k_2\sqrt{D_1}\frac{\xi_2}{m}\right)\times F(m^2t)+\left(k_1\sqrt{D_2}\frac{\eta_1}{n}+k_2\sqrt{D_1}\frac{\eta_2}{n}\right)\cdot F(n^2t)\right\},\end{aligned}\right\}\quad(17)$$

where $q=4\pi r_e^2$ is the surface area of the spherical electrode. From Eqs. (6) it is seen that

$$\left.\begin{aligned}
&\frac{\xi_1}{m}+\frac{\eta_1}{n}=\frac{d_1}{mn}=\frac{a\sqrt{D_2}}{r_e c};\\
&\frac{\xi_2}{m}+\frac{\eta_2}{n}=\frac{d_2}{mn}=\frac{a\sqrt{D_1}}{r_e c};\\
&i_1'=(k_1{}^*C_1-k_2{}^*C_2)\frac{D_1D_2}{r_e{}^2c}\\
&\quad=\frac{(k_1{}^*C_1-k_2{}^*C_2)D_1D_2}{\left(k_1D_2+k_2D_1+\dfrac{D_1D_2}{r_e}\right)r_e}.
\end{aligned}\right\}\quad(18)$$

If the overall reaction rate is governed by the diffusion process, it can be shown asymptotically that

$$\begin{aligned}
i_2'&\sim\frac{K}{\sqrt{\pi t}}\cdot\frac{1}{m^2n^2}\{n^2(k_1\sqrt{D_2}\xi_1+k_2\sqrt{D_1}\xi_2\\
&\quad+m^2(k_1\sqrt{D_2}\eta_1+k_2\sqrt{D_1}\eta_2)\}\\
&=\frac{K}{\sqrt{\pi t}}\cdot\frac{a^2}{c^2}\Big[[k_1\sqrt{D_2}\{-mn+d_1(m+n)\}\\
&\quad+k_2\sqrt{D_1}\{-mn+d_2(m+n)\}]\Big]\\
&=\frac{Ka}{\sqrt{\pi t}}\left\{-\frac{k_1\sqrt{D_2}+k_2\sqrt{D_1}}{c}\right.\\
&\quad\left.+\frac{b}{r_e c^2}(k_1D_2+k_2D_1)\right\}\\
&=\frac{(k_1{}^*C_1-k_2{}^*C_2)(k_1D_2{}^2\sqrt{D_1}+k_2D_1{}^2\sqrt{D_2})}{\sqrt{\pi t}\left(k_1D_2+k_2D_1+\dfrac{D_1D_2}{r_e}\right)^2}.
\end{aligned}\quad(19)$$

Since k_1 is much larger than k_2, D_1 and D_2, it can be written approximately that

$$i_2'\simeq\frac{D_1(k_1{}^*C_1-k_2{}^*C_2)}{\sqrt{\pi D_1t}}\cdot\frac{D_2}{\left(k_1D_2+k_2D_1+\dfrac{D_1D_2}{r_e}\right)}.\quad(20)$$

Thus it follows that

$$i'=i_1'+i_2'\simeq\left(\frac{1}{r_e}+\frac{1}{\sqrt{\pi D_1t}}\right)\cdot\frac{D_1D_2(k_1{}^*C_1-k_2{}^*C_2)}{k_1D_2+k_2D_1+(D_1D_2/r_e)}.\quad(21)$$

On the other hand, it follows from the Eqs. (16) that

$${}^*C_1-{}^\circ C_1(\text{fin.})=\frac{D_2(k_1{}^*C_1-k_2{}^*C_2)}{k_1D_2+k_2D_1+(D_1D_2/r_e)}.\quad(22)$$

It can be, therefore, manifested that

$$i=nFq\cdot D_1\{{}^*C_1-{}^\circ C_1(\text{fin.})\}\cdot\left(\frac{1}{r_e}+\frac{1}{\sqrt{\pi D_1t}}\right).\quad(23)$$

Analogously it can be concluded that

$$i=nFq\cdot D_2\{{}^\circ C_2(\text{fin.})-{}^*C_2\}\cdot\left(\frac{1}{r_e}+\frac{1}{\sqrt{\pi D_2t}}\right).\quad(23\,a)$$

This result derived asymptotically can be readily obtained when we solve the system of Eqs. (1) with the boundary conditions given by

$$t>0,\ r=r_e,\ C_1={}^\circ C_1(\text{fin.}),\ C_2={}^\circ C_2(\text{fin.}),\quad(24)$$

i.e. when we assume that the interfacial concentrations take their final value immediately after the beginning of the electrolysis.

(4) The Current Intensity Controlled by the Electrode Process.—In this case the rate constants k_1 and k_2 being much smaller than the diffusion coefficients, it can be shown approximately that

$$\left.\begin{aligned}
&b=\frac{\sqrt{D_1D_2}}{r_e}(\sqrt{D_1}+\sqrt{D_2});\quad c=\frac{D_1D_2}{r_e{}^2};\\
&b^2-4ac=\frac{D_1D_2}{r_e{}^2}(\sqrt{D_1}-\sqrt{D_2})^2;\\
&m=d_2=\sqrt{D_1}/r_e;\quad n=d_1=\sqrt{D_2}/r_e;\\
&\frac{\xi_1}{m}=\frac{r_e}{\sqrt{D_1}};\quad\frac{\eta_2}{n}=\frac{r_e}{\sqrt{D_2}};\quad\frac{\xi_2}{m}=\frac{\eta_1}{n}=0.
\end{aligned}\right\}\quad(25)$$

Hence it follows that

$$i'=(k_1{}^*C_1-k_2{}^*C_2)\left[1-\frac{k_1r_e}{D_1}\{1-F(m^2t)\}-\frac{k_2r_e}{D_2}\{1-F(n^2t)\}\right].\quad(26)$$

k_1 and k_2 being very small, and upon neglecting the higher powers of k's it is found that

$$i=nFq(k_1{}^*C_1-k_2{}^*C_2),\quad(27)$$

which is a satisfactory result.

(5) Establishment of the Concentration Equilibrium at the Spherical Electrode Surface.—It follows from the Eqs. (16) that

$${}^\circ C_1(\text{fin.})/{}^\circ C_2(\text{fin.})=k_2/k_1,\quad(28)$$

indicating that even after the elapse of the infinite time the concentrations at the interface do not reach strictly to their equilibrium values. This may appear irrational at the first sight, but the same conclusion can be derived very simply as follows. Upon integrating the Eqs. (1) with the boundary condition given by Eq. (24), it can be readily seen that

$$i' = k_1 \cdot {}^{\circ}C_1(\text{fin.}) - k_2 \cdot {}^{\circ}C_2(\text{fin.})$$
$$= D_1\{{}^{*}C_1 - {}^{\circ}C_1(\text{fin.})\} \cdot \left(\frac{1}{\sqrt{\pi D_1 t}} + \frac{1}{r_e}\right)$$
$$= D_2\{{}^{\circ}C_2(\text{fin.}) - {}^{*}C_2\} \cdot \left(\frac{1}{\sqrt{\pi D_2 t}} + \frac{1}{r_e}\right). \quad (29)$$

This relation holds at any time, and it can be immediately found that putting $t=\infty$ gives the Eqs. (16). Owing to the term $1/r_e$, it is seen that the electrolytic current continues to flow *for ever*; this means that the concentrations at the electrode surface are *always* deviated from their equilibrium state. Therefore, it may be said that the curvature of electrode is the essential factor affecting the electrode processes. It is manifested by Kaishev[2] that the equilibrium potential of a reversible metal electrode differs from the value predicted by the Nernst formula when the curvature radius is finite. This opinion is in harmony with the present considerations.

(6) Polarographic Current-Time Curves. —The above treatment for the spherical electrode is much more complicated than that for the plane electrode; but the course of polarographic current-time curve as discussed in our preceding paper[1] is seen to be explained reasonably by the theoretical treatment given here. The oscillographic findings are comprehensible from the present theory; the procedure therefore can be carried out quite analogously to that given in our preceding paper.

(2) R. Kaishev, *Annuaire Univ. Sofia, Faculté phys.-m-at.*, **43**, *Livre* 2, 53—62 (1941~1947); *C. A.* **44**, 3818 (1950).

Summary

Provided that the depolarizer and the electrode reaction product are water soluble, the spherical diffusion equations are integrated. The boundary condition is so chosen that the three elementary processes, i. e., the diffusion of depolarizer, the electrode reaction, and the diffusion of the product, proceed in an equal velocity at the electrode surface. The result thus obtained can explain the essential rôle of the curvature of the electrode in some problems concerning the electrode reaction.

The author wishes to express his sincere thanks to Prof. I. Tachi for his interest to this research.

Agricultural Chemical Laboratory Faculty of Agriculture, Kyoto University, Kyoto

Researches on the Polarographic Diffusion Current. III. Higher Order Approximation of the Ilkovič Equation

By Tomihito KAMBARA and Isamu TACHI

(Received February 22, 1952)

Theoretical revision of the Ilkovič equation was carried out by Strehlow with Stackelberg,[1] Lingane with Loveridge,[2] and by us[3]; there is no doubt that the correction term of the form :

$$(D^{1/2} \cdot m^{2/3} \cdot t^{1/6} + A \cdot D \cdot m^{1/3} \cdot t^{1/3})$$

is required. As for the numerical value of the coefficient A, however, a further discussion is needed. In order to clear up this problem, our new treatment will be given below.

Derivation of the Equation

As reported in our preceding paper,[3] the thickness of diffusion layer, denoted by δ, surrounding any spherical electrode of radius r_e is given by the integral equation:

$$r_e^3(y^2+2y) \equiv \pi D \int_0^t \frac{r_e^2}{\delta} \cdot dt, \qquad (1)$$

where y is given by

(1) H. Strehlow und M. v. Stackelberg, *Z. Elektrochem.*, **54**, 51 (1950).
(2) J. J. Lingane and B. A. Loveridge, *J. Am. Chem. Soc.*, **72**, 438 (1950).
(3) T. Kambara, M. Suzuki, and I. Tachi, This Bulletin, **23**, 219 (1950); T. Kambara and I. Tachi, ibid., 225; *Proc. I. Intern. Polarographic Congress in Prague*, Part I, 126 (1951).

$$y=\delta/(r_e-\delta), \tag{2}$$

and D denotes the diffusion coefficient of the depolarizer. In the case of the dropping mercury electrode, it is seen that

$$\left.\begin{aligned} &r_e=a\cdot t^{1/3};\ a=\alpha\cdot m^{1/3};\\ &\alpha=\frac{1}{10}\left(\frac{3}{4\pi d}\right)^{1/3}=2.602\times10^{-2};\end{aligned}\right\} \tag{3}$$

where m is the rate of flow of mercury in mg./sec. and $d=13.55$ is the specific gravity of mercury at 20°C. Thus Eq. (1) can be transformed into the form :

$$\pi Dat^{1/3}(y+1)=a^3\left\{-y^3+2(y^2+y^2)+2t\,(y+1)y\frac{dy}{dt}\right\}. \tag{4}$$

Writing

$$a^3y^3/(y+1)=Y \tag{5}$$

and regarding this quantity of an infinitesimally small value as having a constant value during the time interval of interest, then it is seen that Eq. (4) is integratable; i. e.

$$\frac{3}{7}\pi Dat^{7/3}=-\frac{Y}{2}t^3+a^3y^3t^2. \tag{6}$$

Combination of the Eqs. (5) and (6) gives the following cubic equation :

$$F(y)=y^3+2y^2-2(\delta_1/r_e)^2y-2(\delta_1/r_e)^2=0, \tag{7}$$

where

$$\delta_1=\sqrt{\frac{3}{7}\pi Dt} \tag{8}$$

is the thickness of diffusion layer derived by Ilkovič.

Since y possesses a small positive value compared with unity, it is seen that one of the approximate solutions of Eq. (7) is given by

$$\eta=\delta_1/r_e\ ; \tag{9}$$

whence the Lingane-Loveridge equation:[2]

$$\frac{1}{\delta}=\frac{1}{r_e}+\frac{1}{\delta_1} \tag{10}$$

can be obtained, the procedure of which was already shown by us.[3] A more precise solution thereof is, according to the differential calculus, given by

$$y=\eta-\left[\frac{F(y)}{F'(y)}\right]_{y=\eta}=\eta\cdot\frac{4+2\eta}{4+\eta}. \tag{11}$$

That Eq. (11) is more accurate than Eq. (10), is made out as follows; i. e., it can be readily seen that

$$F(\eta)=-\eta^3\ ;$$

$$F\left(\eta\frac{4+2\eta}{4+\eta}\right)=\frac{1}{8}\eta^4\left(1+\frac{7}{4}\eta+\frac{1}{2}\eta^2\right)\left(1+\frac{1}{4}\eta\right)^{-3}\ ;$$

accordingly it is seen that a more suitable value for y is found. It may be noticed here, however, that

$$F(\eta)=-\eta^3<0\ ;\quad F(2\eta)=4\eta^3+6\eta^2>0\ ;$$

and also that $F''(y)=6y+4$ and $F'(y)=3y^2+4y-2\eta^2$ are positive in the interval $[\eta,\ 2\eta]$.

Now it follows from the Eqs. (2), (9), and (11) that

$$\frac{1}{\delta}=\frac{1}{r_e}+\frac{1}{\delta_1}\cdot\frac{4+\eta}{4+2\eta}=\frac{1}{\sqrt{\frac{3}{7}\pi Dt}}\cdot f(\eta), \tag{12}$$

where $f(\eta)$ is, according to the Maclaurin's theorem, shown to be

$$\begin{aligned} f(\eta)&=\eta+\frac{4+\eta}{4+2\eta}=\eta+\frac{1}{2}+\frac{1}{2}\left(1+\frac{1}{2}\eta\right)^{-1}\\ &=1+\frac{3}{4}\eta+\frac{1}{8}\eta^2-\frac{1}{16}\eta^3+\frac{1}{32}\eta^4-\frac{1}{64}\eta^5+\frac{1}{128}\eta^6-\cdots. \end{aligned} \tag{13}$$

Hence the instantaneous limiting diffusion current i_d in amp. is given by

$$i_d=nF\cdot4\pi r_e^2\cdot\frac{D\cdot^*C}{\sqrt{\frac{3}{7}\pi Dt}}\cdot f(\eta). \tag{14}$$

Further it is seen that

$$\eta=b\cdot D^{1/2}\cdot m^{-1/3}\cdot t^{1/6}\ ;\ b=44.593. \tag{15}$$

Adopting the usual conventional units, therefore, it is found that i_d in μ amp. is shown by

$$\begin{aligned} i_d=707.6\,nC[&D^{1/2}\cdot m^{2/3}\cdot t^{1/6}+33.45\,D\cdot m^{1/3}\cdot t^{1/3}\\ &+248.6\,D^{7/2}\cdot t^{1/2}-5543\,D^2\cdot m^{-1/3}\cdot t^{2/3}+123.6\\ &\times10^3D^{5/2}\cdot m^{-2/3}\cdot t^{5/6}-2.755\times10^6\cdot D^3\cdot m^{-1}\cdot t\\ &+61.44\times10^6\cdot D^{7/2}\cdot m^{-4/3}\cdot t^{7/6}-\cdots\cdots]. \end{aligned} \tag{16}$$

Thus the mean current is shown by

$$\begin{aligned} \bar{i}_d=606.5\,nC[&D^{1/2}\cdot m^{2/3}\cdot t^{1/6}+29.27\,D\cdot m^{1/3}\cdot t^{1/3}\\ &+171.1\,D^{7/2}\cdot t^{1/2}-3880\,D^2\cdot m^{-1/3}\cdot t^{2/3}+81.38\\ &\times10^3D^{5/2}\cdot m^{-2/3}\cdot t^{5/6}-1.607\times10^6D^3\cdot m^{-1}\cdot t\\ &+33.08\times10^6D^{7/2}\cdot m^{-4/3}\cdot t^{7/6}-\cdots\cdots]. \end{aligned} \tag{17}$$

In this equation t now represents the drop time.

Discussion of the Result

Since the above stated procedures are more exact than our former one, it can be concluded that as for the correction term of the Ilkovič equation, the coefficient 39 previously reported by us is too large. Then which is more adequate of the two coefficients, i. e. 17 given by Strehlow and Stackelberg or 29.27 given here? The answer to this question will become clear by the experimental work in future. It must be

pointed out here, however, that the polarographic current-time curve, especially in the younger age of drop-life, considerably differs from that predicted by the formula of the form

$$i=(k_1\cdot t^{1/6}+k_2\cdot t^{1/3})\ ;$$

this is reasonably comprehensible from the considerations taking the rate of electrode reaction into account.[4] Thus it is expected that also the mean current would be effected for the same reason.

It was reported by Smith[5] that the current-time curve with a very slowly growing mercury drop shows a parabola of one-half order. This phenomenon was first clarified by Strehlow and Stackelberg[1] in a mathematically very simple way. The above theory can elucidate this finding very satisfactorily. It is further expected that with a capillary of small m-value and large t-value, the higher terms will become more and more important.

It must be pointed out here that the coefficient 606.5 in Eq. (16) is more adequate than the former reported value 605; this discrepancy arises from the fact that we used the value $d=13.6$ (0°C) for the density of mercury in the preceding papers.

We made a serious error when, in our preceding papers,[3] we wrote that the transformation of the coordinate system carried out by MacGillavry and Rideal[6] is erroneous. In order to elucidate the relation between the two theories proposed by MacGillavry with Rideal and by Ilkovič,[7] we will show the mathematical proof for the identity of these two theories. Because the quantity $(4\pi/3)\rho^3$ appearing in the MacGillavry theory, represents the volume of the spherical shell of incompressible medium surrounding the mercury drop, it is seen that

$$\frac{4\pi}{3}\rho^3 \doteqdot qx=a^2t^{2/3}\cdot x=a^2u, \qquad (18)$$

where u is the variable appearing in the Ilkovič theory. With the aid of this relationship, the solution given by MacGillavry becomes identical with that given by Ilkovič.

Next we will prove that the MacGillavry-Rideal theory, which starts from the differential equation taking the curvature of mercury drop into consideration, is neglecting the curvature effect in result. Their differential equation, i. e.

$$\frac{1}{D}\frac{\partial C}{\partial t}=\frac{\partial^2 C}{\partial r^2}+\frac{2}{r}\frac{\partial C}{\partial r}-\frac{1}{D}\frac{\gamma}{3r^2}\frac{\partial C}{\partial r} \qquad (19)$$

is converted into the form :

$$\frac{1}{D}\frac{\partial C}{\partial t}=\frac{(\rho^3+\gamma t)^{4/3}}{\rho^5}\left(\rho\frac{\partial^2 C}{\partial \rho^2}+2\frac{\rho^3-\gamma t}{\rho^3+\gamma t}\frac{\partial C}{\partial \rho}\right) \qquad (20)$$

by the transformation of the coordinate system shown by

$$r^3=\rho^3+\gamma t\ ;\quad \gamma=a^3. \qquad (21)$$

Since the condition $\gamma t \gg \rho^3$ holds, Eq. (20) is transformed into

$$\frac{1}{D}\frac{\partial C}{\partial t}=\frac{(\gamma t)^{4/3}}{\rho^5}\left(\rho\frac{\partial^2 C}{\partial \rho^2}-2\frac{\partial C}{\partial \rho}\right). \qquad (22)$$

Upon solving this equation, they derived the original Ilkovič equation.

If we ignore the curvature of drop, it is seen that Eq. (19) is written as

$$\frac{1}{D}\frac{\partial C}{\partial t}=\frac{\partial^2 C}{\partial r^2}-\frac{1}{D}\cdot\frac{\gamma}{3r^2}\cdot\frac{\partial C}{\partial r}. \qquad (23)$$

By the relation shown by Eq. (21), this equation is transformed into

$$\frac{1}{D}\frac{\partial C}{\partial t}=\frac{(\rho^3+\gamma t)^{4/3}}{\rho^5}\left(\rho\frac{\partial^2 C}{\partial \rho^2}-\frac{2\gamma t}{\rho^3+\gamma t}\frac{\partial C}{\partial \rho}\right). \qquad (24)$$

Also this equation can be simplified into Eq. (22), which leads to the same result; accordingly it can be demonstrated that the MacGillavry-Rideal theory ignores the curvature effect.

It is pointed out by Dr. H. Matsuda[8] that the mathematical procedure given in Part II of this research[3] is in some points incorrect, i. e. it holds only as the first order approximation. The procedure solving the MacGillavry-Rideal differential equation given by him, which will be published in the near future, is expected to contribute much to the study of polarographic diffusion current.

Summary

Starting from the integral equation for the thickness of diffusion layer at the spherical electrode, a new equation for the polarographic diffusion current is derived and discussed.

The authors wish to express their hearty thanks to Prof. M. v. Stackelberg and Dr. H. Strehlow for their kind communications of their opinions on this problem and for separate copies of their papers. The authors' thanks are also due to Dr. H. Matsuda for his kind and constructive criticism.

Agricultural Chemical Laboratory, Faculty of Agriculture, Kyoto University, Kyoto

(4) T. Kambara and I. Tachi, This Bulletin, **25**, 135 (1952); T. Kambara, ibid., 281.
(5) G. S. Smith, *Nature*, **163**, 290 (1949).
(6) D. MacGillavry and E. K. Rideal, *Rec. trav. chim. Pays-Bas*, **56**, 1013 (1937).
(7) D. Ilkovic, *Collection Czech. Chem. Communs.*, **6**, 498 (1934); *J. chim. physique*, **35**, 129 (1938).
(8) H. Matsuda, Private communications.

On the Mechanism of the Reduction Process of the Hydrogen Ion at the Dropping Mercury Electrode. I. Theoretical Part

By Reita TAMAMUSHI[1]

(Received June 17, 1952)

Introduction

The study of the irreversible reduction wave of the hydrogen ion at the dropping mercury electrode (D. M. E.) is not only very important in the field of polarography, but also it seems to be highly valuable from the general standpoint of the study of hydrogen overvoltage, because the D. M. E. has the following characteristics in comparison with the usual stationary electrode. It is well known that at the D. M. E. a very good reproducibility can be obtained with many metal ions and organic substances because of its continuous renewal of the surface. The use of the D. M. E. makes it possible to ignore the historical effect of the electrode, and it can be expected that some obstacles in experiments, which appear in the use of the stationary electrode, are eliminated.

The mechanism of the reduction process of the hydrogen ion at the D. M. E. was investigated by J. Tomes,[2] J. Novak[3] and J. Heyrovsky[4] in 1937. The experimental results obtained by them, however, seem to be too complicated to be satisfactorily explained by the former theory on the polarographic current-voltage curve which assumes that the electrode potential of the D. M. E. can be represented by the Nernst equation.[5] Furthermore, it is doubtful whether the Nernst equation could be used in the polarographic reduction process of the hydrogen ion.

The great advances in the experimental technique and theory of polarography have been made during these ten years. By the use of the cathode-ray oscillograph[6] and the method of Kalousek[7] it became possible to examine the reversibility of the electrode process at the D. M. E. A new concept of the polarographic limiting current which is controlled by the adsorption process[8] or the rate of the reaction[9] was introduced by R. Brdicka and others, and the revised Ilkovic equation for the diffusion current was derived by several investigators.[10] In collaboration with Dr. N. Tanaka the present author derived the formulas for the current-voltage curve in polarography from the standpoint of chemical kinetics and presented an interpretation for the experimental results concerning the irreversible polarographic waves.[11]

Under these circumstances it seems to be promising to investigate the reduction process of the hydrogen ion at the D. M. E. from the same theoretical viewpoint as in the previous work.[11] This paper treats the theoretical part of the study; the formulas for the current-voltage curve of the hydrogen ion discharge under the various reaction mechanisms are derived and the discussions on the properties of the half-wave potential and others are presented. The experimental part will follow in other papers.

General Remarks

Many theories have been presented to interpret theoretically Tafel's equation,[12]

$$\eta = a - b \log i,$$

where η is the overvoltage at the current density i and a and b are the constants. These theories can be classified into three types—namely, (i) the slow discharge theory, (ii) the recombination theory and (iii) the electrochemical theory—according to the rate-determin-

(1) Present address: Chemistry Department, Faculty of Science, Ochanomizu Women's University, Tokyo.

(2) J. Tomes, *Collection Czechoslov. Chem. Communs.*, **9**, 150 (1937).

(3) J. Novak, ibid., **9**, 207 (1937).

(4) J. Heyrovsky, ibid., **9**, 271 (1937).

(5) J. Heyrovsky and D. Ilkovic, *Collection Czechoslov. Chem. Communs.*, **7**, 198 (1935).

(6) For example, P. Delahay, *J. Phys. Colloid. Chem.*, **54**, 630 (1950).

(7) M. Kalousek, *Collection Czechoslov. Chem. Communs.*, **13**, 105 (1948).

(8) R. Brdicka, ibid., **12**, 522 (1947).

(9) R. Brdicka and K. Wiesner, ibid., **12**, 138 (1947); etc.

(10) J. J. Lingane and B. A. Loveridge, *J. Am. Chem. Soc.*, **72**, 438 (1950); H. Strehlov and M. v. Stackelberg, *Z. Elektrochem.*, **54**, 51 (1950); T. Kambara, M. Suzuki and I. Tachi, This Bulletin, **23**, 219 (1950); T. Kambara and I. Tachi, ibid., **23**, 225 (1950).

(11) N. Tanaka and R. Tamamushi, This Bulletin, **22**, 187 (1949); R. Tamamushi and N. Tanaka, ibid., **22**, 227 (1949); **23**, 110 (1950); R. Tamamushi, ibid., **23**, 250 (1950); N. Tanaka, ibid., **23**, 253 (1950); R. Tamamushi and N. Tanaka, ibid., **24**, 127 (1951); N. Tanaka and R. Tamamushi, *Proc. I. International Polarographic Congress in Prague, Part I*, p. 468 (1951).

(12) J. Tafel, *Z. physikal. Chem.*, **50**, 641 (1905).

ing process. In the slow discharge theory[13] the rate-determining step is the discharge process of the hydrogen ion (1), while in the recombination theory[14] the process of the formation of the molecular hydrogen (2) is the slowest step.

$$\text{A.}\quad \begin{cases} \mathrm{H^+} + e \underset{\kappa_2 E_2}{\overset{\kappa_1 E_1}{\rightleftharpoons}} \mathrm{H} & (1) \\ \mathrm{H} + \mathrm{H} \underset{k_2}{\overset{k_1}{\rightleftharpoons}} \mathrm{H_2} & (2) \end{cases}$$

In the electrochemical theory of Horiuchi and others,[15] the following reduction process is assumed:

$$\text{B.}\quad \begin{cases} \mathrm{H^+} + e \underset{\kappa_2 E_2}{\overset{\kappa_1 E_1}{\rightleftharpoons}} \mathrm{H}_a & (3) \\ \mathrm{H}_a + \mathrm{H^+} \underset{k_2}{\overset{k_1}{\rightleftharpoons}} \mathrm{H_2^+} & (4) \\ \mathrm{H_2^+} + e \underset{\kappa_4 E_4}{\overset{\kappa_3 E_3}{\rightleftharpoons}} \mathrm{H_2} & (5) \end{cases}$$

H_a: the adsorbed hydrogen atom.

in which the rate-determining step is process (5). The mechanism which is assumed by Heyrovsky to interpret the polarographic current-voltage curve of the hydrogen ion is similar to that of the electrochemical theory, but in this case "molarization" process (4) is the rate-determining step.[4]

In general, the hydrogen atom which is produced, H or H_a, will disappear from the electrode surface by various processes, i. e., recombination process (2), molarization process (4), the diffusion process of H itself, and so on. As far as the reduction process is concerned, the problem which of these processes is predominant will be determined by the magnitudes of the forward rates of these processes. (Hereafter, forward means the direction from left to right of a chemical equation.) For example, if the rate constant of the forward process of (2) is larger than those of the diffusion process of the hydrogen atom from the electrode surface and the other processes, process (2) will be the predominant reaction to consume the hydrogen atom produced. On the other hand, if the diffusion process of the hydrogen atom is much faster than the rates of the other processes, the hydrogen atom will disappear from the electrode surface mainly by the diffusion of itself.

It is assumed throughout the following discussion that the overall electrode process is in a stationary state, i. e., in a dynamic equilibrium. It is to be mentioned here that the electrode potential is used in the following discussion instead of the overvoltage.

The Mechanism A

(I) One Hydrogen Ion participates in Process (1).—Let us consider that the rate constants of the forward (reduction) and the reverse (oxidation) reactions of process (1) are represented by $\kappa_1 E_1$ and $\kappa_2 E_2$ and that those of recombination process (2) by k_1 and k_2, respectively. κ_1, κ_2, E_1 and E_2 are the abbreviations of $s\frac{kT}{h}e^{-\Delta F_1/RT}$, $s\frac{kT}{h}e^{-\Delta F_2/RT}$, $e^{-n\alpha VF/RT}$ and $e^{(1-\alpha)nVF/RT}$, respectively, where ΔF_1 and ΔF_2 are the free energies of activation of the forward and the reverse reactions of process (1), V the electrode potential referred to a certain reference electrode, α the fraction of the potential V which is operative between the initial and the activated states, n the number of electrons which participate in redox reaction (1), and s is a constant which depends on the nature of the electrode. Since the current flowing is represented by the difference of the two rates, i. e., the forwerd and the reverse, the cathodic current at the dropping mercury electrode can be written as follows:

$$I = F(\kappa_1 E_1 [A_H{}^+] - \kappa_2 E_2 [A_H]) \qquad (6)$$

$$I = 2F(k_1' [A_H]^2 - k_2' [A_{H_2}]) \qquad (7)$$

$$k_1' \equiv \sigma k_1 \qquad k_2' \equiv \sigma k_2$$

in which $[A_H{}^+]$, $[A_H]$ and $[A_{H_2}]$ are the activities of the hydrogen ion, the hydrogen atom and the hydrogen molecule at the electrode surface, respectively, and σ is a proportional constant.

The hydrogen ion at the electrode surface is supplied by the diffusion process of this ion from the bulk of the solution where the activity of the hydrogen ion remains constant. Moreover, it is assumed that the molecular hydrogen produced at the electrode will disappear from the electrode surface by diffusion. Taking into consideration these diffusion processes, the current flowing is represented by

$$I = FK_{H^+}([C_{H^+}]^\circ - [C_{H^+}]) = FK'_{H^+}([A_{H^+}]^\circ - [A_{H^+}]) \qquad (8)$$

(13) M. Volmer and T. Erdey-Gruz, *Z. physikal. Chem.*, **150 A**, 203 (1930); R. W. Gurney, *Proc. Roy. Soc.*, **134 A**, 137 (1931); A. Frumkin, *Faraday Society Discussion*, No. 1, p. 57 (1947); etc.

(14) J. Tafel, loc. cit.; J. O'M. Bockris, *Faraday Society Discussion*, No. 1, p. 95 (1947); etc.

(15) G. Okamoto, J. Horiuchi and K. Hirota, *Sci. Papers Inst. Phys. Chem. Res. Tokyo*, **29**, 223 (1936); etc.

$$K'_{H^+} \equiv K_{H^+}/f_{H^+}$$
$$I = 2FK_{H_2}([C_{H_2}] - [C_{H_2}]^\circ)$$
$$= 2FK'_{H_2}([A_{H_2}] - [A_{H_2}]^\circ) \qquad (9)$$
$$K'_{H_2} \equiv K_{H_2}/f_{H_2}$$

where $[C_{H^+}]^\circ$, $[C_{H_2}]^\circ$, $[C_{H^+}]$ and $[C_{H_2}]$ are the concentrations of the hydrogen ion and the hydrogen molecule in the bulk of the solution and at the electrode surface, respectively, $[A_{H^+}]^\circ$ and $[A_{H_2}]^\circ$ the activities of the corresponding terms, and f_{H^+} and f_{H_2} are the activity coefficients of the hydrogen ion and the hydrogen molecule, respectively. We can ignore the existence of the migration current because of the presence of the excess of the supporting electrolyte in the polarographic studies.[16]

By assuming that all processes at the electrode surface including the diffusion processes are kept in a dynamic equilibrium, the current, I, can be expressed as the function of V, $[A_{H^+}]^\circ$ $[A_{H_2}]^\circ$ from Eqs. (6), (7), (8) and (9), i.e.:

$$I = F\kappa_1 E_1\left(\frac{FK'_{H^+}[A_{H^+}]^\circ - I}{FK'_{H^+}}\right) - F\kappa_2 E_2\left(\frac{\Gamma}{2FK'_{H_2}}\left(2FK'_{H_2}[A_{H_2}]^\circ + \frac{K'_{H_2}}{k'_2}I + I\right)\right)^{1/2} \qquad (10)$$
$$\Gamma \equiv k_2'/k_1'$$

This is the general equation for the current-voltage curve of the hydrogen ion discharge under mechanism (A).

(a) **Activation-controlled Case.**—In this case it is assumed that $\kappa_1 E_1$ is much smaller than K'_{H^+} and that the current flowing is negligibly small at the electrode potential, where $\kappa_1 E_1$ is nearly equal to $\kappa_2 E_2 \Gamma^{1/2}$. When the electrode potential becomes more negative, $\kappa_1 E_1$ becomes larger and $\kappa_2 E_2 \Gamma^{1/2}$ tends to be zero. In this potential region the current, which is accompanied by the reduction process, appears.[11] Under this condition the second term of the right-hand side of Eq. (10) can be neglected in comparison with the first term and the reduction current can be represented by

$$I = F\kappa_1 E_1 \frac{FK'_{H^+}[A_{H^+}]^\circ - I}{FK'_{H^+}} \qquad (11)$$
$$I_l = FK'_{H^+}[A_{H^+}]^\circ \qquad (12)$$

where I_l means the limiting current.

(16) I. M. Kolthoff and J. J. Lingane, "Polarography", Interscience Pub. Inc., New York, N. Y., 1946, p. 83.

This relation is quite the same as that for the reduction of the simple (or hydrated) metal ion in the activation-controlled case.[11] It is readily shown that the relation between $\log I$, $(I_l - I)$ and V—so-called "log-plot"—is a straight line whose tangent is equal to $RT/\alpha F$ and that the half-wave potential, $V_{1/2}$, is independent of the limiting current. Moreover, Eq. (12) shows that the limiting current is controlled by the diffusion process and is equal to the diffusion current.

(b) **Diffusion-controlled Case.**—As mentioned in the previous papers[11] it is assumed, in the diffusion-controlled case, that $\kappa_1 E_1$ and $\kappa_2 E_2 \Gamma^{1/2}$ are much larger than K'_{H^+}, K'_{H_2} or k'_2 at the electrode potential where $\kappa_1 E_1$ is nearly equal to $\kappa_2 E_2 \Gamma^{1/2}$. In this potential region Eq. (10) can be reduced to

$$\left(\frac{\kappa_2 E_2}{\kappa_1 E_1}\right)^2 = \frac{2}{F}\frac{K'_{H_2}}{(K'_{H^+})^2}\frac{1}{I'} \times \frac{(FK'_{H^+}[A_{H^+}]^\circ - I)^2}{2FK'_{H_2}[A_{H_2}]^\circ + \frac{K'_{H_2}}{k'_2}I + I} \qquad (13)$$

because the term $1/\kappa_1 E_1$ can be neglected in comparison with the other terms in Eq. (10). When the activity of the hydrogen molecule in the bulk of the solution is equal to zero, the following equation for the reduction wave can be obtained from Eq. (13) by introducing the relation, $I_l = FK'_{H^+}[A_{H^+}]^\circ$, i.e.:

$$V = \text{const.} - \frac{RT}{F}\log\frac{I}{(I_l - I)^2} \qquad (14)$$

From this equation it is shown that the relation between $\log I/(I_l - I)^2$ and V is linear and that the half-wave potential is represented by

$$V_{1/2} = \text{const.} + \frac{RT}{F}\log I_l \qquad (15)$$

Eq. (15) means that the half-wave potential is not independent of the limiting current but it shifts to a more positive one as the limiting current increases.

(II) **Two Hydrogen Ions participate in Process 1.**—If we assume that each of two hydrogen ions takes an electron simultaneously and the hydrogen atoms thus produced combine with each other to form a hydrogen molecule at the electrode surface, the following equation for the discharge reaction should be used instead of process (2), i.e.:

$$2H^+ + 2e \rightleftharpoons 2H \qquad (2')$$

According to this process the current flowing is represented by

$$I \simeq 2F(\kappa_1 E_1[A_H{}^+]^2 - \kappa_2 E_2[A_H]^2) \quad (16)$$

By the use of Eq. (16) instead of Eq. (6), the general equation for the current-voltage curve can be easily obtained by the same method as mentioned before:

$$I \simeq 2F\kappa_1 E_1\left(\frac{FK'_{H}{}^{+}[A_{H+}]^\circ - I}{FK'_{H}{}^{+}}\right)^2 - 2F\kappa_2 E_2 \times\left(\frac{I}{2FK'_{H_2}}\left(2FK'_{H_2}[A_{H_2}]^\circ + \frac{K'_{H_2}}{k_2'}I + I\right)\right) \quad (17)$$

(a) Activation-controlled Case.—In this case the following relations for the reduction wave are derived from Eq. (17):

$$\kappa_1 E_1 = \frac{F(K'_{H}{}^{+})^2 I}{2(I_l - I)^2}$$

or

$$V = \text{const.} - \frac{RT}{\alpha F}\log\frac{I}{(I_l - I)^2} \quad (18)$$

and

$$I_l = FK'_{H}{}^{+}[A_H{}^+]^\circ$$

It is quite obvious in this case that the limiting current is determined by the diffusion process and that the half-wave potential becomes more positive as I_l increases.

(b) Diffusion-controlled Case.—By the same treatment as mentioned in **(I)**-**(b)**, the equation of the current-voltage curve under the present condition can be obtained, the results of which are quite similar to Eqs. (13), (14) and (15).

Electrochemical Mechanism

According to the electrochemical theory, the reduction mechanism of the hydrogen ion is represented by process (B). In this case, besides Eqs. (8) and (9) due to the diffusion processes, the current flowing can be written as follows:

$$I = F(\kappa_1 E_1[A_H{}^+]^\circ - \kappa_2 E_2[A_{Ha}]) \quad (19)$$

$$I = F(k_1'[A_{Ha}][A_H{}^+] - k_2'[A_{H_2}{}^+])$$

$$k_1' \equiv \sigma k_1 \quad k_2' \equiv \sigma k_2 \quad (20)$$

$$I = F(\kappa_3 E_3[A_{H_2}{}^+] - \kappa_4 E_4[A_{H_2}]) \quad (21)$$

$$\kappa_3 E_3 \equiv s\frac{kT}{h}e^{-\Delta F_3/RT}e^{-\beta VF/RT}$$

$$\kappa_4 E_4 \equiv s\frac{kT}{h}e^{-\Delta F_4/RT}e^{(1-\beta)VF/RT}$$

ΔF_3 and ΔF_4 are the free energies of activation of the forward and the reverse processes of (5), respectively, and β has the same meaning as α.

(I) Rate-determining Step is Process (5).—If we assume that process (5) is the slowest step of processes (3), (4) and (5) in the potential region where the reduction wave appears and that these processes are in a dynamic equilibrium at the electrode surface, the relation (22) for the current-voltage curve can be derived from Eqs. (8), (9), (19), (20) and (21): By taking into account the condition of the activation-controlled case, the second term of the right-hand side of Eq. (22) can be neglected in the potential region of the reduction wave, because $\kappa_4 E_4$ is nearly equal to zero under this condition, and Eq. (22) can be reduced to Eq. (23). Furthermore, it seems reasonable to assume that $\kappa_1 E_2/\kappa_1 E_1$ is very small in this potential region and that I is much larger than $K'_{H}{}^{+}I$. By this assumption Eq. (23) can be simplified as follows:

$$I = \kappa_3 E_3\frac{1}{(K'_{H}{}^{+})^2}\frac{(FK'_{H}{}^{+}[A_H{}^+]^\circ - I)^2}{FI\dfrac{\kappa_2 E_2}{\kappa_1 E_1}} \quad (24)$$

When the electrode potential is sufficiently negative and $I/\kappa_3 E_3$ is negligibly small, the limiting current which is controlled by the diffusion process appears and it is represented by Eq. (12). From these equations the following formulas for the current-voltage curve and the half-wave potential are derived, i.e.:

$$V = \text{const.} - \frac{RT}{(1+\beta)F}\log\frac{I}{(I_l - I)^2} \quad (25)$$

and

$$V_{1/2} = \text{const.} + \frac{RT}{(1+\beta)F}\log I_l \quad (26)$$

$$I = F\left\{\kappa_3 E_3\frac{k_1'\kappa_1 E_1[(FK'_{H}{}^{+}[A_H{}^+]^\circ - I)^2 - K'_{H}{}^{+}I(FK'_{H}{}^{+}[A_H{}^+]^\circ - I)] - F(K'_{H}{}^{+})^2\kappa_2 E_2 I}{F^2 k_2'(K'_{H}{}^{+})^2\kappa_2 E_2} - \kappa_4 E_4\frac{2FK'_{H_2}[A_{H_2}]^\circ + I}{2FK'_{H_2}}\right\} \quad (22)$$

$$I = F\kappa_3 E_3\frac{\dfrac{1}{(K'_{H}{}^{+})^2}[(FK'_{H}{}^{+}[A_H{}^+]^\circ - I)(FK'_{H}{}^{+}[A_H{}^+]^\circ - I - K'_{H}{}^{+}I)] - F\dfrac{1}{k_1'}\dfrac{\kappa_2 E_2}{\kappa_1 E_1}I}{F^2\dfrac{k_2'}{k_1'}\dfrac{\kappa_2 E_2}{\kappa_1 E_1}} \quad (23)$$

These results are qualitatively similar to those obtained from Eqs. (14) and (15).

(II) Rate-determining Step is Process (3).—Let us consider that the rate constant, $\kappa_2 E_2$, of the reverse reaction of process (3) is negligibly small in comparison with that of the forward reaction, $\kappa_1 E_1$, in the potential region of the reduction wave, and that the rate constants of the forward reactions of processes (4) and (5) are sufficiently large. In this case the adsorbed hydrogen atom, H_a, produced in process (3) will instantaneously react with H^+ and an electron and give a molecular hydrogen. Under this condition the reduction current can be represented as follows:

$$I=\kappa_1 E_1 \frac{I_l-I}{K'_{H^+}}$$

$$I_l=FK'_{H^+}[A_{H^+}]^\circ$$

This result is quite the same as that of the reduction of the simple metal ion in the activation-controlled case.[11] As far as the reduction process is concerned, processes (4) and (5) do not play any role in the present case, but, if the oxidation process of H_2 is considered, these processes have an important effect on the current-voltage curve.

The Mechanism in which the Adsorption Process of the Hydrogen Ion is taken into Consideration

Let us assume that only the hydrogen ions adsorbed on the electrode surface can be neutralized. This assumption seems probable because it has been pointed out by J. Weiss that only H_3O^+ ion on or very near to the surface of the electrode can discharge.[17] The structure of the double layer near the electrode is considered to consist of two energy barriers, one of which is between the solution side, S, and the adsorption state, A, and the other is between the adsorption state and the electrode side, E. (Fig. 1). As suggested by P. van Rysselberghe, the hydrogen atom produced by the neutralization process will exist in various forms, e. g., adsorbed state H_a, free hydrogen atom, and so on.[18] Moreover, there may be various processes which will take place after the neutralization of the hydrogen ion, e. g., the recombination of the hydrogen atoms, the combination reaction of the hydrogen atom and the hydrogen ion, etc. At any rate, if it is assumed that the rate constant of the oxidation reaction, i. e., the reverse process from E to A, is negligibly small in comparison with that of the neutralization process from A to E in the potential region of the reduction wave, the equation for the reduction wave is not influenced by the processes which follow the neutralization reaction. In the following, only the results derived from this assumption are set down. For convenience' sake, let us call this mechanism "the slow discharge mechanism of the adsorbed hydrogen ion".

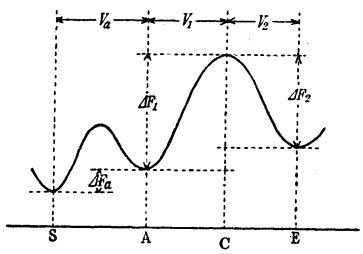

Fig. 1.—The energy barrier between the electrode and the solution.

Under these conditions the overall electrode process of the discharge of the hydrogen ion is represented as follows:

$$H^+(\text{bulk of the solution}) \xrightarrow{\text{diffusion}} H^+(\text{surface})$$

$$H^+(\text{surface}) \underset{}{\overset{\text{adsorption}}{\rightleftharpoons}} H^+(\text{adsorbed})$$

$$H^+(\text{adsorbed}) \underset{\kappa_2 E_2'\ \text{oxidation}}{\overset{\kappa_1 E_1'\ \text{reduction}}{\rightleftharpoons}} H\ (\text{surface})$$

$$H\ (\text{surface}) \longrightarrow \text{disappears from the electrode surface by some processes}$$

According to these processes the current flowing can be written by the next relations:

$$I=FK'_{H^+}([A_{H^+}]^\circ-[A_{H^+}]) \qquad (8)$$

$$I=F(\kappa_1 E_1'[A_{Ha^+}]-\kappa_2 E_2'[A_H]) \qquad (27)$$

$$\kappa_1 E_1' \equiv s\frac{kT}{h}e^{-\Delta F_1/RT}e^{-V_1 F/RT},$$

$$\kappa_2 E_2' \equiv s\frac{kT}{h}e^{-\Delta F_2/RT}e^{V_2 F/RT}$$

where ΔF_1 and ΔF_2 are the free energies of activation of the reduction-oxidation process; V_1 means the difference of the electrical potential between the activated state, C, and the adsorbed state, A, and V_2 means the difference of the electrical potential between the electrode surface, E, and the activated state, C, respectively (Fig. 1). $[A_{Ha^+}]$ is the activity of the hydrogen ion adsorbed on the electrode

(17) J. Weiss, *Faraday Society Discussion*, No. 1, p. 135 (1947).

(18) P. v. Rysselberghe, *J. Chem. Phys.*, **17**, 1226 (1949).

Table 1

Mechanism	Chemical Formula	Formula for C-V Curve	Log-plot	$V_{1/2}$ vs. I_l	I_l
A-(I)					
Diff.	$H^+ + e \rightleftarrows H$	$V = \text{const.} - \frac{RT}{F}\log\frac{I}{(I_l-I)^2}$	unsym. (L)	pos.	I_d
Act.	$H + H \rightleftarrows H_2$	$V = \text{const.} - \frac{RT}{\alpha F}\log\frac{I}{I_l-I}$	sym.	indep.	〃
A-(II)					
Diff.	$2H^+ + 2e \rightleftarrows 2H$	$V = \text{const.} - \frac{RT}{F}\log\frac{I}{(I_l-I)^2}$	unsym. (L)	pos.	〃
Act.	$2H \rightleftarrows H_2$	$V = \text{const.} - \frac{RT}{\alpha F}\log\frac{I}{(I_l-I)^2}$	unsym. (L)	pos.	〃
Electrochem.					
(I)	$H^+ + e \rightleftarrows H_a$; $H_a + H^+ \rightleftarrows H_2^+$	$V = \text{const.} - \frac{RT}{(1+\beta)F}\log\frac{I}{(I_l-I)^2}$	unsym. (L)	pos.	〃
(II)	$H_2^+ + e \rightleftarrows H_2$	$V = \text{const.} - \frac{RT}{\alpha F}\log\frac{I}{I_l-I}$	sym.	indep.	〃
Slow Disch. Ads. H^+ Ion	$H_a^+ + e \rightleftarrows H$; $H + H \rightleftarrows H_2$	$V = \text{const.} - \frac{RT}{\alpha' F}\log\frac{I}{(I_l-I)^\nu}$	unsym. (U)	neg.	〃

Diff.: The diffusion-controlled type. Act.: The activation-controlled type.
unsym. (L): The lower half of the wave is steeper than the upper half.
unsym. (U): The upper half of the wave is steeper than the lower half.
sym.: There is a center of symmetry at half-wave potential, i. e., the relation between $\log I/(I_l-I)$ and V is linear.
pos.: $V_{1/2}$ shifts to more positive with the increase of I_l.
neg.: $V_{1/2}$ shifts to more negative with the increase of I_l.
indep.: $V_{1/2}$ is independent of I_l.

surface. According to the assumption mentioned above we can neglect the second term of the right-hand side of Eq. (27) in the potential region of the reduction wave and, therefore, Eq. (27) can be reduced to the following as an approximation:

$$I = F\kappa_1 E_1' [A_{Ha}^+] \qquad (28)$$

Now, let us assume that the adsorption equilibrium of the Freundlich adsorption isotherm type is kept between the adsorbed ion and the ion in the solution side. It is shown that the Freundlich adsorption isotherm is more satisfactorily applied to the adsorption phenomena in solution than the Langmuir isotherm.[19] If the effect of the electrical potential difference, V_a, between the adsorbed state, A, and the solution side, S, is taken into consideration, this equilibrium can be represented by

$$[A_{Ha}^+] = \gamma [A_H^+]^\nu \exp\left(-\frac{V_a F}{RT}\right) \qquad (29)$$

$$\nu \leqq 1$$

where γ and ν are the constants of adsorption.

From Eqs. (8), (28) and (29) the equation for the current-voltage curve can be obtained as follows:

$$\kappa_1 E_1' \exp\left(-\frac{V_a F}{RT}\right) = \frac{(FK'_{H^+})^\nu}{F\gamma} \frac{I}{(FK'_{H^+}[A_H^+]^\circ - I)^\nu} \qquad (30)$$

by which it is easily shown that at a sufficiently negative potential the limiting current, which is controlled by the diffusion process and represented by Eq. (12) cited before, appears. If the relation between the electrode potential, V, and the terms, V_1, V_2 and V_a,

$$V = V_1 + V_2 + V_a,\ V_1 + V_a = \alpha' V \text{[20]}$$

and Eq. (12) are introduced, the following formula is obtained by rearranging Eq. (30),

(19) J. N. Brönsted, "Physical Chemistry", William Heinemann Ltd., London, 1937, p. 355.

(20) α' is a proportional constant and is related to α by the following equation: $\alpha' = \alpha\{(V-V_a)/V\} + (V_a/V)$, because α can be represented by $V_1/(V_1+V_2)$ in the present case. It is obvious that when V_a is very small α' becomes equal to α.

$$V=\text{const.}-\frac{RT}{\alpha' F}\log\frac{I}{I_l-I}+\frac{RT}{\alpha' F}(\nu-1)\log(I_l-I) \qquad (31)$$

in which,

$$\text{const.}=\frac{RT}{\alpha' F}\left(-\frac{\Delta F_1}{RT}+\log\gamma+\log s+\log\frac{kT}{h}+\log F-\nu\log(F K'_{H^+})\right)$$

It is quite clear that the relation between V and $\log I/(I_l-I)$ is by no means linear in this case. By using the definition for the half-wave potential, $I=I_l/2$, we can get the relation between $V_{1/2}$ and I_l as follows:

$$V_{1/2}=\text{const'.}+\frac{RT}{\alpha' F}(\nu-1)\log I_l \qquad (32)$$

in which,

$$\text{const'.}=\frac{RT}{\alpha' F}\left(-\frac{\Delta F_1}{RT}+\log\gamma+\log s+\log\frac{kT}{h}+\log F-\nu\log(F K'_{H^+})-(\nu-1)\log 2\right)$$

The half-wave potential shifts to more negative side as the limiting current increases, because the term $(\nu-1)$ is negative.

All results on the properties of the current-voltage curve of the hydrogen ion, which are obtained under the various reduction mechanisms, are summarized in Table 1.

Summary

The formulas for the current-voltage curve of the reduction wave of the hydrogen ion under the various mechanisms of the overall deposition process were derived from the standpoint of chemical kinetics. The results on the various properties of the current-voltage curve,—the relation between the half-wave potential and the concentration of the hydrogen ion in the bulk of the solution, the property of the limiting current, and the log-plot analysis of the current-voltage curve—are presented.

It is assumed throughout the present discussion that the processes at the electrode surface, including the diffusion process, are kept in a stationary state, i. e., in a dynamic equilibrium. This assumption seems to be reasonable when the stationary and reproducible current-voltage curve is obtained at the dropping mercury-electrode.

The author expresses his best thanks to Prof. San-ichiro Mizushima and Assist. Prof. Nobuyuki Tanaka for their great encouragement and valuable suggestions in this study. The cost of this research has been defrayed from the Scientific Research Encouragement Grant from the Ministry of Education.

Institute of Science and Technology, Tokyo University, Tokyo

On the Mechanism of the Reduction Process of the Hydrogen Ion at the Dropping Mercury Electrode. II. Experimental Part — The Limiting Current of the Hydrogen Wave

By Reita TAMAMUSHI[1]

(Received June 17, 1952)

In the theoretical part of this work[2] the formulas for the current-voltage curve of the reduction wave of the hydrogen ion have been studied from the standpoint of the chemical kinetics and the theoretical considerations on the properties of the reduction wave have been presented. In this paper the experimental results and the discussion on the limiting current of the hydrogen ion are set down.[3]

Experimental

Apparatus:—A Heyrovsky-Shikata type photo-recording polarograph and a manually operating

(1) Present address: Chemistry Department, Faculty of Science, Ochanomizu Women's University, Tokyo.

(2) R. Tamamushi, This Bulletin, **25**, 287 (1952).

(3) Recently, the discussion on the hydrogen wave was reported by J. Kůta in the Proceedings of the I. International Polarographic Congress in Prague, Part I, p. 852 (1951).

polarograph similar to that used by J. J. Lingane and I. M. Kolthoff[4] were used. An over-damped galvanometer was used to measure the polarographic current.

A specially designed all-glass polarographic cell as shown in Fig. 1 was used throughout this study

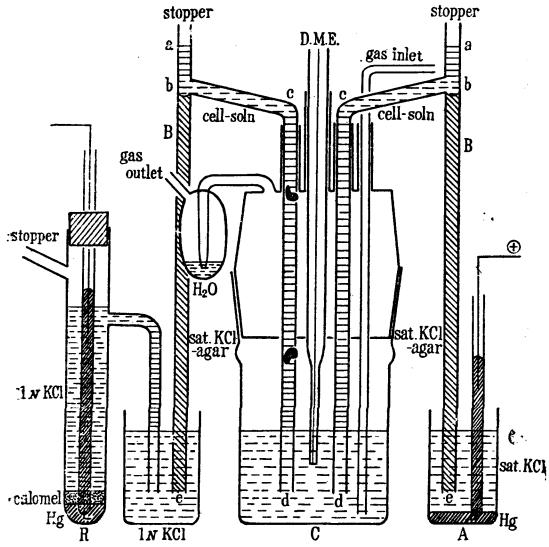

Fig. 1.—All-glass polarographic cell assembly: A: anode; B: h-type sat. KCl-agar-bridge; C, polarographic cell; R: reference electrode (N. C. E.).

to avoid the contamination from the rubber connection. The anode was a large area mercury pool connected with the cell-solution by the saturated KCl solution and a h-type sat. KCl-agar-bridge. The reference electrode for the measurement of the electrode potential of the D.M.E. was a normal calomel electrode connected with the cell-solution by 1N KCl solution and a h-type sat. KCl-agar-bridge. The part **be** of a h-type bridge was filled with a sat. KCl-agar and the cell-solution was sucked into the side-tube **abcd** to make a junction at point **b**. By this method the effect of the high concentration of KCl in agar on the cell-solution can be reduced to a great extent. The liquid junction potential may be greatly reduced by the use of saturated KCl.

The capillary constant, $m^{2/3}\,t^{1/6}$, of the dropping mercury electrode, which was used throughout the present experiment, was 1.028 $mg.^{2/3}\,sec.^{-1/2}$ at the height of the mercury reservior of 53 cm. This value was determined in 0.1N KCl solution open to air without the applied potential.

The dissolved oxygen was removed from the cell-solution by bubbling pure hydrogen gas obtained by the electrolysis of a NaOH solution for about 40 minutes.

A water or a liquid-paraffin thermostat maintained at 25.0° was used throughout the experiments except when the effect of the temperature on the reduction wave of the hydrogen ion was examined.

Materials:—The pure mercury, which was distilled under vacuum after washing several times with dil. HNO_3 solution and dist. water, was used for the dropping mercury electrode. As a supporting electrolyte 0.1N KCl solution was used in the present study. The potassium chloride used was recrystallized from dist. water. Reagent grade HCl and Fixanal HCl were used to make a stock solution, the composition of which is 0.1N KCl–0.01N HCl. No maximum suppressor was used. The concentration of HCl in the original solution was determined by the acid-base titration.

Experimental Results

A typical polarogram with a well-defined limiting current was obtained with the dil. solution of HCl in 0.1N KCl solution, which is due to the deposition of the hydrogen ion of HCl. The various properties of the limiting current, I_l, of the hydrogen ion, — i. e., the relation between I_l and the concentration of the hydrogen ion, $[C_{H^+}]°$, in the bulk of the solution, the relation between I_l and the height of the mercury reservoir, p, the temperature coefficient of I_l, etc.—were studied in this medium.

The Relation between I_l and $[C_{H^+}]°$.— This relation is represented by a straight line as shown in Fig. 2 over the concentration range

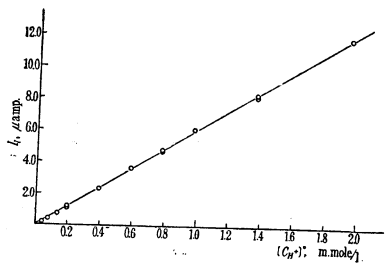

Fig. 2.—The relation between I_l and $[C_{H^+}]°$ at 25°C.

of the hydrogen ion from 0.039 to 1.95 millimole per liter. It is obvious that the relation between I_l and $[C_{H^+}]°$ is represented as follows:

$$I_l = a[C_{H^+}]° \qquad (1)$$

$a = 6.04$ microamp./millimole/l.

The value of a is calculated from the experimental data with the least square method.

The Temperature Coefficient of I_l.—The effect of the temperature of the cell-solution

(4) J. J. Lingane and I. M. Kolthoff, *J. Am. Chem. Soc.*, **61**, 825 (1939).

Table 1

Temperature Coefficient of I_l.

Temp. τ, °C.	I_l, microamp.	$dI_l/d\tau$, microamp./°C.	$(1/I_l)(dI_l/d\tau)$, %	$d\log I_l/d\tau$, %
$[C_H{}^+]^\circ=0.78$ millimole/l.				
5	3.74	0.0866	2.32	1.01
15	4.46	0.0612	1.37	0.61
25	5.03	0.0526	1.05	0.43
35	5.44	0.0316	0.58	0.24
45	5.72	0.0240	0.42	0.17
$[C_H{}^+]^\circ=1.95$ millimole/l.				
5	9.25	0.15	1.62	0.68
15	10.6	0.12	1.13	0.52
25	11.7	0.11	0.94	0.44

on the limiting current was studied over the temperature range of 0 to 50°, the results of which are shown in Table 1 and Fig. 3. In Table 1, the term $[d\log I_l/d\tau]$ represents a tangent of the relation between $\log I_l$ and the temperature, τ, at any temperature, and this is called as the "relative temperature coefficient", while the term $dI_l/d\tau$ represents the "absolute temperature coefficient".

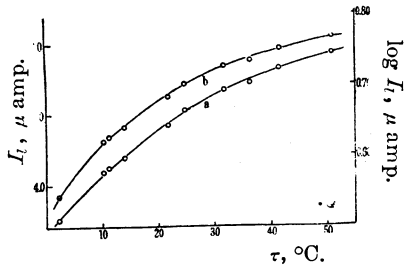

Fig. 3.—The effect of temperature on I_l: a, I_l vs. τ; b, $\log I_l$ vs. τ. $[C_H{}^+]^\circ=0.78$m. mole/l.

The Relation between I_l and p.—In order to examine whether the limiting current of the hydrogen ion under the present condition is controlled only by the diffusion process or not, the experiment on the relation between I_l and was carried out. As shown in Fig. 4, the relation between I_l and $\sqrt{p}$ is linear and represented by the following equation:

$$I_l=0.76\sqrt{p}+2.0 \text{ (microamp.)} \quad (2)$$

The value of p is corrected with the back pressure, p_b, which is calculated by the following relation:[5]

$$p_b=\frac{7.73\times10^{-3}\sigma}{m^{1/3}t^{1/3}}=\frac{3.1}{m^{1/3}t^{1/3}} \text{ (cm.)} \quad (3)$$

$$\sigma=400 \text{ dyne cm.}^{-1}$$

(5) I. M. Kolthoff and J. J. Lingane, "Polarography", nterscience Pub. Inc., New York, N. Y., 1946, p. 67.

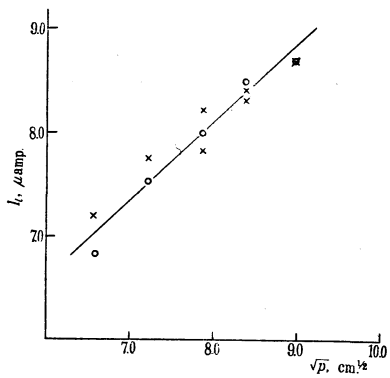

Fig. 4.—The relation between I_l and $\sqrt{p}$: ○, data obtained by the manual apparatus; ×, data obtained by the Heyrovsky-Shikata type polarograph.

where σ is the surface tension of mercury in the electrolyte solution, m the weight of mercury in mg. flowing from the capillary per second, and t the drop-time of one drop in second. If the experimental value, $m^{1/3}t^{1/3}=1.50$, is used, p_b is equal to 2.1 cm. It is apparent from Eq. (3) that p_b is independent of p, because $m^{1/3}t^{1/3}$ is independent of p. It is to be noted here that, when the value of p is changed from about 40 cm. to about 80 cm., the term $t\times p$ is kept nearly constant as shown in Table 2.

Table 2

p, cm.	t, sec.	$p\times t$
80.1	2.98	238
70.2	3.40	238
61.6	4.06	250
51.9	4.56	236
43.4	5.54	240

The Relation between the Diffusion-current Constant and t.—If we assume that the limiting current of the hydrogen ion is

equal to the diffusion current, I_d, it is possible to obtain the relation between the diffusion-current constant, $I_d/m^{2/3}t^{1/6}$, and t from the experiment which was carried out to investigate the relation, I_l vs. $\sqrt{p}$. The value of m at each drop-time, t, can be calculated by assuming the following equation:

$$m = \text{const.} \times p \qquad (4)$$

The value of the constant in Eq. (4) was obtained by inserting the experimental data, $m=0.708$ mg./sec. at $p=52.0$ cm., into this equation.

The result obtained is shown in Fig. 5. It can be said that the diffusion-current constant is not independent of t, but it increases almost linearly with the increase of t over the range of t from 3 to 6 seconds. The diffusion-current constant also is not independent of the term, $m^{-1/3}t^{1/6}$, as shown in Fig. 6.

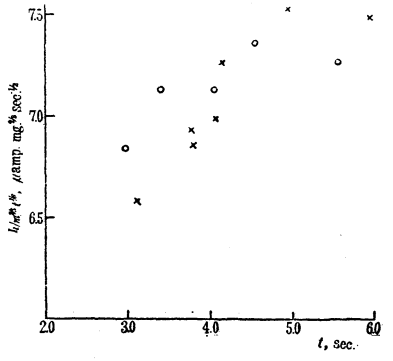

Fig. 5.—The relation between the diffusion current constant and t.

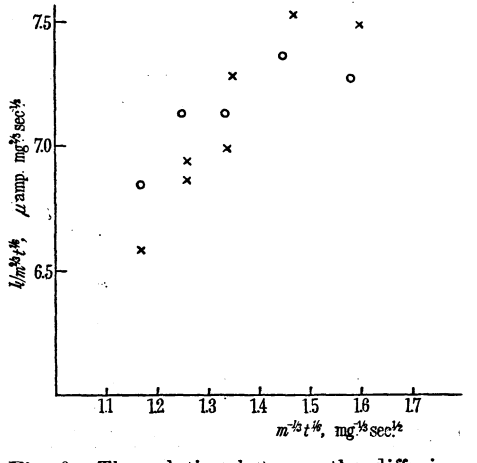

Fig. 6.—The relation between the diffusion current constant and $m^{-1/3}t^{1/6}$.

Discussion

There are several kinds of limiting currents in polarography, i. e., the diffusion current, the kinetic current,[6] the adsorption current[7] and the combination of these currents. The diffusion current, I_d, is represented as follows according to Ilkovic equation (6) or revised Ilkovic equation (7):[8]

$$I_d = 605\, nCD^{1/2}m^{2/3}t^{1/6} \qquad (6)$$

$$I_d = 605\, nCD^{1/2}m^{2/3}t^{1/6}\left(1+\frac{AD^{1/2}t^{1/6}}{m^{1/3}}\right) \qquad (7)$$

where n is the number of the electrons which participate in the redox reaction, C the concentration of the oxidant or the reductant in millimole per liter, D the diffusion coefficient of the corresponding substance in the medium under investigation in cm.^{2} per second, m the weight of mercury flowing from the D. M. E. per second in mg., and t the drop-time in second. In Eq. (7) A is a constant and equal to 39 or 17 according to Lingane-Loveridge and Kambara-Tachi or Strehlov-Stackelberg, respectively.

It is well known that the kinetic current is independent of the height of the mercury reservior, p,[6] and the diffusion current is proportional to the square root of p as readily shown from the Ilkovic equation. Revised Ilkovic equation (7) requires that the relation between I_l and p is represented as follows:

$$I_l = a_0 + a_1\sqrt{p} \qquad (8)$$

where a_0 and a_1 are constants. This relation is quite the same as Eq. (2) obtained from the experiment.

By means of Eq. (7) the constant term, a_0, in Eq. (8) can be written as follows:

$$a_0 = 605\, nADCm^{1/3}t^{1/3}$$

If we use the following numerical values obtained under the present experimental conditions,

$m=0.708$ mg./sec., $t=4.56$ sec.

$D_{H^+}=8.0\times10^{-5}$cm.^{2}/sec., $C=1.30$ millimole/l.

(6) R. Brdicka and K. Wiesner, *Collection Czechoslov. Chem. Communs.*, **12**, 138 (1947); J. Koutecky and R. Brdicka, ibid., **12**, 337 (1947).

(7) R. Brdicka, *Collection Czechoslov. Chem. Communs.*, **12**, 522 (1947).

(8) J. J. Lingane and B. A. Loveridge, *J. Am. Chem. Soc.*, **72**, 438 (1950); H. Strehlov and M. v. Stackelberg, *Z. Elektrochem.*, **54**, 51 (1950); T. Kambara, M. Suzuki and I. Tachi, This Bulletin, **23**, 219 (1950); T. Kambara and I. Tachi, ibid., **23**, 225 (1950).

the constant, a_0, is equal to 3.6 microamp. or 1.6 microamp. according to $A=39$ or $A=17$, respectively. In this calculation it is assumed that n equals one. The value of D_{H^+}—the diffusion coefficient of the hydrogen ion in 0.1 N KCl solution—will be discussed later. The experimental value, $a_0=2.0$ microamp., is in fairly good agreement with the theoretical value mentioned above.

Furthermore, the experimental result, that the diffusion-current constant is not independent of t or $m^{-1/3}t^{1/6}$ as shown in Figs. 5 and 6, suggests that it is more appropriate to use Eq. (7) for the diffusion current of the hydrogen ion rather than Eq. (6). From the slope of the relation between the diffusion-current constant and the term, $m^{-1/3}t^{1/6}$, we can obtain the value of A in Eq. (7). If the value of 8.0×10^{-5} cm.^{2}/sec. is used for D_{H^+} in 0.1 N KCl solution, A is calculated to be equal to about 35, and this value is quite reasonable.

From these results it seems probable to consider that the limiting current of the hydrogen ion in 0.1 N KCl solution is the diffusion current which is represented by Eq. (7).

This conclusion is also confirmed by the temperature coefficient of I_l. If the limiting current of the hydrogen ion is controlled by some other processes different from the diffusion process, *e. g.*, if I_l is equal to the kinetic current, the temperature coefficient of I_l will be much larger than those in Table 1. When it is assumed that the temperature coefficient of the diffusion coefficient is obtained from that of the limiting ionic conductance, λ°, by means of the Nernst equation, the temperature coefficient of the diffusion current can be calculated as follows from the Ilkovic equation:[9]

$$\left[\frac{1}{I_d}\frac{dI_d}{dT}\right]_{298}=0.0053+\left[\frac{1}{2\lambda^\circ}\frac{d\lambda^\circ}{dT}\right]_{298}.^{(10)} \quad (9)$$

According to B. B. Owen and F. H. Sweeton,[11] the temperature coefficient of λ° of the hydrogen ion at 25° is equal to 0.015, so we can obtain from Eq. (9) the temperature coefficient of I_l of the hydrogen ion as follows:

$$\left[\frac{1}{I_d}\frac{dI_d}{dT}\right]_{298}\fallingdotseq 0.013. \quad (10)$$

The result obtained from Eq. (7) differs from that of the Ilkovic equation only by the additional correction term,

$$\frac{d\log(1+AD^{1/2}m^{-1/3}t^{1/6})}{dT}$$
$$=\frac{AD^{1/2}m^{-1/3}t^{1/6}}{1+AD^{1/2}m^{-1/3}t^{1/6}}\left\{\frac{1}{2}\left(\frac{1}{\lambda^\circ}\frac{d\lambda^\circ}{dT}+\frac{1}{T}\right)+\frac{1}{6t}\frac{dt}{dT}-\frac{1}{3m}\frac{dm}{dT}\right\}$$
$$\fallingdotseq\frac{AD^{1/2}m^{-1/3}t^{1/6}}{1+AD^{1/2}m^{-1/3}t^{1/6}}\left\{\frac{1}{2}\left(\frac{1}{\lambda^\circ}\frac{d\lambda^\circ}{dT}+\frac{1}{T}\right)-\frac{1}{3m}\frac{dm}{dT}\right\},$$

where $\frac{1}{6t}\frac{dt}{dT}$ is neglected. By considering this correction term the temperature coefficient of I_d at 25° becomes to be 0.015, when $A=39$ and $\left[\frac{1}{m}\frac{dm}{dT}\right]_{298}\fallingdotseq 0.0037$ are used.

These results derived from Eqs. (7) and (6) are in comparatively good agreement with the experimental value, about 0.010, at 25°.

Under these circumstances, if we use Eq. (1) and Eq. (6) or (7), the values of n in Eqs. (6) and (7) are obtained as follows:

$n=1.09$ (The Ilkovic equation)
$n=0.72$ (The revised equation, $A=39$)
$n=0.89$ (Tht revised equation, $A=17$).

In the calculation of n the diffusion coefficient of the hydrogen ion in 0.1 N KCl solution was assumed to be equal to 8.0×10^{-5} cm.^{2}/sec. These results prove the assumption that n is equal to one in the reduction process of the hydrogen ion at the D. M. E.

Inversely, if we assume that n is equal to one, the polarographic diffusion coefficient of the hydrogen ion in 0.1 N KCl solution can be calculated by Eq. (6) or (7), i. e.,

$D_{H^+}=9.5\times10^{-5}$ cm.^{2}/sec. (Eq. (6))
$D_{H^+}=4.8\times10^{-5}$ 〃 (Eq. (7), $A=39$)
$D_{H^+}=6.6\times10^{-5}$ 〃 (Eq. (7), $A=17$).

To calculate the value of D_{H^+} from Eq. (7), the following relation was used:

$$D^{1/2}=\frac{-a_2+\sqrt{a_2^2+4a_1a_0}}{2a_1}$$
$$a_0=I_d/C$$
$$a_1=605\,Am^{1/3}t^{1/3}$$
$$a_2=605\,m^{2/3}t^{1/6}.$$

(9) I. M. Kolthoff and J. J Lingane, "Polarography", Interscience Pub. Inc., New York, N. Y., 1946 p. 74.

(10) In this case, the temperature coefficient means the value which is obtained by dividing the slope of the relation between I_l and τ at 25°, $(dI_l/dT)_{298}$, by I_l at 25° (Table 1, column 4).

(11) B. B. Owen and F. H. Sweeton, *J. Am. Chem. Soc.*, **63**, 2811 (1941).

The diffusion coefficient of the hydrogen ion, D_{H^+}, in 0.1 N KCl solution, which was employed in the above calculations concerning the limiting current, was computed by the Onsager's limiting law for the diffusion coefficient.[12] As the concentration of the diffusing ion is generally very small in comparision with that of the supporting electrolyte whose composition is sensibly constant in the polarographic measurements, the diffusion coefficient of the hydrogen ion under the present condition can be represented as follows according to this law:

$$D_{H^+} = \frac{\lambda^\circ_{H^+} RT}{|Z_{H^+}| F^2} \times 10^{-7} - \frac{\lambda^\circ_{H^+} |Z_{H^+}| v^2 \varepsilon}{3D} \times 10^{-9} \sqrt{\frac{4\pi}{1000 DRT}} \left(1 - \sqrt{\mathrm{d}(\omega_{H^+})}\right) \sqrt{I}$$

$$\mathrm{d}(\omega_{H^+}) = \left(\frac{|Z_{H^+}|}{|Z_{K^+}| + |Z_{Cl^-}|}\right) \times \left(\frac{|Z_{K^+}| \lambda^\circ_{K^+}}{|Z_{H^+}| \lambda^\circ_{K^+} + |Z_{K^+}| \lambda^\circ_{H^+}} + \frac{|Z_{Cl^-}| \lambda^\circ_{Cl^-}}{|Z_{H^+}| \lambda^\circ_{Cl^-} + |Z_{Cl^-}| \lambda^\circ_{H^+}}\right)$$

$$I = C_{H^+} Z^2_{H^+} + C_{K^+} Z^2_{K^+} + C_{Cl^-} Z^2_{Cl^-} \fallingdotseq C_{K^+} Z^2_{K^+} + C_{Cl^-} Z^2_{Cl^-}$$

where λ° is the ionic conductance of the corresponding ion, Z the valency, C the concentration in mole per liter, R the gas constant per mole, T the absolute temperature, F the Faraday constant, D the dielectric constant, v the velocity of light, and ε the electric charge. In the present calculation the following numerical values were used.

$$\lambda^\circ_{H^+} = 349.8, \quad \lambda^\circ_{K^+} = 73.52, \quad \lambda^\circ_{Cl^-} = 76.34$$
$$Z_{H^+} = Z_{K^+} = Z_{Cl^-} = 1, \quad C_{K^+} = C_{Cl^-} = 0.1$$
$$R = 8.314 \times 10^7, \quad T = 298, \quad F = 96500$$
$$D = 78.55, \quad v = 3.0 \times 10^{10}, \quad \varepsilon = 4.80 \times 10^{-10}.$$

Although the agreement between the theoretical predictions of the Onsager's limiting law and the experimental results is not exact and is only reasonably satisfactory as stated by L. J. Gosting and H. S. Harned,[12] it seems to be more appropriate to use this limiting law rather than the Nernst equation for the diffusion coefficient of the individual ion in the polarographic study. A systematic investigation may be necessary to answer the question: "By which theoretical relation can the diffusion coefficient under the condition of the polarographic study be most adequately computed?"

According to the discussion carried out in the present paper, it can be concluded that the limiting current of the hydrogen ion in the system of dil. HCl in 0.1N KCl solution is controlled by the diffusion process of the hydrogen ion and it is represented by the revised Ilkovic equation. Under these conditions we can apply the theoretical results on the current-voltage curve obtained in the theoretical part[2] of the present study to the actual hydrogen wave, because each mechanism, which was assumed for the reduction process of the hydrogen ion in the theoretical part, requires the limiting current controlled by the diffusion process.

Summary

The properties of the limiting current of the reduction wave of the hydrogen ion were studied in the system of dil. HCl in 0.1 N KCl solution.

The relation between the limiting current and the concentration of the hydrogen ion in the bulk of the solution was linear, and the experimental relation between the limiting current and the height of the mercury reservior was interpreted by the revised Ilkovic equation.

It was shown that the temperature coefficient of the limiting current is nearly equal to 1.0 % at 25° which is in agreement with the theoretical value computed from the revised Ilkovic equation.

From these results it was concluded that the limiting current of the hydrogen ion obtained under the present condition is controlled by the diffusion process of the hydrogen ion.

The author expresses his best thanks to Prof. San-ichro Mizushima and Assist. Prof. Nobuyuki Tanaka for their great encouragement and valuable suggestions in this study. The cost of this research has been defrayed from the Scientific Research Encouragement Grant from the Ministry of Education.

Institute of Science and Technology, Tokyo University, Tokyo

(12) Louis J. Gosting and Herbert S. Harned, *J. Am. Chem. Soc.*, **73**, 159 (1951).

Heats of Sublimation of Condensed Polynuclear Aromatic Hydrocarbons

By Hiroo INOKUCHI, Sukekuni SHIBA, Takashi HANDA and Hideo AKAMATU

(Received June 6, 1952)

Introduction

Wolf and Weghofer[1] have found that there is an additivity in molar heats of sublimation among benzene, naphthalene and anthracene. In the previous investigation,[2] one of the present authors (H. I.) also has found the similar additivity among the condensed polynuclear aromatic compounds of the higher molecular weights. In this previous work, however, the experimental method used was not a legitimate one and the number of compounds investigated was also restricted. In the present investigation, the orthodox molecular effusion method following Knudsen[3] for measurement of vapour pressure was applied to the extended number of hydrocarbons.

Materials

Anthracene was purified from commercial product through anthraquinone and anthrone. Recrystallized from toluene and ethyl alcohol solution. This product, denoted as anthracene I, is white crystal with deep violet coloured fluorescence. Anthracene I was sublimed in vacuum, and obtained a product made of white crystals showing feeble fluorescence. This is denoted as anthracene II (m. p. 219°C.).

Phenanthrene was purified from commercial product by chromatography, recrystallized from ethyl alcohol solution. The product with blue coloured fluorescence was sublimed in vacuum.

Pyrene was synthesized from biphenyl-2, 2'-diacetaldehyde following Weitzenböck,[4] recrystallized from ethyl alcohol solution, and repeatedly sublimed in vacuum. The product shows slightly green coloured fluorescence (m. p. 151°C.).

Naphthacene was synthesized from α-naphthol and phthalic anhydride following Deichler and Weizmann,[5] recrystallized from glacial acetic acid solution and benzene solution, then repeatedly sublimed in vacuum (m. p. 340°C.).

Perylene was synthesized from naphthalene following Scholl,[6] recrystallized from benzene solution and glacial acetic acid solution, then repeatedly sublimed in vacuum. Yellow crystals with green coloured fluorescence (m. p. 261°C.).

Anthanthrene was obtained by reducing anthanthrone with zinc powder in fused mixture of sodium chloride and zinc chloride, recrystallized from benzene solution, and repeatedly sublimed in vacuum. Brownish yellow coloured (m. p. 257.5 ~258°C.).

Meso-naphthodianthrene was obtained by reducing meso-naphthodianthrone which was synthesized from anthrone, recrystallized from benzene solution, and repeatedly sublimed in vacuum. Deep green coloured.

Pyranthrene was obtained by reducing commercial pyranthrone, recrystallized from nitrobenzene solution and sublimed in vacuum.

Ovalene was synthesized from meso-naphthodianthrene following Clar,[7] repeatedly sublimed in vacuum. Reddish orange coloured.

Violanthrene was obtained by reducing commercial violanthrone, repeatedly sublimed in vacuum. Deep red coloured.

All these materials are the same samples as used for the electrical conductivity measurements[8] as well as the magnetic susceptibility measurements carried on in our laboratory.

Experimental Procedure

The apparatus for measuring vapour pressure by the molecular effusion method is illustrated in Fig. 1. A small vessel, sample container, made of pyrex glass is hanging from a quartz spring balance in an evacuated glass tube. The cap of the sample container is made of thin-wall pyrex glass. There is a small hole in the cap through which vapours flow to the evacuated outside by the molecular effusion.

The vapour pressure p can be determined by the well known following relation

$$p = (W/st)(2\pi RT/M)^{1/2} \qquad (1),$$

where M is the molecular weight, T is the absolute temperature, R is the gas constant, s is the

(1) K. L. Wolf and H. Weghofer, *Z. physik. Chem.*, **B 39**, 194 (1938).
(2) H. Inokuchi, *J. Chem. Soc. Japan*, **72**, 552 (1951).
(3) M.Knudsen, *Ann. d. Physik*, **28**. 999 (1909); M. Volmer, *Z. physik. Chem., Bodenstein-Festband*, 863 (1931).
(4) R. Weitzenböck, *Monat. f. Chem.*, **34**, 193 (1913).
(5) C. Deichler and C. Weizmann, *Ber.*, **36**, 547 (1903).
(6) R. Scholl, *Ber.*, **43**, 2202 (1910).
(7) E. Clar and H. Frömmel, *Ber.*, **82**, 46 (1949).
(8) H. Inokuchi, This Bulletin, **24**, 222 (1951).

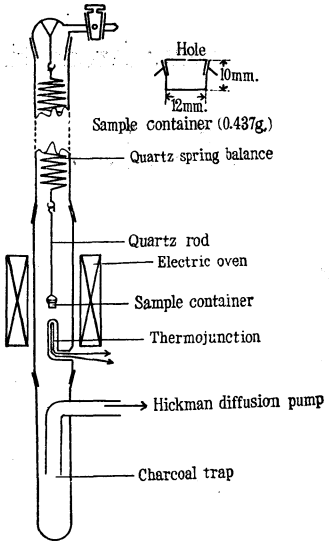

Fig. 1.—The apparatus for measuring the vapour pressure by effusion method.

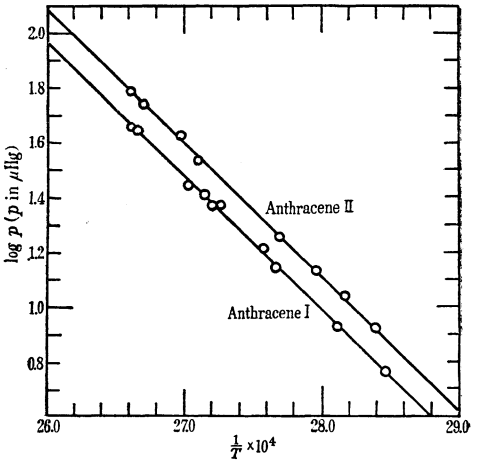

Fig. 2.—The logarithm of vapour pressure plotted against to the reciprocal temperature for anthracene.

area of the hole, and W is the mass which escapes by the effusion in time t. The cross sectional area of the hole, s, was determined by the microscope. Two kinds of hole were used, one is 0.0956 mm.^{2} and the other 0.2276 mm.^{2} in area.

The time t was measured for a constant decrease in mass, W, of the sample. The sensitivity of the spring balance was that one mg. in weight change corresponds to 0.433 mm. in elongation change, and the latter can be determined to 0.001 mm. by a microcomparator which was used as cathetometer. The temperature was controlled by supplying a stationary current to the electric oven; the constancy could be maintained within ± 0.5°C. for each temperature.

Results

A good linear relationship was found between the logarithm of vapour pressure and the reciprocal of temperature for each compound. This is illustrated in Fig. 2 for anthracene.

From the empirical equation of

$$\log p = A - B/T \qquad (2)$$

the heats of sublimation as well as the entropies of sublimation under one atmosphere are calculated by Clausius-Clapeyron's relation; $\Delta H = 2.303 \cdot R \cdot B$ and $\Delta S^\circ = 2.303 \cdot R \cdot (A - 2.8808)$.

The molar heat of sublimation (ΔH) was estimated as 22.0 kcal. for anthracene I and 22.1 kcal. for anthracene II. From these values, the inner heats of sublimation ($\Delta U = \Delta H - RT$) were determined as 21.3 kcal. and 21.4 kcal. respectively. The heat of sublimation of anthracene has been obtained by several investigators; 20.0 kcal. by Mortimer and Murphy,[9] 22.3 kcal. by Wolf and Weghofer,[1] 22.8 kcal. by Nitta, Seki and Momotani[10] and 22.3 kcal. by Magnus, Hartmann and Becker.[11] Of these values, Mortimer's result seems too small, and the others are in good agreement with our result.

The experimental results are summarized in Table 1.

In the second column of Table 1 the number of carbon atoms in each molecule are shown, and in the last column the values of inner heat of sublimation being assigned to one carbon atom are shown. It must be emphasized that the last values are nearly constant to each other. This is well illustrated in Fig. 3, where the inner heats of sublimation are plotted against the number of carbon atoms in each molecule. From the linearity of Fig. 3, the value of inner heat of sublimation assigned to one carbon atom is estimated as 1.51 kcal./mole. This is nothing but showing that there is an additivity in the heats of sublimation among the present series of compounds.[12]

(9) F. S. Mortimer and R. V. Murphy, *Ind. Eng. Chem.*, **15**, 1140 (1923).

(10) I. Nitta, S. Seki and M. Momotani, *J. Chem. Soc. Japan*, **71**, 430 (1950).

(11) A. Magnus, H. Hartmann and F. Becker, *Z. physik. Chem.*, **197**, 75 (1951).

(12) Recently, Magnus et al.[11] have derived the heats of sublimation of some similar compounds from the integral heats of solution in xylene. In their results, five kinds of isomers of $C_{18}H_{12}$ are included. The heats of sublimation of these compounds have been found to vary from 25.4 kcal. of 3,4-benzophenanthrene to 20.7 kcal. of naphthacene. This last value is slightly larger than our result. Nevertheless, the average value of five compounds is 27.1 kcal. and the assigned value to one carbon atom is about 1.51 kcal./mole.

Table 1

Heats of Sublimation of Condensed Polynuclear Aromatic Hydrocarbons

Substance	Number of C-atoms (n)	Mean exp. temperature (C°.)	$\log p = A - B/T$ (p in mm. Hg) A	$B \cdot 10^{-3}$	Inner heat of sublimation (ΔU in kcal.)	Entropy of sublimation ($\Delta S°$ in cal./deg.)	$\Delta U/n$ kcal.
Benzene*	6				9.2		1.53
Naphthalene*	10				15.3		1.53
Anthracene I	14	92	11.420	4.79_5	21.3 ± 0.5	39.1	1.52
Anthracene II	14	91	11.611	4.82	21.4 ± 0.3	40.0	1.53
Phenanthrene	14	42	12.780	4.74	21.1 ± 0.3	45.3	1.51
Pyrene	16	79	12.903	5.23	23.3 ± 0.4	45.9	1.46
Naphthacene	18	186	11.485	6.13	27.1 ± 0.7	39.4	1.51
Perylene	20	142	14.350	6.77	30.2 ± 0.5	52.5	1.51
Anthanthrene	22	206	12.889	7.06	31.3 ± 1.2	45.8	1.42
Coronene**	24	134			35.5		1.48
Meso-naphthodianthrene	28	332	13.789	9.43	42.0 ± 1.2	49.9	1.50
Pyranthrene	30	322	14.825	10.15	45.3 ± 1.6	54.7	1.51
Ovalene	32	327	15.757	11.04	49.4 ± 1.9	58.9	1.54
Violanthrene	34	317	17.532	11.68	52.3 ± 2.1	67.0	1.54

* Wolf and Weghofer's data[1] ** Previous work's data[2]

Table 2

Heats of Sublimation of Anthraquinone, Benzanthrone and Anthanthrone

Substance	Number of C-atoms (n_c)	Number of O-atoms (n_o)	Mean exp. temperature (C.°)	$\log p = A - B/T$ (p in mm. Hg) A	$B \times 10^{-3}$	Inner heat of sublimation (ΔU in kcal.)	Entropy of sublimation ($\Delta S°$ in cal./deg.)	$\Delta U/(n_c+n_o)$ (kcal.)
Anthraquinone	14	2	103	12.457	5.47_5	24.2 ± 0.5	43.8	1.51
Benzanthrone	17	1	125	13.432	6.03	26.8 ± 0.5	48.3	1.49
Anthanthrone	22	2	219	13.684	7.95	35.4 ± 1.2	49.4	1.48

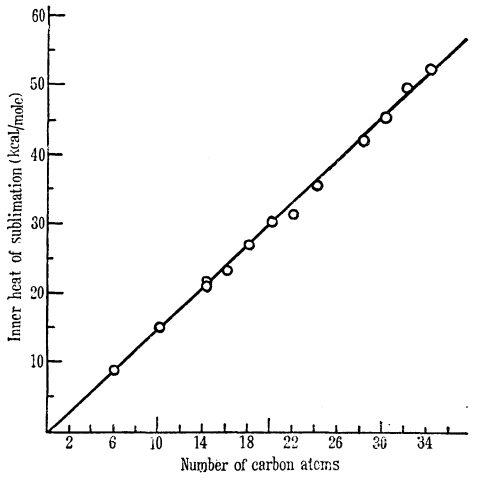

Fig. 3.—Inner heats of sublimation in kcal./mole plotted against number of carbon atoms in a molecule.

It is not unnatural to find such an additivity law, since the crystals of these compounds are made of typical molecular lattice, and the intermolecular forces will be purely based on the dispersion effect.

In the case of compounds with quinonoid structure instead of hydrocarbons, it was found that some polymerization occurs in a part of specimen during the course of sublimation at higher temperature, and the polymerization product covers the surface of specimen. This made the accurate measurement of vapour pressure difficult and the number of reliable results was restricted. In Table 2 the results are shown for anthraquinone, benzanthrone and anthanthrone. In this case too a rough additivity law seems to be found. The contribution of oxygen atom to the heat of sublimation is nearly the same as that of carbon atom.

Recently much attention has been directed to the condensed polynuclear aromatic compounds, for their interesting physical properties due to the π-electron orbitals as well as the components of coal tar. Compounds with higher molecular weights have been synthesized too. Neverthless, as the molecular weight increases, no good solvent can be found for these compounds. In consequence, the technique of separation or purification is mostly

restricted to the sublimation method, instead of the usual method through dissolution process. The additivity law in heats of sublimation will be useful for the separation and identification of these compounds in relation to each other.

Summary

The heats of sublimation of a series of condensed polynuclear aromatic hydrocarbons, from anthracene (C_{14}) to violanthrene (C_{34}), were measured. It has been found that there is an additivity in the inner heats of sublimation among these compounds, i. e., as the number of carbon atoms in each molecule increases by one, the inner heat of sublimation increases by 1.51 kcal./mole.

The authors thank the Ministry of Education for the Grant in Aid for Fundamental Scientific Research.

Department of Chemistry, Faculty of Science, Tokyo University, Tokyo

Closure, Resonance, Bond and Activation Entropy

By Kiyoteru Orozai, Sanshiro Kume and Shouzow Fukushima

(Received December 20, 1951)

Introduction

According to Sackur-Lewis[1] the molecular entropy of the monoatomic gas molecule is given theoretically by the equation:

$$S=5/2\cdot R\ln T-R\ln P+3/2\cdot R\ln M-2.63, \quad (1)$$

where R is universal gas constant, and M is molecular weight. At the state of 298.2°K and 1 atm. eq. (1) becomes

$$S^\circ=26+3/2\cdot R\ln M, \quad (2)$$

where S° is molecular entropy at 298.2°K and 1 atm. As to diatomic molecule Eastman,[2] for example, has given the empirical rule:

$$S^\circ=29+3/2\cdot R\ln(XY)+0.7\ln M. \quad (3)$$

Because of difficulty of expressing the molecular entropy of polyatomic gas molecule by means of a simple equation, the empirical treatment of this entropy has been performed chiefly from the standpoint of atomic group regularity. Parks-Huffman[3] have, for example, systematized the entropy change assigned to the displacement of atomic groups, and Bremner-Thomas[4] have constructed the atomic group equation. The empirical rules of simple form such as Wenner's[5]

$$\log S^\circ=A\log M+\log B \quad (4)$$

and Kobozev's[6]

$$S^\circ=26+3\ln M+1.45\times M^{3/4} \quad (5)$$

are not so accurate for practical use.

From the standpoint of chemical bond we have constructed a new empirical rule for the calculation of molecular entropy of general gas molecule, which has sufficient accuracy and wide range of application, and have discussed the relations of entropy to the molecular structure and the frequency factor of chemical reaction quantitatively.

Empirical Rule

The empirical rule is expressed by the equation:

$$S^\circ=26+3/2\cdot R\ln\overset{n}{\Pi}(X)+0.7\ln\overset{m}{\Pi}\left(\frac{X+Y}{e^{\alpha}}\right), \quad (6)$$

where S° is molecular entropy of ideal gas at 298.2°K and 1 atm., R is universal gas constant, i. e., 1.987 cal·degree^{-1}, X is atomic weight, n is number of atoms in the molecule, $X+Y$ is sum of atomic weights of atoms joined with the bond, m is total number of bonds in the molecule, and finally α is a parameter given by the equation:

(1) O. Sackur, *Ann. Phys.*, **36**, 958 (1911); G. N. Lewis, *Phys. Rev.*, **18**, 121 (1921).
(2) E. D. Eastman, *J. Am. Chem Soc.*, **45**, 80 (1923).
(3) G. S. Parks and H. M. Huffman, "The Free Energy of Some Organic Compounds", New York, 1932.
(4) J. G. M. Bremner and G. D. Thomas, *Trans, Faraday Soc.*, **43**, 779 (1947).
(5) R. P. Wenner, *Chem. Eng. Progress*, **45**, 194 (1949).
(6) N. I. Kobozev, *Zhur. Fiz. Khim.*, **22**, 1002 (1948).

$$\alpha = 9^{3-n} - \frac{15.7}{m} + 1.9^{N} + \frac{B^2}{1.8} + 5/4 \cdot n_X - f. \qquad (7)$$

The third term of eq. (6), which has been derived from the standpoint of chemical bond, is the principal feature of the rule, where m is expressed generally with

$$m = n - 1, \qquad (8)$$

but for the compound of ring structure with

$$m = n,\ n+1,\ \cdots\cdots. \qquad (9)$$

In eq. (7) N is bond order, and so $N=1$ for single bond and $N=3$ for triple bond, but must be taken $N=1$ for double bond and for bond in diatomic molecule. B is the degree of branching of the bond, which is counted as follows:

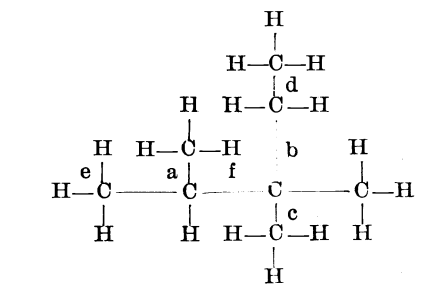

(A)

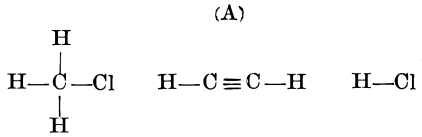

(B) (C) (D)

In molecule (A) $B=2$ for bond a, $B=3$ for bonds b and c, and $B=0$ for all other bonds d, e, f, etc. In molecules (B), (C), and (D), namely in the molecules, which are constructed with the central atom or central atomic pair joined with multiple bond, and surrounding atoms, $B=-1$ for all bonds concerned. In diatomic molecule, therefore, $B=-1$ always.

The fifth term of eq. (7) is the correction term for the bond involving the seventh group non-metallic element, i. e., halogen, where n_X is number of halogen atoms joined to the same atom, but must be taken as zero in diatomic molecule. The sixth term f of eq. (7) is the correction term for the bond involving the fifth and sixth group non-metallic element, and is counted as follows:

$f=3$ (for the single bond joining the central atom and the atomic group, when the molecule is constructed with the central 5th or 6th group atom and surrounding one atomic group and several atoms),

$f=2$ (for the single bond between 5th or 6th group atoms each other),

$f=0$ (for all other bonds).

For example,

$f=3$ (for C—N of amine, C—O of alcohol, C—S of mercaptane),

$f=2$ (for N—N, O—O, S—S, N—O),

and for diatomic molecule $f=0$ inevitably.

Simpler Method of Calculation

In special cases as below the rule becomes simpler. For monoatomic molecule, for example, the bond term of eq. (6) disappears, and so the rule is reduced to

$$S^\circ = 26 + 3/2 \cdot R \ln X, \qquad (10)$$

which agrees with the equation of Sackur-Lewis.

For diatomic molecule $n=2$, $m=1$, $N=1$, $B=-1$, $n_X=0$, and $f=0$, so that the rule becomes

$$\begin{aligned} S^\circ &= 26 + 3/2 \cdot R \ln (XY) + 0.7 \ln (X+Y) \\ &\quad - 0.7 \times \{9 - 15.7 + 1.9 + 0.55\} \\ &= 29 + 3/2 \cdot R \ln (XY) + 0.7 \ln (X+Y), \end{aligned} \qquad (11)$$

which agrees with the equation of Eastman.

For non-branched hydrocarbons involving more than two carbon atoms, excluding ethylene and acetylene, $n \geqq 5$, $B=0$, $n_X=0$, and $f=0$, and so the rule becomes

$$\begin{aligned} S^\circ &= 26 + 3/2 \cdot R \ln \overset{n}{\Pi} (X) + 0.7 \ln \overset{m}{\Pi} (X+Y) \\ &\quad - 0.7 \times \overset{m}{\Sigma} \left\{ -\frac{15.7}{m} + 1.9^{N} \right\} \\ &= 37 + 3/2 \cdot R \ln \overset{n}{\Pi} (X) + 0.7 \ln \overset{m}{\Pi} (X+Y) \\ &\quad - 0.7 \times \overset{m}{\Sigma} 1.9^{N}. \end{aligned} \qquad (12)$$

Finally for non-branched saturated hydrocarbons or non-branched olefines involving more than two carbon atoms, excluding ethylene, $n \geqq 5$, $B=0$, $n_X=0$, $f=0$, and $N=1$, and so the rule becomes from eq. (12)

$$\begin{aligned} S^\circ &= 37 + 3/2 \cdot R \ln \overset{n}{\Pi} (X) + 0.7 \ln \overset{m}{\Pi} (X+Y) \\ &\quad - 1.33\, m. \end{aligned} \qquad (13)$$

As a typical example S° of propane (C_3H_8) is calculated

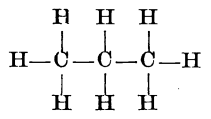

from eq. (13) as follows:

$$\begin{aligned} S^\circ &= 37 + 2.98 \times 3 \ln 12 + 0.7 \times \{8 \ln 13 + 2 \ln 24\} \\ &\quad - 1.33 \times 10 \\ &= 37 + 22.2 + 18.8 - 13.3 = 64.7 \text{ (e.u.)}, \end{aligned}$$

while the observed value of S° is 64.5 e.u.

Application of Empirical Rule

In Table 1 the calculated values of molecular

Table 1

Application of Empirical Rule

(unit e. u.; * exceptions)

Substance		$S°_{calc.}$	$S°_{obs.}$	Δ
H	Hydrogen atom	26.0	25.7	0.3
Cl	Chlorine atom	36.7	36.9	−0.2
Br	Bromine atom	39.1	38.8	0.3
I	Iodine atom	40.6	40.2	0.4
He	Helium atom	30.2	29.2	1.0
A	Argon atom	37.0	36.4	0.6
Cd	Cadmium atom	40.2	40.0	0.2
Hg	Mercury atom	41.9	41.5	0.4
Ca	Calcium atom	37.1	36.7	0.4
K	Potassium atom	37.0	36.6	0.4
Li	Lithium atom	31.8	31.5	0.3
P	Phosphorus atom	36.3	36.0	0.3
Rb	Rubidium atom	39.3	39.0	0.3
S	Sulphur atom	36.4	36.0	0.4
Cs	Caesium atom	40.7	40.3	0.4
Na	Sodium atom	35.4	35.1	0.3
Zn	Zinc atom	38.5	38.2	0.3
H_2	Hydrogen	29.5	31.2	−1.7
F_2	Fluorine	49.1	48.6	0.5
Cl_2	Chlorine	53.2	53.3	−0.1
Br_2	Bromine	58.7	59.1	−0.4
I_2	Iodine	61.9	61.8	0.1
HCl	Hydrogen chloride	42.2	43.3	1.1
HBr	Hydrogen bromide	45.2	47.0	−1.8
HI	Hydrogen iodide	47.0	47.5	−0.5
TlCl	Talium chloride	59.3	59.1	0.2
TlBr	Talium bromide	61.9	61.7	0.2
TlI	Talium iodide	63.5	63.6	−0.1
AgCl	Silver chloride	57.3	56.5	0.8
NaCl	Sodium chloride	51.9	52.9	−1.0
KCl	Potassium chloride	53.5	55.2	−1.7
H_2O	Water	44.4	45.1	−0.7
H_2S	Hydrogen sulphide	47.4	48.2	−0.8
NH_3	Ammonia	45.3	45.9	−0.6
PH_3	Phosphine	49.3	50.2	−0.9
PCl_3	Phosphorus trichloride	74.8	74.5	0.3
PBr_3	Phosphorus tribromide	83.2	83.1	0.1
CH_4	Methane	44.9	44.5	0.4
C_2H_6	Ethane	55.5	54.9	0.6
C_2H_5Cl	Ethyl chloride	66.1	65.9	0.2
$CH_2Cl \cdot CH_2Cl$	1, 2-dichloroethane	76.8	78.2	−1.4
$(CH_3)_2S$	Dimethyl sulphide	67.6	68.3	−0.7
CH_3OH	Methanol	57.8	57.7	0.1
C_2H_5OH	Ethanol	67.2	67.3	−0.1
CH_3SH	Methyl mercaptane	60.7	60.9	−0.2
C_2H_5SH	Ethyl mercaptane	70.1	70.6	−0.5
CH_3NH_2	Methyl amine	57.8	57.7	0.1
$(CH_3)_2NH$	Dimethyl amine	64.8	65.2	−0.4
CH_3F	Methyl fluoride	53.4	53.3	0.1
CH_3Cl	Methyl chloride	55.4	56.0	−0.6
CH_3Br	Methyl bromide	58.4	58.7	−0.3
CH_3I	Methyl iodide	60.2	60.9	−0.7
CH_2Cl_2	Dichloromethane	64.4	64.7	−0.3
CH_2Br_2	Dibromomethane	70.1	70.8	−0.7
$CHCl_3$	Chloroform	71.7	70.8	0.9
$CHBr_3$	Bromoform	80.1	79.1	1.0
PCl_5	Phosphorus pentachloride	84.9	84.3	0.6
CH_3CHO	Acetaldehyde	63.8	63.2	0.6
CH_3OCH_3	Dimethyl ether	65.0	65.6	−0.6
CH_3CN	Methyl cyanide	59.5	58.2	1.3
$(CH_3)_2S_2$	2, 3-Dithiabutane	80.9	80.5	0.4
N_2H_4	Hydrazine	57.4	57.0	0.4
CH_3NHNH_2	Methyl hydrazine	66.6	66.6	0
C_3H_8	Propane	64.7	64.5	0.2
n-C_4H_{10}	n-Butane	73.8	74.1	−0.3
n-C_5H_{12}	n-Pentane	83.0	83.3	−0.3
n-C_6H_{14}	n-Hexane	92.2	92.5	−0.3
n-C_7H_{16}	n-Heptane	101.4	101.6	−0.2
n-C_8H_{18}	n-Octane	110.6	110.8	−0.2
n-C_9H_{20}	n-Nonane	119.8	120.0	−0.2
n-$C_{10}H_{22}$	n-Decane	129.0	129.2	−0.2
n-$C_{11}H_{24}$	n-Undecane	138.2	138.4	−0.2
n-$C_{12}H_{26}$	n-Dodecane	147.4	147.6	−0.2
n-$C_{13}H_{28}$	n-Tridecane	156.6	156.7	−0.1
n-$C_{14}H_{30}$	n-Tetradecane	165.8	165.7	0.1
n-$C_{15}H_{32}$	n-Pentadecane	175.0	175.1	−0.1
n-$C_{16}H_{34}$	n-Hexadecane	184.2	184.3	−0.1
n-$C_{17}H_{36}$	n-Heptadecane	193.4	193.5	−0.1
n-$C_{18}H_{38}$	n-Octadecane	202.6	202.7	−0.1
n-$C_{19}H_{40}$	n-Nonadecane	211.8	211.8	0
n-$C_{20}H_{42}$	n-Eicosane	221.0	221.0	0
C_4H_{10}	2-Methyl propane (Isobutane)	72.0	71.3	0.7
C_5H_{12}	2-Methyl butane (Isopentane)	81.4	82.0	−0.6
$C(CH_3)_4$	2, 2-Dimethyl propane (Neopentane)	76.0	76.9	−0.9
$Si(CH_3)_4$	Silicon tetramethyl	80.4	85.8	−5.4*
C_6H_{14}	2-Methyl pentane	90.6	90.7	−0.1
〃	3-Methyl pentane	90.6	90.8	−0.2
〃	2,2-Dimethyl butane	85.2	85.7	−0.5
〃	2,3-Dimethyl butane	89.0	87.3	1.7
C_7H_{16}	2-Methyl hexane	99.8	99.6	0.2
〃	3-Methyl hexane	99.8	101.4	−1.6
〃	3-Ethyl pentane	99.8	98.5	1.3
〃	2, 2-Dimethyl pentane	94.4	93.6	0.8
〃	2, 3-Dimethyl pentane	98.2	99.0	−0.8
〃	2, 4-Dimethyl pentane	98.2	94.8	3.4*
〃	3, 3-Dimethyl pentane	94.4	95.5	−1.1
〃	2, 2, 3-Trimethyl butane	92.8	92.5	0.3
C_8H_{18}	2-Methyl heptane	109.0	108.8	0.2
〃	3-Methyl heptane	109.0	110.3	−1.3
〃	4-Methyl heptane	109.0	108.4	0.6
〃	3-Ethyl hexane	109.0	109.5	−0.5

Substance		$S°_{calc.}$	$S°_{obs.}$	Δ
C_8H_{18}	2, 2-Dimethyl hexane	101.6	103.1	−1.5
〃	2, 3-Dimethyl hexane	105.4	106.1	−0.7
〃	2, 4-Dimethyl hexane	105.4	106.5	−1.1
〃	2, 5-Dimethyl hexane	105.4	104.9	0.5
〃	3, 3-Dimethyl hexane	101.6	104.7	−3.1*
〃	3, 4-Dimethyl hexane	105.4	104.3	1.1
〃	2-Methyl-3-ethyl pentane	105.4	105.4	0
〃	3-Methyl-3-ethyl pentane	101.6	103.5	−1.9
〃	2, 2, 3-Trimethyl pentane	100.0	101.6	−1.6
〃	2, 2, 4-Trimethyl pentane	100.0	101.6	−1.6
〃	2, 3, 3-Trimethyl pentane	100.0	103.1	−3.1*
〃	2, 3, 4-Trimethyl pentane	103.8	103.0	0.8
〃	2, 2, 3, 3-Tetra-methyl butane	94.6	94.3	0.3
C_2H_4	Ethene (Ethylene)	52.7	52.5	0.2
C_3H_6	Propene (propylene)	63.6	63.8	−0.2
C_4H_8	1-Butene	73.1	73.5	−0.4
〃	2-Butene (cis and trans)	73.1	71.4 (mean)	1.7
〃	2-Methyl-2-propene	71.5	70.2	1.3
C_5H_{10}	1-Pentene	82.3	83.1	−0.8
〃	2-Pentene (cis and trans)	82.3	82.3 (mean)	0
C_5H_{10}	2-Methyl-1-butene	80.7	81.7	−1.0
〃	3-Methyl-1-butene	80.7	79.7	1.0
〃	2-Methyl-2-butene	80.7	80.9	−0.2
C_6H_{12}	1-Hexene	91.5	92.3	−0.8
〃	2-Hexene (cis and trans)	91.5	91.9 (mean)	−0.4
C_2H_2	Ethyne (Acetylene)	48.8	48.0	0.8
C_3H_4	Propyne (Methyl acetylene	59.3	59.3	0
C_4H_6	1-Butyne	68.5	69.5	−1.0
〃	2-Butyne	68.5	67.7	0.8
C_5H_8	1-Pentyne	77.7	79.1	−1.4
〃	2-Pentyne	77.7	79.3	−1.6
〃	3-Methyl-1-butyne	76.2	76.2	0
〃	1, 4-Pentadiene	81.2	79.7	1,5
C_5H_{10}	Trimethylethylene	80.8	79.7	1.1
O_2	Oxygen	48.0	48.0	0
S_2	Sulphur	52.6	53.5	−0.9
N_2	Nitrogen	47.0	45.6	1.4
P_2	Phosphorus	52.4	52.2	0.2
PN	Phosphorus nitride	49.8	50.4	−0.6

entropies of various molecules by means of this rule were compared with the observed values,[7] i. e., the thermal entropies calculated thermodynamically from the calorimetric data, using the third law, or the statistical entropies calculated statistically from the spectroscopic data, excluding the weight of nuclear spin. The error of the observed value is sometimes ±1 e.u., and in special cases often ±2 e.u. absolutely.

In 140 instances shown in Table 1 the present rule is applicable for 136 instances within the error of ±2 e. u., and for 112 instances within the error of ±1 e.u. But in the present rule the difference between the isomers, excluding branched isomers, i.e., *D-L*, cis-trans, *o-m-p*, etc., are not involved. These effects are, however, not so large that they are included within the error of the rule. For the compounds of ring structure and those having resonance effect the present rule is not applicable. The discrepancies in such cases are rather suitable quantities in discussing the relation between entropy and molecular structure as will be stated below.

Abnormal Depression of Entropy

Abnormal depression of entropy, which is defined as the positive difference between the calculated entropy by means of the present rule and the observed entropy, can be interpreted with the depression due to ring closure, *Closure entropy*, and the depression due to resonance effect, *Resonance entropy*.

The values of closure entropies of some substances are tabulated in Table 2. For the ring of 3, 5 and 6 members the closure entropies are about 7, 13 and 18 e.u. respectively. The closure entropy 20.9 e.u. of cyclohexane agrees well with

Table 2

Closure Entropy (unit, e. u.)

Substance		No. of memb. of ring	$S°_{calc.}$	$S°_{obs.}$	Closure entropy
C_3H_6	Cyclopropane	3	64.6	56.8	7.8
O_3	Ozone	3	62.8	57.0	5.8
C_2H_4O	Ethylene oxide	3	64.7	57.9	6.8
C_5H_{10}	Cyclopentane	5	83.3	70.7	12.6
C_6H_{12}	Cyclohexane	6	92.2	71.3	20.9
C_7H_{14}	Methyl cyclohexane	6	99.8	82.1	17.7
C_8H_{16}	Ethyl cyclohexane	6	109.0	91.5	17.5
C_8H_{16}	1, 1-Dimethyl cyclohexane	6	103.6	87.2	16.4
C_8H_{16}	Dimethyl cyclo-hexanes (excluding 1, 1-)	6	107.4	88.8 (mean)	18.6
$C_{10}H_{18}$	Decahydronaph-thalene (trans)	6, 6	129.4	89.4	40.0

(7) "Selected Values of Properties of Hydrocarbons", Natl. Bureau of Standards; E. B. Wilson, JR., *Chem. Rev.*, **27**, 17 (1940); Landolt-Börnstein; *Chem. Abst.*; "*Annual Review of Physical Chemistry*", **1**, (1950), Annual Reviews, Inc., Stanford, California; S. Kaneko, "Thermodynamics", Tokyo, (1941).

the conclusion of Bremner-Thomas[4] from the atomic group method that in cyclohexane the entropy depression due to ring closure is about 20 e.u.

The values of resonance entropies of some substances are tabulated in Table 3. Many substances in the table have been interpreted by Pauling[6] as having resonance effects between various valence structures. The symbol $S°_{calc.}$ is the calculated value for the same typical valence structure as in the case of the resonance energy. The small resonance entropy 1.4 e.u. of carbon monoxide indicates that in diatomic molecule the entropy does not decrease appreciably with the resonance effect.

Table 3

Resonance Entropy (unit, e. u.)

Substance		$S°_{calc.}$	$S°_{obs.}$	Resonance entropy
CH_3NO_2	Nitromethane	73.2	65.7	7.5
CH_2:CHCl	Vinyl chloride	65.0	61.1	3.9
CH_3COOH	Acetic acid	73.2	69.4	3.8
HCOOH	Formic acid	64.0	60.0	4.0
C_4H_6	1, 3-Butadiene	72.0	66.6	5.4
C_5H_8	1, 3-Pentadiene (trans) (Piperylene, trans)	81.2	76.4	4.8
〃	2-Methyl-1, 3-butadiene (Isoprene)	79.6	75.4	4.4
SF_6	Sulphur hexafluoride	83.9	69.4	14.5
CF_4	Carbon tetrafluoride	68.5	62.4	6.1
CCl_4	Carbon tetrachloride	76.9	74.2	2.7
CBr_4	Carbon tetrabromide	88.5	85.6	2.9
SiF_4	Silicon tetrafluoride	72.3	67.4	4.9
BF_3	Boron trifluoride	64.4	61.2	3.2
PF_3	Phosphorus trifluoride	68.6	64.1	4.5
AsF_3	Arsenic trifluoride	72.8	69.1	3.7
CF_3CH_3	1, 1, 1-Trifluoroethane	75.8	66.9	8.9
CCl_3CH_3	1, 1, 1-Trichloro ethane	82.3	77.0	5.3
CH_3NC	Methyl isocyanide	61.0	58.8	2.2
Cl_3PO	Trichlorophosphoxide	84.3	77.6	6.7
Cl_3PS	Trichlorophosphosulphide	86.6	79.3	7.3
$(CH_3)_2CO$	Acetone	73.2	70.1	3.1
$COCl_2$	Phosgene	72.9	69.1	3.8
SO_3	Sulphur trioxide	75.0	61.2	13.8
SO_2	Sulphur dioxide	64.5	59.4	5.1
CO_2	Carhon dioxide	60.9	50.2	10.7
CO	Carbon monoxide	47.0	45.6	1.4

As from thermodynamics

$$\Delta F = \Delta H - T \cdot \Delta S,$$

the degree of stabilization due to resonance effect must be originally discussed with the resonance free energy, but not only the resonance energy. In the extreme case as carbon dioxide the resonance entropy is 10.7 e. u. and the resonance energy is 33 kcal., so that the resonance free energy becomes

$$\Delta F = 33,000 - 298 \times 10.7$$
$$= 33,000 - 3,189 = 29,811 \text{ (cal.)}$$

at ordinary temperature. In general case, however, the resonance entropy is not so large that it may be negligible compared with the resonance energy.

The substances, which have abnormal depressions due to ring closure and resonance effect, are aromatic compounds as shown in Table 4. As

Table 4

Closure plus Resonance Entropy (unit, e. u.)

Substance		$S°_{calc.}$	$S°_{obs.}$	Closure +reson. entropy
C_6H_6	Benzene	89.4	64.3	25.1
—	Alkyl benzenes	—	—	19.3 (mean)
C_8H_8	Styrene	105.4	82.5	22.9
C_9H_{10}	Methyl styrenes	—	—	21.7 (mean)

closure plus resonance entropy of benzene is 25.1 e.u. and closure entropy of benzene must be 20.9 e.u., taken as the same as cyclohexane, the resonance entropy of benzene becomes 4.2 e. u., which agrees well with the conclusion of Bremner-Thomas[4] that the depression of entropy due to resonance effect is about 4 e.u. in benzene.

We have not seen any substance, which has the abnormal elevation of entropy, namely, for which the observed entropy is much larger than the entropy calculated by means of the present rule, excluding some exceptions in Table 1. From this fact it will be said that the present rule gives probably the upper limit of the observed entropy of gas molecule.

Bond Entropy

The quantity *Entropy of formation from atoms* $S°_{af}$ was defined as

$$S°_{af} = (\text{Entropy of atomic state}) - (\text{Entropy of molecular state}), \quad (14)$$

with the analogy of enthalpy of formation from atoms. Entropy of atomic state becomes with the use of eq. (10)

(8) L. Pauling, "The Nature of Chemical Bonds", Cornell Univ. Press, New York, 1940.

(Entropy of atomic state) $= \sum^{n}(26+3/2\cdot R\ln X)$

$$=26n+3/2\cdot R\ln \prod^{n}(X), \quad (15)$$

and entropy of molecular state becomes with the use of eq. (6)

(Entropy of molecular state) =

$$26+3/2\cdot R\ln \prod^{n}(X)+0.7\ln \prod^{m}\left(\frac{X+Y}{e^{\alpha}}\right). \quad (16)$$

From these equations it follows

$$S^{\circ}_{af}=26(n-1)-0.7\ln \prod^{m}\left(\frac{X+Y}{e^{\alpha}}\right).$$

As for the substances excluding those of ring structure

$$m=n-1, \quad (8)$$

it follows

$$S^{\circ}_{af}=\sum^{m}\left\{26-0.7\ln\left(\frac{X+Y}{e^{\alpha}}\right)\right\} \quad (17)$$

$$=\sum^{m}S^{\circ}_{B}, \quad (18)$$

where

$$S^{\circ}_{B}=26-0.7\ln\left(\frac{X+Y}{e^{\alpha}}\right). \quad (19)$$

Although the quantity S°_{B} has the additivity as shown in eq. (18), it has not the independency as shown in eqs. (19) and (7). Namely S°_{B} has, besides the quantities X, Y and N, which are proper to the bond, the quantities n, m, B, n_X and f, which are controlled with the situations of the bond. Consequently it is impossible to build up *true bond entropy*, which has both the additivity and the independency as in the case of bond energy, although it is possible to build up *formal bond entropy* S°_{B}, which has only the additivity as stated above. It is, therefore, also impossible to construct the bond free energy with the sufficient accuracy.

In the special case such as non-branched hydrocarbon involving more than two carbon atoms, excluding ethylene and acethylene, $n\geqq 5$, $B=0$, $n_X=0$ and $f=0$ as stated above, so that eq. (7) becomes

$$\alpha=-\frac{15.7}{m}+1.9^{N}, \quad (20)$$

and eq. (17) becomes

$$S^{\circ}_{af}=\sum^{m}\left\{26-0.7\ln\left(\frac{X+Y}{1.9^{N}}\right)\right\}-11 \quad (21)$$

$$=\sum^{m}S^{\circ}_{B}{}'-11,$$

where $S^{\circ}_{B}{}'$ is defined as

$$S^{\circ}_{B}{}'=26-0.7\ln\left(\frac{X+Y}{1.9^{N}}\right). \quad (22)$$

It follows therefore

$$S^{\circ}_{af}+11=\sum^{m}S^{\circ}_{B}{}'. \quad (23)$$

As shown in eqs. (22) and (23) $S^{\circ}_{B}{}'$ has both the independency and the additivity. However the quantity $S^{\circ}_{B}{}'$ is also not suitable for the name bond entropy, because the range of application of this quantity is very small, and furthermore the meaning of the additivity of this quantity is not clear-cut in the physical sense as shown in eq. (23).

Derivation of Atomic Group Method

Many rules in the atomic group method must be included naturally in the present rule. The typical rules of the atomic group displacement method, for example, are derived as follows:

(1) Displacement of H of C—H with CH_3 (excluding $C_1\rightarrow C_2$)

(a) Non-branched

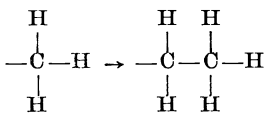

increase: (C, H, H); (C—H×2, C—C×1)

decrease: .....

From eq. (13) the increase of entropy by displacement ΔS° is calculated as

$$\Delta S^{\circ}=2.98\times\ln 12+0.7\times\{2\ln 13+\ln 24\}-1.33\times 3$$
$$=7.4+5.8-4.0=9.2,$$

while the observed mean value of ΔS° is 9.2 e.u.

(b) Branched with two degree

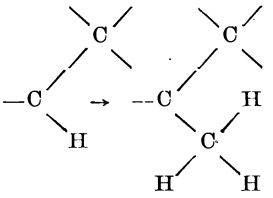

From eqs. (6) and (7)

$$\Delta S^{\circ}=9.2(\text{calculated value in 1a})-0.7\times\frac{2^2}{1.8}$$
$$=9.2-1.6=7.6,$$

while the observed mean value is 7.5 e. u.

(c) Branched with three degree

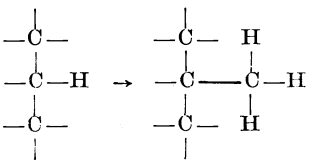

From eqs. (6) and (7)

$$\Delta S^{\circ}=9.2(\text{calculated value in 1a})-0.7$$
$$\times\left\{-\frac{2^2}{1.8}+\frac{3^2}{1.8}\times 2\right\}$$
$$=9.2+1.6-3.5\times 2=3.8,$$

while the observed mean value is 3.8 e.u.

(2) Displacemens of C—C with C=C (excluding ethane to ethylene)

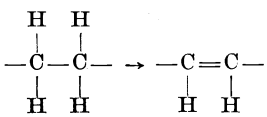

From eqs. (6) and (7)

$$\Delta S^\circ = -2\times\{0.7\ln 13 - 0.7\times 1.9\}$$
$$= -2\times(1.8-1.3) = -1.0,$$

while the observed mean value is −1.0 e.u.

The calculated values of ΔS° as stated above are very convenient for the calculation of S° of hydrocarbons, and are applicable also for the substances involving the abnormal depressions, provided that the latter are not affected by the displacement.

Activation Entropy of Chemical Reaction

According to Eyring et al.[9] the specific reaction rate of bimolecular gas reaction k is expressed by the equation:

$$k = \kappa e^2 \frac{kT}{h} RTe^{\Delta S_p^*/R} e^{-E/RT} \text{ (cc.mole}^{-1}\text{sec.}^{-1}\text{)}, \quad (24)$$

where κ is the transmission coefficient, k is Boltzman constant (1.372×10^{-16} erg·degree^{-1}), h is Planck constant (6.554×10^{-27} erg.sec.), R is universal gas constant (in the terms $e^{\Delta S_p^*/R}$ and $e^{-E/RT}$ R is 1.987 cal·degree^{-1}, and in the term RT, R is 82.06 cc·atm·degree^{-1}), ΔS_p^* is activation entropy when the standard state is chosen as 1 atm., and E is the experimental activation energy. Compared with Arrhenius's equation

$$k = Ae^{-E/RT},$$

the frequency factor A is expressed as

$$A = \kappa e^2 \frac{kT}{h} RTe^{\Delta S_p^*/R}. \quad (25)$$

Putting $\kappa=1$, and introducing the numerical values, it follows

$$A = 1.27\times10^{13}\, T^2 e^{\Delta S_p^*/2} \text{ (cc·mole}^{-1}\text{sec.}^{-1}\text{)}. \quad (26)$$

If ΔS_p^* is given, therefore, the frequency factor of bimolecular gas reaction can be calculated readily with the use of eq. (26)

Activation entropy ΔS_p^* is given from thermodynamics by

$$\Delta S_p^* = \Delta S_p^{\circ *} + \Delta C_p^* \ln\frac{T}{298}, \quad (27)$$

where $\Delta S_p^{\circ *}$ is entropy difference between activated complex and initial state at 298°K and 1 atm., and ΔC_p^* is the difference of molecular heat at constant pressure between activated complex and initial state assuming independent with temperature.

When the initial state converts to activated complex, molecular heat will decrease on the one hand according to the presumed decrease of degrees of freedom of translation and rotation, and will increase on the other hand according to the presumed increase of degrees of freedom of vibration and depressions of vibrational frequencies. As these problems are too complicated to discuss quantitatively, it was assumed that these opposite effects cancel each other, i. e.,

$$\Delta C_p^* = 0. \quad (28)$$

For bimolecular reaction $\Delta S_p^{\circ *}$ is expressed as

$$\Delta S_p^{\circ *} = S^{\circ *} - (S^\circ_A + S^\circ_B), \quad (29)$$

where $S^{\circ *}$, S°_A and S_B° are S° of activated complex, reactant A, and reactant B respectively. S°_A and S°_B can readily be computed by means of the present rule, if the reactants have not abnormal depressions. Compared with the entropies of normal molecules, entropy of activated complex will increase on the one hand according to the presumed elongation of the bond distance and depression of vibrational frequency, and will decrease on the other hand according to the presumed restrictions by the activated bonds[10] and depressions by ring closure and resonance effect. As these effects are too complicated to discuss quantitatively, it was assumed that the entropies of the activated complexes of the triatomic reaction

$$X+Y-Z \rightleftarrows X\cdots Y\cdots Z \dashrightarrow X-Y+Z,$$

and the double decomposition

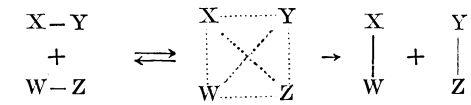

could be computed with the models

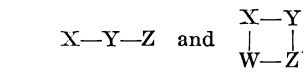

respectively, as the result of cancellation of both effects.

The frequency factors of some simple reactions computed by means of the above-mentioned series of assumptions were compared with the observed values in Table 5. As seen in the table the calculated values agree with the observed within 3~1/6 times, so that the rough assumptions above stated concerning the molecular heat and entropy of

(9) S. Glasstone, K. J Laidler and H. Eyring. "The Theory of Rate Processes", McGraw-Hill, Inc., New York, 1941.

(10) K. Otozai, This Bulletin. **24**, 218 (1951); K. Otozai, *Scient. Papers, Osaka Univ.*, No. 20, (1951).

Table 5

Calculation of Frequency Factor

Reaction	$S°^*$ (e. u.)	$S°_A$ (e. u.)	$S°_B$ (e. u.)	ΔS^*_p (e. u.)	T (°K)	$A_{calc.}$ ($cc \cdot mole^{-1} \cdot sec^{-1}$)	$A_{obs.}$ ($cc \cdot mole^{-1} \cdot sec^{-1}$)	$A_{calc.}/A_{obs.}$
$H+H_2=H_2+H$	33.2	26.0	29.5	−22.3	300	1.6×10^{13}	1.1×10^{13}[9]	1
$Cl+H_2=ClH+H$	45.9	36.7	29.5	−20.3	298	0.5×10^{14}	1.8×10^{14}[9]	1/4
$H+HBr=H_2+Br$	48.8	26.0	45.2	−22.4	500	4.3×10^{13}	1.3×10^{13}[9]	3
$Br+H_2=BrH+H$	48.8	39.1	29.5	−19.8	499	1.6×10^{14}	0.8×10^{14}[9]	2
$H_2+I_2=2HI$	70.1	29.5	61.9	−21.3	700	1.5×10^{14}	2.0×10^{14}[11]	1
$Br_2+Cl_2=2BrCl$	90.8	58.7	53.2	−21.1	—	0.3×10^{14} (298°K)	1.8×10^{14}[12] (room)	1/6
$H_2C:CH_2+H_2=C_2H_6$	54.7	52.7	29.5	−27.5	773	0.8×10^{13}	1.9×10^{13}[13]	1/2

activated complex are approximately correct. This discussion concerning entropy of activation is one of two works of the research on activation energy performed by one of the authors.[10]

Summary

(1) From the standpoint of chemical bond a new empirical rule for the calculation of entropy of polyatomic gas molecule has been proposed. It agrees with the observed value within the error of ±2 e. u., and includes monoatomic and diatomic molecule as a special case, and finally gives the upper limit of the observed value.

(2) The abnormal depression of entropy from the standard of the present rule was interpreted as ring closure entropy and resonance entropy, and respective values were given for some typical substances. Closure entropy 20.9 e. u. of cyclohexane and resonance entropy 4.2 e. u. of benzene agreed well with the conclusion of Bremner-Thomas according to the atomic group method.

(3) It has been shown that resonance entropy is so small that its contribution to the resonance free energy is neglisible compared with resonance energy. In special case, however, the contribution of the resonance entropy is about 10% of the resonance free energy, as in the case of carbon dioxide.

(4) It has been shown that it is impossible to construct the true bond entropy, which is additive and independent. But it is possible to build up the formal bond entropy, which is additive and not independent.

(5) In order to show that the present rule includes naturally the atomic group method, some typical rules of the atomic group displacement method have been derived.

(6) Under some assumptions the frequency factors of some simple chemical reactions have been computed by means of the present rule. The calculated values agreed with the observed within 3～1/6 times.

The authors wish to express their sincere thanks to Prof. T. Titani for his valuable discussions of these problems, and to Dr. S. Seki for his kind guidance concerning thermochemical data.

Faculty of Science, Osaka University, Osaka

(11) M. Bodenstein, *Z. phys. Chem.*, **29**, 295 (1899).
(12) W. Jost, *Z. phys. Chem.*, B **14**, 413 (1931).
(13) R. N. Pease, *J. Am. Chem. Soc.*, **54**, 1876 (1932).

The Relation between the Second Virial Coefficient of Osmotic Pressure and the Molar Volume of Solute (Abstract)[1]

By Gisuke MESHITSUKA

(Received January 29, 1952)

Equation for the Osmotic Pressure in Dilute Ideal Solution

The osmotic pressure P, of a solution is thermodynamically related to the vapour-

(1) Details have been published in *Chemistry of High Polymers, Japan*, **9**, 268 (1952).

pressure of pure solvent $p_1°$, and that of solution p_1 according to the equation

$$P=-\frac{RT}{\bar{v}_1}\ln\frac{p_1}{p_1°} \qquad (1)$$

where $\bar{v}_1$ represents the partial molar volume of solvent in solution, R the gas constant and T absolute temperature. As a special case, when the solution is ideal, the partial molar volume of the solvent $\overline{v_1}$ can be put down as equal to the molar volume of pure solvent $v_1°$, and $p_1/p_1°$ to the mole fraction of the solvent in the solution N_1, according to the Raoult's law, so that eq. (1) becomes

$$P=-\frac{RT}{v_1°}\ln N_1 . \qquad (2)$$

And if the solution is composed from n_1 moles of solvent and n_2 moles of solute, the mole fraction of solvent N_1 is clearly

$$N_1=\frac{n_1}{n_1+n_2} \qquad (3)$$

and the total volume of the solution V can be expressed as

$$V=n_1v_1°+n_2v_2° \qquad (4)$$

where $v_1°$ and $v_2°$ are the molar volumes of the solvent and the solute in pure state respectively.

Putting eqs. (3) and (4) in eq. (2), we obtain

$$P=\frac{n_1RT}{V-n_2v_2°}\ln\left(1+\frac{n_2}{n_1}\right). \qquad (5)$$

This eq. (5) can, however, be further simplified to the eq. (6) for which is shown below for a sufficiently dilute solution by expanding the logarithmic factor in the right hand side and neglecting higher terms than the second

$$P=\frac{n_2RT}{V-n_2v_2°} . \qquad (6)$$

Dilute Solutions of Low Molecular Weight Substances

In real solutions solute molecules are generally solvated, that is, a number of solvent molecules are loosely attached to a solute molecule. But it may be a plausible assumption that the degree of solvation, i. e. the number of solvent molecules attached to a solute molecule increases with increasing dilution; finally a saturated state is reached and thereafter the degree of solvation does not increase with further increase of dilution. Accordingly in this state of saturation the solution may be treated as a sort of ideal solution, when we regard the solvated solute molecule as a whole as a molecule of the solute. Then, by expressing the maximum degree of solvation in this saturated state by $N_{\max}$, we can put the number of free solvent molecules in the solution at a sufficiently large dilution

$$n_1'=n_1-N_{\max}n_2 \qquad (7)$$

the mole fraction of the free solvent

$$N_1'=\frac{n_1'}{n_1'+n_2}=\frac{n_1-N_{\max}n_2}{n_1-N_{\max}n_2+n_2} \qquad (8)$$

and the total volume of the solution

$$V=n_1'v_1°+n_2(v_2°+v_1'N_{\max}) \qquad (9)$$

where v_1' represents the molar volume of the solvent in the solvated state. Hence if we put eqs. (8) and (9) in eq. (2) we obtain for a sufficiently dilute solution

$$P=\frac{n_1'RT}{V-n_2(v_2°+v_1'N_{\max})}\ln\left(1+\frac{n_2}{n_1'}\right) \qquad (10)$$

or

$$P(V-n_2b_{\max})=n_2RT \qquad (11)$$

where

$$b_{\max}=v_2°+N_{\max}v_1' . \qquad (12)$$

The $b_{\max}$ represents the maximum molar volume of the solvated solute, that is, the molar volume of the solvated solute in the state of saturated solvation.

Dilute Solutions of Chain Polymers

As is well known, the abnormal character of the solution of high polymers especially that of chain polymers is generally attributed to the random motion of the sections of the chain molecules in soln. But if we assume the extension of a chain molecule due to its random motion having a saturated or maximum value in sufficient dilution, such a solution can be treated in exactly the same way as the solution of low molecular weight substances in its saturated state of solvation. We obtain exactly the same form of the equation as (11) for the relation between the osmotic pressure, the volume of the solution and the temperature for a sufficiently dilute solution of high polymer, if we assume $b_{\max}$ representing the maximum molar volume of the solute, that is, the volume occupied by the solute molecule at its highest degree of expansion.

The Second Virial Coefficient and the Molar Volume of the Solute

The relation between the osmotic pressure P and the concentration c expressed in gram per liter of a solution is expressed by a well known equation

$$P=RT\left(\frac{c}{M}+A_2c^2+A_3c^3+\cdots\right) \quad (13)$$

where M represents the molecular weight of the solute and A_2 and A_3 are the so-called the second and the third virial coefficient respectively. Hence, it may be of interest to compare eq. (11) obtained above with this eq. (13). For this purpose eq. (11) is deformed into the form

$$P=\frac{n_2RT}{V-n_2b_{\max}}=\frac{RT}{\frac{M}{c}-b_{\max}}$$

$$=RT\frac{c}{M}\left(1-\frac{c}{M}b_{\max}\right)^{-1},$$

and by expanding the right hand side of this equation and neglecting higher terms, we obtain

$$P=RT\left(\frac{c}{M}+\frac{b_{\max}}{M^2}c^2\right). \quad (14)$$

By comparing the second terms in the right hand sides of eqs. (13) and (14) we see that the second virial coefficient A_2 is related to the maximum molar volume $b_{\max}$ and the molecular weight M of the solute according to the equation:

$$A_2=b_{\max}/M^2. \quad (15)$$

As a verification of this eq. (15) we have compared the value of $b_{\max}$ of polystyrene in toluen solution calculated by this equation using the data obtained from the osmotic pressure measurement with that computed from the light scattering measurement. We have obtained namely from the data of osmotic pressure measurement made by Mark and others[2] at 25°C. for the toluene solution of polystyrene having a mean molecular weight of 1,580,000 as a value of $b_{\max}$ 3.74×10^5 liter/mole according to eq. (15). This value agrees, however, sufficiently well with the value of $b_{\max}=3.68\times10^5$ liter/mole obtained from the light scattering measurement made by Zimm and others[3] at 22°C. for the toluene solution of polystyrene having a mean molecular weight of 1,610,000.

Degree of Hydration of Sucrose and Glucose

When we calculate $b_{\max}$ for sucrose in aqueous solution by eq. (15) using the data of osmotic pressure measurement made by Morse[4] at 20°C., we obtain 0.382 liter/mole. But $b_{\max}$ is related with the molar volume of pure solute v_2^0 and the molar volume of the hydrated water v_1' according to eq. (12). Hence, if we assume v_2^0 being equal to the molar volume of pure solid sucrose (0.216 liter/mole) and v_1' being equal to the molar volume of pure water (0.018 liter/mole), we obtain as a maximum degree of hydration $N_{\max}$ of sucrose a value of about 9 accoring to eq. (12). In the same way we obtain as $N_{\max}$ for glucose at 10°C. a value of about 3.5 from the osmotic pressure measurement made by the same author.

The author expresses his hearty thanks to Prof. Toshizo Titani for his kind guidance and encouragement in the course of this study.

Chemical Institute, Faculty of Science, Osaka University, Osaka

(2) T. Alfrey, A. Bartovics and H. Mark, *J. Am. Chem. Soc.*, **65**, 2319 (1943).
(3) P. Outer, C. I. Carr and B. H. Zimm, *J. Chem. Phys.*, **18**, 830 (1950).
(4) H. N. Morse, *Am. Chem. J.*, **48**, 29 (1912).

Ueber die spezielle Reaktionsfähigkeit der beiden Endgruppe von langer Kette

von R. SENZYU und O. ASAYAMA

(Eingegangen am 25, Dezember, 1951)

Einleitung

Bei der Hydrolyse von Polysacchariden z. B. der cellulose,[1] der Stärke,[2] des Inulins[3] und des Lävans[3] nehmen die nach der monomolekularen Gleichung berechneten Reaktionskonstanten mit dem Spaltungsgrad zu. Diese Vorgang ist auch bei der Abspaltung des Polyesters bemerkbar. In früheren Untersuchungen über die Polyesterung von zweibasischen, organischen Säuren und zweiwertigen Alkoholen teilte P. J. Flory[4] mit, dass der Polymerisationsgrad keine Einfluss auf die Realktiosfähigkeit hat. Diese empirischen Ergebnisse deuten darauf hin, dass die beiden Endgruppen von langer Kette eine spezielle Eigenschaft besitzen. Bedauerlicherweise ist es jedoch bisher niemanden gelungen, die speziellen Eigenschaften der beiden Endgruppen von langer Kette unmittelbar zu bestätigen. Will man diese Frage lösen, so ist es am einfachsten, die Verseifungsgeschwindigkeit von Polyäthylenglykol-diacetat, das nur an beiden Enden der langen Kette die funktionellen Gruppen besitzt, mit derselben von β-Methoxyäthylacetat zu vergleichen. Aus diesem Grunde wurden die Untersuchungen über die alkalischen Verseifungen von Polyäthylenglykol-diacetat und β-Methoxyäthylacetat untergenommen.

Herstellung von Versuchsmaterialien

β-Methoxyäthylacetat.— β-Methoxyäthylacetat wurde nach M. H. Palomma[5] aus Aethylenglykolmonoäthyläther und Acetylchlorid in Gegenwart von Pyridin dargestellt. Der Siedepunkt, 145°C.

Polyäthylenglykol-diacetat.— Das Polyäthylenglykol-dihydrat wurde nach H. Staudinger[6] durch Polymerisation des Aethylenoxydes dargestellt. 15 g. des betreffenden Polyäthylenglykoldihydrates wurden mit 100 cc. Essigsäureanhydrid 4 Stunden lang am Rückflusskühler gekocht. Darauf wurde die Hauptmenge Anhydrid im Vakuum abdestilliert. Die höhermolekularen Diacetat wurden durch wiederholtes Umfällen erhaltet. Das Molekulargewicht wurde nach Rast bestimmt. Molekulargewicht 2440, Polymerisationsgrad 55.

Versuchsanordnung

Die Verseifung wurde in der üblichen Weise vorgenommen. In einem Meyerschen Kolben wurde eine bestimmte Menge von 0.1 N NaOH, die durch Verdünnung von 1 N Lauge mit kohlensäurefreiem Wasser in Messkolben dargestellt wurde, auf die gewünschte Tempetatur im Thermostatten vorgewärmt. In einem anderen Meyerschen Kolben wurde dann die wässerige Lösung einer abgewogenen Menge Ester hergestellt und ebenfalls vorgewärmt. Zur Zeit $t=0$ wurden dann die beiden Lösungen unter Rühren gemischt. Der Kolben wurde durch einen Gummistopfen verschlossen. Zum Zweck der Titration wurde stets eine bestimmte Menge der Lösung in 15 cc. 0,05110 N HCl hinzugefügt und dann die Menge von überschüssigen Säuren mit Phenolphtalein zurücktitriert. Die Konzentrationen des Esters und des Alkalis und die zeitlichen Aenderungen sind in den Tabellen stets in cc. von Salzsäure angegeben.

Empirische Ergebnisse

Die Reaktionskonstante in den Tabellen wurden nach der folgenden bimolekularen Gleichung berechnet

$$K=\frac{\log a+\log(a_0-a_\infty)-\log a_0-\log(a-a_\infty)}{0.4343\ a_\infty\ (t-t_0)}.$$

Als Einheitskonzentration wurde jedoch durchweg, um die verschiedenen Konstanten miteinander vergleichen zu können, die 1 N Lösung benutzt. Die Werte für K sind daher mit den entsprechenden Faktoren multipliziert.

Die Tabellen zeigen durch die guten Konstanten der Werte von K, dass die alkalische Verseifung sowohl von Polymer wie auch von Monomer glatt bimolekular verläuft. Die

(1) K. Freudenberg uud Mitarbeiter, *Ber.* **65**, 1179 (1932); **66**, 19 (1933); **68**, 2070 (1935); **69**, 1258 (1936); M. L. Wolfrom und L. W Georges, *J. Am. Chem. Soc.*, **59**, 282 (1937).
(2) K. Meyer, H. Hopff und H. Mark, *Ber.* **62**, 1103 (1929); K. Freudenberg, *Ber.* **69**, 1258 (1936).
(3) H. Hibbert und E. G. V. Percival, *J. Am. Chem. Soc.*, **52**, 3995 (1930); S. Knoop, *Ann.* **504**, 26 (1933); **520**, 34 (1935).
(4) P. J. Flory, *J. Am. Chem. Soc.*, **61**, 3384 (1939).
(5) M. H. Palomma, *Ber.* **71**, 480 (1938).
(6) H. Staudinger, *Ber.* **62**, 2395 (1929).

Tabelle 1

Die Verseifung von β-Methoxyäthylacetat bei 10°C. (Konzent. des Esters = 0.01663 (mol/l.))

Zeit in Sek. $(t-t_0)$	Neutralisierte cc. N/20 HCl für 25 cc. Lös. (a)	K(mol/cc.)$^{-1}$ Sek.$^{-1}$
0	9.43 (a_0)	
214	8.40	4.39
352	7.43	4.30
699	6.60	4.05
1583	5.28	4.05
2177	3.66	4.10
3060	3.01	4.05
4296	2.52	3.80
∞	1.31 (a_∞)	
	Durchschnitt	4.10

Tabelle 2

Die Verseifung von β-Methoxyäthylacetat bei 25°C. (Konzent. des Esters = 0.01603 (mol/l.))

Zeit in Sek. $(t-t_0)$	Neutralisierte cc. N/20 HCl für 25 cc. Lös. (a)	K(mol/cc.)$^{-1}$ Sek.$^{-1}$
0	9.75 (a_0)	
60	7.90	13.6
119	6.80	13.2
187	5.96	13.2
361	4.54	12.4
602	3.55	12.2
902	2.85	12.3
1439	2.33	11.4
2577	1.86	10.5
3418	1.70	10.3
∞	1.44 (a_∞)	
	Durchschnitt	12.3

Tabelle 3

Die Verseifung von Polyäthylenglykol-diacetat bei 10°C. (Konzent. der Estergruppe = 0.01630 (mol/l.))

Zeit in Sek. $(t-t_0)$	Neutralisierte cc. N/20 HCl für 25 cc. Lös. (a)	K(mol/cc.)$^{-1}$ Sek.$^{-1}$
0	8.10 (a_0)	
175	6.56	5.21
345	5.99	4.05
589	4.88	4.40
1457	3.20	4.23
3193	2.02	3.93
5810	1.36	3.78
9650	0.93	3.87
∞	0.37 (a_∞)	
	Durchschnitt	4.21

genügende Uebereinstimmung der K-Werte von Polymer mit denen von Monomer ist von grosser Bedeutung. In der Regel lässt sich

Tabelle 4

Die Verseifung von Polyäthylenglykol-diacetat bei 25°C. (Konzent. der Estergruppe = 0.01490 (mol/l.))

Zeit in Sek. $(t-t_0)$	Neutralisierte cc. N/20 HCl für 20 cc. Lös. (a)	K(mol/cc.)$^{-1}$ Sek.$^{-1}$
0	6.23 (a_0)	
68	5.24	12.9
104	4.74	14.2
159	4.28	13.6
338	3.30	12.8
580	2.63	11.9
878	2.01	12.6
1424	1.56	11.9
2137	1.20	12.2
2980	1.09	10.3
∞	0.61 (a_∞)	
	Durchschnitt	12.5

die Reaktionsgeschwindigkeitskonstante durch folgende Arrheniussche Gleichung darstellen.

$$K = A \cdot \exp(-E/RT)$$

Wenn man von der Temperaturabhängigkeit der Reaktionskonstante nach der Arrheniusschen Gleichung die Aktivierungsenergie und den sterischen Faktor berechnet, so erhält man die in der Tabelle 5 angegebenen Werte.

Tabelle 5

Die kinetischen Daten der alkalischen Verseifungen von β-Methoxyäthylacetat[1] und Polyäthylenglykol-diacetat[2]

Substanz	K(mol/cc.)$^{-1}$ Sek.$^{-1}$ 10°C.	25°C.	E (kcal.)	$A \times 10^{15}$	ΔS^* (cal.)	ΔF^* (kcal.)
1	4.21	12.5	12.81	1.90	−10.5	15.95
2	4.10	12.3	12.71	1.50	−10.8	15.95

Die freie Aktivierungsenergie (ΔF^*) und die Aktivierungsentropie (ΔS^*) wurden nach der folgenden Eyringschen Gleichung berechnet.

$$K = \kappa' \cdot kT/h \cdot \exp(\Delta S^*/R)\exp(-\Delta H^*/RT),$$
$$(\Delta F^* = \Delta H^* - T\Delta S^*).$$

Dass E, A, ΔF^* und ΔS^* von Polymer mit denselben von Monomer gut übereinstimmen, bedeutet, dass die Verseifungsmechanismen von beiden Ester ganz identisch sind. Nach bisherigen Untersuchungen nimmt die Reaktionsfähigkeit mit dem zunehmenden Molekulargewicht ab. Bei solcher Reaktion, bei der sich nur die beiden Endgruppen beteiligen, kann man jedoch annehmen, dass die Reaktionsfähigkeit bei hochmolekularen und niedermolekularen Stoffen keinen Unterschied

aufweist. Früher teilte P. Flory[4] mit, dass bei Polyesterung von zweibasischen, organischen Säuren und zweiwertigen Alkoholen die Reaktionskonstanten stets konstant sind. Diese Ergebnisse bedeuten, dass das Molekulargewicht keinen Einfluss auf die Reaktionsfähigkeit hat. Diese Tatsache wird zwar schwer durch die heutzutage am weitesten verbreiteten Anschauungen aufgeklärt, dass mit Zunahme des Molekulargewichtes die Reaktionsfähigkeit abnehme, aber ist unter Berücksichtigung unserer Ergebnisse leicht verständlich, denn die von P. Flory behandelten Reaktionen sind diejenigen, an denen sich nur die beiden Endgruppen von langer Kette beteiligen.

Zusammenfassung

Um die spezielle Reaktionsfähigkeit der beiden Endgruppen von langer Kette festzustellen, wurden die Untersuchungen über die alkalischen Verseifungen von β-Methoxyäthylacetat und Polyäthylenglykol-diacetat, das an dem beiden Enden von langer Kette die funktionellen Acetylgruppen besitzt durchgeführt. Die Reaktionsfähigkeit der beiden Endgruppen von langer Kette stimmt nicht nur in Reaktionskonstante, sondern auch in Aktivierungsenergie und sterischen Faktor mit denen von Monomer überein. Mindestens bei solcher Reaktion, an der sich nur die beiden Endgruppen beteiligen, kann man annehmen, dass die Reaktionsfähigkeit bei den hochmolekularen und niedermolekularen stoffen keinen Unterschied aufweist.

Institut für Wissenschaft und Industrie,
Kyushu Universität, Fukuoka

Monolayers of Branched-Chain Fatty Acids. II. α-Aromatic Substituted Fatty Acids

By Masami IZAWA

(Received May 26, 1952)

In our previous report, force-area curves for a number of branched-chain fatty acids having aliphatic side chains have been studied.[1] It was concluded that there are close relations between the force-area curves and the position and the length of the side chains. In this report, experiments were carried out for four series of branched-chain fatty acids having aromatic side chains in the α-position, namely, 2-phenyl-, 2-(α-naphthyl)-, 2-benzyl- and 2-(α-naphthomethyl)-n-fatty acids,* which were shown to have antibacterial activities in vitro.[2,3]

Asano and his co-workers[2] and Ukita and his co-workers[3] have postulated that a good antibacterial effect might be expected if a substance occupied a large area when adsorbed on a bacterial cell surface. This assumption led them to syntheses and examination of the antibacterial activities of aromatic ring-substituted compounds mentioned above. Contrary to their expectation, no influence of substituting groups on the antibacterial activity has been found, though substitution of naphthyl and naphthomethyl groups had a little better effect against *S. aureus* than substitution of phenyl group. They assumed implicitly that a naphthalene ring occupies a much larger area on the cell surface than a benzene ring, but this assumption should be verified experimentally. From force-area relation on water substrate, one can estimate the orientation of the molecules of these compounds at the cell surface, and this is one of the reasons for which this study was done.

Materials and Methods

Twenty-three substances were used in this experiment:

α-phenyl series:

$$C_nH_{2n+1}\underset{\displaystyle C_6H_5}{\underset{|}{C}}HCOOH \quad n=2, 8, 10, 12, 13, 14, 16.$$

* For simplicity, the names of these compounds were referred in this paper to α-phenyl-, α-naphthyl-, α-benzyl- and α-naphthomethyl-series respectively.

(1) M. Izawa, This Bulletin, **25**, 182 (1952).

(2) M. Asano, H. Motomatsu and O. Tamemasa, *J. Pharmaceut. Soc. Japan*, **70**, 622 (1950). (In Japanese)

(3) T. Ukita, O. Tamemasa and H. Motomatsu, *J. Pharmaceut. Soc. Japan*, **71**, 289 (1951).

α-naphthyl series:

$C_nH_{2n+1}CHCOOH$ ($C_{10}H_7$) $n=4, 6, 8, 10, 12.$

α-benzyl series:

$C_nH_{2n+1}CHCOOH$ ($CH_2C_6H_5$) $n=4, 6, 8, 10, 12.$

α-naphthomethyl series:

$C_nH_{2n+1}CHCOOH$ ($CH_2C_{10}H_7$) $n=0, 4, 6, 8, 10, 12.$

All these compounds were synthesized by Dr. Tamemasa of the Chemical Department, Institute for Infectious Diseases, Tokyo University. As to their synthetic methods, constants and bactericidal properties, reference should be made to the original papers.[2,3]

Techniques employed were the same as those of the previous report.[1] Langmuir-Adam surface balance was made by Suzuki Scientific Instrument Works, Tokyo. The torsion wire of 0.278 dyne per cm. per degree was used. All experiments were carried out at 20°C. in an air-thermostat, which can be kept closed during the period of all operations.

Results and Discussion

1. Monolayers on 0.01 N Hydrochloric Acid Solution.—a. α-Phenyl series (Fig. 1).—Force-area curves begin to rise at about 60 A.^{2} per molecule, and collapse at 42 A.^{2}, with the equilibrium surface pressure of 27.5 dynes per cm. The effect of the length of the aliphatic portion of the molecules on the force-area curves is not large. Films of $n=8$ or lower members of the series are unstable.

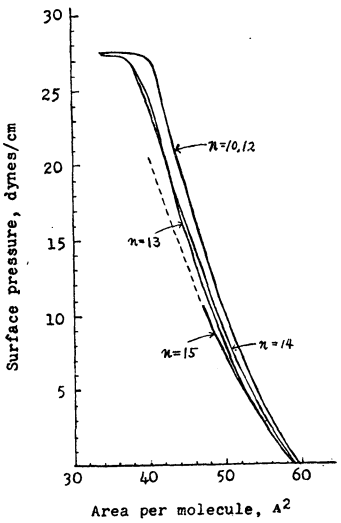

Fig. 1.—Force-area curves for $C_nH_{2n+1}CH(C_6H_5)COOH$ series on 0.01 N HCl solution at 20°C.

b. α-Naphthyl series (Fig. 2).—The limiting area of the monolayers is about 60 A.^{2}, but the curves are steeper than those for α-phenyl series. These monolayers reach equilibrium pressure of 23 dynes at 45 A.^{2} In this case, also, the length of the alkyl chain exhibits a minor effect on the force-area curves, and the members lower than $n=6$ give no stable film.

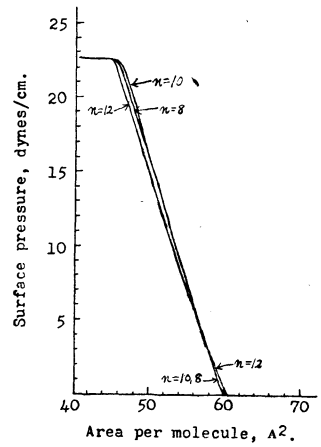

Fig. 2.—Forse-area curves for $C_nH_{2n+1}CH(C_{10}H_7)COOH$ series on 0.01 N HCl solution at 20°C.

c. α-Benzyl series (Fig. 3).—Limiting area of this series is about 67 A.^{2}, and the films collapse at 45 A.^{2} and 24 dynes. Acids of $n=6$ or lower members give unstable films, and $n=8$ acid seems to dissolve considerably.

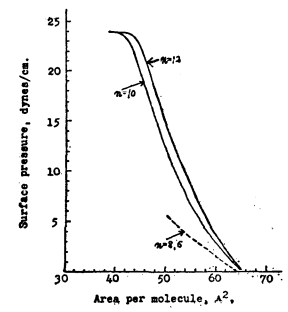

Fig. 3.—Force-area curves for $C_nH_{2n+1}CH(C_6H_5\cdot CH_2)COOH$ series on 0.01 N HCl solution at 20°C.

d. α-Naphthomethyl series (Fig. 4).—Limiting area is about the same as that of α-benzyl series, namely, 66 A.^{2}, but the force-area curves are steeper, and the monolayers collapse at about 50 A.^{2} and 19 dynes. The effect of the length of the aliphatic chain is negligibly small, as shown in the figure. Acids with $n=6$ or lower do not give stable films.

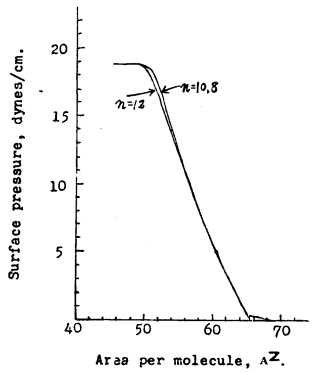

Fig. 4.—Force-area curves for $\begin{matrix} C_nH_{2n+1} \\ C_{10}H_7\cdot CH_2 \end{matrix}\!\!>$ CH·COOH series on 0.01 N HCl solution at 20°C.

These results can be represented schematically as the curves shown in Fig. 5. In every series, the length of the alkyl chains in the molecules has only minor effect upon the force-area curves. Therefore, it was concluded that the force-area curves are determined mainly by the aromatic portion of the molecules. In the case of α-alkyl substituted fatty acids, if the length of the longer aliphatic chain becomes longer, the cross-sectional area per molecule becomes larger at low pressure region, and smaller at higher pressures.[1,4] The fact that there exists no such relation in α-aromatic substituted acids may be due to the stronger interaction between adjacent molecules, probably because of the higher molecular weight of these substances.

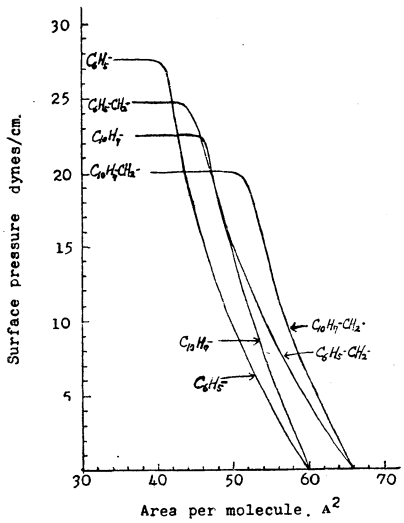

Fig. 5.—Effect of substituting groups on the force-area curves of α-substituted n-fatty acids.

Limiting areas per molecule of α-phenyl and α-naphthyl acids and those of α-benzyl and α-naphthomethyl acids are nearly equal, and are 60 A.^{2} and 66 A.^{2} respectively. Accordingly, phenyl and naphthyl groups are considered to have such an orientation as having equal cross-sectional areas on the surface. From the molecular models, it is shown that phenyl or naphthyl group can orient vertically on the surface of water, that is, the plane of the aromatic ring can be placed perpendicular to the water surface, and that phenyl and α-naphthyl groups are able to have an orientation having nearly equal cross-sectional areas. This is in accordance with the result of the experiment.

Stenhagen has reported that the collapse area for α-cyclohexyl-fatty acids (50 A.^{2}) equals the sum of the area of p-alkylcyclohexanol (30 A.^{2}) and that of hydrocarbon chain(20 A.^{2}). [4]If the additivity of the cross-sectional areas can be applied to any films exhibiting the liquid expanded state, the area for phenyl, naphthyl, benzyl or naphthomethyl group is 22, 25, 25, and 30 A.^{2} respectively. The collapse area for ω-phenyl-n-fatty acids reported by Ställberg and Stenhagen[5] is 21 A.^{2}, which is in agreement with the figure from the molecular models (ca. 20 A.^{2}), and this area corresponds to the experimental data given above for phenyl group (22 A.^{2}). For the figures other than that for phenyl, comparison was not practicable because of the lack of experimental data.

2. Influence of *p*H of the substrate on the force-area curves (Fig. 6).—Fig. 6 shows the force-area curves for α-phenylpalmitic acid on 1/30 M phosphate buffer substrate, pH of which being 5.5, 6.0, 7.0 and 8.0, together with the curve on 0.01 N hydrochloric acid solution.

The curve on the substrate of pH 5.5 coincides well with that on 0.01 N HCl solution but the equilibrium pressure is higher. At pH 6.0 and 7.0, curves are somewhat expanded, and become unstable at high pressure region.

(4) E. Stenhagen, *Trans. Faraday Soc.*, **36**, 597 (1940).
(5) S. Ställberg and E. Stenhagen, *Svensk Kem. Tid.*, **53**, 355, (1941); *C. A.*, **36**, 1536-2 (1942).

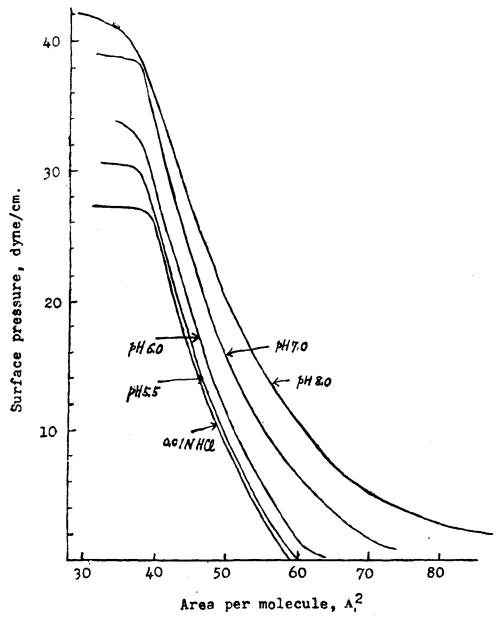

Fig. 6.—Effect of pH on the force-area curves of $\begin{matrix} C_{14}H_{29} \\ C_6H_5 \end{matrix}\!\!>\!CH\cdot COOH$ on M/30 phosphate buffer.

The equilibrium pressure obtained by rapid compression is higher than the pressure at acidic region. At pH 8.0, the film expands much more, and shows a gaseous state, and becomes unstable at 20 dynes per cm. or higher. These findings are in agreement with the data for other fatty acids at different pH.

Effect of pH on other substances examined here was similar to the effect on α-phenylpalmitic acid shown in figure 6, though the stability region was considerably varied from one compound to another, and, therefore, was not shown in this report.

3. Surface behavior and antibacterial properties.—It has been well known that a peak will be found when antibacterial activity is plotted against the total number of carbon atoms of substances of a homologous series. It was reported that for the four series mentioned above the highest activity was found in the member having about 20 carbon atoms.[2,3] It has not been possible to interpret the existence of the activity maximum in terms of the surface behavior only, and there is no direct relation between film properties and antibacterial activity of any one of the four series, nor for the aliphatic substituted fatty acids reported previously.[1] Daniels concluded that the increase in activity in an ascending series paralleled the decrease in water solubility, the increase in lipid solubility, and to a certain extent, the increase in surface activity, and that the rapid decrease beyond the activity maximum was attributable to a limiting water solubility.[6] On the other hand, Work and Work[7] suggested that the bactericidal activity of surface-active compounds should be interpreted solely in terms of their surface activity. They believed that the existence of activity maximum was due to the micelle formation at higher concentrations. Whether Daniels' or Work and Work's conclusion is correct must be examined further in other lines of experiments in the case of aromatic substituted fatty acids.

The effect of substitution upon bactericidal activity was shown to be very small.[3] Considering the relatively large experimental errors of bactericidal tests, it should be concluded from the film experiment that these four series of compounds have equal cross-sectional areas on the surface. Provided that substances which occupy larger area at the cell surface have stronger antibacterial activity than those which possess smaller area, it is not unreasonable to say that the four series have almost equal antibacterial activity. It would be of interest to examine the activity of substances which lie flat on the surface.

Summary

(1) Force-area relations for 2-phenyl-, 2-(α-naphthyl)-, 2-benzyl- and 2-(α-naphthomethyl)-n-fatty acids have been investigated.

(2) Force-area curves are characteristic to each of the four series, showing that the length of alkyl chains in the molecules has only a minor effect upon the curves.

(3) Influence of pH on the force-area curves, so far examined, is shown to be similar to other fatty acids.

(4) It was concluded that the aromatic ring in the α-position of the fatty acids has such an orientation that the plane of the aromatic ring is placed perpendicular to the water surface.

(5) Film properties seem to have no direct relation to the antibacterial activity of these compounds, and some of the regularities for the activity are discussed.

The author wishes to thank Dr. Hamao Umezawa, the chief of the Division of Anti-

(6) T. C. Daniels, *Ann. Rev. Biochem.*, **12**, 447 (1943).
(7) T. S. Work and E. Work, "The Basis of Chemotherapy", Interscience Publishers, Inc., New York, N. Y., 1948, p. 319.

biotics of this Institute, for helpful discussions, and is especially grateful to Dr. Osamu Tamemasa for a number of branched-chain fatty acids.

National Institute of Health, Tokyo

Physicochemical Properties of the Surface of Aqueous Solutions. III. Mechanical Behavior of Surface of Micellar and Macromolecular Solution*

By Tunetaka SASAKI and Hideo KIMIZUKA

(Received May 26, 1952)

Introduction

Recently the methods and concepts of modern rheology have been applied to the investigations on the mechanical properties of the surface of aqueous saponin solution.[1],[2] The present authors have also studied the surface viscosity of aqueous solutions foaming when shaken.[3] The surface viscometer thereby employed was, however, unfortunately unsuitable for the quantitative measurements of surface rigidity and surface viscosity coefficient. So the present authors have attempted further experiments to obtain more detailed results by means of a torsion ring method. The present paper describes the mechanical behaviour of the surfaces of solutions thus measured.

Experimental

The essential part of the apparatus used is shown in Fig. 1. In this figure, A is a platinum ring of 4 cm. in diameter suspended by a phosphorbronze torsion wire, B, of 0·04 mm. in diameter and 30 cm. in length, the torsion constant of which being 0.494 dyne/cm. A shallow glass vessel C of 6 cm. in diameter and 1.3 cm. in depth, contains a solution for measurement. D is a glass cylinder of 1 cm. in diameter and 1.3 cm. in height, and M is a small mirror for the measurement of an angle of deflexion of the platinum ring. C and D are placed concentrically with each other. The apparatus shown in Fig. 1 is set in a closed vessel to keep it free from occasional contamination.

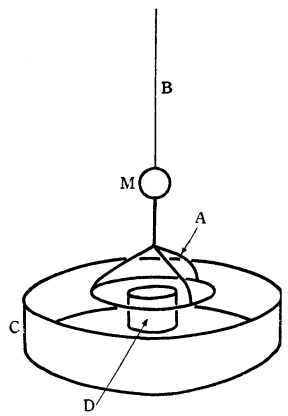

Fig. 1.

To carry out an experiment, the platinum ring is allowed to come in contact with the surface of the solution concentrically both to C and D. After the desired time of aging of the surface, the top of the torsion wire is rotated by a definite angle, and each successive position of the platinum ring expressed by an angle of rotation, θ, is measured with time by means of a lamp and scale method. As the surface film is distorted with the ring, θ is considered to be a strain of the surface.

In case of pure elastic deformation, the relation between a strain, θ, and a stress applied to the surface, $\kappa(\theta_0-\theta)$, κ being a torsion constant of the suspension wire and θ_0, a rotated angle initially given to the top of torsion wire, is expressed by the equation:

$$\theta=\frac{\kappa}{E}(\theta_0-\theta), \qquad (1)$$

where E is a constant proportional to the surface rigidity, G, as shown by the following relationship:

* This work was reported at the meeting for general discussion of colloid chemistry held in Kyoto, on Nov. 19, 1950, under the auspices of the Chemical Society of Japan.

(1) J. R. van Wazer, *J. Coll. Sci.*, **2**, 223 (1947).
(2) A. A. Trapeznikov, *Kolloid Zhur.*, **12**, 67 (1950).
(3) H. Kimizuka and T. Sasaki, This Bulletin, **24**, 230 (1951).

$$G=\frac{E}{4\pi}\frac{\left(\frac{1}{r_1^2}-\frac{1}{r_2^2}\right)\left(\frac{1}{r_2^2}-\frac{1}{r_3^2}\right)}{\left(\frac{1}{r_1^2}-\frac{1}{r_3^2}\right)}\equiv KE \qquad (2)$$

where r_1, r_2 and r_3 are the radii of the shallow glass vessel, wire ring and inner glass cylinder respectively. The value of K was 0.0315 cm.$^{-2}$ in the present case.

In the case of pure viscous flow, the rate of deformation is given by the equation;

$$\frac{d\theta}{dt}=\frac{\kappa}{R}(\theta_0-\theta), \qquad (3)$$

and the constant R is related with surface viscosity coefficient as shown by the following relationship,

$$\eta=KR. \qquad (4)$$

As will be described later, the surface of solutions investigated generally exhibited the mechanical behaviour in which the elastic and viscous deformations were superposed.

As we could not detect any perceptible amount of bulk viscosity, the viscoelasticity observed solely came from the surface itself, just as in the case of the preceding paper.[3] Of samples used, saponin was purified by electrodialysis[4] and crystal violet, by salting out.[5] The horse serum albumin was a highly purified specimen, kindly supplied by Mr. Ômura, of Takeda Pharm. Ind. Ltd. and purified polyvinyl alcohol in degree of polymerization of 1200, kindly supplied by Mr. Kai, of Dep. Applied Chem., Fac. Tech., Kyûsyû University, Both of these were used without further purification. The time of aging was kept to one hour throughout this experiment. The time scale was taken in a range from 60 to 300 sec. The experiments were carried out at room temperature, 17±2°C.

After each meaurement, $\theta\sim t$ curve and $d\theta/dt\sim\theta$ curve were drawn, the corresponding mechanical model was constructed and the related constants were calculated.

Viscous deformation.—The surface of 0.100 g./l. saponin solution exhibited pure viscous deformation. The result was shown in Fig. 2.

Maxwell model.—The surface of 0.002 g./l. polyvinyl alcohol solution behaved according to Maxwell model. The equation of motion, except for $t=0$, is

$$\frac{d\theta}{dt}=\frac{E\kappa}{R(E+\kappa)}(\theta_0-\theta). \qquad (5)$$

The value of E and therefore G can be calculated according to equations (1) and (2) from the measurement of instantaneous elastic deformation. Then the value of R and therefore η can be calculated from the observed data using equations (4) and (5). The result was shown in Fig. 3.

Non-Newtonian flow.—The surface of 10^{-3}mole/l. crystal violet solution exhibited this behaviour. In this case, the empirical relationship between the rate of deformation and the strain could be expressed by the equation;

$$\log\frac{d\theta}{dt}=A-B\theta, \qquad (6)$$

where A and B are constants. The result was shown in Fig. 4.

Maxwell model with non-Newtonian flow.—The surface of 0.500 g./l. horse serum albumin solution exhibited this behaviour. The empirical equation, except for $t=0$, was similar to the equation (6). The result was shown in Fig. 5.

Voigt model.—The surface of 0.250 g./l. saponin solution exhibited this behaviour the result was shown in Fig. 6. The equation of motion is

$$\frac{d\theta}{dt}=-\frac{E+\kappa}{R}\theta+\frac{\kappa}{R}\theta_0. \qquad (7)$$

E can be calculated by the equation;

$$E=\frac{\kappa(\theta_0-\theta_r)}{\theta_r} \qquad (8)$$

in which θ_r is θ when $d\theta/dt=0$. R and η can be calculated according to the equations (4) and (7).

Three parameter model.—The surface of 0.100 g./l. polyvinyl alcohol solution exhibited this behaviour. The result was shown in Fig. 7. The equation of motion, except $t=0$, is

$$\frac{d\theta}{dt}=-\frac{EE'+\kappa(E+E)}{R(E'+\kappa)}\theta+\frac{\kappa(E+E')}{R(E'+\kappa)}\theta_0. \qquad (9)$$

The term of retarded elasticity, E, can be calculated by the equation

$$E=\frac{E'E^*}{(E'-E^*)}. \qquad (10)$$

where E' is instantaneous elasticity and E^* is given by the relationship;

$$E^*=\frac{\kappa(\theta_0-\theta_r)}{\theta_r} \qquad (11)$$

in which θ_r is the value of θ when $d\theta/dt=0$. R can be calculated according to the equation (9).

Discussion

In the deformation of viscous flow and the Maxwell model, θ increases with time, finally reaching θ_0, an angle initially given to the top of torsion wire, and this behaviour permits no

(4) G. Klein, "Handbuch der Pflanzen Analyse" 1932, III, 1109.

(5) C. Robinson and H. A. T. Mills, *Proc. Roy. Soc., A* **131**, 576 (1931).

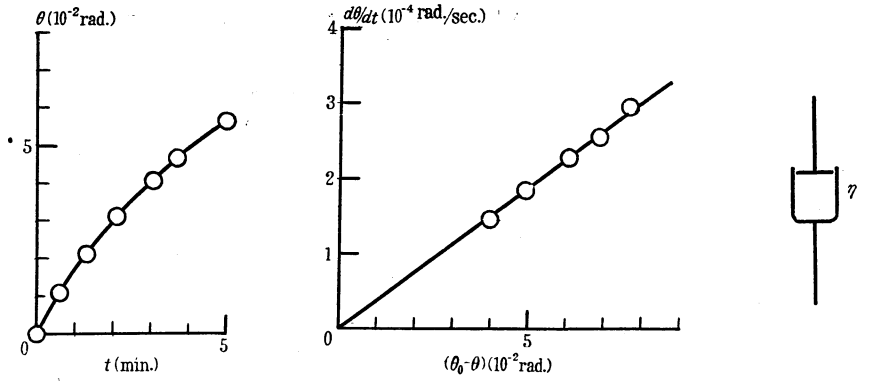

(a) $\theta \sim t$ curve
$\theta_0 = 0.0872$ rad.

(b) $d\theta/dt \sim (\theta_0 - \theta)$ curve

(c) Model
$\eta = 3.89$ g./sec.

Fig. 2.—Saponin solution (0.100 g./l.).

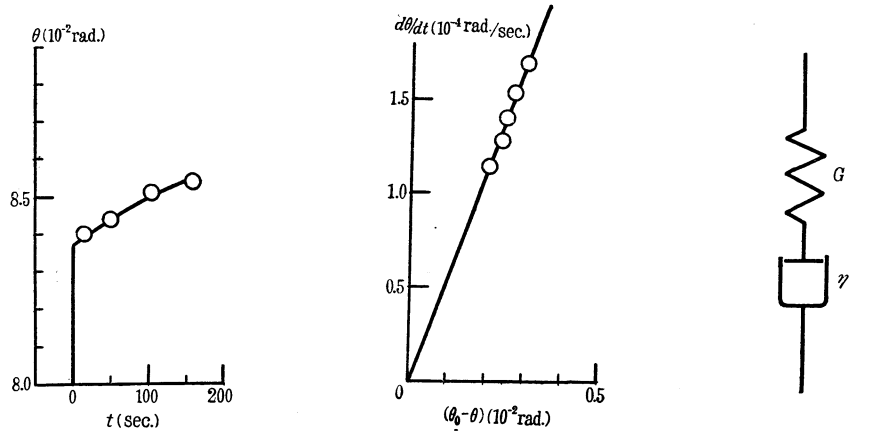

(a) $\theta \sim t$ curve
$\theta_0 = 0.0872$ rad.

(b) $d\theta/dt \sim (\theta_0 - \theta)$ curve

(c) Model
$G = 7.34 \times 10^{-4}$ dyne/cm.
$\eta = 1.15 \times 10^{-2}$ g./sec.

Fig. 3.—Polyvinyl alcohol solution (0.002 g./l.).

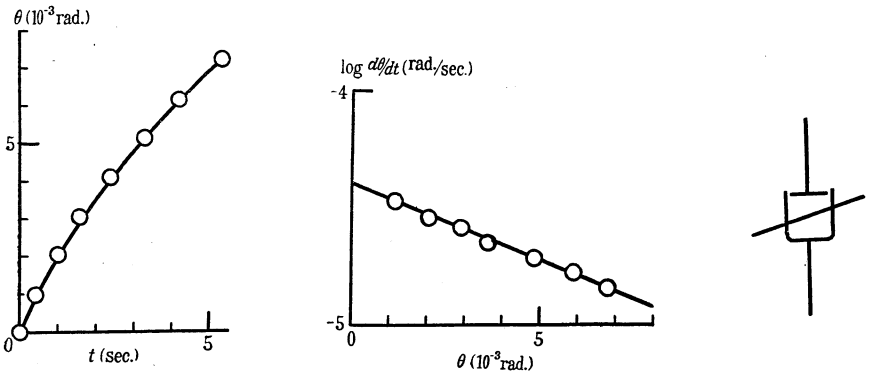

(a) $\theta \sim t$ curve
$\theta_0 = 0.0872$ rad.

(b) $\log \dfrac{d\theta}{dt} \sim \theta$ curve

(c) Model

Fig. 4.—Crystal violet solution (10^{-3} mole./l.).

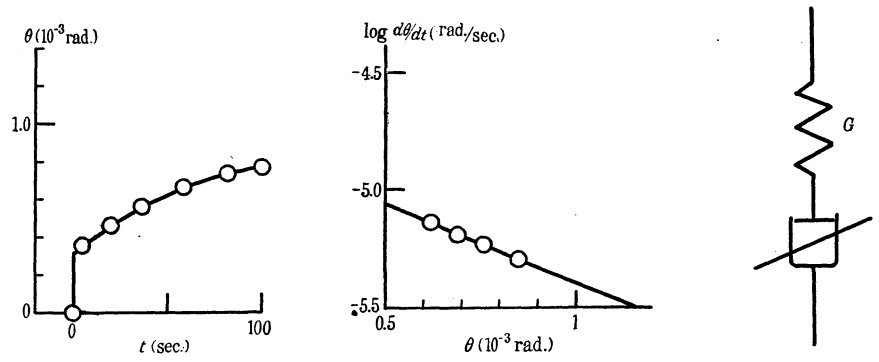

(a) $\theta \sim t$ curve
$\theta_0 = 0.872$ rad.

(b) $\log \frac{d\theta}{dt} \sim \theta$ curve

(c) Model
$G = 4.32$ dyne/cm.

Fig. 5.—Horse serum albumin solution (0.500 g./l.).

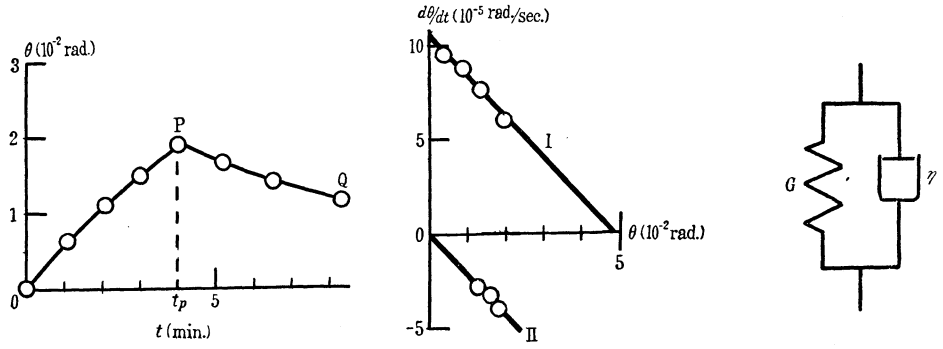

(a) $\theta \sim t$ curve
$\theta_0 = 0.0872$ rad.

(b) $d\theta/dt \sim \theta$ curve
Lines I and II correspond to OP and QP in (a) respectively.

(c) Model
$G = 1.27 \times 10^{-2}$ dyne/cm.
$\eta = 13.3$ g./sec.

Fig. 6.—Saponin solution (0.250 g./l.).

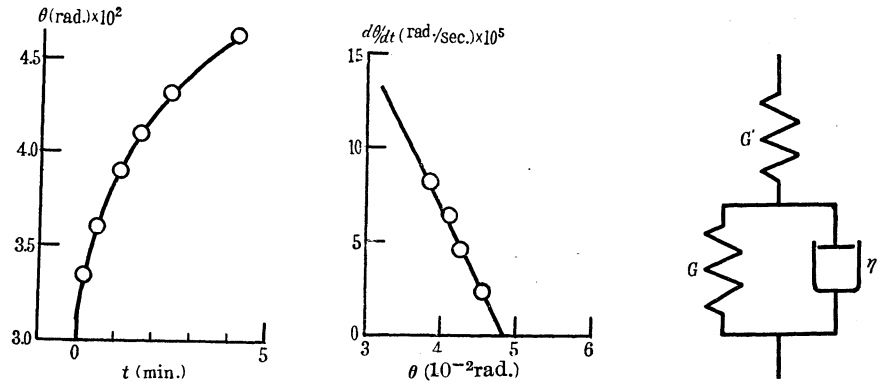

(a) $\theta \sim t$ curve
$\theta_0 = 0.174$ rad.

(b) $d\theta/dt \sim \theta$ curve

(c) Model
$G' = 6.90 \times 10^{-2}$ dyne/cm.
$G = 9.30 \times 10^{-2}$ dyne/cm.
$\eta = 53.2$ g./sec.

Fig. 7.—Polyvinyl alcohol solution (0.100 g./l.).

other interpretation than these mechanical models. On the other hand, the Voigt and three parameter model may be replaced by somewhat different interpretation under the conditions of the present experiment, viz., the Voigt model may possibly be replaced by purely plastic flow and the three parameter model, by the Maxwell model with yield point. In this connection, Fig. 6 might offer the means for the correct interpretation of the mechanical behaviour. In Fig. 6a, the change in effective torque from $\kappa(\theta_0-\theta)$ to $-\kappa\theta$ at time t_p caused the deformation of the film to reduce from θ to zero as shown by the portion PQ. The corresponding $d\theta/dt\sim\theta$ curve was shown as II in Fig. 6b. If the behaviour can be described according to the Voigt model, the following equation must hold

$$\frac{d\theta}{dt}=-\frac{(E+\kappa)\theta}{R}. \qquad (12)$$

In the case of plastic flow, the residual deformation should remain after the torque was changed to-$\kappa\theta$. The result showed an absence of yield value in the surface and the correctness of the Voigt model in this case. For the three parameter model, the similar result can be obtained.

The non-Newtonian flow observed may be interpreted to be either of Eyring's non-Newtonian flow or quasi-viscous flow, which cannot be decided clearly at least in the present experiment.

In the present experiment, the value of θ could be measured down to 10^{-4} radian and the angle of torsion, θ_0, initially given to the top of torsion wire was ranged between 0.1 and 1 radian, so that the rigidity could be measured in the region from 1.5×10^{-5} to 150 dynes/cm., according to equations (1) and (2). The lower limit of viscosity measurement proved to be 1.5×10^{-3} g./sec. by a similar calculation. As was mentioned above, the measurement of low rigidity and viscosity requires a suspension wire of low torsion constant. Since the surface of solution may be of a low yield value if any,[1] it is advisable to use the suspension wire of torsion constant as low as possible for the measurements of mechanical properties of surface without disturbing an adsorbed layer.

It should be noticed that the above viscoelastic constants were obtained referring to the time scale of the present experiment, while the complete description of the mechanical behaviour requires the information of a complete viscoelastic spectrum of the material.[6] For the mechanical model of the surface of saponin solution, Wazer[1] presented the Voigt model, while Trapeznikov,[2] the four parameter model consisting of a series combination of a spring, a Voigt model and a dashpot. Difference between these results is probably due to the difference in the experimental conditions.

Summary

1. A torsion ring method using a suspension wire of low torsion constant was employed for the measurement of a surface viscosity and rigidity of aqueous solutions.

2. The mechanical behaviours of the surfaces of the solutions of saponin, polyvinyl alcohol, crystal violet and horse serum albumin aged for one hour were analysed and expressed using mechanical models. The corresponding rigidity and viscosity were estimated.

3. The mechanical models observed were the Newtonian flow, non-Newtonian flow, Maxwell model with Newtonian or non-Newtonian flow, Voigt model, and three parameter model consisting of a series combination of a spring and a Voigt element.

The authors wish to express their thanks to Dr. T. Nakagawa of the univ, of Tokyo, for the discussion of the results. The cost of this research was defrayed from the Scientific Research Expenditure of the Department of Education given to one of the authors.

Department of Chemistry, Faculty of Science, Kyûsyû University, Fukuoka.

(6) T. Alfrey, Jr., "Mechanical Behavior of High Polymers," Interscience Publishers, Inc., New York, 1948, pp 116-173.

Seasonal Variations of Minor Chemical Constituents in the Waters of the Zunan-Kuroshio Region. I.* On Nitrogen-phosphorus Content Ratio with the Behaviors of Nitrate and Phosphate

By Rinnosuke FUKAI

(Received March 20, 1952)

Introduction

Whereas a large number of observations have been made on nutrient salts in sea water in various periods as well as in various localities of Europe and America, observations made in the western Pacific near Japan have been restricted to coastal waters and such observations were seldom carried out during and after the war.

Determinations of nutrient salts in sea water have been made by the present author on the waters of the Zunan-Kuroshio region, where the Kuroshio, a warm current, is passing over the Izu submarine ridge, in connection with studies on other hydrographical conditions and fisheries resources.

In the present paper, data concerning nitrate and phosphate determinations which were made by the present author are selected from those concerning the observations which had been made from January 1950 to February 1951, by the author and other workers, and their seasonal variations are investigated with reference to N-P ratio.

The relationship between the contents of nitrate-nitrogen and those of phosphate-phosphorus in the sea water, was first suggested by Harvey(1) in 1928. Later, it was discussed by Redfield,(2) Cooper,(3) Fleming(4) and other workers. Of the normal ratio of nitrate-N/phosphate-P, the value, 6.8 (by weight), which was proposed by Cooper is widely accepted.

The purpose of this study is as follows: to answer the question whether the normal ratio of N/P can be accepted for the waters of the Zunan-Kuroshio region, and if any deviation from the normal ratio is found, whether it has a connection with other conditions.

Analytical Methods Adopted

For nitrate: Colorimetric determination with Harvey's reduced strychnine reagent.(5)

For phosphate: Denigès-Atkins' method.(6) Colorimetric determination with blue color resulting from the reaction with complex phosphomolybdic acid and the following reduction by stannous chloride solution.

Stations Under Consideration

Two stations were chosen on a line between Sunosaki and Hachijō as follows: Station 3, on the shelf slope about 20 miles south of Sunosaki (Lat. 34°40'N, Long. 139°45'E); Station 6, in the main current of the Kuroshio (Lat. 33°50'N, Long. 139°45'E). (Fig. 1)

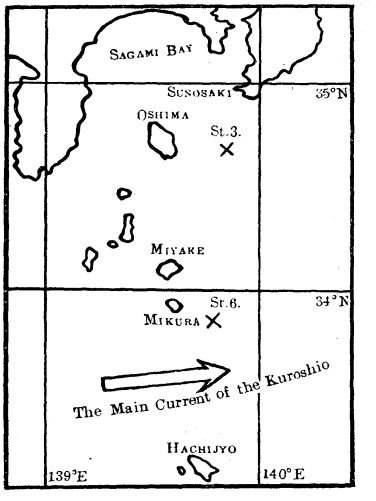

Fig. 1.—Stations under consideration.

Results and Discussion

Attention is called to the fact that in the sea region under examination, the spacial position of the Kuroshio itself may be altered

* Contribution B. No. 64 from Tokai Regional Fisheries Research Laboratory, Tokyo, Japan.

(1) H. W. Harvey, "Biological chemistry and physics of sea water", Cambridge University press, 1928, p. 48.

(2) A. C. Redfield, "James Johnstone Mem. Vol.", 1934, p. 176.

(3) L. H. N. Cooper, *J. Mar. Biol. Assoc.*, **22**, 177 (1938).

(4) R. H. Fleming, "Proc. Sixth Pacific Sci. Congress", Vol. **3** (1939).

(5) H. Wattenberg, *Rapp. et Proc.-Verb. des Reunions*, **103**, 1 (1937).

(6) R. J. Robinson, *J. Mar. Res.*, **7**, 33 (1948).

in course of time. If so, variations in contents of chemical substances which appear in such spacially fixed stations do not always represent those that relate to seasonal changes. From hydrographical data, however, it can be assumed on the whole that a stationary state has been reached in so far as the current is considered.

Considering the data, water columns are assumed, and the columns are divided into several parts in which the integral mean concentrations of chemical substances are calculated (in order to avoid fluctuation of individual datum). Based upon these values, the values of N/P are calculated in each part of the water columns for each month. The vertical distributions of these ratios for each month are shown in Fig. 2 (at Station 3) and Fig. 3 (at Station 6).

In these figures, vertical broken lines represent the normal value of N/P, proposed by Cooper. If the values of N/P in sea water remained constant and had the normal one, the points plotted in the figures should lie on the lines. The results obtained are not in good agreement. But this does not always give the conclusion that the actual values of N/P deviate from the normal one, since considerable errors accompany the estimation of chemical substances in sea water.

In order to obtain reliable ranges for the calculated values of N/P, probable maximum and minimum values of N/P were computed of each value, introducing the numerical values of probable maximum error given in Table 1

Table 1

Probable Maximum Errors in Determination

found Nitrate-N (μg./l.)	Error (μg./l.)	found Phosphate-P (μg./l.)	Error (μg./l.)
< 25	± 5	< 20	± 2
25– 50	± 10	20–50	± 3
50–100	± 15	> 50	± 5
100–300	± 20		
>300	± 30		

in the computation. These probable ranges are shown by two dotted curves for each month in the figures. Then, it can be considered that the deviations from the normal ratio take place only when the normal lines do not lie between two dotted curves.

In Fig. 2, from these points of view, nitrate content below subsurface layers was relatively higher than phosphate content in January and February 1950, while in March and April 1950 and February 1951, phosphate content was predominant. Although these variations in vertical distribution of N/P might suggest some character of a phenomenon occurring in this sea region, any conclusion may not be given until further observations will be accumlated.

In Fig. 3, the distribution of N/P for each month are regular except those in May and July, 1950. In upper layers (0-200 m.) the ratios are much lower than the normal ratio. On the contrary, in deep layers (400-800 m.)

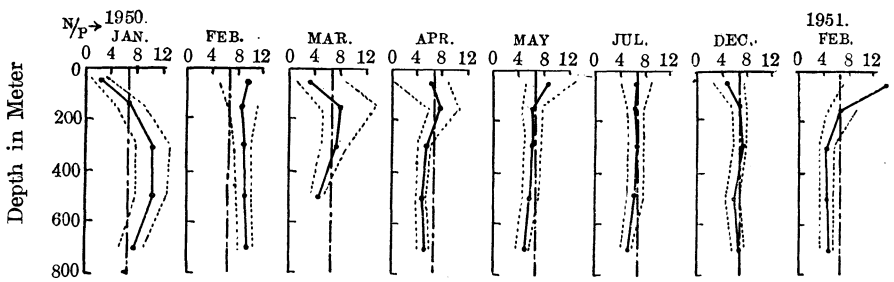

Fig. 2.—Vertical distribution of N-P ratios for each month (at Station 3).

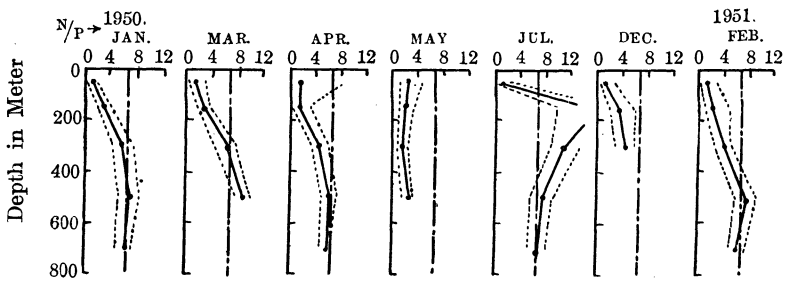

Fig. 3.—Vertical distribution of N-P ratios for each month (at Station 6).

the ratios are nearly equal to the normal ratio.

The average values of N/P in these regular cases are 1.4 and 6.9 for upper layers and deep layers, respectively. The rejection limits are 0-2.8 for upper layers and 4.7-9.1 for deep layers (level of significance: 0.05). These values indicate the possibility of difference of water masses that are present in upper and lower layers.

It is a remarkable fact that the values of N/P in May and July 1950, deviated considerably not only from the normal ratio but also they deviated in opposite directions from each other.

In order to examine the processes of deviation from the normal ratio systematically, the rates of change in nitrate, $\delta[N]/\delta t$, and phosphate, $\delta[P]/\delta t$, were computed. Further, on the base of $\delta[N]/\delta t$, theoretical rates of change of phosphate, $\delta[P']/\delta t$, were also computed. These computations were based upon the assumption that phosphate was accompanied in the ratio of 6.8 by nitrate.

The values of $\delta[P]/\delta t - \delta[P']/\delta t$ are given in Table 2. Due to the experimental errors introduced in the computations, it is impossible

Table 2

Values of $\delta[P]/\delta t - \delta[P']/\delta t$ in Each Layer for Each Period (unit: μg./l./month)

Depth(m.)	0 100	100 200	200 400	400 600	600 800
	at Station 3				
'50 JAN. -FEB.	−10	−4	+ 1	− 2	−16
FEB. -MAR.	+ 4	+2	+ 6	+29*	
MAR.-APR.	− 3	+1	+14	+ 4	
APR. -MAY	− 2	+5	− 7	−13	+ 6
MAY-JUL.	+ 1	0	0	− 2	+ 3
'50 DEC. -'51 FEB.	− 3	0	+ 5	+ 3	+11*
	at Station 6				
'50 JAN. -MAR.	− 2	−1	0	− 4	
MAR.-APR.	− 5	−4	+ 3	− 2	
APR. -MAY	+ 2	+3	+17*	+36*	
MAY-JUL.	− 1	−6*	−14*	−20*	
'50 DEC. -'51 FEB.	0	−1	− 1		

to deduce the correlation between nitrate and phosphate from most of the values. But from the values which were marked by *, it can be concluded that net increase or decrease of phosphate has occurred.

As above mentioned, it is evident that the deviations from Cooper's normal ratio have occurred in this sea region.

As the causes of deviation, the following may be assumed:

1. The effect of coastal water masses in which the ratio of N/P is different from the normal ratio.

2. Increase in amount of planktons, of which the N/P ratios are widely different from the normal ratio.

3. Difference in rates with which nitrate and phosphate are regenerated in decomposition processes of dead marine organisms.

It is difficult to decide among these three causes, which one is the most probable for the elucidation. But in view of the peculiar features of the sea region under question, (1) should be discarded. (2) is the most improbable one. Consequently, (3) is the most probable. But plankton populations in the upper layers of the Kuroshio in the region under question correspond to phosphorus content equivalent to 0.5-2 μg./l., and it can not give a decisive explanation for the deviation of N/P in the intermediate layers. Abundant plankton populations, such as found in the Oyashio, which is a cold current originating in the northern part of the North Pacific and penetrating under the Kuroshio, must be taken into consideration as the cause of deviation in N/P.

Summary

Data of nitrate and phosphate detrminations have been selected from those of the Zunan-Kuroshio observations which were made from January, 1950 to February, 1951, and their seasonal variations were investigated with reference to N/P ratio.

As a result, it was proved that no change was recognised in deep layers (400-800 m.) at Station 6 (in the main current of the Kuroshio) throughout the period, but deviations from Cooper's normal ratio were found in surface and subsurface layers. The cause of these deviations may partly be due to the decomposition processes of dead marine organisms.

The author is sincerely indebted to Prof. K. Kimura, Dr. Garbin, Dr. M. Migita and Dr. T. Abe for their kindness in giving him critical discussions of this subject-matter.

Tokai Regional Fisheries Research Laboratory, Tokyo, Japan.

Adiabatic Compressibility of Aqueous Solution. I. Dicarboxylic and Oxycarboxylic Acid*

By Yutaka MIYAHARA

(Received May 5, 1952)

In a series of investigations, carried out in this laboratory[1][2] and elsewhere,[3][4][5][6] concerning the ultrasonic velocity measurement of aqueous solution, it has been shown that the adiabatic compressibility of solution is intimately related to the hydration of solute. The present study concerns the results obtained with dicarboxylic and oxycarboxylic acid solution.

Experimental

The ultrasonic velocity was measured by an ultrasonic interferometer. The wiring diagram is shown in Fig. 1. The frequency of ultrasonics

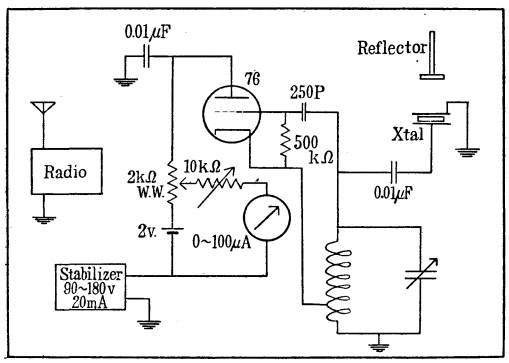

Fig. 1.

was 1090 KC. The constant frequency applied during each measurement was obtained by adjusting it to the same frequency of commercial radio (JOAR) by heterodyne method. The diameter and resonance frequency of X-cut crystal used were 20 mm. and 1270 KC respectively. The precision of each measurement of sound velocity was ±0.02 percent.

The materials used were recrystalized from G. P. or E. P. grade chemicals in trade.

Results and Discussion

As has been well known, adiabatic compressibility is related to sound velocity in the following formula;

$$\kappa = \frac{1}{Dc^2} \tag{1}$$

where D and c are density and velocity of sound respectively. And as reported in the previous paper (see appendix), we have the following relations between compressibility and hydration;

$$K \equiv V_0 - \frac{\kappa}{\kappa_0} = v_h\left(\frac{D_h}{D_0} - \frac{\kappa_h}{\kappa_0}\right) \tag{2}$$

$$V_0 = \frac{D_s - x}{D_0} \tag{3}$$

where we set up the following notations;

κ ····adiabatic compressibility of solution,
κ_h ····adiabatic compressibility of hydrated water,
κ_0 ····adiabatic comresssibility of water,
v_h ····volume of hydrated water in 1 cc. of solution,
D_h ····density of hydrated water,
D_0 ····density of water,
D_s ····density of solution,
x ····concentration of solute in gram per 1 cc. solution.

For a mole of solute, we have

$$K_m = \frac{KM}{x} = v_h'\left(\frac{D_h}{D_0} - \frac{\kappa_h}{\kappa_0}\right) \tag{4}$$

where M is molecular weight, v_h' the volume of hydrated water per mole of solute.

The obtained values of c/c_0 (where c_0 is sound velocity in water), κ/κ_0, V_0 and K at 20°C. are given in Table 1~8.

* Presented at the Fifth Annual Meeting of Chemical Society of Japan held at Tokyo on April 6, 1952.

(1) Y. Miyahara and H. Shiio, *J. Chem. Soc. Japan*, **72** 876 (1951).
(2) Y. Miyahara and H. Shiio, *J. Chem. Soc. Japan*, **73** 1 (1952).
(3) Y. Wada, G. Shinpo, M. Oda and J. Nagumo, Oyo butsuri (*J. Applied Phys. Japan*), **17** 257 (1948).
(4) T. Yasunaga and T. Sasaki, *J. Chem. Soc. Japan*, **72**, 87 (1951).
(5) T. Yasunaga and T. Sasaki, *J. Chem. Soc, Japan*, **72**, 366 (1951).
(6) T. Sasaki, T. Yasunaga and H. Fujiwara, *J. Chem. Soc. Japan*, **73**, 181 (1952).

Table 1
Malonic Acid

No.	x g./cc.	c/c_0	κ/κ_0	V_0	K
1	0.0351	1.0047	0.9782	0.9776	−0.0006
2	0.0462	1.0062	0.9715	0.9705	−0.0010

Table 2
Succinc Acid

No.	x g./cc.	c/c_0	κ/κ_0	V_0	K
1	0.0274	1.0050	0.9822	0.9806	−0.0016
2	0.0384	1.0066	0.9756	0.9732	−0.0024
3	0.0302	1.0054	0.9803	0.9790	−0.0013

Table 3
Glutaric Acid

No.	x g./cc.	c/c_0	κ/κ_0	V_0	K
1	0.0347	1.0076	0.9766	0.9739	−0.0027
2	0.0254	1.0053	0.9834	0.9809	−0.0025

Table 4
Oxalic Acid

No.	x g./cc.	c/c_0	κ/κ_0	V_0	K
1	0.0392	1.0030	0.9761	0.9793	0.0032
2	0.0260	1.0020	0.9838	0.9864	0.0026
3	0.0361	1.0028	0.9780	0.9806	0.0026
4	0.0265	1.0021	0.9832	0.9863	0.0031
5	0.0288	1.0022	0.9822	0.9849	0.0027

Table 5
Tartaric Acid

No.	x g./cc.	c/c_0	κ/κ_0	V_0	K
1	0.0481	1.0095	0.9608	0.9732	0.0124
2	0.0290	1.0053	0.9770	0.9838	0.0068
3	0.0286	1.0054	0.9772	0.9838	0.0066
4	0.0397	1.0076	0.9682	0.9777	0.0095

Table 6
Citric Acid

No.	x g./cc.	c/c_0	κ/κ_0	V_0	K
1	0.0336	1.0053	0.9764	0.9798	0.0034
2	0.0475	1.0079	0.9657	0.9719	0.0062
3	0.0308	1.0048	0.9784	0.9816	0.0032
4	0.0357	1.0057	0.9749	0.9785	0.0036

Table 7
Malic Acid

No.	x g./cc.	c/c_0	κ/κ_0	V_0	K
1	0.0081	1.0014	0.9942	0.9949	0.0007
2	0.0336	1.0058	0.9763	0.9789	0.0026
3	0.0264	1.0045	0.9815	0.9834	0.0019

Table 8
Maleic Anhydride

No.	x g./cc.	c/c_0	κ/κ_0	V_0	K
1	0.0397	1.0054	0.9763	0.9736	−0.0027
2	0.0420	1.0056	0.9752	0.9721	−0.0031
3	0.0488	1.0069	0.9704	0.9677	−0.0027

When a molecule has several radicals which interact with surrounding water molecules, K_m may be represented by the sum of each component of individual radical;

$$K_m=\sum_r K_{m,r} \qquad (5)$$

To testify this we would chose the values of $K_{m,r}$ for each radical rather arbitrarily as are shown in Table 9. In Table 10, the calculated values of K_m using these $K_{m,r}$ values are given. The coincidence between the experimental and calculated values are fairly good except in the case of citric acid.

Table 9

Radical	$K_{m,r}$
−OH	9.5
$-CH_2-$	−7.5
−COOH	4.0

Table 10

Acid	OH	CH_2	COOH	K_m cal.	K_m obs.
Malonic	0	1	2	0.5	−2.0
Succinic	0	2	2	−7.0	−6.6
Glutaric	0	3	2	−14.5	−11.2
Oxalic	0	0	2	8.0	8.0
Malic	1	1	2	10.0	10.1
Tartaric	2	0	2	27.0	37
Citric	1	2	3	6.5	21
Maleic anh.	—	—	—	—	−6.3
Glucose	5	1	0	>40.0	44[1]

It is interesting that the value of $K_{m,r}$ of methylene radical is shown as negative. It means rather formally from (4) that;

$$\frac{D_h}{D_0}<\frac{\kappa_h}{\kappa_0} \qquad \text{for } -CH_2- \qquad (6)$$

However, it is not intended here to discuss the physical meaning of each term in (4) quantitatively. To state qualitatively, it is certain that the negativity of $K_{m,r}$ may be attributed to the hydrophobic nature of methylene radical.

Appendix

Compressibility of diluted aqueous solution.[1][3]

The volume of solution V, containing x_g solute, may be represented by the sum of volume of solute in the solution v_m, of hydrated water v_h and of non-affected water V_0';

$$V=V_0'+v_m+v_h \qquad (1a)$$

If we assume that compressibility of such

solution is represented by the sum of that of each component in their volume ratio, we have;

$$\kappa = \frac{V_0'}{V}\kappa_0 + \frac{v_m}{V}\kappa_m + \frac{v_h}{V}\kappa_h \qquad (2a)$$

where κ_m is compressibility of solute molecule.

For one cc. of solution (2a) becomes

$$\frac{\kappa}{\kappa_0} = V_0' + v_m\frac{\kappa_m}{\kappa_0} + v_h\frac{\kappa_h}{\kappa_0} \qquad (3a)$$

and

$$V_0' = 1 - v_m - v_h \qquad (4a)$$

In terms of density, (4a) takes the form

$$D_0V_0' = D_s - D_mv_m - D_hv_h \qquad (5a)$$

and as

$$v_mD_m = x \qquad (6a)$$

(3a) becomes

$$\frac{D_s - x}{D_0} - \frac{\kappa}{\kappa_0} = v_h\left(\frac{D_h}{D_0} - \frac{\kappa_h}{\kappa_0}\right) - v_m\frac{\kappa_m}{\kappa_0} \qquad (7a)$$

For a molecular solution, the compressibility of the molecule can be assumed to be zero, and we obtain (2).

Chemical Institute, Faculty of Science, Nagoya University, Nagoya

The Crystal Structure of "Dichrochloride", $[Co(NH_3)_3H_2OCl_2]Cl$

By Yoshimichi TANITO, Yoshihiko SAITO and Hisao KUROYA

(Received May 20, 1952)

Introduction

Crystals of dichloro-aquo-triammine-cobalt (III) chloride ("dichrochloride"), $[Co(NH_3)_3H_2OCl_2]Cl$, is well-known for its marked red-blue dichroism. According to Matsuno[1] this modification of $[Co(NH_3)_3H_2OCl_2]Cl$ has trans-configuration with respect to the two chlorine atoms. Stelling[2] has examined the fine structure of K-absorption edge of Cl atoms in this substance and has come to the same conclusion about its configuration.

We have taken up the crystal structure investigation of this complex salt in order to give direct proof of the configuration of the complex ion and also to correlate its structure with its anisotropy in absorption of plane polarized light by crystals.

The Unit Cell and Space Group

The material used in this investigation was prepared according to the method of Meyer, Dirska and Clemens.[3] The crystals for X-ray work have been grown at room temperatures from concentrated solution by adding an equal volume of 6 N hydrochloric acid very slowly through a funnel fitted with a capillary tube. These crystals belong to the hexagonal holohedral class and are usually thin needles, showing faces $(10\bar{1}0)$ and $(10\bar{1}1)$, or rarely tabular in habit with (0001) extended. A crystal rod of less than 0.3 mm. in diameter and another one with no dimension larger than 0.3 mm. were selected for taking oscillation photographs around c- and a-axes. A complete set of oscillation photographs were prepared using Fe K_α radiation ($\lambda = 1.937$ A.), which gave the dimensions:

$$a = 7.37 \text{ A. and } c = 8.75 \text{ A.}^*$$

From the size of the unit cell and the density 1.908 g./cm.^{3},[4] the number of formula units in the unit cell was calculated to be two, the calculated density being 1.891 g./cm.^{3} Oscillation photographs taken about the c-axis with the $[10\bar{1}0]$ as well as $[11\bar{2}0]$ axis at the zero position of oscillation indicated the presence of mirror planes parallel and perpendicular to the c-axis, hence the Laue symmetry was found to be D_{6h}-$6/mmm$. General reflections $(hkil)$ occur in all orders. Reflections $(hh\bar{2}hl)$ are present only with l=even. The space group is therefore one of D^1_{6h}-$C6/mmc$,

(1) K. Matsuno, *J. Coll. Sci. Imp. Univ. Tokyo* **41**, *Art.* 10, 4, (1921).
(2) O. Stelling, *Ber.* **60**, 652(1927); Z. Phys **50**, 520(1928).
(3) J. Meyer, G. Dirska und F. Clemens, *Z. anorg. Ch.* **139**, 357 (1924). S. M. Jörgensen, *Z. anorg. Ch.* **14**, 418 (1897).

* Even very heavy exposure (50 hrs.) indicated no evidence for larger unit cell size.
(4) E. Birk, *Z. anorg. Ch.*, **158**, 114 (1926).

C_{6v}^4-$6/mc$ or D_{3h}^4-$C\bar{6}2c$.

The Atomic Arrangement

The intensities were estimated visually using the timeexposure calibrated strip, taking into account the shape of specimens in relation to absorption. Structure factors were deduced from these intensity data in the usual way, which are shown in Table 1.

At first an attempt has been made to assign approximate co-ordinates for heavy atoms. In the space group D_{6h}^4, C_{6v}^4 and D_{3h}^1 the general positions are 24 fold, 12 fold and 12 fold respectively. Since there are two formula units, $[Co(NH_3)_3H_2OCl_2]Cl$, in the unit cell, 2Co, 4Cl(1) and 2Cl(2) may either occupy sets of two fold special positions, or alternatively Cl(1) may occupy one set of four fold positions. The intensity of reflection (0004) is the strongest by far compared with the rest, which suggests all the atoms might be nearly in phase for this reflection. In general the reflections (*hkil*) are strong when $h-k=3n$ and $l=2n$. These characteristics for reflections combined with the results of trial calculations of structure amplitudes (*hkil*) at once lead to the following arrangement of heavy atoms based on the space group D_{6h}^4-$C6/mmc$:

2Co in 2(*c*) 1/3 2/3 1/4; etc.

2Cl(2) in 2(*a*) 000; etc.

and 4Cl(1) in 4(*f*) 1/3 2/3 z; etc. with $z\approx 0$.

It is almost evident that the signs of the structure factors for a complete unit would be determined mainly by these atoms. In order to determine the z-parameters of Cl more accurately, the three dimensional Fourier synthesis of the electron density along a line (1/3 2/3 z) was evaluated using all the F(*hkil*)'s, whose signs were known from the arrangement of the heavy atoms. As shown in Fig. 1, this lead us to fix the z-parameter at -0.016.

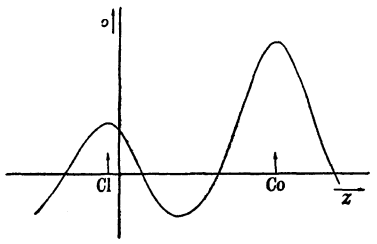

Fig. 1.—$\rho(1/3\ 2/3\ z)$.

It seems reasonable that in this crystal there are complex ions with octahedral co-ordination, —that is, three molecules of ammonia and one water molecule are in the plane of Co atom forming a distorted octahedron together with two Cl (1) atoms up and down the plane, where Co-N and Co-O distances are supposed to be between 1.90~2.00 A. In the space group D_{6h}^4 and its subgroups the proper symmetry of the special position (1/3 2/3 1/4) is ditrigonal or trigonal. Such symmetries cannot be achieved by any regular static arrangement of the complex ions so oriented as the positions of Co and Cl(1) atoms demand. Then we are entitled to assume some kind of statistical arrangement of these octahedral complex ions. The observed intensities are satisfactorily accounted for by means of the space group D_{6h}^4-$C6/mmc$, if the atomic arrangement of N and O atoms are assumed as follows:

6N and 2O in 12 (*j*) $xy\frac{1}{4}$ etc. with

$x_1=0.038$, $y_1=0.451$ and $x_2=0.117$, $y_2=0.372$.

N and O atoms are statistically distributed on these twenty four positions with weights 1/4 and 1/12 respectively.

These parameters were chosen in such a way that the Co-N and Co-O distances become 1.96A. It was not thought worth while to determine these parameter values very accurately as they scatter very poorly compared with other heavy atoms. The electron distribution in the plane of a cobalt atom, $\rho(xy\frac{1}{4})$ was synthesized using all the observed F-values whose sign was calculated from the positions of all the atoms in the unit cell. The result is shown in Fig. 2. The central

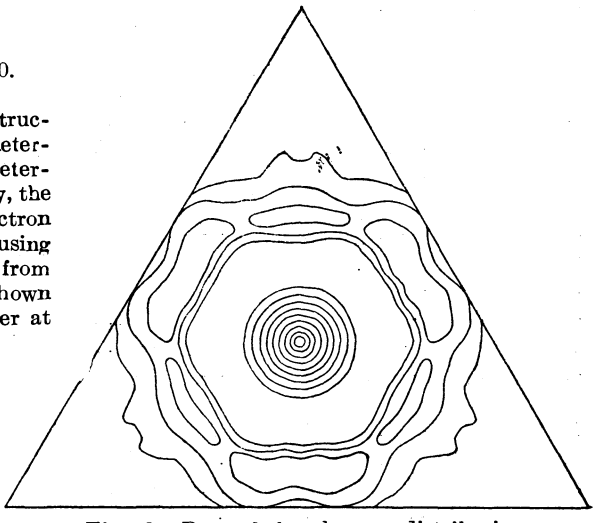

Fig. 2.—Part of the electron distribution, $\rho(xy\frac{1}{4})$. Contours at arbitrary intervals.

peak represents a cobalt atom and the only other regions of high electron density lie about the cobalt peak at distances of about 2 A. and are separated by an almost circular minimum. The maxima making up the region surrounding cobalt are twelve in number, though not fully resolved, and are quite a satiafactory representation of statistical orientation of octahedral complex ion with its Cl-Co-Cl axis normal to the plane of section, as shown in Fig. 3. This result is quite consistent with the previous assumption of Co···NH_3 and Co···H_2O distances.

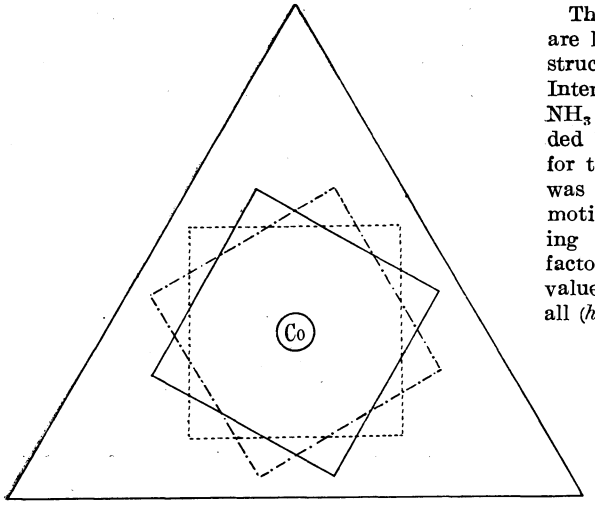

Fig. 3.—Statistical azimuthal orientations of the complex ion. The figure corresponds to Fig. 2.

Table 1
Observed and Calculated F-values

hkil	$F_{obs.}$	$F_{calc.}$	*hkil*	$F_{obs.}$	$F_{calc.}$
$10\bar{1}0$	31	−31.2	$30\bar{3}2$	13	12.8
$20\bar{2}0$	10	−6.7	$40\bar{4}2$	15	13.3
$30\bar{3}0$	101	95.0	$50\bar{5}2$	—	6.8
$40\bar{4}0$	18	−14.0	$11\bar{2}2$	54	50.6
$50\bar{5}0$	9	−6.5	$21\bar{3}2$	14	15.7
$60\bar{6}0$	28	36.9	$31\bar{4}2$	15	17.2
$11\bar{2}0$	112	98.0	$41\bar{5}2$	14	17.2
$21\bar{3}0$	16	−18.0	$51\bar{6}2$	—	8.1
$31\bar{4}0$	19	−18.1	$22\bar{4}2$	9	13.6
$41\bar{5}0$	62	56.0	$32\bar{5}2$	8	9.9
$51\bar{6}0$	9	−8.3	$42\bar{6}2$	—	7.2
$22\bar{4}0$	89	82.0	$33\bar{6}2$	9	17.6
$32\bar{5}0$	18	−10.3			
$42\bar{6}0$	8	−7.1	$10\bar{1}3$	39	48.3
$33\bar{6}0$	46	42.7	$20\bar{2}3$	21	−26.5
$43\bar{7}0$	8	−6.8	$30\bar{3}3$	—	−1.1
			$40\bar{4}3$	22	27.9
$10\bar{1}1$	46	−43.7	$50\bar{5}3$	12	−14.4
$20\bar{2}1$	13	14.4	$21\bar{3}3$	29	32.1
$30\bar{3}1$	—	0	$31\bar{4}3$	28	−32.4
$40\bar{4}1$	25	−21.9	$41\bar{5}3$	—	0
$50\bar{5}1$	12	8.8	$51\bar{6}3$	18	16.9
$60\bar{6}1$	—	1.2	$32\bar{5}3$	22	23.6
$21\bar{3}1$	27	−23.8	$42\bar{6}3$	12	−19.1
$31\bar{4}1$	32	26.8			
$41\bar{5}1$	—	0	0004	127	122.2
$51\bar{6}1$	10	−12.3	$30\bar{3}4$	66	68.4
$32\bar{5}1$	17	−17.2	$11\bar{2}4$	65	63.1
$42\bar{6}1$	10	13.9	$41\bar{5}4$	47	44.6
$43\bar{7}1$	12	−10.3	$22\bar{4}4$	67	68.2
			$42\bar{6}4$	30	36.0
0002	18	−23.6			
$10\bar{1}2$	27	28.0	0008	48	48.6
$20\bar{2}2$	5	8.1	$11\bar{2}8$	28	30.3

The observed and calculated structure factors are listed in Table 1. In the calculation of the structure factors the atomic scattering curves in Internationale Tabellen (1935) were employed. For NH_3 and H_2O appropriate corrections for embedded hydrogen atoms were made. A correction for the anomalous dispersion of the cobalt atom was taken into account. The effect of thermal motion was taken into consideration by multiplying the calculated F-values by a temperature factor $\exp -B(\sin\theta/\lambda)^2$, where $B=2.5$ A.^{2} The value of $R=\sum||Fo|-|Fc||/\sum|Fo|$ was 0.137 for all (*hkil*) reflections.

Description of the Structure

The structure belongs to a new type and the schematic representation is shown in Fig. 4. It is most easily described as NiAs type, consisting of octahedral complex radicals $[Co(NH_3)_3H_2OCl_2]^+$ and Cl^- ions. Interatomic distances are given in the following:

Co···Cl(1) 2.33 A., Cl(2)···Cl(2) 4.38 A.,
Cl(1)···Cl(2) 4.28 A.

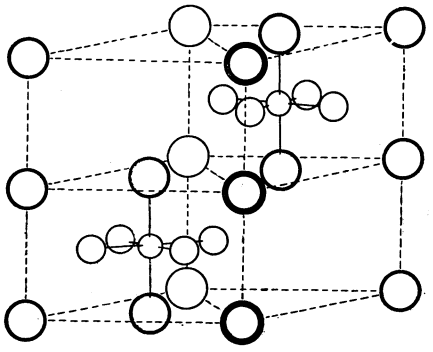

Fig. 4.—Crystal structure of "dichrochloride", $[Co(NH_3)_3H_2OCl_2]Cl$. The small circles represent metal atoms and the medium circles represent NH_3 and H_2O molecules. The largest ones indicate Cl atoms. Each complex ions are shown as taking one of their possible azimuthal orientations.

A complex ion has six Cl^- ions at the apices of a trigonal prism. The proper symmetry of a cobalt atom is $D_{3h}-\bar{6}m2$ and the azimuthal orientations of the octahedral complex radicals are not fixed in space but they are statistically arranged in such a manner that the symmetry becomes D_{3h}; in other words, the octahedral complex ion seems to occupy one of the three equilibrium positions in such a way that one of the four edges of a square consisting of 3N and O atoms becomes parallel to one of the three principal axes, the positions of Co and Cl (1) being fixed. Two chlorine atoms are in trans-coordination, being 2.33 A. from a cobalt atom. This result is in satisfactory agreement with the value 2.33 A.

obtained in the case of $[Coen_2Cl_{2(c)}^{(1)}]Cl \cdot HCl \cdot 2H_2O$.[5]

Some Remarks on the Optical Properties

The crystals of "dichrochloride" have exceptionally marked dichroism. They appear blue when the electric vector is parallel to the c-axis, whereas they appear red when the light is polarized perpendicular to the c-axis. All the complex ions are arranged in the crystal with the Cl-Co-Cl direction parallel to the c-axis. The fact that the crystals appear blue when the light is polarized along the Cl-Co-Cl direction is quite consistent with the results obtained in the case of $[Coen_2Cl_{2(c)}^{(1)}]Cl \cdot HCl \cdot 2H_2O$[5] crystals. Detailed discussion of dichroism of this crystal will be given later, after the quantitative measurement of the absorption spectra with the polarized light has been completed.

Summary

An X-ray diffraction study of crystals of dichloro-aquo-triammine-cobalt (III) chloride eads to a hexagonal unit of structure with $a=7.37$ A. and $c=8.75$ A., containing two formula units in it. The most probable space group is D_{6h}^4-C6/mmc. For an accurate determination of the structure, the method of three dimensional Fourier series was used. The determined structure is most easily described as NiAs type, consisting of $[Co(NH_3)_3H_2OCl_2]^+$ and Cl^- ions. Two chlorine atoms are coordinated to a cobalt atom in trans-positions with respect to each other, each being 2.33 A. from the cobalt atom. The Cl-Co-Cl direction being parallel to the c-axis, the octahedral complex ions seem to have statistical azimuthal orientations in the crystal and the apparent symmetry of the complex ion is $D_{3h}-\bar{6}m2$. Such an arrangement of the complex ions in the crystal may well account for the marked red-blue dichroism of the crystals.

The authors desire to express their hearty thanks to Profs. I. Nitta and R. Tsuchida of the Osaka University for their kind advice and encouragement during the course of this study. Thanks are also due to the Department of Education for a grant.

Institute of Polytechnics, Osaka City University, Osaka

(5) A, Nakahara, Y. Saito and H. Kuroya, This Bulletin, **25**, 331 (1952).

The Crystal Structure of Trans-dichloro-diethylenediamine-cobalt. (III). Chloride Hydrochloride Dihydrate, $[Coen_2Cl_2]Cl \cdot HCl \cdot 2H_2O$

By Akitsugu NAKAHARA, Yoshihiko SAITO and Hisao KUROYA

(Received May 22, 1952)

Introduction

The crystals of hydrochloride dihydrate of trans-dichloro-diethylendiamine-cobalt (III) chloride, $[Coen_2Cl_2]Cl \cdot HCl \cdot 2H_2O$, are grass green in color, and show an easily perceptible pleochroism which may be mainly attributed to the polarized absorption of light by the trans-dichloro-diethylenediamine-cobalt (III) ion itself. We have investigated the crystal structure of this substance for the purpose of determining the shape and size of the complex ion and also to correlate this structure with the absorption spectra of crystals.

Experimental

The substance was prepared by the method of Werner.[1] The crystals used in this investigation were grown from aqueous solution containing strong hydrochloric acid by slow evaporation at room temperatures. They belong to the monoclinic holohedral class and are tabular on (100), showing faces (011) etc. The crystals show well-formed faces, but when exposed to air they rapidly lose part of the water and hydrogen chloride of crystallization and begin to disintegrate. To prevent this, crystals used for X-ray measurements were coated with vacuum grease. Their dimensions were $0.1 \times 0.15 \times 0.01$ cm.

Oscillation photographs about [010] and [001] were prepared using Fe K_α radiation ($\lambda = 1.937$A.). They gave for the dimensions of the unit cell:

$$a = 10.68 \text{ A.}, \quad b = 7.89 \text{ A.}, \quad c = 9.09 \text{ A.}$$

(1) A. Werner, *Ber.*, **34**, 1733 (1901).

and $\beta = 110°26'$.

From the size of the unit cell and the density, 1.653 g./cm.^{3}, determined at 10°C by the pyknometer method, the number of the formula units in the unit cell was calculated to be $2.01 \approx 2$.

Observed extinctions were $(h0l)$ for l=odd and $(0k0)$ for k=odd, whence the space group is $C_{2h}^5 - P2_1/c$.

The intensities of reflections were estimated by comparison with a time-exposure calibrated strip. They were converted into structure amplitudes in the usual way.

Determination of the Structure

In the space group $C_{2h}^5 - P2_1/c$ the general position is fourfold, and since there are two formula units, $[Coen_2Cl_2]Cl \cdot HCl \cdot 2H_2O$, in the unit cell, it follows that the cobalt atoms must lie in special positions. These special positions are the symmetry centers.

As the first step in the structure determination, Patterson projections on (010) and (001) were made, using the $(h0l)$ and $(hk0)$ data respectively. In the projection upon (010) the peaks close to the origin were readily identified as corresponding to the Co—Cl interatomic distances within the $[Coen_2Cl_2]^+$ complex ion and the Cl—Co—Cl direction was found to be nearly parallel to the c-axis. All other peaks on both projections, $P(xz)$ and $P(xy)$, were easily interpreted in terms of the Co—Co, Co—Cl and Cl—Cl interatomic distances. At this stage, however, it was not possible to find the approximate parameter values of Co and Cl atoms without ambiguity, as there exist various possibilities. In order to decide adequate ones among these, (hkl) reflections were considered. Approximate parameter values for Co and Cl atoms could then be determined uniquely, while those for other lighter atoms remained unfixed.

As the next step, the projections of the electron density upon (010) and (001) were synthesized using the $F(h0l)$'s and $F(hk0)$'s respectively, the signs of which were calculated from the arrangement of the heavy atoms. The projections so obtained showed the heavy cobalt and chlorine atoms quite clearly resolved, together with rather faint outlines of other atoms in the unit cell. Particularly the projection upon (001) showed the ethylenediamine ring very clearly resolved. Using these projections, together with our knowledge about interatomic distances, it was possible to assign approximate coordinates for all other lighter atoms including two molecules of water of crystallization. By the method of successive approximation the final projections including all observed F's were obtained. The results are shown in Figs. 2 and 4, which may be interpreted with the aid of Figs. 1 and 3 respectively. The atomic parameters determined in this way were finally adjusted by small amounts to obtain the best

Table 1

Final Parameters

	x/a	y/b	z/c
Co	0	0	0
Cl (1)	0.036	−0.072	0.260
Cl (2)	0.328	−0.363	0.260
N (1)	0.092	0.219	0.069
N (2)	0.175	−0.107	0.019
C (1)	0.225	0.196	0.056
C (2)	0.278	0.015	0.108
O	0.480	−0.340	0.030

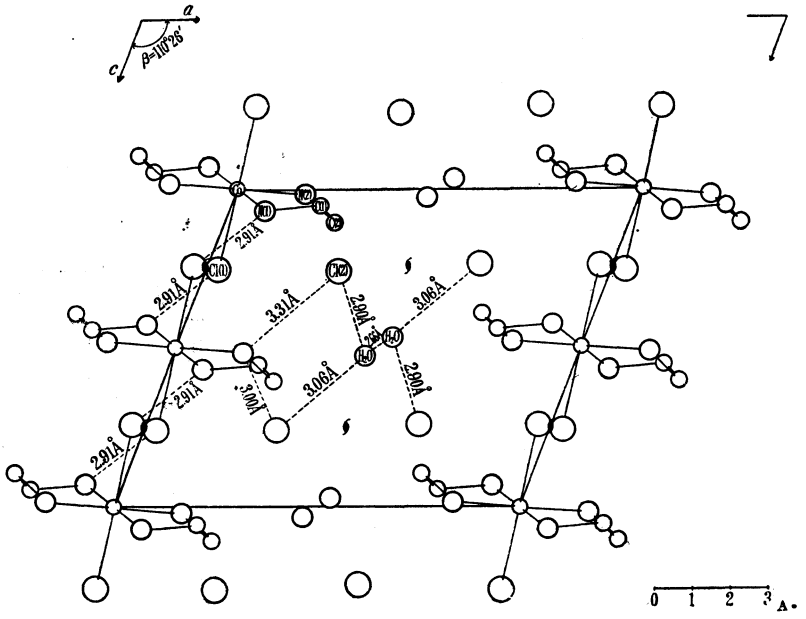

Fig. 1.—Projection of the structure upon the plane (010).

Table 2

Observed and Calculated Structure Factors

hkl	*Fobs.*	*Fcalc.*	*hkl*	*Fobs.*	*Fcalc.*	*hkl*	*Fobs.*	*Ecalc.*
002	3	3	702	9	6	520	6	11
004	29	30	70$\bar{2}$	6	2	530	<1	−3
006	1	−7	704	2	−1	540	1	6
			70$\bar{4}$	<1	5	550	<1	−6
100	22	22	70$\bar{6}$	6	4	560	<1	1
200	14	14	70$\bar{8}$	6	10			
300	25	23				610	<1	0
400	18	18	802	7	9	620	9	8
500	3	2	80$\bar{2}$	9	8	630	7	−6
600	15	16	80$\bar{4}$	<1	−4	640	4	−5
700	2	1	80$\bar{6}$	5	4	650	4	−6
800	<1	−1	80$\bar{8}$	3	−1	660	2	4
900	<1	5						
			902	2	2	710	11	−12
102	1	3	90$\bar{2}$	2	0	720	9	9
102	14	15	90$\bar{4}$	7	7	730	8	−8
104	2	2	90$\bar{6}$	1	−1	740	6	6
10$\bar{4}$	20	21				750	1	1
106	<1	1	100$\bar{2}$	7	6			
10$\bar{6}$	<1	0	100$\bar{4}$	1	1	810	<1	−1
10$\bar{8}$	7	8	100$\bar{6}$	5	3	820	<1	4
						830	3	−1
202	3	3	020	11	12			
20$\bar{2}$	11	11	040	<1	−3	910	2	−3
204	9	9	060	<1	4	920	1	0
20$\bar{4}$	20	18						
206	1	1	110	5	−7	011	19	19
20$\bar{6}$	8	8	120	15	17	012	6	6
20$\bar{8}$	7	4	130	13	−13	013	10	10
			140	15	12	014	<1	−1
302	11	−15	150	4	6	015	7	6
30$\bar{2}$	26	−23	160	6	−4			
304	9	12	170	4	3	021	8	5
30$\bar{4}$	22	19				022	6	0
306	3	−5	210	10	10	023	<1	1
30$\bar{6}$	9	−7	220	12	13	024	10	9
30$\bar{8}$	13	13	230	6	−6			
			240	8	8	031	8	9
402	9	9	250	5	−7	032	<1	−2
40$\bar{2}$	11	9	260	6	−1	033	7	9
404	<1	5	270	3	0			
40$\bar{4}$	13	13				041	8	−12
406	8	7	310	2	−2	042	9	14
40$\bar{6}$	3	−3	320	15	16	043	7	5
40$\bar{8}$	5	6	330	7	−7			
			340	6	3	051	6	7
502	4	4	350	<1	−2	052	<1	2
50$\bar{2}$	12	12	360	4	3	053	4	3
504	4	3	370	2	−2			
50$\bar{4}$	10	10				061	7	−6
50$\bar{6}$	8	9	410	3	−5	062	<1	8
50$\bar{8}$	3	3	420	12	11	063	7	8
			430	7	−8			
602	3	1	440	7	7	071	2	2
60$\bar{2}$	3	−3	450	<1	1			
604	9	11	460	5	6			
60$\bar{4}$	16	17	470	<1	0			
60$\bar{6}$	<1	2						
60$\bar{8}$	9	12	510	8	3			

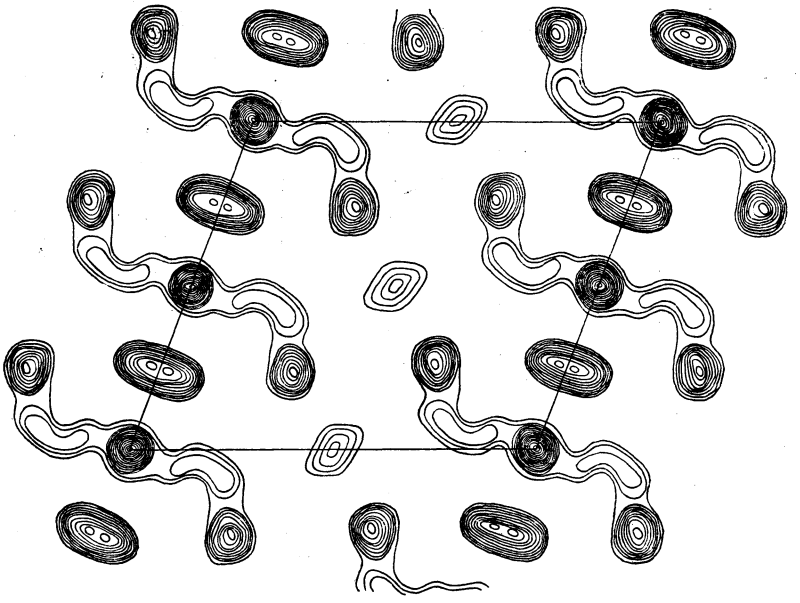

Fig. 2.—A Fourier projection of electron density upon (010). The projection corresponds to Fig. 1. Contours at arbitrary intervals.

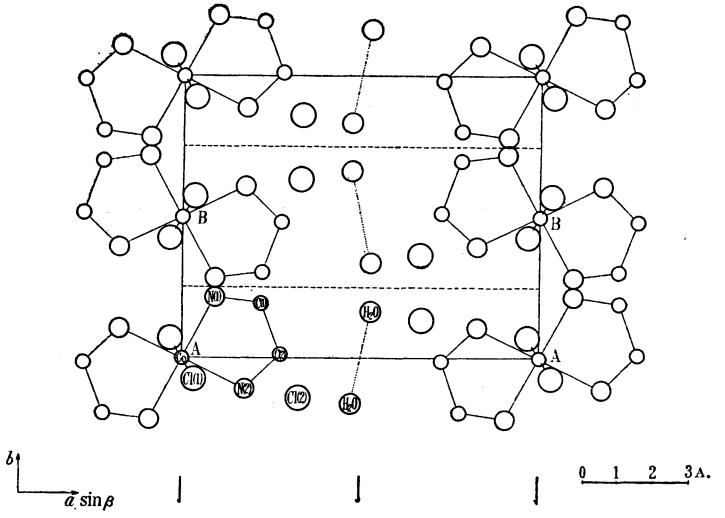

Fig. 3.—Projection of the structure upon a plane normal to the *c*-axis. Units marked B are derived from those marked A by the operation of a glide plane "*c*" parallel to (010). Groups $[H_2O...H...H_2O]^+$ are indicated by dotted lines.

agreements between the observed and calculated *F*'s. A list of the final parameters is given in Table 1. In the calculation of the structure factors, the atomic scattering curves in Internationale Tabellen (1935) were employed and corrected for temperature according to the Debye-Waller formula, the constant B being given the value 2.5 A.[2]

The agreement on the whole is quite good and the values of $R=\sum||Fo|-|Fc||/\sum|Fo|$ are 0.194, 0.228 and 0.279 for (*h*0*l*), (*hk*0) and (0*kl*) respectively. The larger values of R for the (0*kl*) zone may be attributed to the less accurate values due to absorption.

Description of the Structure

Figs. 1 and 3 show the structure projected upon (010) and a plane normal to the *c*-axis respectively. The interatomic distances and interbond angles calculated from the parameter values are listed in Table 3.

In Fig. 5 is shown a perspective drawing of the $[Coen_2Cl_2]^+$ ion. The cobalt atom lies at the center of symmetry. Two chlorine atoms are co-ordinated at a distance of 2.33 A. to a cobalt atom in trans-positions. The line joining them is perpendicular to the plane in which the four nitrogen atoms of the two ethylenediamine mole-

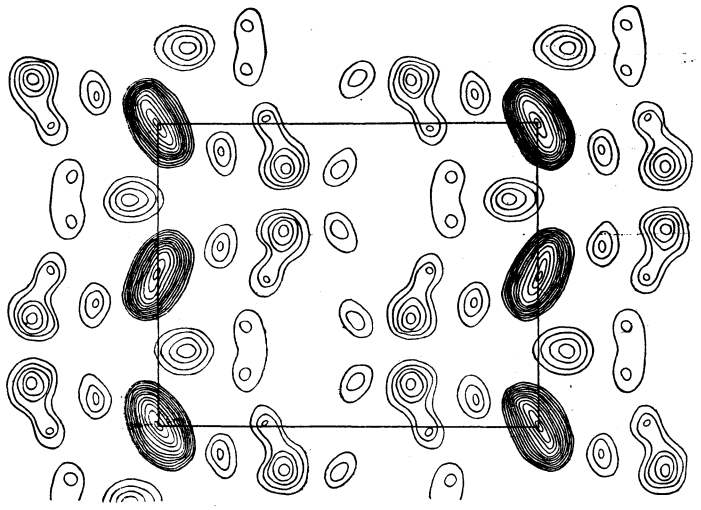

Fig. 4.—A Fourier projection of electron density upon a plane normal to the c-axis. The projection corresponds to Fig. 3. Contours at arbitrary intervals.

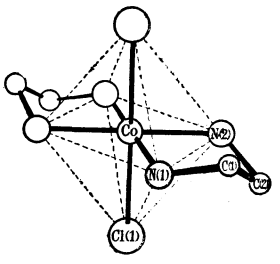

Fig. 5.—A perspective drawing of the complex ion, $[Coen_2Cl_2]^+$.

Table 3

Interatomic distances (in A.) and interbond angles.

Co.....Cl (1)	2.33	Cl (1).....N (1)	2.91
Co.....N (1)	1.98	Cl (1).....Cl (1)	4.01
Co.....N (2)	2.00	Cl (1).....Cl (2)	3.87
N (1)...C (1)	1.48	Cl (2).....H_2O	2.90
N (2)...C (2)	1.47	...H_2O	3.06
C (1)...C (2)	1.55	...N (2)	3.31
$\angle N_1C_1C_2$	110°	...N (2)	3.00
$\angle N_2C_2C_1$	108°	...C (2)	3.25
$\angle CoN_1C_1$	104°	H_2O .....H_2O	2.66
$\angle CoN_2C_2$	106°		

cules were found to lie. Within the errors of experiment these ligand atoms (4 N and 2 Cl) form a distorted octahedron around a cobalt atom. The C—C distance of 1.55 A. as well as the C—N distances, 1.47 A. and 1.48 A., although not very reliable because these atoms were not fully resolved in the projection upon (010), are in good agreement with the well-known values of C—C and C—N distances respectively.

It is interesting to note here that the ethylenediamine molecules are present in the "gauche" forms; there are two kinds of "gauche" molecules in the crystal, the one being the mirror image of the other, and moreover, these two kinds of molecules are co-ordinated to a cobalt atom in such a way that the one is related by the operation of a center of symmetry to the other. Referring to Fig. 1, it is evident that these complex ions are arranged in layers parallel to the plane (100). The Cl—Co—Cl bond direction is inclined to the plane (010) at an angle of 14.5° and the projection of this direction upon (010) makes an angle of 10° with the c-axis. The closest distances of approach between the complex ions in the layer are found to be 2.91 A. between Cl(1) atom of one complex ion and N(1) atom of the adjacent. Thus the complex ions are held together in layers by these Cl...N bonds. A projection of a single layer of $[Coen_2Cl_2]^+$ is shown in Fig. 6. Between these layers are arranged the Cl^- ions and H_2O molecules, both occupying general positions. A complex ion has four nearest Cl^- ions. The closest approach of a complex ion and Cl^- ion is between N(2) and Cl^-. The Cl^-...N(2) distances are 3.00 and 3.31 A. which may be compared with the values found in the case of methyl ammonium chloride crystals.[2]

The positions of H cannot in general be determined by the method of X-rays; however, the fact that two molecules of water of crystallization form a pair with O...O distance of 2.66 A. and this pair is surrounded exclusively by Cl^- ions strongly suggests the existence of a group $[H_2O...H...H_2O]^+$. A molecule of H_2O possesses two Cl^- ions at 2.90 A. and 3.06 A., thus every group, $[H_2O...H...H_2O]^+$, is surrounded by four Cl^- ions.

(2) E. W. Hughes and W. N. Lipscomb, *J. Am. Chem. Soc.*, **68**, 1970 (1946).

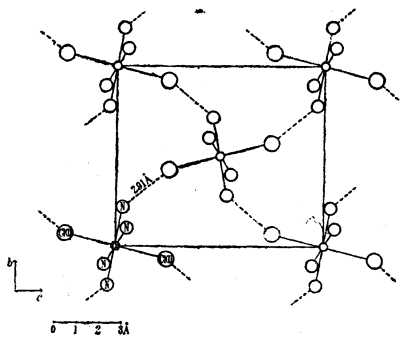

Fig. 6. Projection of a single layer of $[Coen_2Cl_2]^+$ upon the plane (100). Only positions of Co, Cl(1) and N atoms are shown. Cl...N(2) bond directions are indicated by broken lines.

Remarks on the Optical Properties

Thin tabular crystals extended on (100) appear blue when the electric vector is parallel to the c-axis, while they appear yellowish green when the light is polarized along the b-axis. Such striking dichroism may be reasonable, since there is a large component of the Cl—Co—Cl bond along the c-axis. This result cannot be considered to be in full agreement with the conclusion obtained by Yamada and Tsuchida,[3] who have measured microscopically the absorption of the crystals of the praseo-salts.* Detailed discussion will be given in reference to the absorption of the crystals of the "dichrochloride", the crystal structure of which has been determined recently by the present authors;[4] the absorption measurements of the dichrochloride are now in progress.

(3) S. Yamada and R. Tsuchida, This Bulletin, **25**, 127 (1952).

(4) Y. Tanito, Y. Saito and H. Kuroya, This Bulletin, **25**, 328 (1952).

* a, b and c-axes adopted by Yamada and Tsuchida correspond to c, b and a-axes in the present paper respectively.

Summary

The crystal structure of trans-dichloro-diethylenediamine-cobalt (III) chloride hydrochloride has been determined using the rotation method (Fe $K_\alpha\lambda=1.937$ A.). The substance crystallizes in a monoclinic lattice with two formula units in the unit cell, the dimensions of which are $a=10.68$ A., $b=7.89$ A., $c=9.09$ A. with $\beta=110°26'$.

The determined structure seems most easily described as consisting of layers of $[Coen_2Cl_2]^+$ ions parallel to the plane (100) and those of Cl^-, H_2O and H^+. Two chlorine atoms are co-ordinated to a cobalt atom in trans-positions. The line joining them is perpendicular to the plane in which four nitrogen atoms are found to lie. The dimensions of a complex ion are given. The water molecules probably form a group $[H_2O...H...H_2O]^+$ together with a proton, O...O distance being 2.66 A. These groups are located between them. The dichroism of the crystal is discussed on the basis of the determined structure.

The authors desire to express their hearty thanks to Profs. I. Nitta and R. Tsuchida of Osaka University for their kind advice and encouragement in the course of this study. Part of the cost of this study has been defrayed from the Scientific Fund from the Ministry of Education, to which the authors' thanks are due.

Institute of Polytechnics, Osaka City University, Osaka

Notes on The Polymer-Mixed Solvents System. I The refinement of the free energy expression

By Toru KAWAI

(Received January 18, 1952)

Introduction

While the thermodynamic systems involved in the problems of fractionation of high polymer are essentially multicomponent ones, they are normally simplified or approximated by assuming that the mixture of two solvents behaves as a homogeneous liquid with resspect

to the polymer.[1][2] Although this single liquid approximation is useful in obtaining semi-quantitative information concerning the polymer-mixed solvents interaction, it requires that the proportions of the two liquids are the same in both phases or in both sides of the membrane. Employing the single liquid approximation and some other approximation methods, Scott[3] has considered the problems of phase equilibria in a ternary system of polymer and two liquids. The free energy expression in his treatment contains, however, two serious assumptions which are not always applicable to the practical cases. Namely,

(a) the interaction energy between unlike pairs of molecules of the constituents is the geometric mean of those between respective like pairs (the Scatchard's approximation).[4]

From this assumption Scott derived the heat of mixing in the ternary system by employing two constants A_{13}, A_{23} characteristic of the corresponding binary systems, polymer-liquid 1 and polymer-liquid 2.

(b) the unit submolecule of the polymer and the molecules of the two solvents are all the same in shape and size.

Concerning the above two assumptions, the free energy expression will be refined and the single liquid approximation will be discussed in the present paper.

The Heat of Mixing of the System

Scatchard[4] has shown that if we make an assumption entirely equivalent to a binary components system we obtain for the heat of mixing in the ternary system

$$\Delta H^M_{123} = V_m(A_{12}v_1v_2 + A_{13}v_1v_3 + A_{23}v_2v_3), \qquad V_m = x_1V_1 + x_2V_2 + x_3V_3, \quad (1)$$

where the A's are the constants characteristic to each pair of the components, the v's volume fractions, the x's mole fractions and the V's molal volumes of the constituents. Differentiation leads to the partial molal heat of mixing,

$$\Delta\bar{H}_1 = V_1[A_{12}v_2^2 + A_{13}v_3^2 + (A_{12}+A_{13}-A_{23})v_2v_3] \quad (2a)$$

$$\Delta\bar{H}_2 = V_2[A_{12}v_1^2 + A_{23}v_3^2 + (A_{12}+A_{21}-A_{13})v_1v_3] \quad (2b)$$

$$\Delta\bar{H}_3 = V_3[A_{13}v_1^2 + A_{23}v_2^2 + (A_{13}+A_{23}-A_{12})v_1v_2]. \quad (2c)$$

Without the assumption (a) previously noted, we can derive the partial molal heat of mixing $\Delta\bar{H}_0$, corresponding to the single liquid approximation, directly from Eq. (1) as follows; when the ratio of compositions of solvents 1 and 2 is constant,

$$\theta N_1V_1 = N_2V_2, \quad N_1V_1 + N_2V_2 = (1+\theta)N_1V_1 = N_0V_0,$$
$$N_0 = N_1 + N_2, \quad V_0 = (1+\theta)V_1/(1+\theta V_1/V_2),$$

and then, Eq. (1) becomes

$$\Delta H^M_{123} = A_{12}\{N_0V_0/(1+\theta)\} \times \{N_0V_0\theta/(1+\theta)\}/(N_0V_0+N_3V_3) + A_{13}\{N_0V_0/(1+\theta)\} \times N_3V_3/(N_0V_0+N_3V_3) + A_{23}\{N_0V_0\theta/(1+\theta)\} \times N_3V_3/(N_0V_0+N_3V_3). \quad (3)$$

Differentiating with respect to N_0,

$$\Delta\bar{H}_0 = V_0\{[\theta/(1+\theta)^2]A_{12}(1-v_3)^2 + [1/(1+\theta)]A_{13}v_3^2 + [\theta/(1+\theta)]A_{23}v_3^2\} = V_0\{-[\theta(1+\theta)^2]A_{12} + [1/(1+\theta)]A_{13} + [\theta/(1+\theta)]A_{23}\}v_3^2 + [\theta/(1+\theta)^2]V_0A_{12}, \quad (4)$$

where the term $[\theta/(1+\theta)^2]V_0A_{12}$ vanishes when the mixture of solvents 1 and 2 are assumed to be a homogeneous liquid. Hence,

$$\Delta\bar{H}_0 = V_0A_{30}v_3^2, \quad A_{30} = -[\theta/(1+\theta)^2]A_{12} + [1/(1+\theta)]A_{13} + [\theta/(1+\theta)]A_{23}. \quad (5)[5]$$

The Entropy of Mixing of the System

The familiar expression of Huggins[6] and Flory[7] for the entropy of high polymer solutions may be written (binary system)

$$\Delta S = R\ln W = -R\{N_1\ln[N_1/(N_1+xN_3)] + N_3\ln[xN_3/(N_1+xN_3)] + u_s[N_1xN_3/(N_1+xN_3)]\}. \quad (6)$$

(The notation of this equation is similar to what is usually employed.)

Here we adopt an approximate method introducing the effect of volume difference between the polymer submolecule and the solvent molecule. At first, we consider a binary system of polymer 3 and liquid 1, where the molal volume V_1 of the solvent differs from the equivalent quantity V_3 of the polymer submolecule. In hypothetical lattice sites the operation of packing the solvent molecules which are equal in size and shape to the submolecule in the remaining sites is exactly equivalent to that of setting the polymer molecules in the sites without considering the existence of the solvent molecules. (This situation leads to Eq. (6)) When $V_1 > V_3$, however, the configurations of polymer molecules are constrained by larger solvent molecules. The total number of

(1) R. S. Scott, *J. Chem. Phys.*, **13**, 178 (1945).
(2) G. Gee, *Trans. Faraday Soc.*, **40**, 468 (1944).
(3) R. S. Scott, *J. Chem. Phys.*, **17**, 268 (1949).
(4) G. Scatchard, *J. Am. Chem. Soc.*, **56**, 995 (1934); *Trans. Faraday Soc.*, **33**, 160 (1937).

(5) Applying the "geometric mean rule" to Eq. (5), we can easily derive Scott's result $\mu_{30} = [(A\phi_1 - B\phi_2)/(\phi_1+\phi_2)]^2$ in reference 3.
(6) M. L. Huggins, *J. Chem. Phys.*, **9**, 440 (1941); *Ann. N. Y. Acad. Sci.*, **43**, I (1942).
(7) P. J. Flory, *J. Chem. Phys.*, **9**, 666 (1941); Ibid., **13**, 453 (1945).

different configurations in this case W'', will be obtained from W', when N_1V_1/V_3 is substituted for N_1 in the above expression of W (Eq. 6), multiplying by a factor due to the fact that V_1/V_3 sites must be in one group. Thus,

$$W'' = W' \times W_1 \Big/ \binom{N_1V_1/V_3 + xN_3}{N_1V_1/V_3}, \qquad (7)$$

where W_1 is the number of different ways in which N_1 molecules each occupying V_1/V_3 sites can be packed in $(N_1V_1/V_3)+xN_3$ sites without overlapping. Ōsawa[6] calculated W_1 for certain cases, but we may replace $R\ln W_1$ with the usual expression of the entropy of mixing, $-R[N_1\ln v_1+N_2\ln v_2]$. Thus,

$$\begin{aligned}\Delta S'' = \Delta S' - R\{&N_1\ln[N_1V_1/(N_1V_1+xN_3V_3)]\\ &+xN_3\ln[xN_3V_3/(N_1V_1+xN_3V_3)]\}\\ &+R\{(N_1V_1/V_3)\ln[N_1V_1/(N_1V_1+xN_3V_3)]\\ &+xN_3\ln[xN_3V_3/(N_1V_1+xN_3V_3)]\}\end{aligned} \qquad (8)$$

where $\Delta S' = R\ln W'$.
And

$$\begin{aligned}\Delta\bar{S}_1'' &= -R[(V_1/V_3)\{\ln v_1+(1-1/x)v_3+\mu_s v_3^2\}\\ &\quad+\{1-(V_1/V_3)\}(\ln v_1+v_3)]\\ &= R[(V_1/V_3x)v_3+(1/2-\mu_s V_1/V_3)v_3^2+\cdots]. \end{aligned} \qquad (9)$$

When $V_3>V_1$, simply,[9]

$$\Delta S'' = \Delta S' \qquad (10)$$

$$\begin{aligned}\Delta\bar{S}_1'' &= (V_1/V_3)\Delta\bar{S}_1' = -(RV_1/V_3)[\ln v_1+(1-1/x)v_3\\ &\quad+\mu_s v_3^2] = R(V_1/V_3)[v_3/x+(1/2-\mu_s)v_3^2+\cdots]. \end{aligned} \qquad (11)$$

This result agrees with the Flory's formula.[10]

The first bracketed terms in Eq. (8), which correspond to W_1, are considered to be the entropy change in the case when isolated xN_3 molecules were mixed with other N_1 molecules different in size. The second bracketed terms, of course, correspond to $\binom{N_1V_1/V_3+xN_3}{NV_1/V_3}$. Thus it is easily seen that the first bracketed terms may be replaced with the usual expression of the entropy of mixing in a three components system $-R[N_1\ln v_1+N_2\ln v_2+N_3\ln v_3]$, when we deal with polymer-mixed solvents system. Therefore, when $(1+\theta)V_1/(1+\theta V_1/V_2)>V_3$,

$$\begin{aligned}\Delta S'' = \Delta S'_{30} - R\{&N_1\ln[N_1V_1/(N_1V_1+N_2V_2+xN_3V_3)]\\ &+N_2\ln[N_2V_2/(N_1V_1+N_2V_2+xN_3V_3)]\\ &+xN_3\ln[xN_3V_3/(N_1V_1+N_2V_2+xN_3V_3)]\}\\ &+R\{[(N_1V_1+N_2V_2)/V_3]\ln[(N_1V_1\\ &+N_2V_2)/(N_1V_1+N_2V_2+xN_3V_3)]\\ &+xN_3\ln[xN_3V_3/(N_1V_1+N_2V_2+xN_3V_3)]\} \end{aligned} \qquad (12)$$

where $\Delta S'_{30}$ corresponds to $\Delta S'$ in Eq. (8).[11] Hence,

$$\begin{aligned}\Delta\bar{S}_1'' &= -R\{\ln v_1+(1-V_1/V_2)v_2+(1-V_1/V_3)v_3\\ &\quad+(V_1/V_3)[(1-1/x)v_3+\mu_s v_3^2]\} \end{aligned} \qquad (13a)$$

$$\begin{aligned}\Delta\bar{S}_2'' &= -R\{\ln v_2+(1-V_2/V_1)v_1+(1-V_2/V_3)v_3\\ &\quad+(V_2/V_3)[(1-1/x)v_3+\mu_s v_3^2]\} \end{aligned} \qquad (13b)$$

When, $(1+\theta)V_1/(1+\theta V_1/V_2)<V_3$,

$$\begin{aligned}\Delta S'' = \Delta S'_{30} - R[&N_1\ln\{N_1V_1/(N_1V_1+N_2V_2)\}\\ &+N_2\ln\{N_2V_2/(N_1V_1+N_2V_2)\}]. \end{aligned} \qquad (14)[11]$$

Hence,

$$\Delta\bar{S}_1'' = -(RV_1/V_3)[\ln v_1+(1-1/x)v_3+\mu_s v_3^2] \qquad (15a)$$

$$\Delta\bar{S}_2'' = -(RV_2/V_3)[\ln v_2+(1-1/x)v_3+\mu_s v_3^2]. \qquad (15b)$$

Now we can write for the single liquid approximation that

$$\begin{aligned}\Delta S''' &= \Delta S'' + R\{N_1\ln[N_1V_1/(N_1V_1+N_2V_2)]\\ &\quad+N_2\ln[N_2V_2/(N_1V_1+N_2V_2)]\},[11]\\ N_1 &= N_0V_0/(1+\theta)V_1,\ N_2 = \theta N_0V_0/(1+\theta)V_2, \end{aligned}$$

and then, expressing Eqs. (12) and (14) with N_0, N_3, differentiation leads to $\Delta\bar{S}_0'''$; When $V_0>V_3$,

$$\begin{aligned}\Delta\bar{S}_0''' &= -R\{(V_0/V_3)[\ln v_0+(1-1/2)v_3+\mu_s v_3^2]\\ &\quad+(1-V_0/V_3)(\ln v_0+v_3)\} = R[V_0/V_3x)\times v_3\\ &\quad+(1/2-\mu_s V_0/V_3)v_3^2+\cdots\cdots]. \end{aligned} \qquad (16)$$

When $V_0<V_3$,

$$\begin{aligned}\Delta\bar{S}_0''' &= -(RV_0/V_3)[\ln v_0+(1-1/x)v_3+\mu_s v_3^2]\\ &= (RV_0/V_3)[v_3/x+(1/2-\mu_s)v_3^2+\cdots\cdots]. \end{aligned} \qquad (17)$$

The Partial Molal Free Energy

Combining the equations of the previous sections for the partial molal entropy and heat of mixing, there is obtained for the partial molal free energy.

When $V_1(1+\theta)/(1+\theta V_1/V_2)>V_3$,[12]

$$\begin{aligned}\Delta\bar{F}_1 &= RT\{\ln v_1+(1-V_1/V_2)v_2+(1-V_1/V_3)v_3\\ &\quad+(1-1/x)v_3+\mu_s v_3^2+(V_1/RT)[A_{12}v_2^2+A_{13}v_3^2\\ &\quad+(A_{12}+A_{13}-A_{23})v_2v_3]\} \end{aligned} \qquad (18a)$$

(8) F. Osawa, *Busseiron Kenkyu*, **12**, 27 (1948); ibid., **14**, 40 (1949).

(9) Employing Osawa's approximation, the writer estimated the effect of size and shape of solvents on $\Delta\bar{S}_1$ for the solution of rodlike molecules ($V_3>V_1$), and the result is included in Eq, (II) as a special case. This Bulletin, **24**, 264 (1951).

(10) P. J. Flory, *J. Chem. Phys.*, **10**, 51 (1942).

(11) The bracketed terms in Eq. (14) arise from the fact that the term $\Delta S'_{30}$ means the entropy change of mixing polymer molecules with the hypothetical homogeneous liquid assumed in the single liquid approximation. Thus these terms vanish for the single liquid approximation. This is also true for Eq. (12). It is easily seen that Eq. (12) and (14) can be also derived considering two processes, namely, mixing of liquid 1 and 2, and that of polymer 3 and this "new liquid".

(12) These conditions result from our approximate treatment of the entropy term as discussed in the previous section.

$$\Delta\bar{F}_2 = RT\{\ln v_2 + (1-V_2/V_1)v_1 + (1-V_2/V_3)v_3 + (1-1/x)v_3 + \mu_s v_3^2 + (V_2/RT)[A_{13}v_1^2 + A_{23}v_3^2 + (A_{12}+A_{23}-A_{13})v_1v_3]\}. \quad (18b)$$

When $V_1(1+\theta)/(1+\theta V_1/V_2) < V_3$,[12]

$$\Delta\bar{F}_1 = RT\{(V_1/V_3)[\ln v_1 + (1-1/x)v_3 + \mu_s v_3^2] + (V_1/RT)[A_{12}v_2^2 + A_{13}v_3^2 + (A_{12}+A_{13}-A_{23})v_2v_3]\} \quad (19a)$$

$$\Delta\bar{F}_2 = RT\{(V_2/V_3)[\ln v_2 + (1-1/x)v_3 + \mu_s v_3^2] + (V_2/RT)[A_{13}v_1^2 + A_{23}v_3^2 + (A_{12}+A_{23}-A_{13})v_1v_3]\} \quad (19b)$$

For the single liquid approximation,

when $V_0 > V_3$,

$$-\Delta\bar{F}_0 = RT(V_0/V_3x)v_3 + (1/2-\mu_s V_0/V_3 - V_0A_{30}/RT)v_3^2 + \cdots\cdots] \quad (20)$$

when $V_0 < V_3$,

$$-\Delta\bar{F}_0 = RT\{(V_0/V_3)[v_3/x + (1/2-\mu_s - V_3A_{30}/RT)v_3^2 + \cdots\cdots]\}. \quad (21)$$

Using the above Eqs. (18a, b) and (19a, b), we can compute the equilibrium phase diagrams for this ternary system by the usual conditions;

$$\Delta\bar{F}_1' = \Delta\bar{F}_1'', \quad \Delta\bar{F}_2' = \Delta\bar{F}_2'', \quad \Delta\bar{F}_3' = \Delta\bar{F}_3''. \quad (22)$$

(The expression for $\Delta\bar{F}_3$ is easily derived from the heat and entropy expressions which have been obtained previously.)

Now, if we consider the entropy term only, we obtain from Eqs. (15a, b) and (22)

$$(V_1/V_3)[\ln v_1' + (1-1/x)v_3' + \mu_s v_3'^2] = (V_1/V_3)[\ln v_1'' + (1-1/x)v_3'' + \mu_s v_3''^2] \quad (23a)$$

$$(V_2/V_3)[\ln v_2' + (1-1/x)v_3' + \mu_s v_3'^2] = (V_2/V_3)[\ln v_2'' + (1-1/x)v_3'' + \mu_s v_3''^2]. \quad (23b)$$

Hence,

$$\ln(v_1'/v_2') = \ln(v_1''/v_2'') \quad \text{or} \quad \theta' = \theta''. \quad (24)$$

Thus, the single liquid approximation is satisfied only when $\Delta\bar{H}_1 = 0$, and the invalidity of the single liquid approximation in the usual cases is due to the heat term only.[13] As immediately seen from Eqs. (13a, b), this is not true for the case when $V_3 < V_0$. In most of the actual cases, however, V_3 is anticipated to be larger than V_0 from the data of the molecular construction of polymer molecules, although the exact values of V_3 cannot be deduced.[14] From this point of view the problems of the selective adsorption will be discussed in future.

A Special Treatment of Associated Liquids

It is interesting to assume polymer-two liquids systems in which one or two of the liquids are associated liquids as an extreme case when $V_0 > V_3$. In this case, the deviation from the single liquid approximation may be attributable to the entropy term as well as to the heat term. Tobolsky and Bratz,[15] and Flory[16] have treated solutions of associated liquids with high polymer equations. The situation becomes more complicated in our case, but it does not seem to be inadequate to assume that the associated liquid consists of an equiliblium mixture of polymer molecules of various sizes, in order to estimate roughly the above volume effect.

To avoid complications we assume now that the submolecule of polymer and the "submolecule" of associated liquid and the molecule of non-asociated liquid have all the same volume. This assumption may be sufficient to obtain a rough picture of the volume effect on the entropy of mixing in polymer-two liquids systems in which one or two components are associated liquid. First of all, let us consider the binary system polymer 3-associated liquid 1.

(A) Polymer 3-associated liquid 1 system.—We can assume this system as a special case where the size and shape of solvent differ extremely from that of polymer submolecule. Thus, employing Eq. (7), the entropy of mixing in this system may be written,

$$\begin{aligned}\Delta S'' &= \Delta S'_{30} + \Delta S_{10} - \Delta S^0_{31} \\ &= -R[yN_1\ln\{yN_1/(yN_1+xN_3)\} + N_3\ln\{xN_3/(yN_1+xN_3)\}] \\ &\quad - R[N_1\ln\{yN_1/(yN_1+xN_3)\} + xN_3\ln\{xN_3/(yN_1+xN_3)\}] + R[yN_1\ln\{yN_1/(yN_1+xN_3)\} \\ &\quad + xN_3\ln\{xN_3/(yN_1+xN_3)\}] \\ &= -R[N_1\ln\{xN_3/(yN_1+xN_3)\} + N_3\ln\{yN_1/(yN_1+xN_3)\}] \end{aligned} \quad (25)$$

where $\Delta S'_{30} = R\ln W' =$ the entropy of mixing N_3 polymer molecules with randomly distributed yN_1 separate submolecules of liquid 1, $\Delta S_{10} = R\ln W_1 =$ the entropy of mixing N_1 molecules of associated liquid with xN_3 separate submolecules of polymer 3, and ΔS^0_{31} (which corresponds to $\binom{yN_1+xN_3}{yN_1} =$ the entropy of mixing both sorts of the submolecules at random. (the number average degree of "polymerization" of associated liquid 1 $= y$).

The terms containing μ_s in the entropy expression vanishes in this case as can be easily understood from Huggins' theory[17] from which

(13) This is also true for Scott's result of Eqs. (9abc) in reference 3.

(14) One submolecule is supposed to be several times larger than the monomeric unit of the polymer, although the molal volume of the solvent could be a little larger than the equivalent quantity of the monomeric unit of the polymer.

(15) A. V. Tobolsky, P. J, Bratz, *J. Chem. Phys.*, **13**, 379 (1945).

(16) P. J. Flory, *J. Chem. Phys.*, **14**, 49 (1945).

(17) M. L. Huggins, *Ann. N. Y. Acad. Sci.*, **43**, 1 (1942)

the terms were derived.

Differentiating Eq. (25) with respect to N_1,

$$\Delta\bar{S}_1'' = -R[\ln v_1 + (1-y/x)v_3]. \quad (26)$$

This result corresponds to Scott's for the polymer-polymer system[16] (Eq. (1a) in reference 18). Here we attempt to apply a somewhat paradoxical situation to the present problem. Namely, it may be permissible to assume that the associated liquid in both sides of the membrane were diffusible as separate submolecules, although it behaves thermodynamically as if it were a mixture of macromolecules in both sides. Thus, differentiating Eq. (25) with respect to yN_1 (not N_1), we can obtain an "effective" partial molal entropy of mixing,

$$\Delta\bar{S}_1'' = -R[(1/y)\ln v_1 + (1/y - 1/x)v_3] = R[v_3/x + v_3^2/2y + \cdots\cdots] \quad (27).$$

Since the y values are supposed to be considerably large in the polymer-polymer system, two polymers would be often incompatible if there were any positive heat of mixing.[19] Considering that such incompatibility does not appear in the actual polymer-associated liquid systems, the average degree of "polymerization" is supposed to be not so large as that of the actual polymer.

Therefore, it may be rather suitable to assume y as a measure of the effect of "association" of solvent on the partial molal entropy of mixing.

(B) Polymer 3-liquid 1-associated liquid 2.—In this case, we can assume two processes separately, namely, the mixing of polymer 3 and associated liquid 2, ΔS_{23} (which has been given by Eq. (25)), and the dilution of this "mixture" by liquid 1, $\Delta S_{\widehat{231}}$. Then,

$$\begin{aligned}\Delta S'' = \Delta S_{23} + \Delta S_{\widehat{231}} = &-R\{N_2\ln[yN_2/(yN_2+xN_3)] \\ &+N_3\ln[xN_3/(yN_2+xN_3)]\} \\ &-R\{N_1\ln[N_1/(N_1+yN_2+xN_3)] \\ &+(N_2+N_3)\ln[(xN_3+yN_2)/(N_1+yN_2+xN_3)] \\ &+\mu_s^{\widehat{231}}\times N_1(xN_3+yN_2)/(N_1+yN_2+xN_3)\}. \quad (28)^{[20]}\end{aligned}$$

Differentiation leads to

$$\Delta\bar{S}_1'' = -R[\ln v_1 + (1-1/y)v_2 + (1-1/x)v_3 + \mu_s^{\widehat{231}}(v_2+v_3)^2] \quad (29a)$$

$$\Delta\bar{S}_2'' = -R[\ln v_2 + (1-y)v_1 + (1-y/x)v_3 + y\mu_s^{\widehat{231}}v_1^2] \quad (29b)$$

$$\Delta\bar{S}_3'' = -R[\ln v_3 + (1-x)v_1 + (1-x/y)v_2 + x\mu_s^{\widehat{231}}v_1^2]. \quad (29c)$$

When $\mu_s^{12} = \mu_s^{13} = \mu_s^{\widehat{231}}$, these results coincide with the result of Scott' (Eqs. (5a, b, c) in reference 18).

If the single liquid approximation may be applicable, assuming $\theta N_1 = yN_2$, $N_0 = (1+\theta)N_1$, and

$$\begin{aligned}\Delta S''' = \Delta S'' + R\{&N_1\ln[N_1/(N_1+yN_2)] \\ &+N_2\ln[yN_2/(N_1+yN_2)] + \mu_s^{12} \\ &\times N_1yN_2/(N_1+yN_2)\}, \quad (30)^{[11]}\end{aligned}$$

$$\begin{aligned}\Delta\bar{S}_0''' = &-R\{[1/(1+\theta)+\theta/(1+\theta)y]\ln v_0 + [1/(1+\theta) \\ &-1/x+\theta/(1+\theta)y]v_3 + \mu_s^{\widehat{231}}[\theta/(1+\theta)]^2v_3^2\} \\ = &R[v_3/x + \{(1/2)[1/(1+\theta)+\theta/(1+\theta)y] \\ &-\mu_s^{\widehat{231}}[\theta/(1+\theta)]^2\}v_3^2 + \cdots\cdots]. \quad (31)\end{aligned}$$

Combining Eq. (31) with Eq. (5),

$$\begin{aligned}-\Delta\bar{F}_0 = &RT[v_3/x + \{(1/2)[1/(1+\theta)+\theta/(1+\theta)y] \\ &-\mu_s^{\widehat{231}}[\theta/(1+\theta)]^2 - (V_0/RT)[-\theta/(1+\theta)^2\times A_{12} \\ &+1/(1+\theta)\times A_{23}+\theta/(1+\theta)\times A_{13}]\}v_3^2 + \cdots]. \quad (32)\end{aligned}$$

This result shows that the entropy term contributes in some way to the solubility and the phase separation in the system and that whether associated liquid 2 is solvent or non-solvent makes a considerable difference in the above contribution. Namely, the mixed solvents show poorer solvent power than that supposed from the true energetical solvent power, and this is more notable when the associated liquid is solvent than when it is non-solvent.

(C) Polymer 3-associated liquids 1 and 2 system.—The above procedure by which we derived Eq. (28) can be applied to introduce the entropy of mixing in polymer 3- associated liquids 1 and 2 system. Hence,

$$\begin{aligned}\Delta S'' = \Delta S_{31} + \Delta S_{\widehat{312}} = &-R\{N_1\ln[xN_3/(yN_1+xN_3)] \\ &+N_3\ln[yN_1/(yN_1+xN_3)]\} - R\{N_2\ln[zN_2/(yN_1 \\ &+zN_2+xN_3)] + (N_1+N_3)\ln[(yN_1+xN_3)/(yN_1 \\ &+zN_2+xN_3)]\} = -R\{N_1\ln[yN_1/(yN_1+zN_2 \\ &+xN_3)] + N_2\ln[zN_2/(yN_1+zN_2+xN_3)] \\ &+N_3\ln[xN_3/(yN_1+zN_2+xN_3)]\}, \quad (33)\end{aligned}$$

where ΔS_{31} = the entropy of mixing polymer 3 with associated liquid 1, (see Eq. (25)) and $\Delta S_{\widehat{312}}$ = that of mixing this mixture with associated liquid 2. (The average degree of "polymerization" of associated liquid 2 = z.) Hence,

$$\Delta\bar{S}_1'' = -R(\ln v_1 + v_2 + v_3 - yv_2/z - yv_3/x) \quad (34a)$$

$$\Delta\bar{S}_2'' = -R(\ln v_2 + v_3 + v_1 - zv_3/x - zv_1/y) \quad (34b)$$

$$\Delta\bar{S}_3'' = -R(\ln v_3 + v_1 + v_2 - xv_1/y - xv_2/z) \quad (34c)$$

For the single liquid approximation,

$$\theta yN_1 = zN_2, \quad N_0 = yN_1 + zN_2 = (1+\theta)yN_1,$$

$$\begin{aligned}\Delta S''' = \Delta S'' + R\{&N_1\ln[yN_1/(yN_1+zN_2)] \\ &+N_2\ln[zN_2/(yN_1+zN_2)]\}, \quad (35)^{[11]}\end{aligned}$$

(18) R. L. Scott, *J. Chem. Phys.*, **17**, 279 (1949).

(19) For two polymers, the critical value of μ ($\Delta\bar{H}_1 = RTy\mu v_3^2$) is several orders of magnitude smaller than that for two normal liquids (μ=2) or for a polymer-solvent system (μ=1/2) see Eq. (2) in reference 18).

(20) This expression of $\Delta S_{\widehat{23}1}$ is a rough approximation obtained by assuming hypothetically that the mixture of polymer 3 and associated liquid 2 is a homogeneous polymer.

and then,

$$\Delta\bar{S}_0''' = R\{v_3/x + (1/2)[1/(1+\theta)y + \theta/(1+\theta)z]v_3^2 + \cdots\cdots\} . \quad (36)$$

Actually, the problem of "association" is far more complicated than appears above. Thus the present treatment includes many questions to be discussed. First, somewhat questionable situation in separate evaluation of the entropy and energy term may not be permissible especially in the systems in which one or two components are associated liquids. Next, we must distinguish between hydrogen bonded liquids and those associated simply because of the dipole moment of the molecules, and between a three dimentional "polymer" network such as water which is able to form tetrahedral bonds per molecule and the linear "polymer" such as alcohols in which molecules with capacity for only two bonds per molecule are combined with each other. In short, the essential feature of the potentials between like and unlike pairs must be clearer. It is the purpose of this chapter, however, to indicate the possible applicability of the above procedure for rough estimation of the entropy in these systems.

Summary

The free energy expression derived by Scott for the polymer-mixed solvents system are refined and amplified, removing the assumptions which are not always applicable to the actual cases, although it was introduced by him for the sake of simplicity.

Owing to scantiness of the available data and to difficulties of exact calculation, the phase diagrams of the system using the results obtained are not given here. Determination of plait points and the problems in the osmotic pressure measurement in mixed solvents will be discussed elsewhere. Here, we confined ourselves to formulate the free energy expression for various systems also involving the systems in which one or two of the constituents are associated liquids as a special case where the assumption (b) is far from true. Application of the result obtained to some problems in viscosity, osmotic pressure, and swelling phenomena will be presented in the following articles.

This paper was presented at the Annual Meeting of the Tokyo Institute of Technology, where the treatment of associated liquids was discussed with particular reference to the applicability of the above methods to the thermodynamic problems of association.

In the writer's opinion, the generality of the thermodynamic function derived here in the application to equilibria involving transformation between various "polymeric" species of the associated liquid may be accessible when the volume effect of the associated liquid on the entropy term in these systems must be encountered. Obviously the Flory-Tobolsky-Bratz treatment is applicable only to the linear "polymer" such as alcohol, and we may go too far to say that our treatment is also applicable to the three dimentional "polymer". Our treatment is supposed, however, to be not far from true even in such a case, since the entropy of mixing in the above systems containing associated liquids as one or two components was formulated on the assumption that the submolecules of the "polymer" are distributed at random. i. e., this corresponds to the Bragg-Williams approximation.

The author expresses his appreciation to Professor A. Harajima and S. Ichimura for their kind reading and some suggestions, and to the director, K. Makishima, for his encouragement and support to this work.

Laboratory of Textile Chemistry,
Tokyo Institute of Technology, Tokyo

Note on Polymer-Mixed Solvent System II. Application of the Previous Treatment

Tôru KAWAI

(Received January 18, 1952)

Introduction

In order to investigate the state of the polymer molecules in the solvent, it is necessary to draw one's conclusion by summarizing the information obtained from various methods of physico-chemical measurements, i. e., viscosity, osmotic pressure, light scattering,

swelling and others. This paper deals with discussions of the interaction exhibited by several polymer-mixed solvents systems from the results of these measurements. Employing the partial molal free energy expression obtained in Article I, the phenomenon that the first portions of the addition of non-solvent improve the solvent ability of the medium in some cases and the abnormality which arises in the cases in which one or both of the mixed solvents are an associated liquid, will be interpreted.

Relationship between Intrinsic Viscosity and Thermodynamic Quantity μ

We are going to focus our attention on one polymer molecule and consider the equilibrium between an effective volume pervaded by a polymer chain and its environments. As is seen in our treatment applied to the explanation of the Schulz's osmotic pressure equation,[1] the activity a_s of the solvent in the region occupied by a polymer molecule is given by

$$\ln a_s=\Delta\bar{F}_{1s}/RT=\ln(1-v_{2s})+v_{2s}+\mu' v^2_{2s}+Av_{2s}^{1/3}-Bv_{2s}, \quad (1)$$

where $\Delta\bar{F}_{1s}$ is the partial molal free energy of solvent and v_{2s} the volume fraction of polymer, subscript s showing the spherical region in which a polymer molecule is distributed. A and B are constants somewhat dependent on molecular weight, solvent type, etc., and μ' is an interaction parameter, a little different from true thermodynamic quantity μ as was discussed[1] in our previous paper.

An analogous procedure can be applied to the polymer 3-mixed solvents 1 and 2 system, so long as the single liquid approximation may be permissible. Thus,

$$\ln a_s=\Delta\bar{F}_{0s}/RT=\ln(1-v_{3s})+v_{3s}+\mu' v^2_{3s}+Av_{3s}^{1/3}-Bv_{3s}, \quad (1')$$

where μ' is supposed to be a little larger than $\mu_s+\mu_{30}$ used in Article 1 as mentioned above. ($\mu'=\mu_s'+\mu_{30}$). The above procedure is entirely equivalent to that of the swelling equilibrium. All the terms in the right-hand side of Eq. (1') except $Av_{3s}^{1/3}$ are assumed to correspond to the dilution of a polymer molecule with the solvent. Thus, these must be replaced by the partial molal free energy expression derived in Article 1, although some modifications are still required due to the above restriction for the number of configurations. The relationship between intrinsic viscosity and thermodynamic quantity μ can, however, be derived as a rough approximation from Eq. (1'). If the single liquid approximation may be allowed, we may write for the condition of the equilibrium between the above two regions at infinite dilution.

$$\ln a_s=\Delta\bar{F}_{30}/RT=\ln(1-v_{3s})+(1-B)v_{3s}+(\mu_s'+\mu_{30})v^2_{2s}+Av_{3s}^{1/3}=0. \quad (2)$$

Thus we can obtain the relation between v_{3s} and $\mu_s'+\mu_{30}$. The volume fraction v_{3s} in the spherical region is related to intrinsic viscosity $[\mu]$ as follows, including φ function representing the effective permeation of the flowing solvent through the domain of polymer chain in the Debye and Buche's treatment,[2]

$$[\mu]=[(\mu_r-1)/c]_{c\to 0}=0.0025\,\varphi/v_{3s}\rho, \quad (3)$$

where c is the concentration in g. per litre and ρ the density of the polymer.

The above treatment is entirely equivalent to that of Flory who discussed the configurations of a polymer molecule in a binary polymer-solvent system.[3] Although the true thermodynamic equilibrium between the above two regions is discussed for the single liquid approximation here, it is easily seen that the result obtained is reduced to the Flory's when his expression α, the factor by which linear dimension of the distribution of segments becomes larger than that of random flight configurations owing to long range interference is employed. However, further discussion concerning the problems of selective adsorption, volume effect of solvent, etc. may become possible when the free energy expressions in Article 1 are used. Comparison of this treatment with some viscosity data will be presented elsewhere in more detail.

Now the relation Eq. (2) is expressed as follows;

$$F(v_{3s})=-(\mu'_s+\mu_{30})v^2_{3s}, \quad (4)$$

where

$$\mu_{30}=(V_0/RT)[-\theta/(1+\theta)^2\times A_{12}+1/(1+\theta)\times A_{13}+\theta(1+\theta)\times A_{23}]. \quad (5)$$

(The notation of these equations is similar to what was employed in Article 1.)

(1) T. Kawai, This Bulletin, **24**, 69 (1951).

(2) P. Debye and A. M. Buche, *J. Chem. Phys.*, **16**, 573 (1948).

(3) P. J. Flory, *J. Chem. Phys.*, **17**, 303 (1949).

Differentiating Eq. (4) with respect to θ, if $F(v_{3s})$ and μ'_s can be assumed to be independent of θ[4];

$$d\{F(v_{3s})/v^2_{3s}\}/dv_{3s}\times dv_{3s}/d\theta=d\mu_{30}/d\theta. \quad (6)$$

This result shows that the maximum in intrinsic viscosity and the minimum in thermodynamic quantity μ appear in the ratio θ_c of volume fraction of liquid 2 to that of liquid 1, at which the following condition is satisfied,

$$d\mu_{30}/d\theta=-(1-\theta_c)/(1+\theta_c)\times\mu_{12}+\mu_{23}-\mu_{13}=0, \quad (7)$$

where $\mu_{12}=(V_0/RT)A_{12}$, $\mu_{13}=(V_0/RT)A_{13}$, $\mu_{23}=(V_0/RT)A_{23}$.

Here we assume liquid 1 is solvent ($\mu_{13}<1/2$), and liquid 2 non-solvent ($\mu_{23}>1/2$). Then, the sulution of this equation (7) can afford physical meaning only when $(\mu_{23}-\mu_{13})/\mu_{12}<1$. Namely, when $(\mu_{23}-\mu_{13})/\mu_{12}>1$, the solvent ability of the medium decreases uniformly with increasing θ ($d\mu_{30}/d\theta>0$). When $(\mu_{23}-\mu_{13})/\mu_{12}<1$, the solvent ability of the medium is improved until θ_c, at which Eq. (7) is satisfied, and since then it decreases as θ increases. For the same value of μ_{12}, the larger the $(\mu_{23}-\mu_{13})$ values, the smaller the θ_c. In other words, when liquid 1 has a stronger solvent power and liquid 2 has a stronger precipitating power, the solvent power of the mixture shows a maximum value at smaller content of non-solvent and vice versa. It must be noted, however, that the contribution of μ_{12} to the values of μ_{30} should be considered also. For the same values of $(\mu_{23}-\mu_{13})$, the larger the value of μ_{12}, the larger the θ_c. Besides, as is seen from Eq. (5), the solvent ability of the mixture is improved more effectively by larger values of μ_{12}. Various methods of estimation of the interaction parameters, μ_{12}, μ_{13}, and μ_{23} for a few systems are presented in the next section.

Discussion for Several Actual Systems

The parameter μ_{30}, a measure of the energetical interaction in these ternary systems, consists of three parts as seen in Eq. (5). In this connection, these three parameters μ_{12}, μ_{13}, and μ_{23} must be estimated. When polymer 3 is soluble in liquids 1 and 2 ($\mu_s+\mu_{13}<1/2$, $\mu_s+\mu_{23}<1/2$), the quantities μ_{13} and μ_{23} can be evaluated from osmotic pressure measurements. And when one of the two liquids is non-solvent ($\mu_s+\mu_{13}>1/2$, or $\mu_s+\mu_{23}>1/2$), we must calculate the values of μ_{13} or μ_{23} from swelling measurements. The parameter μ_{12} can be evaluated from vapor pressure data for the binary system liquid 1-liquid 2 as follows: When the entropy of mixing in this system may be assumed to be ideal,[5] we may write

$$\ln\gamma_1=\ln a_1-\ln x_1=\Delta\bar{H}_1/RT=(V_1/RT)A_{12}v_2^2 \quad (8)$$

$$\ln\gamma_2=\ln a_2-\ln x_2=\Delta\bar{H}_2/RT=(V_2/RT)A_{12}v_1^2, \quad (8')$$

where the a's are the activity, the γ's the activity coefficient, and the x's the molar fraction of each component. Therefore, if $\ln\gamma_1$, which can be usually obtained from vapor pressure data, is plotted against v_2^2, and similarly $\ln\gamma_2$ against v_1^2, each set of points will generally fall on a straight line. The slope of the line gives the values of $(V_1/RT)A_{12}$ and $(V_2/RT)A_{12}$ respectively. Considering the approximation used in deriving Eq. (7), we may adopt the mean value of them as $(V_0/RT)A_{12}$. Thus, we can estimate μ_{12}, μ_{23} and μ_{12} separately.

In this connection the systematic experiments involving osmotic pressure, viscosity, swelling and the other measurements should be required to investigate the interaction of polymer and mixed solvents. Since such series of systematic experimental results have not been presented for any of the polymer-mixed solvents systems, it is necessary to estimate the μ's from the experimental data involving only one or two of the above various measurements.

Now, in spite of the weakness that we can not determine uniquely the effect of the solvents in such a three-components system, the dilution ratio, which is determined by the addition of a non-solvent to a polymer solution of a standard concentration until phase separation begins, may also be useful to estimate roughly the μ's employing condition as follows;

$$\mu_s+\mu_{30}=\mu_s+[-\theta/(1+\theta)^2\times\mu_{12}+1/(1+\theta)\times\mu_{13}+\theta/(1+\theta)\times\mu_{23}]\fallingdotseq 1/2. \quad (9)$$

(4) The constant A in Eq. (2) is not always independent of θ as was seen from its expression. This assumption, however, may be permissible since its dependency on θ does not have any notable effect on our result.

(5) This is true for two non-polar liquids systems, so long as molal volumes of the two liquids do not differ very largely from each other. (see Hildebrand; "Solubility of Non-electrolytes", 3rd Ed. Reinfold Publishing Corp., New York, 1950)

This relationship (9) and Eq. (7) in the preceding section can be used in estimating the μ's respectively.

Employing the methods mentioned above, we are going to discuss the interaction of polymer and two liquids for several actual cases. Yoshioka measured viscosity of polyvinyl acetate in various mixed solvents.[6] Considering the abnormality in the systems involving some associated liquids as components, these systems are to be divided into three; namely, polymer 3-associated liquid 1-non-associated liquid 2, polymer 3-associated liquids 1 and 2, and polymer 3-non-associated liquids 1 and 2.

1. Polymer 3-Associated Liquids 1 and 2

(a) Polyvinyl Acetate-Acetone-Water System.—From the osmotic data[7][8] for polyvinyl acetate-pure acetone system at different temperatures, there is obtained for the interaction parameters $\mu_s=0.47$, $\mu_{13}=-0.04$. According to Eq.(27)in Article 1, $\mu_s=1/2-1/2y$, and thus, the abnormally large value of μ_s was acceptable, although quantitative discussion is impossible owing to the rough approximate treatment in Article 1. Actually, this value of μ_s is extraordinarily larger than that estimated theoretically for a fairly flexible chain[9] and expected also from many experimental facts. Employing the Yoshioka's data, we obtain

from Eq. (7) $0.9\,\mu_{12}-0.04-\mu_{23}=0$

(the condition for $[\eta]_{max.}$, $\theta/(1+\theta)=0.05$[10]),

(10)

and

from Eq. (9) $-0.197\,\mu_{12}-0.029+0.27\,\mu_{23}=0.03$

(the condition for the precipitating point,

$\theta/(1+\theta)=0.27$[6] $\mu_s=0.47$[11]) (11)

From Eqs. (10) and (11), $\mu_{12}=1.53$, $\mu_{23}=1.33$. Adopting these values for μ_{12}, μ_{13} and μ_{23}, the $\mu_s+\mu_{30}$ values are calculated against $\theta/(1+\theta)$ in Fig. 1, compared with those obtained from the Endo's osmotic data,[8] and with intrinsic

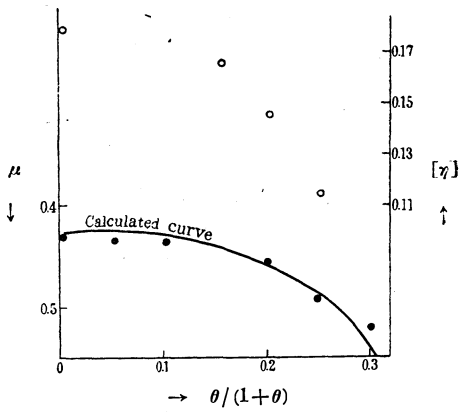

Fig. 1.—Polyvinyl acetate-acetone-water system.

viscosity[6] for various contents of water. On the other hand, the μ_{12} value calculated from the vapor pressure data in the International Critical Table gives extremely large value ($\mu_{12}=7.38$) when Eq. (8) and (8′) are used, but our treatment for two associated liquids system bring out an appropriate value for μ_{12}. From Eq. (26) in Article 1,

$$\ln a_1=\ln v_1+(1-y/x)v_2+\mu_{12}v_2^2 \qquad (12)$$

If we plot $(\ln a_1-\ln v_1)/v_2$ against v_2, the points fall on a line as given in Fig. 2. The slope

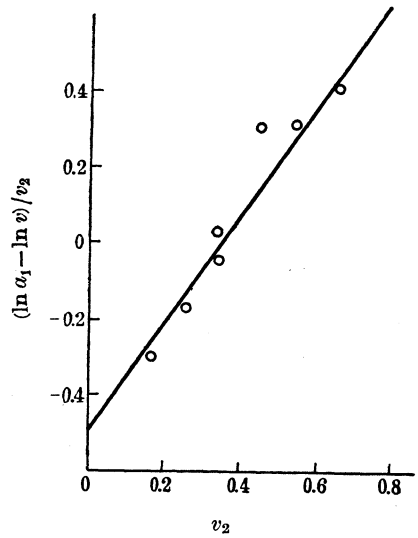

Fig. 2.—An example of calculation of μ_{12} (acetone-water system $\mu_{12}=1.447$).

of the line gives $\mu_{12}=1.45$. The estimation of y/x by exteraporation to $v_3=0$ affords a reasonable value ($y/x=1.5$[12]).

(6) Yoshioka, *J. Chem. Soc. Japan*, **72**, 8 (1951).
(7) G. Browning, J. D. Ferry, *J. Chem. Phys.*, **17**, 1107 (1949).
(8) K. Endo, *J. Chem. Soc. Japan*, **71**, 232 (1950).
(9) B. H. Zimm, A. C. S. Meeting, Sept. (1947) (P. Doty, M. Brownstein and W. Schlener, *J. Phys. Coll.* Chem., **53**, 243 (1949).)
(10) K. Yoshioka, This Bulletin, **23**, 60 (1950).
(11) Comparing Eq. (36) with Eq. (27) in Article I, it is seen that the adoption of this value for μ_s is not unfounded.
(12) Although both x and y may be considerably large, the values of y/x are anticipated in the range from 0.1 to 1.0.

(b) Polyvinyl Acetate-Methanol-Water System.—Endo measured osmotic pressure of polyvinyl acetate in methanol-water mixture of several compositions.[13] The $\mu_s+\mu_{30}$ values for various contents of water are calculated from his data as is shown in Fig. 3. Since the results of the measurements at different

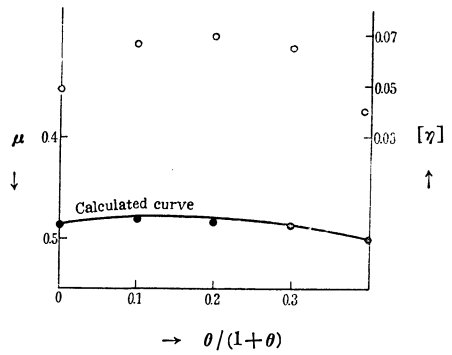

Fig. 3.—Polyvinyl acetate-methanol-water system.

temperatures are not yet published, μ_s and μ_{30} cannot be evaluated separately. It may be said, however, from the information of temperature dependence of intrinsic viscosity[13] that μ_{30} is positive even at θ_c for $[\eta]_{max.}$ in this system. Moreover, the μ_s value is supposed to be not far from 0.45~0.47 and this is acceptable from our procedure as in the case (a). Substituting these values of $\mu_s+\mu_{30}$ for θ in Eq. (9), we can obtain five equations, from which the most appropriate values for the μ's are determined as follows, $\mu_s+\mu_{13}=0.486$, $\mu_s+\mu_{23}=0.714$, $\mu_{12}=0.30$. Then, the composition at which intrinsic viscosity shows a maximum is calculated from Eq. (7) as $\theta=13.6$, $\theta/(1+\theta)=0.12$, showing a satisfactory agreement with experimental results ($\theta/(1+\theta)=0.15$ by Matsumoto,[14] $\theta/(1+\theta)=0.20$ by Endo[13]). Although the change of $\mu_s+\mu_{30}$ with $\theta/(1+\theta)$ is comparatively small in this case, the Endo's measurements[13] show that intrinsic viscosity changes with $\theta/(1+\theta)$ considerably as is shown in Fig. 3. Furthermore, Endo pointed out that in this system the second virial coefficient A_2 in the osmotic pressure equation depends on molecular weight of the polymer to a remarkable degree. These abnormalities cannot yet be explained, but some suggestions may be given for the solution of these problems by our procedure for polymer-two associated liquids system in Article 1.

(13) K. Endo, *J. Chem. Soc. Japan*, **72**, 883 (1951).
(14) S. Matsumoto, *Chem. of High Polymer, Japan*, **6**, 179 (1949).

(2) Polymer 3-Associated liquid 1-Non-associated Liquid 2 System

The above calculation involves implicitly an assumption that the μ_s value in polymer-mixed solvents system equals that of the polymer-one of the mixed solvents system. As can be understood from Eqs. (27) and (36) in Article 1, this assumption may be acceptable for polymer-two associated liquids system, but Eq. (32) in Article 1 shows that it may not be applicable to the present system. It may be said, however, that this assumption may not cause a remarkable error when the associated liquid is solvent (not non-solvent) as easily seen from Eqs. (31) and (27) in Article 1. Actually, the following treatment considering the heat term only can be an explanation of the polymer-mixed solvents interaction in this system, showing a good agreement with experimental data.

(a) Polyvinyl Acetate-Acetone-Ether System.—The binary system of acetone-ether does not show such specific interaction as acetone-water and methanol-water systems and Eq. (8) or (8′) holds its validity. Thus, the μ_{12} value may be calculated from vapor pressure data in International Critical Table ($\mu_{12}=0.54$). Employing this value for μ_{12} and -0.04 for μ_{13}, we can obtain $\mu_{23}=0.34$ from Eq. (7) for the condition of $[\mu]_{max.}$ ($\theta_c/(1+\theta_c)=0.15$.)[6] The $\mu_s+\mu_{30}$ values calculated from these values μ_{12}, μ_{13} and μ_{23} show a good correspondence to intrinsic viscosity for varying compositions of the mixed solvents as is shown in Fig. 4, i. e., the solvent ability of the

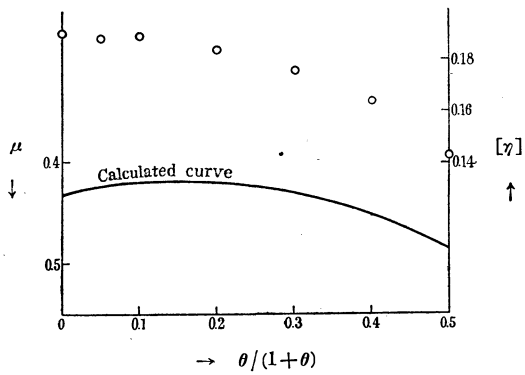

Fig. 4.—Polyvinyl acetate-acetone-ether system.

medium decreases slowly as the content of ether increases without a conspicuous maximum. Obviously, this is due to the small value of μ_{23}. It is not appropriate to say that ether is non-solvent for polyvinyl acetate.

(b) Polyvinyl Chloride-Acetone-Carbon Disulfide System.—As a special case where polymer is soluble only in a certain range of composition of liquids 1 and 2, osmotic pressure, viscosity and swelling are measured in this system by Ishikawa and Kawai.[15] In Fig. 5 the values of μ and $[\mu]$ obtained from

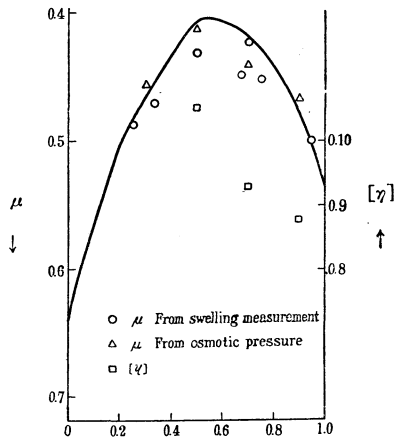

Fig. 5.—Polyvinyl chloride-acetone-carbon disulfide system.

the above three measurements are compared with $\mu_s+\mu_{30}$ calculated from our procedure by adopting $\mu_{12}=0.8$, $\mu_s+\mu_{13}=0.534$, $\mu_s+\mu_{23}=0.650$. The values of $\mu_s+\mu_{13}$ and $\mu_s+\mu_{23}$ are evaluated from the swelling measurement. Although the μ_{12} value calculated from vapor pressure data[16] is 1.04, we adopt $\mu_{12}=0.8$, because this value shows rather better agreement with the experimental facts. Namely, employing this value, there is obtained $\theta/(1+\theta)=0.05$ or 0.78 for the precipitating point and $\theta/(1+\theta)=0.52$ for $[\mu]_{max}$.

Finally, this system is not a special one but is assumed to be one of the systems in which the solvent power of the medium is improved by the addition of diluent until a certain composition is reached, whereas in this case, the polymer is not soluble in the individual constituents of this mixture.[17]

(c) Polyvinyl Acetate-Acetone-Petroleum Benzin System.—Combining Eq. (7) for the condition of $[\mu]_{max}$. ($\theta/(1+\theta)=0.13$[6]) and Eq. (9) for that of the precipitating point ($\theta/(1+\theta)=0.45$[6]), there is obtained $\mu_{12}=0.819$, $\mu_{23}=0.566$, ($\mu_{13}=-0.04$). Considering the approximate treatment used here, it may be questionable to determine the μ's from these two conditions only. Further discussion may, however, be impossible also from the fact that petroleum benzin is a mixture of heptane, hexane and others. In practice, a fairly good correspondence is obtained between thus calculated $\mu_s+\mu_{30}$ and intrinsic viscosity for varying contents of petroleum benzin, as is shown in Fig. 6.

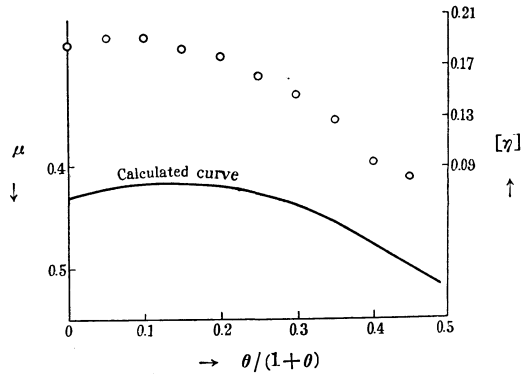

Fig. 6.—Polyvinyl acetate-acetone-petroleum benzin system.

(3) Polymer-3-Non-Associated Liquids 1 and 2

(a) Polyvinyl Acetate-Benzene-Petroleum Benzin System.—From the Nakajima's osmotic data,[18] $\mu_s+\mu_{31}=0.319$ and $\mu_s+\mu_{30}=0.432$ at $\theta/(1+\theta)=0.30$. From these data, calculation follows that $\mu_{12}=0.438$, $\mu_{13}=-0.151$, $\mu_{23}=0.566$, where μ_{23} is that obtained in the case 2(c). Substitution of these values

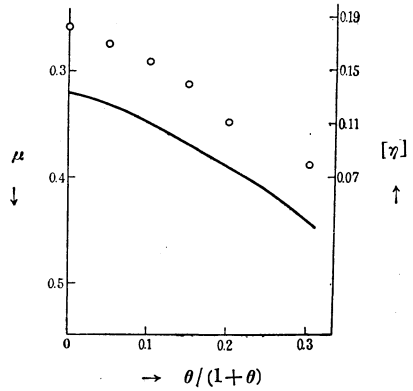

Fig. 7.—Polyvinyl acetone-benzene-petroleum benzin system.

(15) K. Ishikawa and T. Kawai, *J. Chem. Soc. Japan Ind. Chem. Section*, **55**, 173 (1952).

(16) J. V. Zawidzki, *Z. physik. Chem.*, **35**, 129 (1900).

(17) This phenomenon, known as "cosolvency", is seen also in a few other systems, for instance, polystylene-acetone-methylcyclohexane system. (S. P. G. Colombo and H. Mark, *J. Polymer Sci.*, **6**, 295 (1951).)

(18) A. Nakajima, *Chem. of high Polymer, Japan*, **6**, 451 (1949).

for μ_{12}, μ_{13}, and μ_{23} in Eq. (7) gives a negative value for θ_c, which is meaningless in a physical sense. This agrees with the experimental fact that $[\mu]$ decreases uniformly with addition of non-solvent in this system. In Fig. 7, the calculated $\mu_x+\mu_{30}$ values are plotted against $\theta/(1+\theta)$, being compared with the intrinsic viscosity data.[6] Furthermore, the Vold's data[19] of vapor pressure in benzene-heptane system give $\delta_1-\delta_2=2.493$, where δ_1 and δ_2 are the Hildebrand's solubility parameter[20] of the individual liquids. Assuming $V_0=100$, μ_{12} can be estimated as 0.428 from this value of $(\delta_1-\delta_2)$, affording a good coincidence with the above estimation.

Conclusion

Considering the two assumptions which were introduced by Scott in his treatment of phase equilibrium in a ternary system of polymer and two liquids, more general free energy expression to correlate much of the experimental data has been derived in Article 1. When some of the three components are polar, it may be anticipated that the deviation from the Scott's treatment due to invalidity of the assumption (a) is especially important. Thus, our modification of his treatment was checked here with some experimental results principally with regard to the assumption (a). Furthermore, the assumption (b) is far from true especially when one or both of the mixed solvents are associated liquid, but even in such cases, all complicated factors are covered by an approximate method in the present treatment, although this approximate treatment must be discussed in more detail. Actually, the present treatment is applicable to many ternary systems with a fair degree of accuracy. The characteristics of each system are well expressed by the interaction parameters μ_{12}, μ_{13}, and μ_{23}. Thus, the phenomenon that the medium involving non-solvent to some extent behaves as a better solvent than the pure solvent and the abnormal behavior in the systems containing associated liquids as one or two components can be understood from our procedure in Article 1.

The author expresses his appreciation to Mr. K. Yoshioka and K. Endo of the Chemical Laboratory of Tokyo University, for communicating to him privately their experimental data and wishes to thank the director, K. Makishima, for his encouragement and support of this work.

Laboratory of Textile Chemistry,
Tokyo Institute of Technology, Tokyo

(19) R. D. Vold, *J. Am. Chem. Soc.* **59**, 1515 (1937).

(20) The Hildebrand's parameter δi represents the square root of internal pressure (or "cohesive energy density") $(\Delta E^v_i/V_i)^{1/2}$, where ΔE^v_i is the energy of vaporization and V_i the molal volume of liquid i. When the assumption of the "geometric mean' is permissible as in this system where the both two liquids are non-polar, $\Delta H^M_{12}=V_0(\delta_1-\delta_2)^2v_1v_2$, *i. e.*, $\mu_{12}=V_0(\delta_1-\delta_2)^2$.

Formula for the Melting Points of Inorganic Compounds of Type MXO_n

By Shizuo FUJIWARA

(Received March 5, 1952)

General

(**1—a**) Purpose of the present paper is to propose an expression for the melting points of the inorganic compounds of type MXO_n as the function of the ionic radius and the polarizability of the atom, where M^+ is the metal ion and XO_n^- is the anion, e. g., in the case of the alkali nitrates, M^+ denotes lithium, sodium and potassium ion etc., and XO_n^- nitrate ion, NO_3^-.

The melting points of the salts are expressed by T°K and the polarizabilities and the ionic radii of the ions, M^+ and $X^{(2n-1)+}$, are written as α and r respectively. Positive signs are suffixed to α and r of the metal ion, M^+, and the negative signs to those of the ion, $X^{(2n-1)+}$, in the negative ion. The data of the melting points which are necessary for this study have been taken out of the Landolt-Boernstein tables,(1) International critical tables(2) and the

(1) Landolt-Boernstein Physikalisch-chemische Tabellen.

(2) International critical tables.

Smithonian physical tables.[3] Both the values of Goldschmidt[4] and of Pauling,[5] are adopted for the ionic radius. The polarizabilities of the metal ion, M^+, are taken out of the reports of Goldschmidt[6] and of Fajans.[7] The polarizabilities of the ion $X^{(2n-1)+}$ are approximately taken as equal to the cubes of the ionic radius of $X^{(2n-1)+}$. That is, α_- is set as $(r_-)^3$. The values of α given by Goldschmidt and by Fajans have also been utilized.

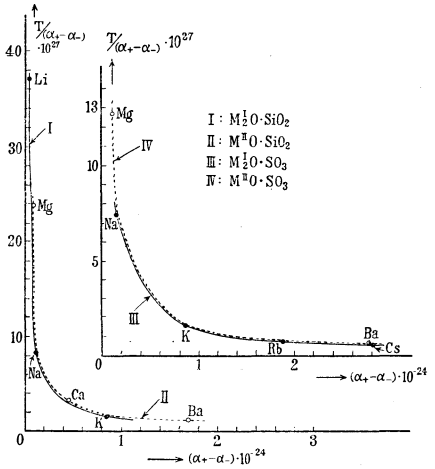

Fig. 1.

In order to find any correlation between T, α and r, these values were presented as graphs in many ways. Considering the results, a simple relation was observed, when the values of $T/(\alpha_+ - \alpha_-)$ was plotted as an ordinate and $(\alpha_+ - \alpha_-)$ as an abscissa. In Fig. 1, the examples of alkali-silicates, alkaliearth-silicates and alkali-sulphates etc. are given. Each line shows very similar type, and the type of the line seems to be approximately 'hyperbolic.' These 'hyperbolic' lines can also be obtained for other series of salts. No other relation has yet been obtained, which is simpler than those in Fig. 1. All the data of T, α and r, necessary for the calculation, are given in Tab. 1. In the table, the data of Pauling, Fajans and Goldschmidt are cited for α and r.

(1—b) Now we consider the series of compounds having different cations and the same anion. According to (1—a), approximate 'hyperbolic' correlation should be observed as a graph of $T/(\alpha_+ - \alpha_-)$ versus $(\alpha_+ - \alpha_-)$ for these compounds. Then an approximate expression (1) is obtained for these salts,

$$T^m \cdot (\alpha_+ - \alpha_-)^n = A \qquad (1)$$

where m and n are the exponent of T and $(\alpha_+ - \alpha_-)$ respectively and A is a constant. In order to find the values of m and n which satisfy (1), the known values of T and $(\alpha_+ - \alpha_-)$ were put into (1) and the values of A were calculated for the several values of m and n. According to the results of calculation, A becomes almost constant for all the members of the series when,

$$m = 1$$

and

$$n = 1/6. \qquad (2)$$

When these values of m and n were applied to other series, the results were also very satisfying. The calculated values of A for several series of salts are also shown in Tab. 2.

Though the values of A remains almost constant in one series of compounds, there are slight differences between the members of the series. These differences are due to the differences between the constituents of the salts. In order to find any regularity in these differences, the present author examined the correlation between the ionic radius of the atom and the values of A. When he has presented these values as a graph of A versus the reciprocal of the ionic radius of the cation, r_+,

Table 1

		Li^+	Na^+	K^+	Rb^+	Cs^+	Mg^{2+}	Ca^{2+}	Sr^{2+}	Ba^{2+}
r_+ (10^{-8}.cm.)	Paul.	0.60	0.95	1.33	1.48	1.69	0.65	0.99	1.13	1.35
	Gold.	0.78	0.98	1.33	1.49	1.65	0.78	1.06	1.27	1.43
α_+ (10^{-24}.cm.^{3})	Faj.	0.08	0.196	0.88	1.56	2.56	0.12	0.51	0.86	1.68
	Gold.	0.067	0.197	0.29	1.90	2.85	0.114	0.57	1.38	2.8
		Al^{3+}	B^{3+}	C^{4+}	Si^{4+}	N^{5+}		P^{5+}		S^{6+}
r^- (10^{-8}.cm.)	Paul.	0.50	0.20	0.15	0.41	0.11		0.34		0.29
	Gold.	0.57		0.2	0.49	0.1~0.2		0.03~0.4		0.34

(3) Smithonian physical tables, P. 254 (1933).
(4) V. M. Goldschmidt *Chem. Ber.* **60**, 1268 (1927).
(5) L. Pauling *J. Am. Chem. Soc.*, **49**, 765 (1927).
(6) V. M. Goldschmidt Geochemische Verteilungsgesetze der Elemente vol. **7**, 60 (1926).
(7) K. Fajans, G. Joos *Z. f. Phys.* **23**, 1 (1924).

Table 2

(1) $(M_2O \cdot B_2O_3)$	α_+(G.), r_+(G), r_-(P), $\alpha_- = (0.2)^3$		
Salt	T°K	A	r_-/r_+
$Li_2O \cdot B_2O_3$	1116	0.069	0.256
$Na_2O \cdot B_2O_3$	1239	0.094	0.204
$K_2O \cdot B_2O_3$	1220	0.120	0.151
$(MO \cdot B_2O_3)$			
$CaO \cdot B_2O_3$	1427 (1)	0.159	0.188
	1373	0.139	〃
$SrO \cdot B_2O_3$	1373	0.145	0.157
$BaO \cdot B_2O_3$	1333	0.158	0.140
(2) $(MO \cdot Al_2O_3)$	α_+(G), r_+(G), r_-(G), $\alpha_- = (0.57)^3$		
$CaO \cdot Al_2O_3$	1960 (1)	0.167	0.54
	1873	0.159	〃
$SrO \cdot Al_2O_3$	2015 (1)	0.207	0.45
	2288	0.237	〃
$BaO \cdot Al_2O_3$	2000 (1)	0.235	0.33
	2273	0.267	〃
(3) $(M_2O \cdot CO_2)$	α_+(G), r_+(G), $r_- = 0.2$, $\alpha_- = (0.2)^3$		
$Li_2O \cdot CO_2$	1005	0.065	0.256
$Na_2O \cdot CO_2$	1124	0.085	0.204
$K_2O \cdot CO_2$	1164	0.114	0.151
$Rb_2O \cdot CO_2$	1170	0.130	0.134
$(MO \cdot CO_2)$			
$SrO \cdot CO_2$	1770	0.187	0.157
$BaO \cdot CO_2$	2013	0.239	0.140
(4) $(M_2O \cdot SiO_2)$	α_+(G), r_+(G), r_-(G), $\alpha_- = 0.04$(G)		
$Li_2O \cdot SiO_2$	1474 (3)	0.0807	0.50
$Na_2O \cdot SiO_2$	1361 (3)	0.0997	0.40
$K_2O \cdot SiO_2$	1249 (3)	0.1218	0.294
$(MO \cdot SiO_2)$			
$MgO \cdot SiO_2$	1830 (3)	0.1185	0.50
$CaO \cdot SiO_2$	1515 (3)	0.136	0.369
$SrO \cdot SiO_2$	1853 (3)	0.1946	0.307
$BaO \cdot SiO_2$	1877 (3)	0.2223	0.274
$(MO_2 \cdot SiO_2)$	$\alpha_+ = [r_+(G)]^3$, $\alpha_- = 0.04$(G)		
$ZrO_2 \cdot SiO_2$	2823 (3)	0.261	0.448
$HfO_2 \cdot SiO_2$	2851 (3)	0.265	0.443
$UO_2 \cdot SiO_2$	2881 (3)	0.323	0.371
$ThO_2 \cdot SiO_2$	2882 (3)	0.372	0.351
(5-2) $(M_2O \cdot N_2O_5)$	α_+(G), r_+(G) $\alpha_- = [r_-(P)]^3 = 0.001$		
$NaNO_3$	581	0.443	0.12
KNO_3	614	0.0603	0.083
$RbNO_3$	583	0.0649	0.074
$CsNO_3$	683	0.196	0.067
(5-3) $(MO \cdot N_2O_5)$	α_+(F), $\alpha_- = [r_-(P)]^3$, r_+(P)		
$Ca(NO_3)_2$	834	0.0759	0.111
$Sr(NO_3)_2$	843	0.0887	0.0975
$Ba(NO_3)_2$	865	0.102	0.0817
(6) (M_3PO_4)	α_+(F), r_+(P), r_-(P) $\alpha_- = [r_-(P)]^3$		
Salt	T°K	A	r_-/r_+
Li_3PO_4	1110	0.061	0.57
Na_3PO_4	1613	0.119	0.35
K_3PO_4	1613	0.157	0.256
(7-3) $(M_2O \cdot SO_3)$	α_+(G), r_+(G), r_-(G), $\alpha_- = [r_-(G)]^3$		
Na_2SO_4	1157	0.085	0.35
K_2SO_4	1340	0.131	0.256
Rb_2SO_4	1325	0.147	0.228
Cs_2SO_4	1281	0.152	0.206
$(MO \cdot SO_3)$			
$MgSO_4$	1393	0.0905	0.436
$CaSO_4$	1723	0.1550	0.32
$BaSO_4$	1853	0.2194	0.23

(1) and (3) of melting points shows the source of reference quotation. Other values of melting points have been taken out of reference (2).

strictly speaking, the ratio of the ionic radii, r_-/r_+, one straight line has been obtained and the following expressions (3), (4) have been given,

$$A = a - b(r_-/r_+) \qquad (3)$$

$$T \cdot (\alpha_+ - \alpha_-)^{1/6} = a - b \cdot (r_-/r_+), \qquad (4)$$

where a and b are the constants of positive sign which are characteristic for one series of the salts. Thus the expression (4) is the formula for the melting points of the inorganic compounds of type MXO_n. Several examples showing the linearity functions of (3) are shown in Fig. 2 and 3.

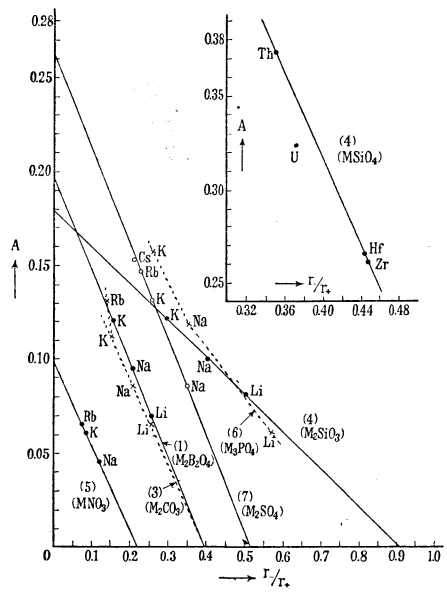

Fig. 2.

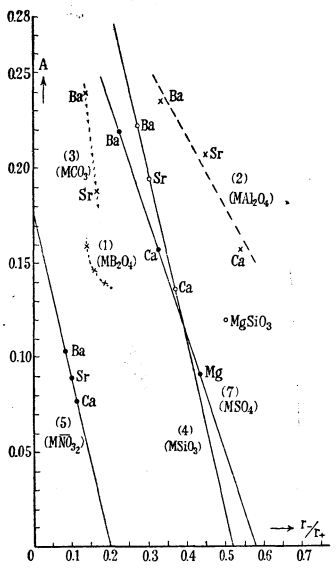

Fig. 3.

Special

(1) **Borates.**—Linear correlation of (4) is observed in the case of borates of lithium, sodium and potassium when the ionic radius of B^{3+}, r_-, is taken as 0.20, and polarizability of B^{3+}, α_-, as $(0.20)^3=0.008(10^{-24}\,cm^3)$. The polarizabilities for the cations are taken from Goldschmidt's data. Such a clear-cut linear correlation was not observed in the case of bivalent métal salts, such as calcium, strontium and barium, as was shown in monovalent metal salts.

Following values of a and b for expression (4) are obtained by the graph, $a=0.195$ and $b=0.482$ for $M_2O\cdot B_2O_3$.

(2) **Alluminates.**—Alluminates of bivalent metals do not give a linear correlation expressed by (4). But when the ionic radius of Al^{3+}, r_-, is taken as 0.57 and the polarizabilities of the cations are taken from Goldschmidt's data, we can obtain an approximately straight line as is shown in Fig. 3. In this case, the polarizability of Al^{3+}, α_-, is set as $(0.57)^3$. When we set α_- as $(0.50)^3$, the cube of the ionic radius given by Pauling for Al^{3+}, the presented graph deviates far from a straight line. Polarizabilities taken out of the data of Fajans and Joos are unsatisfactory. Considering the results of this study, the presented graphs for most of the other series of compounds do not show clear-cut linear correlation when we take the polarizabilities out of the data of Fajans and Joos, and the ionic radii out of those of Pauling. Thus the Goldschmidt's values will be adopted for polarizabilities and ionic radii in the following calculation. When we take the melting points out of the literature (2) as 1873°K for $CaO\cdot Al_2O_3$, 2288°K for $SrO\cdot Al_2O_3$ and 2273°K for $BaO\cdot Al_2O_3$, the presented graph deviates from a straight line exceedingly, whereas, the values taken out of the literature (1) are satisfying. Thus the values given by the latter seem close to the fact, and in this case the following approximate values of a and b are obtained.

$$a=0.350,\quad b=0.327 \quad \text{for} \quad MO\cdot Al_2O_3.$$

This result is an example, where the applicability of the formula (4) for the examination of the observed values of melting points is demonstrated.

(3) **Carbonates.**—The ionic radius for C^{4+}, r_-, is 0.2 and α_- is set as $(0.2)^3=0.008$. The correlation given by the salts of lithium, sodium and potassium is approximately taken as a straight line, and the following values are obtained,

$$a=0.178 \text{ and } b=0.450 \text{ for } M_2O\cdot CO_2.$$

Rubidium carbonate deviates from this line.

The melting points of the bivalent metal carbonates are known only for strontium, and barium, and the linearity can not be examined in this case. But if we make a graph with the two salts, we can obtain the following values,

$$a=0.699, \text{ and } b=3.25 \text{ for } MO\cdot CO_2.$$

(4) **Silicates.**—When the polarizability of Si^{4+} is taken as 0.04, the silicates of lithium, sodium give closely linear correlation and in this case,

$$a=0.183 \text{ and } b=0.200 \text{ for } M_2O\cdot SiO_2.$$

The results are unsatisfactory when α_- is set as $(r_-)^3$.

Calcium, strontium and barium give also another linear correlation, and

$$a=0.472,\ b=0.904 \text{ for } MO\cdot SiO_2.$$

Magnesium compound, $MgO\cdot SiO_2$, deviates from this correlation. The present author examined also the correlation between the compounds of tetravalent metals, $MO_2\cdot SiO_2$. When the ionic radius is taken as 0.87 for Zr^{4+}, 0.88 for Hf^{4+}, 1.05 for U^{4+} and 1.10 for Th^{4+} according to Goldschmidt, and the polalizabilities of these ions are taken as the cubes of the ionic radii respectively, thorium, hafnium and zirconium show linear correlation and in this case,

$$a=0.975 \text{ and } b=1.157 \text{ for } MO_2\cdot SiO_2.$$

Uranium compound deviates from this line.

(5) **Nitrates.**—A linear correlation can be obtained for the nitrates of sodium, potassium and rubidium. In this case, the linear correlation is held for the values both of Fajans and of Goldschmidt. Both of the ionic radii given by Pauling and by Goldschmidt can also be adopted to obtain the linear correlation. And the following values of a and b are obtained for $M_2O\cdot N_2O_5$,

$$\begin{matrix} a=0.113, \\ b=1.57, \end{matrix} \begin{bmatrix} \alpha_+ \text{(Fajans)} \\ r_+ \text{(Pauling)} \end{bmatrix} \quad (5\text{-}1)$$

and

$$\begin{matrix} a=0.097, \\ b=0.440, \end{matrix} \begin{bmatrix} \alpha_+ \text{(Goldschmidt)} \\ r_+ \text{(Goldschmidt)} \end{bmatrix} \quad (5\text{-}2)$$

Cesium nitrate deviates from this correlation. Linearity is better when the Pauling's value is adopted for the ionic radius of sodium than when the Goldschmidt's value is adopted.

Magnesium, strontium and barium give a linear correlation when Fajans' values are adopted for α_+ and Pauling's values for r_+, and in this case.

$$a=0.175 \text{ and } b=0.88 \text{ for } MO\cdot N_2O_5. \quad (5\text{-}3)$$

Goldschmidt's values for α_+ and r_+ are not so satisfying in this case.

(6) **Phosphates.**—The linearity does not sufficiently stand when the values of Fajans are adopted for α_+ and those of Pauling for r_+. The results are also not so satisfying when Goldschmidt's data are utilised. It may be due to the assumption that α_- is set as $(r_-)^3$ and this value is not close to the fact.

(7) **Sulphates.**—Sulphates of monovalent metals give very satisfying results. Especially four compounds of sodium, potassium, rubidium and cesium show a completely linear correlation when Goldschmidt's values are adopted for α_+ and r_+. Cesium salt deviates from the linear correlation slightly when Pauling's value is adopted for the ionic radius. When the polarizability of S^{6+} is set as $(r_-)^3$, following values are obtained for $M_2O\cdot SO_3$,

$$\begin{matrix} a=0.250, \\ b=0.480, \end{matrix} \begin{bmatrix} r_+ \text{(Pauling)} \\ \alpha_+ \text{(Fajans)} \end{bmatrix}, \quad (7\text{-}1)$$

$$\begin{matrix} a=0.255, \\ b=0\cdot495, \end{matrix} \begin{bmatrix} r_+ \text{Golds.)} \\ \alpha_+ \text{(Fajans)} \end{bmatrix}, \quad (7\text{-}2)$$

$$\begin{matrix} a=0.263, \\ b=0.666, \end{matrix} \begin{bmatrix} r_+ \text{(Golds.)} \\ \alpha_+ \text{(Golds.)} \end{bmatrix}. \quad (7\text{-}3)$$

The bivalent metal compounds show satisfying regularity when Goldschmidt's values are adopted for α_+ and r_+, and

$$a=0.36,\ b=0.62 \text{ for } MO\cdot SO_3.$$

The results are not satisfying when the values of α_+ and r_+ given by Fajans and by Pauling are adopted.

Summary

(1) An expression for the melting points of the inorganic compounds of type MXO_n has been obtained as,

$$T\cdot(\alpha_+-\alpha_-)^{1/6}=a-b\cdot(r_-/r_+),$$

and the values of a and b have been given, where T is the melting point in absolute temperature, α_+ and r_+ are the polarizability and the ionic radius of the cation M^+, respectively, and α_-, r_- are the polarizability and the ionic radius of the ion $X^{(2n-1)+}$ respectively.

(2) Considering the results of the practical calculation, the values given by Goldschmidt are to be adopted for the formula as the polarizabilities and ionic radii, and those given by Fajans and by Pauling are less satisfying in some cases. It is probably due to the fact that the Goldschmidt's values correspond to the ions in the solid and those of Fajans and of Pauling to the free ions.

(3) This formula will be useful for the examination of the known values of the melting points and for the estimation of the unknown data.

(4) It is very important that 'melting point' is presented as a function of the variables characteristic for atoms, such as ionic radius and polarizability of atoms.

The author wishes to express his sincere thanks to Prof. Kenjiro Kimura of Tokyo University of Tokyo for his guidance throughout L. this study. Many thanks are also due to Prof. Pauling of California Institute of Technology and Prof. G. T. Seaborg of the University of California, who have taken an interest in the advanced copy of this article and given valuable suggestions.

*Chemical Laboratory, Faculty of Science, Tokyo University, Tokyo**

* Present adress: University of Electro-Communications, 1—5, Shimomeguro, Meguroku, Tokyo.

Synthesis of 2-Amino-4-methyl-5-aminomethylthiazole

By Kiku MURATA and Hideo IKEHATA

(Received March 27, 1952)

For the purpose of obtaining 2-amino-4-methyl-5-aminomethylthiazole presumed as the reduction product of azo-color from thiamin, reduction of 2-amino-4-methyl-5-cyanothiazole, the synthesis of which was reported in a previous report[1], was carried out by several different methods. Among them the reduction by Raney-nickel was successful, although the other methods were not good. The results obtained will be reported here.

Experimental

(1) **Catalytic Reduction with Palladium Charcoal.**—In 30 cc. of acetic and 20 cc. of 20% distilled hydrochloric acid, 1 g. of 2-amino-4-methyl-5-cyanothiazole was dissolved and air in the vessel was replaced by hydrogen gas three times, then 2 g. of palladium charcoal* in acetic acid was added and the mixture was shaken for about 16 hours at room temperature. After absorption of the calculated amount of hydrogen, the solution was separated from the charcoal and condensed in vacuo, and then aqueous sodium carbonate was added to the residue. Orange colored crystal crystallized out from the solution. The crystal was separated from the solvent and recrystallized from hot water. In spite of repeated crystallization, the content of nitrogen in this substance was very low indicating that a loss of ammonia set free from the aminomethyl group produced by the reduction of the cyano group could have taken place. Therefore pure crystal of 2-amino-4-methyl-5-aminomethylthiazole was not obtained.

(2) **Attempted Reduction by Electrolysis.**—One gram of 2-amino-4-methyl-5-cyanothiazole was dissolved in 150 cc. of 20% distilled hydrochloric acid and placed in the cathode chamber of a large cell. In the anode chamber was placed 50 cc of 20% distilled hydrochloric acid. Electrolysis was carried out at the initial current of one ampere and potential of six volts. The electrolyte was evaporated in vacuo. From the residue unreacted 2-amino-4-methyl-5-cyanothiazole was collected again.

(3) **Reduction with Lithium Aluminium Hydride.**—To 50 cc. of absolute ether added with 0.9 g. of lithium aluminium hydride, 130 cc. of absolute ether containing 1 g. of 2-amino-4-methyl-5-cyanothiazole were added drop by drop under stirring in an ice bath, and thereafter the stirring was continued for 30 min. more at room temperature. The destruction of the excess of lithium aluminium hydride was accomplished by 30% solution of sodium hydroxide, and the reaction product was extracted with ether three times. The etherial solution was washed with aqueous sodium bicarbonate, dried with sodium sulfate, and was evaporated. From the residue 0.2 g. of orange colored crystal, m. p. 145—162°C. was obtained, and 0.6 g. of oil containing a mineral substance was obtained from the filtrate. By recrystallization of the crystals from methanol and water needles-shaped crystals, m. p. 165—166°C. were obtained. Mixed melting point with the crystals, m. p. 165—166°C. obtained by the reduction with Raney nickel, did not show depression. However the yield was not satisfactory.

(4) **Catalytic Reduction with Raney Nickel.**—By the method of W. Huber[2], 5 g. of 2-amino-4-methyl-5-cyanothiazole was dissolved in 120 cc. of absolute methanol containing 11 g. of ammonia. This solution was poured into an autoclave with a capacity of 500 cc. and 10 g. of Raney nickel was added.

After filling the autoclave with hydrogen gas until it reached 25 atmosphere, it was shaken at 10—15°C. for two hours. Then the methanol solution was separated from Raney nickel and condensed in vacuo at 35—40°C., and thereby 0.8 g. of crystals containing mineral substance as impurity was obtained. Gaseous hydrochloric acid was passed into the filtrate and allowed to stand overnight in an ice chest. The next day, 4.5 g. of colorless crystals, m. p. 120—225°C. (decomp.) was obtained in 60% yield. The crystals were dissolved in methanol, filtered and recrystallized three times from methanol by adding one third its volume of butanol. Colorless crystals of 2-amino-4-methyl-5-aminomethyl-thiazole hydrochloride m. p. 215—225°C. (decomp.) were obtained (Found: C, 27.56, H. 5.46, Calcd. for $C_5H_9N_3S$. 2HCl; C, 27.68, H. 5.13). On addition of aqueous sodium carbonate to an aqueous solution of the hydrochloride, the free thiazole crystallized out, which after recrystallization from methanol and water, gave orange-colored needles, m. p. 165—167°C.

The authors wish to express their sincere thanks to Dr. Matsukawa of Takeda Institute

(1) K. Murata, This Bulletin, **25**, 16 (1952).

* This charcoal contains 5% of palladium chloride.

(2) W. Huber, *J. Am. Chem. Soc.* **66**, 876 (1944).

who has kindly helped them in this research. Thanks are also due to Mr. Kubomatsu of the Osaka Municipal Institute for Industry who gave them opportunities to use the apparatus in his Institute, and to Dr. Chachin of this Research Institute for his support in executing this work. The cost of this research has been partly defrayed from the Ministry of Education, to which the authors' thanks are due.

Osaka Municipal Institute for Hygiene, Osaka

An Aromatic Hydrocarbon Isolated from Coal Bitumen

By Tsutomu SAKABE and Rokuro SASSA

(Received April 4, 1952)

Introduction

Many studies on the solvent extraction of bituminous coal, especially about specific extraction and extractive disintegration have been done as useful methods to study the chemical constitution of coal. However attempts to isolate a chemically pure substance from the extract and to determine its chemical structure have been scarce, so that no condensed aromatic hydrocarbon which is interesting in reference to the structure of coal has been obtained except methylanthracene isolated by F. Hofmann and P. Damm[1] from pyridine extract of Upper Silesian coal.

E. Donath[2] recognized the existence of anthracene and chrysene from color reactions of the carbon bisulfide and chloroform extracts of Rositzer coking coal, but he was not successful in isolating these substances. A. Pictet and coworkers[3] isolated two hydrogenated derivatives of fluorene from benzene extract of Saar coal.

Analytical compositions of the compounds separated by F. Hofmann and P. Damm suggested the existence of hydrogenated aromatic hydrocarbons having molecular weight of 230—330. From the measurement of molecular weight, boiling point, refractive index and H—C ratio, B. S. Biggs and J. F. Weiler[4] pointed out that the hydrogenation products of benzene extract and residue were both hydrogenated condensed ring compounds and similar in the molecular weight distribution. Therefore it seems reasonable to consider that the extract contains the materials similar to the fundamental unit of coal, in which highly condensed aromatic hydrocarbons may be included.

Furthermore it may be supposed that the crystalline substance noticed by R. V. Wheeler and C. Cockram[5] from the so-called γ_1 fraction of bitumen was a condensed aromatic hydrocarbon. The authors obtained a crystalline substance of high melting point from the benzene extract of Yūbari bituminous coal, and studied its chemical structure by means of ultraviolet absorption spectrum.

Experimental

Preparation of Bitumen—The extraction was carried out in five stages by a rotary bomb of five litres. Six hundred grams of Yūbari coal, ground through 60 Tyler mesh, were extracted once at 220°C., twice at 240°C. and finally twice at 260°C. The duration of each extraction stage was three hours. Two litres of benzene were used in each stage. The benzene solutions obtained from 3 kg. of coal were mixed and benzene was distilled off. The residual material from the extract was separated into the oily bitumen (127 g.) and the solid bitumen (195 g.) according to the ordinary method.

Isolation of Crystalline Substance—The oily bitumen was added to about twice its volume of fresh cold petroleum ether, allowed to stand, and the precipitate which appeared was filtered. The solid bitumen was extracted fifteen times with 500 cc. of petroleum ether each time. The extract was mixed with the precipitate from the oily

(1) F. Hofmann and P. Damm, *Brenn. Chem.*, **3**, 73, 81 (1922): **4**, 65 (1923).
(2) E. Donath, *Chem. Ztg.*, **32**, 1271 (1908).
(3) A. Pictet, L Ramseyer and O. Kaiser, *Compt. rend.*, **165**, 58 (1916).
(4) B. S. Biggs and J. F. Wailer, *J. Am. Chem. Soc.*, **59**, 369 (1937).
(5) C. Cockram and R. V. Wheeler, *J. Chem. Soc.*, **1927**, 700.

bitumen and the fuller's earth. Then the mixture was repeatedly extracted with hot benzene. The benzene solution was concentrated by distillation and allowed to cool to obtain the crystalline substance. After recrystallizing from xylene it was sublimated at 280—290°C. under atmospheric pressure. The pale yellow crystal thus obtained showed the same melting point as that of the material obtained from the mother liquid of recrystallization. The yield of this material was 80 mg., 0.003% of the original coal in dry ash free basis, but the real content of the substance might be higher because of a considerable loss during isolation and purification.

m. p., 304.5—305.5°C.

Anal., Found: C, 94.01; H, 5.99.

Ultraviolet Absorption Spectrum—The ultraviolet absorption spectrum of this material was observed by photo-electric method in *n*-heptane, using Shimazu QM—60 spectrometer as a monochrometer and multiplier photo-tube 1P 28 as the detector of the incident and transmitted light. The estimation of the intensity of monochromatic ray was carried out by direct observation of micro-ammeter. The result obtained is shown in Fig. 1, where the ordinate is the absorbance and the abscissa is the wave length of light in mμ.

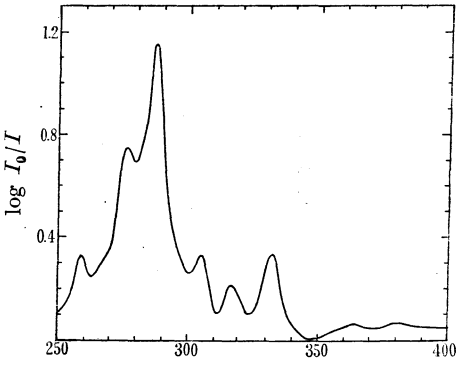

Fig. 1.—Ultraviolet absorption spectrum.

Result

Comparison of the wave numbers calculated from this spectrum with those of many condensed aromatic hydrocarbons having 4 or 5 rings which were reported by H. B. Klevens and J. R. Platt[6] suggests that this material has a skeletal structure of either 1.2-benzanthracene, 3.4-benzophenanthrene or picene. If it is one of the 1.2-benzanthracene or 3.4-benzophenanthrene derivatives, it is considered as one of their methyl derivatives from its analytical composition. But their melting points are so much lower that the material can not be one of them. For instance the highest melting points of their isomers are as follows; 1.2-(3′-methylbenz) anthracence: 194—195°C., 3.4-benzo-6-methylphenanthrene: 80—81°C.[7] If it is a picene derivative, its analytical composition shows very good coincidence with dimethylpicene. Three isomers of dimethylpicene have been synthesized by L. Ruzicka and coworkers, namely 2.11-dimethylpicene,[8] m. p. 293—294°C., 4.9-dimethylpicene,[9] m. p. 380—381°C., and 4.11-dimethylpicene,[10] m. p. 305—306°C. Moreover L. Ruzicka reported that 4.11-dimethylpicene could be sublimated at 260°C. in a high vacuum. Therefore it appears certain that the material is 4.11 (?)-dimethylpicene.

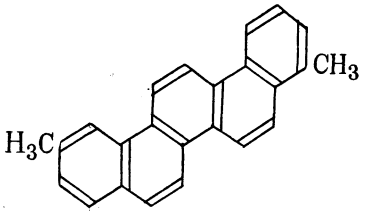

Anal., Calc. for $C_{24}H_{18}$: C, 94.12; H, 5.88.

Discussion

The fact that the Yūbari coal bitumen contains 4.11 (?)-dimethylpicene may suggest that it is one of the hydrocarbon skeletons of fundamental unit of coal and comes in free state by chance. Though definite discussion is impossible owing to our poor knowledge of coal structure, the following facts can be pointed out as the foundation of this opinion;

1. H. C. Howard[11] described that coal had a polymeric character, and that cryoscopic measurement in catechol of the degradation products of Pittsburg seam coal always gave molecular weight of 250—350 due to the dissociating or depolymerizing action of strongly polar solvent catechol, which was considered as the molecular weight of the fundamental unit of coal. The authors found that molecular weight of the fractions of bitumen and pseudobitumen from Yūbari coal were approximately 280—360 when measured by the same

(6) H. B. Klevens and J. R. Platt, *J. Chem. Phys.*, **17**, 470 (1949).

(7) G. Egloff, "Physical Constants of Hydrocarbon IV", Reinhold Publishing Corporation, New York (1947).

(8) L. Ruzicka and E. Mörgeli, *Helv. Chim. Acta*, **19**, 377 (1936).

(9) L. Ruzicka and K. Hofmann, *Helv. Chim. Acta*, **22**, 126 (1939).

(10) L. Ruzicka and K, Hofmann, *Helv. Chim. Acta*, **20**, 1155 (1937).

(11) H. C. Howard, *J. Phys. Chem.*, **40**, 1103 (1936).

method. The molecular weight of dimethylpicene is 306.

2. The coal is considered to be constructed from the crystallite having graphitic hexagonal structure from the viewpoint of X-ray diffraction. The breadths of network along "a" axis of regenerated humic acids from typical Japanese coals were measured by K. Inouye;[12] Yūbetsu coal: 12.4 A., Takamatsu coal: 9.6 A., Takashima coal: 14.3 A., and Shishimachi coal: 7.8 A. It seems to be same order of Yūbari coal. Assuming that the distance between carbon atoms in picene is nearly equal to graphite, the molecular dimension of picene is 11.3 A.

3. By the study about the hydrogenation products of benzene extract and residue from Edenborn coal, B. S. Biggs and J. F. Weiler[4] found that the ratios of the compounds having 5—7 condensed rings in the hydrocarbon skeletons of extract and residue were 23% and 15% respectively.

4. Picene[13] was included in condensed aromatic hydrocarbons obtained from hydrogenation product of coal which were described in the patents of I. G. Farbenindustrie.

The authors are deeply grateful to Mr. Kazuo Shibata of the Tokugawa Institute for Biological Research for spectral measurements and helpful advice.

Fuel Research Institute
Kawaguchi, Saitama

(12) K. Inouye, This Bulletin, **23**, 132 (1950).

(13) I. G. Farbenind., Brit. Pat. 470,338 (1936).

Sterols and other Unsaponifiable Substances in the Fats of Shell Fishes, Crustacea and Echinodermata. X. Corbisterol

By Yoshiyuki TOYAMA, Minoru KITA* and Tatsuo TANAKA

(Received May 28, 1952)

In the 2nd report of this series,[1] a new sterol named corbisterol was separated from the fat of *Corbicula leana*, and the formula $C_{29}H_{44}O$ or $C_{28}H_{42}O$ was assigned to this sterol on the basis of analysis, iodine value and saponification value of its acetate. The iodine value was determined by the pyridine sulfate dibromide method. In a later study described in the 8th report,[2] however, the determination of unsaturation of this sterol by perbenzoic acid showed a value for its acetate, which was half the value obtained by the pyridine sulfate dibromide method and corresponded to the value calculated for two ethylenic linkages. The determination of hydrogen value may afford a sure means to know the numbers of ethylenic linkages of corbisterol, but both corbisterol and its acetate absorbed hydrogen very slowly, even at an elevated temperature, when hydrogenation proceeded to a certain degree, and the quantitative hydrogenation could not be attained. Bergmann and Ottke[3] pointed out that 7-dehydrosterols are prone to give iodine values considerably higher than the theoretical values, and suggested that corbisterol is a 7-dehydrosterol, probably identical with 22, 23-dihydroergosterol.

The present paper is concerned with a further study of corbisterol by bromination, reduction and ozonolysis of corbisteryl acetate and absorption spectrum of corbisterol. In order to ascertain whether or not the reaction involved in the iodine value determination accompanies substitution, and to what extent if it does, the bromination product was prepared by allowing the pyridine sulfate dibromide solution to react with corbisteryl acetate under the same condition as the iodine value determination. The bromine content of bromination product was found to be approximately 6 atom equivalents per one mole of bromination product, while the total consumption of bromine corresponding to the iodine value was 8 atom equivalents per one mole of corbisteryl acetate. These results may be interpreted by assuming that of the total bromine consump-

(1) Taro Matsumoto and Yoshiyuki Toyama, *J. Chem. Soc. Japan*, **64**, 326 (1943).

(2) Minoru Kita and Yoshiyuki Toyama, *J. Chem. Soc. Japan, Pure Chem. Sect.*, **70**, 451 (1949).

(3) W. Bergmann and R. C. Ottke, *J. Org. Chem.*, **14**, 1085 (1949).

* Present address: The Industrial Research Institute, Osaka Prefecture.

tion 4 atom equivalents are attributed to addition reaction while the remaining 4 atom equivalents are attributed to substitution reaction which causes 2 atom equivalents of bromine to enter into the bromination product and forms 2 moles of hydrogen bromide. Formation of hydrogen bromide in bromination was ascertained in another experiment in which a solution of bromine in chloroform was allowed to react with corbisteryl acetate and hydrogen bromide formed during the reaction was estimated by titration with alkali in a specially devised vessel. The result of titration indicated the formation of as much as 2.9 moles of hydrogen bromide per one mole of corbisteryl acetate while the total consumption of bromine was found to be 8 atom equivalents. Although the titration with alkali can not be thought to give the correct value of the amount of hydrogen bromide formed by substitution, the above results show convincingly that substitution occurs to a considerable extent in bromination. However, it can not be assumed that addition of bromine to all ethylenic linkages has occurred quantitatively in this case, though substitution occurs to a considerable extent. Bromination product prepared from corbisteryl acetate by bromination under thorough cooling showed bromine content lying between 4 and 6 atom equivalents per one mole.

If perbenzoic acid titration represents the real unsaturation, corbisterol should be diunsaturated sterol. It is, however, known that perbenzoic acid titration gives a lower value than the theoretical value for some compounds having conjugate double bonds, as shown by Pummerer, Rebmann and Reindel[4] in the case of several carotenoids and isoprene, the unsaturation of the latter based on perbenzoic acid titration being found to correspond to only one double bond. The presence of conjugate double bonds in corbisterol was suspected from the fact that pyridine sulfate dibromide solution developed a peculiar red coloration with corbisteryl acetate as in the case with tung oil which consists substantially of glyceride of elaeostearic acid having conjugate double bonds. Meanwhile Bergmann advised one of the present authors, Toyama, in a private communication to take an ultraviolet absorption spectrum of corbisterol. Fig. 1 shows ultraviolet absorption curve of corbisterol. The typical absorption spectrum of 5, 7-dienoic sterols is seen in the curve. Corbisteryl acetate shows also a positive Tortelli-Jaffe color reaction.

Corbisteryl acetate was subjected to ozonolysis, and a volatile aldehyde was separated from the product of ozonolysis by its 2, 4-dinitrophenyl hydrazone which formed yellow colored needles and had nearly the same melting point 115–116° as 2, 4-dinitrophenyl hydrazone of ethyl isopropyl acetaldehyde obtained by Bergmann and Low[5] from the product of ozonolysis of poriferasterol. These results seem to indicate fairly certainly that corbisterol has the formula $C_{29}H_{46}O$ and that its structure is 5, 7, 22-triunsaturated C_{29}-sterol as shown below.

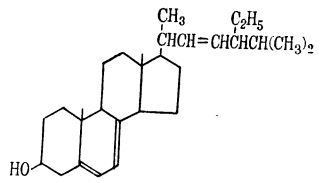

It differs from ergosterol in the group attached to 24–C, the former having ethyl group instead of methyl group at 24–C. It is also to be noted that comparing corbisterol and 7-dehydrostigmasterol prepared from stigmasterol by Linsert,[6] both sterols have nearly the same melting point and specific rotation, but their acetates differ markedly in their melting points.

	Corbisterol	7–Dehydrostigmasterol
M. p.	151–152°	154°
$[\alpha]_D$	−105.5°	−113.1°
M. p. of acetate	152–153°	172°

The results of the biological assay of irradiated corbisterol will be published elsewhere.

Experimental

Crude corbisteryl acetate prepared from the sterol fraction of the fat of *Corbicula leana* was purified by repeated recrystallization. The purified product had m. p. 152–153°, $[\alpha]_D$−72.8°, saponification value 122.1 (calculated for $C_{31}H_{48}O_2$:123.9), and iodine value (pyridine sulfate dibromide method) 221.6 (calculated for $C_{31}H_{48}O_2$:168.2).

Found: C, 81.94%; H, 11.13%.

Calculated for $C_{31}H_{48}O_2$: C, 82.24%; H, 10.69%.

(4) R Pummerer, L. Rebmann and W. Reindel, *Ber.*, **62**, 1411 (1929).

(5) W. Bergmann and E. M. Low, *J. Org. Chem.*, **12**, 67 (1947).

(6) O. Linsert, *Hoppe-Seyler's Z. physiol. Chem.*, **241**, 125 (1936).

Corbisterol obtained from its acetate showed m. p. 151–152°* and $[\alpha]_D$ −105.5° after recrystallization from ethanol.

Found: C. 84.55%; H, 11.58%.

Calculated for $C_{29}H_{46}O$: C, 84.81%; H, 11.29%.

Bromination of corbisteryl acetate.—Bromine in the form of pyridine sulfate dibromide was allowed to react with corbisteryl acetate under the same condition as the iodine value determination. The bromination product was separated using ether, the ether solution washed with water and dried over anhydrous sodium sulfate, and the ether distilled off. Bromide thus obtained was a dark colored solid (Found : Br, 50.00%. Calculated for $C_{31}H_{46}O_2Br_6$: Br, 51.44%). Bromine in chloroform was allowed to react with corbisteryl acetate in a similar way as the iodine value determination. Titration with thiosulfate gave an iodine value 222.5. After titration with thiosulfate, the solution was titrated with sodium hydroxide and it was found that the total amount of acids formed in the course of reaction was 2.9 moles per one mole of corbisteryl acetate.

Corbisteryl acetate (0.123 g.) was dissolved in 5 cc. of ether, and bromine in acetic acid (1:2.5) was added dropwise to the solution under cooling below −10° until the solution became colored by excess of bromine. After keeping the solution under cooling for 2 hours, the insoluble bromide formed was filtered, washed with cold ether and dried under vacuum, yielding 0.0685 g. of white crystalline powder. It melted at 186–188° with darkening (Found : Br, 45.50 %. Calculated for $C_{31}H_{46}O_2Br_6$: Br, 51.44%. Calculated for $C_{31}H_{48}O_2Br_4$: Br, 41.39%). The filtrate from this bromide was washed with thiosulfate solution for the removal of excess bromine. Ether was distilled off under vacuum until the solution became concentrated. On cooling the concentrated solution, 0.046 g. of white crystalline powder was separated. Fractional crystallization of crystalline powder from ether gave 2 fractions, a fraction with m. p. 189–189.5° (decomp.) and Br 46.78% and the other fraction with m. p. 183–184.5° (decomp.) and Br 42.32%.

Absorption spectrum of corbisterol. — Fig. 1 shows ultraviolet absorption spectrum of corbisterol in ethanol (0.0018 g. in 15.5857 g.) The maximum absorptions occurred at 272, 282 and 294 mμ and the molecular extinction coefficients were 9,974, 10,008 and 6,016 respectively.

Reduction of corbisteryl acetate.—Crude corbisteryl acetate (0.085 g.) was dissolved in 20 cc. of warm ethanol, and 3.3 g. of metallic sodium was added in small portions while the solution was refluxed. To the solution then cold water was added and it was extracted with ether. On distilling off ether, there was obtained 0.077 g. of crystalline substance, which had m. p. 144–145°

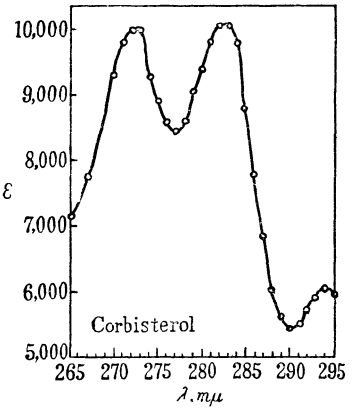

Fig. 1.—Absorption spectrum of corbisterol.

and iodine value 140.6 (calculated for $C_{29}H_{48}O$: 123.0) after recrystallization from ethanol. The molecular extinction coefficients of the reduction product were 503 at 272 mμ, 515 at 282 mμ and 298 at 294 mμ, so that the bulk of original conjugation in corbisteryl acetate must have disappeared by the reduction.

Ozonolysis of corbisteryl acetate.— Corbisteryl acetate (1.4 g.) was suspended in 14 cc. of acetic acid and ozonized oxygen with 3 % of ozone was passed through the solution at a flow rate of 300–400 cc. per minute. After 50 minutes the solution became clear. Ozonized oxygen was passed for further 15 minutes. Zinc powder and a few drops of silver nitrate solution were added to the solution while stirring. After 30 minutes zinc was centrifuged. The solution was poured into water and the emulsion was heated. The volatile matter was distilled and caught in 500 cc. of 2 N-hydrochloric acid solution containing 1 g. of 2, 4-dinitrophenyl hydrazine. The precipitate formed was filtered after standing 20 hours. Yield 0.2 g. On recrystallization from ethanol, its melting point was unaltered at 115–116°. It was optically inactive or very slightly dextrorotatory, if at all.

Summary

From the results of a further study of corbisterol by bromination, reduction and ozonolysis of corbisteryl acetate and absorption spectrum of corbisterol, the structure of corbisterol is believed to be 5, 7, 22-triunsaturated C_{29}-sterol.

The authors are indebted to Prof. W. Bergmann of Yale University for his kind suggestion and advice. The expense of the present study has been defrayed from the Grant in Aid for Fundamental Scientific Research.

Department of Applied Chemistry, Faculty of Engineering, Nagoya University, Nagoya

* The melting points of corbisterol and its acetate recorded in the 8 th report seem to be a little too high. There might have been some error in the melting point determination.

A Note on the Accelerating Action of Biacetyl and Benzil on the Autoxidation of Cyclohexene.

By Osamu SIMAMURA and Motome HAMASHIMA[1]

(Received July, 15 1952)

In view of the recent report by T. Kubota

(1) Present address: Government Chemical Industrial Research Institute, Tokyo, Hatagaya, Tokyo.

and Y. Shimazu[2] that ergosterol reacts with oxygen in the presence of biacetyl in xylene at 30°, we wish to place on record our findings obtained in the course of an investigation of the autoxidation of cyclohexene which was carried out in 1948 to 1949 and the results of which have remained unpublished.

It has frequently been observed that biacetyl accelerates the deterioration of butter and margarine[3] to which it has been added as a flavouring, and promotes the peroxide formation[4] in fat. There seemed to be no doubt that biacetyl played the role of an autoxidation catalyst. The following experiments demonstrated that biacetyl and benzil, probably 1, 2-diketones as a class, act as a catalyst in the autoxidation of cyclohexene. Purified cyclohexene freshly distilled before use was shaken in an atmosphere of 760 to 780 mm. Hg of oxygen in a Warburg manometer in the dark at 27°. After the lapse of an induction period ranging from 8 to 10 hours the oxygen uptake became gradually noticeable (about 0.1 cc. of oxygen per cc. of cyclohexene in the course of 20 hours). When 7.0 mg. of biacetyl per cc. of cyclohexene was present, no induction period was observed and the oxygen uptake began immediately with a rate of 0.12 cc. per hour per cc. of cyclohexene, a further absorption ensuing with a characteristic behaviour of autocatalysis. Biacetyl itself absorbed oxygen at a rate of about 0.0025 cc. per hour per cc. of biacetyl after an induction period of 9 hours. Benzil (20.9 mg. per cc. of cyclohexene) also was found to exert a similar, though somewhat weaker, accelerating effect, the initial rate of oxygen uptake being 0.04 cc. per hour per cc. of cyclohexene. The cyclohexene used in the above experiments could not be considered as quite free from any traces of the peroxide; for, though a freshly distilled sample gave hardly perceptible coloration with ferrous ammonium sulfate and ammonium thiocyanate solutions, 1 cc. of it, added to 5 cc. of acetic acid, 1 g. of potassium iodide and 50 cc. of water and, after 20 minutes, the liberated iodine titrated, consumed 0.08 to 0.15 cc. of N/20 sodium thiosulfate solution.

Incidentally, the addition of 43.2 mg. of bromanil per cc. of cyclohexene inhibited the absorption of oxygen by cyclohexene, the induction period being prolonged to more than 60 hours. This observation may be of interest in view of the action of chloranil as an effective chain transfer agent in the polymerization of styrene.[5]

Department of Chemistry, Faculty of Science, Tokyo University, Tokyo.

(2) T. Kubota and Y. Shimazu, *Proc. Japan Acad.*, **28**, 80 (1952).

(3) N. King, *Chem. Abstr.*, **25**, 4943 (1931). T. Tapernaux, ibid., **27**, 785 (1933). B. W. Hammer, ibid., **29**, 6658 (1935). H. Schmallfuss and U. Stadie, ibid., **39**, 3370 (1945).

(4) W. Ritter and T. Nussbaumer, ibid., **33**, 9467 (1939). Recently A. Reinart (ibid., **44**, 2664 (1950)) reported that biacetyl also has a deleterious effect on the carotene and bixin.

(5) J. W. Breitenbach and V. Taglieber, *Ber.*, **76**, 272 (1943).

Dielectric Dispersion of Copper Sulphate Pentahydrate Crystals

By Ryôiti KIRIYAMA and
Hideko IBAMOTO

(Received August 28, 1952)

Temperature dependences of the dielectric constants and losses of copper sulphate pentahydrate single crystals perpendicular to their ω $(1\bar{1}\bar{1})$ planes have been measured from $-180°$ to 120°C and at frequencies between 300 c and 3 Mc.

In order to approach to equilibrium conditions under the water vapour pressures for given temperatures, we put a considerable amount of the crystal grains in the bottom of the glass cell, thus we were able to obtain reproducible values up to 96°C which coincides with the dehydration temperature.

At temperatures higher than about 70°C, there is a distinct dispersion of the dielectric constants. Up to 96°C they decrease gradually at higher frequencies (600 kc and 3 Mc). The

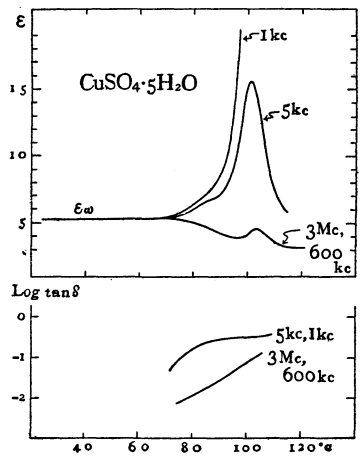

Dielectric Dispersion of Copper Sulphate Pentahydrate Crystals

values are 5.36 at 20° and 4.0 at 95°C. In this frequency region, we have obtained the same values for several specimens, therefore, this fall must be of an essential nature of this crystal. At lower frequencies (500 c to 5 kc), on the contrary, the higher the temperature, the larger is the dielectric constant. In this frequency region, however there has been found no saturation phenomenon and also no loss maximum.

The dielectric constants increase rapidly when dehydration occurs. Such a phenomenon is common in many dehydration processes of hydrated crystals, and this is originated mainly from the proton-conduction in the absorbed layer of dehydrated water molecules on the crystal surfaces.

The reason of the dispersion phenomenon below the dehydration temperature may be attributed to the orientation polarization of the fifth water molecule of this pentahydrate. This water molecule is linked with other water molecules by hydrogen bonds as shown by the determination of crystal structure, and resembles to the molecules in ice. Other four water molecules coordinated directly to the copper ion do not contribute presumably to the orientation polarization.

Next, the reason of the gradual fall of the dielectric constants at higher frequencies must be the diminution of protonic polarization caused by the expansion of the crystal lattice as the temperature rises. Such a protonic polarization may have a larger value when a proton is forming a hydrogen bond between two oxygen atoms than simply in a hydroxyl radical. When the strength of a hydrogen bond is weakened by the lattice loosening at higher temperatures, such an ionic nature of this hydrogen atom will decrease and a covalent nature of it will increase. Then, as the result of such protonic polarization, the dielectric constant at higher frequencies where no orientation polarization takes place falls down gradually with temperature.

Datails will be published in this Bulletin.

Department of Chemistry, Faculty of Science, Osaka University, Osaka

Analytical Chemistry by means of Oxalic Acid. II. On the Quantitative Analysis of Barium[1]

By Tamotsu MATSUMOTO

(Received April 7, 1952)

The methods of precipitating barium as barium oxalate or its various hydrates have been studied by many authors.[2] As to the application of the reaction for determining barium, several investigations[3] have been published, but the results were not effective. The present writer employed 50% alcohol as washing liquid of barium oxalate, and established a method in which barium is estimated gravimetrically as barium oxalate hemihydrate or volumetrically by titrating oxalic acid combined with barium with potassium permanganate.

1. Gravimetric Method.—Procedure:—To 25ml. of hot 0.1 M barium chloride solution which is acidified with dilute hydrochloric acid so that a large quantity of barium oxalate precipitate once formed may be dissolved, a definite quantity of hot 5% ammonium oxalate solution is added with constant stirring. When dilute ammonia water is added drop by drop to the solution until the latter becomes just pink with phenolphthalein, the solution being well agitated all the while, a crystalline precipitate is produced. Now the whole mass in the beaker covered with watch glass is warmed on the water-bath for about 2 hrs., and is left to stand over night. The precipitate after being washed several times by decantation using 50% alcohol solution is filtered with a 1. G. 5. glass filter. Then the precipitate is dried at 100°—105°C. for 2 hrs. in the air-bath, and weighed as barium oxalate hemihydrate.

A) Influences of Amounts of Amm. Oxalate and Dilution of Sample Solution—.In order to find out the most suitable amount of ammonium oxalate which should be taken for the precipitation of barium oxalate and also to learn the influence of dilution of the sample solution, a series of experiments were carried out, the results of which are shown in Table 1.

When the molar ratio of ammonium oxalate to barium exceeds 2.8 and the concentration of the sample solution is less than 0.1 M, the precipitation is not complete. A large quantity of ammonium oxalate seems to form a complex salt of ammonium barium oxalate.[4] So the precipitant should be used in a slight excess, and the sample solution should not be diluted to less than 0.1 M with water.

Table 1

(Ba used is 0.3434 g.)

Water added	5% amm. oxalate		$BaC_2O_4 \cdot 1/2H_2O$	Ba found	Error
		molar ratio			
ml.	ml.	to Ba	g.	g.	mg.
—	10	1.4	0.5860	0.3434	±0
—	20	2.8	0.5858	0.3433	−0.1
—	40	5.6	0.5853	0.3430	−0.4
—	60	8.4	0.5843	0.3424	−1.0
—	80	11.2	0.5834	0.3419	−1.5
25	10	1.4	0.5852	0.3429	−0.5
50	10	1.4	0.5824	0.3413	−2.1
100	10	1.4	0.5805	0.3402	−3.2

Solubilities of Barium Oxalate.—The precipitate of barium oxalate prepared by the above method is dissolved in a solvent, and from the quantity of the precipitate dissolved the solubility of barium oxalate is calculated. Table 2 shows the solubilities of barium oxalate in distilled water as well as in 50% alcohol at 25°—26°C.

Table 2

Solvent	Time that solvent is in contact with ppt. hr.	$BaC_2O_4 \cdot 1/2H_2O$ dissolved in 50 ml mg.	Solubility (25°—26°C) mg./l.	Solubility (25°—26°C) mol/l.	Solubility product
water	8	6.1	121	5.4×10^{-4}	2.9×10^{-7}
	24	6.3			
	32	6.3			
50% alc.	8	trace	3.9	1.7×10^{-5}	2.9×10^{-10}
	24	0.2			
	32	0.2			

From the above results it has been found that the 50% alcohol solution is suitable to the washing-

(1) Read before at the 6 th Ordinary Meeting of the Chugoku-Shikoku Branch of the Chemical Society of Japan in January, 1952.

(2) A. Souchay and E. Lenssen, *Ann.*, **99**, 36 (1856); Groschuff, *Chem. Ber.*, **34**, 3313 (1901); Herz and Muss, *Chem. Ber.*, **36**, 3718 (1903).

(3) Barbu N. Angelescu, *Bulet. Soc. de Chimie din Romania*, **5**, 12 (1923); J. Haslam, *Analyst*, **60**, 668 (1935), C. Diaz Villamil, *An. Soc. espan. Fisica Quim.*, **34**, 580.

(4) R. Scholder, E. Gadenne and H. Niemann, *Chem. Ber.*, **60**, 1489 (1927).

of barium oxalate. Moreover the solubility of this salt in water is 3.8×10^{-4} mol/l. (18°C.) according to F. Kohlrausch[5] and 6.8×10^{-4} mol/l. (26°C.) to Herz and Muss.[6]

B) Influence of Various Salts Present.—In order to observe the influence of various salts on the precipitation of barium oxalate, 25 ml. of 0.1 M barium chloride solution was mixed with a definite quantity of various salts, and this solution was treated in the manner described before. The results are shown in Table 3.

Table 3

(Ba used is 0.3434 g.)

Salt mixed	g.	$BaC_2O_4\cdot1/2H_2O$ g.	Ba g.	Error mg.
NaCl	2	0.5857	0.3432	−0.2
〃	〃	0.5859	0.3433	−0.1
KCl	2	0.5859	0.3433	−0.1
〃	〃	0.5860	0.3434	±0
KNO_3	2	0.5858	0.3433	−0.1
〃	〃	0.5859	0.3433	−0.1
NH_4Cl	2	0.5857	0.3432	−0.2
〃	〃	0.5860	0.3434	±0
NH_4NO_3	2	0.5855	0.3431	−0.3
〃	〃	0.5852	0.3429	−0.5
〃	5	0.5825	0.3413	−2.1
〃	〃	0.5830	0.3416	−1.8

Sod. chloride, pot. chloride, pot. nitrate and amm. chloride show almost no bad influence, but amm. nitrate seems to form a complex salt with barium oxalate, which makes the value of barium a little low.

2. Volumetric Method.—J. Haslam[7] studied the titration of the barium oxalate which was formed in perchloric acid solution. The present writer applied the following method to the volumetric analysis of barium.

Procedure:—From a definite volume of 0.1 M barium chloride solution the precipitate of its oxalate is prepared under the best condition required in the former method. When dilute nitric acid is added to the precipitate in a glass filter, oxalic acid is liberated. Then the solution in the filter is filtered out with suction and the filter is well washed with distilled water. All the filtrate is kept in a measuring flask and diluted accurately to 250 ml. 10 ml. of the filtrate, acidified with sulfuric acid, is titrated with 0.1 N potassium permanganate in the usual way. The results are shown in Table 4.

Table 4

Ba taken g.	(0.1M-$BaCl_2$) (ml.)	0.1N-$KMnO_4$ (factor = 0.9479) ml.	Ba found g.	Error mg.
0.3434	(25)	52.65	0.3428	−0.6
0.3434	(25)	52.72	0.3432	−0.2
0.3434	(25)	52.70	0.3431	−0.3
0.1374	(10)	21.08	0.1372	−0.2
0.1374	(10)	21.05	0.1370	−0.4
0.1374	(10)	21.08	0.1372	−0.2
0.0687	(5)	10.52	0.0685	−0.2
0.0687	(5)	10.55	0.0687	±0
0.0687	(5)	10.48	0.0682	−0.5

It has been found that the volumetric analysis by means of oxalic acid produces almost satisfactory results.

Summary

(1) Quantitative precipitation of barium as its oxalate hemihydrate was made possible by employing 50% alcohol as washing solution and by drying the precipitate at 100°—105°C. for 2 hrs.

(2) Sod. chloride, pot. chloride, pot. nitrate and amm. chloride produce little influence on this determination, while amm. nitrate positively effects the estimation.

(3) It was found that barium can be determined volumetrically by titrating with potassium permanganate the oxalic acid which is formed when the barium oxalate is decomposed with nitric acid.

The writer wishes here to express his hearty thanks to Prof. Masayoshi Ishibashi in Kyoto Univ. for his kind guidance and encouragement throughout this experiment. The expenses to this research have been defrayed from the Grant in Aid for Fundamental Scientific Research from the Department of Education, to which the writer's thanks are due.

Chemical Institute, Faculty of Science, Okayama Univ., Osaka

(5) Landolt-Boernstein, "Physik. Chem. Tabellen" (1905-36).
(6) Herz and Muss, *Chem. Ber.*, **36**, 3718 (1903).
(7) J. Haslam, *Analyst*, **60**, 668 (1936).

On the Vapor Pressure of Liquid Mixture[1]

By Michio KURATA*

(Received May 22, 1952)

Introduction

The theories of "*regular solutions*" were developed by Hildebrand[2] and others[3] with good success in qualitative description of various properties concerning the vapor pressure of liquid mixture. But these theories seem not to be enough for quantitative discussion, especially for the systems exhibiting appreciable departure from "*regular solution*".

In this paper, we shall develop a theory based on the kinetic theory and derive an equation which relates the vapor pressure of a mixture to its composition and the vapor pressures of its constituents. Of course, it is desirable to develop the statistical theory of "*real solutions*", not of "*regular solutions*", because the statistical method gives the most rigorous approach to the problem in question. However, the equation of vapor pressure which results from this approach will come to have a complex form[4], and this is undesirable for the present purpose of deriving a practical equation.

Vapor Pressure of Regular Solution

At first, we will treat of regular solution and confirm that the kinetic method coincides with the statistical method. The treatment of this section corresponds to Penner's method for the vapor pressure of pure liquid[5].

Let us consider the regular solution composed of liquids A and B and denote the molar fractions of each component by x_A and x_B. According to the kinetic theory of gases, the velocities of condensation of each kind of molecule per unit area of surface of the solution, C_A and C_B, may be given by

$$\left.\begin{aligned} & C_A = p_A/(2\pi m_A kT)^{1/2} \\ \text{and} \quad & C_B = p_B/(2\pi m_B kT)^{1/2}, \end{aligned}\right\} \qquad (1)$$

where k is the Boltzmann constant and T the absolute temperature. And p_A and p_B represent the partial vapor pressures of the indicated components, m's are the masses of molecule of the indicated species. Here the condensation coefficient is assumed to be unity for simplicity's sake. On the other hand, if we use the theory of absolute rate[6], the velocities of vaporization per unit area, D_A and D_B, are given by

$$\left.\begin{aligned} & D_A = (x_A n)[(kT/h)(F_A^{\ddagger}/F_A)\exp(-\tilde{u}_A/kT)] \\ \text{and} \quad & D_B = (x_B n)[(kT/h)(F_B^{\ddagger}/F_B)\exp(-\tilde{u}_B/kT)], \end{aligned}\right\} \qquad (2)$$

Here n is the total number of molecules per unit area, h is the Planck constant and $\tilde{u}_A$ and $\tilde{u}_B$ are the activation energies of vaporization of molecule-A and -B respectively. And F_A (or F_B) represents the partition function of molecule A (or B) at the equilibrium state, $F_A^{\ddagger}$ (or $F_B^{\ddagger}$) represents the partition function of the activated molecule, which does not include the contribution due to translational motion in the one degree of freedom along the coordinate of vaporization, and they are connected with the free volumes ω_A (or ω_B) and $\omega_A^{\ddagger}$ (or $\omega_B^{\ddagger}$) by the familiar relations[7],

$$\left.\begin{aligned} & F_A = (2\pi m_A kT/h^2)^{3/2}\cdot\omega_A \\ \text{and} \quad & F_A^{\ddagger} = (2\pi m_A kT/h^2)\cdot\omega_A^{\ddagger 2,3} \text{ etc.}, \end{aligned}\right\} \qquad (3)$$

respectively. Further, as is shown in Fig. 1 schematically, $\omega_A^{\ddagger}$ and $\omega_B^{\ddagger}$ can be approximated by the cell volume, v, of the quasi-crystalline lattice or by the volume occupied by one liquid molecule; i. e.

$$\omega_A^{\ddagger} = \omega_B^{\ddagger} = v = (1/n)^{3/2}. \qquad (4)$$

---

* Present address; Department of Industrial Chemistry, Faculty of Engineering, Kyoto University, Kyoto.

(1) Read at the 2nd Annual Meeting of the Society in April, 1949.

(2) J. H. Hildebrand, "Solubility of Non-electrolytes", New York, 1939.

(3) For example, R. H. Fowler and E. A. Guggenheim, "Statistical Thermodynamics", Cambridge, 1939, Chap. VIII.

(4) T. S. Chang, (*Proc. Camb. Phil. Soc.*, **35**, 265 (1939)) had treated of liquid mixture of single size molecule and double size molecule.

(5) S. S. Penner, *J. Phys. Colloid Chem.*, **52**, 949, 1262 (1948); See also, M. Mizushima, *Kagaku*, **16**, 67 (1946), in Japanese.

(6) S. Glasstone, K. J. Laidler and H. Eyring, "The Theory of Rate Processes", New York, 1941.

(7) See ref. (6) or ref. (2).

Then Eq. (2) with Eqs. (3) and (4) becomes

$$\left.\begin{aligned} &D_A=x_A(kT/2\pi m_A)^{1/2}(1/\omega_A)\exp(-\tilde{u}_A/kT) \\ &\text{and} \\ &D_B=x_B(kT/2\pi m_B)^{1/2}(1/\omega_B)\exp(-\tilde{u}_B/kT). \end{aligned}\right\} \quad (5)$$

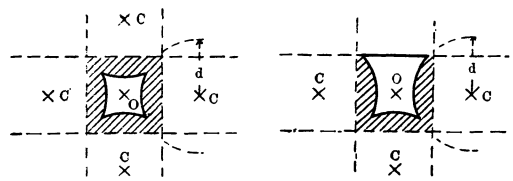

(i) free vol. of liquid molecule, ω. (ii) free vol. of surface molecule.

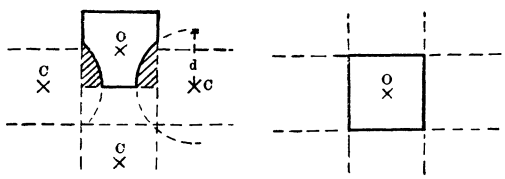

(iii) free vol. of activated molecule, $\omega^{\ddagger}$. (iv) free vol. of gas molecule, v.

o: center of the molecule whose free volume is in question.
c: center of the adjacent molecules of o-molecule.
d: diameter of molecule.
Shaded area: Region excluded by c-molecules.

Fig. 1.—Schema of free volume.

As the velocities of condensation should be equal to those of vaporization in equilibrium, we put $C_A=D_A$ and $C_B=D_B$ and then obtain

$$\left.\begin{aligned} &p_A=x_A(kT/\omega_A)\exp(-\tilde{u}_A/kT), \\ &p_B=x_B(kT/\omega_B)\exp(-\tilde{u}_B/kT). \end{aligned}\right\} \quad (6)$$

Now if we denote the potential energies of A and B molecules surrounded only by A (or B) molecules by $-u_A$ (or $-u_{AB}$) and $-u_{AB}$ (or $-u_B$), respectively, and use the Bragg-Williams approximation, the total energy U of a solution composed of $N(=N_A+N_B)$ molecules is given by

$$U=N_Au_A+N_Bu_B+2x_Ax_B\cdot N\Delta u \quad (7a)$$

$$\text{with} \quad \Delta u\equiv u_{AB}-\{(u_A+u_B)/2\}, \quad (7b)$$

and then $\tilde{u}_A$ and $\tilde{u}_B$ are given by

$$\left.\begin{aligned} &\tilde{u}_A=(\partial U/\partial N_A)_{N_B}=u_A+2x_B^2\Delta u \\ &\text{and} \quad \tilde{u}_B=(\partial U/\partial N_B)_{N_A}=u_B+2x_A^2\Delta u. \end{aligned}\right\} \quad (8)$$

Inserting Eq. (8) into Eq. (6) and putting

$$\left.\begin{aligned} &P_A=(kT/\omega_A)\exp(-u_A/kT) \\ &\text{and} \quad P_B=(kT/\omega_B)\exp(-u_B/kT), \end{aligned}\right\} \quad (9)$$

we can get the well-known formulae

$$\left.\begin{aligned} &p_A=x_AP_A\exp(-2x_A^2\Delta u/kT) \\ &\text{and} \quad p_B=x_BP_B\exp(-2x_B^2\Delta u/kT), \end{aligned}\right\} \quad (10)$$

which coincide with the ones obtained by the statistical method[3]. Of course, P_A and P_B are the vapor pressures of pure liquids A and B respectively. And u_A and u_B are connected with the heats of vaporization, λ_A and λ_B, by

$$\lambda_A=u_A-(kT/2) \text{ and } \lambda_B=u_B-(kT/2). \quad (11)$$

Derivation of Practical Equation for the Total Vapor Pressure, P

In order to take into consideration the difference of sizes between A and B molecules which has been ignored in the preceding section, we should use rather the expression of energy of van Laar's type[8],

$$U-(N_Au_A+N_Bu_B)=\varphi_A\varphi_BB\equiv\Delta U, \quad (12)$$

than Eq. (7). Here φ's are the volume fractions and B is the parameter corresponding to $2N\Delta u$ in Eq. (7). As is well-known, Eq. (12) is derived from the consideration that each molecule is surrounded by A and B molecules in proportion of φ_A and φ_B.

In this paper, we will use the following assumption, instead of Eq. (12), for the purpose of deriving a practical equation.

Assumption.—φ_AN_A molecules of A are surrounded by A molecules only and they have the potential energy of $-u_A$. The remaining φ_BN_A molecules of A are surrounded by B molecules only and they have the potential energy of $-u_{AB}$. Similarly, φ_AN_B molecules of B and the remaining φ_BN_B have the potential energies of $-u_{AB}$ and $-u_B$ respectively.

Using this assumption and denoting the free volume of a molecule surrounded by the molecules of different species only by ω_{AB}, we get

$$\left.\begin{aligned} &D_A=x_A(kT/2\pi m_A)^{1/2}[(\varphi_A/\omega_A)\cdot \\ &\exp(-u_A/kT)+(\varphi_B/\omega_{AB})\exp(-u_{AB}/kT)], \\ &D_B=x_B(kT/2\pi m_B)^{1/2}[(\varphi_A/\omega_{AB}) \\ &\exp(-u_{AB}/kT)+(\varphi_B/\omega_B)\exp(-u_B/kT)]. \end{aligned}\right\} \quad (13)$$

These equations correspond to Eq. (5) for regular solution.

(8) J. J. van Laar, *Z. phys. Chem.*, **A 137**, 421 (1928).

Now let us define the "mutual vapor pressure" P_{AB} by the similar relation as Eq. (9),

$$P_{AB}=(kT/\omega_{AB})\exp(-u_{AB}/kT). \quad (14)$$

Then, equating Eqs. (1) and (13) and using Eqs. (9) and (14), we can easily obtain

$$\left.\begin{aligned} p_A&=x_A\varphi_A P_A+x_A\varphi_B P_{AB} \\ \text{and}\quad p_B&=x_B\varphi_A P_{AB}+x_B\varphi_B P_B. \end{aligned}\right\} \quad (15)$$

For practical purposes, we may put

$$x_A\varphi_B+x_B\varphi_A=2(x_Ax_B\varphi_A\varphi_B)^{1/2}, \quad (16)$$

obtaining our final result,

$$P=p_A+p_B=x_A\varphi_A P_A+x_B\varphi_B P_B +2(x_Ax_B\varphi_A\varphi_B)^{1/2}P_{AB}. \quad (17)$$

Comparison of Eq. (17) with the Experimental Data

To make comparison of Eq. (17) with the experimental values, we must evaluate P_{AB}, which is the sole unknown parameter in the equation. In this section, we will use for P_{AB} the value evaluated from the observed value of P, P_{obs}, at a composition $x_A \fallingdotseq x_B$.

Table 1

List of the Systems Compared and the Results Obtained.—I.

System (Ref.*)	°C.	P_{AB}	$\bar{\Delta}$, %
$CCl_4+C_6H_6$ (i)	0	33.3	0.3
	10	58.0	0.3
	20	90.5	0.2
	30	138.0	0.1
	40	206.5	0.1
$CS_2+C_6H_6$ (ii)	0	120.0	2.2
	10	177.0	2.2
	20	263	2.0
	30	380	1.3
	40	530	1.3
$CCl_4+C_2H_5OH$ (i)	34.8	328	3.4
	50	626	3.5
	60	928	3.7
	66	1162	3.9
$CCl_4+C_6H_5CH_3$ (ii)	10	40.8	0.8
	20	60.5	1.1
	30	94.7	1.3
	40	138.0	0.8
	50	210.5	0.5
	60	304	0.5
	70	420	0.4
CS_2+CHCl_3 (ii)	0	141.0	1.4
	10	217	1.4
	20	322	1.7
	30	467	1.0
	40	660	0.9
$CS_2+CH_3COCH_3$ (ii)	0	235	5.9
	10	371	5.3
	20	557	4.5
	30	817	3.8
	35	960	3.6
$CS_2+C_6H_5CH_3$ (ii)	10	147	4.3
	20	222	4.0
	30	324	3.5
	40	460	1.8
$C_6H_6+CHCl_3$ (ii)	0	45.4	0.6
	20	122.5	1.1
	40	266	0.3
	60	574	0.2
$C_6H_6+CH_3OH$ (ii)	0	81.9	5.6
	10	144.0	5.4
	20	236	4.9
	30	379	5.5
	40	590	6.7
	60	1300	7.8
$C_6H_6+CH_3COOH$ (ii)	20	95.0	2.2
	30	157.0	2.8
	40	239	4.0
	50	357	3.2
	60	520	3.0
	70	737	2.0
$C_6H_6+C_2H_5OH$ (i)	34.8	288	5.0
	50	557	5.3
	60	830	5.5
	66	1057	5.8
$C_6H_6+n\text{-}C_3H_7OH$ (ii)	10	63.0	8.4
	20	106.0	6.3
	30	172.0	5.7
	40	270	5.5
	50	410	6.4
$C_6H_6+C_2H_5OC_2H_5$ (ii)	0	98.0	0.4
	10	157.0	0.4
	20	242	0.2
	30	347	0.3
$C_6H_6+CH_3CO_2C_2H_5$ (ii)	10	84.5	3.3
	20	138.3	0.9
	30	214	1.3
	40	330	1.4
	50	466	1.4
	60	657	1.1
$C_6H_6+C_6H_5CH_3$ (ii)	10	34.7	1.6
	20	59.4	1.1
	30	98.5	0.9
	40	149.0	1.1
	50	214	0.9
	60	303	0.4
	80	574	0.5

* References:

(i) *International Critical Tables*, Vol. III, pp. 285, 358 (1928).
(ii) Schmidt, *Z. Phys. Chem.*, **121**, 221 (1926).

The comparison of P_{calc} with P_{obs} has been performed in regard to about 20 systems which are chosen from various types of mixtures as shown in Tables 1 and 2. In these tables are arranged the systems in three classes: mixtures of (A) non-polar and non-polar liquids, (B) non-polar and polar liquids and (C) polar and polar liquids, for convenience's sake. In these tables are also tabulated P_{AB} in terms of mm. Hg and $\overline{\Delta}$ which is the arithmetical mean of $|P_{calc}-P_{obs}|\times 100/P_{obs}$ at various compositions. $\overline{\Delta}$ is regarded as a kind of measure of the coincidence of P_{calc} with P_{obs}. Some of the results of calculations are plotted in Figs. 2 and 3, where the circles and the full lines represent the observed and the calculated values respectively. The agreement of P_{calc} with P_{obs} seems to be fairly good for all of the systems listed in Tables 1 and 2.

Table 2

List of the Systems Compared and the Results Obtained.—II.

System (Ref.*)	°C.	P_{AB}	$\overline{\Delta}$, %
H_2O+CH_3OH (i)	39.9	165	3.3
	59.4	416	2.8
$H_2O+C_2H_5OH$ (i)	40	159	4.4
	55	338	4.4
	75	823	4.2
$H_2O+n\text{-}C_3H_7OH$ (i)	30.3	83.0	3.7
	49.9	240	4.9
	65.9	510	4.2
	79.8	930	3.7
$CHCl_3+CH_3COCH_3$ (ii)	0	43.8	0.9
	10	65.2	2.1
	20	112.3	1.9
	30	178	2.0
	40	270	1.7
	50	395	1.5
$CHCl_3+C_2H_5OC_2H_5$ (ii)	0	86.4	2.2
	10	135.0	1.0
	20	213	0.6
	30	309	0.3
$CH_3OH+C_2H_5OH$ (ii)	10	41.6	1.4
	20	74.2	0.4
	30	134.0	0.7
	40	215	0.2
	50	345	0.3
	60	528	0.4
$CH_3OH+n\text{-}C_3H_7OH$ (ii)	10	40.6	0.6
	20	72.5	1.3
	30	134.0	0.3
	40	217	0.8
	50	346	0.6
	60	495	0.5
$C_2H_4Br_2+C_3H_6Br_2$ (i)	85.1	152.0	0.4
$C_2H_5OH+C_2H_5CO_2H_5$ (i)	0	173	5.6
	10	269	5.0
	20	405	4.6
	30	594	3.9
	35	713	4.0
CH_3COCH_3	20	432	0.7
$+C_2H_5OC_2H_5$ (i)	30	642	1.4
$CH_3CO_2C_2H_5$	0	109.0	0.3
$+C_2H_5OC_2H_5$ (ii)	10	167.0	0.2
	20	258	0.2
	30	388	0.8

* References are given in Table 1.

Further, if we plot log P_{AB} against $1/T$, a straight line will be obtained according to the definition of P_{AB}, Eq. (14). That is, defining the "mutual heat of vaporization", λ_{AB}, by

$$\lambda_{AB}=u_{AB}-(kT/2), \tag{18}$$

and putting

$$b=\lambda_{AB}/2.303\,k, \tag{19}$$

we can write Eq. (14) in the form,

Table 3

Values of a and λ_{AB}.

System A	System B	a	b	λ_{AB}	$(\lambda_A+\lambda_B)/2$	$\lambda_A(\lambda_B)$*
				(kcal./mole)		
CCl_4	C_6H_6	7.720	1691	7.74	7.77	7.67
CS_2	C_6H_6	7.265	1420	6.50	7.25	6.65
CCl_4	EtOH	8.490	1840	8.42	8.83	
CCl_4	$PhCH_3$	7.600	1705	7.80	7.96	(8.24)
CS_2	$CHCl_3$	7.388	1431	6.55	7.03	
CS_2	Me_2CO	7.672	1445	6.61	7.17	
CS_2	$PhCH_3$	7.335	1463	6.69	7.44	
C_6H_6	$CHCl_3$	7.850	1694	7.75	7.64	7.86
C_6H_6	MeOH	8.590	1823	8.34	8.43	
C_6H_6	AcOH	8.096	1792	8.20	8.73	(9.60)
C_6H_6	EtOH	8.671	1915	8.76	8.93	
C_6H_6	PrOH	8.396	1868	8.55	9.48	(11.10)
C_6H_6	Et_2O	7.766	1578	7.22	7.31	
C_6H_6	AcOEt	7.875	1682	7.70	8.15	
C_6H_6	$PhCH_3$	7.714	1742	7.97	8.05	
H_2O	MeOH	9.063	2143	9.81	9.65	10.30
H_2O	EtOH	9.316	2228	10.19	10.15	
H_2O	PrOH	9.411	2273	10.40	10.70	
$CHCl_3$	Me_2CO	7.850	1698	7.77	7.56	7.42
$CHCl_3$	Et_2O	7.538	1530	7.00	7.08	(6.75)
MeOH	EtOH	8.962	2077	9.50	9.50	9.00
MeOH	PrOH	9.114	2125	9.72	10.05	
EtOH	Et_2O	7.648	1478	6.76	8.37	10.00
Me_2CO	Et_2O	7.847	1528	6.99	7.23	7.70
AcOEt	Et_2O	7.632	1530	7.00	7.60	8.45

* Values in parentheses are the heat of vaporization of B-component given in the same row.

$$\log_{10} P_{AB} = a - (b/T), \qquad (20)$$

to a good approximation. The demand for this linearity is, indeed, satisfied by the values

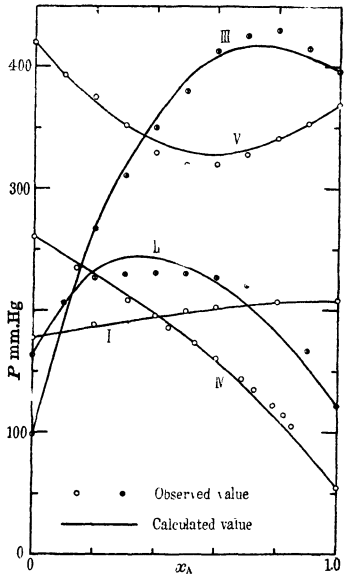

Fig. 2.—Observed and calculated values of P–1: Curve I, A=CCl_4, B=C_6H_6 (40°C.); Curve II, A=C_6H_6, B=CH_3OH (30°C.); Curve III, A=C_6H_6, B=CH_3COOH (60°C.); Curve IV, A=H_2O, B=CH_3OH (39.9°C.); Curve V, A=$CHCl_3$, B=CH_3COCH_3 (40°C).

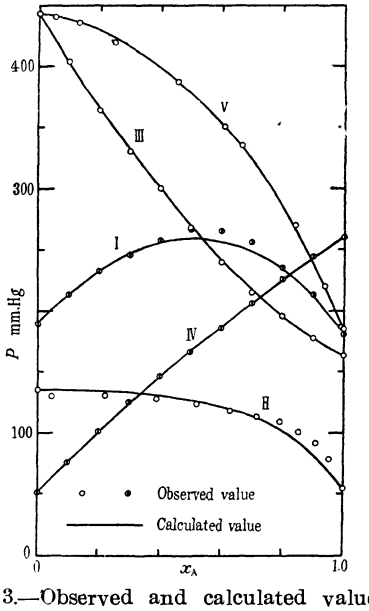

Fig. 3.—Observed and calculated values of P–2: Curve I, A=C_6H_6, B=$CH_3CO_2C_2H_5$ (40°C.); Curve II, A=H_2O, B=C_2H_5OH (40°C.); Curve III, A=$CHCl_3$, B=$C_2H_5OC_2H_5$ (20°C.); Curve IV, A=CH_3OH, B=n-C_3H_7OH (40°C.); Curve V, A=CH_3COCH_3, B=$C_2H_5OC_2H_5$ (20°C.).

of P_{AB} tabulated in Tables 1 and 2. In Table 3 are given the values of a and b in Eq. (20). Using these values, we can obtain P_{AB} at any temperature. In this Table, are also tabulated λ_{AB} in terms of kcal./mole and, for comparison's sake, $(\lambda_A+\lambda_B)/2$ and λ_A (or λ_B). It should be noticed that the signs of $\Delta\lambda$ defined by

$$\Delta\lambda = \lambda_{AB} - \{(\lambda_A+\lambda_B)/2\} = \Delta u \qquad (21)$$

are consistent with the sign of the heat of mixing for all of the systems cited here. Especially,

$$\Delta\lambda = (6.99-7.23) = -0.24 \text{ kcal./mole}$$

for the mixture of acetone and ethyl ether, which is regarded as "regular solution", coincides with the value of Δu evaluated by Porter[9] from Eq. (10), $2\Delta u/kT = -0.741$ at 30°C., quantitatively. These results are to be compared with the fact that the sign of Δu evaluated by Eq. (10) conflicts some times with the one expected from the heat of mixing for the system exhibiting appreciable departure from regular solution (for example, H_2O+CH_3OH). And λ_{AB} obtained from the present method is consistent with the value of "activation energy of flow" estimated from the data of the viscosity coefficient as was illustrated in our previous paper[10].

However, our formula for the partial vopor pressure shows, unfortunately, only poor agreement with the experimental data. So, we cannot calculate the so-called "x to y diagram" (diagram of the composition of solution to that of vapor) from the present theory.

Estimation of $\Delta\lambda$ from Heat of Mixing

In this section, we will compare λ_{AB} or $\Delta\lambda$ given in Table 3 with those estimated from the heat of mixing, ΔH.

As the difference between H (enthalpy) and U (energy) can be neglected in liquid phase, we get from Eqs. (12) and (21)

$$\Delta H \equiv \Delta U = 2\varphi_A\varphi_B(N\Delta\lambda), \qquad (22)$$

where plus sign of ΔH represents the heat evolved by the solution. Using this relation, we can again estimate $\Delta\lambda$ from the observed values of ΔH. In Table 4 are given the results of calculation for some examples.

Though the constancy of $\Delta\lambda$ to x_A is not enough in examples 2 or 3, the values of $\Delta\lambda$ thus estimated will give, at least, their correct

(9) A. W. Porter, *Trans. Farad. Soc.*, **16**, 336 (1920).
(10) M. Tamura and M. Kurata, This Bulletin, **25**, 32 (1952), Eq. (17) and Table 3.

order. As the values of $\Delta\lambda$ obtained from Table 3 are in agreement with the ones estimated here within small error, 50~60 cal./mol., we can conclude that λ_{AB} tabulated in Table 3 gives the correct measure of energy of molecular contact of A—B type within small error, probably less than 0.1 kcal./mole (or less than 2%).

Table 4

Estimation of $\Delta\lambda$ from Heat of Mixing.

Example 1. A=CCl_4, B=C_6H_6 at 25°C.

x_A	ΔH kjoule/mole	$\Delta\lambda$ kcal./mole Eq. (22)	Table 3
0.300	−0.091	−0.050	
0.351	−0.106	−0.054	
0.501	−0.107	−0.051	−0.03
0.618	−0.104	−0.053	
0.731	−0.089	−0.056	

Example 2. A=C_6H_6, B=C_2H_5OH at 15°C.

x_A	ΔH joule/g. soln.	$\Delta\lambda$ kcal./mole Eq. (22)	Table 3
0.202	−6.067	−0.194	
0.282	−6.867	−0.197	
0.469	−7.556	−0.230	−0.17
0.579	−7.338	−0.264	
0.702	−6.706	−0.331	

Example 3. A=C_6H_6, B=$CHCl_3$ at 18°C.

x_A	ΔH joule/g. soln.	$\Delta\lambda$ kcal./mole Eq. (22)	Table 3
0.219	2.64	0.170	
0.396	3.31	0.160	
0.496	3.31	0.157	0.11
0.604	3.18	0.160	
0.723	2.89	0.178	

Data of ΔH are adopted from "*International Critical Tables*" Vol. V, p. 154.

Table 5

Total Vapor Pressure of the Mixture of CCl_4 (A), C_2H_5OH (B) and C_6H_6 (C).

x_A	x_B	34.8°C. P_{obs}	P_{calc}	Δ, %	60°C. P_{obs}	P_{calc}	Δ, %
0.131	0	153	153	0	407	404	− 0.7
0.126	0.040	191	161	−15.7	515	431	−16.3
0.112	0.144	201	181	− 9.9	559	492	−12.0
0.094	0.288	204	200	− 2.0	580	556	− 4.1
0.078	0.408	204	209	+ 2.5	585	591	+ 1.0
0.058	0.561	199	208	+ 4.5	577	603	+ 4.5
0.045	0.661	193	199	+ 3.1	564	588	+ 4.3
0.035	0.736	186	188	+ 1.1	546	562	+ 2.9
0.022	0.833	167	165	− 1.2	508	509	+ 0.2
0.013	0.900	143	144	+ 0.7	462	457	− 1.1
0.007	0.945	130	127	− 2.3	421	415	− 1.4
0.386	0	163	162	− 0.6	426	426	0
0.363	0.061	203	175	−13.8	551	466	−15.4
0.342	0.116	208	185	−11.1	575	499	−13.2
0.289	0.253	212	205	− 3.3	599	564	− 5.8
0.232	0.400	212	217	+ 2.3	603	611	+ 1.3
0.178	0.540	208	216	+ 3.8	598	619	+ 3.5
0.100	0.742	190	192	+ 1.1	560	572	+ 2.1
0.058	0.850	167	163	− 2.4	508	506	− 0.4
0.035	0.909	147	143	− 2.7	465	455	− 2.2
0.019	0.951	128	126	− 1.6	417	415	− 0.5
0.587	0	166	167	− 0.6	435	436	+ 0.2
0.550	0.063	207	181	−12.6	561	480	−14.4
0.501	0.147	215	196	− 8.8	600	532	−11.3
0.432	0.266	218	212	− 2.8	612	583	− 4.7
0.329	0.440	216	224	+ 3.7	615	632	+ 2.8
0.269	0.542	213	221	+ 3.8	608	634	+ 4.3
0.190	0.675	203	207	+ 2.0	588	608	+ 3.4
0.134	0.773	187	188	+ 0.5	559	566	+ 1.3
0.094	0.839	173	170	− 1.7	522	519	− 0.6
0.045	0.921	144	141	− 2.1	459	448	− 2.4
0.013	0.978	115	114	− 0.9	387	382	− 1.3
0.745	0	170	170	0	441	442	+ 0.2
0.538	0.277	221	218	− 1.4	625	596	− 4.6
0.420	0.436	219	227	+ 3.7	624	637	+ 2.1
0.323	0.566	215	223	+ 3.7	615	640	+ 4.1
0.204	0.726	199	202	+ 1.5	583	595	+ 2.1
0.141	0.811	184	180	− 2.2	543	548	+ 0.9
0.093	0.875	163	160	− 1.8	497	496	− 0.2
0.045	0.940	137	133	− 2.9	437	429	− 1.8
0.497	0.503	223	232	+ 4.0	637	655	+ 2.8
0.416	0.421	220	226	+ 2.7	628	633	+ 0.8
0.357	0.361	217	220	+ 1.4	617	612	− 0.8
0.284	0.288	213	209	− 1.9	602	579	− 3.8
0.215	0.218	209	197	− 5.7	589	542	− 8.0
0.139	0.141	201	180	−10.4	566	489	−13.6
0.083	0.085	194	169	−12.9	535	455	−14.9
0.041	0.042	182	158	−13.2	490	411	−16.1
0.018	0.019	170	152	−10.6	446	404	− 9.4
0.190	0.810	187	185	− 1.1	554	558	+ 0.7
0.178	0.760	194	194	0	571	576	+ 0.9
0.168	0.717	199	201	+ 1.0	581	593	+ 2.1
0.157	0.669	202	206	+ 2.0	586	603	+ 2.9
0.139	0.590	205	212	+ 3.4	589	615	+ 4.4
0.114	0.486	205	214	+ 4.4	589	611	+ 3.7
0.079	0.334	203	205	+ 1.0	583	573	− 1.7
0.052	0.221	200	191	− 4.5	570	526	− 7.7
0.033	0.140	194	176	− 9.3	548	481	−12.2
0.013	0.057	185	160	−13.5	509	429	−15.7
0.006	0.027	172	154	−10.5	457	408	−10.7

	P_A	P_B	P_C	P_{AB}	P_{BC}	P_{AC}
34.8°C.	173	103	147	328	288	170
60°C.	446	354	389	928	830	443

Data of P_{obs} are adopted from Ref. (i) in Table 1.

Total Vapor Pressure of Ternary Liquid Mixture

Extending the treatment mentioned above to ternary mixture of liquids composed of A, B and C components, we can easily obtain the relation having the similar type to Eq. (17);

$$P=x_A\varphi_A P_A+x_B\varphi_B P_B+x_C\varphi_C P_C +2(x_Ax_B\varphi_A\varphi_B)^{1/2}P_{AB}+2(x_Bx_C\varphi_B\varphi_C)^{1/2}P_{BC} +2(x_Cx_A\varphi_C\varphi_A)^{1/2}P_{AC}. \quad (23)$$

Then, if we know P_{obs} at least at three compositions, for example, (i) $x_A=x_B=1/2$, (ii) $x_B=x_C=1/2$ and (iii) $x_A=x_C=1/2$, it will be possible to calculate P at any composition. In Table 5 are given the results of calculation for the system, carbon tetrachloride+benzene +ethyl alcohol. The degree of agreement of P_{calc} with P_{obs} is the same order as the one obtained for the binary mixture. The values of P_A, P_B, P_C, P_{AB}, P_{BC} and P_{AC} used in this calculation are tabulated in the last part of this table. Among these values, P_{AB} and P_{BC} were already given in Table 1 and P_{AC} was calculated by Eq. (20) with a and b given in Table 3.

It seems to be a strong point of the present method that the extension to the multi-component system can be performed very easily as shown here.

Summary

(1) The kinetic method was applied to the vapor pressure of regular solution; the result being in agreement with that of the statistical method.

(2) New semi-empirical equations having simple form were derived for the vapor pressures of binary and ternary mixtures of liquids and satisfactory agreements of these equations with the experimental data were illustrated in regard to about 20 examples.

In conclusion the author wishes to express sincere thanks to Professor Mikio Tamura for his kind guidance throughout this work. The cost of this research has been defrayed from the Grant in Aid for Fundamental Scientific Research from the Ministry of Education.

Laboratory of Physical Chemistry, Tokyo Institute of Technology, Tokyo and Department of Industrial Chemistry, Faculty of Engineering, Kyoto University, Kyoto

Ultraviolet Absorption Spectra of Troponoids[1]

By Masamichi TSUBOI

(Received May 8, 1952)

Introduction

In connection with a serial study by T. Nozoe and his coworkers[2] on "troponoids"—a group of compounds with a seven-membered carbon ring, (cycloheptatriene-2, 4, 6-one-1),—the present writer has had an opportunity to observe the ultraviolet absorption spectra of more than twenty compounds of this group. It is the purpose of this paper to present what the writer has observed of the general relations between the spectral features and the molecular structures of these compounds and to give explanations concerning these relations.

Data

In Figs. 1—20 are shown graphically the data of the ultraviolet absorption spectra of troponoids, as obtained by means of a Beckman spectrophotometer model DU. Samples used are listed in Table 1, with remarks on them. All of these samples were prepared by Nozoe and his co workers. The structural formulas of most of these compounds were determined

(1) T. Nozoe and his co-workers give the general name "troponoids" to tropone, tropolone, and related compounds.

(2) T. Nozoe, *Sci. Rep. Tohoku Univ.*, Ser. I, **34**, 199 (1950); *Nature*, **167**, 1055 (1951); *Chem and Chem. Industry (Chem. Soc. Japan)*, **4**, 348 (1951).

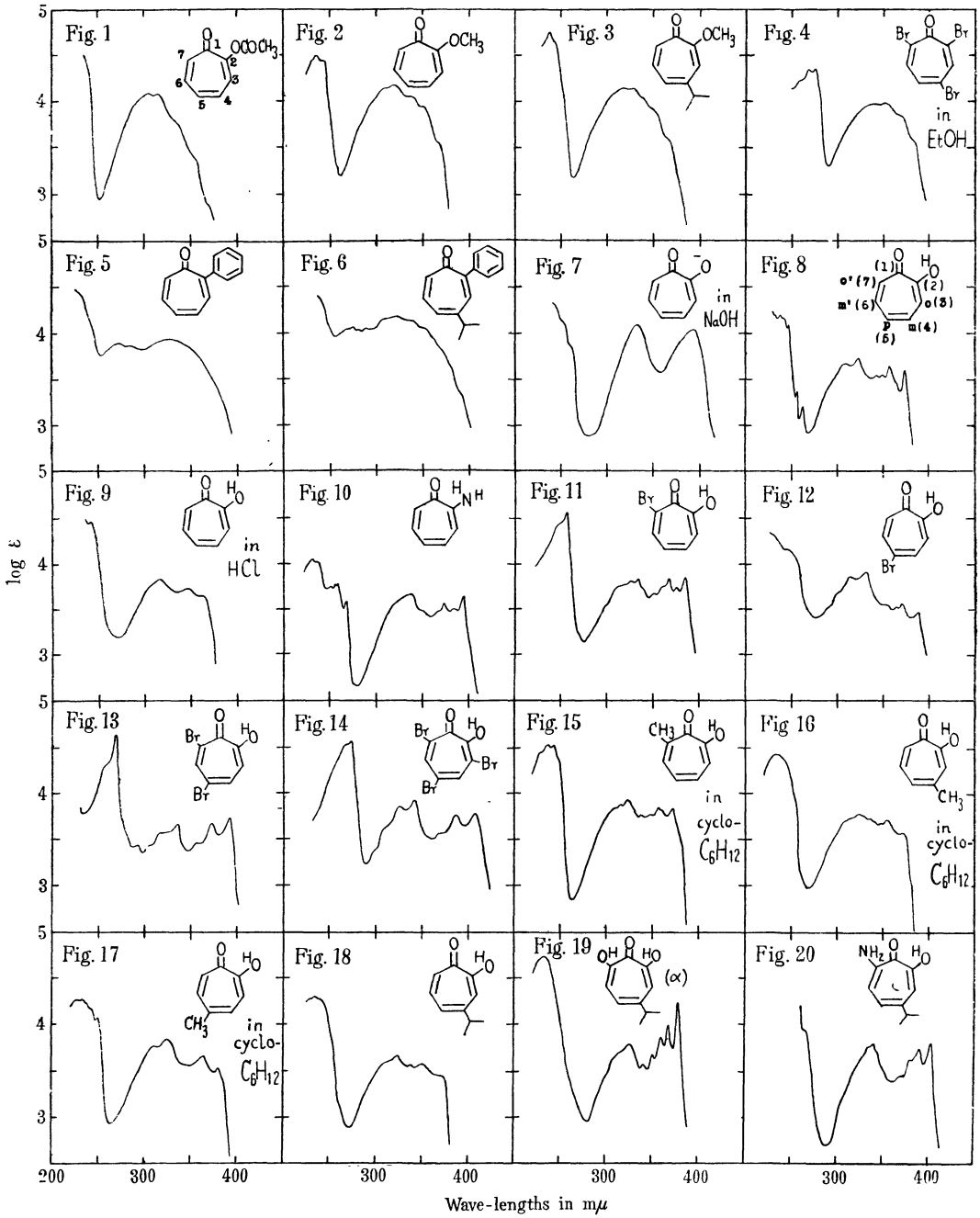

Figs. 1—20.—Ultraviolet Absorption Spectra of Troponoids
(Solvent: iso octane unless otherwise stated)

Table 1

Substances	Melting Points, °C.	References	Structural Formulas and Ultraviolet Absorption Spectra
Tropolone acetate	69.5-70.5	(3)	Cf. Fig. 1
Tropolone methyl ether	(oil)	(4)	Cf. Fig. 2
Hinokitiol methyl ether	(oil)	(5)	Cf. Fig. 3
2, 4, 7-Tribromotropone	185	(6)	Cf. Fig. 4
2-Phenyltropone	85-86	(7)	Cf. Fig. 5
2-Phenyl-4-(or 6)-isopropyl-tropone	93-94	(7)	Cf. Fig. 6
Tropolone	50-51	(8)	Cf. Figs. 7, 8 and 9
2-Aminotropone	106-107	(9)	Cf. Fig. 10
o-Bromotropolone	107-108	(8) and (10)	Cf. Fig. 11
p-Bromotropolone	190-191	(8)	Cf. Fig. 12
o, *p*-Dibromotropolone	152-153	(10)	Cf. Fig. 13
o, *o'*, *p*-Tribromotropolone	125-126	(8)	Cf. Fig. 14
o-Methyltropolone	51	(11)	Cf. Fig. 15
m-Methyltropolone	76	(12)	Cf. Fig. 16
p-Methyltropolone	110	(5)	Cf. Fig. 17
Hinokitiol (β-Thujaplicin) (*m*-Isopropyl-tropolone)	51-52	(13)	Cf. Fig. 18
o'-Hydroxyhinokitiol	60(α), 52(β), 46(γ)	(14)	Cf. Fig. 19(α)
o'-Aminohinokitiol	99	(15)	Cf. Fig. 20

also by them.[3]~[15] In the present experiments, iso-octane was used as the solvent in most cases, but in the cases where the measurements corresponding to Figs. 4, 7, 9, and 15—17 were made, ethanol, NaOH solution, HCl solution, and cyclohexane were used respectively as the solvents.

Discussion

I. General Features.—Each of the absorption spectra of troponoids so far observed is divisible, without exception, into two parts—one ranging from 200 to 300 mμ which is composed of the absorption bands with ε-values of 10^4-10^5. and the other ranging from 300 to 400 mμ which is composed of the absorption bands a little weaker in intensity ($\varepsilon = 10^3$-10^4). This is a characteristic feature common to all the troponoids spectra.

In detail, however, the spectra of troponoids may be classified into two types:

Type A (Tropone type)—This is represented by the spectrum of tropone, which shows only one electronic band in the 300-400 mμ region.[16] The spectra of Figs. 1—6 belong to this type. All of these spectra are of tropone derivatives with no hydrogen bonds.

Type B (Anion type)—This is represented by the spectrum of tropolone anion (Fig. 7), which is observed when tropolone is dissolved in an alkaline solution. Each of the spectra of this type shows two electronic bands in the 300-400 mμ region. The spectra of Figs. 8—20 belong to this type. All of these spectra are of tropone derivatives which have either OH or NH_2 radical on the 2-carbon atom (C_2) (carbon atom adjacent to the carbonyl carbon atom) and an intramolecular hydrogen bond between the OH or NH_2 and the carbonyl oxygen atom.

All the compounds examined have C=O and C=C's conjugated with each other. According to McMurry,[17] it is expected, with such compounds, that two kinds of electronic bands will

(3) T. Nozoe, S. Seto, and T. Sato, to be published.
(4) T. Nozoe, S. Seto, T. Ikemi, and T. Arai, *Proc. Japan Acad.*, **27**, 102 (1951).
(5) T. Nozoe, *Science of Drugs*, **3**, 171 (1949).
(6) T. Nozoe, Y. Kitahara, T. Ando, and S. Masamune, *Proc. Japan Acad.*, **27**, 415 (1951); H. J. Dauben and H. J. Ringold, *J. Am. Chem. Soc.*, **73**, 876 (1951).
(7) T. Nozoe, T. Mukai, and J. Minegishi, *Proc. Japan Acad.*, **27**, 419 (1951).
(8) T. Nozoe, S. Seto, Y. Kitahara, M. Kunori, and Y. Nakayama, Ibid., **26**, 38 (1950).
(9) T. Nozoe, S. Seto, H. Takeda, S.Morosawa, and K. Matsumoto, Ibid., **27**, 556 (1951).
(10) T. Nozoe, Y. Kitahara, K. Yamane and A. Yoshikoshi, Ibid., **27**, 18 (1951).
(11) T. Nozoe, T. Mukai, and K. Matsui, Ibid., **27**, 646 (1951).
(12) T. Mukai, M. Kunori, H. Kishi, T. Muroi, and K. Matsui, Ibid., **27**, 410 (1951).
(13) T. Nozoe, *Science of Drugs*, **3**, 174 (1949); *Sci. Rep. Tohoku Univ.*, **34**. 199 (1950).
(14) T. Nozoe, Y. Kitahara, and K. Doi, *Proc. Japan Acad.*, **27**, 156 (1951).
(15) T. Nozoe, Y. Kitahara, and K. Doi, *J. Am. Chem. Soc.* **73**, 1895 (1951).
(16) W. von E. Doering and F. L. Detert, *J. Am. Chem. Soc.*, **73**. 876 (1951).
(17) H. L. McMurry, *J. Chem. Phys.*, **9**. 231, 241 (1941); Cf. also M. Kasha, Discussions of the Faraday Society, 1950, p. 14.

appear: one due to the N→Vn type transitions and the other due to the N→En type transitions. The bands of the first kind are related to the π-electrons extending along the entire system of conjugated bonds and are strong in intensity ($\varepsilon \fallingdotseq 10^4$); while the bands of the second kind are related to the electrons in the non-bonding molecular orbital, largely localized on the oxygen atom and are weak in intensity ($\varepsilon \fallingdotseq 10^1$). All the observed bands of the compounds now at issue are strong in intensity ($\varepsilon \fallingdotseq 10^4$), and hence may be assigned to the transitions of the N→Vn type, but not to the transitions of the N→En type.

The two bands in the 300—400 mμ and 200—300 mμ regions in the spectra of type A may be regarded as due respectively to N→V_1 and to N→V_2 transitions in a seven-sided ring system composed of conjugated three C=C's and one C=O, viz. a system composed of the field; 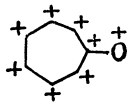 and eight π-electrons. Octatrienal, which has also conjugated three C=C's and one C=O, shows a band at 306 mμ, and this was explained by McMurry[17] as due to the N→V_1 transition. The 300 mμ band in the spectra of type A may be of the same nature as this 306 mμ band.

Tropolone anion may be regarded as a system composed of a field; 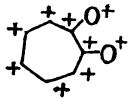 and ten π-electrons. According to Dewar's molecular orbital treatment,[18] the two bands in the 300—400 mμ region as well as the bands in the 200—300 mμ region may be explained as due to the N→Vn transitions in the system just mentioned. The fact that tropolone and its derivatives exhibit spectra of type B, as tropolone anion, may be taken as indicating that they bear a closer resemblance in the electronic state to tropolone anion than to tropolone methyl ether and tropolone acetate, which exhibit spectra of type A. This may in turn indicate that there is a resonance in tropolone somewhat similar,

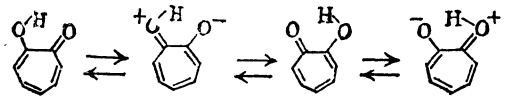

which resembles the resonance in tropolone anion,

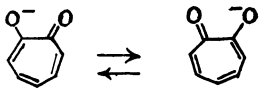

The resonance as above cannot occur in tropolone methyl ether and tropolone acetate, there being no intramolecular hydrogen bond in these compounds. The spectrum of aminotropone (Fig. 10) belongs also to the "Anion type" (type B), indicating that its electronic state resembles that of tropolone anion. The intramolecular N-H...O bonding in this compound seems to act like the O-H...O bonding in tropolone.

II. Effect of Substitution on the Positions of the Bands.—Though, as has been stated above, various spectra belonging to both type A and type B resemble one another in their general feature, they differ from ons another in the positions of their corresponding bands. Of the spectra of type A, that of tropone shows the bands at the shortest wave-lengths, and when Br, isoC_5H_7, OCH_3, or $OCOCH_3$ are substituted for the hydrogen atoms of tropone, they shift toward longer wave-lengths. Of the pectra of type B, that of tropolone shows thee bands at the shortest wave-lengths, and the substitution of Br, CH_3, etc. for the hydrogen atoms of tropolone also causes the shifting of the bands toward longer wave-lengths.[19] The amounts of these shifts ($\Delta\nu$) are shown in Table 2. As may be seen from the table, the shift of the bands is greatest when the substituent is NH_2, and it becomes less in the order of OH, Br, and alkyl radicals. This order of the amount of shift for different substituent radicals is reverse to the order of the ionization potentials of the radicals.[20] There is a tendency that *p* (or 5)-substitution of tropolone (Figs. 12 and 17) gives in general a larger red-shift than *m* (or 4)- or *o* (or 3)-substitution (Figs. 11, 15, and 16); and the amount of the red-shift is approximately additive when two or more radicals are substituted for the hydrogen atoms in one tropolone ring.

These shifts of the bands caused by substitution may be explained as due to the electron migration from the substituent radicals toward the seven-membered ring of the tropone. K. F. Herzfeld[21] advanced a general theory on the electron migration from the substituent radicals toward the conjugated double-bond

(18) M. J. S. Dewar, *Nature*, **166**, 790 (1950).

(19) *O* (or 3)-and *m* (or 4)-alkyl substitut'ons are exceptional; they cause a little shifting of the bands towards shorter wave-lengths.

(20) A. L. Sklar, *J. Chem. Phys.*, **7**, 984 (1939).

(21) K. F. Herzfeld, *Chem. Rev.*, **41**, 233 (1947).

Table 2

Fundamental System	Substituents	Positions of Absorption Peaks of the Longest Wave-Lengths		Shiftings due to the Substitution ($\Delta\nu$), cm^{-1}
		$m\mu$	cm^{-1}	
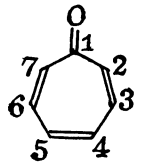	Nothing	310	32200	—
	2-$OCOCH_3$	317	31500	−700
	2-OCH_3	321	31100	−1100
	2-OCH_3-4-$isoC_3H_7$	325	30700	−1500
	2,4,7-Br_3	349	28600	−3600
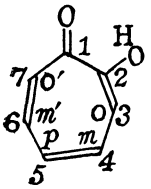	Nothing	374	26700	—
	o(or 3)-CH_3	372	26800	+100[19]
	m(or 4)-CH_3	372	26800	+100[19]
	p(or 5)-CH_3	379	26400	−300
	m(or 4)-$isoC_3H_7$	372	26800	+100[19]
	o(or 3)-Br	385	25900	−800
	p(or 5)-Br	389	25700	−1000
	o,*p*(or 3,5)-Br_2	392	25500	−1200
	o,*p*,*o'*(or 3,5,7)-Br_3	407	24500	−2200
	m(or 4)-$isoC_3H_7$-*o'*(or 7)-OH	379	26400	−300
	m(or 4)-$isoC_3H_7$-*o'*(or 7)-NH_2	402	24800	−1900

system, and H. Baba and S. Nagakura[22] made a correction and a supplement to it. According to this theory, the lower the ionization potential of the substituent is, the greater must be the extent of the migration, and accordingly the greater must be the shift of the band caused by the migration; and when the substituent radicals are more than one, the amount of the shift must be the sum of the shifts caused by respective radicals. All these consequences of the theory are in good agreement with what has been observed of the shifts of the bands due to substitutions in tropone and tropolone.

The Baba-Nagakura theory claims that the band due to $N\rightarrow E_n$ transition should shift on substitution toward shorter wave-lengths. Then, the fact that all the bands of tropone and tropolone that have been treated in this paper shift on substitution toward longer wave-lengths must be, according to the theory, an indication that these bands are not due to $N\rightarrow E_n$ transitions. This is what has already been concluded from the intensity measurements of these bands (page 372).

III. Miscellanies.—Some interesting facts which have come to the writer's notice in the course of the present work are recorded below:

(1) The spectrum of 2-phenyltropone as well as that of 2-phenyl-4 (or 6)-isopropyltropone corresponds nearly to the superposition of the spectra of tropone and benzene. This fact shows that there is but little interaction between π-electrons of the seven-membered ring and the benzene ring in 2-phenyltropone or 2-phenyl-4 (or 6)-isopropyl-tropone.

(2) The spectrum of tropolone in neutral water corresponds exactly to the superposition in a certain proportion of the spectra of tropolone in NaOH (Fig. 7) and of tropolone in HCl (Fig. 9). This fact shows that in the aqueous solution of tropolone two forms of molecules 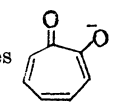 and 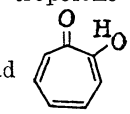 coexist.

(3) The absorption bands of tropolone acetate (Fig. 1) are situated at slightly shorter wave-lengths than those of tropolone methyl ether (Fig. 2). An explanation of this fact may be that the nonbonding electrons on the oxygen atom attached to the 2-carbon atom (C_2) in tropolone acetate migrate partly toward the acetyl group and partly toward the seven-membered ring, while those of tropolone methyl ether migrate exclusively toward the seven-membered ring.

(4) The vibrational structures of the spectra of *o*-, *m*-, and *p*-methyl tropolones are considerably different from one another (Figs. 15, 16, and 17), while they bear a striking resemblance respectively to those of *o*-, *m*-, and *p*-isopropyl tropolones (α, β, and γ-thujaplicins).[23] Similarly the vibrational structures of the spectra of *o*- and *p*-methyl tropolones

(22) H. Baba and S. Nagakura, *J. Chem. Soc. Japan*, **72**, 72, 74 (1951).

(23) A. Aulin-Erdtman, *Acta. Chem. Scand.*, **4**, 1031 (1950).

resemble respectively to those of *o*-, and *p*-bromotropolones (Figs. 11 and 12). In general, the features of the vibrational structures in the spectra of the tropolone ring appear to be determined by the positions, rather than the kinds, of the substituent radicals.

(5) Of *o'*-hydroxyhinokitiol (Fig. 19), three isomers, α(m. p. 60°C.), β(m. p. 52°C.), and γ(m. p. 46°C.) have been obtained by T. Nozoe et al.[14] The spectra of these three isomers are exactly alike in the positions of all the absorption peaks, but differ from one another in the absorption intensities of the bands. According to the present writer's near infra-red absorption studies, there is evidence which indicates that these three isomers differ from one another in the state of their intramolecular hydrogen bonds.

The writer wishes to express his sincere thanks to Professors San-ichiro Mizushima, Takehiko Shimanouchi, and Saburo Nagakura of Tokyo University for their kind guidance in this work, and to professor Tetsuo Nozoe, Messrs. Shuichi Seto, Yoshio Kitahara, Toshio Mukai, and their co-workers in Tohoku University for placing the samples at the writer's disposal and for their valuable advice.

Department of Chemistry, Faculty of Science, Tokyo University, Tokyo

Mechanical Properties of Concentrated Hydrogels of Agar-agar. I. Modulus of Elasticity in Compression

By Hiroshi FUJITA, Kazuhiko NINOMIYA and Terutake HOMMA

(Received January 31, 1952)

Introduction

The variation in mechanical properties of gels of high-polymeric substances is perhaps one of the most interesting problems of research in the field of rheology. Recent advances in rheology have resulted in the development of theories which permit interpretation of various mechanical properties of high polymers in terms of molecular quantities. However, papers dealing with the mechanical properties of polymer gels from the rheological point of view are still few in the literature. Remarkable progress has recently been made by Ferry[1] and his coworkers for the mechanical behavior in a variety of protein gels such as gelatin and fibrinogen gels. The experimental data accumulated in their studies have since been almost all concerned with the elasticity of the materials investigated, and few data have yet been obtained for the viscoelastic behavior of the materials.

Various aspects of physico-chemical properties of agar-agar gels have been reported, but there is little information available on their mechanical properties. For this reason, Nakagawa et al.[2~5] have set up a series of experimental studies on the rheological properties of hydrogels of agar-agar, and have published several interesting papers which are chiefly concerned with the elastic behavior at very low concentrations. In order to complete our understanding of the mechanical behavior of hydrogels of agar-agar, it is also of considerable interest to extend their research to a region of higher concentrations than they treated.

In this paper, the results of a study of the elastic behavior in compression of agar-agar hydrogels at concentrations between 2g./100 cc. and 4 g./100 cc. are reported.

Material and Apparatus

The material used was a grade of powdered agar-agar, from which the test pieces of agar-agar hydrogels were made according to the procedure which will be described below. No fractionation of the sample was made. It is well realized that the physico-chemical properties of any gel-system are appreciably influenced by the

(1) See, for example, J. D. Ferry, "Advances in Protein Chemistry," IV, Academic Press Inc., Publishers, New York, 1948, p. 1-78.

(2) T. Nakagawa, *Kagaku*, **20**, 130 (1950).
(3) T. Nakagawa, *J. Chem. Soc. Japan*, **72**, 390 (1951).
(4) T. Nakagawa and T. Danno, *J. Chem. Soc. Japan*, **72**, 518 (1951).
(5) T. Danno, *J. Chem. Soc. Japan*, **72**, 1061 (1951).

conditions under which the gel to be studied was formed. Accordingly, in order to produce experimental data which will ultimately be suited for quantitative discussions, it is necessary to take a consistent process in the course of preparing the sample gels. In this investigation the following procedure was employed consistently.

A mixture of the agar-agar powder and distilled water which was prepared to a desired concentration was boiled for 30 min. to make it sol. The sol was transferred into a glass cylinder, whose height and inner diameter were both about 3 cm., and chilled for 1 hr. in rest air kept at 25°C. to make it hard. Picking out the gel thus formed from the cylinder, a rod-shaped test specimen was obtained; over the concentration range as was treated in this work (2 g./100 cc.~4 g./100 cc.), all the specimens were rigid enough to support their own weight, or to be amenable to measurements by means of an apparatus which will be described below. The specimen was then quickly inserted in the apparatus and stood there for 30 min. The apparatus was installed in an air thermostat which had been previously controlled to a desired temperature. Some preliminary observations indicated that the test piece, as a whole, reached a temperature almost equal to that in the thermostat when it was placed there for about 30 min. In the case of as low temperature as 5° to 10°C., a somewhat longer time was required before arriving at the thermal equilibrium. For these reasons, except in the case of investigating the effect of gelation time, all the measurements were taken after 30 min. from the introduction of the specimen into the apparatus.

The apparatus used in this experiment was a modified form of the chainomatic balance used by Dart and Guth[6] for the study of the mechanical properties of natural cork. A schematic diagram of the apparatus is shown in Figure 1. Differing from Dart and Guth's original apparatus where desired compression stress-strain curves had to be determined manually, the present apparatus was designed so that a continuous smooth locus corresponding to a compression stress-strain curve could be recorded automatically on a chart paper mounted on the rotating cylinder. Because of the limit of space, accounts of the mechanical principle of the apparatus as well as the method of measurement must be omitted here; detailed descriptions of them will be made in a separate paper.[7]

Temperatures inside the thermostat (from about 5° to 60°C.) were controlled to about ±0.25°C. over the entire operating range in a particular run. Humidity was maintained at an almost saturated state to prevent drying of the specimen gel as much as possible.

The bundle of chains in the apparatus was

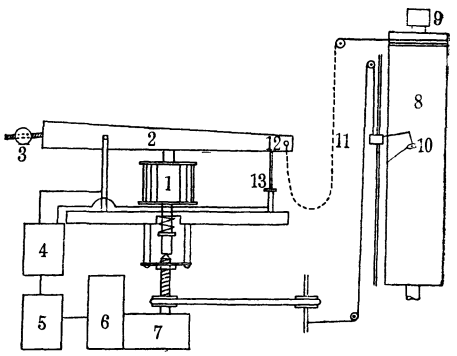

Fig. 1.—Experimental apparatus; 1: sample. 2: balance arm. 3: balast. 4: relay. 5: battery. 6: motor. 7: gear box. 8: chart cylinder. 9: driving clock. 10: pen. 11: chains. 12: hanger. 13: contact point.

lowered at a constant rate of falling with rotation of the chart cylinder at a constant speed. Accordingly, all the stress-strain curves obtained in this experiment should be accepted as the stress-strain curve for a constant rate of loading, or approximately, for a constant rate of increase in stress. The rate used herein was about 1000 dynes/cm.^{2}/sec. In converting the locus recorded on the chart cylinder to the corresponding stress-strain curve it was necessary to know the value of Poisson's ratio for the sample. In this study, it was simply presumed to be 0.5 without making any experimental determination for it.

Results and Discussion

Typical compression stress-strain curves obtained at various conditions are shown in Figures 2 and 3, where γ denotes the strain and S the stress. All the stress-strain curves obtained invariably have a general tendency similar to that found in the curves in the

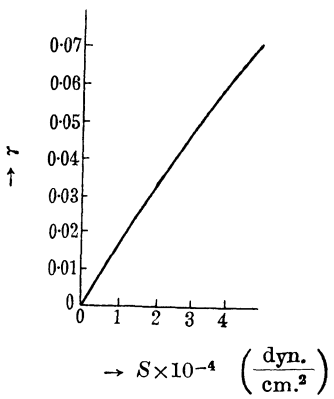

Fig. 2.—Stress-strain curve for a sample of 3 g./100 cc. conc. at 25°C. after 90 min. chilling.

(6) S. L. Dart and E. Guth, *J. Appl. Phys.*, **17**, 314 (1946); ibid., **18**, 476 (1947). See, also, R. S. Witte and R. L. Anthony, *J. Appl. Phys.*, **22**, 689 (1951).

(7) K. Ninomiya, *J. Chem. Soc. Japan*, in preparation.

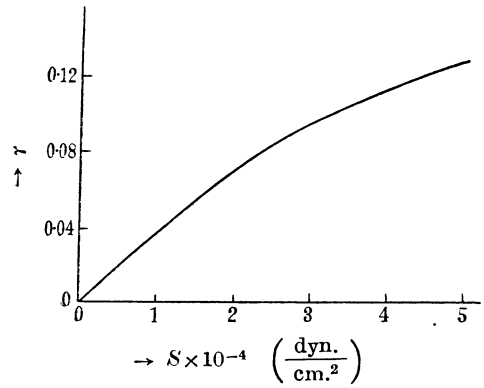

Fig. 3.—Stress-strain curve for a sample of 2 g./100 cc. at 23°C. after 90 min. chilling.

figures; for moderately small values of stress the strain increases linearly with the stress, while at higher stresses the plot is gradually curved toward the stress-axis, thus revealing a certain non-linearity. Relative length of the portion where Hooke's law holds very closely was found to be largely affected by experimental conditions. Some hysteresis loop was observed in the stress-strain curve when a cyclic process of loading was applied to the specimen. Since, however, it was almost negligible within the limits of deformations tested, it was presumed that all test pieces used in this work would be purely elastic for at least sufficiently small strains. The modulus of elasticity (Young's), E, was evaluated using the slope of the linear part in the stress-strain curve, and it was found that, in the range of test conditions herein adopted, the value of E fell in a range of about 10^5 dynes/cm.^{2}~10^6 dynes/cm.^{2}; for example, E for an agar-agar hydrogel of concentration 4 g./100 cc. was about 10^6 dynes/cm.^{2} at temperature 25°C. This value is, in effect, almost comparable to the value of E for a gelatin hydrogel of concentration 18.6 g./100 cc.[8] Generally speaking, it may be concluded that an agar-agar hydrogel is considerably more rigid than a gelatin gel.

There have been various opinions regarding the origin of the elasticity of a hydrogel of agar-agar, but no definite conclusion has yet been attained. Recently, Hirai[9] has attempted to interpret the elastic behavior of an agar-agar gel in terms of the kinetic theory of rubber-like elasticity, by taking partly into account the energy contribution due to interactions between the chain molecules of agar-agar.

(8) R. Houwink, "Elasticity, Plasticity and Structure of Matter" Cambridge University Press, London, 1937, p. 275.

(9) N. Hirai, *J. Chem. Soc. Japan*, **73**, 65 (1952).

Although he has reached a result which is apparently in accordance with the experimental results on the relation between the modulus of elasticity and the temperature, there seem to be some ambiguous points in his development concerning the consideration of the energy contribution.

Dependence of the Modulus of Elasticity upon Concentration.—This is a primarily interesting problem in the study of mechanical properties of a gel-system. Experiments were performed at 25°C. by varying the concentration from 2 g./100 cc. to 4 g./100 cc. The results obtained are plotted in Figure 4, where C is the concentration in percentages. From this figure the data prove to fit the following simple relation:

$$E=k \cdot C^{1.7}, \qquad (1)$$

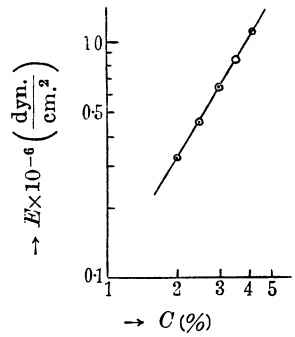

Fig. 4.—Concentration dependence of the modulus of elasticity, E, at 25°C. after 90 mim. chilling.

where k is a proportionality constant. With hydrogels of gelatin, it was frequently reported by many workers[10~12] that the relation:

$$E=k \cdot C^2 \qquad (2)$$

well described the data, though in some cases the exponent in Eq. (2) had to be taken as slightly less than 2. With fibrin clots (gel of fibrinogen containing small amount of thrombin), Ferry and Morrison[13] provided the relation:

$$E=k \cdot C^{1.57}. \qquad (3)$$

Ferry[11] also showed for hydrogels of gelatin that the exponent 2 in Eq. (2) was hardly affected by change in temperature.

(10) S. E. Sheppard and S. S. Sweet, *J. Am. Chem. Soc.*, **43**, 539 (1921).

(11) J. D. Ferry, *J. Am. Chem. Soc.*, **70**, 2244 (1948); See, also, reference (1).

(12) N. Hirai, *J. Chem. Soc. Japan*, **72**, 837 (1951).

(13) J. D. Ferry and P. R. Morrison, *J. Am. Chem. Soc.*, **69**, 388 (1947); See, also, reference (1).

Dependence of the Modulus of Elasticity upon Temperature.—Keeping the agar-agar concentration at 4 g./100 cc., measurements were made at several temperatures between 5° and 63°C., and the plot indicated in Figure 5 was obtained, where θ is the temperature in centigrades. This plot is seen to have a similar appearance to that obtained by Ferry et al.[14][11] for gelatin hydrogels and, also, to that by Nakagawa et al.[4][5] for agar-agar hydrogels of very low concentrations. At higher temperatures than about 60°C. the test pieces used became less rigid even at a concentration as high as 4 g./100 cc. The apparatus used in this work, however, was safely applicable only to the specimen rigid enough. Accordingly, the data given above would necessarily be somewhat incorrect in such an elevated temperature region. Hysteresis of the modulus in a cyclic temperature change was not studied in this work.

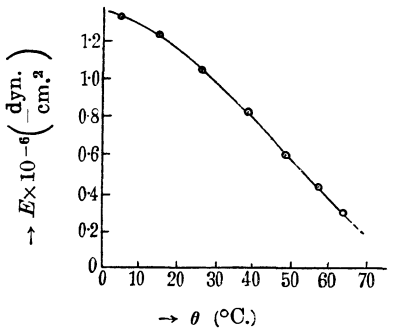

Fig. 5.—Temperature dependence of the modulus of elasticity, E, at 4 g./100 cc. after 90 min. chilling.

Effect of Gelation Time upon the Modulus of Elasticity.—For hydrogels of gelatin and fibrin clots, the effect of gelation time upon their rigidity was investigated in detail by Ferry et al.,[11][13][1] but for agar-agar gels there is no information on this problem. In view of this, the following experiment was conducted.

A number of glass cylinders filled with a hydrosol of agar-agar of known concentration were inserted simultaneously in the thermostat kept at 25°C. and allowed to stand there for an appropriate time (from 40 to 60 min.) to make the sol hard. The specimen gels were then successively subjected to measurements one by one at a suitable interval of time. The measurement was extended over an interval of about 170 min. for each concentration. Thus, the results plotted in Figure 6 were obtained, where t_g is the gelation time in minutes, being defined as the time which has elapsed after the cylinders were introduced in the cooling chamber. It is seen that within the first several ten minutes there was a fairly rapid increase of the modulus of elasticity but this increase was followed by a very gradual approach to a constant value. The higher the concentration, the more rapid the initial development of E resulted. It is worthy of notice here that the plotted curves indicate that the 90 min. chilling procedure as used in all other measurements than those described in this section was almost enough to assure the steady state values of E. Similar plots as shown in Figure 6 were already obtained by Ferry et al.[11][13] for both gelatin hydrogels and fibrin clots; for gelatin hydrogels the plot did not approach a final state even after more than 10 hr. had elapsed for all the cases investigated, while for fibrin clots it required only about 1 hr. before attaining a steady state. The latter result may be compared with our result for hydrogels of agar-agar.

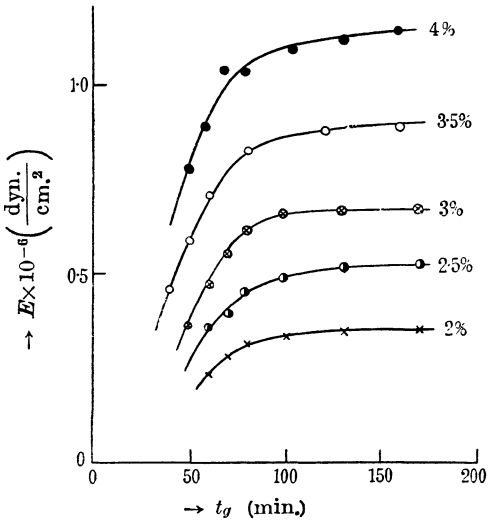

Fig. 6.—Effect of gelation time, t_g, on the modulus of elasticity, E, at various concentrations.

Summary

As the first step in a series of works on the mechanical behavior of a concentrated hydrogel of agar-agar, the experimental determination of its elastic behavior in compression was made. An apparatus which could record a compression stress-strain curve automatically

(14) J. D. Ferry and J. E. Eldridge, *J. Phys. & Colloid Chem.*, **53**, 184 (1949).

was devised and used to obtain the results reported in this paper. Influences of temperature, concentration, and gelation time upon the modulus of elasticity (Young's) were considered and plotted in Figures 4, 5 and 6.

The authors wish to thank Mr. T. Nakagawa of the University of Tokyo for helpful advice and encouragement given in the course of this study. Thanks are also due to Mr. T. Maki of this laboratory for his assistance in measurements.

Applied Physics Laboratory, Department of Fisheries, Faculty of Agriculture, Kyoto University, Maizuru

The Spectroscopic properties of Conjugated Systems

By Kazuo SHIBATA

(Received April 11, 1952)

The spectroscopic properties of conjugated systems in organic molecules have already been the subject of repeated investigations, and many efforts have been devoted to finding out the relationship existing between the positions of absorption maxima and the structures of the molecules. Based on the observations made on a large number of cyanine dyes, especially by Hamer[1] and Brooker[2], it has been stated that there exists an approximately linear relationship between the wave length of the absorption maximum and the length of conjugated system, whereas Kuhn and Hausser[3] showed that in the case of other types of conjugated systems such as diphenyl polyenes, the square of the wavelength of absorption maximum is related linearly to the length of conjugated systems.

These relationships, especially the one found for cyanine dyes were interpreted by Lewis and Calvin[4] semi-classically and later by Sklar and Herzfeld[5] and Bayliss[6] quantum mechanically. It should, however, be noticed that the linear relationships in question are not only the approximate ones, but also that there have been found a number of cases that are apparently at variance with them. In order to obtain a coherent understanding of the electronic states of conjugated systems, it is desirable to scrutinize more in detail and more systematically the spectroscopic properties of conjugated systems with a large variety of chemical compounds. From this point of view the present work was devoted to investigations of the spectroscopic properties of a large number of cyanine dyes and styryl dyes as well as polyene type compounds.*

(1) The Effect of Substitutions and the Solvents upon the Position of Absorption Maximum.—Preliminary observations were

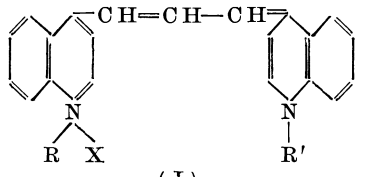

(I)

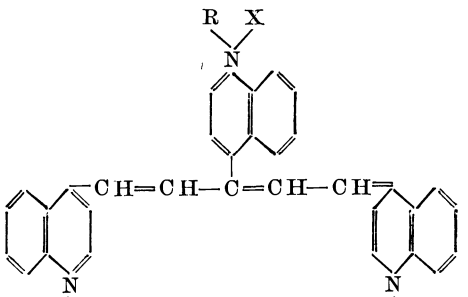

(II)

(1) Hamer, *J. Chem. Soc.* 125, 1348 (1924); **1930**, 995 **1936**, 1225; **1932**, 251; **1928**, 206.

(2) Brooker, *J. Am. Chem. Soc.* **57**, 2480, 2488, 2492 (1935); **58**, 659, 662 (1936); **59**, 67, 74 (1937).

(3) Hausser and Kuhn, *Z. Physik. Chem.*, B, **29**, 371, 378, 384, 391, 417 (1935).

(4) Lewis and Calvin, *Chem. Rev.*, **25**, 273 (1939); Branch and Calvin, "The Theory of Organic Chemistry", 1941, p. 155.

(5) Herzfeld and Sklar, *J. Chem. Phys.* **10**, 508, 521 (1942).

(6) Bayliss, *J. Chem. Phys.* **16**, 287 (1948).

* The observations were made by photoelectric measurements, the accuracy of which was about ± 10 A.

The styryl and cyanine dyes used in this work were synthesized in the laboratories of Prof. E. Ochiai and of Dr. T. Ogata, to whom the writer wishes to express his hearty thanks for their kindness in placing the materials at the author's disposal.

made with various derivatives of cryptocyanine (I) and neocyanine (II), using water as the solvent.

As a rule, these cyanine compounds display two absorption bands in the visible region, the one at longer wave length being always stronger than the other. In some cases the existence of the weaker band is more or less obscured by the other. In the following, these two bands are referred to as the "first" (stronger) and the "second" absorption band. To begin with, we shall restrict our consideration only to the first absorption band. The results of our observations are summarized in Table 1 and 2, where λ_1 (in A.) means the wave length of the maximum of the first absorption band. From these data it may be seen that in so far as it concerns alkyl groups, the substitution of R and R′ does not cause any profound difference in λ_1, the maximum difference observed being only a few mμ. Nor does the substitution of the halogen X cause any significant shift of λ_1. Quite the same was true when, instead of water, ethanol was used as the solvent, for which the comprehensive data will be given in the latter part of this paper.

Table 1

Absorption Maxima of Cryptocyanines

R	R′	X	λ_1 in A.
$-CH_3$	—R	—I	6940
$-C_2H_5$	—R	:	6960
:	$-isoC_5H_{11}$	:	6960
:	$-CH_2-CH_2-OAc$	:	6950
$-CH_2-CH_2-\phi$	—R	:	7320
$-CH_2-CO-NH_2$	—R	:	7220
$-CH_2-COOC_2H_5$	—R	—Cl	6960

Table 2

Absorption Maxima of Neocyanines

R	X	λ_1 in A.
$-CH_3$	—I	7560
$-C_2H_5$	:	7590
$-nC_3H_7$	:	7570
$-isoC_3H_7$	:	7540
$-nC_4H_9$	:	7590
$-isoC_4H_9$	:	7560
$-nC_5H_{11}$	:	7590
$-isoC_5H_{11}$	:	7550
$-CH_2-CH_2-OAc$	:	7580
$-CH_2-CH_2-\phi$	:	7620
$-CH_2-CH_2-O-CH_2-\phi$	:	7610
$-C_2H_5$	:	7590
:	—Cl	7520
:	—SCN	7520
:	$-NO_2$	7520
:	$-NO_3$	7530
:	$-SO_3-OC_2H_5$	7520
:	$-SO_3-\phi CH_3$	7510

Table 3

The Absorption Maxima of (I) and (II) observed in Various Solvents

Solvents	(I)	(II)
Water	6960	7610
Acetnitrile	7020	—
Acetic anhydride	7040	7720
Acetaldehyde	7045	—
Methanol	7050	7720
Ethyl acetate	7055	7750
Nitromethane	7055	7750
Acetone	7060	7730
Ethylene glycol	7085	—
Ethanol	7090	7760
Formamide	7090	7800
Chloroform	—	7830
Acetyl acetone	7100	—
Isobutanol	7110	—
Amyl acetate	7115	—
Pyridine	7155	8100
Benzyl alcohol	7185	—
Tetra-chloroethylene	7190	7730
Aniline	7205	—
Nitrobenzene	7235	7990

Using the compounds having ethyl group as R and R′ and iodine as X, the effect of solvents upon the value of λ_1 was investigated. The results obtained are summarized in Table 3. From this table it is apparent that λ_1 has the smallest value when water is used as solvent. It should be noticed that the absorption spectra observed in that case were markedly different from those observed in other organic solvents. Moreover, for reasons not yet clear, the light absorption in that case did not obey Beer's law which was found to hold satisfactorily true when ethanol or acetone were used as the solvent. Significant is the fact that ethanol gave the values of λ_1 which coincided within the limit of only ± 40 A. with those observed with the following solvents;

Acetic anhydride, Acetaldehyde, Methanol, Ethyl acetate, Nitromethane, Acetone, Ethylene glycol, Formamide and Chloroform.

Based on these findings, the measurements of λ in our further experiments were carried out, using exclusively ethanol as the solvent. In the discussions to be made later, reference will also be made to a number of data reported by other workers, especially those by Brooker[2]

and Hamer.[1] All data to be referred to are those obtained by using either ethanol or methanol as the solvent.

(2) The Relationship between λ^2 and the Number of Bonds in the Conjugated Systems of Various Symmetric Cyanine Dyes. — For various kinds of symmetric cyanine dyes, we made the plot of the square of λ_1 against the number of bonds in the conjugated systems, after the precedent of Lewis and Calvin[4] for the polyene type compounds. In this plot, only those substances having alkyl groups as R or R′ were taken into consideration, and taking into account the fact established in our preliminary experiments, the differences in those alkyl groups as well as in the halogen X were disregarded.

For a series of substances having the same terminal nuclei, a curve bending concavely towards the λ_1^2-axis was obtained, and for another series of symmetric cyanine dyes with different kinds of terminal nuclei, another curve bending also in the same way was obtained. These curves do not generally coincide, but run almost exactly parallel to each other. This is schematically illustrated in Fig. 1, where n′ means the number of bonds between the two terminal nuclei and the curves CGD and EHF are those obtained for

$$A-(CH=CH)_l-CH=A \qquad (III)$$

and

$$B-(CH=CH)_l-CH=B \qquad (IV)$$

respectively. For this rule we shall adduce a large number of concrete examples in later paragraphs. Interesting is the fact that the similar relation also holds for the second absorption band, as will be discussed later.

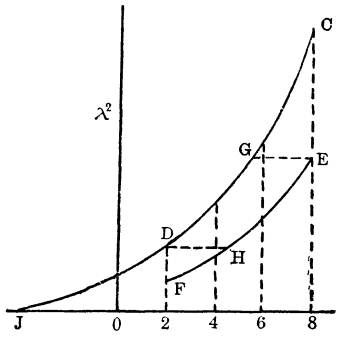

Fig. 1.

(3) The Concept of the "Color Factor" and its Characteristics.—The fact that the curves mentioned above run parallel to each other indicates that the lateral position of each curve is determined by the nature of the terminal nuclei. Let us assume a corresponding curve starting from the origin of the coordinate. Referring to this standard curve, the length JO may be regarded as due to the effect of the two nuclei of A.

In the following this value will be called the "color factor" of the nuclei of A. Color factors found experimentally for various kinds of nuclei are listed in Table 4. About half of the data given in the table are those obtained for polyene type compounds, which will be considered in later discussions.

Of great interest is the fact that in some cases there exists an additivity relation in the values of color factors. The difference between the color factor for a nucleus and that of the corresponding benzo-nucleus was found to be always 0.3. Therefore, the color factor of benzothiazole, for example, can be calculated by adding 0.3 to the color factor of thiazole (1.80).

Extending the concept of the color factor to the whole molecule of a compound, its value can be computed by adding the color factors of nuclei in the molecule and the number of bonds in the conjugated system. For example, the color factor of cryptocyanine is 11.10, because the color factor of quinoline linked at the position 4 is 3.55, and the number of bonds connecting the two quinoline nuclei is 4. We shall designate the color factor of a molecule by n in later discussions.

(4) Empirical Formula for the Standard λ^2-n-curve. — The significance of the color factor of each compound lies in the fact that it enables us to calculate the value of λ_1 with appreciable accuracy. It was found that the following equations fit in well with the standard curves for λ_1 (in $10^3 \times$A. unit).

$$\lambda_1^2 = n/(0.36-0.0123\,n) \qquad (1)$$

The curve C_1 in Fig. 2 is drawn according to Eq. (1) by plotting the square of the observed values of λ_1 against n, which in turn was calculated from the values given in Table 4.

By plotting the square of the observed values of λ_2 against the same values of n, as was done for the first absorption bands, we obtain the standard curve for λ_2. In this case, Eq. (2) of the same form fits in fairly well.

$$\lambda_2^2 = n/(0.40-0.0124\,n) \qquad (2)$$

The curve C_2 in Fig. 2 is drawn according to this equation.

Table 4

The Values of "Color Factors" for Various Nuclei

CH—CH=CH	2.00	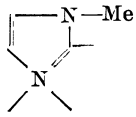	0.98	C=O	2.00
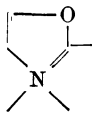	0.98		2.30		4.0
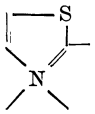	1.80	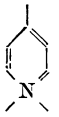	3.25	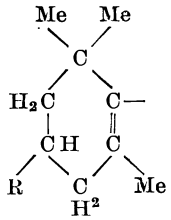	2.0
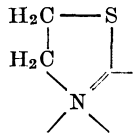	0.85	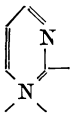	2.35	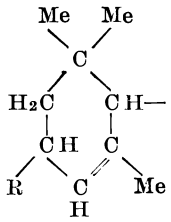	1.5
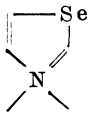	1.85		+0.30	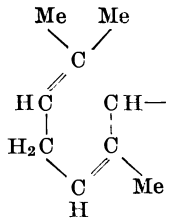	3.5
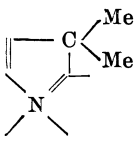	1.63		3.00	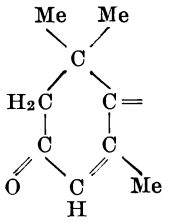	5.0

For some important symmetric and asymmetric cyanine dyes, the calculated and observed values of λ_1 are compared in Tables 5 and 6. As may be seen from these tables, the agreement between the two values is satisfactory for symmetric dyes, while the values calculated for asymmetric dyes are always somewhat lower than the observed ones. The reason of this disagreement will be discussed later.

(5) **Analogous Relation Existing for Polyene and some other Compounds.**—It may be highly interesting to note that what we have established for cyanine type compounds was also found to hold, mutatis mutandis, for other types of compounds with conjugated systems. The polyene type compounds are known to have, in general, three absorption bands, among which the second one is the strongest and the other two have almost the same intensity. For these compounds a close examination of the λ^2-n'-relation shows that it is non-linear; contrary to the case of cyanine dyes, the curves bend concavely toward the n'-axis. Using the spectroscopic data for diphenyl polyenes ϕ—$(CH=CH)_l$—ϕ reported by Kuhn and Hausser[3], and assuming the color factor of

Table 5

The Symmetric Cyanine Dyes
A—(CH=CH)$_l$—CH=A

A	l	$\lambda_{cal.}$	$\lambda_{obs.}$
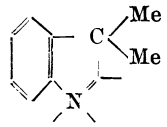	1	5460	5450
	2	6420	6360
	3	7430	7450
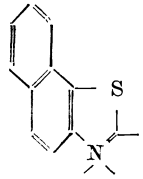	0	4980	4550
	1	5930	5950
	2	6910	6890
	3	7970	7990
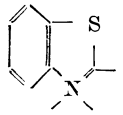	0	4650	4220
	1	5590	5570
	2	6570	6500
	3	7590	7620
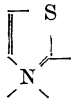	0	4380	4380
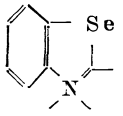	1	5670	5700
	2	6640	6600
	3	7670	7700
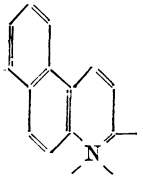	0	5430	5530
	1	6400	6350
	2	7400	7380
	1	6290	6300
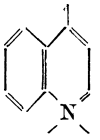	0	6050	5910
	1	7040	7090
	2	8100	8100
	3	9290	9320
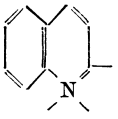	0	5150	5220
	1	6100	6050
	2	7090	7080
	3	8160	8080
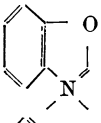	0	3870	3720
	1	4840	4850
	2	5790	5800
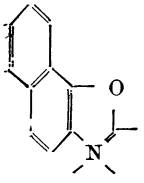	0	4170	3990
	1	5130	5140
	2	6070	6070

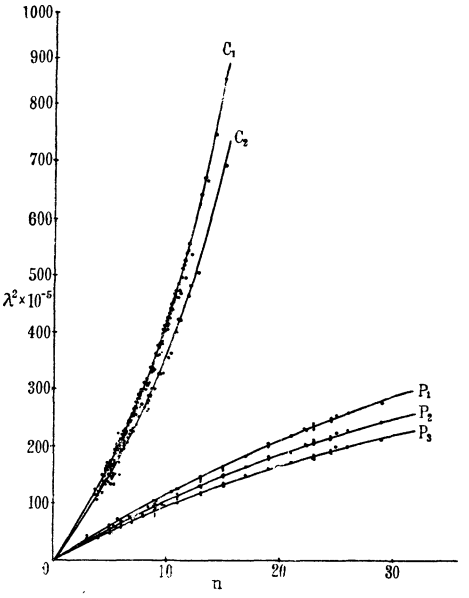

Fig. 2.

Table 6

The Asymmetric Cyanine Dyes

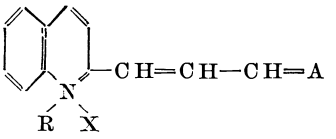

A	$\lambda_{cal.}$	$\lambda_{obs.}$
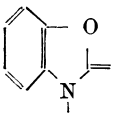	5470	5450
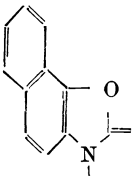	5610	5640
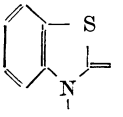	5850	5600
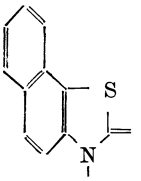	6020	5990
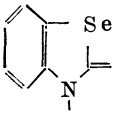	5880	5820

the phenyl group to be 3, we obtain the following empirical formulas for the standard curves of the three bands, which are again of the same form as before;

$$\lambda_1^2 = n/(0.80+0.008\,n) \quad (3)$$

$$\lambda_2^2 = n/(0.84+0.012\,n) \quad (4)$$

$$\lambda_3^2 = n/(0.92+0.015\,n) \quad (5)$$

Striking is the fact that these empirical formulas not only fit in well with diphenyl polyenes but also with the other compounds listed in Table 7 and with carotinoids (α- and β-carotene, lycopine, cryptoxanthine, crocetin etc.) if we assume the suitable values of the color factors given in the last column of Table 4. These assumed values of color factors are resonable from the consideration of the number of double bonds in the nucleus.

Table 7

Compounds	l
ϕ—(CH=CH)$_l$—ϕ	1—7
CH_3—(CH=CH)$_l$—CH_3	4—6
CH_3—(CH=CH)$_l$—CH_2—OH	1—4
ϕ—(CH=CH)$_l$—H	1—2
CH_3—(CH=CH)$_l$—COOH	1—3
CH_3—(CH=CH)$_l$—CHO	1—3
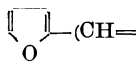	0—3
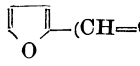	0—3

The curves P_1, P_2 and P_3 in Fig. 2 were drawn according to these equations and the points on these curves are those obtained by plotting the observed values of λ^2 against n, which were calculated from the values of color factors given in Table 4.

Besides cyanine and polyene compounds, there is another group of coloring substances which apparently, and in a peculiar manner, obey the above mentioned rule. The compounds listed in Table 8 have the property in common that they have two distinct absorption bands separated rather widely. If we plot the square of λ_2 (the absorption band at shorter wave length) on the standard line P_2 in Fig. 2, the point for the square of λ_1 was found to fall exactly upon curve C_1 against one and the same value of the color factor. For example, the points for λ_1 and λ_2 of thiobenzophenone fall on curves C_1 and P_2, respectively, with the color factor of 9.5. The same was true with all other compounds listed in Table 8, in which the color factors estimated in the above mentioned manner are also given for comparison.

Table 8

Compounds	λ^2 (λ in $10^3\times$A. unit)		n
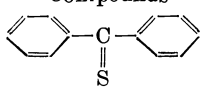	9.9	38.4	9.5
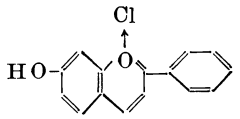	5.9	19.8	5.7
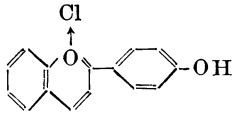	6.3	21.2	6.0
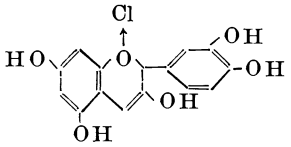	7.3	26.0	7.0
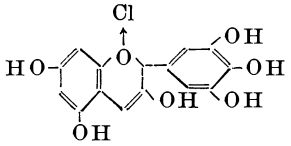	7.6	27.6	7.2
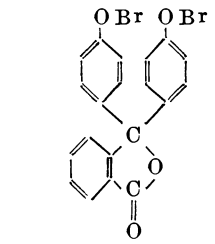	9.3	32.1	8.3

From the facts described above, it may be inferred that the compounds listed in Table 8 have both cyanine and polyene types of absorption bands. It should, however, be added that while unsubstituted thiobenzophenone follows our rule satisfactorily, the applicability of the rule is rather unsatisfactory in the case of some substituted thiobenzophenones. In Table 9 are shown the data reported by Burawoy[7]. For substituted thiobenzophenones we cannot find any definite value of color factor, on the basis of which the points for the two bands may be brought exactly upon the curves C_1 and P_2, respectively, in Fig. 2. If we assume for these substances the value of color factor which had been used for unsubstituted thiobenzophenone, the point for λ_1 falls lower than curve C_1 and the point for λ_2 falls above curve P_2.

(7) Burawaoy; *J. Chem. Soc.*, **1939**, 1177.

Table 9

Compounds	λ^2 (λ in $10^3\times$ A. unit)		Solvents
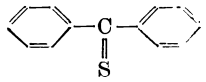	9.9	38.4	hexane
	—	36.9	ether
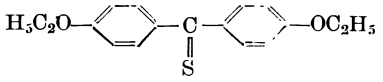	11.8	35.5	hexane
	12.5	33.5	ethanol
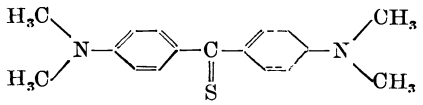	—	32.8	hexane

The similar discrepancy from our rule was observed with styryl dyes. In Table 10, are given the values of λ which we have found for some styryl dyes. The value of color factors of these compounds can be calculated from the values given in Table 4. When we plot the square of λ against the color factor, the point for λ falls between curves C_1 and P_2. This was the case with all styryl dyes investigated.

Table 10

The Absorption Maxima of Styryl Dyes

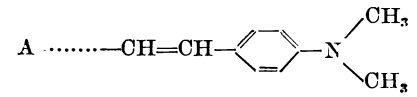

Compounds	$\lambda_{(max.)}$ in A. unit
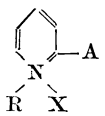	4670
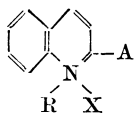	5270
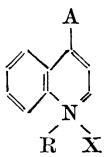	5460

As we have seen, our rule has proved to be quite satisfactory for certain groups of compounds, while it gives more or less deviating values for some other groups of compounds. In the following, an attempt will be made to elucidate the causes underlying the diversity of spectroscopic properties of different types of compounds.

(6) Interpretations of the Different λ^2-n-Relationships shown by Different Groups of Compounds.—In 1939 Burawoy[7], investigating the spectroscopic properties of various kinds of compounds, made the interesting observation that the two absorption bands shown by thiobenzophenones behave differently under certain conditions. On changing the solvent from a non-polar one to a polar one, it was found that the band at longer wave length was shifted towards shorter wave length, while the other band was displaced towards longer wave length (See Table 9). A similar phenomenon was observed when the dipole moment of the substance was enhanced by introducing some radical in it. These phenomena indicate that the structures in the molecules, which are responsible for the two bands are essentially different in nature. According to Burawoy, the band situated at longer wave length is caused by a chromophore of ionic nature ("chromophore R"), while the band at shorter wave length is brought about by a non-ionic chromophore ("chromophore K").

We have already seen that the first band of thiobenzophenone follows the rule of the bands of cyanine compounds, while its second band behaves exactly like the bands of polyene compounds. The data given in Table 3 show that the bands of cyanine compounds, like the band of thiobenzophenone at longer wave length, are shifted to violet by a change of the solvent which increases the dipole moment of the substances. Just the reverse phonomena are observed with polyene compounds; their bands, like the second absorption band of thiobenzophenone, are shifted to red with the increase of dipole moment by the effect of solvent. The same effect is brought about also by the substitution entailing an increase of dipole moment of polyene compounds.

It may safely be asserted that the polyene type compounds are non-ionic in any kind of solvent, while cyanine compounds will very likely assume ionic form in various solvents. At any rate, it may be certain that the Burawoy's chromophore R and K correspond to the conjugated double bond systems of cyanine and polyene compounds, respectively.

From this point of view, the compounds listed in Table 8 may be regarded as having the property of producing two types of molecule, ionic and non-ionic, in the solution.

(7) **Conclusion.**—By careful and detailed studies of a large number of absorption spectra of organic compounds with conjugated systems, we have found a rule governing quantitatively the relationship existing between the length of conjugated system and the absorption maximum. In alignment with these newly found λ^2-n-relationships, improvement of theoretical explanations such as Herzfeld and Sklar's is awaited with great interest.

As was remarked already, the rule we have found for symmetric cyanine dyes and polyene compounds does not apply with sufficient accuracy to some substituted thiobenzophenone and styryl dyes, nor for some asymmetric cyanine dyes. In these cases, our rule gives always higher values of λ for cyanine type absorption and lower values of λ for polyene type absorption. Systematic deviations in these cases indicate that in these compounds, besides the number of conjugated double bonds and the "color factor" of the terminal nuclei, some other factor plays a role in determining the position of the absorption band. The fact that our rule gives deviating values for substituted thiobenzophenone, while it applies satisfactorily to unsubstituted thiobenzophenone, suggests that the factor in question may be related to the dipole or the symmetry of the compounds. A theoretical explanation of this factor will be reported later in another work with more sufficient data on styryl dyes.

The author wishes to express his sincere thanks to Prof. E. Ochiai and Dr. T. Ogata for their kindness in placing the precious amples at the author's disposal.
s

The Tokugawa Institute for Biological Research, Tokyo

On Hydrogen Bonds Intimately Related with π-Electron Systems

By Masamichi TSUBOI

(Received May 29, 1952)

R. S. Rasmussen et al.[1),2)] pointed out that molecules such as, enolized β-diketones and salicyl aldehyde, which are characterized by the possession of both intramolecular hydrogen bond and C=O bond conjugated with other double bonds, show C=O vibration of abnormally low frequency. They suggested that in such molecules the hydrogen bond and the conjugated double bond system (or π-electron system) are intimately related to each other, and they called such molecules "conjugated chelate system". K. Kuratani, M. Tsuboi and T. Shimanouchi[3),4)] regarded that in tropolone (an isomer of salicyl aldehyde) the O—H···O bonding is intimately related to the seven-sided π-electron system. T. Shimanouchi and S. Mizushima[5)] and M. G. Evans and J. Gergely[6)] showed the possibility of electron transfer along the hydrogen-bonded long chain, ···HN—C=O···HN—C=O···, in proteins. This implies that the N—H···O bondings in it are intimately related to the π-electrons of C=O's. In general, in those molecules in which hydrogen bonds cooperate with π-electron systems to form a ring or a long chain, there are indications of a specially intimate relation between the hydrogen bonds and the π-electron systems.

The purpose of this paper is to present infrared and ultraviolet evidences which indicate that in these special molecules the hydrogen nuclei of the hydrogen-bonded OH

(1) R. S. Rasmussen, D. D. Tunnicliff and R. R. Brattain. *J. Am. Chem. Soc.*, **71**, 1068 (1949).
(2) R. S. Rasmussen and R. R. Brattain, *J. Am. Chem. Soc.*, **71**, 1073 (1949).
(3) K. Kuratani, M. Tsuboi and T. Shimanouchi. This Bulletin **25**, 250 (1952).
(4) M. Tsuboi, This Bulletin, **25**, 369 (1952).
(5) T. Shimanouchi and S. Mizushima, This Bulletin, **21**, 1 (1948).
(6) M. G. Evans and J. Gergely, *Biochemica et Biophysica Acta.* **3**, 188 (1949).

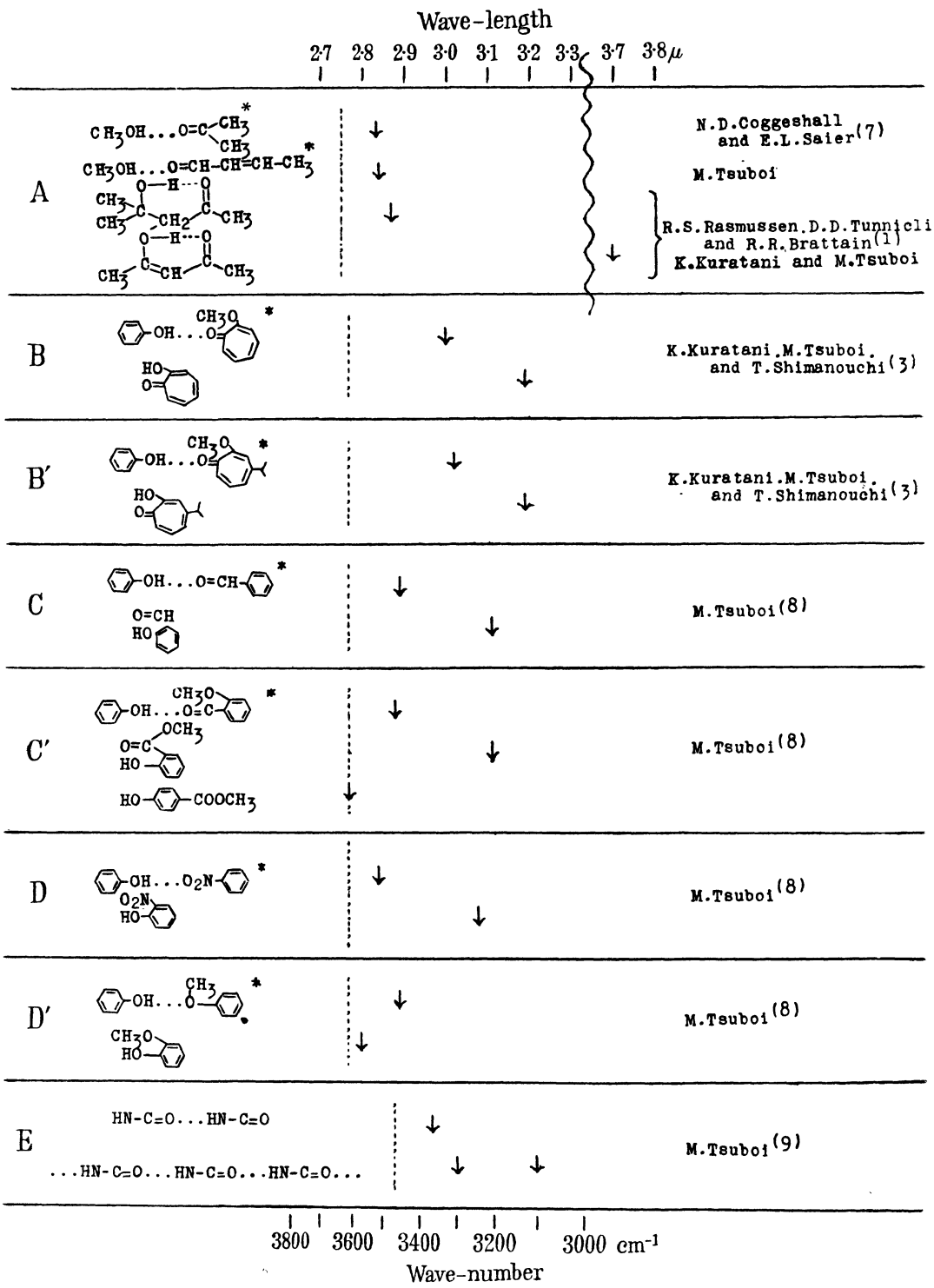

Fig. 1.

(7) N. D. Coggeshall and E. L. Saier. *J. Am. Chem. Soc*, **73**. 5414 (1951).

(8) M. Tsuboi, This Bulletin, **25**, 60 (1952).

(9) M. Tsuboi, This Bulletin, **22**, 215, 255 (1949).

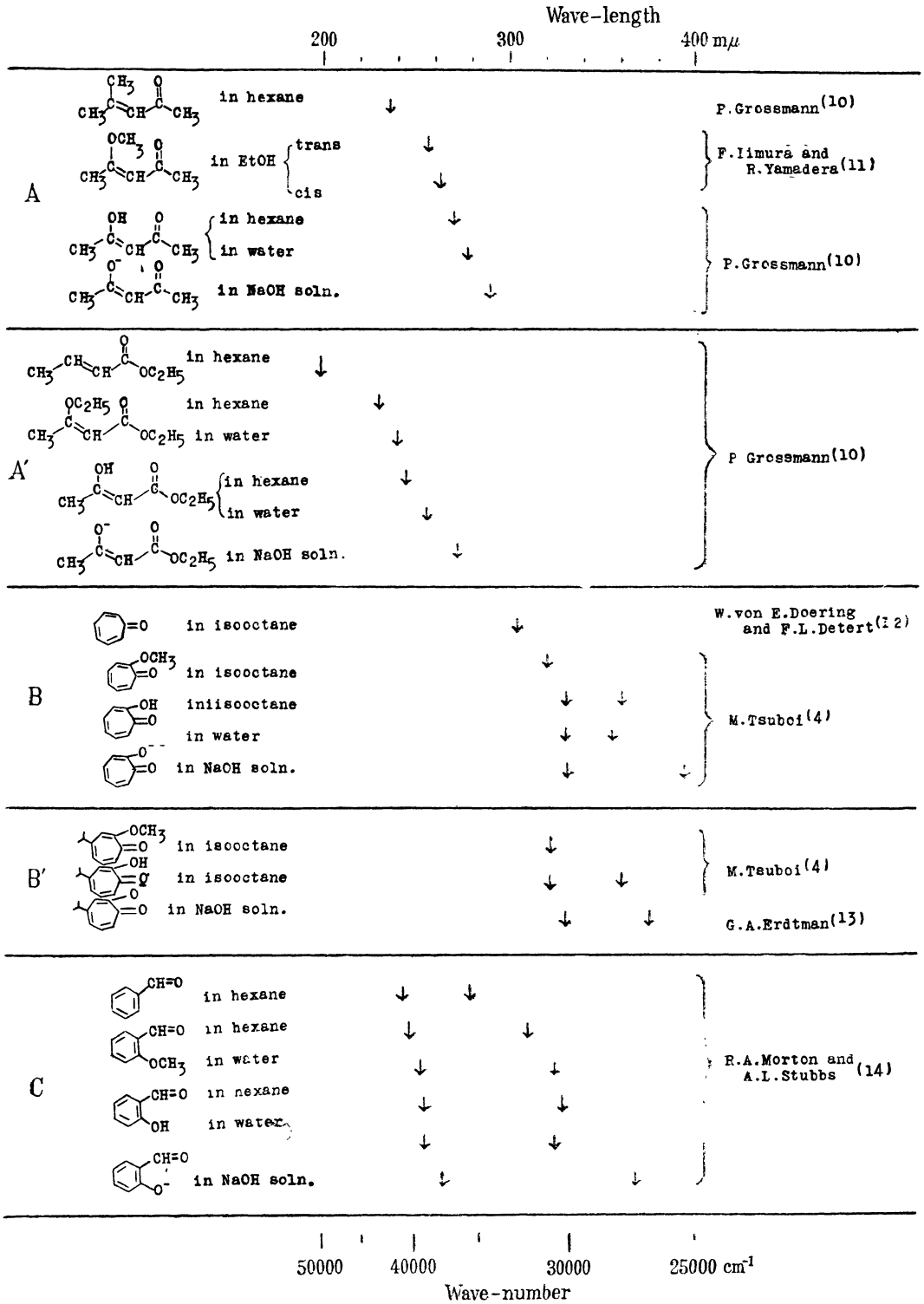

Fig. 2.

(10) P. Grossmann, *Z. Physik. Chem.*, **109**. 305 (1924).
(11) F. Iimura and R. Yamadera. Private communications.
(12) W. von E. Doering and F. L. Detert, *J. Am. Chem. Soc.*, **73**. 876 (1951).
(13) G. A. Erdtman, *Acta Chemica Scandinavica*, **4**, 1031 (1950).
(14) R. A. Mortman and A. L. Stubbs. *J. Chem. Soc.*, **1940**, 1347.

or NH groups are halfway dissociated and consequently two of the electrons of the O or N atom become partly π-electronic, having specially strong interactions with the adjacent π-electron systems, or, in other words, there occurs in these molecules a conjugation across the hydrogen bonds.

In this paper, the following five kinds of molecules are discussed. The resonance formulas tentatively given for these molecules may be considered to represent extreme cases where the relations between the hydrogen bonds and the π-electron systems are most intimate.

(A) Enolized β-diketones

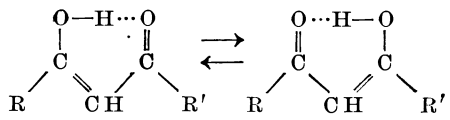

(B) Tropolone, etc.

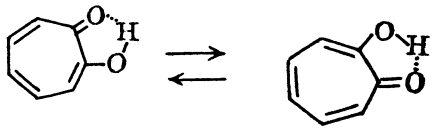

(C) Salicyl aldehyde, etc.

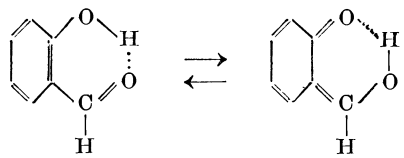

(D) *o*-Nitrophenol

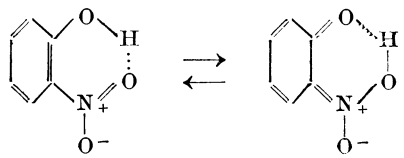

(E) Peptides

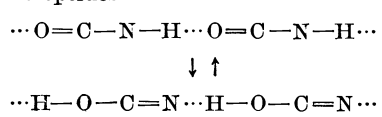

Data

The infrared and ultraviolet data are given in Figs. 1 and 2 respectively.

Fig. 1 shows the degrees in which the O—H or N—H bonds in the above-mentioned five kinds of molecules are weakened compared with the normally hydrogen-bonded O—H or N—H bonds. The arrows in the figure indicate the positions of the infrared absorption bands due to the vibrations of O—H's and N—H's in various hydrogen-bonded states, and the dotted lines, the positions of free O—H bands of alcohol and phenol and of free N—H bands of N-methylacetamide. The formulas with * in Fig. 1 represent molecular complexes which are formed in ternary solutions composed of proton-donator (phenol, etc.), proton-acceptor (benzaldehyde, etc.), and carbon tetrachloride.[8]

From Fig. 2, it may be seen that the electronic bands of the molecules now under consideration lie halfway between those of the methyl (or ethyl) ethers and anions of these molecules. The arrows in the figure indicate the positions of the ultraviolet absorption bands of several conjugated double bond systems with carbonyl groups. All of these bands, being too strong in intensity ($\varepsilon \fallingdotseq 10^4$) to be assigned to the transitions of $N \rightarrow E_n$ type,[15] may be assigned to those of $N \rightarrow V_n$ type.[15]

Discussions

A. Enolized β-diketones. (Cf. Figs. 1A, 2A and 2A') — The O—H band of enolized acetylacetone is diffuse, broad, and weak, and is situated at a position (3.7 μ), much displaced from the proper position of O—H (2.75 μ). On the other hand, the O—H bands in ordinary O—H···O=C bondings are rather sharp and strong, and are situated at about 2.85 μ. These facts reveal that the O—H bond in enolized acetylacetone (one of the conjugated chelate systems) is weaker than the O—H bonds in the normal O—H···O=C bondings. (The force constant of the former is as small as 60% of that of the latter).

The so-called $N \rightarrow V_1$ band[15] of enolized acetylacetone methyl ether, a compound in which the OCH_3 group replaces the CH_3 group in mesityloxyde, is situated at 260 mμ the position shifted as much as 25 mμ from that of the corresponding band of mesityloxyde (235 mμ)[16]. The $N \rightarrow V_1$ band shifts further to about 270 mμ when the OH group replaces the OCH_3 group in enolized acetylacetone methyl ether to form enolized acetylacetone. The shifting of electronic bands due to mere $OCH_3 \rightarrow OH$ replacement being usually not so great (for instance anisole and phenol give their electronic bands almost at the same positions in nonpolar solvents), the above-mentioned shift of the $N \rightarrow V_1$ band may be something special in electronic structure. It is noteworthy in connection with this that the

(15) H. L. McMurry, *J. Chem. Phys.*, **9**, 231, 241 (1941).

(16) This shift may be due to the electron migration from the OCH_3 toward the π-electron system of the enolized acetylacetone methyl ether. See K. F. Herzfeld, *Chem. Rev.*, **41**, 233 (1947); H. Baba and S. Nagakura, *J. Chem. Soc. Japan*, **72**, 72, 74 (1951).

$N\rightarrow V_1$ band of enolized acetylacetone is situated at an intermediate position between the bands of its methyl ether and its anion. This fact shows that the enolized acetylacetone is intermediate in the electronic state between its methyl ether and its anion; its methyl ether being composed of the field

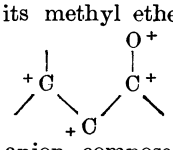

and four π-electrons, and its anion composed of the field

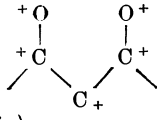

and six π-electrons (see Appendix).

R. S. Rasmussen et al[1] assumed a resonance:

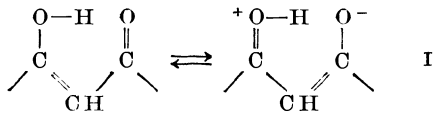

I

to occur in enolized acetylacetone. No evidence is contradictory to this theory, but the present writer is inclined to attach importance to the resonance:

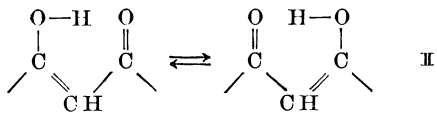

II

Thus, in the writer's view, the hydrogen atom is situated on the perpendicular bisector of the line connecting the two oxygen atoms, and the molecule has a symmetry plane which involves the bisector and is perpendicular to the molecular plane. Facts which favour the preference of resonance II rather than resonance I are:

(i) The observed dipole moment of enolized acetylacetone (about 3 D. U.) is much smaller than it should be if resonance I were predominant.[17]

(ii) Infrared absorption band due to the O—H stretching vibration of this molecule is abnormally weak in intensity.

(iii) $CH_3C(OCH_3)=CH-CO-CH(CH_3)_2$ has four isomers,

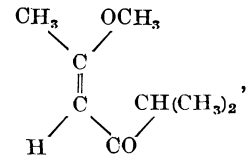

,

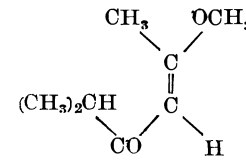

,

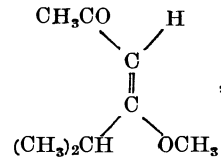

, and

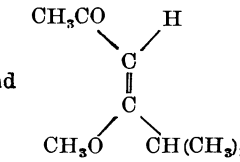

while $CH_3C(OH)=CH-CO-CH(CH_3)_2$ has only one[11].

B. Tropolone, etc. (Cf. Fig. 1B, 1B′, 2B and 2B′) — Phenol-tropolone methyl ether, a complex with *inter*-molecular O—H···O=C bonding, gives its O—H band at 3.00 μ. Here, the carbonyl O of O—H···O=C bonding is considered to be situated on the prolongation of the line representing the O—H bond vector. On the other hand in tropolone, with *intra*-molecular O—H···O=C bonding, the position of the carbonyl oxygen atom deviates greatly from the prolongation of the O—H bond vector line. Merely from molecular geometrical considerations, the above facts might appear to show that the intramolecular O—H···O=C bonding of tropolone must be much weaker than the intermolecular O—H···O=C bonding between phenol and tropolone methyl ether, and accordingly that the O—H band must be situated at much shorter wave-length than 3.00 μ. However, the actually observed O—H band of tropolone in carbon tetrachloride is situated at 3.19 μ, much longer wavelength than 3.00 μ, and is weaker and broader than the above 3.00 μ band[3]. This is an indication that the O—H bond in tropolone is weakened under a special circumstance due to the intimate relation between the O—H···O bonding and the conjugated double bonds in the seven-membered ring.

The ultraviolet absorption spectrum of tropolone exhibits features intermediate between those of tropolone methyl ether and tropolone anion. This may be taken as indicating that the intramolecular hydrogen bonding in tropolone gives an effect upon tropone ring to transform its electronic structure halfway toward that of tropolone anion.

As may be seen from Fig. 1B′ and 2B′ the O—H···O bonding in hinokitiol is the same in nature as that of tropolone.

C. Salicyl aldehyde, etc. (Cf. Fig. 1C, 1C′, and 2C)—The O—H bands of salicyl aldehyde and methyl salicylate are situated

(17) According to J. B. Conant and A. F. Thompson (*J. Am. Chem. Soc.*, **54**, 4039 (1932)), keto-enol equilibrium in β-diketones shifts toward keto-form in polar solvents, and toward enol-form in nonpolar solvents, indicating that the enol-form of β-diketones is in general less polar than the keto-form. According to C. T. Zahn (*Physik. Z.*, **34**, 570 (1933)) the mean dipole moment of acetylacetone molecule is 3 D. U. in gas phase, where more than 90% of molecules take the enol-form.

at longer wave-lengths respectively than those of intermolecular complexes: phenol-benzaldehyde and phenol—methyl benzoate. This fact shows that the O—H bond in salicyl aldehyde and methyl salicylate are weakened by the intimate relations between the O—H···O bondings and the conjugated double bond systems in these molecules.

Each of the ultraviolet absorption bands of salicyl aldehyde is intermediate in its position between the corresponding bands of its methyl ether and its anion.

A. E. Martin[18] found that in 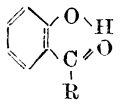 type molecules a broad O—H band is associated with the structure where R is H or CH_3, but a sharp band is produced when R is OH or OCH_3. As is known, the OH and OCH_3 groups are lower in ionization potential than the alkyl groups[19]. Then, what Martin found may be expressed as follows: the relation between the hydrogen bond and the conjugated double bond system in 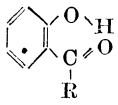 type molecules becomes less intimate as the ionization potential of R becomes lower.

D. *o*-Nitrophenol. (Cf. Fig. 1D and 1D′)—The shifting of the O—H band of phenol due to its forming an intermolecular hydrogen bond with nitrobenzene is only from 2.77 μ to 2.84 μ. From this it is seen that the oxygen atom of nitro group attached to the benzene ring is not a strong proton acceptor. Nevertheless, the O—H band of *o*-nitrophenol is situated at 3.08 μ, a much displaced position. Then, the intramolecular hydrogen bond in *o*-nitrophenol must also be related intimately with the π-electron system*.

E. Peptides. (Cf. Fig. 1E)—The dimer of N-methylacetamide with a single N—H···O=C bonding gives one N—H association bands at 2.97 μ, while its *long* chain polymer gives two N—H association bands at 3.03 μ and 3.22 μ[9]. This fact is considered to have some connections with the view advanced by T. Shimanouchi and S. Mizushima[5] as well as by M. G. Evans and J. Gergely[6], that a "conjugation"[20] is possible along the hydrogen-bonded long chain, ···HN—C=O··· HN—C=O···, in protein.

The appearance of the second N—H band at 3.22 μ is characteristic of this system. Recently, I. Oshida and Y. Oshika,[21] showed theoretically that, if in a hydrogen bond, X—H···Y, there are two almost equally stable positions of the proton between the two atoms X and Y, and if the potential barriers between these two stable positions are of certain appropriate height (Fig. 3, A), there must occur two bands in the 3 μ region from this system.

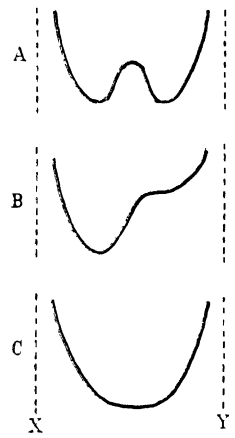

Fig. 3.—Three types (A, B and C) of the potential curve of proton in X—H···Y bonding.

It is possible that the two N—H bands of the N—H···O bondings in the long chain, ···HN—C=O···HN—C=O···, and in the ring dimers of δ-valerolactam[9,22], ε-caprolactam[9] and diketopiperazine[9] correspond to the theoretically expected bands. Further, it is possible that in ordinary hydrogen bonds one of the potential valley is much deeper than the other (Fig. 3, B) and in the conjugated chelate system there is only one wide potential valley near the centre of the line connecting X and Y atoms (Fig. 3, C).

Appendix

Electronic states of acrolein type molecule 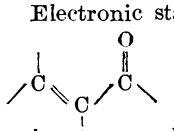 and enolized acetylacetone anion type molecule 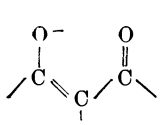 will be

(18) A. E. Martin, *Nature*, **166**, 474 (1950).
(19) A. L. Sklar, *J. Chem. Phys*, **7**, 984 (1939).
(20) H. C. Longuet-Higgins and G. W. Wheland, *Annual Rev. Phys. Chem.*, **1**, 133 (1949).
* The O-H band due to the intramolecular hydrogen bond not related with the π-electron system is situated at a position not much displaced from 2.77μ, as is exemplified by guaiacol which gives an O-H band at 2.80μ. (Cf. Fig. 1 D.).

(21) I. Oshida and Y. Oshika, *Busseiron Kenkyu*, **46**, 95 (1952).
(22) M. Tsuboi, This Bulletin, **24**, 75 (1951).

treated here according to the simple molecular orbital methods.

(I) Treatment by the LCAO Method.—Neglecting the overlap integrals, we can write the secular equation for the approximate molecular orbitals, which may be expressed as linear combinations of $2p\pi$ atomic orbitals of the C and O atoms composing these molecules, in the form:

$$\begin{vmatrix} \alpha_O-E & \gamma_{CO} & 0 & 0 \\ \gamma_{CO} & \alpha_C-E & \gamma_{CC} & 0 \\ 0 & \gamma_{CC} & \alpha_C-E & \gamma_{CC} \\ 0 & 0 & \gamma_{CC} & \alpha_C-E \end{vmatrix} = 0 \text{(acrolein)},$$

$$\begin{vmatrix} \alpha_O-E' & \gamma_{CO} & 0 & 0 & 0 \\ \gamma_{CO} & \alpha_C-E' & \gamma_{CC} & 0 & 0 \\ 0 & \gamma_{CC} & \alpha_C-E' & \gamma_{CC} & 0 \\ 0 & 0 & \gamma_{CC} & \alpha_C-E' & \gamma_{CO} \\ 0 & 0 & 0 & \gamma_{CO} & \alpha_O-E' \end{vmatrix} = 0$$

(enolized acetylacetone anion)

where α_C and α_O are the Coulomb terms for the C and O atoms, and γ_{CC} and γ_{CO} are the resonance integrals of the adjacent C—C and C—O respectively. If we assume, according to M. J. S. Dewar,[23] that

$$\alpha_C-\alpha_O=\beta$$
$$\gamma_{CO}=\sqrt{2}\beta$$
$$\gamma_{CC}=\beta \qquad \beta=-73.2 \text{ kcal./mol.}$$
$$(25600 \text{ cm.}^{-1}),$$

we obtain the following values for energy levels of the π-electrons:

$$E=\alpha_C-2.22\beta,\ \alpha_C-\beta,\ \alpha_C+0.45\beta,$$
$$\alpha_C+1.67\beta \text{ (acrolein)}$$
$$E'=\alpha_C-2.34\beta,\ \alpha_C-2\beta,\ \alpha_C-0.47\beta,$$
$$\alpha_C+\beta,\ \alpha_C+1.81\beta$$
(enolized acetylacetone anion).

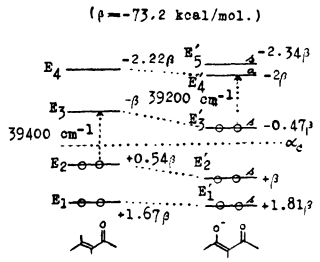

Fig. 4.

These energy levels are shown graphically in Fig. 4, in which s or a designates whether the wave function belonging to the level is symmetrical or antisymmetrical with respect to the symmetry plane of enolized acetylacetone anion molecule, which is perpendicular to the molecular plane. The observed 235 mμ (42600 cm.$^{-1}$) band of mesityloxyde may correspond to the $E_2 \rightarrow E_3$ transition (See Fig. 4, calculated 39400 cm.$^{-1}$), and the observed 290 mμ (34500 cm.$^{-1}$) band of enolized acetylacetone anion to the $E_3' \rightarrow E_4'$ transition (See Fig. 4, calculated 39200 cm.$^{-1}$).

(II) Treatment by the Free Electron Model Method.—The method assumes a model where the π-electrons in the systems

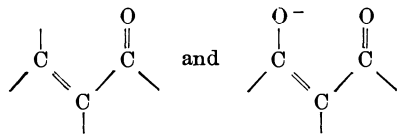

are one-dimensional electron-gases in the fields, A and B, of uniform potential, whose lengths are x and y respectively. | A | ←x→ | B | ←y→

The solution[24] of the Schrödinger equation for this model gives the energy levels shown in Fig. 5, and based on this, the wave-numbers

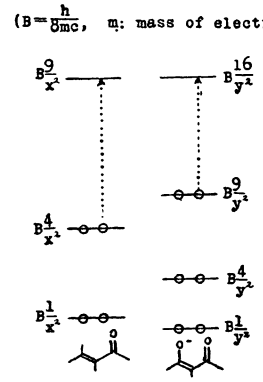

Fig. 5.

of the $N \rightarrow V_1$ bands of acrolein and enolized acetylacetone anion should be

$$\nu_1 = B\frac{5}{x^2} \quad \text{and} \quad \nu'_1 = B\frac{7}{y^2}$$

respectively. If we put here

$$\frac{x}{y} = \frac{3}{4}$$

(23) M. J. S. Dewar, *J. Chem. Soc.*, **1950**, 2329.

(24) N. S. Bayliss, *J. Chem. Phys.*, **16**, 287 (1948).

then $$\frac{\nu_1}{\nu_1'} \fallingdotseq \frac{5}{4}$$

This is in agreement with the observed ratio,

$$\frac{\nu_{obs.}}{\nu'_{obs.}} = \frac{42600\ \text{cm.}^{-1}}{34500\ \text{cm.}^{-1}} \fallingdotseq \frac{5}{4}.$$

This agreement shows that the magnitude of red-shift of the $N \rightarrow V_1$ band due to the change:

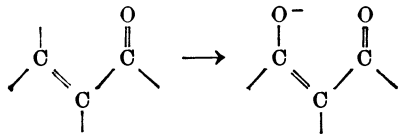

may be well explained on the basis of the free electron model.

The writer wishes to express his sincere thanks to Professors Sanichiro Mizushima, Takehiko Shimanouchi, and Saburo Nagakura, and to Mr. Hiroaki Baba, for their kind guidance and valuable suggestions. The expense of this research has been partly defrayed from Grant in Aid for Scientific Research from Ministry of Education.

Department of Chemistry, Faculty of Science, Tokyo University, Tokyo

On the Thermal Dissociation of Organic Compounds. II. The Dissociation of the Urea Linkage in Sym-dimethylurea, Asym-dimethylurea and Asym-phenylethylurea in Butyric Acid

By Toshio Hoshino, Teruaki Mukaiyama and Hiroko Hoshino

(Received April 28, 1952)

Introduction

The results of measurements of the rate constants and the activation energy of the thermal dissociation of aryl urea have already been shown in the preceeding report.[1] Then we tried to determine the same constants in alkyl urea.

On heating, alkyl urea dissociates to isocyanate and amine by the same mechanism as in sym-diphenylurea which was shown in the preceeding report. The dissociated isocyanate reacts instantaneously with butyric acid which was used as solvent and forms carbaminic acid-butyric acid-anhydride and then easily decomposes to butyrated amine and carbon dioxide.

The thermal dissociation of sym-dimethylurea in butyric acid involves the following reactions:

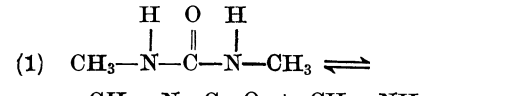

(1) $CH_3-N(H)-C(=O)-N(H)-CH_3 \rightleftharpoons CH_3-N=C=O + CH_3-NH_2$

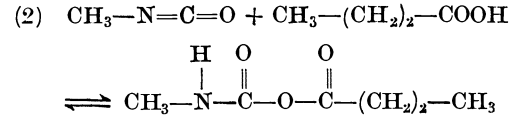

(2) $CH_3-N=C=O + CH_3-(CH_2)_2-COOH \rightleftharpoons CH_3-N(H)-C(=O)-O-C(=O)-(CH_2)_2-CH_3$

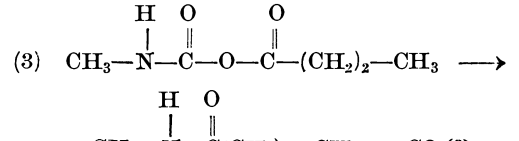

(3) $CH_3-N(H)-C(=O)-O-C(=O)-(CH_2)_2-CH_3 \longrightarrow CH_3-N(H)-C(=O)(CH_2)_2-CH_3 + CO_2$[2]

(1) T. Hoshino, T. Mukaiyama and H. Hoshino, *J. Am. Chem. Soc.*, **74**, 3097 (1952).

(2) The mechanism of process (3) can be considered as follows;. Conceivably it will proceed by way of an intramolecular nucleophilic displacement as sketched below. The use of isotropic carbon should be serviceable to demonstrate that the carbon dioxide which was evolved originated from the urea molecule.

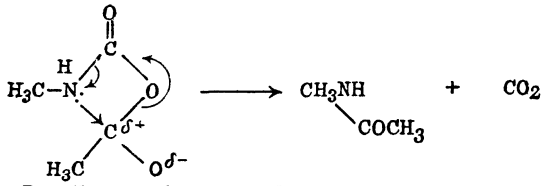

Recently, as we have assumed on the mechanism of the decarboxylation of anhydride of carbamic and fatty acids, it was proved[2]' by using C^{13} atom that carbon dioxide which was evolved originated from the urea molecule.

(2)' H. R. V. Arnstein and Ronald Bentley, *J. Chem. Soc.*, **1951**, 3509.

(4) $CH_3—NH_2 + CH_3—(CH_2)_2—COOH \rightleftharpoons CH_3—\underset{\displaystyle H}{\overset{|}{N}}—\overset{\displaystyle O}{\overset{\|}{C}}—(CH_2)_2—CH_3 + H_2O.$

If reaction (1) is rate-determining, the rate of dissociation becomes measurable if one determines the amount of carbon dioxide evolved according to (3).

Unlike the case of sym-diphenylurea described in the previous report, sym-dimethylurea could not be dissociated in acetic acid even at the boiling point (118°C), so butyric acid was adopted as the solvent and the reaction was carried above 130°C.

Asym-dimethylurea and asym-phenylethylurea dissociate, respectively, to dimethylamine and isocyanic acid, phenylethylamin and isocyanic acid in acetic acid. It was found that the reactions are similar to the case of sym-diphenylurea in acetic acid as shown in the first report. The dissociation reaction and the reaction of isocyanic acid with acetic acid proceed at comparable rate.

The rate constants and the activation energy of thermal dissociation in butyric acid were derermined.

Experimental Part

A 35 ml. long-necked, round-bottomed flask was connected to a gas buret by means of a capillary tube. Halfway along the capillary tube, a 10 ml. bulb was inserted which was maintained at 0°C. to condense reaction products less volatile than carbon dioxide. The reaction vessel was maintained at a desired, constant temperature by immersion into the vapors above a suitable boiling liquid contained in a three-necked flask equipped with condenser and thermometer; the reaction vessel was inserted in the centre neck of the flask. Vapors of the following liquid were used as heating agents: water, isoamylalcohol, xylene and anisole. The liquid was distilled prior to each run; during the course of an experiment (one to two hours) the temperature remained satisfactorily constant as long as the atmospheric pressure did not fluctuate.

Sym-dimethylurea (m. p. 108.5°C.), asym-dimethylurea (m. p. 181.0°C.) and asym-phenylethylurea (m. p. 60~61°C.) were used. Acetic acid was distilled after prolonged boiling with acetic anhydride. Butyric acid was carefully purified by vacuum distillation.

The ratio of urea to fatty acid was 1 mole: 100 moles.

To compute the rate constant of the reaction of the thermal dissociation of urea, we have used the following treatment. The first order rate law can be expressed as

$$Y = A(1-e^{-kt}), \qquad (1)$$

in which A is initial concentration of urea and Y is the amount of dissociated urea at any time. Therefore

$$\ln \Delta Y = [\ln A + \ln(1-e^{-k\Delta t})] - kt. \qquad (2)$$

As $[\ln A + \ln(1-e^{-k\Delta t})]$ is considered as independent term with respect to t, equation (2) can be expressed as follows;

$$\ln \Delta Y = \text{Constant} - kt$$

For the reaction of the first order, it requires the plot of $\ln \Delta Y$ against t to be a straight line. The rate constant is given by the gradient of the $t-\ln \Delta Y$ diagram shown in the Fig. 1, 3, and 5. For example, the experiment gave the following results. (Table 1, 2 and 3) Thermal dissociation of sym-dimethylurea in butyric acid.

Table 1

Sym-dimethylurea in Butyric Acid at 409.0°K.
Calculated with the Value of $\Delta t = 60$ min.

time (min.)	CO_2 evolved(cc.)	time (min.)	CO_2 evolved(cc.)	ΔY
10	4.2	70	24.0	19.8
15	6.1	75	25.3	19.2
20	8.1	80	26.7	18.6
25	9.9	85	27.9	18.0
30	11.6	90	29.3	17.7
35	13.3	95	30.5	17.2
40	15.0	100	31.7	16.7
45	16.6	105	32.9	16.3
50	18.2	110	34.0	15.8
55	19.7	115	35.0	15.3
60	21.2	120	36.1	14.9
65	22.6	125	37.2	14.6

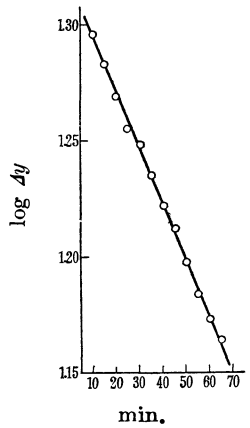

Fig. 1.—The plot of t against $\log \Delta Y$. Sym-dimethylurea in butyric acid at 409.0°K.

First order kinetics with respect to sym-dimethylurea was observed.

The rate constant (min.$^{-1}$)

$T = 409.0$°K. $k = 5.64 \times 10^{-3}$
$T = 413.2$°K. $k = 8.42 \times 10^{-3}$
$T = 421.5$°K. $k = 1.62 \times 10^{-2}$

The activation energy

$E = 34.3$ kcal.

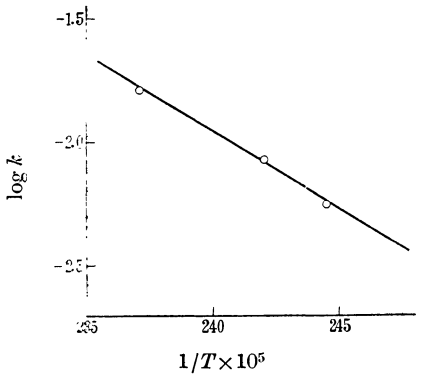

Fig. 2.—Thermal dissociation of sym-dimethylurea in butyric acid: the plot of $1/T'$ against $\log k$.

It may be noted again that the thermal dissociation of sym-dimethylurea does not occur in acetic acid.

Thermal dissociation of asym-dimethylurea in butyric acid.

Table 2

Asym-dimethylurea in Butyric Acid at 402.8°K.' Calculated with Value of $\Delta t = 60$ min.

time (min.)	CO_2 evolved(c.c.)	time (min.)	CO_2 evolved(c.c.)	ΔY
10	1.4	70	8.7	7.3
15	2.0	75	9.2	7.2
20	2.8	80	9.8	7.0
25	3.4	85	10.3	6.9
30	4.1	90	10.8	6.7
35	4.7	95	11.2	6.5
40	5.2	100	11.7	6.5
45	5.8	105	12.2	6.4
50	6.4	110	12.6	6.2
55	7.0	115	13.1	6.1
60	7.5	120	13.5	6.0
65	8.2	125	13.9	5.7

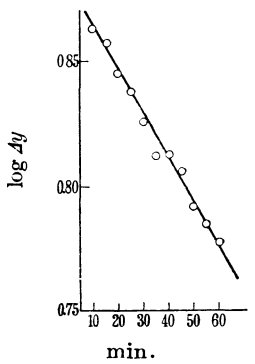

Fig. 3.—The plot of t against $\log \Delta Y$. Asym-dimetylurea in butyric acid. at 402.8°K.

First order kinetics with respect to asym-dimethylurea was observed.

The rate constant (min.$^{-1}$)

$T = 402.8$°K. $k = 3.98 \times 10^{-3}$

$T' = 409.0$°K. $k = 5.94 \times 10^{-3}$

$T' = 422.0$°K. $k = 1.70 \times 10^{-2}$

The activation energy

$E = 26.7$ kcal.

When asym-dimethylurea is heated in acetic acid, the result does not satisfy the requirement for first order kinetics. As shown in Fig. 4, the reaction belongs to the successive one.

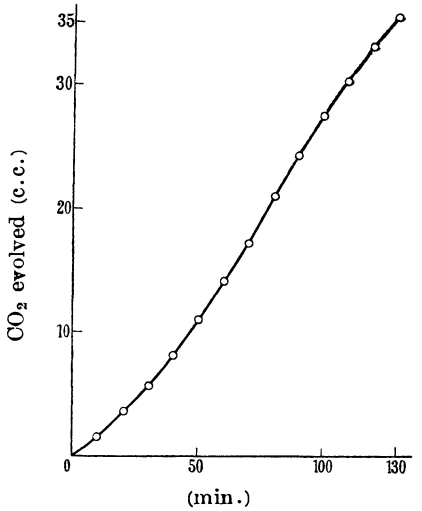

Fig. 4.—Thermal dissociation of asym-dimethylurea in acetic acid at 372.1°K.

The thermal dissociation of asym-phenylethylurea in butyric acid.

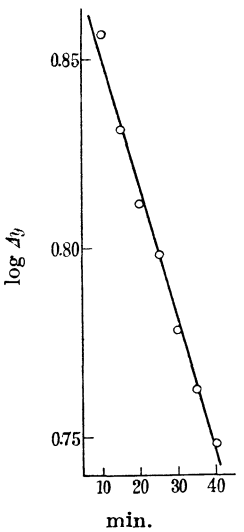

Fig. 5.—The plot of t against $\log \Delta Y$. Asym-phenylethylurea in butyric acid at 409.8°K.

Table 3

Asym-phenylethylurea in Butyric Acid at 409.8°K., Calculated with the Value of $\Delta t = 35$ min.

time (min.)	CO_2 evolved(c.c.)	time (min.)	CO_2 evolved(c.c.)	ΔY
10	1.4	45	8.6	7.2
15	2.7	50	9.5	6.8
20	3.9	55	10.4	6.5
25	4.9	60	11.2	6.3
30	5.9	65	11.9	6.0
35	6.9	70	12.7	5.8
40	7.8	75	13.4	5.6

First order kinetics with respect to asym-phenylethylurea were observed.

The rate constant (min.$^{-1}$)

$T = 400.5$°K. $k = 1.47 \times 10^{-3}$

$T = 409.8$°K. $k = 4.07 \times 10^{-3}$

$T = 411.8$°K. $k = 4.93 \times 10^{-2}$

The activation energy

$E = 30.2$ kcal.

When asym-phenylethylurea is heated in acetic acid, the result was similar to that described in the case of asym-dimethylurea in acetic acid.

Discussion

The dissociation of urea may be considered to proceed over tautomerizations:

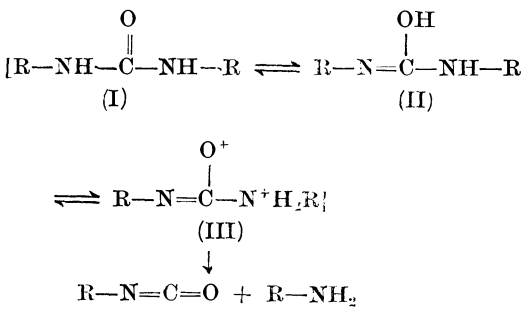

As the tautomerization occurs by an intramolecular proton transfer, the ability of proton-donors or proton-acceptors of nitrogen of urea is considered as one of the important factors for the reaction to proceed. In the tautomerization above mentioned, the tautomer (III) may be considered as activated state, which ready to dissociate into isocyanate and amine.

Experiment shows that the activation energy of sym-dimethylurea (34.3 kcal.) is larger than that of sym-diphenylurea (28.0 kcal.). By resonance effect of phenyl group, the basic strength of aromatic amine is less than that of alkyl amine as shown in Table 4 by pKh values. The tautomer (II) formed in sym-diphenylurea has more tendency to dissociate proton than in sym-dimethylurea which will be proportional to the basic charactor of corresponding amines. Also, when the tautomer (III) is formed the stability of dissociated products in arylurea introduced by resonance energy will promote the reaction more than in alkylurea. Consequently, the dissociation reaction of alkylurea needs more energy than that of arylurea.

Table 4

The pKh value for amines reported by Hall and Sprinkle[3]

ammonia	9.27	dimethylamine	10.71
methylamine	10.64	phenylethylamine	5.11
aniline	4.62		

The activation energy of asym-dimethylurea (26.7 kcal.) is smaller than that of sym-dimethylurea. In case of asym-dimethylurea, one nitrogen of urea is the primary and the other is the tertiary. In asym-dimethylurea, the tautomer (II) has more tendency to dissociate proton and to accept proton in the tautomer (III). These considerations are deduced from the basic strength of the corresponding amines. By these two effects, the reason for the lower activation energy of dissociation can be explained.

The activation energy of asym-phenylethylurea (30.2 kcal.) is larger than that of asym-dimethylurea. In these ureas, the ability of dissociating proton from the tautomer (II) is the same and that of accepting proton in the tautomer (III) is different. The tertiary nitrogen of asym-phenylethylurea has aliphatic- and phenyl-groups. By the resonance effect of the phenyl-group, the basic strength decreased as compared with that in asym-dimethylurea. Consequently, it is clear that the larger activation energy will be required.

Summary

(1) The rate constants and the activation energies of the thermal dissociation of sym-dimethylurea, asym-dimethylurea and asym-phenylethylurea were determined.

(2) It was demonstrated that the substituents have great influence on the dissociation reaction.

Laboratory of Organic Chemistry,
Tokyo Institute of Technology

(3) Norris F. Hall and Marshall R. Sprinkle, *J. Am. Chem. Soc.*, **54**, 3469 (1932).

On the Thermal Dissociation of Organic Compounds. III. The Dissociation of Ester Linkage in Phenylcarbaminic acid phenylester in Butyric acid.

By Toshio HOSHINO, Teruaki MUKAIYAMA and Hiroko HOSHINO

(Received April 28, 1952)

Introduction

That phenylcarbaminic acid phenylester decomposes to phenyisocyanate and phenol on heating has already been reported.[1] It can be considered that the carbaminic acid ester linkage of phenylcarbaminic acid phenylester dissociates to phenylisocyanate and phenol by the same mechanism as described in the preceding report[2][3] in the urea linkage which showed that it dissociates to isocyanate and amine.

In the present work, we tried to determine the rate constant and the activation energy of dissociation by the same method used in the thermal dissociation of urea linkage.

The thermal dissociation of phenylcarbaminic acid phenylester in butyric acid involves the following reactions:

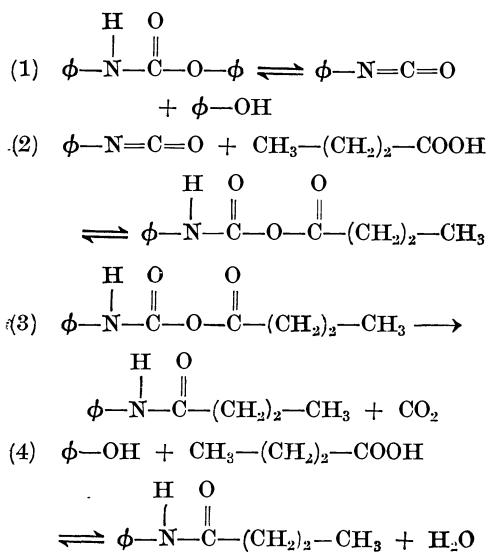

Even at the boiling point of acetic acid, the thermal dissociation of ester linkage of phenylester could not be observed. Then ester was heated in butyric acid and the dissociation reaction was observed above 130°.

As the rate of reaction of the isocyanate dissociated with butyric acid is thirty times faster than that of dissociation as it was observed by our previous experiment, we were able to determine the rate constant and the activation energy of dissociation of ester by measuring the volume of carbon dioxide evolved throughout the reaction.

Experiment Part

The apparatus was the same as that described in the first report and the volume of carbon dioxide evolved during the reaction was measured.

The sample was prepared from phenylisocyanate and phenol, recrystallized from alcohol. (m. p. 127.0°C.) Butyric acid was carefully purified by vacuum distillation.

The reaction was carried out with the ratios of 1mole of ester to 100 moles of butyric acid.

The rate of reaction was computed using the same procedure as described in the previous report.

Table 1

Phenylcarbaminic acid phenylester in butyric acid at 409.1°K, calculated with the value of $\Delta t = 50$ min.

time (min.)	CO_2 evolved(cc.)	time (min.)	CO_2 evolved(cc.)	ΔY
10	6.2	60	28.7	22.5
15	9.3	65	30.5	21.2
20	12.0	70	32.0	20.0
25	14.2	75	33.7	19.5
30	16.5	80	35.2	18.7
35	18.7	85	36.4	17.7
40	20.7	90	37.6	16.9
45	22.9	95	38.8	15.9
50	24.9	100	39.7	14.8
55	26.7	105	40.6	13.9

The rate satisfied the requirement for first order kinetics with respect to the ester.

(1) R. Leuckart, *J. prakt. Chem.*, **41**, 318 (1890).
(2) T. Hoshino, T. Mukaiyama and H. Hoshino, *J. Am Chem. Soc.*, **74**, 3097 (1952).
(3) T. Hoshino, T. Mukaiyama and H. Hoshino, This Bulletin, **25**, 392 (1952).

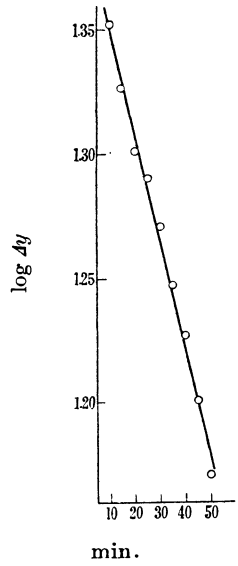

Fig. 1.—The plot of t against $\log \Delta Y$. Phenylcarbaminic acid phenylester in butyric acid at 409.1°K.

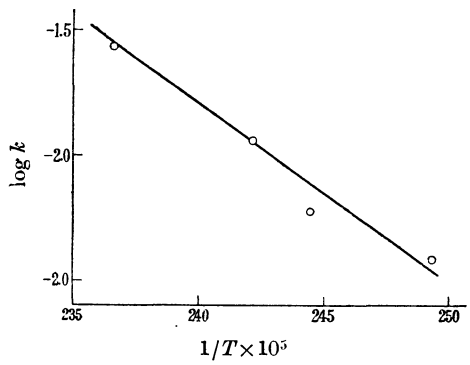

Fig. 2.—Thermal dissociation of phenylcarbaminic acid phenylester in butyric acid: the plot of $1/T$ against $\log k$.

The rate constant (min.$^{-1}$)

$T=401.1$°K. $k=3.98\times10^{-3}$
$T=409.1$°K. $k=5.94\times10^{-3}$
$T=413.0$°K. $k=1.23\times10^{-2}$
$T=422.6$°K. $k=2.71\times10^{-2}$

The activation energy

$E=33.3$ kcal.

It may be noted again that the thermal dissociation of ester does not occur in acetic acid even at the boiling point.

Discussion

As the result of the experiment, the activation energy of thermal dissociation of ester is shown to be larger than that of urea. This explains the fact that the dissociation of ester does not occur even at the boiling point of acetic acid.

The activation energy of dissociation of diphenylurea in butyric acid is 28.0 kcal. and that of phenylcarbaminic acid phenylester is 33.3 kcal.. This difference between the two substances can be explained by the following considerations.

In phenylcarbaminic acid phenylester, it may be shown that the equilibrium will take place between (II) and (III) by a intramolecular proton transfer. The equilibrium shifts in the direction of (II) and (III) on heating. The (III) dissociates to phenol and phenylisocyanate.

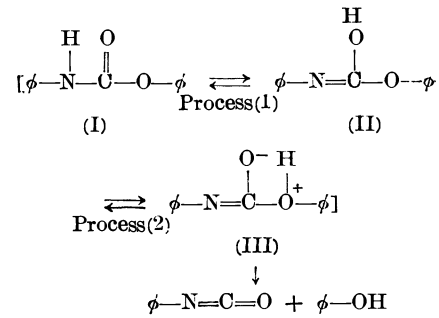

The urea, as shown in the first report, dissociates by the same mechanism.

The difference of the activation energies required for dissociation between urea and ester will be explained by using the terms, "chemical driving force" and "chemical inertia," introduced by Evans and Polanyi[4]. In the tautomerization above mentioned, (III) may be considered as activated state, which is ready to dissociate into isocyanate and alcohol. The difference between urea and ester may depend on process (2), because no appreciable difference can be found in process (1).

With the aid of this consideration, the energy required for dissociation depends on the following factors.

The chemical inertia may be attributed to the work in overcoming the interference action against the dissociating proton from $-\overset{\overset{\displaystyle O-H}{|}}{C}-$ to $-\overset{\overset{\displaystyle O^-}{|}}{C}-$ $+H^+$ and to that breaking the C—O linkage or C—N linkage. These two compounds may have a similar tendency for the former factor. According to Pauling[5] the bond energy of C—N linkage is smaller than that of C—O linkage as shown in Table 2. In this case, however, instead of neutral atoms, they should be considered as $C-N^+\rightarrow C^+:N$ or $C-O^+\rightarrow C^+:O$, and the numerical values can not be designated exactly. These considerations suggest that the chemical inertia of ester is larger than that of urea.

The chemical driving force necessary for the rupture of the ester or urea linkages may be

(4) Reviewed by Evans and Polanyi, *Trans. Fard. Soc.*, **34**, 11. (1938).

(5) L. Pauling, "The nature of the Chemical Bond", Cornell University Press, 1939, p. 57.

attributed to the formation of alcohol or amine. The heat of formation of aniline from $H^{+}+-\overset{H}{\underset{\cdot\cdot}{N}}-\phi$ or phenol from $H^{+}+-\underset{\cdot\cdot}{\ddot{O}}\phi$ and the proton acceptability of nitrogen of urea or oxygen of ester are considered as the chemical driving force in these reactions. The basity of aniline is much larger than that of phenol and this suggests that the chemical driving force is larger in urea than in ester.

The difference of the chemical inertia and the chemical driving force is the necessary potential energy of activation. On these considerations, it can be concluded that ester requires more activation energy than urea.

Table 2

Single bond energy for neutral atoms as shown by Pauling[5]

N—C	48.6 kcal.
O—C	70.0 kcal.

Summary

(1) The rate constant and the activation energy of thermal dissociation of phenylcarbaminic acid phenylester in butyric acid are determined.

(2) It has been made clear on the basis of reaction mechanism that dissociation of ester linkage requires larger activation energy than that of urea linkage.

Laboratory of Organic Chemistry, Tokyo Institute of Technology, Tokyo

Theory of Monolayer. I. Heat of Surface Vaporization in the Monolayer

By Hiroshi HOTTA

(Received April 28, 1952)

The estimation of the heat of surface vaporization in the monolayer has been tried by several investigators by applying the two-dimensional Clapeyron-Clausius' equation.[1],[2] For the estimation by this method, however, we must have both the knowledge of the area occupied by a molecule in the gaseous film as well as in the liquid film at the transition pressure, and the knowledge of the temperature depend ence of the transition pressure. These measurements are experimentally not very simple. However, the new method presented here provides the information on the heat of surface vaporization in the monolayer without any experimental difficulty.

In general the free volume in a liquid can be estimated from the vapour pressure.[3] Conversely the heat of surface vaporization must be obtained by the definition of the free surface area from a surface pressure-area curve as follows. For this purpose we shall begin with the construction of the partition function. The molecular[4] complete partition function for the monolayer, f, would be given as usual by

$$f=\frac{2\pi mkT}{h^2}\times\frac{kT}{h\nu}\times j(T)\times\Omega(T), \qquad (1)$$

where the first term is the partition function for translation in the surface, the second for vibration normal to the surface, $j(T)$ for the internal degrees of freedom of the molecule in the surface, and $\Omega(T)$ for the configurational potential energy.

Since we can write $\Omega(T)$ for the perfect gaseous film in the form

$$\Omega(T)=A=\frac{kT}{F}, \qquad (2)$$

where A is the molecular surface area and F the surface pressure, the partition function (1) is rewritten as

$$f^G=\frac{2\pi m(kT)^2}{h^2F^G}\cdot\frac{kT}{h\nu^G}\cdot j^G(T), \qquad (3)$$

where the superscript G refers to the gaseous film. On the other hand, $\Omega(T)$ for the liquid film can be expressed in the form

$$\Omega(T)=A_f e^{(U+kT)/kT}, \qquad (4)$$

according to the smoothed potential model[5], where U is the potential energy of the molecule when it is at the centre of its cell referred to an energy zero at infinite separation of the molecule,

(1) J. Sameshima, *Proc. Imp. Acad. Japan*, **10**, 155 (1934).
(2) N. K. Adam and G. Jessop, *Proc. Roy. Soc.*, **A 110**, 423 (1926).
(3) R. H. Fowler and E. A. Guggenheim, "Statistical Thermodynamics," 1939, p. 332.
(4) Since only the molecular quantity is treated in this paper, the word "*molecular*" is omitted hereafter, as far as the omission does not cause confusion.
(5) Reference 3, p. 325.

A_f the free surface area, of which definition will be given in the later part of this paper. Then, the partition function (1) is rewritten as

$$f^L=\frac{2\pi mkTA_f}{h^2}\cdot\frac{kT}{h\nu^L}\cdot j^L(T)\cdot e^{(U+kT)/kT}, \quad (5)$$

where the superscript L refers to the liquid film.

Hence we have for the chemical potential, μ, as usual

$$\mu^G=-kT\log f^G$$
$$=kT\log F^G-kT\log\frac{2\pi m(kT)^2}{h^2}-kT\log\frac{kT}{h\nu^G}$$
$$-kT\log j^G(T), \quad (6)$$

and

$$\mu^L=-kT\log f^L+F^LA^L$$
$$=-U-kT-kT\log\frac{2\pi mkTA_f}{h^2}-kT\log\frac{kT}{h\nu^L}$$
$$-kT\log j^L(T)+F^LA^L. \quad (7)$$

The equilibrium condition between gaseous and liquid film is

$$\mu^G=\mu^L. \quad (8)$$

Hence, equating (6) and (7), and assuming $j(T)$ to be equal in both films we obtain

$$\frac{F^GA_f}{kT}\cdot\frac{\nu^L}{\nu^G}=e^{-\frac{U+kT-F^LA^L}{kT}}. \quad (9)$$

Furthermore, assuming ν to be equal in both films, the propriety of which will be criticised in the following paper, we can rewrite (9) as

$$\frac{F^GA_f}{kT}=e^{-\frac{U+kT-F^LA^L}{kT}}, \quad (10)$$

where all the quantities in (10) correspond of course to these at the transition point.

On the other hand, the heat content, H, is as usual

$$H^G=-T^2\left(\frac{\partial\mu^G/T}{\partial T}\right)_F$$
$$=2kT+E^G_{int}, \quad (11)$$
$$H^L=-T^2\left(\frac{\partial\mu^L/T}{\partial T}\right)_F$$
$$=-U+kT+E^L_{int}+F^LA^L. \quad (12)$$

If we assume the internal contribution, E_{int}, including the vibration normal to the surface, to be equal in both films, corresponding to the assumption for the equality of $j(T)$ and ν, the heat of surface vaporization L^v, is written as

$$L^v=H^G-H^L=U+kT-F^LA^L \quad (13)$$

Introducing this relation into (10), it becomes

$$\frac{F^GA_f}{kT}=e^{-\frac{L^v}{kT}}. \quad (14)$$

The larger the molecular area in the liquid film is, the more accurate this equation is, because the state is more ideal and it is assumed implicitly in the above derivation that the configuration of molecule in the surface is similar in both films. In this sense the following calculation listed in Table 1 is rational.

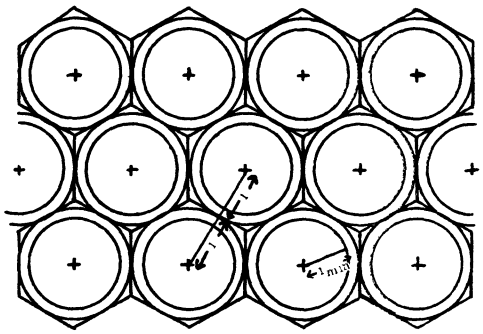

Fig. 1.

For the estimation of the heat of surface vaporization, it is necessary to define the free surface area with the measurable quantities. Since the molecules in the liquid film are supposed to be closely packed and each of them is free to move in each cell, the observed surface area may be the area of a hexagon as shown in Fig. 1. When the radius of an inscribed circle is r, the area must be

$$A=3.464\,r^2. \quad (15)$$

If it is supposed, that the minimum compressible surface area, A_{min}, *in this state* is equal to the area at the kink point for the next transition or at the collapse point, A_{min} is similarly expressed by

$$A_{min}=3.464\,r^2_{min}, \quad (16)$$

where r_{min} is the radius of an inscribed circle in this case. Therefore, the free surface area might be expressed by

$$A_f=3.464(2r-2r_{min})^2, \quad (17)$$

as the modification of a model used by Lennard-Jones and Devonshire.[6] Substituting from (15) and (16) into (17) we can obtain

$$A_f=4g(\sqrt{A}-\sqrt{A_{min}})^2, \quad (18)$$

where g is the form factor as the measure of the deviation of the chain molecule from the rigid disk model. Although there is no physical evidence that the hexagon model should be especially accepted to the free surface, this correction is also contained in this form factor. For simplicity, this factor is assumed hereafter to be unity even though it may be slightly more than unity.

We can now attain the first object by inserting (18) into (14), that is,

$$\frac{4F^G(\sqrt{A}-\sqrt{A_{min}})^2}{kT}=e^{-\frac{L^v}{kT}}. \quad (19)$$

(6) Lennard-Jones and Devonshire, *Proc. Roy. Soc.*, **A 163**, 59 (1937).

Table 1[7][8][9]

Substance	Temperature in °C.	F^G in dyn./cm.	A	A_{min}	A_f	U	U^*	Literature
			in A.^{2}			in 10^{-14} erg/molecule		
Myristic acid	7.2	0.130	46.3	43.0	0.78	28.2		
	9.1	0.149	47.5	40.8	1.08	26.3		
	14.1	0.199	51.0	35.0	6.86	18.4	18	(2) (7)
	17.0	0.228	51.6	33.2	6.97	17.9		
	18.0	0.238	51.8	32.2	9.36	16.7		
	22.3	0.281	52.5	30.5	9.98	16.0		
Pentadecylic acid	17.9	0.142	43.8	41.4	0.032	41.4	61	(2) (9)
α-Bromo C_{17} acid	13	0.013	46.5	36.0	2.07	33.7		(7)
α-Monomyristin	12.5	0.017	70.0	41.5	12.0	16.7		(8)

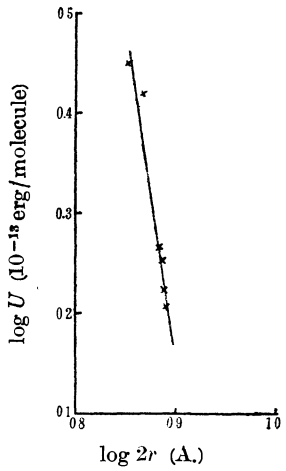

Fig. 2.—Relation between potential energy and intermolecular distance for myristic acid. The straight line is expressed by formula (20).

Unfortunately, the suitable experimental data for the comparison with this estimation are sparse. The values thus estimated of some substances, on which the reliable experimental data are available, are listed in Table 1 with the related matter. The surface vapour pressure of fatty acid, F^G at definite temperature, in the Table was calculated from the experimental data at the room temperature by assuming that dF^G/dT is 0.01 dyn./cm.,[2] and U^* in the Table is the value of U obtained by Adam and Jessop at about 14°C. with aid of Clapeyron-Clausius' equation.[2] The agreement with both values of myristic acid is satisfactory. On the contrary, the disagreement with the data of pentadecylic acid may be caused from the combination of data of different authors.

If $\log U$ for myristic acid is plotted against $\log 2r$ as shown in Fig. 2 in order to obtain the relation between the potential energy and the intermolecular distance, these points lie nearly on a straight line expressed by the formula

$$U = \frac{3.8\times10^{-8}}{(2r)^6} \text{ erg/molecule,} \qquad (20)$$

where r is in A. unit. The most reliable data at the room temperature, is taken as standard. In this case we assume implicitly that U is independent of temperature. If this assumption is justified it may be concluded from (20) that the energy of cohesion in the liquid expanded film is mainly due to van der Waals' force. However, the Harkins' data on the myristic acid[8] are not so regular. We must, of course, remember that all the data cited here were measured on the acidulated substrate, so that the dissociation was repressed. The deviation from the line shown in Fig. 2 may be corrected by the exact measurement of the surface vapour pressure.

In conclusion, although the theory contains some assumption, it is sure that a new measure has been presented for the surface phenomena, and that the problems proposed here may be brought to a settlement only by the exact and systematic experiment. Nevertheless, if the adequate data for the homologous series can be obtained, it may be possible to describe the interaction between the molecules in the liquid film.

The author wishes to express his sincere thanks to Prof. T. Isemura for his kind advice and encouragement.

The Institute of Scientific and Industrial Research, Osaka University, Sakai, Osaka

(7) N. K. Adam and G. Jessop, *Proc. Roy. Soc.*, **A 112**, 862 (1926).
(8) N. K. Adam and G. Jessop, ibid., **A 117**, 532 (1927).
(9) G. C. Nutting and W. D. Harkins, *J. Am. Chem. Soc.*, **61**, 2040 (1939).

On a Relation between Dielectric Constant and Heat of Vaporization of Non-polar Liquids.

By Akiyoshi WADA

(Received May 6, 1952)

The nature of the attractive force between two molecules with no permanent electric moment was first explained by London[1] as a "dispersion force". As is well known, it is due to the polarization of each molecule by the other. Even though each molecule is centro-symmetrical, that is, a non-polar molecule, it always has some instantaneous dipole moment caused by the internal electronic oscillation. Such an instantaneous dipole moment of each molecule polarizes the other and produces an attractive force.

On the other hand, according to Onsager[2], if an electric dipole μ is immersed in a dielectric, whose dielectric constant, ε, is larger than 1, it is stabilized by the amount ΔE:

$$\Delta E=\frac{(\varepsilon-1)}{2\varepsilon+1}\cdot\frac{\mu^2}{a^3}\cdot N, \qquad (1)$$

where a is the radius of the molecule, and N is Avogadro's number.

Now if we take ε of Eq. (1) equal to the dielectric constant of the non-polar liquid and μ its instantaneous dipole moment, then the energy of vaporization, E_{evap}, is approximately equal to the mean energy of the ΔE given by Eq. (1);

$$E_{evap}=\frac{(\varepsilon-1)}{2\varepsilon+1}\cdot\frac{\bar{\mu}^2}{a^3}\cdot N. \qquad (2)$$

The effective dipole moment of the molecule is estimated as follows: The "dispersion energy" between two molecules separated by distance R is

$$-\frac{3}{4}\cdot\frac{I_0\alpha^2}{R^6}, \qquad (3)$$

where α is polarizability and I_0 is the ionization potential of the molecule. While the energy of interaction between polarizability α and the mean dipole moment $\bar{\mu}^2$ is

$$-\frac{2\bar{\mu}^2\alpha}{R^6}. \qquad (4)$$

By equating Eqs. (3) and (4), we have

$$\bar{\mu}^2=\frac{3I_0\alpha}{8}. \qquad (5)$$

Following Onsager, if the molecule is regarded as a sphere of radius a with a polarizability α, the dielectric constant ε is expressed by the Lorenz-Lorentz formula in the case of non-polar liquid;

$$\alpha=\frac{\varepsilon-1}{\varepsilon+2}\cdot a^3. \qquad (6)$$

Using Eqs. (2), (5) and (6), we obtain the final relation between the heat of vaporization H_{evap} and the dielectric constant:

$$H_{evap}=E_{evap}+RT=\frac{(\varepsilon-1)^2}{(2\varepsilon+1)(\varepsilon+2)}\cdot\frac{3NI_0}{8}+RT. \qquad (7)$$

This equation provides the temperature dependence of heat of vaporization in terms of the dielectric constant at each temperature.

The ionization potential I_0 can be given by the spectroscopic data, but unfortunately we have no such accurate data extending over the all ranges of frequency, so that it shall now be treated as an empirical parameter.

Table 1

	t°C.	H_{evap}(calc.) kcal./mol.	H_{evap}(obs.) kcal./mol.
Benzene	20	8.08	8.11
	60	7.60	7.61
	100	7.08	7.08
	140	6.59	6.46
	180	6.04	5.80
Carbon bisulphide	0	6.80	6.82
	20	6.67	6.67
	46	6.41	6.41

In Table 1, the heat of vaporization H_{evap}(calc.) of benzene and carbon bisulphide calculated by Eq. (7) is compared with the observed values. The experimental data of ε and H_{evap} are taken from the "International Critical Tables". The parameter I_0 is assumed as 12.4 eV. and 8.0e V. respectively, and these figures seem reasonable for these molecules compared with observed values 6.0 eV. and 9.6 eV.[3] in the case of benzene. It will be seen that the temperature dependence of the heat of vaporization is well expressed by this relation.

The writer wishes to express his sincere thanks to Professor Yonezo Morino for his kind advice.

Department of Chemistry, Faculty of Science, Tohyo University, Tokyo

(1) F. London, *Z. Physik.* **63**, 245 (1930).
(2) L. Onsager, *J. Am. Chem. Soc.* **58**, 1486 (1936).
(3) P. E. Boucher, *Phys. Rev.* **19**, 189 (1922). "Int. Crit. Table," Vol. 6, P. 72.

On the Molecular Structures of synthetic Estrogens. I. On *meso*-Hexestrol Dimethyl Ether and *trans* $\alpha\alpha'$-Bis (methylthio) stilbene

By Wataru SUETAKA

(Received March 18, 1952)

Since several years ago a certain number of synthetic estrogens have been prepared, and a hypothesis on the reason of their efficacy was presented: they are effective because their molecular structures are closely similar to those of natural ones[1]. In order to discuss the molecular structures of synthetic estrogens, the dipole moment of two substances, *meso*-hexestrol dimethyl ether and *trans* $\alpha\alpha'$-bis (methylthio)-stilbene, were measured. The former is an estrogenic diphenylethane, and the latter probably has the same molecular structure as that of *pp'*-dimethoxy *trans* $\alpha\alpha'$-bis (methylthio) stilbene, an estrogenic stilbene, because these two substances were prepared by the same reaction.

Experimental Part

The density d and the dielectric constant ε of the solutions in benzene or in carbon tetrachloride were measured with pycnometre and a heterodyne beat apparatus. The apparatus and the method used here were already reported elsewhere[2]. The wavelength used is about 150 metres.

The molar polarization P_2 of the solute was calculated by the following equation:

$$P_2 = M_2\{(p_{12}-p_1)/w+p_1\},$$

where

p_{12}: the specific polarization of the solution
p_1: the specific polarization of the solvent
w: the weight fraction of the solute
M_2: the molecular weight of the solute

If $P_{2\infty}$ designates P_2 at the infinite dilution, the dipole moment at the temperature T is calculated by the equation

$$\mu = 0.0127\sqrt{\{P_{2\infty}-(P_E+P_A)\}T} \quad \text{(in Debye unit)}$$

where

P_E: the electronic polarization of the compound
P_A: the atomic polarization of the compound

P_E was taken to be equal to the molar refraction MR_D for D sodium line, which was calculated by atomic refraction given in "Landolt-Börnstein Tabellen", and P_A was assumed to be 5% of MR_D. The solution, with which the experiment was carried out, were so dilute, that $P_{2\infty}$ was safely taken to be equal to the mean value of P_2's.

The solvent benzene was made free from thiophene by aluminium chloride. It was then dried over metallic sodium and distilled; the fraction boiled within 0.5°C. was collected for use. Carbon tetrachloride is the highest commercial grade, which was distilled, dried over calcium chloride and redistilled; the fraction boiled within 0.3°C. was collected for use. One of the samples *trans* $\alpha\alpha'$-bis (methylthio) stilbene, was kindly prepared by Dr. R. Ikeda of the Chemical Laboratory, Faculty of Science, Tokyo University and the other was prepared by Teikoku Zoki Co. Their purity was confirmed by the measurement of melting points: m. p. 143.9—144.0°C. for *meso*-hexestrol dimethyl ether, and 146.5—148.0°C. for *trans* $\alpha\alpha'$-bis (methylthio)-stilbene.

The results of the measurements are given in Table 1, 2 and 3.

Table 1

The Dielectric Constants and the Densities of *meso*-Hexestrol Dimethyl Ether in Carbon Tetrachloride Solutions at 25°C.

w	ε	d (g./cc.)	P_2 (cc.)
0.00000	2.2260	1.58329	—
0.00629	2.2421	1.57907	158.6
0.01098	2.2529	1.57360	162.8
0.01606	2.2632	1.56901	159.1

$P_{2\infty}=160.2$ cc. $\mu=1.77$ (D)

Table 2

The Dielectric Constants and the Densities of *meso*-Hexestrol Dimethyl Ether in Benzene Solutions at 25°C.

w	ε	d (g./cc.)	P_2 (cc.)
0.00000	2.2720	0.87236	—
0.01374	2.2861	0.87408	145.0
0.03509	2.3109	0.87736	146.6

$P_{2\infty}=145.8$ cc. $\mu=1.57$ (D)

(1) E. C. Dodds, L. Goldberg, W. Lauson and R. Robinson: *Nature*, **141**, 248 (1938).
(2) S. Mizushima, Y. Morino and K. Higasi: *Sci. Papers Inst. Phys-Chem. Res. (Tokyo)*, **25**, 159 (1934).

Table 3

The Dielectric Constants and the Densities of *trans* αα'-Bis (methylthio) stilbene in Benzene Solutions at 30°C.

w	ε	d (g./cc.)	P_2 (cc.)
0.00000	2.2620	0.86610	—
0.01172	2.2741	0.86908	120.0
0.01531	2.2774	0.86990	118.9

$P_{2\infty} = 119.5$ cc. $\mu = 1.24$ (D)

Discussion of the Result

1. *meso*-Hexestrol Dimethyl Ether—As this compound has a C—C rotational axis in its center, two isomers may exist in principle with regard to this axis, the one being the trans form, and the other the gauche form, as shown in Fig. 1.

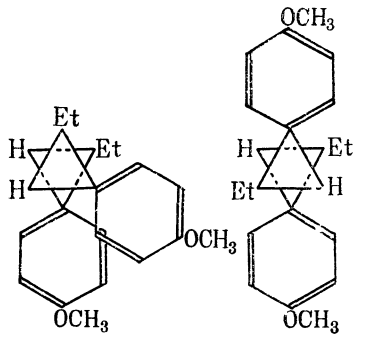

cis $\mu = 2.06$ D *trans* $\mu = 1.75$ D

Fig. 1.

The dipole moments of two isomers were estimated by vector addition. For the moment of CH_3—O bond the value 1.29 D estimated from the dipole moment of hydroquinone dimethyl ether 1.70 D[3] under the assumption of the value of 111°[4] for the C—O—C bond angle was used, and for the moment of C—O bond the value 0.78 D* estimated from the dipole moment of anisole 1.35 D[5] under the same assumption. It is assumed that the methyl group makes free rotation about C—O axis. For both the moments of H—C and C_2H_5—C bonds, the value of 0.3 D was assumed. The resultant moment of the *trans* and the *gauche* form thus computed are 1.75 D and 2.06 D respectively.

On comparing them with the observed moments, the value 1.77D* observed in carbon tetrachloride solution is almost equal to that of the *trans* form. Hence it may be concluded that, if ever exist, there is only small amount of the *gauche* form in carbon tetrachloride solution. This conclusion may be justified, when taking into account the fact that in the *gauche* form two *p*-methoxyphenyl groups and two ethyl groups come mutually too near to make this form stable. The fact that this compound is of the *trans* form makes it favourable that this compound has the molecular structure similar to that of natural estrogen. The observed moment in benzene solution 1.57 D is lower than that in carbon tetrachloride solution. But the interpretation of this result seems to be difficult.

2. αα'-Bis (methylthio) stilbene—This compound has two isomers: the *trans* and the *cis* isomers with regard to the central C=C bond. The isomer used for the measurement was obtained as crystal and the other isomer remained in the solution as oil. Since these *trans* isomers generally have higher melting points than that of the *cis* isomers, the isomer used for the measurement seems to be the *trans* one. The determination whether this compound has *trans* or *cis* form is also an object of this research.

If this compound has a structure closely similar to that of natural estrogen, it must have the configuration as shown in Fig. 2.

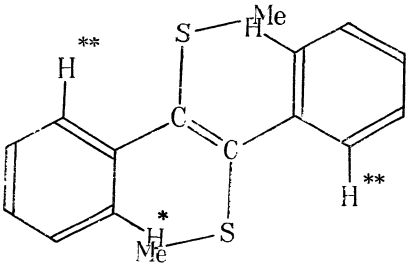

Fig. 2.

This configuration has a center of symmetry and hence has a dipole moment equal to zero. The experimental value, however, does not satisfy this expectation, so evidently this compound is not fixed in this configuration. Then the decision of the structure of this compound is interesting. At first sight it might be considered that the benzene planes are fixed on the same plane as that of the four bonds neibouring to the C=C bond by the quantum mechanical resonance between the phenyl groups and central C=C bond. But if the benzene rings are fixed on this plane, the distances between the methyl groups and the H* or H** atoms attatched to the phenyl groups at the *ortho*-positions must be shorter than 2.7 A. This distance is definitely shorter than 3.2 A., the sum of the van der Waals' radii, therefore probably the benzene rings are twisted from the plane. This conjecture agrees with the result of the ultraviolet absorption spectra of the similar compounds. The resultant moment of this molecule depends on the relative positions of the two methyl

* For this value, from the dipole moment of phenyl ether 1.35D, (5) 0.89D is estimated under the same assumption.

(3) S. Mizushima, Y. Morino, and H. Okazaki: *Sci. Papers Inst. Phys-Chem. Res. (Tokyo)*, **34**, 1147 (1943).

(4) R. Maxwell: *J. Opt. Soc. Am.*, **30**, 374 (1940).

(5) L. G. Groves and S. Sugden: *J. Chem. Soc.*, **1937** 1782.

groups, which can rotate around the S—C bond. Using the moment 1.15 D for CH_3—S bond, which has been obtained from the moment 1.40 D[6] of dimethyl sulphide and the C—S—C bond angle 105°[4], the observed value 1.24 D of this compound provides the value 112° of angle between the two S—CH_3 bonds. If both of the S—CH_3 bonds rotate in reverse directions, starting from the *trans* position as shown in Fig. 2, the positions of rotational angles 34°, 146°, and a pair of 30° and 222°, give the observed moment. Of these positions only that of the rotational angle 34° is favourable for this compound to maintain the molecular structure similar to that of natural estrogen. Assuming the values of C—C: 1.54 A., C=C: 1.34 A., C—S: 1.82 A., C—H: 1.07 A., $<C=C—C$: 120° and $<C—S—CH_3$: 105°, when the rotation by 34° around the S—C bond is assumed, the benzene rings must be twisted circa 75° from the plane, in order to keep the H* atom at the distance 3.2 A. from the methyl groups. This structure has the distances 3.12 A. between CH_3 groups and H** atoms, but the distances among the groups in a molecule generally can be shorter than the van der Waals' distances, thus probably this structure is realized.

In this place it is worth while to compute the moment of the *cis* isomer. The *cis* isomer has also the axes of rotation around S—C bonds. Assuming the moment 0.85 D for C—S bond, 1.15 D for CH_3—S bond, and 0.3 D for H—C bond, the simple vector addition gives the value from 0.40 D to 3.12 D for the moment of the *cis* isomer. But if the configurations are excluded, in which the distance between the two methyl groups is within 4.0 A., the sum of the van der Waals radii, the structure having the moment smaller than 1.30 D are not allowed to exist. The observed value 1.24 D lies in this unallowed region. Thus it might be concluded that this compound is not the *cis* isomer. But taking into account the basic assumtion for this calculation, it seems unreasonable to insist only from this reason that this compound is the *trans* isomer.

From the discussion described above it seems that these substances have general resemblance to natural estrogen in their molecular structures.

I wish to express my deep gratitude to Prof. Y. Morino and Dr. I. Miyagawa of the Chemical Laboratory, Faculty of Science, University of Tokyo, for their many helpfull suggestions and discussions. I am also indebted to Dr. T. Takahashi and Dr. M. Ōki of the Chemical Laboratory, Faculty of Science, University of Tokyo, for their kind supply of the sample and their encouragement throughout this work.

Research Laboratory of Fuel Science, Tokyo Institute of Technology, Tokyo

(6) H. Staude "Physikalisch-chemisches Taschenbuch" (1945).

Electrolytic Reduction of Aromatic Carboxylic Acids. I. Reduction of Benzoic Acid under Pressure[1]

By Shin-ichi ONO and Tsuneo YAMAUCHI

(Received May 7, 1952)

A number of investigations have been carried out on the electrolytic reduction of benzoic acid, but all of them were made at ordinary pressure in an open vessel. The authors, therefore, studied this problem under the pressure of hydrogen and carbon dioxide to find out the effect of the pressure on the reduction products.

(1) Reduction of Benzoic Acid to Benzylalcohol.—C. Mettler[2], Fr. Fichter and Israel Stein,[3] H. Inoue,[4] Sherlock Swann and G. D. Lucker,[5] studied this problem in the alcoholic sulfuric acid solution by using a lead cathode with good yields. The authors carried out electrolysis in alcoholic sulfuric acid solution by using a lead cathode and compared the yield of benzyl-alcohol obtained under the various pressures of hydrogen and carbon dioxide with that obtained in an open

(1) Presented at the annual meeting of the Chem. Soc. of Japan in 1950.

(2) C. Mettler, *Ber.*, **38**, 1745 (1905).

(3) Fr. Fichter, Israel Stein, *Helv. Chim. Acta.*, **12**, 821 (1929).

(4) H. Inoue, *J. Soc. Chem. Ind. Japan*, **24**, 806 (1921).

(5) Sherlock Swann and G. D. Lucker, *Trans. Electrochem. Soc.*, **75**, 411 (1939).

vessel. Not only hydrogen but also carbon dioxide had an important effect on the yield of the reduction product. The yield increased in proportion to the pressures of hydrogen or carbon dioxide respectively. (Table 1)

(2) Reduction of Benzoic Acid to Benzaldehyde. — Hugo Weil[6] and Mettler[7] studied this problem by using a mercury cathode and benzene, and obtained benzaldehyde with 30—50% yield. Benzaldehyde was removed to a benzene layer from a water layer and protected from reduction to alcohol.

S. Tesh. Alexander Low[8] obtained 50% benzaldehyde by using sodium bisulfite which combined with benzaldehyde instead of benzene, but only 20% by Mettler's method.

The authors carried out the electrolysis by using a mercury cathode in a mixture of boric acid, sodium sulfate solution and benzene. The yield increased in accordance with the pressure of hydrogen. In case of carbon dioxide the yield decreased as the pressure increased. (Table 2)

(3) Reduction of Benzoic Acid to Ethyl Hexahydrobenzoate.—Emill Müller[9] electrolysed benzoic acid in alcoholic sulfuric acid solution by using a lead cathode, and obtained a hydro-compound, but F. Somlb[10] identified this to be dihydro benzoic acid ethylester. Fr. Fichter[11] obtained benzylalcohol mainly by the same method, and predicted that one will obtain hydro-compound when the current density is small.

The authors carried out the electrolysis in alcoholic sulfuric acid solution by using a platinized platinum cathode. When the pressure of hydrogen or carbon dioxide was increased, the yield of ethylhexahydrobenzoate decreased but the yield of hexahydrobenzoic acid increased.

It was thought that ethyl benzoate was formed from benzoic acid under this condition and the ester was reduced to ethyl hexahydrobenzoate.

It was found that the electrolytic reduction of benzoic acid at a platinized platinum cathode in alcoholic sulfuric acid solution gave rise to hexahydrobenzoic acid and its ester, but no benzylalcohol.

These results contrast sharply with that obtained from a lead cathode. It was assumed that there would be an essential difference between the nature of lead and platinized platinum cathode in the course of reduction.

Examination of the Table 4 shows that the hydrogen pressure has an effect on the reduction products.

(6) Hugo Weil, D. R. P. 196, 293 (1906).
(7) C. Mettler, *Ber.*, **41**, 4148 (1906).
(8) Alexander Low, *Tran. Am. Elec. Chem. Soc*, **45**, (1924).
(9) E. Baur and E. Müller, *Zeit. Elektrochem.*, **34**, 98 (1928).
(10) F. Somlb, *Zeit. Elektrochem.*, **35**, 264 (1929).
(11) Fr. Fichter, *Helv. Chim, Acta.*, **12**, 821 (1929).

Experimental

(1) Reduction of Benzoic acid to Benzylalcohol.—The electrolytic conditions were as follows: cathode: lead plate, 1 dm.^{2}; cathodic solution: 10 g. of benzoic acid, 70 g. of sulfuric acid, 60 g. of ethyl alcohol; anode: lead; anodic solution: 30% sulfuric acid; current density: 5 amp./dm.^{2}; Temperature: 30—50°C.; current quantity: 10 amp. hrs.; Pressure: 1—30 atmosphere.

The temperature was kept under 50°C. by using a water bath and by stirring the cathodic solution vigorously; the current was passed until 10 amp. hrs. were reached.

When the electrolytic reduction was completed, the catholyte was poured into water and extracted with ether. The ether solution was dried with anhydrous sodium sulphate. After the vapourization of the ether, the pale yellow fragrant oil was fractionated at 180—220°C. The fraction was saponified with 2N caustic soda and was extracted with ether and distilled. The fraction between 196—203°C. has specific gravity of 1.045 at 20°C. and refractive index $n_D^{25}=1.5283$ (those of benzylalcohol are $D^{15}=1.0507$, $n_D^{25}=1.53866$ respectively). It dissolved calcium chloride and gave the odour of benzaldehyde when warmed with nitric acid. Thus we regarded this fraction as benzylalcohol. When the residual water solution at the above mentioned extraction was acidified by adding sulfuric acid, the precipitation was gained. This was identified as benzoic acid, judging from its freezing point. Hydrobenzoin and benzene were not detected.

To study the effect of pressure, the electrolytic cell with a stirrer was placed in an autoclave specially designed* for this purpose. The gas was introduced to remove the air, and then the desired pressure was maintained and a series of electrolytic reductions was made under pressures of 1—30 atmosphere.

Result are summerized in Table 1.

Table 1

Pressure of H_2	Yield		Current Efficiency
1 atm.	4.5 g.	50.8%	44.6%
10	5.6	63.2	55.4
15	6.5	73.4	64.4
30	7.2	81.3	71.4
Pressure of CO_2	Yield		Current Efficiency
1 atm.	4.5 g.	50.8%	44.6%
10	5.0	56.4	49.5
20	5.2	58.7	51.5
30	5.5	62.1	54.5

* S. Ono, *J. Chem. Soc. Japan*, **73**, 852 (1952).

(2) Reduction of Benzoic Acid to Benzaldehyde.—The electrolytic conditions were as follows: cathode: mercury (16.2 cm.^{2}); cathodic solution: 6.5 g. of sodium sulphate, 6.5 g. of boric acid, and 5 g. of sodium benzoate were dissolved into 85 cc. of water and 50 cc. of benzene for fixation of the aldehyde added to this solution.

anode: lead; anodic solution: 10% aquous solution of sodium sulphate; current density: 6 amp./dm.^{2}; current quantity: 4 amp. hrs.; temperature: 20—25°C.; presure: 1—30 atm.

After breaking the current, we continued the stirring further on for about one hour to utilize the reducing power of sodium amalgam. Then the catholyte was separated from mercury and 100 cc. of 10% sulfuric acid was added and steamdistilled. The distillate was extracted with ether and the ether solution was neutralized with sodium bicarbonate to remove the unreduced benzoic acid to the water layer.

The ether solution was dried with anhydrous sodium sulphate. After stripping the ether, we gained benzaldehyde with boiling point 179°C. The water solution was acidified and the precipitated benzoic acid was recovered. On the contrary, aldehyde was not obtained in the case of lead-, platinized platinum-, or copper-cathode. This reason is explained as follows: Mercury acts as sodium amalgam by which benzoic acid is reduced to aldehyde, and then sodium amalgam turns back to mercury. In this case, the system of the mercury and sodium amalgam was circulated by electrolysis. Thus the yield of aldehyde was increased by keeping the experimental conditions to suit the formation of sodium amalgam. If the catholyte became alkaline, the velocity of the action of sodium amalgam on benzoic acid was slowed down. On the contrary, by maintaining it in a condition to make the above-said velocity speedy, the formation of sodium amalgam was decreased.

When the electrolytic reduction was undertaken at high pressure of hydrogen atmosphere, the yield of aldehyde was increased with the pressure, but in the carbon dioxide atmosphere the yield was decreased with the increase of the pressure. The latter can be illustrated as follows: the increase of the amount of carbon dioxide dissolved in catholyte decomposes sodium benzoate to benzoic acid and the catholyte increases acidity, so that the yield decreases. It seems that the dissolution of carbondioxide and benzoic acid in benzene makes the dissolution of aldehyde in benzene more difficult.

Results are summarized in Table 2.

Table 2

Pressure of H_2	Yield		Current Efficiency
1 atm.	0.6 g.	16.3%	7.6%
20	1.1	29.9	13.9
30	1.6	43.3	20.1
Pressure of CO_2	Yield		Current Efficiency
1 atm.	0.6 g.	16.3%	7.6%
10	0.3	8.2	3.8
20	trace	—	—

(3) Reduction of Benzoic Acid to Ethyl Hexahydrobenzoate.—The electrolytic conditions were as follows: cathode: platinized platinum (84.2 cm.^{2}); cathodic solution: 10 g. of benzoic acid, 120 cc. of 95% alcohol, 30 g. of sulfuric acid; anode: lead; anodic solution: 30% sulfuric acid; current density: 0.5—1.0 amp./dm.^{2}; temperature: 20—30°C.; current quantity: 15—20 amp. hrs.; pressure: 1—30 atm. After electrolysis, the catholyte was filtered and the greater part of solvent was taken off under reduced pressure. The results of fractional distillation of 20 g. products are shown in Table 3.

Table 3

	fraction	yield	D_4^{25}	n_D^{25}
(1)	185—195°	5 g. (25%)	0.9506	1.4373
(2)	195—200°	9 (45)	0.9525	1.4396
(3)	200—225°	4 (20)	1.0500	1.4525
(4)	225—240°	1.6 (8)	—	—

The fraction (2) which is a colorless liquid ought to be ethyl hexahydrobenzoate from its physical constant and the hydrolysis of the fraction (2) produced hexahydrobenzoic acid. The fraction (3) seemed to be the mixture of hexahydrobenzoic acid and its ethyl ester from its physical constant. Saponification of (3) with 20% alcoholic potassium hydroxide, gave a hexahydrobenzoic acid, M. P. 28°C. The fraction (4) a greater portion of which was distilled at 233—237°C., seemed to be hexahydrobenzoic acid, but we could not confirm it as its amount was too small.

The relation between the amounts of four fractions and the pressure is shown in Table 4.

Table 4

Press. atm. / Fraction	1(H_2)	5(H_2)	10 (H_2)	30 (H_2)	10 (CO_2)	20 (CO_2)
(1) 185—195°	25%	25%	20%	23%	30%	25%
(2) 195—200°	45	40	35	23	30	25
(3) 200—225°	20	20	28	35	25	30
(4) 225—240°	8	10	12	17	10	15

In the case of the electrolytic reduction under pressure, the fraction (2), that is the ethyl hexahydrobenzoate was decreased and the fraction (3) (4) that is the mixture of ethyl hexahydrobenzoate and its acid was increased with the increase of the pressure of hydrogen. When ethyl benzoate is catalytically reduced, either hexahydro-compound or benzyl alcohol is obtained according to the catalyst. In the case of the electrolytic reduction of benzoic acid (benzoic ester) using a platinized-platinum cathode, the authors obtained ethyl hexahydrobenzoate and its acid but no benzylalcohol with small current density at ordinary or high pressures. But the yields of the réduction products differ according to the pressure.

Summary

The authors studied the electrolytic reduction of benzoic acid and compared the yield of the reduction product obtained under various pressures of hydrogen and carbon dioxide with that obtained in an open vessel. The effect of pressure in the course of electrolytic reduction was discussed and it was found that the reduction product differed according to the pressure.

The authors express their gratitude to Dr. N. Sugiyama, Professor of the Tokyo University of Education and Dr. B. Sakurai, professor of the Shinshu University for their kind advice. The expense of this work has been defrayed from the Grant in Aid for Scientific Research from the Ministry of Education, to which the authors' thanks are due.

Department of Chemistry, Faculty of Engineering, Naniwa University, Osaka

Fractionation of Cellulose Acetate and Distribution of Non-Cellulosic Components between the Fractions

By Kei MATSUZAKI, Setsuo FUKUHARA, Akira HATANO and Hiroshi SOBUE

(Received May 14, 1952)

Introduction

As raw materials for the production of cellulose acetate, cotton linters have usually been used, but recently wood pulps purified more than 95% α have been used, mixed with or without cotton linters. Also in Japan, studies of high-grade pulp for cellulose ester are now in progress.

It has generally been observed[1] that acetone solutions of cellulose acetates from wood pulp are hazy, and films and fibers produced are weaker in strength than those from cotton linters. It is important and interesting to make clear the cause of these defects of wood pulp although the haziness of the solution does not prevent their application to fibers.

In this research, secondary cellulose acetates from linters and pulp were fractionated and their chain-length distributions were compared, and viscosities in acetone and cupriethylene diamine solutions, acetic acid contents and pentosan contents of the individual fractions were determined.

Much[2] has been written about fractionation of secondary cellulose acetate but only recent investigations will be referred to here. Sookne et al.[3] fractionated cellulose acetate by precipitation with ethanol from acetone solution and obtained fifteen fractions. The acetic acid content remained constant for all fractions except three of very low chain length which showed slightly higher values. Most of the haze-producing material in the acetate was found to be contained in the higher-molecular fraction. But details of the experiment are not known in Japan. Howlett and Urquhart[4] fractionally dissolved acetate and found that the high-molecular fraction, which was low in acetic acid content, gave a hazy acetone solution. Scherer and Thompson[5] used the acetone-water-heptane system and D. P. of the first fraction was lower than that of the second. The acetic acid content of the fractions increased from 51.1 to 54.9% as the D. P. decreased on account of acetolysis. Wales and Swanson[6] believed the incomplete solubility of the first fraction to be caused by association between calcium ions and sulfuric half-ester groups or carboxyl groups of the polymer. Any further study of the incompletely soluble fraction has not yet been made.

(1) C. J. Malm, *Svensk Papperstidn.*, **50**, Hägglund Issue 135 (1947).

(2) L. H. Cragg and H. Hammerschlag, *Chem. Rev.*, **39**, 79 (1946).

(3) A. M. Sookne, H. A. Rutherford, H. Mark and M. Harris, *J. Res. Nat. Bur. Standards*, **29**, 123 (1942).

(4) F. Howlett and A. R. Urquhart, *J. Textile Institute*, **37**, T89 (1946).

(5) P. C. Scherer and R. B. Thompson, *Rayon & Synthetic Textiles*, **32**, No, 9, 69; No. 10, 51 (1951).

(6) M. Wales and D. L. Swanson, *J. Phys. & Colloid Chem.* **55**. 203 (1951).

Experimental Procedures and Results

The samples used were cellulose acetates from cotton linters, Rayaceta and a domestic pulp. The samles (each 5 g.) were dissolved in acetone to give 1% solution and fractionally precipitated with ethanol. The precipitant was added to give a slight precipitate in the solution, then the solution was warmed in a water bath to make it clear and kept standing in an incubator for 24 hours. The precipitate formed was separated from the supernatant liquid, washed with water and dried in a vacuum desiccator. The last fraction was obtained by evaporating and concentrating the solution and by filtering the precipitate on a glass filter. The D. P. calculated from the viscosity of acetone solution and the pentosan content of each fraction were tabulated in Tables 1—3. (in acetone $Km=9\times10^{-4}$ at 20°C.). The acetic acid content of each fraction was also determined. Fractions incompletely soluble in acetone showed slightly lower acetic acid content but the result was not clear as the accuracy of the determination was low, on account of the small quantity of the sample (0.1 g.). Then 20 g. of another acetate from Rayaceta was fractionated into five fractions and the D. P. from acetone solution, the D. P. from cupriethylene diamine solution, the acetic acid content and the pentosan content of each fraction were determined. The results are shown in Table 4. In this case, the first fraction was divided into two fractions by redissolving in acetone, the upper hazy solution (F1S) and the under gel-like precipitate (F1P).

Table 1

Fractionation of Cellulose Acetate from Cotton Linters. AcOH 54.7%, D. P. 200, Pentosan under 0.02%

Fraction	Weight %	D. P.	Solubility in Acetone	Pentosan %
1	0.60	400	81.7	—
2	6.72	352	hazy	0.07
3	8.72	290	100	<0.02
4	9.30	276	100	<0.02
5	9.97	255	100	<0.02
6	8.88	224	100	<0.02
7	11.50	189	100	<0.02
8	3.68	184	100	<0.02
9	4.57	158	100	<0.02
10	4.70	140	100	<0.02
11	4.22	126	100	<0.02
12	6.98	111	100	<0.02
13	5.63	103	100	<0.02
14	15.16	59	hazy	0.04

Table 2

Fractionation of Cellulose Acetate from Rayaceta. AcOH 54.7%, D. P. 210, Pentosan 0.1%

Fraction	Weight %	D. P.	Solubility in Acetone	Pentosan %
1	0.20	—	—	—
2	3.63	260	85.3	0.5
3	4.25	300	26.9	1.0
4	3.58	353	92.4	0.25
5	5.11	396	100	<0.02
6	2.23	340	100	<0.02
7	14.50	308	100	<0.02
8	7.39	267	100	<0.02
9	6.23	233	100	<0.02
10	4.81	205	100	<0.02
11	7.35	189	100	<0.02
12	8.57	162	100	<0.02
13	5.35	131	100	<0.02
14	3.15	118	100	<0.02
15	9.87	101	100	<0.02
16	6.17	63	100	<0.02
17	7.58	35	yellowish hazy	0.1

Table 3

Fractionation of Cellulose Acetate from a Domestic Pulp. AcOH 55.7%, D. P. 261, Pentosan 0.3%

Fraction	Weight %	D. P.	Solubility in Acetone	Pentosan %
1	10.79	260	precipitate, soly. not determined	1.0
2	8.37	429	precipitate, soly. not determined	1.5
3	5.79	440	hazy	0.2
4	5.22	411	100	<0.02
5	8.95	342	100	<0.02
6	10.49	316	100	<0.02
7	5.39	277	100	<0.02
8	4.75	245	100	<0.02
9	8.71	197	100	<0.02
10	4.90	170	100	<0.02
11	5.78	147	100	<0.02
12	5.34	116	100	<0.02
13	4.23	83	100	<0.02
14	6.13	66	100	<0.02
15	5.16	35	82	0.1

Table 4

Fractionation of Cellulose Acetate from Rayaceta

Fraction	Weight %	D. P. in Acetone*	D. P. in $Cu(En)_2$**	Solubility in Acetone	AcOH %	Pentosan %
original	—	165	163	100	54.8	0.1
1S	8.52	217	203	hazy	54.8	0.3
1P	3.25	184	176	58	—	0.7
2	33.79	227	227	100	54.8	<0.02
3	17.36	162	163	100	54.6	<0.02
4	16.22	107	133	100	54.8	<0.02
5	20.86	66	68	100	55.0	0.03

* $Km=9.0\times10^{-4}$ for cellulose acetate at 20°C.
** $Km=8.8\times10^{-4}$ for cellulose at 20°C.

Discussion

From Tables 1—3, it is seen that the acetate from linters gives only 0.60% of the first incompletely soluble fraction and inversion of D. P. is not observed when solubility of the fraction is taken into consideration, whereas, in the case of the acetate from Rayaceta, the fractions from the first to the fourth are incompletely soluble in acetone and considerable inversion of viscosity is observed even when solubility of the fractions is considered. Scherer and Thompson[5] thought that this was due to the migration of the low-molecular portion into the acetone-insoluble fraction. But we believe this is not the case. It seems these fractions may have actually a low D. P..

In Table 4, the D. P.s of both F1S and F1P are lower than that of F2. We could not decide whether this was due to the presence of the haziness which would prevent the accurate determination of the concentration of the solution, or due to associated products in the solution. If the former is true the D. P. determined from the viscosity of the completely dissolved solution of the fraction would be higher. Therefore viscosity in cupriethylene diamine solution was determined.

Cellulose acetates are saponified and dissolved in cupriethylene diamine solution. Unesterified cellulose and esterified pentosan would be also dissolved and associated products would dissociate into molecular dispersion. The determination in diamine solution shows the same results as in acetone. D. P. of F1S is higher than that of F1P. This indicates that a part of F1S is a normal fraction which should have a higher D. P. than that of F2, if separately precipitated from the abnormal fraction in F1S, and have normal molecular shape. Then Scherer's opinion might be wrong. Abnormal materials included mainly in F1P and partly in F1S, having actually a low D. P., are responsible for the inversion of the D. P.

A comparison between chain-length distributions of the acetates from cotton linters and Rayaceta shows that the latter has a rather heterogeneous distribution, although their average D. P.s are almost the same. Our previous investigation,[7] as those of others,[8] showed that the chain-length distribution of a wood pulp is more heterogeneous than that of purified cotton and the heterogeneity does not disappear even if acid-hydrolysis takes place. Both the difference in the heterogeneity of the chain-length distribution of the acetates, which Malm could not prove experimentally, and the heterogeneity in chemical composition e. g. acetone-insoluble fractions, may account for the weakness in their mechanical properties and for their viscometric behavios.

Next, the pentosan content of each fraction was determined. The determination by phloroglucin gives about 1% of pentosan content even to pentosan-free materials such as glucose or linters, on account of oxymethyl furfural produced from hexose. The error due to oxymethyl furfural increases as the pentosan content decreases. A part of the error can be corrected by treating the wet precipitate of the phloroglucide with ethanol,[9] but a trace of pentosan (under 0.1% of the sample) would not be detected and determined. Therefore, determination of pentosan by paperchromatography[10] was adopted.

Tables 1—3 indicate that all fractions which give a hazy acetone solution or show incomplete solubility in acetone, include pentosan. The last fractions obtained by evaporating the solvent also include pentosan, but its quantity is small.

It is noticed that even the acetate from linters include pentosan, though it can not be detected from the acetate itself. It is concentrated in the first, second and the last fraction. The acetate from Rayaceta contains 0.1—1.0% pentosan in its initial fractions and the last fraction. The behavior of the acetate from a domestic pulp was almost the same.

These indicate that there is a clear relationship between pentosan content and the haziness of acetone solution of acetates as Jayme and Schenck[11] proved. It is observed that the greater the pentosan content of a fraction, the greater the haziness of its acetone solution or its acetone-insolubility. The acetates from wood pulp invariably include a higher content of the portions which show incomplete solubility in acetone and a higher content of pentosan. Table 4 shows that F1P contains more pentosan than F1S. The acetic acid content of each fraction remained almost constant. Since the acetic acid content of F1P could not be determined, it is still uncertain that the acetone-insoluble fractions are low-esterified cellulose.

Thus, it can not be decided whether the

(7) K. Matsuzaki and H. Sobue, This Bulletin, **24**, 184 (1951).

(8) L. Jörgensen, Dissertation, Oslo 1950; N. Glarén, Dissertation, Uppsala 1944.

(9) H. Sobue, K. Matsuzaki and T. Abe, unpublished work.

(10) H. Sobue, K. Matsuzaki, A. Hatano and U. Arisawa, *J. Soc. Tex. Cell. Ind. Japan*, **8**, 79 (1952); H. Sobue and A. Hatano, *J. Chem. Soc. Japan, Ind. Chem. Sec.*, **55**, 131 (1952).

(11) G. Jayme and U. Schenck, *Melliand Textilberichte*, **31**, 153, 230 (1950).

insoluble fractions are due to association by the salt bridge effect of calcium ions between carboxyl or sulfuric half-ester groups as Wales and Swanson[6] suggested, or due to the remaining structure (e. g. incompletely digested fragments) of the wood tissues which could be considerably acetylated but would not yield a mono-molecularly dispersed solutiou. In our opinion, both are responsible but the latter more so, because the hazy portions are always accompanied by pentosan, and the determination of the protein content of each fraction by paper chromatography revealed that the acetone insoluble fractions include it more than acetone soluble fractions. But it does not seem that all pentosan is combined with cellulose, a part of it is molecularly dispersed, and acetylated, saponified and precipitated, though most of it is removed in the saponification stage. (e. g. Rayaceta contained 0.5% pentosan, the acetate 0.15% based on cellulose)

Now we may say the following as to the acetylation and refining of wood pulp.

1. Pentosan in pulp must be removed as far as possible although most of it is removed during the ripening stage as above mentioned. Pentosan itself or pentosan-cellulose complex cause haziness of the acetone solution and result in heterogeneity of the acetate. Pentosan remained as an important index for the degree of the refinement of pulp.

2. Carboxyl and sulfuric acid groups must be removed as far as possible. Sulfuric acid groups can be removed in the stabilization process. Carboxyl groups are mainly formed during bleaching stages. In this respect, bleaching which does not accompany modification and degradation of cellulose, such as by sodium chlorite, is prefered.

3. Jayme classified acetylation characteristics of pulp into those inherent to pulp and those produced by pretreatments etc. All the above mentioned are referred to the characteristics inherent to pulp. Of course, pretreatments and drying conditions etc. (e. g. boiling after cold alkali refinement and the drying temperature must not be raised over 60°C. and the drying must not be continued until they become bone-dry) should be controlled strictly.

Experimental

Pentosan content was determined as follows. 0.2—0.3 g. of a sample was dissolved and degraded in 70% sulfuric acid, diluted to 2—3% and boiled under reflux for 8 hours. Saccharide solution refined by the usual method was developed by butanol-water-acetic acid mixture (4:1:1). Quantitative estimation was made by determination of the area of the spot or of the intensity of the light transmitted through the spot colored by aniline hydrogen phthalate. As the spots of glucose and xylose were overlapped slightly, the area method was generally adopted. Amino acid was colored by ninhydrine, and approximate estimation was made by its color intensity.

Cupriethylene diamine solution was prepared after T230 Sm—50.[12] The acetates were dissolved in this solution and kept under nitrogen atmosphere for 24 hours.

Acetic acid content was determined as follows. About 0.5 g. of a sample was dissolved in 50 cc. of acetone, saponified with 50 cc. of 0.2N potassium hydroxide solution. After three hours, 50 cc. of 0.2N hydrochloric acid solution was added and back titrated with the alkali.

As the D. P.s were determined in 0.6% solution, the solubilities were also determined in this solution. D. P.s of the incompletely soluble fractions were corrected for the solubilities when they were known. It was observed that the insoluble fractions became gradually dispersed as the concentration of the solutions was lowered. This is seen from the fact that F1P which was at first a gel-like precipitate showed 58% solubility by redissolving in acetone.

Summary

1. Three cellulose acetates from cotton linters, Rayaceta and a domestic pulp were fractionally precipitated from acetone solution with ethanol, and viscosity measurements in acetone solution and pentosan determinations by paper chromatography of the individual fractions were made.

2. Another acetate from Rayaceta was again fractionated into five fractions and viscosities in acetone and cupriethylene diamine solution and pentosan contents of the individual fractions were determined.

3. The results showed a close relationship between the initial acetone-insoluble fractions or in acetone haze-producing fractions and their pentosan content. These fractions include abnormal materials which show low viscosity (probably low D. P.) in cupriethylene diamine solution as well as in acetone. They are included much in the acetates from wood pulps.

4. It could not be decided whether these acetone-insoluble fractions were due to association by salt bridge effect of calcium ions between carboxyl or sulfuric half-ester groups, or due to the remaining structure of wood tissues.

5. The chain-length distributions of the cellulose acetates from wood pulp seem to be more heterogeneous than those from cotton linters.

(12) Tappi Standard.

The authors express thanks to Mr. T. Ueki and Miss K. Saito for their earnest aid to the experiment. The expense of the work was defrayed from the Scientific Research Encouragement Grant of the Department of Education.

Department of Applied Chemistry, Faculty of Engineering, Tokyo University, Tokyo

Vat Dyes of Acenaphthene Series. IV. Condensation of Perylenetetracarboxylic Acid Anhydride with *o*-Phenylenediamine[1]

By Toshio MAKI and Harukichi HASHIMOTO

(Received July 5, 1952)

By the condensation of perylenetracarboxylic acid anhydride (I) with aromatic amines scarlet or red vat dyes of N, N'-diaryl-tetracarboxyldiimide type are generally obtained.[2] We have found, however, that the relation is quite particular in the case of *o*-phenylenediamine. At lower condensation temperature (160°) the main product (67.1% of the theory) was N, N'-di (*o*-amino) phenyl-perylenetetracarboxyl-diimide (II), which is soluble in alkaline hydrosulfite and insoluble in 90% sulfuric acid. It dyes cotton in weak, dull-red violet of low value as a vat dye.

At moderate condensation temperature (190°) a new valuable violet vat dye was obtained as the principal product (60.6%), which is easily soluble in alkaline hydrosulfite and also soluble in 90% sulfuric acid. This dye has a very strong dyeing power and deep violet shade is produced on cotton with 2% dye (1W method). It is really remarkable that this new vat dye has the maximum light fastness (8 grade), highest of all-hitherto known synthetic organic dyes of violet shades. The fastness against chlorine is also maximum. The constitution of this dye is 3, 4-benzimidazole-9, 10-(*o*-amino) phenyl - perylenetetracarboxyl - diimide (III), simply called by us as "Acenaphthene Violet". The remaining amino group is diazotizable.

At the temperatures higher than 200° the main product is 3, 4, 9, 10-perylenetetracarboxyl-bis-benzimidazole (IV), which is a violet blue substance insoluble in alkaline hydrosulfite and for this reason it has no dyeing ability.[3]

As another route N, N'-di (*o*-nitro) phenyl-perylenetetracaboxyl-diimide (V) was prepared by the condensation of perylenetetracarboxylic acid anhydride with *o*-nitroaniline and then

(I)

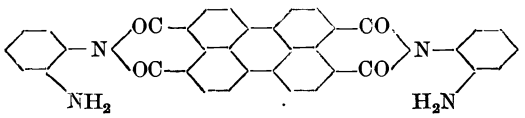

(II)

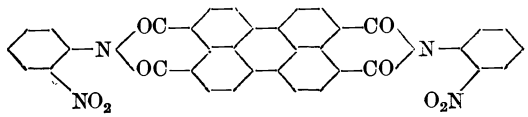

(V)

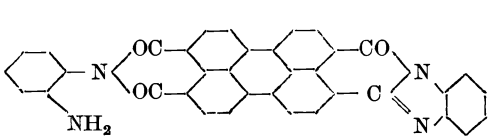

(III)

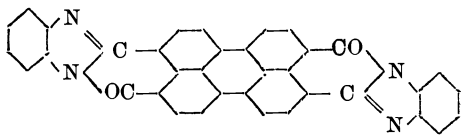

(IV)

(1) Read before the 5th Annual Meeting of the Chemical Society of Japan on April 5, 1952.

(2) T. Maki and H. Hashimoto, *J. Chem. Soc. Japan, Ind. Chem. Section*, **54**, 544 (1951).

(3) G. P. 502352, *Frdl.* **17**, 1395.

reduced with alkaline hydrosulfite containing sodium sulfide at 60°. The diamino compound thus obtained was completely identical with that (II), above mentioned, which had been prepared directly from *o*-phenylenediamine. The effect of thermal treatment on the stability of the three compounds is interesting. Thus, the diamino compound (II) is converted mainly into Acenaphthene Violet (III) by boiling with nitrobenzene for 1~1.5 hours. Acenaphthene Violet can be almost entirely changed into the unvattable bis-imidazole (IV) when boiled with nitrobenzene for 5 hours. The quantitative separation of the three compounds can be carried out using alkaline hydrosulfite and 90% sulfuric acid.

Experimental Part

Condensation of Perlyenetetracarboxylic Acid Anhydride with *o*-Phenylenediamine.—A mixture of 1.96 g. (1/200 mole) of finely powdered perylenetetracarboxylic acid anhydride and 7.5 g. (14/200 mole) of *o*-phenylenediamine was kept in an oil bath without stirring for 4 hours at 190° (bath temperature). In order to remove the excess of *o*-phenylene diamine, 50 cc. of alcohol was added to the product, stirred at 70° for 30 minutes, filtered and washed with alcohol. From this residue the unchanged perylenetetracarboxylic acid anhydride was extracted by heating with 500 cc. of aqueous 1% sodium hydroxide on a water bath, filtering and thoroughly washing with water. Crude condensation product 2.77 g.

Separation.—The crude product was finely powdered, kept with 560 cc. (200 parts) of water, 11 g. (4 parts) of sodium hydroxide and 11 g. (4 parts) of sodium hydrosulfite at 45° for 15 minutes, filtered, and the residue was once more treated with the same amount of the alkaline hydrosulfite solution, filtered, washed with the alkaline hydrosulfite till the filtrate became colorless. The residue was then suspended in 500 cc. of water, acidified with hydrochloric acid, filtered and washed neutral. Yield (IV) is 0.41 g. (15.2% of the theory).

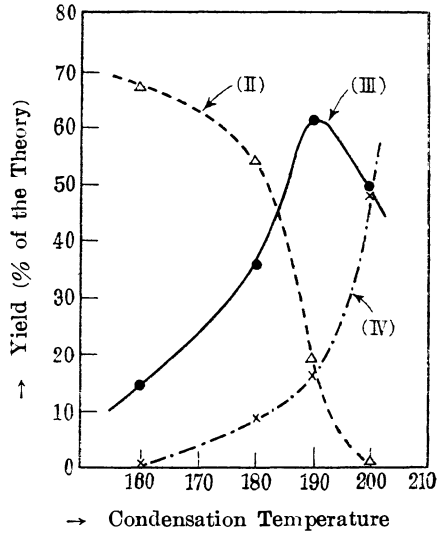

Fig. 1.

The combined violet red filtrate was oxidized by a current of air, the precipitate collected and washed neutral. Yield is 2.27 g. This was then dissolved in 115 g. (50 parts) of 98.7% sulfuric acid, 11.1 cc. of water added dropwise with external ice cooling to produce 90% sulfuric acid and allowed to stand over-night. The precipitate was collected on a glass filter, washed with 90% sulfuric acid, suspended in water and neutralized with sodium carbonate. Yield (II) is 0.55 g. (19.2% of the theory). The 90% snlfuric acid filtrate was poured into 1 l. of ice water, the resulting precipitate collected and washed neutral. Yield (III) is 1.68 g. (60.6% of the theory). The further relations between the condensation temperatures and yields of the three compounds are illustrated in Fig. 1.

3,4-Benzimidazolo-9,10-(*o*-amino)phenylperylenetetracarboxyl-diimide (Acenaphthene Violet) (III).—Black violet powder, insoluble in organic solvents of lower boiling points, sparingly soluble in boiling *o*-dichlorobenzene or nitrobenzene with violet red color and weak red fluorescence. Soluble in conc. sulfuric acid and the solution shows blue (thin layer) and violet blue (thick layer) dichroism with weak red fluorescence. Soluble also in 90% sulfuric acid. Easily soluble in alkaline hydrosulfite and gives violet red vat with weak red fluorescence. Cotton is dyed in deep violet shade with 2% dye (IW method). These cotton dyeings have the maximum fastness against light (8 grade), chlorine (5 grade) and washing (40°—5 grade, 90°—4 grade). Staple fibre is dyed in deep red violet shade even with 1% dye. Found: N, 9.76; Calculated for $C_{36}H_{18}O_3N_4$ (III): N, 10.10%.

When the violet cotton dyeing was diazotized on the fibre and treated with alkaline β-naphthol solution the shade became more red and its light fastness suddenly depressed to 2 grade. By boiling 1.00 g. of the violet dye (III) with 2.0 g. of benzoyl chloride in 20 g. of *o*-dichlorobenzene under reflux for 10 hours 0.54 g. of insoluble violet powder and 0.50 g. of soluble violet red powder were obtained, apparently consisting of the bis-imidazole (IV) (the former) and benzoylated product of (III) (the latter). Both of them were no more vattable with alkaline hydrosulfite. When 1 part of Acenaphthene Violet (III) is heated with 200 parts of nitrobenzene at the boiling point (ca. 211°) for 5 hours the substance is nearly completely converted into the unvattable bis-imidazole (IV).

3,4,9,10-Perylenetetracarboxyl-bis-benzimidazole (IV).—Violet grey powder, insoluble in organic solvents of lower boiling points, sparingly soluble in boiling nitrobenzene giving faint violet red solution with weak red fluorescence. Conc.

sulfuric acid solution is blue without dichroism and fluorescence, from which violet blue precipitate resulted by the addition of water. Insoluble in alkaline hydrosulfite. Found: N, 10.07; Calculated for $C_{76}H_{16}O_2N_4$ (IV): N, 10.44%.

N, N'-Di (*o*-amino) phenyl-perylenetetracarboxyl-diimide (II).—Red violet powder, insoluble in organic solvents of lower boiling points, sparingly soluble in boiling *o*-dichlorobenzene with violet red color and weak red fluorescence. Conc. sulfuric acid solution shows red violet (thin layer) and red (thick layer) dichroism with strong red fluorescence. The color of the sulfuric acid solution is changed into blue of the imidazoles when heated to 150°. Insoluble in 90% sulfuric acid. Soluble in alkaline hydrosulfite forming violet red vat with weak red fluorescence, from which cotton is dyed in weak dull red violet entirely different form the dyeings of (III). Found: N, 9.56; Calculated for $C_{36}H_{20}O_4N_4$ (II): N, 9.79%.

When the cotton dyeing was diazotized on the fibre and coupled with alkaline β-naphthol the shade was changed into red brown. By heating 1 part of the substance (II) with 200 parts of nitrobenzene at the boiling point for 1.5 hours 57% of the substance converted into Acenaphthene Violet (III) and 43% into the unvattable bis-imidazole (IV). If the boiling is continued for 5 hours the substance is nearly completely converted into the unvattable bis-imidazole.

Condensation of Perylenetetracarboxylic Acid Anhydride with *o*-Nitroaniline.—

N, N'-Di(*o*-nitro)phenyl-perylenetetracarboxyl-diimide (V).—Perylenetetracarboxylic acid anhydride (1.96 g., 1/200 mole) was heated with 6.90 g. (10/200 mole) of *o*-nitroaniline and 1.20 g. (4/200 mole) of glacial acetic acid in an oil bath under reflux with stirring at 230° (bath temperature) for 10 hours. The product was heated up with 50 cc. of alcohol and hot solution filtered. The collected precipitate was then treated with 200 cc. of hot aqueous 1% sodium hydroxide to remove the unchanged tetracarboxylic acid anhydride (recovered anhydride 0.48 g. or 24.4% of the starting material). Yield of (V) is 2.48 g. (78.5% of the theory). Dark brown powder, sparingly soluble in boiling nitrobenzene with red orange color and yellow fluorescence. Soluble in conc. sulfuric acid with strong red fluorescence and red violet (thin layer) and red (thick layer) dichroism. The color of the sulfuric acid solution is not changed into blue by heating to 150° and brown red precipitate is produced by pouring into water. Hydrosulfite vat (IW method) is violet red with weak red fluorescence and cotton is dyed in weak dull red violet, which is identical with the dyeing of the corresponding diamino compound. Found: N, 8.82; Calculated for $C_{36}H_{16}O_8N_4$ (V): N, 8.86%.

Reduction of N, N'-Di (*o*-nitro) phenyl-perylenetetracarboxyl-diimide. — The di (*o*-nitro) phenyl-diimide (V) (1.00 g.) was vatted by heating with 2.0 g. of sodium hydroxide, 2.0 g. of sodium hydrosulfite and 100 cc. of water to 60°, 0.80 g. of 55% sodium sulfide was added and kept further 2 hours at 60°. Water (100 cc.) was then added, oxidized by a current of air, the precipitate collected, thoroughly washed with water and dried at 110°. Yield is 0.84 g. Dark brown powder of violet red streak, soluble in conc. sulfuric acid with red violet (thin layer) and red (thick layer) dichroism and strong red fluorescence. All other chemical and dyeing properties are completely identical with the di (*o*-amino) phenyl-diimide (II) obtained directly with *o*-phenylenediamine. Converted also into Acenaphthene Violet (III) and then into the unvattable bis-imidazole (IV) by boiling with nitrobenzene.

Found: N, 9.45; Calculated for $C_{36}H_{20}O_4N_4$ (II); N, 9.79%.

Dyestuffs Research Laboratory, Department of Applied Chemistry, Tokyo University, Tokyo

The Bitter Substance, Produced in Black-rotten Sweet Potato. III. On the Constitution of Ipomoeamarone. Part 2.

By Takashi OHNO and Misao TOYAO

(Received May 10, 1952)

It was shown in our previous report[1] that ipomoeamarone was an open-chain sesquiterpenic compound containing a ketonic group, two oxide rings and two ethylenic linkages. It gave a keto-acid (named ceratonic acid) and oxalic acid by oxidation with potassium permanganate at room temperature, and gave acetone, acetic acid, oxalic acid and a liquid

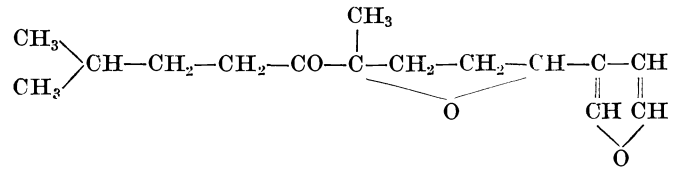

I.

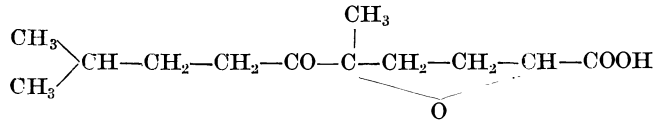

II.

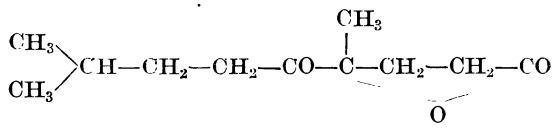

III.

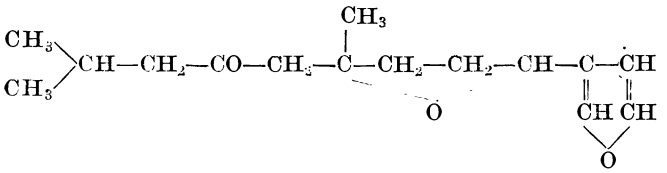

I′.

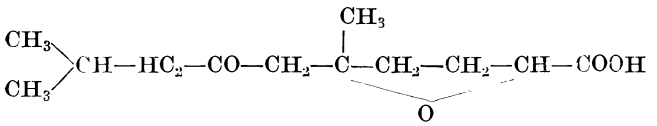

II′.

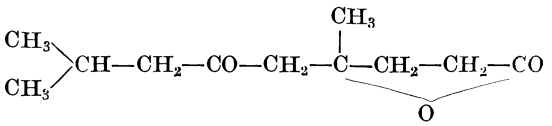

III′.

(1) T. Ohno, This Bulletin **25**, 222-225 (1952).

acid by the same oxidation procedure at 100°.

At the general meeting of the Agricultural Chemical Society of Japan, held at Tokyo on April 5, 1952, we proposed tentatively formula I for ipomoeamarone, II for ceratonic acid, and III for the keto-lactone, the latter two of which were the degradation products of the former by oxidation with potassium permanganate.

T. Kubota and his collaborators of the Osaka City College of Polytechnics also announced the results of their own research on ipomoeamarone at the general meeting of the Chemical Society of Japan, held at Tokyo on April 3, 1952, and put forward the formulae of ipomoeamarone (I′), ipomeanic acid (II′) and ipomic lactone (III′), the latter two of which were ozonolysis products of the former.

Some part of their results, including the structures of ipomeanic acid and ipomic lactone, has already been published,[2][3] and their report read at the general meeting of the Chemical Society of Japan was published recently[4].

Though, between Kubota et al. and us, there is an essential disagreement in the interpretation of the structure of ipomoeamarone, we wish to postpone detailed discussion of this and to publish our results read at the general meeting of the Agricultural Chemical Society of Japan as it stands.

As regards the nomenclature of the substances, we think it preferable to use "ceratonic acid", because this name apparently was in print prior to "ipomeanic acid", but we agree with Kubota et al. in adopting the name "ipomic lactone" for the keto-lactone (III or III′).

By oxidation of ipomoeamarone with potassium permanganate at room temperature, a non-volatile liquid acid showing ketonic color reaction was obtained. This was converted into *p*-phenylphenacyl ester (m. p. 79°) and by its analysis a molecular formula, $C_{12}H_{20}O_4$, can be given to the acid. However, neither crystalline semicarbazone nor 2,4-dinitrophenylhydrazone of the acid was obtained. It is now obvious from the results of following experiments that this acid retains the original ketonic and oxidic groups, both present in ipomoeamarone. This acid was named ceratonic acid in our previous paper, and may be identical with the ipomeanic acid of Kubota et al.

Ipomoeamarone semicarbazone was now oxidized in dilute acetone with potassium permanganate at room temperature, and a crystalline semicarbazone and a mixture of non-volatile liquid acids were obtained. The former was identified with the semicarbazone of ceratonic acid (ipomeanic acid), $C_{13}H_{23}O_4N_3$, m. p. 172°, $[\alpha]_D^{24} = -86.7°$ (in alcohol and pyridine, 4:1). The latter, admixed with some of this crystalline semicarbazone, was then hydrolysed with dilute sulfuric acid in methanol, and fractionated into two parts. The lower boiling fraction (b. p. 99—103°/0.3mm.) coincided with the formula $C_{11}H_{18}O_3$ and was considered to be a keto-lactone, because of its difficult neutralizability at room temperature. It gave positive color reaction for a ketone, but its 2,4-dinitrophenylhydrazone was a liquid and semicarbazone crystallized only partially This lactone was considered to be the ipomic lactone of Kubota et al. The higher boiling fraction, (b. p. 123—135°/0.3 mm.), ceratonic acid, accorded with $C_{12}H_{20}O_4$; *p*-phenylphenacyl ester melted at 79°, and is identical with the ester of the acid, obtained by direct oxidation of ipomoeamarone; the semicarbazone melted at 172° and is identical with the above mentioned semicarbazone. The non-volatile acid was thus proved to be a mixture of ipomic lactone and ceratonic acid.

Ipomoeamarone was treated with phenylmagnesium bromide, and the resulting compound was dehydrated with acetic anhydride and zinc chloride, followed by oxidation with potassium permanganate. Formic, isovaleric, and oxalic acids were obtained besides a non-volatile acid and a lactone.

From the properties of these degradation products obtained by various oxidation methods, it is concluded that: (1) Ceratonic acid is an open-chain acid containing the original ketonic group and one of the original oxide rings, losing three carbon atoms, two ethylenic linkages and an oxide oxygen, and ipomoeamarone possesses therefore, beyond all doubt, a furan-nucleus involving a carbon atom which might have been converted to a carboxylic group of ceratonic acid and three other carbon atoms which might have been lost by oxidation. That is, ipomoeamarone is a furan derivative substituted at α or β position with a side chain of C_{11} which contains a ketonic group and an oxide ring. (2) Ipomic lactone, which is a carbon shorter than ceratonic acid, retains also an original ketonic group, the oxide ring of ceratonic acid being transformed into a lactone ring. The carbon atom of α-position of ceratonic acid may therefore be a

(2) T. Kubota and T. Matsuura, *Proc. Japan Acad.* **28**, 44-47 (1952). They proposed the name "Ipomeamarone" instead of "Ipomoeamarone" for the sake of simplifying the spelling.

(3) T. Kubota and T. Matsuura, ibid. **28**, 83-84 (1952).

(4) T. Kubota and T. Matsuura, ibid. **28**, 198-199 (1952).

secondary one, with which oxide oxygen connects, and the oxide ring forms a hydrofuran-nucleus, because the properties of the lactone is considered to be a γ-lactone. (3) The formation of isovaleric acid by the oxidation of the reaction product of Grignard's reagent may establish the constitution of ipomoeamarone to be an isoamyl ketone, and the reaction involved would have taken place in the following manner;

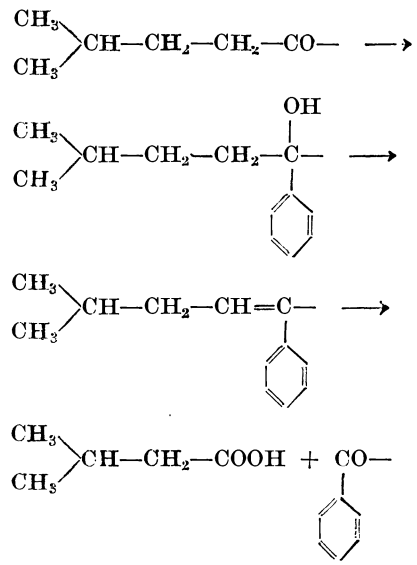

Ipomoeamarone gave dark green color in the pine-shaving test, and an adduct with maleic anhydride, although in a liquid form. In addition, the facts that absorption of hydrogen proceeds only slowly by catalytic reduction, the unsuccessfulness of obtaining dihydro-compound, and the stability of double bonds against sodium ethanolate reduction, are only understood by assuming that two ethylenic linkages of ipomoeamarone form a furan-nucleus.

In consequence, if ipomoeamarone is presumed to be a sesquiterpene derivative and to have a skeleton of an oridinary openchain three-isoprene-structure, such as farnesol or nerolidol, the conclusion may be drawn from the results that ipomoeamarone has a tentative formula (I), ceratonic acid (II), and ipomic lactone (III), respectively.

The only difference between the constitutional formulae of ipomoeamarone of Kubota and of us is the position of ketonic group, and it will be discussed in a future communication.

Experimental

(1) **Ipomoeamarone semicarbazone.**—The yield of semicarbazone by the pyridine-method (see our last communication) from the crude bitter oil was as follows; 60—70 g. of crude semicarbazone from 100 g. fraction 1 (b. p. 140—145°/7 mm.). This product gave 21—25 g. of pure crystals by recrystallization; 80—90 g. of crude semicarbazone from 100 g. fraction 2 (b. p. 145—150°/7 mm.), giving 28—31 g. of pure crystals by recrystallization.

(2) **Hydrolysis of ipomoeamarone semicarbazone.** (a) **By oxalic acid.**—A mixture of the semicarbazone (20 g.) and oxalic acid (30 g.) in water (1 l.) was boiled vigorously for one hour. The product was isolated by means of ether, and ether was washed with aqueous alkali and evaporated. Pure ipomoeamarone (13.6 g.) was obtained by vacuum distillation (yield; 83.4%).

(b) **By potassium bisulfate.**—A mixture of the semicarbazone (5 g.) in benzene (80 cc.) and potassium bisulfate (25 g.) in water (50 cc.) was shaken at room temperature for 175 hours. The benzene layer was separated, washed with saturated sodium bicarbonate solution followed by drying with anhydrous sodium sulfate. After the complete removal of benzene, petroleum ether was added and undecomposed semicarbazone (1 g.) precipitated was filtered off. Free ipomoeamarone was obtained as colorless oil after vacuum distillation of the filtrate; b. p. 112—3°/0.6 mm., $[\alpha]_D^{20} = +11.07°$ (c, 2.8 in benzene). (Found: C, 72.24; H, 8.62. Calc. for $C_{15}H_{22}O_3$: C, 72.00; H, 8.80%

(3) **Oxidation of ipomoeamarone.**—Free ipomoeamarone (2.0 g.), which was regenerated from the semicarbazone, was suspended in water (100 cc.), and powdered potassium permanganate was added to the mixture in small portions under shaking and occasional cooling. After 6 g. of potassium permanganate (corresponding to 7.1 atoms of oxygen) were added, no further decolorisation occurred. Manganese dioxide was then filtered off and washed with hot water. The filtrate and washings were combined, concentrated, decolorized with active charcoal, extracted with ether to remove neutral substances, and acidified with concentrated hydrochloric acid. The separated oil was extrated twice with chloroform, and dried with anhydrous sodium sulfate. A brown viscous acid (1.6 g.) was obtained after the removal of chloroform. The liquid acid showed positive color reaction for ketone with sodium nitroprusside, although it gave no crystalline semicarbazone. Its *p*-bromophenacyl ester was liquid, but *p*-phenylphenacyl ester was obtained as leaflet crystals mixed with oily substance, m. p. 79° from alcohol. Analysis showed that the ester corresponds to the formula $C_{26}H_{30}O_5$, showing that the acid is $C_{12}H_{26}O_4$. (Found: C, 73.43; H, 6.98. Calc. for $C_{26}H_{30}O_5$: C, 73.94; H, 7.11%)

It is obvious that the acid, as shown in the next experiment, preserves the original ketonic

group and one of the oxide rings, and we proposed the name ceratonic acid to this acid in our previous paper. It may be the same compound as the ipomeanic acid of Kubota et al.

The aqueous layer, separated from chloroform solution, was neutralized with aqueous ammonia, and a solution of calcium chloride was added to it. Calcium oxalate was precipitated; 0.16 g. (namely 0.16 equivalent).

(4) **Oxidation of ipomoeamarone semicarbazone.**—To a solution of ipomoeamarone semicarbazone (20 g.) in acetone (200 cc.), treated beforehand with potassium permanganate, water (200 cc.) was added, followed by the addition of powdered potassium permanganate in small portions under shaking and occasional cooling. Forty-seven grams (equivalent to 6.85 atoms of oxygen) were consumed. After manganese dioxide was decomposed by passing sulfur dioxide gas through the reaction mixture, it was concentrated to half its volume under diminished pressure, and inorganic substances were filtered off and washed with ether. The filtrate was extracted repeatedly with ether, the combined ether extract was washed with 10% sodium hydroxide solution repeatedly, and 3.6 g. of a neutral oil, which crystallized immediately, was obtained after evaporation; colorless powder, m. p. 119° (from ether and petroleum ether). Mixed melting point determination and analytical value showed that it was the unreacted semicarbazone. (Found: C, 62.78; H, 7.98; N, 13.48. Calc. for $C_{16}H_{25}O_3N_3$: C, 62.54; H, 8.14; N, 13.68%)

Aqueous layer mixed with sodium hydroxide solution was acidified with dilute sulfuric acid, fractionating into a part soluble in ether and crystals soluble in ether with difficulty. The latter was ceratonic acid semicarbazone; colorless powder from ether, m. p. 172° (decomp.), $[\alpha]_D^{24} = -86.7°$ (*c*, 6.0 in ethanol and pyridine, 4:1). (Found: C, 54.81, 54.51; H, 8.57, 7.94; N, 14.97, 14.73. Calc. for $C_{13}H_{23}O_4N_3$: C, 54.74; H, 8.07; N, 14.74%) The former was a viscous liquid (11 g.) admixed with some crystals of the semicarbazone. The oil was refluxed with 25% sulfuric acid (50 cc.) in methanol (100 cc.) for 3 hours, the methanol was removed, and the separated oil was extracted with ether and the ether extract distilled in a vacuum. A viscous oil (6.6 g.) was obtained; b. p. up to138°/0.15 mm., $[\alpha]_D^{20} = +18.0°$ (*c*, 2.0 in ether). *p*-Phenylphenacyl ester melted at 79°, which was identical with the ester above mentioned, was contaminated by an oily substance; no crystallien semicarbazone was obtained. By analysis of the acid it was shown to be a mixture of two substances, $C_{12}H_{20}O_4$ and $C_{11}H_{18}O_3$. (Found: C, 64.54, 64.24; H, 9.59, 9.19. Calc. for $C_{12}H_{20}O_4$: C, 63.16; H, 8.77. Calc. for $C_{11}H_{18}O_3$: C, 66.67; H, 9.07%.)

The mixture of the acid (5.0 g.) was fractionated as follows: (A) b. p. 99—103°/0.3 mm., 2.5 g., (B) b. p. 103—123°/0.3 mm., 0.5 g., (C) b. p. 123—135°/0.3 mm., 1.5 g. The first fraction, a pale yellow mobile oil, was considered to be a lactone, because it was neutralized with N/10 potassium hydroxide solution only when warmed. *p*-Phenylphenacyl ester was not obtained. The first and second fraction in ether were treated with sodium bicarbonate solution to remove acidic substances if any, and the lactone was obtained by shaking it repeatedly with 10% sodium hydroxide solution, followed by acidifying, extracting with ether, and distilling in vacuo, b. p. 134—140°/4 mm., 1.0 g. (Found: C, 67.01; H, 9.00. Calc. for $C_{11}H_{18}O_3$: C, 66.76; H, 9.09%)

The lactone gave a color reaction with sodium nitroprusside, but the semicarbazone was crystallized only partially. The 2,4-dinitrophenylhydrazone remained oily; yellow crystals, which were formed in an alcoholic solution by cooling with a mixture of dry ice and ether, melted at room temperature. This ketolactone may be the same compouud as the ipomic lactone of Kubota et al.

The third fraction, a viscous yellow oil, proved to be ceratonic acid. The acid was converted into *p*-phenylphenacyl ester, m. p. 79° and also into semicarbazone, m. p. 168° (decomp.); these proved to be identical with the derivatives which were mentioned above, respectively. Analysis of the oil corresponds to $C_{12}H_{20}O_4$. (Found: C, 63.20; H, 8.69. Calc. for $C_{12}H_{20}O_4$: C, 63.16; H, 8.78%)

(5) **Reaction of phenylmagnesium bromide upon ipomoeamarone and oxidation of the product by potassium permanganate.**—To an ice-cooled solution of ipomoeamarone (5.6 g., regenerated from the semicarbazone) in ether was added a solution of phenylmagnesium bromide in ether (2.7 N, 15 cc.) dropwise and the mixture was refluxed for 30 minutes. The reaction product was poured into a mixture of ice and dilute sulfuric acid. The ethereal layer was separated, washed with saturated bicarbonate solution, and dried. To the viscous product obtained by removal of the ether, 4 g. of acetic anhydride and a small portion of zinc chloride were added. After refluxing for 30 minutes, the mixture was poured into water. Ether was added, washed with 10% potassium hydroxide solution and dried. The removal of the ether left 6 g. of a viscous dark-brown oil.

The oil obtained was oxidized with potassium permanganate in dilute pyridine (100 cc. pyridine and 300 cc. water). Thirteen grams of potassium permanganate were required (corresponding to 6.8 atoms of oxygen). Manganese dioxide was now removed by filtration and washed with hot water. From the filtrate and washings pyridine was distilled off with steam. The residual solution, after concentration to half its volume, was treated with ether to remove non-volatile neutral substances (0.1 g.), and the aqueous layer was distilled with steam after acidification. The distillate was neutralized and treated with potassium permanganate solution for decomposition of formic acid. The filtrate from manganese dioxide was concentrated to dryness, acidified, and extracted with ether. The volatile acid (250 mg.) was converted to *p*-bromophenacyl ester, m. p. 64°. This was proved to be the ester of isovaleric

acid by mixed melting point determination and analysis. (Found: C, 52.00; H, 5.60, Calc. for $C_{13}H_{15}O_3Br$: C, 52.17; H, 5.02. Calc. for $C_{12}H_{13}O_3Br$: C, 50.53; H, 4.56%) The mixed melting point with the ester of isobutyric acid showed a depression of about 10°.

From the residual solution of steam-distillation, there were obtained a non-volatile acid (0.9 g.), a lactone (0.1 g.) and oxalic acid.

Summary

By oxidation of ipomoeamarone and its semicarbazone with potassium permanganate, ceratonic acid (ipomeanic acid) (II), $C_{12}H_{20}O_4$, and ipomic lactone (III), $C_{11}H_{18}O_3$, were obtained. The ketonic group of ipomoeamarone was proved to be an isoamyl ketone by the oxidation of the reaction product of Grignard's reagent. These experiments led us to conclude that ipomoeamarone is represented by the provisional constitution (I).

We wish to express our sincere gratitude to Prof. S. Takei and Dr. M. Ohno of the University of Kyoto for their guidance and to Dr. M. Matsui of our Laboratory for his helpful advice given to us during our research.

Nissin Chemical Co., Osaka Works, Osaka